

2009

# Proazaphosphatranes: versatile molecules with applications in fuel cell technology, biodiesel production and important organic transformations

Kuldeep Wadhwa  
Iowa State University

Follow this and additional works at: <https://lib.dr.iastate.edu/etd>

 Part of the [Chemistry Commons](#)

## Recommended Citation

Wadhwa, Kuldeep, "Proazaphosphatranes: versatile molecules with applications in fuel cell technology, biodiesel production and important organic transformations" (2009). *Graduate Theses and Dissertations*. 10802.  
<https://lib.dr.iastate.edu/etd/10802>

This Dissertation is brought to you for free and open access by the Iowa State University Capstones, Theses and Dissertations at Iowa State University Digital Repository. It has been accepted for inclusion in Graduate Theses and Dissertations by an authorized administrator of Iowa State University Digital Repository. For more information, please contact [digirep@iastate.edu](mailto:digirep@iastate.edu).

**Proazaphosphatranes: versatile molecules with applications in fuel cell technology,  
biodiesel production and important organic transformations**

by

**Kuldeep Wadhwa**

A dissertation submitted to the graduate faculty  
in partial fulfilment of the requirement of the degree of  
DOCTOR OF PHILOSOPHY

Major: Organic Chemistry

Program of Study Committee:

John G. Verkade, Major Professor

George A. Kraus

Richard C. Larock

Victor S. Lin

Klaus Schmidt-Rohr

Iowa State University

Ames, Iowa

2009

Copyright © Kuldeep Wadhwa, 2009. All rights reserved

**DEDICATION**

**In memory of my mother the late Mrs. Geeta Wadhwa**

## TABLE OF CONTENTS

CHAPTER 1. GENERAL INTRODUCTION	1
CHAPTER 2. P( <i>i</i> -PrNCH <sub>2</sub> CH <sub>2</sub> ) <sub>3</sub> N: EFFICIENT CATALYST FOR SYNTHESIZING β-HYDROXYESTERS AND α,β-UNSATURATED ESTERS USING α-TRIMETHYLSILYLETHYLACETATE (TMSEA)	11
Abstract	11
Introduction	12
Results and Discussion	14
Conclusion	20
Experimental Section	23
Acknowledgment	23
References	23
CHAPTER 3. P( <i>i</i> -PrNCH <sub>2</sub> CH <sub>2</sub> ) <sub>3</sub> N: AN EFFICIENT CATALYST FOR TMS-1,3-DITHIANE ADDITION TO ALDEHYDES	27
Abstract	27
Introduction	27
Results and Discussion	30
Conclusion	35
Experimental Section	36
Acknowledgment	36
References	36
CHAPTER 4. P( <i>i</i> -PrNCH <sub>2</sub> CH <sub>2</sub> ) <sub>3</sub> N AS A LEWIS-BASE CATALYST FOR THE SYNTHESIS OF β-HYDROXYNITRILES USING TMSAN	39
Abstract	39
Introduction	39
Results and Discussion	42
Conclusion	50
Experimental Section	51
Acknowledgment	52
References	52
CHAPTER 5. P(PhCH <sub>2</sub> NCH <sub>2</sub> CH <sub>2</sub> ) <sub>3</sub> N: AN EFFICIENT LEWIS-BASE CATALYST FOR THE SYNTHESIS OF PROPARGYLIC ALCOHOLS AND MORITA-BAYLIS-HILLMAN ADDUCTS VIA ALDEHYDE ALKYNYLATION	56
Abstract	56
Introduction	57
Results and Discussion	59
Conclusion	74
Experimental Section	75



Acknowledgment	75
References	76
<b>CHAPTER 6. P(PhCH<sub>2</sub>NCH<sub>2</sub>CH<sub>2</sub>)<sub>3</sub>N CATALYSIS OF MUKAIYAMA ALDOL REACTIONS OF ALIPHATIC, AROMATIC, HETEROCYCLIC ALDEHYDES AND TRIFLUOROMETHYL PHENYL KETONE</b>	<b>79</b>
Abstract	79
Introduction	80
Results and Discussion	85
Conclusion	104
Experimental Section	106
Acknowledgment	124
References	124
<b>CHAPTER 7: DETERMINATION OF THE STRUCTURE OF A NOVEL ANION EXCHANGE FUEL CELL MEMBRANE BY SOLID-STATE NUCLEAR MAGNETIC RESONANCE SPECTROSCOPY</b>	<b>132</b>
Abstract	132
Introduction	133
Experimental Section	138
Results and Discussion	140
Conclusion	155
Acknowledgment	155
References	155
<b>CHAPTER 8. SYNTHESIS OF LINEAR OR BRANCHED POLYMERS POSSESSING CHEMICALLY BONDED PHOSPHATRANIUM NITRATE AS EFFICIENT NITRATE CONDUCTING MEMBRANES</b>	<b>158</b>
Objective	158
Introduction	158
Experimental Section	168
Results and Discussion	176
Conclusion	182
References	182
<b>CHAPTER 9. PROAZAPHOSPHATRANE CATALYSTS MOUNTED ON PERHALOGENATED POLYMERS</b>	<b>185</b>
Introduction	185
Results and Discussion	190
Conclusion	193
Experimental Section	194
References	196

CHAPTER 10. GENERAL CONCLUSIONS AND FUTURE WORK	200
ACKNOWLEDGEMENTS	207
APPENDIX A FOR CHAPTER 2	210
APPENDIX B FOR CHAPTER 3	284
APPENDIX C FOR CHAPTER 4	346
APPENDIX D FOR CHAPTER 5	423
APPENDIX E FOR CHAPTER 6	581

**LIST OF ABBREVIATIONS**

Ac	Acetyl
aq	aqueous
atm	atmospheric pressure
Bn	Benzyl
br	broad
Br	Bromide
bs	broad singlet
<i>i</i> -Bu	<i>iso</i> -butyl
<i>n</i> -Bu	Butyl
<i>t</i> -Bu	<i>tertiary</i> -butyl
°C	degree celsius
cat.	catalytic
Cl	Chloride
Cy	Cyclohexyl
d	doublet
DMF	<i>N,N</i> -dimethylformamide
equiv	equivalent
Et	Ethyl
h	hour(s)
HMPT	Hexamethylphosphorus triamide

HRMS	High resolution mass spectroscopy
Hz	Hertz
LDA	Lithium diisopropylamide
m	multiplet
Me	Methyl
min	minute(s)
mL	mililiters
mmol	milimol(s)
m.p.	melting point
N	Normal
NMR	Nuclear magnetic resonance
Nu	Nucleophile
<i>o</i>	ortho
<i>p</i>	para
neo-Pent	neo-Pentyl
Ph	Phenyl
<i>i</i> -Pr	iso-propyl
rt (RT)	room temperature
s	singlet
t	triplet
TBAF	Tetrabutylammonium fluoride
tert	tertiary

THF

Tetrahydrofuran

TLC

Thin layer chromatography

TMS

Trimethylsilyl

## CHAPTER 1. GENERAL INTRODUCTION

### Thesis Organization

This thesis is composed of ten chapters including the present chapter. The  $^1\text{H}$ ,  $^{13}\text{C}$ , and  $^{31}\text{P}$  NMR spectra for the reaction products have been compiled in the appendices, which appear at the end of the thesis.

The present chapter contains an introduction and a brief description of each of the remaining chapters. Then follows a general introduction to phosphatranes and phosphatranium ions and their uses as efficient catalysts for various transformations and also as cations for anionic conductors.

The second chapter entitled “*P(i-PrNCH<sub>2</sub>CH<sub>2</sub>)<sub>3</sub>N: Efficient Catalyst for Synthesizing  $\beta$ -Hydroxyesters and  $\alpha,\beta$ -Unsaturated Esters using  $\alpha$ -Trimethylsilylethylacetate (TMSEA)*” consists of a paper published in the *Journal of Organic Chemistry*, which describes the use of the commercially available proazaphosphatrane  $\text{P}(i\text{-PrNCH}_2\text{CH}_2)_3\text{N}$  as an efficient catalyst for the synthesis of  $\beta$ -hydroxyesters and  $\alpha,\beta$ -unsaturated esters via activation of the silicon-carbon bond of  $\alpha$ -trimethylsilylethylacetate. Selectivity for either of these two products was achieved simply by altering the catalyst loading and reaction temperature to afford the addition or stereoselective condensation product.

The third chapter entitled “*P(i-PrNCH<sub>2</sub>CH<sub>2</sub>)<sub>3</sub>N: An Efficient Catalyst for TMS-1,3-Dithiane Addition to Aldehydes*” consists of a communication published in *Tetrahedron Letters* describing an efficient methodology for the addition of 2-trimethylsilyl-1,3-dithiane (TMS-dithiane) to aldehydes at room temperature using the proazaphosphatrane  $\text{P}(i$

$\text{PrNCH}_2\text{CH}_2)_3\text{N}$ . The catalyst loading required for these reactions (5 mol %) is the lowest recorded in the literature, and the majority of the reaction times for this transformation were the shortest thus far reported.

The fourth chapter entitled “*P(i-PrNCH<sub>2</sub>CH<sub>2</sub>)<sub>3</sub>N as a Lewis-Base Catalyst for the Synthesis of β-Hydroxynitriles Using TMSAN*” consists of a paper published in the *Journal of Organic Chemistry* describing an efficient method of synthesizing β-hydroxynitriles in good to excellent yields using a wide variety of aldehydes (possessing various functional groups), enolizable aliphatic aldehydes, and a wide array of heterocyclic aldehydes. These reactions are facilitated using only 2 mol % catalyst, which, to the best of our knowledge, is the lowest catalyst loading thus far reported for this methodology.

The fifth chapter entitled “*P(PhCH<sub>2</sub>NCH<sub>2</sub>CH<sub>2</sub>)<sub>3</sub>N: An Efficient Lewis-base Catalyst for the Synthesis of Propargylic Alcohols and Morita-Baylis-Hillman adducts via Aldehyde Alkynylation*” reports the contents of a paper submitted for publication on the use of  $\text{P(PhCH}_2\text{NCH}_2\text{CH}_2)_3\text{N}$  as an efficient catalyst for the addition of aryl trimethylsilyl alkynes to various aromatic, aliphatic and heterocyclic aldehydes in THF at room temperature. Only propargylic alcohols were isolated in good to excellent isolated yields in the cases of electron-rich, electron-neutral, heterocyclic and aliphatic aldehydes, whereas β-branched Morita-Baylis-Hillman-type adducts were isolated with electron-deficient aromatic aldehydes after conventional acid hydrolysis of the TMS ethers.

The sixth chapter entitled “*P(PhCH<sub>2</sub>NCH<sub>2</sub>CH<sub>2</sub>)<sub>3</sub>N Catalysis of Mukaiyama Aldol Reactions of Aliphatic, Aromatic, Heterocyclic Aldehydes and Trifluoromethyl Ketone*” describes a paper in preparation reporting Mukaiyama reactions catalyzed by the title

proazaphosphatranane, which activates the silicon of the Si-O bond of trimethylsilyl enolates for reaction with aldehydes to yield the corresponding aldol products in good to excellent isolated yields. Among ketones, only the activated ketone 2,2,2-trifluoroacetophenone underwent clean aldol product formation with a variety of trimethylsilyl enolates. The reaction conditions were mild; operationally simple; and a variety of functional groups, such as nitro, amino, ester, chloro, trifluoromethyl, bromo, iodo, cyano and fluoro groups were tolerated. Product yields were generally better than or comparable to those recorded in the literature. With bulky (2,2-dimethyl-1-methylenepropoxy)trimethylsilane, only  $\alpha,\beta$ -unsaturated esters were isolated. Several heterocyclic aldehydes examined gave good product yields.

The seventh chapter entitled “*Determination of the Structure of a Novel Anion Exchange Fuel Cell Membrane by Solid-State Nuclear Magnetic Resonance Spectroscopy*” consists of a paper published in *Macromolecules* in collaboration with Prof. Klaus Schmidt-Rohr’s group, which reports the synthesis of a novel anion exchange fuel cell membrane by chemically attaching proazaphosphatranium and phosphatranium cations under microwave conditions to the sulfonic groups of Nafion-F<sup>®</sup>. Solid-state NMR techniques were employed to determine the structure and composition of this anion exchange membrane. The <sup>31</sup>P NMR spectrum showed two main signals with a 2:1 intensity ratio and chemical shift changes of +89 ppm and +46 ppm, respectively, from the main peak of phosphatranium chloride. <sup>1</sup>H-<sup>31</sup>P heteronuclear correlation NMR spectroscopy and <sup>1</sup>H-<sup>31</sup>P recoupling experiments indicated that the proton originally bonded to phosphorus in phosphatranium chloride is replaced in the major component of the Nafion<sup>®</sup>-proazaphosphatranium/phosphatranium composite. <sup>19</sup>F



NMR experiments showed that the fluorine in the  $-\text{SO}_2\text{F}$  group of the Nafion-F<sup>®</sup> precursor is completely replaced.  $^{31}\text{P}\{^{19}\text{F}\}$  rotational-echo double resonance (REDOR) experiments measured a P–F internuclear distance of  $\sim 0.4$  nm, which showed that the proazaphosphatranium is covalently attached to Nafion<sup>®</sup> through an S–P bond.  $^{13}\text{C}$  NMR and  $^1\text{H}$ – $^{13}\text{C}$  HetCor spectra indicated that the proazaphosphatranium structure is maintained even after the microwave treatment at  $180$  °C, and also showed the presence of entrapped dimethylformamide solvent.

The eighth chapter entitled “*Synthesis of Linear or Branched Polymers Possessing Chemically Bonded Phosphatranium Nitrate as Efficient Nitrate Conducting Membranes*” describes the synthesis of polymers containing phosphatranium nitrate bound to polymer backbones. These polymers are designed to function as efficient nitrate ion conductors for carbamide-fueled electrochemical cells.

The ninth chapter entitled “*Proazaphosphatranane Catalysts Mounted on Perhalogenated Polymers*” describes the synthesis of a novel Teflon<sup>®</sup>-bound azidoproazaphosphatranane catalyst for improving the recyclability of a heterogeneous catalyst for biodiesel synthesis by transesterification of soybean oil with methanol.

The thesis ends with the tenth chapter entitled “*General Conclusions and Future Work*,” which summarizes the findings in chapters 2-9 and provides a prospective outlook for the chemistry of proazaphosphatrananes. Included in this chapter are a proposed synthesis of perhalogenated polymer-bound proazaphosphatrananes and their application in Lewis-base catalyzed reactions and as a recyclable ligand for palladium-catalyzed cross-couplings. Also

included in this chapter is a proposed new strategy for the room temperature synthesis of polydifluoroacetylene (PDFA) facilitated by a proazaphosphatrane. PDFA is a potentially important polymer because of its unusual chemical, electronic and optical properties. The only synthetic route known in the literature involves prior synthesis of the monomer, which is notoriously explosive and pyrophoric.

### General Introduction

Proazaphosphatranes (**1**) are an important class of compounds that find advantageous uses as base catalysts and as ligands for palladium-catalyzed cross-couplings.<sup>1</sup> The first synthesis of a proazaphosphatrane, namely,  $P(\text{MeNCH}_2\text{CH}_2)_3\text{N}$ , was carried out in our laboratory by Lensink *et al.* in 1989.<sup>2</sup> Several such compounds soon became commercially available from Aldrich, Fluka and Strem and they are still available today. The unusual basicity of these compounds is evident from their facile P- (rather than N-) protonation to form  $\text{N}_{\text{basal}} \rightarrow \text{P}$  transannulated phosphatranium ions of type **2** shown in Figure 1. We have found that proazaphosphatranes, such as those in (Figure 1), are strongly basic as seen from their  $\text{pK}_a$  values in this figure.<sup>3,4</sup>

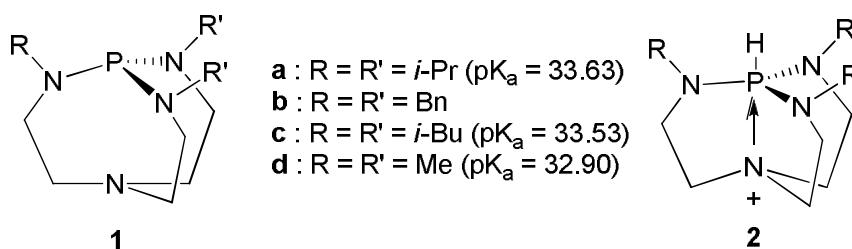
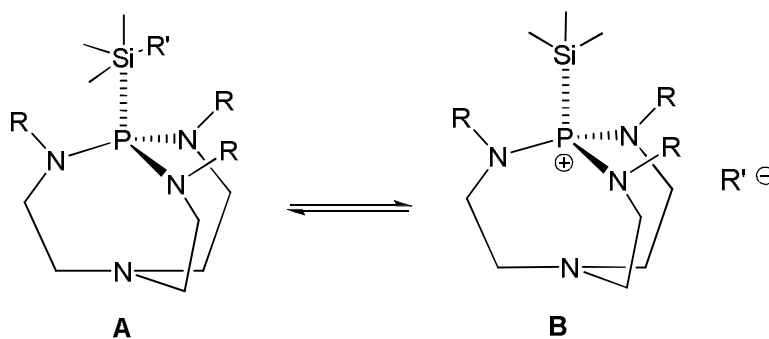


Figure 1

With the discovery of these novel molecules, a consistently growing array of reactions, catalyzed by strong Lewis bases emerged from our group. For example, Wroblewski and D'Sa synthesized the very strongly basic **1a**,<sup>5</sup> which D'Sa *et al.* then used for the silylation of alcohols.<sup>6</sup> Subsequently, reports from our group appeared in which the use of proazaphosphatranes for the activation of the silicon, e.g., is reported. Thus D'Sa *et al.* reported the silylation of alcohols using *tert*-butyldimethylsilyl chloride<sup>6,7</sup> and Wang and Fetterly reported evidence for the activation of the silyl group of TMSiCN and TBDMSCN for the synthesis of cyanohydrins using the reaction between trialkylsilyl nitrile and carbonyl compounds.<sup>8,9</sup> Proazaphosphatrane **1d** was found to be an efficient catalyst for the desilylation of TBDMS ethers.<sup>10</sup> In 2005, Urgaonkar *et al.* reported the nucleophilic aromatic substitution of aryl fluorides with aryl silyl ethers using **1c**.<sup>11</sup> Recently, the same reaction was reported by Raders<sup>12</sup> using proazaphosphatrane **1c** under microwave conditions with a lower catalyst loading. Wang *et al.* described the allylation of aromatic aldehydes with allyltrimethylsilanes<sup>13</sup> and the reduction of aldehydes and ketones using poly(methylhydrosiloxane)<sup>14</sup> in the presence of proazaphosphatrane **1d**.<sup>14</sup>

Wang *et al.* also described a mechanistic investigation of the activation of crotyltrimethylsilane using **1a** for the catalytic crotylation of aromatic aldehydes.<sup>13</sup> The formation of both  $\alpha$ - and  $\gamma$ -addition products in 1:1 ratio in this reaction was observed. The authors proposed the formation of an intermediate of type **B** depicted in Figure 2, which was later substantiated experimentally by Wang *et al.*<sup>8</sup> via <sup>29</sup>Si and <sup>31</sup>P NMR spectroscopic studies. The peak shown at <sup>29</sup>Si  $\delta = 7$  ppm was attributed to the formation of intermediate **B** wherein the anion was displaced.



**Figure 2**

The above results showed that a proazaphosphatranes were an excellent catalysts for silyl activation to synthesize useful organic intermediates. Part of the goal of this thesis was to develop the use of proazaphosphatranes to synthesize various useful small organic molecules by the activation of Si-O and Si-C bonds, along with efforts to gain further evidence for silicon group activation (Chapters 2-6).

Previously, Fetterly *et al.* in our group demonstrated that a phosphatranium cation of type **2** in Figure 1 for which the counter anion is nitrate, is an excellent catalyst for aza- and thia-Michael reactions.<sup>15</sup> Evidence was presented that such a nitrate salt in which the cation was bound to a solid support was superior to a commercially available nitrate anion exchange resin. This improved action was attributed to the poor anion-cation attractive interaction in our phosphatranium salts, which was rationalized on the basis of: (i) resonance stabilization of the phosphatranium cation (discussed further in Chapter 7 and 8), and (ii) the bulky size of the cation. Both factors render the nitrate ion “naked”. These results prompted us to chemically bind phosphatranium salts to polymeric membrane supports to function as nitrate ion conducting membranes for fuel cell applications (discussed in Chapter 8). Subsequently

this technique was utilized to develop a novel Nafion<sup>®</sup>-phosphatranium composite membrane, which showed excellent hydroxide ion conductivity (Chapter 7).

A thermally and air stable derivative of a proazaphosphatranane discovered in our laboratory is shown in Figure 3.<sup>16</sup> This compound was initially believed to be **3a**, but later it was determined to be **3b**, using X-ray crystallographic analysis of a homogeneous analog.<sup>17</sup> Merrifield resin is a polystyrene-based resin cross-linked by divinylbenzene. Heterogeneous catalysts of type **3c** have been shown by us to be useful in the acetylation of alcohols with vinyl acetate<sup>16</sup> and in 1,4 addition reactions.<sup>18</sup> Reddy *et al.* reported the use of catalyst **3c** for

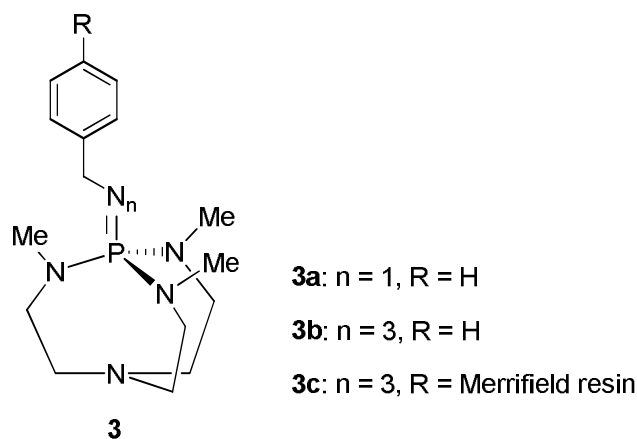


**Figure 3**

the synthesis of biodiesel, but found it to be deactivated after 11 cycles.<sup>17</sup> It was then discovered via solid state <sup>13</sup>C NMR techniques (in collaboration with Professor Schmidt-Rohr of this Department) that the catalyst was plugged with organic impurities accumulated during the catalyst cycles, thereby deactivating the catalyst by blocking the active sites.

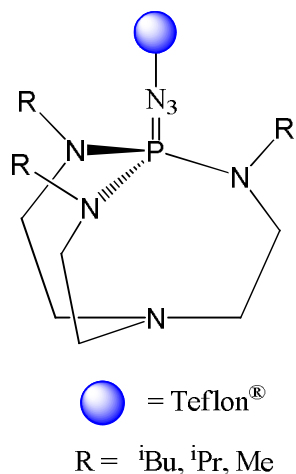


**Figure 4**

These observations prompted us to attempt the synthesis of a Teflon<sup>®</sup>- or Nafion<sup>®</sup>-bound azidoproazaphosphatane (Figure 4), which is discussed in Chapter 9. Such a solid support would enable our catalyst system to be stable to elevated temperatures and hydrolytic conditions. Moreover, high recyclability and resistance to plugging of the polymer pores by organic impurities would also be a very beneficial potential outcome.

### References

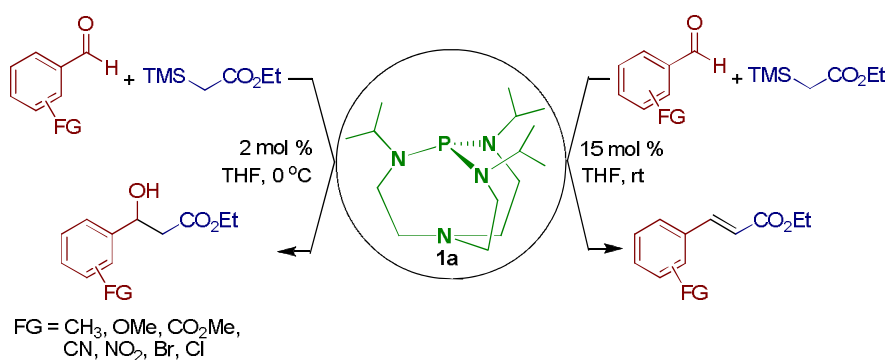
1. For reviews on proazaphosphatane chemistry, see: (a) Verkade, J. G. In *New Aspects of Phosphorus Chemistry II*, *Top. Curr. Chem.* Majoral, J. P. Ed., **2002**, 233, 1–44. (b) Verkade, J. G.; Kisanga, P. B. *Tetrahedron* **2003**, 59, 7819–7858. (c) Verkade, J. G.; Kisanga, P. B. *Aldrichimica Acta* **2004**, 37, 3–14. (d) Uргаonkar, S.; Verkade, J. G. *Specialty Chemicals* **2006**, 26, 36–39.

2. Lensink, C.; Xi, S.-K.; Daniels, L. M.; Verkade, J. G. *J. Am. Chem. Soc.* **1989**, *111*, 3478–3479.
3. Laramay, M. A. H.; Verkade, J. G. *J. Am. Chem. Soc.* **1990**, *112*, 9421–9422.
4. Kisanga, P. B.; Verkade, J. G. *J. Org. Chem.* **2000**, *65*, 5431–5432.
5. (a) Wroblewski, A.; Pinkas, J.; Verkade, J. G. *Main Group Chemistry* **1995**, *1*, 69. (b) D'Sa, B.; Verkade, J. G. *Phosphorus Sulfur Silicon* **1997**, *123*, 301.
6. D'Sa, B. Verkade, J. G. *J. Am. Chem. Soc.* **1996**, *118*, 12832–12833.
7. D'Sa, B. A.; McLeod, D.; Verkade, J. G. *J. Org. Chem.* **1997**, *62*, 5057–5061.
8. Wang, Z.; Fetterly, B. M.; Verkade, J. G. *J. Organometallic Chem.* **2002**, *646*, 161–166.
9. Fetterly, B. M.; Verkade, J. G. *Tetrahedron Lett.* **2005**, *46*, 8061–8066.
10. Yu, Z.; Verkade, J. G. *J. Org. Chem.* **2000**, *65*, 2065–2068.
11. Uргаonkar, S.; Verkade, J. G. *Org. Lett.* **2005**, *7*, 3319–3322.
12. Raders, S. M.; Verkade, J. G. *Tetrahedron Lett.* **2008**, *49*, 3507–3511.
13. Wang, Z.; Kisanga, P. B.; Verkade, J. G. *J. Org. Chem.* **1999**, *64*, 6459–6461.
14. Wang, Z.; Wroblewski, A. E.; Verkade, J. G. *J. Org. Chem.* **1999**, *64*, 8021–8023.
15. Fetterly, B. M.; Jana, N. K.; Verkade, J. G. *Tetrahedron* **2006**, *62*, 440–456.
16. Ilankumaran, P.; Verkade, J. G. *J. Org. Chem.* **1999**, *64*, 9063–9066.
17. Venkat Reddy, Ch.; Fetterly, B. M.; Verkade, J. G. *Energy Fuels* **2007**, *21*, 2466–2472.
18. Venkat Reddy, Ch.; Verkade, J. G. *J. Org. Chem.*, **2007**, *72*, 3093–3096.

CHAPTER 2. P(*i*-PrNCH<sub>2</sub>CH<sub>2</sub>)<sub>3</sub>N: EFFICIENT CATALYST FOR SYNTHESIZING  
 β-HYDROXYESTERS AND α,β-UNSATURATED ESTERS USING α-  
 TRIMETHYLSILYLETHYLACETATE (TMSEA)

Kuldeep Wadhwa, and John G. Verkade

*J. Org. Chem.* **2009**, *74*, 4368–4371



**Abstract:** In this report we present an efficient synthesis for β-hydroxyesters and α,β-unsaturated esters via activation of the silicon-carbon bond of α-trimethylsilylethylacetate using catalytic amounts of commercially available proazaphosphatane, P(*i*-PrNCH<sub>2</sub>CH<sub>2</sub>)<sub>3</sub>N **1a** (see above scheme). Selectivity for either of these two products can be achieved simply by altering the catalyst loading and reaction temperature to afford addition or stereoselective condensation. This method is mild and tolerates a wide array of functional groups.



## Introduction

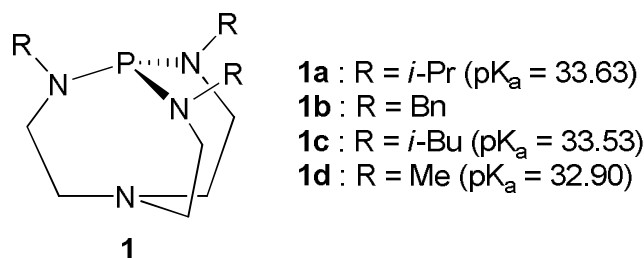
$\beta$ -Hydroxyesters are one of the most important classes of intermediates in the synthesis of natural products.<sup>1</sup> The most common method for the synthesis of such intermediates is the use of the carbon-carbon bond-forming Reformatsky reaction first discovered in 1887<sup>2</sup> which has been extensively studied since then.<sup>3,4</sup> The classical Reformatsky reaction utilizes elevated reaction temperatures and is typically carried out in aromatic solvents such as benzene, which are generally not environmentally friendly.<sup>2-4</sup> An improvement of the Reformatsky reaction involves the use of activated zinc reagents,<sup>5</sup> although the main drawback of this approach is the necessity for preparing fresh metal catalyst in advance, owing to instability of these reagents.<sup>5</sup> As an alternative to the conventional Zn-based Reformatsky methodology, other metals such as iron,<sup>6a</sup> nickel,<sup>6b</sup> magnesium,<sup>6c</sup> manganese<sup>6d</sup> and indium can be employed.<sup>6e,6f</sup> However, such metals are required in stoichiometric amounts,<sup>6b,6d</sup> and some of them must be reduced by the addition of a reducing metal.<sup>6a,6b,6d,6e</sup> The formation of side products is also an issue in the case of magnesium.<sup>6c</sup>

A later development involved the use of the reaction between an  $\alpha$ -silylester and a carbonyl (i.e., the silyl-Reformatsky reaction) to yield the corresponding  $\beta$ -hydroxyester.<sup>7,8a</sup> TBAF (6 mol %) has been employed as a source of fluoride ion for activating the  $\alpha$ -silyl group to generate a naked carbanion which then adds to the electrophilic carbonyl. However, product yield was only moderate and the substrate scope was limited.<sup>7a</sup> Use of an  $\alpha$ -dimethylsilylester in DMF solvent at 50 °C for 48 h, gave a 39-93% yield of the corresponding  $\beta$ -hydroxyester.<sup>7b</sup> The very strong Schwesinger base P4-*t*Bu (pK<sub>a</sub> 40 in

$\text{CH}_3\text{CN}$ ,<sup>9a</sup> 10 mol %) at  $-78\text{ }^\circ\text{C}$  gave the corresponding  $\beta$ -hydroxyester of the substrate acetophenone in poor yield (29%).<sup>8a</sup>

TBAF (3 mol %) is an effective catalyst for silicon activation in the reaction of TMSEA with aldehydes and ketones at low temperature ( $-20\text{ }^\circ\text{C}$ ) affording 24–88% yields of corresponding aldol products.<sup>7c</sup> Activation of the Si–C bond of TMSEA in a reaction with benzaldehyde using 20 mol % of *tris*(2,4,6-trimethoxyphenyl)phosphine at  $100\text{ }^\circ\text{C}$  in DMF was reported by Imamoto *et al.*<sup>7d</sup> to give a moderate yield (60%) of corresponding product, but no scope for aldehyde substrates was reported. Hamelin *et al.* reported silyl-Reformatsky reactions of TMSEA with three aromatic aldehydes using 8 equivalents of CsF as catalyst, which gave 62–75% yields of product at ambient temperature, and 62–84% yields using 440 W microwave radiation.<sup>7e</sup> Wieden *et al.* reported the use of  $\text{K}[\text{Al}(\text{OCH}_3)_4]$  (1 mol %) in refluxing pyridine as solvent in silyl-Reformatsky reactions between TMSEA and three aromatic aldehydes, but only moderate yields (39 and 46%) and a good yield of 81% was observed for the aldol products.<sup>7f</sup>

**FIGURE 1.** Proazaphosphatranes



Because of their significant Lewis basicities, proazaphosphatranes **1** in  $\text{CH}_3\text{CN}$ <sup>9b</sup> have been of interest to us as catalysts and reagents ever since their first synthesis in our laboratories. A key structural feature of **1** is the potential for  $\text{N}_{\text{basal}} \rightarrow \text{P}$  transannulation that

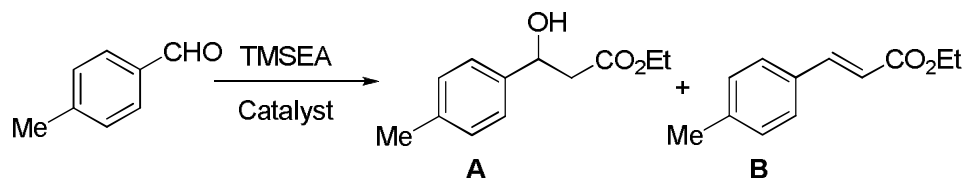
would enhance the nucleophilicity of the phosphorus. We have reported several instances in which **1** is apparently capable of activating a silicon center, e.g., in the silylation of alcohols using a silyl chloride,<sup>10a,10b</sup> the synthesis of cyanohydrins from the addition of trimethylsilyl nitrile to carbonyl compounds,<sup>10c,10d</sup> the desilylation of TBDMS ethers,<sup>10e</sup> and in the nucleophilic aromatic substitution of aryl fluorides with aryl silylethers.<sup>10f,10g</sup>

## Results and Discussion

In the present work, we report the use of **1a** as a catalyst for the efficient synthesis of  $\beta$ -hydroxyesters via a silyl-Reformatsky reaction, and  $\alpha,\beta$ -unsaturated esters via Peterson olefination from aldehydes with TMSEA as shown in the scheme in the Abstract. For optimization of the conditions, the reaction between *p*-tolualdehyde and TMSEA was selected. Excellent catalytic efficiency of **1a** and its commercial availability<sup>11</sup> favored its selection for the aforementioned syntheses. Using 5 mol % **1a**, this reaction at room temperature underwent mainly condensation to give the corresponding  $\alpha,\beta$ -unsaturated ester **B** in 75% yield and the desired aldol product **A** in 19% isolated yield, which is in accord with the **B/A** ratio of 8:2 observed by proton NMR spectroscopy in the crude reaction mixture (Table 1, entry 1). Increasing the catalyst loading to 10 mol % under the same reaction conditions increased the yield of the condensation product to 77% while decreasing the yield of aldol product (Table 1, entry 2). Raising the temperature to 80 °C, while keeping the loading of **1a** at 10 mol %, had no significant effect on the yield of condensation product (Table 1, entry 3). A further increase in loading of **1a** to 15 mol % at 25 °C led to a rise in yield of condensation product **B** (83%, Table 1, entry 4). However, reducing the reaction time gave only a 56% yield (Table 1, entry 4).

Gratifyingly, reducing the loading of **1a** to 5 mol % and lowering the temperature to 0 °C resulted in an 82% yield of aldol product **A** (Table 1, entry 5). Further lowering the loading of **1a** to 4 and 2 mol % at 0 °C increased the yield of **A** to 83 and 86% (Table 1, entries 6 and 7, respectively). When the reaction was carried out for 12 h, incomplete conversion and a lower yield was observed (62%, Table 1, entry 7). Lowering the temperature to –20 °C did not increase the yield of aldol product at 2 mol % loading of **1a** (87%, Table 1, entry 8) compared with that attained at 0 °C (86%, Table 1, entry 7). The yields of **A** obtained with **1a–d** screened under the optimized conditions given in Table 1, entry 7 for **1a** were good (Table 1, entries 5-7 and 9-12). The yield did not appear to correlate with steric or basicity trends of the proazaphosphatranes, however.

**TABLE 1:** Survey of Proazaphosphatranes as Catalysts for the Synthesis of  $\beta$ -Hydroxyesters and  $\alpha,\beta$ -Unsaturated Esters<sup>a</sup>



Entry	Catalyst	Mol %	Temp (°C)	Yield of <b>A</b> (%) <sup>b</sup>	Yield of <b>B</b> (%) <sup>b</sup>
1	<b>1a</b>	5	25	19	75
2	<b>1a</b>	10	25	14	77
3	<b>1a</b>	10	80	7	78
4	<b>1a</b>	15	25	-	83(56) <sup>c</sup>
5	<b>1a</b>	5	0	82	5
6	<b>1a</b>	4	0	83	-

**Table 1 continued**

7	<b>1a</b>	2	0	86(62) <sup>c</sup>	-
8	<b>1a</b>	2	-20	87	-
9	<b>1a</b>	1	0	81	-
10	<b>1b</b>	2	0	79	-
11	<b>1c</b>	2	0	81	-
12	<b>1d</b>	2	0	85	-

<sup>a</sup>Reaction conditions: (a) aldehyde (2 mmol), TMSEA (2.4 mmol), THF (2 mL), 24 h, 1N HCl (3 mL). <sup>b</sup>Yields represent isolated yields after silica gel column chromatography. <sup>c</sup>Reaction was carried out for 12 h.

To explore the scope of our methodology for the synthesis of  $\beta$ -hydroxyesters, a variety of aromatic, aliphatic and heterocyclic aldehydes were tested with **1a** under the optimized conditions given in Table 1, entry 7. Both electron donating and withdrawing groups were well tolerated, affording excellent yields of corresponding aldol product with only traces of dehydrated product detectable by <sup>1</sup>H NMR spectroscopy in the crude reaction mixtures (Table 2). Electron donating groups such as methyl (Table 1, entry 7), methoxy at both the *p*- and *o*- position (entries 2 and 3, respectively) and halogen groups (entries 4, 5 and 6); and electron withdrawing groups such as nitro (entry 7), cyano (entry 8) and ester (entry 9) afforded good yields of corresponding aldol products. The enolizable aliphatic aldehydes in entry 10 and 11 also underwent the silyl Reformatsky transformation, providing good yields of products. Interestingly,  $\alpha,\beta$ -unsaturated *trans*-cinnamaldehyde gave the desired aldol product in excellent isolated yield without significant contamination by 1,4 addition product (entry 12). Sterically hindered aldehydes such as 2,6-dimethylbenzaldehyde (entry 13) and biphenyl-2-carboxaldehyde (entry 14) gave good isolated yields of their corresponding aldol

products. Heterocyclic aldehydes also tolerated our reaction conditions. Both 5- and 6-membered ring aldehydes bearing N-, O- and S- heteroatoms gave excellent yields of their corresponding aldols (entries 15-17).

We then investigated the synthesis of  $\alpha,\beta$ -unsaturated esters, which are useful synthons in natural product synthesis.<sup>12</sup> Prime methodologies for the synthesis of  $\alpha,\beta$ -unsaturated esters are the Wittig<sup>13</sup> and Horner-Wadsworth-Emmons reactions.<sup>14</sup> The most important disadvantage of both these approaches is the necessity to employ an equivalent amount of strong base.<sup>13,14</sup> The decarboxylation of malonic acid half-esters is also an important route to the synthesis of  $\alpha,\beta$ -unsaturated esters.<sup>15</sup> Advantages of the Knoevenagel reaction are the inexpensive nature of the starting materials, and the easy removal of by-products ( $\text{CO}_2$  and  $\text{H}_2\text{O}$ ) to provide pure compounds.<sup>15a-c</sup> However, disadvantages of this method include the use of strongly basic conditions (e.g., the use of pyridine as solvent), excess malonic acid esters, and elevated temperatures. Moreover, the Knoevenagel reaction is not stereoselective, and enolizable aldehydes do not yield the desired products.<sup>15d-g</sup>

Another common approach to the synthesis of  $\alpha,\beta$ -unsaturated esters is the Peterson olefination reaction<sup>16</sup> which has advantages over the Wittig and Horner-Wadsworth-Emmons reactions, including easy reaction work up and product purification. Moreover, isolated-product yields are high. Disadvantageously, however, conventional Peterson olefination reactions consume an equivalent amount of a lithium base.<sup>16</sup> Recently Kondo *et al.* reported the use of a catalytic amount of P4-*t*Bu as an efficient base for the condensation reaction of TMSEA with aldehydes, ketones or formamides to yield the corresponding  $\alpha,\beta$ -unsaturated

esters.<sup>8a</sup> Ozanne *et al.* have reported the use of catalytic cesium fluoride (12 mol %) in DMSO as solvent for Peterson olefination of  $\alpha$ -silylestere with aldehydes or imines.<sup>8b</sup>

As we show in the present work, the conditions in Table 1, entry 4 are suitable for the condensation of TMSEA with aryl and heterocyclic aldehydes to yield the corresponding  $\alpha,\beta$ -unsaturated esters (Table 3). Aliphatic aldehydes, on the other hand, did not give the corresponding  $\alpha,\beta$ -unsaturated ester under our reaction conditions. Along with good tolerance of various functional groups and good to excellent isolated product yields, the reactions in Table 3 were also stereoselective, yielding only *trans*- products as determined by <sup>1</sup>H NMR spectroscopy. Electron donating groups such as methyl (entry 1) and methoxy (entry 2) provided the corresponding *trans* condensation products in excellent yields. The electron withdrawing cyano group allowed complete conversion to the desired product in excellent yield (entry 4). The reaction of *trans*-cinnamaldehyde with TMSEA also showed stereoselectivity, affording the corresponding condensation product as a mixture of two stereoisomers in a 9:1 ratio as determined by <sup>1</sup>H NMR spectroscopy (entry 5). Sterically hindered 2,6-dimethylbenzaldehyde gave the desired product in excellent yield (entry 6). Screening of heterocyclic aldehydes for the condensation reaction gave both good stereoselectivity and very good isolated product yield as was shown for 2-thiophenecarboxaldehyde and 2-benzofurancarboxaldehyde (entries 7 and 8, respectively).

**TABLE 2:** Scope of the Addition Reaction of Aldehydes with TMSEA Catalyzed by **1a**<sup>a</sup>

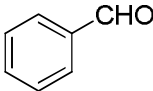
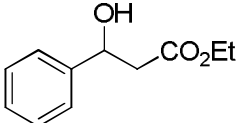
Entry	Aldehyde	Product	yield (%) <sup>b</sup>	lit. yield (%)
1			71	76, <sup>c</sup> 60, <sup>d</sup> 70, <sup>e</sup> 46, <sup>f</sup> 91 <sup>g</sup>

Table 2 continued

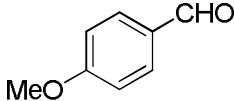
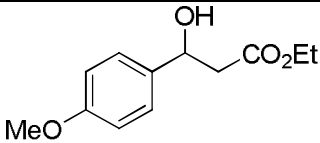
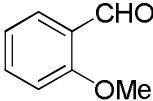
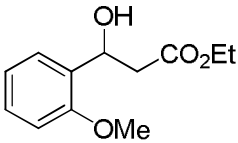
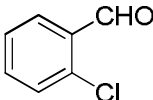
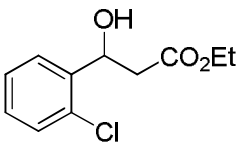
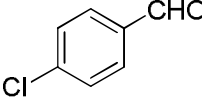
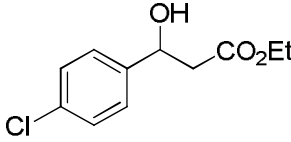
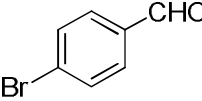
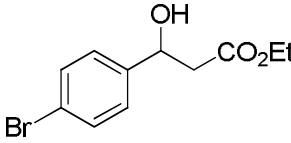
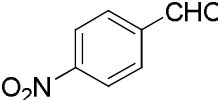
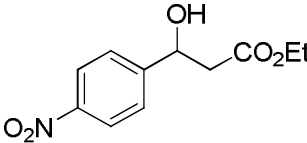
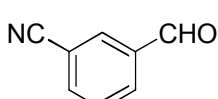
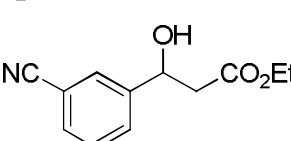
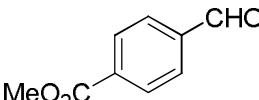
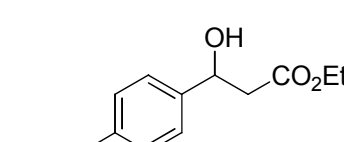
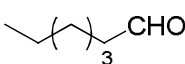
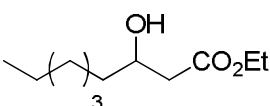
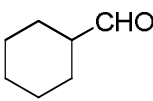
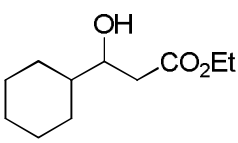
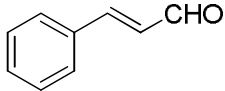
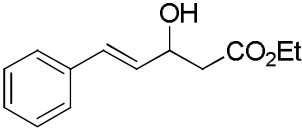
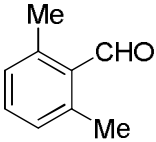
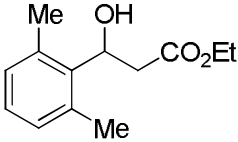
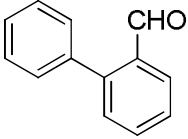
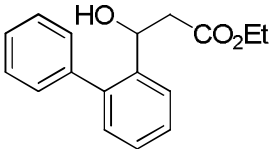
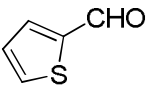
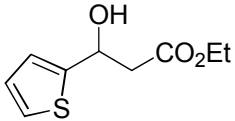
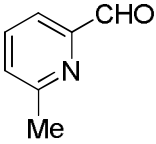
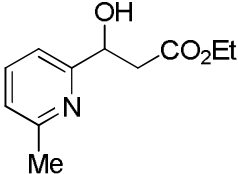
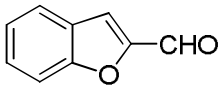
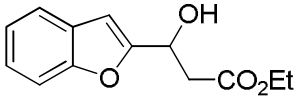
2			76	62 <sup>e</sup>
3			77	-
4			87	-
5			78	75 <sup>e</sup>
6			87	-
7			92	38 <sup>g</sup>
8			84	-
9			71	-
10			73	-
11			77	-



Table 2 continued

12			76	-
13			87	-
14			78	-
15			76	-
16			81	-
17			79	-

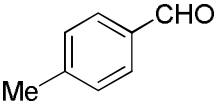
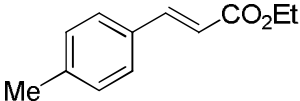
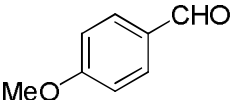
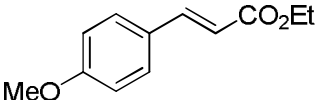
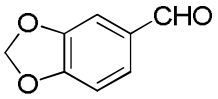
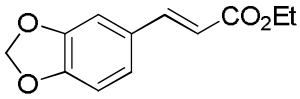
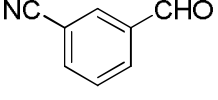
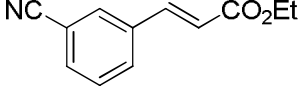
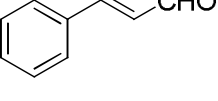
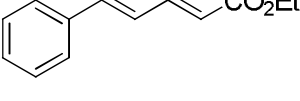
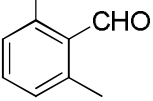
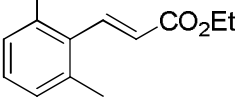
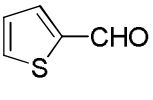
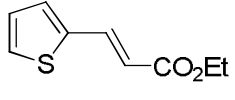
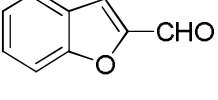
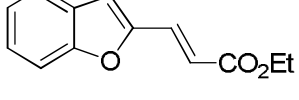
<sup>a</sup>Reaction conditions: (a) aldehyde (2 mmol), TMSEA (2.4 mmol), **1a** (2 mol %), THF (2 mL), 0 °C, 24 h, 1N HCl (3 mL). <sup>b</sup>Isolated yield after column chromatography. <sup>c</sup>See ref 7c. <sup>d</sup>See ref 7d. <sup>e</sup>See ref 7e. <sup>f</sup>See ref 8b. <sup>g</sup>See ref 7f.

## Conclusion

In conclusion, we have described a very mild and effective method for the synthesis of aldol products and  $\alpha,\beta$ -unsaturated esters by a simple change in **1a** loading and temperature. This method is general for aromatic, aliphatic and heterocyclic aldehydes, it tolerates a wide

spectrum of functional groups (including acid- and base-sensitive examples) and it leads to excellent isolated yields of aldol products. High stereoselectivity is achieved in the condensation reactions, yielding *trans*-products in good to very good isolated yields. The selectivity of the two products upon changing the reaction conditions can be rationalized using the two-stage mechanism proposed by Kondo *et al.* for the P4-*t*Bu-catalyzed reactions of TMSEA with carbonyl compounds to synthesize  $\alpha,\beta$ -unsaturated esters.<sup>8a</sup> In the 1st stage, the anion of a P4-*t*Bu-TMS<sup>+</sup> <sup>-</sup>CH<sub>2</sub>CO<sub>2</sub>Et (an intermediate formed from P4-*t*Bu and TMSEA) 1,2-adds to a carbonyl to produce a silylated  $\beta$ -hydroxyester, which in the 2<sup>nd</sup> stage eliminates HP4-*t*Bu<sup>+</sup> <sup>-</sup>OTMS. This elimination product catalyzes formation of the  $\alpha,\beta$ -unsaturated ester from the silylated  $\beta$ -hydroxyester. Commercial availability of catalyst **1a** and the environmentally desirable lack of metal usage in the syntheses reported here renders our methodology attractive. In comparing yields of  $\beta$ -hydroxyesters attained in our methodology with those found in the literature for the five of the methods cited in four entries of Table 2, we found that only one literature yield is higher than is attained with our method, four yields are lower, and three are comparable. In the case of the  $\alpha,\beta$ -unsaturated esters in Table 3, we compared two literature methods cited in three entries of this table, and found that one literature yield was higher than that attained with our methodology and two were lower. Our methodology was ineffective for the ketones (e.g., acetophenone, 4-chloroacetophenone and benzophenone).

**TABLE 3:** Scope of the Condensation Reaction of Aldehydes with TMSEA Catalyzed by **1a**<sup>a</sup>

Entry	Aldehyde	Product	Yield (%) <sup>b</sup>	Lit. Yield (%) <sup>c</sup>
1			83	91 <sup>c</sup>
2			83	69 <sup>c</sup>
3			79	-
4			90	-
5			84(9:1) <sup>d</sup>	65 <sup>c</sup>
6			80	-
7			89	-
8			79	-

<sup>a</sup>Reaction conditions: (a) aldehyde (2 mmol), TMSEA (2.4 mmol), **1a** (15 mol %), THF (2 mL), rt, 24 h, 1N HCl (3 mL). <sup>b</sup>Isolated yield after column chromatography. <sup>c</sup>See ref 8a. <sup>d</sup>Determined by NMR. <sup>e</sup>See ref 8b.

## Experimental Section

**General Reaction Procedure for the Synthesis of  $\beta$ -Hydroxyesters and  $\alpha,\beta$ -Unsaturated esters.** In a nitrogen-filled glove box, a round bottom flask was charged with **1** (2 mol % for  $\beta$ -hydroxyesters, 15 mol % for  $\alpha,\beta$ -unsaturated esters). Anhydrous THF (2.0 mL) was syringe under argon into the flask, followed by TMSEA (2.40 mmol) at 0 °C (r.t. for  $\alpha,\beta$ -unsaturated esters). The reaction mixture was stirred at 0 °C (r.t. for  $\alpha,\beta$ -unsaturated esters) for 15 min and then aldehyde (2.0 mmol) was added over 5–10 min. The reaction mixture was stirred for 24 h at 0 °C (r.t. for  $\alpha,\beta$ -unsaturated esters) and then it was quenched with 3 mL of aqueous HCl (1*N*). The reaction mixture was stirred at 0 °C (r.t. for  $\alpha,\beta$ -unsaturated esters) for 1 h and then it was neutralized with saturated aqueous NaHCO<sub>3</sub> and extracted with CH<sub>2</sub>Cl<sub>2</sub> (3 × 30 mL). The product was purified by column chromatography on silica gel using 10% EtOAc/hexanes, except for heterocyclic substrates (20–25% EtOAc/hexanes).

## Acknowledgment

The National Science Foundation is gratefully acknowledged for financial support of this research in the form of grant 0750463. We also thank Dr. Ch. Venkat Reddy for helpful discussions.

## References

- (1) (a) Sánchez, M.; Bermejo, F. *Tetrahedron Lett.* **1997**, 38, 5057–5060. (b) Gabriel, T.; Wessjohann, L. A. *Tetrahedron Lett.* **1997**, 38, 1363–1366. (c) Wittenberg, R.; Beier, C.;

Drager, G.; Jas, G.; Jasper, C.; Monenschein, H.; Kirschning, A. *Tetrahedron Lett.* **2004**, *45*, 4457–4460. (d) Servi, S. *Synthesis* **1990**, 1–25 and references therein.

(2) Reformatsky, S. *Chem. Ber.* **1887**, *20*, 1210–1211.

(3) (a) Gensler, W. J. *Chem. Rev.* **1957**, *57*, 191–280. (b) Diaper, D. G. M.; Kuksis, A. *Chem. Rev.* **1959**, *59*, 89–178.

(4) (a) Fürstner, A. *Synthesis* **1989**, 571–590. (b) Ocampo, R.; Dolbier, W. R. *Tetrahedron* **2004**, *60*, 9325–9374. (c) Orsini, F.; Sello, G. *Curr. Org. Synth.* **2004**, *1*, 111–135.

(5) (a) Rieke, R. D.; Uhm, S. J. *Synthesis* **1975**, 452–453. (b) Santaniello, E.; Manzocchi, A. *Synthesis* **1977**, 698–699. (c) Csuk, R.; Fürstner, A.; Weidmann, H. *J. Chem. Soc., Chem. Commun.* **1986**, 775.

(6) (a) Durandetti, M.; Périchon, J. *Synthesis* **2006**, 1542–1548. (b) Inaba, S.-I.; Rieke, R. D. *Tetrahedron Lett.* **1985**, *26*, 155–156. (c) Moriwake, T. *J. Org. Chem.* **1996**, *31*, 983–985. (d) Suh, Y. S.; Rieke, R. D. *Tetrahedron Lett.* **2004**, *45*, 1807–1809. (e) Chao, L. C.; Rieke, R. D. *J. Org. Chem.* **1975**, *40*, 2253–2255. (f) Babu, S. A.; Yasuda, M.; Shibata, I.; Baba, A. *J. Org. Chem.* **2005**, *70*, 10408–10419.

(7) (a) Nakamura, E.; Shimizu, M.; Kuwajima, I.; Sakata, J.; Yokoyama, K.; Noyori, R. *J. Org. Chem.* **1983**, *48*, 932–945 (b) Miura, K.; Sato, H.; Tamaki, K.; Ito, H.; Hosomi, A. *Tetrahedron Lett.* **1998**, *39*, 2585–2588. (c) Nakamura, E.; Shimizu, M.; Kuwajima, I. *Tetrahedron Lett.* **1976**, *20*, 1699–1702. (d) Matsukawa, S.; Okano, N.; Imamoto, T. *Tetrahedron Lett.* **2000**, *41*, 103–107. (e) Latouche, R.; Texier-Boulet, F.; Hamelin, J. *Bull. Soc. Chim. Fr.* **1993**, *130*, 535–546. (f) Birkofer, L.; Ritter, A.; Wieden, H. *Chem. Ber.* **1962**, *95*, 971–976.

(8) (a) Kobayashi, K.; Ueno, M.; Kondo, Y. *Chem. Commun.* **2006**, 3128–3130. (b) Bellassoued, M.; Ozanne, N. *J. Org. Chem.* **1995**, *60*, 6582–6584.

(9) (a) Schwesinger, R.; Schlemper, H.; Hasenfratz, C.; Willaredt, J.; Dambacher, T.; Breuer, T.; Ottaway, C.; Fletchinger, M.; Boele, J.; Fritz, H.; Putzas, D.; Rotter, H. W.; Bordwell, F. G.; Statish, A. V.; Ji, G. Z.; Peters, E. M.; Peters, K.; von Schnering, H. G.; Walz, L. *Liebigs Ann.* **1996**, 1055–1081. (b) Kisanga, P. B.; Verkade, J. G. Schwesinger, R. *J. Org. Chem.* **2000**, *65*, 5431–5432.

(10) (a) D'Sa, B. A.; Verkade, J. G. *J. Am. Chem. Soc.* **1996**, *118*, 12832–12833. (b) D'Sa, B. A.; McLeod, D.; Verkade, J. G. *J. Org. Chem.* **1997**, *62*, 5057–5061. (c) Wang, Z.; Fetterly, B. M.; Verkade, J. G. *J. Organomet. Chem.* **2002**, *646*, 161–166. (d) Fetterly, B. M.; Verkade, J. G. *Tetrahedron Lett.* **2005**, *46*, 8061–8066. (e) Yu, Z.; Verkade, J. G. *J. Org. Chem.* **2000**, *65*, 2065–2068. (f) Uргаonkar, S.; Verkade, J. G. *Org. Lett.* **2005**, *7*, 3319–3322. (g) Raders, S. M.; Verkade, J. G. *Tetrahedron Lett.* **2008**, *49*, 3507–3511.

(11) Proazaphosphatranes **1a**, **1c**, and **1d** are commercially available.

(12) (a) Xia, C.; Heng, L.; Ma, D. *Tetrahedron Lett.* **2002**, *43*, 9405–9409. (b) Chen, D.; Guo, L.; Liu, J.; Kirtane, S.; Cannon, J. F.; Li, G. *Org. Lett.* **2005**, *7*, 921–924. (c) Ryu, D. H.; Corey, E. J. *J. Am. Chem. Soc.* **2003**, *125*, 6388–6390. (d) López, F.; Harutyunyan, S. R.; Meetsma, A.; Minnaard, A. J.; Feringa, B. L. *Angew. Chem., Int. Ed.* **2005**, *44*, 2752–2756. (e) Srikanth, G. S. C.; Castle, S. L. *Tetrahedron* **2005**, *61*, 10377–10441. (f) Hayashi, T.; Yamasaki, K. *Chem. Rev.* **2003**, *103*, 2829–2844.

(13) (a) Murphy, P. J.; Brennan, J. *Chem. Soc. Rev.* **1988**, *17*, 1–30. (b) Maryanoff, B. E.; Reitz, A. B. *Chem. Rev.* **1989**, *89*, 863–927. (c) Murphy, P. J.; Lee, S. E. *J. Chem. Soc., Perkin Trans. I*, **1999**, 3049–3066.

(14) (a) Motoyoshiya, J. *Trends in Organic Chemistry* **1998**, *7*, 63–73. (b) Nicolaou, K. C.; Harter, M. W.; Gunzner, J. L.; Nadin, A. *Liebigs Ann.* **1997**, *7*, 1283–1301.

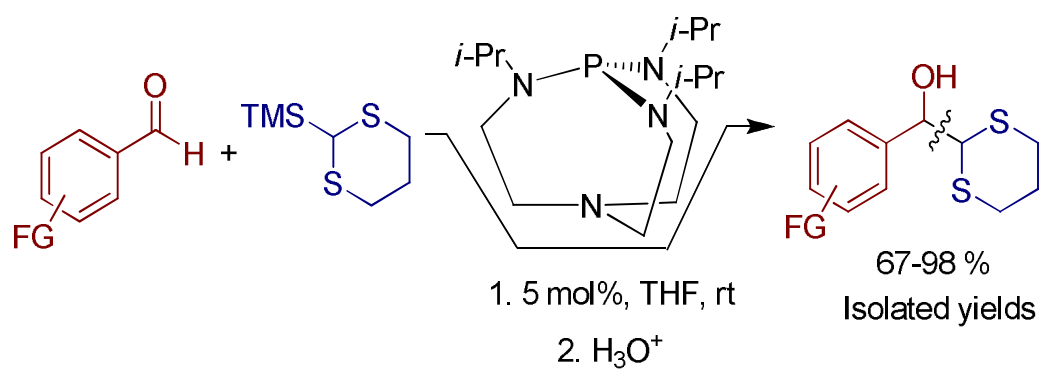
(15) (a) Galat, A. *J. Am. Chem. Soc.* **1945**, *68*, 376–377. (b) Klein, J.; Bergmann, E. D. *J. Am. Chem. Soc.* **1957**, *79*, 3452–3454. (c) Shabtai, J.; Ney-Igner, E.; Pines, H. *J. Org. Chem.* **1981**, *46*, 3795–3802. (d) Carmona, A. T.; Robina, F. J.; Garcia, R. E.; Demange, R.; Vogel, P.; Winters, A. L. *J. Org. Chem.* **2003**, *68*, 3874–3883. (e) Yamanaka, H.; Yokoyama, M.; Sakamoto, T.; Shiraishi, T.; Sagi, M.; Mizugaki, M. *Heterocycles* **1983**, *20*, 1541–1544. (f) Ragoussis, N.; Ragoussis, V. *J. Chem. Soc. Perkin Trans. I* **1998**, 3529–3533.

(16) (a) Staden, L. F. V.; Gravestock, D.; Ager, D. J. *Chem. Soc. Rev.* **2002**, *31*, 195–200. (b) Peterson, D. J. *J. Org. Chem.* **1968**, *33*, 780–784. (c) Ager, J. *Org. React.* **1990**, *38*, 1–223.

**CHAPTER 3. P(*i*-PrNCH<sub>2</sub>CH<sub>2</sub>)<sub>3</sub>N: AN EFFICIENT CATALYST FOR TMS-1,3-DITHIANE ADDITION TO ALDEHYDES**

Kuldeep Wadhwa and John G. Verkade

*Tetrahedron Lett.* **2009**, *50*, 4307–4309



**Abstract**— Herein we report the use of P(*i*-PrNCH<sub>2</sub>CH<sub>2</sub>)<sub>3</sub>N (**1a**) as an efficient catalyst for 2-trimethylsilyl-1,3-dithiane (TMS-dithiane) addition to aldehydes at room temperature. The catalyst loading required for these reactions (5 mol %) is the lowest recorded in the literature, and the majority of the reaction times for this transformation are the shortest thus far reported. A variety of functional groups are tolerated on the aryl aldehyde substrates.

### Introduction

The addition of 1,3-dithiane (a masked acylcarbanion) to various electrophiles (e.g., aldehydes, ketones, alkyl halides) is one of the most practiced methodologies in synthetic organic chemistry for the formation of C-C bonds.<sup>1-6</sup> Also known as an “umpolung”, “dipole inversion” or “inversion of reactivity” reaction, this process at the S<sub>2</sub>C carbon of the dithiane



allows facile generation of a carbonyl functionality under mild oxidation conditions using reagents such as  $\text{Hg}(\text{ClO}_4)_2$ ,  $\text{CuCl}_2/\text{CuO}$ ,  $\text{AgNO}_3$ ,  $\text{Tl}(\text{NO}_3)_3$  and [bis(trifluoroacetoxy)iodo]benzene.<sup>6-10</sup> The most common deprotonating agent for converting a 1,3-dithiane to a nucleophile for addition to an electrophilic carbon center is the use of a stoichiometric amount of BuLi.<sup>1-6</sup>

Umpolung of a dithiane for its addition to ketones and aldehydes has also been accomplished via catalytic activation of a silyl group in a 2-silyl-1,3-dithiane.<sup>11-14</sup> Thus Pollicino *et al.* reported the use of a stoichiometric amount of cesium fluoride as a base in DMF solvent using 2-trimethylsilyl-4,6-dimethyl-1,3-dithiane and benzaldehyde to obtain a product yield of 72%, but the substrate scope was limited to benzaldehyde.<sup>11</sup> Corey *et al.* utilized an equivalent of CsF in a 1:1 mixture with CsOH at 0 °C for 2 h for the reaction of *p*-methoxybenzaldehyde with TMS-dithiane which achieved a product yield of 85%.<sup>12</sup> A catalytic amount (10 mol %) of the fluoride ion source [*n*-Bu<sub>4</sub>N][Ph<sub>3</sub>SiF<sub>2</sub>] was reported by DeShong *et al.* to achieve a 96% yield of product from the reaction of benzaldehyde (the only substrate tested) with TMS-dithiane.<sup>13</sup> Very recently, Mukaiyama *et al.* reported that the use of 30 mol % of [*n*-Bu<sub>4</sub>N][OPh] as a general catalyst for promoting the addition (TMS-dithiane at 0 °C in DMF to aldehydes and ketones to provide product yields of 60-97% and 63-93%, respectively.<sup>14</sup> This significantly improved methodology does, however, require a highly polar aprotic solvent and a high mol % of catalyst.<sup>14</sup>

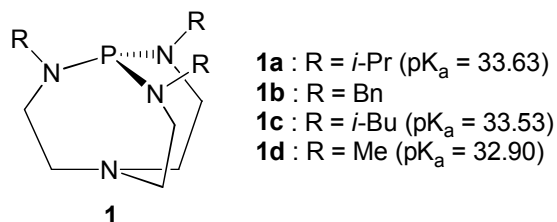
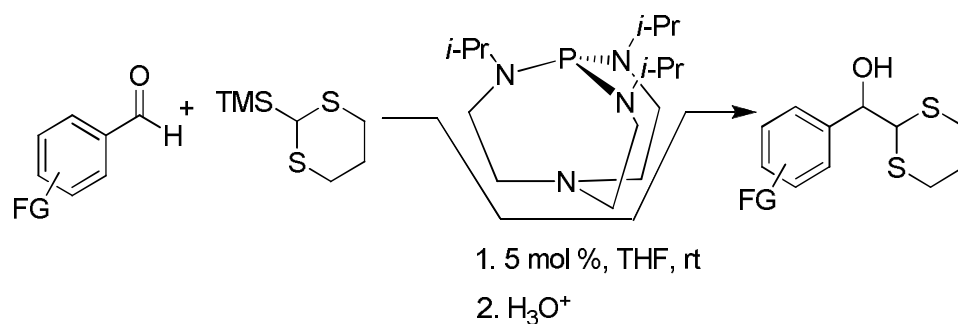


**Figure 1.** Proazaphosphatrane **1**

We have found<sup>15</sup> that proazaphosphatranes such as those in Figure 1 are strongly basic with pK<sub>a</sub> values in the range 32-34 in MeCN for their P-protonated N<sub>basal</sub>→P transannulated conjugate acids.<sup>16</sup> To the extent that N<sub>basal</sub>→P transannulation may be occurring during reactions catalyzed by **1**, the nucleophilicity of the phosphorus may be enhanced.<sup>15b</sup> We previously reported reactions in which proazaphosphatranes can activate silicon functionalities,<sup>17-23</sup> as for example in the silylation of alcohols using *tert*-butyldimethylsilyl chloride,<sup>17,18</sup> the synthesis of cyanohydrins from the addition of a trialkylsilylcyanide to carbonyl compounds,<sup>19,20</sup> the desilylation of TBDMS ethers,<sup>21</sup> and the nucleophilic aromatic substitution of aryl fluorides with aryl silylethers.<sup>22,23</sup>

Because proazaphosphatranes activate silicon functional groups<sup>17-23</sup> in addition to functioning as strong Lewis bases,<sup>15,16</sup> it occurred to us that in view of the paucity of reports in which the catalytic activation of TMS-dithiane for carbonyl umpolung<sup>13,14</sup> has been utilized, proazaphosphatranes might function well in such reactions. Here we report use of a proazaphosphatrane as an efficient catalyst for 1,3-dithiane addition to the carbonyl of aldehydes as shown in Scheme 1.



**Scheme 1.** General Reaction Scheme

### Results and Discussion

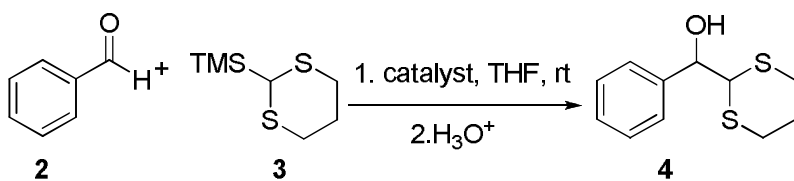
For optimization studies (Table 1) we chose the reaction of an electron-neutral aldehyde (**2**) with TMS-dithiane (**3**). With 2 mol % of **1a**, the isolated yield of product **4** was only 52% (entry 1). Increasing the catalyst loading to 5 mol %, however, augmented that yield to 98% (entry 2) over the same time period. Gratifyingly, this reaction time could be shortened to 30 min without compromising yield (entry 3). The conditions of entry 3 for proazaphosphatranes **1b-d** also gave excellent yields of product **4** (Table 1, entry 4-6). Proazaphosphatranes **1a** was our catalyst of choice, however, because of the combination of its superior performance, commercial availability,<sup>24</sup> and ease in handling owing to its crystalline nature when purified by sublimation.<sup>25</sup> It is noteworthy that our catalyst loading of 5 mol % is the lowest recorded in the literature for this methodology. According to NMR spectroscopy, no reaction was observed in the absence of catalyst (entry 7).

With the conditions in entry 3 of Table 1, a variety of aldehydes were screened to generalize the scope of catalyst **1a** (Table 2). Electron donating groups such as methoxy (entry 1) and methyl (entry 2) resulted in excellent isolated product yields. Electron withdrawing and acid sensitive groups such as ester (entry 3) and cyano (entry 4) gave

excellent and good yields, respectively. A halogen-containing aryl aldehyde (entry 5) and an enolizable aliphatic aldehyde (entry 6) provided excellent product yields. With the sterically congested aldehyde 2-biphenyl carboxaldehyde (Table 2, entry 7) a good isolated yield of product (81%) was realized.

Because only two heterocyclic aldehydes were previously examined in this reaction,<sup>14</sup> we examined five five- and two six-membered ring examples with our protocol, in which the low catalyst loading of 5 mol % was maintained. The oxygen-containing benzofuran-2-carboxaldehyde participated in its reaction with dithiane (Table 2, entry 8) as did the halogenated nitrogen heterocycle in entry 9 and the N- and S-containing heterocycle in entry 10; all giving excellent product yields. Although the heterocycle containing two nitrogens in entry 11 gave a rather moderate yield of product, excellent product yields were achieved with thiophene-2-carboxaldehyde (entry 12), 6-methyl-2-pyridinecarboxaldehyde (entry 13) and N-methylindole-2-carboxaldehyde (entry 14).

**Table 1:** Survey of Proazaphosphatranes (**1**)<sup>a</sup>



Entry	Catalyst	Mol %	Time	Yield (%) <sup>b</sup>
1	<b>1a</b>	2	24 h	52
2	<b>1a</b>	5	24 h	98
3	<b>1a</b>	5	30 min	98 (96) <sup>c</sup>

**Table 1 continued**

4	<b>1b</b>	5	30 min	95
5	<b>1c</b>	5	30 min	97
6	<b>1d</b>	5	30 min	95
7	none	-	24 h	0

<sup>a</sup>Reaction conditions: catalyst (x mol %), benzaldehyde (2.0 mmol), **3** (2.4 mmol), THF (2 mL), rt followed by 1N HCl (3 ml). <sup>b</sup>Isolated yield after column chromatography. <sup>c</sup>Lit. yield see refs 13 and 14.

From the variety of aldehydes included in the scope of our protocol, it appears that our methodology is general for those possessing electron withdrawing or donating groups and additionally for acid- or base-labile functional groups. Heterocyclic and enolizable aliphatic aldehydes are also amenable to our protocol.

**Table 2:** Reaction Scope of Aldehydes with 2-Trimethylsilyl-1,3-dithiane Catalyzed by **1a**<sup>a</sup>

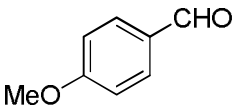
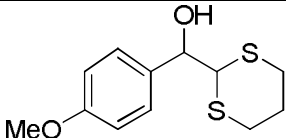
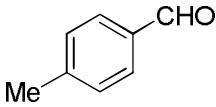
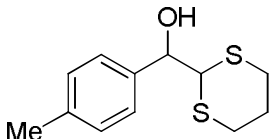
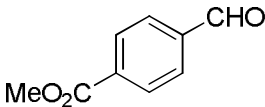
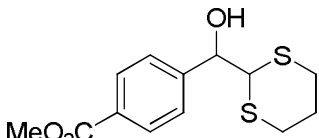
Entry	Aldehyde	Product	Yield (%) <sup>b</sup>	Lit. Yield (%)
1			95	85 <sup>c</sup> , 95 <sup>d</sup>
2			98	97 <sup>d</sup>
3			93	-

Table 2 continued

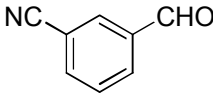
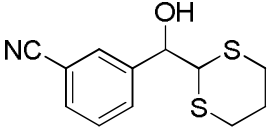
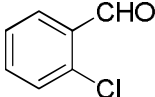
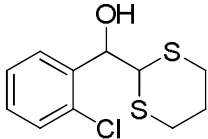
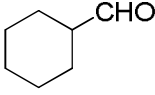
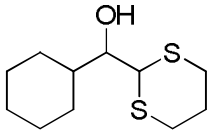
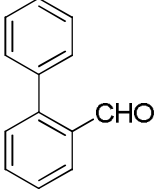
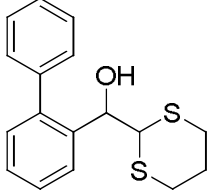
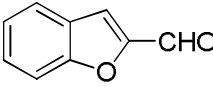
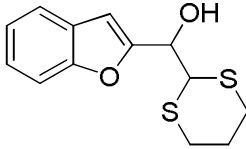
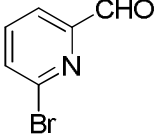
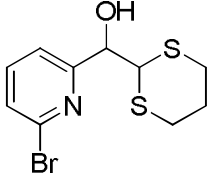
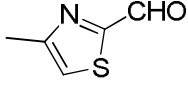
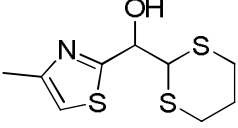
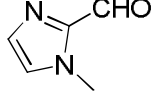
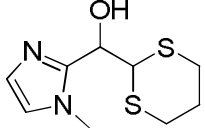
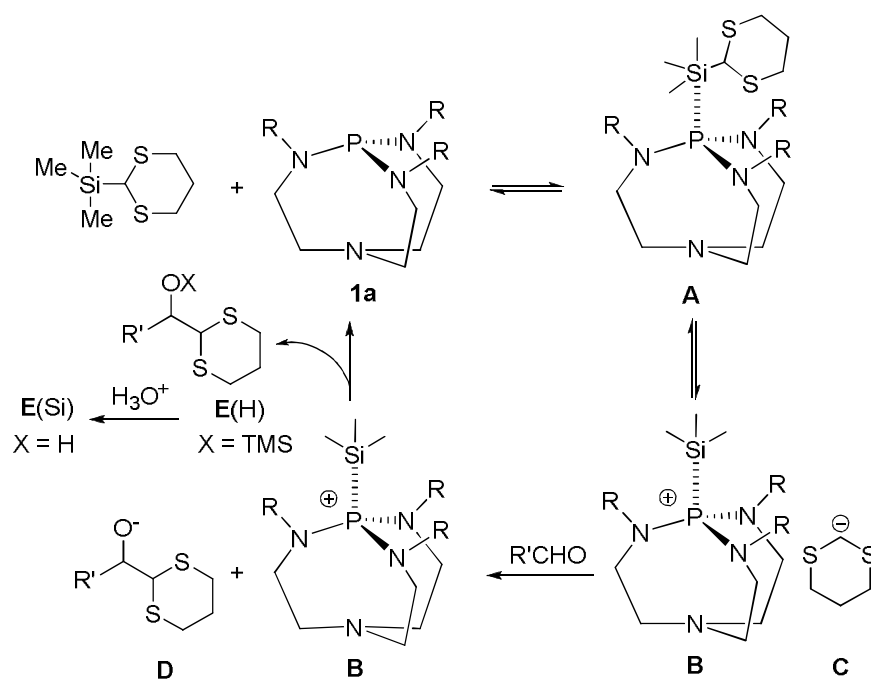
4			80	-
5			96	95 <sup>d</sup>
6			94	83 <sup>d</sup>
7			81	-
8			95	-
9			92	-
10			94	-
11			67	-

Table 2 continued

12			97	-
13			98	-
14			94	-

<sup>a</sup>Reaction conditions: aldehyde (2 mmol), **3** (2.4 mmol), THF (2 mL), **1a** (5 mol %) rt, 30 min followed by 1N HCl (3 mL). <sup>b</sup>Isolated yield after silica gel column chromatography. <sup>c</sup>See ref 12. <sup>d</sup>See ref 14.

A proposed mechanism for the addition of TMS-dithiane to aldehydes under our conditions is depicted in Scheme 2. Initially, **1** forms a pentacoordinated silicate TMS-dithiane adduct **A** which enriches the electron density on the silicon, consequently weakening the bonds around this atom and thus favoring ionization to species **B** and **C**. Thereafter, the dithiane anion **C** nucleophilically attacks the aldehyde carbon giving **D** which then nucleophilically attacks cation **B** giving intermediate **E**(Si). This intermediate is subsequently hydrolyzed in a second step to give the product **E**(H) with regeneration of the catalyst **1a**.



**Scheme 2.** Proposed mechanism for TMS-1,3-dithiane addition reactions of aldehydes catalyzed by **1a**

### Conclusion

In summary, we found the nonionic strongly Lewis basic proazaphosphatane **1a** to be an efficient catalyst for the addition of 2-trimethylsilyl-1,3-dithiane to aldehydes. To the best of our knowledge, ours is the first report of a low catalyst loading for the synthesis of  $\beta$ -hydroxydithianes using a TMS-dithiane reagent. Our protocol operates efficiently at room temperature in 30 min with a commercially available catalyst, and product yields are generally excellent. Compared with literature reports of the highest yields for five of the products in Tables 1 and 2, our methodology gave a substantially higher yield in one instance and equal yields (within 1%) in the remaining 4 cases.



## Experimental Section

**General reaction procedure.** A round-bottomed flask was charged with **1** (0.1 mmol, 5 mol %) in a nitrogen filled glove-box. To this was added 2.0 mL of anhydrous tetrahydrofuran (THF) followed by the addition of aldehyde (2.0 mmol) at room temperature. The resulting solution was stirred at room temperature for 15 min and then 2-trimethylsilyl-1,3-dithiane **3** (2.4 mmol) was added over a period of two min. Progress of the reaction was monitored by proton NMR spectroscopy. The reaction mixture was stirred for 30 min and followed by quenching with 3 mL of an aq. solution 1N HCl. The mixture was stirred for an additional 1 h and then it was neutralized with saturated aq. NaHCO<sub>3</sub> solution and extracted with CH<sub>2</sub>Cl<sub>2</sub> (3 × 30 mL). The combined organic extracts were dried over anhydrous MgSO<sub>4</sub>. The crude product was purified by column chromatography using 30% EtOAc/hexane as eluent, whereas in the case of entry 11 of Table 2, 20% (v/v) MeOH/CH<sub>2</sub>Cl<sub>2</sub> was employed.

## Acknowledgment

The National Science Foundation is gratefully acknowledged for financial support of this research through grant 0750463. We also thank Dr. Ch. Venkat Reddy for helpful discussions.

## References

1. Smith III, A. B.; Adams, A. C. *Acc. Chem. Res.* **2004**, *37*, 365–377.
2. Corey, E. J.; Seebach, D. *Angew. Chem., Int. Ed. Engl.* **1965**, *4*, 1075–1077.
3. Corey, E. J.; Seebach, D. *Angew. Chem., Int. Ed. Engl.* **1965**, *4*, 1077–1078.
4. Corey, E. J.; Seebach, D.; Freedman, R. *J. Am. Chem. Soc.* **1967**, *89*, 434–436.

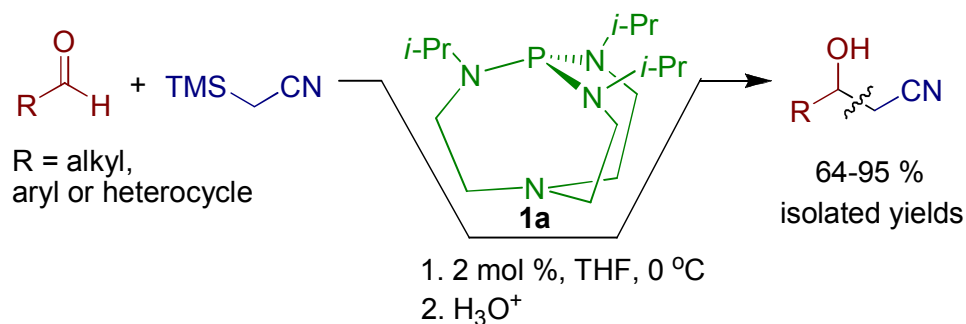
5. Seebach, D.; Corey, E. J. *J. Org. Chem.* **1975**, *40*, 231–237.
6. Gröbel, B.-T.; Seebach, D. *Synthesis* **1977**, 357–402.
7. Corey, E. J.; Erickson, B. W. *J. Org. Chem.* **1971**, *36*, 3553–3560.
8. Fetizon, M.; Jurion, M. *J. Chem. Soc., Chem. Commun.* **1972**, 382–383.
9. Stork, G.; Zhao, K. *Tetrahedron Lett.* **1989**, *30*, 287–290.
10. Greene, T. W.; Wuts, P. G. M. in *Protective Groups in Organic Synthesis*, 3rd ed., John Wiley & Sons, New York, **1999**; pp. 329–344.
11. Capperucci, A.; Cere, V.; Innocenti, A. D.; Nocentini, T.; Pollicino, S. *Synlett.* **2002**, 1447–1450.
12. Busch-Petersen, J.; Bo, Y.; Corey, E. J. *Tetrahedron Lett.* **1999**, *40*, 2065–2068.
13. Pilcher, A. S.; DeShong, P. *J. Org. Chem.* **1996**, *61*, 6901–6905.
14. Michida, M.; Mukaiyama, T. *Chem. Lett.* **2008**, *37*, 26–27.
15. For reviews of proazaphosphatrane chemistry, see: (a) Verkade, J. G. In *New Aspects of Phosphorus Chemistry II*, *Top. Curr. Chem.* Majoral, J. P. Ed., **2002**, *233*, 1–44. (b) Verkade, J. G.; Kisanga, P. B. *Tetrahedron* **2003**, *59*, 7819–7858. (c) Verkade, J. G.; Kisanga, P. B. *Aldrichimica Acta* **2004**, *37*, 3–14. (d) Urgaonkar, S.; Verkade, J. G. *Specialty Chemicals* **2006**, *26*, 36–39.
16. Kisanga, P. B.; Verkade, J. G. Schwesinger, R. *J. Org. Chem.* **2000**, *65*, 5431–5432.
17. D'Sa, B. A.; Verkade, J. G. *J. Am. Chem. Soc.* **1996**, *118*, 12832–12833.
18. D'Sa, B. A.; McLeod, D.; Verkade, J. G. *J. Org. Chem.* **1997**, *62*, 5057–5061.
19. Wang, Z.; Fetterly, B. M.; Verkade, J. G. *J. Organomet. Chem.* **2002**, *646*, 161–166.
20. Fetterly, B. M.; Verkade, J. G. *Tetrahedron Lett.* **2005**, *46*, 8061–8066.

21. Yu, Z.; Verkade, J. G. *J. Org. Chem.* **2000**, *65*, 2065–2068.
22. Urgaonkar, S.; Verkade, J. G. *Org. Lett.* **2005**, *7*, 3319–3322.
23. Raders, S. M.; Verkade, J. G. *Tetrahedron Lett.* **2008**, *49*, 3507–3511.
24. Proazaphosphatranes **1a**, **1c**, and **1d** are commercially available from sources such as Aldrich and Strem Chemicals.
25. Wroblewski, A. E.; Pinkas, J.; Verkade, J. G. *Main Group Chem.* **1995**, *1*, 69–79.

CHAPTER 4. P(*i*-PrNCH<sub>2</sub>CH<sub>2</sub>)<sub>3</sub>N AS A LEWIS-BASE CATALYST FOR THE  
SYNTHESIS OF β-HYDROXYNITRILES USING TMSAN

Kuldeep Wadhwa and John G. Verkade\*

*J. Org. Chem.* **2009** ASAP



**Abstract:** Proazaphosphatrane **1a** was found to be an efficient catalyst for synthesis of β-hydroxynitriles via the reaction of trimethylsilylacetonitrile (TMSAN) with aldehydes under mild reaction conditions and typically low catalyst loading (ca. 2 mol %). A variety of functional groups were tolerated and good to excellent product yields were obtained.

### Introduction

Carbon-carbon bond forming reactions are extensively utilized in modern organic synthesis<sup>1</sup> and one of the most common approaches to this process is via nucleophilic addition to carbonyl compounds.<sup>1</sup> β-Hydroxynitriles are important building blocks in many natural product syntheses<sup>2</sup> owing to the stability of nitriles to handling,<sup>3</sup> and the versatility of the nitrile group to conversion to a variety of other functionalities such as amines,<sup>4a</sup> amides,<sup>4b</sup> aldehydes,<sup>4c</sup> esters,<sup>4d</sup> alcohols<sup>4e</sup> or carboxylic acids.<sup>5</sup>

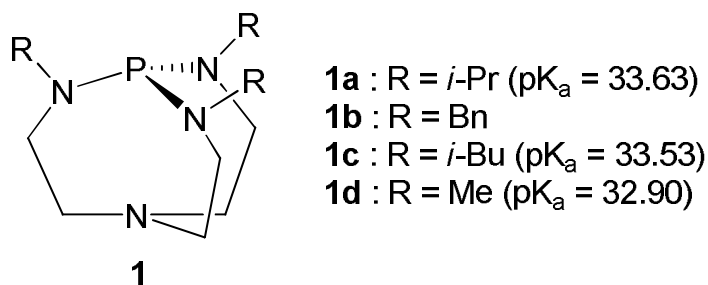
Generally,  $\beta$ -hydroxynitriles have been synthesized with the aid of an equivalent amount of strong alkali metal base (for example,  $(\text{CH}_3)_2\text{CHMgBr}$ , BuLi, or alkali amides) to deprotonate the alpha proton of acetonitrile or benzyl nitrile to generate a nucleophile that attacks the carbonyl group.<sup>6</sup> Low yields commonly encountered with these methods<sup>6</sup> have been attributed<sup>7</sup> to reversibility of the reaction or facile product dehydration to give  $\alpha,\beta$ -unsaturated nitriles.

More recently, several other methods aimed at improving the yields of  $\beta$ -hydroxynitrile syntheses have appeared in the literature.<sup>8</sup> Using an equivalent amount of *n*-BuLi, additional TMSCl was added to trap the alkoxide, resulting in a favorable shift of the equilibrium.<sup>8a</sup> Other reported methods include the use of toxic metal catalysts such as Mn/PbCl<sub>2</sub>/TMSCl,<sup>8d</sup> Hg(ONC)<sub>2</sub><sup>3</sup> and PbCl<sub>2</sub>/Ga.<sup>8k</sup> A two step synthesis of  $\beta$ -hydroxynitriles has been reported involving the prior generation of an aryl anion using aryl halide in an electrochemical cell,<sup>8e</sup> which then deprotonates acetonitrile for subsequent addition of the resulting anion to ketones, aldehydes, alkyl halides and esters. However, this method is cumbersome, providing only moderate product yields (52–74%). Another commonly utilized approach is the use of 1,2-epoxides in the presence of a nitrile or LiClO<sub>4</sub>/KCN to promote nucleophilic ring opening of the epoxide. However, this method generally favors the use of aliphatic epoxides and yields vary from 35–98%.<sup>8f-j</sup> Additional reported methods for the synthesis of  $\beta$ -hydroxynitriles involve multi-step approaches.<sup>8l-m</sup>

TMSAN has been utilized for prior formation of the *O*-silyl ether in several attempts to overcome the reaction reversibility problem. In one such reaction,  $\beta$ -hydroxynitriles were produced in 70-73% yield via acid hydrolysis of the *O*-silyl adduct formed via the use of

toxic potassium cyanide as the catalyst.<sup>9a</sup> The use of KF as a catalyst resulted in quantitative conversion of the *O*-silyl ether to product, but 25 mol % of KF was required, and only benzaldehyde was explored as a substrate.<sup>9b</sup> KF (50 mol %) loaded on alumina with prior catalyst activation at 673 K using benzaldehyde as the sole substrate gave a low yield of product plus 15% of  $\alpha,\beta$ -unsaturated nitrile.<sup>9d</sup> Utilizing 10 mol % of tris(dimethylamino)sulfonium difluorotrimethylsiliconate (TASF) at -15 °C resulted in product yields of 20–93% for a variety of aldehydes and ketones.<sup>9c</sup> Using 2.5 mol % of [Cu(PPh<sub>3</sub>)<sub>3</sub>][(EtO)<sub>3</sub>SiF<sub>2</sub>] as a catalyst in the presence of 1.2 equivalents of (EtO)<sub>3</sub>SiF as an additive for the cyanomethylation of aldehydes using TMSAN,<sup>5</sup> gave good product yields (75-100%), but no scope of functional groups was reported. The use of LiOAc and CsOAc as Lewis base catalysts has been described<sup>7</sup> and although the yields are good, a high catalyst loading (10 mol %) as well as a relatively inconvenient solvent (DMF) is required. Piperidine (24 mol %) functioned as a catalyst under microwave conditions in the absence of solvent, but product yields were low to moderate (ca. 38-73%) and reactions were typically conducted at elevated temperature (85 °C).<sup>9e</sup> Recently Kitazaki *et al.* reported the use of *tris*(2,4,6-trimethoxyphenyl)phosphine (10 mol %) for TMSAN addition to aldehydes and ketones with product yields of 56-99%, and to imines with 0-85% product yields in DMF and DMPU.<sup>9f</sup>

**FIGURE 1.** Proazaphosphatranes



We found earlier<sup>10</sup> that proazaphosphatranes (**1**) bearing various organic groups on the PN<sub>3</sub> nitrogens (Figure 1) are strongly basic with pK<sub>a</sub> values of the their P-protonated N<sub>basal</sub>→P transannulated conjugate acids in the range 32-34 in MeCN.<sup>11</sup> To the extent that N<sub>basal</sub>→P transannulation may be occurring during reactions catalyzed by **1**, the nucleophilicity of the phosphorus may be enhanced.<sup>10b</sup> We previously reported reactions in which proazaphosphatranes can activate silicon functionalities as, for example, in the silylation of alcohols using silyl chloride,<sup>12a,12b</sup> synthesis of cyanohydrins from the addition of trimethylsilyl nitrile to carbonyl compounds,<sup>12c,12d</sup> desilylation of TBDMS ethers,<sup>12e</sup> nucleophilic aromatic substitution of aryl fluorides with aryl silylethers,<sup>12f,12g</sup> allylation of aromatic aldehydes,<sup>12h</sup> and reduction of aldehydes and ketones using poly(methylhydrosiloxane).<sup>12i</sup>

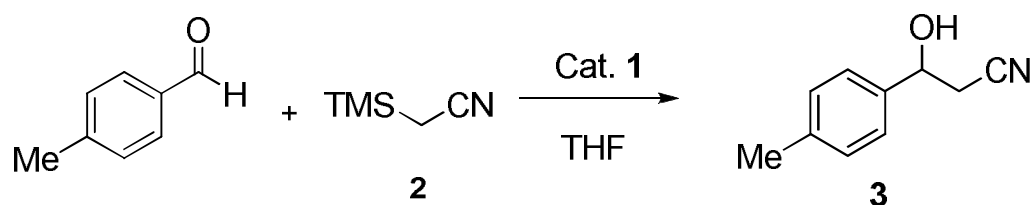
In the present work, we report the use of proazaphosphatrane **1a** as an efficient catalyst for the synthesis of β-hydroxynitriles from aldehydes with TMSAN as shown in the scheme in the Abstract.

## Results and Discussion

To optimize the reaction conditions, we chose the reaction of *p*-tolualdehyde with TMSAN (Table 1) as a model. We selected proazaphosphatrane **1a** as the screening catalyst owing to its efficiency in this reaction and its commercial availability.<sup>13</sup> Using 10 mol % of **1a** at room temperature, dehydration to the corresponding α,β-unsaturated nitrile dominated β-hydroxynitrile formation (Table 1, entry 1). Lowering the temperature to 0 °C under the

same conditions increased the yield of the desired product to 46% (entry 2) but lowering the temperature to  $-15\text{ }^{\circ}\text{C}$  revealed essentially no change in product yield (entry 3).

**TABLE 1.** Survey of Proazaphosphatranes as Catalysts for the Synthesis of  $\beta$ -Hydroxynitriles<sup>a</sup>



Entry	Catalyst	Mol %	Yield (%) <sup>b</sup>
1 <sup>c</sup>	<b>1a</b>	10	30
2	<b>1a</b>	10	46
3 <sup>d</sup>	<b>1a</b>	10	45
4	<b>1a</b>	5	56
5	<b>1a</b>	4	74
6	<b>1a</b>	2	91 <sup>e</sup>
7	<b>1a</b>	1	86
8	<b>1b</b>	2	87 <sup>e</sup>
9	<b>1c</b>	2	90 <sup>e</sup>
10	<b>1d</b>	2	90 <sup>e</sup>

<sup>a</sup>Reaction conditions: (a) aldehyde (2.0 mmol), TMSAN (2.4 mmol), THF (2 mL),  $0\text{ }^{\circ}\text{C}$ , 24 h, followed by 1N HCl (3 mL). <sup>b</sup>Isolated yield after silica gel column chromatography. <sup>c</sup>Reaction was carried out at rt. <sup>d</sup>Reaction was carried out at  $-15\text{ }^{\circ}\text{C}$ . <sup>e</sup>Average of three runs.

Since higher loading of a basic catalyst can lead to undesired formation of  $\alpha,\beta$ -



unsaturated nitrile via a Peterson olefination pathway,<sup>14</sup> we reduced the catalyst loading to 5 mol % and found that the yield of  $\beta$ -hydroxynitrile was substantially enhanced (Table 1, entry 4). Further lowering of the catalyst loading increased the yield of  $\beta$ -hydroxynitrile to 74 and 91% (entries 5 and 6, respectively). However, lowering the catalyst loading below 2% inhibited completion of the reaction, resulting in only a good product yield (86%, entry 7). Thus we decided to proceed with 2 mol % catalyst at 0 °C to screen proazaphosphatranes **1b–d**, and those results are also summarized in Table 1 (entries 8–10). We found that changing the R group on the PN<sub>3</sub> nitrogens gave comparable yields of the desired product, although **1a** was slightly better than the others. We do not have a reasonable explanation for this observation.

Given the higher activity of **1a** as a catalyst and its commercial availability, we proceeded with **1a** under the conditions optimized in Table 1, entry 6 to extend the scope of our protocol for the synthesis of  $\beta$ -hydroxynitriles. Thus a variety of aromatic and aliphatic aldehydes were employed under the optimized conditions in Table 1, entry 6. The product yields shown in Table 2 are comparable in most cases to those reported in the literature. Both electron donating and withdrawing groups afforded excellent isolated yields, with only a trace of, or no dehydrated product detectable by <sup>1</sup>H NMR spectroscopy. Electron donating groups such as methyl (Table 1, entry 6), methoxy at both para and ortho positions (Table 2, entries 2 and 3), and halogen (Table 2, entry 4) were tolerated under our conditions, giving excellent isolated product yields. Electron withdrawing groups such as *p*-nitro (entry 6), *m*-cyano (entry 7) and *p*-ester (entry 8) were also well tolerated, affording the desired respective products in excellent isolated yields. *Trans*-cinnamaldehyde gave the desired product in

good isolated yield (entry 9) with no observable evidence from NMR spectroscopy of the corresponding Michael addition product. Aliphatic enolizable aldehydes also gave good isolated product yields (Table 2, entries 10 and 11). Unfortunately our methodology was ineffective for the ketones tested (acetophenone, 4-chloro-acetophenone and benzophenone).

**TABLE 2.** Scope of the Reaction of Aldehydes with TMSAN Catalyzed by **1a**<sup>a</sup>

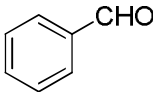
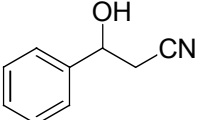
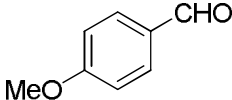
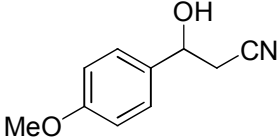
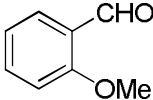
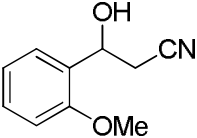
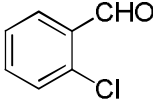
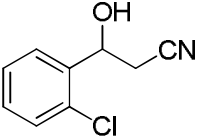
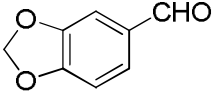
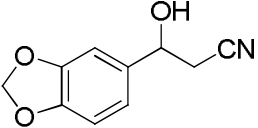
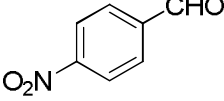
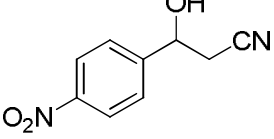
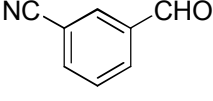
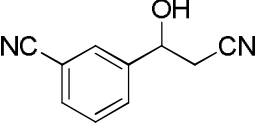
Entry	Reactant	Product	Yield (%) <sup>b</sup>	Lit. Yield (%)
1			89	62-100 <sup>c-h</sup>
2			83	80-96 <sup>e,f,g,i</sup>
3			77	-
4			94	-
5			82	-
6			94	94 <sup>g</sup>
7			89	-

Table 2 continued

8			93	73 <sup>e</sup>
9			94	45-99 <sup>c,e,f,i</sup>
10			85	80 <sup>f</sup>
11			86	80-86 <sup>f,g</sup>

<sup>a</sup>Reaction conditions: (a) aldehyde (2.0 mmol), TMSAN (2.4 mmol), **1a** (2 mol %), THF (2 mL), 0 °C, 24 h, followed by 1N HCl (3 mL). <sup>b</sup>Isolated yield after column chromatography. <sup>c</sup>See ref 9a. <sup>d</sup>See ref 9b. <sup>e</sup>See ref 9c. <sup>f</sup>See ref 5. <sup>g</sup>See ref 7. <sup>h</sup>See ref 9e. <sup>i</sup>See ref 9f.

With a range of 5- and 6-membered ring heterocycle-bearing aldehydes possessing representation of O-, N- and S-heterocycle types, good to excellent yields of the desired product were obtained (Table 3). Thus the thiophenic aldehydes in entries 1 and 2 gave very good and excellent product yields, respectively; the pyridinyl aldehydes in entries 3 and 4; and quinolyl aldehyde in entry 5 afforded the corresponding products in excellent to good yields, respectively; N-containing 2-formyl-1-methylindole gave an excellent isolated product yield (entry 6), the S,N-heterocycle in entry 7 facilitated an excellent yield of product; and the benzofuran, coumarin and furan carboxaldehydes in entries 8, 9 and 10 permitted a modest, moderate and good yield of products, respectively. The moderate

product yield in entry 9 was pleasantly surprising in view of the sensitivity of lactones to acid and base.

**TABLE 3.** Scope of the Reaction of Heterocyclic Aldehydes with TMSAN Catalyzed by **1a**<sup>a</sup>

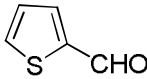
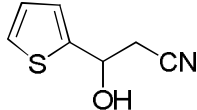
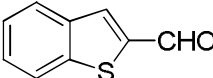
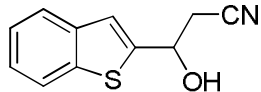
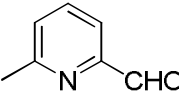
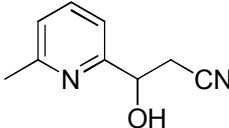
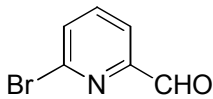
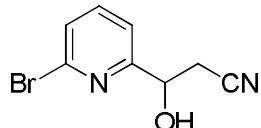
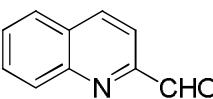
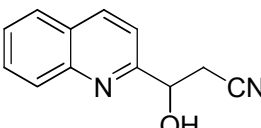
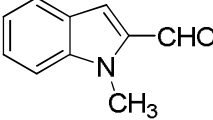
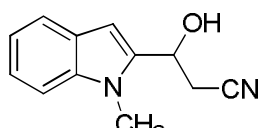
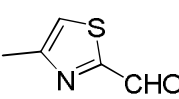
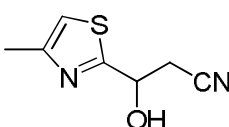
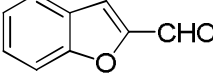
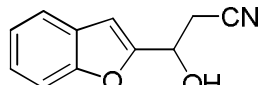
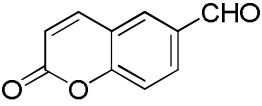
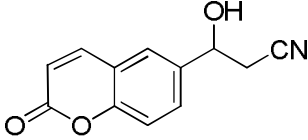
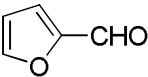
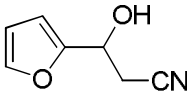
Entry	Aldehyde	Product	Yield (%) <sup>b</sup>
1			88
2			93
3			92
4			87
5			93 (97) <sup>c</sup>
6			81
7			95
8			64

Table 3 continued

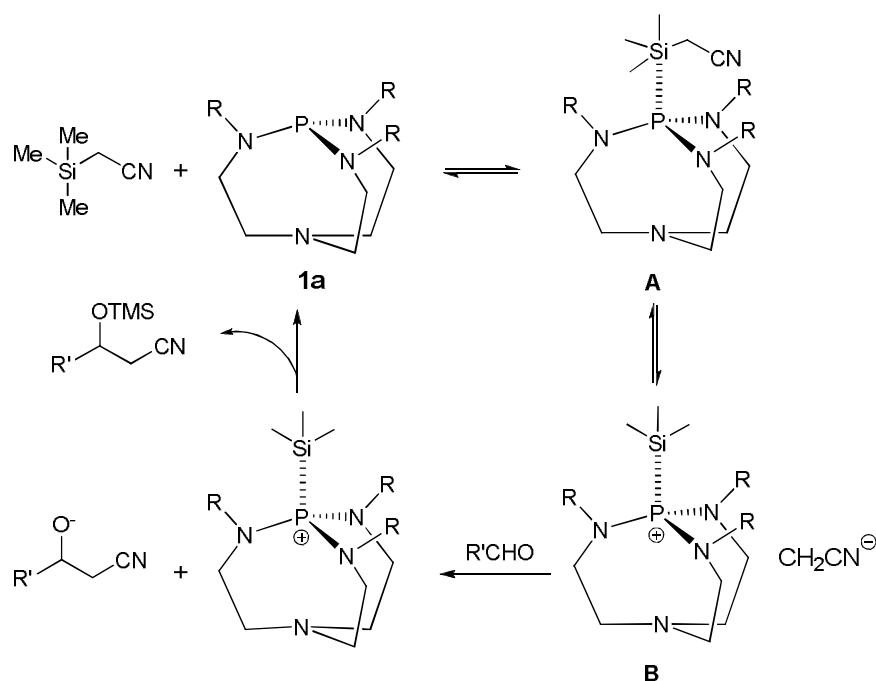
9			70
10			81 (99, <sup>c</sup> 65 <sup>d</sup> )

<sup>a</sup>Reaction conditions: (a) aldehyde (2.0 mmol), TMSAN (2.4 mmol), **1a** (2 mol %), THF (2 mL), 0 °C, 24 h, followed by 1N HCl (3 mL). <sup>b</sup>Isolated yield after column chromatography. <sup>c</sup>See ref 7. <sup>d</sup>See ref 9f.

A proposed mechanistic pathway for the addition of TMSAN to aldehydes is shown in Scheme 1. To obtain some insight into this pathway, we carried out <sup>29</sup>Si NMR experiments at -40 °C in which a THF solution of TMSAN ( $\delta^{29}\text{Si}$  5.02 ppm in THF) was treated with an equimolar amount of **1a**. A new peak, which then appeared at  $\delta^{29}\text{Si}$  9.16, was attributed to the tetracoordinate silicon species **B** in which the anionic  $\text{CH}_2\text{CN}^-$  has been displaced. This chemical shift is in the same region as a peak we reported previously for a 1:1 mixture of TMSAN and **1d** in  $\text{C}_6\text{D}_6$  ( $\delta^{29}\text{Si}$  7.5) in which  $\text{CN}^-$  had been displaced. If the anion had not been displaced in both cases, an upfield rather than a downfield shift from the parent TMSAN molecule would have been observed since the silicon would have become 5-coordinate.<sup>12c</sup> We used similar reasoning to account for the formation of both  $\alpha$ - and  $\gamma$ -addition products in the reaction of crotyltrimethylsilane with aldehydes in the presence of **1a**.<sup>12h</sup> After transient **A** forms **B** in Scheme 1, an aldehyde molecule reacts with  $\text{CH}_2\text{CN}^-$  to form the alkoxide shown, which after trimethylsilylation is acid-hydrolyzed to give the corresponding  $\beta$ -hydroxynitrile as the final product, plus the regenerated catalyst **1a**.

Although we have  $^{29}\text{Si}$  NMR evidence consistent with the formation of **B**, we have no convincing  $^{31}\text{P}$  NMR evidence for this species.  $^{31}\text{P}$  chemical shifts for  $\text{PR}_4^+$  cations are generally in the range of 90-140 ppm.<sup>15</sup> The chemical shift for **B** is 119 ppm at  $-40\text{ }^\circ\text{C}$  in THF, which is virtually unchanged from the value of **1a** under the same conditions. This result perhaps suggests a minimal perturbation of the phosphorus shielding environment as a result of a weak Si-P interaction.

Since six-coordinate silicon species are also well known, **A** in Scheme 1 may undergo nucleophilic attack by the carbonyl oxygen of the aldehyde to give rise to the six-coordinate intermediate **C** shown in Scheme 2. This intermediate may then decompose to product and regenerated catalyst **1a** via the 4-center intermediate depicted in **D**. The unreactivity of ketones in our protocol can be rationalized on the basis of their increased steric hindrance in the formation of intermediates **C** and **D**.

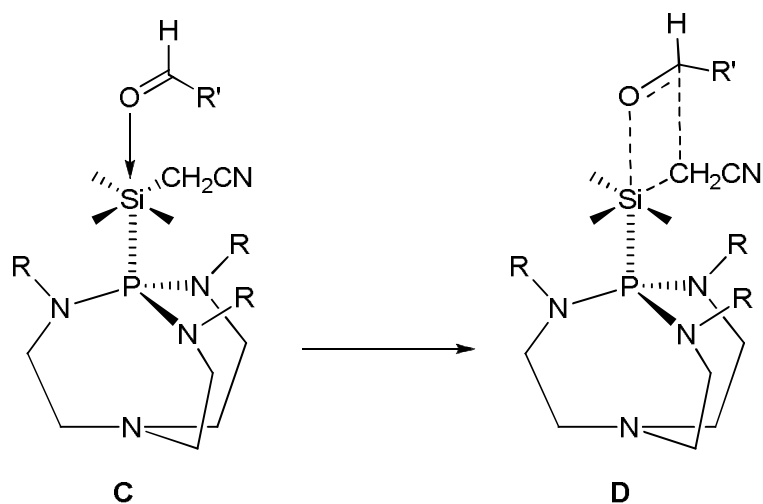
**Scheme 1.** Proposed Mechanism of TMSAN Addition to Aldehydes

### Conclusion

In summary, commercially available **1a** is an excellent catalyst for the synthesis of  $\beta$ -hydroxynitriles via the reaction of TMSAN with aldehydes. Our reaction conditions are mild and our catalyst loadings are the lowest we were able to find in the literature for this transformation. In the case of aryl aldehydes, both electron withdrawing and donating groups are well tolerated, both heterocyclic and aliphatic aldehydes function well, and both acid- and base-sensitive functionalities favor the reaction. Comparing our yields to the maximum yields for seven different methods in the literature using seven different catalyst systems, our yields were lower in two cases, comparable ( $\pm 5\%$ ) in four, and higher in one case. For the two literature yields that were larger than ours, one literature preparation involved the use of LiOAc in DMF and in the other, 2.5 mol % of  $[\text{Cu}(\text{PPh}_3)_3][(\text{EtO})_3\text{SiF}_2]$  and 120 mol % of

(EtO)<sub>3</sub>SiF as an additive were present. In Table 3 our yields for two substrates when compared to the maximum yields in the literature, were comparable in one case ( $\pm 5\%$ ) and lower in the other, the literature method for these two cases involved the use of 10 mol % of LiOAc in DMF. From an environmental standpoint, it is worth noting that our catalyst is metal-free.

**Scheme 2.** Alternative Proposed Mechanism of TMSAN Addition to Aldehydes



### Experimental Section

**General reaction procedure.** A round bottom flask was charged with the required amount of proazaphosphatrane (**1**) (2 mol %), in a nitrogen-filled glove-box. Anhydrous THF (2.0 mL) was added to the flask via syringe, followed by addition of TMSAN (2.40 mmol) at 0 °C via syringe under an argon atmosphere. The reaction mixture was stirred at 0 °C for 15 min and then aldehyde (2.0 mmol) was added over a period of 5–10 min. The reaction mixture was stirred for 24 h at 0 °C and then it was quenched with 3 mL of aqueous HCl (1*M*). The reaction mixture was stirred at 0 °C for 1 h and then it was neutralized with



saturated aq. NaHCO<sub>3</sub> and extracted with CH<sub>2</sub>Cl<sub>2</sub> (3 × 30 mL). The crude product was purified by column chromatography on silica gel using 10% EtOAc/hexanes, except for heterocyclic substrates, in which case 20–25% EtOAc/hexanes was used as the eluent.

### Acknowledgment

We are grateful to the Aldrich Chemical Co. for their generous gift of **1a**. The National Science Foundation is gratefully acknowledged for financial support of this research through grant 0750463. We also thank Dr. Ch. Venkat Reddy for helpful discussions.

### References

- (1) *Comprehensive Organic Synthesis*, Ed. B. M. Trost, Pergamon Press, Oxford, 1991, vol. 2. p. 1–502.
- (2) (a) Corey, E. J.; Wu, Y.-J. *J. Am. Chem. Soc.* **1993**, *115*, 8871–8872. (b) Fukuda, Y.; Okamoto, Y. *Tetrahedron* **2002**, *58*, 2513–2521. (c) Fülöp, F.; Huber, I.; Bernáth, G.; Hönig, H.; Seuffer-Wasserthal, P. *Synthesis* **1991**, 43–46. (d) Elnagdi, M. H.; Elmoghayar, M. R. H.; Elgemeie, G. E. H. *Synthesis* **1984**, 1–26. (e) Fleming, F. F.; Shook, B. C. *Tetrahedron* **2002**, *58*, 1–23. (f) Fleming, F. F.; Iyer, P. S. *Synthesis* **2006**, 893–913.
- (3) You, Z.; Lee, H. *Tetrahedron Lett.* **1996**, *37*, 1165–1168.
- (4) (a) Koenig, T. M.; Mitchell, D. *Tetrahedron Lett.* **1994**, *35*, 1339–1342. (b) Djoman, M. C. K.-B.; Ajjou, A. N. *Tetrahedron Lett.* **2000**, *41*, 4845–4849. (c) Khai, B. T.; Arcelli, A. *J. Org. Chem.* **1989**, *54*, 949–953. (d) Luo, F.-T.; Jeevanandam, A. *Tetrahedron Lett.*

**1998**, 39, 9455–9456. (e) Xie, Y. P.; Men, J.; Li, Y. Z.; Chen, H.; Cheng, P. M.; Li, X. J. *Catal. Commun.* **2004**, 5, 237–238.

(5) Suto, Y.; Kumagai, N.; Matsunaga, S.; Kanai, M.; Shibasaki, M. *Org. Lett.* **2003**, 5, 3147–3150.

(6) (a) Kaiser, E. W.; Hauser, C. R. *J. Am. Chem. Soc.* **1967**, 89, 4566–4567. (b) Kaiser, E. W.; Hauser, C. R. *J. Org. Chem.* **1968**, 33, 3402–3404. (c) Li, N.-S.; Yu, S.; Kabalka, G. W. *J. Org. Chem.* **1995**, 60, 5973–5974.

(7) Kawano, Y.; Kaneko, N.; Mukaiyama, T. *Chem. Lett.* **2005**, 34, 1508–1509.

(8) (a) Zhou, J. J. P.; Zhong, B.; Silverman, R. B. *J. Org. Chem.* **1995**, 60, 2261–2262. (b) Kisanga, P.; McLeod, D.; D'Sa, B.; Verkade, J. G. *J. Org. Chem.* **1999**, 64, 3090–3094. (c) Kumagai, N.; Matsunaga, S.; Shibasaki, M. *J. Am. Chem. Soc.* **2004**, 126, 13632–13633. (d) Takai, K.; Ueda, T.; Ikeda, N.; Moriwake, T. *J. Org. Chem.* **1996**, 61, 7990–7991. (e) Barhdadi, R.; Gal, J.; Heintz, M.; Troupel, M.; Perichon, J. *Tetrahedron* **1993**, 49, 5091–5098. (f) Ciaccio, J.; Stanescu, C.; Bontemps, J. *Tetrahedron Lett.* **1992**, 33, 1431–1434. (g) Chini, M.; Crotti, P.; Favero, L.; Macchia, F. *Tetrahedron Lett.* **1991**, 32, 4775–4778. (h) Mitchell, D.; Koenig, T. *Tetrahedron Lett.* **1992**, 33, 3281–3284. (i) Gorzynski Smith, J. *Synthesis* **1984**, 629–656. (j) Ohno, H.; Mori, A.; Inoue, S. *Chem. Lett.* **1993**, 6, 975–978. (k) Zhang, X. L.; Han, Y.; Tao, W.-T.; Huang, Y.-Z. *J. Chem. Soc., Perkin Trans. 1* **1995**, 189–191. (l) Wade, P.; Bereznak, J. F. *J. Org. Chem.* **1987**, 52, 2973–2977. (m) Araki, S.; Yamada, M.; Butsugan, Y. *Bull. Chem. Soc. Jpn.* **1994**, 67, 1126–1129. (n) Kumagai, N.; Matsunaga, S.; Shibasaki, M. *Tetrahedron* **2007**, 63, 8598–8608.

(9) (a) Gostevskii, B. A.; Kruglaya, O. A.; Albanov, A. I.; Vyazankin, N. S. *J. Organomet. Chem.* **1980**, *187*, 157–166. (b) Latouche, R.; Texier-Boullet, F.; Hamelin, J. *Tetrahedron Lett.* **1991**, *32*, 1179–1182. (c) Palomo, C.; Aizpurua, J. M.; López, M. C.; Lecea, B. *J. Chem. Soc. Perkin Trans. 1*, **1989**, 1692–1694. (d) Kawanami, Y.; Yuasa, H.; Toriyama, F.; Yoshida, S.; Baba, T. *Catal. Commun.* **2003**, *4*, 455–459. (e) Jolivet, S.; Abdallah-El Ayoubi, S.; Mathe, D.; Texier-Boullet, F.; Hamelin, J. *J. Chem. Res. Synop.* **1996**, *6*, 300–301. (f) Matsukawa, S.; Kitazaki, E. *Tetrahedron Lett.* **2008**, *49*, 2982–2984.

(10) For reviews on proazaphosphatrane chemistry, see: (a) Verkade, J. G. In *New Aspects of Phosphorus Chemistry II*, *Top. Curr. Chem.* Majoral, J. P. Ed., **2002**, *233*, 1–44. (b) Verkade, J. G.; Kisanga, P. B. *Tetrahedron* **2003**, *59*, 7819–7858. (c) Verkade, J. G.; Kisanga, P. B. *Aldrichimica Acta* **2004**, *37*, 3–14. (d) Urgaonkar, S.; Verkade, J. G. *Specialty Chemicals* **2006**, *26*, 36–39.

(11) Kisanga, P. B.; Verkade, J. G.; Schwesinger, R. *J. Org. Chem.* **2000**, *65*, 5431–5432.

(12) (a) D'Sa, B. A.; Verkade, J. G. *J. Am. Chem. Soc.* **1996**, *118*, 12832–12833. (b) D'Sa, B. A.; McLeod, D.; Verkade, J. G. *J. Org. Chem.* **1997**, *62*, 5057–5061. (c) Wang, Z.; Fetterly, B. M.; Verkade, J. G. *J. Organomet. Chem.* **2002**, *646*, 161–166. (d) Fetterly, B. M.; Verkade, J. G. *Tetrahedron Lett.* **2005**, *46*, 8061–8066. (e) Yu, Z.; Verkade, J. G. *J. Org. Chem.* **2000**, *65*, 2065–2068. (f) Urgaonkar, S.; Verkade, J. G. *Org. Lett.* **2005**, *7*, 3319–3322. (g) Raders, S. M.; Verkade, J. G. *Tetrahedron Lett.* **2008**, *49*, 3507–3511. (h) Wang, Z.; Kisanga, P.; Verkade, J. G. *J. Org. Chem.* **1999**, *64*, 6459–6461. (i) Wang, Z.; Wroblewski, A. E.; Verkade, J. G. *J. Org. Chem.* **1999**, *64*, 8021–8023.

(13) Proazaphosphatranes **1a**, **1c**, and **1d** are commercially available.

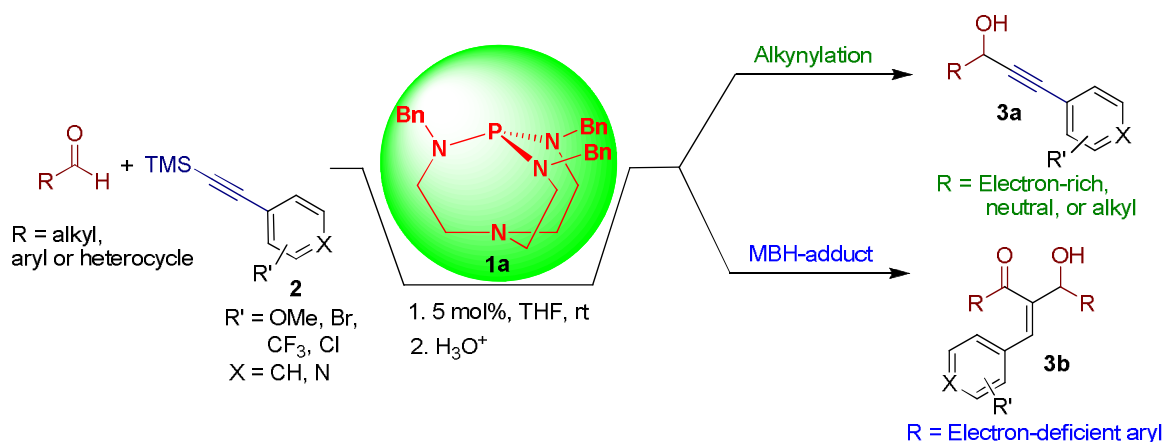
(14) (a) Kojima, S.; Fukuzaki, T.; Yamakawa, A.; Murai, Y. *Org. Lett.* **2004**, *6*, 3917–3920. (b) Palomo, C.; Aizpurua, J. M.; Aurrekoetxea, N. *Tetrahedron Lett.* **1990**, *31*, 2209–2210. (c) Birkofer, L.; Ritter, A.; Wieden, H. *Chem. Ber.* **1962**, *95*, 971–976. (d) Matsuda, I.; Murata, S.; Ishii, Y. *J. Chem. Soc. Perkin Trans. 1*, **1979**, 26–30. (e) Yamakado, Y.; Ishiguro, M.; Ikeda, N.; Yamamoto, H. *J. Am. Chem. Soc.* **1981**, *103*, 5568–5570.

(15) *Handbook of Phosphorus Nuclear Magnetic Resonance Data*, Ed. J. C. Tebb, CRC Press Inc. 1991.

**CHAPTER 5. P(PhCH<sub>2</sub>NCH<sub>2</sub>CH<sub>2</sub>)<sub>3</sub>N: AN EFFICIENT LEWIS-BASE CATALYST  
FOR THE SYNTHESIS OF PROPARGYLIC ALCOHOLS AND MORITA-BAYLIS-  
HILLMAN ADDUCTS VIA ALDEHYDE ALKYNYLATION**

Kuldeep Wadhwa, Venkat Reddy Chintareddy, John G. Verkade

*Accepted in J. Org. Chem.*



**Abstract:** Proazaphosphatranane P(PhCH<sub>2</sub>NCH<sub>2</sub>CH<sub>2</sub>)<sub>3</sub>N (**1a**) is an efficient catalyst for the addition of aryl trimethylsilyl alkynes to a variety of aromatic, aliphatic and heterocyclic aldehydes in THF at room temperature. The reaction conditions are mild and employ a low catalyst loading (*ca.* 5 mol %). Only propargylic alcohols were isolated in good to excellent isolated yields when electron-rich, electron-neutral, heterocyclic and aliphatic aldehydes were employed, whereas  $\beta$ -branched Morita-Baylis-Hillman (MBH) type adducts were isolated with electron-deficient aromatic aldehydes after conventional acid hydrolysis of the TMS ether products. Alkynes containing heterocyclic, and aromatic groups bearing electron-withdrawing or -donating substituents underwent clean addition to

cyclohexanecarboxaldehyde and to electron-rich aromatic aldehydes to give propargylic alcohols in excellent isolated yields.  $\beta$ -Branched Morita-Baylis-Hillman (MBH) type adducts were isolated when electron-deficient aromatic aldehydes were employed. Reaction pathways to both types of products are proposed.

### Introduction

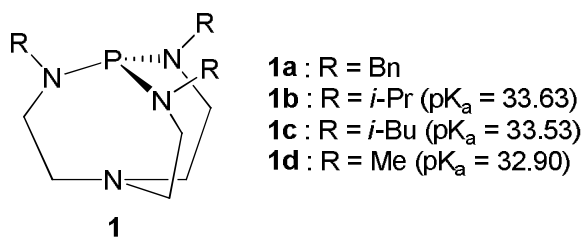
Propargylic alcohols are useful in the synthesis of complex multi-functional natural products, such as (–)-Reveromycin B, Aspinolide B, ( $\pm$ )-Blastmycinone, (–)-Methylenolactocin, (+)-Sterpurene, and (–)-Chlorothricolide via carbon-carbon bond forming reactions.<sup>1-3</sup> Several methods have been described in the literature over the decades for the synthesis of propargylic alcohols,<sup>4-7</sup> and the most common technique for their synthesis is via the use of metal bases (*e.g.*, *n*-BuLi) to generate the acetylide ion.<sup>4-6</sup> Heavy metals have also been used in the preparation of propargylic alcohols.<sup>5,6</sup> For example, Carreira *et al.* have worked extensively on stereoselective alkynylations of aldehydes, mainly with Zn metal-based catalytic systems.<sup>5</sup> In addition, Ag-, In- and Ru-based catalyst systems for terminal alkyne addition have also been reported.<sup>6</sup>

In recent years, several reports on Lewis-base activation of various organosilyl reagents to yield important organic intermediates have been published.<sup>8</sup> Pertinent to the present work on activation of silyl-terminated alkynes to generate the corresponding acetylide nucleophiles, are past examinations of this process.<sup>7</sup> In 1976, Kuwajima *et al.* first reported the use of tetrabutylammonium fluoride (3-5 mol %) for the reaction between 1-trimethylsilyl-2-phenylacetylene with aldehydes and ketones, providing products in yields ranging from 5 to 87%.<sup>7a,7b</sup> Shioiri *et al.* reported the use of a quaternary ammonium fluoride

salt derived from cinchonine (10 mol %) at -20 °C to facilitate the reaction of 1-trimethylsilyl-2-phenylacetylene with aldehydes, Morita-Baylis-Hillman (MBH) type adducts, were isolated in 23-92% yields. Among the eleven aldehydes screened, alkynylation product was obtained in the case of benzaldehyde and *o*-phthalaldehyde in minor quantities. Whereas alkynylation was observed as a major product with *p*-anisaldehyde and 3,4-dimethoxybenzaldehyde.<sup>7c</sup> The use of 10 mol % of KOEt in THF as solvent at 0 °C was reported by Sheidt *et al.* to provide good yields of alkynylated product when triethoxysilylacetylenes were used as reagents with aldehydes, ketones and imines.<sup>7d</sup> In 2006, Mukaiyama *et al.* reported that 10 mol % of [Bu<sub>4</sub>N][OPh] at -78 °C in THF as solvent gave 39-100% isolated alkynylated product yields with aldehydes and four ketone substrates.<sup>7e</sup> Matsukawa *et al.* reported the synthesis of propargylic alcohols using tris(2,4,6-trimethoxyphenyl)phosphine (10 mol %) as a catalyst for reaction between 1-trimethylsilyl-2-phenylacetylene and various aldehydes in DMF as solvent at 100–120 °C yielding product 74-96% isolated yield.<sup>7f</sup> Tetrabutylammonium triphenyldifluorosilicate was used (10 mol %)<sup>7g</sup> to promote the reaction between 1-trimethylsilyl-2-phenylacetylene and benzaldehyde yielded the alkynylated product in 81% yield. However, the generality of this process remains to be determined.<sup>7g</sup> The use of tetraphenylphosphonium hydrogen difluoride (3-8 mol %) to catalyze the reaction of 1-trimethylsilyl-2-phenylacetylene with one aldehyde and three ketones in DMF solvent at 50 °C provided moderate product yields (46-64%).<sup>7h</sup> Corey *et al.* utilized a 1:1 mixture of CsF and CsOH for silyl activation of 1-trimethylsilyl-2-phenylacetylene in the alkynylation of two aldehydes, which gave good product yields (85 and 90%,) although 1.6 equiv. of fluoride ion was required.<sup>7i</sup>

Discovered for the first time in our laboratories, proazaphosphatranes of the type shown in Figure 1 are strongly basic, with  $pK_a$  values of 32–34 in  $CH_3CN$  for their P-protonated  $N_{\text{basal}} \rightarrow P$  transannulated conjugated acids.<sup>9</sup> If such transannulation occurs during a catalytic cycle, the nucleophilicity of the phosphorus center would be enhanced. The catalytic activation of silicon centers by the phosphorus of proazaphosphatranes has been invoked, for example, for silylation of alcohols using silyl chloride,<sup>10a,10b</sup> for the synthesis of cyanohydrins by the addition of trimethylsilyl nitrile to carbonyl compounds,<sup>10c,10d</sup> for desilylation of TBDMS ethers,<sup>10e</sup> for nucleophilic aromatic substitution of aryl fluorides with aryl silylethers,<sup>10f,10g</sup> for allylation of aromatic aldehydes,<sup>10h</sup> and for the reduction of aldehydes and ketones with poly(methylhydrosiloxane).<sup>10i</sup>

**Figure 1.** Proazaphosphatranes

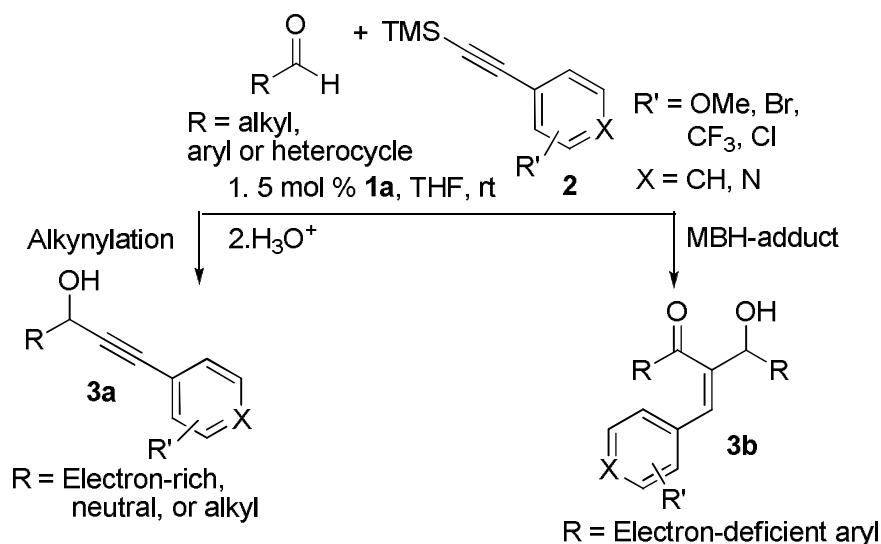


## Results and Discussion

In the present work, we report the use of proazaphosphatrane **1a** as an efficient catalyst for the synthesis of propargylic alcohols using electron-rich, electron-neutral, heterocyclic and aliphatic aldehydes with trimethylsilylacetylenes, whereas  $\beta$ -branched Morita-Baylis-Hillman (MBH) type adducts are obtained as the sole products in the case of electron-deficient aromatic aldehydes (Scheme 1).



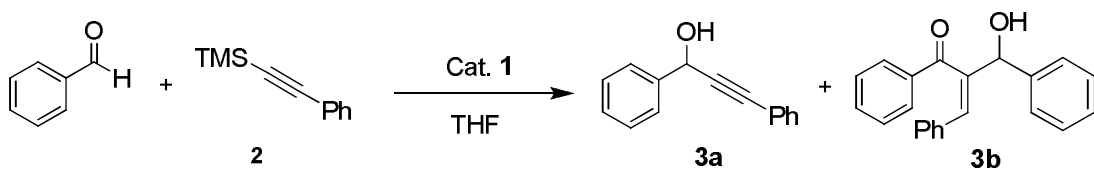
**Scheme 1. 1a-Catalyzed Alkynylation and MBH Reactions**



We first screened the reaction between benzaldehyde and 1-trimethylsilyl-2-phenylacetylene (**2**) (as shown in the Scheme in Table 1) using **1a** as a catalyst. With 5 mol % catalyst and 1 equivalent of alkyne **2** in THF solvent, complete conversion to a mixture of **3a** and **3b** was observed by  $^1\text{H}$  NMR spectroscopy. Silica gel column chromatography allowed **3a** to be isolated in 79% yield and the MBH type adduct **3b** in 6% yield (Table 1, entry 1). We then attempted to minimize formation of the MBH product **3b** by lowering the catalyst **1a** loading to 3 mol % (Table 1, entry 2). Unfortunately, the corresponding alkynylation product **3a** was isolated in only 20% yield and only starting aldehyde was recovered from the remainder of the reaction mixture. Gratifyingly, increasing the trimethylsilyl alkyne to two equivalents (Table 1, entry 3) increased the yield of the alkynylation product **3a** to 82% with only a 2% yield of the MBH side product **3b**. Lowering the temperature to 0 °C had no significant effect on the ratio of the two products (Table 1,

entry 4). We then screened proazaphosphatranes **1b-1d** in the reaction in Table 1 using the best catalytic conditions reported in this table (entry 3) and the results are recorded in Table 1, entries 5-7. From these results, it is seen that **1a** functioned best for making **3a** under the conditions in entry 3 of Table 1. No reaction was observed under our conditions in the absence of catalyst (Table 1, entry 8).

**Table 1.** Survey of proazaphosphatranes as catalysts for the synthesis of propargylic alcohols.<sup>a</sup>



entry	catalyst	mol (%)	<b>2</b> (Equiv.)	temp (°C)	yield of <b>3a</b> (%) <sup>b</sup>	yield of <b>3b</b> (%) <sup>b</sup>
1	<b>1a</b>	5	1.5	25	79	6
2	<b>1a</b>	3	1.5	25	20	-
3	<b>1a</b>	5	2.0	25	82 (27-100) <sup>c-i</sup>	2
4	<b>1a</b>	5	2.0	0	81	2
5	<b>1b</b>	5	2.0	25	72	10 <sup>j</sup>
6	<b>1c</b>	5	2.0	25	42	-
7	<b>1d</b>	5	2.0	25	69	-
8	none	-	2.0	25	n.r. <sup>k</sup>	n.r. <sup>k</sup>

<sup>a</sup> Reaction conditions: aldehyde (2.0 mmol), THF (2 mL), 24 h, followed by 1N HCl (3 mL).

<sup>b</sup> Isolated yield after silica gel column chromatography. <sup>c</sup> 76% yield using 3 mol % <sup>n</sup>Bu<sub>4</sub>NF (ref 7a). <sup>d</sup> 76% yield using 5 mol % <sup>n</sup>Bu<sub>4</sub>NF (ref 7b). <sup>e</sup> 27% yield using 10 mol % of the quaternary ammonium fluoride salt derived from cinchonine (ref 7c). <sup>f</sup> 100% yield using 10

mol % NBu<sub>4</sub>(OPh) (ref 7e). <sup>g</sup>95% yield using 10 mol % tris(2,4,6-trimethoxyphenyl)phosphine (ref 7f). <sup>h</sup>81% yield using 10 mol % <sup>n</sup>Bu<sub>4</sub>N(Ph<sub>3</sub>SiF<sub>2</sub>) (ref 7g). <sup>i</sup>64% yield using 3 mol % Ph<sub>4</sub>P(HF<sub>2</sub>) (ref 7h). <sup>j</sup>Determined by <sup>1</sup>H NMR spectroscopic integration. <sup>k</sup>No reaction.

To examine the scope of this methodology a wide variety of aldehydes consisting of electron-rich, electron-poor, heterocyclic and aliphatic examples were screened under the optimized conditions in Table 1, entry 3, and the results are summarized in Tables 2 and 3. Electron-deficient *o*-fluorobenzaldehyde reacted efficiently with alkyne **2** to yield the desired alkylation product in an excellent isolated yield (Table 2, entry 1). Aldehydes with electron-donating substituents, such as *p*-tolualdehyde (Table 2, entry 2), *m*-methoxybenzaldehyde (Table 2, entry 3) and *m*-tolualdehyde (Table 2, entry 4) resulted in very good isolated yields of alkylation products, except in the case of *m*-tolualdehyde, wherein 6% of the MBH adduct was isolated. Pleasingly, excellent isolated yields with no observable MBH side product were obtained when sterically hindered aldehydes, such as *o*-phenylbenzaldehyde (Table 2, entry 5), *o*-tolualdehyde (Table 2, entry 6) and 2,6-dimethylbenzaldehyde (Table 2, entry 7) were employed under our conditions. The versatility of our protocol was extended to the heterocyclic aldehyde, thiophene-2-carboxaldehyde, providing a 91% yield of alkylation product (Table 2, entry 8). Unfortunately, pyridine- and furan-2-carboxaldehyde gave complicated mixtures the reason for which is not clear at this time (Table 2, entry 9 and 10 respectively).

**Table 2.** Reactions of electron-rich aromatic, and heterocyclic aldehydes with 1-trimethylsilyl-2-phenylacetylene (**2**) using proazaphosphatrane **1a** as the catalyst.<sup>a</sup>

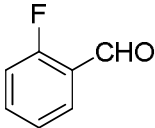
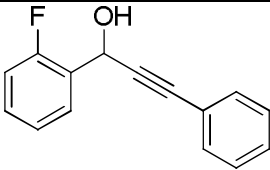
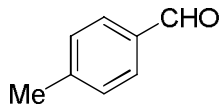
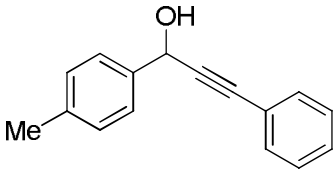
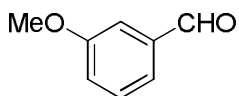
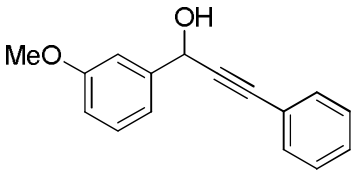
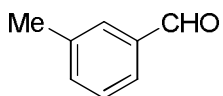
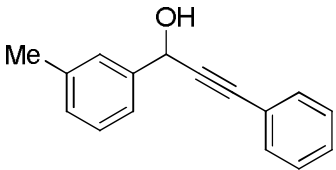
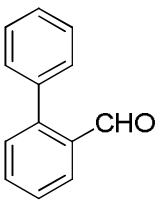
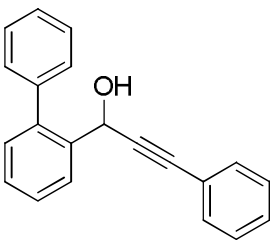
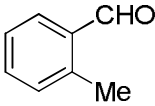
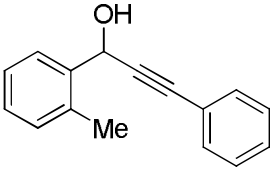
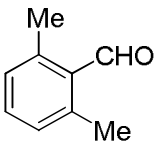
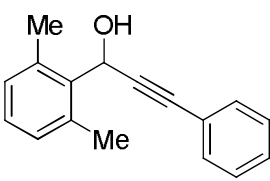
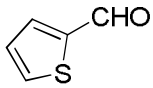
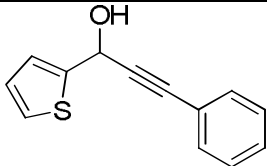
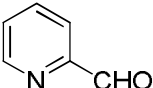
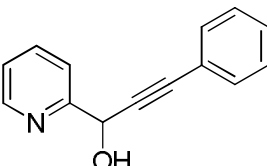
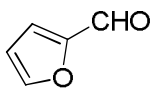
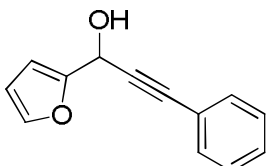
Entry	Aldehyde	Product	Yield (%) <sup>b</sup>	Lit. Yield (%)
1			95	-
2			82	100 <sup>c</sup>
3			91	-
4			83	-
5			91	-
6			97	99 <sup>c</sup>
7			96	-

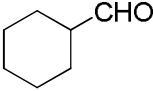
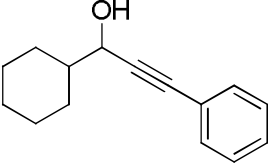
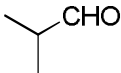
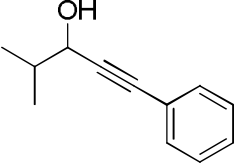
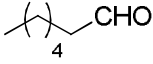
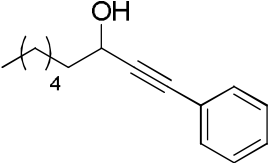
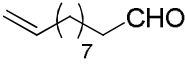
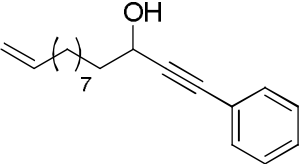
Table 2 continued

8			91	87 <sup>c</sup>
9 <sup>d</sup>			-	-
10 <sup>d</sup>			-	-

<sup>a</sup> Reaction conditions: aldehyde (2.0 mmol), **2** (4.0 mmol), **1a** (5 mol %), THF (2 mL), rt, 24 h, followed by 1N HCl (3 mL). <sup>b</sup> Isolated yield after column chromatography. <sup>c</sup> 10 mol % NBu<sub>4</sub>(OPh) (ref 7e). <sup>d</sup> Inseparable complex mixture was observed.

After screening aromatic aldehydes, we tested several aliphatic examples (Table 3). All the substrates in this table selectively gave propargylic alcohols, and MBH type adduct formation was not observed. We conjecture that this is because the intermediate **E** (shown in scheme 2) required for MBH type adduct formation cannot be stabilized by aliphatic aldehydes (*vide infra*). Cyclohexanecarboxaldehyde (Table 3, entry 1), isobutyraldehyde (Table 3, entry 2) and heptaldehyde (Table 3, entry 3) led to generally excellent isolated yields of alkynylated product (96, 94 and 84%, respectively). Interestingly, catalyst **1a** was efficient in producing a high yield of alkynylation product with a long-chain unsaturated aliphatic aldehyde (Table 3, entry 4).

**Table 3.** Reactions of aliphatic aldehydes with 1-trimethylsilyl-2-phenylacetylene (**2**) using proazaphosphatane **1a** as the catalyst.<sup>a</sup>

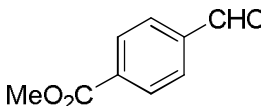
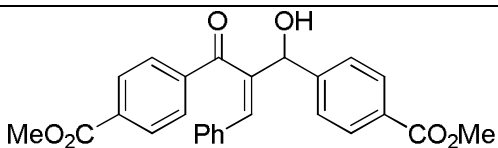
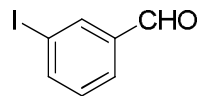
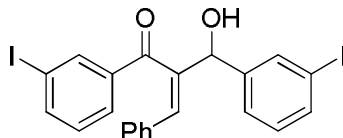
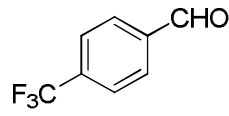
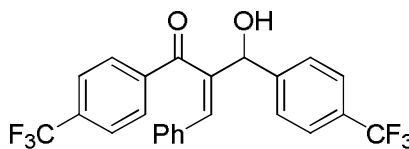
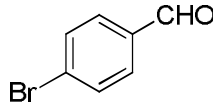
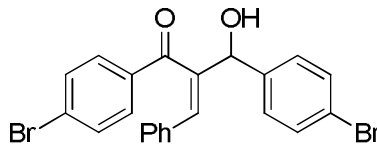
Entry	Aldehyde	Product	Yield (%) <sup>b</sup>	Lit. Yield (%)
1			96	79 <sup>c</sup> , 85 <sup>d</sup> , 88 <sup>e</sup>
2			94	-
3			84	-
4			79	-

<sup>a</sup> Reaction conditions: aldehyde (2.0 mmol), **2** (4.0 mmol), **1a** (5 mol %), THF (2 mL), rt, 24 h, followed by 1N HCl (3 mL). <sup>b</sup> Isolated yield after column chromatography. <sup>c</sup> Using 10 mol % NBu<sub>4</sub>(OPh) (ref 7e). <sup>d</sup> Using 3.2 equiv. of a 1:1 mixture of CsOH/CsF (ref 7i). <sup>e</sup> 88% yield using 10 mol % tris(2,4,6-trimethoxyphenyl)phosphine (ref 7f).

We next screened several electron-poor aldehydes and observed the  $\beta$ -branched MBH type adducts formed exclusively under our conditions (Table 4), this may be because of the formation of stabilized intermediate **E** as shown in scheme 2 (*vide infra*). Acid-sensitive electron-deficient methyl 4-formylbenzoate selectively gave the MBH adduct in good isolated yield (Table 4, entry 1). Electron-poor halogen-containing 3-iodobenzaldehyde

(Table 4, entry 2) and 4-bromobenzaldehyde (Table 4, entry 4) also stereoselectively afforded the MBH type adducts in good isolated yields and electron-deficient 4-(trifluoromethyl)benzaldehyde yielded the MBH adduct in excellent isolated yield (Table 4, entry 3).

**Table 4.** Reactions of electron-deficient aldehydes with 1-trimethylsilyl-2-phenylacetylene (**2**) using **1a** as the catalyst.<sup>a</sup>

Entry	Aldehyde	Product	Yield (%) <sup>b</sup>
1			85
2			78
3			93
4			79

<sup>a</sup> Reaction conditions: aldehyde (2.0 mmol), **2** (4.0 mmol), **1a** (5 mol %), THF (2 mL), rt, 24 h, followed by 1N HCl (3 mL). <sup>b</sup> Isolated yield after column chromatography.

We then screened alkynes with various electron-withdrawing, electron-donating and heterocyclic functionalities. Gratifyingly they all tolerated our reaction conditions well, giving good to excellent isolated yields of alkynylation products (Table 5). We also examined substituents on the alkyne phenyl group. With an electron-donating methoxy

group, an excellent isolated product yield of 92% was realized (Table 5, entry 1). An electron-deficient trifluoromethyl group at the *para* position (Table 5, entry 2) led to a good isolated yield of the desired product and halogens (both bromo and chloro at *ortho* and *meta* positions, respectively) resulted in good isolated product yields (Table 5, entry 4 and 5). Heterocyclic functionalities (such as pyridyl or thiophenyl) on the alkynes also underwent complete conversion, good to excellent isolated yields of the desired product under our reaction conditions (Table 5, entries 3 and 6). The use of terminally silylated aliphatic alkynes, such as hex-1-ynyltrimethylsilane (Table 5, entry 7), produced no observable product using the reaction conditions reported in Table 5, footnote a.

**Table 5.** Reactions of cyclohexanecarboxaldehyde with substituted 1-trimethylsilylacetylenes using **1a** as the catalyst.<sup>a</sup>

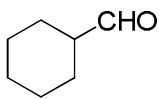
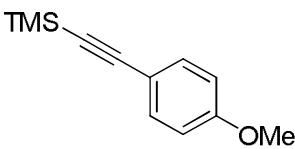
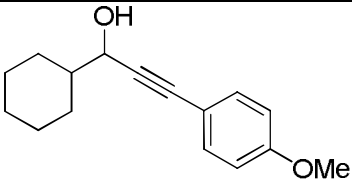
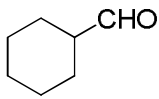
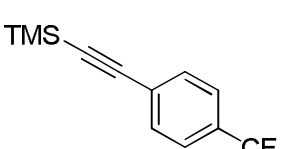
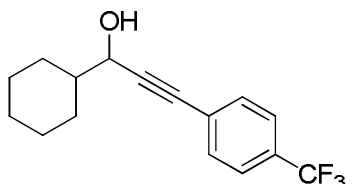
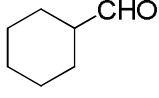
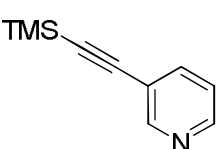
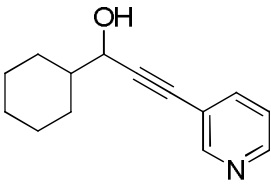
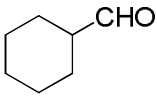
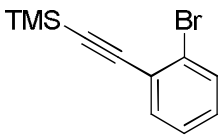
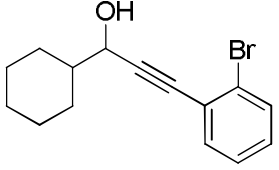
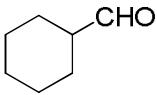
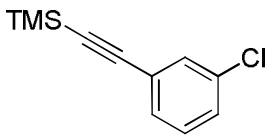
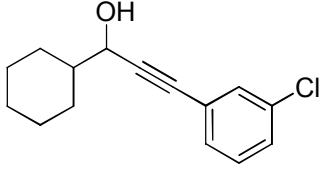
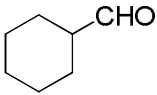
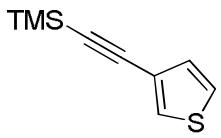
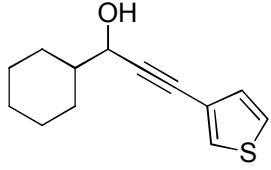
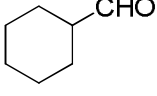
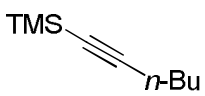
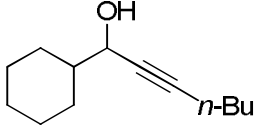
Entry	Aldehyde	Alkyne	Product	Yield (%) <sup>b</sup>
1				92
2				84
3				88



Table 5 continued

4				86
5				84
6				91
7				nr <sup>c</sup>

<sup>a</sup> Reaction conditions: aldehyde (2.0 mmol), **2** (4.0 mmol), **1a** (5 mol %), THF (2 mL), rt, 24 h, followed by 1N HCl (3 mL). <sup>b</sup> Isolated yield after column chromatography. <sup>c</sup> No reaction.

Electron-rich aromatic aldehydes were also evaluated in the presence of a variety of aromatic-substituted alkynes (Table 6). Bulky 2,6-dimethylbenzaldehyde reacted with the electron-rich alkyne in entry 1 of Table 6 giving a quantitative conversion to the alkynylated product in excellent isolated yield (92%). A terminal silylated aromatic alkyne substituted with a bromine at the *ortho* or a chloro group at the *meta* position afforded the desired products with 2-biphenylcarboxaldehyde and *o*-tolualdehyde (Table 6, entries 2–4) in good to moderate isolated yields. *o*-Tolualdehyde in the presence of an electron-deficient or electron-rich alkyne (having a *p*-trifluoromethyl group or a *p*-methoxy group on the terminal phenylacetylene) gave good isolated yields of the alkynylated product (Table 6, entries 5 and 6, respectively). Heterocyclic alkynes, such as thiophenyl and pyridyl, also underwent

complete conversion to give modest to good isolated yields of the desired product with *o*-tolualdehyde under our reaction conditions (Table 6, entries 7 and 8, respectively).

In accord with the results shown in Table 4, we obtained MBH type adducts stereoselectively as the *cis*-isomer (as determined by 2D NOESY NMR, Table 4, entry 2) when the reaction was carried out between electron-deficient aldehydes and substituted terminally-silylated alkynes (Table 7). Here the product yields ranged from modest (65%) to moderate (74%).

**Table 6.** Reactions of electron-rich aromatic aldehydes with variously substituted 1-trimethylsilylacetylenes using **1a** as catalyst.<sup>a</sup>

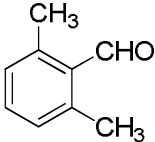
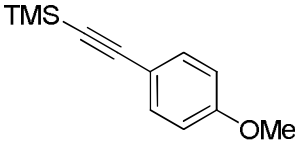
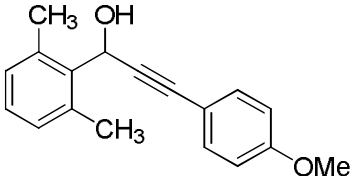
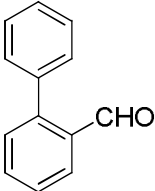
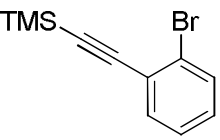
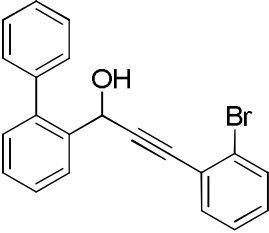
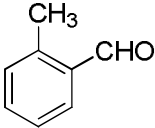
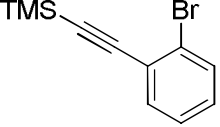
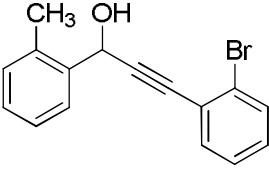
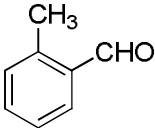
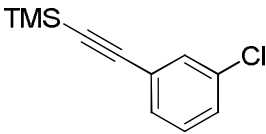
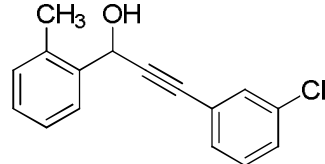
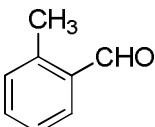
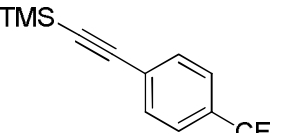
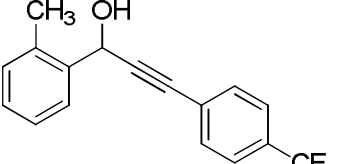
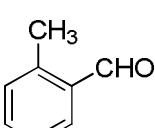
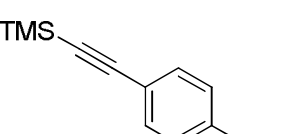
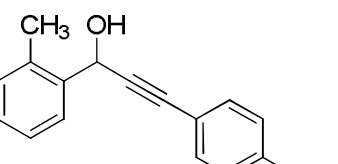
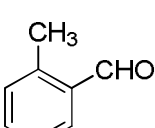
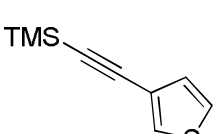
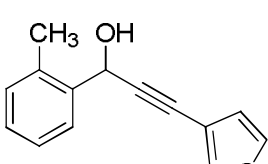
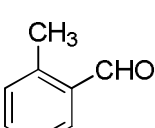
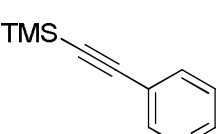
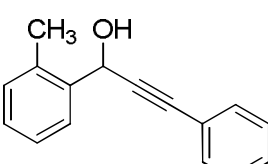
Entry	Aldehyde	Alkyne	Product	Yield (%) <sup>b</sup>
1				92
2				81
3				78

Table 6 continued

4				72
5				83
6				86
7				67
8				88

<sup>a</sup> Reaction conditions: aldehyde (2.0 mmol), **2** (4.0 mmol), **1a** (5 mol %), THF (2 mL), rt, 24 h, followed by 1N HCl (3 mL). <sup>b</sup> Isolated yield after column chromatography.

A rationale for the selectivity in the formation of the two different types of products we observed, can be given using a combination of mechanisms for the two reactions<sup>11</sup> (Scheme 2). After activation of the silyl group of **2** by proazaphosphatranes **1a** to form the activated pentacoordinated silicon species **A**, **A** dissociates to form the cationic intermediate **B** and the

acetylide counter anion. To obtain some insight into this pathway, we carried out  $^{29}\text{Si}$  NMR experiments at  $-40\text{ }^{\circ}\text{C}$  in which we combined 1-trimethylsilyl-2-phenylacetylene ( $\delta\text{ }^{29}\text{Si}$  NMR,  $-18.5\text{ ppm}$  in THF) with proazaphosphatrane **1a** in equimolar ratio in THF. A new  $^{29}\text{Si}$  peak appeared at  $\delta\text{ }7.17\text{ ppm}$ , which was attributed to the tetracoordinate silicon species **B** from which the acetylide anion had been displaced. This chemical shift accords with the previously reported value for a 1:1 mixture of TMSCN and **1d** in  $\text{C}_6\text{D}_6$  ( $\delta\text{ }^{29}\text{Si}$   $7.5\text{ ppm}$ ) in which  $\text{CN}^-$  had presumably been displaced.<sup>10c</sup> If the anion had not been displaced in both cases, an upfield rather than a downfield shift from the parent TMSCN molecule would have been observed since the silicon would have become 5-coordinate.<sup>10c</sup> We used similar reasoning to account for the formation of both  $\alpha$ - and  $\gamma$ -addition products in the reaction of crotyltrimethylsilane with aldehydes in the presence of **1b**.<sup>10h</sup> The acetylide ion in Scheme 2 then nucleophilically attacks the aldehyde to give the ionic intermediate **C**. Transfer of the silyl group to the alkoxide regenerates catalyst **1a** and the alkynylated product **D** is formed concomitantly. In the case of electron-deficient aldehydes, **D** can undergo a deprotonation step to form intermediate **E**, followed by rearrangement of **E** to give the allenic anion **F**. Anion **F** could abstract a proton from **D** to generate **E** and give allene **G**, which has been previously isolated as a crude product and which, after addition of an aldehyde produced **H**, which in turn was converted to the MBH type adduct upon acid hydrolysis.<sup>11</sup>

**Table 7.** Reactions of electron-deficient aldehydes with substituted 1-trimethylsilylacetylenes using **1a** as catalyst.<sup>a</sup>

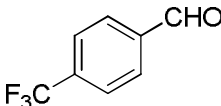
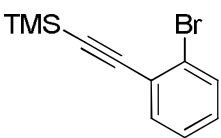
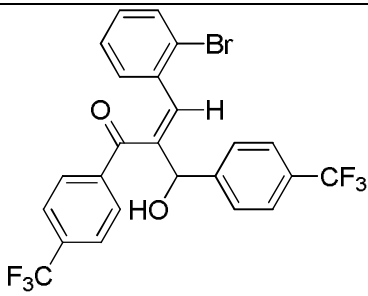
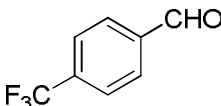
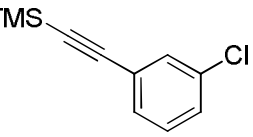
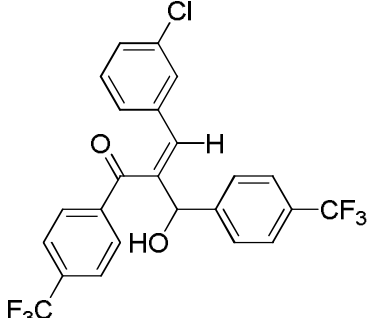
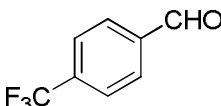
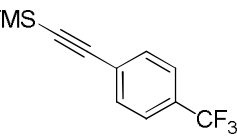
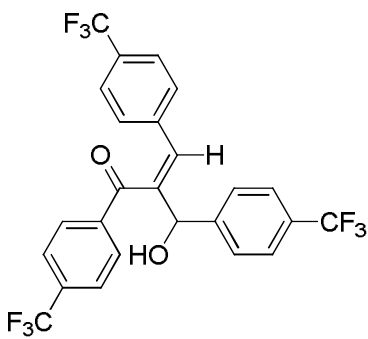
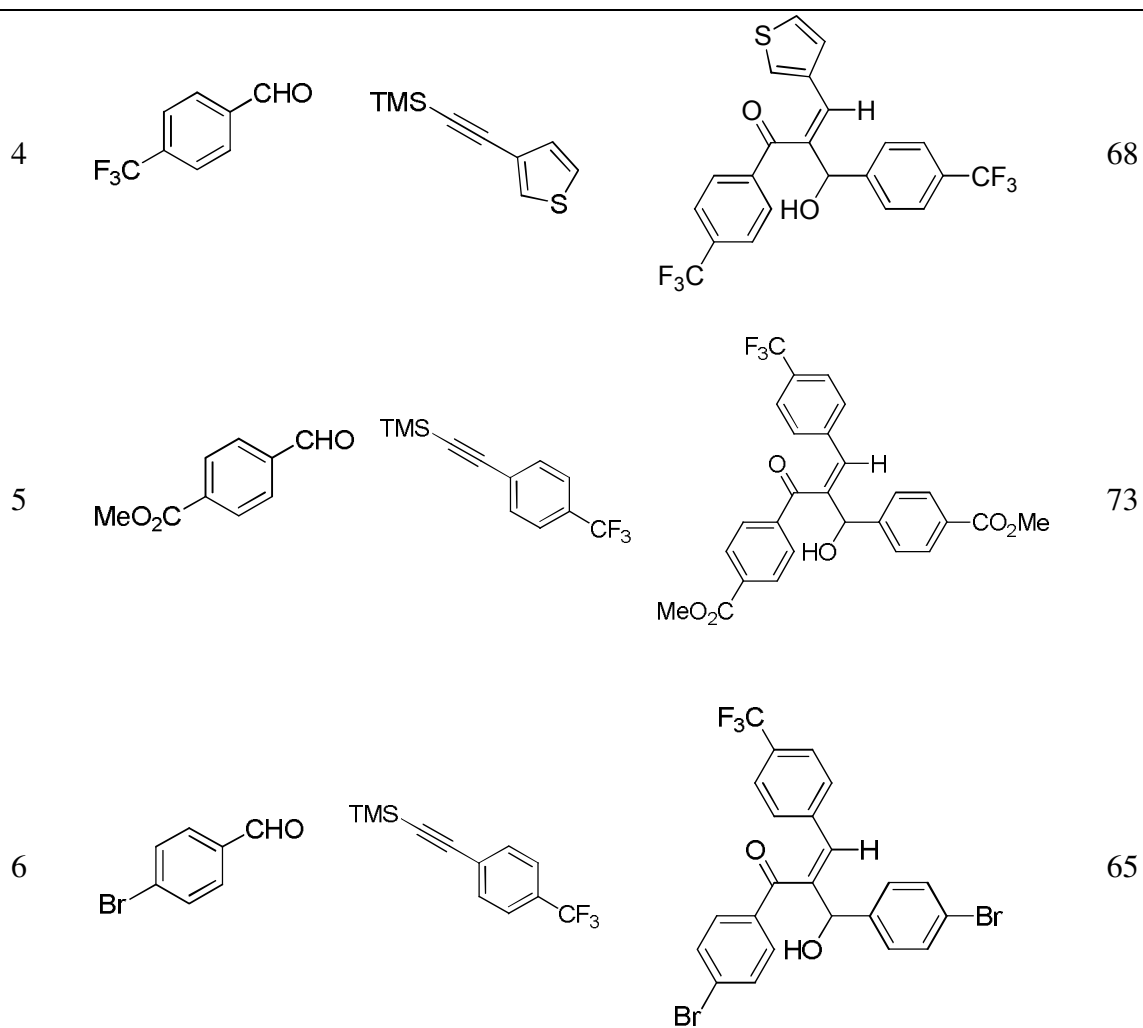
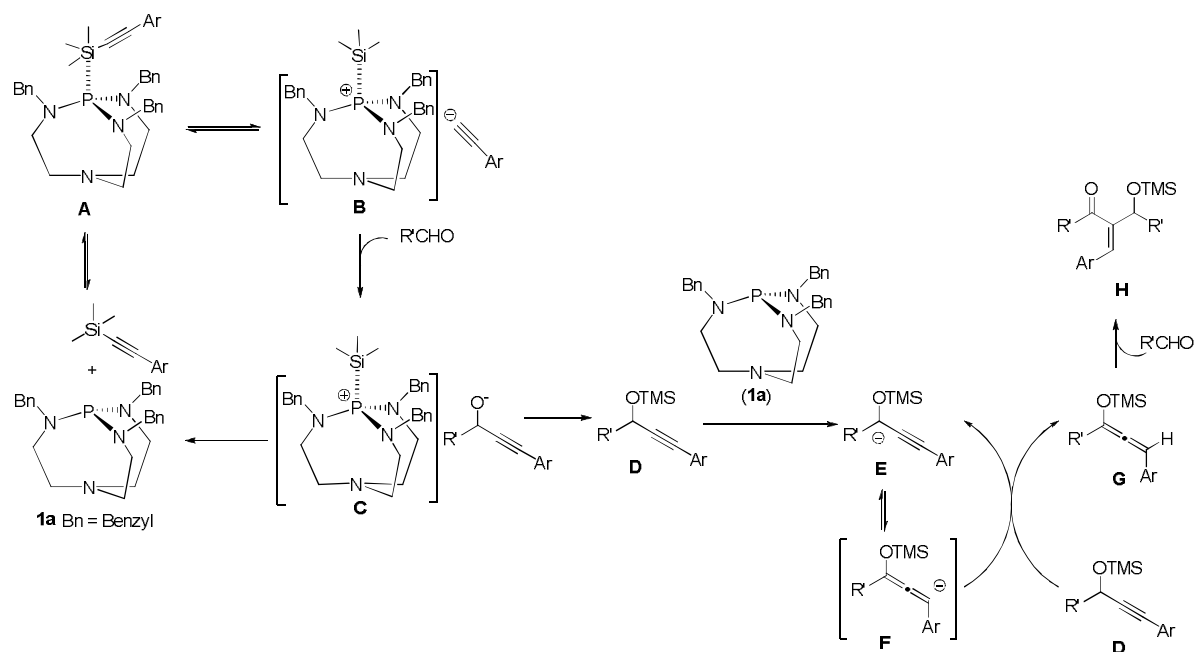
Entry	Aldehyde	Alkyne	Product	Yield (%) <sup>b</sup>
1				68
2				74
3				72

Table 7 continued



<sup>a</sup> Reaction conditions: aldehyde (2.0 mmol), **2** (4.0 mmol), **1a** (5 mol %), THF (2 mL), rt, 24 h, followed by 1N HCl (3 mL). <sup>b</sup> Isolated yield after column chromatography.

**Scheme 2.** Proposed Mechanism for the Alkynylation and MBH Reactions

### Conclusion

We have found that the non-ionic Lewis basic proazaphosphatrane **1a** is an efficient catalyst for addition of 1-aryl-2-(trimethylsilyl)acetylenes to aldehydes at room temperature. The selectivity of this reaction for the synthesis of propargylic alcohols is facilitated by electron-rich, electron-neutral, heterocyclic and aliphatic aldehydes, whereas MBH type adducts are isolated when electron-deficient aldehydes are employed, regardless of the substituents on the propargylic alcohol and despite the use of excess alkyne. Attempts to maximize yields of MBH type adducts by using a ratio of 0.5 equiv. of alkyne to aldehyde and by increasing the catalyst loading to 10 mol %, resulted in a 1:1 ratio of alkynylation to MBH product. We

believe our protocol will find many applications in organic syntheses, including the synthesis of a variety of useful polyfunctional aromatics. The use of low metal-free catalyst loading (*ca.* 5 mol %), the high isolated product yields, the broad scope, and room temperature reaction conditions are attractive features of this protocol.

### Experimental Section

**General Procedure for Alkynylation and MBH reactions.** A flat bottom screw-capped vial was charged with proazaphosphatrane catalyst **1a** (44.4 mg, 0.1 mmol, 5 mol %) in a nitrogen filled glove box. To the vial was added at room temperature, 2.0 mL of anhydrous THF, followed by the addition of aldehyde (2.0 mmol). The resulting solution was stirred at room temperature for 15 min and then aryl(trimethylsilyl)acetylene (4.0 mmol) was added over a period of two min. Progress of the reaction was monitored by TLC. The reaction mixture was stirred for 24 h and quenched with 3 mL of an aq. solution of HCl (*1N*). The mixture was stirred for an additional 1 h and then neutralized with saturated aq. NaHCO<sub>3</sub> solution. The crude product was extracted with CH<sub>2</sub>Cl<sub>2</sub> (3 × 30 mL) and the combined organic extracts were dried over anhydrous MgSO<sub>4</sub> (*ca.* 2.0 g). The crude product was purified by column chromatography using 30% EtOAc/hexane as eluent.

### Acknowledgment

The National Science Foundation is gratefully acknowledged for financial support of this research in the form of grant 0750463.



### References

- (1) For a review, see: Cozzi, P. G.; Hilgraf, R.; Zimmermann, N. *Eur. J. Org. Chem.* **2004**, 4095–4105.
- (2) (a) Marshall, J. M.; Bourbeau, M. P. *Org. Lett.* **2003**, *5*, 3197–3199. (b) Cuzzupe, A. N.; Hutton, C. A.; Lilly, M. J.; Mann, R. K.; McRae, K. J.; Zammit, S. C.; Rizzacasa, M. A. *J. Org. Chem.* **2001**, *66*, 2382–2393. (c) Pilli, R. A.; Victor, M. M.; De-Meijere, A. *J. Org. Chem.* **2000**, *65*, 5910–5916. (d) Overman, L. E.; Bell, K. L. *J. Am. Chem. Soc.* **1981**, *103*, 1851–1853. (e) Stork, G.; Nakamura, E. *J. Am. Chem. Soc.* **1983**, *105*, 5510–5512. (f) Noyori, R.; Tomino, I.; Yamada, M.; Nishizawa, M. *J. Am. Chem. Soc.* **1984**, *106*, 6717–6725. (g) Midland, M. M.; Nguyen, N. H. *J. Org. Chem.* **1981**, *46*, 4107–4108. (h) Gibbs, R. A.; Okamura, W. H. *J. Am. Chem. Soc.* **1988**, *110*, 4062–4063. (i) Zhu, G.; Lu, X. *J. Org. Chem.* **1995**, *60*, 1087–1089. (j) Mukai, C.; Kataoka, O.; Hanaoka, M. *J. Org. Chem.* **1993**, *58*, 2946–2952. (k) Leder, J.; Fujioka, H.; Kishi, Y. *Tetrahedron Lett.* **1983**, *24*, 1463–1466.
- (3) (a) Fried, J.; Sih, J. C. *Tetrahedron Lett.* **1973**, *40*, 3899–3902. (b) Roush, W. R.; Spada, A. P. *Tetrahedron Lett.* **1982**, *23*, 3773–3776. (c) Cheon, S. H.; Christ, W. J.; Hawkins, L. D.; Jin, H.; Kishi, Y.; Taniguchi, M. *Tetrahedron Lett.* **1986**, *27*, 4759–4762. (d) Nicolaou, K. C.; Webber, S. E. *J. Am. Chem. Soc.* **1984**, *106*, 3734–3736. (e) Chemin, D.; Linstrumelle, G. *Tetrahedron Lett.* **1992**, *48*, 1943–1952. (f) Vourlournis, D.; Kim, K. D.; Peterson, J. L.; Magriotis, P. A. *J. Org. Chem.* **1996**, *61*, 4848–4852. (g) Corey, E. J.; Niimura, K.; Konishi, Y.; Hashimoto, S.; Hamada, Y. *Tetrahedron Lett.* **1986**, *27*,

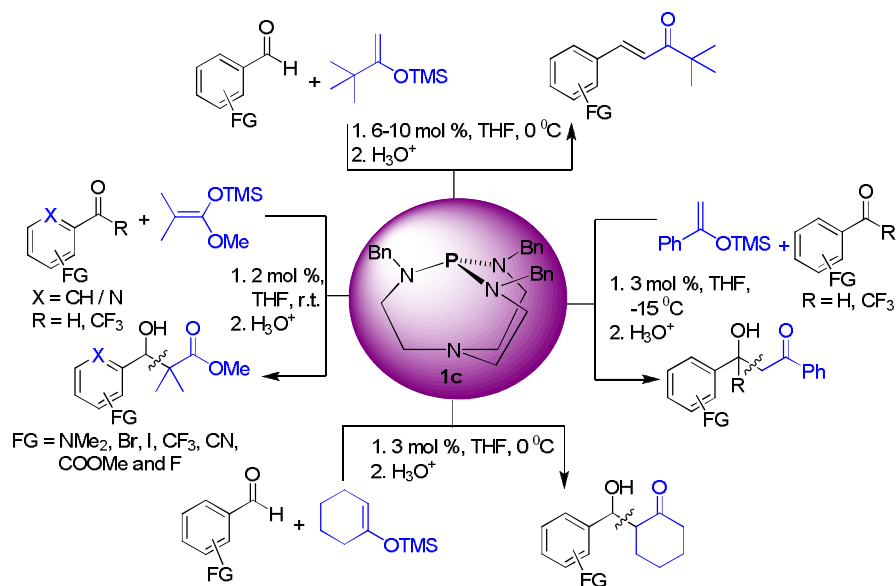
- 2199–2202. (h) Marshall, J. A.; Wang, X. *J. Org. Chem.* **1992**, *57*, 1242–1252. (i) Roush, W. R.; Sciotti, R. J. *J. Am. Chem. Soc.* **1994**, *116*, 6457–6458. (j) Evans, D. A.; Halstead, D. P.; Allison, B. D. *Tetrahedron Lett.* **1999**, *40*, 4461–4462. (k) Fox, M. E.; Li, C.; Marino, J. P.; Overman, L. E. *J. Am. Chem. Soc.* **1999**, *121*, 5467–5480.
- (4) (a) Viehe, H. G.; Reinstein, M. *Chem. Ber.* **1962**, *95*, 2557–2562. (b) Brandsma, L. *Preparative Acetylenic Chemistry*, 2<sup>nd</sup> ed., Elsevier, Amsterdam, 1988. (c) Eaton, P. E.; Srikrishna, A.; Uggeri, F. *J. Org. Chem.* **1984**, *49*, 1728–1732.
- (5) (a) Frantz, D. E.; Fässler, R.; Tomooka, C. S.; Carreira, E. M. *Acc. Chem. Res.* **2000**, *33*, 373–381. (b) Anand, N. K.; Carreira, E. M. *J. Am. Chem. Soc.* **2001**, *123*, 9687–9688. (c) Frantz, D. E.; Fässler, R.; Carreira, E. M. *J. Am. Chem. Soc.* **2000**, *122*, 1806–1807. (d) Boyall, D.; Frantz, D. Z.; Carreira, E. M. *Org. Lett.* **2002**, *4*, 2605–2606.
- (6) (a) Takita, R.; Fukuta, Y.; Tsuji, R.; Ohshima, T.; Shibasaki, M. *Org. Lett.* **2005**, *7*, 1363–1366. (b) Wei, C.; Li, C.-J. *Green Chem.* **2002**, *4*, 39–41. (c) Yao, X.; Li, C.-J. *Org. Lett.* **2005**, *7*, 4395–4398.
- (7) (a) Nakamura, E.; Kuwajima, I. *Angew. Chem., Int. Ed. Engl.* **1976**, *15*, 498–499. (b) Kuwajima, I.; Nakamura, E.; Hashimoto, K. *Tetrahedron* **1983**, *39*, 975–982. (c) Yoshizawa, K.; Shioiri, T. *Tetrahedron Lett.* **2005**, *46*, 7059–7063. (d) Lettan, II, R.; Sheidt, K. *Org. Lett.* **2005**, *7*, 3227–3230. (e) Kitazawa, T.; Minowa, T.; Mukaiyama, T. *Chem. Lett.* **2006**, *35*, 1002–1003. (f) Matsukawa, S.; Sekine, I.; *Synth. Commun.* **2009**, *39*, 1718–1721. (g) Pilcher, A. S.; DeShong, P. *J. Org. Chem.* **1996**, *61*, 6901–6905. (h) Bohsako, A.; Asakura, C.; Shioiri, T. *Synlett.* **1995**, *10*, 1033–1034. (i) Busch-Peterson, J.; Bo, Y.; Corey, E. J. *Tetrahedron Lett.* **1999**, *40*, 2065–2068.

- (8) (a) Hatano, M.; Takagi, E.; Ishihara, K. *Org. Lett.* **2007**, *9*, 4527–4530. (b) Matsukawa, S.; Okano, N.; Imamoto, T. *Tetrahedron Lett.* **2000**, *41*, 103–107. (c) Michida, M.; Mukaiyama, T. *Chem. Lett.* **2008**, *37*, 26–27. (d) Matsukawa, S.; Kitazaki, E. *Tetrahedron Lett.* **2008**, *49*, 2982–2984. (e) Kobayashi, K.; Ueno, M.; Kondo, Y. *Chem. Commun.* **2006**, 3128–3130.
- (9) For reviews on proazaphosphatrane chemistry, see: (a) Verkade, J. G. in *New Aspects of Phosphorus Chemistry II*, *Top. Curr. Chem.* Majoral, J. P. Ed., **2002**, *233*, 1–44. (b) Verkade, J. G.; Kisanga, P. B. *Tetrahedron* **2003**, *59*, 7819–7858. (c) Verkade, J. G.; Kisanga, P. B. *Aldrichimica Acta* **2004**, *37*, 3–14. (d) Urgaonkar, S.; Verkade, J. G. *Specialty Chemicals* **2006**, *26*, 36–39.
- (10) (a) D'Sa, B. A.; Verkade, J. G. *J. Am. Chem. Soc.* **1996**, *118*, 12832–12833. (b) D'Sa, B. A.; McLeod, D.; Verkade, J. G. *J. Org. Chem.* **1997**, *62*, 5057–5061. (c) Wang, Z.; Fetterly, B.; Verkade, J. G. *J. Organomet. Chem.* **2002**, *646*, 161–166. (d) Fetterly, B. M.; Verkade, J. G. *Tetrahedron Lett.* **2005**, *46*, 8061–8066. (e) Yu, Z.; Verkade, J. G. *J. Org. Chem.* **2000**, *65*, 2065–2068. (f) Urgaonkar, S.; Verkade, J. G. *Org. Lett.* **2005**, *7*, 3319–3322. (g) Raders, S. M.; Verkade, J. G. *Tetrahedron Lett.* **2008**, *49*, 3507–3511. (h) Wang, Z.; Kisanga, P. B.; Verkade, J. G. *J. Org. Chem.* **1999**, *64*, 6459–6461. (i) Wang, Z.; Wroblewski, A. E.; Verkade, J. G. *J. Org. Chem.* **1999**, *64*, 8021–8023.
- (11) Yoshizawa, K.; Shioiri, T. *Tetrahedron Lett.* **2006**, *47*, 757–761.

**CHAPTER 6. P(PhCH<sub>2</sub>NCH<sub>2</sub>CH<sub>2</sub>)<sub>3</sub>N CATALYSIS OF MUKAIYAMA ALDOL REACTIONS OF ALIPHATIC, AROMATIC, HETEROCYCLIC ALDEHYDES AND TRIFLUOROMETHYL PHENYL KETONE**

Venkat Reddy Chintareddy, Kuldeep Wadhwa, and John G. Verkade

*manuscript in preparation*



**Abstract:** Herein we find that proazaphosphatane **1c** is a very efficient catalyst for Mukaiyama aldol reactions of aldehydes with trimethylsilyl enolates in THF solvent. Only the activated ketone 2,2,2-trifluoroacetophenone underwent clean aldol product formation with a variety of trimethylsilyl enolates under similar conditions as the aldehydes. The reactions were carried out at room temperature using (1-methoxy-2-methyl-1-propenyloxy)trimethylsilane, whereas the temperature was  $-15\text{ }^{\circ}\text{C}$  in the case of 1-phenyl-1-(trimethylsilyloxy)ethylene. The reaction conditions are mild and operationally simple, and a variety of aryl functional groups, such as nitro, amino, ester, chloro, trifluoromethyl, bromo, iodo, cyano, and fluoro groups are tolerated. Product yields are generally better than or

comparable to those in the literature. 1-Phenyl-1-(trimethylsilyloxy)ethylene, 1-(trimethylsilyloxy)cyclohexene and 2-(trimethylsilyloxy)furan underwent clean conversion to  $\beta$ -hydroxy carbonyl compounds under our reaction conditions. In the case of bulky (2,2-dimethyl-1-methylenepropoxy)trimethylsilane, only  $\alpha,\beta$ -unsaturated esters were isolated. Heterocyclic aldehydes, such as pyridine-2-carboxaldehyde, benzofuran-2-carboxaldehyde, benzothiophene-2-carboxaldehyde, and 1-methyl-2-imidazolecarboxaldehyde gave good yields of Mukaiyama products. An optimized synthesis for the catalyst **1c** is also reported herein.

### Introduction

The Mukaiyama aldol reaction<sup>1</sup> is a versatile carbon-carbon bond forming reaction, which occurs between an enoxysilane and a carbonyl compound to form  $\beta$ -hydroxy carbonyl compounds. The most common application of this transformation involves complex molecule synthesis<sup>2</sup> (such as fragment coupling<sup>3</sup> and chiral building block construction)<sup>4</sup> and it has been the subject of intensive investigation for the past three decades.<sup>2</sup> Moreover, the Mukaiyama reaction has significant advantages over the classical aldol reaction,<sup>5</sup> such as mild reaction conditions, non-reversibility, good yields of aldol products and lower production of dehydrated side products.<sup>6</sup> Initially, stoichiometric amounts of Lewis acids were used to promote Mukaiyama transformations, but it is now more common to employ catalytic loadings of these promoters whose role is believed to be the activation of the electrophilic carbonyl carbon substrate. Among the considerable number of such catalysts are  $\text{Me}_3\text{SiOTf}$ ,<sup>7</sup>  $\text{Me}_3\text{SiI}$ ,<sup>8</sup>  $\text{Me}_3\text{SiCl}/\text{SnCl}_2$ ,<sup>9</sup>  $\text{Ph}_3\text{CCl}/\text{SnCl}_2$ ,<sup>10</sup>  $\text{Ph}_3\text{CClO}_4$ ,<sup>11</sup> trityl salts;<sup>12</sup> various

rhodium complexes;<sup>13</sup> trivalent lanthanum,<sup>14a</sup>  $\text{Ln}(\text{OTf})_3$  ( $\text{Ln} = \text{Yb}^{14b}$ , Gd, Lu),<sup>14c</sup> and scandium<sup>14e</sup> triflates;  $\text{Yb}[\text{C}(\text{SO}_2\text{C}_8\text{F}_{17})_3]_3$  and  $\text{Sc}[\text{C}(\text{SO}_2\text{C}_8\text{F}_{17})_3]_3$ ;<sup>14f</sup> iron,<sup>15a,15b</sup> ruthenium,<sup>15c</sup> palladium<sup>15c,15d</sup> and bis[(bis(1,3-trimethylsilyl)cyclopentadienyl)ytterbium(III) chloride]<sup>16a</sup> complexes; and  $[\text{Et}_3\text{Si}(\text{toluene})]\text{B}(\text{C}_6\text{F}_5)_4$ ,<sup>16b</sup>  $[\text{Cp}_2\text{Zr}(\text{OtBu})\text{THF}[\text{BPh}_4]]$ ,<sup>16c</sup>  $\text{BiCl}_3\text{-NaI}$ ,<sup>16d</sup>  $\text{Sc}(\text{OTf})_3\text{-water}$ ,<sup>16e</sup>  $(\text{PfoBu}_2\text{SnOSnBu}_2\text{OPf})_2$ ,<sup>16f</sup>  $\text{Bi}(\text{OTf})_3$ ,<sup>16g</sup>  $\text{Bi}(\text{OTf})_3/\text{ionic liquids}$ ,<sup>16h</sup>  $\text{Cp}_2\text{Zr}(\text{OTf})_3$ ,<sup>16i</sup> complexes of Ti(IV),<sup>17a</sup> 1,3-dihalotetraalkyldistannoxane,<sup>17c</sup>  $[\text{Mo}_2(\text{OAc})_4]/\text{O}_2$ ,<sup>17d</sup>  $\text{LnBr}_3$ ,<sup>17e</sup> scandium trisdodecanesulfonate,<sup>17f</sup> B-[3,5-bis(trifluoromethyl)phenyl]oxazaborolidine,<sup>17g</sup>  $\text{SmI}_2$ ,<sup>18a</sup>  $\text{MgI}_2\cdot(\text{OEt}_2)_n$ ,<sup>18b</sup> polymer-supported  $\text{Sc}(\text{OTf})_3$ ,<sup>18c,d</sup> titanium silicates,<sup>18e,f</sup> montmorillonite K10,<sup>18g</sup>  $\text{SmCl}_3$ ,<sup>18h</sup>  $\text{FeCl}_2$ ,<sup>18i</sup> zinc triflate,<sup>18j</sup>  $\text{Sc}(\text{OTf})_3$  in PEG,<sup>18k,l</sup> a dinuclear titanium(IV) complex of *p*-tert-butylthiacalix[4]arene,<sup>18m</sup> aluminum bis(trifluoromethylsulfonyl)amides,<sup>18n</sup> sulfated-metal oxides,<sup>18o</sup>  $\text{Sc}(\text{OTf})_3/\text{amphiphilic calix}[6]\text{arene complex}$ ,<sup>18p</sup>  $\text{InCl}_3$ ,<sup>18q</sup> sulfated- $\text{ZrO}_2$ ,<sup>18r</sup> MCM-41,<sup>18s</sup> diphenyltin sulfide/silver perchlorate,<sup>18t</sup>  $\text{BF}_3\cdot\text{OEt}_2$ ,<sup>18u</sup> Sn-MCM-48,<sup>18v</sup> mesoporous- $\text{Mn}^{2+}$  catalyst,<sup>18w</sup>  $\text{CuF}\cdot 3\text{PPh}_3\cdot 2\text{EtOH}/(\text{EtO})_3\text{SiF}$ ,<sup>18x</sup> and tris(pentafluorophenyl)boron.<sup>18y</sup>

Lewis bases that have been employed to nucleophilically activate the enoxysilane substrate include 0.5 mol % of sodium phenoxide-phosphine oxides,<sup>19</sup> 20 mol % tris(2,4,6-trimethoxyphenyl)phosphine,<sup>20</sup> 1 mol % quaternary ammonium dendrimers containing iodide counterions,<sup>21a</sup> 1 mol % SBA-15 functionalized TBD {1,5,7-triazabicyclo[4.4.0]dec-5-ene},<sup>21b</sup> 20 mol % of DBU,<sup>21c</sup> 10 mol % a polystyrene-bound-phosphoramidate,<sup>21d</sup> quaternary ammonium fluoride salts,<sup>21e</sup> 5-10 mol % fluorides,<sup>22</sup> 10 mol % lithium alkoxides,<sup>23a</sup> 10 mol % lithium acetate,<sup>23b,23c</sup> 10 mol % *N*-oxides,<sup>24</sup> and 10 mol % *N*-methylimidazole.<sup>25</sup> Mukaiyama *et al.* also reported such reactions employing 1 equivalent of lithium amide<sup>26</sup> or

10 mol % acetate catalysts<sup>27</sup> and recently, Song *et al.* reported a catalytic method with 0.5 mol % N-heterocyclic carbenes as catalysts.<sup>28</sup>

It has also been reported that Mukaiyama aldol reactions can proceed without catalysts in highly polar solvents, such as DMF,<sup>29a</sup> DMSO,<sup>29a</sup> water,<sup>29b</sup> and ionic liquids.<sup>29c</sup> Another catalytic system utilizes iodine whose mechanism of action is suggested to involve an electron transfer pathway.<sup>30</sup>

The activation of silyl enolates in which the Lewis acidity of the silicon atom has been enhanced by a Lewis base has been studied by Denmark *et al.* who introduced phosphoramidate Lewis bases to catalyze the aldol reaction of trichlorosilyl enolates with aldehydes.<sup>31</sup> Similarly, Hosomi and co-workers reported a Mukaiyama reaction using a dimethylsilyl enolate in the presence of an aldehyde or imine substrate and CaCl<sub>2</sub> in dry or aqueous DMF solvent.<sup>32</sup>

Previous work in our laboratories has established that bicyclic proazaphosphatranes<sup>33</sup> (Figure 1) bearing methyl, *iso*-butyl or benzyl groups on the PN<sub>3</sub> nitrogens are highly effective catalysts, promoters, and ligands for Pd-catalyzed cross-coupling reactions, such as Buchwald-Hartwig aminations,<sup>34a</sup> Stille couplings,<sup>34b</sup> and Suzuki reactions.<sup>34c</sup>

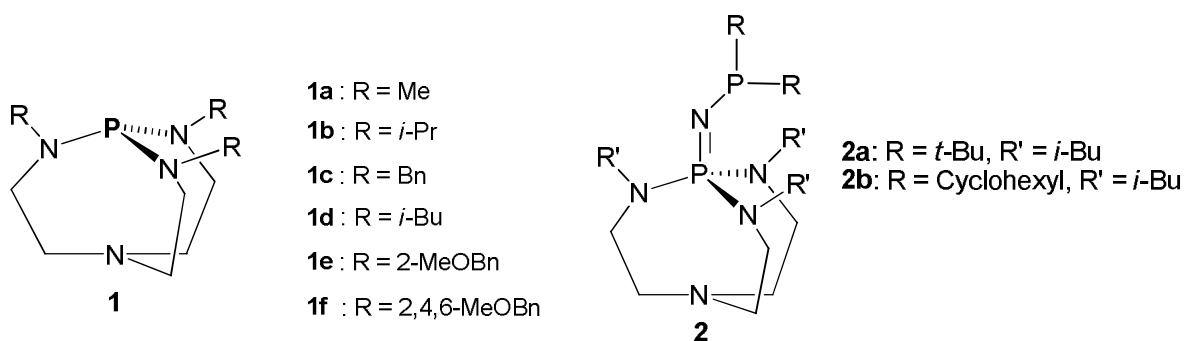
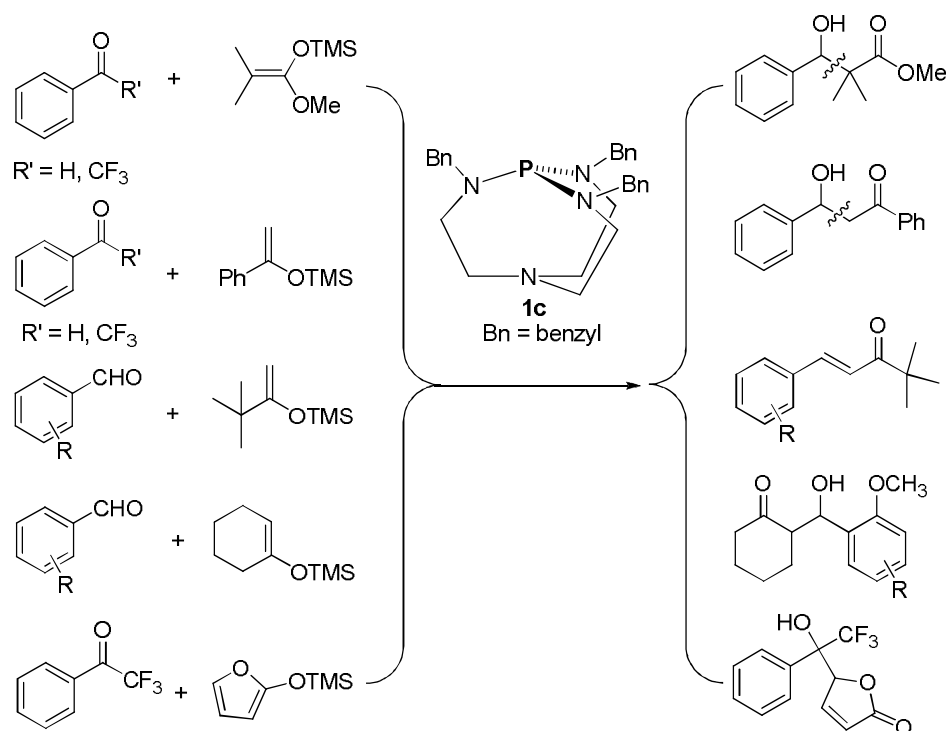


**Figure 1.** Proazaphosphatranes (**1**) and imino-proazaphosphatranes (**2**).

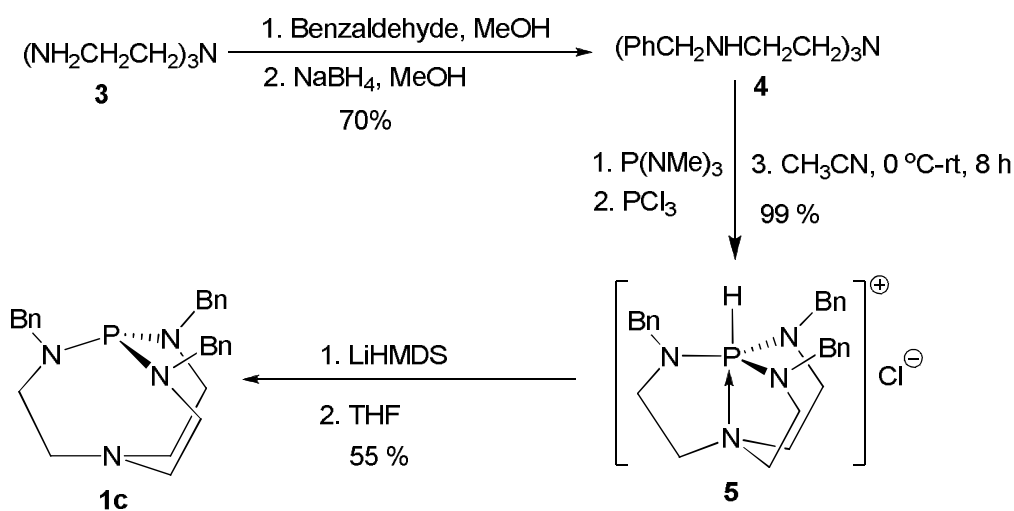
Proazaphosphatranes are strongly basic, with  $pK_a$  values of their P-protonated  $N_{\text{basal}} \rightarrow P$  transannulated conjugate acids in the range 32-34 in MeCN.<sup>34d</sup> To the extent that  $N_{\text{basal}} \rightarrow P$  transannulation may be occurring during reactions catalyzed by **1**, the nucleophilicity of the phosphorus may be enhanced.<sup>33b</sup> Earlier we reported the activation of silicon-carbon bonds by strongly Lewis basic proazaphosphatranes in the silylation of alcohols with *tert*-butyldimethylsilyl chloride (TBDMSCl),<sup>35</sup> desilylation of TBDMS ethers,<sup>36</sup> addition of TMS-CN to carbonyl compounds,<sup>37</sup> and nucleophilic aromatic substitution of aryl fluorides with aryl TBDMS (or TMS) ethers.<sup>38</sup> As part of our ongoing efforts to expand synthetic methodologies facilitated by the use of proazaphosphatranes as catalysts, we report here efficient activation of silicon in silyl enolates using **1c** as a catalyst in Mukaiyama aldol reactions (Scheme 1).





**Scheme 1.** Mukaiyama aldol reactions of various silyl enol ethers catalyzed by **1c**.

Although we reported the synthesis of **1c** previously,<sup>39</sup> we now describe a more convenient set of reaction conditions (Scheme 2). Both synthetic methods involve three steps, but step 1 is now better optimized and in step 3 the more convenient base LiHMDS is employed instead of KO<sup>t</sup>Bu. Although our overall yield of 38% for **1c** is lower than that obtained via our previously reported route (48%), the present protocol provides more consistent yields in the deprotonation step.



**Scheme 2.** Synthesis of catalyst **1c**.

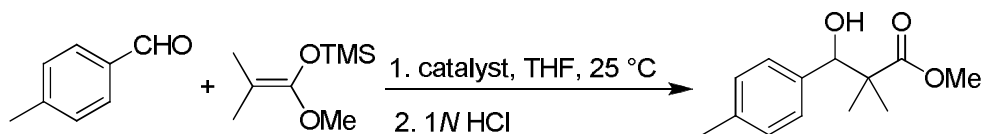
## Results and Discussions

For optimization of the Mukaiyama reaction conditions, the room temperature aldol reaction of the electron-neutral aryl aldehyde shown in the model reaction in (Table 1) was chosen. All the proazaphosphatranes screened (**1a-f**) resulted in good to excellent isolated yields of aldol products, which were obtained after room temperature acid hydrolysis. Since catalysts **1b** and **1c** produced nearly the same product yield (entries 2 and 3, respectively), we reduced the catalyst loading to 0.5 mol % which revealed the somewhat better performance of **1c** (entries 7 and 8). Although we found that the bulky catalyst **1d** showed better activity in a variety of transformations,<sup>33</sup> **1c** was best in the present transformation, as well as in Stille reactions on which we reported earlier.<sup>33b</sup> The origin of the beneficial influence of the benzyl groups of catalyst **1c** and the *i*-Bu substituents of **1d** on different reactions is not clear.

Very recently, we reported the synthesis of **2a**<sup>40a</sup> and **2b**<sup>40a</sup> and their applications as bulky, air-stable, and electron-rich ligands in both palladium-catalyzed Suzuki<sup>40b</sup> and in

Buchwald-Hartwig aminations.<sup>40c</sup> In the Mukaiyama aldol screening reaction in Table 1, both catalysts showed comparable results under the same reaction conditions (entries 9 and 10 in Table 1). The control experiment shown in Table 1, entry 11 reveals the need for a catalyst to presumably activate the silicon center in the Mukaiyama aldol reaction. It is interesting that 8 out of the 12 methods found in the literature employ 5–20 mol % of catalyst (see footnote *c* of Table 1 to reach moderate to high product yields. On the other hand, NHC's<sup>28</sup> and a 1,3-dihalotetraalkyldistannoxane<sup>17c</sup> produced 83 and 99% product yields using only 0.5 and 0.025 mol % of catalyst, respectively.

**Table 1.** Survey of Proazaphosphatranes in a Mukaiyama Aldol Reaction using (1-Methoxy-2-methyl-1-propenyloxy)trimethylsilane.<sup>a</sup>



Entry	Catalyst	Yield (%) <sup>b</sup>
1	<b>1a</b>	82
2	<b>1b</b>	91
3	<b>1c</b>	92
		(79-99) <sup>c</sup>
4	<b>1d</b>	77
5	<b>1e</b>	89
6	<b>1f</b>	90
7 <sup>d</sup>	<b>1b</b>	87

∨

**Table 1 continued**

8 <sup>d</sup>	<b>1c</b>	90
9	<b>2a</b>	90
10	<b>2b</b>	91
11	none	nr <sup>e</sup>

<sup>a</sup> Reaction conditions: catalyst (2.0 mol %), aldehyde (2 mmol), silyl ether (2.4 mmol), THF (4 mL), 24 h, room temperature, followed by 1N HCl (4.0 mL), 12 h. <sup>b</sup> Isolated yields after silica gel column chromatography. <sup>c</sup> Refs 15c, 17c, 18c, 20, 21c, 23a, 23b, 26a, 26c, 27b, 27c, and 28. <sup>d</sup> Using 0.5 mol % of the catalyst **1c**. <sup>e</sup> nr = No reaction after 24 h.

A variety of aldehydes were tested (Table 2) using the optimized reaction conditions reported in footnote a of Table 1 (unless stated otherwise in Table 2). As is evident from Table 2, both electron-neutral and electron-donating aldehydes reacted with equal ease with  $\text{Me}_2\text{C}=\text{C}(\text{OMe})\text{OSiMe}_3$ , affording the desired aldols in good to excellent yields. Electron-neutral aryl aldehydes, such as benzaldehyde (Table 2, entry 1), 1-naphthaldehyde (entry 2), and *o*-phenylbenzaldehyde (entry 3) also underwent clean addition reactions with  $\text{Me}_2\text{C}=\text{C}(\text{OMe})\text{OSiMe}_3$  to give the expected aldol products in good to excellent yields. Aldehydes with electron-donating substituents, such as *m*-methoxybenzaldehyde (entry 4), *o*-tolualdehyde (entry 5), 2,6-dimethylbenzaldehyde (entry 6), *p*-methoxybenzaldehyde (entry 7), 3,4-dimethoxybenzaldehyde (entry 8), and 2-methoxy-1-naphthaldehyde (entry 9) resulted in moderate to excellent isolated yields of aldol products. Excellent isolated yields were obtained when sterically hindered aldehydes, such as *o*-tolualdehyde (Table 2, entry 5), 2,6-dimethylbenzaldehyde (entry 6), and *o*-phenylbenzaldehyde (entry 3) were employed under our reaction conditions. Di-substituted isophthalaldehyde also participated in this reaction by providing a 93% combined yield of mono- and di-substituted products (entry 10)

when the ratio of isophthalaldehyde/(1-methoxy-2-methyl-1-propenyloxy)trimethylsilane was 1:2.4.

It is interesting to note that the reaction of  $\text{Me}_2\text{C}=\text{C}(\text{OMe})\text{OSiMe}_3$  with *p*-(*N,N*-dimethylamino)benzaldehyde gave a poor yield of product (47%) when the neutralization work up step was carried out with saturated aqueous  $\text{NaHCO}_3$ . However, an excellent isolated yield (96%) was obtained when the product was isolated as the TMS-protected alcohol in a separate experiment. Using the stronger base  $\text{NaOH}$ , instead of  $\text{NaHCO}_3$ , gratifyingly gave an excellent isolated yield of aldol product (90%) (Table 2, entry 11).

**Table 2.** Scope of the Mukaiyama Aldol reaction of Aldehydes with  $(\text{CH}_3)_2\text{C}=\text{C}(\text{OCH}_3)\text{OSi}(\text{CH}_3)_3$  Catalyzed by **1c<sup>a</sup>**

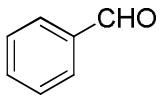
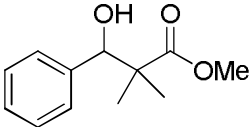
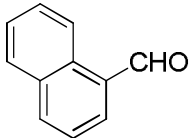
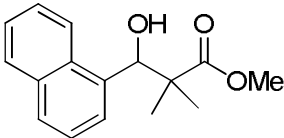
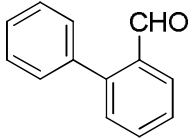
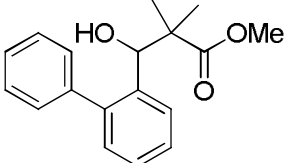
Entry	Aldehyde	Product	Yield (%) <sup>b</sup>	Lit. Yield (%)
1			93	20-100 <sup>c</sup>
2			81	82-97 <sup>d</sup>
3 <sup>e</sup>			92	-

Table 2 continued

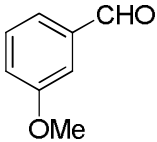
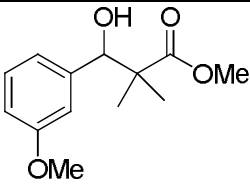
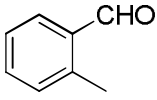
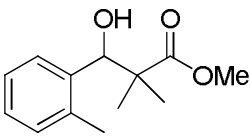
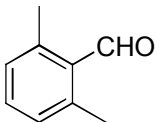
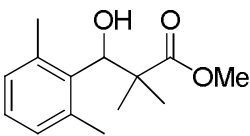
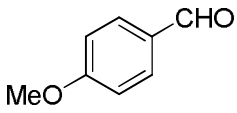
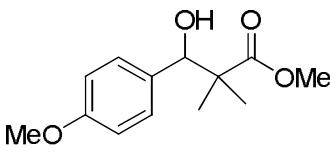
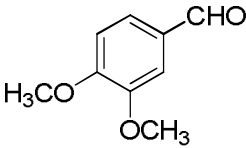
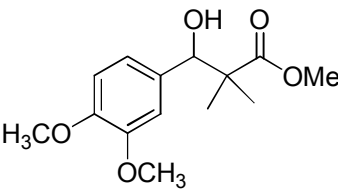
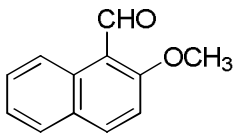
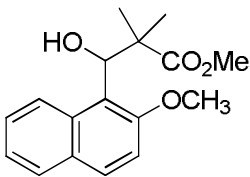
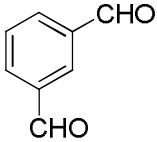
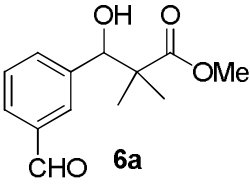
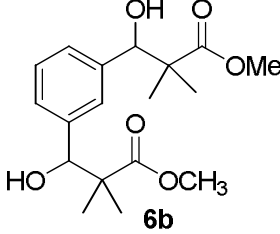
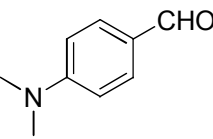
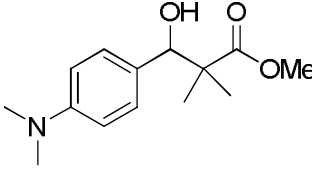
4			88	-
5 <sup>e</sup>			92	93 <sup>f</sup>
6			86	-
7			90	44-98 <sup>g</sup>
8 <sup>e</sup>			91	-
9 <sup>e</sup>			69	-
10 <sup>h</sup>			93 <sup>i</sup>	-

Table 2 continued

		 <b>6b</b>		
11 <sup>j</sup>			47 <sup>k</sup>	
			96 <sup>m</sup>	83 <sup>l</sup>
			90 <sup>n</sup>	

<sup>a</sup> Reaction conditions: aldehyde (2.0 mmol), TMS-ether (2.4 mmol), **1c** (3.0 mol % unless otherwise stated), THF (4.0 mL), room temperature for 24 h. <sup>b</sup> Isolated yields after silica-gel chromatography. <sup>c</sup> Refs 17d, 17e, 17f, 18c, 18d, 18e, 18f, 18g, 20, 21c, 23a, 23c, 24, 25, 26a, 28, 29a, 29b, 29c, 30. <sup>d</sup> Refs 17d, 23a, 26a, 28. <sup>e</sup> Using 6 mol % of **1c**. <sup>f</sup> Ref 18c. <sup>g</sup> Ref 15c, 17e, 18e, 20, 21b, 23a, 24, 25, 26a, 27b, 27c, 28, 29a, 29c. <sup>h</sup> Using 10 mol % of **1c** and 4.8 mmol Me<sub>2</sub>C=C(OMe)OSiMe<sub>3</sub>. <sup>i</sup> Combined isolated yield of **6a** (49%) and **6b** (44%). <sup>j</sup> Using 10 mol % of catalyst **1c**. <sup>k</sup> NaHCO<sub>3</sub> was used for neutralizing excess HCl used for the hydrolysis of the TMS-ether. <sup>l</sup> Ref 28. <sup>m</sup> Isolated yield as the TMS-ether. <sup>n</sup> NaOH was used in place of NaHCO<sub>3</sub> for neutralizing excess HCl used for the hydrolysis of the TMS-ether.

A variety of aldehydes bearing electron-withdrawing groups were screened with Me<sub>2</sub>C=C(OMe)OSiMe<sub>3</sub> under the optimized conditions mentioned in Table 1, entry 3, and the results are summarized in Table 3. *o*-Chlorobenzaldehyde and *o*-fluorobenzaldehyde provided excellent isolated product yields (entries 1 and 2, respectively), while 3-iodobenzaldehyde (Table 3, entry 3) and 4-bromobenzaldehyde (entry 4) both gave good yields of product. Electron-deficient 4-(trifluoromethyl)benzaldehyde gave a moderate yield (entry 5) as did the *p*-nitro (entry 6), *m*-cyano (entry 7) and *p*-cyano (entry 8) analogues. *p*-Chloro and ester-functionalized aldehydes underwent clean reactions giving good to excellent yields of products (entries 9 and 10, respectively).

**Table 3.** Scope of the Mukaiyama Aldol Reaction of Functionalized Aldehydes with  $(\text{CH}_3)_2\text{C}=\text{C}(\text{OCH}_3)\text{OSi}(\text{CH}_3)_3$  Catalyzed by **1c**<sup>a</sup>

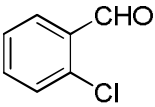
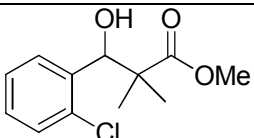
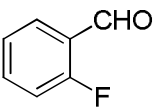
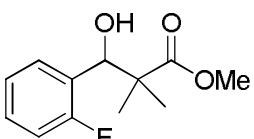
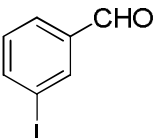
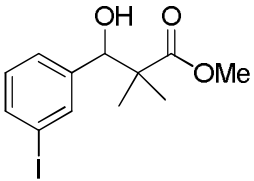
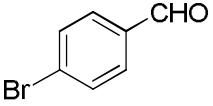
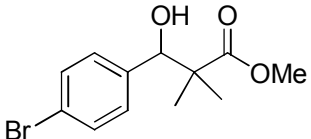
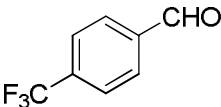
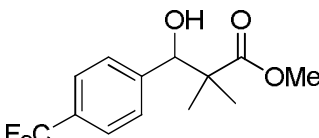
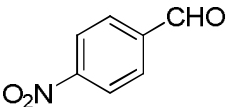
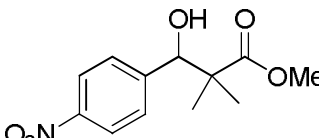
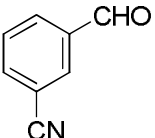
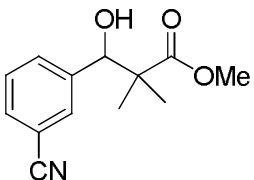
Entry	Aldehyde	Product	Yield (%) <sup>b</sup>	Lit. Yield (%)
1			91	(65 <sup>c</sup> , <5 <sup>d</sup> )
2			77	-
3 <sup>e</sup>			95	-
4 <sup>f</sup>			72	34-92 <sup>g</sup>
5 <sup>f</sup>			84	33-68 <sup>h</sup>
6			62	32-97 <sup>i</sup>
7 <sup>f</sup>			58	-



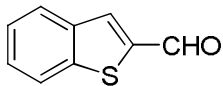
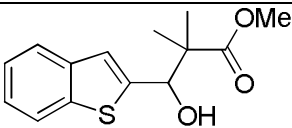
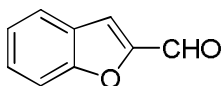
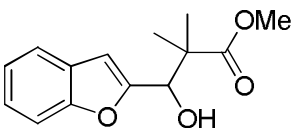
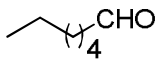
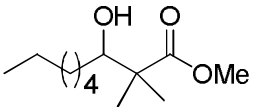
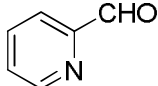
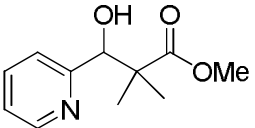
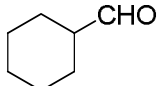
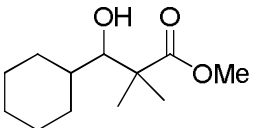
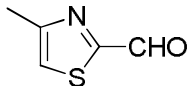
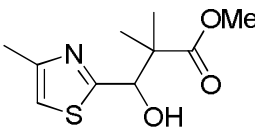
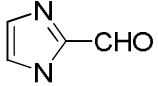
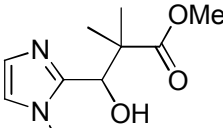
Table 3 continued

8			74	69-90 <sup>j</sup>
9 <sup>f</sup>			91	63-94 <sup>k</sup>
10			82	99 <sup>l</sup>

<sup>a</sup> Reaction conditions: aldehyde (2.0 mmol), TMS-ether (2.4 mmol), **1c** (3.0 mol % unless otherwise stated), THF (4.0 mL), room temperature, 24 h. <sup>b</sup> Isolated yields after silica-gel chromatography. <sup>c</sup> Ref 24. <sup>d</sup> Ref 15c. <sup>e</sup> Using 10 mol % of catalyst **1c**. <sup>f</sup> Using 6 mol % of catalyst **1c**. <sup>g</sup> Refs 15c, 17e, 23a, 26a, 26c. <sup>h</sup> Ref 17d. <sup>i</sup> Refs 17e, 18f, 21b, 23a, 23b, 24, 25, 26a, 26c, 26b, 27b, 27c, 28. <sup>j</sup> Refs 18f, 23a, 26a, 26c, 28. <sup>k</sup> Refs 15c, 17e, 18c, 21c, 23a, 23b, 24, 25, 26a, 26c, 27b, 27c, 28, 29c, 30. <sup>l</sup> Refs 23b, 27b.

We then turned our attention to screening various heterocyclic and aliphatic aldehydes with  $\text{Me}_2\text{C}=\text{C}(\text{OMe})\text{OSiMe}_3$  (Table 4). Both 5- and 6-membered ring aldehydes bearing N, O or S heteroatoms afforded the expected aldol product in poor to excellent isolated yields. Sulfur-containing 2-benzothiophenecarboxaldehyde afforded an excellent isolated product yield (Table 4, entry 1), 2-benzofurancarboxaldehyde gave a very good yield (Table 4, entry 2), and an enolizable aliphatic aldehyde (entry 3) also provided a good yield of the corresponding aldol product. However, 2-pyridinecarboxaldehyde and cyclohexanecarboxaldehyde gave only modest isolated product yields (entries 4 and 5, respectively). Nevertheless, the yield in entry 5 exceeded that previously reported in the literature. The two 5-membered heterocyclic aldehydes in Table 4 (entries 6 and 7) gave only low yields of the corresponding products.

**Table 4.** Scope of the Mukaiyama Aldol Reaction of Heterocyclic Aldehydes with  $(\text{CH}_3)_2\text{C}=\text{C}(\text{OCH}_3)\text{OSi}(\text{CH}_3)_3$  Catalyzed by **1c**<sup>a</sup>

Entry	Aldehyde	Product	Yield (%) <sup>b</sup>	Lit. Yield (%)
1 <sup>c</sup>			92	-
2			89	-
3			80	47-80 <sup>d</sup>
4			67	53-97 <sup>e</sup>
5			67	35-48 <sup>f</sup>
6 <sup>c</sup>			36	-
7 <sup>c</sup>			52	-

<sup>a</sup> Reaction conditions: aldehyde (2.0 mmol), TMS-ether (2.4 mmol), **1c** (3.0 mol % unless otherwise stated), THF (4 mL), room temperature. <sup>b</sup> Isolated yields after silica-gel column chromatography. <sup>c</sup> Using 10 mol % of catalyst **1c**. <sup>d</sup> Refs 14a, 18g, 18h. <sup>e</sup> Refs 23b, 26b, 27b, 29b, 29c. <sup>f</sup> Refs 20, 27b.

In screening the reaction of  $\text{PhC(=CH}_2\text{)OSiMe}_3$  with *o*-anisaldehyde using proazaphosphatranes **1a-1d** (Table 5, entry 1), **1c** gave the best product yield (82%) in accord with the previous findings in the present work. We then screened several aldehydes with the same silyl enol ether. Thus, electron-rich *p*-tolualdehyde and electron-poor *p*-chlorobenzaldehyde gave a moderate and a modest yield of product, respectively (entries 2 and 3). A sterically bulky and an enolizable aliphatic acyclic aldehyde gave a modest and a good product aldol yield, respectively (entries 4 and 5) and  $\text{C}_6\text{H}_9\text{OSiMe}_3$  with electron-deficient *p*-nitrobenzaldehyde provided an excellent isolated product yield as the *syn* isomer selectively (entry 6). Electron-neutral benzaldehyde and electron-rich *o*-anisaldehyde afforded good and excellent isolated product yields, respectively, with predominant *syn* isomer selectivity in both cases (entries 7 and 8).

**Table 5.** Scope of the Mukaiyama Aldol Reaction of Aldehydes with  $\text{C}_6\text{H}_5\text{C(=CH}_2\text{)OSi(CH}_3\text{)}_3$  and  $\text{C}_6\text{H}_9\text{OSi(CH}_3\text{)}_3$  Catalyzed by **1c**<sup>a</sup>

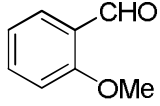
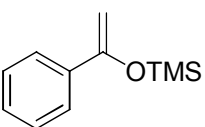
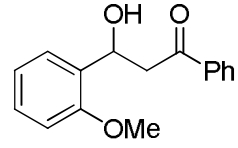
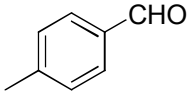
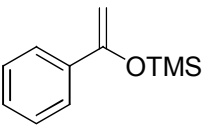
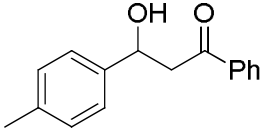
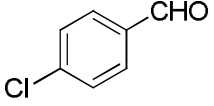
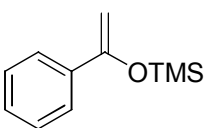
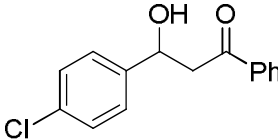
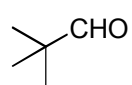
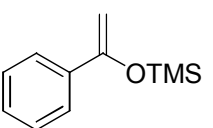
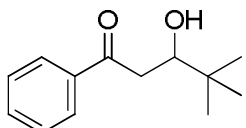
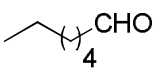
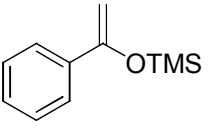
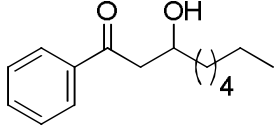
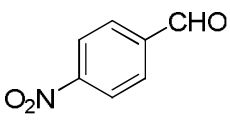
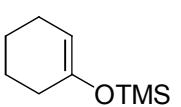
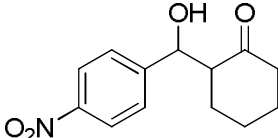
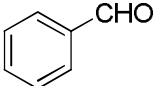
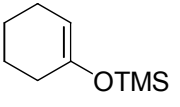
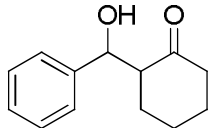
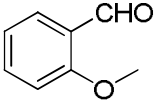
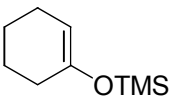
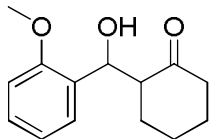
Entry	Aldehyde	TMS-enolate	Product	Yield (%) <sup>b</sup>	Lit. Yield (%)
1				82 <sup>c</sup>	39-94 <sup>d</sup>
				60 <sup>e</sup>	
				79 <sup>f</sup>	
				55 <sup>g</sup>	
2				77	74-89 <sup>h</sup>

Table 5 continued

3				69	48-93 <sup>i</sup>
4				74	88 <sup>j</sup>
5				80	-
6				91	66-92 <sup>k</sup>
7 <sup>l</sup>				76 (94/6) <sup>m</sup>	18-99 <sup>n</sup>
8 <sup>l</sup>				91 (78/22) <sup>m</sup>	(89) <sup>o</sup>

<sup>a</sup> Reaction conditions: aldehyde (2.0 mmol), TMS-ether (2.4 mmol), **1c** (3.0 mol %), otherwise stated), THF (4 mL), 0 °C, 72 h. <sup>b</sup> Isolated yields after silica-gel chromatography. <sup>c</sup> Using 3 mol % **1c**. <sup>d</sup> Refs 17d, 18i, 18j. <sup>e</sup> Using 3 mol % **1a**. <sup>f</sup> Using 3 mol % **1b**. <sup>g</sup> Using 3 mol % **1d**. <sup>h</sup> Refs 18k, 18l, 18m, 28. <sup>i</sup> Refs 18j, 18k, 18l, 18m, 25, 28. <sup>j</sup> Ref 18n. <sup>k</sup> Refs 22b, 30. <sup>l</sup> Using 6 mol % of catalyst **1c**. <sup>m</sup> The syn/anti ratio was determined by using proton NMR spectroscopy. <sup>n</sup> Refs 1a, 14b, 14e, 15d, 16d, 17g, 18j, 18o, 18p, 18q, 18r, 18s, 18t, 18y, 21e, 22b, 30. <sup>o</sup> Ref 18u.

The use of bulky  $\text{Me}_3\text{CC}(=\text{CH}_2)\text{OSiMe}_3$  was then investigated as shown in Table 6. To our surprise, the unsaturated ketone **7b** was obtained, rather than the desired aldol product **7a** when we carried out the reaction at 0 °C (Table 6, entry 1). An attempt to optimize the reaction to selectively produce aldol product by lowering the reaction temperature to -20 °C failed to give aldol product, and the same yield of dehydrated product (entry 2) was produced as was the case at 0 °C. Lowering the temperature to -78 °C did not produce any observable product and only starting materials were recovered (entry 3). At room temperature, this reaction did not proceed to complete conversion and only a moderate yield of  $\alpha,\beta$ -unsaturated ketone **7b** (entry 4) was isolated. We then expanded the scope of this trimethylsilyl enol ether to a diverse range of aldehydes using the conditions in entry 1 of Table 6.

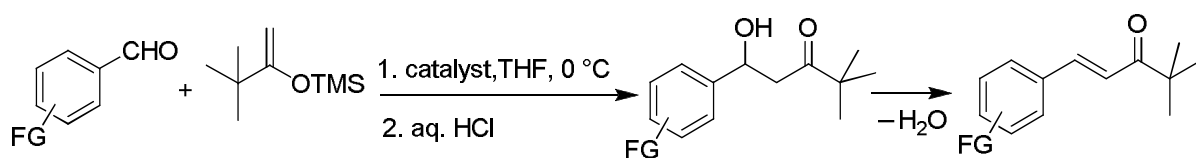
**Table 6.** Scope of the Mukaiyama Aldol Reaction of 2-Fluorobenzaldehyde with  $(\text{CH}_3)_3\text{CC}(=\text{CH}_2)\text{OSi}(\text{CH}_3)_3$  Catalyzed by **1c**<sup>a</sup>

Entry	Catalyst <b>1c</b> (mol %)	Temp (°C)	Time (h)	Yield <b>7a</b> (%) <sup>b</sup>	Yield <b>7b</b> (%) <sup>b</sup>
1	6	0	72	0	92
2	6	-20	72	0	90
3	6	-78	12	n.r.	n.r. <sup>c</sup>
4	6	25	72	0	60 <sup>d</sup>

<sup>a</sup>Reaction conditions: aldehyde (2.0 mmol), (2,2-dimethyl-1-methylenepropoxy)trimethylsilane (2.4 mmol), THF (2.0 mL), followed by 1N HCl. <sup>b</sup>Isolated yields after silica-gel column chromatography. <sup>c</sup>No reaction. <sup>d</sup><sup>1</sup>H NMR spectroscopy revealed that 40% of the reaction consisted of unreacted aldehyde.

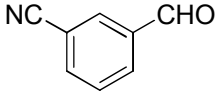
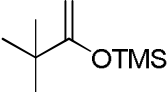
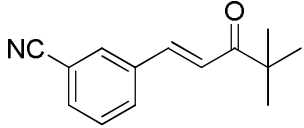
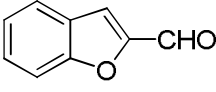
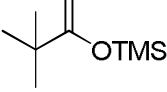
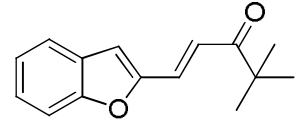
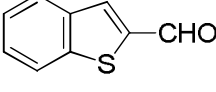
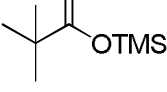
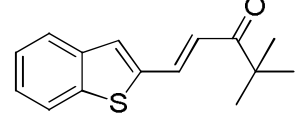
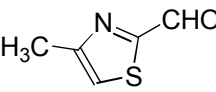
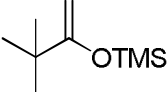
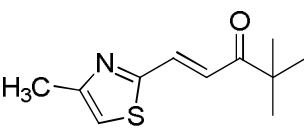
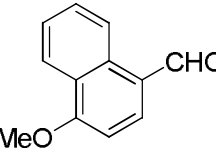
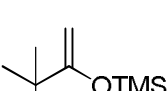
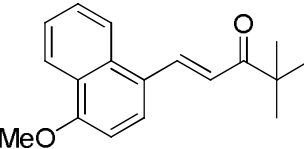
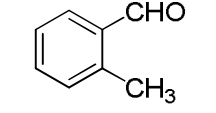
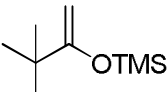
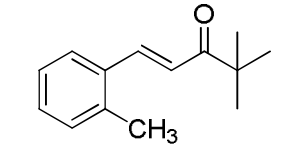
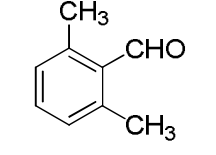
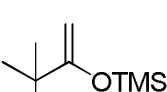
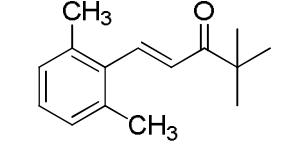
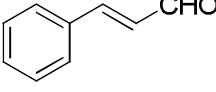
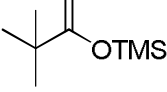
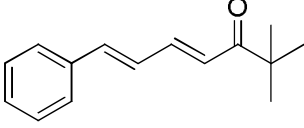
As seen in Table 7, catalyst **1c** gave good to excellent isolated yields of the corresponding  $\alpha,\beta$ -unsaturated bulky ketones for aldehydes bearing a variety of functional groups. Our methodology is compatible with fluoro (Table 6, entry 1), iodo (Table 7, entry 1), and acid-sensitive cyano (Table 7, entry 2) substituents; the heterocyclic aldehydes benzofuran-2-carboxaldehyde (entry 3), benzothiophene-2-carboxaldehyde (entry 4) and 4-methyl-2-thiazolecarboxaldehyde (entry 5); and also electron rich 4-methoxy-1-naphthaldehyde (entry 6) and *o*-tolualdehyde (entry 7). The bulky *ortho*-disubstituted aldehyde in entry 8 afforded a moderate product yield, and *trans*-cinnamaldehyde (entry 9) produced the conjugated bulky ketone shown in excellent isolated yield (95%). The latter yield exceeded that previously reported in the literature using 110 mol % CsF as catalyst at 80 °C.<sup>41</sup> The other products listed in this table have not, to our knowledge, been reported in the literature.

**Table 7.** Synthesis of  $\alpha,\beta$ -Unsaturated Bulky Ketones from Aldehydes with  $(\text{CH}_3)_3\text{CC}(\text{=CH}_2)\text{OSi}(\text{CH}_3)_3$  Catalyzed by **1c**<sup>a</sup>



Entry	Aldehyde	TMS-enolate	Product	Yield (%) <sup>b</sup>
1				95

Table 7 continued

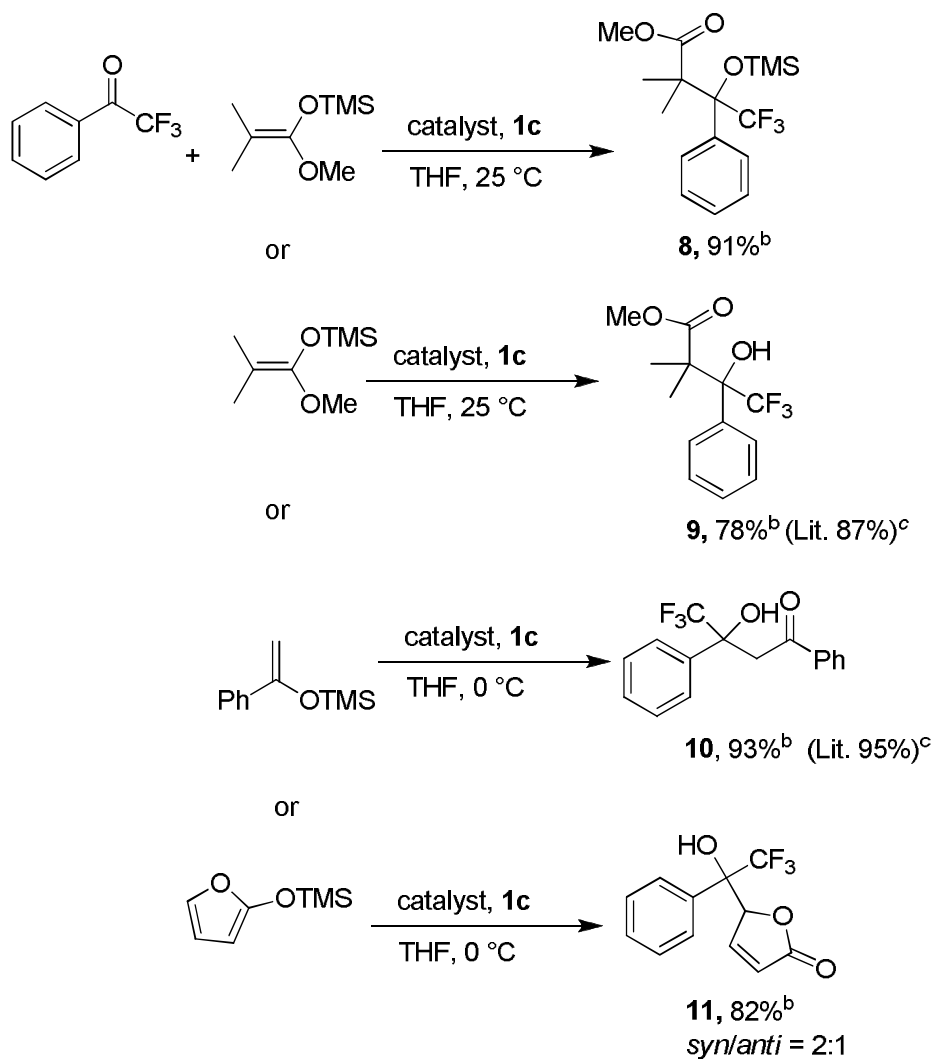
2				94
3				77
4				83
5 <sup>c</sup>				94
6				78
7 <sup>c</sup>				90
8 <sup>c</sup>				72
9 <sup>c</sup>				95 (65) <sup>d</sup>

<sup>a</sup>Reaction conditions: aldehyde (2.0 mmol), (2,2-dimethyl-1-methylenepropoxy)trimethylsilane (2.4 mmol), **1c** (6.0 mol %), THF (4.0 mL), 0 °C, 72 h, followed by 1N HCl (3.0 mL) <sup>b</sup> Isolated yields after silica-gel chromatography. <sup>c</sup> Using 10 mol % of **1c**. <sup>d</sup> Ref. 41.

Our attempts to accomplish Mukaiyama aldol addition to acetophenone, benzophenone and 4-chloroacetophenone were unsuccessful. However, 2,2,2-trifluoroacetophenone reacted with a variety of trimethylsilyl enolates to provide products **8-11** in moderate to excellent yields as shown in Scheme 3. The reaction of  $\text{Me}_2\text{C}(\text{=C})\text{OMe}(\text{OSiMe}_3)$  with 2,2,2-trifluoroacetophenone afforded the corresponding Mukaiyama aldol product in 91% yield as the TMS-protected product **8**. In a separate experiment, hydrolyzed product **9** was obtained in 78% yield. Interestingly, both **8** and **9** possess two vicinal quaternary carbon centers. Not surprisingly, 2,2,2-trifluoroacetophenone was found to be an excellent substrate for this reaction with  $\text{PhC}(\text{=CH}_2)(\text{OSiMe}_3)$  and product **10** was isolated in 93% yield, which is comparable to the yield reported in the literature.<sup>28</sup> The reaction of 2,2,2-trifluoroacetophenone with 2-(trimethylsilyloxy)furan gave a good yield of product **11** with a *syn/anti* ratio of 2:1. Neither **8** nor **11** have been previously reported in the literature.



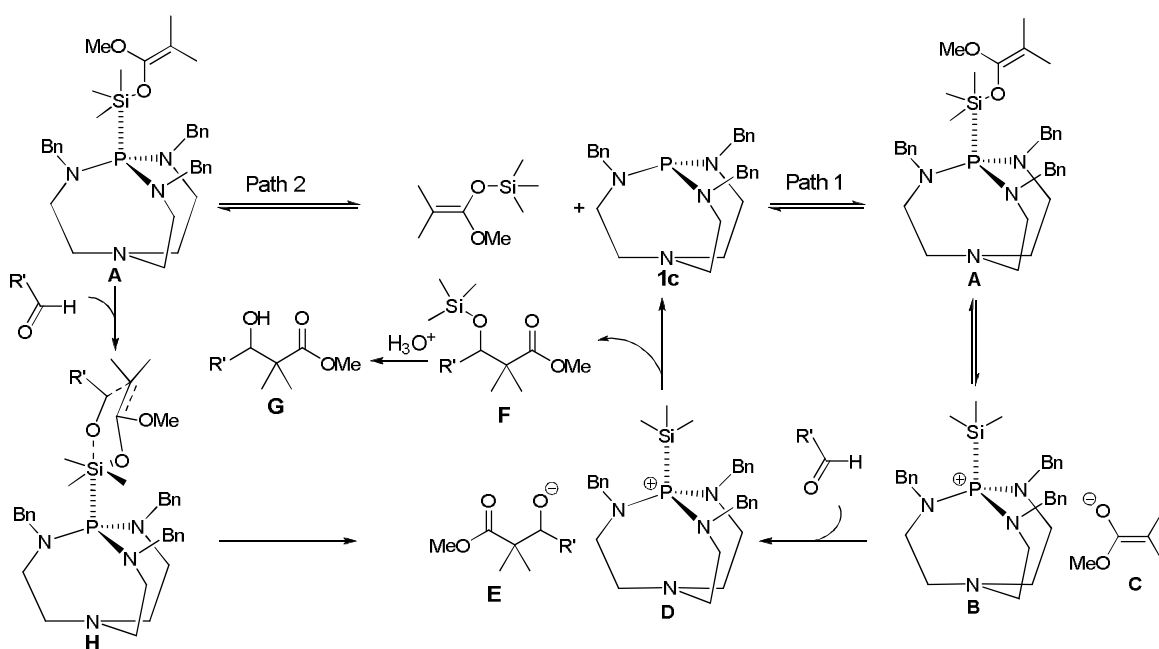
**Scheme 3.** Mukaiyama Aldol Reaction of a Trifluoromethyl Ketone with a Variety of TMS Ethers Catalyzed by **1c**.<sup>a</sup>



<sup>a</sup> Reaction conditions: aldehyde (2.0 mmol), TMS-ether (2.4 mmol), **1c** (5 mol % for **8**, 6 mol % for **9** and 10 mol % for **10**), room temperature. <sup>b</sup> Isolated yields after silica-gel chromatography. <sup>c</sup> Ref. 28.

A mechanism suggested for the Mukaiyama aldol reaction of trimethylsilyl enolates with aldehydes<sup>42</sup> under our conditions is depicted in Scheme 4. In the literature, the Lewis base-

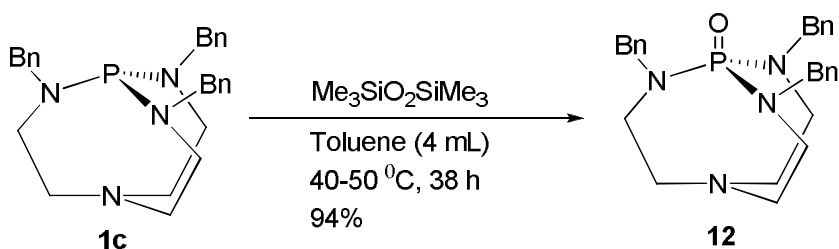
catalyzed Mukaiyama aldol reaction is proposed to proceed through the formation of a pentavalent silicon complex via Lewis-base activation, which generates the naked enolate anion **C** in the presence of a large counter cation.<sup>22b,23,26a,27b,28</sup> In Path 1, **1c** initially forms a pentacoordinated silicon complex **A** in which the electron density on the silicon is enriched, consequently weakening the bonds around this atom, and thus favoring ionization to species **B** and **C**. Evidence for the existence of naked anion **C** was previously presented by our group to account for the formation of both  $\alpha$ - and  $\gamma$ -addition products in the reaction of crotyltrimethylsilane with aldehydes in the presence of **1a**.<sup>43</sup> Enolate anion **C** then nucleophilically attacks the aldehyde carbon giving the corresponding alkoxide **E**, which then nucleophilically attacks cation **D** giving the TMS-protected aldol product **F**. Product **F** is subsequently hydrolyzed in a separate step to give the desired aldol product **G** with accompanying regeneration of the catalyst **1c**. Another proposed route is depicted in Path 2 in Scheme 4. Initially **1c** forms a pentacoordinated silicate TMS-ketene acetal adduct **A** (as was suggested for Path 1), which then coordinates with the incoming aldehyde concomitantly to form hexacoordinated cyclic intermediate **H**<sup>44,20</sup> in which a six-membered cyclic intermediate between the silyl enol ether and the aldehyde is formed. Subsequent steps are as discussed for Path 1 to give product and regenerated catalyst **1c**.



**Scheme 4.** Proposed reaction pathway for the Mukaiyama aldol reaction of aldehydes with  $\text{Me}_2\text{C}=\text{C}(\text{OMe})\text{OSiMe}_3$  catalyzed by **1c**.

To elucidate the nature of the active species in the mechanism in Scheme 4, we conducted  $^{31}\text{P}$  NMR spectroscopic experiments aimed at monitoring changes in the environment of **1c**. Initially, we examined the room temperature  $^{31}\text{P}$  NMR spectrum of **1c** in THF in the presence of equimolar amounts of  $\text{Me}_2\text{C}=\text{C}(\text{OMe})\text{OSiMe}_3$  and *p*-toluialdehyde. A peak at 24 ppm (~5-10% intensity) was observed, which was attributed to the corresponding oxide **12**; a conclusion that was confirmed by synthesizing a sample of **12** as depicted in Scheme 5. The formation of **12** could arise from the formation of an epoxide due to the putative self-condensation of *p*-toluadehyde as was observed previously in the presence of **1a**.<sup>45</sup> We then carried out a  $^{29}\text{Si}$  NMR experiment at  $-40\text{ }^\circ\text{C}$  on a THF solution of  $\text{Me}_2\text{C}=\text{C}(\text{OMe})\text{OSiMe}_3$  ( $\delta^{29}\text{Si}$  19.56, THF) in the presence of an equimolar amount of **1c**. No change was observed in the  $^{29}\text{Si}$  NMR chemical shift. Similarly, TMSOPh ( $\delta^{29}\text{Si}$  18.21 ppm

in THF) under the same conditions using **1c** as a catalyst also produced no change in the  $^{29}\text{Si}$  NMR chemical shift. However, when we used the less bulky **1a**, a new peak at  $\delta^{29}\text{Si}$  6.98 ppm was observed after 2 h and 10 min, which we attribute to the tetracoordinate silicon species **B** in which the anionic species **C** has been displaced. This chemical shift is in the same region as a peak we reported previously for a 1:1 mixture of TMSCN and **1a** in  $\text{C}_6\text{D}_6$  ( $\delta^{29}\text{Si}$  7.5 ppm) in which  $\text{CN}^-$  had been displaced. If the anion had not been displaced in both cases, an upfield rather than a downfield shift from the parent TMSX molecule would have been observed, since the silicon would have become 5-coordinate.<sup>37a</sup> We used similar reasoning to account for the formation of both  $\alpha$ - and  $\gamma$ -addition products in the reaction of crotyltrimethylsilane with aldehydes in the presence of **1a**.<sup>43</sup> After transient **A** forms **B** and **C** in Scheme 4, an aldehyde molecule reacts with **C** to form the alkoxide **E**, which after trimethylsilylation is acid-hydrolyzed to give the corresponding species **G** as the final product, plus the regenerated catalyst **1c**. Although we have  $^{29}\text{Si}$  NMR evidence consistent with the formation of **B**, we have no convincing  $^{31}\text{P}$  NMR evidence for this species.  $^{31}\text{P}$  chemical shifts for  $\text{PR}_4^+$  cations are generally in the range of 90-140 ppm.<sup>46</sup> The  $^{31}\text{P}$  NMR chemical shift for **B** is 128 ppm at  $-40^\circ\text{C}$  in THF, which is virtually unchanged from the value of **1a** under the same conditions. This result perhaps suggests a minimal perturbation of the phosphorus shielding environment as a result of a relatively weak Si-P interaction.



**Scheme 5.** Synthesis of the phosphorus oxide of catalyst **1c**.

### Conclusion

In summary, we have demonstrated that proazaphosphatrane **1c** is an active catalyst for the C-C bond-forming Mukaiyama aldol transformation, furnishing aldol products in generally high yields. Our methodology is compatible with electron-donating and withdrawing aryl aldehyde functional groups (e.g., methoxy, nitro, trifluoromethyl, amino, cyano, bromo, ester, fluoro and chloro) and aliphatic and heterocyclic aldehydes, which also function well in these reactions. Moreover, a variety of silyl enol ethers are compatible with our reaction conditions. Our methodology using **1c** represents an advantageous catalytic alternative to arylphosphines (wherein 20 mol % of catalyst is routinely employed).  $\alpha,\beta$ -Unsaturated bulky ketone products were isolated in good to excellent yields under our reaction conditions.

From Table 8, it is seen that of the total of 26 known Mukaiyama aldol products we found in the literature, we have observed in this work higher yields for 5, comparable yields for 6 and lower yields for 15 of them. While the latter number might be considered somewhat disappointing, it is also to be noted from this table that our catalyst loadings were lower than the minimum catalyst loading (associated with the maximum yield) found in the literature in

well over half (68%) of all of the cases. It should also be mentioned that our protocol resulted in the synthesis of 24 new compounds of which 12 were obtained in excellent yields, 4 in good yields, 4 in moderate yields, 1 in only a modest yield and 3 in poor yields. The facile synthesis of catalyst **1c**, the broad range of amenable silyl enol ethers and aldehydes which can be utilized, the relatively low catalyst loading and the environmentally desirable lack of metal usage in the syntheses reported here renders our methodology attractive.

**Table 8.** A Comparison of the Efficiency of our Catalytic Protocol with Literature Protocols.

Our Product Yields Compared with Maximum Literature Yields and Our Catalyst Loadings Compared with the Lowest found in the Literature			
Table	No. of Our Products with Higher Yields and Our Catalyst Loadings compared with Lit.	No. of Our Products with Comparable <sup>a</sup> Yields and Our Catalyst Loadings compared with Lit	No. of Our Products with Lower Yields and Our Catalyst Loadings compared with Lit.
Table 1	-	-	1 (higher)
Table 2	1 (higher)	1 (higher)	3 (lower)
Table 3	2 (lower)	1 (lower)	4 (lower for 3; higher for 1)
Table 4	1 (lower)	1 (lower)	1 (lower)
Table 5	-	2 (lower)	5 (lower for 4; higher for 1)
Table 7	1 (lower)	-	-

**Table 8 continued**

Scheme 3	1 (higher)	1 (higher)
5 (3 lower)	6 (3 lower)	15 (11 lower)

<sup>a</sup>Taken here to be within  $\pm 5\%$ .

### Experimental Section

**General Considerations.** All reactions were performed under an atmosphere of argon in oven-dried glassware. Toluene, pentane and tetrahydrofuran (THF) were freshly distilled over sodium/benzophenone and stored over 4 Å molecular sieves under an argon atmosphere. <sup>1</sup>H (300 or 400 Hz) and <sup>13</sup>C (100.6 MHz) NMR spectra were recorded in CDCl<sub>3</sub> (unless otherwise stated); the chemical shifts are referenced to the residual peaks of CHCl<sub>3</sub> in CDCl<sub>3</sub>. <sup>31</sup>P NMR spectra were recorded at ambient temperature on a 400 MHz spectrometer using standard procedures. Thin layer chromatography (TLC) was performed using commercially prepared 60 mesh silica gel plates visualized with short-wavelength UV light (254 nm). Column chromatography was performed on silica gel (40–140 mesh) for purification of the product. Electron impact ionization experiments were performed on a triple quadrupole mass spectrometer fitted with a EI/CI ion source. Accurate mass measurements were performed using a double focusing MS-50 mass spectrometer. All commercially available reagents were used as received. All products described in Tables 1–7 and Schemes 2 and 3 are known in the literature (unless indicated otherwise) and were characterized by comparing their <sup>1</sup>H and <sup>13</sup>C NMR spectra to the previously reported data. In all cases, the comparisons were very favorable. New compounds were characterized by <sup>1</sup>H, <sup>13</sup>C, mass (EI) and HRMS analysis.

**Preparation of P(PhCH<sub>2</sub>NCH<sub>2</sub>CH<sub>2</sub>)<sub>3</sub>N (1c):**

**Synthesis of tribenzyl-tren (4).** To 14.6 g (0.100 mol, 1.0 equiv) of freshly distilled [tris(2-aminoethyl)amine] in 75 mL of MeOH was added (30.48 mL, 0.320 mol, 3.2 equiv) of benzaldehyde. The mixture was allowed to stir at room temperature over 8 h. To this mixture was added 100 mL MeOH and then the reaction mixture was cooled to 0-5 °C using an ice bath. NaBH<sub>4</sub> (5.67 g, 0.150 mol, 1.5 equiv) was added slowly to the mixture portion-wise over a period of 1 h. Excess solvent was removed completely using a rotary evaporator, followed by dissolving the resultant slurry in 200 mL water and extracted with CH<sub>2</sub>Cl<sub>2</sub> (3 × 100 mL). The organic extracts were combined and dried over anhydrous Na<sub>2</sub>SO<sub>4</sub> and filtered to remove Na<sub>2</sub>SO<sub>4</sub>. Excess solvent was removed under reduced pressure using a rotary evaporator. The crude light yellow oil was purified using silica gel chromatography (eluent: 10 % MeOH/CH<sub>2</sub>Cl<sub>2</sub>) to afford 29.12 g (70%) of yellow oil.

**Synthesis of [HP(PhCH<sub>2</sub>NCH<sub>2</sub>CH<sub>2</sub>)<sub>3</sub>N]Cl (5).** Anhydrous acetonitrile (50 mL) was charged to a single-neck round bottom flask. The flask was cooled to 0–5 °C in an ice bath. Hexamethylphosphorous triamide (HMPT, 4.72 mL, 26.7 mmol, 2.0 equiv) was added to the flask under argon and the mixture was stirred for 5 min. PCl<sub>3</sub> (1.13 mL, 13.33 mmol, 1.0 equiv) was then slowly added to the mixture via syringe. After stirring the mixture at 0–5 °C for 15 minutes, tribenzyl-tren, **4** (16.6g, 40.05 mmol, 3.0 equiv) dissolved in 50 mL anhydrous acetonitrile was added slowly through a cannula under a positive flow of argon to remove the liberated by-product dimethylamine formed during the reaction. The reaction was continued under constant stirring overnight at room temperature. The excess solvent was then removed under reduced pressure using a rotary evaporator, and then 300 mL of ether and 5.0



mL of THF was added and the reaction mixture was stirred at room temperature for 1 h. The crystalline white solid obtained was filtered and washed with ethyl ether (200 mL) to remove any organic impurities. The product was further dried under reduced pressure to obtain a free-flowing white solid (19.05 g, 99%).

**Synthesis of P(PhCH<sub>2</sub>NCH<sub>2</sub>CH<sub>2</sub>)<sub>3</sub>N (1c).** To a 500 mL round-bottom Schlenk flask was added [HP(PhCH<sub>2</sub>NCH<sub>2</sub>CH<sub>2</sub>)<sub>3</sub>N]Cl (**5**) (7.684 g, 16.0 mmols) and lithium bis(trimethylsilyl)amide (6.21 g, 37.12 mmol) in an argon-filled glove-box. The flask was then evacuated under reduced pressure after which ca 50 mL of anhydrous THF was added to the heterogeneous reaction mixture under a flow of argon. The resulting light yellow solution was stirred for about 12 h at room temperature to complete the deprotonation process (while monitoring by <sup>31</sup>P NMR spectroscopy). The reaction flask was then connected to a vacuum line and kept under reduced pressure for removal of volatiles, after which 200 mL of anhydrous pentane was added with further stirring for an additional 10 h at room temperature. The resulting solution was filtered through a frit under an argon atmosphere and volatiles were removed under reduced pressure on a vacuum line. The solid remaining (6.12 g) was recrystallized from anhydrous pentane three times (3 × 100 mL). The colorless crystalline solid **1c** was dried under vacuum for 3 h to give 3.89 g (55% yield) of product. <sup>31</sup>P NMR (162.8 MHz, C<sub>6</sub>D<sub>6</sub>): 127.97 ppm.<sup>33b</sup>

**General reaction procedure for the (1-methoxy-2-methyl-1-propenyloxy)trimethylsilane:**

In a nitrogen-filled glove-box, a 10 mL flat-bottom flask equipped with a magnetic stir bar was charged with proazaphosphatrane catalyst **1** (2 mol % unless otherwise stated). The flask

was sealed with a rubber septum and then (1-methoxy-2-methyl-1-propenyloxy)trimethylsilane (2.4 mmols) was added, followed by the aldehyde [(2 mmols) (if solid, dissolved in 2 ml of anhydrous THF under an argon atmosphere)] and freshly distilled THF (2 mL) was then syringed into the solution. The reaction was magnetically stirred for a specified length of time (see Tables 1–4), and the progress of the reaction was monitored by thin layer chromatography. After completion of the reaction, 5 mL of 2*N* HCl was added and after stirring for 12 h at room temperature, the reaction mixture was transferred into a 250 mL round-bottom flask. The reaction vessel was washed with ethyl acetate (3 × 10 mL) and then all organic solvents were removed under reduced pressure using a rotary evaporator apparatus. To the flask, 30 mL of dichloromethane was added, then its contents were transferred to a separatory funnel. The reaction mixture was neutralized with satd. aq. NaHCO<sub>3</sub> solution and the product was extracted with dichloromethane (3 × 30 mL). The combined organics were dried over anhydrous MgSO<sub>4</sub> (2.0 g) and then the solvent was removed under reduced pressure. The crude product was purified by using short-path silica gel (140 mesh) chromatography with ethyl acetate/hexanes as eluents in all cases.

**General reaction procedure for the silyl enol ethers 1-phenyl-1-(trimethylsilyloxy)ethylene and 1-(trimethylsilyloxy)cyclohexene:**

To a solution of proazaphosphatane **1** (3 mol %) in 4 mL of anhydrous tetrahydrofuran (THF) at –20 °C was added the silyl enol ether [1-phenyl-1-(trimethylsilyloxy)ethylene or 1-(trimethylsilyloxy)cyclohexene (2.4 mmol)] and then the mixture was stirred at the same temperature for 30 min. The aldehyde (2.0 mmol) was then added and then the reaction mixture was brought to –5 °C and stirring was continued for 72 h. Addition of 1*N* HCl

solution (3 mL) to this mixture and further stirring for 3 h at  $-5\text{ }^{\circ}\text{C}$ , was followed by bringing the reaction mixture to room temperature. The reaction mixture was neutralized with satd. aq.  $\text{NaHCO}_3$  solution and then it was extracted with ethyl acetate ( $3 \times 30\text{ mL}$ ). The organic layers were collected and dried over anhydrous  $\text{Na}_2\text{SO}_4$  followed by solvent removal under reduced pressure using a rotary evaporator apparatus. The crude product was purified by flash chromatography (hexane:ethyl acetate = 90:10) on silica gel (140 mesh) to give the desired aldol product.

**Methyl 3-hydroxy-3-(2-biphenyl)-2,2-dimethylpropionate (Table 2, entry 3).** The general procedure was followed using 2-biphenylcarboxaldehyde (0.323 mL, 2.0 mmol), (1-methoxy-2-methyl-1-propenyloxy)trimethylsilane (0.486 mL, 2.4 mmol), **1c** (56.0 mg, 6 mol %), and THF (4.0 mL). The reaction mixture was purified by column chromatography on silica gel (eluent: 20% ethyl acetate/hexanes) to afford 0.527 g (92%) of the desired product as a white solid.  $^1\text{H}$  NMR ( $\text{CDCl}_3$ , 400 MHz):  $\delta$  7.58 (d, 1H,  $J = 8.0\text{ Hz}$ ), 7.42–7.30 (m, 7H), 7.20 (d, 1H,  $J = 7.6\text{ Hz}$ ), 5.27 (s, 1H), 3.75 (bs, 1H), 3.64 (s, 3H), 1.02 (s, 3H), 0.83 (s, 3H) ppm;  $^{13}\text{C}$  NMR ( $\text{CDCl}_3$ , 100 MHz):  $\delta$  178.8, 142.5, 141.9, 137.7, 130.5, 129.9, 128.5, 127.7, 127.7, 127.4, 127.1, 74.1, 52.4, 48.4, 24.2, 19.5 ppm; HRMS  $m/z$  Calcd for  $\text{C}_{18}\text{H}_{20}\text{O}_3$ : 284.14124. Found: 284.14179.

**Methyl 3-hydroxy-3-(3-methoxyphenyl)-2,2-dimethylpropionate (Table 2, entry 4).** The general procedure was followed using 3-methoxybenzaldehyde (0.272 g, 2.0 mmol), (1-methoxy-2-methyl-1-propenyloxy)trimethylsilane (0.486 mL, 2.4 mmol), **1b** (12.00 mg, 2 mol %), and THF (4.0 mL). The reaction mixture was purified by column chromatography on silica gel (eluent: 15% ethyl acetate/hexanes) to afford 0.418 g (88%) of the desired

product as a colorless oil.  $^1\text{H}$  NMR ( $\text{CDCl}_3$ , 400 MHz):  $\delta$  7.26–7.21 (m, 1H), 6.88–6.82 (m, 3H), 4.86 (d, 1H,  $J = 4.4$  Hz), 3.79 (s, 3H), 3.72 (s, 3H), 3.05 (d, 1H,  $J = 4.0$  Hz), 1.15 (s, 3H), 1.12 (s, 3H) ppm;  $^{13}\text{C}$  NMR ( $\text{CDCl}_3$ , 100 MHz):  $\delta$  178.3, 159.3, 141.9, 128.9, 120.3, 113.6, 113.3, 78.8, 55.4, 52.3, 47.9, 23.2, 19.4 ppm; HRMS  $m/z$  Calcd for  $\text{C}_{13}\text{H}_{18}\text{O}_4$ : 238.12050. Found: 238.12115.

**Methyl 3-hydroxy-3-(2,6-dimethylphenyl)-2,2-dimethylpropionate (Table 2, entry 6).**

The general procedure was followed using 2,6-dimethylbenzaldehyde (0.268 g, 2.0 mmol), (1-methoxy-2-methyl-1-propenyloxy)trimethylsilane (0.486 mL, 2.4 mmol), **1c** (18.32 mg, 2 mol %), and THF (4.0 mL). The reaction mixture was purified by column chromatography on silica gel (eluent: 8% ethyl acetate/hexanes) to afford 0.407 g (86%) of the desired product as a white solid.  $^1\text{H}$  NMR ( $\text{CDCl}_3$ , 400 MHz):  $\delta$  7.06–6.99 (m, 3H), 5.59 (s, 1H), 3.73 (s, 3H), 2.95 (s, 1H), 2.56 (s, 3H), 2.38 (s, 3H), 1.26 (s, 3H), 1.13 (s, 3H) ppm;  $^{13}\text{C}$  NMR ( $\text{CDCl}_3$ , 100 MHz):  $\delta$  178.8, 138.6, 137.5, 135.5, 131.3, 128.6, 127.4, 76.1, 52.5, 50.3, 24.2, 22.6, 20.9 ppm; HRMS  $m/z$  Calcd for  $\text{C}_{14}\text{H}_{20}\text{O}_3$ : 236.14124. Found: 236.14177.

**Methyl 3-hydroxy-3-(3,4-dimethoxyphenyl)-2,2-dimethylpropionate (Table 2, entry 8).**

The general procedure was followed using 3,4-dimethylbenzaldehyde (0.332 g, 2.0 mmol), (1-methoxy-2-methyl-1-propenyloxy)trimethylsilane (0.486 mL, 2.4 mmol), **1c** (56.0 mg, 6 mol %), and THF (4.0 mL). The reaction mixture was purified by column chromatography on silica gel (eluent: 8% ethyl acetate/hexanes) to afford 0.489 g (91%) of the desired product as a colorless oil.  $^1\text{H}$  NMR ( $\text{CDCl}_3$ , 400 MHz):  $\delta$  6.86–6.83 (m, 2H), 6.75 (s, 1H), 5.25 (s, 1H), 3.83 (s, 3H), 3.82 (s, 3H), 3.66 (s, 3H), 1.29 (s, 3H), 1.07 (s, 3H) ppm;  $^{13}\text{C}$

NMR (CDCl<sub>3</sub>, 100 MHz):  $\delta$  175.8, 149.2, 148.4, 129.9, 121.6, 112.2, 110.3, 68.8, 56.1, 56.1, 52.4, 49.9, 23.3, 20.3 ppm; HRMS *m/z* Calcd for C<sub>14</sub>H<sub>20</sub>O<sub>5</sub>: 268.13107. Found: 268.13179.

**Methyl 3-hydroxy-3-(2-methoxynaphthalen-1-yl)-2,2-dimethylpropanoate (Table 2, entry 9).** The general procedure was followed using 2-methoxy-1-naphthaldehyde (0.372 g, 2.0 mmol), (1-methoxy-2-methyl-1-propenyloxy)trimethylsilane (0.486 mL, 2.4 mmol), **1c** (54.0 mg, 6 mol %), and THF (4.0 mL). The reaction mixture was purified by column chromatography on silica gel (eluent: 8% ethyl acetate/hexanes) to afford 0.397 g (69%) of the desired product as a colorless oil. <sup>1</sup>H NMR (CDCl<sub>3</sub>, 400 MHz):  $\delta$  8.10 (bs, 1H), 7.81–7.74 (m, 2H), 7.46 (t, 1H, *J* = 8.0 Hz), 7.32 (t, 1H, *J* = 8.0 Hz), 7.27–7.23 (m, 1H), 5.90 (d, 1H, *J* = 8.0 Hz), 4.90 (bs, 1H), 3.94 (s, 3H), 3.67 (s, 3H), 1.20 (s, 3H), 1.15 (s, 3H) ppm; <sup>13</sup>C NMR (CDCl<sub>3</sub>, 100 MHz):  $\delta$  177.5, 155.5, 133.1, 130.2, 129.3, 128.6, 126.6, 123.6, 119.9, 112.8, 75.2, 55.9, 52.0, 50.3, 24.1, 20.7 ppm; HRMS *m/z* Calcd for C<sub>17</sub>H<sub>20</sub>O<sub>4</sub>: 288.13615. Found: 299.13656.

**Methyl 3-(3-formylphenyl)-3-hydroxy-2,2-dimethylpropanoate (Table 2, entry 10, 6a).** The general procedure was followed using isophthalaldehyde (0.268 g, 2.0 mmol), (1-methoxy-2-methyl-1-propenyloxy)trimethylsilane (0.486 mL, 2.4 mmol), **1c** (88.8 mg, 10 mol %), and THF (4.0 mL). The reaction mixture was purified by column chromatography on silica gel (eluent: 20% ethyl acetate/hexanes) to afford 0.221 g (49%) of the desired product as a colorless oil. <sup>1</sup>H NMR (CDCl<sub>3</sub>, 400 MHz):  $\delta$  9.95 (s, 1H), 7.76–7.73 (m, 2H), 7.54–7.52 (m, 1H), 7.44 (t, 1H, *J* = 8.0 Hz), 4.93 (s, 1H), 3.67 (s, 3H), 3.48 (bs, 1H), 1.01 (s, 3H), 1.06 (s, 3H) ppm; <sup>13</sup>C NMR (CDCl<sub>3</sub>, 100 MHz):  $\delta$  192.4, 177.9, 141.2, 135.9, 133.8, 129.2, 128.9, 128.5, 76.8, 52.3, 47.7, 22.7, 19.1 ppm; HRMS *m/z* Calcd for C<sub>13</sub>H<sub>16</sub>O<sub>4</sub>: 236.10485. Found: 236.10533.

**Dimethyl 3,3'-(1,3-phenylene)bis(3-hydroxy-2,2-dimethylpropanoate)** (Table 2, entry 10, 6b). The general procedure was followed using isophthalaldehyde (0.268 g, 2.0 mmol), (1-methoxy-2-methyl-1-propenyloxy)trimethylsilane (0.486 mL, 2.4 mmol), **1c** (88.8 mg, 10 mol %), and THF (4.0 mL). The reaction mixture was purified by column chromatography on silica gel (eluent: 20% ethyl acetate/hexanes) to afford 0.301 g (44%) of the desired product as a colorless oil. <sup>1</sup>H NMR (CDCl<sub>3</sub>, 400 MHz): δ 7.15–7.14 (m, 4H), 4.79 (d, 1H, *J* = 4.4 Hz), 3.64 (s, 6H), 3.48 (bs, 1H), 1.05 (s, 3H), 1.04 (s, 3H), 1.02 (s, 3H), 1.01 (s, 3H) ppm; <sup>13</sup>C NMR (CDCl<sub>3</sub>, 100 MHz): δ 178.2, 139.7, 139.6, 127.2, 127.2, 127.1, 126.9, 78.5, 78.4, 52.2, 47.8, 47.8, 23.1, 22.8, 19.2, 19.1 ppm; HRMS *m/z* Calcd for C<sub>18</sub>H<sub>26</sub>O<sub>6</sub>: 338.17293. Found: 338.17906.

**Methyl 3-hydroxy-3-(2-chlorophenyl)-2,2-dimethylpropionate** (Table 3, entry 1): The general procedure was followed using 2-chlorobenzaldehyde (0.224 mL, 2.0 mmol), (1-methoxy-2-methyl-1-propenyloxy)trimethylsilane (0.486 mL, 2.4 mmol), **1c** (28.0 mg, 3 mol %), and THF (4.0 mL). The reaction mixture was purified by column chromatography on silica gel (eluent: 10% ethyl acetate/hexanes) to afford 0.440 g (91%) of the desired product as a colorless oil. <sup>1</sup>H NMR (CDCl<sub>3</sub>, 400 MHz): δ 7.46–7.44 (m, 1H), 7.27–7.14 (m, 3H), 5.45 (s, 1H), 3.66 (s, 3H), 3.54 (bs, 1H), 1.12 (s, 3H), 1.10 (s, 3H) ppm; <sup>13</sup>C NMR (CDCl<sub>3</sub>, 100 MHz): δ 178.3, 137.9, 133.5, 129.6, 129.3, 128.8, 126.5, 73.4, 52.3, 48.6, 23.1, 18.7 ppm; HRMS *m/z* Calcd for C<sub>12</sub>H<sub>15</sub>ClO<sub>3</sub>: 242.07097. Found: 242.07153.

**Methyl 3-hydroxy-3-(2-fluorophenyl)-2,2-dimethylpropionate** (Table 3, entry 2). The general procedure was followed using 2-fluorobenzaldehyde (0.210 mL, 2.0 mmol), (1-methoxy-2-methyl-1-propenyloxy)trimethylsilane (0.486 mL, 2.4 mmol), **1c** (28.0 mg, 3 mol

%), and THF (4.0 mL). The reaction mixture was purified by column chromatography on silica gel (eluent: 10% ethyl acetate/hexanes) to afford 0.350 g (77%) of the desired product as a colorless oil.  $^1\text{H}$  NMR ( $\text{CDCl}_3$ , 400 MHz):  $\delta$  7.47–7.43 (m, 1H), 7.27–7.23 (m, 1H), 7.16–7.12 (m, 1H), 7.03–6.98 (m, 1H), 5.28 (d, 1H,  $J = 4.4$  Hz), 3.73 (s, 3H), 3.37 (d, 1H,  $J = 5.7$  Hz), 1.15 (s, 3H), 1.14 (s, 3H) ppm;  $^{13}\text{C}$  NMR ( $\text{CDCl}_3$ , 100 MHz):  $\delta$  178.4, 160.1 (d,  $J = 260$  Hz), 129.4, 129.3 (d,  $J = 4.2$  Hz), 127.4 (d,  $J = 12.9$  Hz), 124.0 (d,  $J = 3.3$  Hz), 115.2 (d,  $J = 22.8$  Hz), 71.7, 52.4, 48.2, 23.1, 18.8 ppm; HRMS  $m/z$  Calcd. for  $\text{C}_{12}\text{H}_{15}\text{FO}_3$ : 226.10052. Found: 226.10078.

**Methyl 3-hydroxy-3-(3-iodophenyl)-2,2-dimethylpropionate (Table 3, entry 3).** The general procedure was followed using 3-iodobenzaldehyde (0.464 g, 2.0 mmol), (1-methoxy-2-methyl-1-propenyloxy)trimethylsilane (0.486 mL, 2.4 mmol), **1c** (88.0 mg, 10 mol %), and THF (4.0 mL). The reaction mixture was purified by column chromatography on silica gel (eluent: 20% ethyl acetate/hexanes) to afford 0.637 g (95%) of the desired product as a colorless oil.  $^1\text{H}$  NMR ( $\text{CDCl}_3$ , 400 MHz):  $\delta$  7.63–7.58 (m, 2H), 7.23 (d, 1H,  $J = 8.0$  Hz), 7.02 (t, 1H,  $J = 8.0$  Hz), 4.79 (d, 1H), 3.70 (s, 3H), 3.13 (bs, 1H), 1.10 (s, 3H), 1.08 (s, 3H) ppm;  $^{13}\text{C}$  NMR ( $\text{CDCl}_3$ , 100 MHz):  $\delta$  178.1, 142.4, 136.8, 136.6, 129.5, 127.0, 93.9, 76.8, 52.3, 47.7, 22.9, 19.2 ppm; HRMS  $m/z$  Calcd. for  $\text{C}_{12}\text{H}_{15}\text{IO}_3$ : 334.00659. Found: 334.00734.

**Methyl 3-hydroxy-2,2-dimethyl-3-(4-(trifluoromethyl)phenyl)propanoate (Table 3, entry 5):** The general procedure was followed using 4-(trifluoromethyl)benzaldehyde (0.272 mL, 2.0 mmol), (1-methoxy-2-methyl-1-propenyloxy)trimethylsilane (0.486 mL, 2.4 mmol), **1c** (28.0 mg, 3 mol %), and THF (4.0 mL). The reaction mixture was purified by column chromatography on silica gel (eluent: 10% ethyl acetate/hexanes) to afford 0.463 g (84%) of the desired product as a white solid.  $^1\text{H}$  NMR ( $\text{CDCl}_3$ , 400 MHz):  $\delta$  7.52 (d, 2H,  $J = 8.0$  Hz),

7.36(d, 2H,  $J = 8.0$  Hz), 4.87 (d, 2H,  $J = 2.8$  Hz), 3.66 (s, 3H), 3.50 (d, 2H,  $J = 4.0$  Hz), 1.08 (s, 3H), 1.04 (s, 3H) ppm;  $^{13}\text{C}$  NMR ( $\text{CDCl}_3$ , 100 MHz):  $\delta$  177.9, 144.1, 129.9 (q,  $J = 32.2$  Hz), 128.0, 124.2 (q,  $J = 270.4$  Hz), 124.6 (q,  $J = 3.7$  Hz), 77.9, 52.2, 47.6, 22.7, 19.0 ppm; HRMS  $m/z$  Calcd for  $\text{C}_{13}\text{H}_{15}\text{F}_3\text{O}_3$ : 276.09732. Found: 276.09812.

**Methyl 3-hydroxy-3-(3-cyanophenyl)-2,2-dimethylpropionate (Table 3, entry 7).** The general procedure was followed using 3-cyanobenzaldehyde (0.262 g, 2.0 mmol), (1-methoxy-2-methyl-1-propenyloxy)trimethylsilane (0.486 mL, 2.4 mmol), **1c** (28.0 mg, 3 mol %), and THF (4.0 mL). The reaction mixture was purified by column chromatography on silica gel (eluent: 10% ethyl acetate/hexanes) to afford 0.271 g (58%) of the desired product as a colorless oil.  $^1\text{H}$  NMR ( $\text{CDCl}_3$ , 400 MHz):  $\delta$  7.58 (s, 1H), 7.55–7.50 (m, 2H), 7.40 (t, 1H,  $J = 7.6$  Hz), 4.89 (d, 1H,  $J = 3.6$  Hz), 3.69 (s, 3H), 3.53 (d, 1H,  $J = 3.6$  Hz), 1.09 (s, 3H), 1.06 (s, 3H) ppm;  $^{13}\text{C}$  NMR ( $\text{CDCl}_3$ , 100 MHz):  $\delta$  177.9, 141.8, 132.4, 131.6, 131.5, 128.8, 119.0, 112.1, 77.7, 52.6, 47.9, 22.8, 19.3 ppm; HRMS  $m/z$  Calcd. for  $\text{C}_{13}\text{H}_{15}\text{NO}_3$ : 233.10519. Found: 233.10548.

**Methyl 3-(benzo[*b*]thiophen-2-yl)-3-hydroxy-2,2-dimethylpropanoate (Table 4, entry 1).** The general procedure was followed using 2-benzothiophenecarboxaldehyde (0.324 g, 2.0 mmol), (1-methoxy-2-methyl-1-propenyloxy)trimethylsilane (0.486 mL, 2.4 mmol), **1c** (88.8 mg, 10 mol %), and THF (4.0 mL). The reaction mixture was purified by column chromatography on silica gel (eluent: 10% ethyl acetate/hexanes) to afford 0.488 g (92%) of the desired product as a pale yellow solid.  $^1\text{H}$  NMR ( $\text{CDCl}_3$ , 400 MHz):  $\delta$  7.79 (d, 1H,  $J = 7.6$  Hz), 7.72 (d, 1H,  $J = 8.0$  Hz), 7.36–7.29 (m, 2H), 7.18 (s, 1H), 5.15 (d, 1H,  $J = 4.0$  Hz), 3.76 (s, 3H), 3.51 (d, 1H,  $J = 4.8$  Hz), 1.28 (s, 6H) ppm;  $^{13}\text{C}$  NMR ( $\text{CDCl}_3$ , 100 MHz):  $\delta$



178.1, 145.1, 139.7, 139.4, 124.5, 124.4, 123.7, 122.5, 122.4, 76.1, 52.6, 48.1, 23.0, 20.5 ppm; HRMS  $m/z$  Calcd. for  $C_{14}H_{16}O_3S$ : 264.08202. Found: 264.08256.

**Methyl 3-(benzofuran-2-yl)-3-hydroxy-2,2-dimethylpropanoate (Table 4, entry 2).** The general procedure was followed using 2-benzofurancarboxaldehyde (0.242 mL, 2.0 mmol), (1-methoxy-2-methyl-1-propenyloxy)trimethylsilane (0.486 mL, 2.4 mmol), **1c** (28.0 mg, 3 mol %), and THF (4.0 mL). The reaction mixture was purified by column chromatography on silica gel (eluent: 10% ethyl acetate/hexanes) to afford 0.442 g (89%) of the desired product as a colorless oil.  $^1H$  NMR ( $CDCl_3$ , 400 MHz):  $\delta$  7.53 (d, 1H,  $J = 7.6$  Hz), 7.44 (d, 1H,  $J = 8.4$  Hz), 7.28–7.20 (m, 2H), 6.64 (s, 1H), 4.94 (s, 1H), 3.75 (s, 3H), 3.71 (bs, 1H), 1.28 (s, 3H), 1.27 (s, 3H) ppm;  $^{13}C$  NMR ( $CDCl_3$ , 100 MHz):  $\delta$  177.8, 156.9, 154.8, 128.1, 124.4, 123.1, 121.2, 111.5, 105.0, 74.0, 52.5, 47.4, 23.1, 20.5 ppm; HRMS  $m/z$  Calcd. for  $C_{14}H_{16}O_4$ : 248.10486. Found: 248.10539.

**Methyl 3-hydroxynonanoate (Table 4, entry 3):** The general procedure was followed using heptaldehyde (0.280 mL, 2.0 mmol), (1-methoxy-2-methyl-1-propenyloxy)trimethylsilane (0.486 mL, 2.4 mmol), **1c** (28.0 mg, 3 mol %), and THF (4.0 mL). The reaction mixture was purified by column chromatography on silica gel (eluent: 10% ethyl acetate/hexanes) to afford 0.345 g (80%) of the desired product as a colorless oil.  $^1H$  NMR ( $CDCl_3$ , 400 MHz):  $\delta$  3.67 (s, 3H), 3.57 (d, 1H,  $J = 4.0$  Hz), 1.26–1.14 (m, 16H), 0.87–0.84 (m, 4H) ppm;  $^{13}C$  NMR ( $CDCl_3$ , 100 MHz):  $\delta$  178.3, 76.7, 51.9, 47.2, 31.8, 31.7, 29.3, 26.7, 22.7, 22.3, 20.4, 14.1 ppm; HRMS  $m/z$  Calcd. for  $C_{12}H_{24}O_3$ : 216.17254. Found: 216.17291.

**Methyl 3-hydroxy-2,2-dimethyl-3-(4-methylthiazol-2-yl)propanoate (Table 4, entry 6).**

The general procedure was followed using 4-Methyl-2-thiazolecarboxaldehyde (0.254 g, 2.0

mmol), (1-methoxy-2-methyl-1-propenyloxy)trimethylsilane (0.486 mL, 2.4 mmol), **1c** (56.0 mg, 6 mol %), and THF (4.0 mL). The reaction mixture was purified by column chromatography on silica gel (eluent: 10% ethyl acetate/hexanes) to afford 0.153 g (36%) of the desired product as a pale yellow solid. <sup>1</sup>H NMR (CDCl<sub>3</sub>, 400 MHz): δ 6.81 (s, 1H), 5.08 (d, 1H, *J* = 4.0 Hz), 4.22 (d, 1H, *J* = 8.0 Hz), 3.71 (s, 3H), 2.38 (s, 3H), 1.21 (s, 3H), 1.21 (s, 3H) ppm; <sup>13</sup>C NMR (CDCl<sub>3</sub>, 100 MHz): δ 177.5, 170.3, 152.1, 114.0, 76.4, 52.4, 48.1, 21.6, 20.9, 17.2 ppm; HRMS *m/z* Calcd. for C<sub>10</sub>H<sub>15</sub>NO<sub>3</sub>S :229.07726. Found: 229.07763.

**Methyl 3-hydroxy-2,2-dimethyl-3-(1-methyl-1*H*-imidazol-2-yl)propanoate (Table 4, entry 7).** The general procedure was followed using 1-Methyl-2-imidazolecarboxaldehyde (0.220 g, 2.0 mmol), (1-methoxy-2-methyl-1-propenyloxy)trimethylsilane (0.486 mL, 2.4 mmol), **1c** (28 mg, 3 mol %), and THF (4.0 mL). The reaction mixture was purified by column chromatography on silica gel (eluent: methanol) to afford 0.221 g (52%) of the desired product as a colorless solid. <sup>1</sup>H NMR (CDCl<sub>3</sub>, 400 MHz): δ 6.82 (d, 1H, *J* = 1.2 Hz), 6.72 (d, 1H, *J* = 0.8 Hz), 4.73 (s, 1H), 4.50 (bs, 1H), 3.66 (s, 3H), 3.65 (s, 3H), 1.23 (s, 3H), 1.22 (s, 3H) ppm; <sup>13</sup>C NMR (CDCl<sub>3</sub>, 100 MHz): δ 177.9, 147.0, 127.2, 121.5, 71.7, 52.3, 47.5, 33.5, 23.1, 21.3 ppm; HRMS *m/z* Calcd. for C<sub>10</sub>H<sub>16</sub>N<sub>2</sub>O<sub>3</sub>: 212.11609. Found: 212.11649.

**3-Hydroxy-1-phenyl-1-nonanone (Table 5, entry 5):** The general procedure was followed using heptaldehyde (0.280 mL, 2.0 mmol), 1-phenyl-1-trimethylsiloxyethylene (0.486 mL, 2.4 mmol), **1c** (28.0 mg, 3 mol %), and THF (4.0 mL). The reaction mixture was purified by column chromatography on silica gel (eluent: 10% ethyl acetate/hexanes) to afford 0.374 g (80%) of the desired product as a colorless oil. <sup>1</sup>H NMR (CDCl<sub>3</sub>, 300 MHz): δ 7.97–7.94 (m, 2H), 7.60–7.44 (m, 3H), 4.21 (bs, 1H), 3.26–2.98 (m, 3H), 1.63–1.29 (m, 10H), 0.89–0.86

(m, 3H) ppm;  $^{13}\text{C}$  NMR ( $\text{CDCl}_3$ , 75 MHz):  $\delta$  201.3, 131.9, 133.8, 128.9, 128.3, 68.0, 45.2, 36.7, 32.0, 29.5, 25.7, 22.8, 14.3 ppm; HRMS  $m/z$  Calcd. for  $\text{C}_{10}\text{H}_{16}\text{N}_2\text{O}_3$ : 212.11609. Found: 212.11649.

**(E)-1-(2-Fluorophenyl)-4,4-dimethylpent-1-en-3-one (Table 6, entry 1).** The general procedure was followed using 2-fluorobenzaldehyde (0.248 g, 2.0 mmol), 3,3-dimethyl-2-trimethylsiloxy-1-butene (0.518 mL, 2.4 mmol), **1c** (54.0 mg, 6 mol %), and THF (4.0 mL). The reaction mixture was purified by column chromatography on silica gel (eluent: 10% ethyl acetate/hexanes) to afford 0.380 g (92%) of the desired product as a colorless oil.  $^1\text{H}$  NMR ( $\text{CDCl}_3$ , 400 MHz):  $\delta$  7.75 (d, 1H,  $J = 16$  Hz), 7.54 (t, 1H,  $J = 8$  Hz), 7.34–7.29 (m, 1H), 7.22 (d, 1H,  $J = 16.0$  Hz), 7.13 (t, 1H, 8.0 Hz), 7.07 (t, 1H,  $J = 8.0$  Hz), 1.21 (s, 9H) ppm;  $^{13}\text{C}$  NMR ( $\text{CDCl}_3$ , 100 MHz):  $\delta$  204.3, 161.8 (d,  $J = 250$  Hz), 135.8 (d,  $J = 2.0$  Hz), 131.6 (d,  $J = 9$  Hz), 129.9 (d,  $J = 3.0$  Hz), 124.6 (d,  $J = 3.0$  Hz), 123.5 (d,  $J = 7$  Hz), 123.2 (d,  $J = 12.0$  Hz), 116.4 (d, 22.0 Hz), 43.4, 26.4 ppm; HRMS  $m/z$  Calcd for  $\text{C}_{13}\text{H}_{15}\text{FO}$ : 206.11069. Found: 206.11108.

**(E)-1-(3-Iodophenyl)-4,4-dimethylpent-1-en-3-one (Table 7, entry 1).** The general procedure was followed using 3-iodobenzaldehyde (0.348 g, 1.5 mmol), 3,3-dimethyl-2-trimethylsiloxy-1-butene (0.432 mL, 2.0 mmol), **1c** (40.0 mg, 6 mol %), and THF (4.0 mL). The reaction mixture was purified by column chromatography on silica gel (eluent: 10% ethyl acetate/hexanes) to afford 0.443 g (95%) of the desired product as a yellow oil.  $^1\text{H}$  NMR ( $\text{CDCl}_3$ , 400 MHz):  $\delta$  7.88 (s, 1H), 7.65 (d, 1H,  $J = 8.0$  Hz), 7.51 (d, 1H,  $J = 16.0$  Hz), 7.47 (d, 1H,  $J = 8.0$  Hz), 7.10–7.05 (m, 2H), 1.20 (s, 9H) ppm;  $^{13}\text{C}$  NMR ( $\text{CDCl}_3$ , 100 MHz):

$\delta$  204.0, 141.3, 139.0, 137.3, 136.8, 130.7, 128.0, 122.0, 95.0, 43.5, 26.5 ppm; HRMS  $m/z$  Calcd for  $C_{13}H_{15}OI$ : 314.0176. Found: 314.0168.

**(E)-3-(4,4-Dimethyl-3-oxopent-1-enyl)benzotrile (Table 7, entry 2).** The general procedure was followed using 3-cyanobenzaldehyde (0.262 g, 2.0 mmol), 3,3-dimethyl-2-trimethylsiloxy-1-butene (0.518 mL, 2.4 mmol), **1c** (54.0 mg, 6 mol %), and THF (4.0 mL). The reaction mixture was purified by column chromatography on silica gel (eluent: 10% ethyl acetate/hexanes) to afford 0.402 g (94%) of the desired product as a colorless oil.  $^1H$  NMR ( $CDCl_3$ , 400 MHz):  $\delta$  7.82 (s, 1H), 7.74 (d, 1H,  $J = 8.0$  Hz), 7.62–7.60 (m, 1H), 7.58 (d, 1H,  $J = 16.0$  Hz), 7.48 (t, 1H,  $J = 8.0$  Hz), 7.15 (d, 1H,  $J = 16.0$  Hz), 1.21 (s, 9H) ppm;  $^{13}C$  NMR ( $CDCl_3$ , 100 MHz):  $\delta$  203.8, 140.2, 136.3, 133.2, 132.6, 131.4, 129.9, 123.2, 118.4, 113.4, 43.6, 26.3 ppm; HRMS  $m/z$  Calcd for  $C_{14}H_{15}NO$ : 213.11536. Found: 213.11582.

**(E)-1-(Benzofuran-2-yl)-4,4-dimethylpent-1-en-3-one (Table 7, entry 3).** The general procedure was followed using 2-benzofurancarboxaldehyde (0.292 g, 2.0 mmol), 3,3-dimethyl-2-trimethylsiloxy-1-butene (0.518 mL, 2.4 mmol), **1c** (54.0 mg, 6 mol %), and THF (4.0 mL). The reaction mixture was purified by column chromatography on silica gel (eluent: 10% ethyl acetate/hexanes) to afford 0.362 g (77%) of the desired product as a yellow oil.  $^1H$  NMR ( $CDCl_3$ , 400 MHz):  $\delta$  7.53 (d, 1H,  $J = 16.0$  Hz), 7.53 (bs, 1H), 7.47 (d, 1H,  $J = 8.0$  Hz), 7.31 (dt, 1H,  $J = 8.0$  Hz,  $J = 1.2$  Hz), 7.24 (d, 1H,  $J = 16.0$  Hz), 7.20 (d, 1H,  $J = 8.0$  Hz), 6.90 (s, 1H), 1.24 (s, 9H) ppm;  $^{13}C$  NMR ( $CDCl_3$ , 100 MHz):  $\delta$  204.0, 155.6, 153.2, 129.5, 128.7, 126.6, 123.5, 121.9, 121.3, 112.0, 111.5, 43.5, 26.5 ppm; HRMS  $m/z$  Calcd for  $C_{15}H_{16}O_2$ : 228.11503. Found: 228.11549.

**(E)-1-(Benzo[*b*]thiophen-2-yl)-4,4-dimethylpent-1-en-3-one** (Table 7, entry 4). The general procedure was followed using 2-benzothiophenecarboxaldehyde (0.326 g, 2.0 mmol), 3,3-dimethyl-2-trimethylsiloxy-1-butene (0.518 mL, 2.4 mmol), **1c** (54.0 mg, 6 mol %), and THF (4.0 mL). The reaction mixture was purified by column chromatography on silica gel (eluent: 10% ethyl acetate/hexanes) to afford 0.404 g (83%) of the desired product as a yellow oil. <sup>1</sup>H NMR (CDCl<sub>3</sub>, 400 MHz): δ 7.87 (d, 1H, *J* = 16.0 Hz), 7.79–7.74 (m, 2H), 7.49 (s, 1H), 7.39–7.33 (m, 2H), 6.95 (d, 1H, *J* = 16.0 Hz), 1.24 (s, 9H) ppm; <sup>13</sup>C NMR (CDCl<sub>3</sub>, 100 MHz): δ 203.9, 140.4, 140.1, 139.8, 136.1, 129.5, 126.4, 125.0, 124.6, 122.6, 122.2, 43.4, 26.5 ppm; HRMS *m/z* Calcd for C<sub>15</sub>H<sub>16</sub>OS: 244.09219. Found: 244.09266.

**(E)-4,4-Dimethyl-1-(4-methylthiazol-2-yl)pent-1-en-3-one** (Table 7, entry 5). The general procedure was followed using 4-methyl-2-thiazolecarboxaldehyde (0.254 g, 2.0 mmol), 3,3-dimethyl-2-trimethylsiloxy-1-butene (0.518 mL, 2.4 mmol), **1c** (90.0 mg, 10 mol %), and THF (4.0 mL). The reaction mixture was purified by column chromatography on silica gel (eluent: 10% ethyl acetate/hexanes) to afford 0.391 g (94 %) of the desired product as a yellow oil. <sup>1</sup>H NMR (CDCl<sub>3</sub>, 400 MHz): δ 7.60 (d, 1H, *J* = 16.0 Hz), 7.35 (d, 1H, *J* = 16.0 Hz), 6.96 (s, 1H), 2.45 (s, 3H), 1.18 (s, 9H) ppm; <sup>13</sup>C NMR (CDCl<sub>3</sub>, 100 MHz): δ 203.8, 163.2, 155.3, 133.8, 124.2, 116.7, 43.6, 26.3, 17.4 ppm; HRMS *m/z* Calcd for C<sub>11</sub>H<sub>15</sub>NOS: 209.08743. Found: 209.08770.

**(E)-1-(4-Methoxynaphthalen-1-yl)-4,4-dimethylpent-1-en-3-one** (Table 7, entry 6). The general procedure was followed using 4-methoxy-1-naphthaldehyde (0.372 g, 2.0 mmol), 3,3-dimethyl-2-trimethylsiloxy-1-butene (0.518 mL, 2.4 mmol), **1c** (54.0 mg, 6 mol %), and THF (4.0 mL). The reaction mixture was purified by column chromatography on silica gel

(eluent: 10% ethyl acetate/hexanes) to afford 0.421 g (78%) of the desired product as a white solid.  $^1\text{H}$  NMR ( $\text{CDCl}_3$ , 400 MHz):  $\delta$  8.49 (d, 1H,  $J = 15.6$  Hz), 8.31 (d, 1H,  $J = 8.0$  Hz), 8.20 (d, 1H,  $J = 8.0$  Hz), 7.79 (d, 1H,  $J = 8.0$  Hz), 7.61–7.50 (m, 2H), 7.14 (d, 1H,  $J = 16.0$  Hz), 6.83 (d, 1H,  $J = 8.0$  Hz), 4.04 (s, 3H), 1.27 (s, 9H) ppm;  $^{13}\text{C}$  NMR ( $\text{CDCl}_3$ , 100 MHz):  $\delta$  204.4, 157.6, 140.0, 133.0, 125.8, 124.9, 123.5, 122.8, 121.3, 103.8, 55.9, 43.4, 26.7 ppm; HRMS  $m/z$  Calcd for  $\text{C}_{18}\text{H}_{20}\text{O}_2$ : 268.14632. Found: 268.14673.

**(E)-4,4-Dimethyl-1-o-tolylpent-1-en-3-one (Table 7, entry 7).** The general procedure was followed using *o*-tolualdehyde (0.240 g, 2.0 mmol), 3,3-dimethyl-2-trimethylsiloxy-1-butene (0.518 mL, 2.4 mmol), **1c** (90.0 mg, 10 mol %), and THF (4.0 mL). The reaction mixture was purified by column chromatography on silica gel (eluent: 10% ethyl acetate/hexanes) to afford 0.364 g (90 %) of the desired product as a white solid.  $^1\text{H}$  NMR ( $\text{CDCl}_3$ , 400 MHz):  $\delta$  7.99 (d, 1H,  $J = 16.0$  Hz), 7.60 (d, 1H,  $J = 8.0$  Hz), 7.27–7.19 (m, 3H), 7.05 (d, 1H,  $J = 16.0$  Hz), 2.44 (s, 3H), 1.24 (s, 9H) ppm;  $^{13}\text{C}$  NMR ( $\text{CDCl}_3$ , 100 MHz):  $\delta$  204.5, 140.7, 138.4, 134.2, 131.1, 130.1, 126.5, 126.4, 122.1, 43.5, 26.6, 20.1 ppm; HRMS  $m/z$  Calcd for  $\text{C}_{14}\text{H}_{18}\text{O}$ : 202.13576. Found: 202.13610.

**(E)-1-(2,6-Dimethylphenyl)-4,4-dimethylpent-1-en-3-one (Table 7, entry 8).** The general procedure was followed using 2,6-dimethylbenzaldehyde (0.268 g, 2.0 mmol), 3,3-dimethyl-2-trimethylsiloxy-1-butene (0.518 mL, 2.4 mmol), **1c** (88.8 mg, 10 mol %), and THF (4.0 mL). The reaction mixture was purified by column chromatography on silica gel (eluent: 10% ethyl acetate/hexanes) to afford 0.310 g (72%) of the desired product as a white solid.  $^1\text{H}$  NMR ( $\text{CDCl}_3$ , 400 MHz):  $\delta$  7.80 (d, 1H,  $J = 16.0$  Hz), 7.12–7.06 (m, 3H), 6.74 (dd, 1H,  $J = 16.0$  Hz,  $J = 1.2$  Hz), 2.34 (s, 6H), 1.21 (s, 9H) ppm;  $^{13}\text{C}$  NMR ( $\text{CDCl}_3$ , 100 MHz):  $\delta$

204.4, 141.4, 136.9, 135.1, 128.4, 128.3, 127.1, 43.4, 26.3, 21.3 ppm; HRMS  $m/z$  Calcd for  $C_{15}H_{20}O$ : 216.15141. Found: 216.15173.

**(4E,6E)-2,2-Dimethyl-7-phenylhepta-4,6-dien-3-one (Table 7, entry 9).** The general procedure was followed using *trans*-cinnamaldehyde (0.264 g, 2.0 mmol), 3,3-dimethyl-2-trimethylsilyloxy-1-butene (0.518 mL, 2.4 mmol), **1c** (90.0 mg, 10 mol %), and THF (4.0 mL). The reaction mixture was purified by column chromatography on silica gel (eluent: 10% ethyl acetate/hexanes) to afford 0.412 g (95%) of the desired product as a yellow oil.  $^1H$  NMR ( $CDCl_3$ , 400 MHz):  $\delta$  7.50–7.46 (m, 3H), 7.37–7.30 (m, 3H), 6.94–6.92 (m, 2H), 6.69 (d, 1H,  $J = 12.0$  Hz), 1.20 (s, 9H) ppm;  $^{13}C$  NMR ( $CDCl_3$ , 100 MHz):  $\delta$  204.6, 143.1, 141.3, 136.4, 129.2, 129.0, 127.3, 127.1, 124.5, 43.3, 26.6 ppm; HRMS  $m/z$  Calcd for  $C_{15}H_{18}O$ : 214.13576. Found: 214.13625.

**Methyl 4,4,4-trifluoro-2,2-dimethyl-3-phenyl-3-(trimethylsilyloxy)butanoate (Scheme 3, product 8).** The general procedure was followed using 2,2,2-trifluoroacetophenone (0.348 g, 2.0 mmol), (1-methoxy-2-methyl-1-propenyloxy)trimethylsilane (0.486 mL, 2.4 mmol), **1c** (54.0 mg, 6 mol %), and THF (4.0 mL). The reaction mixture was purified by flash column chromatography on silica gel (eluent: 10% ethyl acetate/hexanes) to afford 0.633 g (91%) of the desired product as yellow oil.  $^1H$  NMR ( $CDCl_3$ , 400 MHz):  $\delta$  7.48–7.45 (m, 2H), 7.35–7.33 (m, 3H), 3.60 (s, 3H), 1.22 (s, 3H), 1.19 (s, 3H), 0.14 (s, 9H) ppm;  $^{13}C$  NMR ( $CDCl_3$ , 100 MHz):  $\delta$  174.8, 136.5, 128.5, 127.8, 127.3, 126.1 (q,  $J = 288$  Hz) 84.6 (q,  $J = 26.9$  Hz), 51.9, 50.9, 26.8, 22.7, 1.8 ppm; HRMS  $m/z$  Calcd for  $C_{16}H_{17}F_3O$ : 348.13686. Found: 348.13754.

**5-(2,2,2-Trifluoro-1-hydroxy-1-phenylethyl)furan-2(5H)-one (Scheme 3, product 11).**

The general procedure was followed using 2,2,2-trifluoroacetophenone (0.348 g, 2.0 mmol), 2-(trimethylsiloxy)furan (0.403 mL, 2.4 mmol), **1c** (54.0 mg, 6 mol %), and THF (4.0 mL). The reaction mixture was purified by column chromatography on silica gel (eluent: 10% ethyl acetate/hexanes) to afford a combined isolated yield of 0.404 g (83%). *Syn* isomer (white solid)  $^1\text{H}$  NMR ( $\text{CDCl}_3$ , 400 MHz):  $\delta$  7.61–7.60 (m, 2H), 7.49–7.45 (m, 3H), 6.84–6.82 (m, 1H), 6.18–6.16 (m, 1H), 5.71 (t, 1H,  $J = 4.0$  Hz), 4.1 (s, 1H) ppm;  $^{13}\text{C}$  NMR ( $\text{CDCl}_3$ , 100 MHz):  $\delta$  173.0, 152.5, 133.4, 129.8, 129.2, 125.6, 124.5 (q,  $J = 280$  Hz), 124.0, 83.6, 76.6 (q,  $J = 29$  Hz) ppm; HRMS  $m/z$  Calcd for  $\text{C}_{12}\text{H}_9\text{F}_3\text{O}_3$ : 258.05038. Found: 258.05075. *Anti* isomer (yellow oil)  $^1\text{H}$  NMR ( $\text{CDCl}_3$ , 400 MHz):  $\delta$  7.56–7.54 (m, 3H), 7.42–7.39 (m, 3H), 6.04–6.02 (m, 1H), 5.58 (s, 1H), 3.66 (s, 1H) ppm;  $^{13}\text{C}$  NMR ( $\text{CDCl}_3$ , 100 MHz):  $\delta$  172.2, 152.5, 133.3, 129.8, 128.9, 126.4, 124.5 (q,  $J = 280$  Hz), 124.0, 83.2, 77.9 (q,  $J = 20$  Hz) ppm; HRMS  $m/z$  Calcd for  $\text{C}_{12}\text{H}_9\text{F}_3\text{O}_3$ : 258.05038. Found: 258.05076.

**2,8,9-Trimethyl-2,5,8,9-tetraaza-1-phosphabicyclo[3.3.3]undecane 1-oxide (12):** To a solution of **1c** (0.133 g, 0.30 mmol) in 4.0 mL of toluene was added excess  $\text{Me}_3\text{SiOOSiMe}_3$  (0.320 g, 1.80 mmol). The resulting clear solution was stirred at 40–50 °C. After 38 h, all the volatiles were removed under vacuum giving an off-white residue which upon recrystallization from anhydrous pentane yielded **12** as a colorless solid (0.130 g, 94%).  $^{31}\text{P}$  NMR ( $\text{CDCl}_3$ , 162 MHz): 24.24 ppm.  $^1\text{H}$  NMR ( $\text{CDCl}_3$ , 400 MHz): 7.61–7.59 (m, 6H), 7.37–7.26 (m, 9H), 4.25 (d, 6H,  $J = 8.0$  Hz), 2.88–2.79 (m, 12H) ppm.  $^{13}\text{C}$  NMR ( $\text{CDCl}_3$ , 100 MHz): 139.9 (d,  $J = 2.3$  Hz), 128.9, 128.5, 127.4, 50.9 (d,  $J = 5.0$  Hz), 50.0, 47.4 (d,  $J = 3.3$  Hz) ppm. HRMS  $m/z$  calcd for  $\text{C}_{27}\text{H}_{33}\text{N}_4\text{OP}$ : 460.23919. Found: 460.24045.



### Acknowledgement

The authors gratefully acknowledge the National Science Foundation for financial support of this investigation through Grant 0750463.

### References

- [1] (a) Mukaiyama, T.; Banno, K.; Narasaka, K. *J. Am. Chem. Soc.* **1974**, *96*, 7503–7509. (b) Mukaiyama, T.; Izawa, T.; Saigo, K. *Chem. Lett.* **1974**, 323–326. (c) Mukaiyama, T.; Narasaka, K.; Banno, K. *Chem. Lett.* **1973**, 1011–1114. (d) Gawronski, J.; Wascinska, N.; Gajewy, J. *Chem. Rev.* **2008**, *108*, 5227–5252.
- [2] For excellent recent reviews, see: (a) Mukaiyama, T. *Angew. Chem., Int. Ed.* **2004**, *43*, 5590–5614. (b) Carreira, E. M. in *Comprehensive Asymmetric Catalysis I-III*, Eds: Jacobsen, E. N.; Pfaltz, A.; Yamamoto, H. **1999**, *3*, 997–1065. (c) Gawronski, J.; Wascinska, N.; Gajewy, J. *Chem. Rev.* **2008**, *108*, 5227–5252. (d) Ishihara, K.; Yamamoto, H. *Modern Aldol Reactions* **2004**, *2*, 25–68. (e) Kobayashi, S.; Manabe, K.; Ishitani, H.; Matsuo, J.-I. *Science of Synthesis* **2002**, *4*, 317–369. (f) Palomo, C.; Oiarbide, M.; Garcia, J. M. *Eur. J. Chem.* **2002**, *8*, 36–44.
- [3] (a) For recent examples, see: Rech, J. C.; Floreancig, P. E. *Org. Lett.* **2005**, *7*, 5175–5178. (b) Terauchi, T.; Terauchi, T.; Sato, I.; Shoji, W.; Tsukada, T.; Tsunoda, T.; Kanoh, N.; Nakata, M. *Tetrahedron Lett.* **2003**, *44*, 7741–7745. (c) Savall, B. M.; Blanchard, N.; Roush, W. R. *Org. Lett.* **2003**, *5*, 377–379.
- [4] (a) For examples of the construction of chiral building blocks, see: Ishitani, H.; Yamashita, Y.; Shimizu, H.; Kobayashi, S. *J. Am. Chem. Soc.* **2000**, *122*, 5403–

5404. (b) Evans, D. A.; Kozlowski, M. C.; Murry, J. A.; Burgey, C. S.; Campos, K. R.; Connell B. T.; Staples, R. J. *J. Am. Chem. Soc.* **1999**, *121*, 669–685. (c) Carreira, E. M.; Singer R. A.; Lee, W. *J. Am. Chem. Soc.* **1994**, *116*, 8837–8838.
- [5] (a) Nelson, S.G. *Tetrahedron: Asymmetry* **1998**, *9*, 357–389. (b) Mahrwald, R. *Chem. Rev.* **1999**, *99*, 1095–1120. (c) Machajewski, T. D.; Wong, C.-H. *Angew. Chem., Int. Ed.* **2000**, *39*, 1352–1374.
- [6] (a) Hagiwara, H.; Inoguchi, H.; Fukushima, M.; Hoshi, T.; Suzuki, T. *Synlett* **2005**, 2388–2390. (b) Hollis, T.K.; Bosnich, B. *J. Am. Chem. Soc.* **1995**, *117*, 4570–4581. (c) Kantam, M. L.; Choudary, B. M.; Ch. Venkat Reddy, Rao, K. K.; Figueras, F. *Chem. Commun.* **1998**, 1033–1034.
- [7] (a) Murata, S.; Suzuki, M.; Noyori, R. *J. Am. Chem. Soc.* **1980**, *102*, 3248–3249. (b) Mukai, C.; Hashizume, S.; Nagami, K.; Hanaoka, M. *Chem. Pharm. Bull.* **1990**, *38*, 1509–1512. (c) Downey, C. W.; Johnson, M. W. *Tetrahedron Lett.* **2007**, *48*, 3559–3562.
- [8] Sakurai, H.; Sasaki, K.; Hosomi, A. *Bull. Chem. Soc. Jpn.* **1983**, *56*, 3195–3196.
- [9] Iwasawa, N.; Mukaiyama, T. *Chem. Lett.* **1987**, 463–466.
- [10] Mukaiyama, T.; Kobayashi, S.; Tamura, M.; Sagawa, Y. *Chem. Lett.* **1987**, 491–496.
- [11] (a) Mukaiyama, T.; Kobayashi, S.; Murakami, M. *Chem. Lett.* **1985**, 447–450. (b) Mukaiyama, T.; Kobayashi, S.; Murakami, M. *Chem. Lett.* **1984**, 1759–1762.
- [12] Kobayashi, S.; Murakami, M.; Mukaiyama, T. *Chem. Lett.* **1985**, 1535–1538.
- [13] (a) Reetz, M. T.; Vougioukas, A. E. *Tetrahedron Lett.* **1987**, *28*, 793–796. (b) Sato, S.; Matsuda, I.; Izumi, Y. *Tetrahedron Lett.* **1987**, *28*, 6657–6660; (c) Sato, S.; Matsuda, I.;

- Izumi, Y. *Tetrahedron Lett.* **1986**, 27, 5517–5520. (d) Mukaiyama, T.; Soga, T.; Takenoshita, H. *Chem. Lett.* **1989**, 1273–1276.
- [14] (a) Kobayashi, S.; Hachiya, I.; Takahori, T. *Synthesis* **1993**, 371–373. (b) Kobayashi, S.; Hachiya, I. *J. Org. Chem.* **1994**, 59, 3590–3596. (c) Kobayashi, S.; Hachiya, I. *Tetrahedron Lett.* **1992**, 33, 1625–1628. (d) Kobayashi, S. *Chem. Lett.* **1991**, 2187–2190. (e) Kobayashi, S.; Hachiya, I.; Ishitani, H.; Araki, M. *Synlett* **1993**, 472–474. (f) Mikami, K.; Mikami, Y.; Matsuzawa, H.; Matsumoto, Y.; Nishikido, J.; Yamamoto F.; Nakajima, H. *Tetrahedron* **2002**, 58, 4015–4021.
- [15] (a) Bach, T.; Fox, D. N. A.; Reetz, M. T. *J. Chem. Soc., Chem. Commun.* **1992**, 1634–1636. (b) Colombo, L.; Ulgheri, F.; Prati, L. *Tetrahedron Lett.* **1989**, 30, 6435–6436. (c) Doucet, H.; Parrain, J.-L.; Santelli, M. *Synlett* **2000**, 871–873. (d) Sodeoka, M.; Ohrai, K.; Shibasaki, M. *J. Org. Chem.* **1995**, 60, 2648–2649.
- [16] (a) Gong, L.; Streitwieser, A. *J. Org. Chem.* **1990**, 55, 6235–6236. (b) Hara, K.; Akiyama, R.; Sawamura M. *Org. Lett.* **2005**, 7, 5621–5623. (c) Hong, Y.; Norris, D. J.; Collins, S. *J. Org. Chem.* **1993**, 58, 3591–3594. (d) Le Roux, C.; Gaspard-Iloughmane, H.; Dubac, J. *J. Org. Chem.* **1993**, 58, 1835–1839. (e) Tian, H.-Y.; Chen, Y.-J.; Wang, D.; Bu Y.-P.; Li, C.-J. *Tetrahedron Lett.* **2001**, 42, 1803–1805. (f) An, D. L.; Peng, Z.; Orita, A.; Kurita, A.; Man-E, S.; Ohkubo, K.; Li, X.; Fukuzumi, S.; Otera, J. *Eur. J. Chem.* **2006**, 12, 1642–1647. (g) Le Roux, C.; Ciliberti, L.; Laurent-Robert, H.; Laporterie, A.; Dubac, J. *Synlett* **1998**, 1249–1251. (h) Ollevier, T.; Desyroy, V.; Debailleul, B.; Vaur, S. *Eur. J. Org. Chem.* **2005**, 4971–4973. (i) Lin, S.; Bondar, G. V.; Levy, C. J.; Collins, S. *J. Org. Chem.* **1998**, 63, 1885–1892.

- [17] (a) Mukaiyama, T.; Hara, R. *Chem. Lett.* **1989**, 1171–1174. (b) Hara, R.; Mukaiyama, T. *Chem. Lett.* **1989**, 1909–1912. (c) Li, X.; Kurita, A.; Man-E, S.; Orita, A.; Otera, J. *Organometallics* **2005**, *24*, 2567–2569. (d) Yamashita, Y.; Salter, M. M.; Aoyama, K.; Kobayashi, S. *Angew. Chem., Int. Ed.* **2006**, *45*, 3816–3819. (e) Lannou, M.-I.; Helion, F.; Namy, J.-L. *Tetrahedron* **2003**, *59*, 10551–10565. (f) Manabe, K.; Mori, Y.; Nagayama, S.; Odashima, K.; Kobayashi, S. *Inorg. Chim. Acta* **1999**, *296*, 158–163. (g) Ishihara, K.; Kondo, S.; Yamamoto, H. *J. Org. Chem.* **2000**, *65*, 9125–9128.
- [18] (a) Giuseppone, N.; Van de Weghe, P.; Mellah, M.; Collin, J. *Tetrahedron* **1998**, *54*, 13129–13148. (b) Li, W.-D. Z.; Zhang, X.-X. *Org. Lett.* **2002**, *4*, 3485–3488. (c) Takeuchi, M.; Akiyama, R.; Kobayashi, S. *J. Am. Chem. Soc.* **2005**, *127*, 13096–13097. (d) Iimura, S.; Manabe, K.; Kobayashi, S. *Tetrahedron* **2004**, *60*, 7673–7678 (e) Sasidharan, M.; Raju, S. V. N.; Srinivasan, K. V.; Paul, V.; Kumar, R. *Chem. Commun.* **1996**, 129–130. (f) Sasidharan, M.; Kumar, R. *J. Catal.* **2003**, *220*, 326–332. (g) Loh, T.-P.; Li, X.-R. *Tetrahedron* **1999**, *55*, 10789–10802. (h) Vougioukas, A. E.; Kagan, H. B. *Tetrahedron Lett.* **1987**, *28*, 5513–5516. (i) Jankowska, J.; Paradowska, J.; Rakiel, B.; Mlynarski, J. *J. Org. Chem.* **2007**, *72*, 2228–2231. (j) Jankowska, J.; Mlynarski, J. *J. Org. Chem.* **2006**, *71*, 1317–1321. (k) Komoto, I.; Kobayashi, S. *J. Org. Chem.* **2004**, *69*, 680–688. (l) Komoto, I.; Kobayashi, S. *Chem. Commun.* **2001**, 1842–1843. (m) Morohashi, N.; Hattori, T.; Yokomakura, K.; Kabuto, C.; Miyano, S. *Tetrahedron Lett.* **2002**, *43*, 7769–7772. (n) Marx, A.; Yamamoto, H. *Angew. Chem., Int. Ed.* **2000**, *39*, 178–181. (o) Nakamura, H.; Matsuhashi, H.; Arata, K. *Synlett* **2000**, 668–670. (p) Tian, H.; Chen, Y.; Wang, D.; Zeng, C.; Li, C. *Tetrahedron Lett.* **2000**, *41*, 2529–2532. (q) Loh, T.; Pei, J.; Koh, K. S.; Cao, G.; Li, X. *Tetrahedron Lett.* **1997**,

- 38, 3465–3468. (r) Raju, S. V. N.; Ponrathnam, S.; Rajan, C. R.; Srinivasan, K. V. *Synlett* **1996**, 239–240. (s) Ishitani, H.; Iwamoto, M. *Tetrahedron Lett.* **2003**, *44*, 299–301. (t) Mukaiyama, T.; Saito, K.; Kitagawa, H.; Shimomura, N. *Chem. Lett.* **1994**, 789–792. (u) Mukai, C.; Cho, W. J.; Kim, I. J.; Kido, M.; Hanaoka, M. *Tetrahedron* **1991**, *47*, 3007–3036. (v) Taralkar, U. S.; Kalita, P.; Kumar, R.; Joshi, P. N. *App. Catal. A: Gen.* **2009**, *358*, 88–94. (w) Horike, S.; Dinca, M.; Tamaki, K.; Long, J. R. *J. Am. Chem. Soc.* **2008**, *130*, 5854–5855. (x) Oisaki, K.; Suto, Y.; Kanai, M.; Shibasaki, M. *J. Am. Chem. Soc.* **2003**, *125*, 5644–5645. (y) Ishihara, K.; Hananki, N.; Yamamoto, H. *Synlett* **1993**, 577–579.
- [19] Hatano, M.; Takagi, E.; Ishihara, K. *Org. Lett.* **2007**, *9*, 4527–4530.
- [20] Matsukawa, S.; Okano, N.; Imamoto, T. *Tetrahedron Lett.* **2000**, *41*, 103–107.
- [21] (a) Mizugaki, T.; Hetrick, C. E.; Murata, M.; Ebitani, K.; Amiridis, M. D.; Kaneda, K. *Chem. Lett.* **2005**, 420–421. (b) Srivastava, R. *J. Mol. Catal. A: Chem.* **2007**, *264*, 146–152. (c) Shen, Z.-L.; Ji, S.-J.; Loh, T.-P. *Tetrahedron Lett.* **2005**, *46*, 507–508. (d) Flowers, R. A.; Xu, X.; Timmons, C.; Li, G. *Eur. J. Org. Chem.* **2004**, *14*, 2988–2990. (e) Ooi, T.; Doda, K.; Maruoka, K. *Org. Lett.* **2001**, *3*, 1273–1276.
- [22] (a) Noyori, R.; Nishida, I.; Sakata, J. *J. Am. Chem. Soc.* **1983**, *105*, 1598–1608. (b) Nakamura, E.; Shimizu, M.; Kuwajima, I.; Sakata, J.; Yokoyama, K.; Noyori, R. *J. Org. Chem.* **1983**, *48*, 932–945.
- [23] (a) Fujisawa, H.; Nakagawa, T.; Mukaiyama, T. *Adv. Synth. Catal.* **2004**, *346*, 1241–1246. (b) Nakagawa, T.; Fujisawa, H.; Mukaiyama, T. *Chem. Lett.* **2003**, *32*, 696–697. (c) Fujisawa, H.; Takahashi, E.; Mukaiyama, T. *Eur. J. Chem.* **2006**, *12*, 5082–5093.

- [24] Hagiwara, H.; Inoguchi, H.; Fukushima, M.; Hoshi, T.; Suzuki, T. *Synlett* **2005**, 2388–2390.
- [25] Hagiwara, H.; Inoguchi, H.; Fukushima, M.; Hoshi, T.; Suzuki, T. *Tetrahedron Lett.* **2006**, *47*, 5371–5373.
- [26] (a) Mukaiyama, T.; Fujisawa, H.; Nakagawa, T. *Helv. Chim. Acta* **2002**, *85*, 4518–4531.  
(b) Fujisawa, H.; Mukaiyama, T. *Chem. Lett.* **2002**, 182–183. (c) Fujisawa, H.; Mukaiyama, T. *Chem. Lett.* **2002**, 858–859.
- [27] (a) Nakagawa, T.; Fujisawa, H.; Mukaiyama, T. *Chem. Lett.* **2004**, 92–93. (b) Nakagawa, T.; Fujisawa, H.; Nagata, Y.; Mukaiyama, T. *Bull. Chem. Soc. Jpn.* **2004**, *77*, 1555–1567. (c) Nakagawa, T.; Fujisawa, H.; Mukaiyama, T. *Chem. Lett.* **2003**, 462–463.
- [28] Song, J. J.; Tan, Z.; Reeves, J. T.; Yee, N. K.; Senanayake, C. H. *Org. Lett.* **2007**, *9*, 1013–1016.
- [29] (a) Genisson, Y.; Gorrichon, L. *Tetrahedron Lett.* **2000**, *41*, 4881–4884. (b) Loh, T.-P.; Feng, L.-C.; Wei, L.-L. *Tetrahedron* **2000**, *56*, 7309–7312. (c) Chen, S.-L.; Ji, S.-J.; Loh, T.-P. *Tetrahedron Lett.* **2004**, *45*, 375–377.
- [30] Phukan, P. *Synth. Commun.* **2004**, *34*, 1065–1070.
- [31] For an excellent review of the reactions of trichlorosilyl enolates with aldehydes, see: Denmark, S. E.; Stavenger, R. A. *Acc. Chem. Res.* **2000**, *33*, 432–440.
- [32] Miura, K.; Nakagawa, T.; Hosomi, A.; *J. Am. Chem. Soc.* **2002**, *124*, 536–537.
- [33] For reviews of proazaphosphatrane chemistry, see: (a) Verkade, J. G. In *New Aspects of Phosphorus Chemistry II*, *Top. Curr. Chem.* Majoral, J. P. Ed., **2002**, *233*, 1–44. (b)

- Verkade, J. G.; Kisanga, P. B. *Tetrahedron* **2003**, *59*, 7819–7858. (c) Verkade, J. G.; Kisanga, P. B. *Aldrichimica Acta* **2004**, *37*, 3–14. (d) Uргаonkar, S.; Verkade, J. G. *Specialty Chemicals* **2006**, *26*, 36–39.
- [34] (a) Venkat Reddy, Ch.; Uргаonkar, S.; Verkade, J. G. *Org. Lett.* **2005**, *7*, 4427–4430. (b) Su, W.; Uргаonkar, S.; Verkade, J. G. *Org. Lett.* **2004**, *6*, 1421–1424. (c) Uргаonkar, S.; Nagarajan, M.; Verkade, J. G. *Tetrahedron Lett.* **2002**, *43*, 8921–8924. (d) Kisanga, P. B.; Verkade, J. G.; Schwesinger, R. *J. Org. Chem.* **2000**, *65*, 5431–5432.
- [35] (a) D'Sa, B. A.; Verkade, J. G. *J. Am. Chem. Soc.* **1996**, *118*, 12832–12833. (b) D'Sa, B. A.; McLeod, D.; Verkade, J. G. *J. Org. Chem.* **1997**, *62*, 5057–5061.
- [36] Yu, Z; Verkade, J. G. *J. Org. Chem.* **2000**, *65*, 2065–2068.
- [37] (a) Wang, Z; Fetterly, B; Verkade, J. G. *J. Organomet. Chem.* **2002**, *646*, 161–166. (b) Fetterly, B. M.; Verkade, J. G. *Tetrahedron Lett.* **2005**, *46*, 8061–8066.
- [38] Uргаonkar, S.; Verkade, J. G. *Org. Lett.* **2005**, *7*, 3319–3322.
- [39] Su, W.; Uргаonkar, S.; McLaughlin, P. A.; Verkade, J. G. *J. Am. Chem. Soc.* **2004**, *126*, 16433–16439.
- [40] (a) Kingston, J. V.; Ellern, A.; Verkade, J. G. *Angew. Chem., Int. Ed.* **2005**, *44*, 4960–4963. (b) Kingston, J. V.; Verkade, J. G. *J. Org. Chem.* **2007**, *72*, 2816–2822. (c) Venkat Reddy, Ch.; Kingston, J. V.; Verkade, J. G. *J. Org. Chem.* **2008**, *73*, 3047–3062.
- [41] Boyer, J.; Corriu, R. J. P.; Perz, R.; Reye, C. *J. Organomet. Chem.* **1980**, *184*, 157–166.

- [42] For useful discussions of the mechanism of Mukaiyama reactions, see: (a) Wang, L.; Wong, M. W. *Tetrahedron Lett.* **2008**, *49*, 3916–3920. (b) Denmark, S. E.; Lee, W. *Asian J. Chem.* **2008**, *3*, 327–341. (c) Patel, S. G.; Wiskur, S. L. *Tetrahedron Lett.* **2009**, *50*, 1164–1166.
- [43] Wang, Z.; Kisanga, P.; Verkade, J. G. *J. Org. Chem.* **1999**, *64*, 6459–6461.
- [44] Wang, Z.; Fetterly, B. M.; Verkade, J. G. *J. Organomet. Chem.* **2002**, *646*, 161–166.
- [45] Liu, X.; Verkade, J. G. *J. Org. Chem.* **2000**, *65*, 4560–4564.
- [46] *Handbook of Phosphorus Nuclear Magnetic Resonance Data*, Ed. J. C. Tebby, CRC Press Inc. 1991.



**CHAPTER 7. DETERMINATION OF THE STRUCTURE OF A NOVEL ANION  
EXCHANGE FUEL CELL  
MEMBRANE BY SOLID-STATE NUCLEAR MAGNETIC RESONANCE  
SPECTROSCOPY**

Xueqian Kong, Kuldeep Wadhwa, John G. Verkade, and Klaus Schmidt-Rohr\*

*Macromolecules* **2009**, *42*, 1659-1664

**Abstract:** A novel anion exchange fuel cell membrane was successfully synthesized by chemically attaching proazaphosphatranium/phosphatranium cations under microwave treatment to the sulfonic groups of Nafion-F<sup>®</sup>. Solid-state nuclear magnetic resonance (NMR) techniques were employed to determine the actual structure and composition of this anion exchange membrane. <sup>31</sup>P NMR showed two main signals with a 2:1 intensity ratio and chemical shift changes of +89 ppm and +46 ppm, respectively, from the main peak of phosphatranium chloride. <sup>1</sup>H-<sup>31</sup>P heteronuclear correlation (HetCor) NMR and <sup>1</sup>H-<sup>31</sup>P recoupling experiments indicated that the proton originally bonded to phosphorus in phosphatranium chloride is replaced in the major component of the Nafion<sup>®</sup>-proazaphosphatranium/phosphatranium composite. <sup>19</sup>F NMR experiments showed that the fluorine in the -SO<sub>2</sub>F group of the Nafion-F<sup>®</sup> precursor is fully replaced. <sup>31</sup>P{<sup>19</sup>F} rotational-echo double resonance (REDOR) experiments measured a P-F internuclear distance of ~0.4 nm, which showed that the proazaphosphatranium is covalently attached to Nafion<sup>®</sup> through a S-P bond. <sup>13</sup>C NMR and <sup>1</sup>H-<sup>13</sup>C HetCor spectra indicated that the proazaphosphatranium

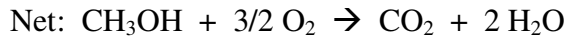
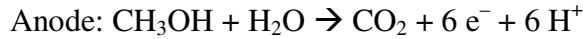
structure is maintained even after the microwave treatment at 180 °C and also showed the presence of entrapped dimethylformamide solvent.

*Keywords: Nafion<sup>®</sup>; Phosphatranium; Proazaphosphatranium, Solid-state nuclear magnetic resonance spectroscopy; Fuel cell; Anion exchange membrane;*

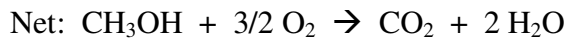
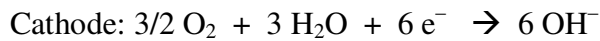
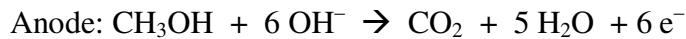
### Introduction

The increasing demand for alternative sources of energy<sup>1-4</sup> has placed direct methanol-based fuel cells (DMFCs) at the forefront of the search for alternatives to fossil fuels. DMFCs are projected to be the first fuel cells that will be commercially available for use by the general population. Among the advantages of DMFCs are their high energy density (5–10 times greater than that of commonly available batteries), moderate operating temperatures, and easy replacement of the methanol fuel cartridge; all of which make DMFCs ideal for usage in portable electronic devices.<sup>5-7</sup> In many modern fuel cells, a proton exchange membrane (PEM) is utilized to transport protons produced in the anodic half reaction for consumption on the cathodic side of the cell (Scheme 1a). However, PEMs in DMFCs suffer from (i) parasitic crossover of methanol, which leads to a lowering of cell voltage and efficiency; (ii) electro-osmosis of water from anode to cathode, which causes severe flooding at the cathode; (iii) reduced catalyst kinetics in the acidic environment requiring high loadings of costly precious-metal catalysts, e.g. platinum.<sup>8</sup> For these reasons, alkaline fuel cells (AFCs) with the same net reaction but exploiting different half reactions as shown in Scheme 1b have become attractive to investigate. The most important advantages of AFCs are that they can operate at a lower catalyst loading owing to more facile methanol oxidation in alkaline media,<sup>9-11</sup> and that they may utilize a broader range of catalysts, such as nickel and silver.<sup>12-14</sup>

(a)



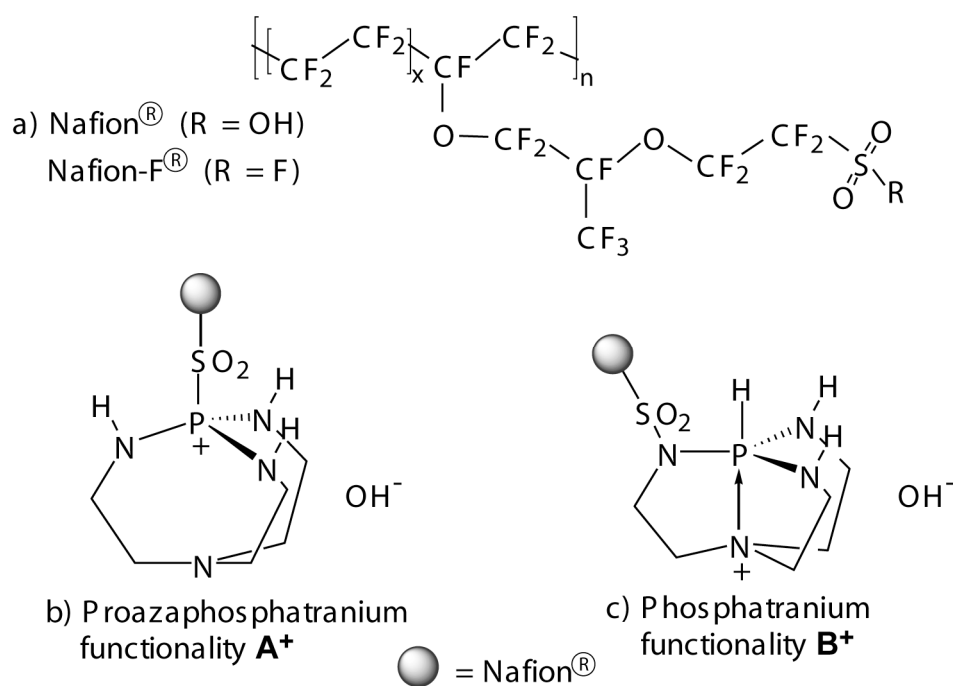
(b)



**Scheme 1:** Half-reactions and the overall net reaction in a methanol fuel cell. (a) Protonic half reactions in a conventional fuel cell. (b) Reactions in an alkaline fuel cell.

In the past, methanol was not suitable as a fuel in AFCs because such cells utilized liquid alkaline electrolytes such as hydroxide ion conductors, which are vulnerable to precipitation of carbonate (e.g.  $\text{K}_2\text{CO}_3$ ) that destroys the catalyst layer, which forms from  $\text{CO}_2$  released in the cell reaction (Scheme 1b).<sup>15-17</sup> As a result, solid alkaline anion exchange membranes (AAEMs) containing hydroxide ions were developed. They combine the advantages of PEMs (flexibility, durability, small volume, and no leakage) and traditional AFCs (good catalyst kinetics) and they can operate when carbonate species are present.<sup>8</sup> Some efforts have been

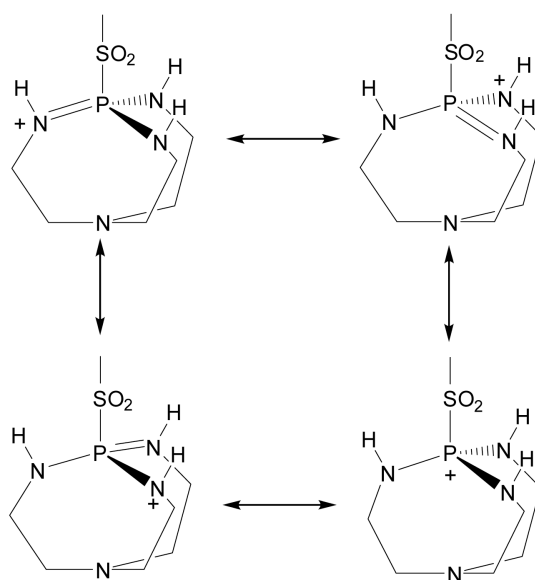
made to use fluorinated polymers as AAEMs. For example, poly(vinylidene fluoride) (PVDF) and poly(tetrafluoroethene-co-hexafluoropropylene) (FEP) have been grafted with 4-vinylbenzyl chloride, followed by modification of the benzyl chloride functionality with trimethylamine to give the trimethylbenzyl ammonium salt, which was then tested as an AAEM.<sup>18</sup> While the FEP-based AAEM gave conductivities of ca. 0.02 S/cm at ambient temperature and an atmospheric relative humidity of 100%, the PVDF-based AAEM degraded on subsequent amination and hydroxide ion exchange.



**Scheme 2.** a) Representation of the average chemical structure of Nafion<sup>®</sup> and Nafion-F<sup>®</sup>. b) Representation of Nafion<sup>®</sup> polymer segments attached to proazaphosphatranium functional groups **A**<sup>+</sup>. c) Representation of the same Nafion<sup>®</sup> polymer segments bonded to phosphatranium functional groups **B**<sup>+</sup>.

An important feature of AAEMs is that their conductivities are directly proportional to the ionophore densities. Commonly studied ionophores tethered to AAEM backbones are quaternary ammonium salts. However, these salts experience relatively intense cation–anion interactions which further impede hydroxide ion mobility. Here we report the synthesis and characterization of a potentially improved AAEM that incorporates novel types of phosphonium cations as depicted in Scheme 2b and 2c. These ionophores have a reduced charge density due to their resonance structures that distribute the positive charge (Scheme 3) and thus diminish ionic interaction, which should facilitate hydroxide ion mobility.

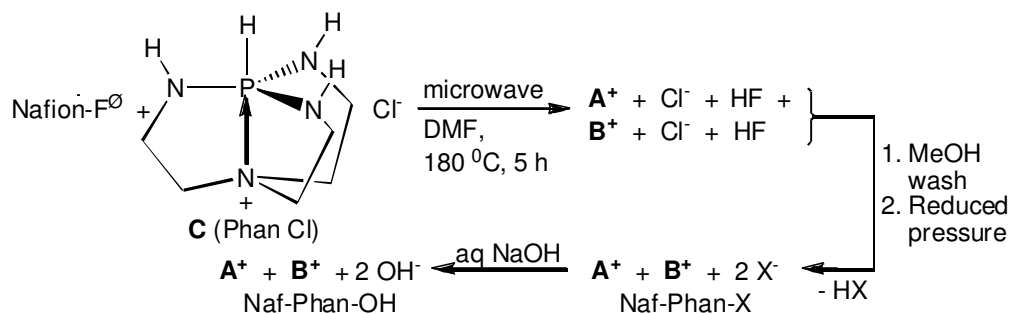
These phosphonium sidegroups have been attached to Nafion<sup>®</sup> (Scheme 2a), a tetrafluoroethylene copolymer bearing sulfonic acid ( $-\text{SO}_2\text{OH}$ ) functional groups that is extensively used as a PEM in fuel cells. Being perfluorinated and semicrystalline, Nafion<sup>®</sup> (a proton cation conductor commercially derived via base hydrolysis of Nafion-F<sup>®</sup>) and its precursor, Nafion-F<sup>®</sup> (which contains  $-\text{SO}_2\text{F}$  functionalities), possess good thermal and mechanical stability, which are particular advantages of Nafion<sup>®</sup> compared with many other potential PEM materials. Nafion<sup>®</sup> is stable up to 300 °C.<sup>19</sup> Its excellent conductivity stems from its combination of a hydrophobic polymer backbone and hydrophilic functional groups which self-organize to form water channels of ~2.5-nm diameter through which small ions can be easily transported.<sup>20</sup>



**Scheme 3:** Resonance structures for a proazaphosphatranium cation.

The synthesis steps for our material are summarized in Scheme 4, wherein Phan denotes the incorporation into the Nafion<sup>®</sup> (Naf) polymer of the two structurally different types of phosphorus cations [i.e., proazaphosphatranium (**A**<sup>+</sup> in Scheme 2) and phosphatranium (**B**<sup>+</sup> in Scheme 2)] and "X" designates the anions Cl<sup>-</sup> or F<sup>-</sup>. Solid state nuclear magnetic resonance (NMR) is a promising tool for assessing the relative levels of **A**<sup>+</sup>, **B**<sup>+</sup> or other functionalities incorporated, and for detailing their chemical structure, since the material is rich in NMR-active spin-1/2 isotopes, namely <sup>1</sup>H, <sup>13</sup>C, <sup>31</sup>P, <sup>19</sup>F and <sup>15</sup>N. The characteristic chemical shifts of the <sup>31</sup>P, <sup>1</sup>H, <sup>19</sup>F, <sup>13</sup>C and <sup>15</sup>N in Naf-Phan-X were detected in quantitative direct polarization (DP) experiments (for <sup>31</sup>P and <sup>19</sup>F) and in cross polarization (CP) experiments (for <sup>31</sup>P, <sup>13</sup>C, and <sup>15</sup>N). The potential bonding of the three latter isotopes to hydrogen was determined by recoupling the dipolar interaction with <sup>1</sup>H. The correlations between phosphorus or carbon and their nearest protons were determined by 2D <sup>1</sup>H-<sup>31</sup>P and <sup>1</sup>H-<sup>13</sup>C heteronuclear correlation (HetCor) NMR. The bonding between Nafion<sup>®</sup> and

proazaphosphatranium/phosphatranium moieties was elucidated using  $^{31}\text{P}\{^{19}\text{F}\}$  rotational echo double resonance (REDOR)<sup>25</sup>.  $^{13}\text{C}$  spectra were edited with CH and  $\text{CH}_2$  selection sequences<sup>33,34</sup> to identify such segments unambiguously.



**Scheme 4:** Synthesis of Naf-Phan-X and Naf-Phan-OH.

### Experimental Section

**Samples.** Nafion-F<sup>®</sup> membrane (6 cm x 6 cm), with a 0.9 mmol/g loading of  $\text{SO}_2\text{F}$  functionality and a thickness of 25 microns (a product of Du Pont supplied by Ion Power Inc.) was charged to a microwave vial. To this was added excess phosphatranium chloride (Phan-Cl in Scheme 4; 500 mg, 2.3 mmol) prepared according to a literature method<sup>21</sup> and dry dimethyl formamide (ca 8 mL) such that the membrane was completely immersed in the solution. The mixture was microwaved at 180 °C for 5 hours using a 300 watt CEM Discover apparatus and then the membrane was washed with copious amounts of methanol to remove any unreacted phosphatranium salt, HX and solvent. For solid state NMR characterization, the Naf-Phan-X membrane was dried at room temperature under reduced pressure. For

electrical measurements (to be reported in due course) the Naf-Phan-X membrane was soaked in aq. NaOH to exchange the halide ions for hydroxide, giving Naf-Phan-OH in Scheme 4. The change in counterion is unlikely to result in significant structural changes of the polymer or sidegroups.

**NMR parameters.** All NMR experiments were performed on a Bruker DSX-400 spectrometer at a resonance frequency of 400 MHz for  $^1\text{H}$ , 100 MHz for  $^{13}\text{C}$ , 162 MHz for  $^{31}\text{P}$ , 376 MHz for  $^{19}\text{F}$  and 40.5 MHz for  $^{15}\text{N}$ , using double-resonance or triple-resonance magic-angle spinning (MAS) probes.  $^{13}\text{C}$  experiments were performed in 7-mm rotors at 6.5 kHz with a  $90^\circ$  pulse length of 4  $\mu\text{s}$ , and with 3-s recycle delays.  $^{31}\text{P}$  experiments were performed in 4-mm rotors at 7 kHz with a  $90^\circ$  pulse length of 4  $\mu\text{s}$ , and with either 2-s recycle delay for cross polarization or 100 s for direct polarization.  $^{19}\text{F}$  experiments were performed in 2.5-mm rotors at 30 kHz, which reduces  $^{19}\text{F}$  dipolar couplings enough to resolve various sidegroup- and backbone signals in Nafion<sup>®</sup>, with a  $90^\circ$  pulse length of 1.85  $\mu\text{s}$ , and with 3-s recycle delays.  $^{15}\text{N}$  experiments were performed in 7-mm rotors at 5 kHz with a  $90^\circ$  pulse length of 9.2  $\mu\text{s}$ , and with 2.5-s recycle delays; the number of scans was 6,144 for phosphatranium chloride and 28,672 for Naf-Phan-X. Two-pulse phase-modulation (TPPM) was used for  $^1\text{H}$ - $^{13}\text{C}$ ,  $^1\text{H}$ - $^{31}\text{P}$ , or  $^1\text{H}$ - $^{15}\text{N}$  heteronuclear dipolar decoupling.  $^{31}\text{P}$  and  $^{15}\text{N}$  chemical shifts were indirectly referenced to  $\text{H}_3\text{PO}_4$  and  $\text{NH}_4^+$ , respectively, using hydroxyapatite ( $^{31}\text{P}$  chemical shift at +3 ppm) and N-acetyl valine ( $^{15}\text{N}$  chemical shift at +122 ppm). All experiments were carried out at ambient temperature.

*$^1\text{H}$ - $^{31}\text{P}$  and  $^1\text{H}$ - $^{13}\text{C}$  HetCor.* Two-dimensional (2D)  $^1\text{H}$ - $^{31}\text{P}$  and  $^1\text{H}$ - $^{13}\text{C}$  heteronuclear correlation (HetCor) NMR experiments<sup>22,23</sup> were performed at spinning frequencies of 7 kHz



and 6.5 kHz, respectively. Frequency-switched Lee-Goldburg<sup>24</sup> homonuclear decoupling was applied during the evolution period  $t_1$ . Lee-Goldburg cross polarization was used to suppress  $^1\text{H}$ - $^1\text{H}$  spin diffusion during polarization transfer and to show mostly one- and two-bond  $^1\text{H}$ - $^{13}\text{C}$  connectivities. For  $^1\text{H}$ - $^{31}\text{P}$  HetCor, the cross polarization time was 0.7 ms, the number of scans was 128, and the number of  $t_1$  increments was 100. For  $^1\text{H}$ - $^{13}\text{C}$  HetCor, the cross polarization time was 0.2 ms, the number of scans was 128, and the number of  $t_1$  increments was 72.

$^{31}\text{P}\{^{19}\text{F}\}$  REDOR.  $^{31}\text{P}\{^{19}\text{F}\}$  REDOR experiments<sup>25</sup> were performed in 2.5-mm rotors at a spinning frequency of 30 kHz, which avoids excessive dephasing losses and allows semi-quantitative  $^{31}\text{P}\{^{19}\text{F}\}$  distance measurements. The dephasing of  $^{31}\text{P}$  magnetization in the field of the  $^{19}\text{F}$  spins was observed.  $^{19}\text{F}$  composite  $180^\circ$  pulses were applied spaced by  $t_r/2$  during a period of  $Nt_r$  in order to recouple the dipolar interaction between  $^{31}\text{P}$  and  $^{19}\text{F}$ . EXORCYCLE was used for the single  $180^\circ$  pulse on the  $^{31}\text{P}$  channel.<sup>26</sup> The recoupling  $^{19}\text{F}$  pulses were turned off to obtain the reference signal  $S_0$ .

## Results and Discussion

**$^{31}\text{P}$  NMR: chemical bonding of phosphorus.** The  $^{31}\text{P}$  MAS NMR spectra (Figure 1a, b) of phosphatranium chloride (Phan-Cl) show a dominant centerband at an isotropic chemical shift of  $-48$  ppm with spinning sidebands (labeled with asterisks) spaced by the spinning frequency  $\omega$ . The signal was quickly dephased by the H-P dipolar coupling during gated recoupling, see Figure 1c, as expected for a P-H group (“protonated phosphorus”). The  $^{31}\text{P}$  chemical shift is close to the value of  $-43$  ppm for the phosphatranium ion in solution as reported in the literature.<sup>27</sup> Peaks at 0 ppm and +41 ppm must be assigned to impurities or

more likely degradation products due to decomposition of Phan-Cl in the presence of water; these peaks do not appear in solution spectra of fresh Phan-Cl in organic solvents.<sup>27</sup> In the spectra of the product Naf-Phan-X (Figure 1d, e), two major peaks at +41 ppm and ~ +5 ppm are observed, with an area ratio of 2:1 in the quantitative DP spectrum. The peak at 41 ppm is associated with a non-protonated phosphorus as indicated by slow CP and slow dephasing by gated recoupling (see Figure 1f). The peak near 5 ppm consists of two components (which are confirmed by  $^1\text{H}$ - $^{13}\text{C}$  correlation below): (i) a broader band at centered at 3 ppm, with significant spinning sidebands, and fast H-P dephasing indicative of P bonded to H, and (ii) the peak at 5 ppm, which shows slower H-P dephasing that may suggest a phosphorus close to a proton but with a smaller H-P dipolar coupling due to a larger internuclear distance or motional averaging. The peak at 41 ppm is assigned to Naf-Phan-X of functionality  $\text{A}^+$ . This assignment is proven below using  $^1\text{H}$ - $^{31}\text{P}$  HetCor spectra, and further supported by chemical-shift analysis. The peaks at ~5 ppm can be tentatively assigned to the  $\text{B}^+$  functionality; the ~3-ppm variation in chemical shifts might be due to different hydrogen bonding. According to the peak areas in the quantitative  $^{31}\text{P}$  NMR spectrum, the Naf-Phan-X functionality  $\text{A}^+$  accounts for 67% of the total phosphorus content in our sample.

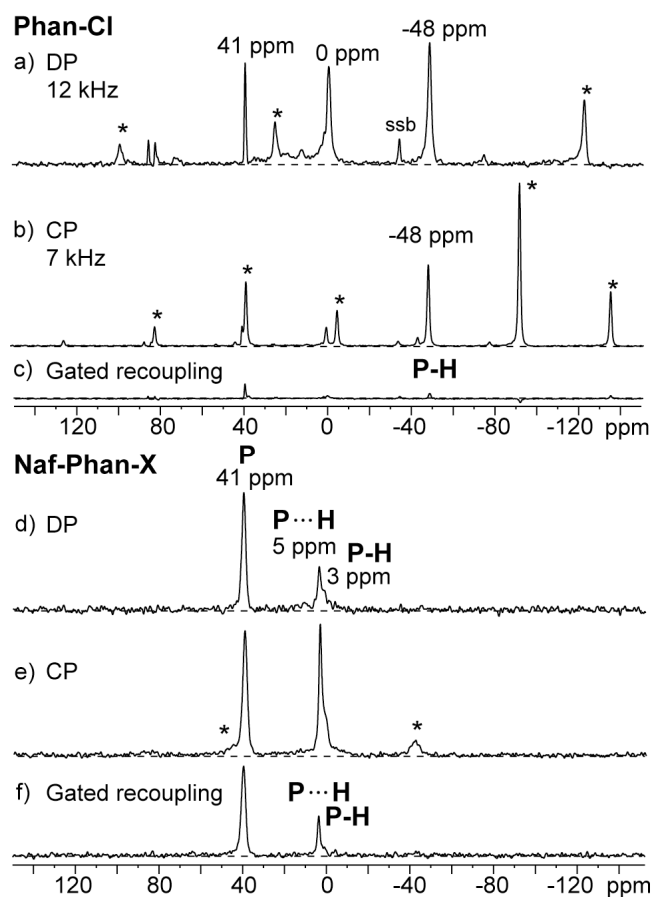


**Figure 1.**  $^{31}\text{P}$  spectra of phosphatranium chloride (Phan-Cl, a - c) and Naf-Phan-X membrane (d - f). For Phan-Cl, a) direct polarization (DP) at  $\nu_r = 12$  kHz with a recycle delay of 100 s and b)  $^1\text{H}$ - $^{31}\text{P}$  cross polarization (CP) at  $\nu_r = 7$  kHz with a recycle delay of 100 s show the centerband of the main  $^{31}\text{P}$  signal with an isotropic chemical shift of -48 ppm; its spinning sidebands are labeled with asterisks. A sideband of the +41-ppm peak is labeled “ssb”. c) CP spectrum after gated recoupling for one rotation period, which confirms that the peak at -48 ppm is the signal of a protonated phosphorus. For the Naf-Phan-X membrane, the DP spectrum d) at  $\nu_r = 12$  kHz with a recycle delay of

100 s, shows two resolved  $^{31}\text{P}$  peaks (at 41 ppm and ~5 ppm) with an area ratio of 2:1. e) CP spectrum at  $\nu_r = 7$  kHz. Sidebands of the shoulder at 3 ppm are labeled by asterisks. f) CP spectrum after gated recoupling for one rotation period.

In order to identify  $^1\text{H}$  near phosphorus, two-dimensional  $^1\text{H}$ - $^{31}\text{P}$  HetCor experiments (Figure 2) were performed with mixing times of 0.05 ms (nearest  $^1\text{H}$ ) and 50 ms ( $^1\text{H}$  within ~3 nm). For phosphatranium chloride, the proton bonded to the phosphorus resonates at 5.6 ppm,<sup>28</sup> which is shown by the stronger cross peak to the  $^{31}\text{P}$  at -48 ppm and its spinning sideband in the spectrum of Figure 2a. In the spectrum after 50 ms of spin diffusion (Figure 2b), the cross peaks for longer distance  $^1\text{H}$ - $^{31}\text{P}$  correlation, i.e. between phosphorus and protons in NH and NCH<sub>2</sub> groups ( $^1\text{H}$  chemical shift at ~3 ppm), surpass those for the direct P-H bonding, due to their larger number. The  $^1\text{H}$  band of protons in P-NH groups, whose chemical shift varies between ~ 4 and 5.1 ppm in the literature,<sup>27,28</sup> is not clearly recognizable in the 2D HetCor spectra. For Naf-Phan-X, the phosphorus at 41 ppm correlates only to the NH and NCH<sub>2</sub> protons. The phosphorus at 5 ppm seems to be close to a proton at ~10 ppm (Figure 2c), which might suggest a strongly H-bonded proton (P-H...X where X = O or N). This could occur in structure **B**<sup>+</sup>, wherein the presence of a five-membered -N-S-O-H-P- ring is conceivable. Further, a distinct set of cross peaks is seen at +3 ppm in the  $^{31}\text{P}$  dimension and ~ 6 ppm in  $^1\text{H}$ , assigned to P-H groups, confirming the presence of two components resonating near 5 ppm in the  $^{31}\text{P}$  spectrum of Naf-Phan-X. It is interesting to note that an impurity with quite similar  $^{31}\text{P}$  and  $^1\text{H}$  chemical shifts is visible in the spectrum of Phan-Cl,

see Figure 2a.

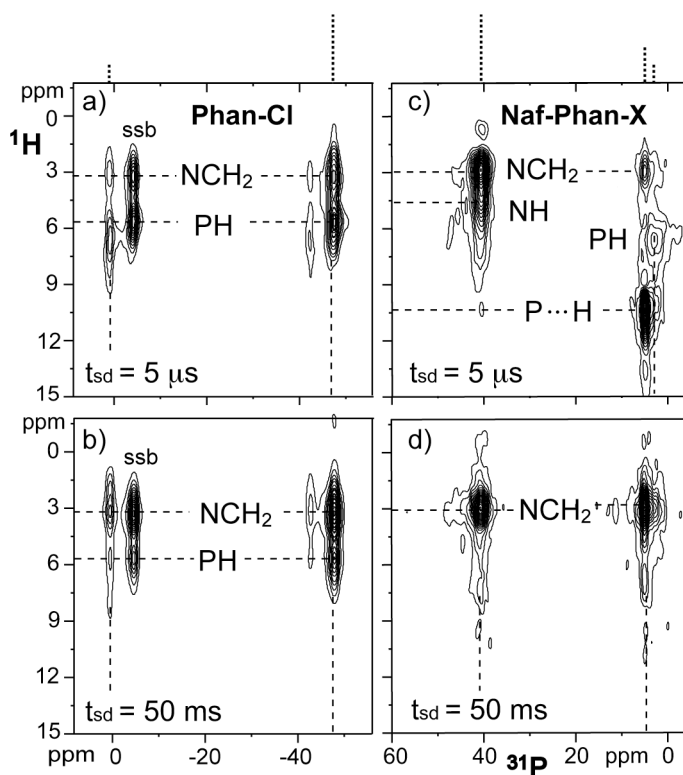


**Figure 2.**  $^1\text{H}$ - $^{31}\text{P}$  HetCor spectra of (a, b) phosphatranium chloride (Phan-Cl) and (c, d) Naf-Phan-X with a CP time of 0.7 ms and at  $\nu_r = 7$  kHz for mixing times of 5  $\mu\text{s}$  and 50 ms. For Phan-Cl, the HetCor spectra show the centerband at  $-48$  ppm in the  $^{31}\text{P}$  dimension, a spinning sideband (“ssb”) near  $-5$  ppm, and an impurity peak at  $+1$  ppm. The centerband positions are indicated by dashed lines at the top of the figure.

**$^{19}\text{F}$  and  $^{31}\text{P}\{^{19}\text{F}\}$  REDOR NMR: changes in the Nafion<sup>®</sup> sidechain.** The  $^{31}\text{P}$  NMR results have proven the change in phosphorus bonding from protonated to non-protonated for the primary product  $\text{A}^+$  in the Naf-Phan-X sample.  $^{19}\text{F}$  NMR spectra (Figure 3) show that the fluorine in  $\text{SO}_2\text{F}$  groups in the precursor Nafion-F<sup>®</sup>, which originally resonated at +46.5 ppm, have totally disappeared in the  $^{19}\text{F}$  spectrum for Naf-Phan-X membrane. This confirms that Nafion<sup>®</sup> side-chains have reacted by losing a fluorine atom. In addition, the  $^{19}\text{F}$  spectral lines have become broader, which indicates reduced mobility of the perfluoropolymer matrix <sup>29</sup>, likely due to attached large molecules.

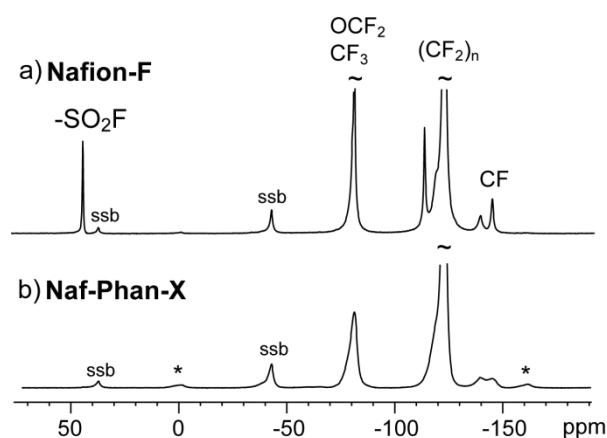


**Figure 3.**  $^{19}\text{F}$  NMR spectra of a) Nafion-F<sup>®</sup> and b) Naf-Phan-X by direct polarization at  $\nu_r = 30$  kHz. The peak of the  $^{19}\text{F}$  directly bonded to sulfur at +46.5 ppm in Nafion-F<sup>®</sup> has disappeared in the Naf-Phan-X sample. In addition, the  $^{19}\text{F}$  peaks of the Naf-Phan-X sample are broader than those of Nafion-F<sup>®</sup>, which indicates reduced mobility. Spinning sidebands of the  $(\text{CF}_2)_n$  peak are labeled “ssb” and those of the main

sidegroup signal by asterisks.

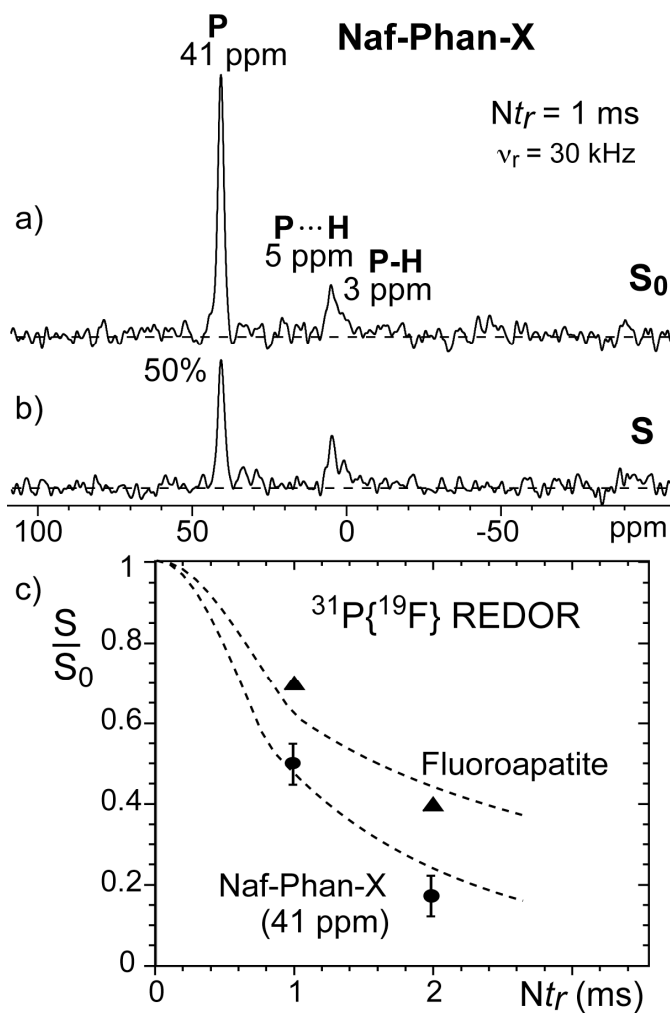


**Figure 4.**  $^{31}\text{P}\{^{19}\text{F}\}$  REDOR spectra of Naf-Phan-X at  $Nt_r = 1$  ms with recycle delay of 30 s and 256 scans. a) Reference spectrum ( $S_0$ ) and b) spectrum after recoupling ( $S$ ) which shows dephasing for  $^{31}\text{P}$  peak at 41 ppm of 50% but little, if any, dephasing for the peak at 5 ppm. c) REDOR  $S/S_0$  curve of Naf-Phan-X (circles) with comparison to fluoroapatite (triangles), which has an F–P distance of  $\sim 0.36$  nm.

Dashed lines are simulation curves, with a closest  $^{31}\text{P}$ - $^{19}\text{F}$  distance of 0.4-nm for Naf-Phan-X (further details see text).

$^{31}\text{P}\{^{19}\text{F}\}$  REDOR experiments (Figure 4) were performed to confirm the bonding between the perfluoropolymer matrix and the proazaphosphatranium cations by estimating the distance between phosphorus and fluorine. Figures 4a and 4b show  $^{31}\text{P}\{^{19}\text{F}\}$  REDOR reference ( $S_0$ ) and dephased (S) spectra, respectively, for Naf-Phan-X at  $Nt_r = 1$  ms. The  $^{31}\text{P}$  peak at 41 ppm, tentatively assigned to  $\mathbf{A}^+$  functionality from  $^1\text{H}$ - $^{31}\text{P}$  spectra, was dephased to 50%, while the peak at 5 ppm, (possibly associated with  $\mathbf{B}^+$  from  $^1\text{H}$ - $^{31}\text{P}$  spectra) showed no significant dephasing. The REDOR experiment was also run at  $Nt_r=2$  ms, where the peak at 41 ppm had dephased to about 17% (circles in Figure 4c). The dephasing rate was compared to that of fluoroapatite, a crystalline mineral solid with a F–P distance of  $\sim 0.36$  nm,<sup>30</sup> (triangles in Figure 4c). The dephasing of the phosphorus peak in Naf-Phan-X of functionality  $\mathbf{A}^+$  is faster than for the phosphorus in fluoroapatite. This suggests an F–P distance comparable to  $\sim 0.4$  nm, which corresponds approximately to a three-bond fluorine–phosphorus distance. This is confirmed by REDOR simulations, see dashed lines in Figure 4, of one  $^{31}\text{P}$  spin coupled to many  $^{19}\text{F}$  spins on a cubic lattice of 0.28-nm spacing ( $45$   $^{19}\text{F}/\text{nm}^3$ ), analogous to simulations described in ref. [31] and [32]. A time scaling factor of 0.73 was used, as determined from the fluoroapatite dephasing and consistent with the expected finite-pulse length effects (75% of a rotation period are without pulses). Adequate fits of the dephasing in Naf-Phan were obtained for a closest  $^{31}\text{P}$ - $^{19}\text{F}$  distance of  $0.4 \pm 0.1$  nm. Thus, the 41 ppm feature is again consistent with  $\mathbf{A}^+$  functionality, while the 5 ppm feature matches the



larger P-F distance of the  $\mathbf{B}^+$  functionality.

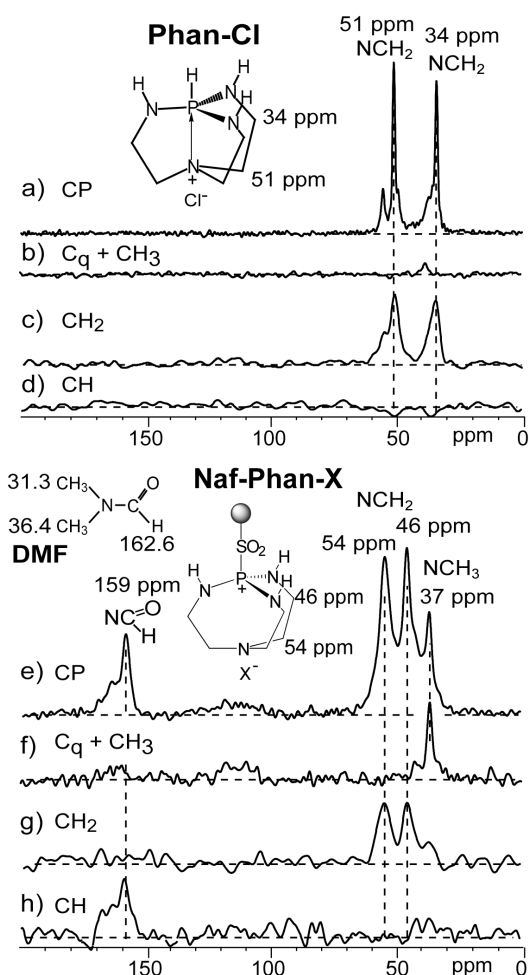


**Figure 5.**  $^{13}\text{C}$  spectra of phosphatranium chloride (Phan-Cl, a-d) and Naf-Phan-X membrane (e-h). (a, e) CP and (b, f) CP/gated decoupling experiments, run at  $\nu_r = 6.5$  kHz; (c, g) CH<sub>2</sub>- and (d, h) CH-selection experiments at  $\nu_r = 5.787$  kHz. For phosphatranium chloride, two peaks of CH<sub>2</sub> bonded to nitrogen are seen, at 34 ppm and 51 ppm. For Naf-Phan-X, the two CH<sub>2</sub> peaks shift to 46 ppm and 54 ppm, respectively. In addition, a protonated carbonyl group and a nitrogen-bonded methyl group are present in a ~1:1 ratio. These are most likely from the swelling

agent N,N-dimethyl formamide (DMF) trapped in the membrane. The structure of DMF is shown, with solution state  $^{13}\text{C}$  chemical shifts indicated.

**$^1\text{H}$ - $^{13}\text{C}$  NMR: structure of the proazaphosphatranium cation.** To ensure that the primary structure of the phosphatranium chloride has not been altered during the synthesis of the Naf-Phan-X membrane, a set of one-dimensional NMR spectra with spectral editing<sup>33,34</sup> was recorded (Figure 5). For phosphatranium chloride, the  $^{13}\text{C}$  spectra clearly show two  $\text{NCH}_2$  signals, at 34 ppm and 51 ppm. This assignment is confirmed by spectral editing that selects signals of  $\text{CH}_2$  groups, see Figure 5c. The  $^{13}\text{C}$  chemical shifts are in good agreement with literature values (see below). However, for Naf-Phan-X, four  $^{13}\text{C}$  peaks were observed. In addition to signals at 54 ppm and 46 ppm, assigned to  $\text{NCH}_2$  groups of the proazaphosphatranium cations bonded to Nafion<sup>®</sup>, additional bands are seen at 159 ppm, from a protonated carbonyl group (aldehyde,  $\text{HC}=\text{O}$ ), and at 37 ppm, from a methyl group which persists in the spectrum after gated decoupling due to motional averaging of C-H coupling by fast uniaxial rotation. The carbonyl and methyl groups are most likely from dimethylformamide (DMF), the swelling agent used, which may be trapped in the membrane. The structure and solution state  $^{13}\text{C}$  chemical shifts of DMF are shown in Figure 5. As expected, in the  $^1\text{H}$ - $^{13}\text{C}$  HetCor spectra (Figure 6) the carbonyl carbon correlates to a proton at ~8 ppm, and all other carbons correlate to  $\text{NCH}_n$  protons at ~3 ppm. Interestingly, one methyl group of DMF, which resonates at 31.3 ppm, is not observed in the  $^{13}\text{C}$  spectra of Naf-Phan-X. The second correlation of the 159 ppm  $^{13}\text{C}$  resonance to a  $^1\text{H}$  at 3 ppm is consistent with a more distant coupling to  $\text{NCH}_n$  protons, as confirmed by its relative prominence with a longer delay for spin diffusion, see Fig. 6(b).

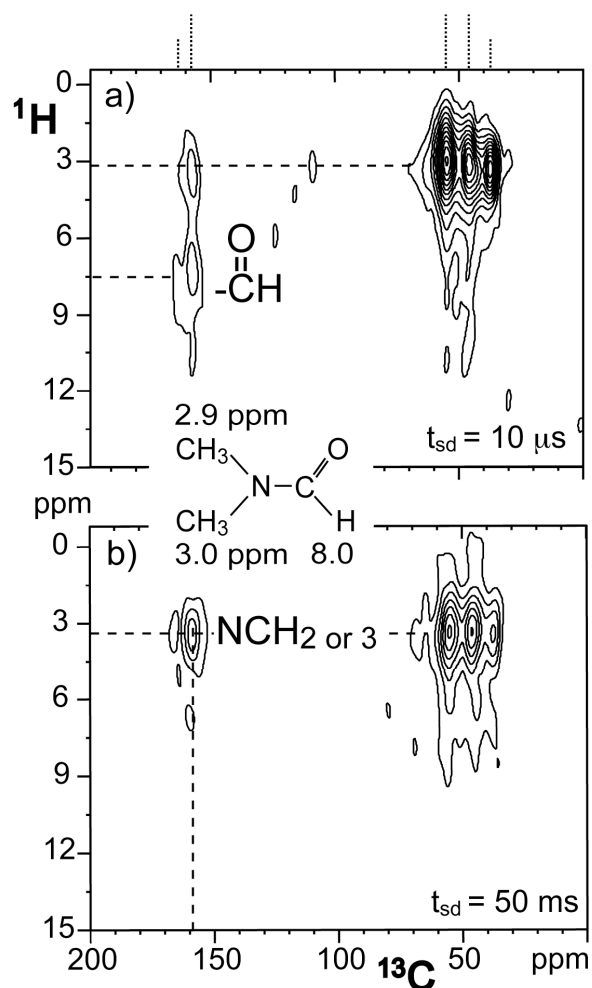


**Figure 6.**  $^1\text{H}$ - $^{13}\text{C}$  HetCor spectra of Naf-Phan-X with spin-diffusion times of a)  $10\ \mu\text{s}$  and b)  $50\ \text{ms}$  at  $\nu_r = 6.5\ \text{kHz}$ .  $^{13}\text{C}$  signal positions are indicated by dashed lines at the top of the figure. Solution state  $^1\text{H}$  NMR chemical shifts for DMF are shown with the structure.

**$^{15}\text{N}$  NMR.** The  $^{15}\text{N}$  NMR spectrum of phosphatranium chloride obtained by cross

polarization from  $^1\text{H}$  (Figure 7) shows a peak at 50 ppm (referenced to liquid  $\text{NH}_4^+$ ) from protonated nitrogen, and a peak at 37 ppm from non-protonated (tertiary) nitrogen, so assigned due to signal persistence in the CP/gated experiment, see Fig 7b. A small signal is also observed at 23 ppm, but due to limited sensitivity it is uncertain whether this is protonated or not. The relative peak areas are 1.6:1:0.5, which does not match the expected 3:1 ratio. However, it should be noted that a significant level of degradation products are detected in the  $^{31}\text{P}$  spectrum of this sample, see Figure 1a, and similar degradation might account for the 23 ppm  $^{15}\text{N}$  resonance. The signal of the protonated nitrogen has been shifted to 25 ppm in the spectrum for Naf-Phan-X (Figure 7c). No peak of non-protonated nitrogen is seen, which may be due to low cross-polarization efficiency of this tetra-coordinated nitrogen strongly diluted in the polymer matrix; the cross-polarization condition may have shifted due to power absorption by the slightly conductive sample. The  $^{15}\text{N}$  peak at 116 ppm can be assigned to an amide ( $\text{N-C=O}$ ) structure; it may come from DMF, but the nitrogen appears to be protonated ( $\text{HN-C=O}$ ).

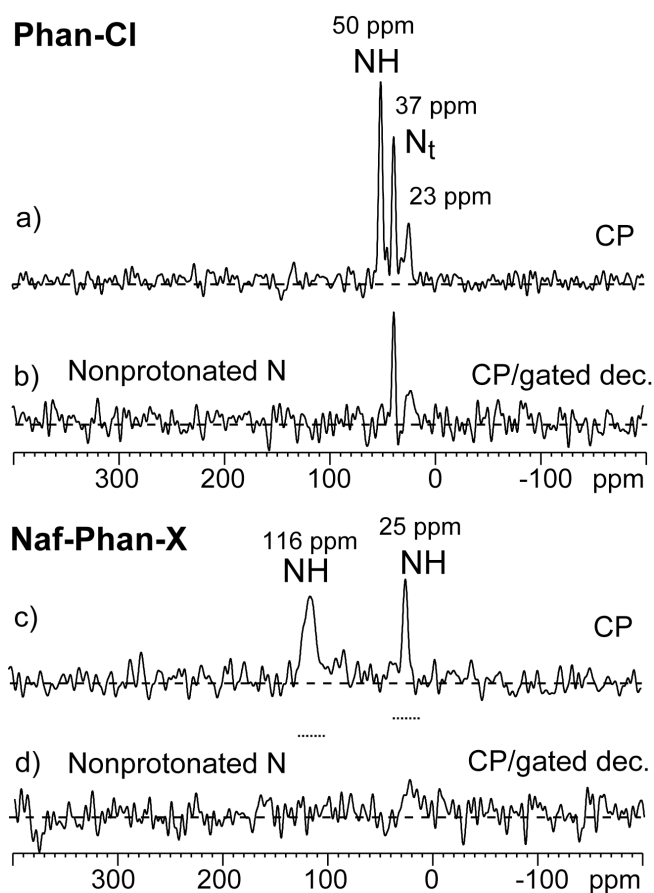


**Figure 7.**  $^{15}\text{N}$  spectra of phosphatranium chloride (a, b) and Naf-Phan-X (c, d) obtained after CP and CP with recoupled gated decoupling, respectively, at  $\nu_r = 5$  kHz. Dashed horizontal lines in d) mark the intensity expected if the N observed in c) was not protonated.

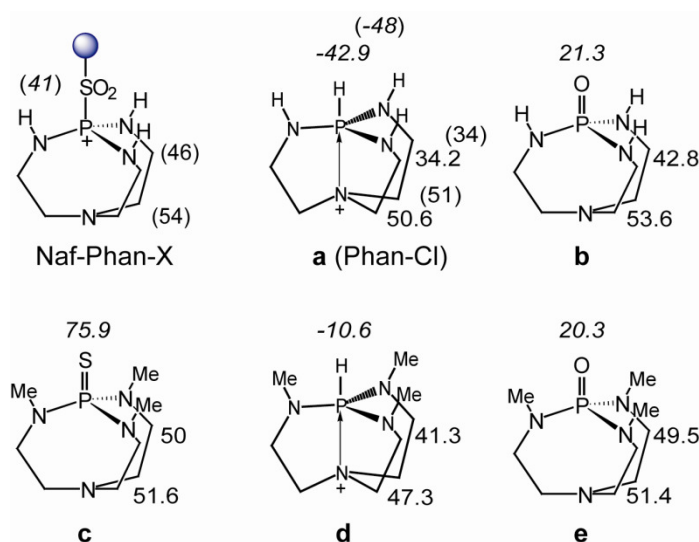


**Figure 8.** Chemical shifts of structures similar to phosphatranium chloride from reference 26.  $^{31}\text{P}$  chemical shifts are in italics, while  $^{13}\text{C}$  chemical shifts are in regular font. The results from our experiments are given in parentheses.

**Analysis of chemical shifts.** In Figure 8, literature chemical shift values<sup>27</sup> of  $^{31}\text{P}$  (in italics) and  $^{13}\text{C}$  (in regular font) are listed for phosphatranium chloride and its derivatives. For phosphatranium chloride, the literature values agree well with the results from our experiments (given in parentheses). Though none of the derivatives have the same structure as Naf-Phan-X, we can analyze them to obtain insights into chemical shift trends. For example, substituting the proton on phosphorus by a sulfur (from structure **d** to **c**) changes the  $^{31}\text{P}$  chemical shift by +87 ppm, which is similar to the change by +89 ppm from phosphatranium chloride to the chemical shift assigned to the proazaphosphatranium functionality **A**<sup>+</sup> in Naf-Phan-X. In addition, the similar  $^{13}\text{C}$  chemical shifts for structures **b**, **c**, **e** and Naf-Phan-X may

indicate elongation of the cage-like molecular structure of the proazaphosphatranium functionality  $\mathbf{A}^+$  in Nafion-Phan-X. Such elongation is relative to structures a (Phan-X) and d of Fig. 8, with their shorter P-N distances due to transannular donation of a nitrogen lone pair to phosphorous. This bonding yields correspondingly unique  $^{13}\text{C}$  shifts and a P-N distance of  $\sim 0.2$  nm, in contrast to  $\sim 0.3$  nm for structures **b**, **c** and **e**,<sup>35</sup> whose  $^{13}\text{C}$  shifts are more akin to the Naf-Phan-X system.

**Structural implications.** The new AAEM possesses several interesting features which we now discuss. Resonance structures of proazaphosphatranium cations of type  $\mathbf{A}^+$  in Scheme 2b can distribute the positive charge in the P–N bonds surrounding the phosphorus (Scheme 3). Such resonance structures minimize coulombic attractions between the cations and anions, and hence can improve the mobility of the anion. It is interesting that analogous cations representative of  $\mathbf{A}^+$  and  $\mathbf{B}^+$  {i.e.,  $[-\text{CS}(\text{O})_2\text{P}(\text{N}-)_3]^+$  and  $[-\text{CS}(\text{O})_2\text{N}(\text{C})\text{P}(\text{N}-)_2]^+$ , respectively} are completely unprecedented in the literature. The robust mechanical, oxidative, hydrolytic and thermal stability of the Nafion<sup>®</sup> framework, the diffuse distribution of positive charge and hydrolytic stability of 4-coordinate proazaphosphatranium and 5-coordinate phosphatranium cations are combined in the novel "hybrid" AAEM depicted in Scheme 2. Thus we have in a formal sense transformed Nafion<sup>®</sup> from a PEM material into a halogenide- and a hydroxide-containing AAEM. We accomplished this "ion polarity inversion" of Nafion<sup>®</sup> by a simple experimental procedure using commercially available Nafion-F<sup>®</sup> as shown in Scheme 4. The Naf-Phan-OH film may be an excellent candidate in AFC fuel cell applications according to preliminary studies showing that it retains good conductivity under strongly basic conditions as well as at elevated temperatures.

## Conclusions

A Nafion<sup>®</sup>-proazaphosphatranium/phosphatranium composite cationic film, a potential anion exchange membrane for direct methanol-based fuel cells, was successfully synthesized via a microwave process from Nafion-F<sup>®</sup> and phosphatranium chloride. Most of the latter was converted to proazaphosphatranium cations attached to the Nafion<sup>®</sup> via a P-S bond (structure **A**<sup>+</sup>), as shown by <sup>31</sup>P{<sup>1</sup>H}, <sup>19</sup>F, and <sup>31</sup>P{<sup>19</sup>F} REDOR NMR. These ionophores have a reduced charge density due to resonance structures that distribute positive charge to diminish ionic interaction, which should facilitate hydroxide ion mobility. Electrical measurements to complement the present structural study and further test these hypotheses are underway. The 4-coordinate stereochemistry of phosphorus in the novel proazaphosphatranium cation was substantiated by <sup>13</sup>C and <sup>15</sup>N NMR. About 1/3 of phosphatranium is converted into two other structures, with S not bonded to P but most likely to N as in structure **B**<sup>+</sup>. In addition, moieties derived from the solvent, DMF, were found in the final product. Efforts to inhibit formation of these impurities are underway.

## Acknowledgements

Work by XK and KSR at the Ames Laboratory was supported by the Department of Energy – Basic Energy Sciences under contract number DE-AC02-07CH11358. Work by KW and JGV was supported by the Department of Defense AFRL under contract number FA8650-05-C-2541.

## References

1. Chu, D.; Jiang, R. *Solid State Ionics* **2002**, *148*, 591.



2. Dyer, C. K. *J. Power Sources* **2002**, *106*, 31.
3. Chang, H.; Kim, J. R.; Cho, J. H.; Kim, H. K.; Choi, K. H. *Solid State Ionics* **2002**, *148*, 601.
4. Meyers, J. P.; Maynard, H. L. *J. Power Sources* **2002**, *109*, 76.
5. *Eye for Fuel Cells conference on Fuel Cells for Portable Applications* Hilton Back Bay, Boston, MA, USA, September 5th-6th **2002**.
6. Ren, X.; Zelenay, P.; Thomas, S.; Davey, J.; Gottesfeld, S. *J. Power Sources* **2000**, *86*, 111.
7. Raadschelders, J. W.; Jansen, J. *J. Power Sources* **2001**, *96*, 160.
8. Varcoe, J. R.; Slade, R. C. T., *Fuel Cells* **2005**, *5*, 187.
9. Lamy, C.; Belgsir, E. M.; Leger, J.-M., *J. Appl. Electrochem.* **2001**, *31*, 799.
10. Tripkovic, A. V.; Popovic, K. D.; Grgur, B. N.; Blizanac, B.; Ross, P. N.; Markovic, N. M., *Electrochim. Acta*, **2002**, *47*, 3707.
11. Yu, E. H.; Scott, K.; Reeve, R. W., *J. Electroanal. Chem.* **2003**, *547*, 17.
12. Gamburgzev, S.; Petrov, K.; Appleby, C. L., *J. Appl. Electrochem.* **2002**, *32*, 805.
13. Wagner, N.; Schulze, M.; Gulzow, E., *J. Power Sources* **2004**, *127*, 264.
14. Schulze, M.; Gulzow, E., *J. Power Sources* **2004**, *127*, 252.
15. McLean, G. F.; Niet, T.; Prince-Richard, S.; Djilali, N. *Int. J. Hydrogen Energy* **2002**, *27*, 507.
16. Schulze, M.; Gulzow, E., *J. Power Sources* **2004**, *127*, 243.
17. Cifrain, M.; Kordesch, K. V., *J. Power Sources* **2004**, *127*, 234.
18. Danks, T. N.; Slade, R. C. T.; Varcoe, J. R. *J. Mater. Chem.* **2002**, *12*, 3371.
19. Sun, L.; Thrasher, J.S. *Polymer Degradation and Stability* **2005**, *89*, 43.

20. Schmidt-Rohr, K.; Chen, Q. *Nature Materials* **2008**, *7*, 75.
21. Laramay, M. A. H.; Verkade, J. G. Z. *Anorg. Allg. Chem.* **1991**, *605*, 163-174
22. Bielecki, A.; Burum, D. P.; Rice, D. M.; Karasz, F. E. *Macromolecules* **1991**, *24*, 4820.
23. Clauss, J.; Schmidt-Rohr, K.; Spiess, H. W. *Acta Polymer.* **1993**, *44*, 1.
24. Bielecki, A.; Kolbert, A.C.; de Groot, H. J. M.; Griffin, R. G.; Levitt, M. H. *Adv. Magn. Reson.* **1990**, *14*, 111.
25. Gullion, T.; Schaefer, J. J. *Magn. Reson.* **1989**, *81*, 196.
26. Sinha, N.; Schmidt-Rohr, K.; Hong, M. J. *Magn. Reson.* **2004**, *168*, 358.
27. Galasso, V. J. *Phys. Chem. A* **2004**, *108*, 4497-4504.
28. Reddy, C. R. V.; Verkade, J. G. *J. Org. Chem.* **2007**, *72*, 3093.
29. Chen, Q.; Schmidt-Rohr, K. *Macromolecules* **2004**, *37*, 5995.
30. Nikcevic, I.; Jokanovic, V.; Mitric, M.; Nedic, Z.; Makovec, D.; Uskokovic, D. J. *Solid State Chem.* **2004**, *177*, 2565.
31. Rawal, A.; Wei, X.; Akinc, M.; Schmidt-Rohr, K., *Chem. Mat.* **2008**, *20*, 2583.
32. Schmidt-Rohr, K.; Rawal, A.; Fang, X.-W., *J. Chem. Phys.* **2007**, *126*, 05401-(1-16).
33. Schmidt-Rohr, K.; Mao, J.-D. *J. Am. Chem. Soc* **2002**, *124*, 13938.
34. Mao, J.-D.; Schmidt-Rohr, K. *J. Magn. Reson.* **2005**, *176*, 1.
35. Verkade, J. G. In *New Aspects of Phosphorus Chemistry II*, *Top. Curr. Chem.* Majoral, J. P. Ed., **2002**, *233*, 1.

**CHAPTER 8. SYNTHESIS OF LINEAR OR BRANCHED POLYMERS  
POSSESSING CHEMICALLY BONDED PHOSPHATRANIUM NITRATE AS  
EFFICIENT NITRATE CONDUCTING MEMBRANES**

Kuldeep Wadhwa and John G. Verkade

In Collaboration with Energetics Inc.

**Objective**

Synthesize materials that possess high nitrate ion mobility for anionic electrically conducting membranes containing linear or branched polymers bearing cationic phosphatranium cations bonded to the backbone framework (Figure 1) with nitrate counter ions ( $X^-$ ).

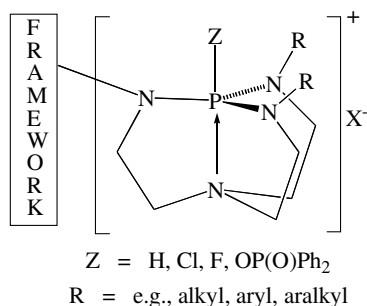


**Figure 1.** Polymer Bound Phosphatranium Salt

**Introduction**

Fuel cells using either metal hydrides or methanol solutions have seen significant research and development in recent years. The Direct Methanol Based Fuel Cell (DMFC) is the dominant candidate to replace the Li-ion battery.<sup>1-4</sup> Several companies are already involved in the R & D of fuel cell technologies for providing power to portable electronic

instruments. However, none of these firms are developing direct-oxidation ammonia fuel cells because of the technical and environmental issues associated with this approach.<sup>5-10</sup> Considerable attention has been focused in recent years on research on the DMFC. However, current DMFC technology requires high catalyst loading of precious metals such as Pt and Ru, and an expensive cationic membrane. Methanol is one of the most electroactive organic fuels in the low temperature range mainly because it has low carbon content, it possesses a readily oxidizable group (hydroxyl) and it has high solubility in aqueous electrolytes. The advantages of the DMFC are that methanol is a liquid which is quite soluble in water, thus reducing concentration polarization problems associated with gaseous fuels; methanol is cheap and easy to handle and store, and it has good electroactivity even though it is an organic fuel. Aqueous ammonia solutions have not been considered to date for fuel cells, even though the good energy potential and hydrogen-storage density of ammonia is widely recognized.<sup>11-13</sup> Ammonia is nitrogen hydride which is cheaply manufactured in bulk. Ammonia is the second largest synthetic commodity product of the chemical industry, with world production exceeding 140 million metric tons. Although ammonia is a toxic noxious gas, ammonia and its derivatives are potential fuels for portable fuel cells. Thus ammonia is a major source of hydrogen, containing 17.6% by weight of hydrogen in its anhydrous state.<sup>14</sup>

Forty-five percent of the world's ammonia production is used to manufacture urea (carbamide). Urea is a major worldwide source of ammoniacal fertilizer, which is environmentally benign and safe in transit and storage. Ammonia derived from urea is a low-cost, readily available, environmentally clean, high-density hydrogen storage medium. Urea contains 8.7 wt% H<sub>2</sub>. There exists an extensive knowledge base in industry for the hydrolysis of urea to ammonia. The cost per kWh for ammonia is comparable to methanol,

and lower than high purity hydrogen. Carbamide (urea) solutions are safe, benign, transportable and environmentally acceptable sources of ammonia.

The proposed Carbamide Fueled Electrochemical Cell (CFC) (Figure 2) has several advantages including:

- Higher energy density, particularly the higher efficiency of alkaline fuel cells [as compared to acid electrolyte methanol fuel cells and hydrogen-based proton exchange membrane (PEM) fuel cells].
- The activation polarization of CFC's is substantially lower than methanol in a DMFC.
- The CFC exhibits significant advantages over the Nickel Metal Hydride, Zinc-Air, and Lithium-Ion / Lithium Polymer battery systems, owing to their higher energy and power density, easy replenishment of fuel, and lower costs.
- The CFC provides significant advantages over other primary hydride-based fuel cells using metal hydrides and borohydrides in terms of cost, safety and environmental considerations.

The development of a direct-oxidation, high energy density, carbamide-derived aqueous-ammonia electrochemical cell (CFC) takes advantage of the high hydrogen content of the ammonia molecule (17.6 wt%) and its high electrochemical reactivity in alkaline media to improve energy density. This technology solves both technical and environmental hurdles by providing a novel integration of existing technology (the use of enzymes to liberate ammonia benignly from urea in bio-reactors) and new technologies (anionic membranes with high conductivity, ammonia coordination chemistry for low activation energy losses, non-noble

catalysts for lower costs, and a novel electrochemistry to yield high cell voltages). This will result in a high-energy, high-power density battery / fuel cell system.

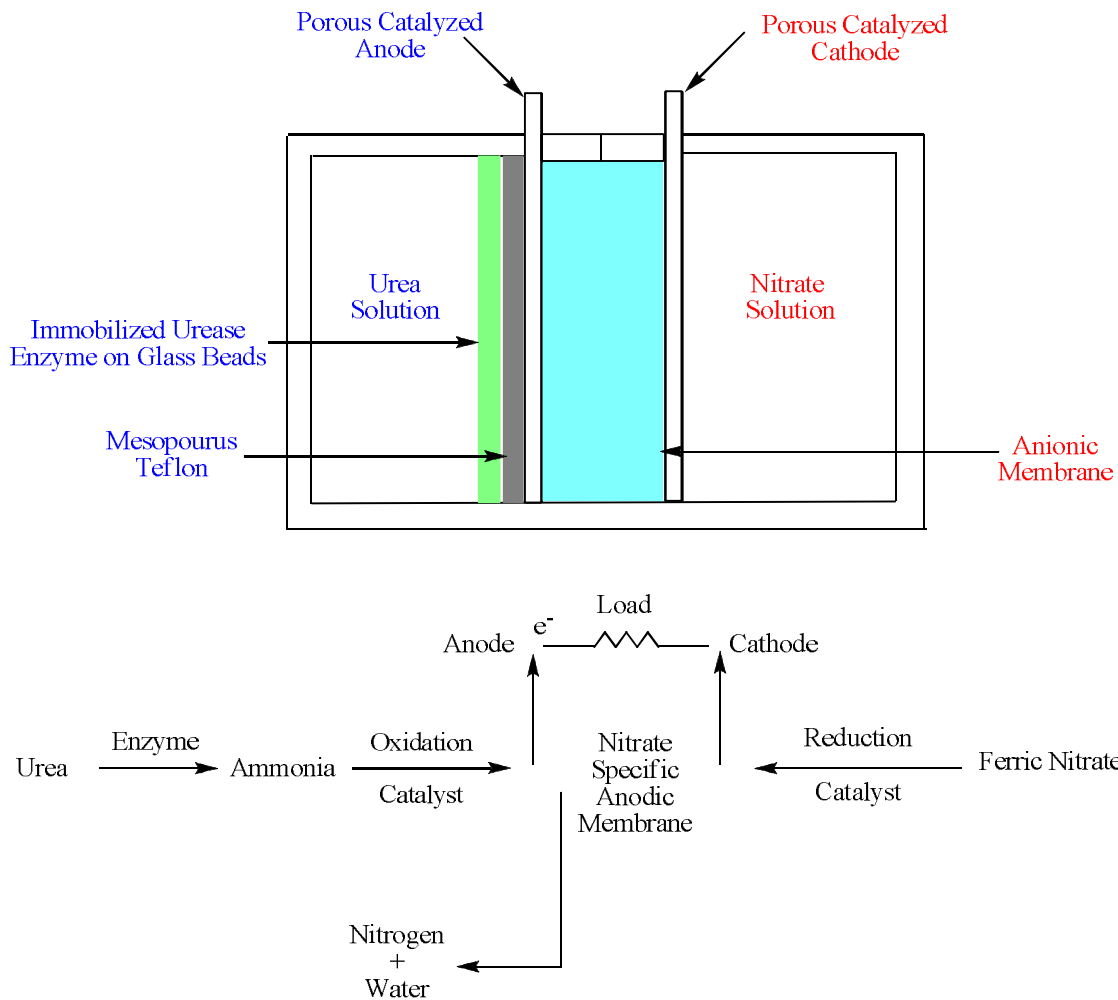


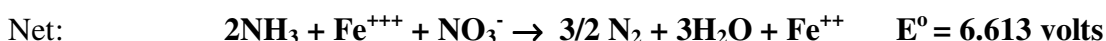
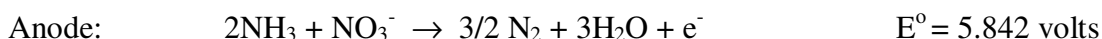
**Figure 2.** Conceptual Carbamide Fueled Electrochemical Cell (CFC)

There are several technical and environmental risks associated with the proposed CFC:

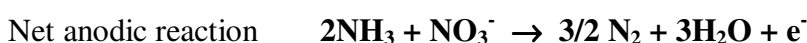
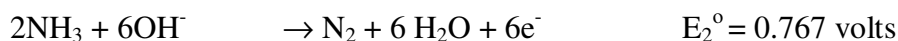
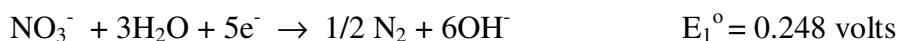
- The conversion of carbamide to ammonia, with high efficiency / throughputs, and its safe containment, involves major engineering and scientific challenges.

- The low ideal voltages for ammonia oxidation reported in literature need to be appreciably improved by at least a factor of two, for successful commercialization of these fuel cells, thus requiring new cell chemistry for such improvements.
- Low ionic conductivities in current anionic membranes have limited their applications in fuel cells, and will need to be improved by a factor of one hundred.
- The high costs of catalysts and their high loading in the electrodes of current fuel cells will need to be decreased by a factor of one hundred for successful commercialization.

**Proposed cell chemistry:** The successful Air Force-funded proposal generated in collaboration with Energetics Inc involved the use of ferric nitrate as the oxidizer/catholyte, nitrate-selective salts / membranes as a solid polymer electrolyte, and cuprated carbamide solutions (with urease-immobilized membranes) as the anolyte (for safe and benign ammonia generation). The expected fuel cell reactions are as follows:



The anodic reaction consists of the following sub-reactions:



Since there is a net loss of electrons, the thermodynamic voltage for the net reaction can be determined as follows using free energy calculations:

$nE^{\circ} = 5E_1^{\circ} + 6E_2^{\circ} = 5(0.248) + 6(0.767) = 5.842 \text{ v}$ , where  $n = 1$ . Therefore,  $E^{\circ} = 5.842 \text{ volts}$ .

The preferred electrolyte for the above described fuel cell chemistry would be a solid polymer anion exchange membrane. The following anionic membranes were tested by Energetics in the past, and their comparison to Nafion<sup>®</sup> is also shown in the table below. The main technical hurdles were membrane thickness and aerial resistance. If improved specific conductivity can be achieved, the higher efficiency of anionic fuel cells would be an enormous advantage to the proposed CFC.

Manufacturer	Designation	Aerial Resistance (ohm- cm <sup>2</sup> )	Thickness (microns)
Membranes Intl.	AMI-7001	22 +/- 1	457.2
Electropure Excellion	I-200	5-10	320-340
Sybron Chemicals	MA-3475	25	400
DuPont Chemicals	<i>Nafion</i> <sup>®</sup>	<b>0.05</b>	<b>50</b>

In order to synthesize materials that possess high nitrate mobility for membranes and chemically modified electrodes, our objective was to synthesize linear polymers containing



phosphatranium derivatives bonded to the backbone framework (as shown schematically in Figure 1) in which the anion  $X^-$  is nitrate. In Figure 3 is shown the variety of bicyclic precursors, the vast majority of them having been made for the first time in our laboratories.

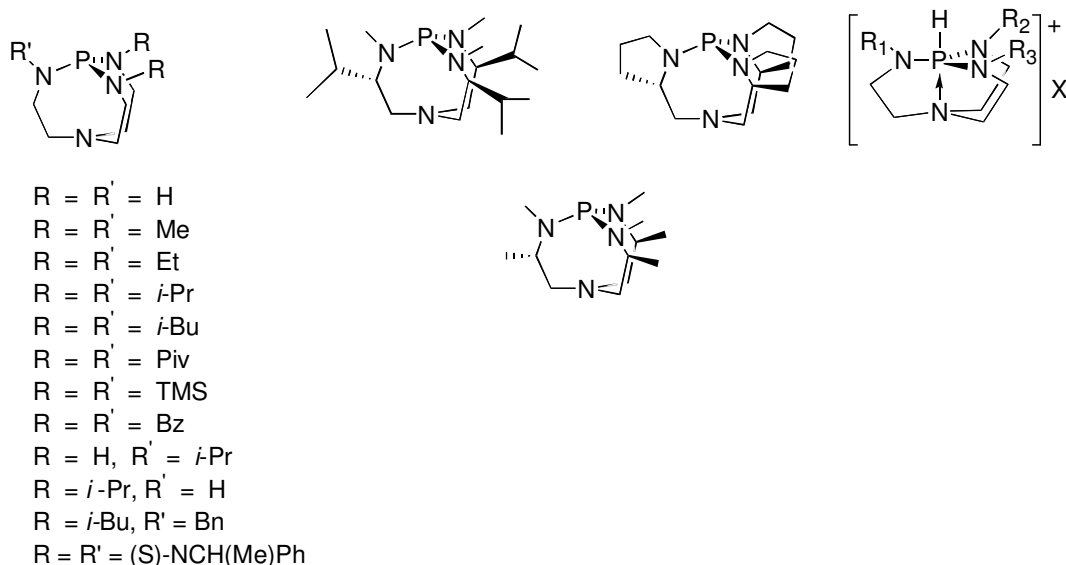


**Figure 3.** Structure of various proazaphosphatranes and phosphatranium ions

All of the proazaphosphatrane precursors are readily converted to the phosphatranium salts in which the phosphorus is protonated as depicted on the right side of Figure 3. Because these phosphatranium cations are very weak acids (having  $\text{pK}_a$  values of 33 to 34 in acetonitrile)<sup>15</sup> the precursors shown are very strong bases; a property which has led us to uncover a very rich chemistry of these species in effecting a wide variety of important Arrhenius or Lewis base-dependent organic reactions both stoichiometrically and catalytically.<sup>16</sup> It may be noted, that we have, in a single step, synthesized several examples of phosphatranium salts in which the axial H substituent is replaced by F, Cl or  $\text{OP}(\text{O})\text{Ph}_2$  which also were shown to exhibit strong transannular  $\text{N} \rightarrow \text{P}$  bonds. We were also successful in chemically bonding to a Merrifield resin in one step, a phosphatranium cation of the type

shown in Figure 3 where  $X^-$  is nitrate.<sup>17</sup> That work was aimed at carrying out aza-Michael and thia-Michael reactions catalyzed by nitrate. This was very successful and it was found that the polymeric catalyst is very stable and highly recyclable. Even when the catalyst dies, it is readily regenerated. The results of this work showed that the nitrate in our resin is superior to that in commercially available nitrate anion exchange resins, and we attribute this improved action to the poor anion-cation interaction in our phosphatranium salts.

The justification for the use of phosphatranium cations of the type shown in Figure 1 is that there is a large body of experimental evidence garnered over the past ten years supporting the following four conclusions:

1) The cations represented in the structure shown in Figure 3 are very robust to air and moisture owing in large measure to their chelated strainless configuration and the existence of the very stabilizing bridgehead-bridgehead nitrogen-to-phosphorus bond.

2) Anions are effectively inhibited from forming interactive ion pairs with these types of cations, owing to extensive resonance delocalization of the positive charge among the four nitrogens and the phosphorus in the cage moiety of the cation shown in Figure 4.

3) Phosphatranium ions can be “decorated” with a wide variety of substituents on the cage core.

4) The upper axial substituent on the phosphatranium cation can be not only a hydrogen, but also a chlorine or a phosphinate group

Conclusion 1 bodes well for stability of the systems we proposed to investigate, and conclusions 3 and 4 offer possibilities for increasing stability through steric hindrance of the

phosphatranium skeleton. Conclusion 2 bodes well for unimpeded membrane transport and hence providing high conductivity of nitrate anions in our proposed system.

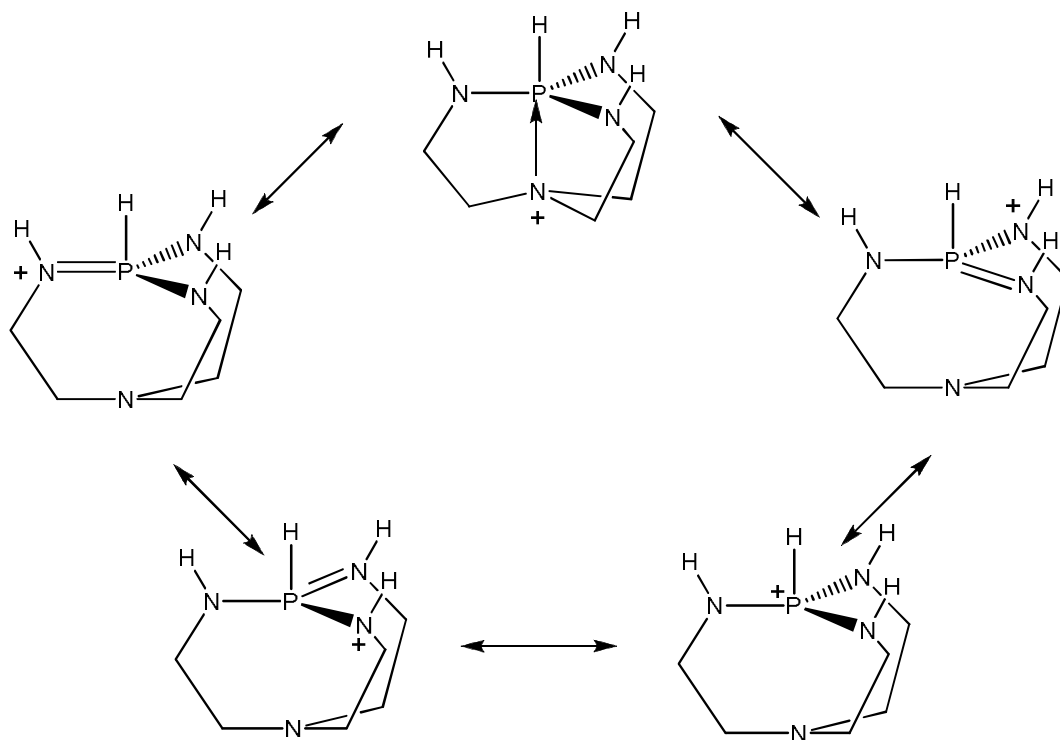
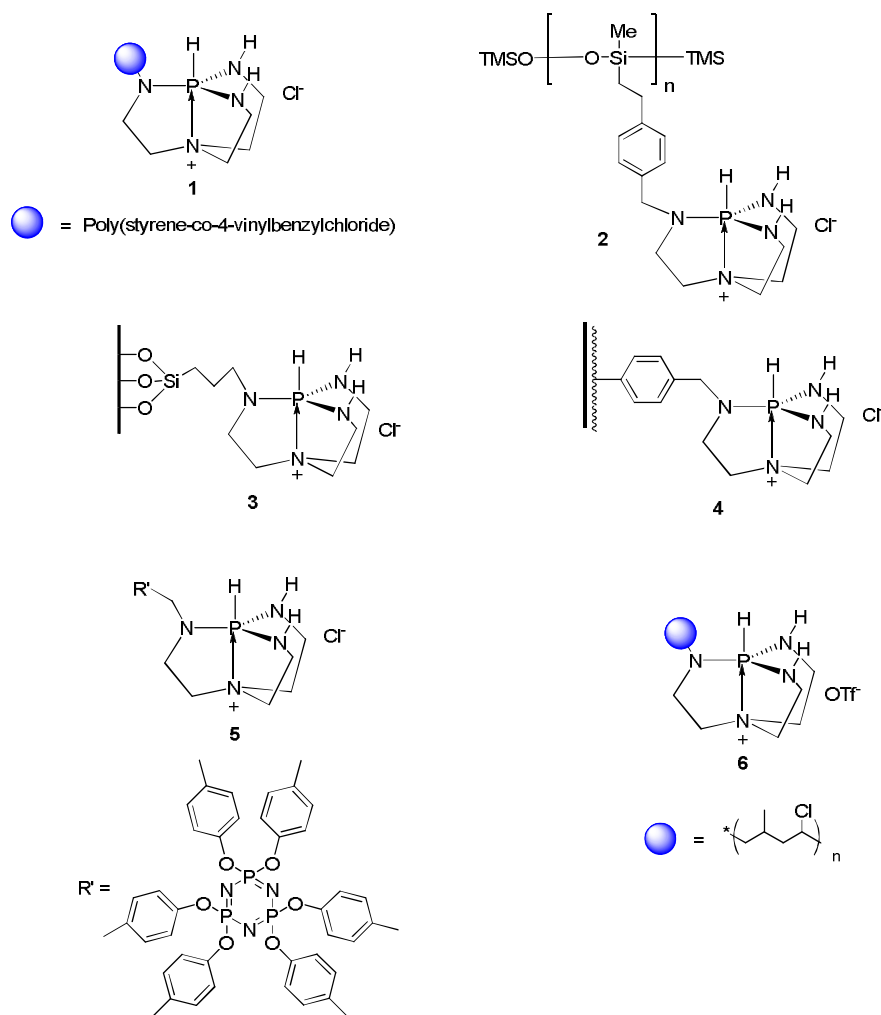


**Figure 4** Resonance structures for a phosphatranium ion

Our objective for developing a suitable conducting film for a membrane or chemically modified electrode entailed two strategies:

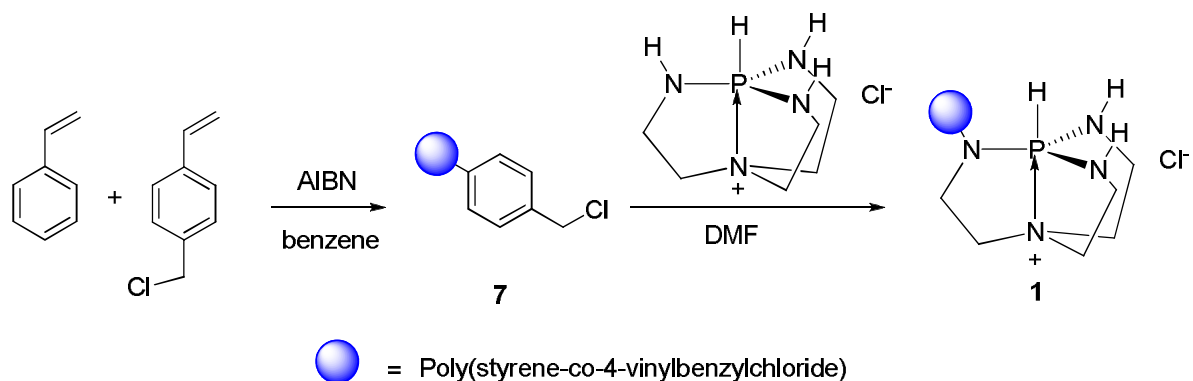
- 1) Development of a nitrate salt that will meet the requirements for withstanding the temperature and the aqueous, basic and oxidative environment of the fuel cell for the period of time required.
- 2) Development of a polymer backbone that will also meet the requirements for withstanding the temperature and the aqueous, basic and oxidative environment of the fuel cell for the period of time required.

We used various polymeric backbones containing benzyl chloride or alkyl chloride functionalities to attach trihydrophosphatranium chloride to the polymeric backbone via C-N linkages. We synthesized cationic polymer membranes **1-6** as shown in Figure 5 and then tested them for their conductive properties.



. **Figure 5.** Structure of cationic polymers

## Experimental



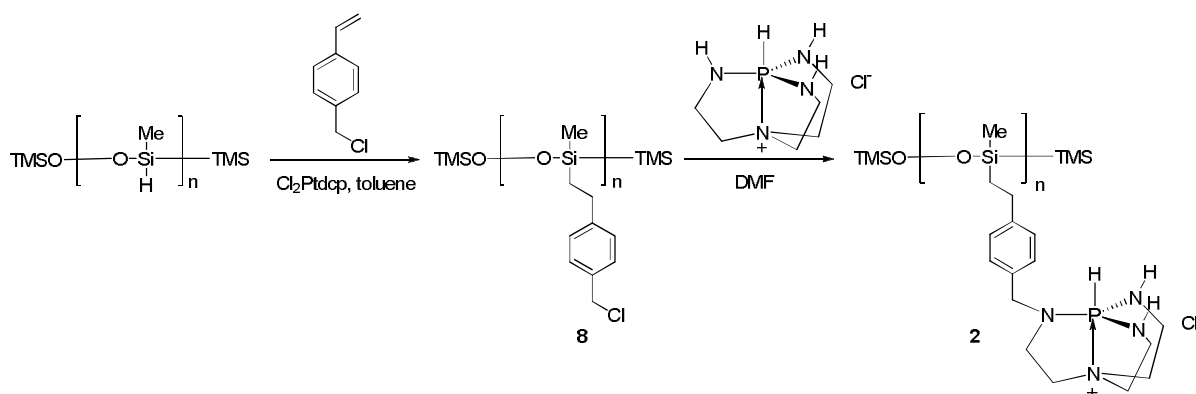
**Scheme 1.** Synthesis of **1**

**Synthesis of 7:** Polymer backbone **7** was synthesized (Scheme 1) according to a literature procedure.<sup>18</sup> To a solution of styrene (20.0 g, 194 mmol) and 4-(chloromethyl)styrene (0.91 g, 6 mmol) in benzene (70 mL) was added 2,2'-azobisisobutylnitrile (AIBN) (0.16 g, 1 mmol). The vessel was purged of oxygen using a vacuum/nitrogen evacuation flushing cycle (3 times) and then the solution was stirred at 70 °C for 40 h. The mixture was poured into methanol drop wise to obtain a THF soluble chloromethylated polystyrene **7** (Cl = 0.3 mmol/g via elemental analysis).

**Synthesis of 1a:** To the solution of chloromethylated polystyrene **7** (1 g, 0.3 mmol chlorine/g) and trihydrophosphatranium chloride (0.084 g, 0.4 mmol) in dry DMF (20 mL) was added triethylamine (0.04 g, 0.4 mmol). The vessel was purged of oxygen using a vacuum/nitrogen evacuation cycle (3 times) and the solution was stirred at 110 °C for 72 h (Scheme 1). The mixture was poured into methanol drop wise to obtain DMF/MeOH (1:1)-

soluble polymer-bound phosphatrane chloride **1a** in quantitative yield. This product was then washed with aq. NaNO<sub>3</sub> solution to replace the chloride ions with nitrate anion.

**Synthesis of 1b:** To the solution of chloromethylated polystyrene **7** (3 g, 0.3 mmol of chlorine/g) and trihydrophosphatranium chloride (1.44 g, 6.8 mmol) in dry DMF (20 mL) was added triethylamine (6.8 mmol). The vessel was purged of oxygen using a vacuum/nitrogen evacuation cycle (3 times) and the solution was stirred at 110 °C for 72 h (Scheme 1). The mixture was poured into methanol drop wise to obtain soluble polymer bound phosphatrane chloride **1b** in quantitative yield. This was then washed with aq. NaNO<sub>3</sub> solution to replace the chloride ions with nitrate anion.

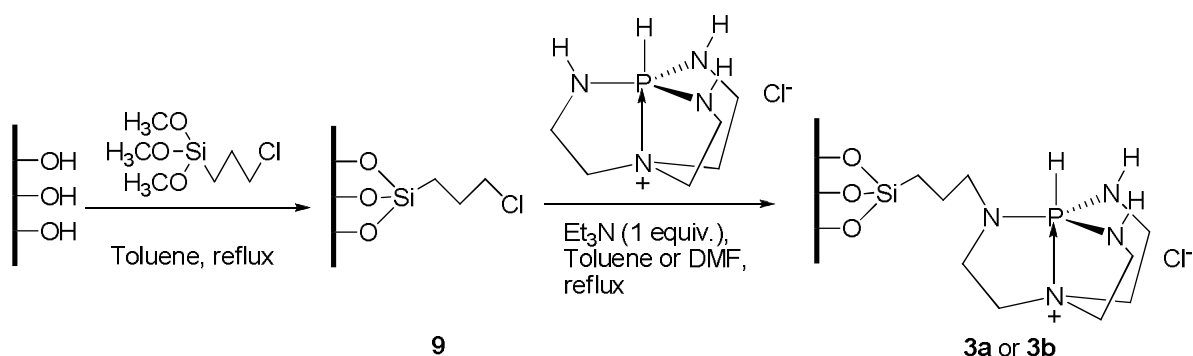


**Scheme 2.** Synthesis of **2**

**Synthesis of 8:** To a solution of poly(methylhydrosiloxane) (PMHS, 0.2-0.3M, 1 equiv.) under argon, was added 4-vinylbenzylchloride (1.3 equiv.) followed by dichlorodi(cyclopentadienyl)platinum(II) (1 mg) as a catalyst (Scheme 2). The mixture was stirred at 60–65 °C for 40 h. The reaction mixture was then cooled to room temperature after which the reaction mixture was added drop-wise into a large volume (ca 50 mL) of hexanes. The precipitate was collected via centrifugation/decantation. Then the precipitated polymer

was collected and dissolved in the minimum amount of THF needed to dissolve the crude polymer completely. The polymer was re-precipitated in hexanes for a repeat of the purification process after which this process was repeated 2–3 times to remove monomer from the crude polymer. Residual solvents were removed under reduced pressure (Cl content = 3.7 mmol/g via elemental analysis).

**Preparation of 2:** To a solution of **8** (3.2 g, 3.7 mmol/g via elemental analysis) in toluene was added trihydrophosphatranium chloride (4.62 g, 22 mmol) followed by triethylamine (2.2 g, 22 mmol) (Scheme 2). The solution was refluxed for 3 days and then the mixture was cooled to room temperature and the product was added drop-wise to excess methanol. The product was filtered, washed with methanol and dried under vacuum to obtain **2**.



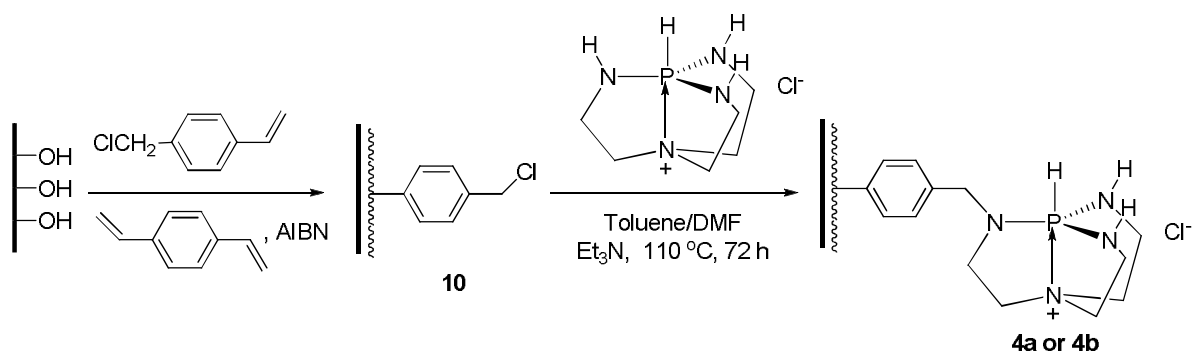
**Scheme 3.** Synthesis of **3a** and **3b**

**Synthesis of 9:** Functionalized silica **9** was prepared according to a literature procedure (Scheme 3).<sup>19</sup> a suspension of 5.96 g of (3-chloropropyl)trimethoxysilane and 20 g of activated silica gel<sup>20</sup> in 100 mL of dry toluene was refluxed with stirring. After 1.5 h ca 25 mL methanol containing some toluene was distilled from the mixture. After an additional hour of refluxing, an additional 25 mL methanol–toluene was distilled out. Finally the

mixture was refluxed for one hour, cooled and filtered, and then the silica was washed several times with skelly F and air dried (Cl content = 1.29 mmol/g via elemental analysis).

**Synthesis of 3a:** Trihydrophosphatranium chloride (1.05 g, 5 mmol) was reacted with 2 g of **9** (Scheme 3) in refluxing toluene for 3 days in the presence of triethylamine (0.5 g, 5 mmol). After cooling to room temperature, the reaction mixture was filtered and the solid product was washed with THF, methanol and ether.

**Synthesis of 3b:** Phosphatranium chloride (1.05 g, 5 mmol) was reacted with 2 g of **9** (Scheme 3) in refluxing DMF for 3 days in the presence of triethylamine (0.5 g, 5 mmol). After cooling to room temperature, the reaction mixture was filtered and the solid product was washed with THF, methanol and ether.



**Scheme 4.** Synthesis of **4a** and **4b**

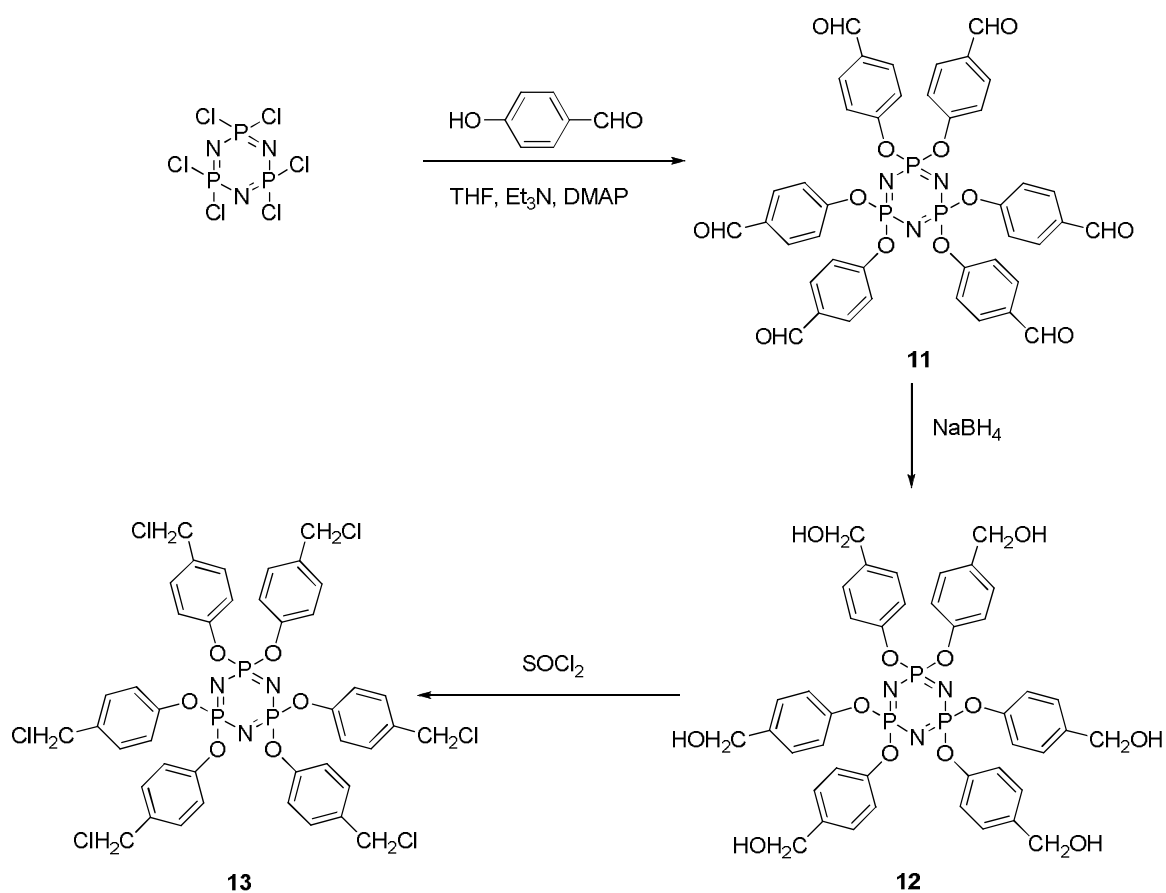
**Synthesis of 10:**<sup>21</sup> Activated silica gel<sup>21</sup> 10 g (Scheme 4) was immersed in a DMF solution (6 mL) containing chloromethylstyrene (6.6 g), divinylbenzene (0.7 g) and AIBN (0.1 g). The mixture was allowed to stand for 30 min while cooling at -5 °C and then filtered. The vinyl monomers on the silica surface were copolymerized by heating the beads at 80 °C for 5



h under Ar atmosphere. The product was washed with benzene for 6 h in a Soxhlet extractor and dried under reduced pressure (Cl content = 1.40 mmol/g via elemental analysis).

**Preparation of 4a:** A mixture of trihydrophosphatranium chloride (1.16 g, 5.54 mmol), **10** (2 g) and triethylamine (0.554 g, 5.54 mmol) was heated in toluene at 110 °C for 72 h (Scheme 4). The solid product was filtered off after cooling the reaction mixture to room temperature and washed with copious amounts of THF, methanol and ether.

**Preparation of 4b:** A mixture of trihydrophosphatranium chloride (1.16 g, 5.54 mmol), **10** (2 g) and triethylamine (0.554 g, 5.54 mmol) was heated in DMF at 110 °C for 72 h (Scheme 4). The solid product was filtered off after cooling the reaction mixture to room temperature and washed with copious amounts of THF, methanol and ether.



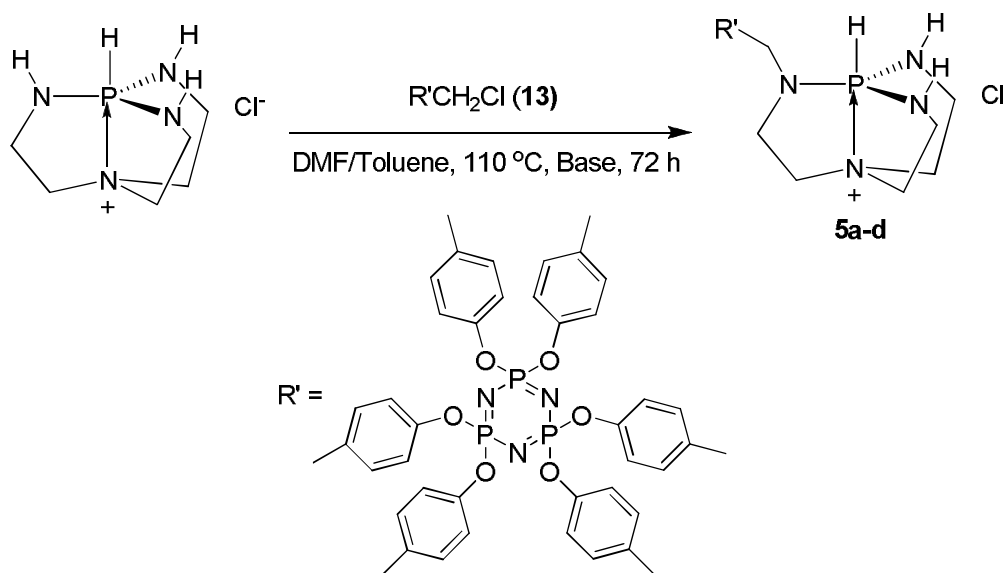
**Scheme 5.** Synthesis of 13

**Synthesis of Hexakis(4-formylphenoxy)cyclotriphosphazene 11:**<sup>22</sup> To a solution of hexakischlorophosphazene (10.2 g, 0.03 mol) in THF was added a solution of *p*-hydroxybenzaldehyde (23 g, 0.19 mol) and triethylamine (24.1 g, 0.24 mol) in THF. The mixture was refluxed for 48 h. After filtration, the solvent was removed under reduced pressure and the residue was recrystallized to give hexakis(4-formylphenoxy)cyclotriphosphazene 11.

**Synthesis of Hexakis(4-hydroxymethylphenoxy)cyclotriphosphazene 12:**<sup>22</sup> To a solution of hexakis(4-formylphenoxy)cyclotriphosphazene 11 (2 g, 2.3 mmol) in THF-MeOH (140

mL, 1:1) was added sodium borohydride (0.56 g, 15 mmol) at room temperature (Scheme 5). The reaction mixture was stirred overnight at room temperature. After evaporation of the solvents, the resulting solids were recrystallized from 90% ethanol to give 1.5 g (75% yield) of hexakis(4-hydroxymethylphenoxy)cyclotriphosphazene **12**.

**Synthesis of Hexakis(4-chloromethylphenoxy)cyclotriphosphazene **13**:**<sup>22</sup> To a solution of hexakis(4-hydroxymethylphenoxy)cyclotriphosphazene **12** (5.0 g, 5.7 mmol) was added thionyl chloride (82 g, 0.69 mol). The solution was stirred at room temperature for 24 h (Scheme 5) and after removal of excess of thionyl chloride under reduced pressure, the product was recrystallized from chloroform in quantitative yield.

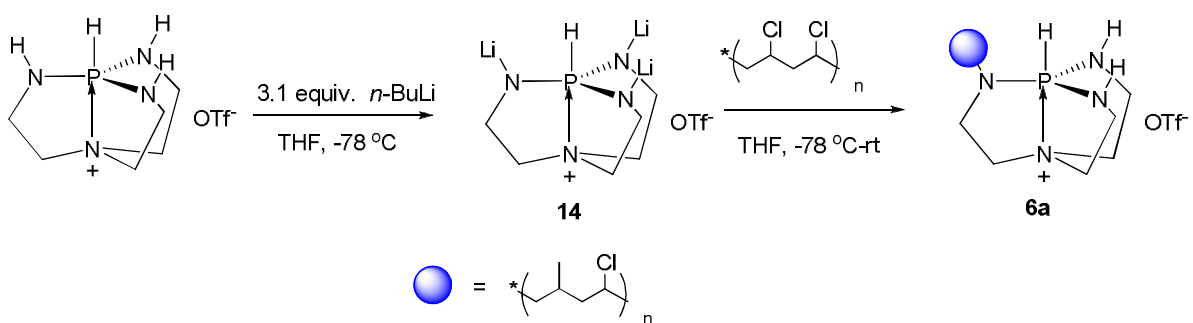


**Scheme 6.** Synthesis of **5a-d**

**Synthesis of 5a-d:** To a solution of hexakis(4-chloromethylphenoxy)cyclotriphosphazene **13** (0.67 g, 0.68 mmol), phosphatranium chloride (0.79 g, 3.7 mmol) in DMF or toluene (Scheme 6), was added a base (see Table 6) (3.7 mmol). The reaction mixture was stirred at

110 °C for 72 h. The product was then precipitated in ethyl ether and filtered off. Impurities were removed by extracting the product with copious amounts of methanol, acetone and THF.

**Synthesis of 6a:** Compound **14** was prepared *in situ* using a literature procedure (Scheme 7).<sup>23</sup> To a solution of phosphatranium triflate<sup>24</sup> (0.648 g, 2 mmol) in THF was added 3.1 equivalents of *n*-BuLi (3.1 equiv., 2.5 mL in hexane) at -78 °C. To this mixture was slowly added a solution of polyvinyl chloride (2.0 g) in 10 mL of THF at -78 °C. The reaction mixture was stirred while allowing it to come to room temperature slowly. Polymer **6a** was precipitated by adding the reaction mixture drop-wise to ethanol.



### Scheme 7. Synthesis of **6a**

**Synthesis of 6b:** Phosphatranium triflate (0.648 g, 2 mmol) prepared according to a literature procedure<sup>24</sup> was dissolved in 10 mL of THF. *n*-BuLi (1.5 equiv., 1.25 mL in Hexane) at -78 °C (Scheme 8) was then added followed by slow addition of a solution of polyvinyl chloride (2.0 g) in 10 mL of THF at -78 °C. The reaction mixture was stirred while allowing it to come to room temperature slowly. The polymer was precipitated by adding the reaction mixture drop-wise to ethanol.



**1b'**: A membrane was cast via molten solid casting with a 1:2 mixture of **1b** and Low Density Polyethylene (LDPE).

**Table 2:** AC impedance tests of **1b** and **1b'**

Sample	Resistivity (Ohm cm)	Resistance (ohm)	Conductivity (Ohm <sup>-1</sup> cm <sup>-1</sup> )	Cross Over
<b>1b</b>	105,000	19	1 x 10 <sup>-5</sup>	No
<b>1b'</b>	420,000	86	2 x 10 <sup>-6</sup>	No

#### Discussion:

1. The mechanical strength of the polymer was poor mainly because the polymer was of low molecular weight.
2. The resistances of both **1a** and **1b** were very high, although, when the loading of phosphatrane was increased in **1b**, the resistance was 10 times lower. The conductivity of both membranes was low.
3. The membrane did not show any crossover of ammonia in the fuel cell.
4. Attempts were made to react other amines such as triethylamine and tributylamine with polymer **7**, but unfortunately all the polymers with quaternary ammonium salts were soluble in water.

#### Results for AC impedance test of **2**:

A membrane was cast via molten solid casting with a 1:4 mixture of **2** and Low Density Polyethylene (LDPE).

**Table 3:** AC impedance test of **2**

Sample	Thickness (micron)	Resistance (ohm)	Conductivity (Ohm <sup>-1</sup> cm <sup>-1</sup> )	Cross Over
<b>2</b>	58.6	56.07	2.72 x 10 <sup>-6</sup>	Yes

Discussion:

1. The resistance of **2** was very high and its conductivity was low.
2. The most important drawback was crossover of ammonia, which decreases the shelf life of fuel cells.

Results of AC impedance test of **3a/3b**: Sample **3a** and **3b** was cast into membrane via molten solid casting with a 20% w/w mixture of **3a** or **3b** and polyvinylchloride (PVC).

**Table 4:** AC impedance tests of **3a** and **3b**

Sample	Resistivity (Ohm cm)	Resistance (ohm)	Conductivity (Ohm <sup>-1</sup> cm <sup>-1</sup> )	Cross Over
<b>3a</b>	6750	9.6	1.5 x 10 <sup>-4</sup>	Yes
<b>3b</b>	10316	1.8	1 x 10 <sup>-4</sup>	Yes

Discussion:

1. The mechanical strength of the polymer membrane was good up to <30% w/w conc with PVC. Brittleness was observed at higher concentrations.

2. The resistance of both **3a** and **3b** was very low with good conductivity for both membranes.
3. Unfortunately crossover of ammonia in the fuel cell was observed.

Results of AC impedance tests of **4a/4b**: A sample of **4a** was cast into a membrane via molten solid casting as a 1:2 mixture by weight with polystyrene, and **4b** was cast as a 10% mixture by weight with polymethylmethacrylate.

**Table 5:** AC Impedance tests of **4a** and **4b**

Sample	Resistivity (Ohm cm)	Resistance (ohm)	Conductivity (Ohm <sup>-1</sup> cm <sup>-1</sup> )	Cross Over
<b>4a</b>	1035	1.5	9 x 10 <sup>-4</sup>	Yes
<b>4b</b>	7430	10.5	1.3 x 10 <sup>-4</sup>	Yes

Discussion:

1. The mechanical strength of **4a** was poor because it was very brittle. On the other hand, **4b** had good mechanical strength.
2. The resistance of both **4a** and **4b** was very low. High conductivity and low resistance was observed for **4b** but its membrane strength was poor.
3. Unfortunately crossover of ammonia in the fuel cell was observed.

Results of AC impedance tests of **5a-d**: Samples of **5a-d** were cast into membranes via molten solid casting as follows:



**5a:** 20% w/w blended with polymethylmethacrylate.

**5b:** 1:2 weight ratio with low density polyethylene (LDPE).

**5c:** 1:3 weight ratio with low density polyethylene (LDPE).

**5d:** 20% w/w blended with polymethylmethacrylate.

**Table 6: AC impedance tests of 5a-d/polymer blends**

Sample	Solvent	Base	Resistance (ohm)	Conductivity (ohm <sup>-1</sup> cm <sup>-1</sup> )	Resistivity (ohm cm)	Cross over
<b>5a</b>	Toluene	Et <sub>3</sub> N	30	$6 \times 10^{-6}$	170,262	No
<b>5b</b>	DMF	Et <sub>3</sub> N	25	$6 \times 10^{-5}$	21,240	No
<b>5c</b>	DMF	Bu <sub>3</sub> N	20	$1 \times 10^{-5}$	116.463	No
<b>5d</b>	DMF	-	11	$2 \times 10^{-5}$	60,864	No

Discussion:

1. Base was used to quench HCl liberated in the reaction between the amine and the benzyl chloride group.
2. The mechanical strengths of **5a-d** were good but the membranes became brittle when the loading of **5** was increased.
3. Resistances were high and conductivities were low.

4. The best conductivity and lowest resistance was obtained when only phosphatranium chloride was used in DMF as solvent.

**The AC impedance test of 6a and 6b:** Samples **6a** and **6b** were cast as membranes via solution casting using THF as solvent.

**Table 7:** AC impedance tests of **6a**, **6b** and **6b'**

Sample	Phosphatrane loading (w.r.t PVC)	Resistance (ohm)	Conductivity (ohm <sup>-1</sup> cm <sup>-1</sup> )	Cross Over
<b>6a</b>	5 mol %	6	$5 \times 10^{-5}$	No
<b>6b</b>	6.25 mol %	1	$6 \times 10^{-4}$	No
<b>6b'</b>	12.5 mol %	-	$9 \times 10^{-5}$	No

Discussion:

1. The mechanical strengths of the **6a**, **6b** and **6b'** membranes were excellent and the membranes were easy to handle.
2. Resistances were low and good conductivities were observed.
3. However, fluctuation in the conductivity was observed was observed in **6b** when a duplicate run was carried out.

## Conclusion

A wide variety of polymeric samples with phosphatranium nitrate attached to the polymer backbone were prepared. Moderate to good values of conductivities were obtained and the best conductivities were obtained for samples **3**, **4**, **5** and **6**. Our results suggest that **6** was the best candidate for fuel cell application. This result suggests that a halogenated polymeric backbone provides low resistances and greater thermolytic stability. Phosphatranium nitrate as shown above is a good candidate for a nitrate ion conductor owing to its bulky cationic nature which reduces anion-cation interactions. A more detailed study of these polymers should be carried out to better understand the relationship between their structures and their properties as anion transport membranes.

## Reference

1. Chu, D.; Jiang, R. *Solid State Ionics* **2002**, *148*, 591.
2. Dyer, C. K. *J. Power Sources* **2002**, *106*, 31.
3. Chang, H.; Kim, J. R.; Cho, J. H.; Kim, H. K.; Choi, K. H. *Solid State Ionics* **2002**, *148*, 601.
4. Meyers, J. P.; Maynard, H. L. *J. Power Sources* **2002**, *109*, 76.
5. Wojcik, A.; Middleton, H.; Damopoulos, I.; Van Herle, J. *J. Power Sources* **2003**, *118*, 342–348.
6. Maffei, N.; Pelletier, L.; Charland, J. P.; McFarlan, A. *J. Power Sources* **2005**, *140*, 264–267.
7. McFarlan, A.; Pelletier, L.; Maffei, N. *J. Electrochem. Soc.* **2004**, *151*, A930–A932.

8. Fournier, G. G. M.; Cumming, I. W.; Hellgardt, K. *J. Power Sources* **2006**, *162*, 198–206.
9. Ma, Q.; Peng, R.; Lin, Y.; Guo, J.; Meng, G. *J. Power Sources* **2006**, *161*, 95–98.
10. Ma, Q.; Ma, J.; Zhou, S.; Yan, R.; Guo, J.; Meng, G. *J. Power Sources* **2007**, *161*, 86–89.
11. *Eye for Fuel Cells conference on Fuel Cells for Portable Applications* Hilton Back Bay, Boston, MA, USA, September 5th-6th **2002**.
12. Ren, X.; Zelenay, P.; Thomas, S.; Davey, J.; Gottesfeld, S. *J. Power Sources* **2000**, *86*, 111.
13. Raadschelders, J. W.; Jansen, J. *J. Power Sources* **2001**, *96*, 160.
14. Chellappa, A.S.; Fischer C.M.; Thomson, W.J. *Appl. Catal.* **2002**, *227*, 231–240.
15. Kisanga, P. B.; Verkade, J. G. *J. Org. Chem.* **2000**, *65*, 5431–5432.
16. For reviews on proazaphosphatrane chemistry, see: (a) Verkade, J. G. In *New Aspects of Phosphorus Chemistry II*, *Top. Curr. Chem.* Majoral, J. P. Ed., **2002**, 233, 1–44. (b) Verkade, J. G.; Kisanga, P. B. *Tetrahedron* **2003**, *59*, 7819–7858. (c) Verkade, J. G.; Kisanga, P. B. *Aldrichimica Acta* **2004**, *37*, 3–14. (d) Uргаonkar, S.; Verkade, J. G. *Specialty Chemicals* **2006**, *26*, 36–39.
17. Fetterly, B. M.; Jana, N. K.; Verkade, J. G. *Tetrahedron* **2006**, *62*, 440–456.
18. Chen, S.; Janda, K.D. *J. Am. Chem. Soc.* **1997**, *119*, 8724–8725.
19. Carpino, L. A.; Mansour, E. M. E; Knapczyk, J. *J. Org. Chem.*, **1983**, *48*, 666–669.
20. Fritz, J. S.; King, J. N. *Anal. Chem.*, **1976**, *48*, 570-572.
21. Suzuki, M. T.; Itabashi, O.; Goto, T.; Yokoyama, T.; Kimura, T. *Anal. Sci.* **1986**, *2*, 391–392

22. Inoue, K.; Negayama, S.; Itaya, T.; Sugiyama, M. *Macromol. Rapid Commun.* **1997**, *18*, 225–231.
23. Liu, X.; Bai, Y.; Verkade, J. G. *J. Organomet. Chem.* **1999**, *582*, 16–24.
24. Laramay, M. A. H.; Verkade, J. G. *Z. Anorg. Allg. Chem.* **1991**, *605*, 163–174.

## CHAPTER 9. PROAZAPHOSPHATRANE CATALYSTS MOUNTED ON PERHALOGENATED POLYMERS

Kuldeep Wadhwa, Venkat Reddy Chintareddy, and John G. Verkade

### Introduction

Biodiesel, obtained from plant oils, is an advantageous alternative to fossil diesel fuel.<sup>1-15</sup> It has many advantages such as biodegradability, biorenewability, very low sulfur content and toxicity, low volatility/flamability, good transport and storage properties, higher cetane number, and its good atmospheric CO<sub>2</sub> balance for production. Transesterification of plant oils with methanol is the most common approach to biodiesel production. The byproduct glycerin, formed during transesterification, also has numerous applications in the food, cosmetic, and pharmaceutical sectors.<sup>16,17</sup> Biodiesel not only has applications as a diesel fuel additive, but it also has a market as green industrial degreasing solvents; as diluents for pigments, paints, and coatings; and for fuel applications in military engines.<sup>18,19</sup>

The most common catalysts for the transesterification of plant oils to biodiesel have included the use of homogeneous strong-base catalysts, such as alkaline metal hydroxides, alkoxides, and acid catalysts, such as HCl and H<sub>2</sub>SO<sub>4</sub>.<sup>9-15,20-28</sup> Alkaline alkoxides and hydroxides are more effective catalysts than acid catalysts and operate at lower temperatures.<sup>29-31</sup> However, the most common disadvantage of homogeneous alkaline catalysts is soap formation, leading to product loss and problems with product separation and purification. Heterogeneous catalysts for biodiesel production have various advantages such as reusability and eco-

compatibility. Moreover, product separation from a heterogeneous catalyst is easier and since no water washes are required during work up, product purity is good. Some heterogeneous catalysts have been reported in the literature such as guanidines or amines anchored to the backbone of organic polymers. Their main drawback is that they operate at the reflux temperature of the solvent used for the reaction.<sup>32-35</sup> Recently, the use of  $\text{WO}_3/\text{ZrO}_2$  (stable up to 100 h at 250 °C) has been employed as a heterogeneous solid acid catalyst at 250 °C to produce biodiesel.<sup>36</sup> However, the recyclability of this catalyst was not reported. Other drawbacks that heterogeneous catalyst systems possess are insufficient catalyst reusability, handling difficulties, the need for elevated temperatures, multistep catalyst synthesis, and, most importantly, frequent problems with adaptability to large-scale preparations.

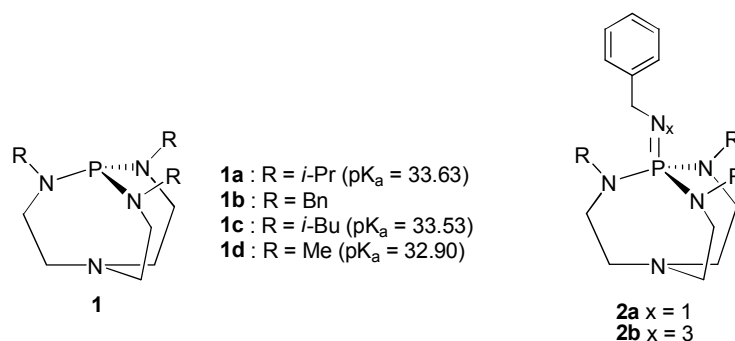


**Figure 1**

First discovered in our laboratory, proazaphosphatranes<sup>37</sup> **1a-d** are exceedingly strong commercially available nonionic bases (pK<sub>a</sub> 32–34 in  $\text{CH}_3\text{CN}$ <sup>38b</sup>) which are useful as homogeneous catalysts and as stoichiometric reagents in a wide variety of important organic transformations, including transesterifications.<sup>38a</sup> Though catalyst **1** is a very efficient catalyst for transesterification, the trivalent aminophosphine moiety in **1** is fairly sensitive to

oxygen and proton sources (including water). However, modification of this catalyst system to less basic but stable iminophosphoranes **2a** (Figure 1) was found to be effective.<sup>39</sup> Subsequently it was found that these structures were erroneously reported as imines<sup>39</sup> and that the correct structures had the azidoproazaphosphatrane **2b** framework as determined by X-ray crystallography for a member of this class of compounds.<sup>40</sup> We also demonstrated that a dendrimer functionalized with an azidoproazaphosphatrane (**3**) shown in Figure 2 is a good catalyst for C-C bond-forming Michael and Henry reactions.<sup>41</sup> As part of our efforts to develop green chemical methods for organic synthesis, homogeneous proazaphosphatranes (**1**) were converted to heterogeneous Merrifield resin-bound analogs of type **4** (Figure 3).<sup>39,40</sup>

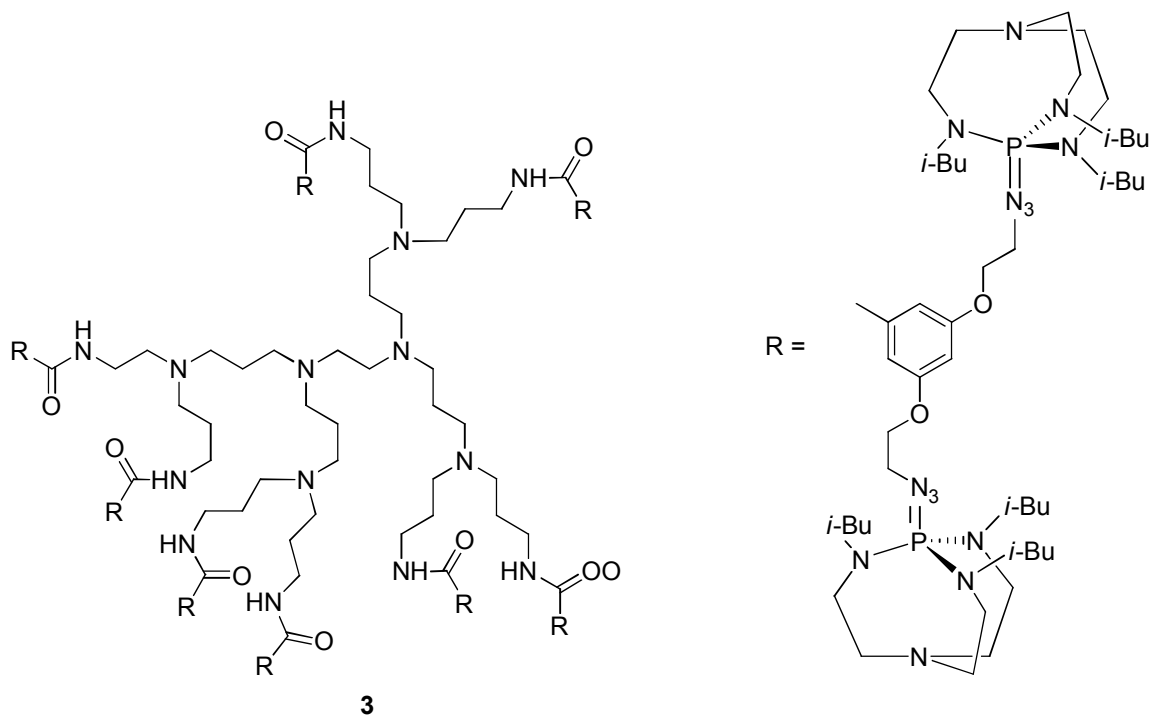
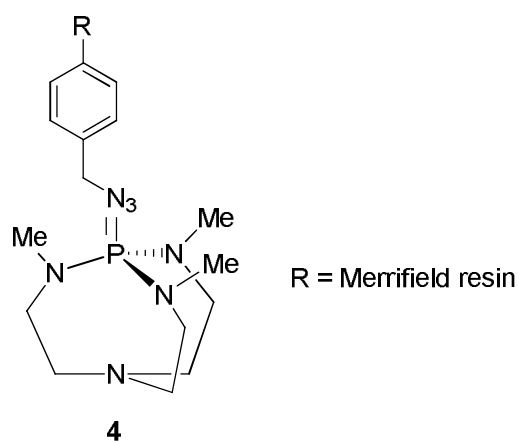


Figure 2



Heterogeneous catalysts of type **4** have been shown by us to be useful in the acetylation of alcohols with vinyl acetate<sup>39</sup> and in 1,4 addition reactions.<sup>42</sup> Verkade *et al.* reported the use of catalyst **4** in the synthesis of biodiesel and showed it to be deactivated after 11 cycles.<sup>40</sup> It was then found by solid state <sup>13</sup>C NMR techniques (in collaboration with Professor Schmidt-Rohr of this Department) that the catalyst was plugged with organic impurities accumulated during the catalyst cycles, thereby deactivating the catalyst by blocking the active sites.<sup>43</sup>



**Figure 3**

To overcome the recyclability problem of catalyst **4**,<sup>40</sup> we proposed a heterogeneous catalyst composed of a molecule such as **4** bonded to a Teflon<sup>®</sup> substrate for the transesterification of plant oils to biodiesel as depicted in Figure 4. The proposed catalyst would have the following advantages.

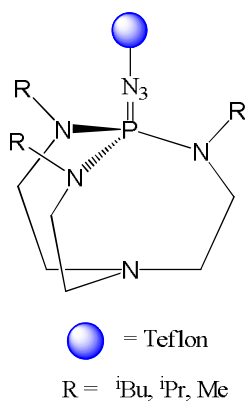
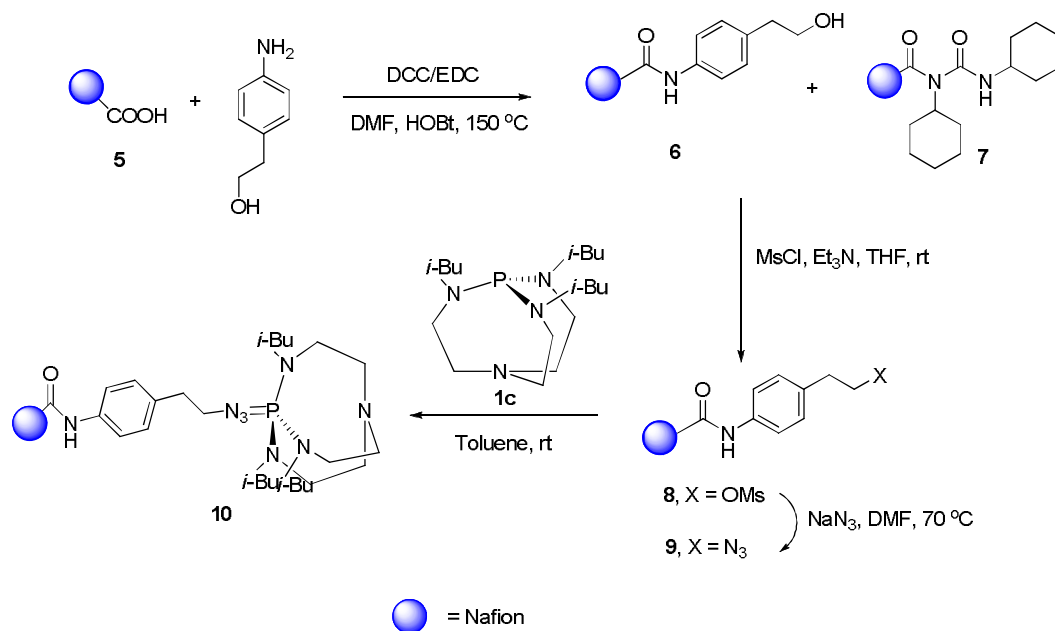


**Figure 4.** Structure of Teflon<sup>®</sup> bound azidoproazaphosphatane

- 1) The highly robust nature of azidoproazaphosphatanes, which we had already shown in the past to be efficient catalysts for transesterification as well as a number of other organic transformations.<sup>39-42</sup>
- 2) These catalysts would be attached to perhalogenated polymer backbones, such as Teflon<sup>®</sup>, which would enable this catalyst system to be stable to elevated temperatures and hydrolytic conditions.
- 3) These catalyst systems would be highly recyclable since they would have no lipophilic pores for plugging by organic impurities.

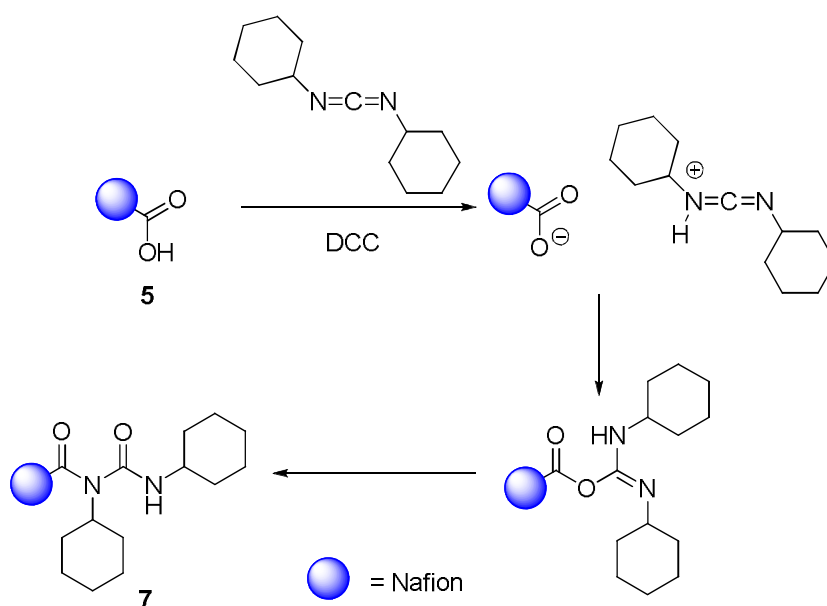
## Results and Discussion



**Scheme 1.** Synthesis of Nafion<sup>®</sup>-bound azidoproazaphosphatrane

As shown in Scheme 1, commercially available Nafion-CO<sub>2</sub>H<sup>®</sup> (**5**) resin was reacted with *p*-aminophenethyl alcohol to form amide linkages (**6**), followed by conversion of the Nafion<sup>®</sup>-bound-phenethyl alcohol (**6**) to the corresponding mesylate (**8**), which was then converted to a phenethyl azide linkage (**9**) using NaN<sub>3</sub>. Nafion<sup>®</sup> bound-phenethyl alcohol (**6**) along with formation of **7** as side product were observed using solid state <sup>13</sup>C NMR spectroscopy. The formation of **7** was rationalized as shown in Scheme 2. Nafion<sup>®</sup>-bound azidoproazaphosphatrane (**10**) was prepared in a procedure similar to that employed for the synthesis of Merrifield-resin bound azidoproazaphosphatrane.<sup>40</sup> However, in the present case,

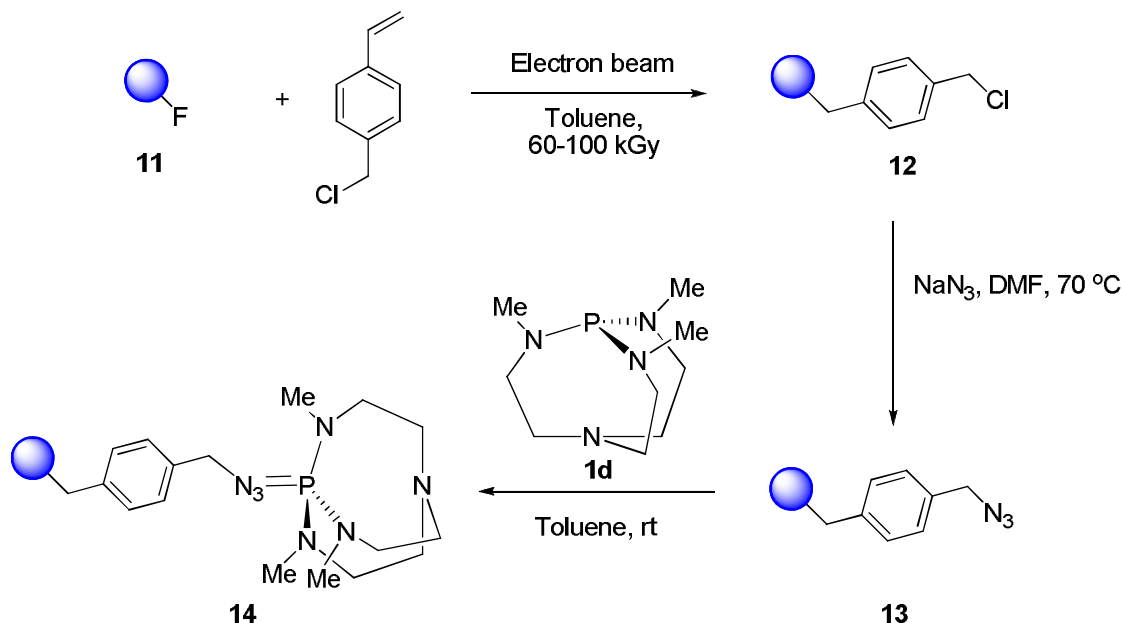
we noticed cleavage of the amide linkage in the  $^1\text{H}$  NMR spectrum. At this stage it is not clear what causes the cleavage of this linkage.



**Scheme 2**

In an attempt to synthesize a Teflon<sup>®</sup>-bound azidoproazaphosphatrane as shown in Figure 4, free radicals were generated on the surface of Teflon<sup>®</sup> (**11**) in the presence of *p*-vinylbenzyl chloride (VBC) using high-energy electron beam (EB) radiation (Scheme 3) yielding **12**.<sup>44</sup> Compound **12** was converted to **13** using  $\text{NaN}_3$ . Compound **13** was then reacted with proazaphosphatrane (**1d**) to generate a Teflon<sup>®</sup>-bound azidoproazaphosphatrane (**14**). We obtained a  $^{31}\text{P}$  NMR peak at 37 ppm that we assigned to **14**, which is in accordance with  $^{31}\text{P}$  NMR of **2b**.<sup>40</sup> When **14** was tested in a reaction of SBO with MeOH to obtain the transesterification product, no reaction was observed by  $^1\text{H}$  NMR spectroscopy. We attribute

this disappointing result to the very low content of the azidoproazaphosphatrane present in the polymer (ca. < 0.17 mmol/g via phosphorus elemental analysis).



**Scheme 3.** Synthesis of Teflon<sup>®</sup>-bound azidoproazaphosphatrane

In these EB grafting experiments, reactions were carried out in a reaction vessel exposed to a radiation dose of 20-100 kGy. Table 1 shows the trend of VBC grafting to Teflon<sup>®</sup> (12-100 micron mesh). The highest loading we obtained was 0.77 mmol/g of benzyl chloride as shown by elemental analysis of chlorine retained. Unfortunately, this loading was not high enough to display observable catalytic activity for the transesterification of soybean oil with methanol.

**Table 1.** Grafting of VBC on Teflon<sup>®</sup> Powder<sup>a</sup> Using EB Radiation

Sample	Size (micron)	Dosage (kGy)	Chlorine (wt %)
1	12	22.32	0.4
2	12	22.32	<0.1
3	55	22.32	0.2
4	100	22.32	0.6
5	55	47.49	2.4
6	100	47.49	1.7
7	55	76.22	2.5
8	100	76.22	2.1
9	55	93.0	2.7
10	100	93.0	1.9

<sup>a</sup>Teflon<sup>®</sup> powder was obtained from Aldrich.

### Conclusion

In conclusion, we have shown that a new perhalogenated polymer-bound azidoproazaphosphatane catalyst for the transesterification of plant oil was synthesized successfully. However, the loading of the catalytic sites on the polymer is very low and needs significant improvement. The use of gamma radiation to graft VBC to Teflon<sup>®</sup> is underway in a collaboration with Dr. Inderjeet Kaur, Himachal Pradesh University, Simla, India, who has demonstrated this technology for VBC-Teflon<sup>®</sup> grafting.<sup>45</sup> Switching the source of energy for EB to gamma radiation from <sup>60</sup>Co has dramatically increased the VBC loading

from 0.77 to 28.5–42.8 mmol/g Cl for a sample of Teflon<sup>®</sup> (55 micron particle size) which we sent her. A one-gram sample of the 150% grafted sample is projected to be sent to us by Dr. Kaur at the end of June, after which we will attach the azidoproazaphosphatane. If this effort is successful, we hope that the new heterogeneous catalyst for the transesterification of soybean oil as well as other important organic transformations will be efficient and highly recyclable.

### Experimental

**Synthesis of 6:** Nafion-CO<sub>2</sub>H<sup>®</sup> **5** (2 g, 3.6 mmol) was weighed in nitrogen filled glove box in a round-bottom flask. To this was added *p*-amino-phenethyl alcohol (1 g, 7.2 mmol), DCC (1.48 g, 7.2 mmol) or EDC (1.1 g, 7.2 mmol), N-hydroxybenzotriazole (0.972 g, 7.2 mmol) in 30 mL DMF. This was heated in a closed vessel at 110 °C for 48 h. Product **6** was filtered and washed with excess water and methanol and then dried under vacuum.

**Synthesis of 8:** To **6** was added triethylamine (1 g, 10.0 mmol) and MsCl (1.14 g, 10.0 mmol) in a round-bottom flask. The solution was stirred at room temperature for 24 h and then filtered under vacuum. The filtered solid was washed with excess water and methanol. Product **8** was dried under vacuum.

**Synthesis of 9:** In a dry round-bottomed flask was added NaN<sub>3</sub> (1.3 g, 20.0 mmol), **8** (1.0 g) and 20 mL of anhydrous DMF. The flask was submerged in a pre-heated (80 °C) oil bath for 48 h. The polymer was filtered and washed with excess water and methanol. Product **9** was dried under vacuum.

**Synthesis of 10:** To a 50 mL round-bottomed flask under inert atmosphere charged with **9** (1.0 g) was added proazaphosphatane **1c** (3.42 g, 10 mmol) and dry toluene (5 mL) which was added via syringe. The mixture was stirred at room temperature for 48 h and then it was filtered and washed with dry toluene under an inert atmosphere.

**Synthesis of 12:** To a thick-walled glass tube was added Teflon<sup>®</sup> powder (**11**) (2 g) and VBC such that the polymer was completely immersed in the VBC. The tubes were then sealed under vacuum. These tubes were exposed to EB radiation for a total dose of 60-100 kGy and then they were heated in an oil bath at 60 °C for 24 h. The polymer was then filtered and washed with copious amounts of toluene to remove any unreacted or homopolymerized VBC. The polymer was then dried under vacuum to obtain the grafted polymer **12**. The maximum grafting of VBC on the polymer was 2.7% (Table 1, entry 9)

**Synthesis of 13:** In a dry round-bottomed flask was added NaN<sub>3</sub> (1.3 g, 20 mmol) and **12** (1.0 g, Cl = 0.77 mmol/g via elemental analysis). To this was added dry DMF (20 mL) and the mixture was heated in a closed flask at 80 °C for 48 h. The polymer was filtered and then washed with excess water, THF and acetone. Product **13** was then dried under vacuum.

**Synthesis of 14:** To a 50 mL round-bottomed flask charged with **13** (0.77 mmol/g) under inert atmosphere was added proazaphosphatane (**1d**, 340 mg, 1.54 mmol) followed by the addition of 10 mL of dry toluene via syringe. The mixture was stirred at room temperature for 48 h and then the solid was filtered and washed with dry toluene under inert atmosphere. The phosphorus loading on polymer **14** was found to be <0.16 mmol/g of phosphorus via elemental analysis.



**General Procedure for Transesterification of SBO to Biodiesel.** A round-bottom flask containing the catalyst **14** (0.5 g) was equipped with a rubber septum and two magnetic stir bars for stirring efficiency. After the tube was flushed with argon, SBO (2 mL) and MeOH (5 mL) were added separately via a syringe. The reaction mixture was stirred vigorously at room temperature (23-25 °C), and the progress of the reaction was monitored by solution  $^1\text{H}$  NMR spectroscopy. The reaction mixture was centrifuged and the vast majority of the supernatant was carefully removed by cannulation to avoid disturbing the catalyst. Excess methanol was removed from the separated supernatant liquid via rotavapor, leaving the biodiesel, which was subjected to  $^1\text{H}$  NMR analysis. The relevant signals chosen for integration were those of methoxy groups in the biodiesel (3.66 ppm, singlet) and those of the R-methylene protons present in the triglycerides (2.3 ppm, triplet) of the SBO.<sup>40</sup> Conversion of SBO to biodiesel was also observed visually by the disappearance of the mutually immiscible SBO and methanol phases. As noted above, however, no SBO transesterification was observed for **14**.

### References

- 1) Toda, M.; Takagaki, A.; Okamura, M.; Kondo, J. N.; Hayashi, S.; Domen, K.; Hara, M. *Nature* **2005**, *438*, 178.
- 2) Srivastava, A.; Prasad, R. *Renewable Sustainable Energy Rev.* **2000**, *4*, 111.
- 3) Shay, E. G. *Biomass Bioenergy* **1993**, *4*, 227.
- 4) Schwab, A. W.; Bagby, M. O.; Friedman, B. *Fuel* **1987**, *66*, 1372.
- 5) Freedman, B.; Butterfield, R. O.; Pryde, E. H. *J. Am. Oil Chem. Soc.* **1986**, *63*, 1375.
- 6) Freedman, B.; Pryde, E. H.; Mounts, T. L. *J. Am. Oil Chem. Soc.* **1984**, *61*, 1638.

- 7) Leclercq, E.; Finiels, A.; Moreau, C. *J. Am. Oil Chem. Soc.* **2001**, 78, 1161.
- 8) Xie, W.; Peng, H.; Chen, L. *J. Mol. Catal. A: Chem.* **2006**, 246, 24.
- 9) Schuchardt, U.; Sercheli, R.; Vargas, R. M. *J. Braz. Chem. Soc.* **1998**, 9, 199.
- 10) Kinney, A. J.; Clemente, T. E. *Fuel Process. Technol.* **2005**, 86, 1137.
- 11) Haas, M. J. *Fuel Process. Technol.* **2005**, 86, 1087.
- 12) Knothe, G. *Fuel Process. Technol.* **2005**, 86, 1059.
- 13) Van Gerpen, J. *Fuel Process. Technol.* **2005**, 86, 1097.
- 14) Lotero, E.; Liu, Y.; Lopez, D. E.; Suwannakaran, A.; Bruce, D. A.; Goodwin, J. G., Jr. *Ind. Eng. Chem. Res.* **2005**, 44, 5353.
- 15) Fukuda, H.; Kondo, A.; Noda, H. *J. Biosci. Bioeng.* **2001**, 92, 405.
- 16) Vicente, G.; Martinez, M.; Aracil, J. *Bioresour. Technol.* **2004**, 92, 297.
- 17) Patel, D. C.; Ebert, C. D. U.S. Patent 4,855,294, 1989; TheraTech, Inc.: UT; *Chem. Abstr.* **1989**, 112, 62666m.
- 18) Wildes, S. *Chem. Health Saf.* **2002**, 24.
- 19) Mushrush, G. W.; Beal, E. J.; Hughes, J. M.; Wynne, J. H.; Sakran, J. V.; Hardy, D. R. *Ind. Eng. Chem. Res.* **2000**, 9, 3945.
- 20) Shah, S.; Sharma, S.; Gupta, M. N. *Energy Fuels* **2004**, 18, 154.
- 21) Dorado, M. P.; Ballesteros, E.; Lopez, F. J.; Mittelbach, M. *Energy Fuels* **2004**, 18, 77.
- 22) Encinar, J. M.; Gonzalez, J. F.; Rodriguez, J. J.; Tejedor, A. *Energy Fuels* **2002**, 16, 443.
- 23) Chang, D. Y. Z.; Van Gerpen, J. H.; Lee, I.; Johnson, L. A.; Hammond, E. G.; Marley, S. J. *J. Am. Oil Chem. Soc.* **1996**, 73, 1549.

- 24) Freedman, B.; Bagby, M. O. *J. Am. Oil Chem. Soc.* **1990**, *67*, 565.
- 25) Abreu, F. R.; Lima, D. G.; Hamu, E. H.; Einloft, S.; Rubim, J. C.; Suarez, P. A. Z. *J. Am. Oil Chem. Soc.* **2003**, *80*, 601.
- 26) Watanabe, Y.; Shimada, Y.; Sugihara, A.; Noda, H.; Fukuda, H.; Tominaga, Y. *J. Am. Oil Chem. Soc.* **2000**, *77*, 355.
- 27) Abreu, F. R.; Lima, D. G.; Hamu, E. H.; Wolf, C.; Suarez, P. A. Z. *J. Mol. Catal. A: Chem.* **2004**, *209*, 29.
- 28) Schuchardt, U.; Vargas, R. M.; Gelbard, G. *J. Mol. Catal. A: Chem.* **1996**, *109*, 37.
- 29) Formo, M. W. *J. Am. Oil Chem. Soc.* **1954**, *31*, 548.
- 30) Nye, M. J.; Southwell, P. H. *Vegetable Oils Diesel Fuel*; Seminar III, ARM-NC-28; Bagby, M. O., Pryde, E. H., Eds.; U.S. Department of Agriculture: Peoria, IL, 1983; p 78.
- 31) Harrington, K. J.; D'Arcy-Evans, C. *Ind. Eng. Chem. Prod. Res. Dev.* **1985**, *24*, 314.
- 32) Schuchardt, U.; Vargas, R. M.; Gelbard, G. *J. Mol. Catal. A: Chem.* **1996**, *109*, 37.
- 33) Schuchardt, U.; Vargas, R. M.; Gelbard, G. *J. Mol. Catal. A: Chem.* **1995**, *99*, 65.
- 34) Sercheli, R.; Vargas, R. M.; Schuchardt, U. *J. Am. Oil Chem. Soc.* **1999**, *76*, 1207.
- 35) Suppes, G. J.; Dasari, M. A.; Doslak, E. J.; Mankidy, P. J.; Goff, M. J. *Appl. Catal. A* **2004**, *257*, 213.
- 36) Furuta, S.; Matsushashi, H.; Arata, K. *Catal. Commun.* **2004**, *5*, 721.
- 37) (a) Verkade, J. G. "P(RNCH<sub>2</sub>CH<sub>2</sub>)<sub>3</sub>N: Very Strong Non-Ionic Bases Useful in Organic Synthesis", *Topics Curr. Chem.* **2002**, *223*, 1–44 and references therein. (b) Verkade, J. G.; Kisanga, P. B. "Proazaphosphatranes: A Synthesis Methodology Trip From Their Discovery to Vitamin A", *Tetrahedron* **2003**, *59*, 7819-7858 and

- references therein. (c) Verkade, J. G.; Kisanga, P. B. "Recent Applications of Proazaphosphatranes in Organic Synthesis", *Aldrichimica Acta* **2004**, *37*, 3–14 and references therein. (d) Urgaonkar, S.; Verkade, J. G., "Proazaphosphatrane Catalysts for Key Industrial Reactions", *Specialty Chemicals* **2006**, *26*, 36–39 and references therein. e) Fetterly, B. M.; Jana, N. K.; Verkade, J. G. Symposium in Print on Organocatalysis, *Tetrahedron*, **2006**, *62*, 440–456.
- 38) a) Ilankumaran, P.; Verkade, J. G. *J. Org. Chem.* **1999**, *64*, 3086–3089. b) Kisanga, P.; Verkade, J. G.; Schwesinger, R. "pKa Measurements of P(RNCH<sub>2</sub>CH<sub>2</sub>)<sub>3</sub>N," *J. Org. Chem.* **2000**, *65*, 5431–5432.
- 39) Ilankumaran, P.; Verkade, J. G. *J. Org. Chem.* **1999**, *64*, 9063–9066.
- 40) Venkat Reddy, Ch.; Fetterly, B. M.; Verkade, J. G. *Energy Fuels* **2007**, *21*, 2466–2472.
- 41) Sarkar, A.; Ilankumaran, P.; Kisanga, P.; Verkade, J. G. *Adv. Synth. Catal.* **2004**, *346*, 1093.
- 42) Venkat Reddy, Ch.; Verkade, J. G. *J. Org. Chem.*, **2007**, *72*, 3093–3096
- 43) In collaboration with Professor K. Schmidt-Rohr at Iowa State University.
- 44) (a) Xi, Z-Y.; Xu, Y-Y.; Zhu, L-P.; Zhu, B.-K. *J. Memb. Sci.* **2009**, *339*, 33–38. (b) Lappan, U.; Geißler, U.; Uhlmann, S. *Nucl. Instrum Meth B* **2005**, *236*, 413–419.
- 45) (a) Kaur, I.; Misra, B.N.; Kohli, A. *Desalination* **2001**, *139*, 357–365. (b) Inderjeet Kaur, I.; Singh, B.; Gupta, N. *Rad. Phys. Chem.* **2005**, *72*, 489–495. (c) Kaur, I., Kumar, R., Singh, B., Misra, B.N., Chauhan, G.S. *J. Appl. Polym. Sci.* **2000**, *78*, 1171 and references therein.

## CHAPTER 10. GENERAL CONCLUSIONS AND FUTURE WORK

### 1. General conclusions and future possibilities for silyl activation using proazaphosphatranes

The work in Chapters 2–6 further demonstrates that proazaphosphatranes are potentially capable of becoming widely used catalysts for the synthesis of various organic intermediates. In those chapters, we showed that proazaphosphatranes are efficient catalysts for the synthesis of  $\beta$ -hydroxyesters,  $\alpha,\beta$ -unsaturated esters,  $\beta$ -hydroxynitriles, propargylic alcohols, Morita-Baylis-Hillman (MBH) type adducts and Mukaiyama aldols, and for catalytic umpolung addition of dithiane to aldehydes. Our group is currently developing syntheses of chiral proazaphosphatranes. It will be interesting to apply these P-center chiral catalysts for enantioselective syntheses of some of the aforementioned intermediates.

In Chapters 5 and 6, we demonstrated the use of *N*-benzyl substituted proazaphosphatrane as an efficient catalyst for Mukaiyama aldol reactions and for the synthesis of propargylic alcohols and Morita-Baylis-Hillman (MBH) type adducts. These studies suggest that the synthesis of other analogs of proazaphosphatranes will be of interest to explore for potentially expanding the growing list of transformations catalyzed by such Lewis bases. Such analogues might also grow the commercial market for phosphatranes beyond the three that are currently available from Aldrich and Strem.

### 2. General conclusions and future plans for the use of phosphatranium salts in ion transport membranes

In Chapter 7 is described a potentially important discovery regarding the synthesis of a Nafion<sup>®</sup>-proazaphosphatrane composite membrane. Initial studies have shown that it is an excellent conductor of hydroxide ion with a low resistance of 0.5 ohm and a high conductivity of 2-5 mS/cm. It is interesting to note here that the membrane contains impurities that seem to be associated with DMF, which may be a factor in lowering the conductivity. Further work is planned aimed at improving the purity of the membrane and optimizing it to obtain very high conductivities of hydroxide or nitrate ion. Such membranes would have the potential to be used in fuel cell applications.

### **3. General conclusions and future plans for the use of Teflon<sup>®</sup>-bound azidoproazaphosphatranes and proazaphosphatranes as efficient catalysts**

We have synthesized a new perhalogenated polymer-bound azidoproazaphosphatrane catalyst for biodiesel production. However, the loading of the catalytic sites on the polymer is low and needs substantial improvement. The use of gamma radiation to graft VBC to Teflon<sup>®</sup> is underway in a collaboration with Dr. Inderjeet Kaur, Himachal Pradesh University, Simla, India, who has successfully demonstrated this technology for VBC-Teflon<sup>®</sup> grafting. Switching the source of energy from EB to <sup>60</sup>Co gamma radiation has dramatically increased the VBC loading from 0.77 to 28.5–42.8 mmol/g Cl for a sample of Teflon<sup>®</sup> (particle size 55 micron), which we sent to Dr. Kaur. A one gram sample of the 150% grafted sample is projected to be sent to us by Dr. Kaur, after which we will attach the azidoproazaphosphatrane. If this effort is successful, we hope that the new heterogeneous catalyst for the transesterification of soybean oil, as well as for other important organic transformations will be efficient and highly recyclable.

Recently, Fetterly *et al.* in our laboratory successfully demonstrated the utility of the Merrifield resin-bound proazaphosphatrane **1** shown in Figure 1 for the efficient synthesis of diaryl ethers via nucleophilic substitution of fluoroarenes with trialkylsilyl ethers with good recyclability (20 times) of the catalyst. With the increasing demand for recyclable catalysts for economic and environmental reasons, it will be interesting to see if perhalogenated polymers grafted with 4-vinylbenzyl chloride, followed by proazaphosphatrane attachment, can meet these requirements. Perhalogenated polymer backbones for such catalysts can potentially increase the mechanical and thermal stability, as well as the recyclability of these catalyst systems.

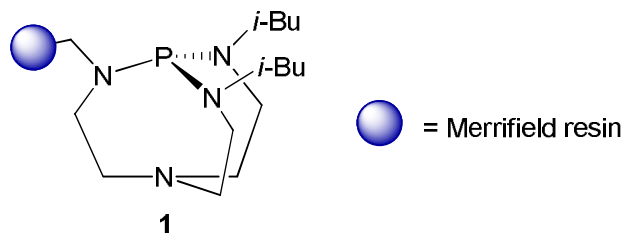


**Figure 1**

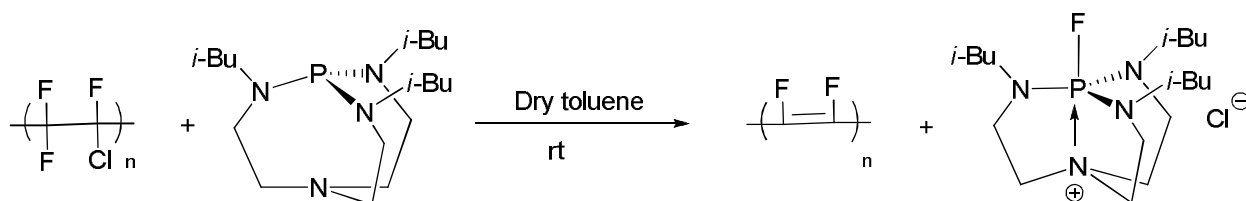
#### **4. Proposed use of proazaphosphatranes for the synthesis of polydifluoroacetylene (PDFA)**

PDFA has attracted attention in the recent past owing to its numerous commercial applications as a semiconducting material and its unique optical and chemical properties. Initial studies have revealed that structural features of not only PDFA, but also of polymonofluoroacetylene (PMFA), make these polymers better alternatives to the more common non-fluorinated polyacetylene as an intrinsic semiconducting material.<sup>1-4</sup>

Advancement in the synthesis of PDFA has been largely hampered by handling problems with both the starting monomer and the target polymer.

Only a few literature reports of the synthesis of PDFA exist.<sup>5-7</sup> Two patents have claimed the synthesis of the desired polymer,<sup>5,6</sup> but the method the inventors described was irreproducible and the polymer obtained does not have the desired properties. Also, decomposition of the polymer was observed in the presence of the catalyst, which the inventors claimed for synthesis of the polymer.<sup>7</sup>

Recently, an attempted synthesis of polydifluoroacetylene was published,<sup>7</sup> involving the polymerization of the parent monomeric molecule difluoroacetylene under cryogenic polymerization conditions (chemical vapor deposition onto a substrate at a temperature of -198 °C to -90 °C). While this approach did yield the desired polymer, the most important drawback of this method is the difficulty in handling the difluoroacetylene monomer owing to its highly unstable nature. It decomposes at higher temperatures and is highly explosive even at liquid nitrogen temperature (-198 °C) in the presence of even trace amounts of oxygen.<sup>8,9</sup>

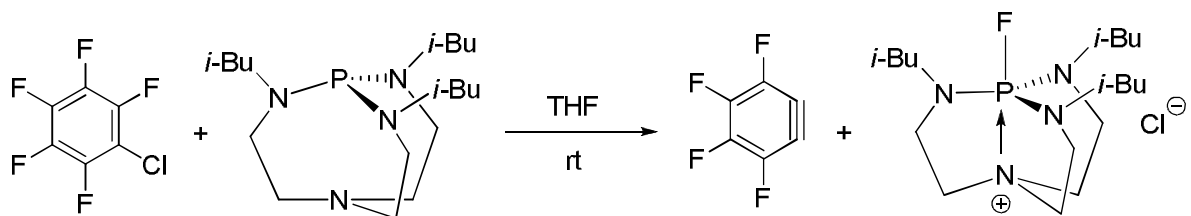


**Scheme 1. Proposed synthesis of PDFA**

It was observed during the course of my research that a proazaphosphatrane can be effectively employed for the synthesis of PDFA at room temperature; however, we presently have no firm data to support this observation. When we treated polychlorotrifluoroethylene

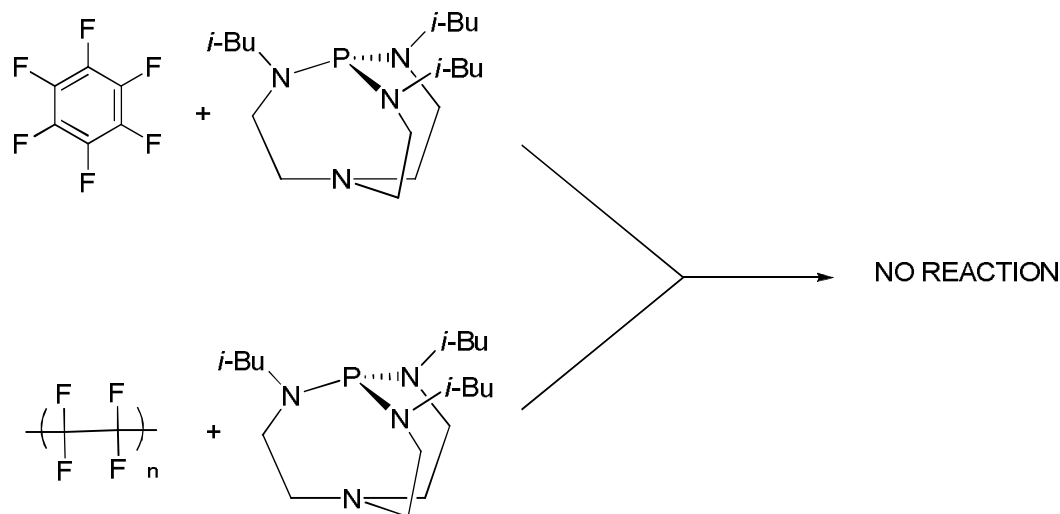


with an equivalent amount of proazaphosphatrane in dry toluene (Scheme 1), we observed the formation of a deep red polymer, which is the typical color of PDFA as described in the literature.<sup>7</sup> When the solution was examined by <sup>31</sup>P NMR spectroscopy, the formation of a fluorinated phosphatranium salt  $\delta^{31}\text{P}$  -40.9 (d,  $J = 730.0$  Hz) with chlorine as a likely counterion as shown in Scheme 1 was observed. A related observation was made by Dr. Kingston in our group during the reaction of a proazaphosphatrane with pentafluorochlorobenzene, which he monitored by <sup>31</sup>P NMR spectroscopy (Scheme 2). Attempts to trap the benzyne presumably formed (Scheme 2) were unsuccessful.



### Scheme 2. Reaction of pentafluorochlorobenzene with proazaphosphatrane

When Teflon<sup>®</sup> was reacted with a proazaphosphatrane, no fluorinated phosphatranium salt was observed, and this was also the case when hexafluorobenzene was reacted with proazaphosphatrane. Although we have no proof for the identity of the counterion (Scheme 3), and we see that the fluorinated phosphatranium salt is formed only when there is chlorine adjacent to fluorine in the substrate. Thus, we believe the counterion to be chloride.



Scheme 3

The advantages of our proposed synthesis compared with the competing methods are:

- 1) Handling monomeric difluoroacetylene is difficult as it is potentially explosive even at liquid nitrogen temperatures in the presence of trace amounts of oxygen.<sup>8,9</sup> Whereas, our method employs a very stable starting material, namely, commercially available polychlorotrifluoroethane.
- 2) Handling the product PDFA is difficult, as it is also sensitive to air, light and water. Thus, it might be difficult to cast the polymer into the desired form after the polymer is synthesized by conventional methods. In our invention, we can cast the starting parent polymer polychlorotrifluoroethane and then carry out the transformation of this material in precast form to PDFA using a proazaphosphatane.

### References

- 1) Metzger, K. C.; Welch, W. J. *Polym. Prepr. (Am. Chem. Soc. Div. Polym. Chem.)* **1984**, 25, 195-196.

- 2) Yamabe, T.; Tanaka, K.; Terama-E, H.; Fukui, K.; Shirakawa, H.; Ikeda, S. *Synth. Met.* **1980**, *1*, 321-327.
- 3) Bakshi, A. K.; Ladik, J.; Liegener, C.M. *Synth. Met.* **1987**, *20*, 43-55.
- 4) Groh, W.; Zimmerman, A. *Macromolecules* **1991**, *24*, 6660-6663.
- 5) Showa Denko K. K., Japanese Patent JP 83-87726 830520, **1983**.
- 6) Matsushita Electric Industrial Co., Japanese Patent JP 81-161657 811009, **1981**.
- 7) Gould, G. L.; Eswara, V.; Trifu, R. M.; Castner, D. G. *J. Am. Chem. Soc.* **1999**, *121*, 3781-3782.
- 8) Middleton, W. J.; Sharkey, W. H. *J. Am. Chem. Soc.* **1959**, *81*, 803-804.
- 9) Runge, A.; Wolfman, W. S. *Tetrahedron. Lett.* **1990**, *31*, 5453-5456.

## ACKNOWLEDGEMENTS

First and foremost, I would like to thank my greatest teacher of all: God. I will do my best in never forgetting what a great fortune I had in just being at Iowa State, and that coming to know Him comes with lessons in living and with serious responsibilities. I hope I am doing the work He has planned for me to do.

I would like to express my sincere gratitude to my supervisor, Prof. John G. Verkade, for having faith in my project proposals, for giving me the opportunity and financial support to work on them, and for guidance. I thank him for being more like my father than a supervisor and for being there when I needed his moral support the most.

I would like to thank my POS committee members Prof Richard C. Larock, Prof. George A. Kraus, Prof. Victor S. Lin, and Prof. Klaus Schmidt-Rohr for their encouragement and helpful suggestions.

I am grateful to Dr. Ch. Venkat Reddy for his guidance for the work in chapters 2, 3 and 4 and for his collaboration in the work described in chapters 5, 6 and 9 of my thesis. My gratitude also goes to Dr. Klaus Schmidt-Rohr and his student Xueqian Kong for their collaboration in the realization of the work described in chapter 7.

I would like to thank Dr. George A. Kraus, for inviting our group to attend his group meetings and for all the helpful discussion and suggestions he provided.

I would like to acknowledge the staff of the Chemistry Instrumentation Facility: Dr. Dave Scott and Dr. Shu Xu for their help in NMR spectroscopic experiments, Dr. Kamal Harratta for MS data, and Steve Veysey for MS and elemental analysis data.

I would like to also thank past and present Prof. Verkade group members for discussions, suggestions and guidance. Among those members are Dr. Nandankumar Valsan, Dr. Weiping Su, Dr. Sameer Urgaonkar, Dr. Brandon Fetterly, Reed Oshel, Steve Raders and Dr. Yibo Zhou.

I would like to acknowledge Energetics Inc, IPRT, the Iowa Department of Transportation, and the National Science Foundation for funding my research.

My sincere thanks go to Reverend Thomas Niehof, PhD of the Trinity Christian Reformed Church for his unconditional love and support. Thanks also go to my TCRC church family for showing faith in me and providing spiritual nourishment.

Most importantly my thanks and love go to my family. Without their love and support nothing I achieved in my life would have been possible. Thanks go to my parents for bringing me into this world and providing me with the best education. Thanks go to my sisters Kamini Sachdeva and Ruchi Kher, my brothers-in-law Ajay Sachdeva and Rajiv Kher, my brother Kuljit Wadhwa who has been more like a second father to me, and to my sister-in-law Nitika Wadhwa. Thanks also go to my niece and nephews Harsh Vardhan Kher, Punya Sachdeva, Achint Wadhwa and Bhuvi Sachdeva for all their love.

I would like to thank my friends who were there for me with all their support during the course of my PhD work. Thanks to Dr. Shilpa Worlikar for being a true supportive friend

during my tough times. Thanks also go to Neha Sawhney, Lekha Gupta, Satish Reddy, Ashutosh Tiwari, Smita Kakar, Vijay Walia, Ganesh Kumar, Saurabh Mehta, Divya Sinha and Yashdeep Phanse.

**APPENDIX A**

**CHAPTER 2**

**General Information**

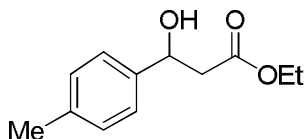
**References for known compounds and characterization data for the new compounds**

**$^1\text{H}$ ,  $^{13}\text{C}$  and HRMS for all compounds**

### General Information

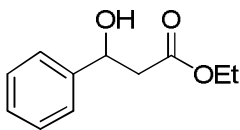
All reactions were carried out under inert atmosphere using oven dried glassware and a magnetic stirrer. THF was distilled and dried over sodium. Trimethylsilylethylacetate (TMSEA), proazaphosphatane **1a** and all aldehydes were purchased from Aldrich Chemical and used without further purification. Products were purified via column chromatography using hexane/ethyl acetate.  $^1\text{H}$  and  $^{13}\text{C}$  nmr spectra were obtained on a VXR-300 and a VXR-400 Varian NMR spectrometer, respectively. All NMR spectra were taken in  $\text{CDCl}_3$ . Thin layer chromatography was used to monitor reaction progress.

#### Ethyl-3-hydroxy-3-(4-methylphenyl)propionate (Table 1, entry 7)<sup>1</sup>:



The general procedure was followed for the synthesis and purification; product was afforded as a colorless oil in 86% isolated yield.

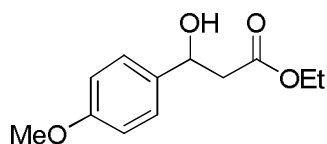
#### Ethyl-3-hydroxy-3-phenylpropionate (Table 2, entry 1)<sup>1</sup>:



The general procedure was followed for the synthesis and purification; product was afforded as a colorless oil in 71% isolated yield.

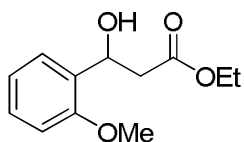
#### Ethyl-3-hydroxy-3-(4-methoxyphenyl)propionate (Table 2, entry 2)<sup>1</sup>:





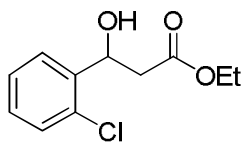
The general procedure was followed for the synthesis and purification; product was afforded as a colorless oil in 76% isolated yield.

**Ethyl-3-hydroxy-3-(2-methoxyphenyl)propionate (Table 2, entry 3)<sup>2</sup>:**



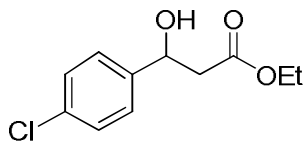
The general procedure was followed for the synthesis and purification; product was afforded as a colorless oil in 77% isolated yield.

**Ethyl-3-hydroxy-3-(2-chlorophenyl)propionate (Table 2, entry 4)<sup>3</sup>:**



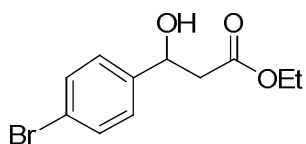
The general procedure was followed for the synthesis and purification; product was afforded as a colorless oil in 87% isolated yield.

**Ethyl-3-hydroxy-3-(4-chlorophenyl)propionate (Table 2, entry 5)<sup>1</sup>:**



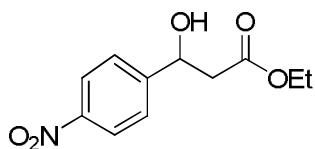
The general procedure was followed for the synthesis and purification; product was afforded as a colorless oil in 78% isolated yield.

**Ethyl-3-hydroxy-3-(4-bromophenyl)propionate (Table 2, entry 6)<sup>1</sup>:**



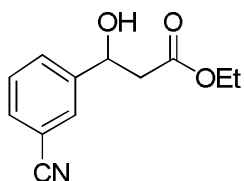
The general procedure was followed for the synthesis and purification; product was afforded as a colorless oil in 87% isolated yield.

**Ethyl-3-hydroxy-3-(4-nitrophenyl)propionate (Table 2, entry 7)<sup>3</sup>:**



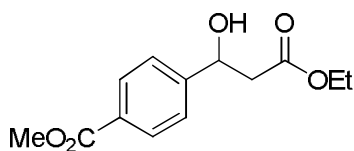
The general procedure was followed for the synthesis and purification; product was afforded as a yellow oil in 92% isolated yield.

**Ethyl-3-hydroxy-3-(3-cyanophenyl)propionate (Table 2, entry 8):**



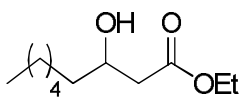
The general procedure was followed for the synthesis and purification, affording the product as a colorless oil in 84% isolated yield. <sup>1</sup>H NMR (CDCl<sub>3</sub>, 400 MHz): δ 7.68 (s, 1H), 7.60 (d, 1H, *J* = 8.0 Hz), 7.56 (d, 1H, *J* = 8.0 Hz), 7.45 (t, 1H, *J* = 8.0 Hz), 5.14 (t, 1H, *J* = 4.0 Hz), 4.17 (q, 2H, *J* = 8.0 Hz), 3.69 (bs, 1H), 2.70–2.68 (m, 2H), 1.25 (t, 3H, *J* = 8.0 Hz) ppm; <sup>13</sup>C NMR (CDCl<sub>3</sub>, 100.6 MHz): δ 172.2, 144.3, 131.6, 130.4, 129.6, 129.5, 118.9, 112.8, 69.5, 61.4, 43.3, 14.4 ppm; HRMS *m/z* Calcd. for C<sub>12</sub>H<sub>13</sub>NO<sub>3</sub>: 219.08954. Found: 219.09013.

**4-(2-Ethoxycarbonyl-1-hydroxy-ethyl)-benzoic acid methyl ester (Table 2, entry 9)<sup>4</sup>:**



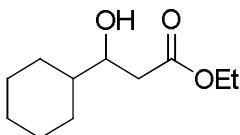
The general procedure was followed for the synthesis and purification; product was afforded as a colorless oil in 71% isolated yield.

**Ethyl-3-hydroxynonanoate (Table 2, entry 10)<sup>5</sup>:**



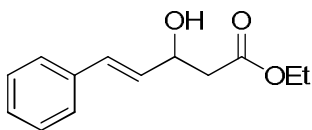
The general procedure was followed for the synthesis and purification; product was afforded as a colorless oil in 73% isolated yield. <sup>13</sup>C NMR (CDCl<sub>3</sub>, 100.6 MHz): δ 173.4, 68.3, 60.9, 41.5, 36.7, 32.0, 29.4, 25.7, 22.8, 14.4, 14.3 ppm.

**Ethyl 3-cyclohexyl-3-hydroxypropanoate (Table 2, entry 11)<sup>6</sup>:**



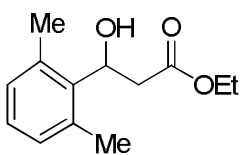
The general procedure was followed for the synthesis and purification; product was afforded as a colorless oil in 77% isolated yield.

**Ethyl-3-Hydroxy-5-phenylpent-4-enoate (Table 2, entry 12)<sup>1</sup>:**



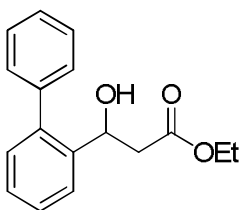
The general procedure was followed for the synthesis and purification; product was afforded as a colorless oil in 76% isolated yield.

**Ethyl-3-hydroxy-3-(2,6-dimethylphenyl)propionate (Table 2, entry 13):**



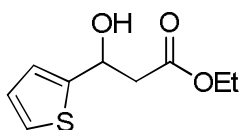
The general procedure was followed for the synthesis and purification; product was afforded as a colorless oil in 87% isolated yield.  $^1\text{H}$  NMR ( $\text{CDCl}_3$ , 400 MHz):  $\delta$  7.07–6.99 (m, 3H), 5.64 (d, 1H,  $J = 10.4$  Hz), 4.21 (q, 2H,  $J = 8.0$  Hz), 3.09–2.97 (m, 2H), 2.58–2.53 (m, 1H), 2.46 (s, 6H), 1.29 (t, 3H,  $J = 8.0$  Hz) ppm;  $^{13}\text{C}$  NMR ( $\text{CDCl}_3$ , 100.6 MHz):  $\delta$  172.3, 137.3, 135.9, 129.2, 127.2, 67.4, 60.6, 39.7, 20.6, 14.0 ppm; HRMS  $m/z$  Calcd. for  $\text{C}_{13}\text{H}_{18}\text{O}_3$ : 222.12559. Found: 222.12604.

**Ethyl-3-hydroxy-3-(2-biphenyl)propionate (Table 2, entry 14):**



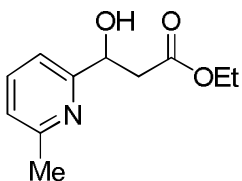
The general procedure was followed for the synthesis and purification; product was afforded as a colorless oil in 78 % isolated yield.  $^1\text{H}$  NMR ( $\text{CDCl}_3$ , 400 MHz):  $\delta$  7.67 (d, 1H,  $J = 8.0$  Hz), 7.43–7.33 (m, 7H), 7.24 (d, 1H,  $J = 8.0$  Hz), 5.27 (d, 1H,  $J = 9.0\text{Hz}$ ), 4.13–4.07 (m, 2H), 3.45 (s, 1H), 2.73–2.52 (m, 2H), 1.21 (t, 3H,  $J = 8.0$  Hz) ppm;  $^{13}\text{C}$  NMR ( $\text{CDCl}_3$ , 100.6 MHz):  $\delta$  172.6, 141.0, 140.8, 139.9, 130.4, 129.4, 128.6, 128.2, 127.8, 127.5, 126.2, 67.0, 61.0, 42.8, 14.4 ppm; HRMS  $m/z$  Calcd. for  $\text{C}_{17}\text{H}_{18}\text{O}_3$ : 270.12559. Found: 270.12608.

**Ethyl-3-hydroxy-3-(2-thienyl)-propionate (Table 2, entry 15)<sup>7</sup>:**



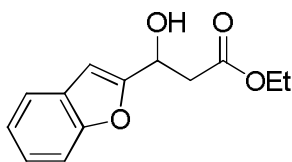
The general procedure was followed for the synthesis and purification; product was afforded as a yellow oil in 76% isolated yield.

**Ethyl-3-hydroxy-3-(6-methylpyridin-2-yl)propanoate (Table 2, entry 16):**

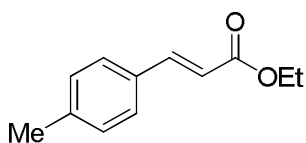


The general procedure was followed for the synthesis and purification; product was afforded as a colorless oil in 81% isolated yield.  $^1\text{H}$  NMR ( $\text{CDCl}_3$ , 400 MHz):  $\delta$  7.59 (t, 1H,  $J = 8.0$  Hz), 7.15 (d, 1H,  $J = 8.0$  Hz), 7.04 (d, 1H,  $J = 8.0$  Hz), 5.12 (d, 1H,  $J = 4.0$  Hz), 4.53 (d, 1H,  $J = 4.0$  Hz), 4.15 (q, 2H,  $J = 8.0$  Hz), 2.80–2.66 (m, 2H), 2.51 (s, 3H), 1.23 (t, 3H,  $J = 8.0$  Hz) ppm;  $^{13}\text{C}$  NMR ( $\text{CDCl}_3$ , 100.6 MHz):  $\delta$  172.1, 159.9, 157.5, 137.3, 122.3, 117.3, 70.0, 60.9, 43.3, 24.5, 14.4 ppm; HRMS  $m/z$  Calcd. for  $\text{C}_{11}\text{H}_{15}\text{NO}_3$ : 209.10519. Found: 209.10557.

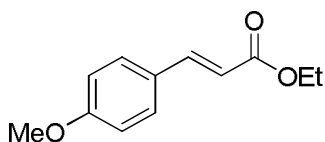
**Ethyl-3-(benzofuran-2-yl)-3-hydroxypropanoate (Table 2, entry 17):**



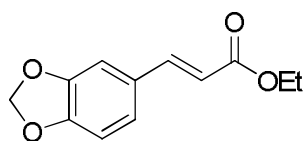
The general procedure was followed for the synthesis and purification; product was afforded as a yellow oil in 79% isolated yield.  $^1\text{H}$  NMR ( $\text{CDCl}_3$ , 400 MHz):  $\delta$  7.53 (d, 1H,  $J = 8.0$  Hz), 7.45 (d, 1H,  $J = 8.0$  Hz), 7.28–7.19 (m, 2H), 6.66 (s, 1H), 5.28 (d, 1H,  $J = 8.0$  Hz), 4.19 (q, 2H,  $J = 8.0$  Hz), 3.71 (d, 1H,  $J = 4.0$  Hz), 2.95 (d, 1H,  $J = 4.0$  Hz), 1.26 (t, 3H,  $J = 8.0$  Hz) ppm;  $^{13}\text{C}$  NMR ( $\text{CDCl}_3$ , 100.6 MHz):  $\delta$  172.0, 157.7, 155.0, 128.2, 124.5, 123.1, 121.4, 111.5, 103.2, 65.0, 61.3, 40.1, 14.4 ppm; HRMS  $m/z$  Calcd. for  $\text{C}_{13}\text{H}_{14}\text{O}_4$ : 234.08921. Found: 234.08965.

**Ethyl (*E*)-3-(4-methylphenyl)-2-propenoate (Table 3, entry 1)<sup>8</sup>:**

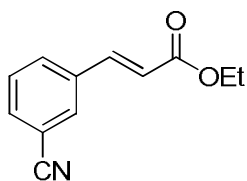
The general procedure was followed for the synthesis and purification; product was afforded as a colorless oil in 83% isolated yield.

**Ethyl (*E*)-3-(4-methoxyphenyl)-2-propenoate (Table 3, entry 2)<sup>8</sup>:**

The general procedure was followed for the synthesis and purification; product was afforded as a colorless oil in 83% isolated yield.

**Ethyl-3-benzo[1,3]dioxol-5-yl-(*E*)-acrylate (Table 3, entry 3)<sup>9</sup>:**

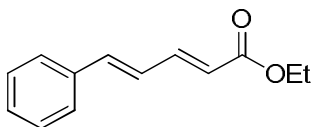
The general procedure was followed for the synthesis and purification; product was afforded as a colorless oil in 79% isolated yield.

**Ethyl (*E*)-3-(3-cyanophenyl)-2-propenoate (Table 3, entry 4):**

The general procedure was followed for the synthesis and purification; product was afforded as a white solid in 90% isolated yield. <sup>1</sup>H NMR (CDCl<sub>3</sub>, 400 MHz): δ 7.47 (s, 1H), 7.70–7.56 (m, 3H), 7.47 (t, 1H, *J* = 8.0 Hz), 6.44 (d, 1H, *J* = 16.0 Hz), 4.22 (q, 2H, *J* = 8.0 Hz), 1.29 (t,

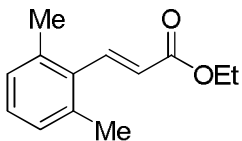
3H,  $J = 8.0$  Hz) ppm;  $^{13}\text{C}$  NMR ( $\text{CDCl}_3$ , 100.6 MHz):  $\delta$  166.3, 141.9, 135.9, 133.3, 132.1, 131.5, 130.0, 121.7, 118.4, 113.5, 61.1, 14.5 ppm; HRMS  $m/z$ . Calcd. for  $\text{C}_{12}\text{H}_{11}\text{NO}_2$ : 201.07897. Found: 201.07925.

**Ethyl (*E,E*)-5-phenylpenta-2,4-dienoate (Table 3, entry 5)<sup>8</sup>:**



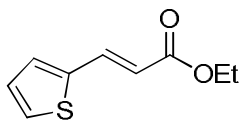
The general procedure was followed for the synthesis and purification; product was afforded as a colorless oil in 84% (9:1 mixture of EE/EZ) isolated yield.

**Ethyl (*E*)-3-(2,6-dimethylphenyl)-2-propenoate (Table 3, entry 6)<sup>8</sup>:**



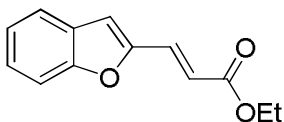
The general procedure was followed for the synthesis and purification; product was afforded as a colorless oil in 80% isolated yield.

**Ethyl-3-thiophen-3-yl-(*E*)-acrylate (Table 3, entry 7)<sup>9</sup>:**



The general procedure was followed for the synthesis and purification; product was afforded as a colorless oil in 89% isolated yield.

**Ethyl (*E*)-3-(benzo[*b*]furan-2-yl)-2-propenoate (Table 3, entry 8)<sup>10</sup>:**



The general procedure was followed for the synthesis and purification; product was afforded as a white solid in 79 % isolated yield.  $^{13}\text{C}$  NMR ( $\text{CDCl}_3$ , 100.6 MHz):  $\delta$  166.8, 155.7, 152.6, 131.4, 128.6, 126.6, 123.5, 121.9, 119.2, 111.6, 111.3, 60.9, 14.6 ppm.

#### Reference:

1. Chen, X.; Zhang, C.; Wu, H.; Yu, X.; Su, W.; Cheng, J. *Synthesis* **2007**, 3233–3239.
2. Dede, R.; Michaelis, L.; Fuentes, D.; Yawer, M. A.; Hussain, I.; Fischer, C.; Langer, P. *Tetrahedron* **2007**, *63*, 12547–12561.
3. Xu, C.; Yuan, C. *Tetrahedron* **2005**, *61*, 2169–2186.
4. Hlavinka, M. L.; Hagadorn, J. R. *Tetrahedron Lett.* **2006**, *47*, 5049–5053.
5. Chattopadhyay, A.; Salaskar, A. *Synthesis* **2000**, 561–564.
6. Beignet, J.; Jarvis, P. J.; Cox, L. R. *J. Org. Chem.* **2008**, *73* 5462–5475.
7. Cozzi, P. G.; Benfatti, F.; Capdevila, M. G.; Mignogna, A. *Chem. Comm.* **2008**, 3317–3318.
8. Chen, Y.; Huang, L.; Ranade, M. A.; Zhang, X. P. *J. Org. Chem.* **2003**, *68*, 3714–3717.
9. Zeitler, K. *Org. Lett.* **2006**, *8*, 637–640.
10. Matsunaga, N.; Kaku, T.; Itoh, F.; Tanaka, T.; Hara, T.; Miki, H.; Iwasaki, M.; Aono, T.; Yamaoka, M.; Kusaka, M.; Tasaka, A. *Bioorg. Med. Chem.* **2004**, *12*, 2251–2273.



KW422, CDCI3  
400 MHz  
COLORLESS OIL  
NOV 08 2007

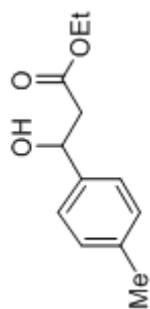
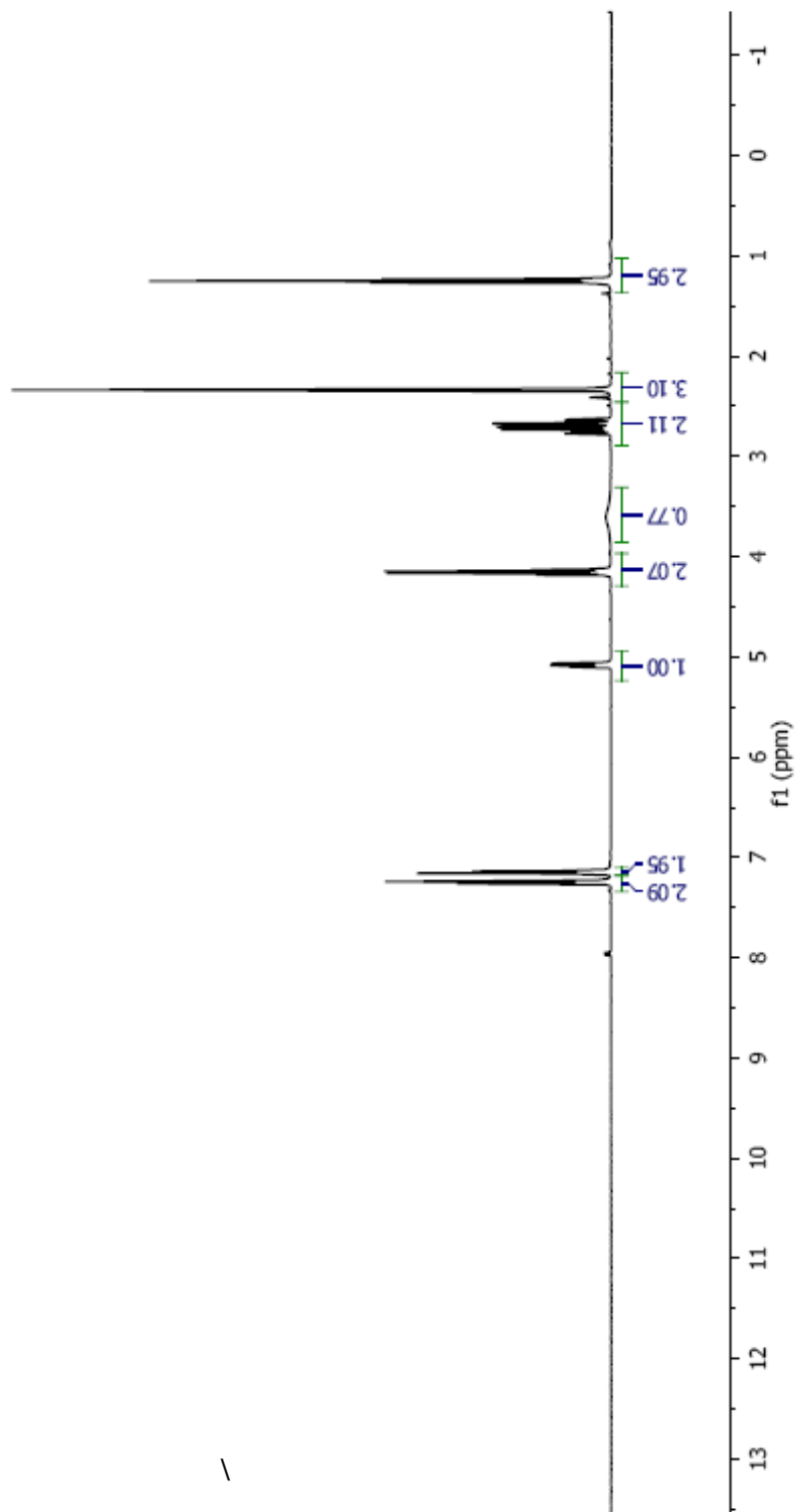
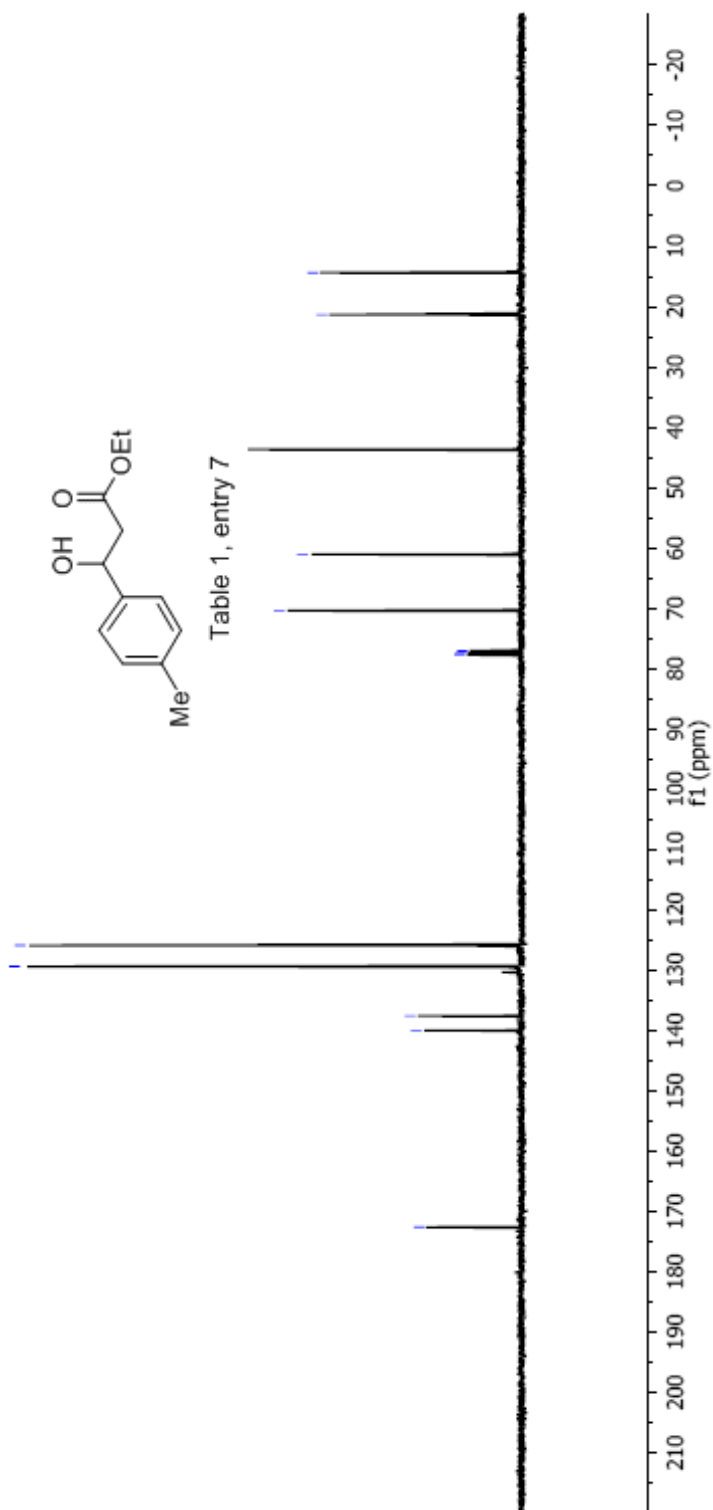
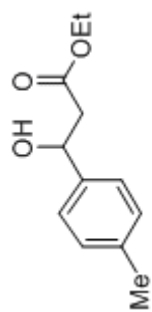


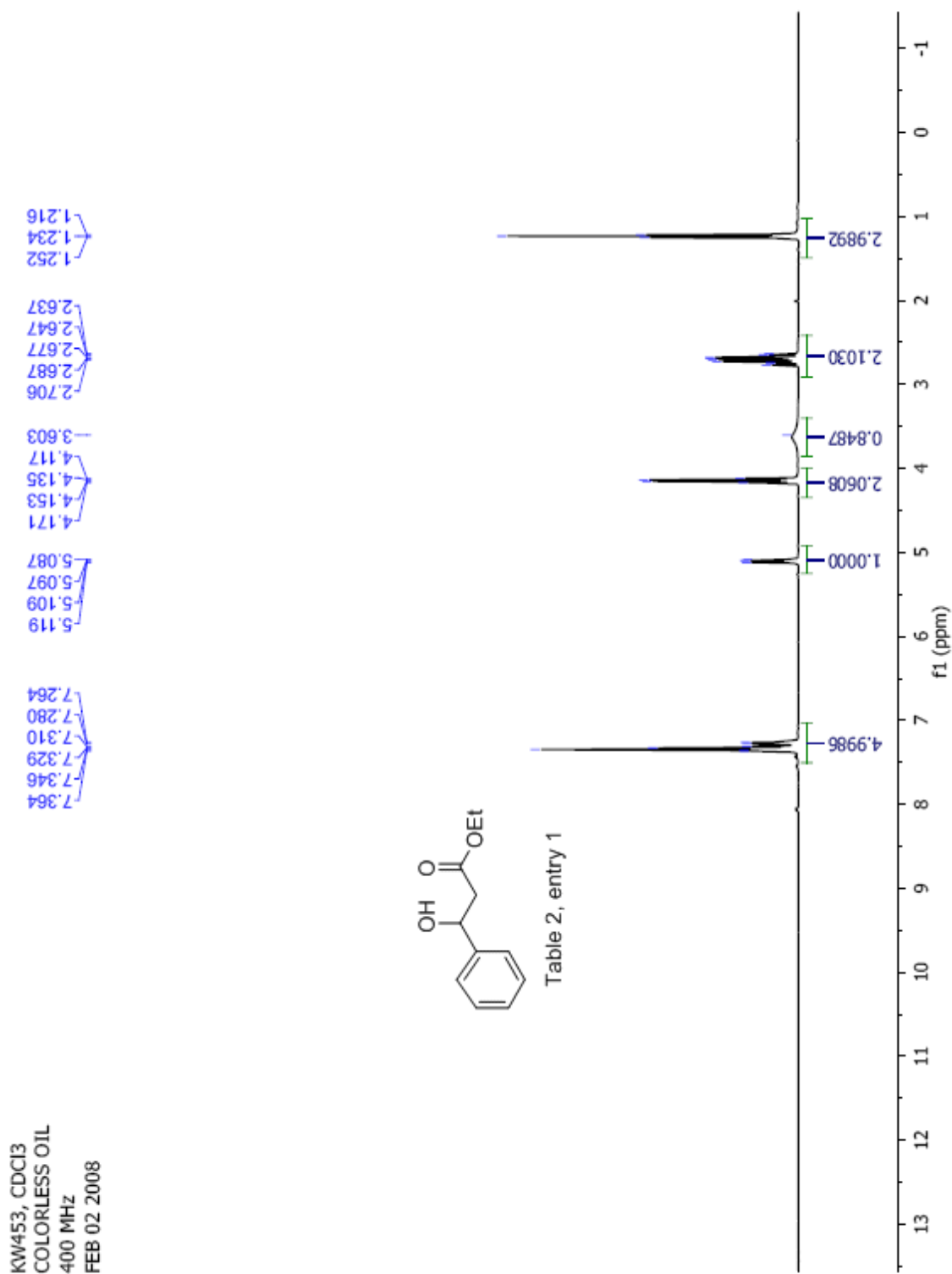
Table 1, entry 7

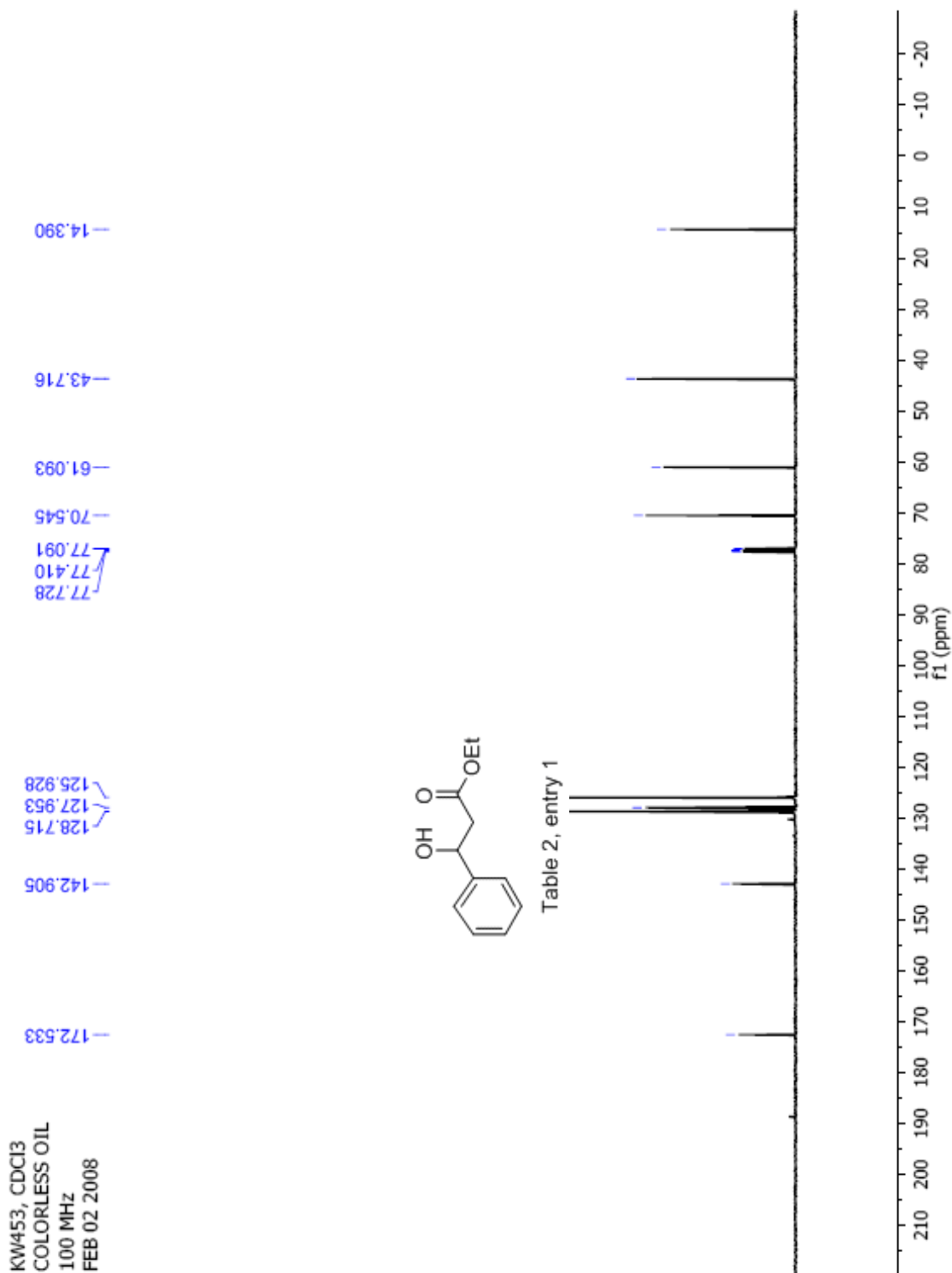


KW422, CDCl<sub>3</sub>  
100 MHz  
COLORLESS OIL  
NOV 08 2007

172.581  
139.967  
137.592  
129.380  
125.885  
77.724  
77.405  
77.088  
70.416  
61.056  
43.699  
21.371  
14.403







KW452, CDCI3  
400 MHz  
COLORLESS OIL  
JAN 29 2008

7.292  
7.270  
6.877  
6.855  
5.082  
5.073  
5.059  
5.050  
4.167  
4.131  
3.782  
3.782  
3.401  
2.710  
2.676  
2.667  
2.636  
2.626  
1.264  
1.247  
1.229

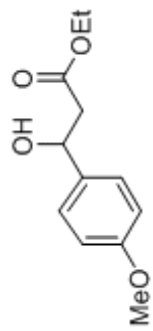
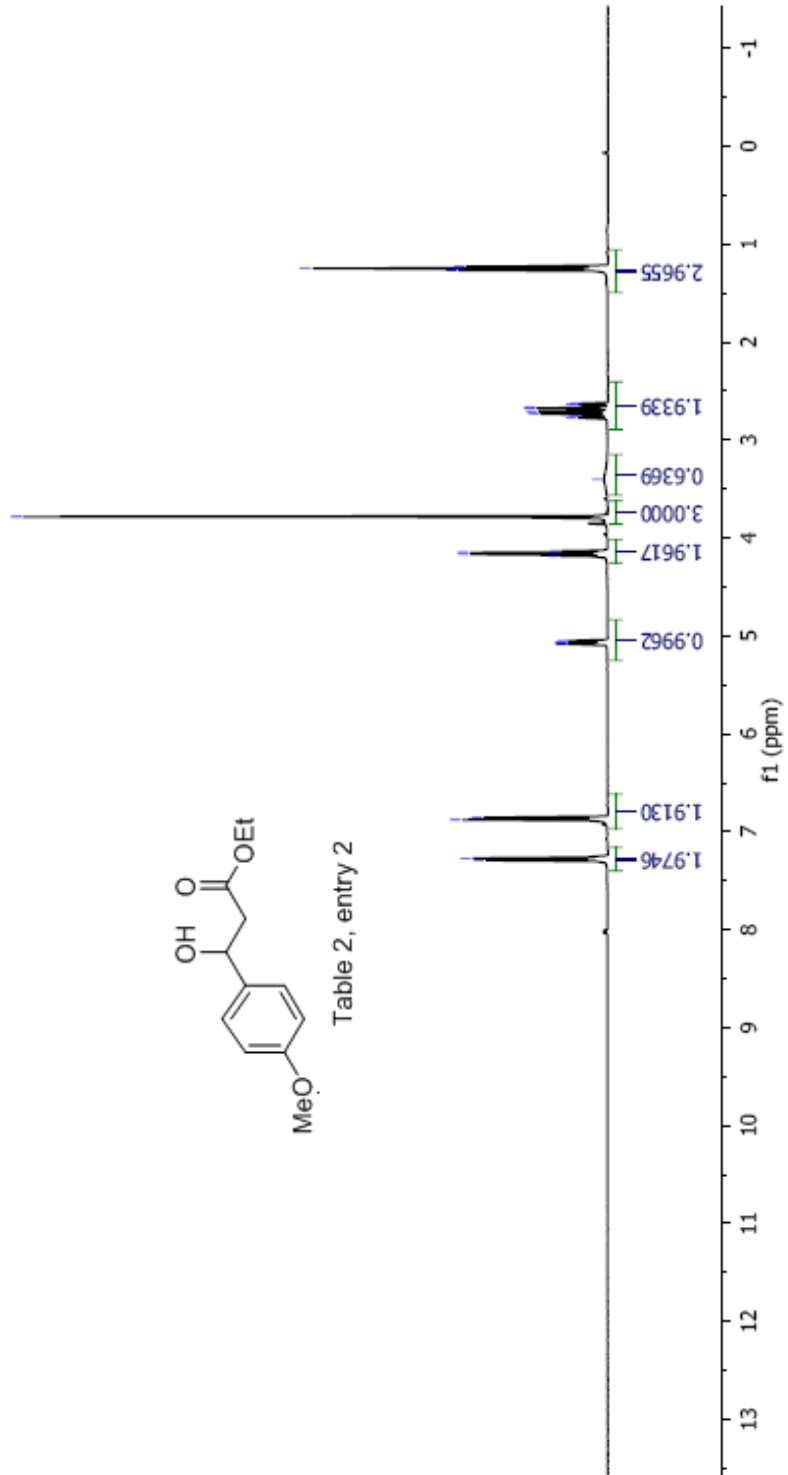
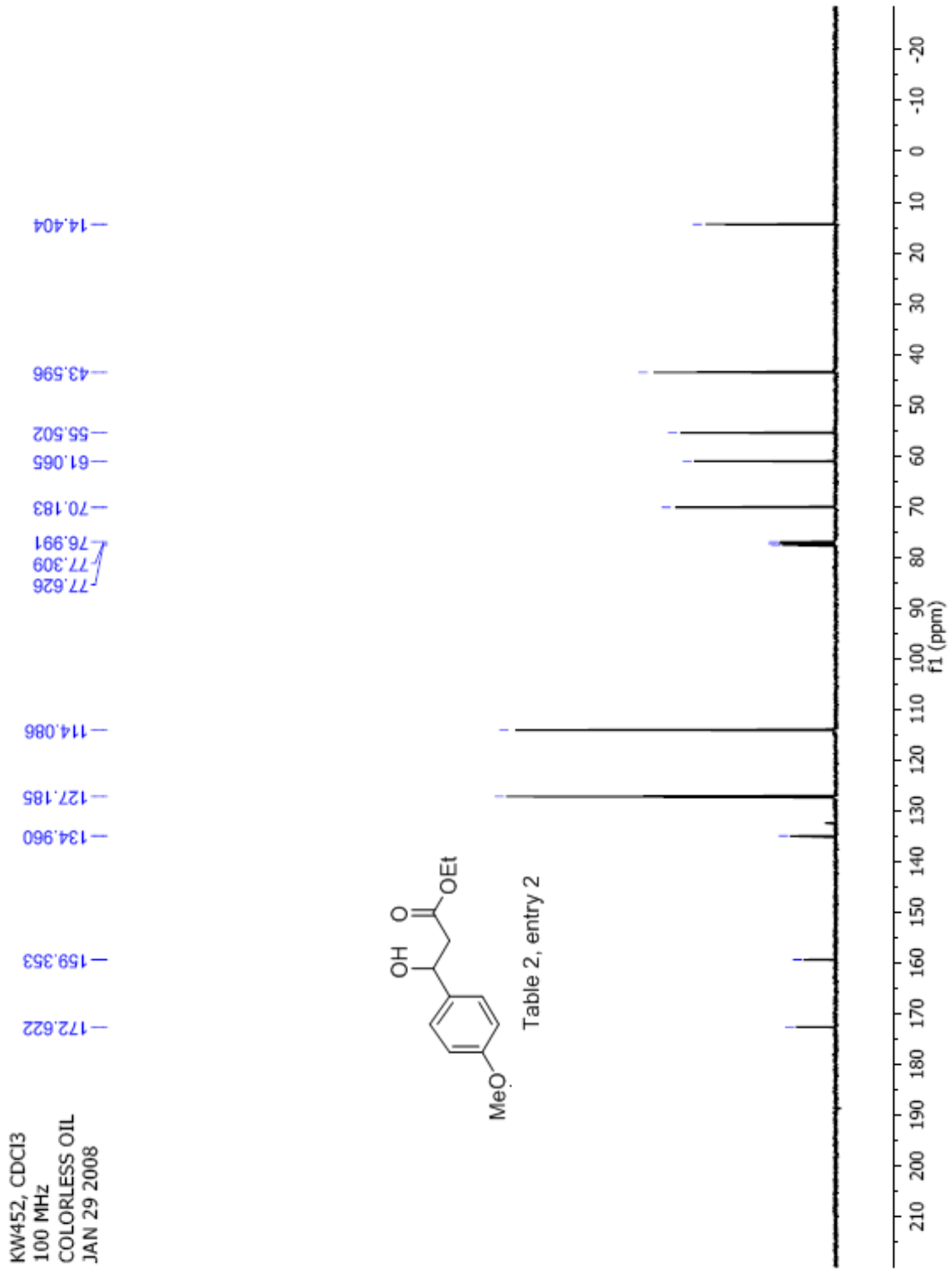


Table 2, entry 2





KW425, CDCl<sub>3</sub>  
300 MHz  
COLORLESS OIL

7.43  
7.41  
7.40  
7.26  
7.23  
7.21  
7.20  
6.95  
6.92  
6.85  
6.83  
5.36  
5.35  
5.33  
4.15  
4.13  
4.11  
3.81  
3.62  
3.61  
2.78  
2.77  
2.70  
2.67  
2.65  
2.62  
1.25  
1.23  
1.21

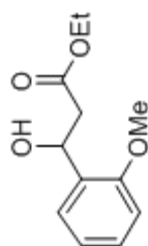
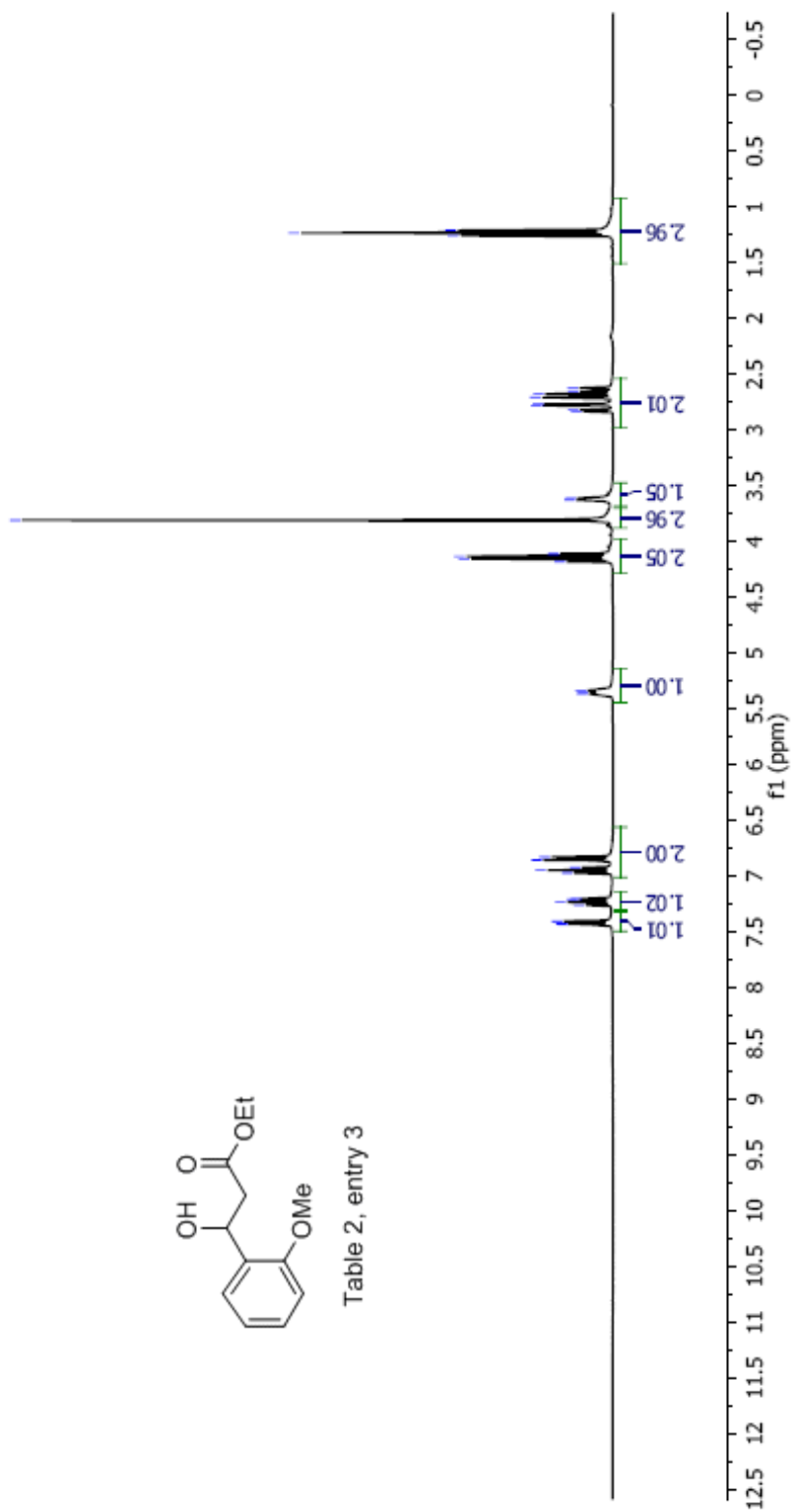
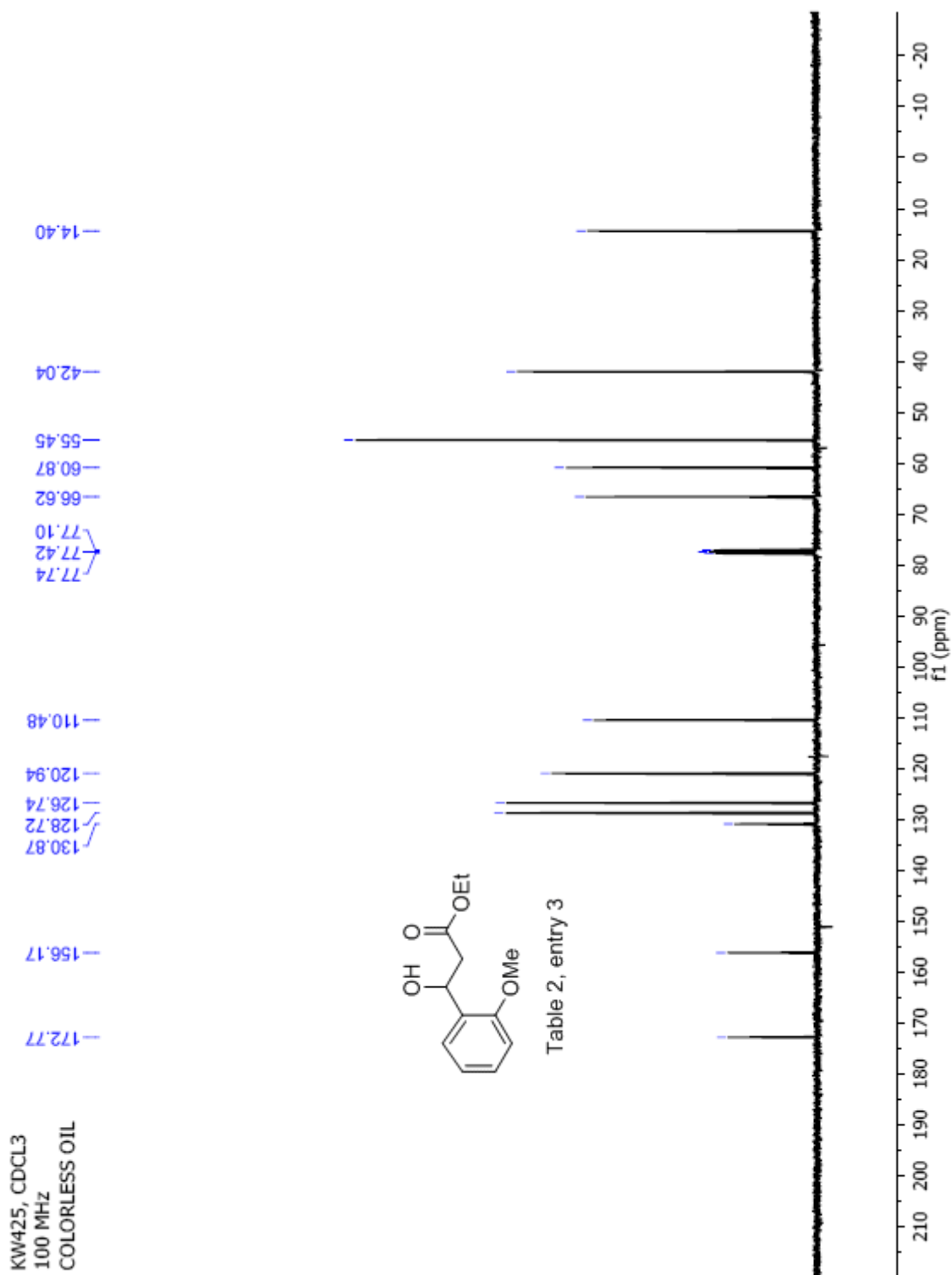


Table 2, entry 3







KW473, CDCl<sub>3</sub>  
400MHz  
COLORLESS OIL

7.629  
7.625  
7.609  
7.606  
7.303  
7.225  
7.201  
5.497  
5.489  
5.482  
5.473  
5.465  
5.458  
4.193  
4.176  
4.158  
3.678  
3.669  
2.821  
2.600  
2.576  
2.558  
2.534  
1.279  
1.261  
1.243

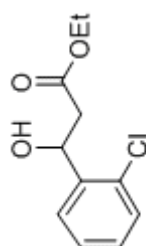
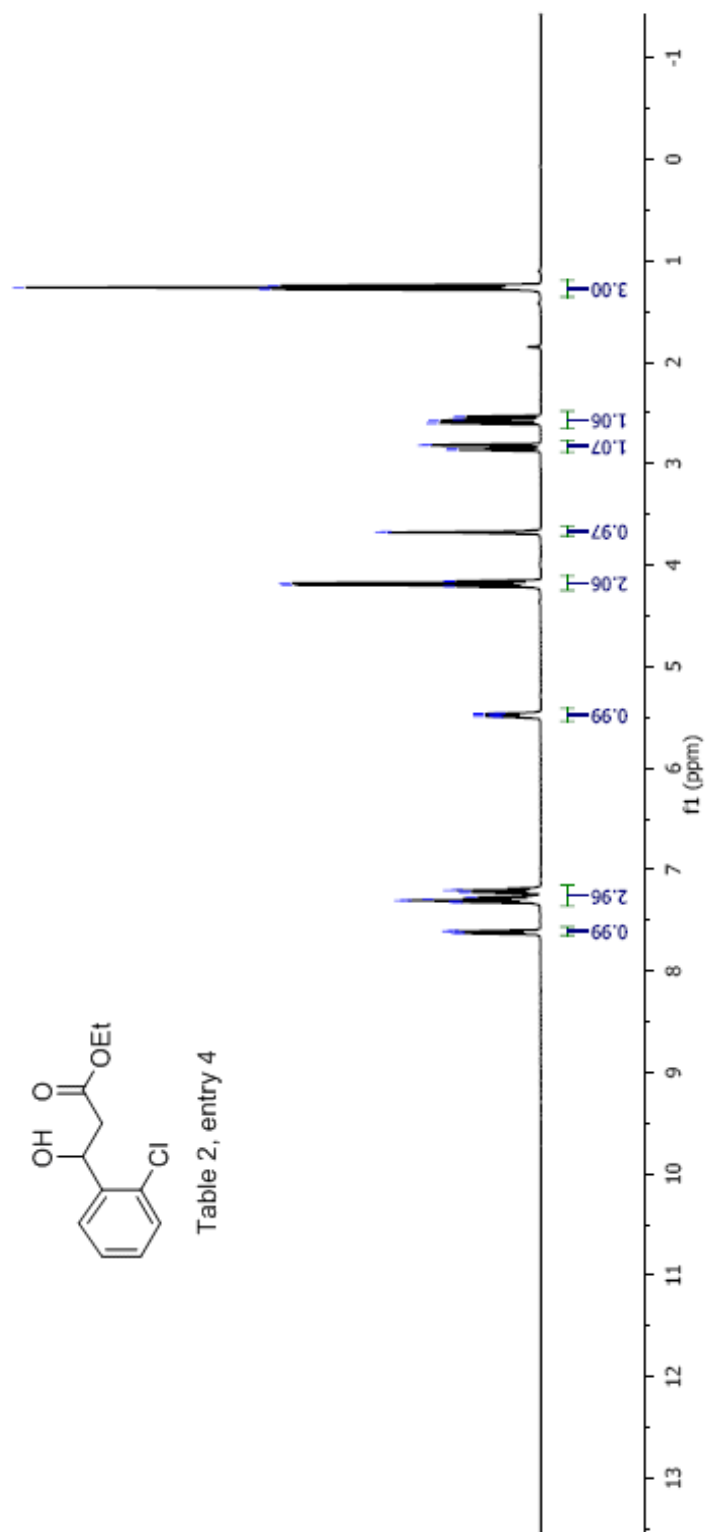
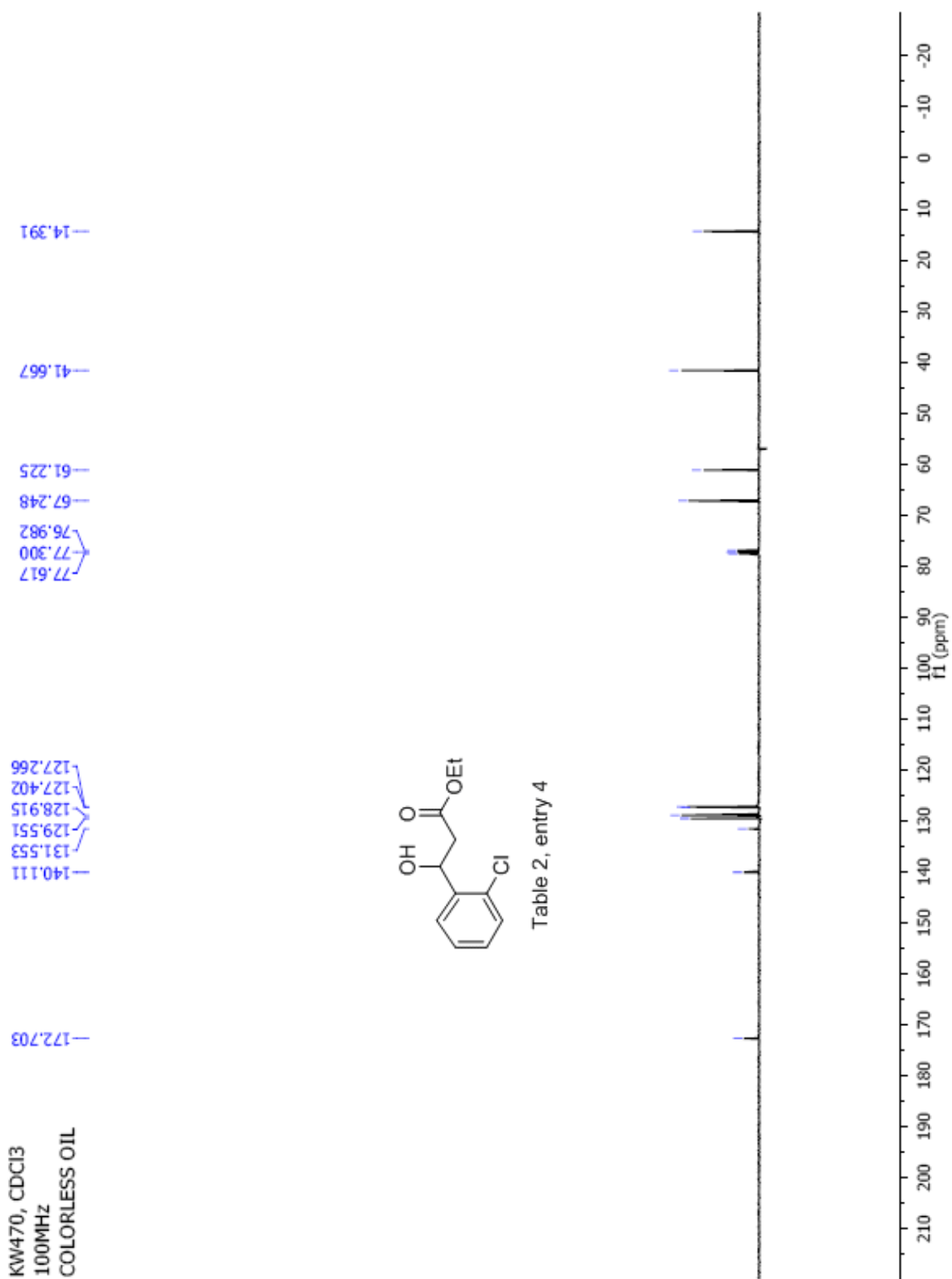


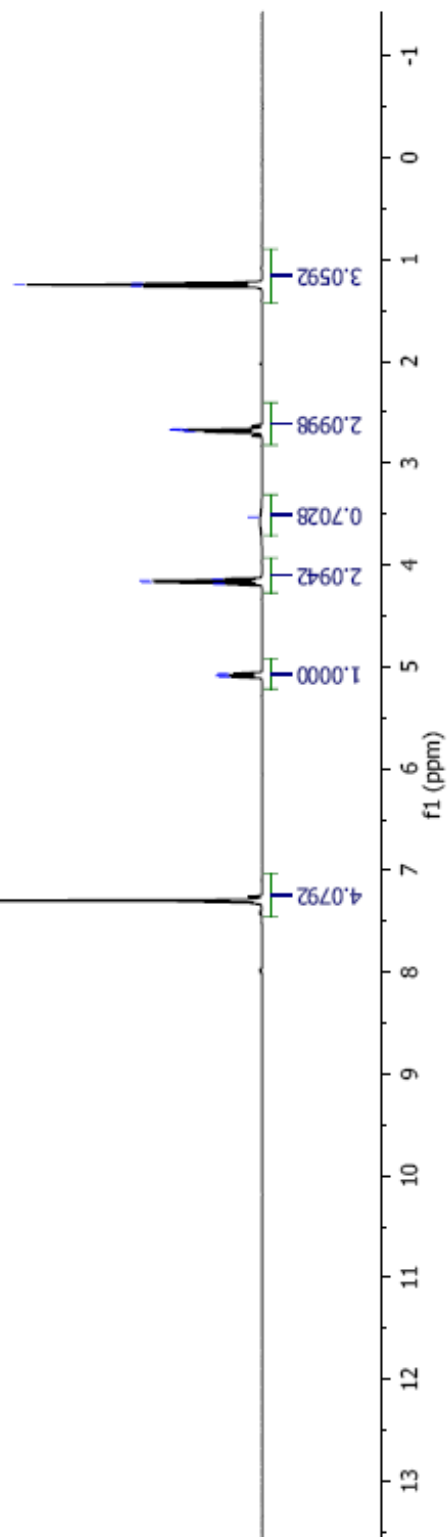
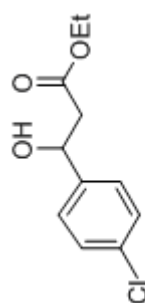
Table 2, entry 4

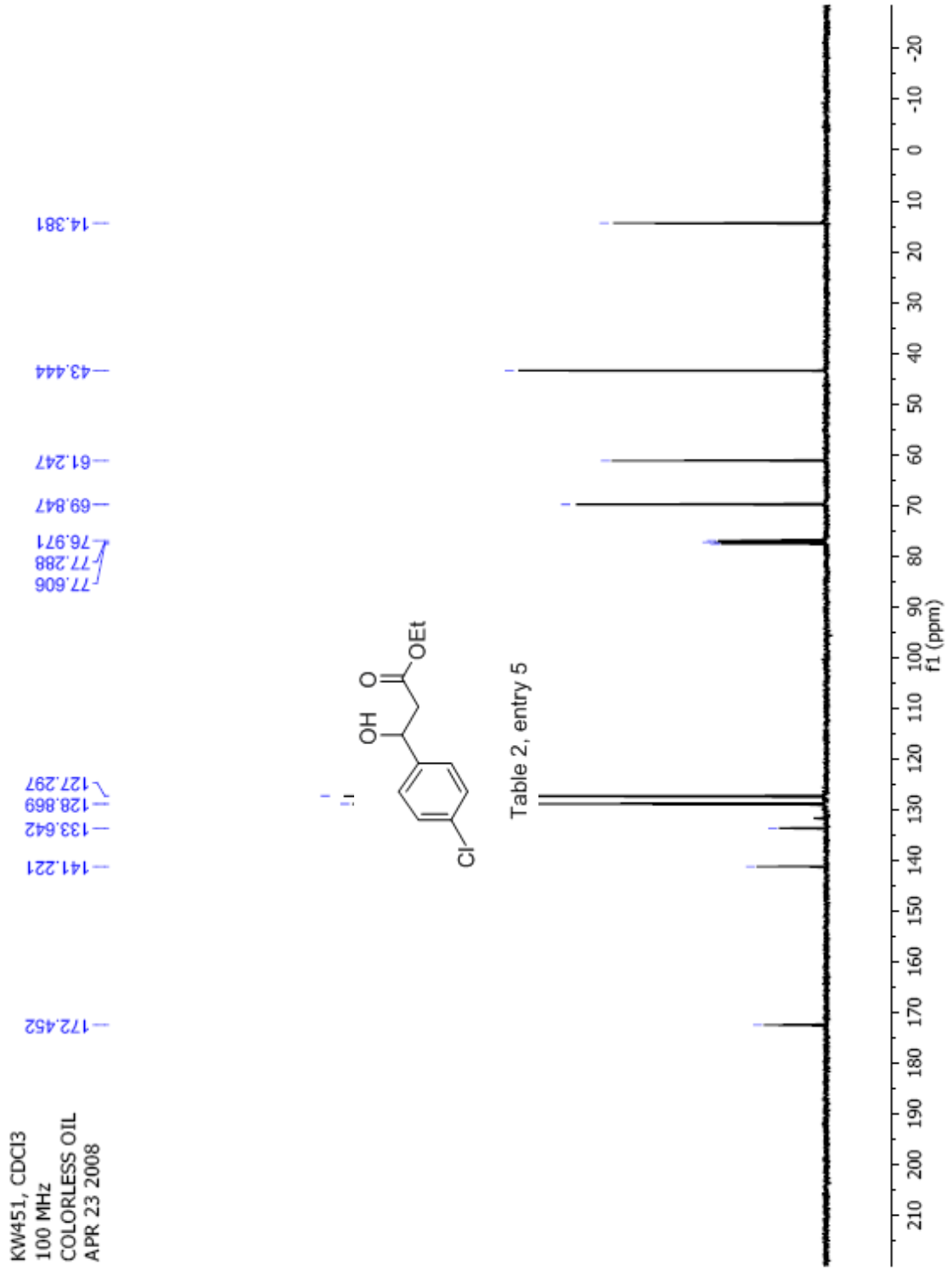




KW451, CDCI3  
400 MHz  
COLORLESS OIL  
APR 23 2008

1.230  
1.248  
1.266  
2.666  
2.672  
2.678  
2.692  
3.531  
4.135  
4.153  
4.171  
4.188  
5.068  
5.079  
5.088  
5.100  
7.299





KW456, CDCI3  
300 MHz  
COLORLESS OIL

7.468  
7.443  
7.244  
7.216  
5.061  
4.169  
4.145  
4.143  
4.122  
3.502  
2.682  
2.674  
2.671  
2.657  
1.269  
1.266  
1.246  
1.242  
1.222  
1.219

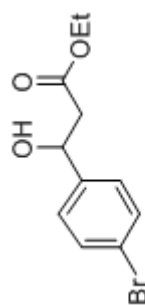
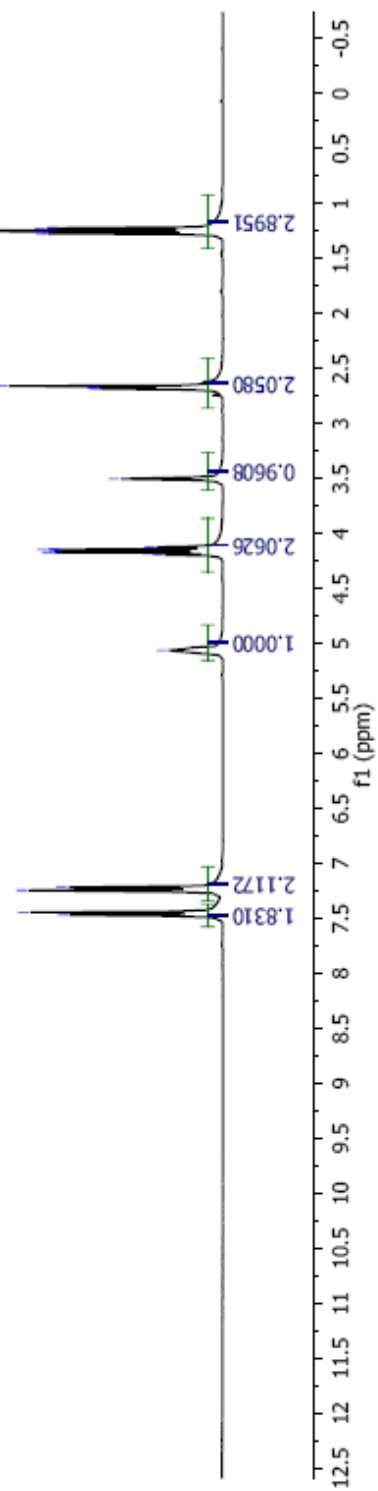
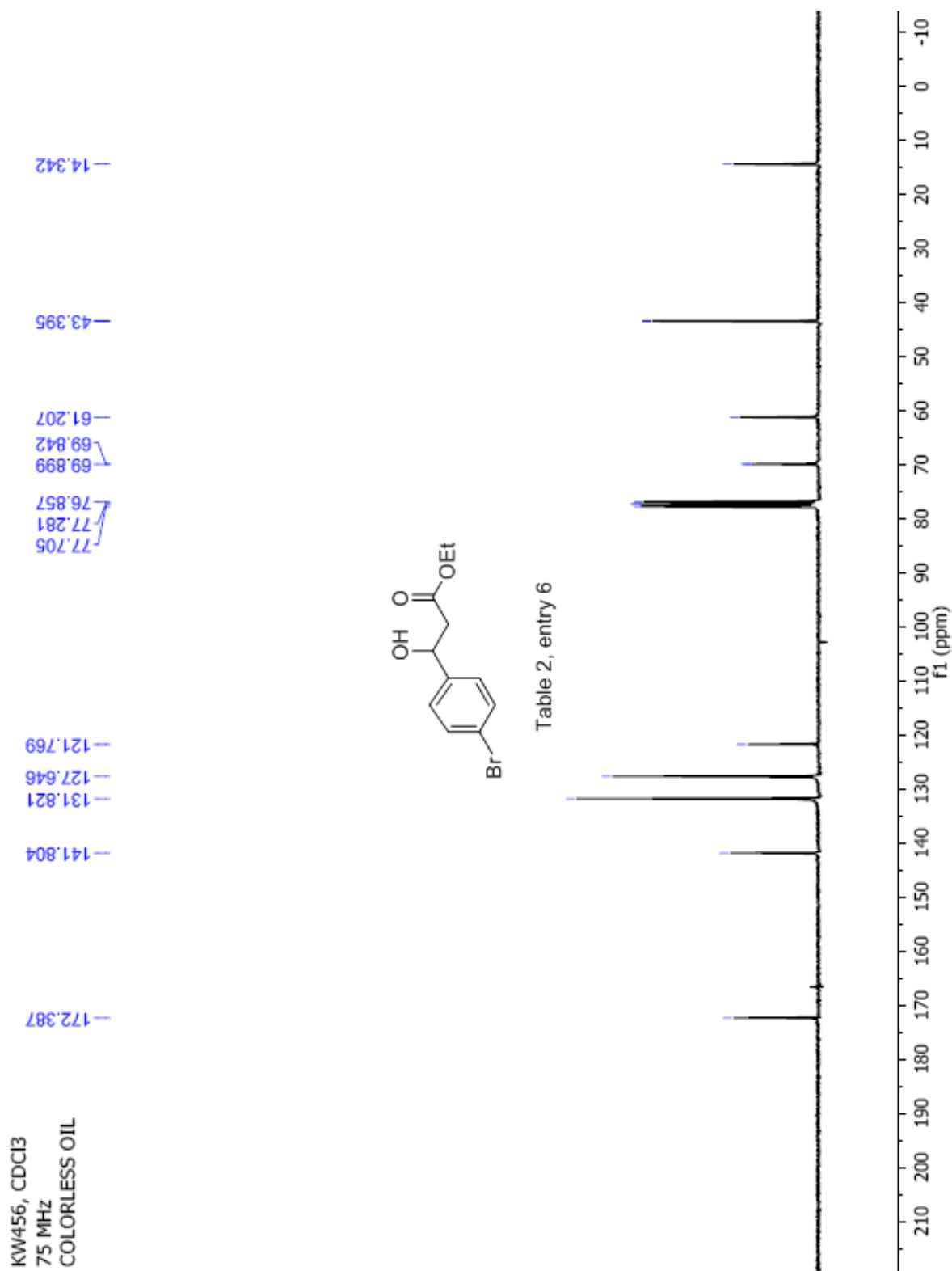


Table 2, entry 6





KW457, CDC13  
 YELLOW OIL  
 400 MHz  
 FEB 02 20 2008

8.174  
 8.170  
 8.157  
 8.152  
 7.542  
 7.521  
 5.218  
 5.200  
 5.188  
 4.161  
 4.143  
 4.125  
 3.786  
 2.710  
 2.706  
 2.698  
 2.686  
 1.248  
 1.230  
 1.212

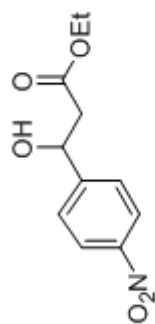
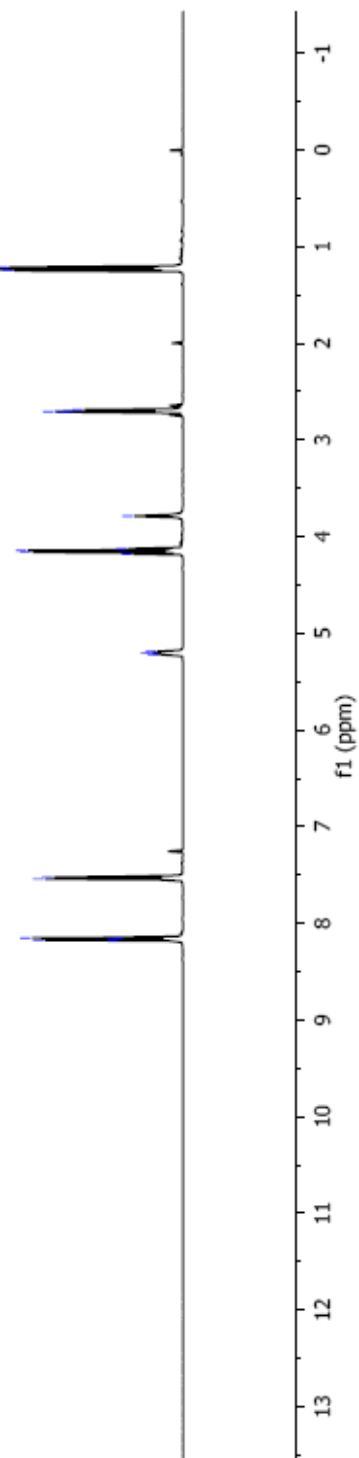
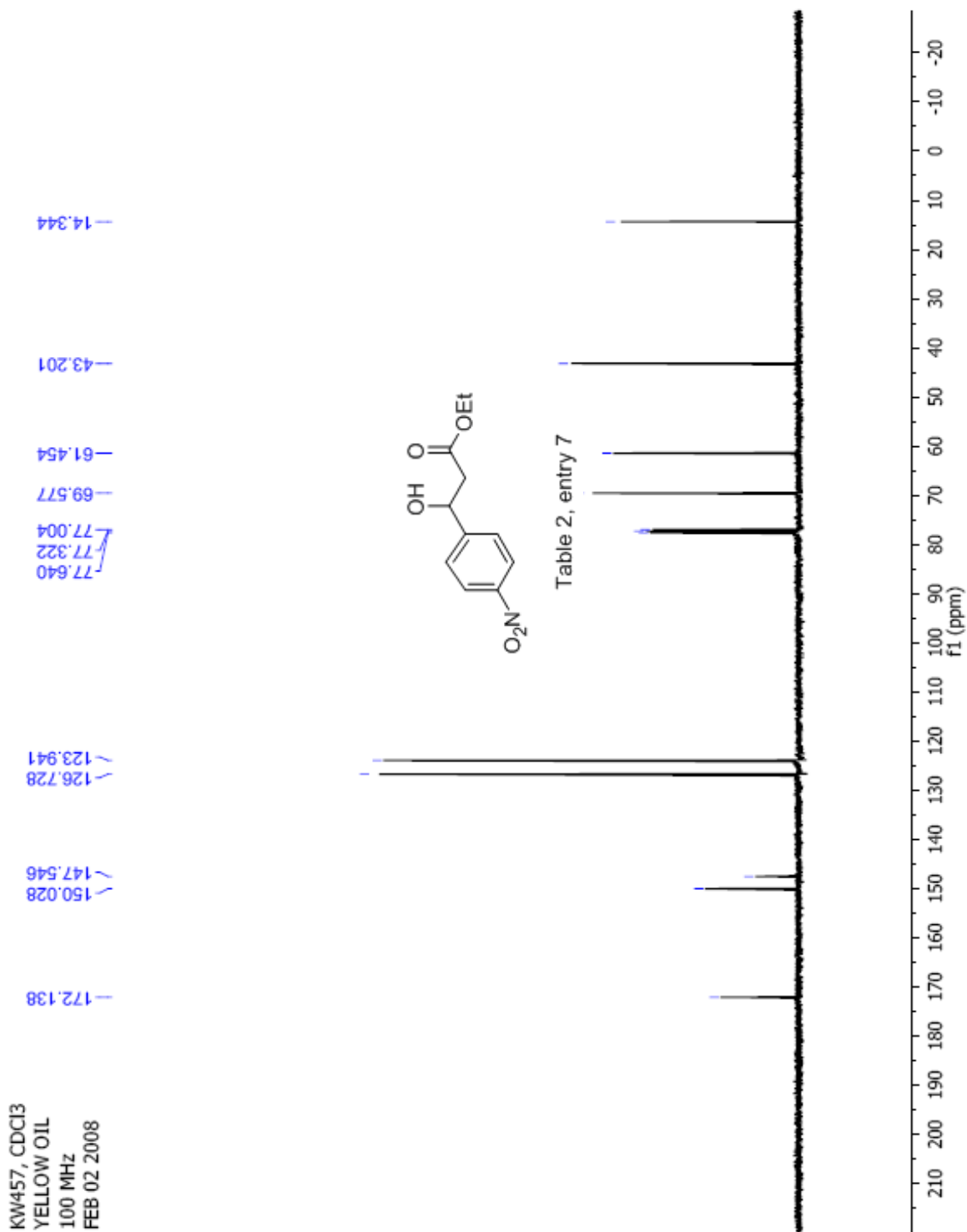


Table 2, entry 7







KW491, CDCl<sub>3</sub>  
400MHz  
COLORLESS OIL

7.685, 7.610, 7.590, 7.569, 7.550, 7.469, 7.450, 7.430  
5.155, 5.138, 5.123, 4.180, 4.162, 4.144, 3.698  
2.701, 2.686, 2.683  
1.266, 1.248, 1.231

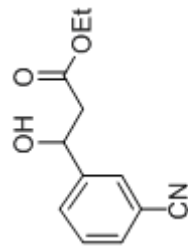
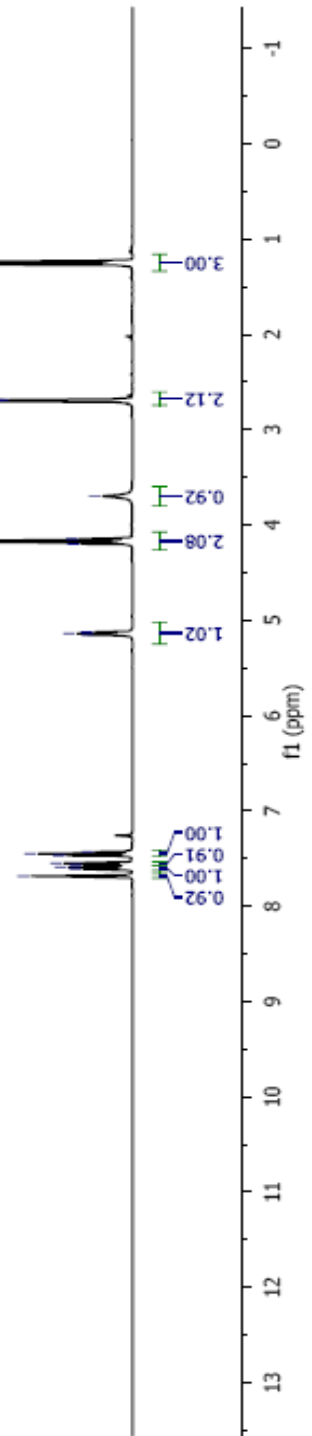
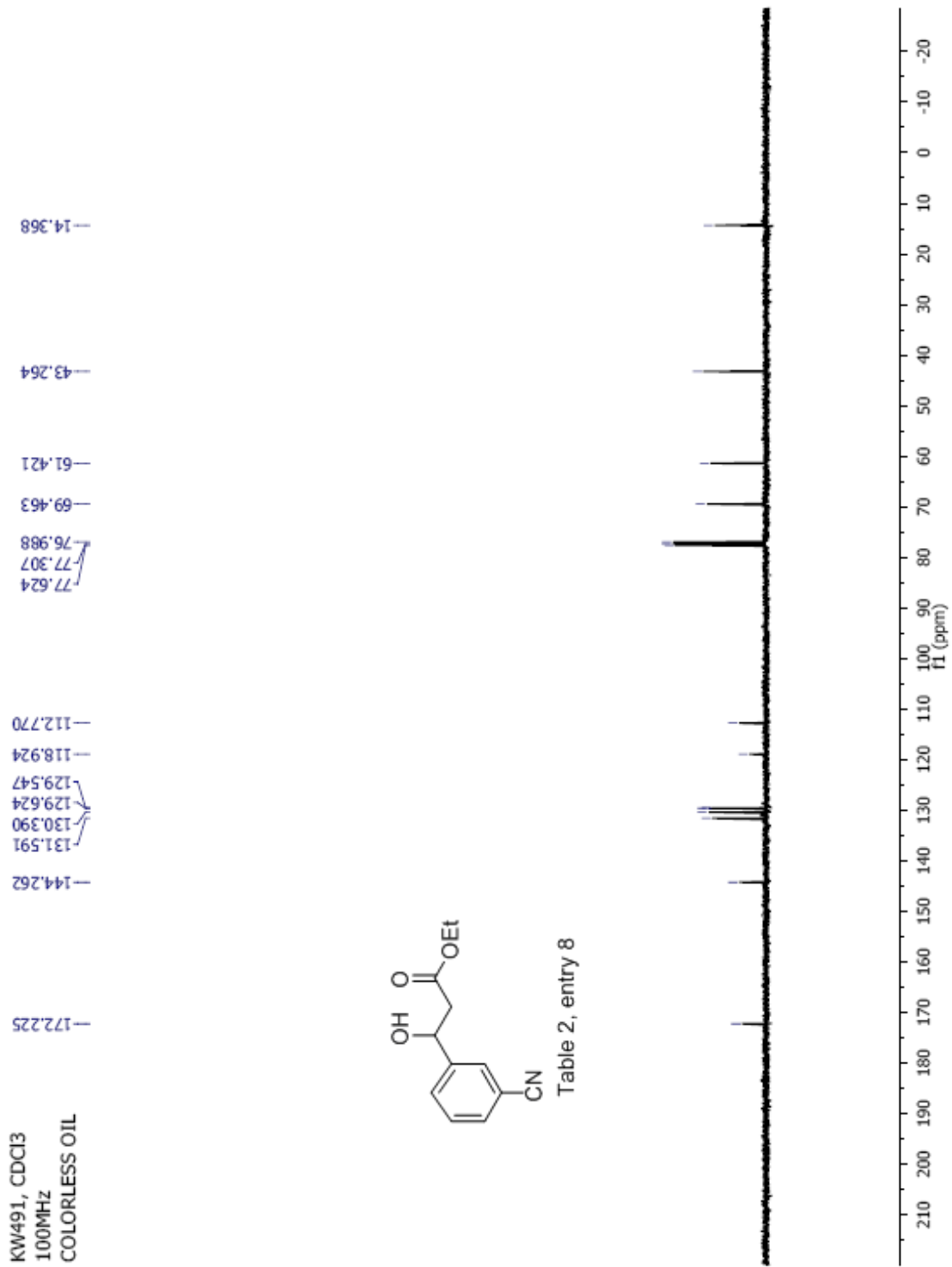


Table 2, entry 8





## Manual Peak Matching Report For Accurate Mass Determination

Theoretical mass	Experimental mass	PFK matching mass	Deviation*
219.08954	219.09013	180.98882	2.7 ppm

\* The deviation is obtained from the following equation:

$$\text{deviation} = \frac{\text{experimental mass} - \text{theoretical mass}}{\text{nominal mass}}$$

Where nominal mass takes in account only  $^{12}\text{C}$ ,  $^1\text{H}$ ,  $^{16}\text{O}$ ,  $^{14}\text{N}$  etc...

Theoretical mass correspond to the mass of the most abundant isotope peak

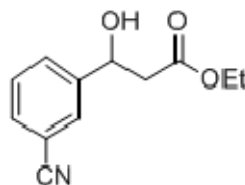
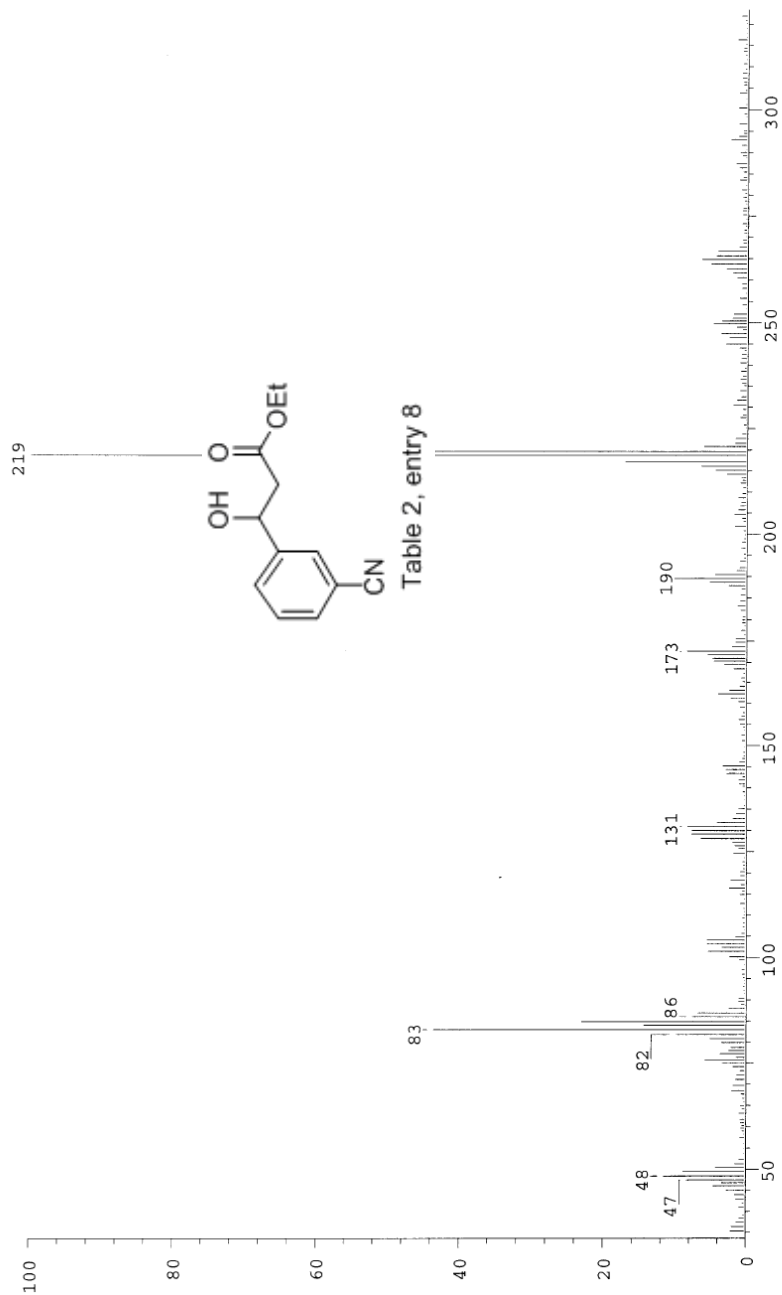


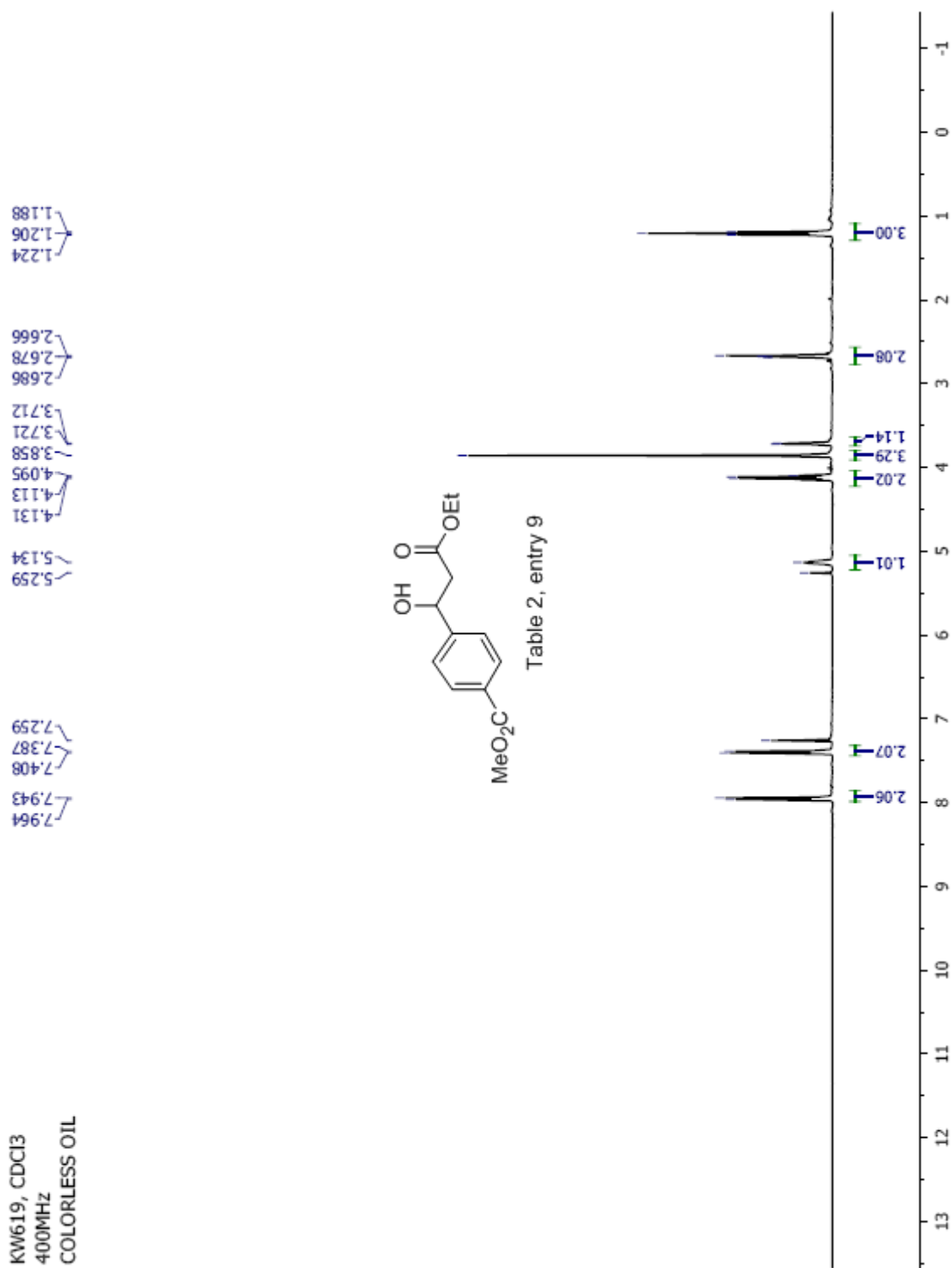
Table 2, entry 8

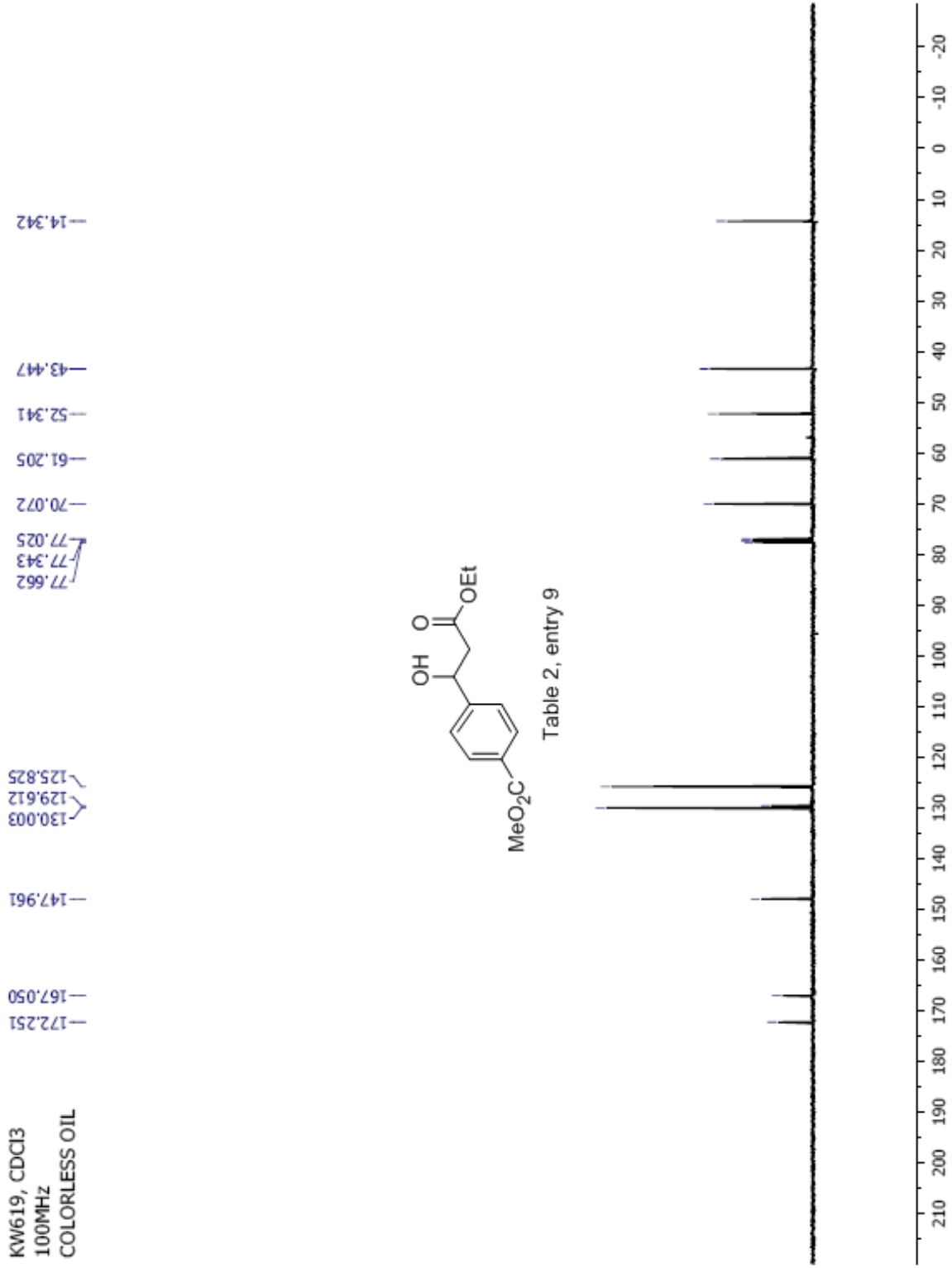
SPEC: fin084256.dat (18-FEB-09 10:42:07)  
 Samp: kw491  
 Comm: DP 70 eV EI  
 Oper: kh  
 Base: 218.68  
 Peak: 1000.0 mmu  
 Scan 24 @ 0.65 min (EI +QIMS LMR UP LR)

Study: ms services  
 Masses: 35.01 > 650.00  
 Intensity: 504804

Scans: 1 > 32  
 Client: Kuldip  
 #Peaks: 633  
 RIC: 3800167  
 5.0E+05







KW487, CDCl<sub>3</sub>  
300MHz  
COLORLESS OIL

4.205  
4.181  
4.157  
4.134  
3.995  
2.938  
2.471  
2.400  
2.345  
1.96  
1.272  
1.249  
0.897  
0.876  
0.853

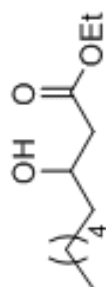
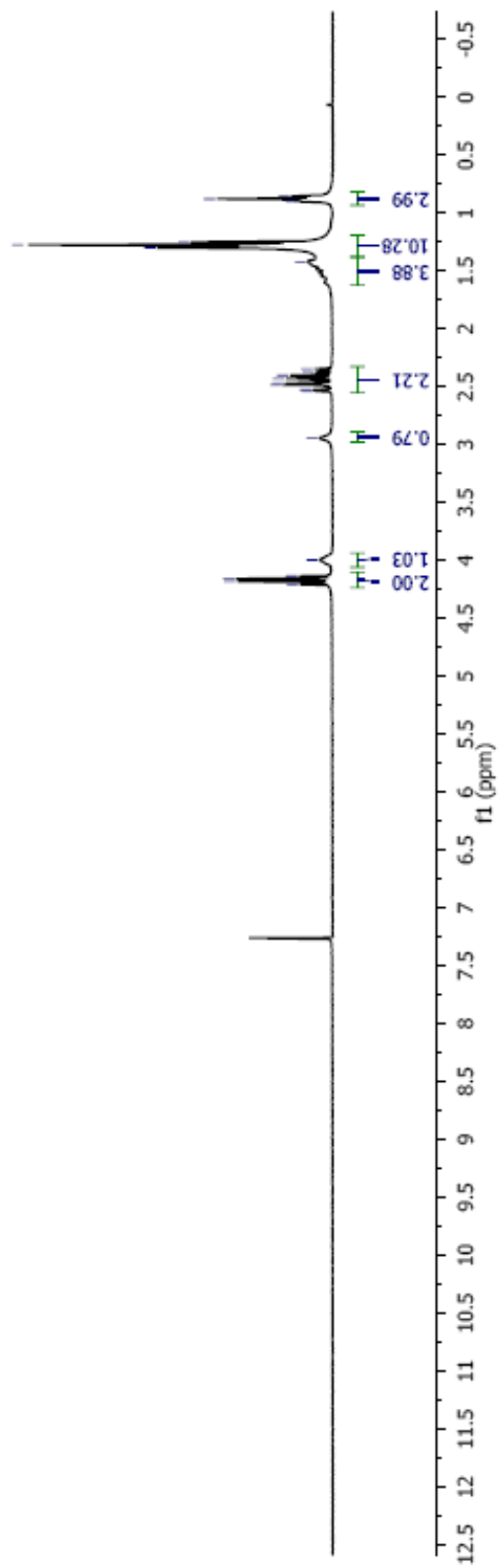


Table 2, entry 10



KW487, CDCl<sub>3</sub>  
100MHz  
COLORLESS OIL

—173.386

—77.568  
—77.251  
—76.933  
—68.253  
—60.917  
—41.497  
—36.736  
—29.439  
—25.683  
—22.844  
—14.438  
—14.339

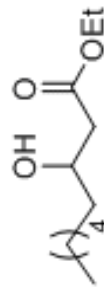
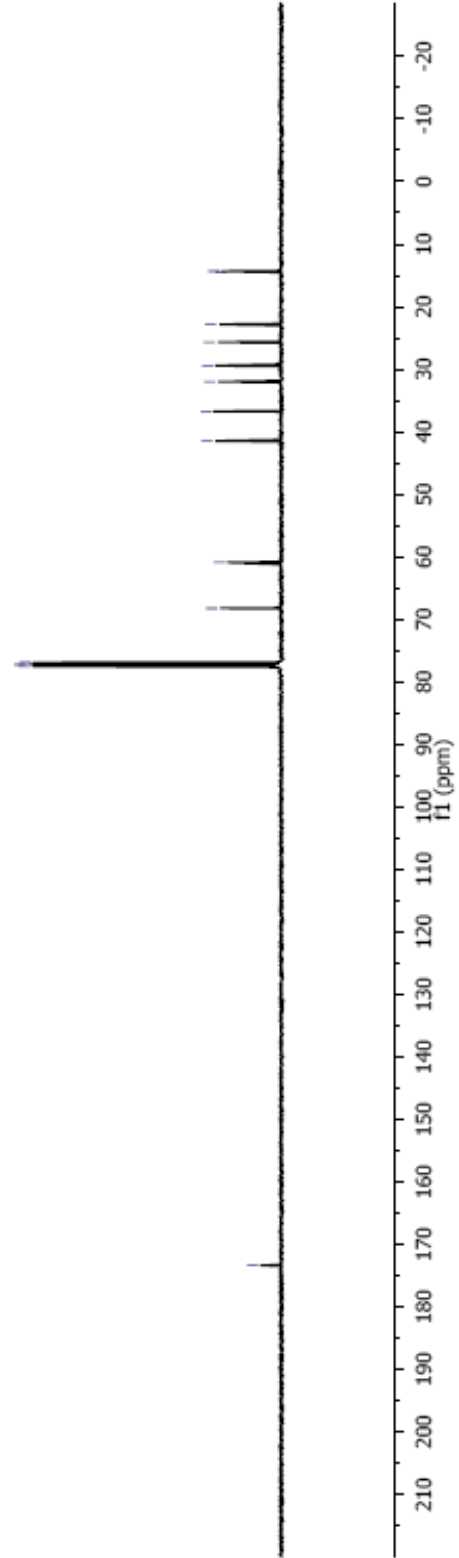


Table 2, entry 10





KW811, CDCI3  
400 MHz  
COLORLESS OIL  
APR 01 2009

0.98  
1.02  
1.05  
1.11  
1.14  
1.17  
1.21  
1.25  
1.27  
1.28  
1.37  
1.64  
1.74  
2.37  
2.39  
2.41  
2.43  
2.49  
3.76  
4.14  
4.15  
4.17  
4.19  
-7.26

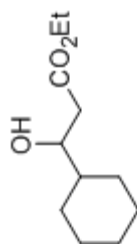
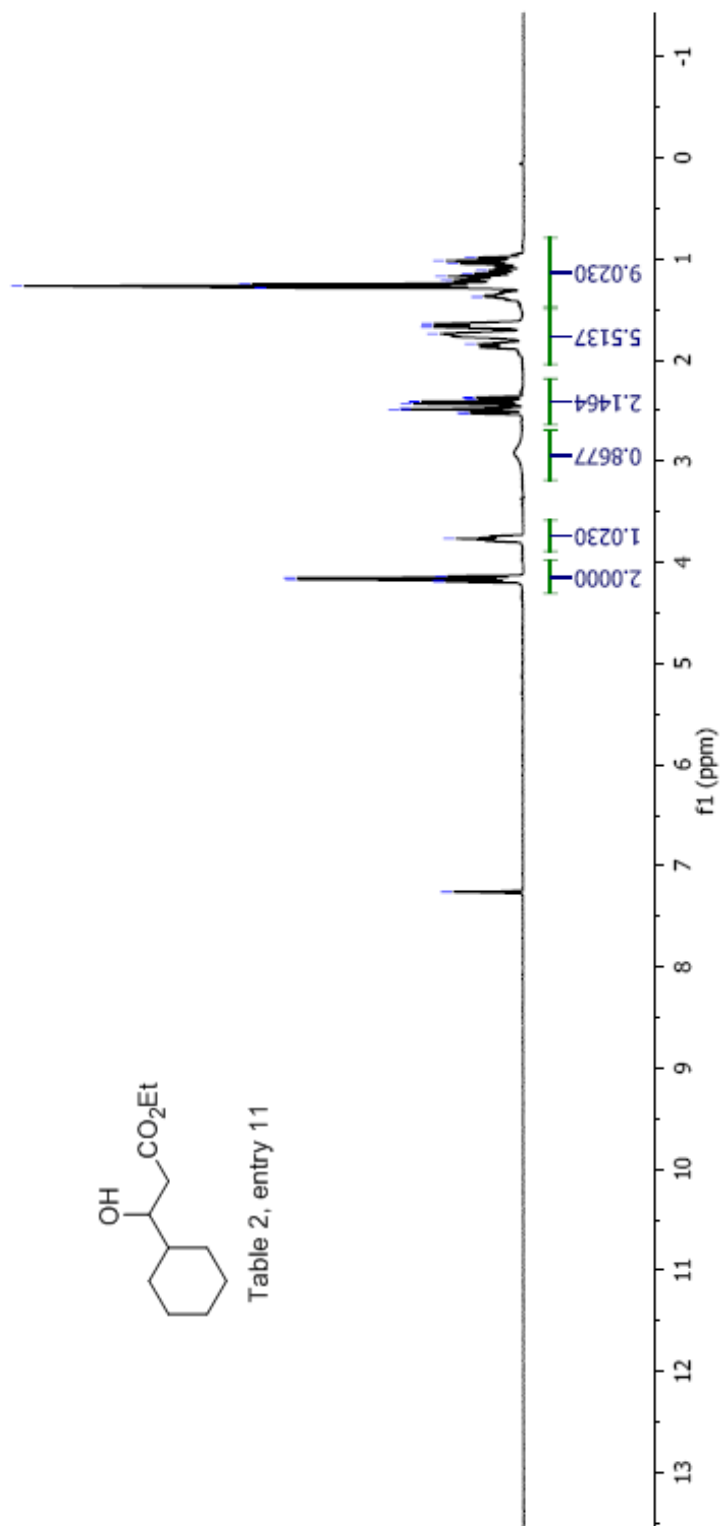


Table 2, entry 11



KW811, CDCI3  
100 MHz  
COLORLESS OIL  
APR 01 2009

—173.76

—77.56  
—77.24  
—76.92  
—72.37  
—60.90  
—57.01  
—43.29  
—38.81  
—28.49  
—26.66  
—26.39  
—26.28  
—14.42

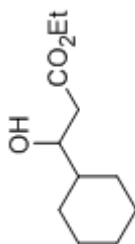
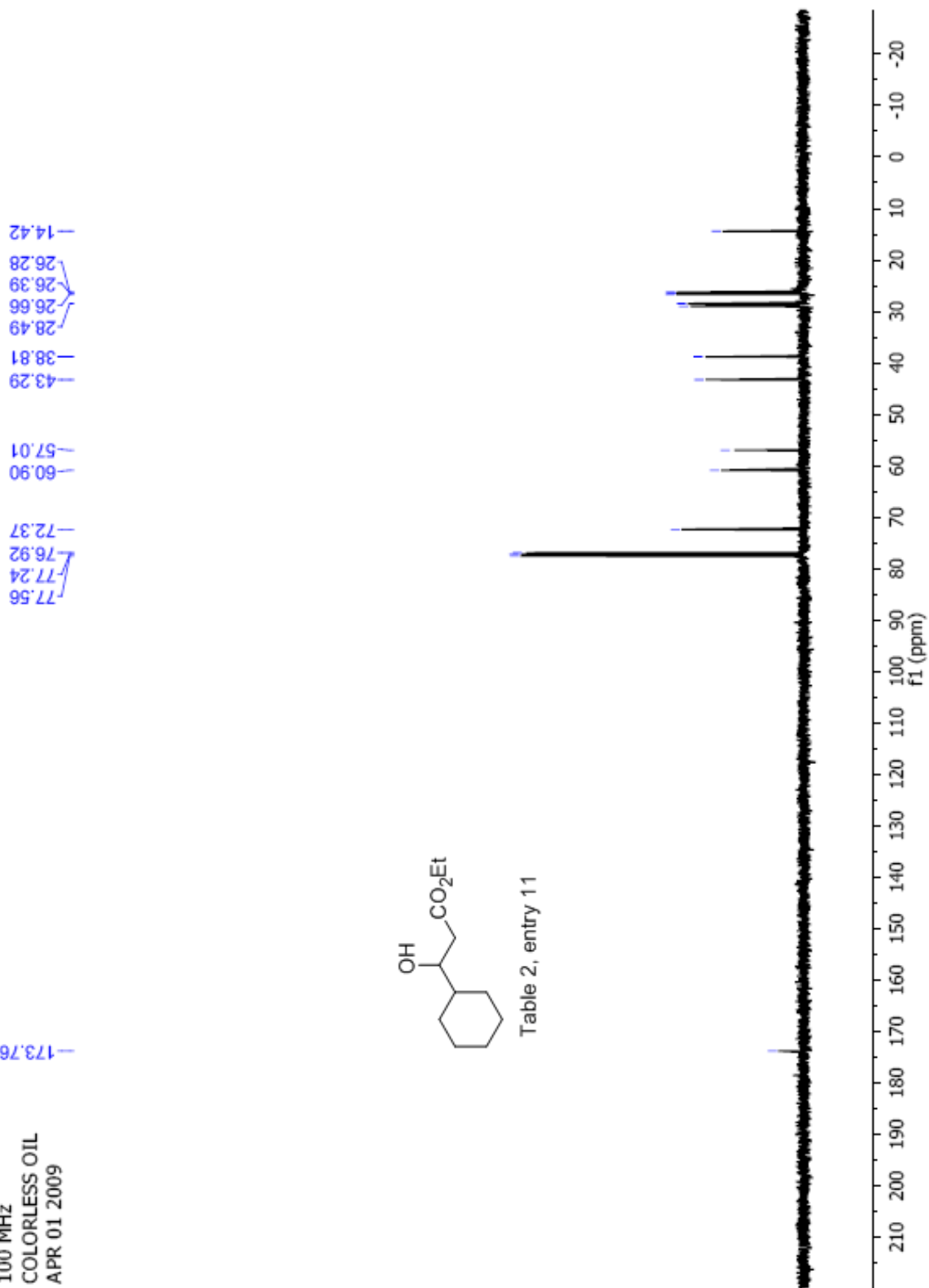
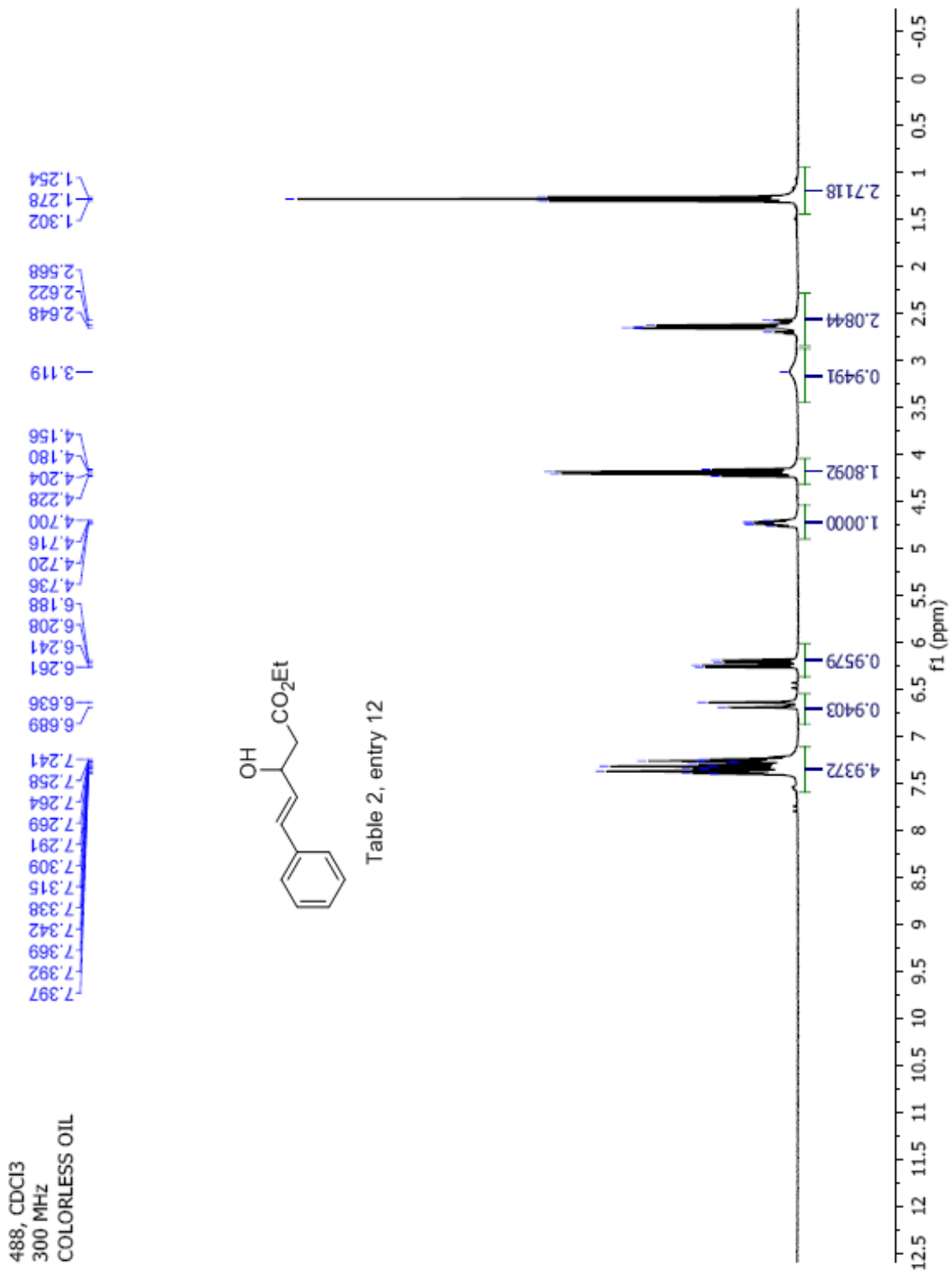
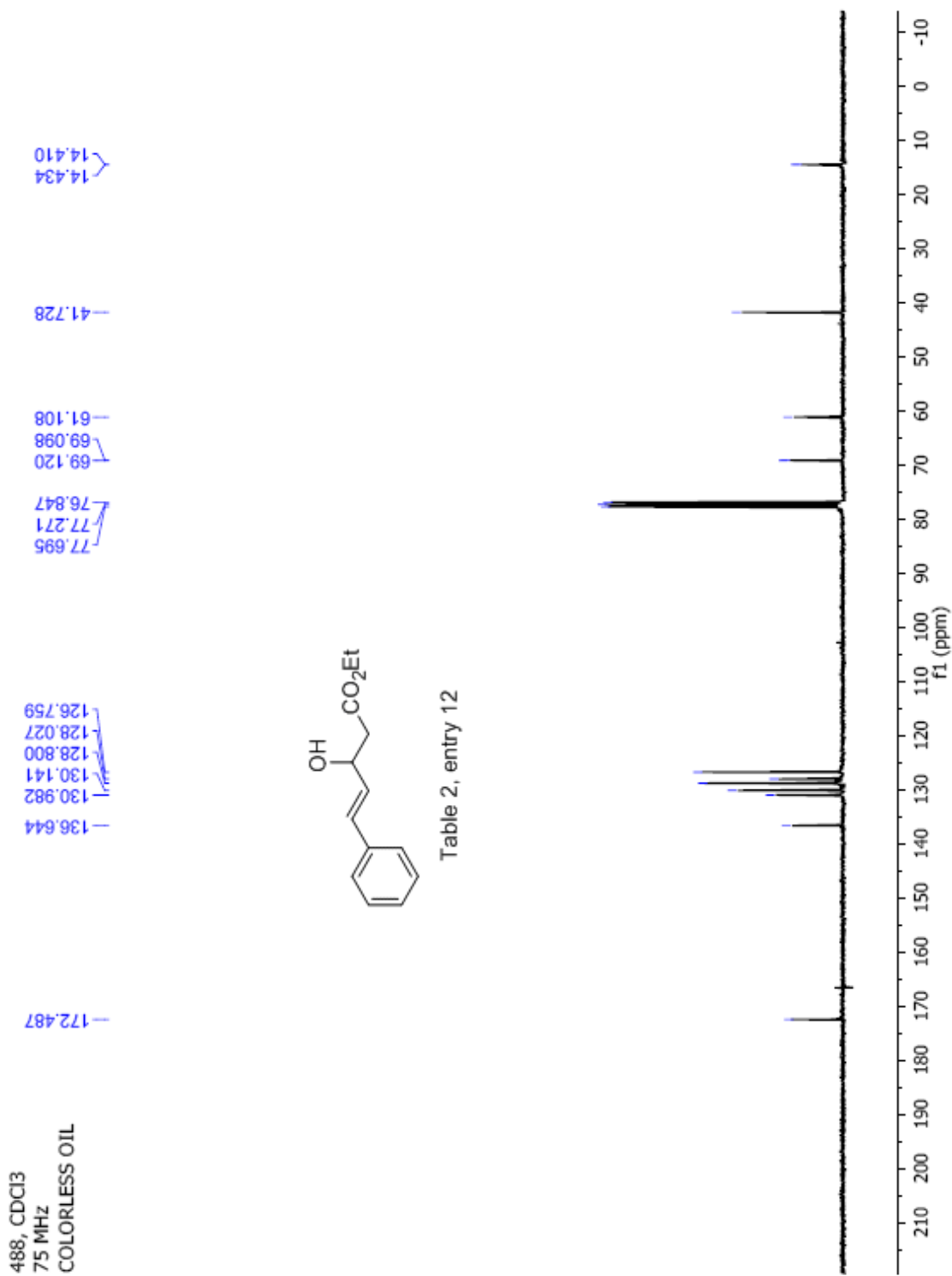


Table 2, entry 11







KW609, CDCI3  
400MHz  
COLORLESS OIL

7.262  
7.071  
7.053  
7.009  
6.990  
5.628  
4.236  
4.218  
4.200  
4.182  
3.055  
3.028  
2.978  
2.576  
2.535  
2.466  
1.312  
1.294  
1.276

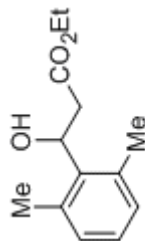
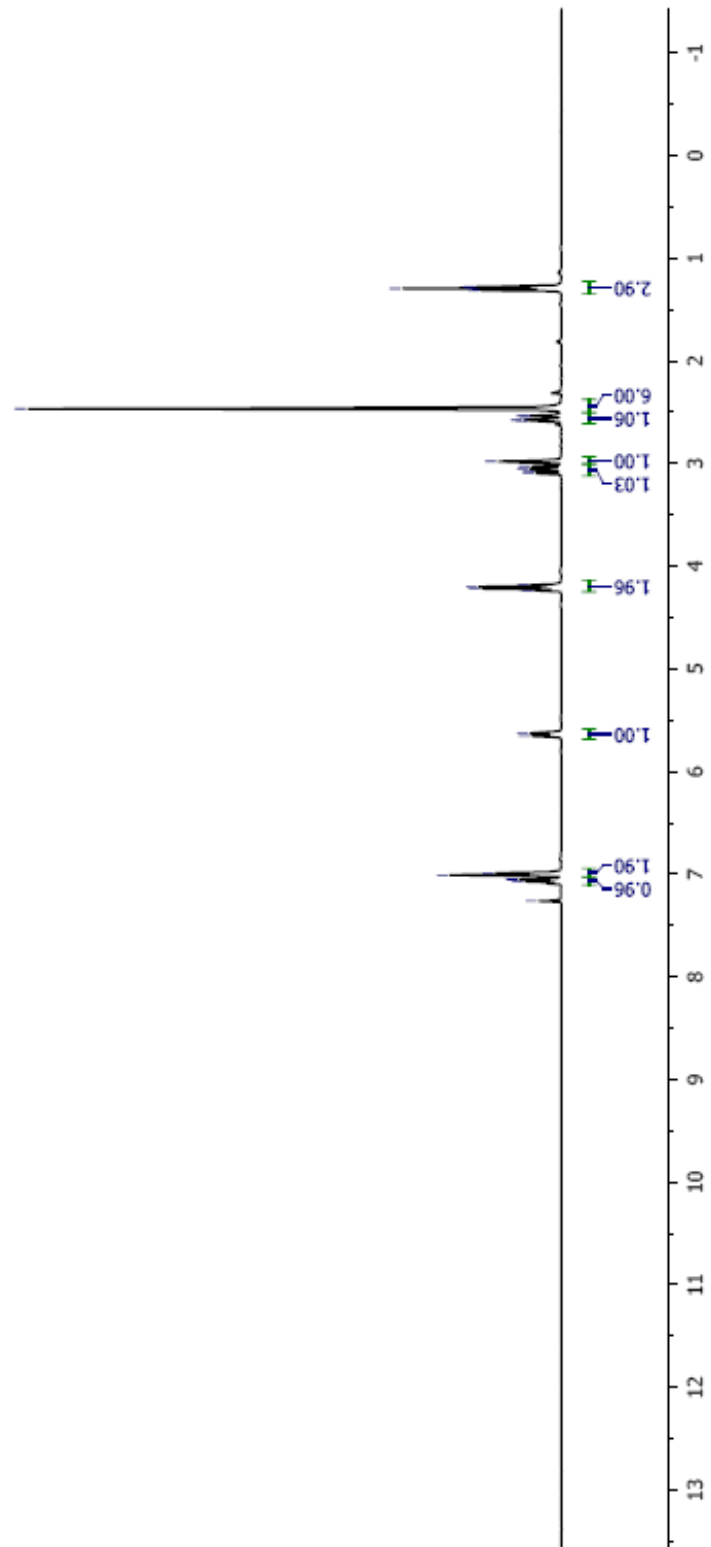
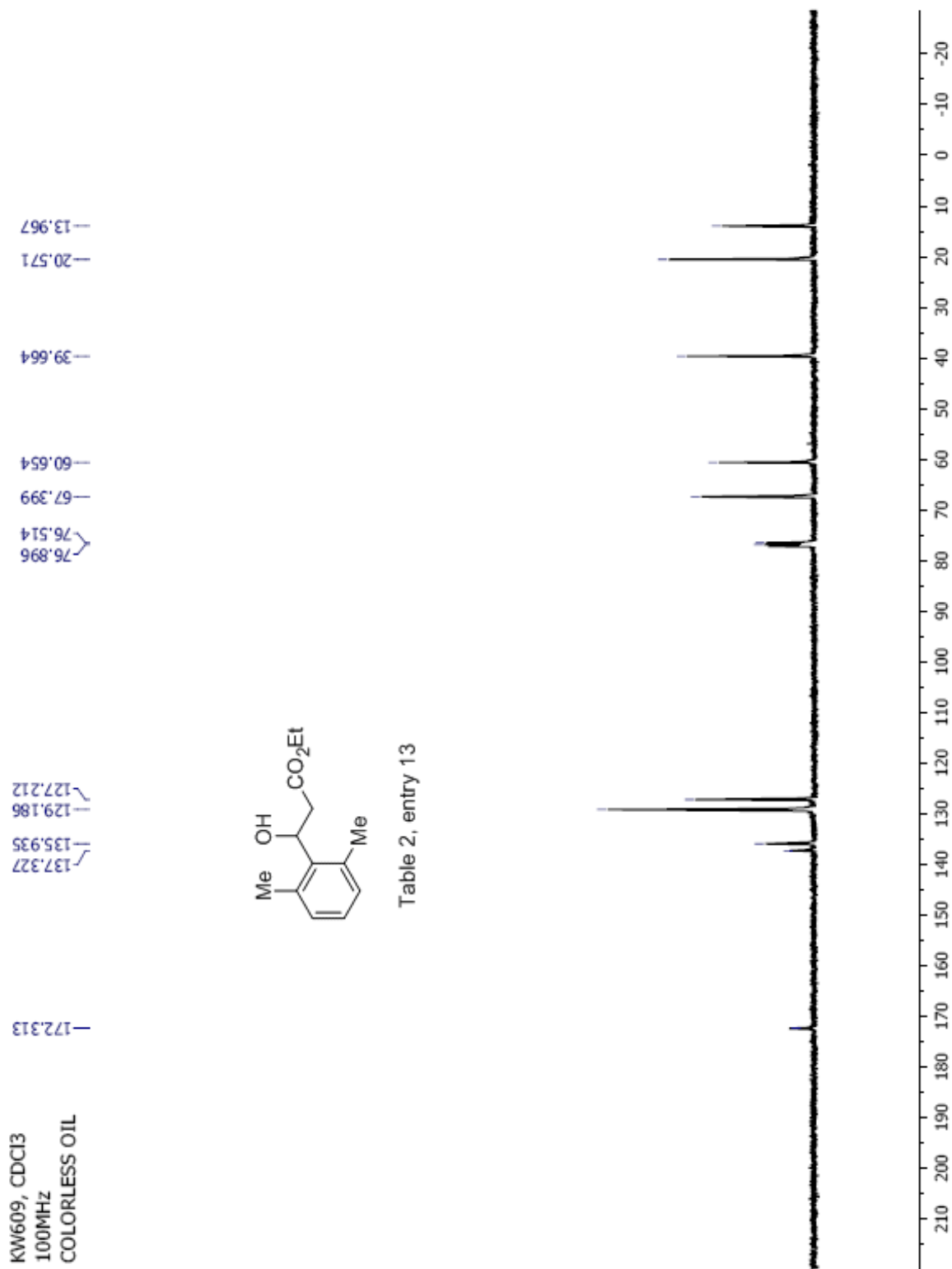


Table 2, entry 13





## Manual Peak Matching Report For Accurate Mass Determination

Theoretical mass	Experimental mass	PFK matching mass	Deviation*
222.12559	222.12604	218.98562	2 ppm

\* The deviation is obtained from the following equation:

$$\text{deviation} = \frac{\text{experimental mass} - \text{theoretical mass}}{\text{nominal mass}}$$

Where nominal mass takes in account only  $^{12}\text{C}$ ,  $^1\text{H}$ ,  $^{16}\text{O}$ ,  $^{14}\text{N}$  etc...

Theoretical mass correspond to the mass of the most abundant isotope peak

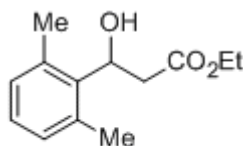


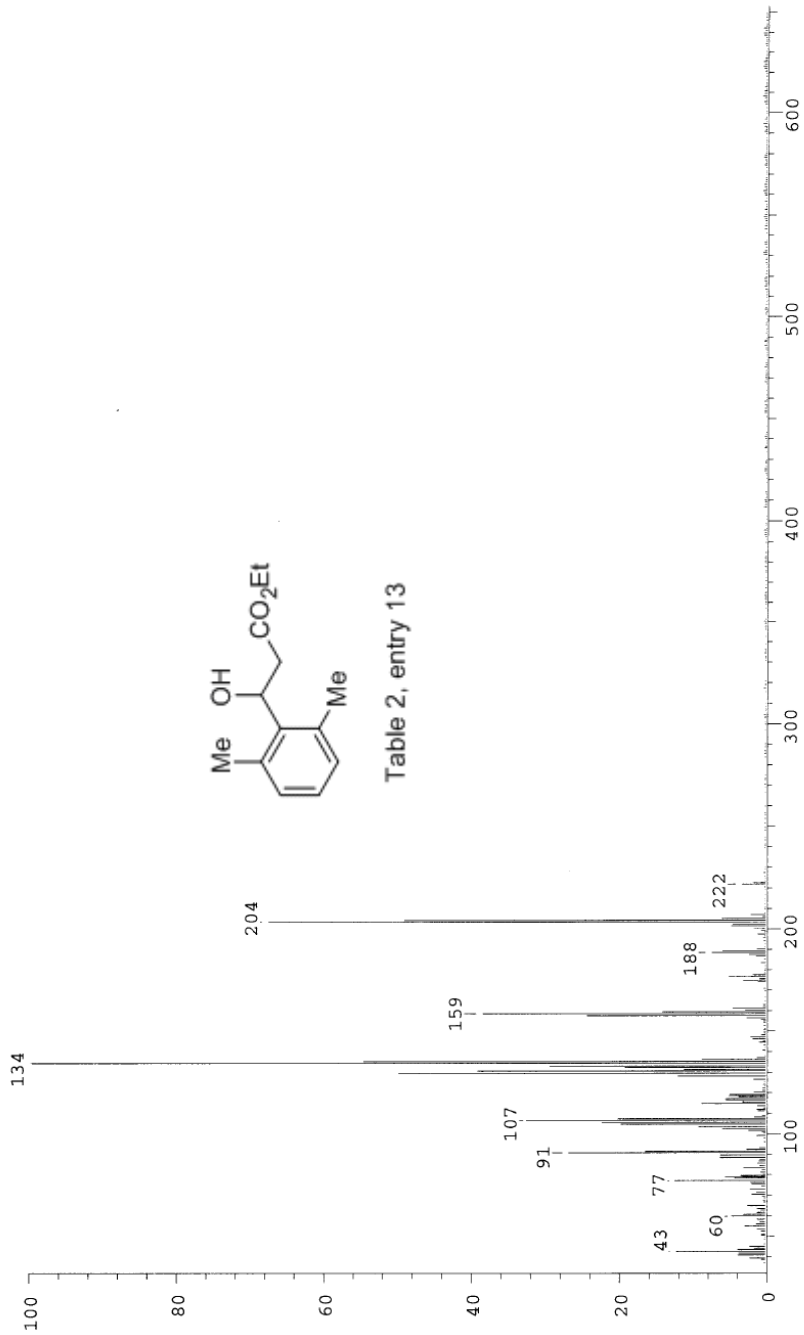
Table 2, entry 13

*Handwritten initials*

SPEC: fin063601.dat (02-MAY-08 11:02:34)  
 Samp: KW609  
 Comm: 70 eV EI  
 Oper: kh  
 Base: 134.44  
 Peak: 1000.0 mmu  
 Scan 1 @ 0.18 min (EI +Q1MS LMR UP LR)

Study: MS Services  
 Masses: 35.01 > 650.00  
 Intensity: 9193

Scans: 1 > 10  
 Client: Kuldup  
 #Peaks: 460  
 RIC: 87292  
 9.2E+03



Date: Fri May 2 11:03:17 2008 ICIS: 8.3.0 SP2 for OSF1 (V4.0) build 98-238 from 26-Aug-98



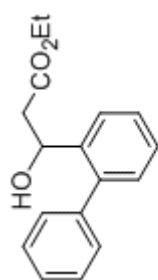
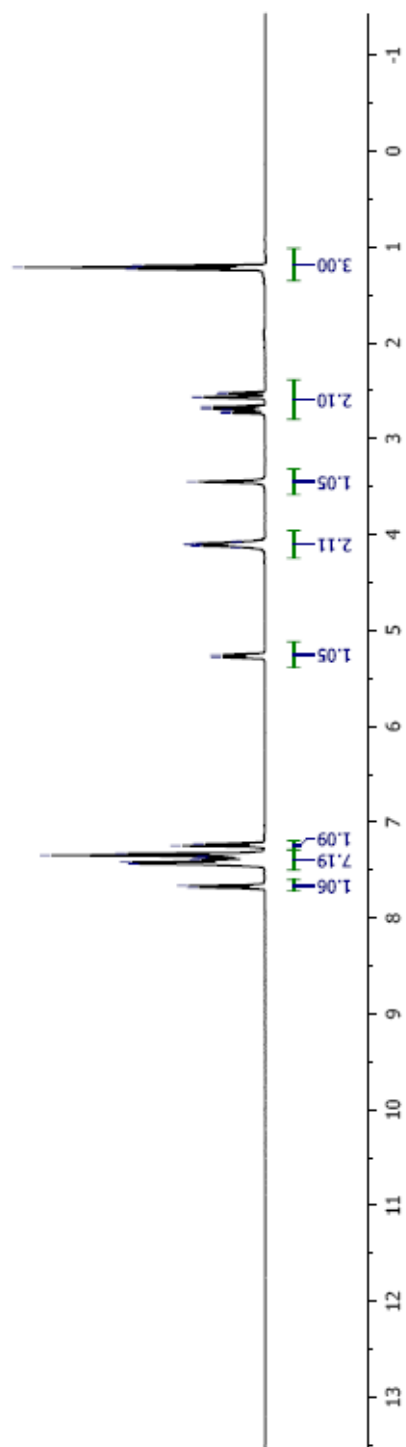
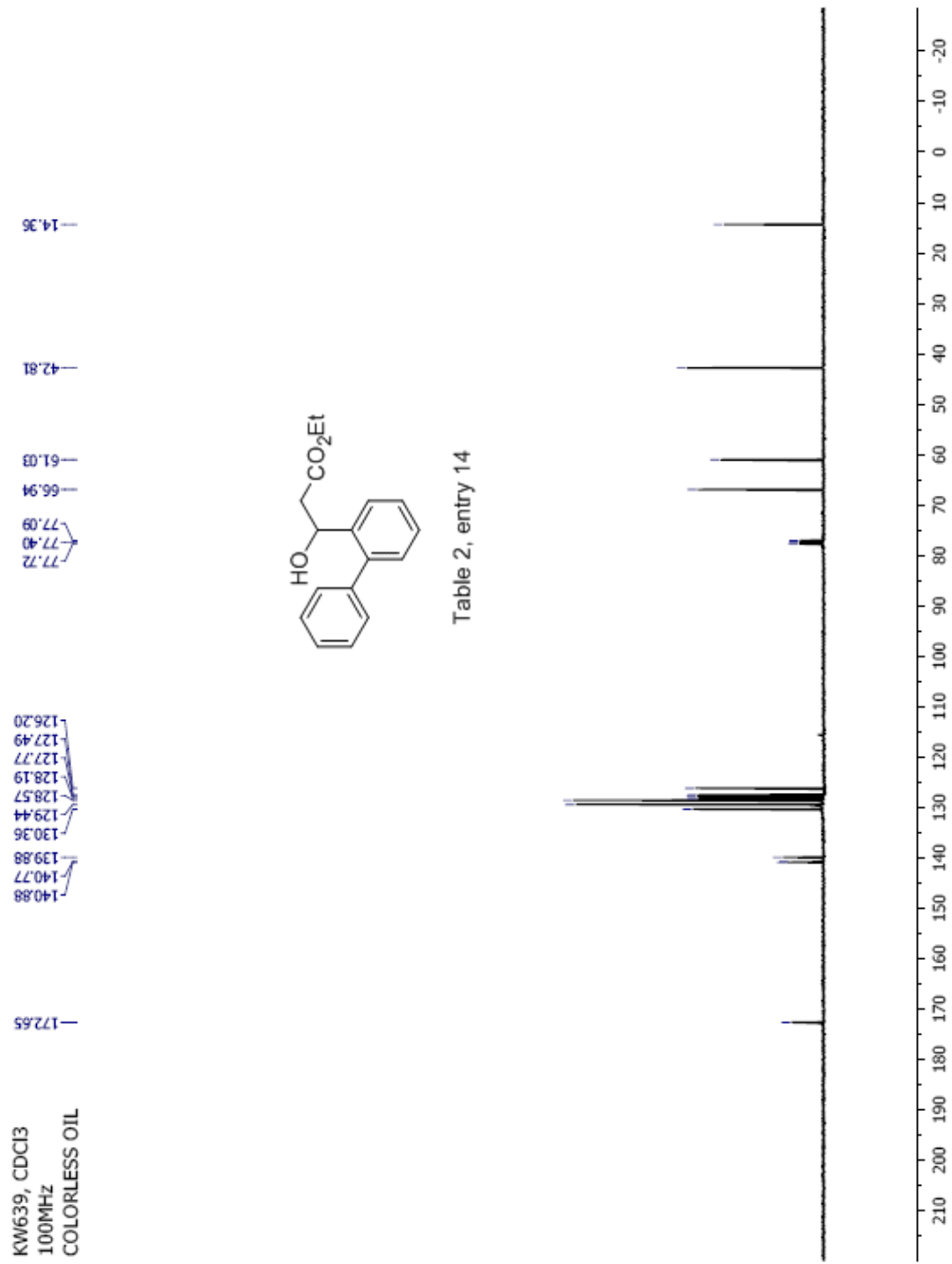


Table 2, entry 14





### Manual Peak Matching Report For Accurate Mass Determination

Theoretical mass	Experimental mass	PFK matching mass	Deviation*
270.12559	270.12608	230.98562	1.8 ppm

\* The deviation is obtained from the following equation:

$$\text{deviation} = \frac{\text{experimental mass} - \text{theoretical mass}}{\text{nominal mass}}$$

Where nominal mass takes in account only  $^{12}\text{C}$ ,  $^1\text{H}$ ,  $^{16}\text{O}$ ,  $^{14}\text{N}$  etc...

Theoretical mass correspond to the mass of the most abundant isotope peak

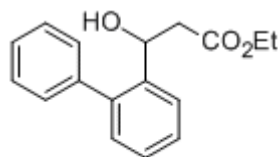


Table 2, entry 14

*Handwritten signature*

Scans: 1 > 20  
 Client: Kuldup  
 #Peaks: 612  
 RIC: 240947  
 4.7E+04

SPEC: fin063688.dat (06-JUN-08 14:38:21)  
 Samp: KW639  
 Comm: 70 eV EI  
 Oper: kh  
 Study: Service  
 Masses: 35.01 > 650.00  
 Base: 164.92  
 Peak: 1000.0 mmu  
 Intensity: 46574  
 Scan 19 @ 0.40 min (EI +QIMS LMR UP LR)

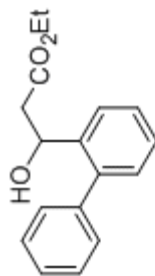
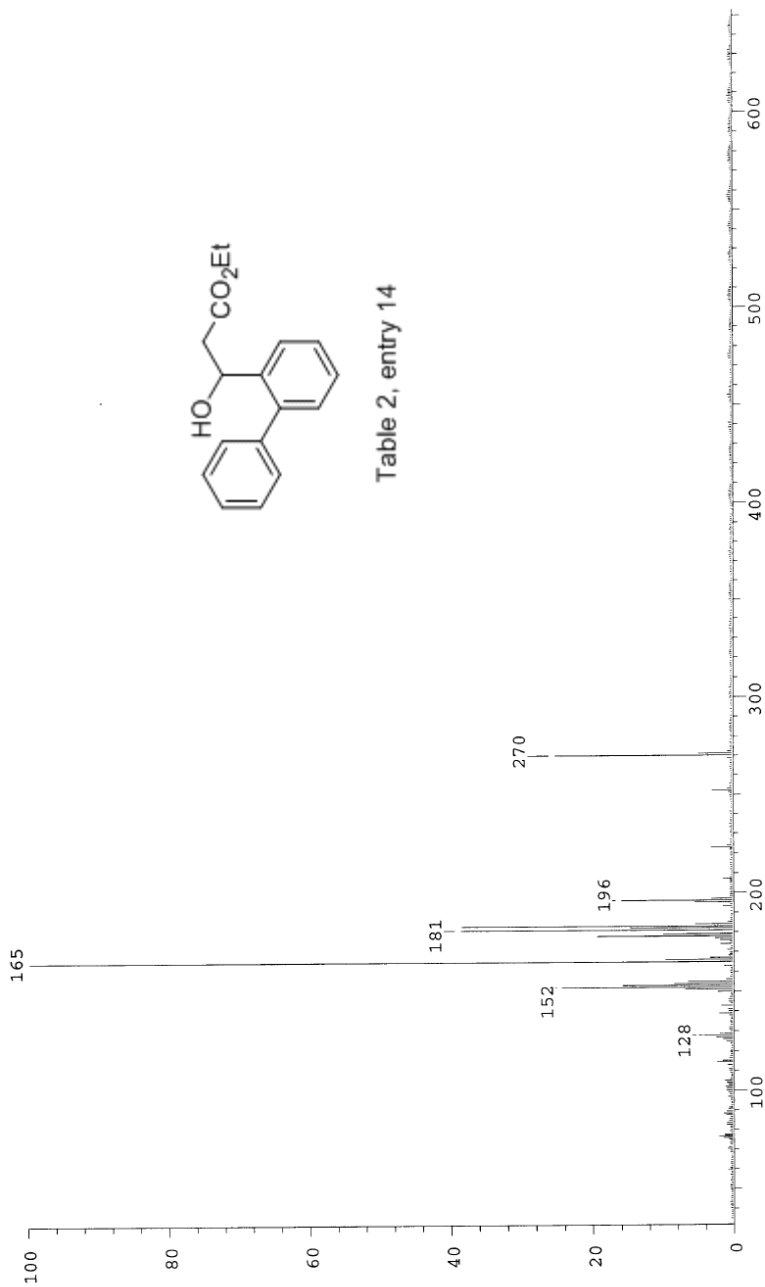
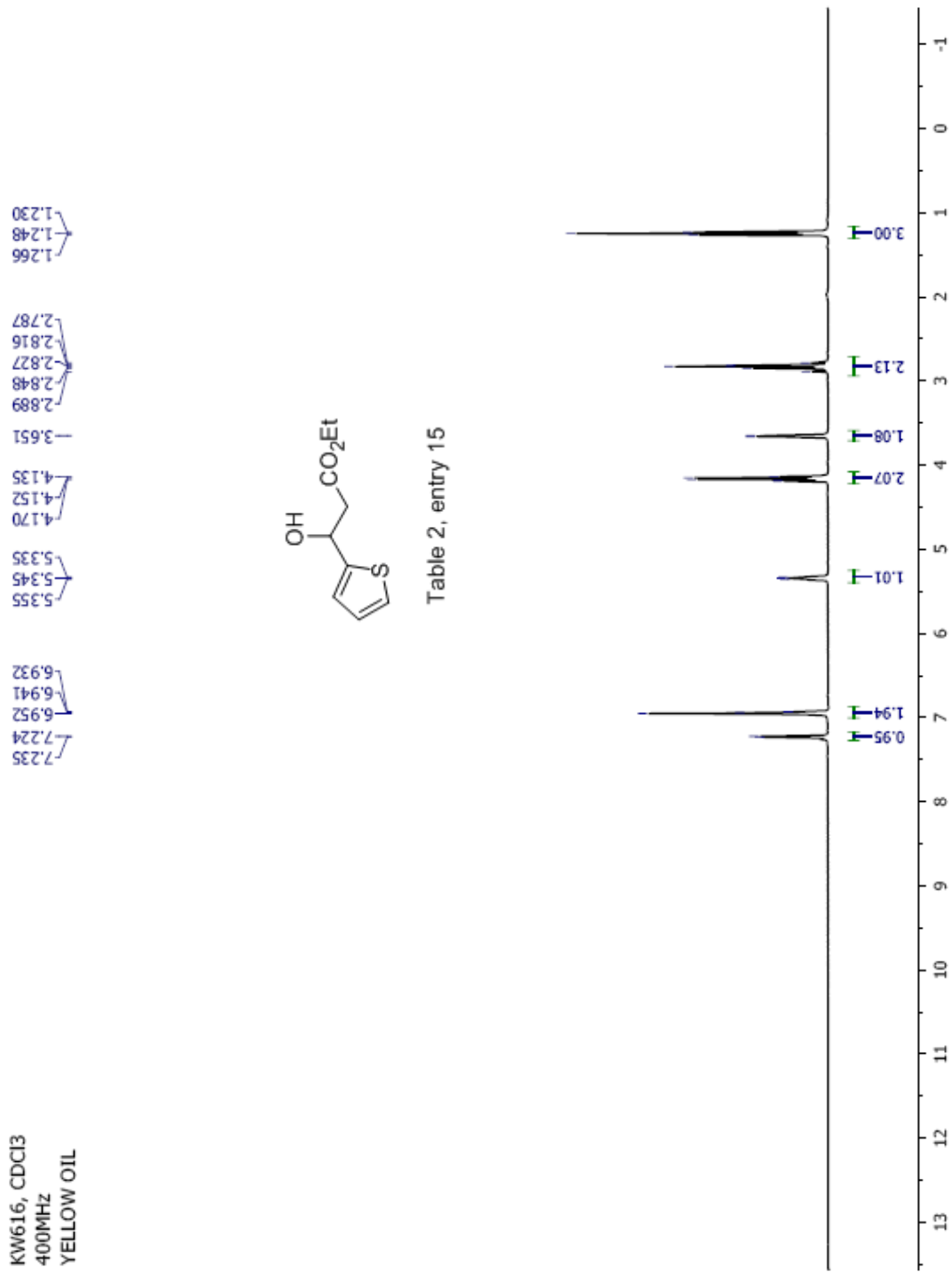
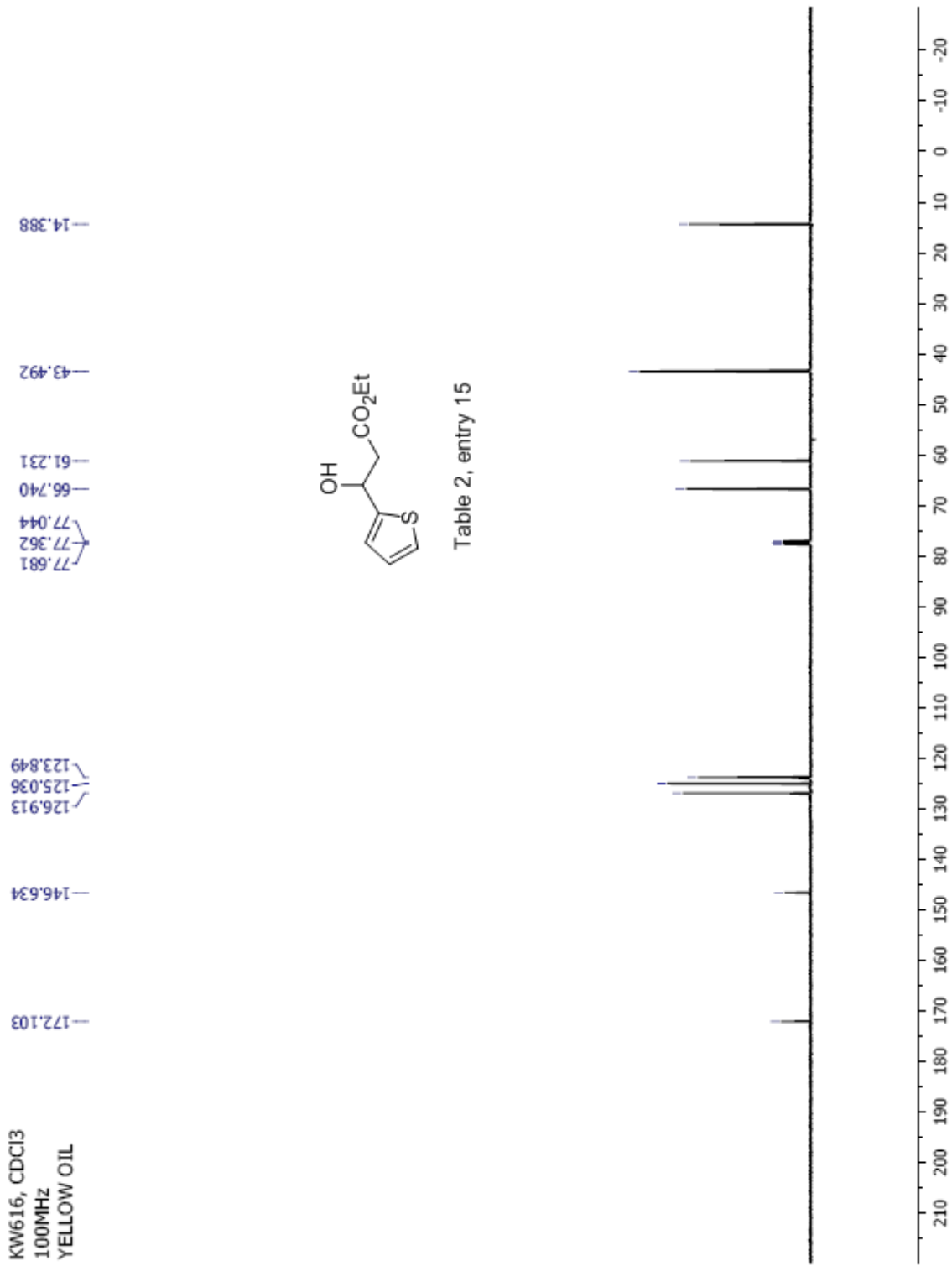


Table 2, entry 14

Date: Fri Jun 6 14:39:12 2008 ICIS: 8.3.0 SP2 for OSF1 (V4.0) build 98-238 from 26-Aug-98





KW622, CDCI3  
400MHz  
COLORLESS OIL

7.579  
7.559  
7.540  
7.162  
7.143  
7.049  
7.030  
5.135  
5.125  
5.115  
4.540  
4.530  
4.166  
4.148  
4.130  
2.806  
2.772  
2.701  
2.683  
2.663  
2.514  
1.253  
1.235  
1.217

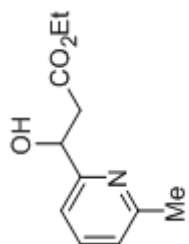
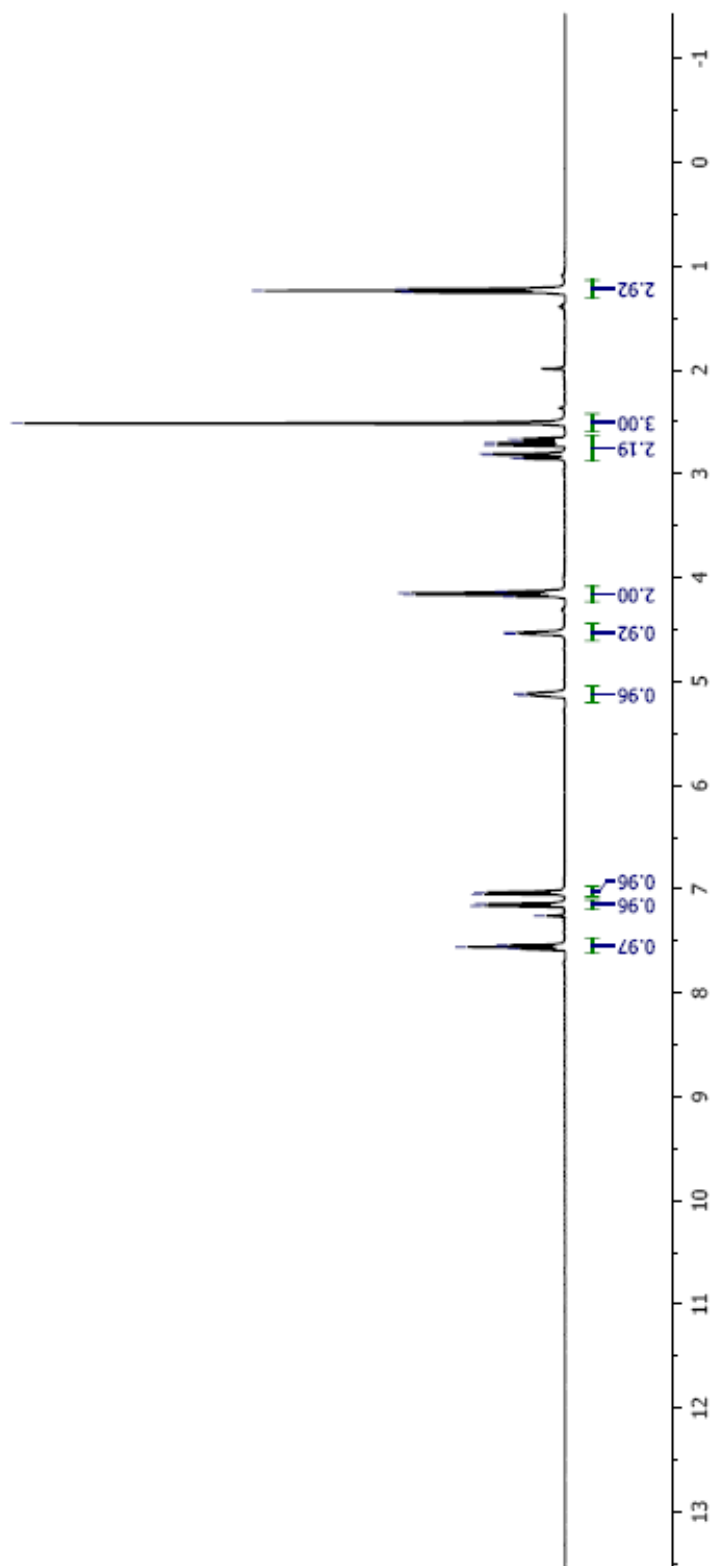
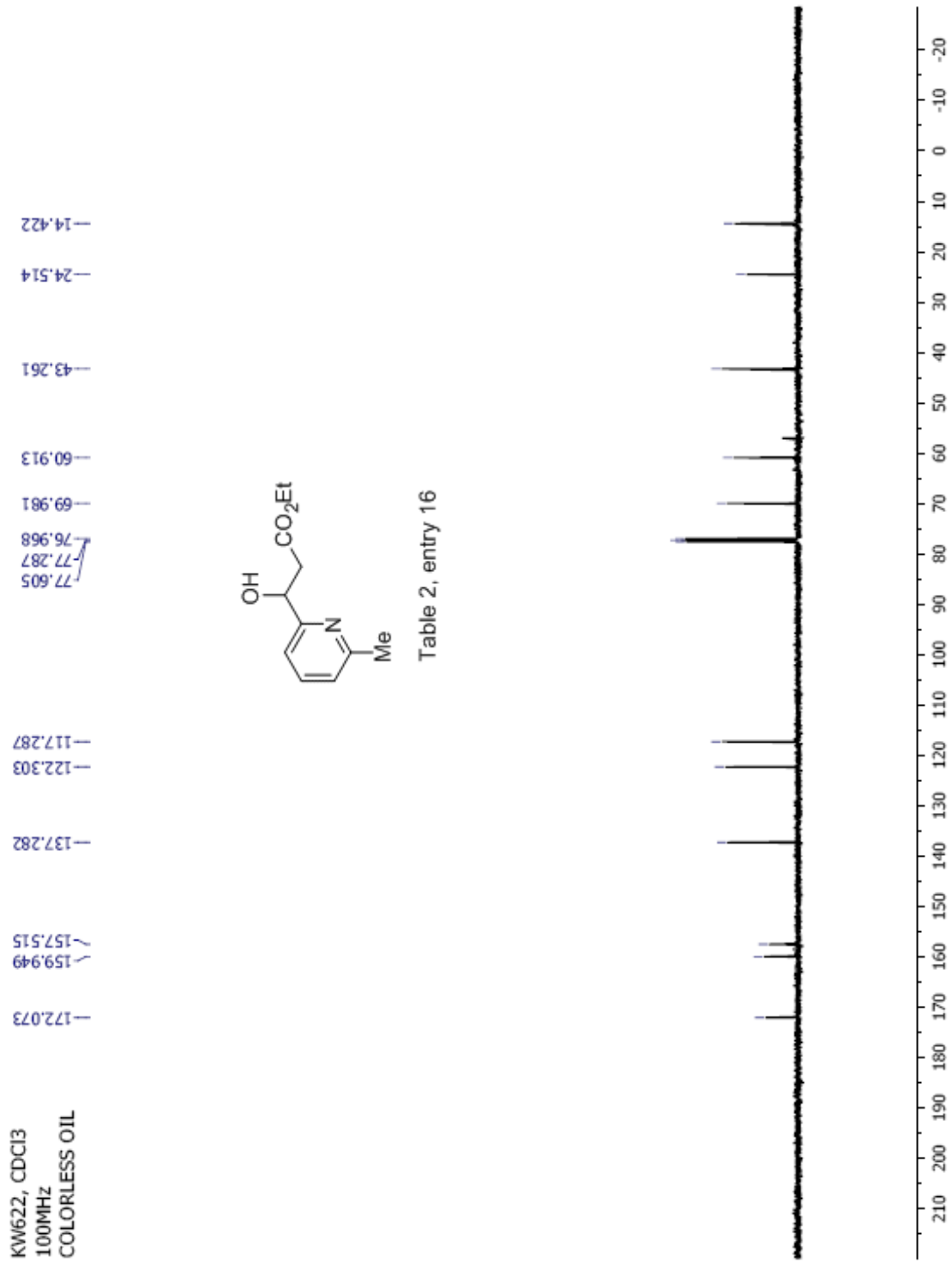


Table 2, entry 16







### Manual Peak Matching Report For Accurate Mass Determination

Theoretical mass	Experimental mass	PFK matching mass	Deviation*
209.10519	209.10557	180.98882	1.8 ppm

\* The deviation is obtained from the following equation:

$$\text{deviation} = \frac{\text{experimental mass} - \text{theoretical mass}}{\text{nominal mass}}$$

Where nominal mass takes in account only  $^{12}\text{C}$ ,  $^1\text{H}$ ,  $^{16}\text{O}$ ,  $^{14}\text{N}$  etc...

Theoretical mass correspond to the mass of the most abundant isotope peak

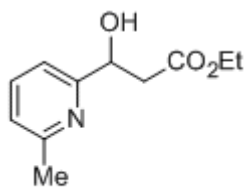


Table 2, entry 16

*Handwritten signature*

SPC: Fin063648.dat (19-MAY-08 10:45:52)  
 Samp: KW622  
 Comm: 70 eV EI  
 Oper: kh  
 Study: Service  
 Base: 122.32  
 Messs: 35.0% > 650.00  
 Peak: 1000.0 mmu  
 Intensity: 2355377  
 Scan 18 @ 0.39 min (EI +QIMS LMR UP LR)

Scans: 1 &gt; 51

Client: Kulcup  
 #Peaks: 641  
 RIC: 31060452 2.4E+06

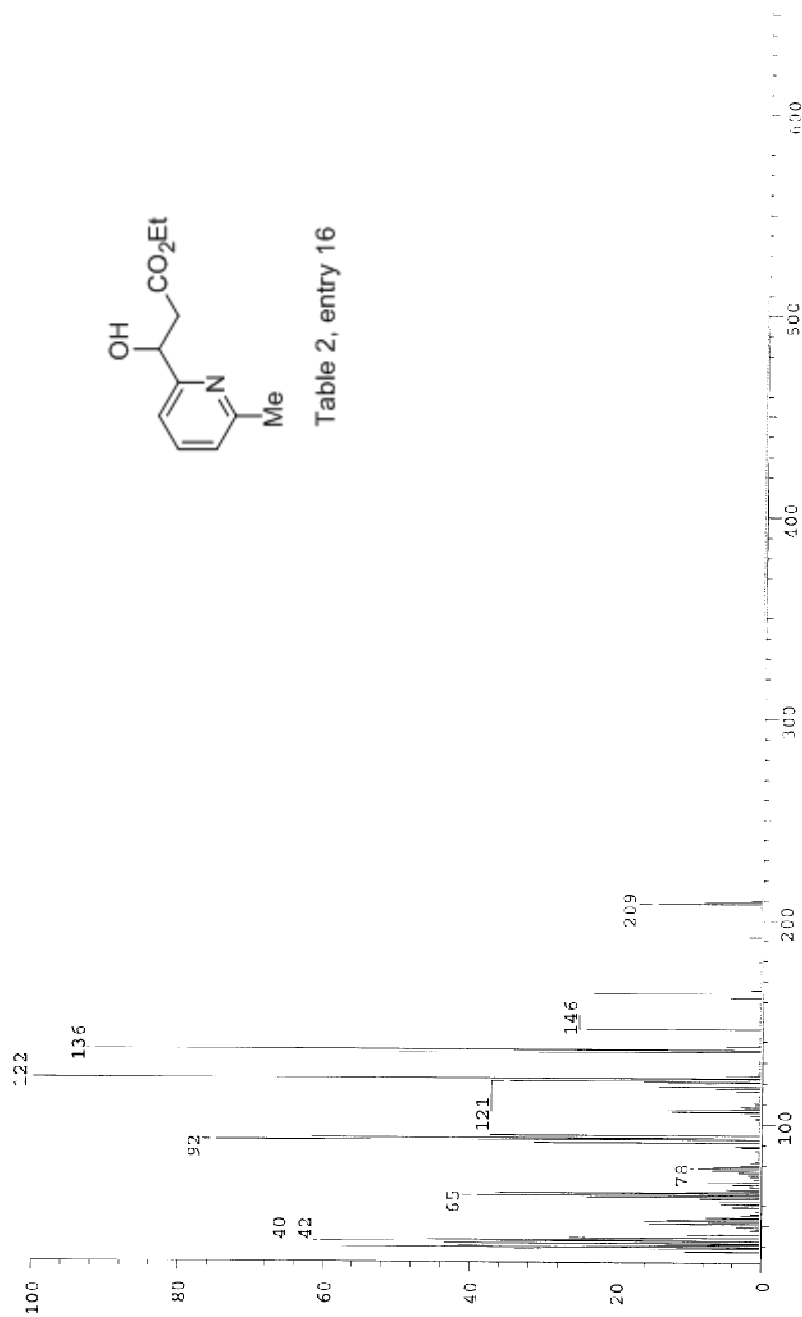


Table 2, entry 16

Date: Mon May 19 10:45:23 2008 ICIS: 8.3.0 SP2 for GDFI (V4.0) build 98-238 from 26-Aug-98

KW637, CDCl<sub>3</sub>  
400MHz  
YELLOW OIL

7.54  
7.52  
7.46  
7.44  
7.28  
7.27  
7.25  
7.23  
7.21  
7.19  
6.66  
5.29  
5.27  
4.20  
4.18  
4.16  
3.72  
3.71  
2.96  
2.95  
1.28  
1.26  
1.24

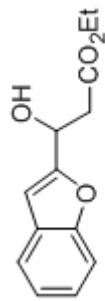
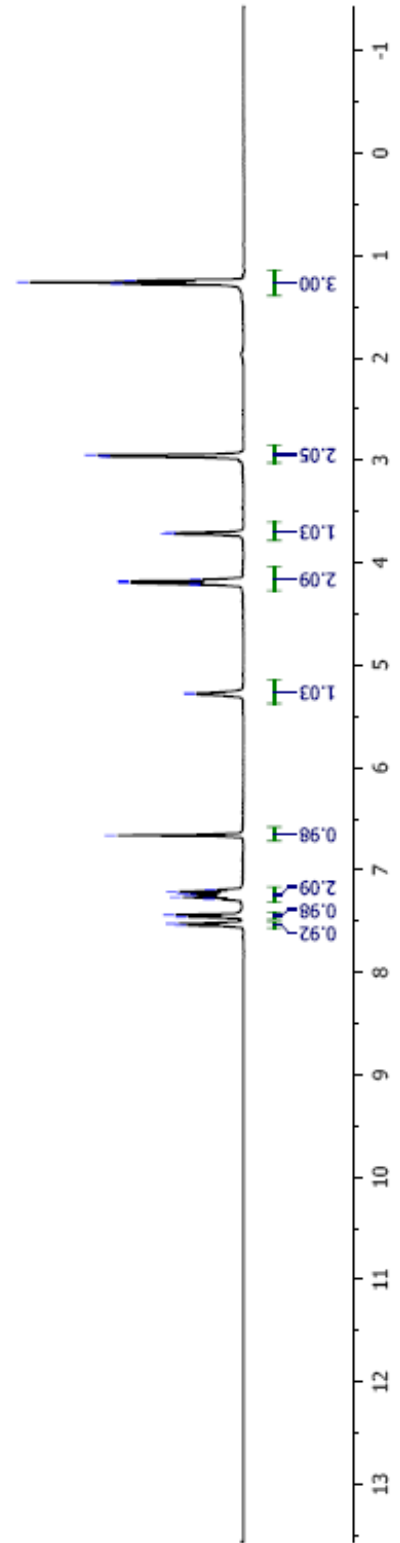
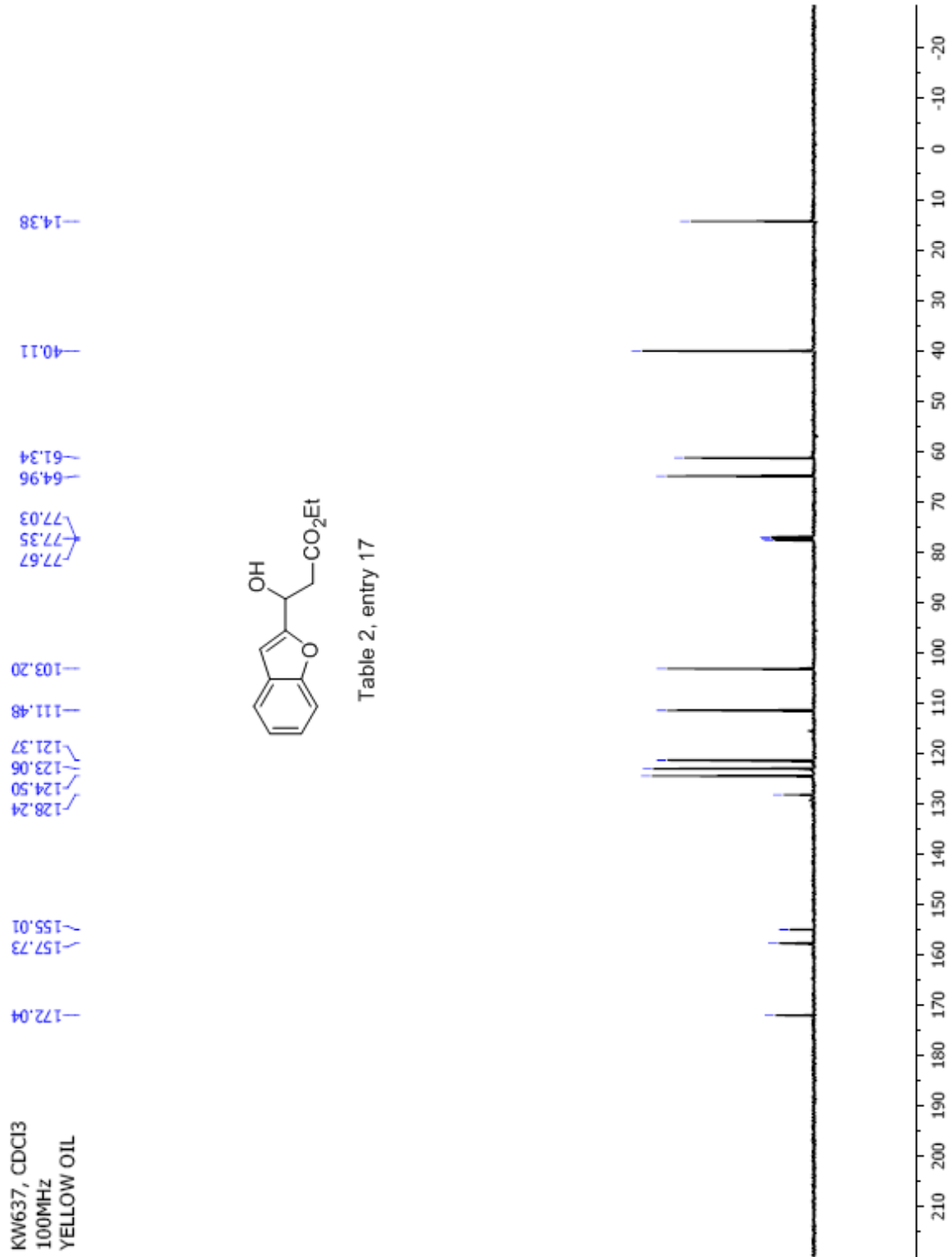


Table 2, entry 17





## Manual Peak Matching Report For Accurate Mass Determination

Theoretical mass	Experimental mass	PFK matching mass	Deviation*
234.08921	234.08965	230.98562	1.9 ppm

\* The deviation is obtained from the following equation:

$$\text{deviation} = \frac{\text{experimental mass} - \text{theoretical mass}}{\text{nominal mass}}$$

Where nominal mass takes in account only  $^{12}\text{C}$ ,  $^1\text{H}$ ,  $^{16}\text{O}$ ,  $^{14}\text{N}$  etc...

Theoretical mass correspond to the mass of the most abundant isotope peak

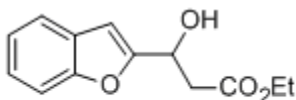


Table 2, entry 17

Scans: 1 > 11  
 Client: Kuldup  
 #Peaks: 609  
 RIC: 498055  
 8.1E+04

SPEC: fin063650.dar (06-JUN-08 14:42:43)  
 Samp: KW637  
 Conn: 70 eV EI  
 Oper: kh  
 Name: 147.04  
 Peak: 1000.0 mmu  
 Scan 10 @ 0.27 min (EI -Q1MS LMR UP LR)

Study: Service  
 Masses: 35.01 > 650.00  
 Intensity: 80757

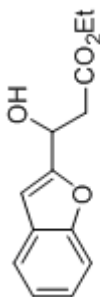
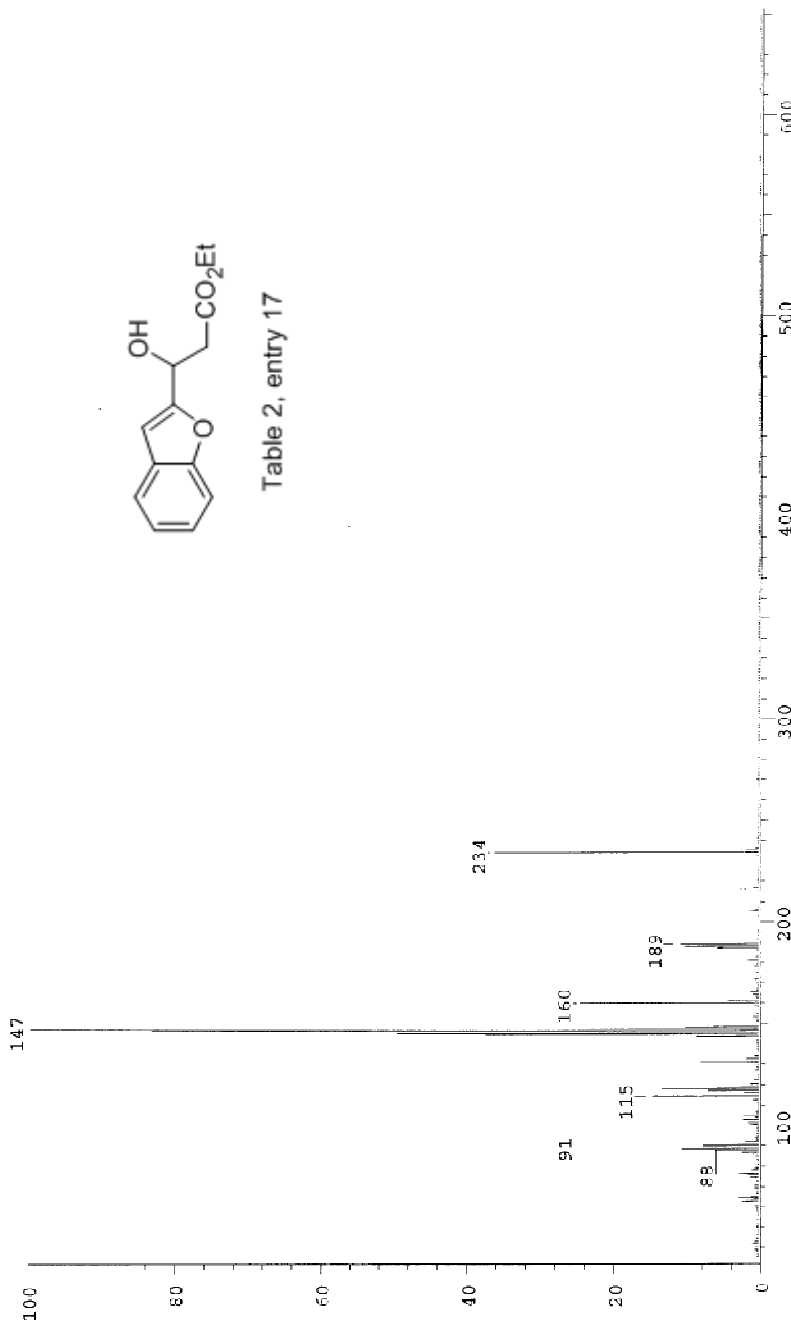
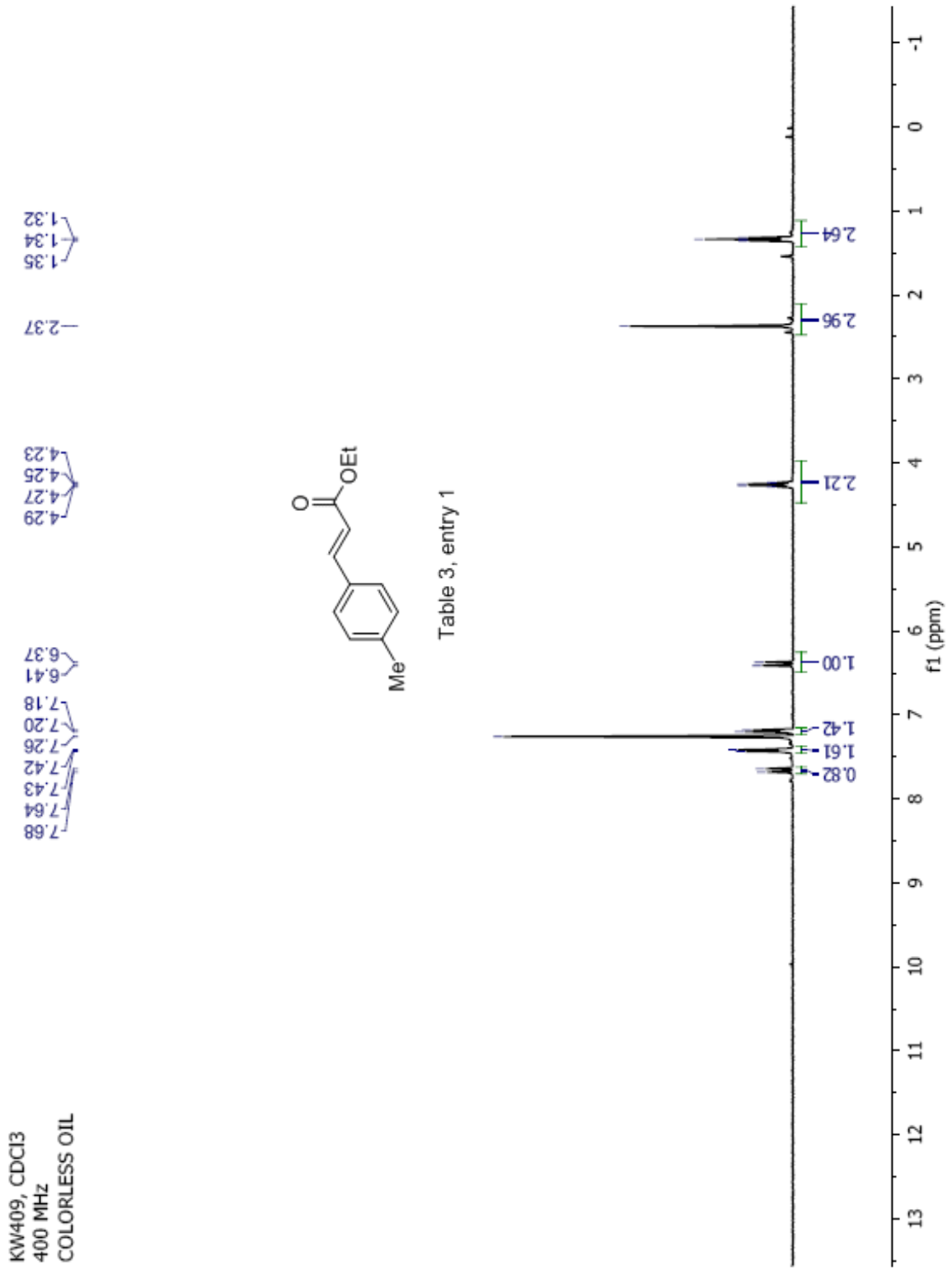
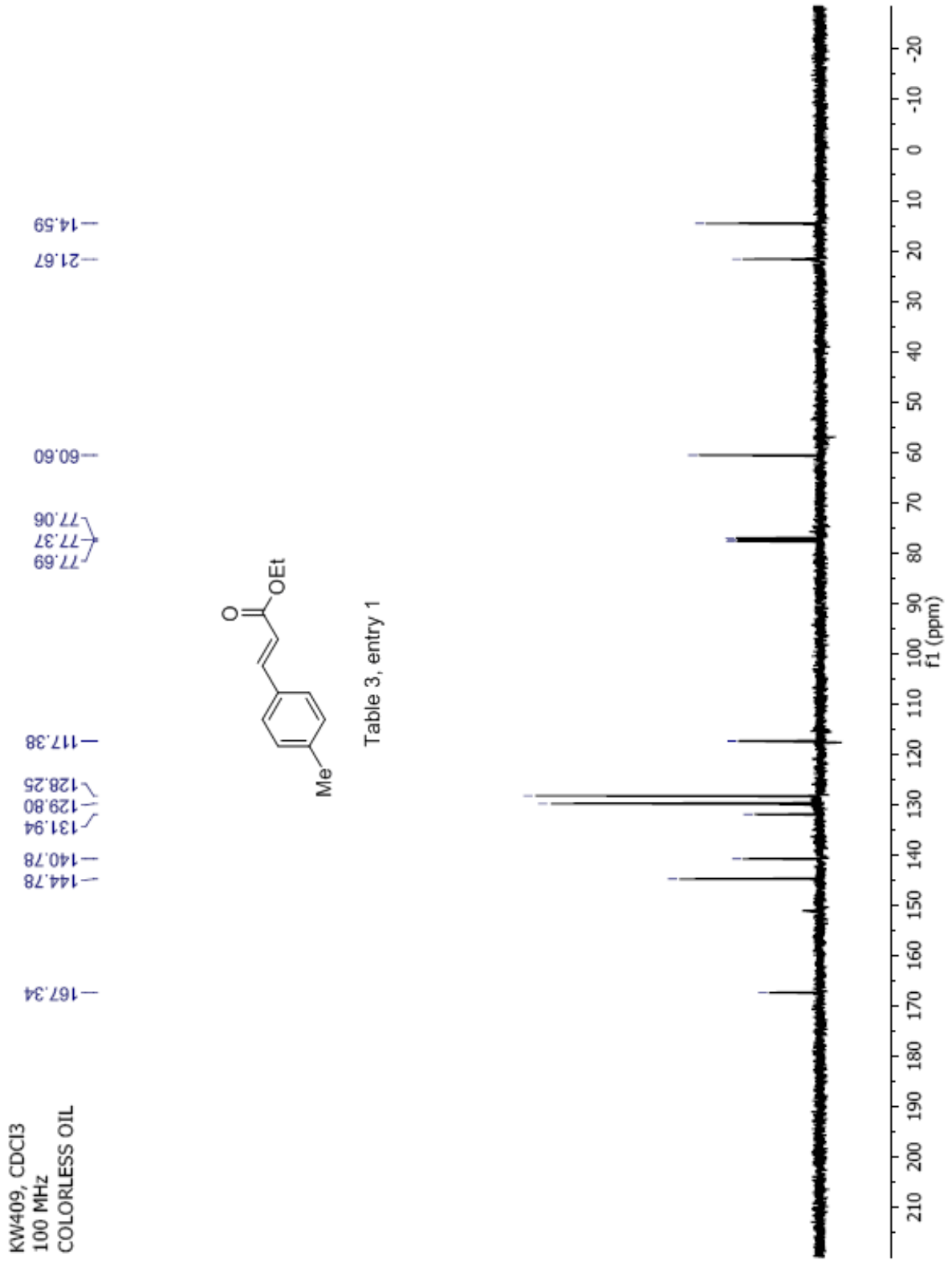


Table 2, entry 17

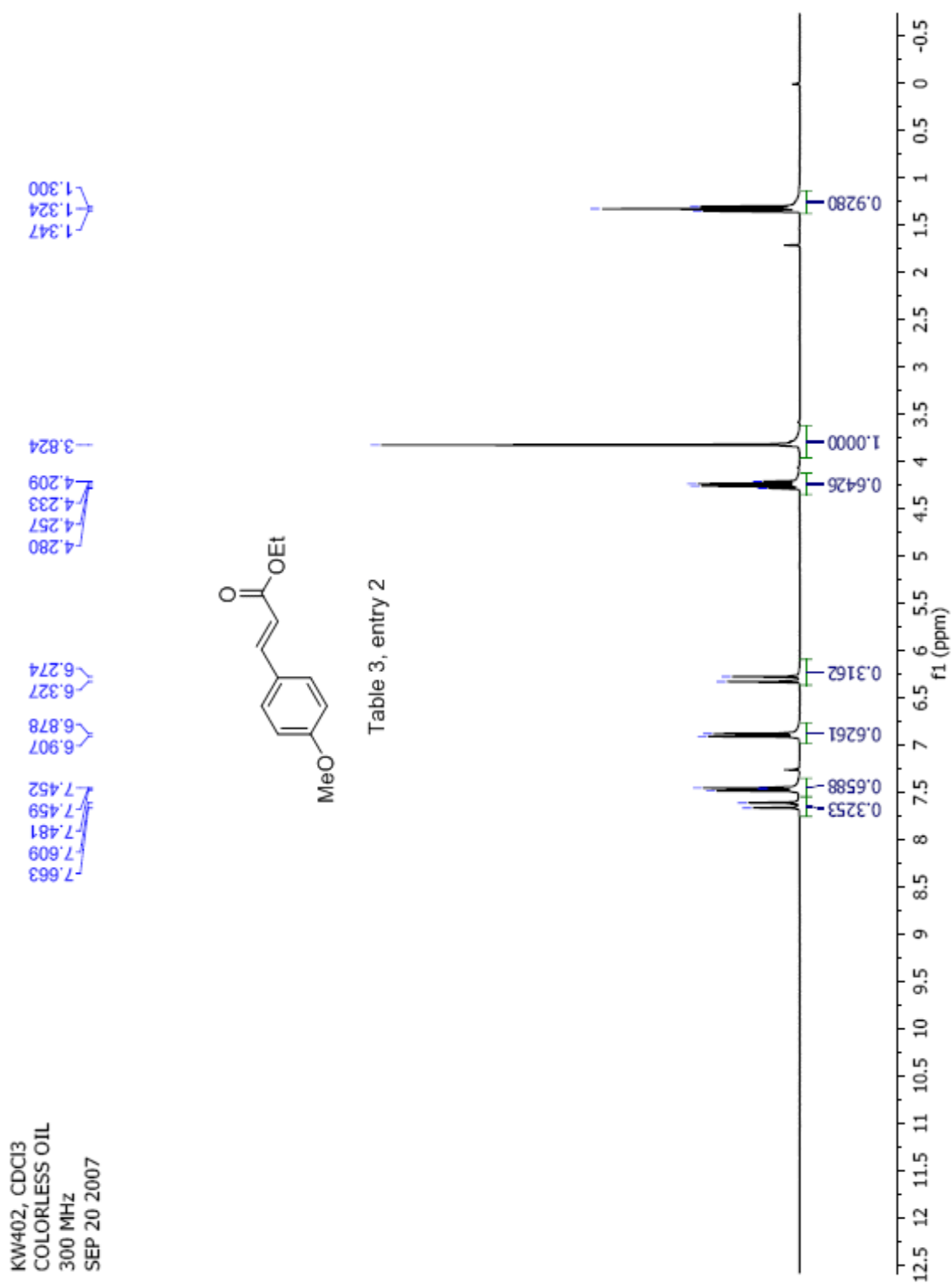


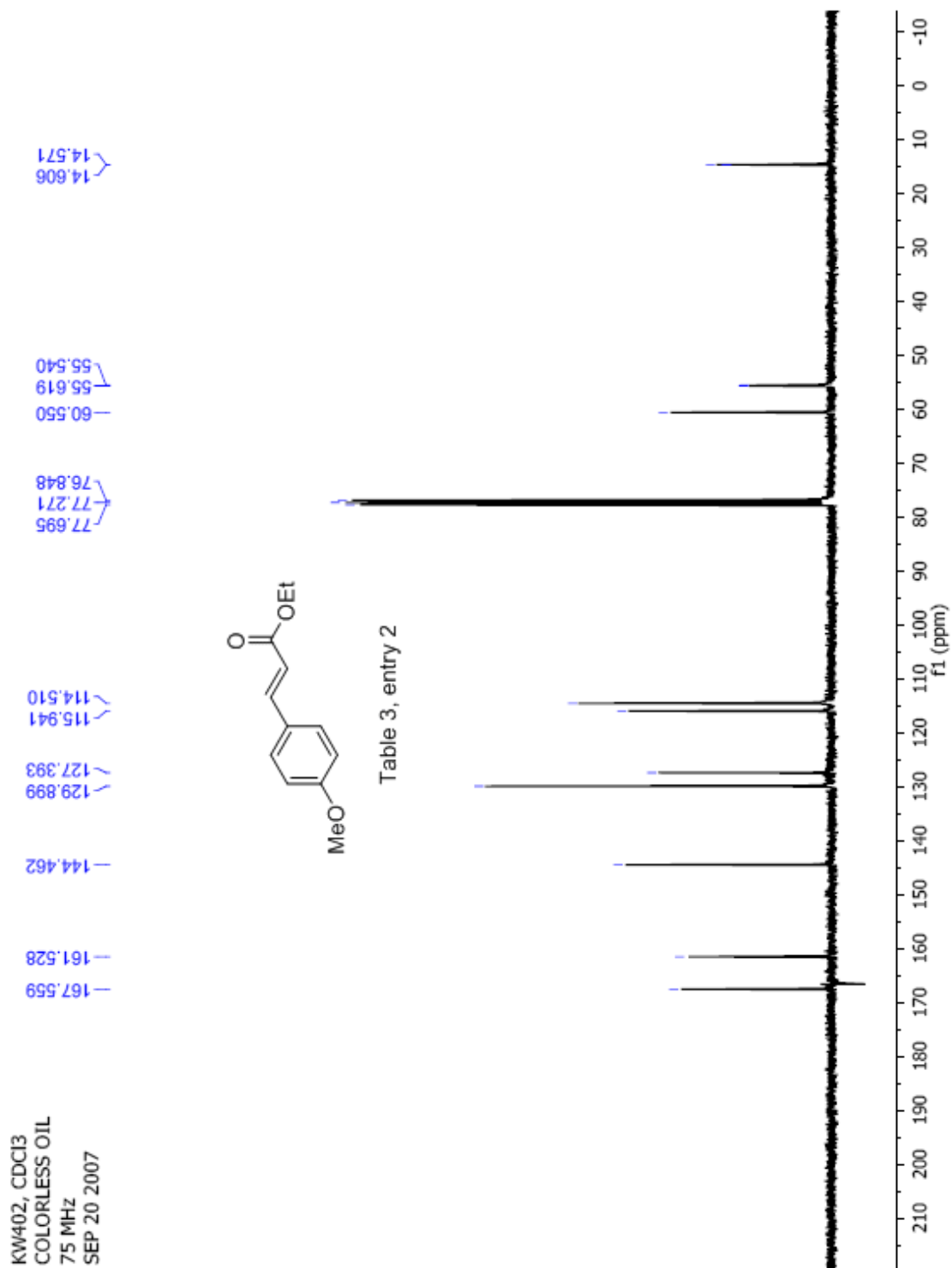
Date: Fri Jun 6 14:43:21 2008 ICIS: 8.2.0 SP2 for OSFI (V4.0) build 98-238 from 26-Aug-98











KW403, CDCI3  
 COLORLESS OIL  
 300 MHz  
 SEP 20 2007

1.301  
 1.325  
 1.349

4.282  
 4.258  
 4.234  
 4.210

7.614  
 7.561  
 7.092  
 6.793  
 6.283  
 6.230  
 6.002

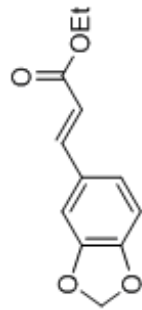
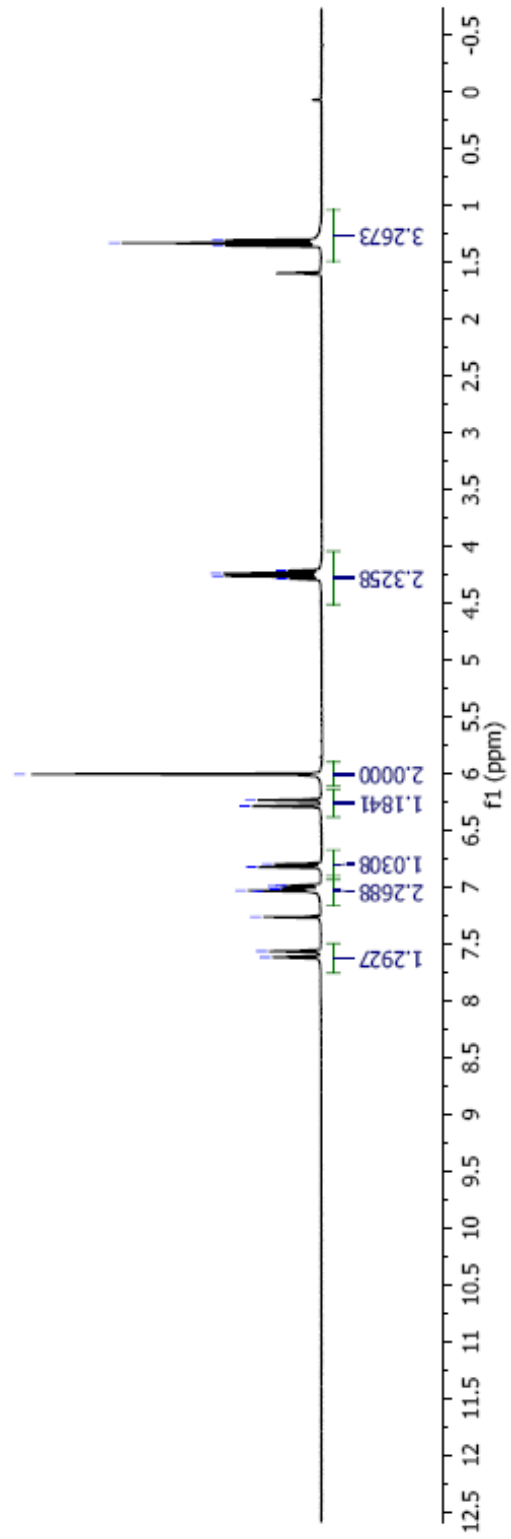
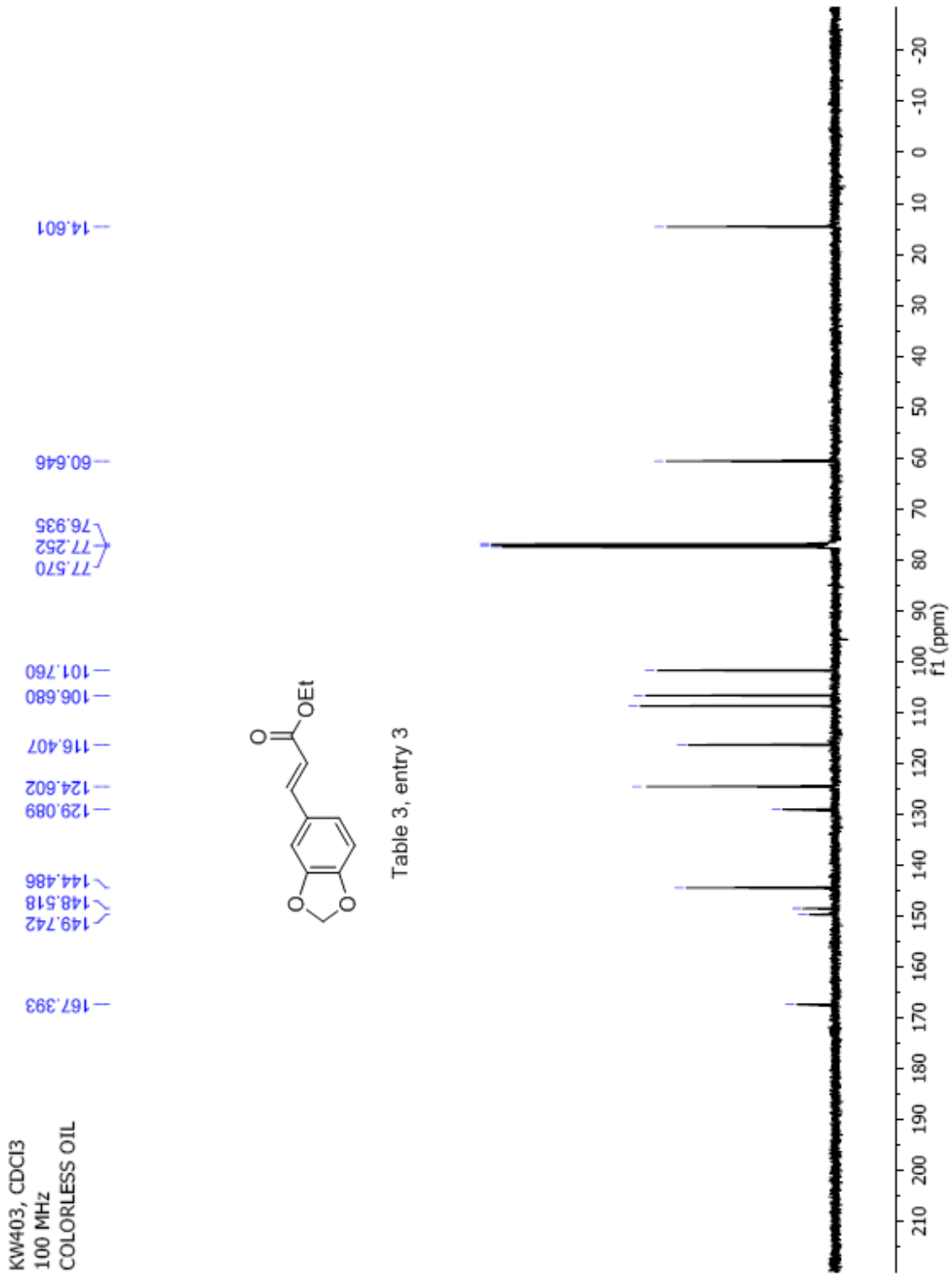
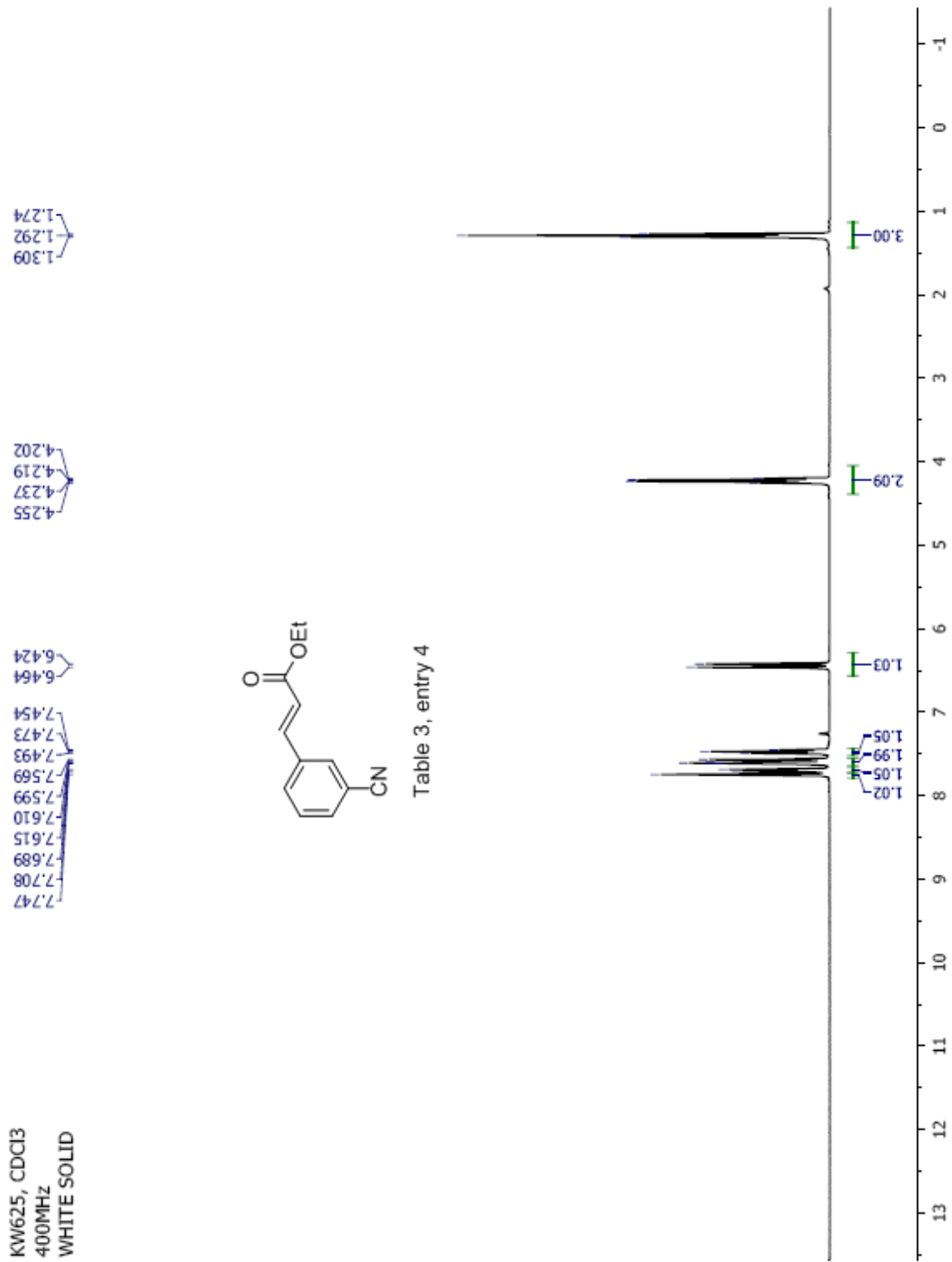


Table 3, entry 3







KW625, CDCl<sub>3</sub>  
100 MHz  
WHITE SOLID

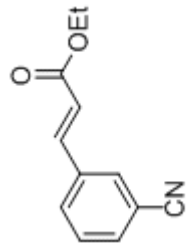
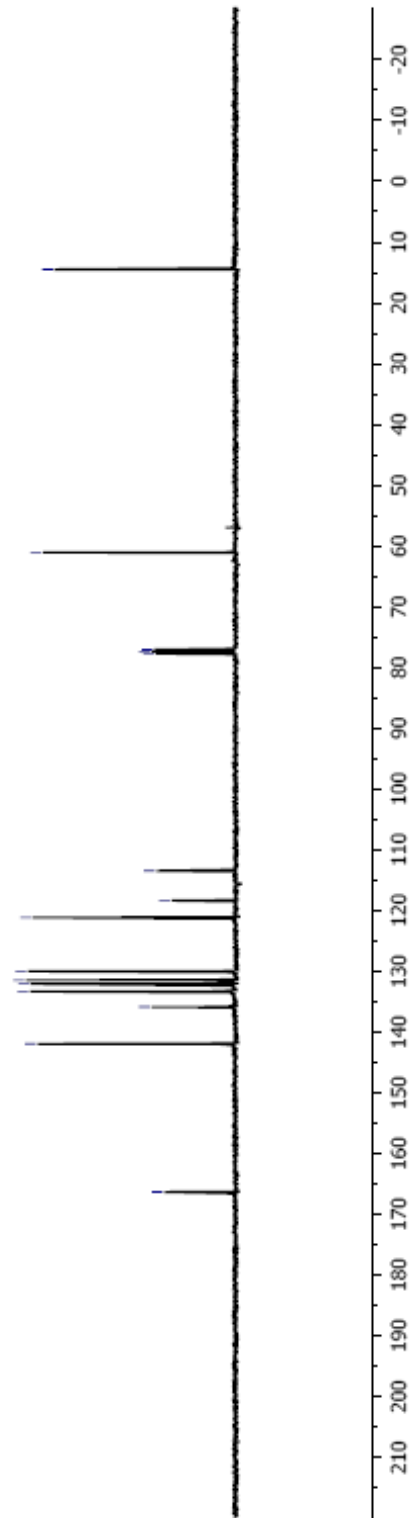


Table 3, entry 4



## Manual Peak Matching Report For Accurate Mass Determination

Theoretical mass	Experimental mass	PFK matching mass	Deviation*
201.07897	201.07925	180.98882	1.4 ppm

\* The deviation is obtained from the following equation:

$$\text{deviation} = \frac{\text{experimental mass} - \text{theoretical mass}}{\text{nominal mass}}$$

Where nominal mass takes in account only  $^{12}\text{C}$ ,  $^1\text{H}$ ,  $^{16}\text{O}$ ,  $^{14}\text{N}$  etc...

Theoretical mass correspond to the mass of the most abundant isotope peak

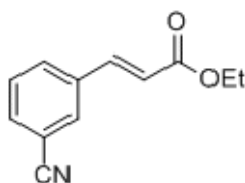


Table 3, entry 4

*br*

Scans: 1 > 21  
 Client: Koldup  
 #Peaks: 637  
 RTC: 89602129  
 1.4E+07

SPEC: FAR084260.dat (23-FEB-09 11:31:43)  
 Samp: kw525  
 Comm: DF 70 ev EI  
 Oper: kh  
 Study: ms services  
 Base: 201.21  
 Masses: 35.01 > 650.00  
 Peak: 1000.0 umu  
 Intensity: 13907968  
 Scan 1 @ 0.19 min (EI -QIMS LMR UP LR)

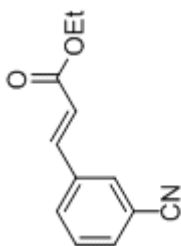
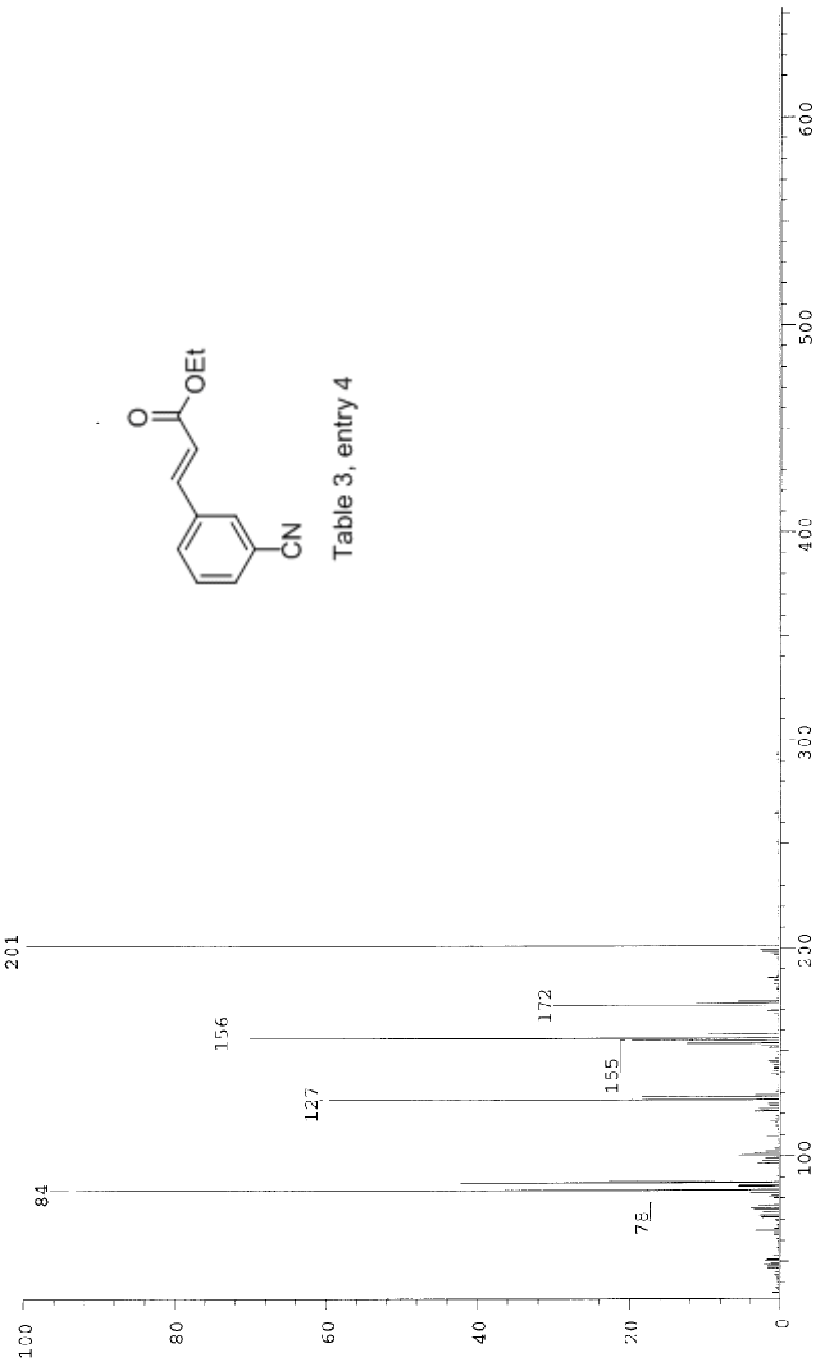
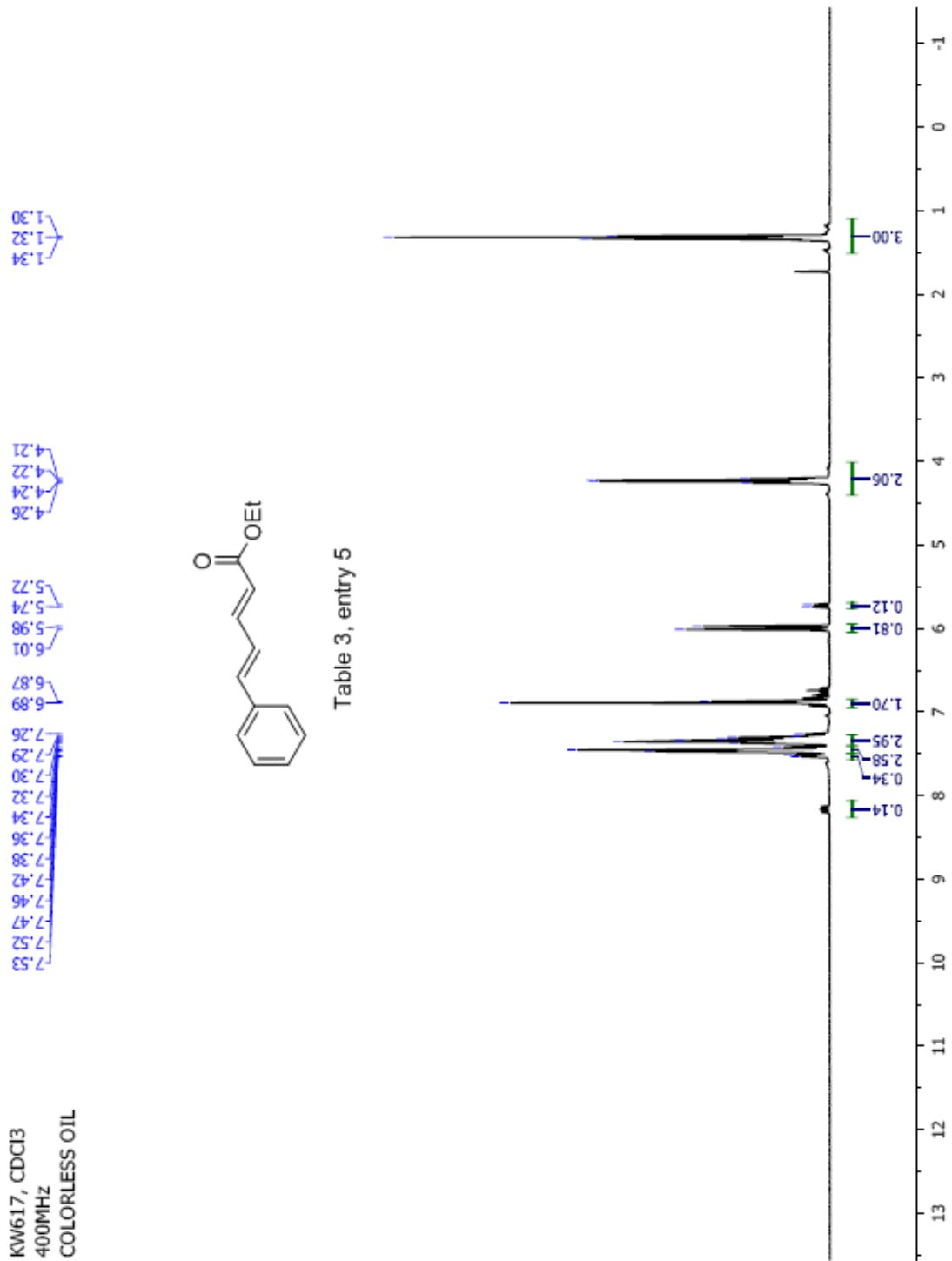
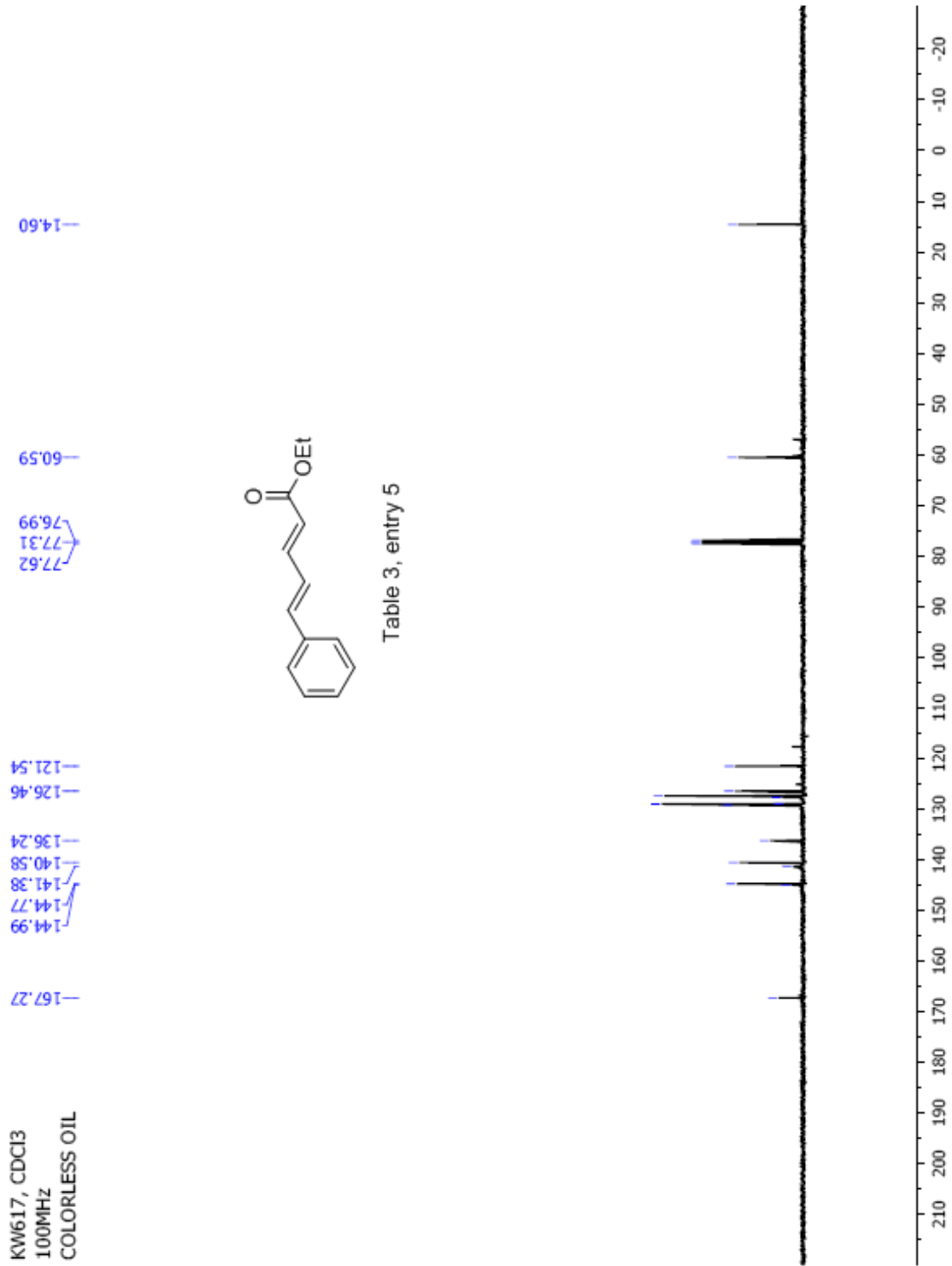


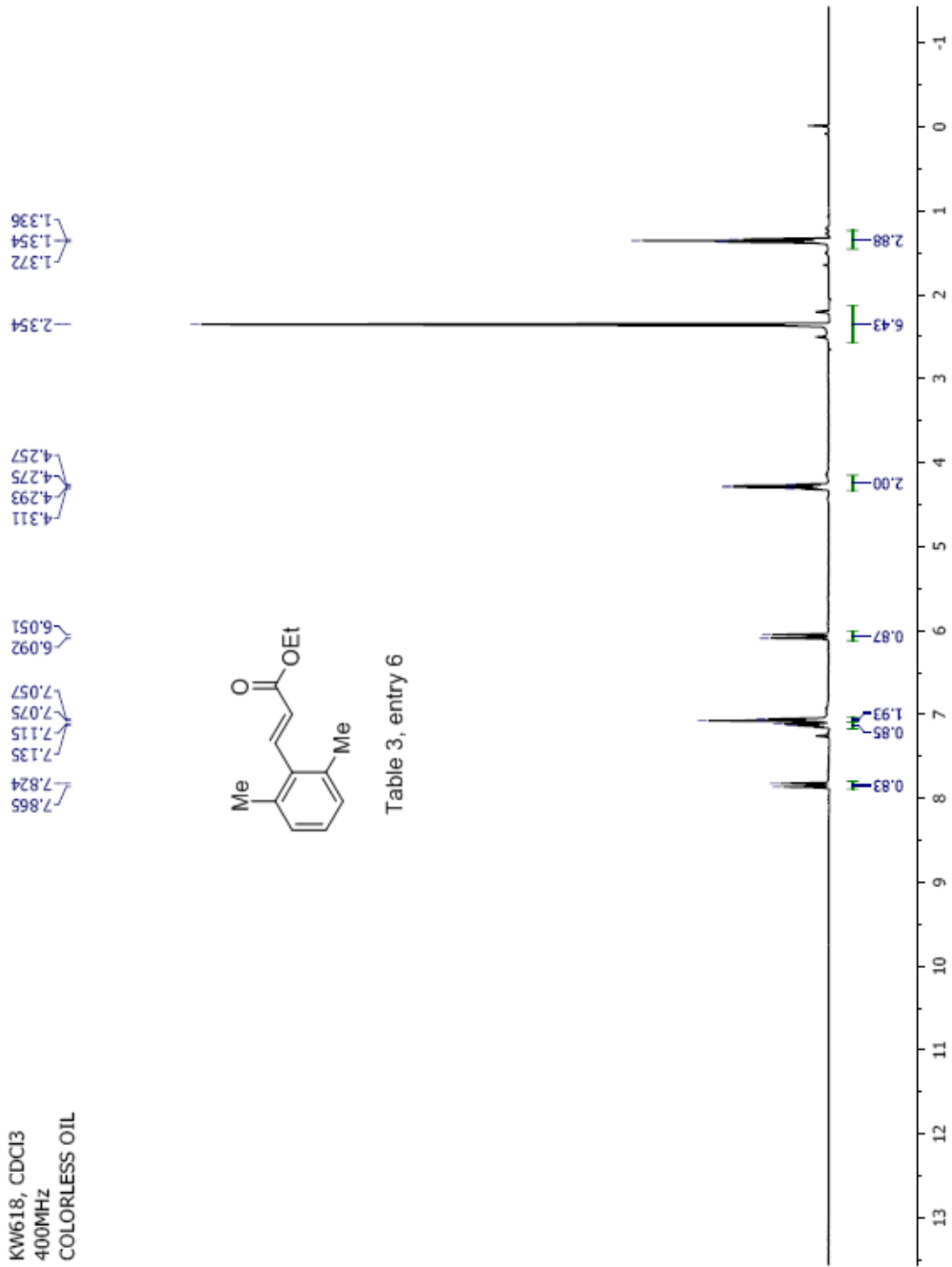
Table 3, entry 4

Date: Mon Feb 23 11:32:45 2009 ICIS: 8.3.0 SP2 for OSF1 (V4.0) build 98-238 From 26-Aug-98









KW618, CDCl<sub>3</sub>  
100MHz  
COLORLESS OIL

167.034  
143.488  
134.230  
128.422  
124.172  
77.597  
77.279  
76.961  
60.803  
21.341  
14.589

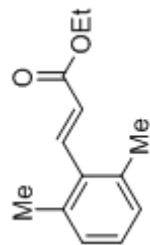
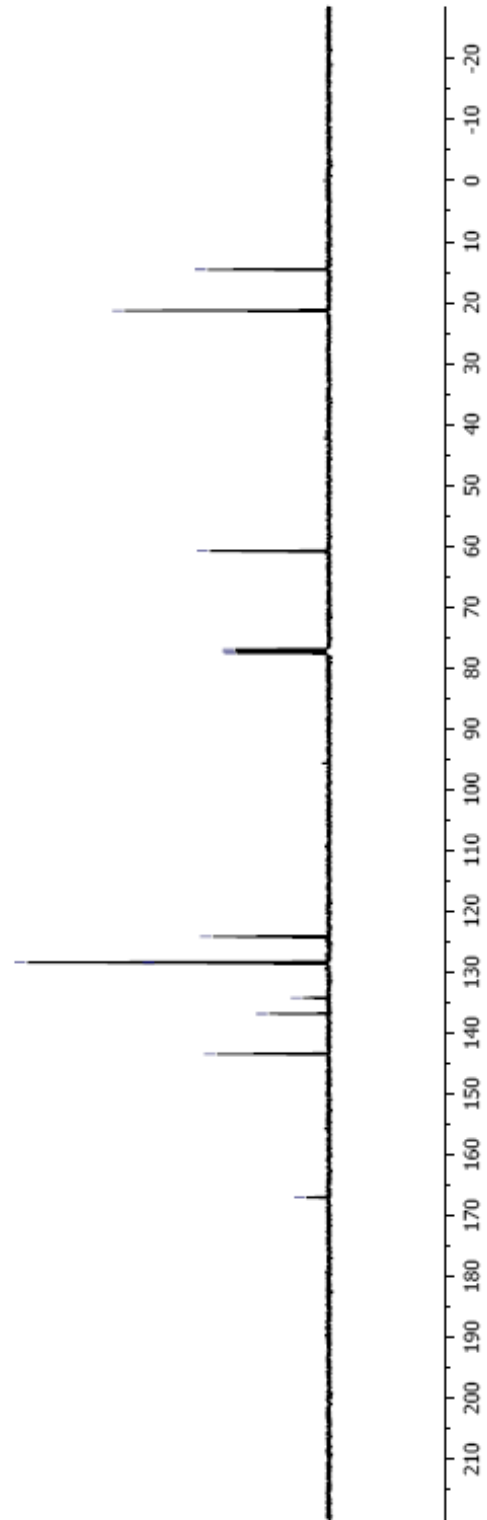
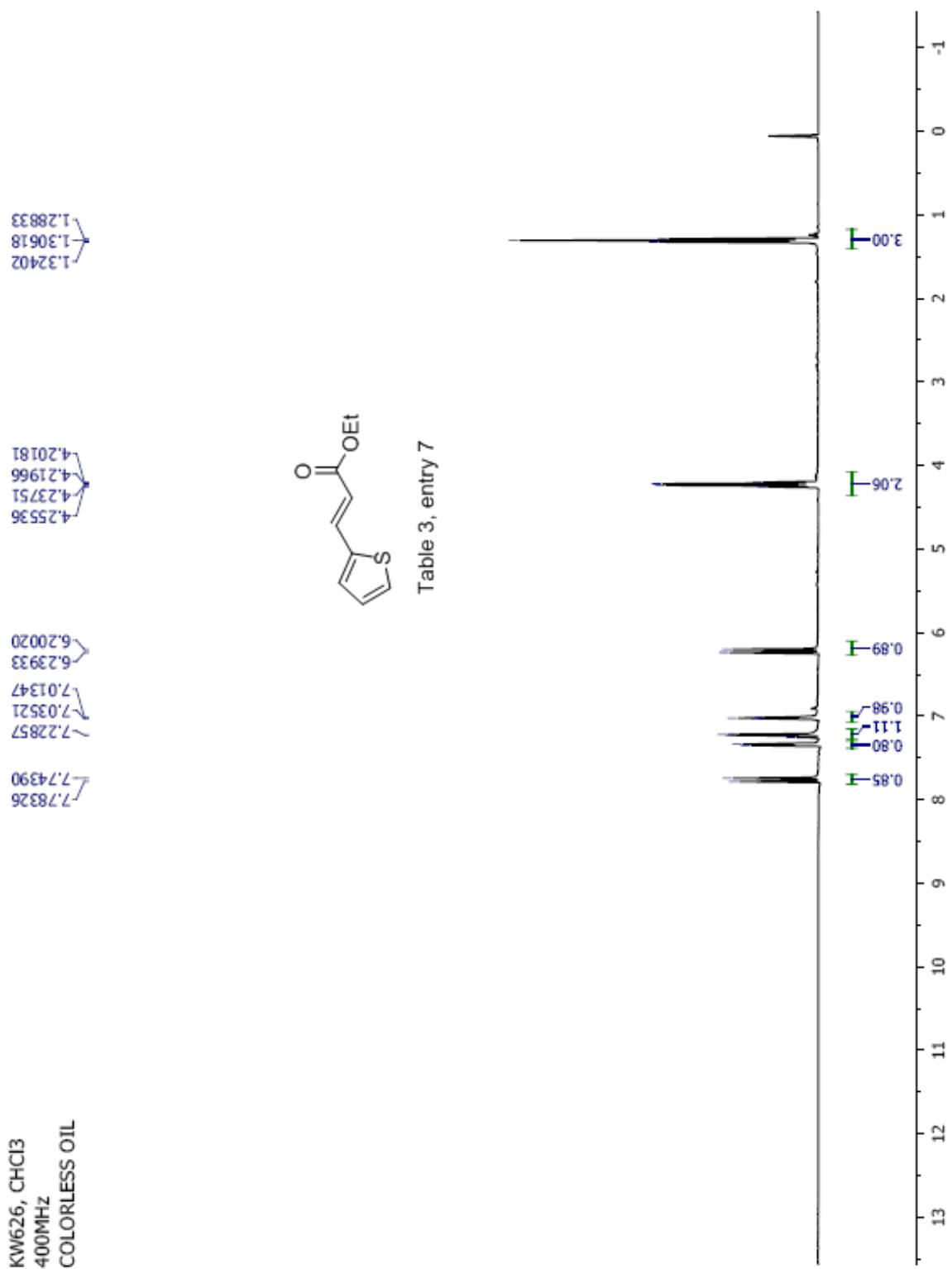
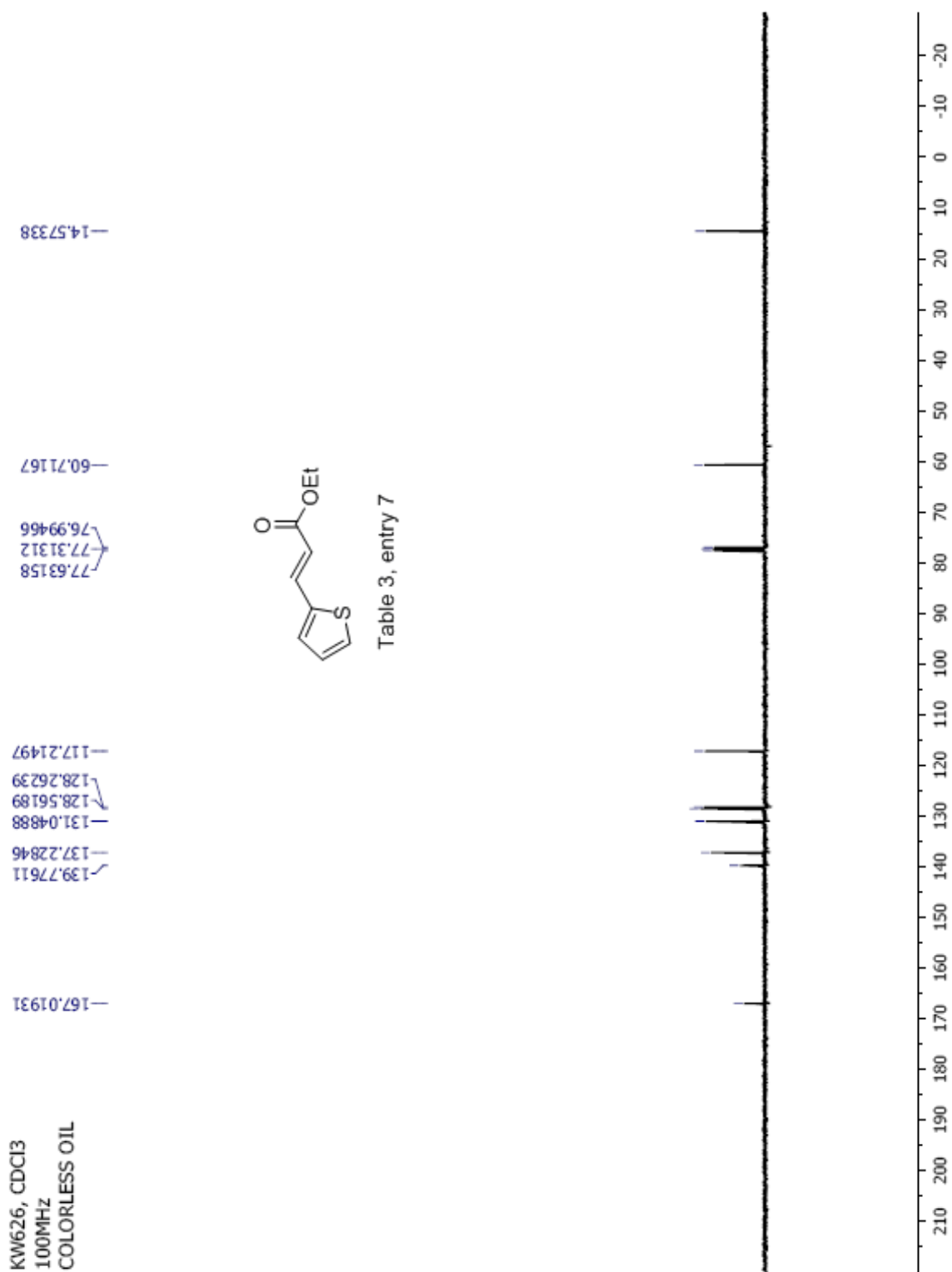


Table 3, entry 6







1.36  
1.34  
1.32

4.30  
4.28  
4.26  
4.24

7.56  
7.55  
7.54  
7.51  
7.47  
7.45  
7.35  
7.33  
7.31  
7.24  
7.22  
7.20  
6.89  
6.59

KW643, CDCl<sub>3</sub>  
400MHz  
WHITE SOLID

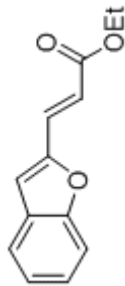
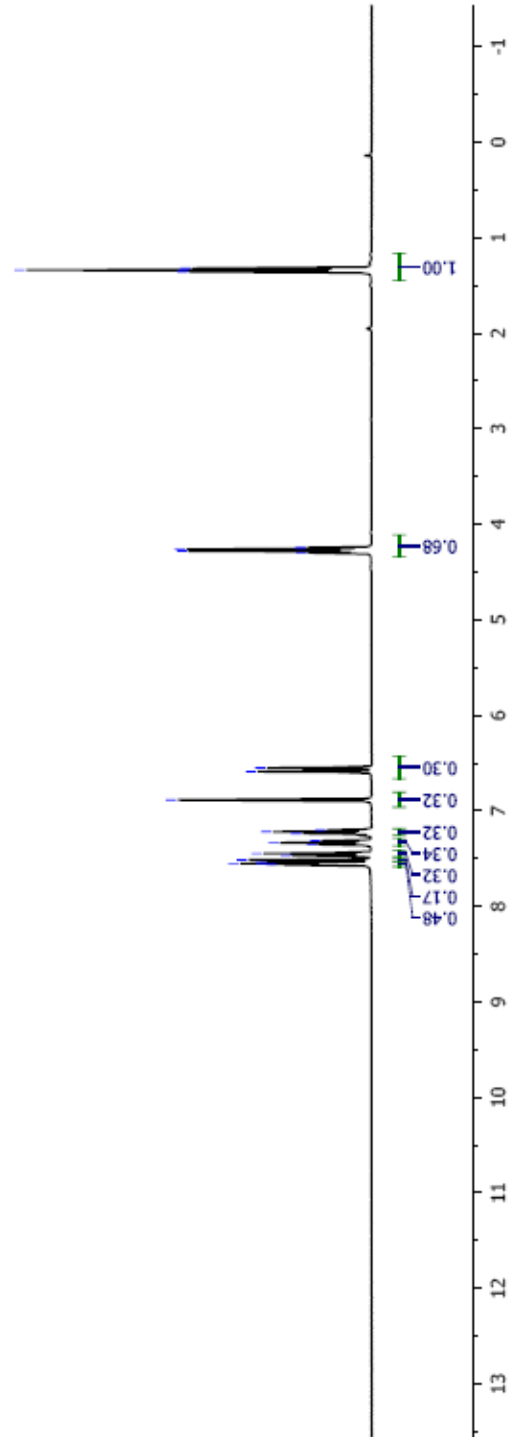


Table 3, entry 8



KW643, CDCl<sub>3</sub>  
 100MHz  
 WHITE SOLID

166.85  
 155.72  
 152.56  
 131.41  
 128.57  
 126.62  
 123.52  
 121.96  
 119.19  
 111.61  
 111.26

77.70  
 77.38  
 77.06

60.89

14.57

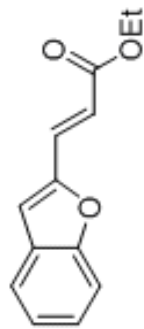
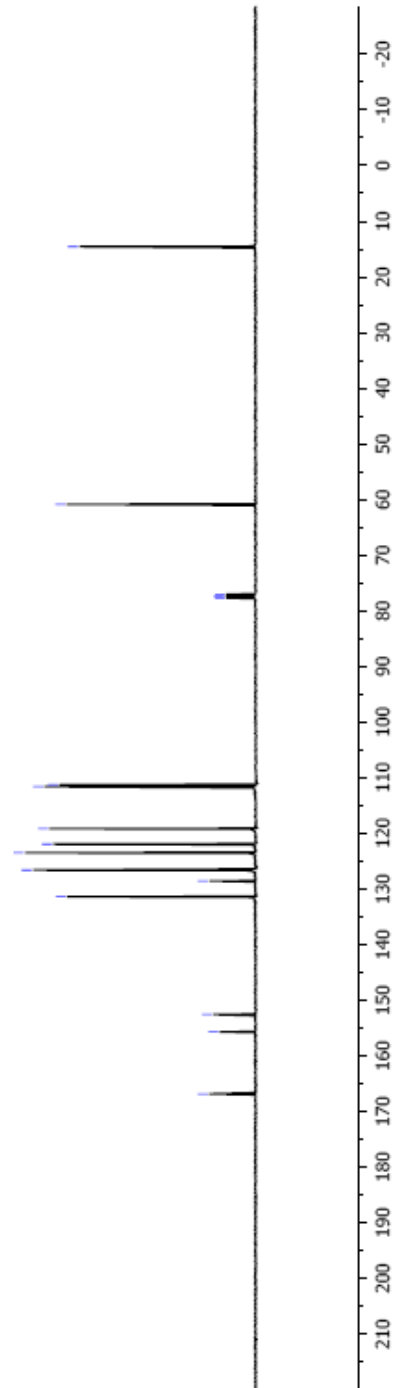


Table 3, entry 8





**APPENDIX B**

**CHAPTER 3**

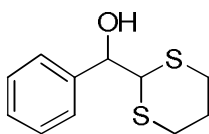
**General Information**

**Reference for known compounds and characterization data for new compounds  
<sup>1</sup>H, <sup>13</sup>C and HRMS for all compounds**

### General Information

All reactions were carried out under inert atmosphere using oven dried glassware and a magnetic stirrer. THF was distilled and dried over sodium. Trimethylsilyl-1,3-dithiane, proazaphosphatane **1a** and all aldehydes were purchased from Aldrich Chemical and used without further purification. Products were purified via column chromatography using hexane/ethyl acetate.  $^1\text{H}$  and  $^{13}\text{C}$  nmr spectra were obtained on a VXR-300 and VXR-400 Varian NMR spectrometer, respectively. All NMR spectra were taken in  $\text{CDCl}_3$ . Thin layer chromatography was used to monitor reaction progress.

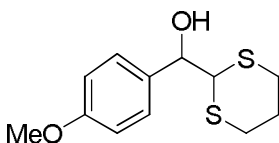
#### 1,3-Dithian-2-yl-phenylmethanol (Table 1, entry 1)<sup>1</sup>:



The general procedure was followed for the synthesis and purification; product was afforded as a colorless oil in 98 % isolated yield.

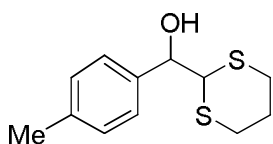
$^{13}\text{C}$  NMR ( $\text{CDCl}_3$ , 100.6 MHz):  $\delta$  140.4, 128.6, 128.5, 127.1, 74.9, 53.1, 28.5, 27.9, 25.6 ppm.

#### 1,3-Dithian-2-yl-4-methoxyphenylmethanol (Table 2, entry 1)<sup>1</sup>:



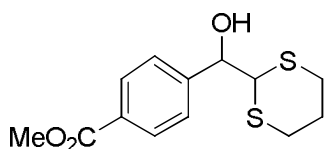
The general procedure was followed for the synthesis and purification; product was afforded as a white solid in 95% isolated yield.

#### 1,3-Dithian-2-yl-4-methylphenylmethanol (Table 2, entry 2):



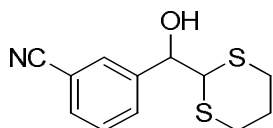
The general procedure was followed for the synthesis and purification; product was afforded as a colorless oil in 98% isolated yield.  $^1\text{H}$  NMR ( $\text{CDCl}_3$ , 400 MHz):  $\delta$  7.32–7.29 (m, 2H), 7.19–7.16(m, 2H), 4.88 (d, 1H,  $J = 8.0$  Hz), 4.09 (d, 1H,  $J = 8.0$  Hz), 2.91–2.68 (m, 4H), 2.35 (s, 3H), 2.07–1.98 (m, 2H) ppm ;  $^{13}\text{C}$  NMR ( $\text{CDCl}_3$ , 100.6 MHz):  $\delta$  138.4, 137.3, 129.3, 126.9, 74.9, 53.2, 28.6, 28.0, 25.6, 21.5 ppm. HRMS  $m/z$  Calcd for  $\text{C}_{12}\text{H}_{16}\text{OS}_2$ : 240.06425. Found: 240.06462.

**Methyl 4-((1,3-dithian-2-yl)(hydroxy)methyl)benzoate** (Table 2, entry 3):



The general procedure was followed for the synthesis and purification; product was afforded as a white solid in 93% isolated yield.  $^1\text{H}$  NMR ( $\text{CDCl}_3$ , 400 MHz):  $\delta$  7.94 (d, 2H,  $J = 8.0$  Hz), 7.42 (d, 2H,  $J = 8.0$  Hz), 4.90 (d, 1H,  $J = 8.0$  Hz), 4.02 (d, 1H,  $J = 8.0$  Hz), 3.84 (s, 3H) 3.52 (s, 1H), 2.88–2.83 (m, 2H), 2.69–2.61 (m, 2H), 1.97–1.89 (m, 2H) ppm ;  $^{13}\text{C}$  NMR ( $\text{CDCl}_3$ , 100.6 MHz):  $\delta$  167.0, 145.7, 130.0, 129.6, 127.1, 74.5, 52.8, 52.4, 28.5, 27.9, 25.5 ppm; HRMS  $m/z$  Calcd for  $\text{C}_{13}\text{H}_{16}\text{O}_3\text{S}_2$ : 284.05409. Found: 284.05447.

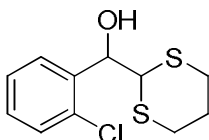
**1,3-Dithian-2-yl-3-cyanophenylmethanol** (Table 2, entry 4):



The general procedure was followed for the synthesis and purification affording a colorless oil in 80% isolated yield.  $^1\text{H}$  NMR ( $\text{CDCl}_3$ , 400 MHz):  $\delta$  7.71 (s, 1H), 7.64 (d, 1H,  $J = 8.0$  Hz), 7.56 (d, 1H,  $J = 8.0$  Hz), 7.44 (t, 1H,  $J = 8.0$  Hz), 4.92 (dd, 1H,  $J = 8.0$  Hz,  $J = 2.0$  Hz), 3.94 (d, 1H,  $J = 8.0$  Hz), 3.36 (d, 1H,  $J = 2.4$  Hz), 2.94–2.91 (m, 2H), 2.75–2.66 (m, 2H), 2.06–1.96 (m, 2H) ppm ;  $^{13}\text{C}$  NMR

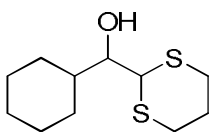
(CDCl<sub>3</sub>, 100.6 MHz):  $\delta$  142.0, 132.0, 131.6, 130.9, 129.1, 119.0, 112.3, 73.7, 52.4, 28.1, 27.4, 25.3 ppm; HRMS  $m/z$  Calcd for C<sub>12</sub>H<sub>13</sub>NOS<sub>2</sub>: 251.04386. Found: 251.04414.

**1,3-Dithian-2-yl-2-chlorophenylmethanol** (Table 2, entry 5):



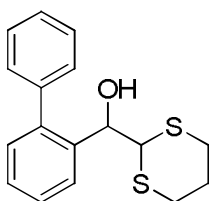
The general procedure was followed for the synthesis and purification affording a colorless oil in 96% isolated yield. <sup>1</sup>H NMR (CDCl<sub>3</sub>, 400 MHz):  $\delta$  7.56–7.54 (m, 1H), 7.34–7.20 (m, 3H), 5.40 (q, 1H,  $J$  = 4.0 Hz), 4.12 (d, 1H,  $J$  = 4.0 Hz), 3.23 (s, 1H), 2.94–2.75 (m, 2H), 2.68–2.62 (m, 2H), 2.02–1.98 (m, 2H) ppm ; <sup>13</sup>C NMR (CDCl<sub>3</sub>, 100.6 MHz):  $\delta$  138.3, 133.3, 129.5, 129.4, 128.4, 127.1, 71.2, 51.6, 28.9, 27.6, 25.6 ppm; HRMS  $m/z$  Calcd for C<sub>11</sub>H<sub>13</sub>ClOS<sub>2</sub>: 260.00963. Found: 260.01002.

**Cyclohexyl(1,3-dithian-2-yl)methanol** (Table 2, entry 6):



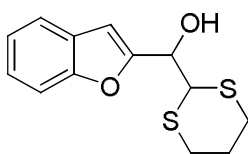
The general procedure was followed for the synthesis and purification affording a colorless oil in 94% isolated yield. <sup>1</sup>H NMR (CDCl<sub>3</sub>, 400 MHz):  $\delta$  4.06 (d, 1H,  $J$  = 8.0 Hz), 3.55 (s, 1H), 2.90–2.73 (m, 4H), 2.34 (s, 1H), 1.90–1.62 (m, 8H), 1.24–1.07 (m, 5H) ppm ; <sup>13</sup>C NMR (CDCl<sub>3</sub>, 100.6 MHz):  $\delta$  76.5, 50.6, 39.9, 30.2, 29.2, 28.4, 26.9, 26.5, 26.5, 26.1, 25.9 ppm; HRMS  $m/z$  Calcd for C<sub>11</sub>H<sub>20</sub>OS<sub>2</sub>: 232.09555. Found: 232.09597.

**1,3-Dithian-2-yl-2-biphenylmethanol** (Table 2, entry 7):



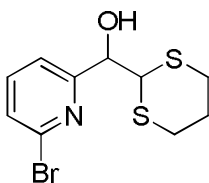
The general procedure was followed for the synthesis and purification giving a colorless oil in 81% isolated yield.  $^1\text{H}$  NMR ( $\text{CDCl}_3$ , 400 MHz):  $\delta$  7.60 (d, 1H,  $J = 8.0$  Hz), 7.42–7.35 (m, 7H), 7.26–7.25 (m, 1H), 5.17 (d, 1H,  $J = 8.0$  Hz), 3.81 (d, 1H,  $J = 8.0$  Hz), 3.19 (s, 1H), 2.76–2.70 (m, 1H), 2.52–2.47 (m, 1H), 2.29–2.24 (m, 1H), 2.08–2.04 (m, 1H), 1.88–1.81 (m, 2H) ppm;  $^{13}\text{C}$  NMR ( $\text{CDCl}_3$ , 100.6 MHz):  $\delta$  142.8, 141.2, 138.1, 130.0, 129.9, 128.4, 128.1, 128.1, 127.2, 126.3, 69.1, 51.6, 26.8, 25.9, 25.2 ppm; HRMS  $m/z$  Calcd for  $\text{C}_{17}\text{H}_{18}\text{OS}_2$ : 302.07991. Found: 302.08031.

**Benzofuran-2-yl(1,3-dithian-2-yl)methanol** (Table 2, entry 8):



The general procedure was followed for the synthesis and purification giving a white solid in 95% isolated yield.  $^1\text{H}$  NMR ( $\text{CDCl}_3$ , 400 MHz):  $\delta$  7.54 (d, 1H,  $J = 8.0$  Hz), 7.47 (d, 1H,  $J = 8.0$  Hz), 7.27 (t, 1H,  $J = 8.0$  Hz), 7.21 (t, 1H,  $J = 8.0$  Hz), 6.79 (s, 1H), 5.095 (q, 1H,  $J = 4.0$  Hz), 4.38 (d, 1H,  $J = 8.0$  Hz), 3.47 (d, 1H,  $J = 4.0$  Hz), 2.90–2.85 (m, 2H), 2.69–2.63 (m, 2H), 1.98–1.92 (m, 2H) ppm;  $^{13}\text{C}$  NMR ( $\text{CDCl}_3$ , 100.6 MHz):  $\delta$  155.3, 155.0, 128.1, 124.7, 123.1, 121.5, 111.6, 105.7, 69.5, 49.4, 28.1, 27.5, 25.5 ppm; HRMS  $m/z$  Calcd for  $\text{C}_{13}\text{H}_{14}\text{O}_2\text{S}_2$ : 266.04352. Found: 266.04411.

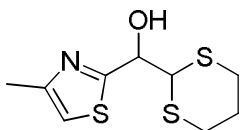
**(6-Bromopyridin-2-yl)(1,3-dithian-2-yl)methanol** (Table 2, entry 9):



The general procedure was followed for the synthesis and purification giving a yellow oil in 92% isolated yield.  $^1\text{H}$  NMR ( $\text{CDCl}_3$ , 400 MHz):  $\delta$  7.56 (t, 1H,  $J = 8.0$  Hz), 7.43–7.40 (m, 2H), 4.96 (bs, 1H), 4.21 (d, 1H,  $J = 8.0$  Hz), 3.66 (bs, 1H), 3.00–2.72 (m, 4H), 2.10–1.88 (m, 2H) ppm;  $^{13}\text{C}$  NMR

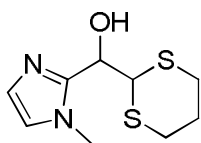
(CDCl<sub>3</sub>, 100.6 MHz):  $\delta$  160.4, 141.5, 139.0, 127.7, 120.9, 75.3, 52.5, 29.2, 28.8, 25.7 ppm; HRMS  $m/z$  Calcd for C<sub>10</sub>H<sub>12</sub>BrNOS<sub>2</sub>: 305.95437. Found: 305.95475.

**(1,3-Dithian-2-yl)(4-methylthiazol-2-yl)methanol** (Table 2, entry 10):



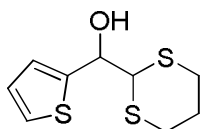
The general procedure was followed for the synthesis and purification affording a yellow oil in 94% isolated yield. <sup>1</sup>H NMR (CDCl<sub>3</sub>, 400 MHz):  $\delta$  6.89 (s, 1H), 5.25 (d, 1H,  $J$  = 8.0 Hz), 4.21 (d, 1H,  $J$  = 4.0 Hz), 3.72 (bs, 1H), 3.03–2.73 (m, 4H), 2.45 (s, 3H), 2.10–1.92 (m, 2H) ppm; <sup>13</sup>C NMR (CDCl<sub>3</sub>, 100.6 MHz):  $\delta$  170.0, 152.8, 114.4, 73.6, 51.9, 28.7, 28.2, 25.5, 17.3 ppm; HRMS  $m/z$  Calcd for C<sub>9</sub>H<sub>13</sub>NOS<sub>3</sub>: 247.01593. Found: 247.01623.

**(1,3-Dithian-2-yl)(1-methyl-1H-imidazol-2-yl)methanol** (Table 2, entry 11):



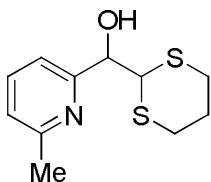
The general procedure was followed for the synthesis and purification producing a white solid in 67% isolated yield. <sup>1</sup>H NMR (CDCl<sub>3</sub>, 400 MHz):  $\delta$  7.02 (s, 1H), 6.81 (s, 1H), 5.21 (bs, 1H), 4.94 (d, 1H,  $J$  = 8.0 Hz), 4.49 (d, 1H,  $J$  = 8.0 Hz), 3.73 (s, 3H), 2.89–2.68 (m, 4H), 2.14–1.92 (m, 2H) ppm; <sup>13</sup>C NMR (CDCl<sub>3</sub>, 100.6 MHz):  $\delta$  147.1, 127.5, 121.7, 67.5, 50.5, 33.4, 28.3, 27.6, 25.6 ppm; HRMS  $m/z$  Calcd for C<sub>9</sub>H<sub>14</sub>N<sub>2</sub>OS<sub>2</sub>: 230.05476. Found: 230.05518.

**1,3-Dithian-2-yl-2-thienylmethanol** (Table 2, entry 12)<sup>1</sup>:



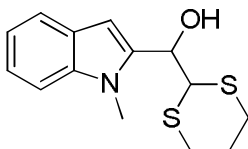
The general procedure was followed for the synthesis and purification giving a white solid in 97% isolated yield.

**(1,3-Dithian-2-yl)(6-methylpyridin-2-yl)methanol** (Table 2, entry 13):



The general procedure was followed for the synthesis and purification giving a white solid in 98% isolated yield.  $^1\text{H}$  NMR ( $\text{CDCl}_3$ , 400 MHz):  $\delta$  7.52 (t, 1H,  $J = 4.0$  Hz), 7.13 (d, 1H,  $J = 8.0$  Hz), 7.02 (d, 1H,  $J = 8.0$  Hz), 4.88 (bs, 1H), 4.84 (bs, 1H), 4.36 (d, 1H,  $J = 3.6$  Hz), 2.84–2.65 (m, 4H), 2.46 (s, 3H), 2.00–1.86 (m, 2H) ppm;  $^{13}\text{C}$  NMR ( $\text{CDCl}_3$ , 100.6 MHz):  $\delta$  157.4, 157.4, 137.0, 122.9, 118.8, 75.2, 53.6, 29.7, 29.4, 25.9, 24.5 ppm; HRMS  $m/z$  Calcd for  $\text{C}_{11}\text{H}_{15}\text{NOS}_2$ : 241.05951. Found: 241.06000.

**(1,3-Dithian-2-yl)(1-methyl-1H-indol-2-yl)methanol** (Table 2, entry 14):



The general procedure was followed for the synthesis and purification affording a yellow oil in 94% isolated yield.  $^1\text{H}$  NMR ( $\text{CDCl}_3$ , 400 MHz):  $\delta$  7.61 (d, 1H,  $J = 8.0$  Hz), 7.32–7.25 (m, 2H), 7.12 (t, 1H,  $J = 8.0$  Hz), 6.61 (s, 1H), 5.10 (d, 1H,  $J = 8.0$  Hz), 4.37 (d, 1H,  $J = 8.0$  Hz), 3.78 (s, 3H), 3.11 (s, 1H), 2.96–2.71 (m, 4H), 2.05–1.91 (m, 2H) ppm;  $^{13}\text{C}$  NMR ( $\text{CDCl}_3$ , 100.6 MHz):  $\delta$  138.2, 138.0, 127.2, 122.2, 121.2, 119.9, 109.5, 101.5, 68.7, 50.9, 30.8, 28.6, 27.9, 25.5 ppm; HRMS  $m/z$  Calcd for  $\text{C}_{14}\text{H}_{17}\text{NOS}_2$ : 279.07516. Found: 279.07569.

**Reference**

1. Ong, C. W.; Yu, C. Y. *Tetrahedron* **2003**, *59*, 9677–9682.



KW602, CDCI3  
 400MHz  
 COLORLESS OIL

7.422  
 7.403  
 7.385  
 7.368  
 7.348  
 7.343  
 7.326  
 7.259  
 4.906  
 4.887  
 4.087  
 2.919  
 2.745  
 2.712  
 2.678  
 2.067  
 2.058  
 2.049  
 2.039  
 2.032  
 2.024  
 2.013  
 1.989  
 1.981  
 1.974  
 1.966  
 1.959  
 1.944  
 1.931

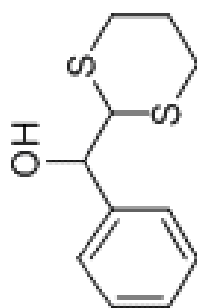
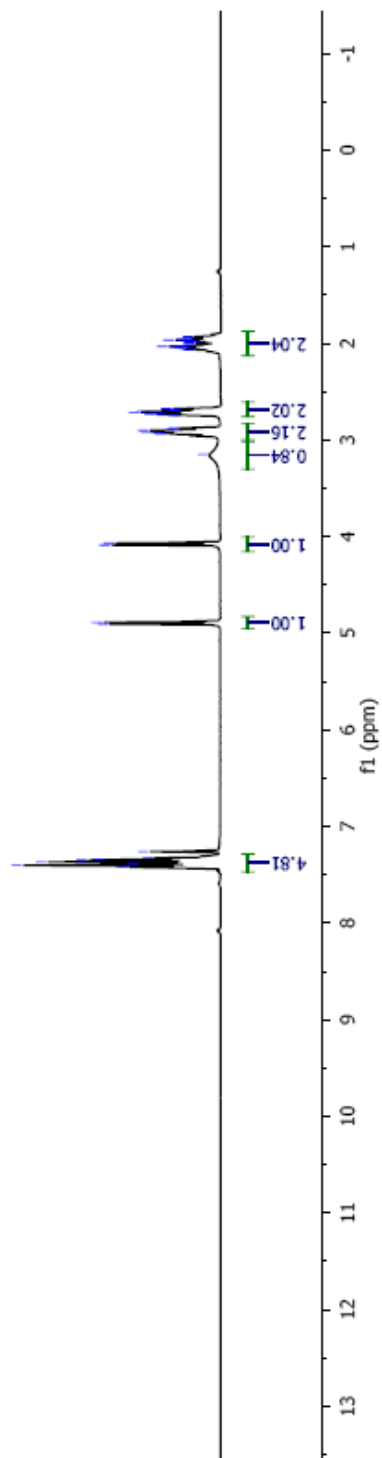


Table 1, entry 1



KW602, CDCl<sub>3</sub>  
100MHz  
COLORLESS OIL

140.431  
128.637  
128.498  
127.079  
77.738  
77.420  
77.103  
74.956  
53.068  
28.541  
27.927  
25.639

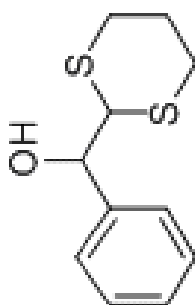
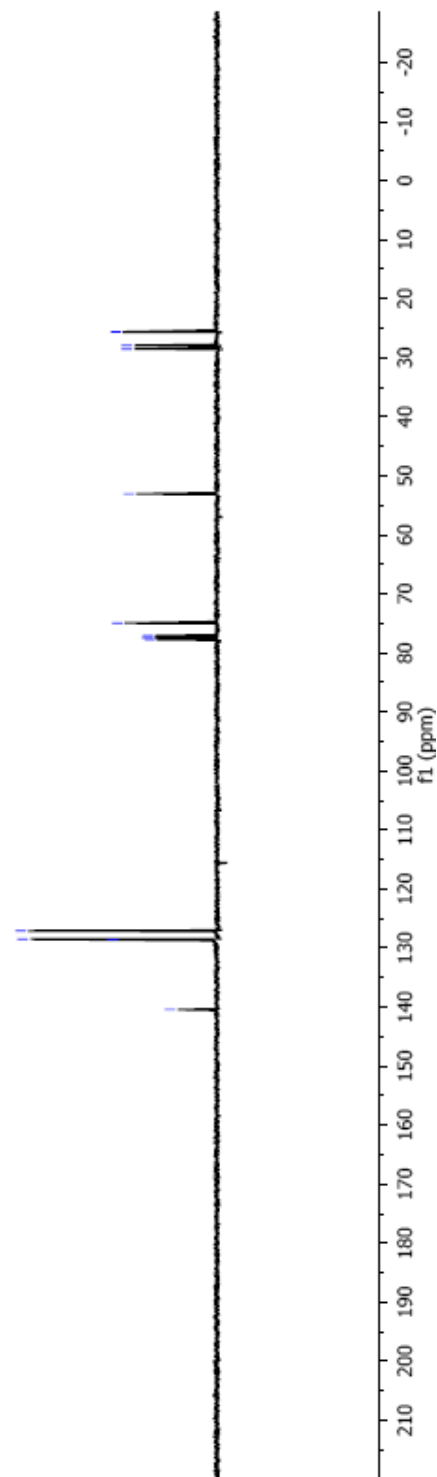
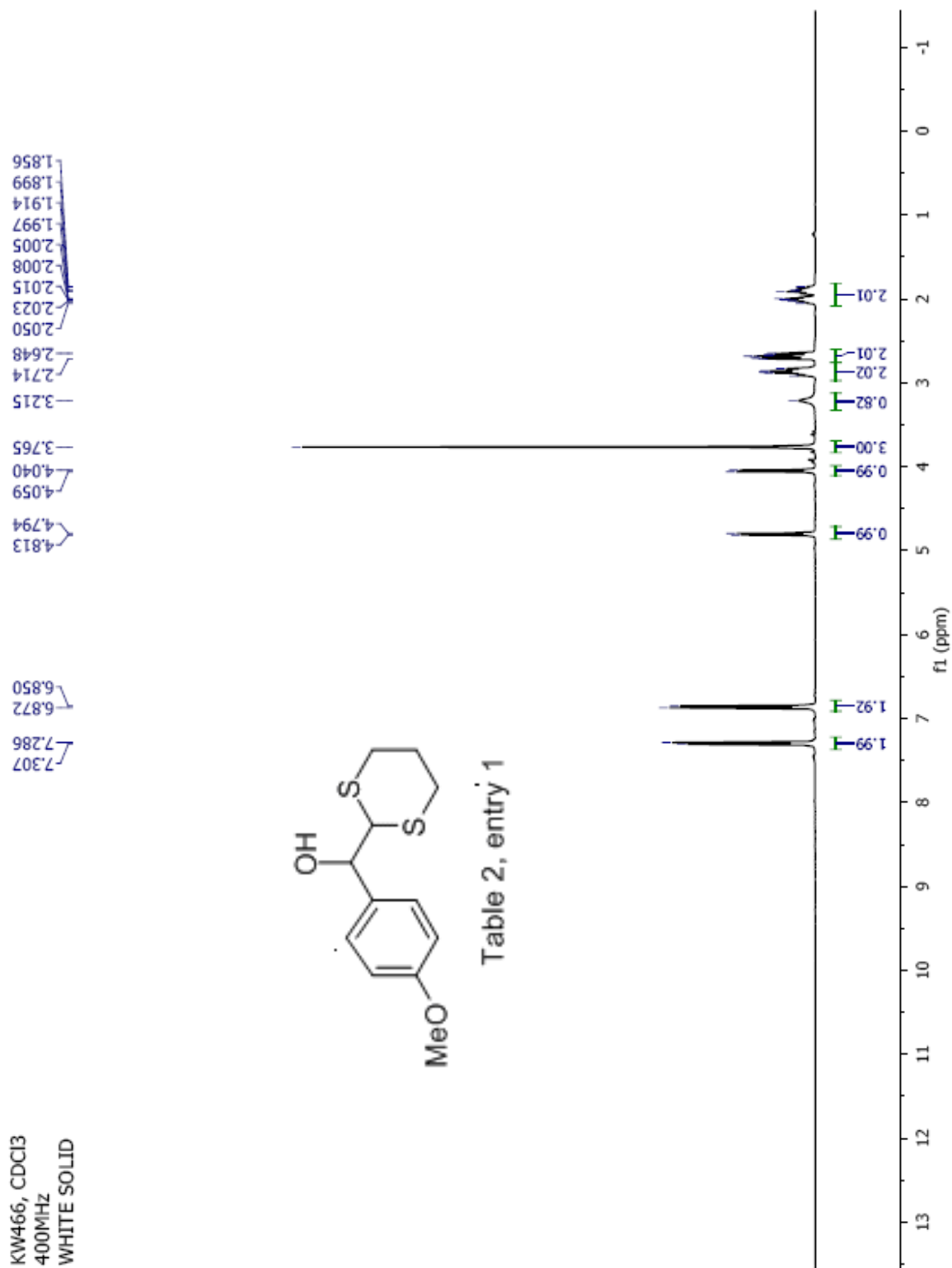
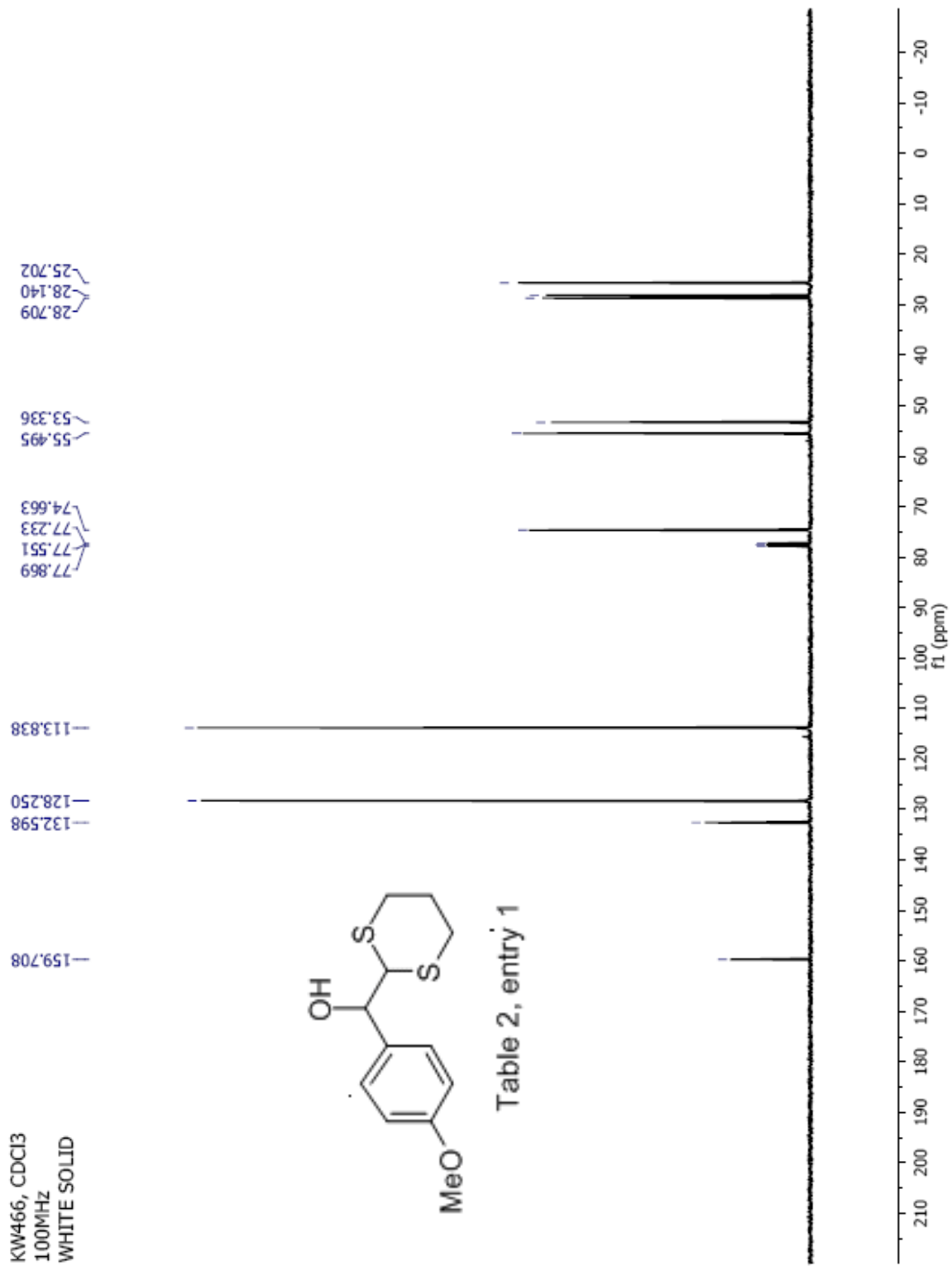


Table 1, entry 1







KW484, CDCl<sub>3</sub>  
 300MHz  
 03/08/2008  
 COLORLESS OIL

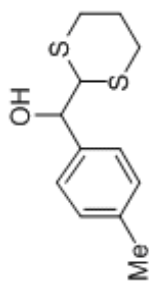
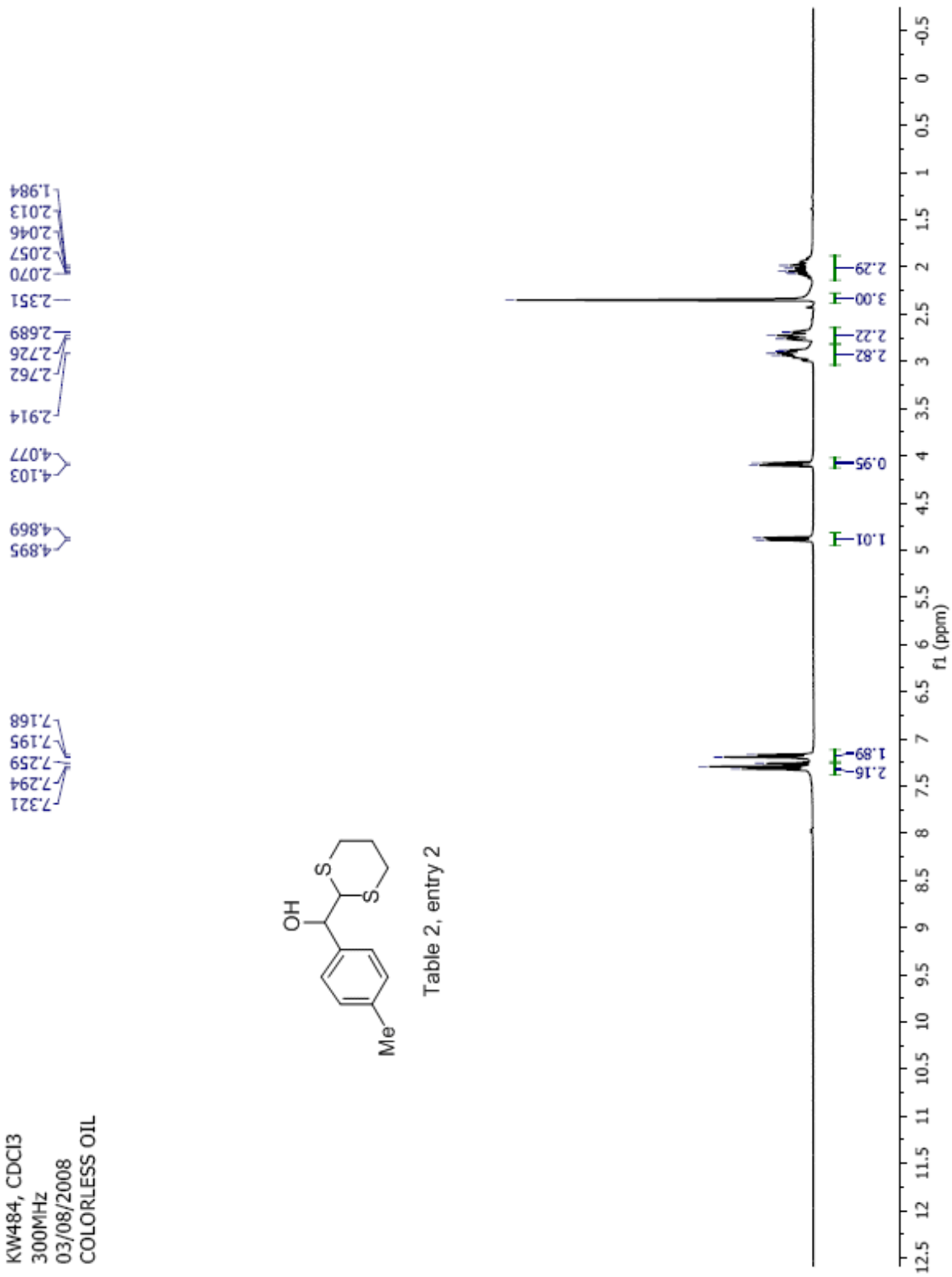


Table 2, entry 2



KW484, CDCl<sub>3</sub>  
75MHz  
COLORLESS OIL  
03/08/2008

138.408  
137.399  
129.269  
126.929  
77.761  
77.336  
76.912  
74.870  
53.200  
28.609  
28.000  
25.657  
21.556

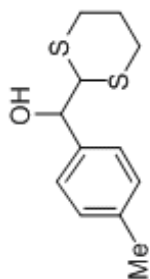
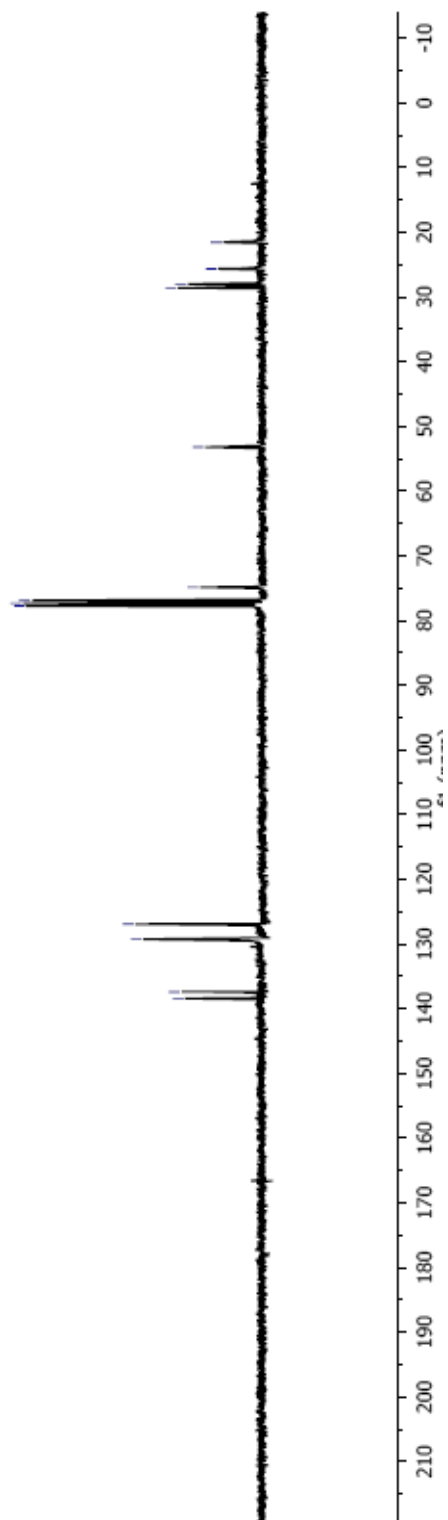


Table 2, entry 2



### Manual Peak Matching Report For Accurate Mass Determination

Theoretical mass	Experimental mass	PFK matching mass	Deviation*
240.06425	240.06462	230.98562	1.6 ppm

\* The deviation is obtained from the following equation:

$$\text{deviation} = \frac{\text{experimental mass} - \text{theoretical mass}}{\text{nominal mass}}$$

Where nominal mass takes in account only  $^{12}\text{C}$ ,  $^1\text{H}$ ,  $^{16}\text{O}$ ,  $^{14}\text{N}$  etc...

Theoretical mass correspond to the mass of the most abundant isotope peak

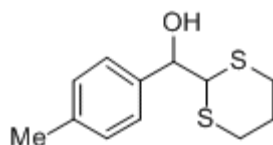
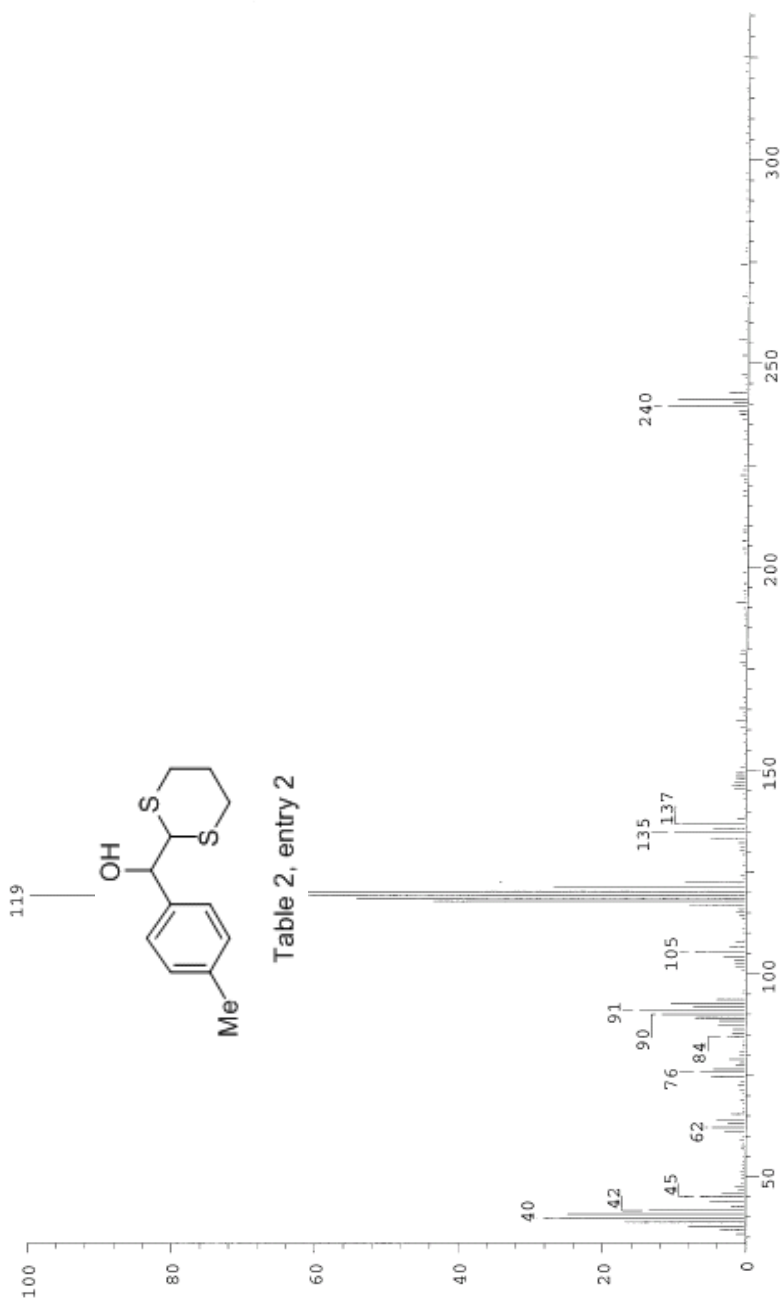


Table 2, entry 2

SPEC: fin084052.dat (08-DEC-08 14:46:14)  
 Samp: kw484  
 Comm: 70 eV EI  
 Oper: kh  
 Base: 119.28  
 Peak: 1000.0 mmu  
 Scan 84 @ 1.88 min (EI +Q1MS LMR UP LR)  
 Study: ms services  
 Masses: 35.01 > 650.00  
 Intensity: 68280  
 Scans: 1 > 84  
 Client: Kuldup  
 #Peaks: 293  
 RIC: 457767  
 6.8E+04



Date: Mon Dec 8 14:49:03 2008 ICIS: 8.3.0 SP2 for OSF1 (V4.0) build 98-238 from 26-Aug-98



KW620, CDCl<sub>3</sub>  
400MHz  
WHITE SOLID

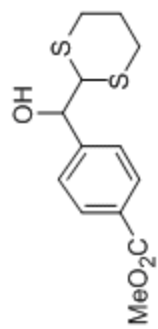
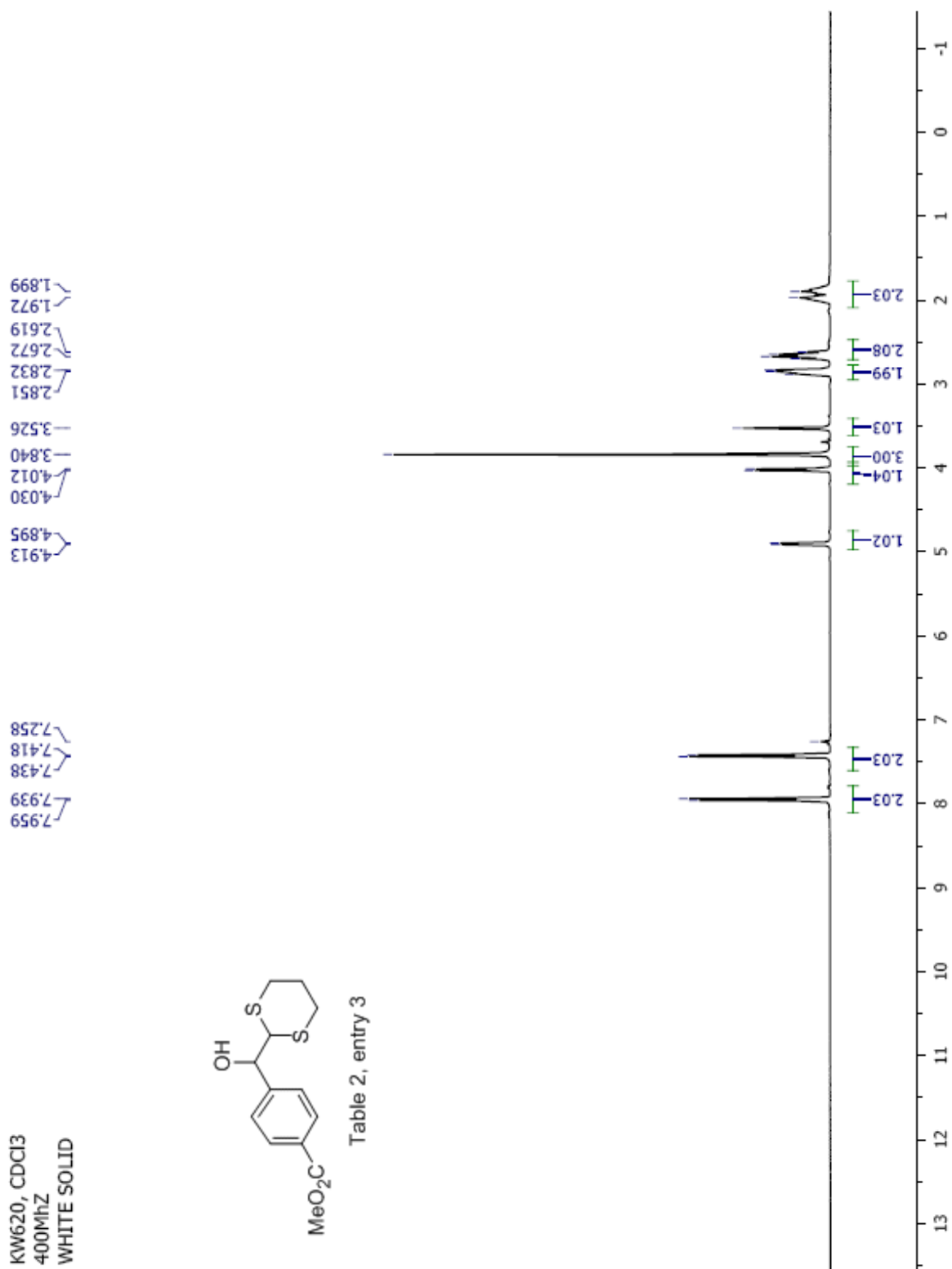
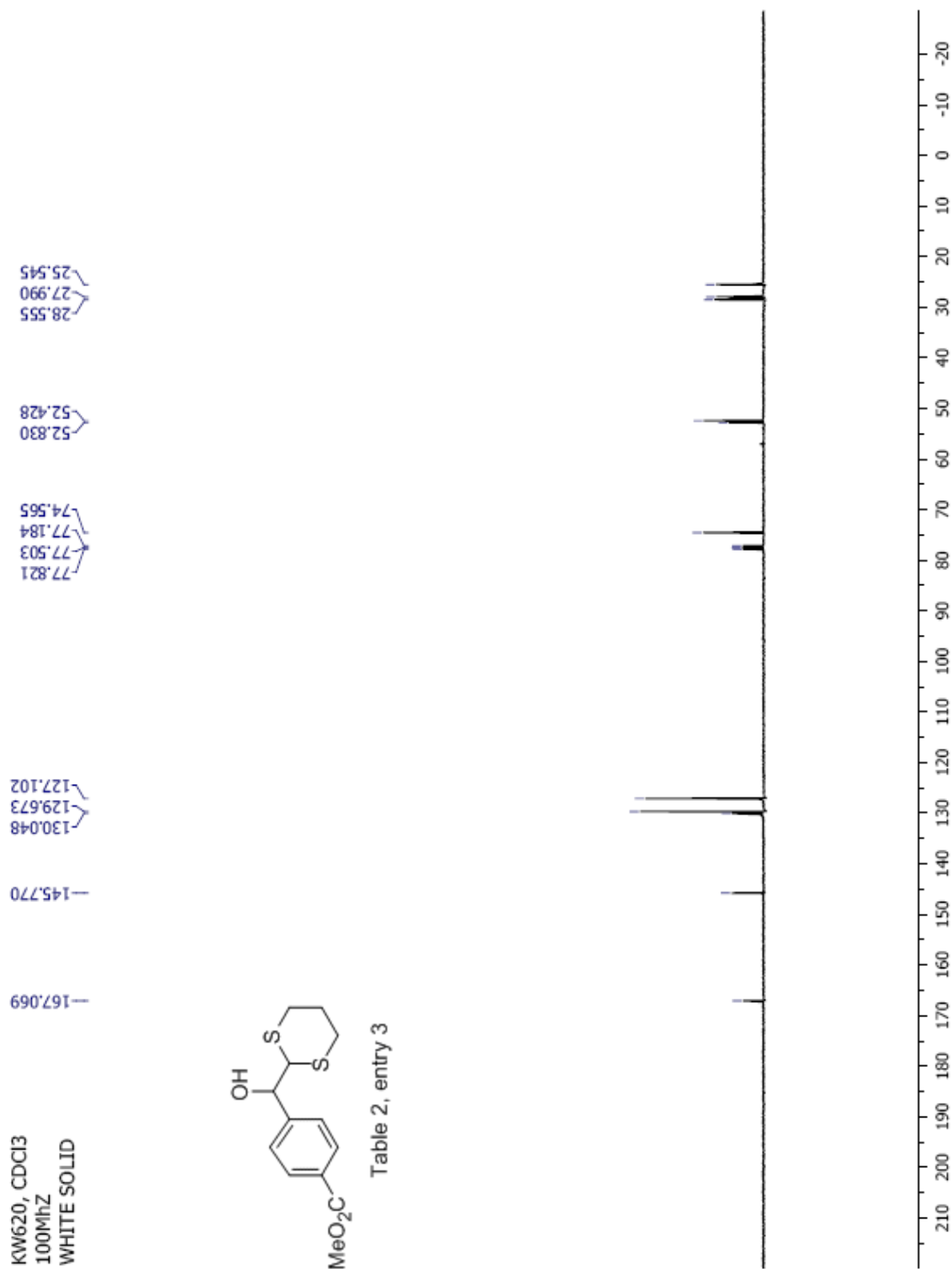


Table 2, entry 3





## Manual Peak Matching Report For Accurate Mass Determination

Theoretical mass	Experimental mass	PFK matching mass	Deviation*
284.05409	284.05447	280.98242	1.3 ppm

\* The deviation is obtained from the following equation:

$$\text{deviation} = \frac{\text{experimental mass} - \text{theoretical mass}}{\text{nominal mass}}$$

Where nominal mass takes in account only  $^{12}\text{C}$ ,  $^1\text{H}$ ,  $^{16}\text{O}$ ,  $^{14}\text{N}$  etc...

Theoretical mass correspond to the mass of the most abundant isotope peak

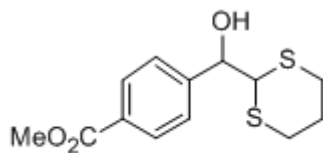
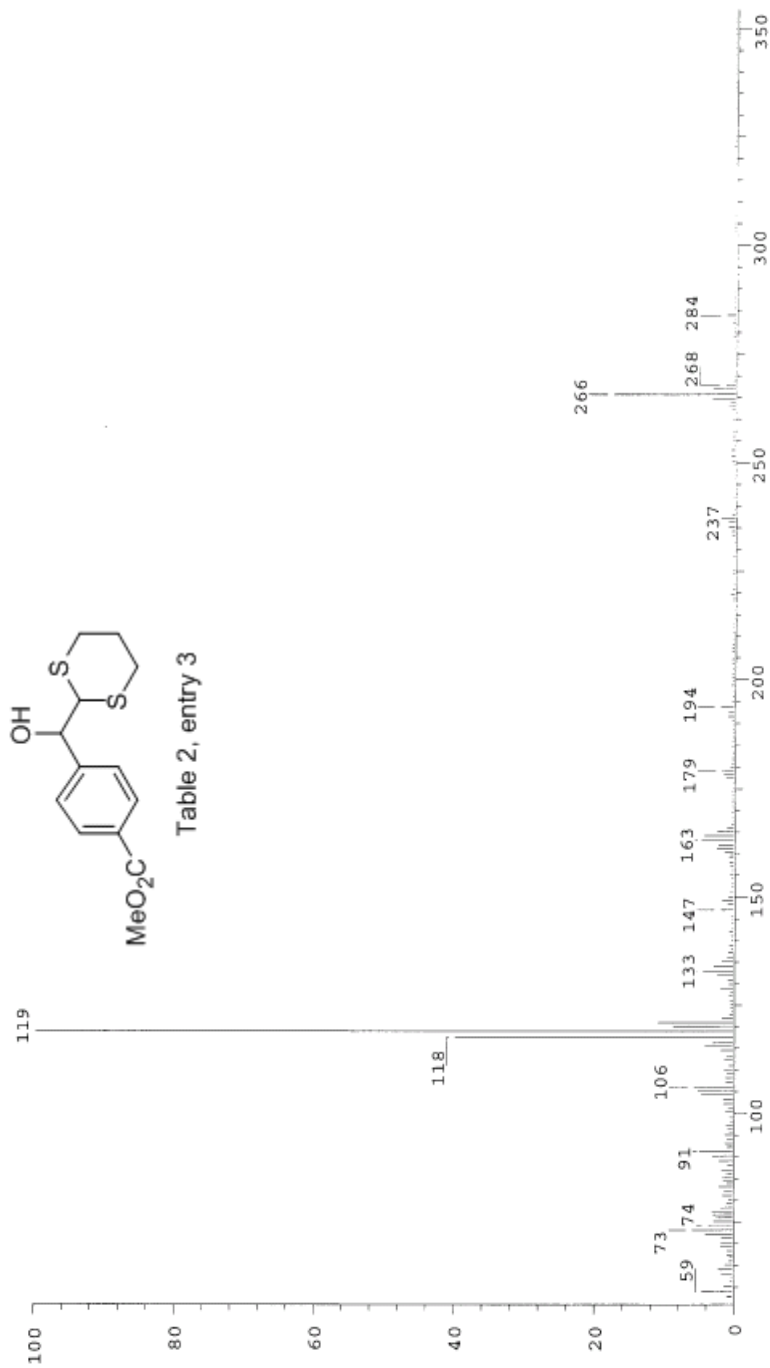


Table 2, entry 3

SPEC: fin063603.dat (06-MAY-08 11:36:23)  
 Samp: KW620  
 Comm: 70 eV EI  
 Oper: kh  
 Base: 118.94  
 Peak: 1000.0 mmu  
 Scan 12 @ 0.40 min (EI +QIMS LMR UP LR)  
 Study: MS Services  
 Masses: 35.01 > 650.00  
 Intensity: 25932  
 Scans: 1 > 45  
 Client: Kuldup  
 #Peaks: 553  
 RIC: 113925  
 2.6E+04



Date: Tue May 6 11:39:23 2008 ICIS: 8.3.0 SP2 for OSP1 (V4.0) build 98-238 from 26-Aug-98

KW624, CDCl<sub>3</sub>  
400MHz  
COLORLESS OIL

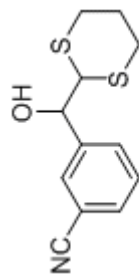
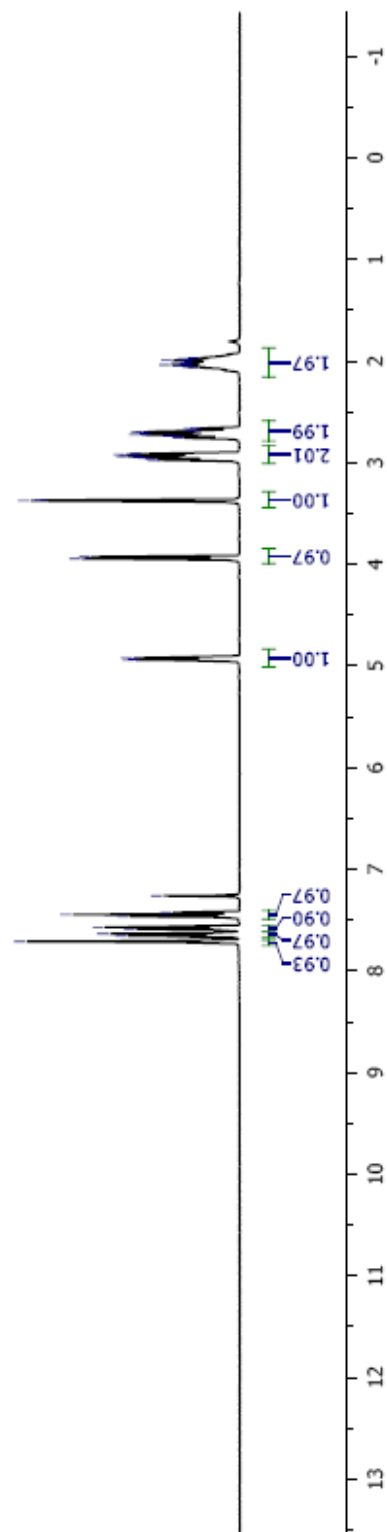


Table 2, entry 4



KW624, CDCl<sub>3</sub>  
100MHz  
COLORLESS OIL

142.077  
132.080  
131.655  
130.924  
129.187  
119.031  
112.366  
77.711  
77.393  
77.074  
73.712  
52.455  
28.119  
27.490  
25.374

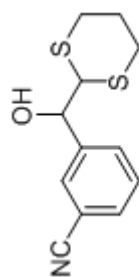
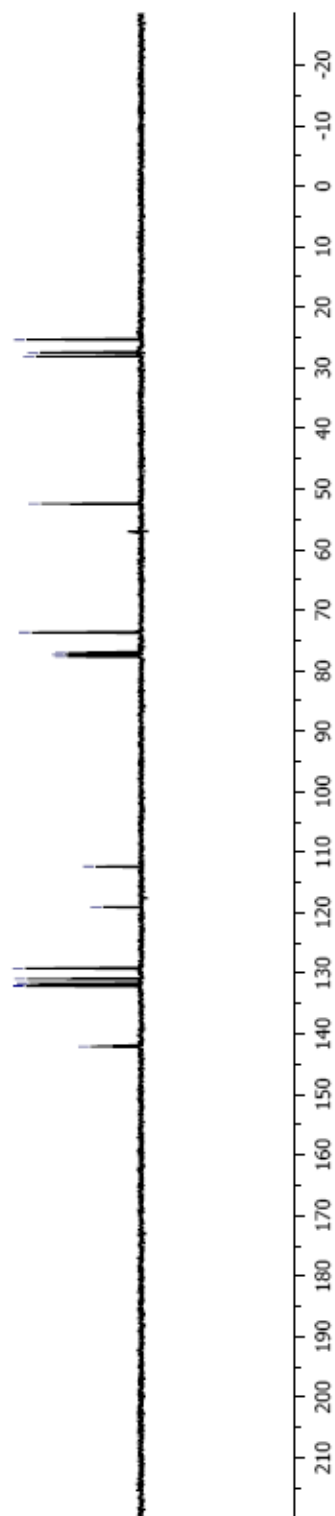


Table 2, entry 4



## Manual Peak Matching Report For Accurate Mass Determination

Theoretical mass	Experimental mass	PFK matching mass	Deviation*
251.04386	251.04414	242.98562	1.1 ppm

\* The deviation is obtained from the following equation:

$$\text{deviation} = \frac{\text{experimental mass} - \text{theoretical mass}}{\text{nominal mass}}$$

Where nominal mass takes in account only  $^{12}\text{C}$ ,  $^1\text{H}$ ,  $^{16}\text{O}$ ,  $^{14}\text{N}$  etc...

Theoretical mass correspond to the mass of the most abundant isotope peak

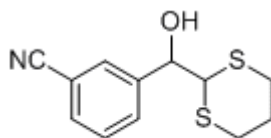


Table 2, entry 4

*JW*

SPEC: fin063692.dat (09-JUN-08 10:41:31)  
 Samp: KW624  
 Comm: 70 eV EI  
 Oper: kh  
 Base: 118.75  
 Peak: 1000.0 mmu  
 Scan 49 @ 1.16 min (EI +QIMS LMR UP LR)  
 Study: Service  
 Masses: 35.01 > 650.00  
 Intensity: 2727781  
 Scans: 1 > 50  
 Client: Kuldup  
 #Peaks: 638  
 RIC: 5575073  
 1.7E+04

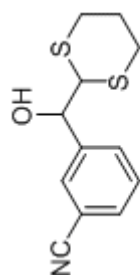
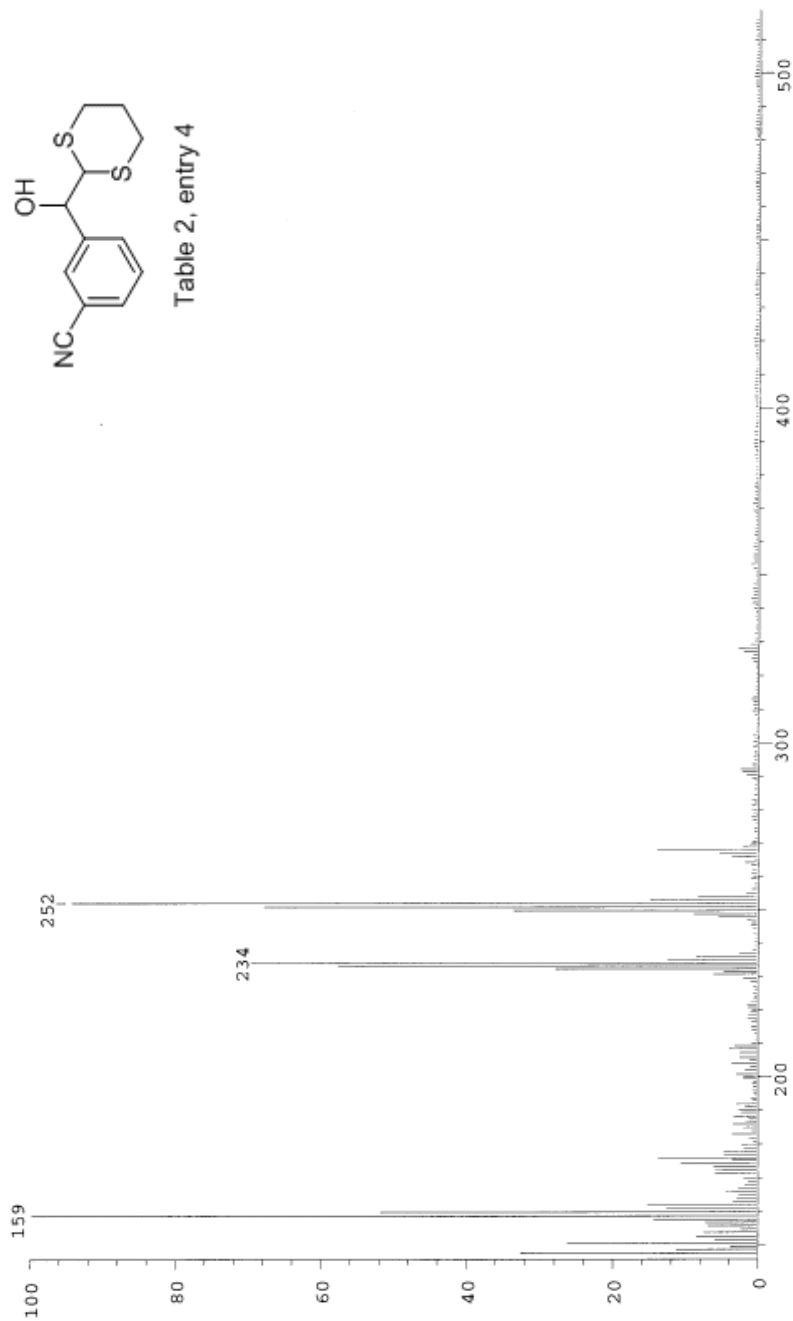


Table 2, entry 4



Date: Mon Jun 9 10:44:04 2008 ICIS: 8.3.0 SP2 for OSF1 (V4.0) build 98-238 from 26-Aug-98



KW603, CDCl<sub>3</sub>  
400MHz  
COLORLESS OIL

7.560  
7.541  
7.344  
7.325  
7.301  
7.283  
7.264  
7.261  
7.242  
7.223  
7.205  
5.427  
5.421  
5.411  
5.404  
4.137  
4.121  
3.234  
2.940  
2.752  
2.677  
2.622  
2.022  
2.013  
2.005  
1.994  
1.984

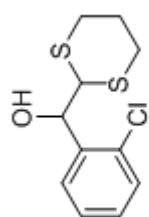
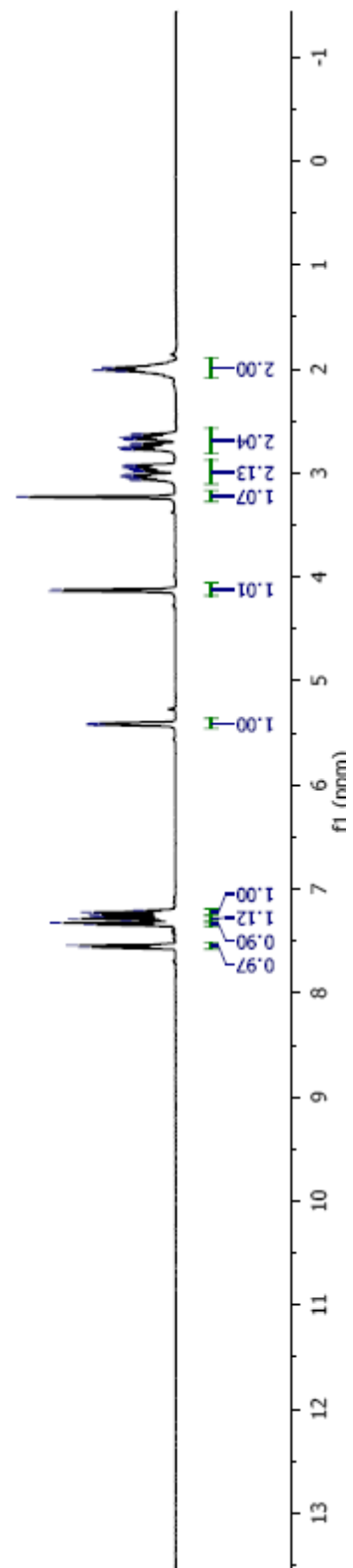


Table 2, entry 5



KW603, CDCl<sub>3</sub>  
100MHz  
COLORLESS OIL

138.320  
133.355  
129.528  
129.450  
128.429  
127.153  
77.777  
77.458  
77.141  
71.285  
51.609  
28.880  
27.633  
25.577

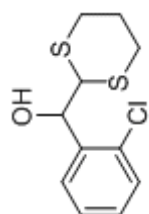
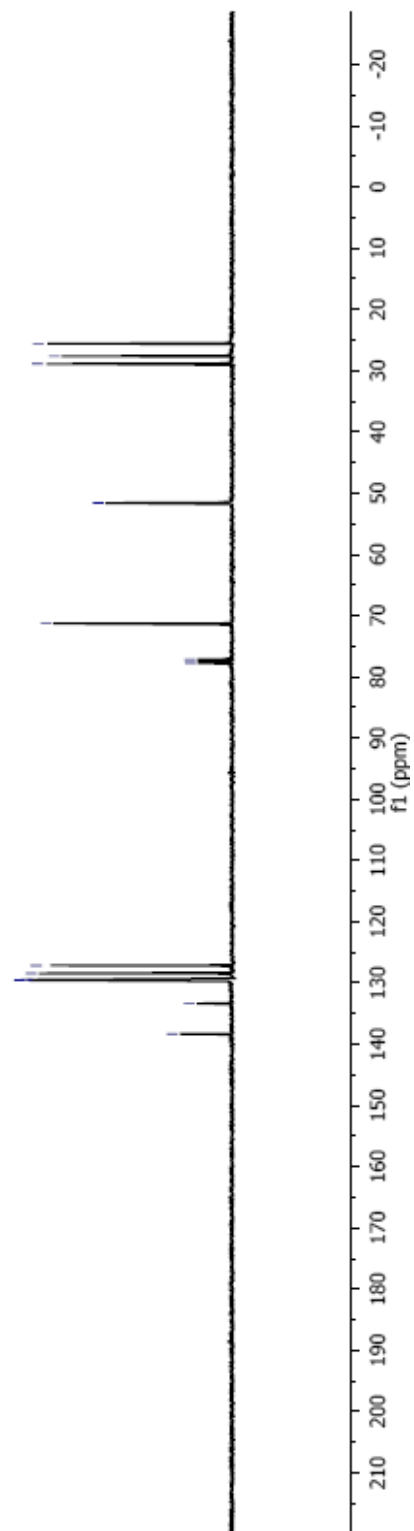


Table 2, entry 5



### Manual Peak Matching Report For Accurate Mass Determination

Theoretical mass	Experimental mass	PFK matching mass	Deviation*
260.00963	260.01002	260.98562	1.5 ppm

\* The deviation is obtained from the following equation:

$$\text{deviation} = \frac{\text{experimental mass} - \text{theoretical mass}}{\text{nominal mass}}$$

Where nominal mass takes in account only  $^{12}\text{C}$ ,  $^1\text{H}$ ,  $^{16}\text{O}$ ,  $^{14}\text{N}$  etc...

Theoretical mass correspond to the mass of the most abundant isotope peak

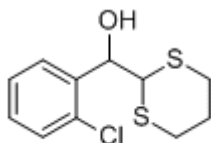
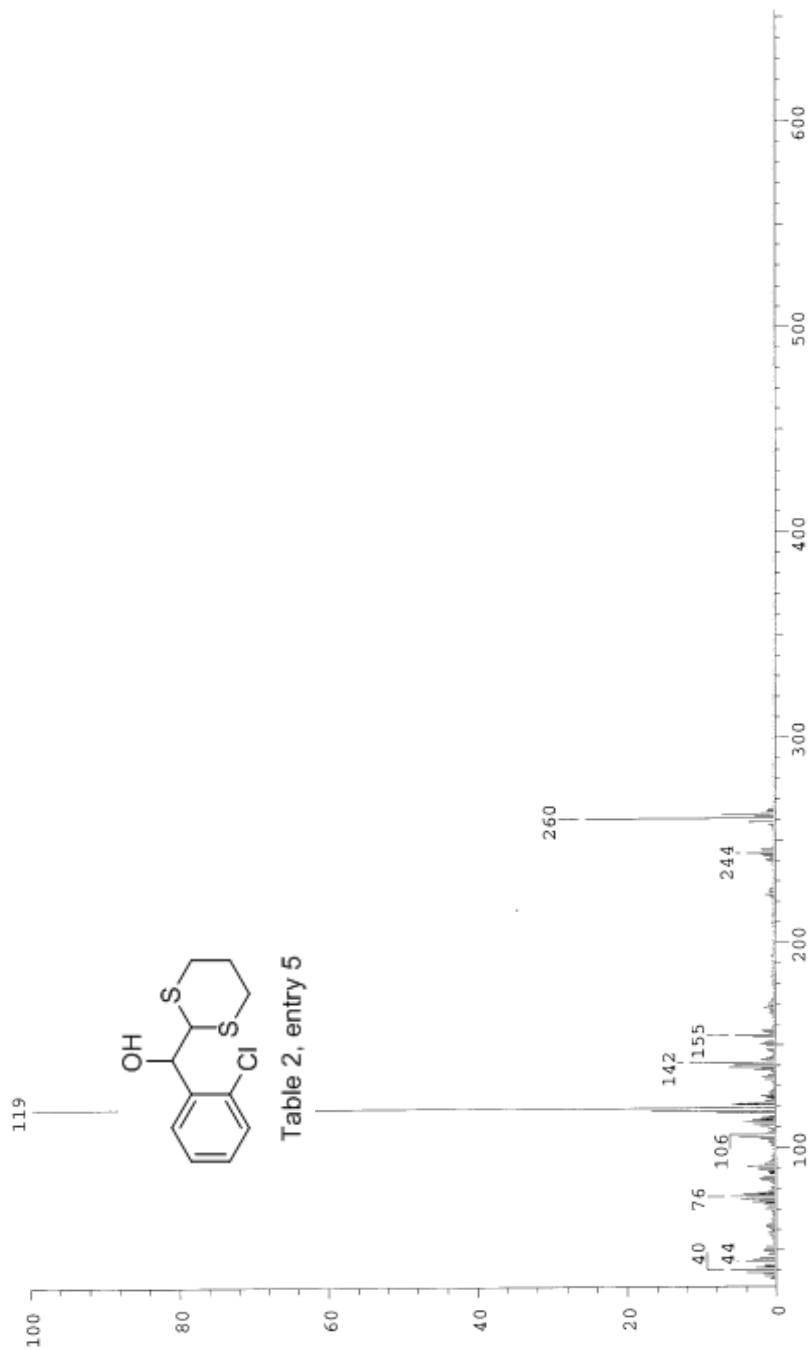


Table 2, entry 5

20

Scans: 1 > 41  
 Client: Kuldup  
 #Peaks: 337  
 RIC: 4342076  
 1.1E+06

SPEC: fin084053.dat (08-DEC-08 14:52:47)  
 Samp: kw484  
 Comm: 70 eV EI  
 Oper: kh  
 Study: ms services  
 Base: 119.27  
 Masses: 35.01 > 650.00  
 Peak: 1000.0 mmu  
 Intensity: 1088172  
 Scan 41 @ 0.99 min (EI +Q1MS LMR UP LR)



Date: Mon Dec 8 14:54:20 2008 ICIS: 8.3.0 SP2 for OSF1 (V4.0) build 98-238 from 26-Aug-98

KW607, CDCl<sub>3</sub>  
400MHz  
COLORLESS OIL

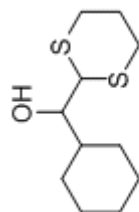
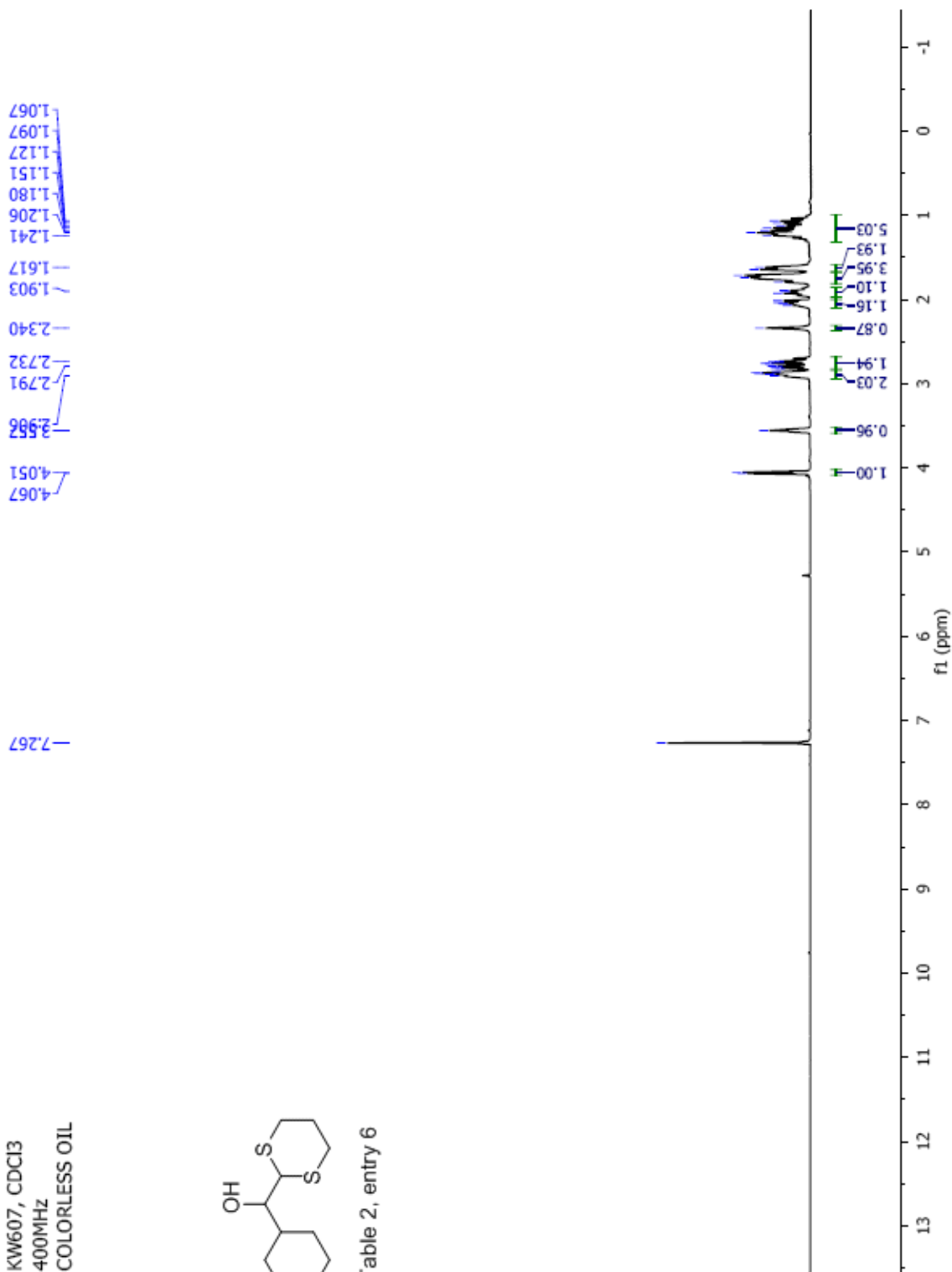


Table 2, entry 6



KW607, CDCl<sub>3</sub>  
100MHz  
COLORLESS OIL

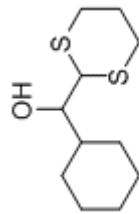
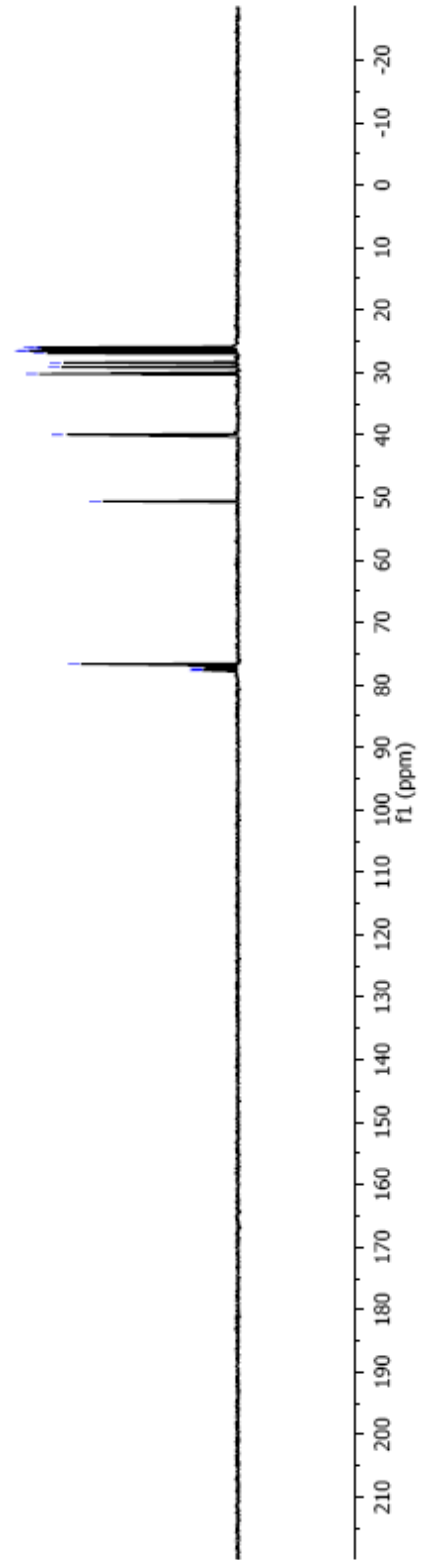


Table 2, entry 6

77.685  
77.571  
77.366  
76.653  
50.604  
39.956  
30.239  
29.166  
28.431  
26.944  
26.558  
26.518  
26.118  
25.993



## Manual Peak Matching Report For Accurate Mass Determination

Theoretical mass	Experimental mass	PFK matching mass	Deviation*
232.09555	232.09597	230.98562	1.8 ppm

\* The deviation is obtained from the following equation:

$$\text{deviation} = \frac{\text{experimental mass} - \text{theoretical mass}}{\text{nominal mass}}$$

Where nominal mass takes in account only  $^{12}\text{C}$ ,  $^1\text{H}$ ,  $^{16}\text{O}$ ,  $^{14}\text{N}$  etc...

Theoretical mass correspond to the mass of the most abundant isotope peak

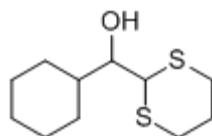


Table 2, entry 6

510

Scans: 1 > 18  
 Client: Kuldup  
 #Peaks: 395  
 RIC: 71790956  
 8.3E+06

SPEC: fin084054.dat (08-DEC-08 14:58:53)  
 Samp: kw607  
 Comm: 70 eV EI  
 Oper: kh  
 Base: 119.70  
 Peak: 1000.0 mmu  
 Scan 1 @ 0.20 min (EI +QIMS LMR UP LR)

Study: ms services  
 Masses: 35.01 > 650.00  
 Intensity: 8310352

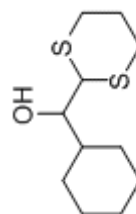
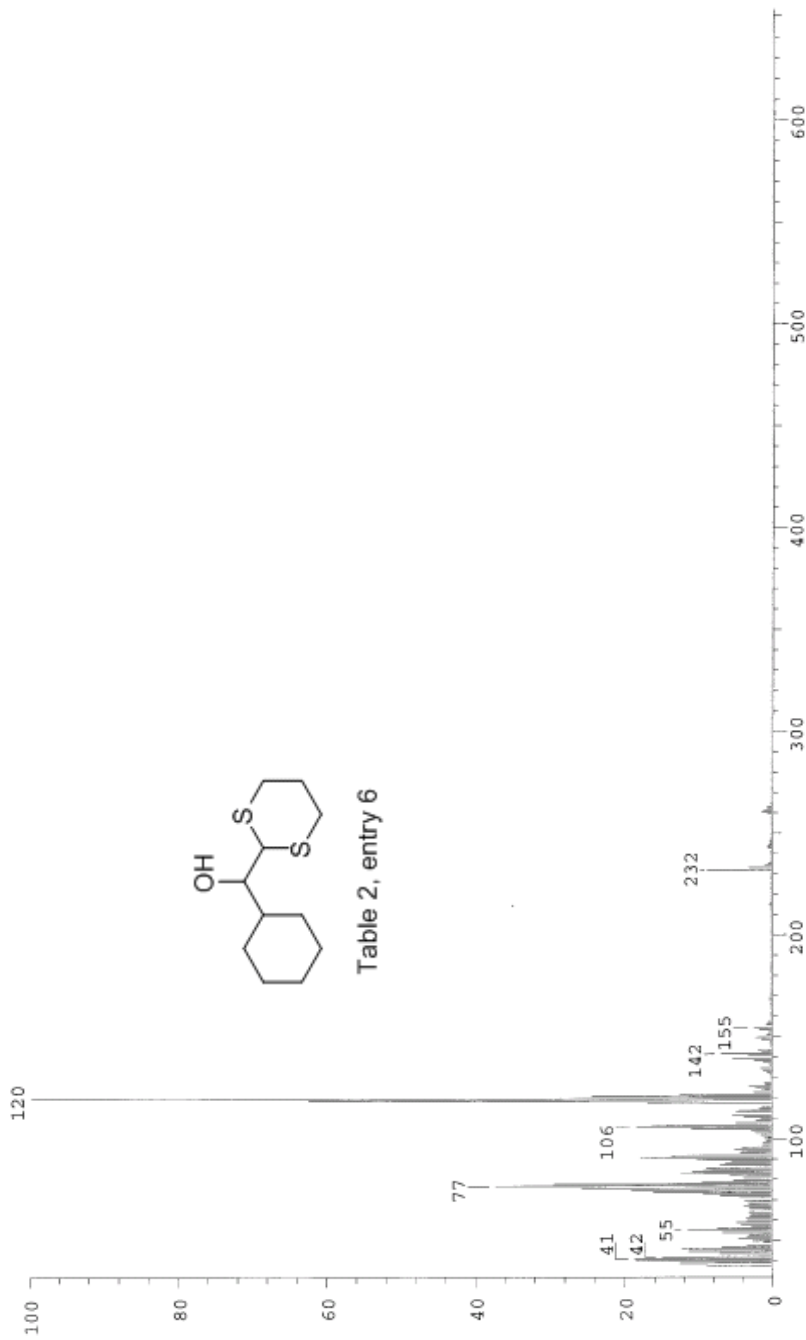
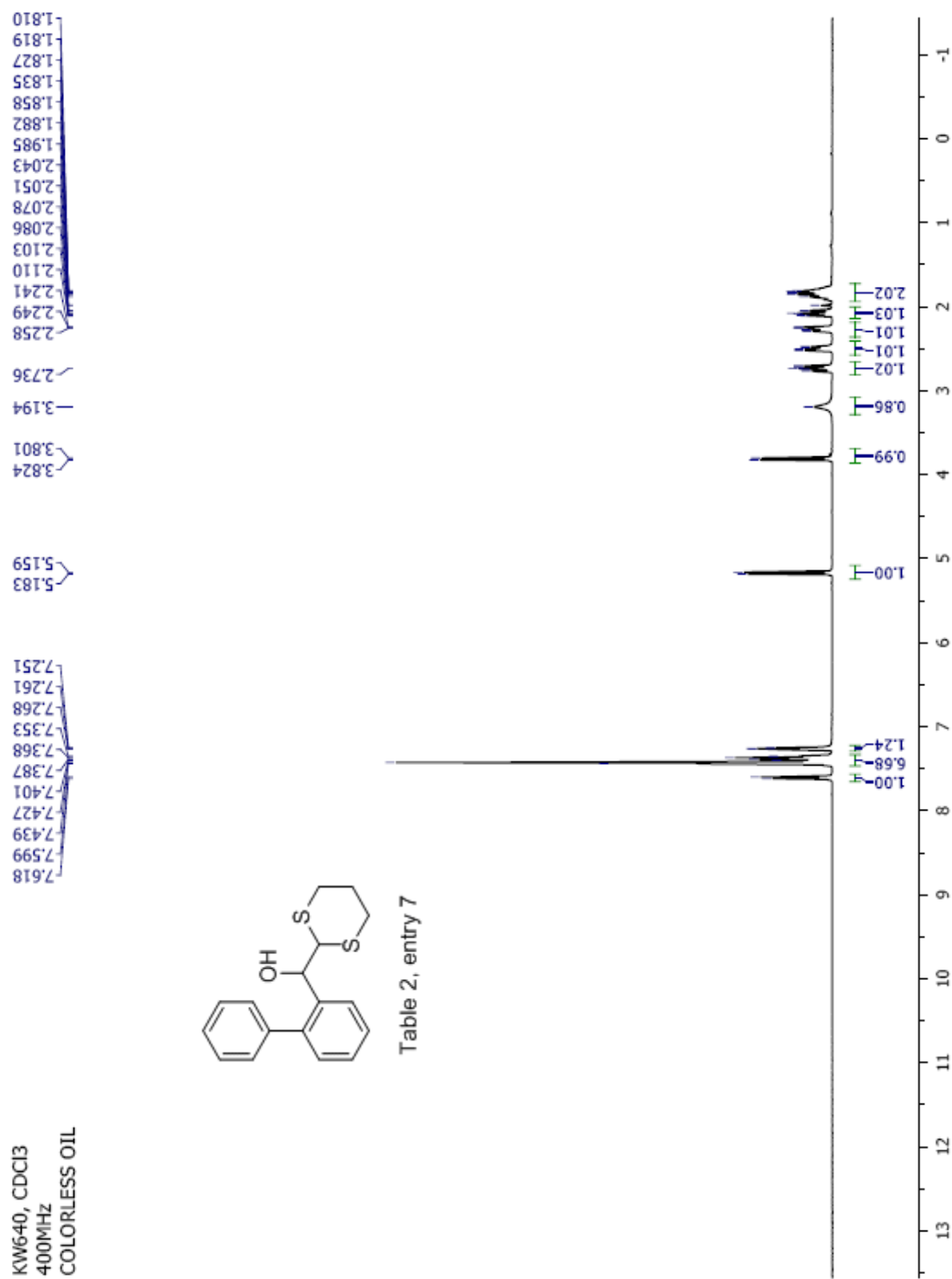


Table 2, entry 6



Date: Mon Dec 8 15:00:03 2008 ICIS: 8.3.0 SP2 for OSF1 (V4.0) build 98-238 from 26-Aug-98





KW640, CDCl<sub>3</sub>  
100MHz  
COLORLESS OIL

142.873  
141.255  
138.104  
129.976  
128.471  
128.156  
128.107  
127.284  
126.344  
77.681  
77.362  
77.048  
69.113  
51.636  
26.864  
25.996  
25.276

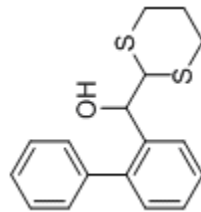
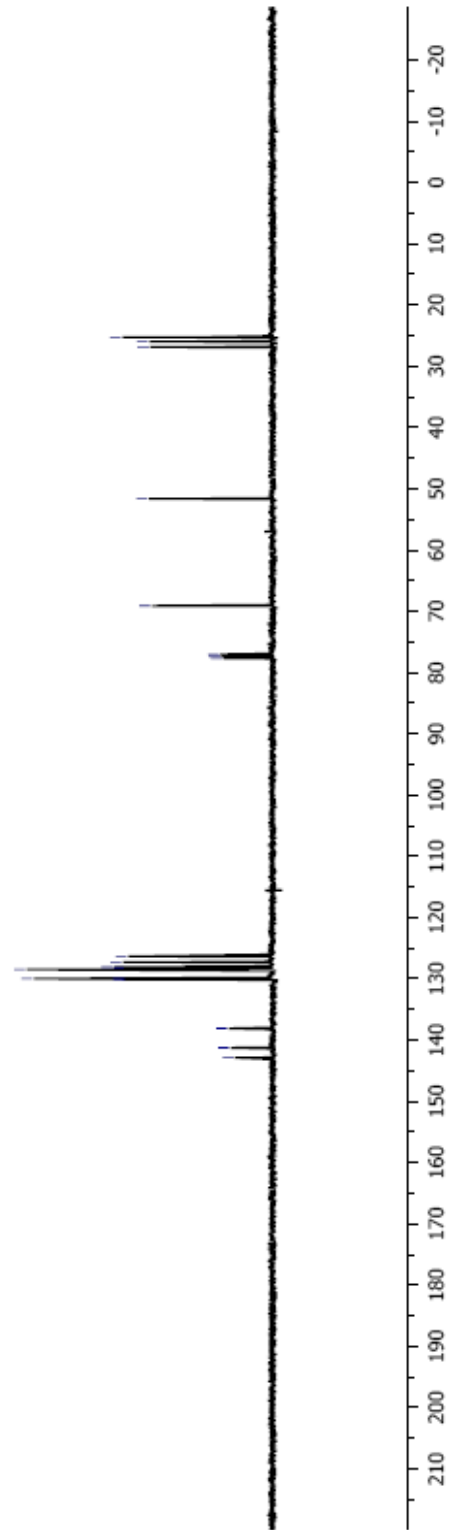


Table 2, entry 7



## Manual Peak Matching Report For Accurate Mass Determination

Theoretical mass	Experimental mass	PFK matching mass	Deviation*
302.07991	302.08031	280.98242	1.3 ppm

\* The deviation is obtained from the following equation:

$$\text{deviation} = \frac{\text{experimental mass} - \text{theoretical mass}}{\text{nominal mass}}$$

Where nominal mass takes in account only  $^{12}\text{C}$ ,  $^1\text{H}$ ,  $^{16}\text{O}$ ,  $^{14}\text{N}$  etc...

Theoretical mass correspond to the mass of the most abundant isotope peak

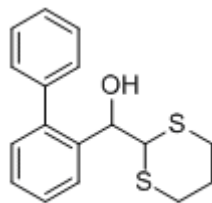


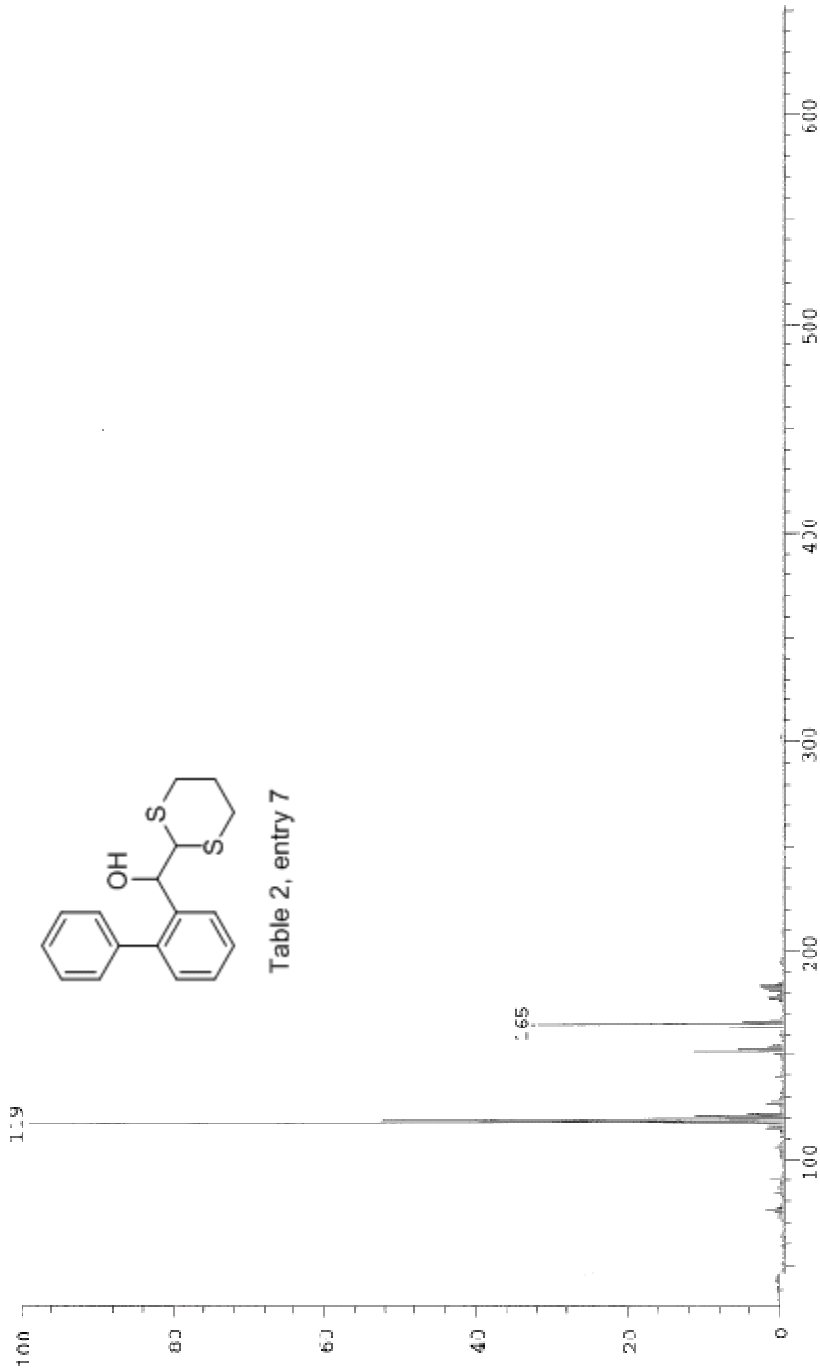
Table 2, entry 7

*Handwritten signature*

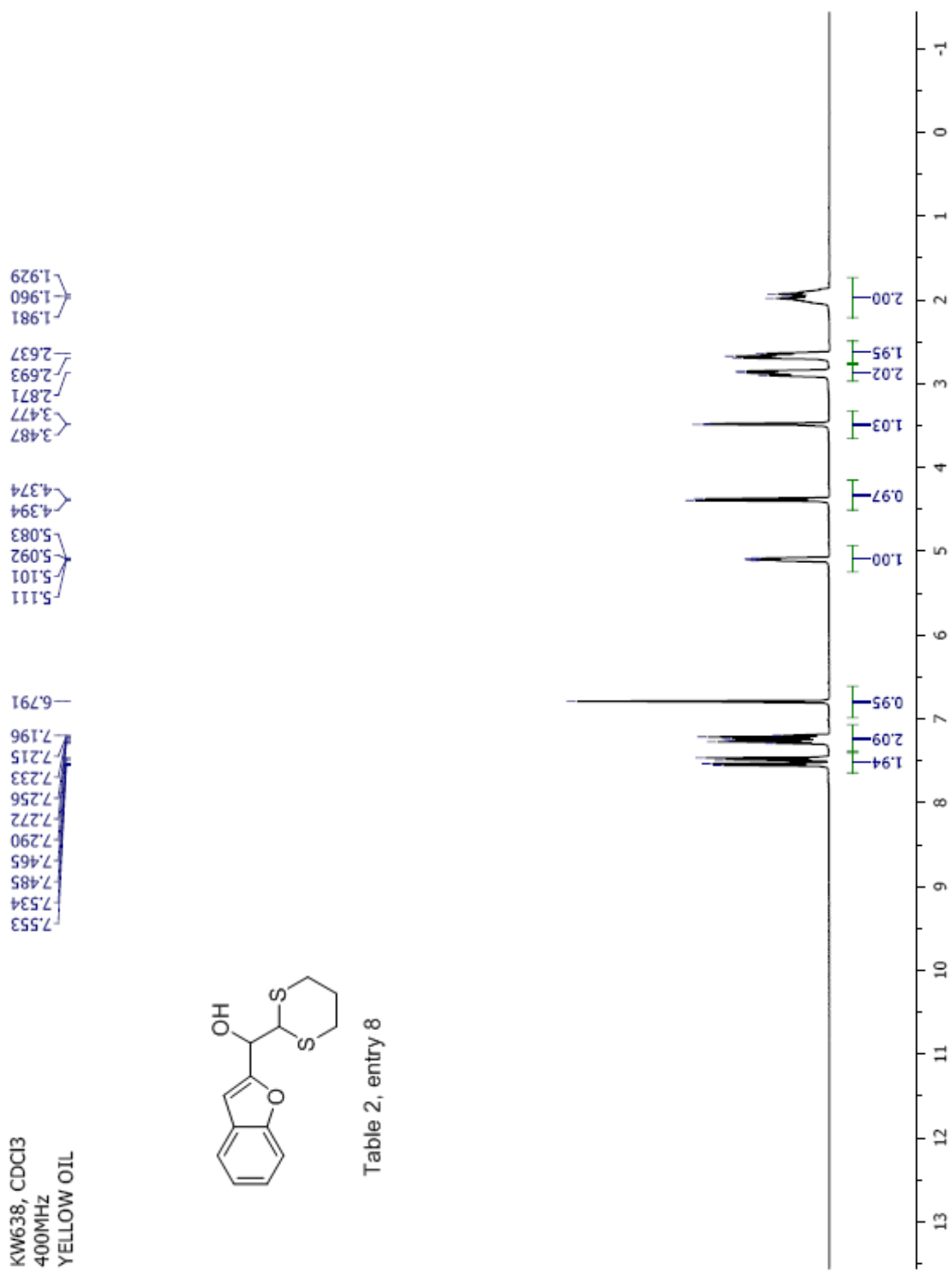
Scans: 1 > 119  
 Client: Kuldup  
 #Peaks: 627  
 RIC: 2294274 9.5E+05

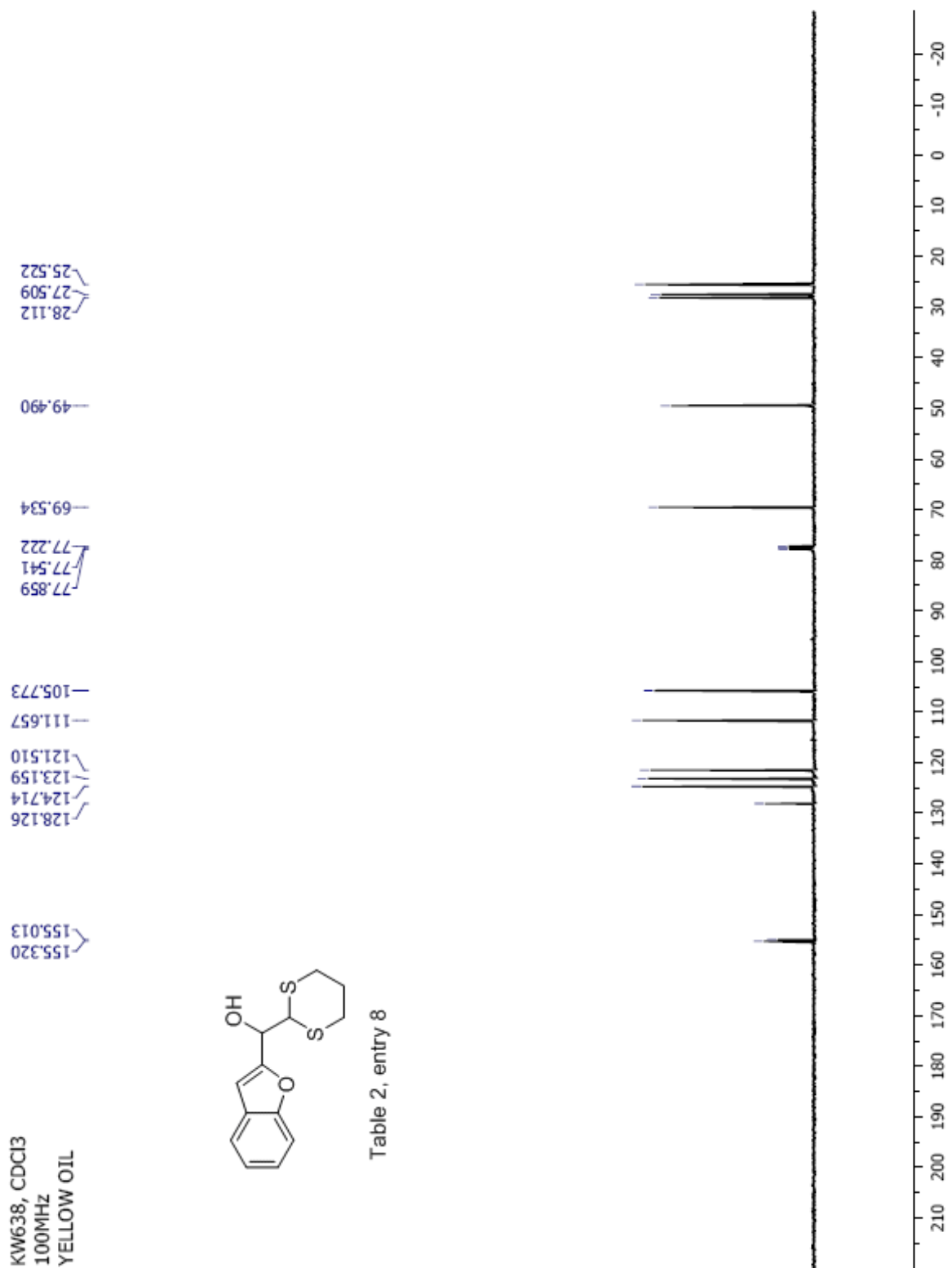
SPEC: f:\063693\data (09-JUN-08 10:45:20)  
 Samp: KUC  
 Comm: 74  
 Oper: M  
 Base: 119.74  
 Peak: 1000.0 mmu  
 Scan: 116 @ 2.53 min (EI -CLMS LMR UP IR)

Study: Service  
 Masses: 35.01 > 650.00  
 Intensity: 585452



Date: Mon Jun 9 10:48:47 2008 ICIS: 8.3.0 SP2 for OSF1 (V1.0) build 58-238 from 26-Aug-98





## Manual Peak Matching Report For Accurate Mass Determination

Theoretical mass	Experimental mass	PFK matching mass	Deviation*
266.04352	266.04411	230.98562	2.2 ppm

\* The deviation is obtained from the following equation:

$$\text{deviation} = \frac{\text{experimental mass} - \text{theoretical mass}}{\text{nominal mass}}$$

Where nominal mass takes in account only  $^{12}\text{C}$ ,  $^1\text{H}$ ,  $^{16}\text{O}$ ,  $^{14}\text{N}$  etc...

Theoretical mass correspond to the mass of the most abundant isotope peak

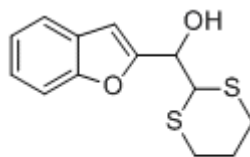


Table 2, entry 8

*JK*

SPEC: fin053654.dat 109-JUN-08 10:53:20

Sample: KW008 G YD

Comm: 70 av EI

Operator: kh

Base: 118.56

Peak: 1000.0 mmu

Scan: 26 @ 6.68 min (EI -QIMS LMR UP LK)

Study: Service

Masses: 35.31 > 650.00

Intensity: 384893

Scans: 1 > 82

Client: Kuldup

#Peaks: 630

RIC: 1100694

3.8E+05

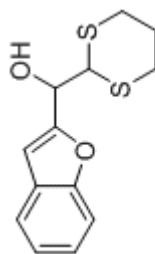
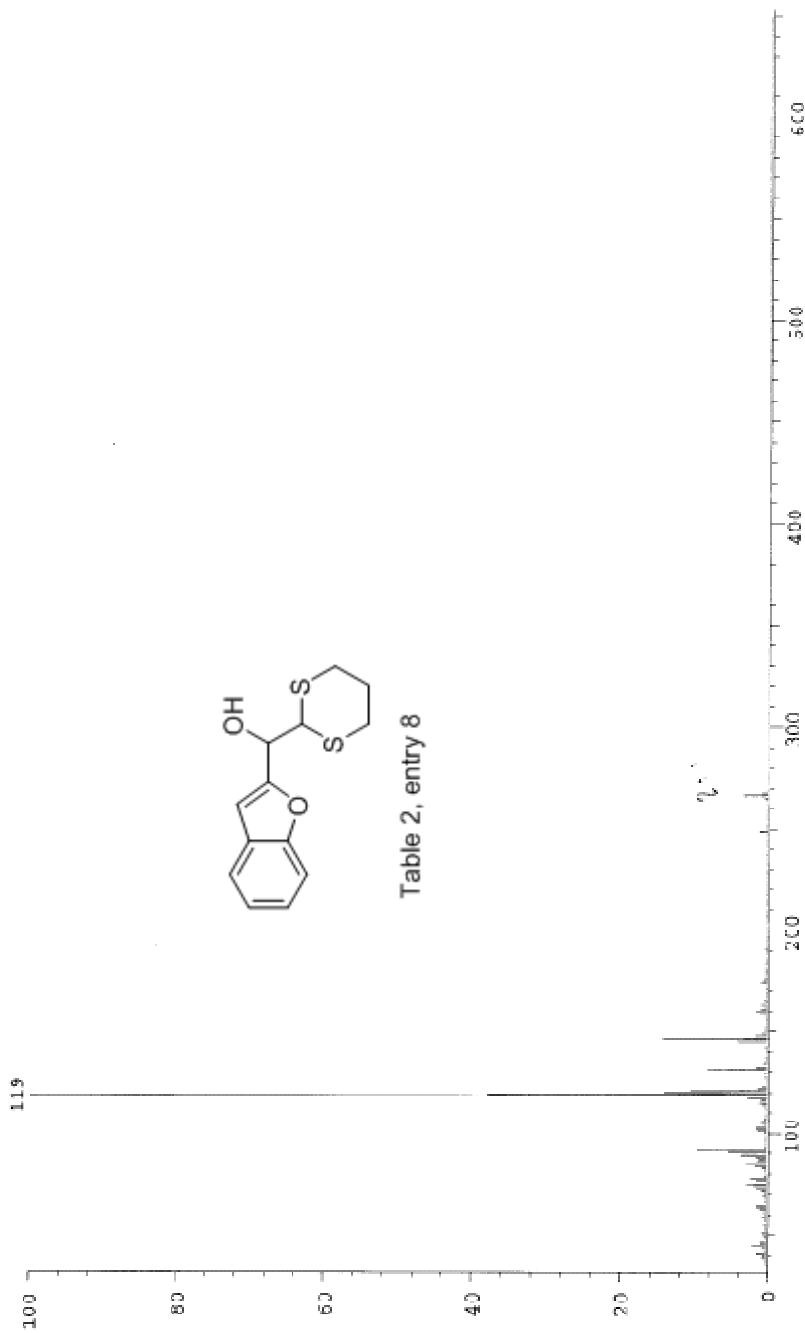


Table 2, entry 8

Date: Mon Jun 9 10:55:42 2008 ICIS: 8.3.0 SP2 for OSF1 (V4.0) build 93-238 From 26-Aug-98



KW633, CDCl<sub>3</sub>  
400MHz  
YELLOW OIL

7.58  
7.54  
7.48  
7.48  
7.40  
7.36  
4.95  
4.62  
4.40  
3.66  
2.99  
2.81  
2.72  
2.30  
2.08  
2.05  
1.95  
1.90  
1.88

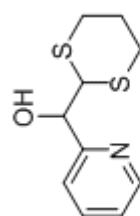
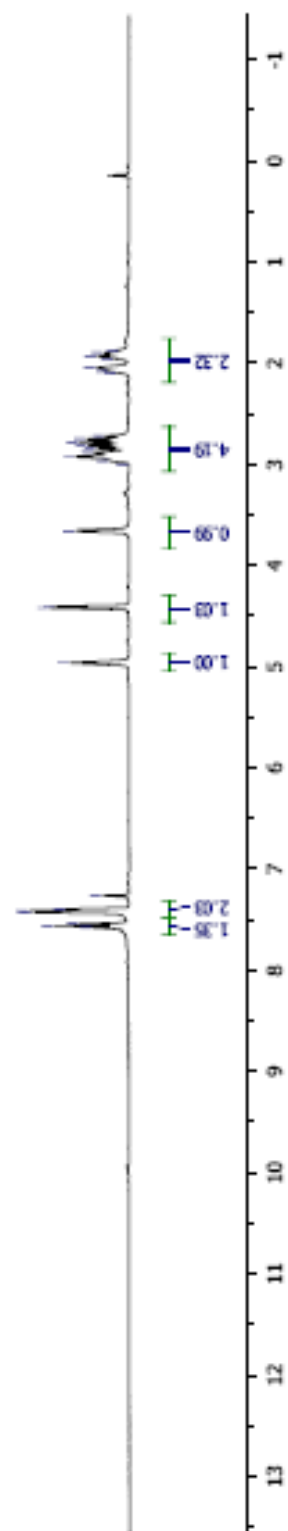


Table 2, entry 9



KW633, CDCl<sub>3</sub>  
100 MHz  
YELLOW OIL

360.46  
141.55  
139.02  
127.75  
120.90  
77.64  
77.32  
77.01  
75.36  
22.54  
21.29  
20.86  
20.70

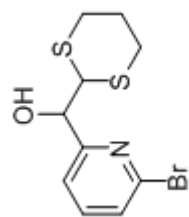
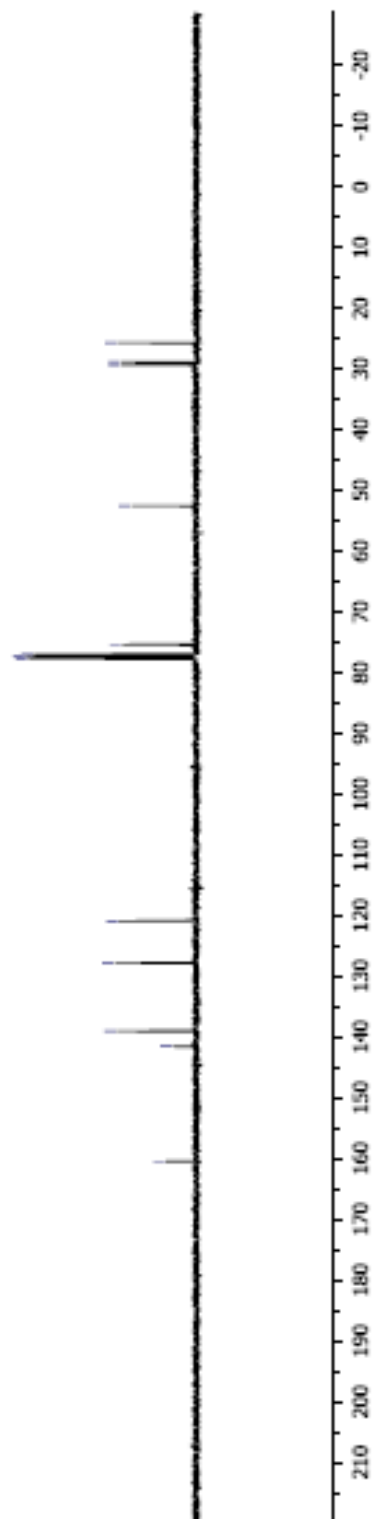


Table 2, entry 9



## Manual Peak Matching Report For Accurate Mass Determination

Theoretical mass	Experimental mass	PFK matching mass	Deviation*
305.95437	305.95475	280.98242	1.3 ppm

\* The deviation is obtained from the following equation:

$$\text{deviation} = \frac{\text{experimental mass} - \text{theoretical mass}}{\text{nominal mass}}$$

Where nominal mass takes in account only  $^{12}\text{C}$ ,  $^1\text{H}$ ,  $^{16}\text{O}$ ,  $^{14}\text{N}$  etc...

Theoretical mass correspond to the mass of the most abundant isotope peak

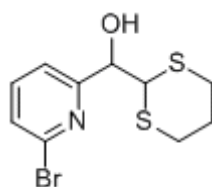


Table 2, entry 9

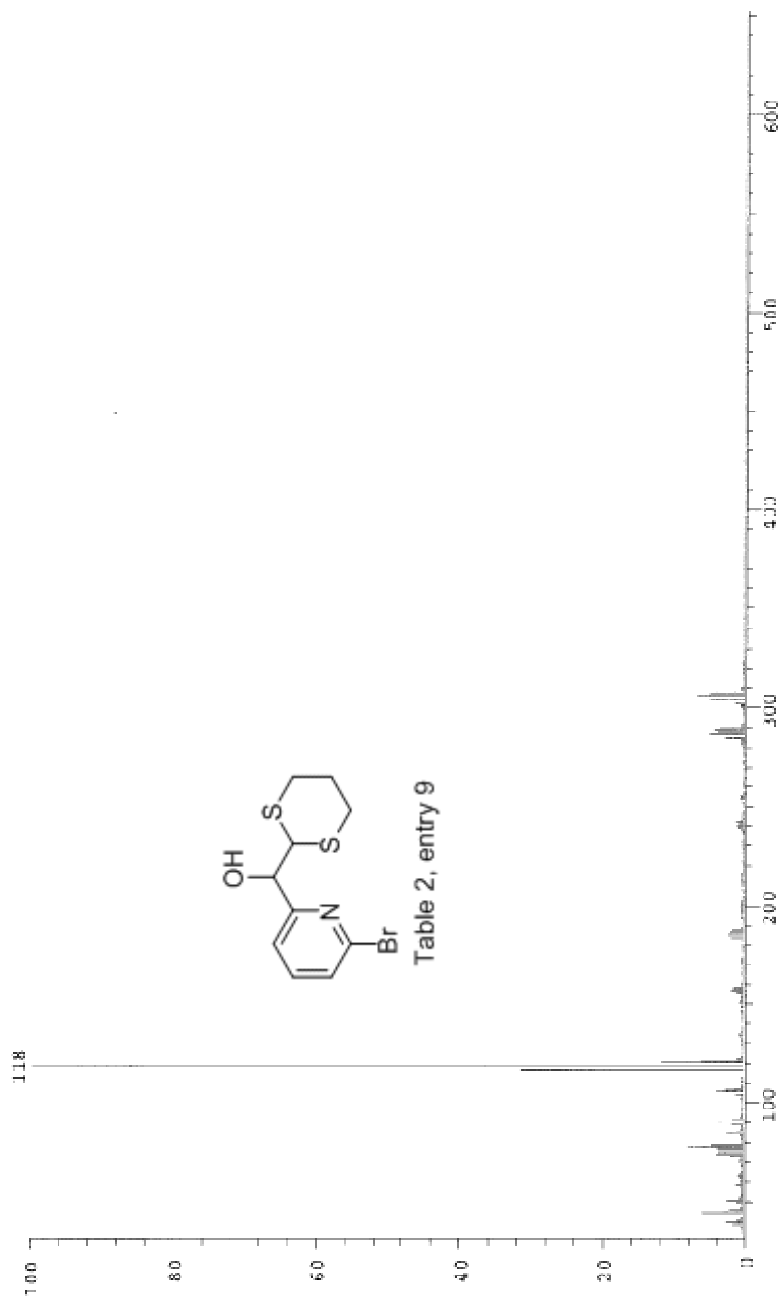
*no*

SPEC: E:\2006095.dat (09-TUR-08 10:57:56)  
 Comp: RWS33  
 Conv: 70 eV EI  
 Oper: kh  
 Study: Service  
 Base: 113.46  
 Masses: 15.01 > 650.00  
 Peak: 1000.0 mm1  
 Intensity: 609353  
 Scan 45 @ 1.08 min (EI +QIMS LMR UP IR)

Scans: 1 > 53

Client: Kuldep  
 #Beaks: 637  
 RIC: X20R604

8.1D+05



Date: Mon Jan 9 10:59:43 2006 ICIS: 8.3.0.SP2 for OSF1 (V4.0) build 98-238 from 26-Aug-98

KW631, CDCl<sub>3</sub>  
400MHz  
YELLOW OIL

7.26  
6.89  
5.24  
4.40  
4.40  
3.72  
2.97  
2.79  
2.73  
2.46  
2.06  
1.99

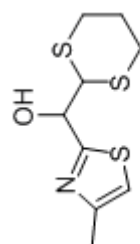
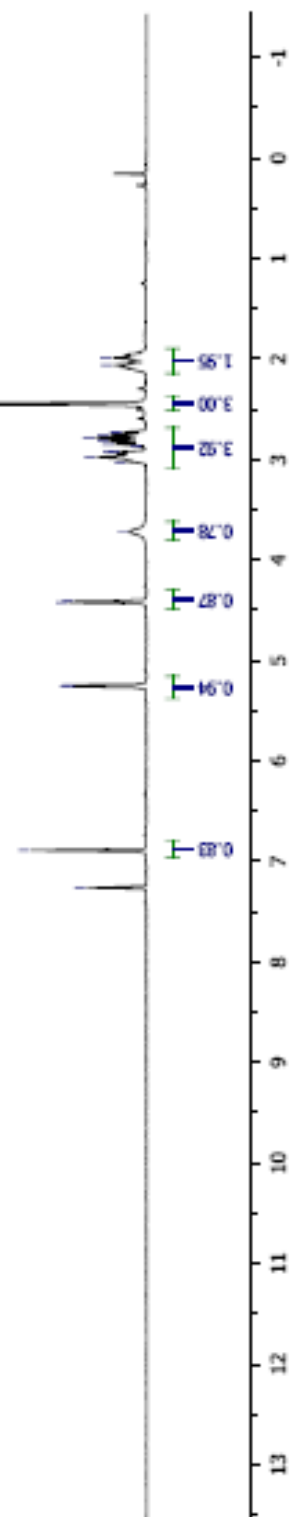
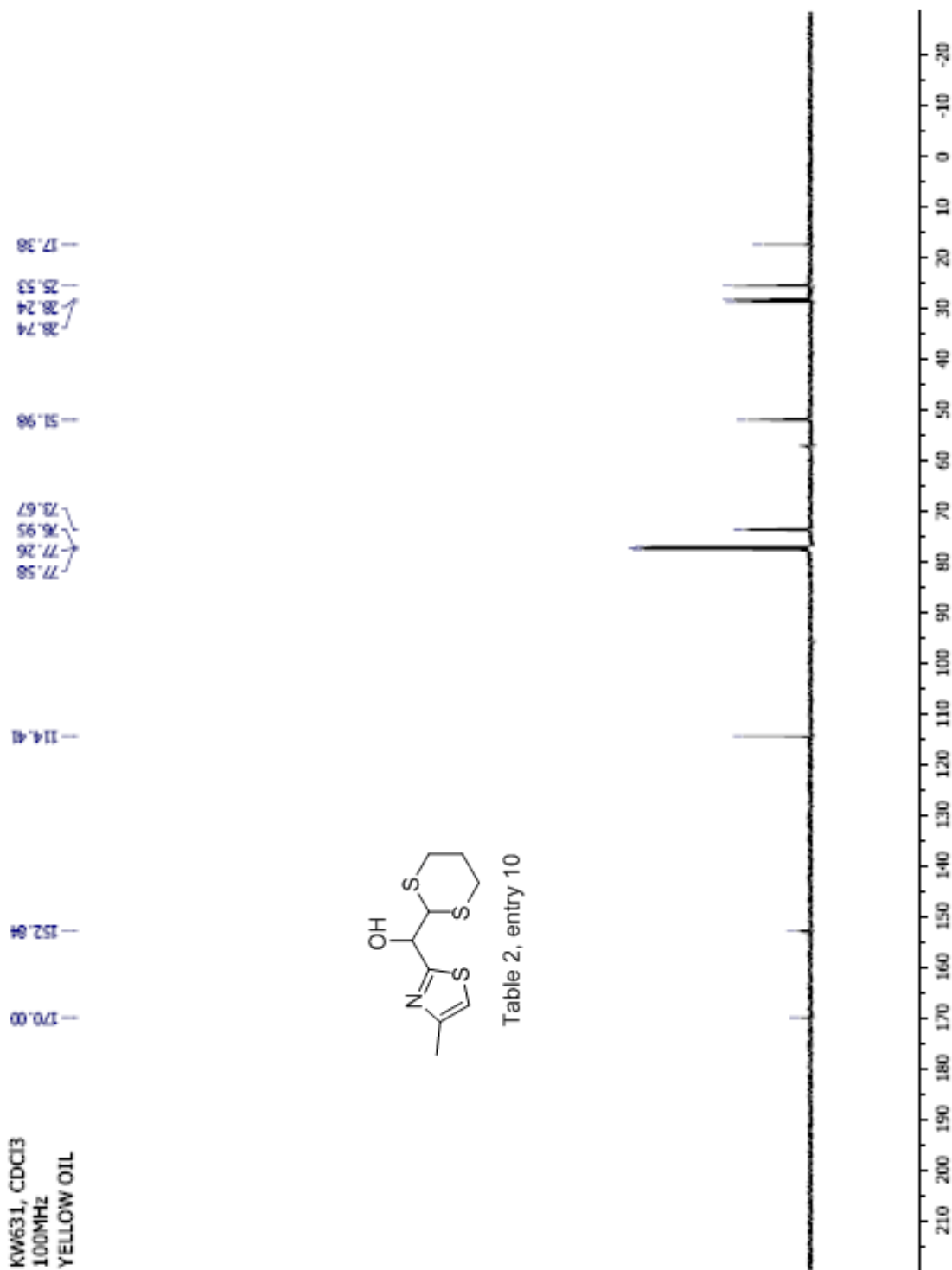


Table 2, entry 10





## Manual Peak Matching Report For Accurate Mass Determination

Theoretical mass	Experimental mass	PFK matching mass	Deviation*
247.01593	247.01623	230.98562	1.2 ppm

\* The deviation is obtained from the following equation:

$$\text{deviation} = \frac{\text{experimental mass} - \text{theoretical mass}}{\text{nominal mass}}$$

Where nominal mass takes in account only  $^{12}\text{C}$ ,  $^1\text{H}$ ,  $^{16}\text{O}$ ,  $^{14}\text{N}$  etc...

Theoretical mass correspond to the mass of the most abundant isotope peak

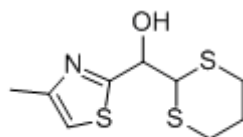
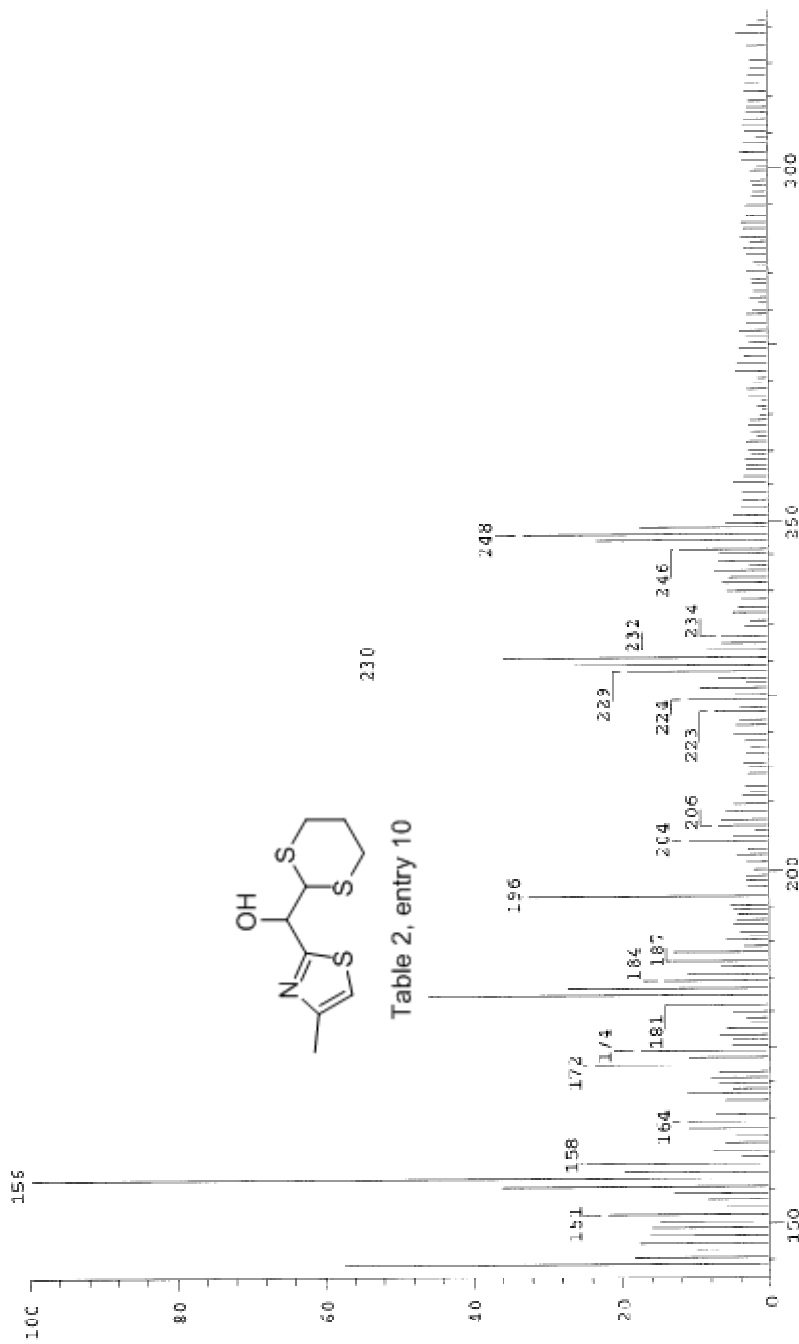


Table 2, entry 10

*Handwritten signature*

Scans: 1 > 42  
 Client: Kuldeep  
 #Peaks: 653  
 RIC: 1147335  
 5.4E+03

SPGC: fir083703.dat (11-JUN-08 11:13:45)  
 Samp: KMEJ1  
 Comp: 70 eV EI  
 Oper: Kh  
 Study: MS services  
 Masses: 35.01 > 650.00  
 Base: 76.18  
 Intensity: 46145  
 Peak: 1000.0 mmu  
 Scan 25 @ 0.67 min (BI +Q1MS IAR UP LR)



Date: Wed Jun 11 11:20:59 2008 -CIS: 8.3.0 SP2 for CSPI (V4.0) build 58-338 from 26-Aug-98



KW635, CDCl<sub>3</sub>  
400MHz  
WHITE SOLID

7.26  
7.02  
6.81  
5.21  
4.93  
4.51  
4.48  
3.73  
2.86  
2.73  
2.71  
2.68  
2.03  
1.96

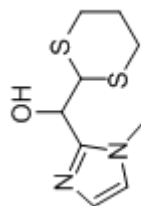
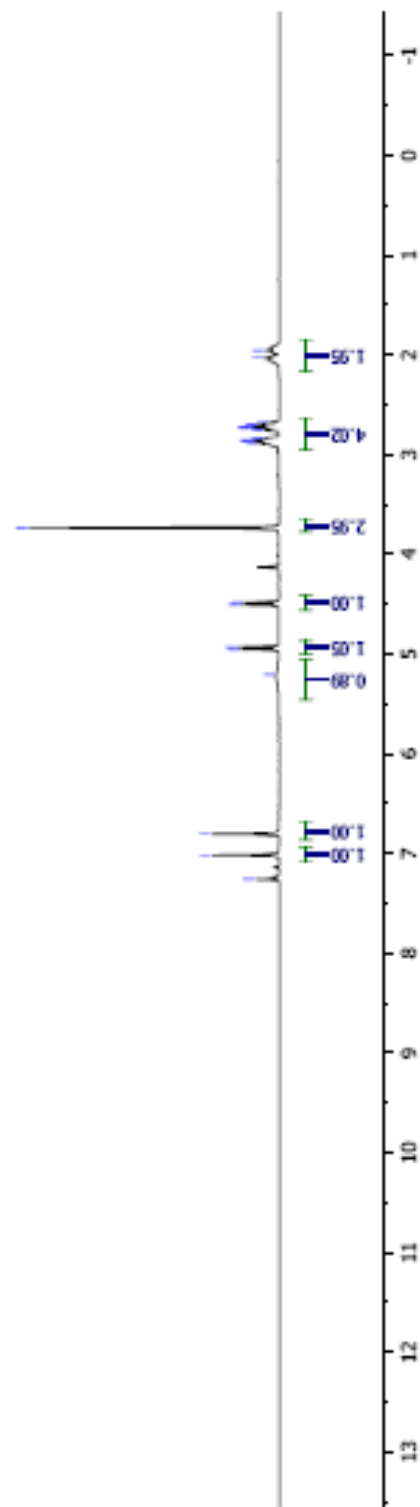


Table 2, entry 11



KW635, CDCl<sub>3</sub>  
100MHz  
WHITE SOLID

167.11  
127.58  
121.72  
77.60  
77.28  
76.96  
67.59  
30.51  
33.49  
28.33  
27.65  
25.66

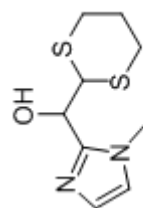
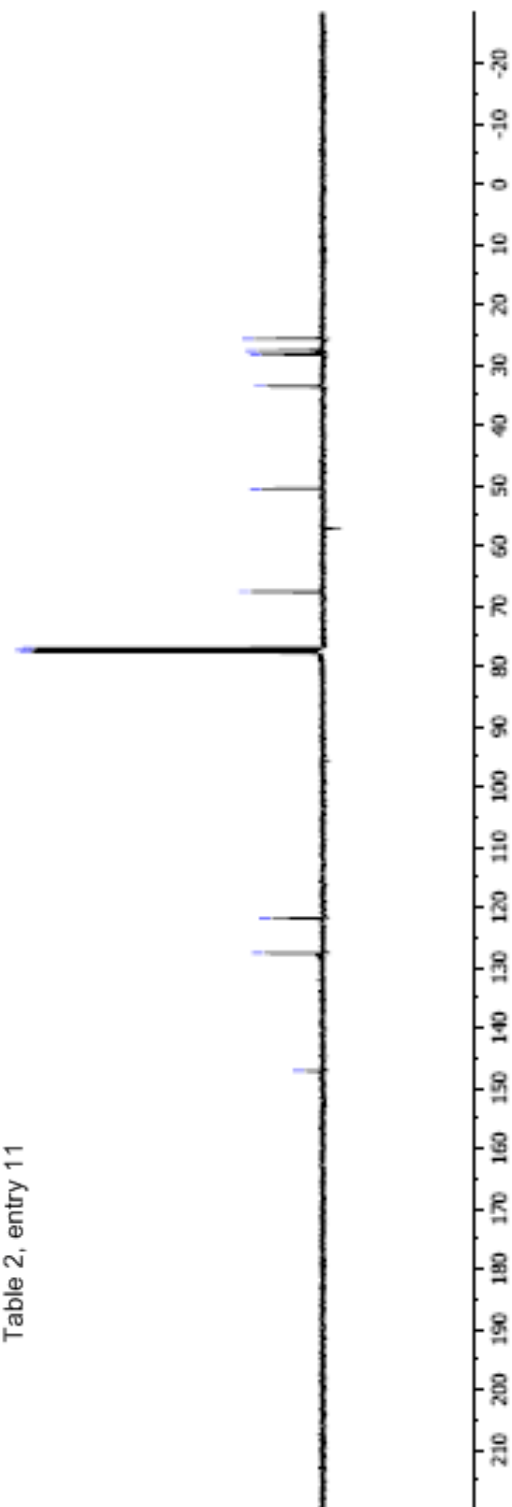


Table 2, entry 11



## Manual Peak Matching Report For Accurate Mass Determination

Theoretical mass	Experimental mass	PFK matching mass	Deviation*
230.05476	230.05518	218.98562	1.8 ppm

\* The deviation is obtained from the following equation:

$$\text{deviation} = \frac{\text{experimental mass} - \text{theoretical mass}}{\text{nominal mass}}$$

Where nominal mass takes in account only  $^{12}\text{C}$ ,  $^1\text{H}$ ,  $^{16}\text{O}$ ,  $^{14}\text{N}$  etc...

Theoretical mass correspond to the mass of the most abundant isotope peak

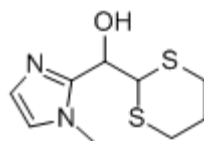


Table 2, entry 11

*MO*

SPEC: E:\n082700.dat (11-JUN-09 10:52:14)  
 Samp: KW635  
 Comm: 70 eV EI  
 Oper: Kh  
 Base: 111.16  
 Peak: 1000.0 mmu  
 Scan 33 @ 0.83 min (EI (QING DME UP LR))

Study: MS services  
 Masses: 35.01 > 550.00  
 Intensity: 65138  
 Client: Kaidup  
 #Peaks: 552  
 RIC: 143609  
 4.6E+03

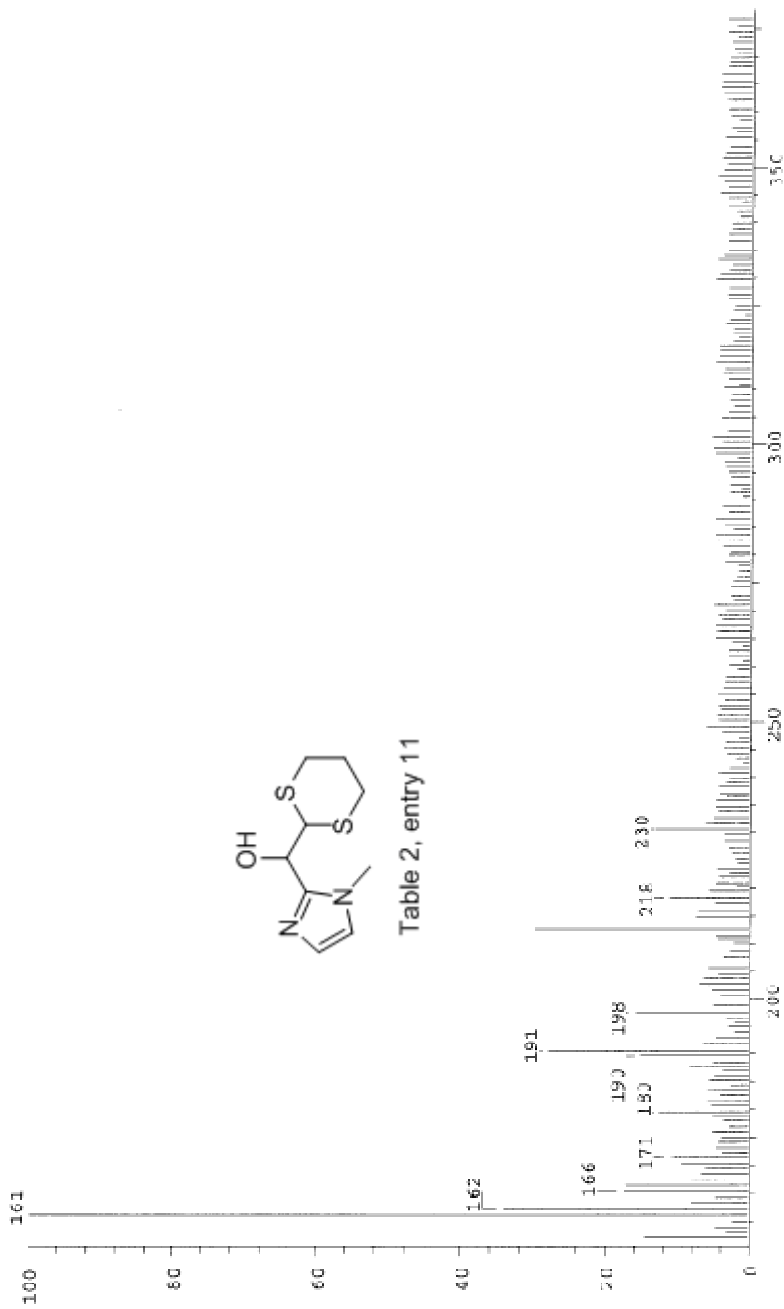


Table 2, entry 11

Date: Wed Jun 11 10:54:21 2008 TOTS: 3.1 0 SP2 for OSE1 (04.0) build 98-258 from 26-Aug-98

1.947  
 1.961  
 1.975  
 1.982  
 1.990  
 2.004  
 2.016  
 2.027  
 2.036  
 2.044  
 2.055  
 2.063  
 2.071  
 2.684  
 2.918  
 3.298  
 4.042  
 4.061  
 5.167  
 5.186  
 6.970  
 6.980  
 6.992  
 7.099  
 7.106  
 7.257  
 7.281  
 7.293

KW608, CDCl3  
 400MHz  
 PALE RED OIL

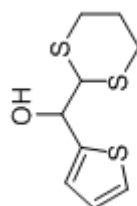
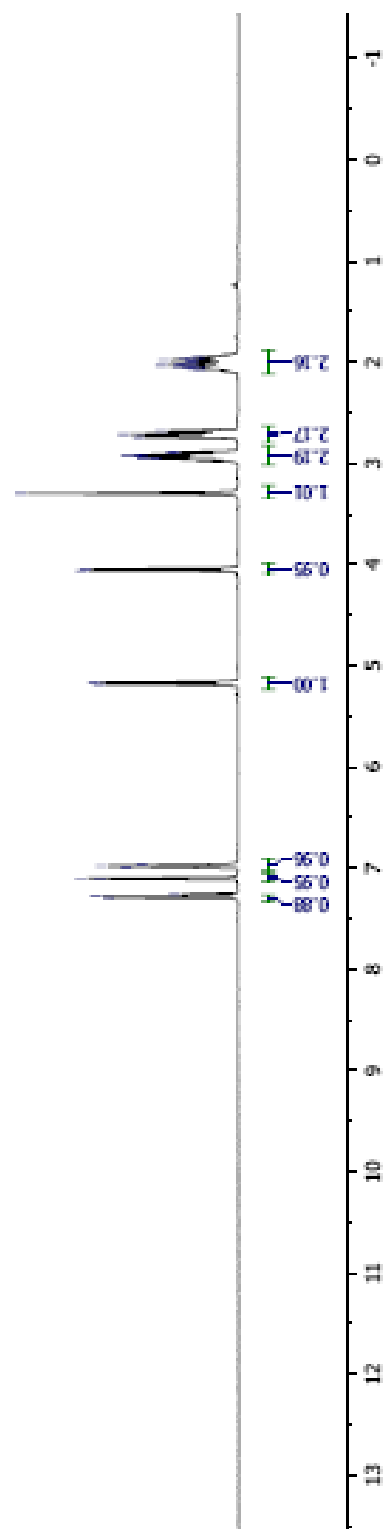


Table 2, entry 12



KW608, CDCl<sub>3</sub>  
100MHz  
PALE RED OIL

148.854  
126.767  
126.158  
125.586  
77.723  
77.405  
77.087  
71.216  
52.872  
28.175  
27.672  
25.300

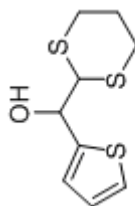
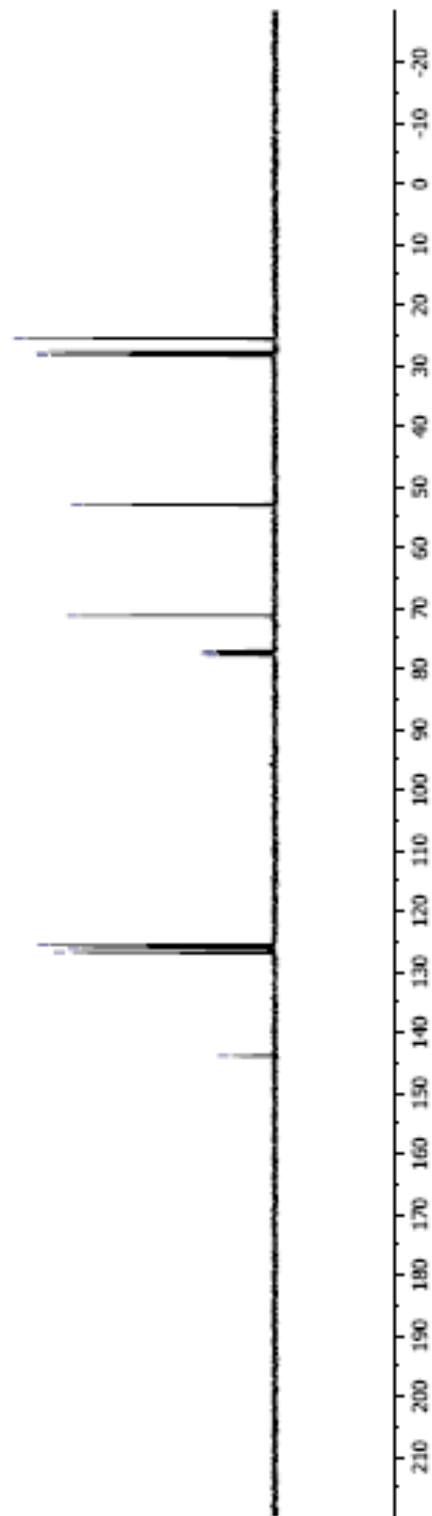
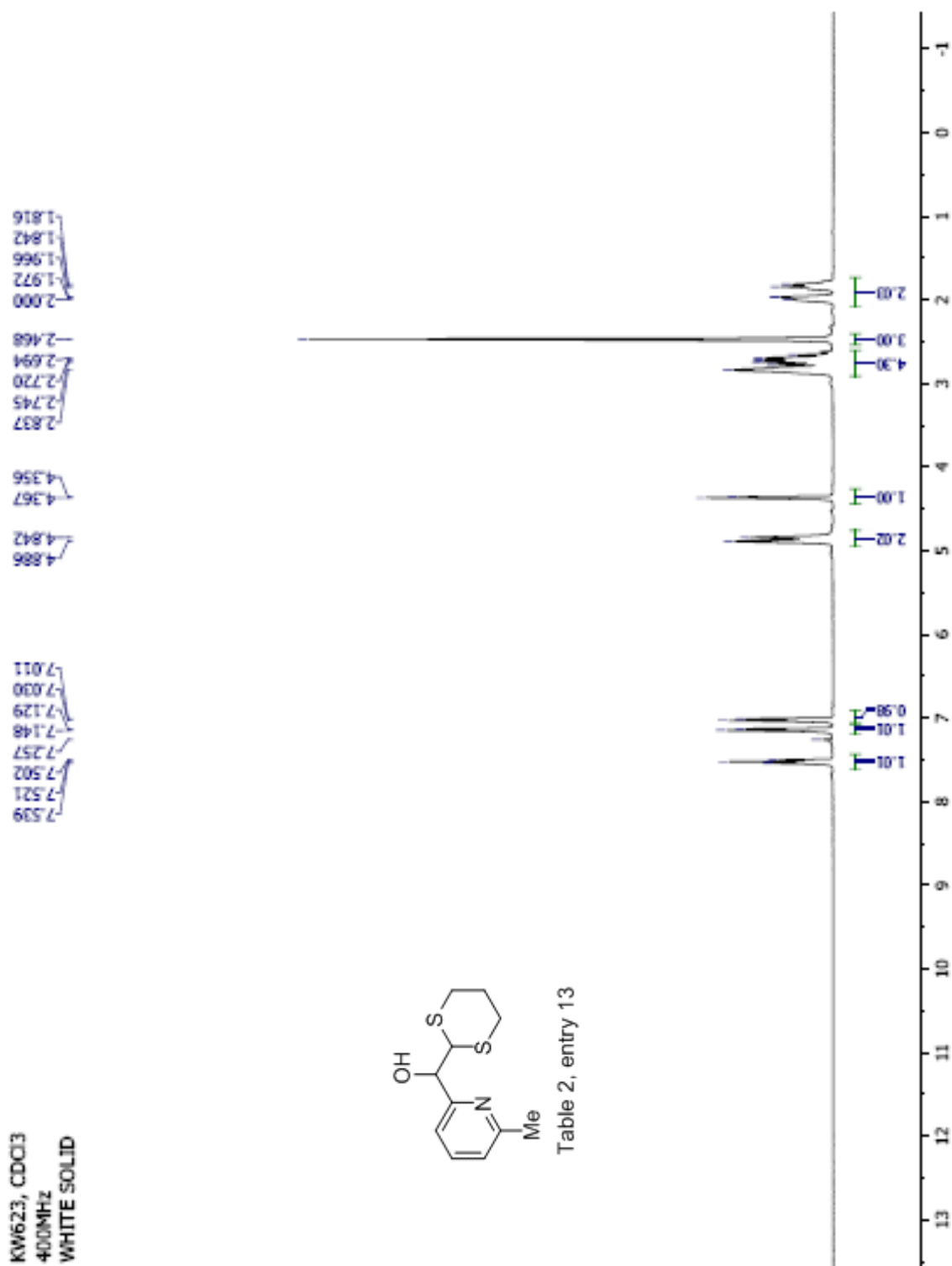


Table 2, entry 12





KW623, CDCl<sub>3</sub>  
100MHz  
WHITE SOLID

157.43  
157.416  
137.024  
122.943  
118.879  
77.886  
77.867  
77.249  
75.262  
53.611  
29.734  
29.446  
25.909  
24.544

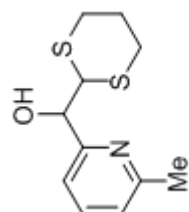
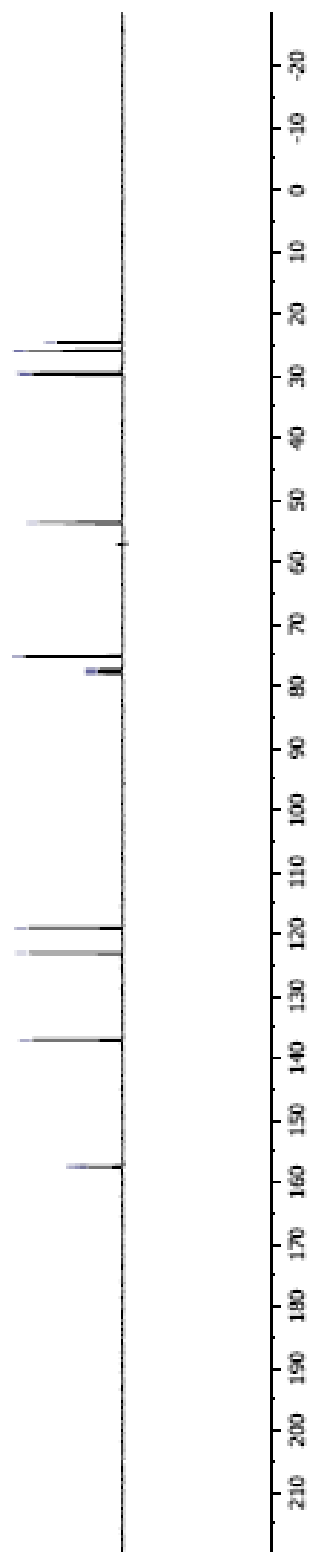


Table 2, entry 13





## Manual Peak Matching Report For Accurate Mass Determination

Theoretical mass	Experimental mass	PFK matching mass	Deviation*
241.05951	241.06000	230.98562	2 ppm

\* The deviation is obtained from the following equation:

$$\text{deviation} = \frac{\text{experimental mass} - \text{theoretical mass}}{\text{nominal mass}}$$

Where nominal mass takes in account only  $^{12}\text{C}$ ,  $^1\text{H}$ ,  $^{16}\text{O}$ ,  $^{14}\text{N}$  etc...

Theoretical mass correspond to the mass of the most abundant isotope peak

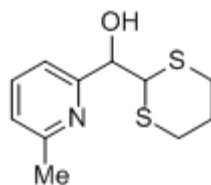


Table 2, entry 13

STBC: fia063650.dat (10-MAY-08 10:50:47)  
 Samp: KW623  
 Conn: 70 eV EI  
 Oper: kh  
 Base: 133.07  
 Peak: 1000.0 mmu  
 Scan 36 @ 0.62 min (RT +QIMS LMR UP LR)  
 Study: Survive  
 Masses: 35.01 > 650.00  
 Intensi.y: 6C5392  
 Client: Kuldap  
 #Peaks: 640  
 RIC: 1934249  
 1.8E+04



Date: Mon May 19 10:53:07 2008 ICIS: 8.3.0 SF2 for CSF1 (V4.0) build 98-23E from 26-Aug-98

KM629, CDCl<sub>3</sub>  
400MHz  
YELLOW OIL

7.626  
7.607  
7.104  
6.614  
5.114  
5.094  
4.385  
4.364  
3.787  
2.966  
2.911  
2.863  
2.762  
2.711  
2.051  
1.978

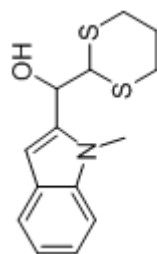
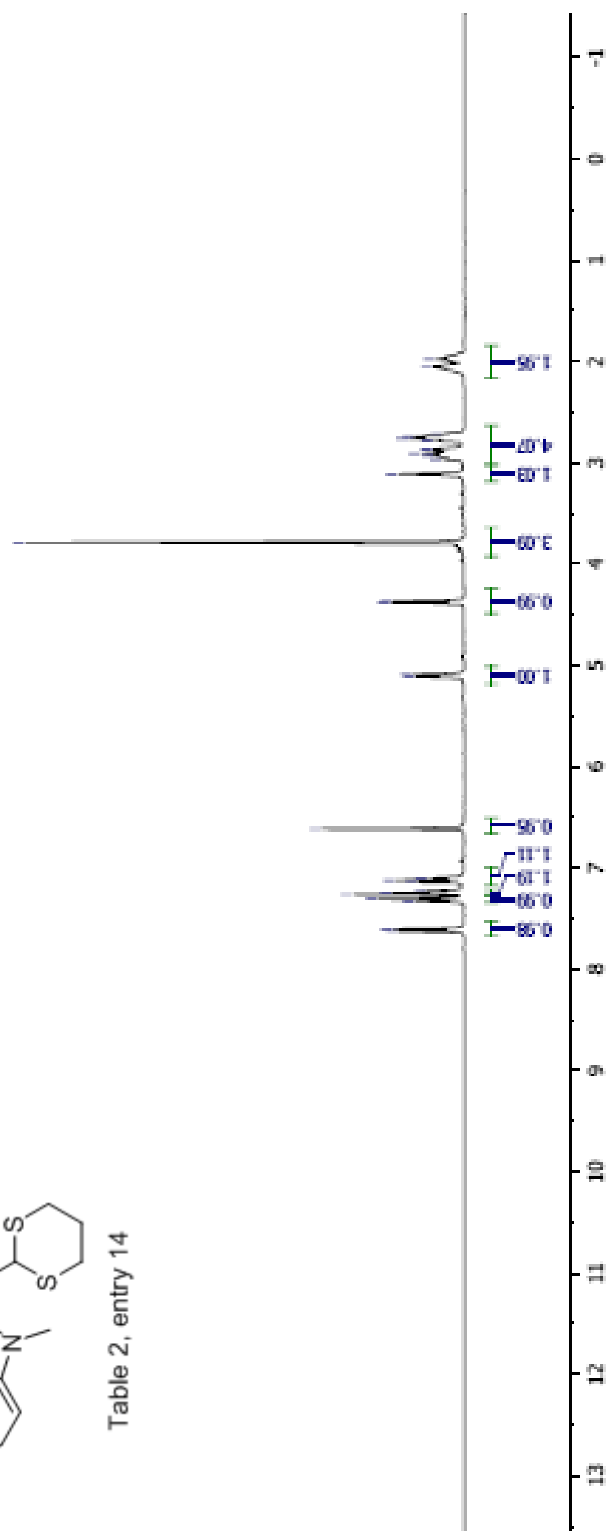


Table 2, entry 14



KW629, CDCl<sub>3</sub>  
100MHz  
YELLOW OIL

138.229  
138.017  
127.280  
122.227  
119.907  
109.527  
101.535  
77.745  
77.427  
77.112  
68.798  
50.927  
30.807  
28.665  
27.911  
25.556

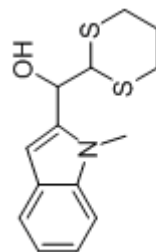
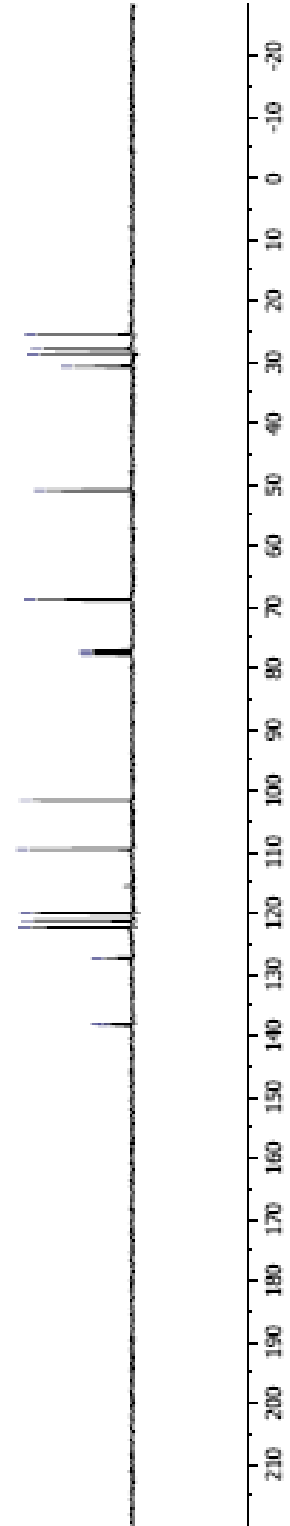


Table 2, entry 14



## Manual Peak Matching Report For Accurate Mass Determination

Theoretical mass	Experimental mass	PFK matching mass	Deviation*
279.07516	279.07569	242.98562	1.9 ppm

\* The deviation is obtained from the following equation:

$$\text{deviation} = \frac{\text{experimental mass} - \text{theoretical mass}}{\text{nominal mass}}$$

Where nominal mass takes in account only  $^{12}\text{C}$ ,  $^1\text{H}$ ,  $^{16}\text{O}$ ,  $^{14}\text{N}$  etc...

Theoretical mass correspond to the mass of the most abundant isotope peak

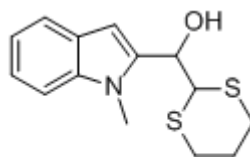


Table 2, entry 14

*Handwritten signature*

Scans: 1 > 48  
 Client: KulAp  
 Peaks: 626  
 RIC: 2450871  
 3.58+13

SPEC: fln003031.d: (09-JUN-08 10:38:15)  
 Samp: 50629  
 Conn: 73 eV EI  
 OPER: KJ  
 Study: Service  
 Masses: 35.01 > 650.00  
 Base: 139.96  
 Peak: 1000.0 rnu  
 Intencty: 352586  
 Scan 47 @ 1.12 min (EI +QMS IMR UP LR)

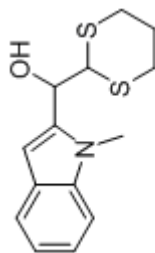
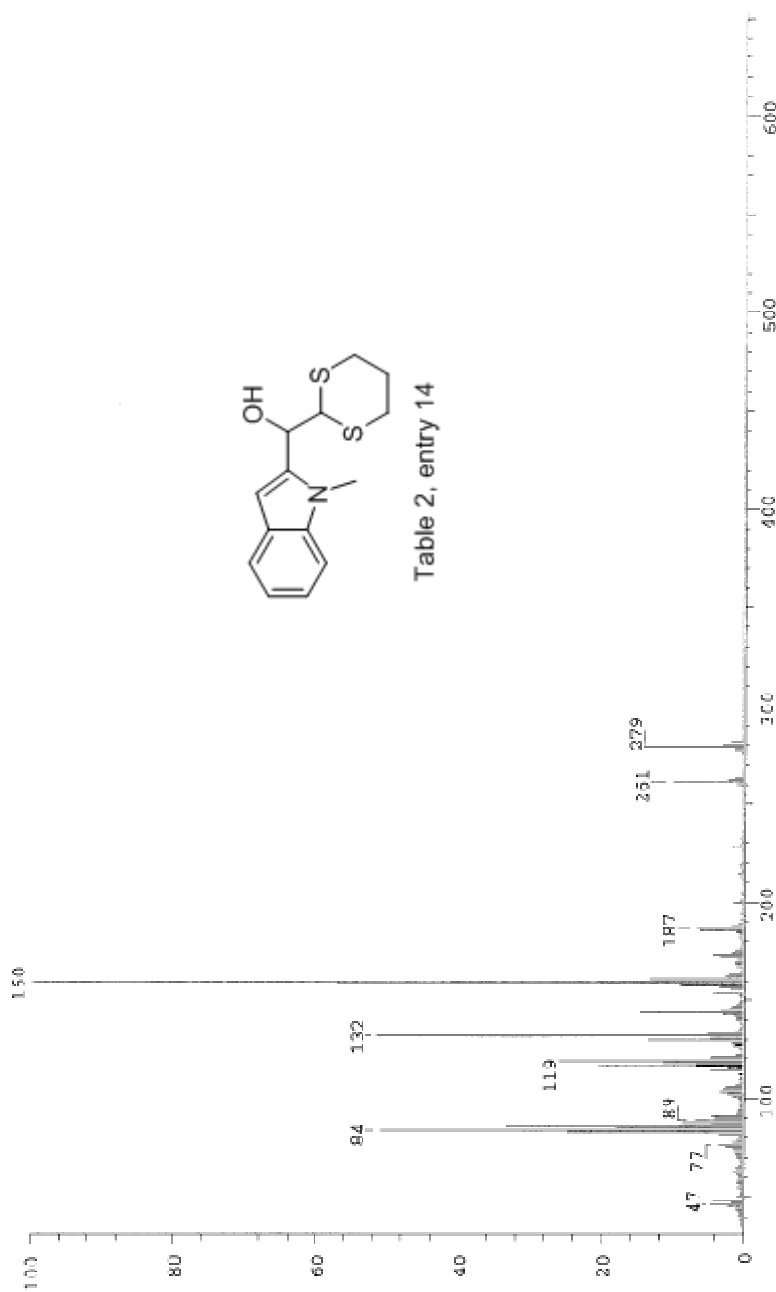


Table 2, entry 14

Date: Mon Jun 9 10:39:54 2006 ICIS: 6.3.0 SP2 for OSPI (V4.0) build 98-238 from 26-Aug-98

**APPENDIX C**

**CHAPTER 4**

**General Information**

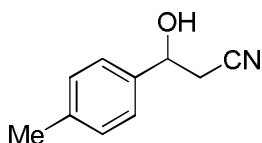
**References for known compounds and characterization data for the new compounds**

**$^1\text{H}$ ,  $^{13}\text{C}$  and HRMS for all compounds**

## General Information

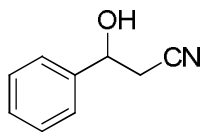
All reactions were carried out under inert atmosphere using oven dried glassware and a magnetic stirrer. THF was distilled and dried over sodium. Trimethylsilylacetonitrile (TMSAN), proazaphosphatane **1a** and all aldehydes were purchased from commercial sources and were used without further purification. Products were purified via column chromatography using hexane/ethyl acetate.  $^1\text{H}$  and  $^{13}\text{C}$  nmr spectra were obtained on a VXR-300 and a VXR-400 NMR spectrometer, respectively. All NMR spectra were taken in  $\text{CDCl}_3$ . Thin layer chromatography was used to monitor reaction progress.

### $\beta$ -Hydroxy-4-methyl- benzenepropanenitrile (Table 1, entry 6)<sup>1</sup>:



The general procedure was followed for the synthesis and purification; product was afforded as a colorless oil in 91% isolated yield.

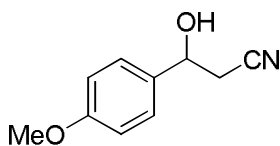
### $\beta$ -Hydroxybenzenepropanenitrile (Table 2, entry 1)<sup>2</sup>:



The general procedure was followed for the synthesis and purification; product was afforded as a colorless oil in 89% isolated yield.

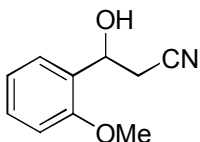
### $\beta$ -Hydroxy-4-methoxy- benzenepropanenitrile (Table 2, entry 2)<sup>2</sup>:





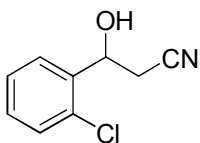
The general procedure was followed for the synthesis and purification; product was afforded as a colorless oil in 83% isolated yield.

**$\beta$ -Hydroxy-2-methoxy- benzenepropanenitrile (Table 2, entry 3)<sup>3</sup>:**



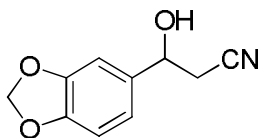
The general procedure was followed for the synthesis and purification; product was afforded as a white solid in 77% isolated yield.

**$\beta$ -Hydroxy-2-chlorobenzenepropanenitrile (Table 2, entry 4)<sup>3</sup>:**



The general procedure was followed for the synthesis and purification; product was afforded as a colorless oil in 94% isolated yield.

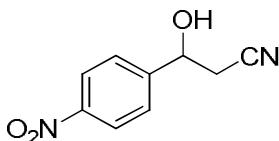
**$\beta$ -Hydroxy-1,3-benzodioxole-5-propanenitrile (Table 2, entry 5):**



The general procedure was followed for the synthesis and purification; product was afforded as a white solid in 82% isolated yield. <sup>1</sup>H NMR (CDCl<sub>3</sub>, 400 MHz):  $\delta$  6.86–6.76 (m, 3H), 5.95 (s, 2H), 4.93–4.89 (m, 1H), 2.81 (d, 1H,  $J$  = 4.0 Hz), 2.70–2.69 (m, 2H) ppm; <sup>13</sup>C NMR

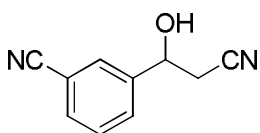
(CDCl<sub>3</sub>, 100.6 MHz):  $\delta$  148.1, 135.1, 119.3, 117.6, 108.5, 106.1, 101.4, 69.9, 28.1 ppm;  
HRMS  $m/z$  Calcd. for C<sub>10</sub>H<sub>9</sub>NO<sub>3</sub>: 191.05824. Found: 191.05876.

**$\beta$ -Hydroxy-4-nitrobenzenepropanenitrile (Table 2, entry 6)<sup>1</sup>:**



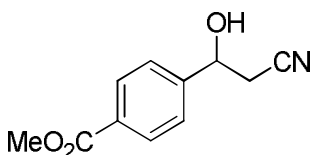
The general procedure was followed for the synthesis and purification; product was afforded as a yellow solid in 94% isolated yield.

**$\beta$ -Hydroxy-3-cyanobenzenepropanenitrile (Table 2, entry 7):**



The general procedure was followed for the synthesis and purification; product was afforded as a yellow oil in 89% isolated yield. <sup>1</sup>H NMR (CDCl<sub>3</sub>, 400 MHz):  $\delta$  7.70 (s, 1H), 7.65–7.59 (m, 2H), 7.50 (t, 1H,  $J$  = 8.0 Hz), 5.08 (q, 1H,  $J$  = 4.8 Hz), 3.62 (d, 1H,  $J$  = 4.4 Hz), 2.82–2.71 (m, 2H) ppm; <sup>13</sup>C NMR (CDCl<sub>3</sub>, 100.6 MHz):  $\delta$  142.9, 132.4, 130.5, 129.9, 129.5, 118.7, 117.2, 112.7, 68.8, 28.3 ppm; HRMS  $m/z$  Calcd. for C<sub>10</sub>H<sub>8</sub>N<sub>2</sub>O: 172.06366. Found: 172.06395.

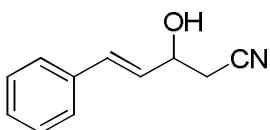
**Methyl 4-(2-cyano-1-hydroxyethyl)benzoate (Table 2, entry 8):**



The general procedure was followed for the synthesis and purification; product was afforded as a yellow oil in 93% isolated yield. <sup>1</sup>H NMR (CDCl<sub>3</sub>, 300 MHz):  $\delta$  8.99 (d, 2H,  $J$  = 8.0

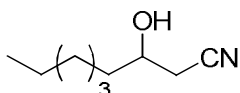
Hz), 7.45 (d, 2H,  $J = 8.0$  Hz), 5.07 (q, 1H,  $J = 4.0$  Hz), 3.89 (s, 3H), 3.27 (d, 1H,  $J = 4.0$  Hz), 2.76–2.74 (m, 2H) ppm;  $^{13}\text{C}$  NMR ( $\text{CDCl}_3$ , 75 MHz):  $\delta$  166.9, 146.2, 130.5, 130.3, 125.8, 117.3, 69.7, 52.6, 28.1 ppm; HRMS  $m/z$  Calcd. for  $\text{C}_{11}\text{H}_{11}\text{NO}_3$ : 205.07389. Found: 205.07416.

**3-Hydroxy-5-phenyl-, 4-pentenitrile (Table 2, entry 9)<sup>4</sup>:**



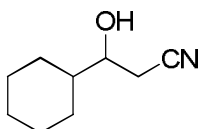
The general procedure was followed for the synthesis and purification; product was afforded as a yellow oil in 94% isolated yield.  $^{13}\text{C}$  NMR ( $\text{CDCl}_3$ , 100.6 MHz):  $\delta$  135.8, 133.1, 128.9, 128.7, 128.3, 127.0, 117.5, 68.8, 26.6 ppm.

**3-Hydroxynonanenitrile (Table 2, entry 10)<sup>5</sup>:**



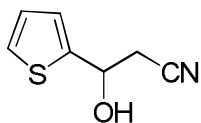
The general procedure was followed for the synthesis and purification; product was afforded as a colorless oil in 85% isolated yield.

**3-Cyclohexyl-3-hydroxypropionitrile (Table 2, entry 11)<sup>5</sup>:**



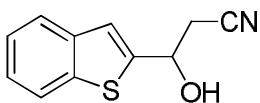
The general procedure was followed for the synthesis and purification; product was afforded as a colorless oil in 88% isolated yield.

**$\beta$ -Hydroxy- 2-thiophenepropanenitrile, (Table 3, entry 1)<sup>6</sup>:**



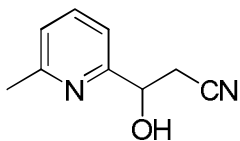
The general procedure was followed for the synthesis and purification; product was afforded as a yellow oil in 88% isolated yield.

**$\beta$ -Hydroxy-benzo[*b*]thiophene-2-propanenitrile (Table 3, entry 2)<sup>6</sup>::**



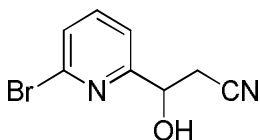
The general procedure was followed for the synthesis and purification; product was afforded as a yellow solid in 93% isolated yield.

**3-hydroxy-3-(6-methylpyridin-2-yl)propanenitrile (Table 3, entry 3):**



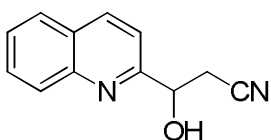
The general procedure was followed for the synthesis and purification; product was afforded as a yellow oil in 92% isolated yield. <sup>1</sup>H NMR (CDCl<sub>3</sub>, 400 MHz):  $\delta$  7.61 (t, 1H, *J* = 8.0 Hz), 7.18 (d, 1H, *J* = 8.0 Hz), 7.10 (d, 1H, *J* = 8.0 Hz), 5.09 (s, 1H), 4.97 (t, 1H, *J* = 4.0 Hz), 2.87–2.75 (m, 2H), 2.51 (s, 3H) ppm; <sup>13</sup>C NMR (CDCl<sub>3</sub>, 100.6 MHz):  $\delta$  157.9, 157.4, 137.8, 123.3, 117.6, 117.5, 68.6, 27.4, 24.4 ppm; HRMS *m/z* Calcd. for C<sub>9</sub>H<sub>10</sub>N<sub>2</sub>O: 162.07931. Found: 162.07961.

**3-(6-bromopyridin-2-yl)-3-hydroxypropanenitrile (Table 3, entry 4):**



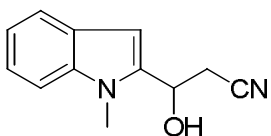
The general procedure was followed for the synthesis and purification; product was afforded as a yellow oil in 87% isolated yield.  $^1\text{H}$  NMR ( $\text{CDCl}_3$ , 400 MHz):  $\delta$  7.62 (t, 1H,  $J = 8.0$  Hz), 7.46 (d, 2H,  $J = 4.0$  Hz), 5.03 (m, 1H), 4.02 (d, 1H,  $J = 4.0$  Hz), 2.97–2.82 (m, 2H) ppm;  $^{13}\text{C}$  NMR ( $\text{CDCl}_3$ , 100.6 MHz):  $\delta$  160.4, 141.7, 139.8, 128.1, 119.7, 117.3, 69.1, 27.0 ppm; HRMS  $m/z$  Calcd. for  $\text{C}_8\text{H}_7\text{BrN}_2\text{O}$ : 225.97417. Found: 225.97456.

### $\beta$ -hydroxy-2-Quinolinepropanenitrile (Table 3, entry 5)



The general procedure was followed for the synthesis and purification; product was afforded as a red oil in 93% isolated yield.  $^1\text{H}$  NMR ( $\text{CDCl}_3$ , 300 MHz):  $\delta$  8.25 (d, 1H,  $J = 9.0$  Hz), 8.10 (d, 1H,  $J = 9.0$  Hz), 7.87 (d, 1H,  $J = 9.0$  Hz), 7.77 (t, 1H,  $J = 9.0$  Hz), 7.59 (t, 1H,  $J = 9.0$  Hz), 7.46 (d, 1H,  $J = 9.0$  Hz), 5.25 (bs, 1H), 5.19 (bs, 1H), 2.96–2.93 (m, 2H) ppm;  $^{13}\text{C}$  NMR ( $\text{CDCl}_3$ , 100.6 MHz):  $\delta$  157.8, 146.7, 138.1, 130.6, 129.1, 128.1, 127.9, 127.4, 118.1, 117.2, 68.9, 27.3 ppm; HRMS  $m/z$  Calcd. for  $\text{C}_{12}\text{H}_{10}\text{N}_2\text{O}$ : 198.07931. Found: 198.07973.

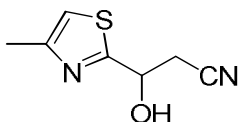
### 3-hydroxy-3-(1-methyl-1H-indol-2-yl)propanenitrile (Table 3, entry 6)



The general procedure was followed for the synthesis and purification; product was afforded as a yellow solid in 81% isolated yield.  $^1\text{H}$  NMR ( $\text{CD}_3\text{CN}$ , 400 MHz):  $\delta$  7.59 (d, 1H,  $J = 8.0$  Hz), 7.41 (d, 1H,  $J = 8.0$  Hz), 7.24 (t, 1H,  $J = 8.0$  Hz), 7.09 (t, 1H,  $J = 8.0$  Hz), 6.54 (s, 1H), 5.23 (q, 1H,  $J = 8.0$  Hz), 3.97 (d, 1H,  $J = 8.0$  Hz), 3.80 (s, 3H), 3.08–3.06 (m, 2H) ppm;  $^{13}\text{C}$

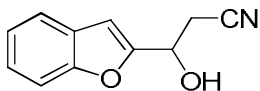
NMR (CD<sub>3</sub>CN, 100.6 MHz):  $\delta$  139.9, 138.1, 127.3, 122.1, 120.8, 119.7, 118.2, 117.5, 109.6, 99.2, 62.6, 29.9, 25.3 ppm; HRMS  $m/z$  Calcd. for C<sub>12</sub>H<sub>12</sub>N<sub>2</sub>O: 200.09496. Found: 200.09532.

**3-Hydroxy-3-(4-methylthiazol-2-yl)propanenitrile (Table 3, entry 7):**



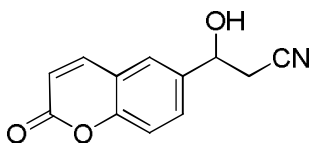
The general procedure was followed for the synthesis and purification; product was afforded as a yellow oil in 95% isolated yield. <sup>1</sup>H NMR (CDCl<sub>3</sub>, 400 MHz):  $\delta$  6.90 (s, 1H), 5.28 (s, 1H), 5.11 (s, 1H), 3.06–2.87 (m, 2H), 2.40 (s, 3H) ppm; <sup>13</sup>C NMR (CDCl<sub>3</sub>, 100.6 MHz):  $\delta$  171.1, 153.1, 117.2, 114.8, 67.5, 27.2, 17.1 ppm; HRMS  $m/z$  Calcd. for C<sub>7</sub>H<sub>8</sub>N<sub>2</sub>OS: 168.03573. Found: 168.03606.

**3-(Benzofuran-2-yl)-3-hydroxypropanenitrile (Table 3, entry 8):**



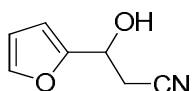
The general procedure was followed for the synthesis and purification; product was afforded as a yellow oil in 64% isolated yield. <sup>1</sup>H NMR (CDCl<sub>3</sub>, 400 MHz):  $\delta$  7.58–7.55 (m, 1H), 7.48–7.45 (m, 1H), 7.34–7.28 (m, 1H), 7.27–7.22 (m, 1H), 6.77 (s, 1H) 5.17 (q, 1H,  $J$  = 8.0 Hz), 3.05–2.91 (m, 3H) ppm; <sup>13</sup>C NMR (CDCl<sub>3</sub>, 100.6 MHz):  $\delta$  155.4, 155.0, 127.8, 125.1, 123.4, 121.7, 117.1, 111.6, 104.4 64.4, 25.2 ppm; HRMS  $m/z$  Calcd. for C<sub>11</sub>H<sub>9</sub>NO<sub>2</sub>: 187.06333. Found: 187.06371.

**3-hydroxy-3-(2-oxo-2H-chromen-6-yl)propanenitrile (Table 3, entry 9):**



The general procedure was followed for the synthesis and purification; product was afforded as a yellow solid in 70% isolated yield.  $^1\text{H}$  NMR ( $\text{CDCl}_3$ , 400 MHz):  $\delta$  7.71–7.68 (m, 1H), 7.57–7.54 (m, 2H), 7.30–7.25 (m, 1H), 6.40 (d, 1H,  $J = 12.4$  Hz), 5.13 (t, 1H,  $J = 6.0$  Hz), 3.34 (s, 1H), 2.80 (d, 2H,  $J = 4.0$  Hz) ppm;  $^{13}\text{C}$  NMR ( $\text{CDCl}_3$ , 100.6 MHz):  $\delta$  160.7, 154.1, 143.3, 137.6, 129.2, 125.2, 119.1, 117.7, 117.6, 116.9, 115.5, 69.4, 28.4 ppm; HRMS  $m/z$  Calcd. for  $\text{C}_{12}\text{H}_9\text{NO}_3$ : 215.05824. Found: 215.05862.

**$\beta$ -Hydroxy-2-furanpropanenitrile (Table 3, entry 10)<sup>7</sup>:**



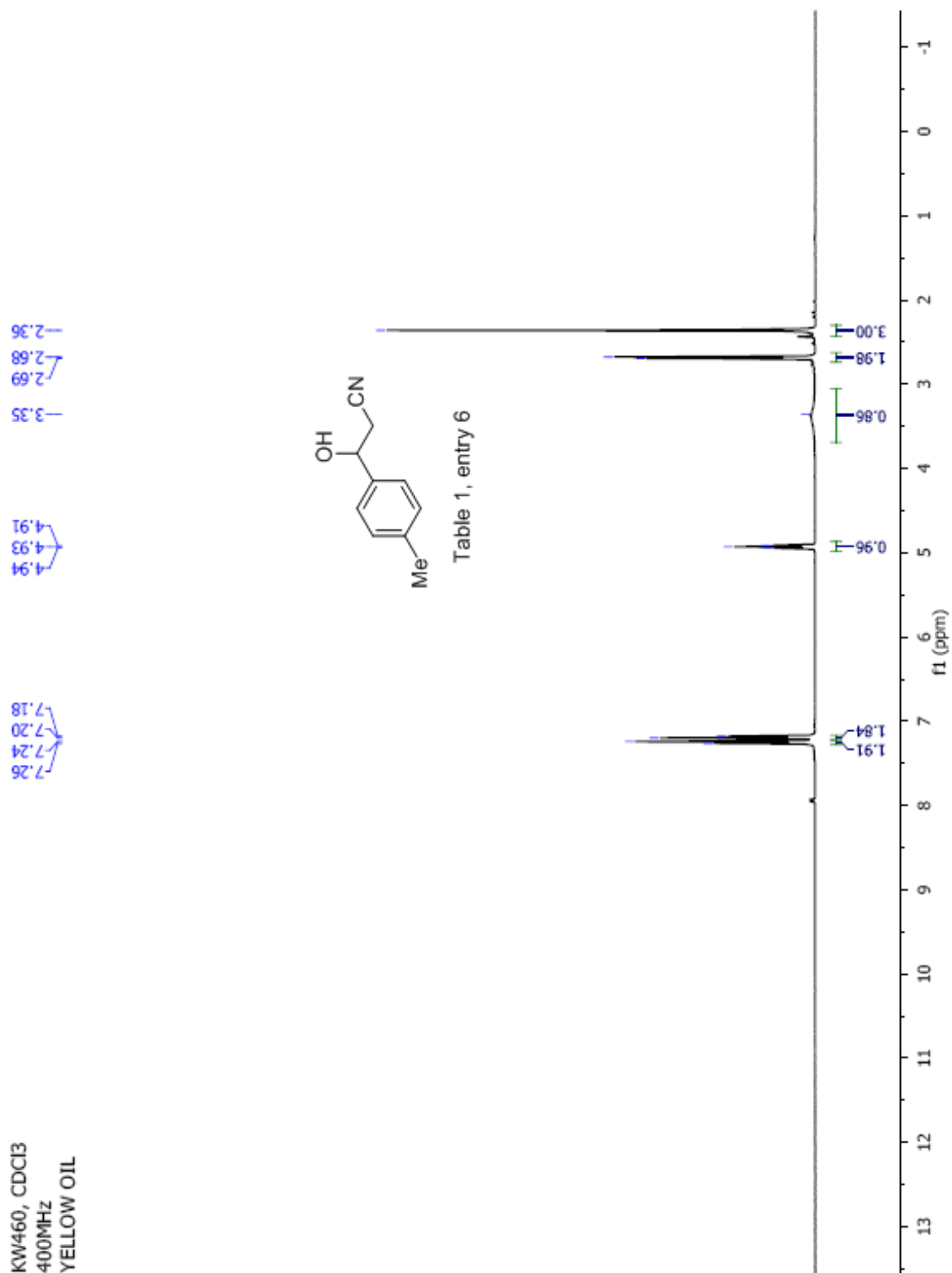
The general procedure was followed for the synthesis and purification; product was afforded as a colorless oil in 88% isolated yield.  $^{13}\text{C}$  NMR ( $\text{CDCl}_3$ , 100.6 MHz):  $\delta$  153.1, 143.1, 117.3, 110.8, 107.7, 63.9, 25.1 ppm.

### Reference

1. Ankati, H.; Zhu, D.; Yang, Y.; Biehl, E. R.; Hua, L. *J. Org. Chem.* **2009**, *74*, 1658–1662.
2. Feroci, M.; Orsini, M.; Sotgiu, G.; Inesi, A. *Electrochim. Acta* **2008**, *53*, 2346–2354.
3. Kamila, S.; Zhu, D.; Biehl, E. R.; Hua, L. *Org. Lett.* **2006**, *8*, 4429–4431.
4. Itoh, T.; Takagi, Y.; Nishiyama, S. *J. Org. Chem.* **1991**, *56*, 1521–1524.
5. Elenkov, M. M.; Hauer, B.; Janssen, D. B. *Adv. Synth. Catal.* **2006**, *348*, 579–585.
6. Turcu, M. C.; Perkiö, P.; Kanerva, L. T. *ARKIVOC* **2009**, *3*, 251–263.

7. Kashin, A. N.; Tul'chinskii, M. L.; Beletskaya, I. P. *J. Organomet. Chem.* **1985**, 292, 205–215.





KW460, CDCl<sub>3</sub>  
100MHz  
YELLOW OIL

138.74  
138.40  
129.73  
125.76  
117.88  
77.73  
77.41  
77.09  
69.95  
28.09  
21.44

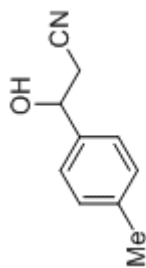
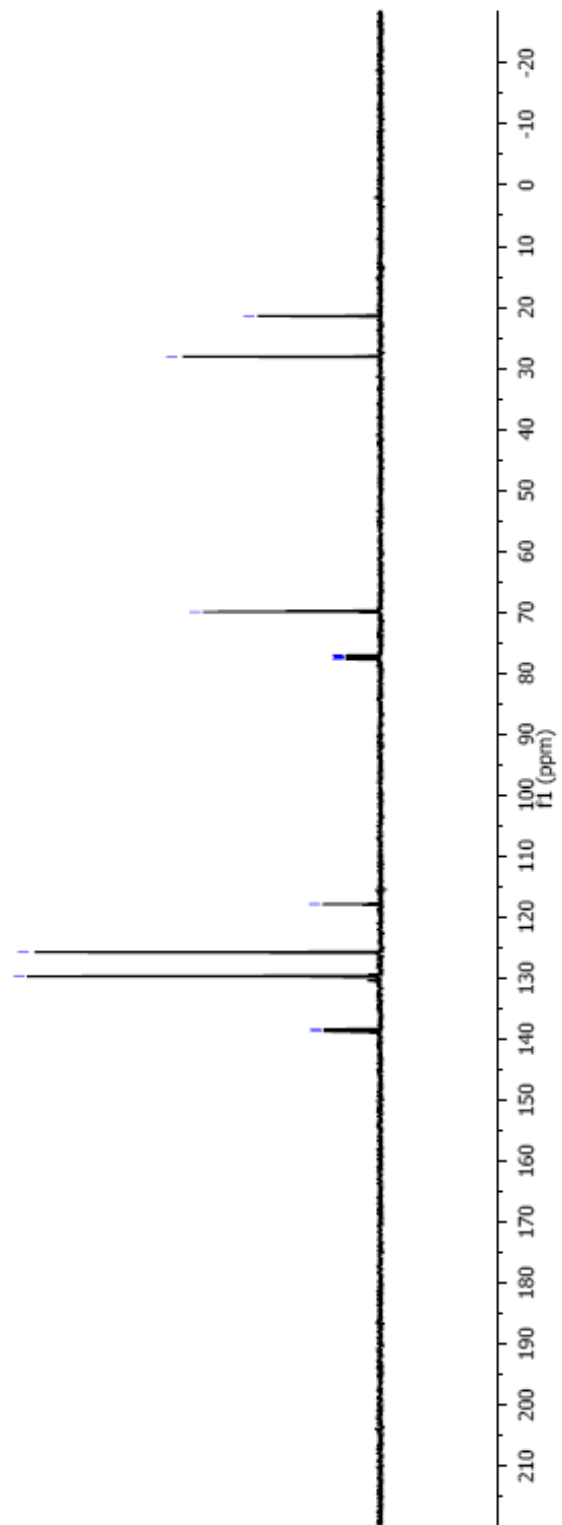


Table 1, entry 6



KW461, CDCl<sub>3</sub>  
400MHz  
YELLOW OIL

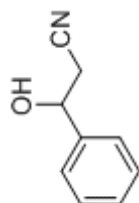
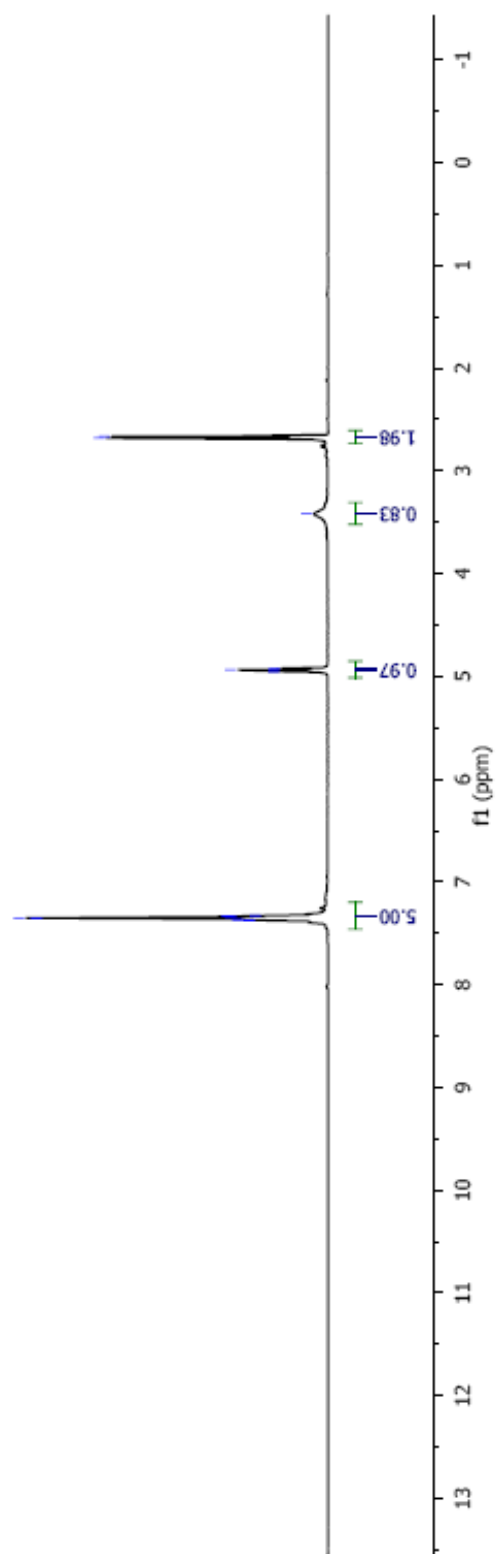
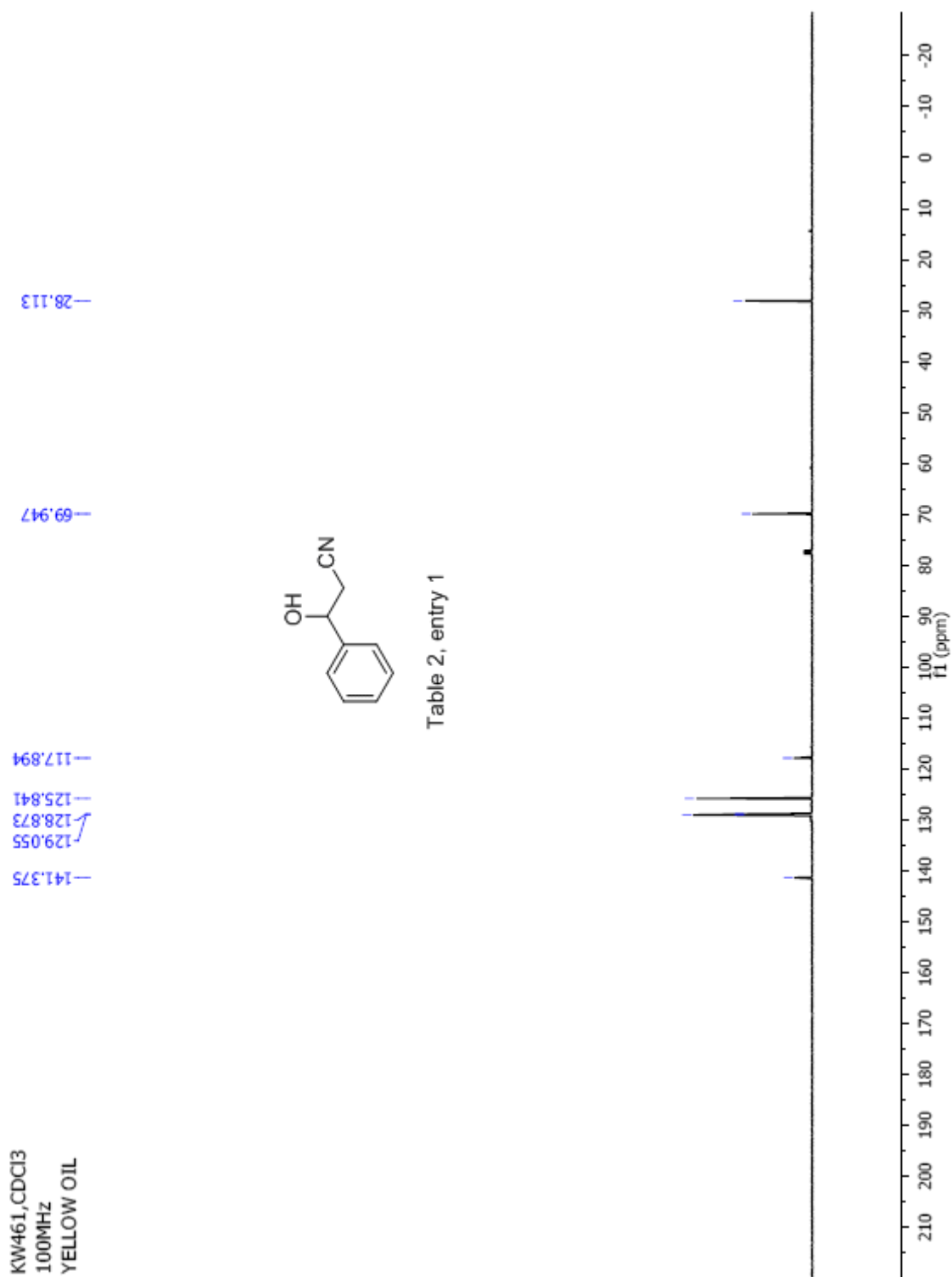


Table 2, entry 1







KW458, CDCl<sub>3</sub>  
400MHz  
02/14/08

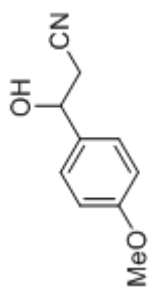
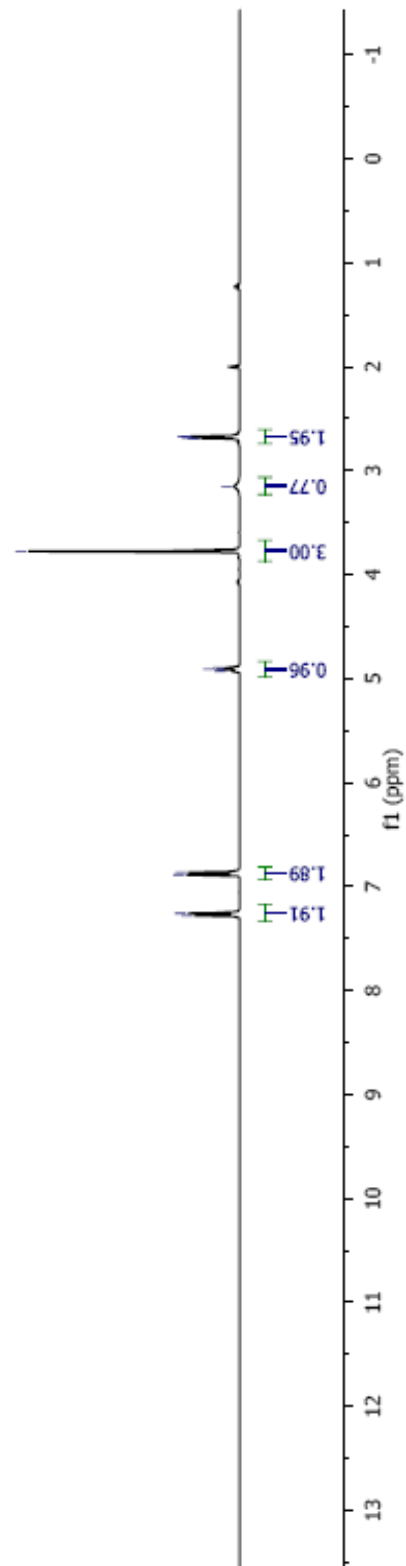
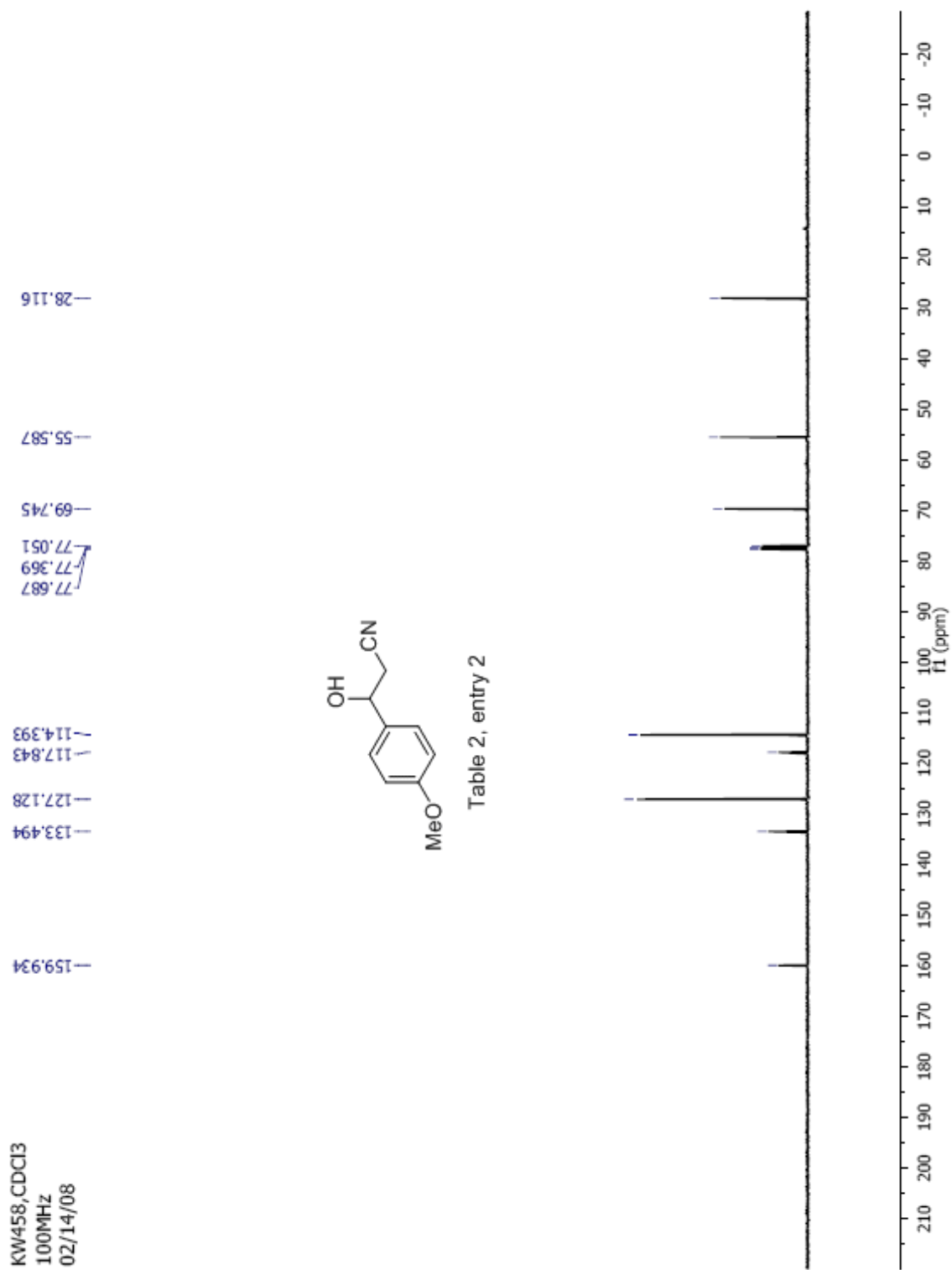
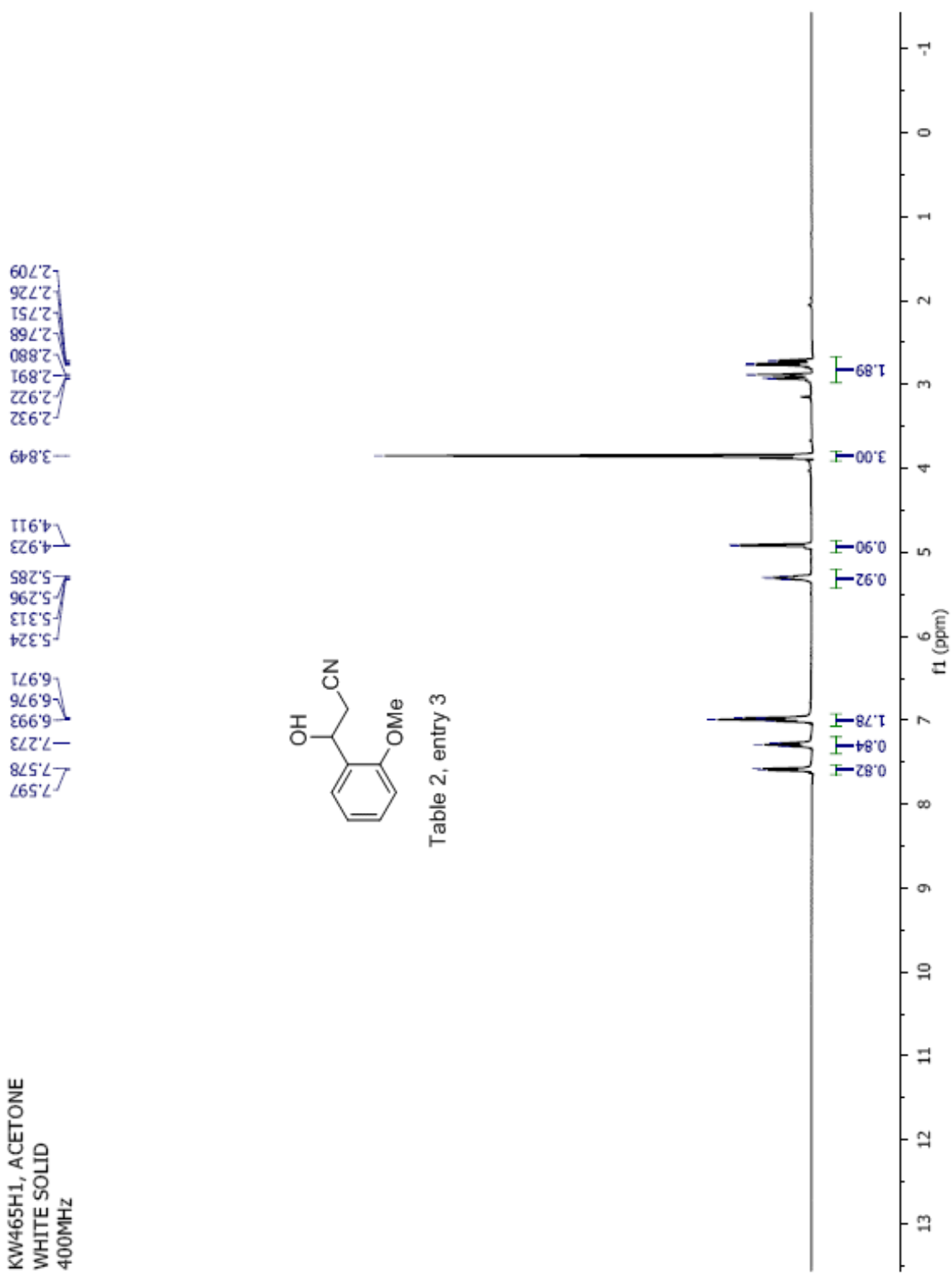
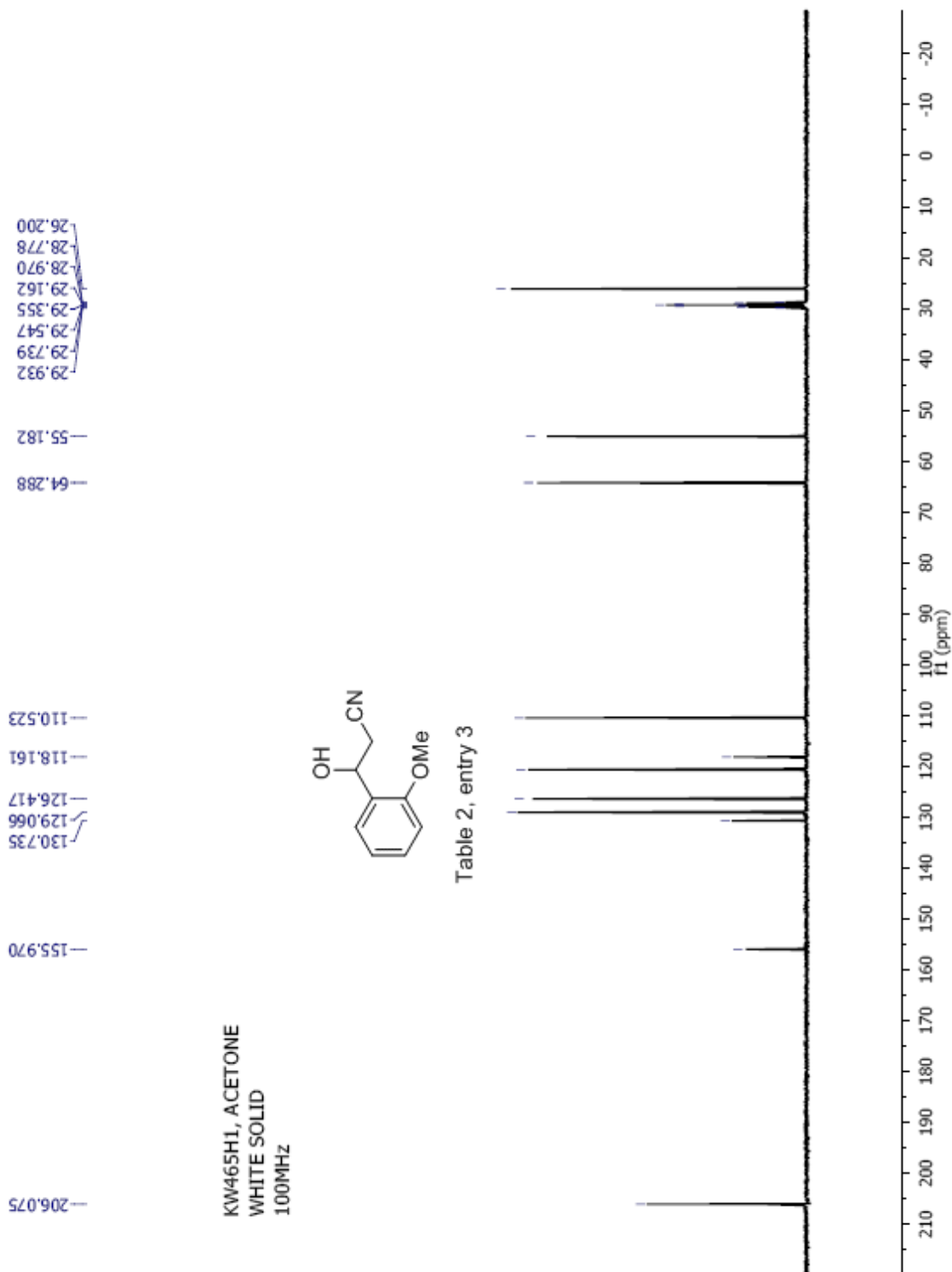


Table 2, entry 2











KW469, CDCl<sub>3</sub>  
400MHz  
COLORLESS OIL

7.668  
7.649  
7.644  
7.336  
7.289  
7.266  
7.247  
5.409  
5.400  
5.391  
3.180  
3.170  
2.912  
2.902  
2.870  
2.860  
2.722  
2.704  
2.680  
2.662

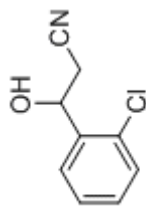
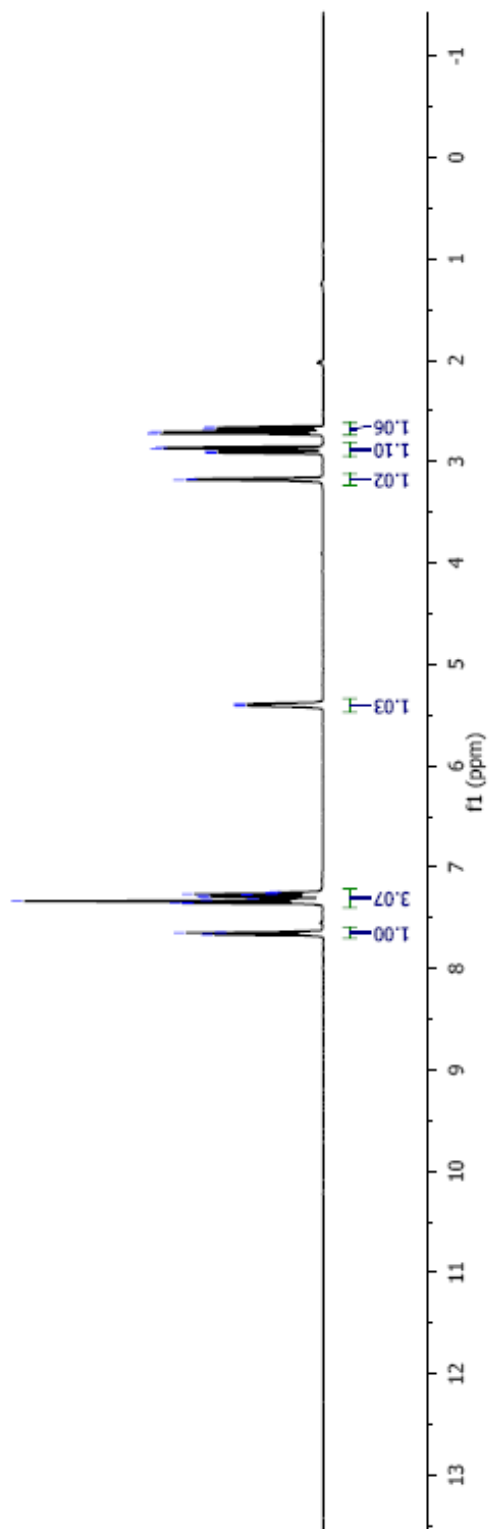


Table 2, entry 4



KW469, CDCl<sub>3</sub>  
100MHz  
COLORLESS OIL

138.579  
129.889  
127.764  
127.238  
117.507  
77.657  
77.339  
77.021  
66.547  
26.558

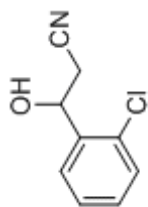
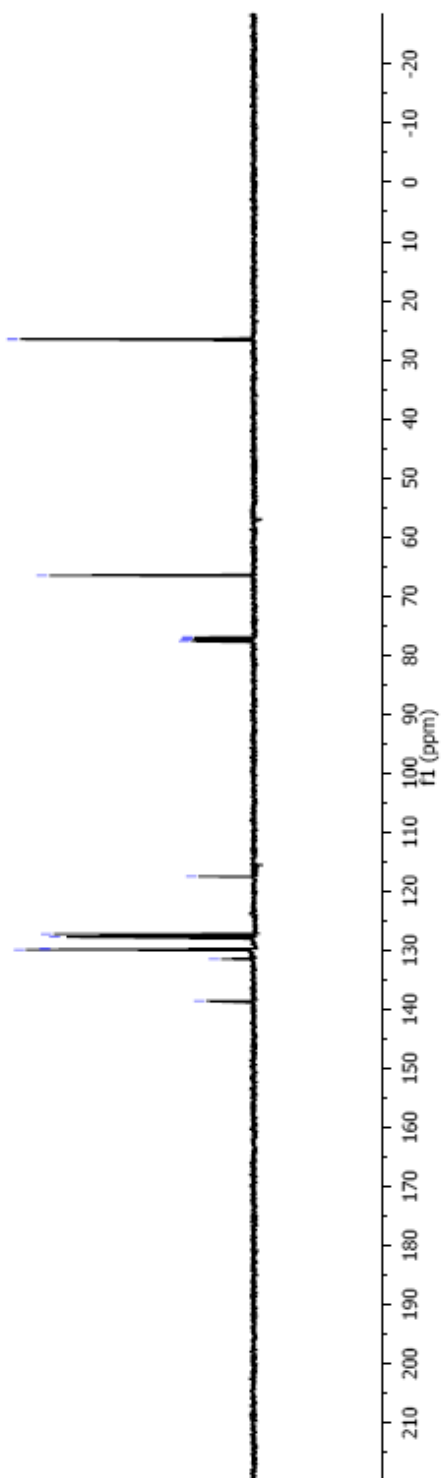


Table 2, entry 4



KW462, CDCl<sub>3</sub>  
400MHz  
WHITE SOLID

7.265  
6.829  
6.805  
6.767  
5.953  
4.935  
4.919  
4.912  
4.896  
2.821  
2.813  
2.709  
2.702  
2.693  
2.687

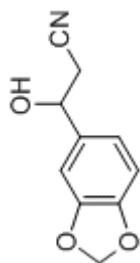
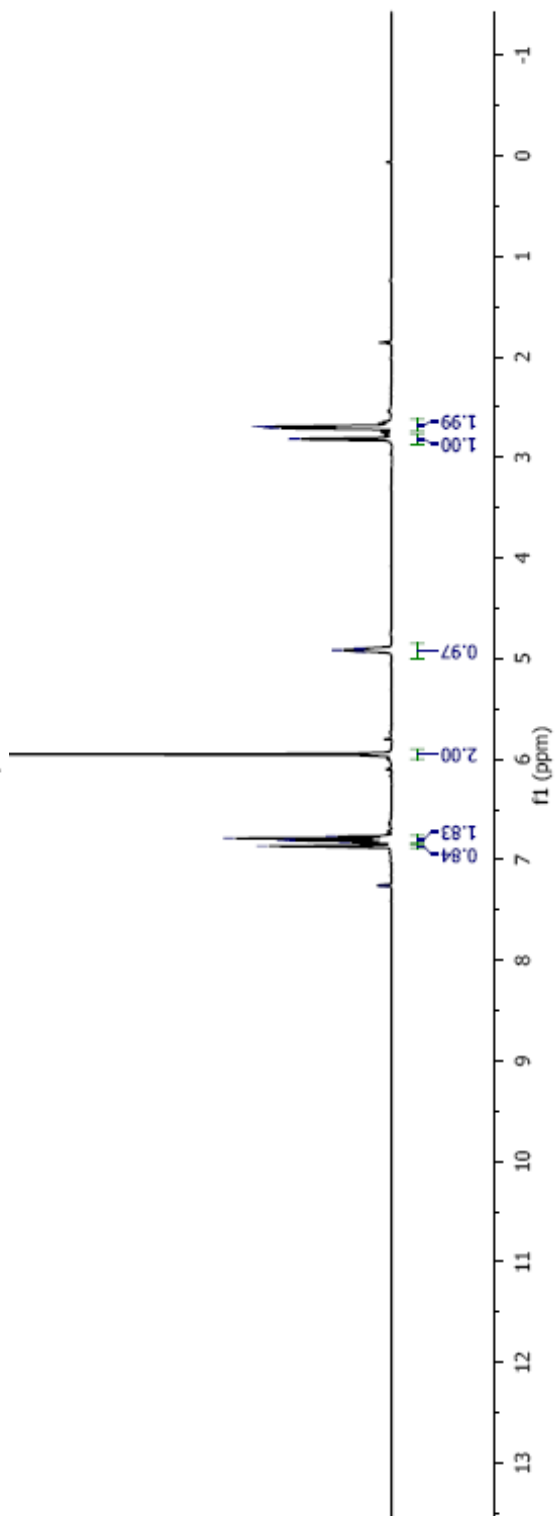
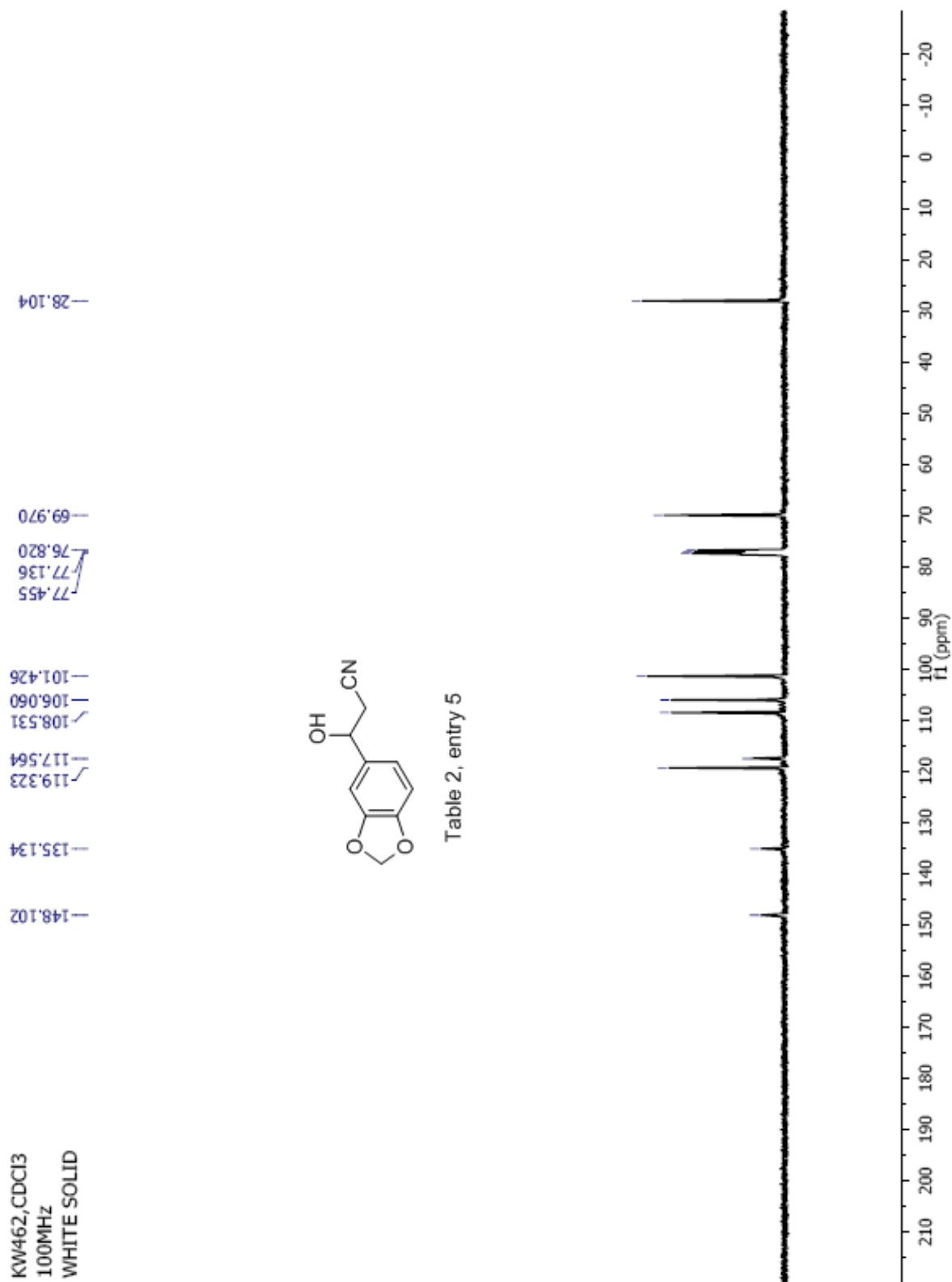


Table 2, entry 5





### Manual Peak Matching Report For Accurate Mass Determination

Theoretical mass	Experimental mass	PFK matching mass	Deviation*
191.05824	191.05876	180.98882	2.7 ppm

\* The deviation is obtained from the following equation:

$$\text{deviation} = \frac{\text{experimental mass} - \text{theoretical mass}}{\text{nominal mass}}$$

Where nominal mass takes in account only  $^{12}\text{C}$ ,  $^1\text{H}$ ,  $^{16}\text{O}$ ,  $^{14}\text{N}$  etc...

Theoretical mass correspond to the mass of the most abundant isotope peak

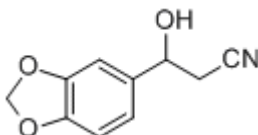
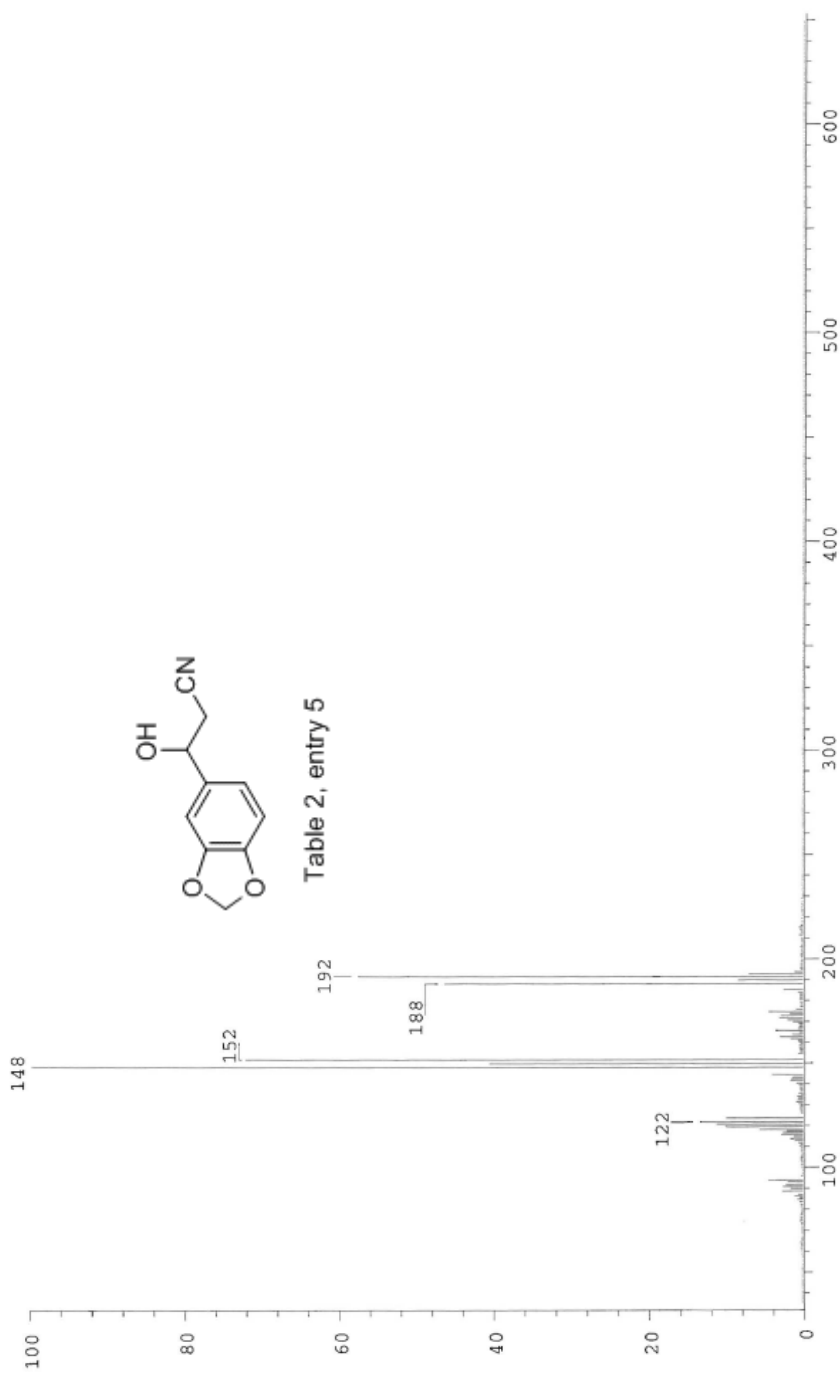


Table 2, entry 5

SPEC: fin084362.dat (06-APR-09 14:49:32)  
 Samp: KW462  
 Comm: DP/EI  
 Oper: kh  
 Base: 147.93  
 Peak: 1000.0 mmu  
 Scan 42 @ 0.71 min (EI +QlMS LMR UP LR)

Study: ms services  
 Masses: 35.01 > 650.00  
 Intensity: 5766834

Scans: 1 > 44  
 Client: Kuldeep  
 #Peaks: 633  
 RIC: 28025415  
 5.8E+06



Date: Mon Apr 6 14:51:42 2009 ICIS: 8.3.0 SP2 for OSFI (V4.0) build 98-238 from 26-Aug-98

KW463, ACETONE  
YELLOW SOLID  
400MHz

8.269  
8.248  
7.802  
7.780  
5.465  
5.454  
5.318  
5.306  
5.292  
5.280  
3.053  
3.041  
3.011  
2.999  
2.964  
2.948  
2.922  
2.906

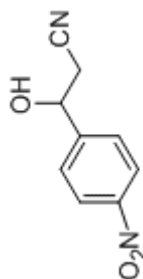
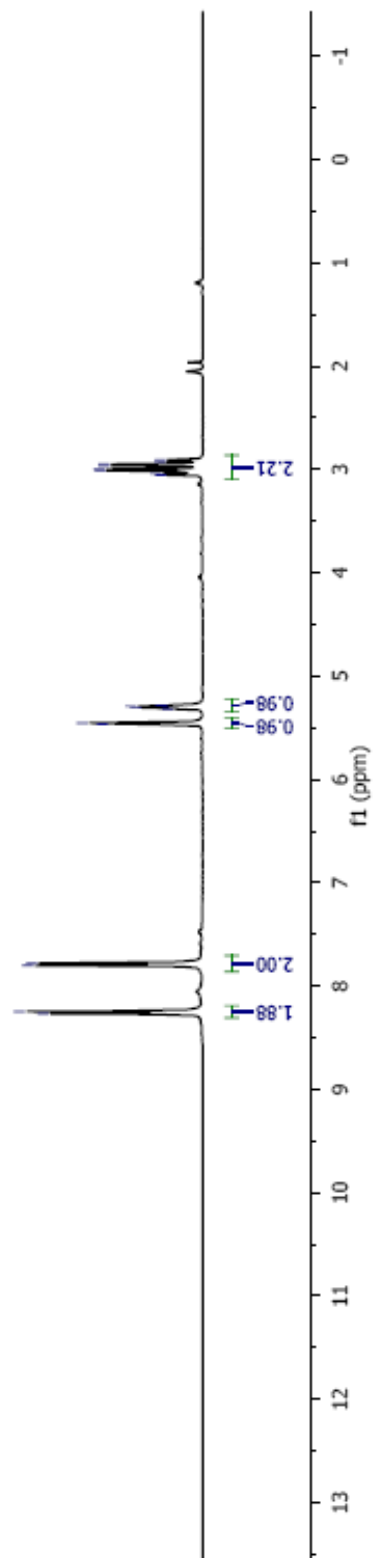
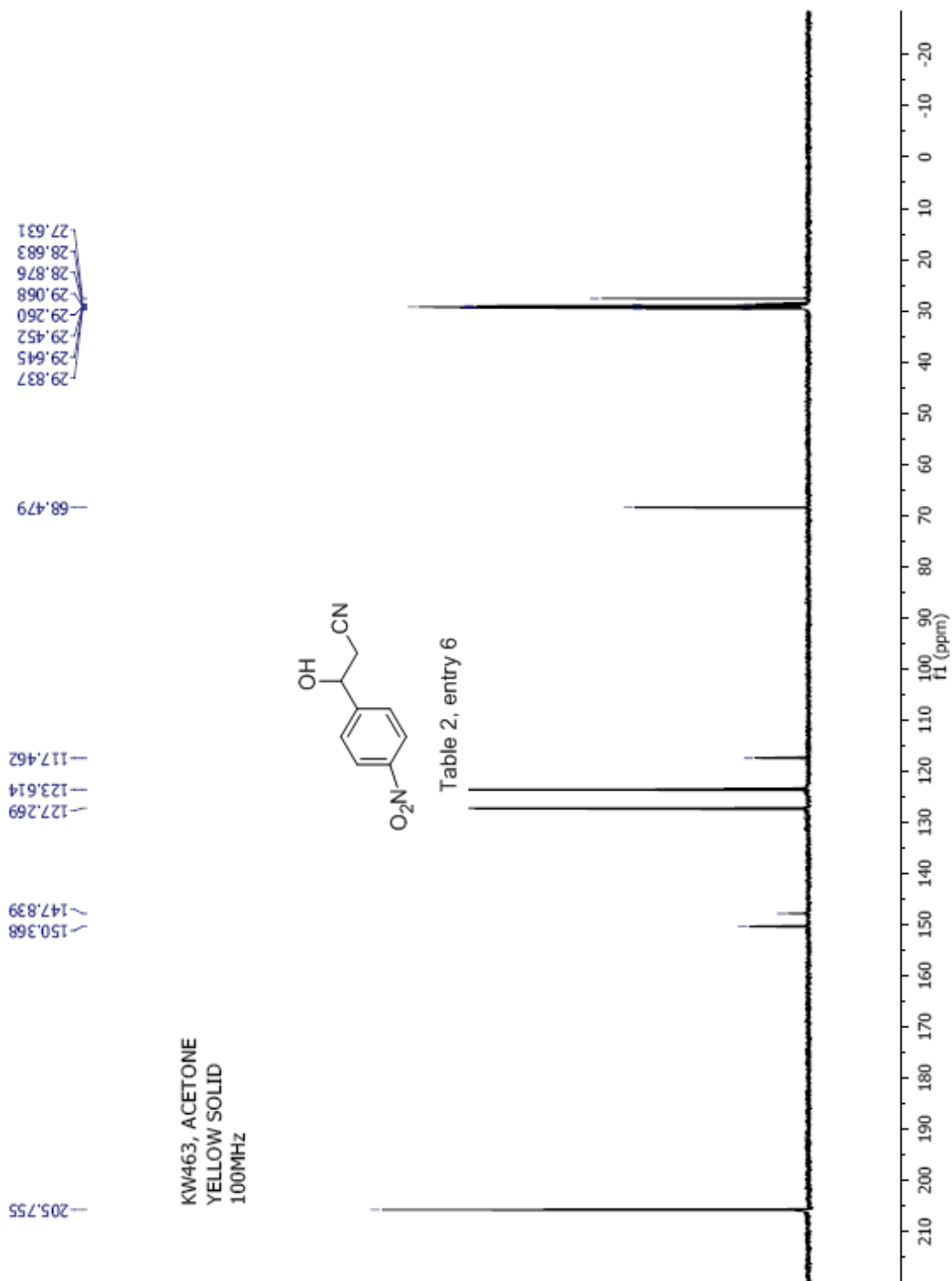


Table 2, entry 6









KW489H, CDCl<sub>3</sub>  
400MHz  
YELLOW OIL

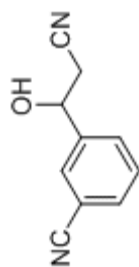
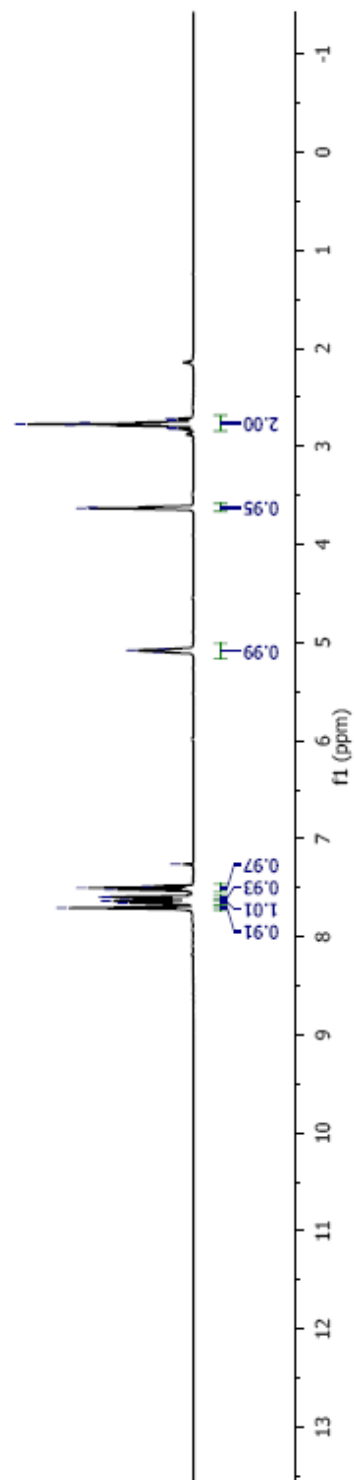


Table 2, entry 7



KW489C, CDCI3  
100MHz  
YELLOW OIL

142.942  
130.524  
129.597  
118.785  
117.232  
112.776  
77.683  
77.365  
77.047  
68.850  
28.300

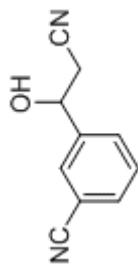
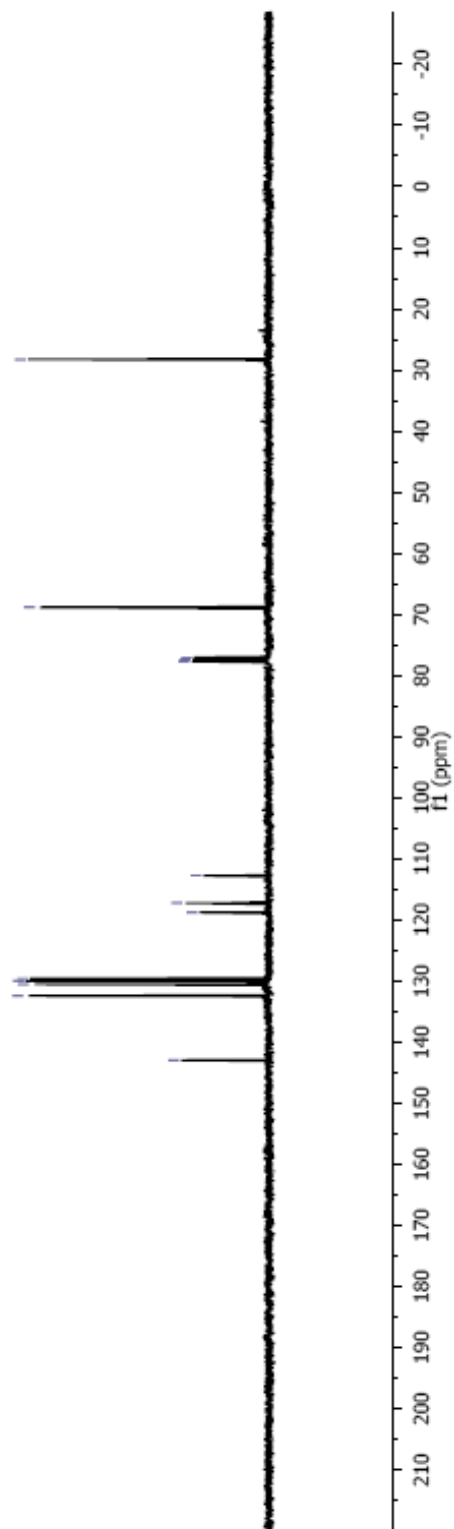


Table 2, entry 7



### Manual Peak Matching Report For Accurate Mass Determination

Theoretical mass	Experimental mass	PKF matching mass	Deviation*
172.06366	172.06395	168.98882	1.7 ppm

\* The deviation is obtained from the following equation:

$$\text{deviation} = \frac{\text{experimental mass} - \text{theoretical mass}}{\text{nominal mass}}$$

Where nominal mass takes in account only  $^{12}\text{C}$ ,  $^1\text{H}$ ,  $^{16}\text{O}$ ,  $^{14}\text{N}$  etc...

Theoretical mass correspond to the mass of the most abundant isotope peak

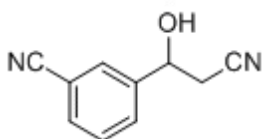


Table 2, entry 7

1/20

SPEC: fin083791.dat (22-JUL-08 11:05:49)  
 Samp: KW489  
 Comm: SP 70 eV EI  
 Oper: kh  
 Base: 131.91  
 Peak: 1000.0 mmu  
 Scan 73 @ 1.65 min (EI +Q1MS LMR UP LR)  
 Study: MS services  
 Masses: 35.01 > 650.00  
 Intensity: 16777215  
 Scans: 1 > 74  
 Client: Kuldup  
 #Peaks: 651  
 RIC: 137516812  
 1.7E+07

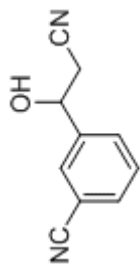
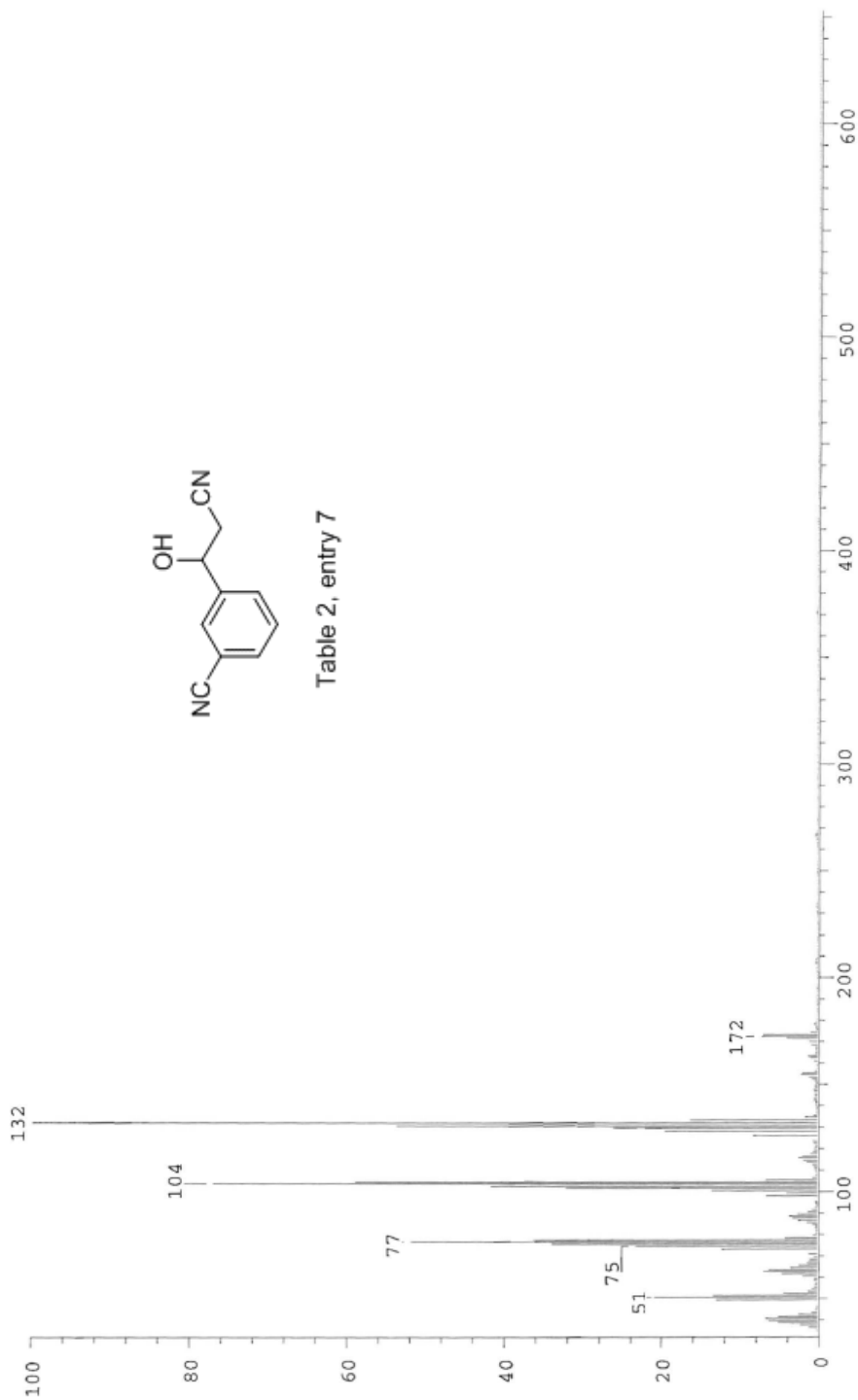


Table 2, entry 7



Date: Tue Jul 22 11:07:55 2008 ICIS: 8.3.0 SP2 for OSFI (V4.0) build 98-238 from 26-Aug-98

KW482, CDC13  
300MHz  
YELLOW OIL

8.01  
7.98  
7.46  
7.43  
5.08  
5.07  
3.89  
3.28  
3.27  
2.76  
2.74

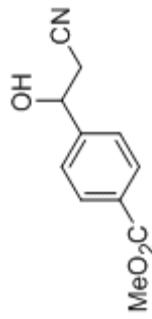
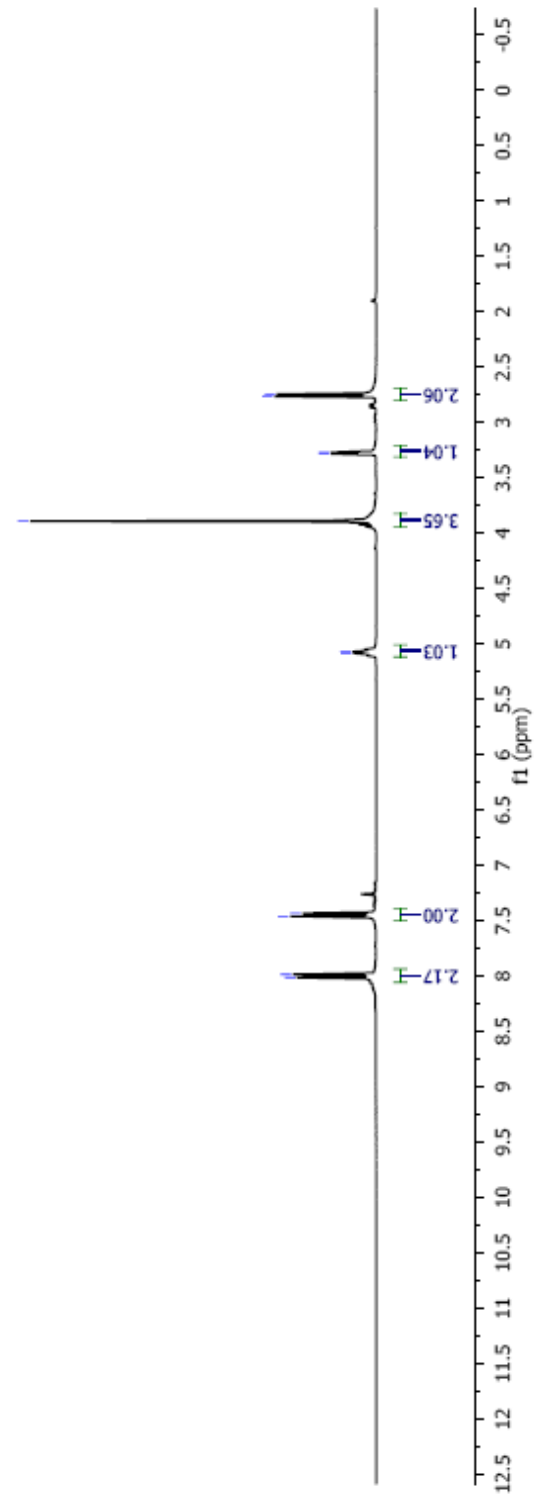
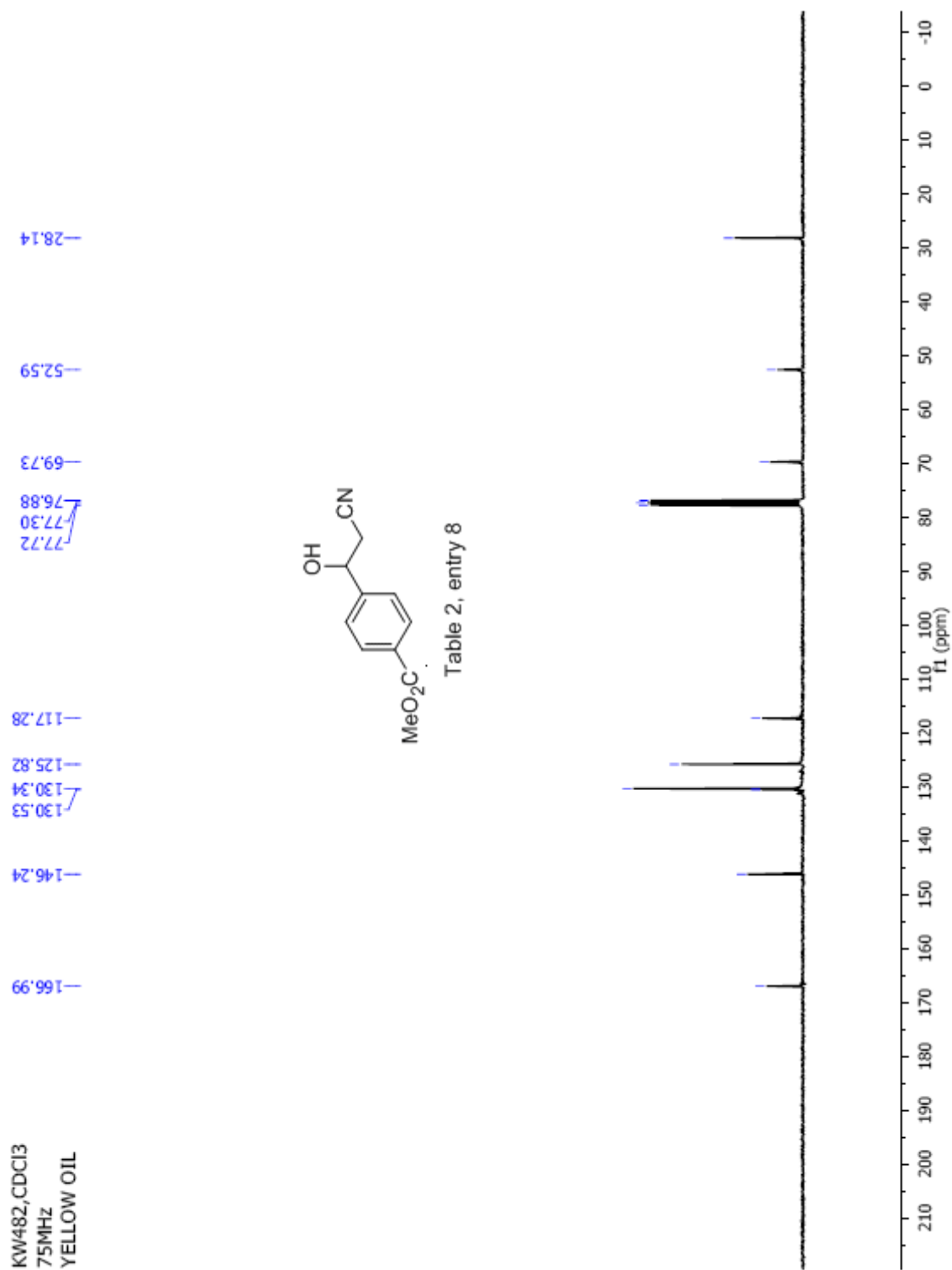


Table 2, entry 8





### Manual Peak Matching Report For Accurate Mass Determination

Theoretical mass	Experimental mass	PFK matching mass	Deviation*
205.07389	205.07416	180.98882	1.3 ppm

\* The deviation is obtained from the following equation:

$$\text{deviation} = \frac{\text{experimental mass} - \text{theoretical mass}}{\text{nominal mass}}$$

Where nominal mass takes in account only  $^{12}\text{C}$ ,  $^1\text{H}$ ,  $^{16}\text{O}$ ,  $^{14}\text{N}$  etc...

Theoretical mass correspond to the mass of the most abundant isotope peak

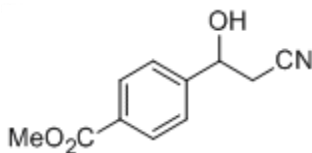


Table 2, entry 8

*Handwritten signature*

Scans: 1 > 84  
 Client: Kuldeep  
 #Peaks: 637  
 RIC: 18425668  
 6.8E+06

SPEC: fin084361.dat (06-APR-09 14:45:04)  
 Samp: KW482  
 Comm: DP/EI  
 Oper: kh  
 Base: 164.65  
 Peak: 1000.0 mmu  
 Scan 60 @ 0.94 min (EI +QIMS LMR UP LR)

Study: ms services  
 Masses: 35.01 > 650.00  
 Intensity: 6828005

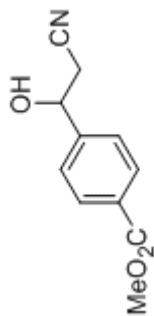
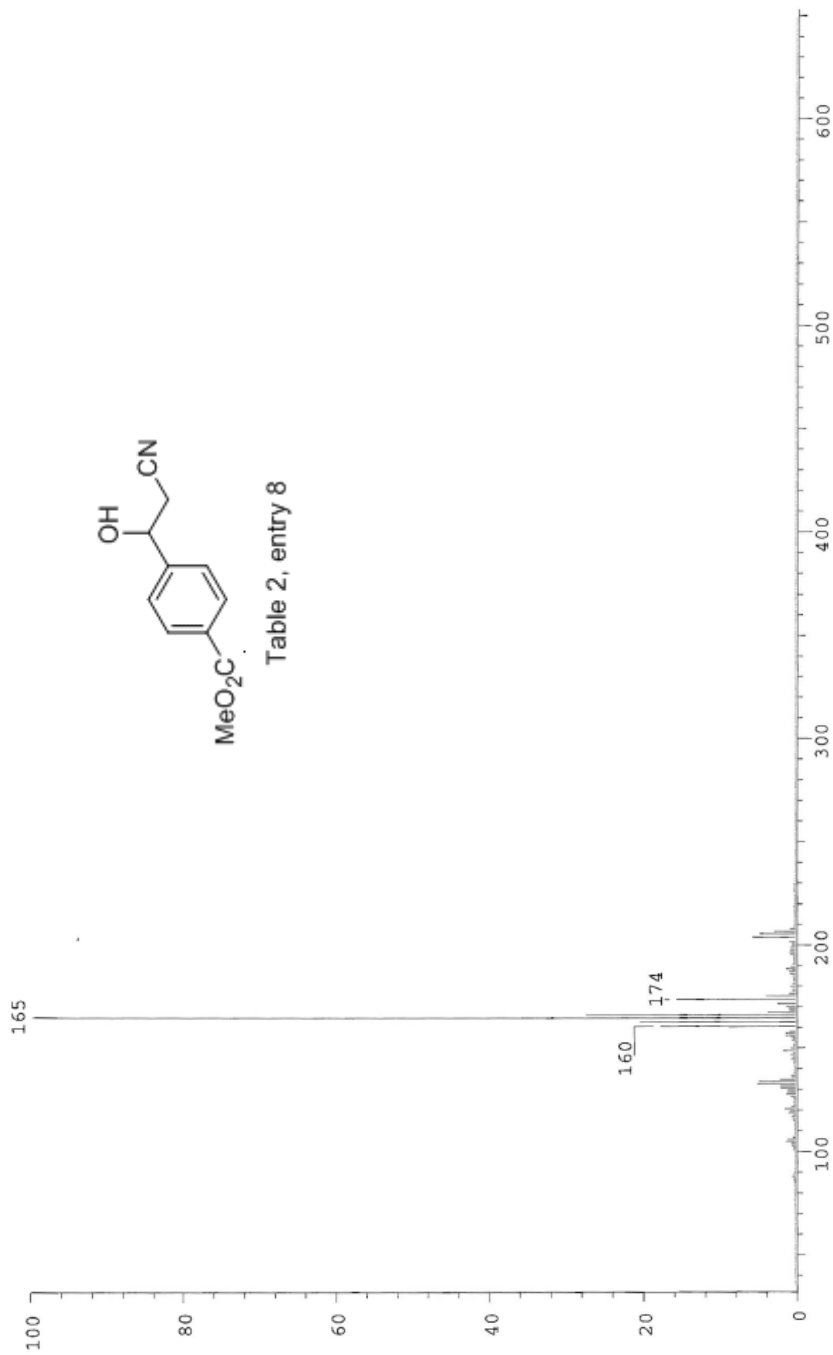
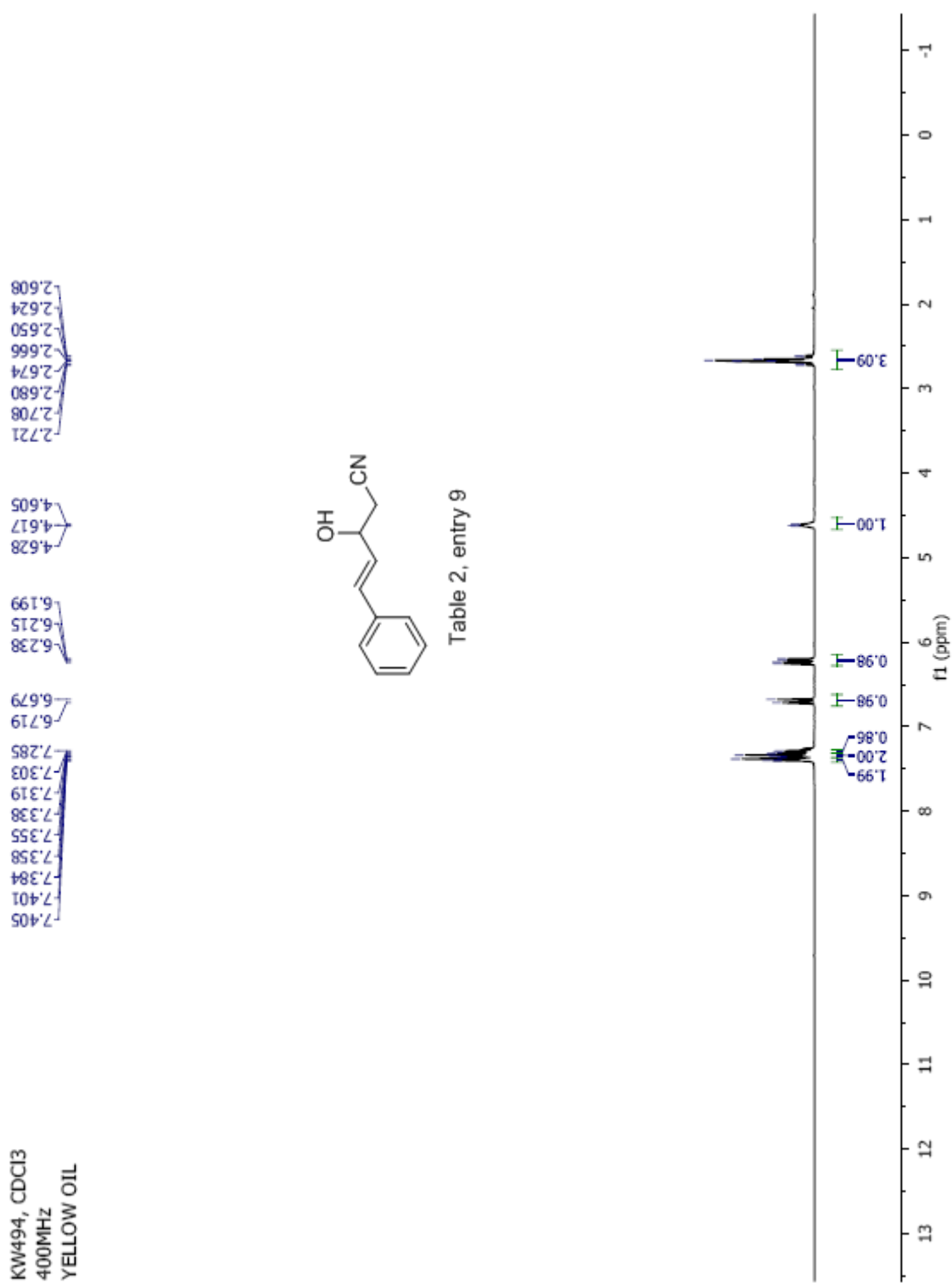
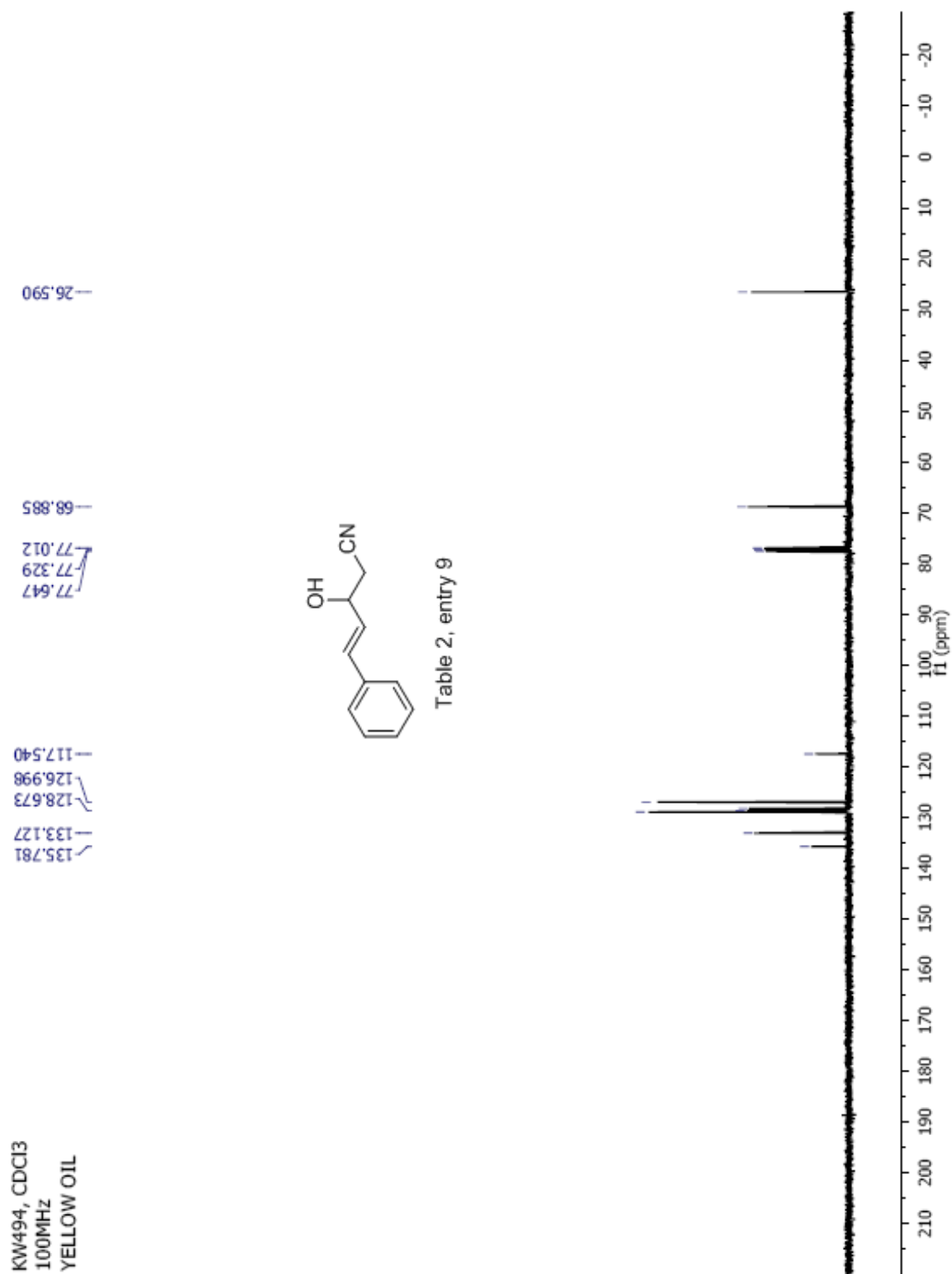


Table 2, entry 8

Date: Mon Apr 6 14:47:58 2009 ICIS: 8.3.0 SP2 for OSF1 (V4.0) build 98-238 from 26-Aug-98







KW486H, CDCl<sub>3</sub>  
300MHz  
COLORLESS OIL

3.901  
2.521  
2.504  
2.486  
2.464  
2.430  
2.409  
1.545  
1.258  
0.851  
0.833

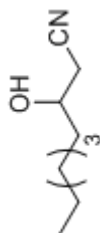
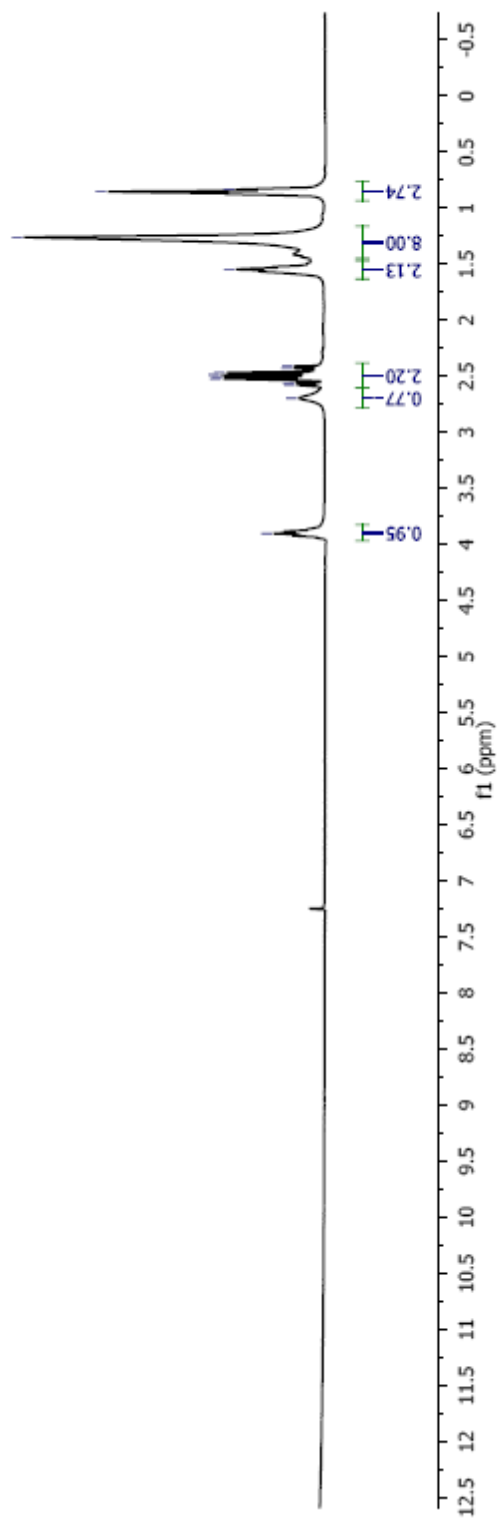


Table 2, entry 10



KW486C, CDC13  
75MHz  
COLORLESS OIL

36.705  
31.863  
26.286  
25.551  
22.747  
14.246

77.725  
77.301  
76.877  
67.907

118.131

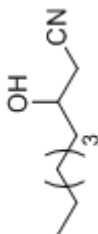
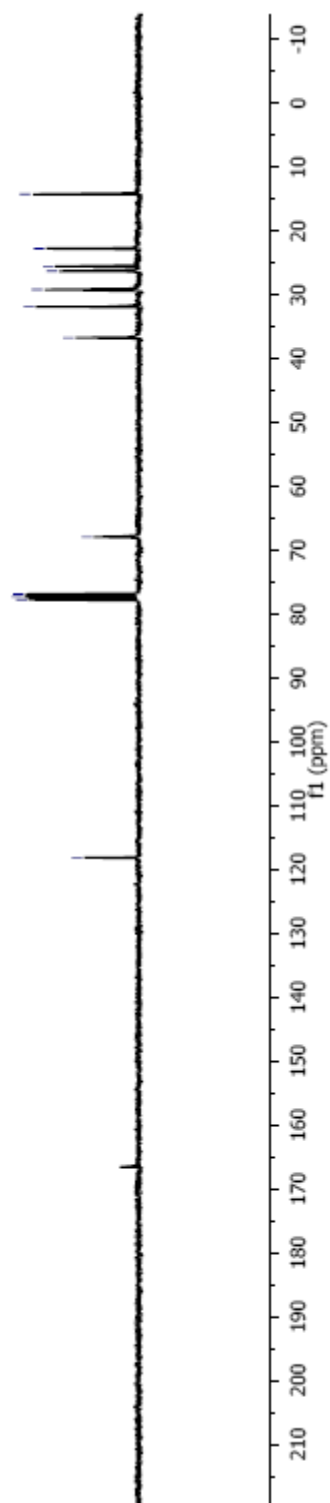


Table 2, entry 10



KW495, CDCl<sub>3</sub>  
400MHz  
COLORLESS OIL

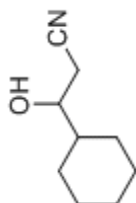
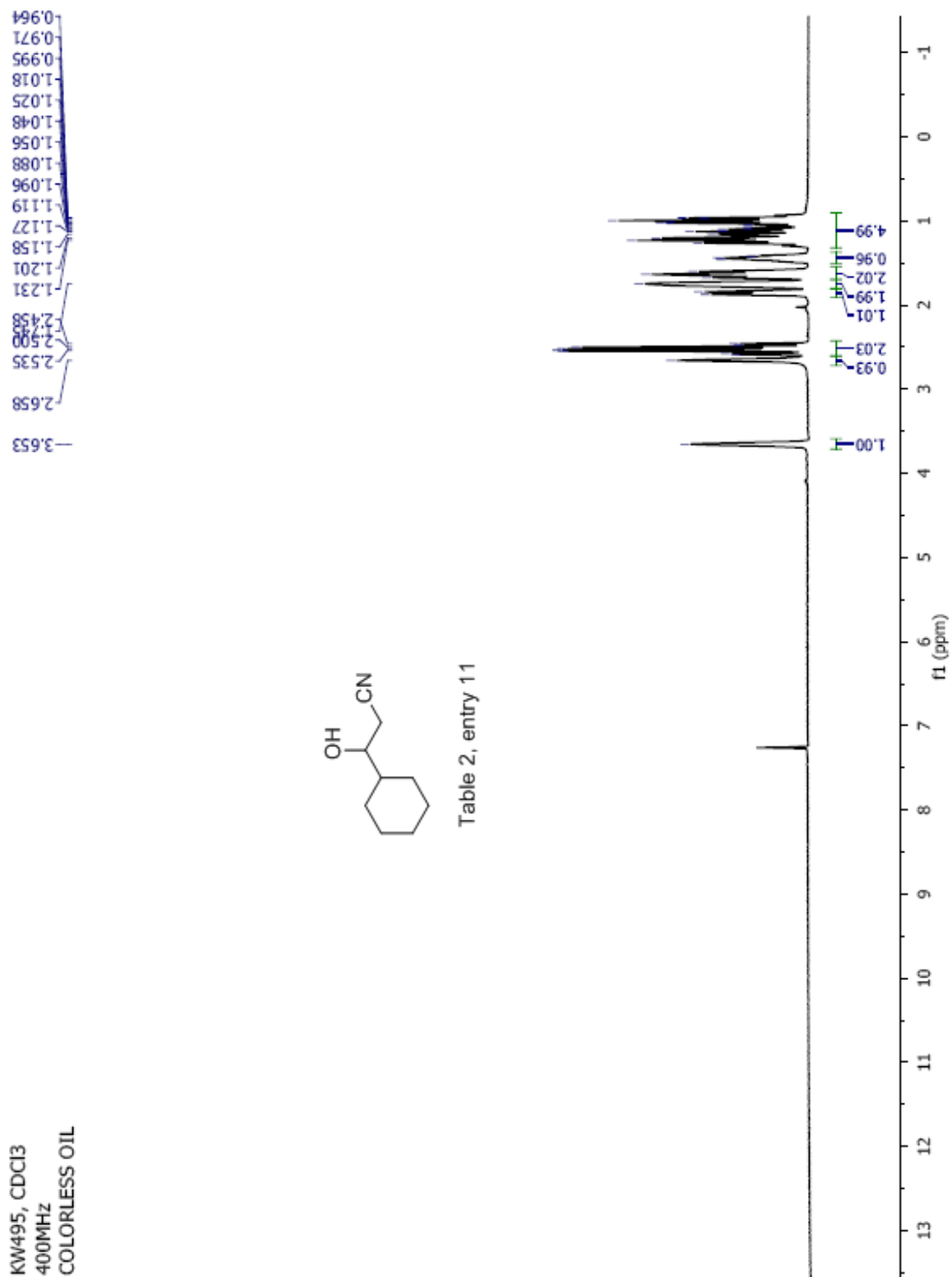


Table 2, entry 11



KW495, CDCl<sub>3</sub>  
100MHz  
COLORLESS OIL

118.612  
77.654  
77.336  
77.018  
72.080  
43.032  
29.118  
28.099  
26.345  
26.094  
25.927  
23.818

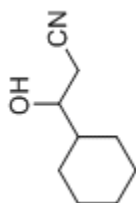
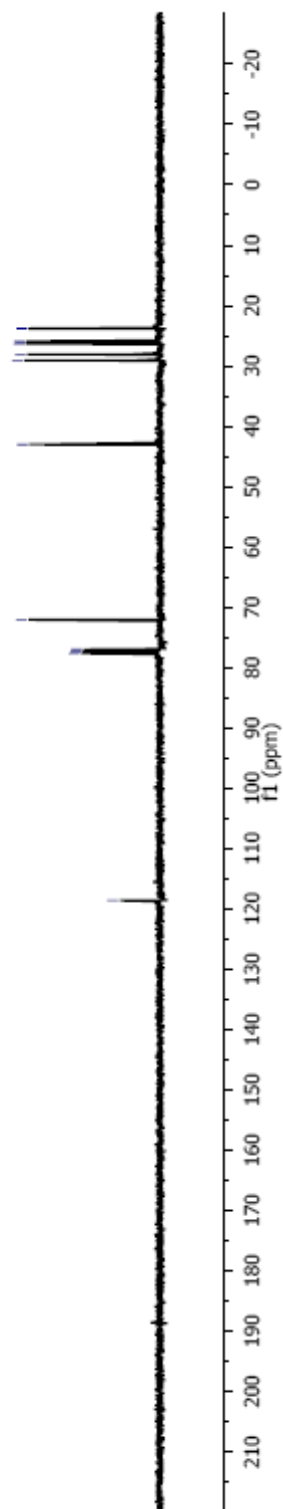


Table 2, entry 11



KW485, CDCl<sub>3</sub>  
400MHz  
YELLOW OIL

7.324  
7.322  
7.312  
7.309  
7.258  
7.086  
7.077  
7.015  
7.006  
7.003  
6.994  
5.306  
5.290  
5.279  
5.264  
2.876  
2.871  
2.859  
2.856  
2.844

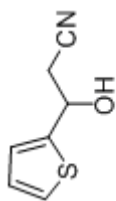
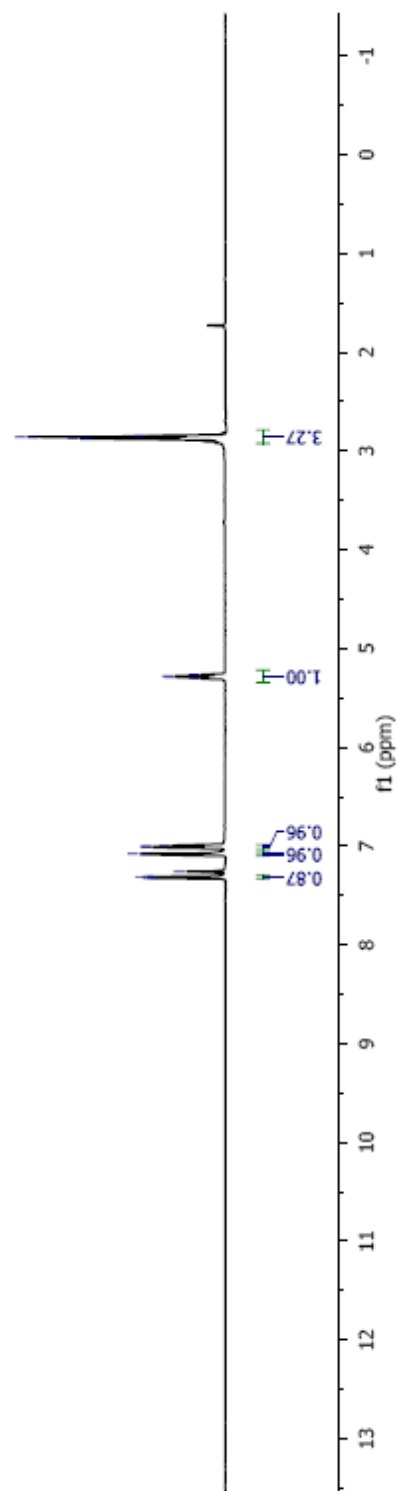
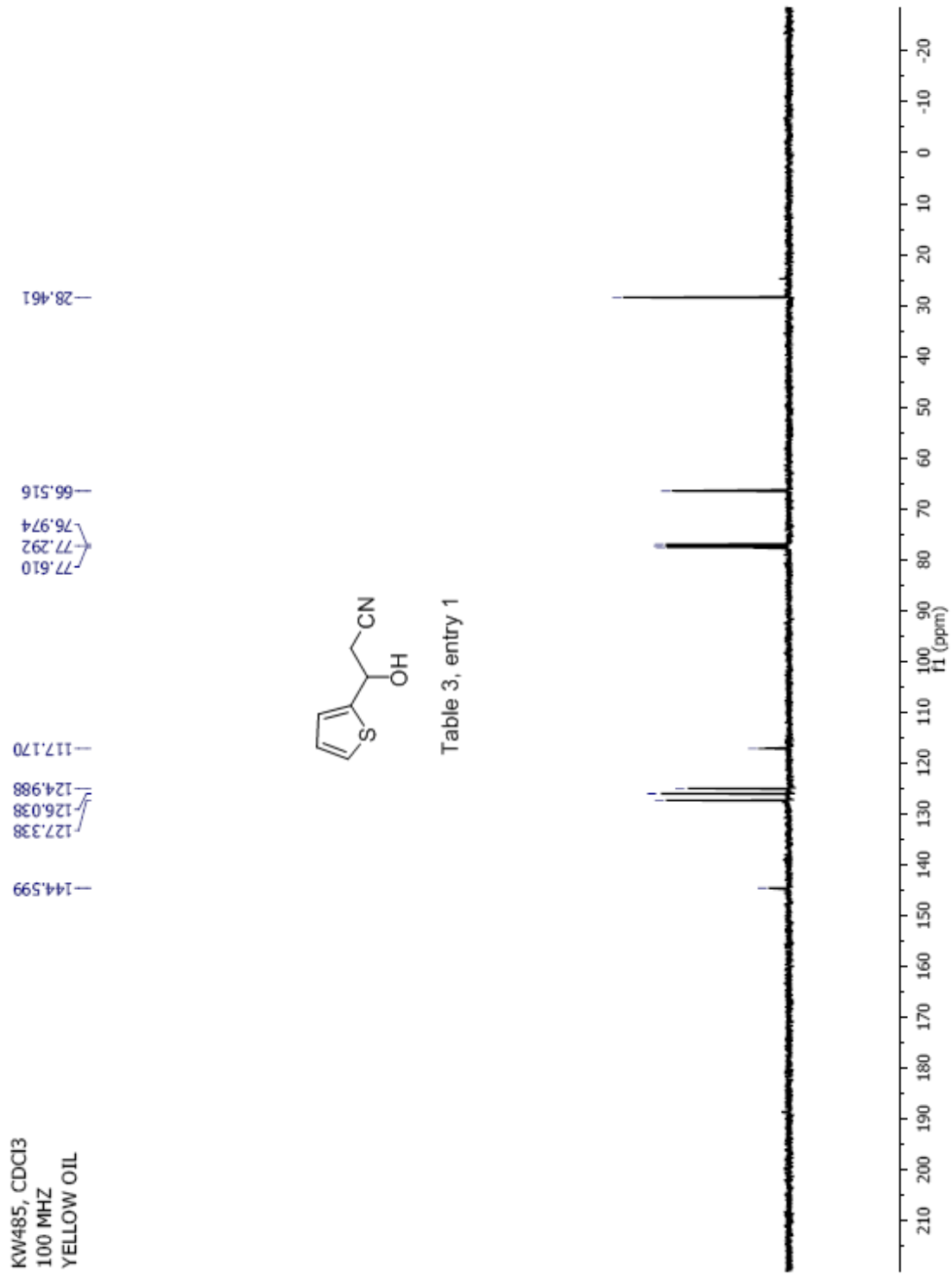


Table 3, entry 1







KW612, ACETONE  
400MHz  
YELLOW SOLID

7.92  
7.90  
7.81  
7.79  
7.40  
7.34  
7.32  
5.68  
5.67  
5.45  
5.44  
5.43  
3.87  
3.08  
3.06  
3.04  
2.05

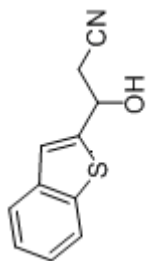
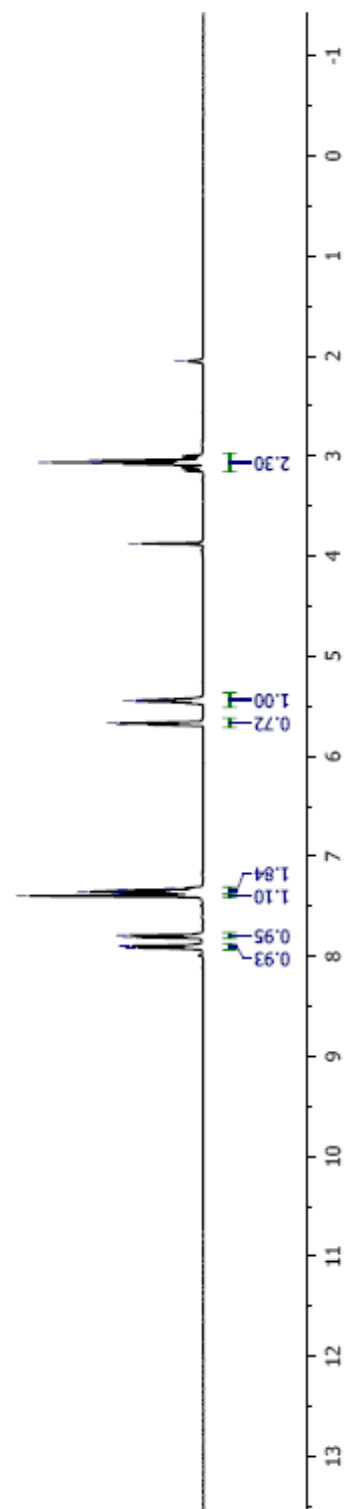
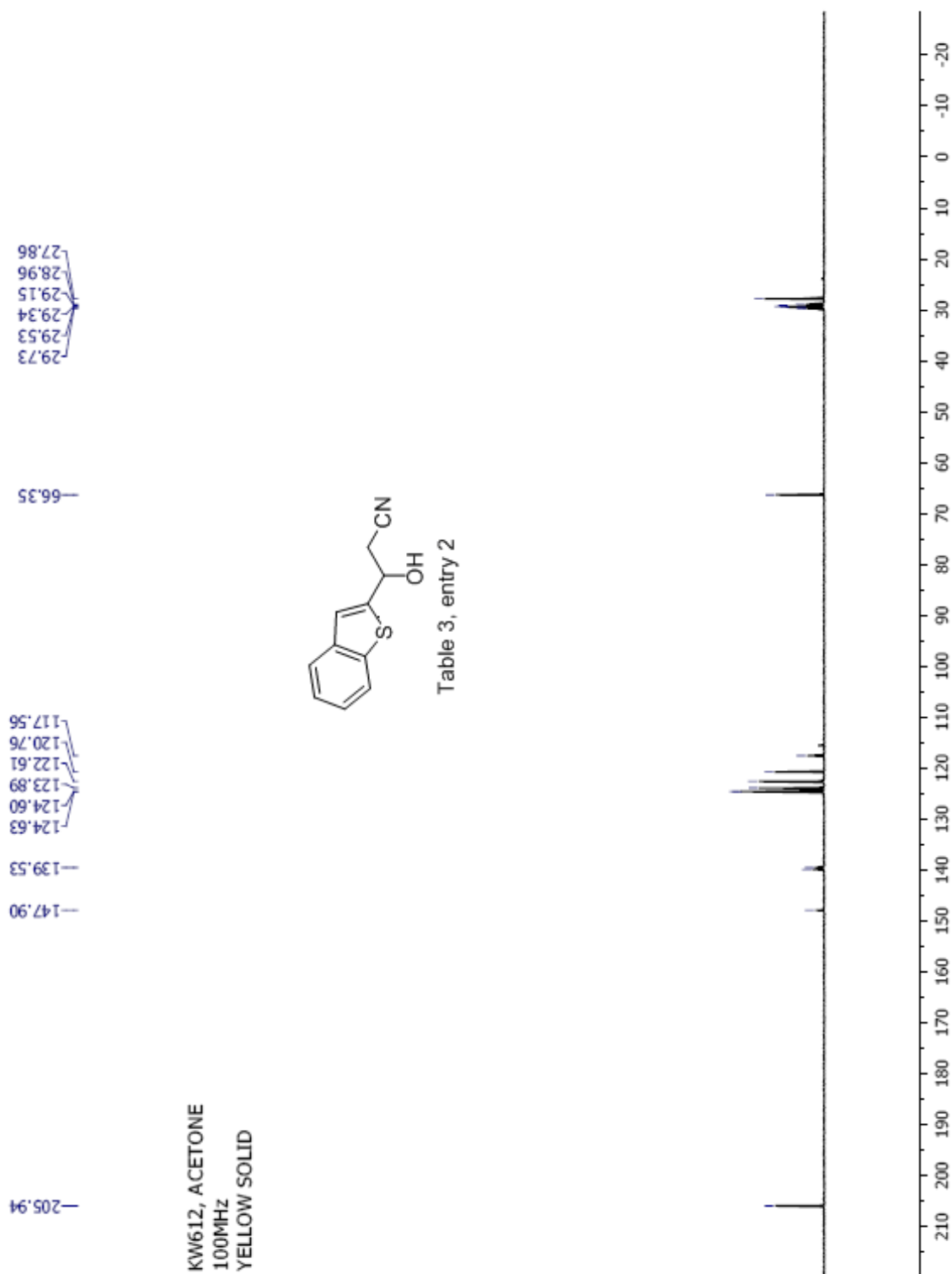
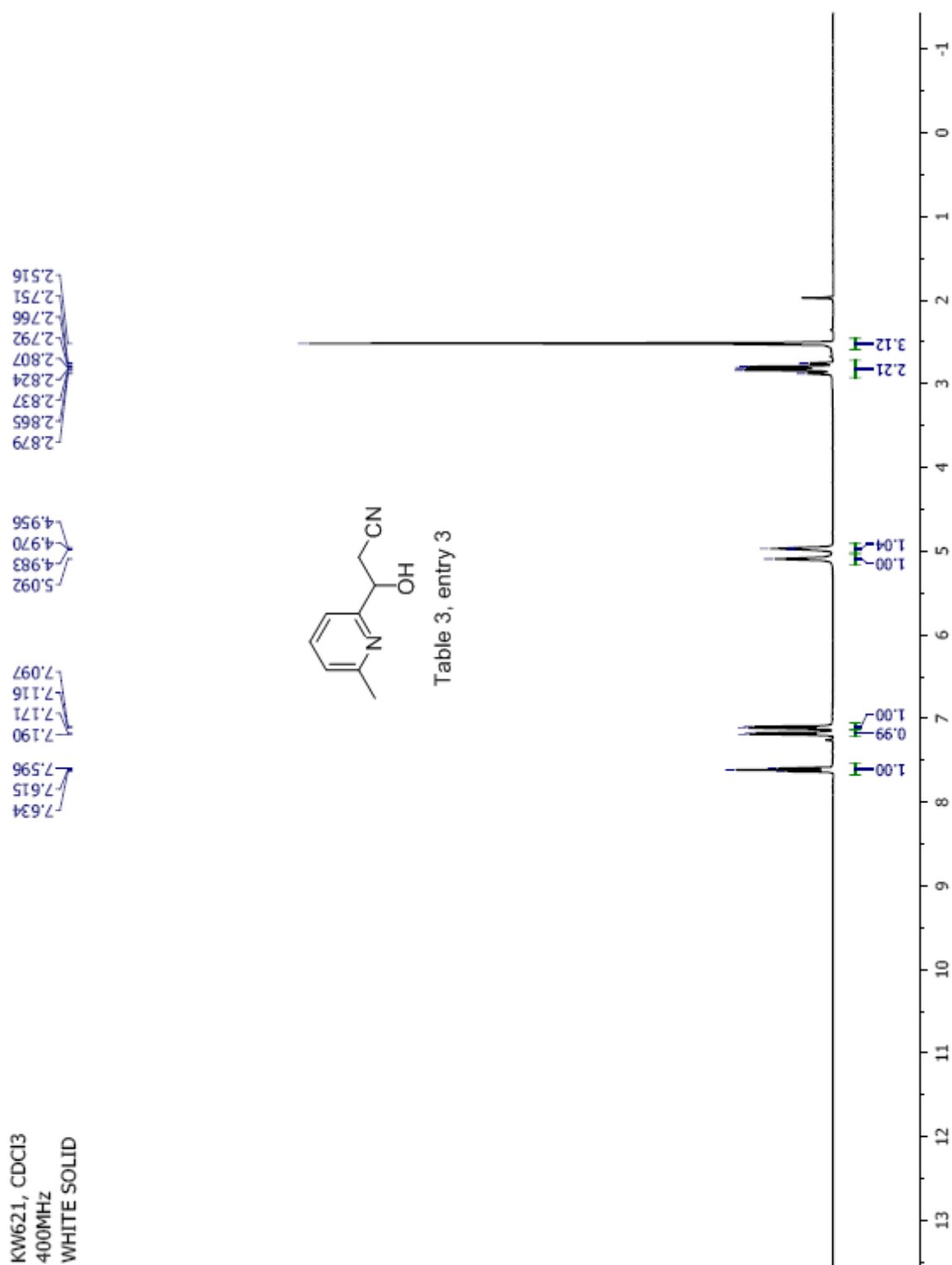
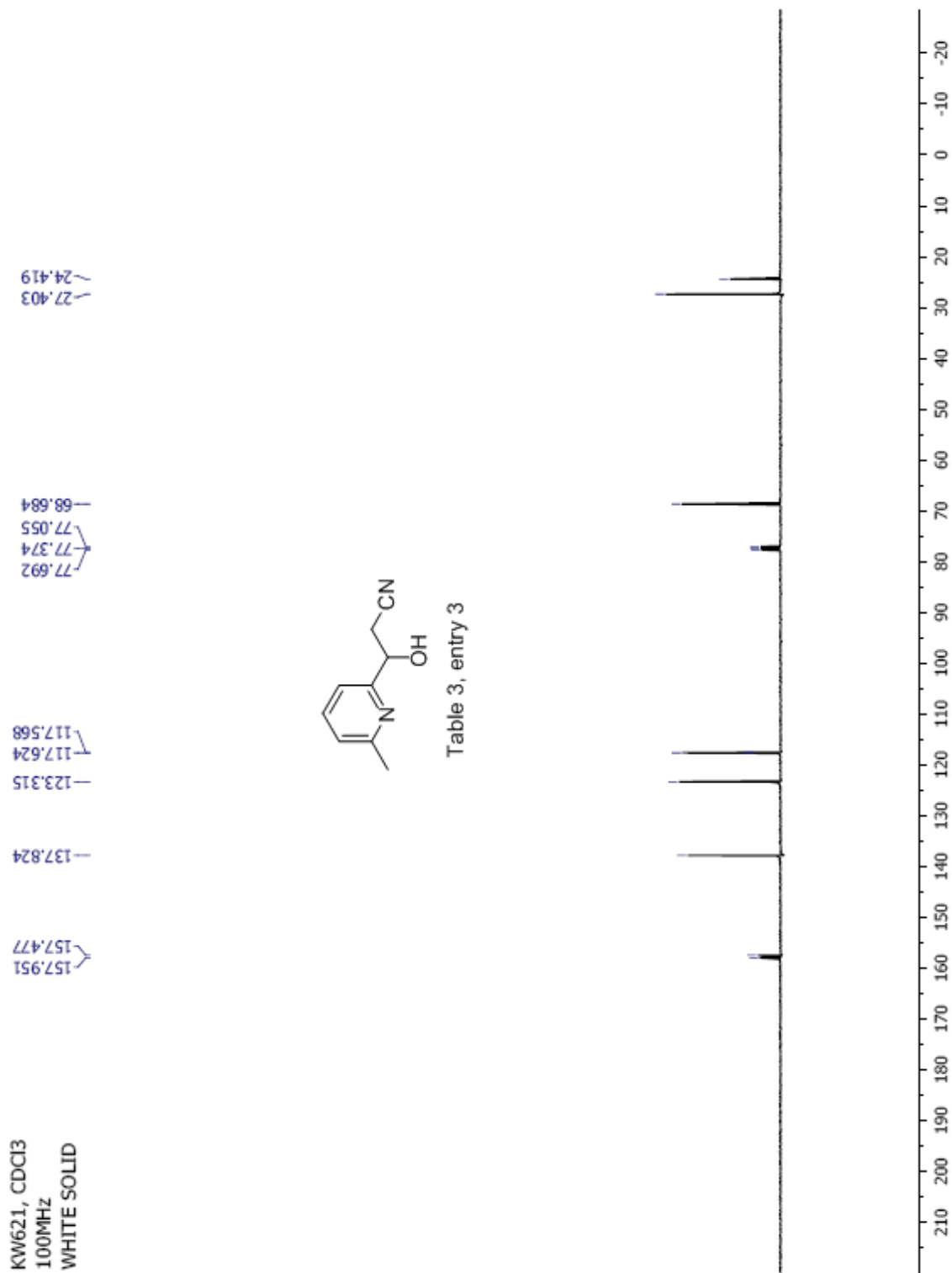


Table 3, entry 2









### Manual Peak Matching Report For Accurate Mass Determination

Theoretical mass	Experimental mass	PFK matching mass	Deviation*
162.07931	162.07961	130.99201	1.8 ppm

\* The deviation is obtained from the following equation:

$$\text{deviation} = \frac{\text{experimental mass} - \text{theoretical mass}}{\text{nominal mass}}$$

Where nominal mass takes in account only  $^{12}\text{C}$ ,  $^1\text{H}$ ,  $^{16}\text{O}$ ,  $^{14}\text{N}$  etc...

Theoretical mass correspond to the mass of the most abundant isotope peak

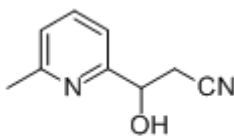


Table 3, entry 3

*Handwritten signature*

Scans: 1 > 13  
 Client: Kuldup  
 #Peaks: 665  
 RIC: 2630508 2.4E+05

SPEC: fin063649.dat (19-MAY-08 10:47:44)  
 Samp: KW621  
 Comm: 70 eV EI  
 Oper: kh  
 Base: 64.82  
 Peak: 1000.0 mmu  
 Scan 1 @ 0.16 min (EI +QIMS LMR UP LR)

Study: Service  
 Masses: 35.01 > 650.00  
 Intensity: 237074

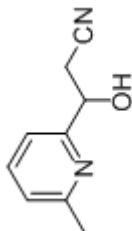
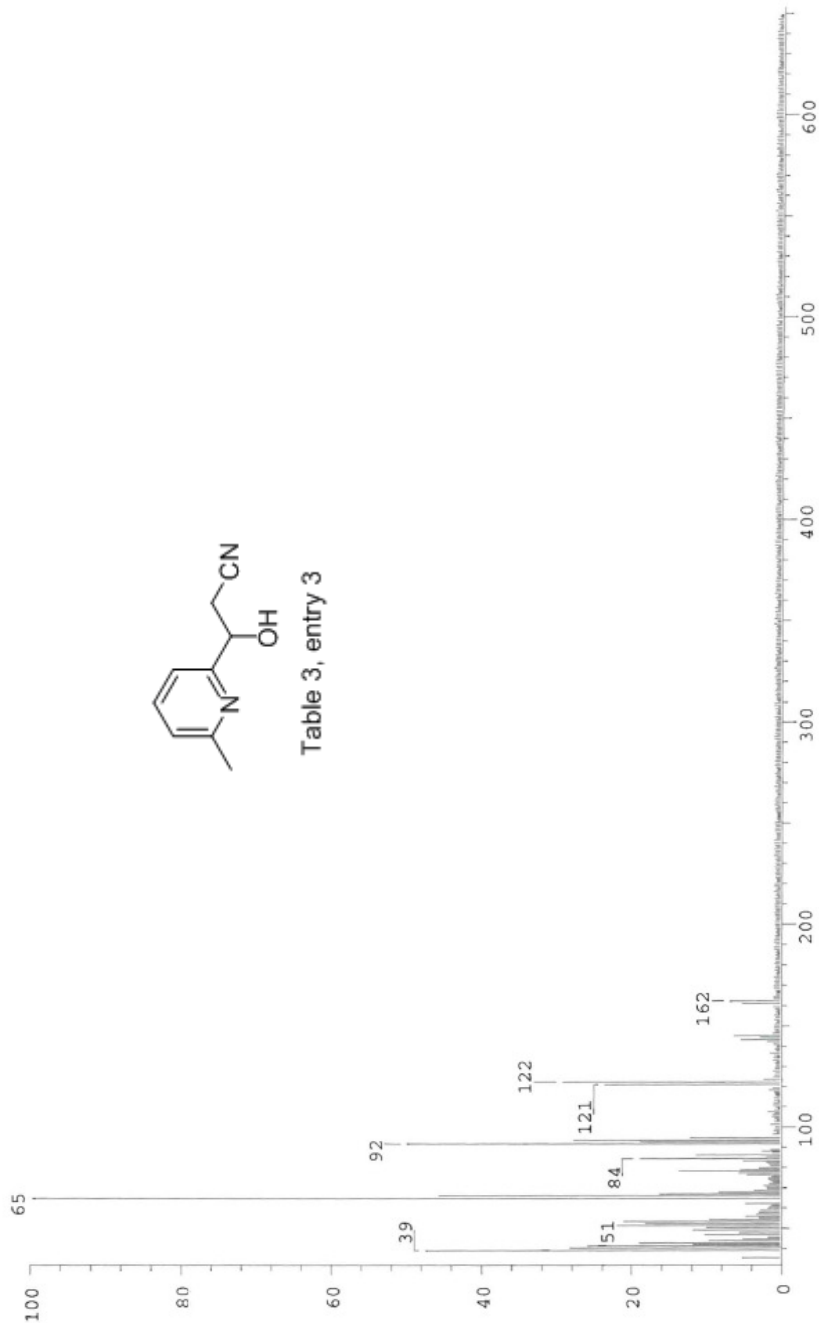


Table 3, entry 3



Date: Mon May 19 10:48:26 2008 ICIS: 8.3.0 SP2 for OSF1 (V4.0) build 98-238 from 26-Aug-98

KW632, CDCL<sub>3</sub>  
400MHz  
YELLOW OIL

7.6418  
7.6228  
7.6034  
7.4693  
7.4521  
7.2592  
5.0483  
5.0350  
4.0382  
4.0245  
2.9764  
2.9636  
2.9345  
2.9220  
2.9096  
2.8792  
2.8634  
2.8377  
2.8217

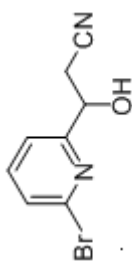
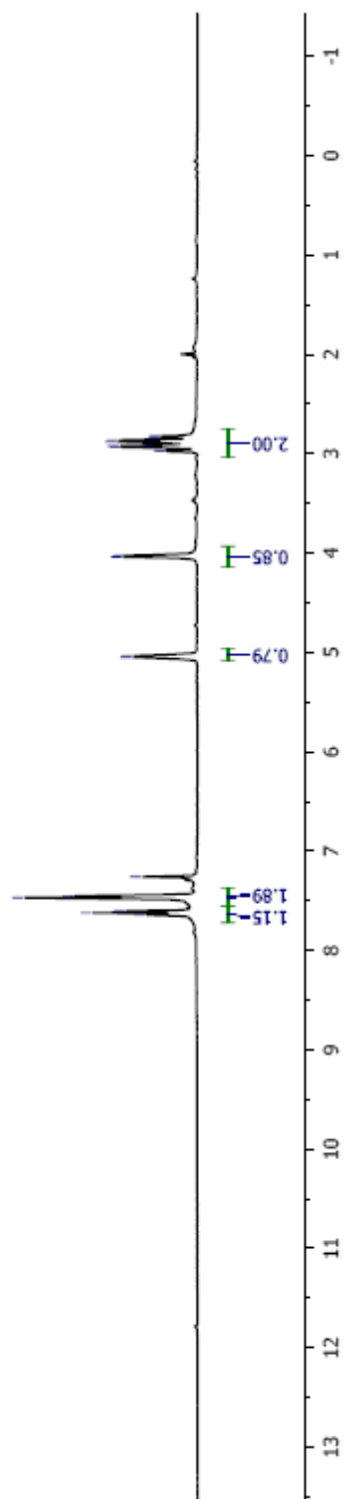
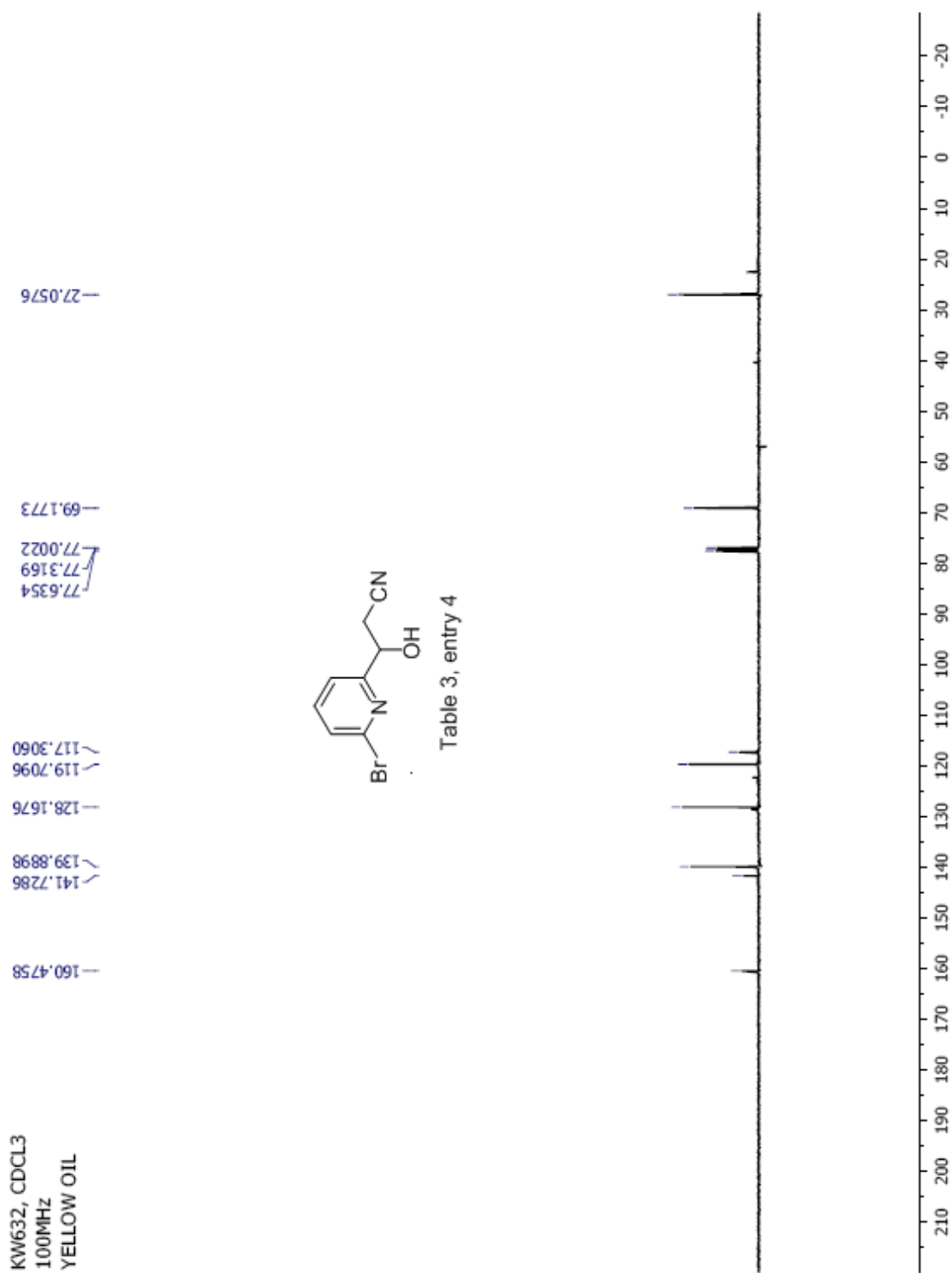


Table 3, entry 4







### Manual Peak Matching Report For Accurate Mass Determination

Theoretical mass	Experimental mass	PFK matching mass	Deviation*
225.97417	225.97456	218.98562	1.7 ppm

\* The deviation is obtained from the following equation:

$$\text{deviation} = \frac{\text{experimental mass} - \text{theoretical mass}}{\text{nominal mass}}$$

Where nominal mass takes in account only  $^{12}\text{C}$ ,  $^1\text{H}$ ,  $^{16}\text{O}$ ,  $^{14}\text{N}$  etc...

Theoretical mass correspond to the mass of the most abundant isotope peak

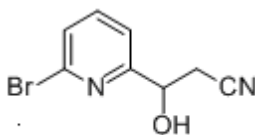


Table 3, entry 4

SPEC: fin083701.dat (11-JUN-08 10:57:21)  
 Samp: KW632  
 Conn: 70 eV EI  
 Oper: kh  
 Study: MS services  
 Base: 186.27  
 Masses: 35.01 > 650.00  
 Peak: 1000.0 mmu  
 Intensity: 27336  
 Scan 13 @ 0.42 min (EI +Q1MS LMR UP LR)

Scans: 1 > 159

Client: Kuldup  
 #Peaks: 663  
 RIC: 319370

2.7E+04

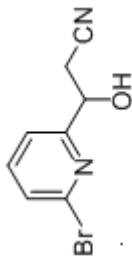
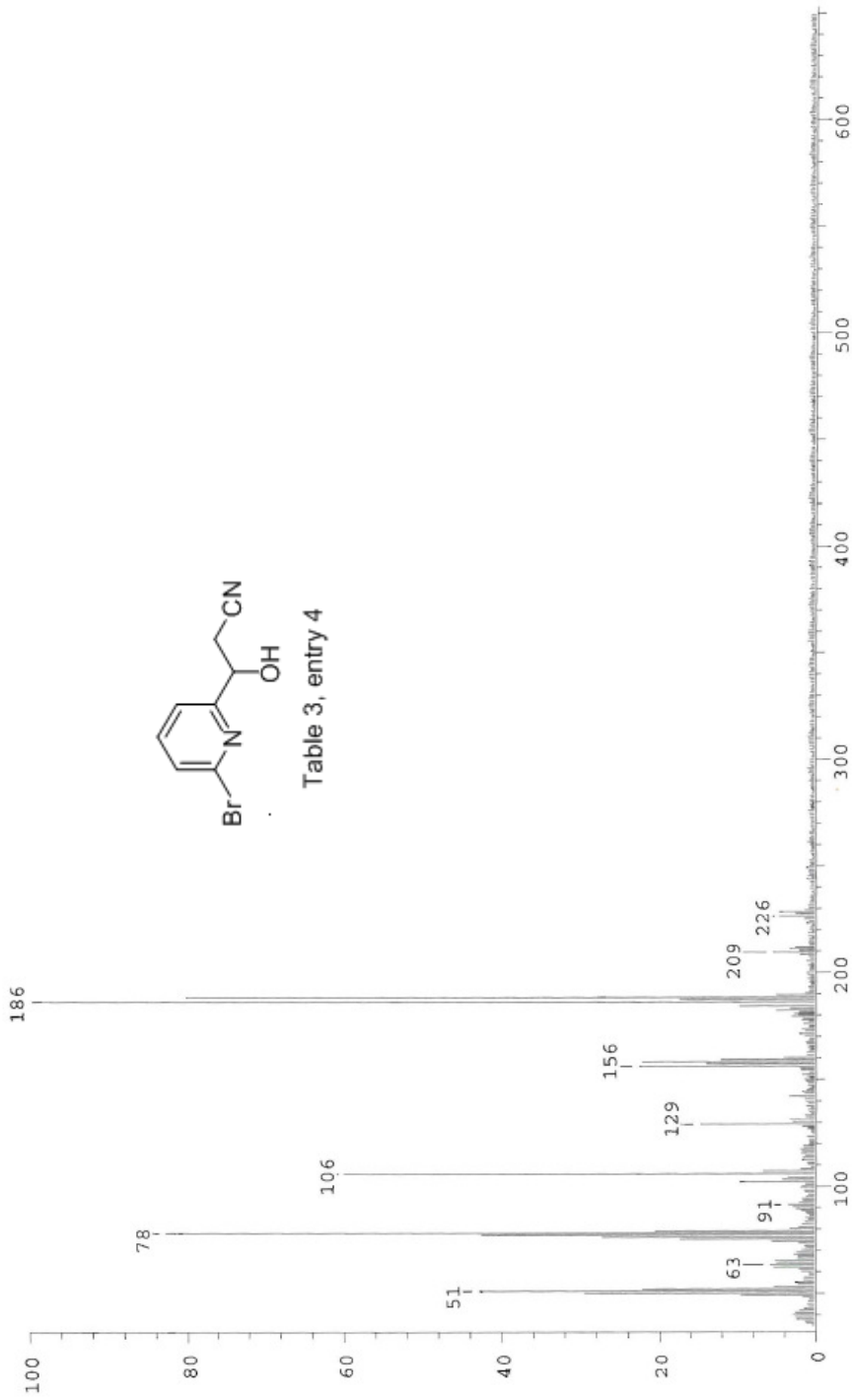


Table 3, entry 4



Date: Wed Jun 11 11:08:22 2008 ICIS: 8.3.0 SP2 for OSF1 (V4.0) build 98-238 from 26-Aug-98

KW790, CDCl3  
300 MHz  
RED OIL  
FEB 20 2009

2.96  
2.95  
2.94  
2.93

5.19

8.26  
8.23  
8.11  
8.08  
7.88  
7.85  
7.77  
7.74  
7.62  
7.59  
7.47  
7.44  
7.26

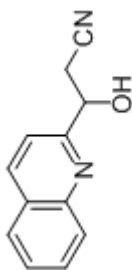
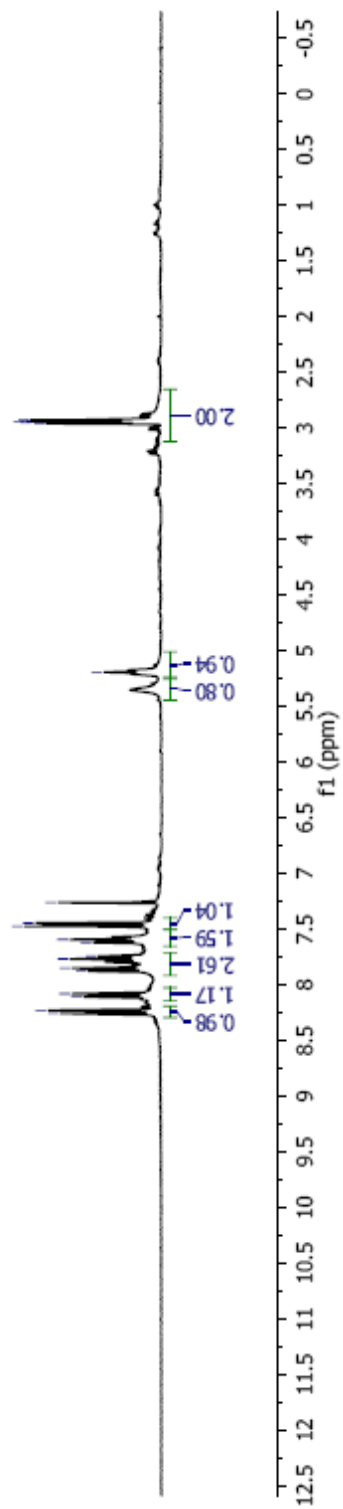


Table 3, entry 5



KW790, CDCl<sub>3</sub>  
100 MHz  
RED OIL  
20 FEB 2009

157.85  
146.69  
138.10  
127.36  
118.04  
117.18  
77.57  
77.26  
76.94  
68.86  
27.26

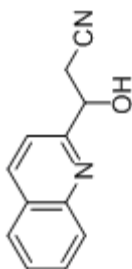
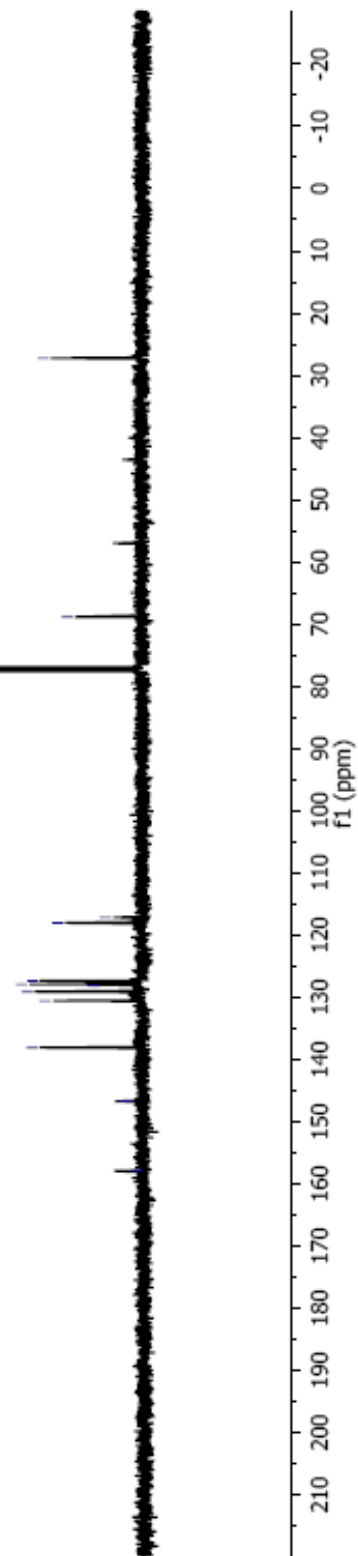


Table 3, entry 5



### Manual Peak Matching Report For Accurate Mass Determination

Theoretical mass	Experimental mass	PFK matching mass	Deviation*
198.07931	198.07973	180.98882	2.1 ppm

\* The deviation is obtained from the following equation:

$$\text{deviation} = \frac{\text{experimental mass} - \text{theoretical mass}}{\text{nominal mass}}$$

Where nominal mass takes in account only  $^{12}\text{C}$ ,  $^1\text{H}$ ,  $^{16}\text{O}$ ,  $^{14}\text{N}$  etc...

Theoretical mass correspond to the mass of the most abundant isotope peak

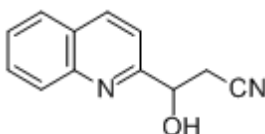


Table 3, entry 5

*ba*

SPC: fin084295.dat (06-MAR-09 11:04:28)  
 Samp: KW790  
 Comm: DP/EI  
 Oper: kh  
 Base: 196.33  
 Peak: 1000.0 mmu  
 Scan 29 @ 0.76 min (EI +QIMS LMR UP LR)

Study: ms services  
 Masses: 35.01 > 650.00  
 Intensity: 137676

Scans: 1 > 32  
 Client: Kuldeep  
 #Peaks: 635  
 RIC: 1469464  
 1.4E+05

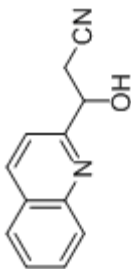
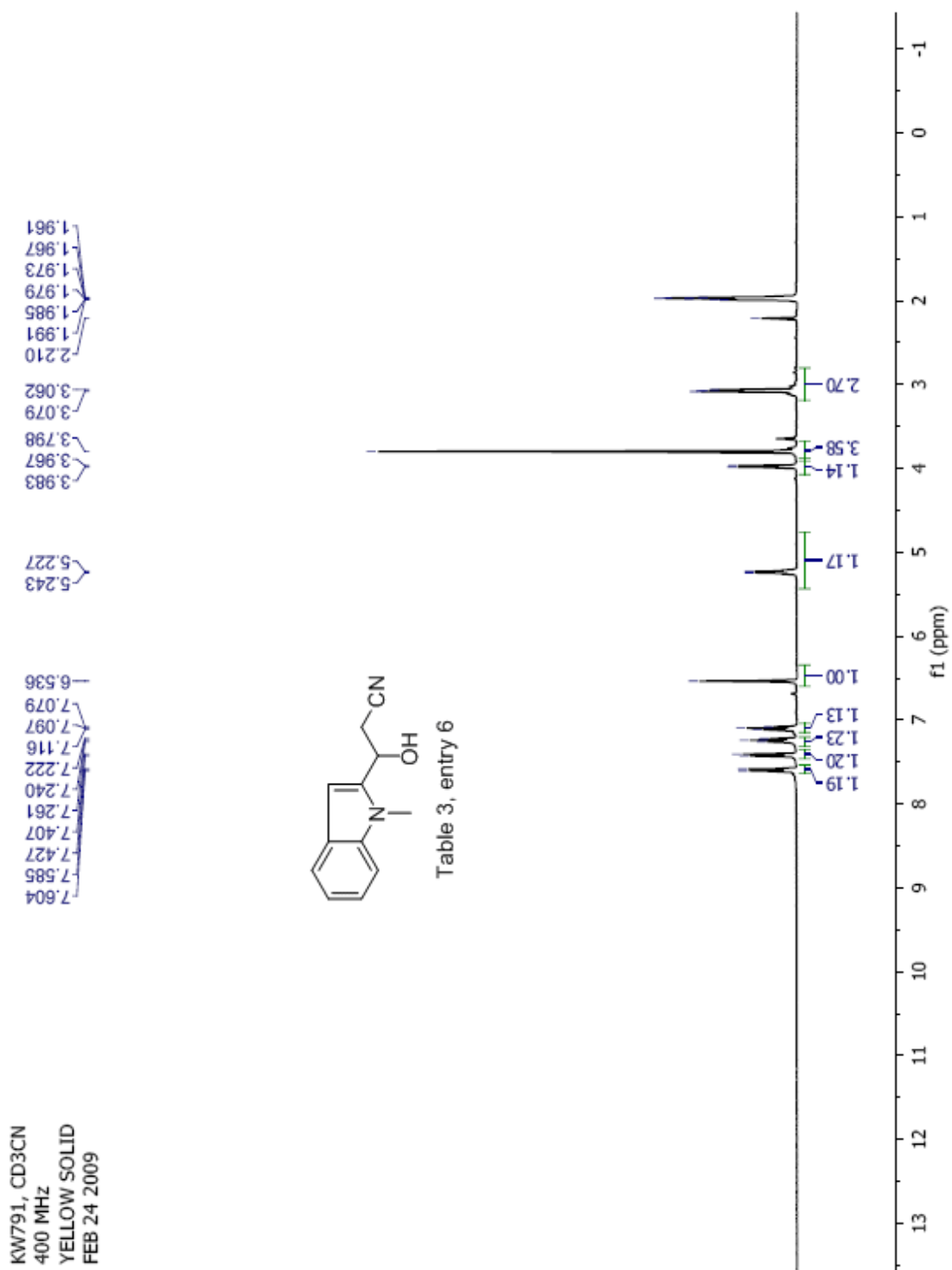
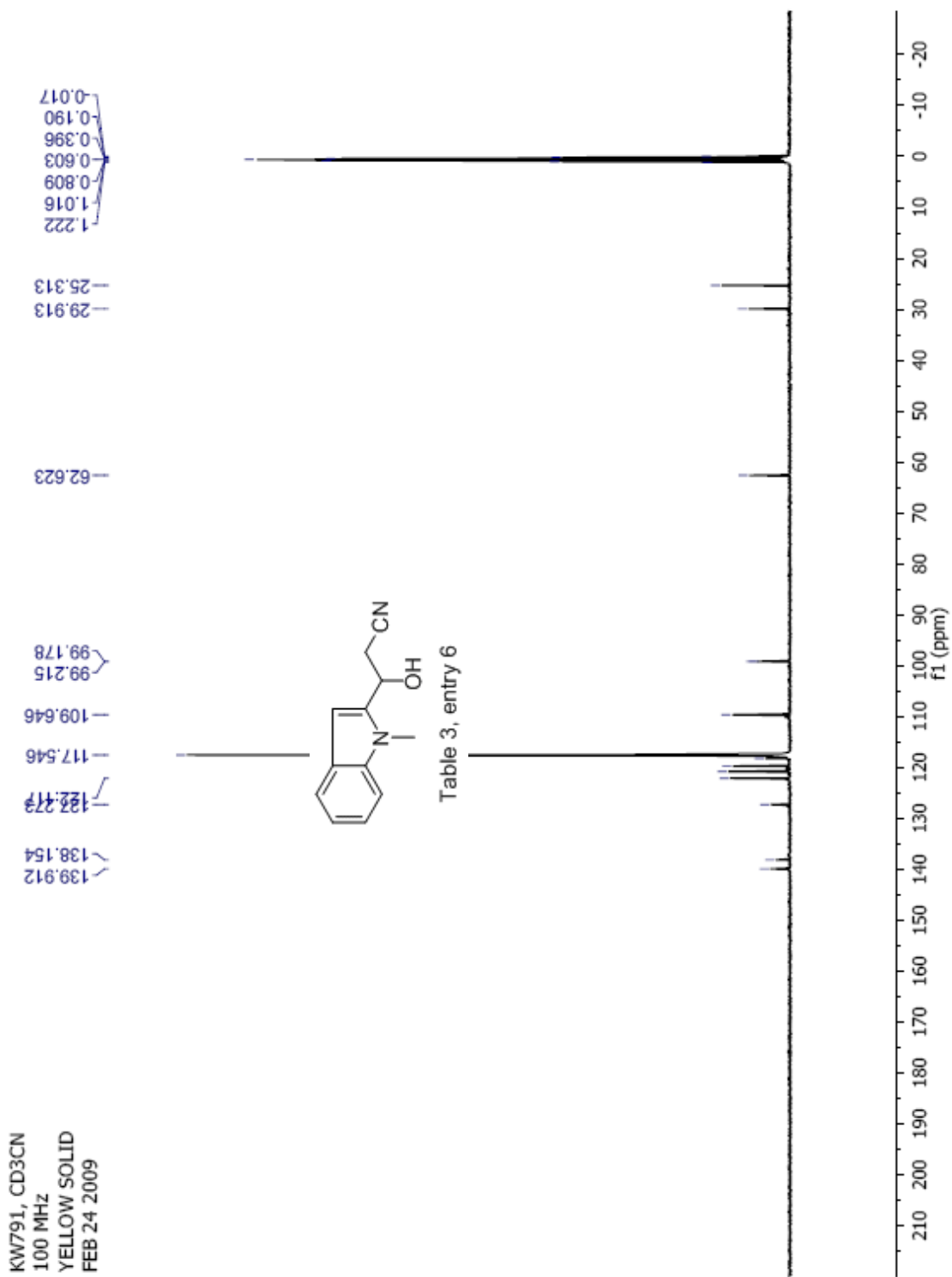


Table 3, entry 5

Date: Fri Mar 6 11:06:37 2009 ICIS: 8.3.0 SP2 for OSF1 (V4.0) build 98-238 from 26-Aug-98







### Manual Peak Matching Report For Accurate Mass Determination

Theoretical mass	Experimental mass	PFK matching mass	Deviation*
200.09496	200.09532	180,98882	1.8 ppm

\* The deviation is obtained from the following equation:

$$\text{deviation} = \frac{\text{experimental mass} - \text{theoretical mass}}{\text{nominal mass}}$$

Where nominal mass takes in account only  $^{12}\text{C}$ ,  $^1\text{H}$ ,  $^{16}\text{O}$ ,  $^{14}\text{N}$  etc...

Theoretical mass correspond to the mass of the most abundant isotope peak

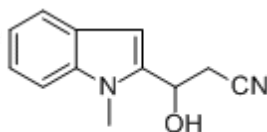
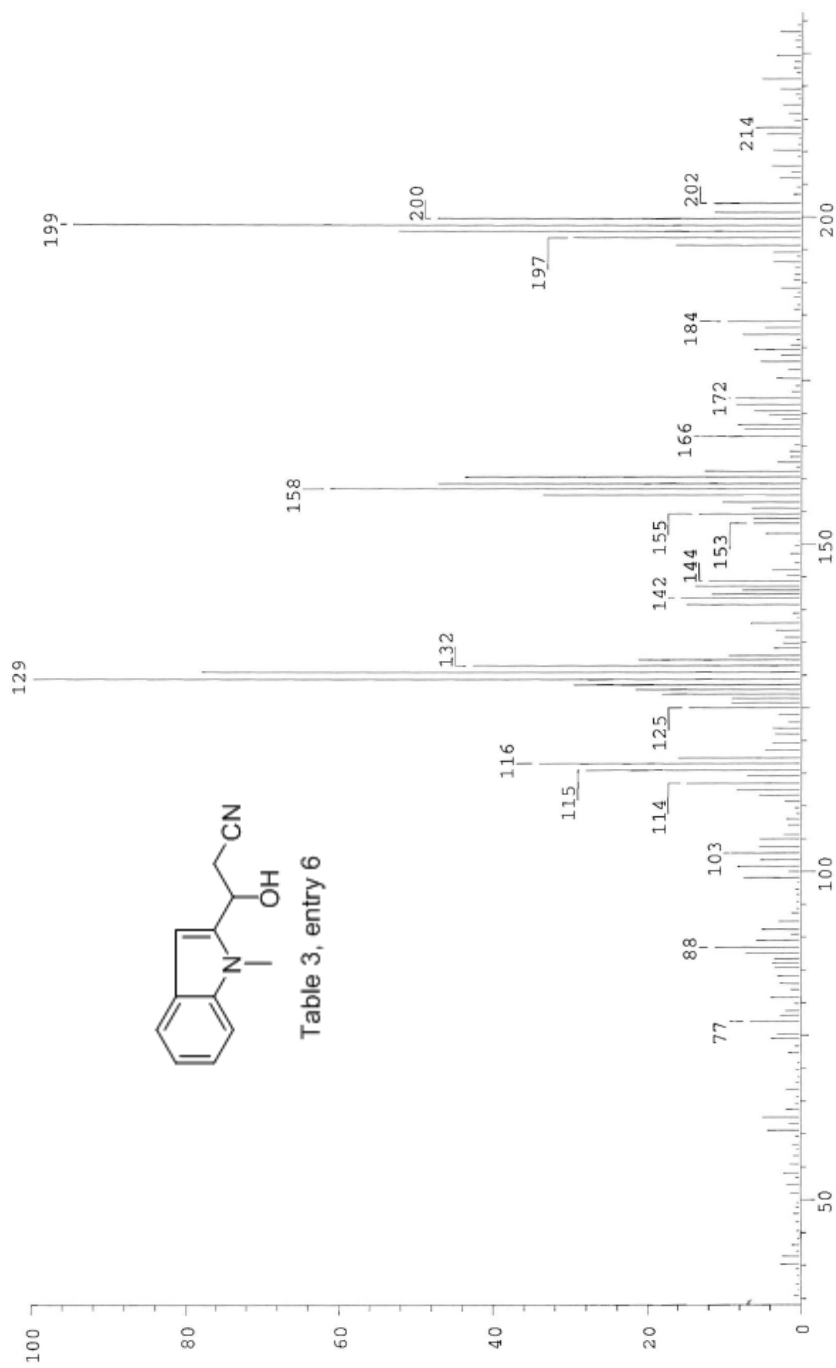


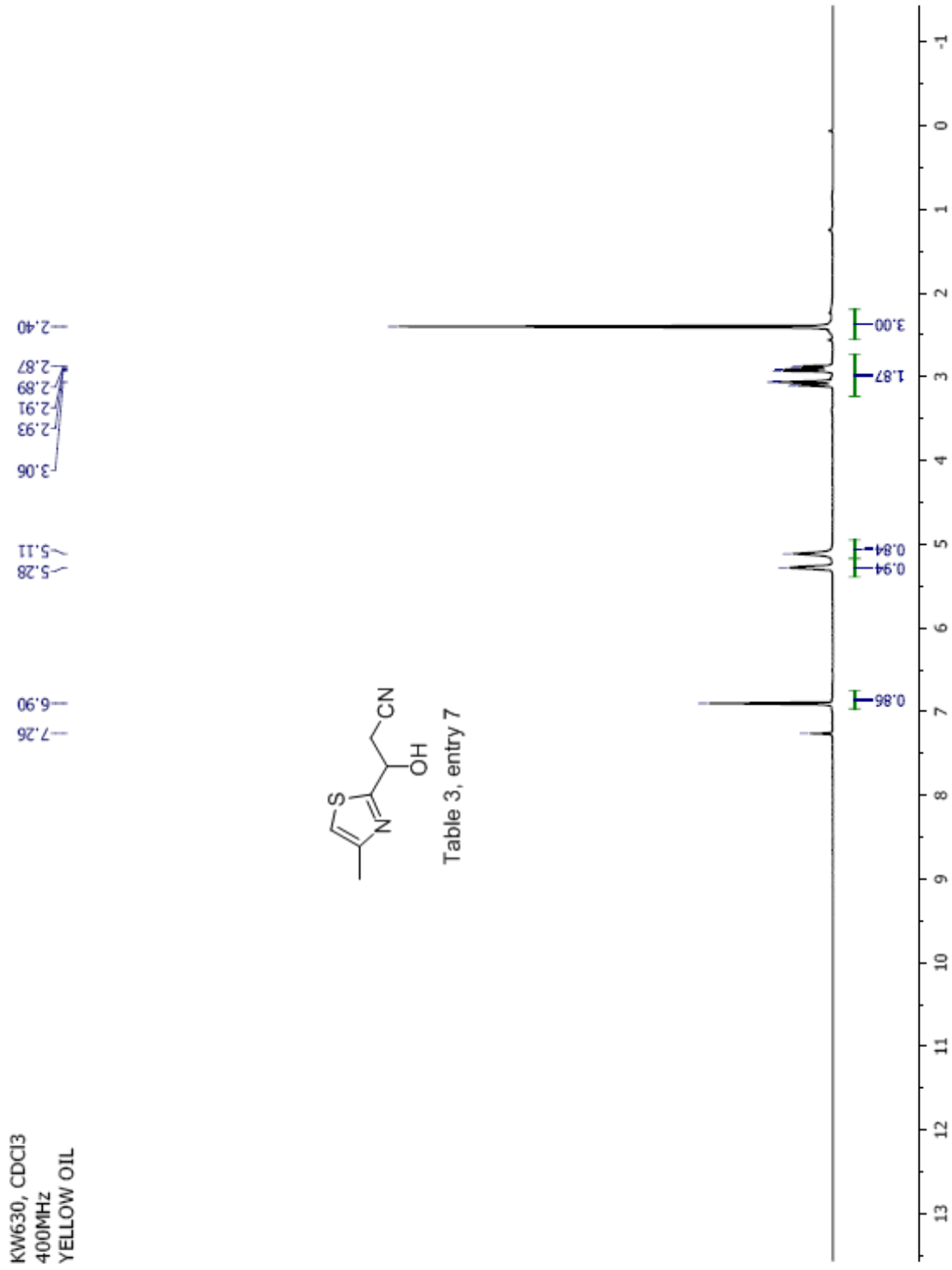
Table 3, entry 6

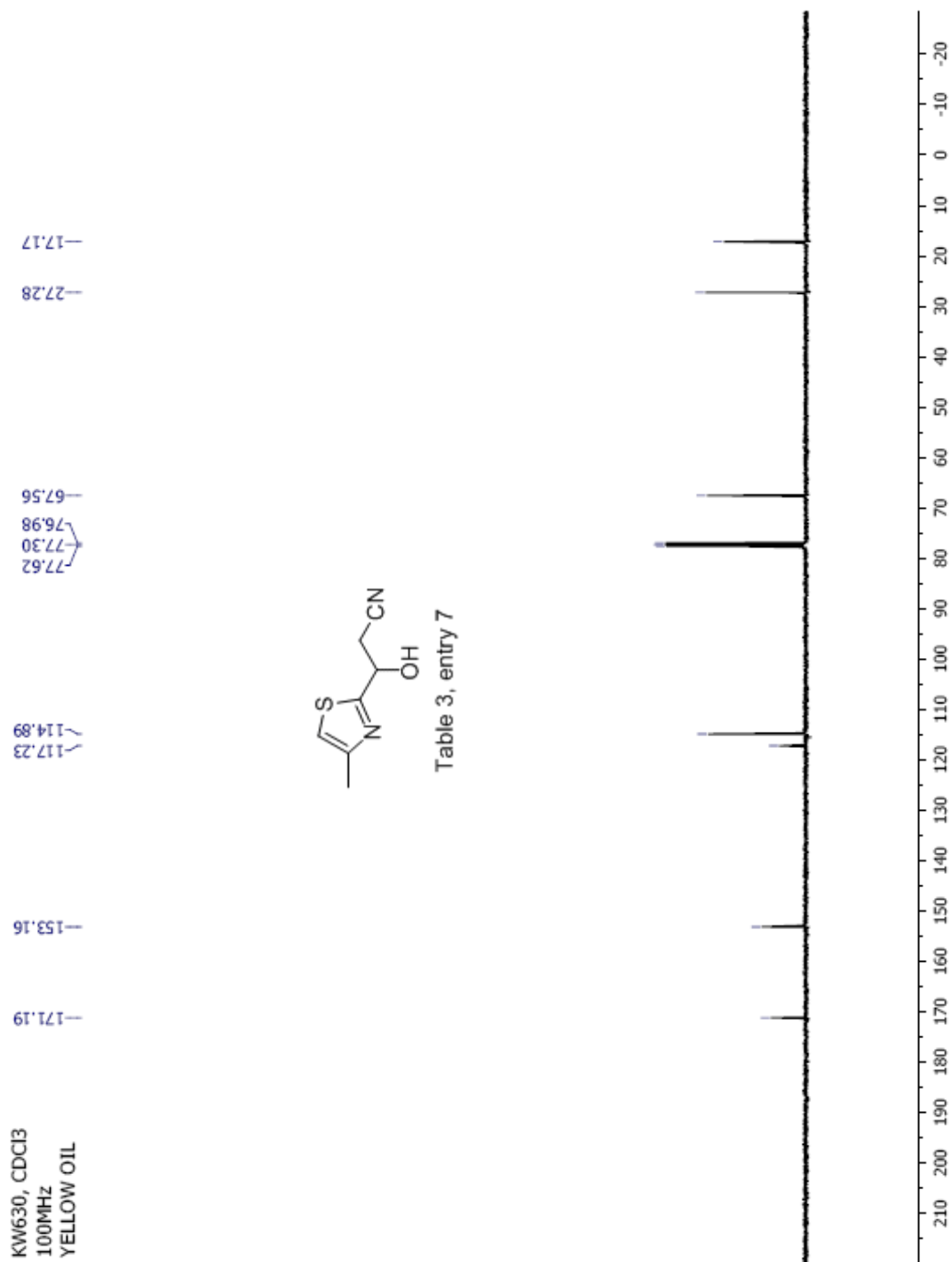
*Handwritten signature*

SPEC: fin084294.dat (06-MAR-09 10:59:25)  
 Samp: KW791  
 Comm: DP/EI  
 Oper: Kh  
 Base: 129.35  
 Peak: 1000.0 mmu  
 Scan 57 @ 1.33 min (EI +QIMS LMR UP LR)  
 Study: ms services  
 Masses: 35.01 > 650.00  
 Intensity: 10149  
 Scans: 1 > 67  
 Client: Kuldeep  
 #Peaks: 635  
 RIC: 210253  
 1.0E+04



Date: Fri Mar 6 11:02:24 2009 ICIS: 8.3.0 SP2 for OSFI (V4.0) build 98-238 from 26-Aug-98





### Manual Peak Matching Report For Accurate Mass Determination

Theoretical mass	Experimental mass	PFK matching mass	Deviation*
168.03573	168.03606	130.99201	2 ppm

\* The deviation is obtained from the following equation:

$$\text{deviation} = \frac{\text{experimental mass} - \text{theoretical mass}}{\text{nominal mass}}$$

Where nominal mass takes in account only  $^{12}\text{C}$ ,  $^1\text{H}$ ,  $^{16}\text{O}$ ,  $^{14}\text{N}$  etc...

Theoretical mass correspond to the mass of the most abundant isotope peak

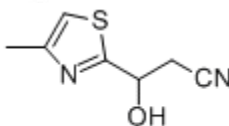


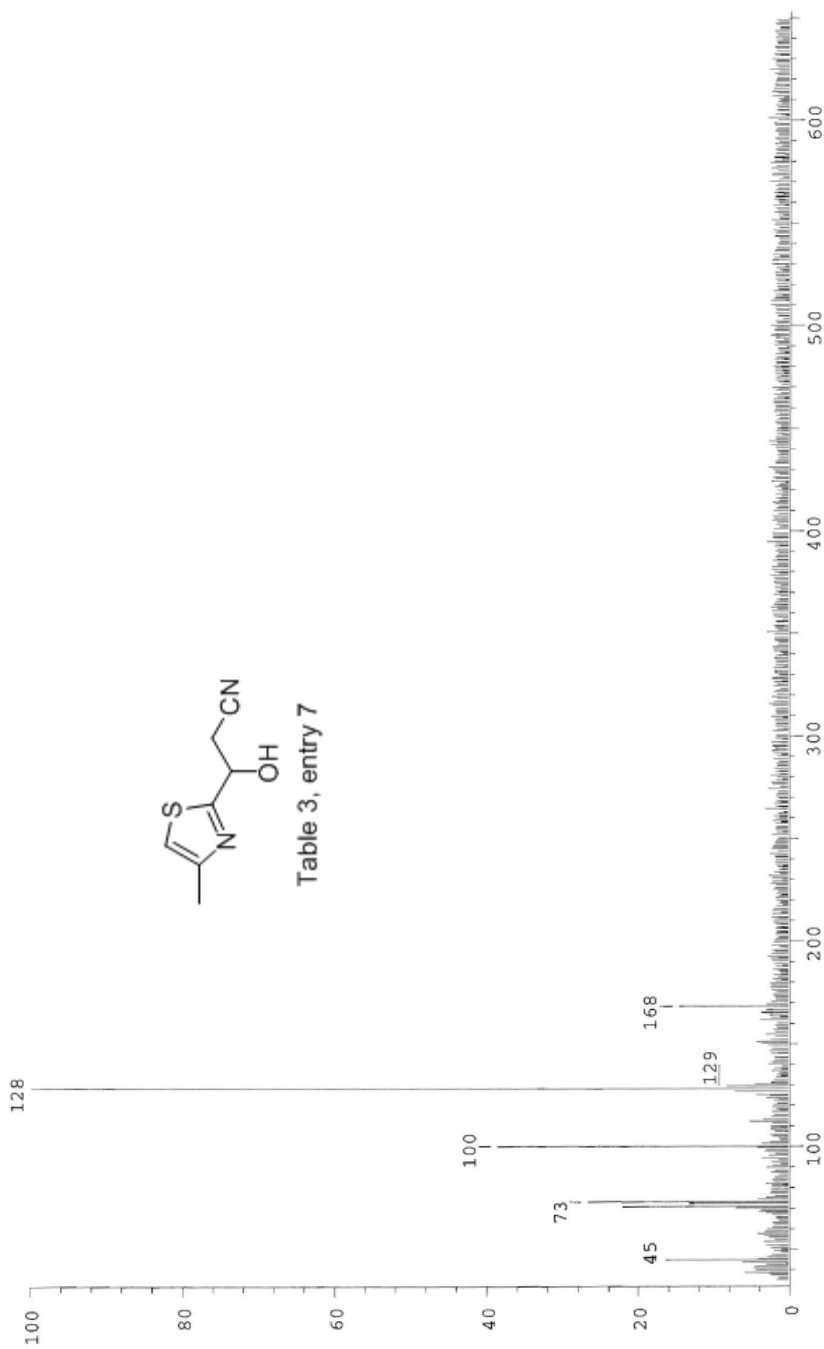
Table 3, entry 7

Scans: 1 > 22  
 Client: Kuldup  
 #Peaks: 662  
 RIC: 768012  
 5.6E+04

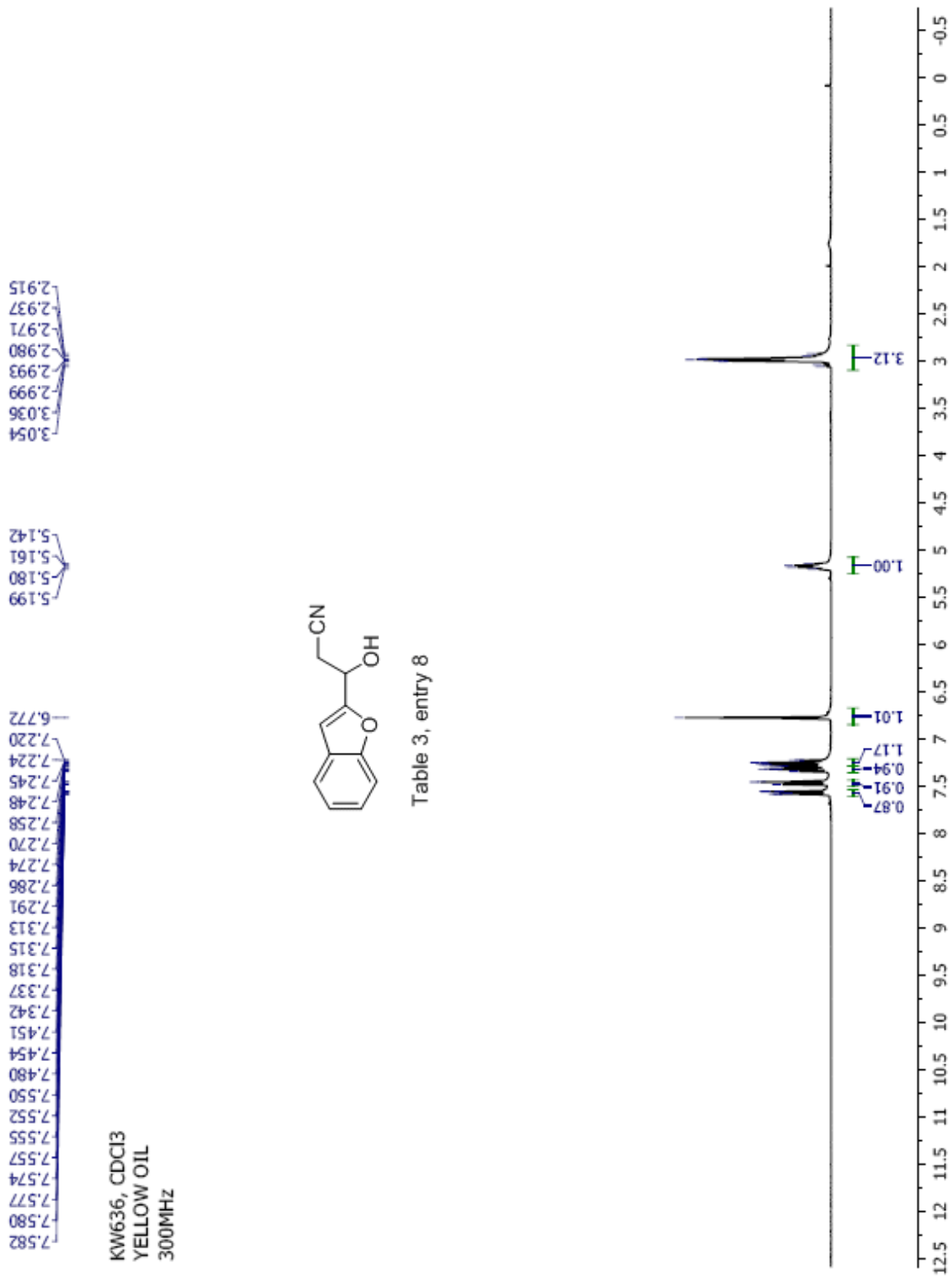
SPEC: fin083702 (11-JUN-08 11:12:31)

Sampl: KW630  
 Comm: 70 eV EI

Study: MS services  
 Oper: kh  
 Masses: 35.01 > 650.00  
 Base: 128.15  
 Intensity: 55743  
 Peak: 1000.0 mmu  
 REG #9 @ 0.41 min (EI +Q1MS LMR UP LR) (+13>19)



Date: Wed Jun 11 11:13:41 2008 ICIS: 8.3.0 SP2 for OSF1 (V4.0) build 98-238 from 26-Aug-98



KW636, CDC13  
100MHz  
YELLOW OIL

155.49  
155.07  
127.83  
125.18  
123.46  
121.74  
117.12  
111.60  
104.40  
77.64  
77.32  
77.01  
64.49  
25.23

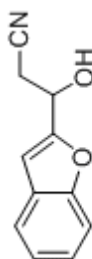
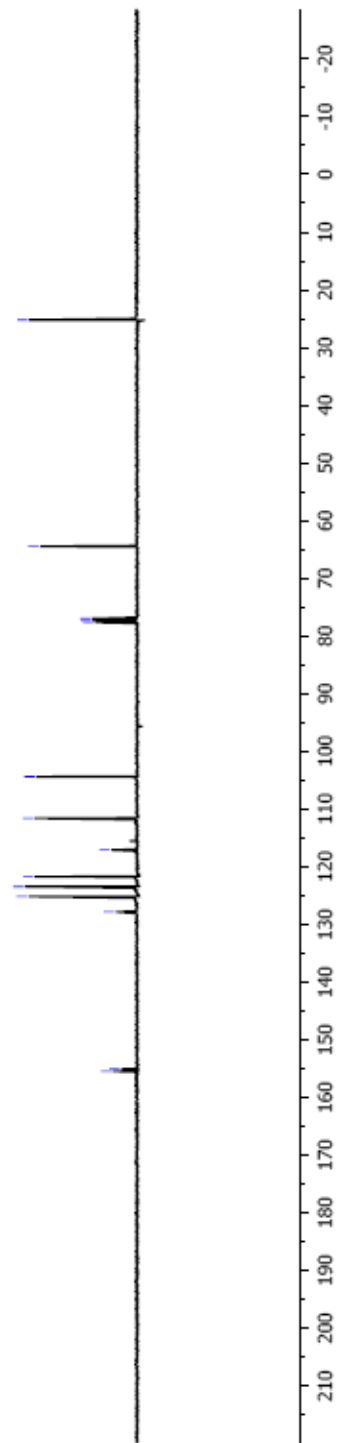


Table 3, entry 8





### Manual Peak Matching Report For Accurate Mass Determination

Theoretical mass	Experimental mass	PFK matching mass	Deviation*
187.06333	187.06371	180.98882	2 ppm

\* The deviation is obtained from the following equation:

$$\text{deviation} = \frac{\text{experimental mass} - \text{theoretical mass}}{\text{nominal mass}}$$

Where nominal mass takes in account only  $^{12}\text{C}$ ,  $^1\text{H}$ ,  $^{16}\text{O}$ ,  $^{14}\text{N}$  etc...

Theoretical mass correspond to the mass of the most abundant isotope peak

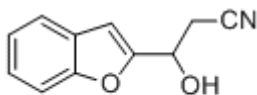


Table 3, entry 8

no

SPEC: fin063689.dat (06-JUN-08 14:40:38)  
 Samp: KW636  
 Comm: 70 eV EI  
 Oper: kh  
 Base: 146.88  
 Peak: 1000.0 mmu  
 Scan 30 @ 0.52 min (EI +QMS LMR UP LR)  
 Study: Service  
 Masses: 35.01 > 650.00  
 Intensity: 22691  
 Scans: 1 > 35  
 Client: Kuldup  
 #Peaks: 623  
 RIC: 114141  
 2.3E+04

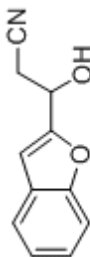
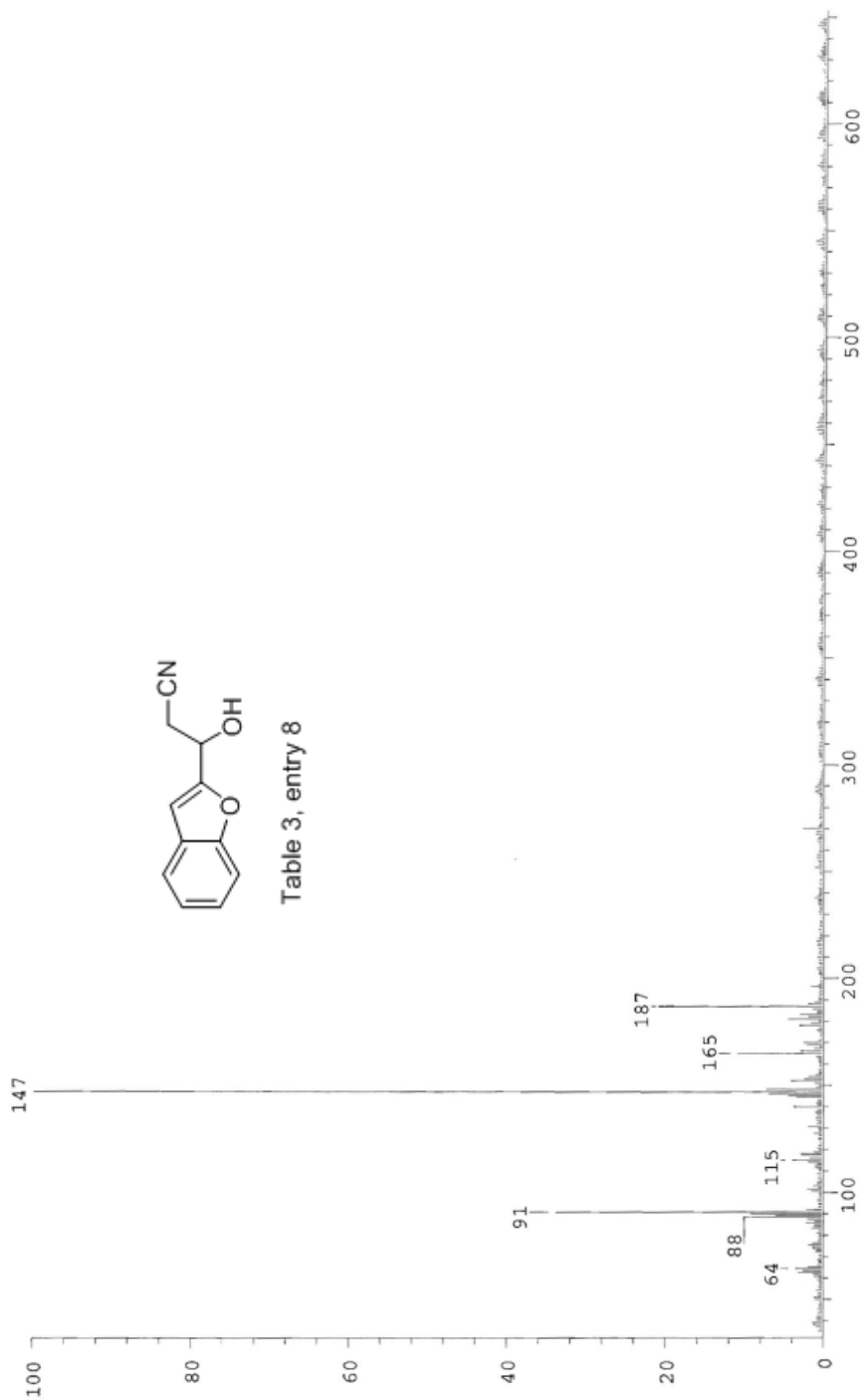


Table 3, entry 8



Date: Fri Jun 6 14:41:33 2008 ICIS: 8.3.0 SP2 for OSF1 (V4.0) build 98-238 from 26-Aug-98

7.13  
7.682  
7.640  
7.571  
7.541  
7.534  
7.306  
7.257  
6.419  
6.387  
5.146  
5.126  
5.106  
3.349  
2.819  
2.799

KW641, CDCI3  
300MHZ  
YELLOW SOLID

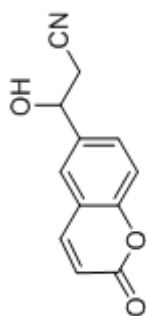
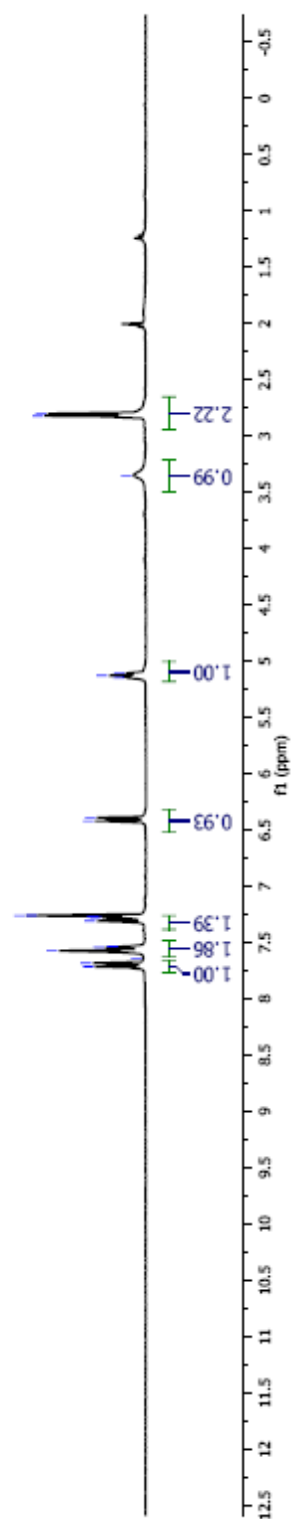
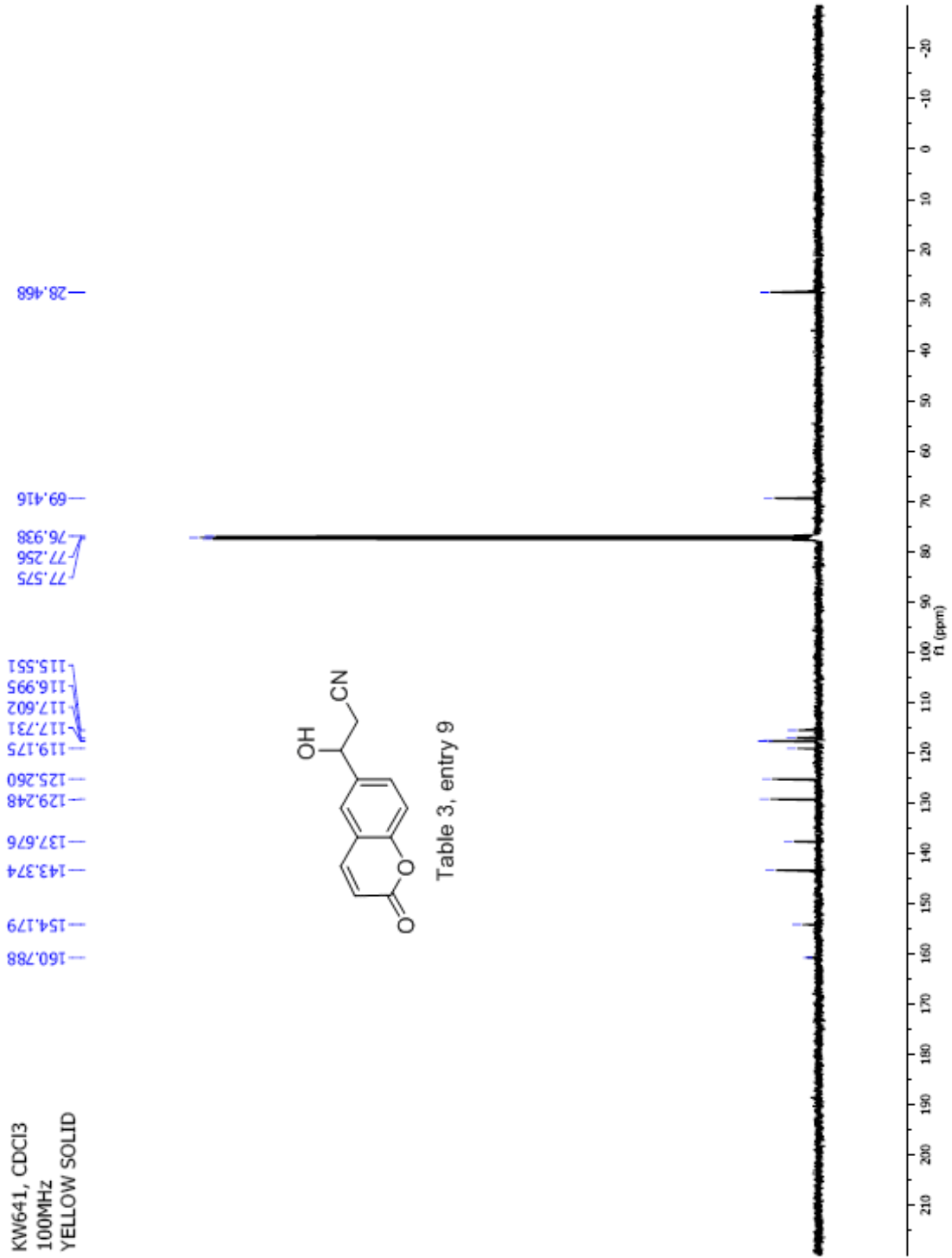


Table 3, entry 9





### Manual Peak Matching Report For Accurate Mass Determination

Theoretical mass	Experimental mass	PFK matching mass	Deviation*
215.05824	215.05862	180.98882	1.8 ppm

\* The deviation is obtained from the following equation:

$$\text{deviation} = \frac{\text{experimental mass} - \text{theoretical mass}}{\text{nominal mass}}$$

Where nominal mass takes in account only  $^{12}\text{C}$ ,  $^1\text{H}$ ,  $^{16}\text{O}$ ,  $^{14}\text{N}$  etc...

Theoretical mass correspond to the mass of the most abundant isotope peak

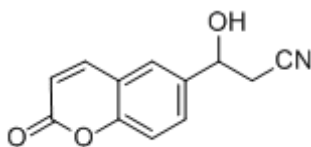


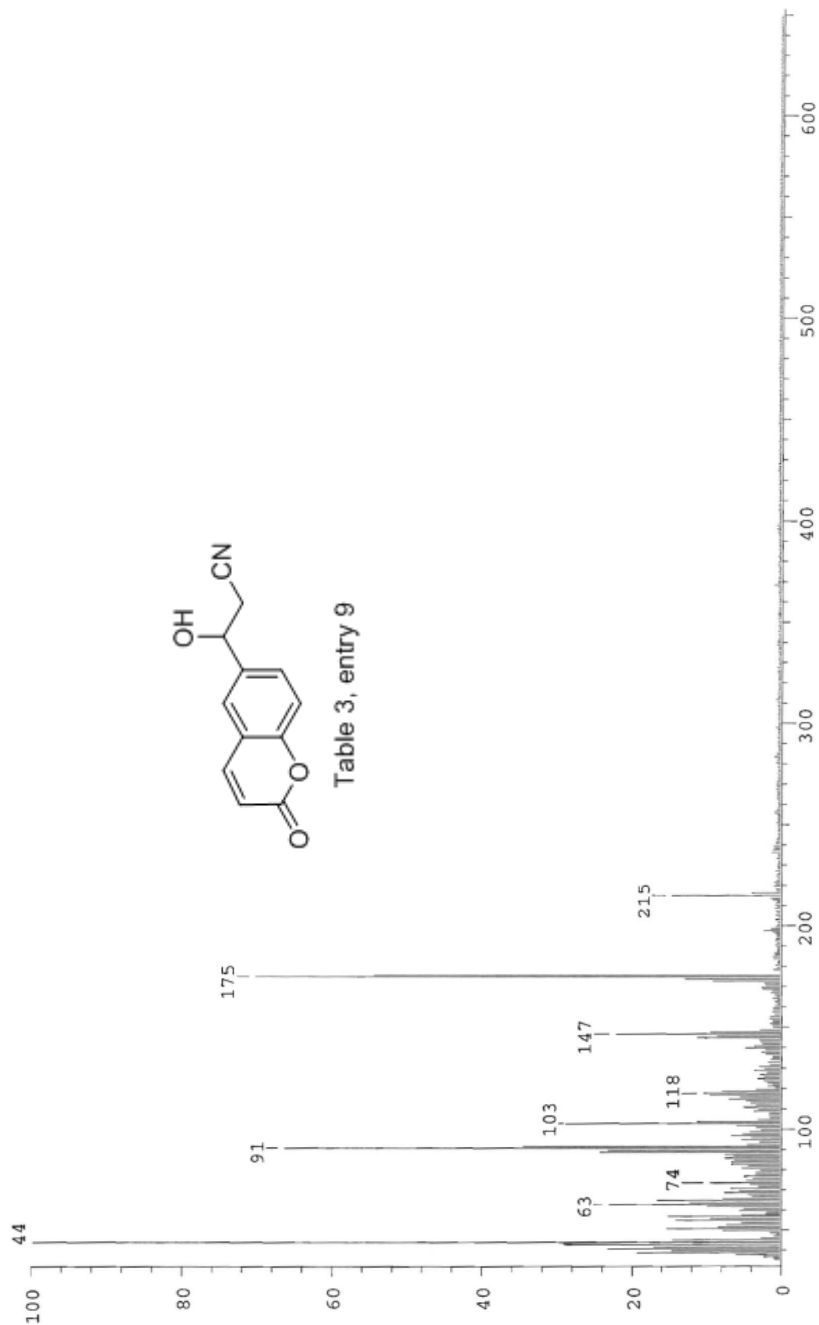
Table 3, entry 9

*M*

SPEC: fin083760.dat (02-JUL-08 12:53:17)  
 Samp: KW641  
 Comm: 70 eV EI  
 Oper: kh  
 Base: 43.96  
 Peak: 1000.0 mmu  
 Scan 54 @ 1.27 min (EI +Q1MS LMR UP LR)

Study: MS services  
 Masses: 35.01 > 650.00  
 Intensity: 644784

Scans: 1 > 56  
 Client: Kuldup  
 #Peaks: 661  
 RIC: 8035415  
 6.4E+05



Date: Wed Jul 2 12:55:02 2008 ICIS: 8.3.0 SP2 for OSF1 (V4.0) build 98-238 from 26-Aug-98

KW806, CDCl<sub>3</sub>  
 400 MHz  
 COLORLESS OIL  
 MAR 05 2009

7.39  
 6.36  
 5.01  
 5.00  
 4.98  
 4.97  
 3.38  
 3.37  
 2.87  
 2.85

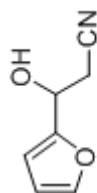
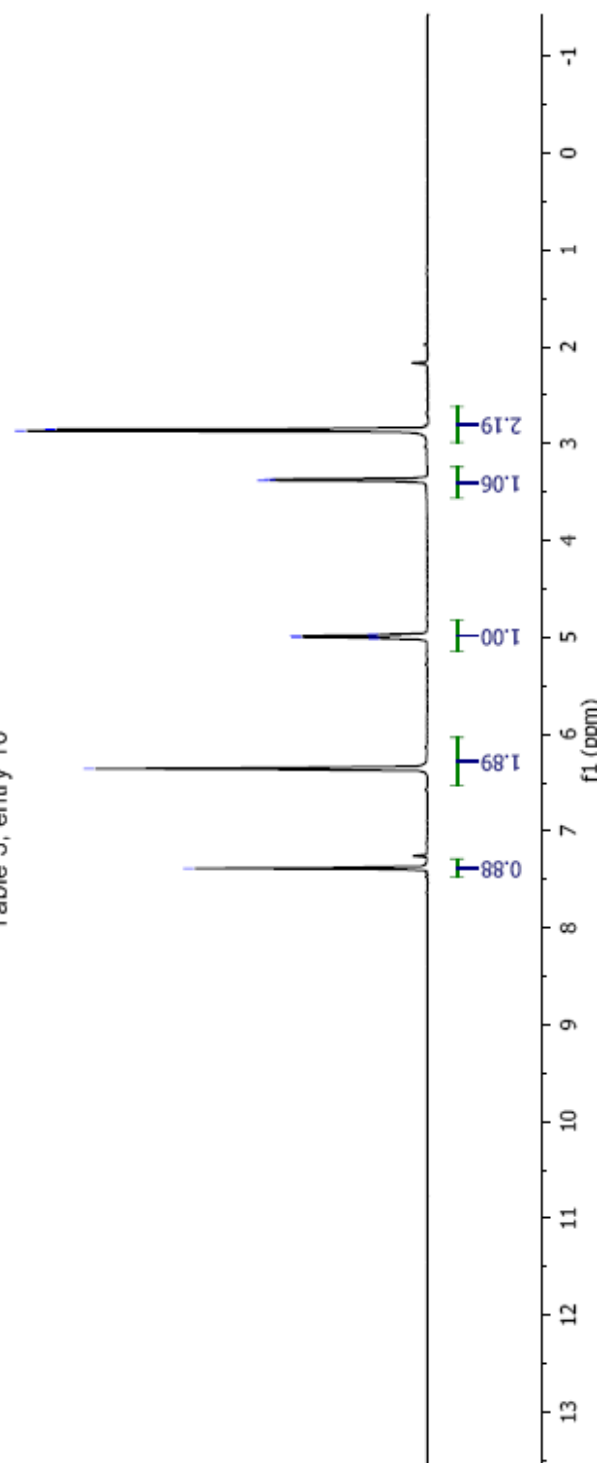
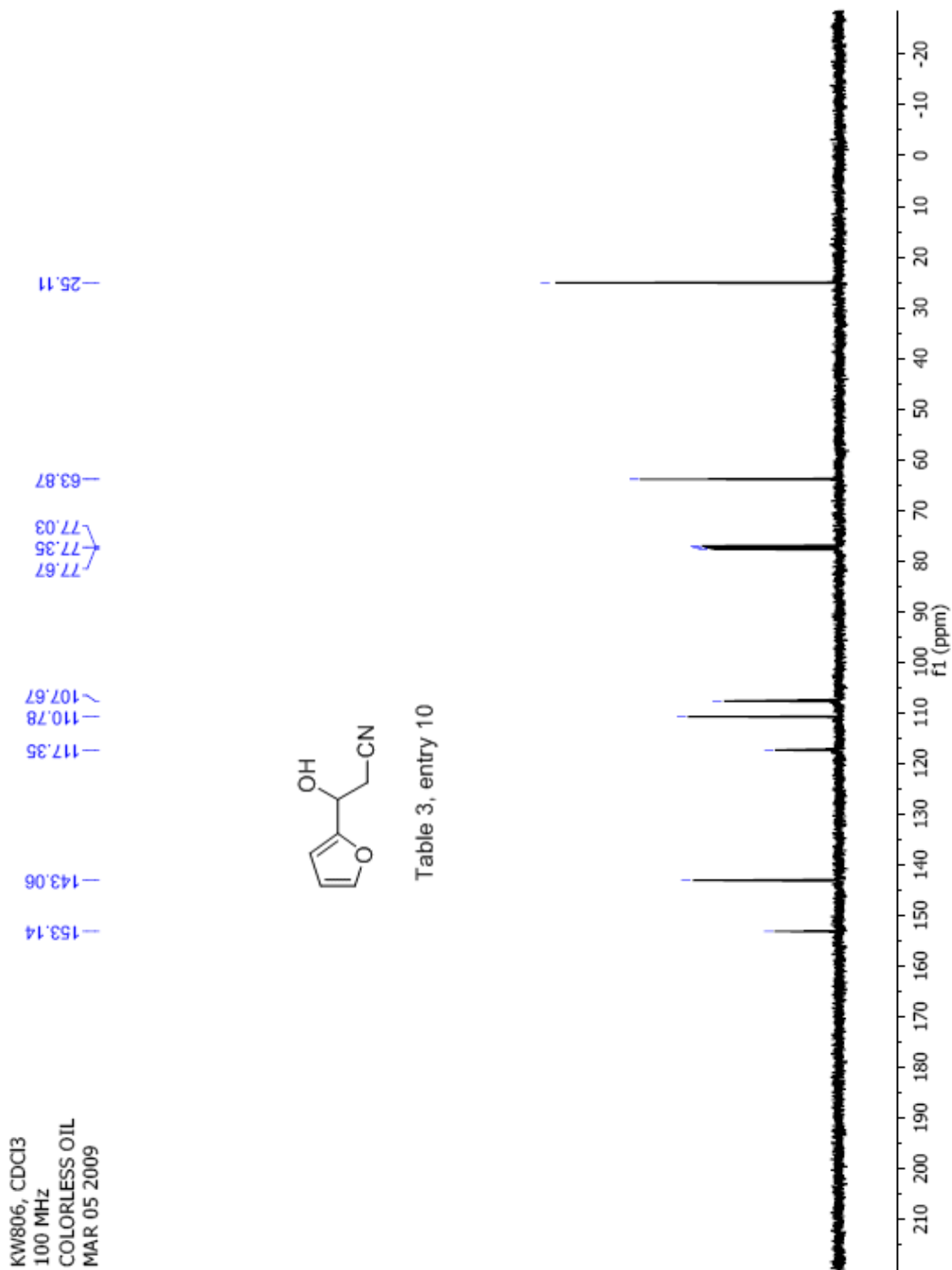


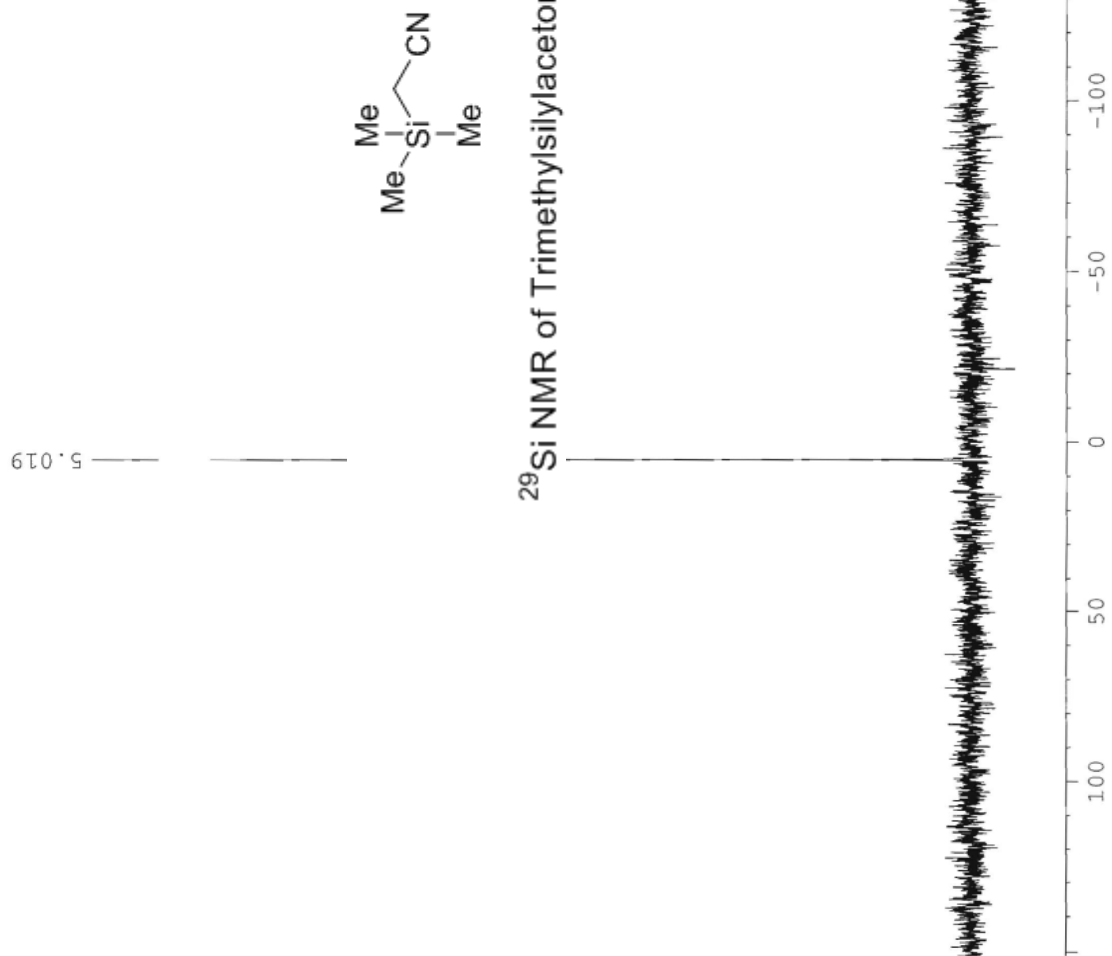
Table 3, entry 10



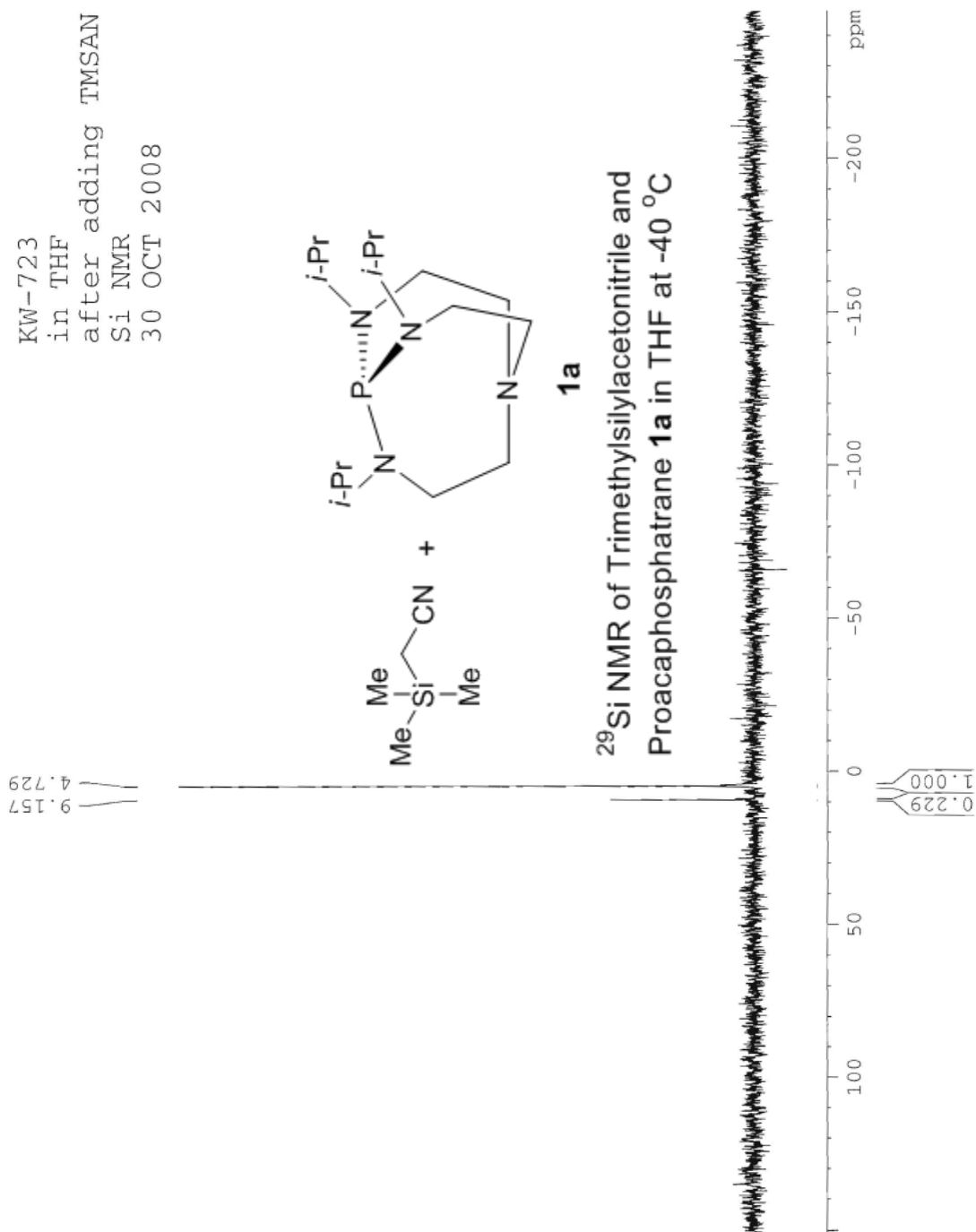




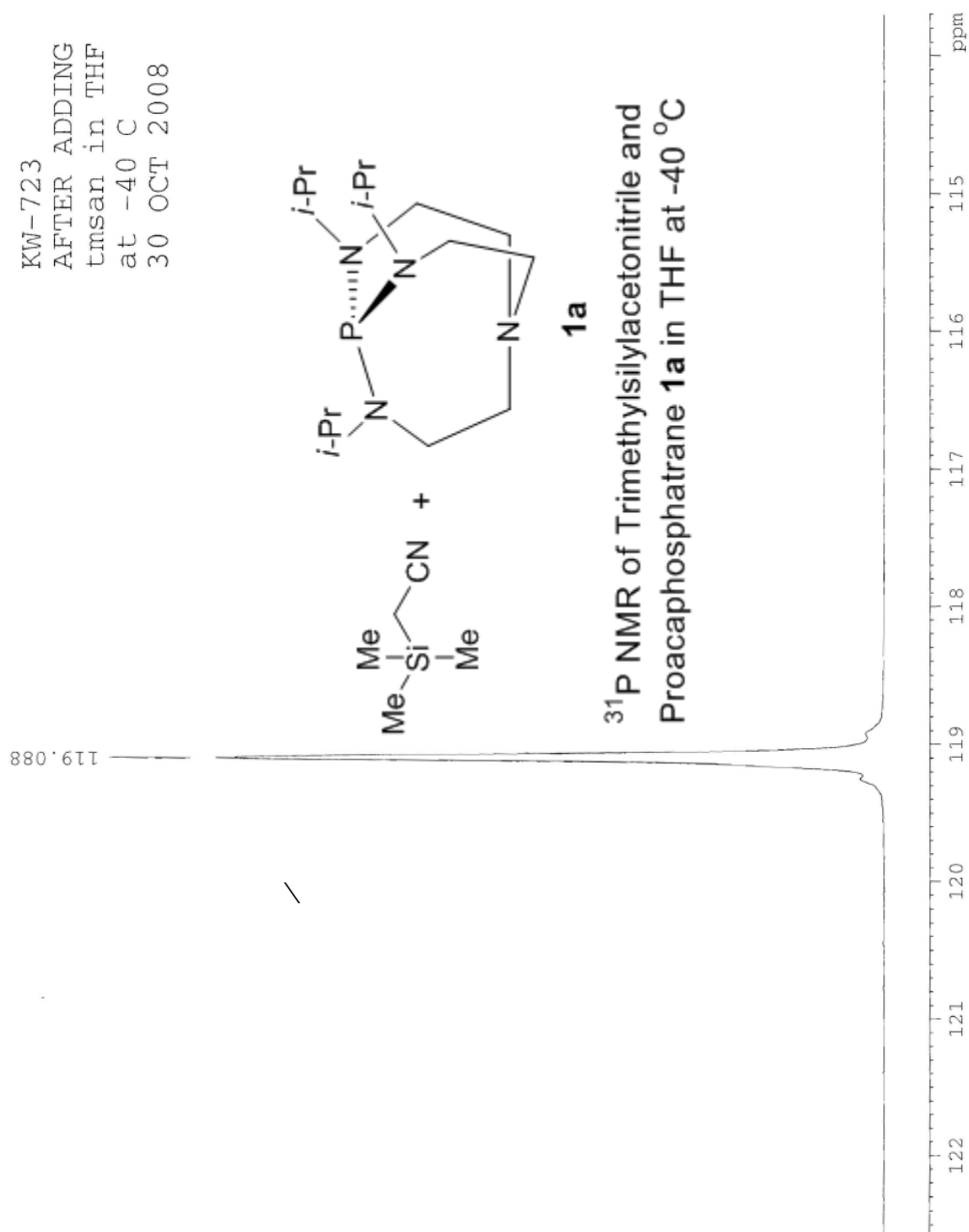
KW 723  
Starting TMS<sub>AN</sub>  
in THF  
31 oct 2008



KW-723  
 in THF  
 after adding TMSAN  
 Si NMR  
 30 OCT 2008



KW-723  
 AFTER ADDING  
 tmsan in THF  
 at -40 C  
 30 OCT 2008



**APPENDIX D**

**CHAPTER 5**

**General Information**

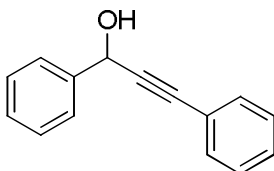
**References for known compounds and characterization data for the new compounds**

**$^1\text{H}$ ,  $^{13}\text{C}$  and HRMS for all compounds**

### General Information

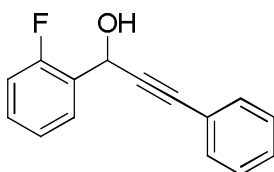
All reactions were carried out under inert atmosphere using oven dried glassware and a magnetic stirrer. THF was distilled and dried over sodium. Aryltrimethylsilylacetylenes, and all aldehydes were purchased from commercial sources and were used without further purification. Proazaphosphatrane **1a** was synthesized using literature procedure.<sup>1</sup> Products were purified via column chromatography using hexane/ethyl acetate. <sup>1</sup>H and <sup>13</sup>C nmr spectra were obtained on a VXR-300, VXR 400 and DRX-400 NMR spectrometer, respectively. All NMR spectra were taken in CDCl<sub>3</sub>. Thin layer chromatography was used to monitor reaction progress.

#### 1,3-Diphenylprop-2-yn-1-ol (Table 1, entry 3)<sup>2</sup>:

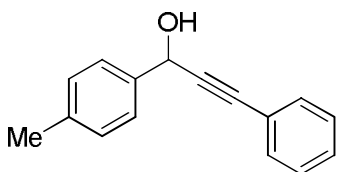


The general procedure was followed for the synthesis and purification; product was afforded as a colorless oil in 82% isolated yield.

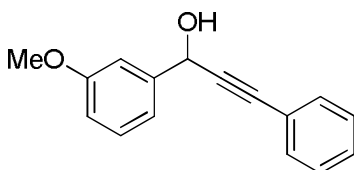
#### 1-(2-Fluorophenyl)-3-phenyl-prop-2-yn-1-ol (Table 2, entry 1)<sup>3</sup>:



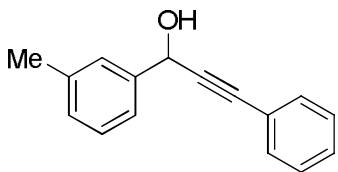
The general procedure was followed for the synthesis and purification; product was afforded as a colorless oil in 95% isolated yield.

**1-(4-Methylphenyl)-3-phenylprop-2-yn-1-ol (Table 2, entry 2)<sup>2</sup>:**

The general procedure was followed for the synthesis and purification; product was afforded as a yellow oil in 82% isolated yield.

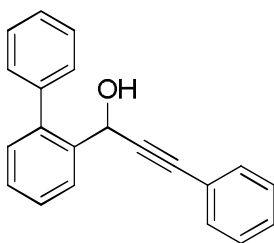
**1-(3-Methoxyphenyl)-3-phenyl-prop-2-yn-1-ol (Table 2, entry 3)<sup>4</sup>:**

The general procedure was followed for the synthesis and purification; product was afforded as a colorless oil in 91% isolated yield.

**3-Phenyl-1-*m*-tolyl-prop-2-yn-1-ol (Table 2, entry 4)<sup>5</sup>:**

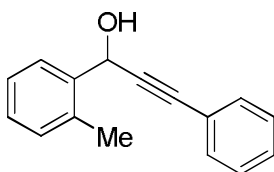
The general procedure was followed for the synthesis and purification; product was afforded as a colorless oil in 83% isolated yield. <sup>13</sup>C NMR (CDCl<sub>3</sub>, 100.6 MHz): δ 140.8, 138.6, 132.1, 129.5, 128.8, 128.8, 128.5, 127.7, 124.1, 122.8, 89.3, 86.7, 65.3, 21.7 ppm.

**1-(2-Phenylphenyl)-3-phenylprop-2-yn-1-ol (Table 2, entry 5)<sup>6</sup>:**



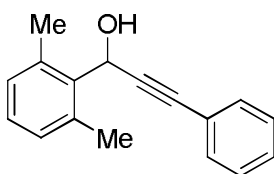
The general procedure was followed for the synthesis and purification; product was afforded as a yellow oil in 91% isolated yield.

**3-Phenyl-1-*o*-tolyl-prop-2-yn-1-ol (Table 2, entry 6)<sup>3</sup>:**



The general procedure was followed for the synthesis and purification; product was afforded as a colorless oil in 97% isolated yield.

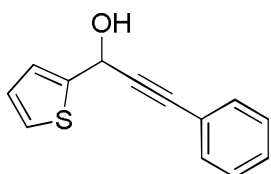
**1-(2,6-dimethylphenyl)-3-phenylprop-2-yn-1-ol (Table 2, entry 7):**



The general reaction procedure was followed for the synthesis and purification; product was afforded as colorless oil in 96% isolated yield. <sup>1</sup>H NMR (CDCl<sub>3</sub>, 400 MHz): δ 7.49–7.46 (m, 2H), 7.34–7.33 (m, 3H), 7.16–7.15 (m, 1H), 7.09–7.08 (m, 2H), 6.16 (s, 1H), 2.62 (s, 6H), 2.52 (s, 1H) ppm; <sup>13</sup>C NMR (CDCl<sub>3</sub>, 100.6 MHz): δ 136.9, 136.6, 131.9, 129.5, 128.7, 128.5,

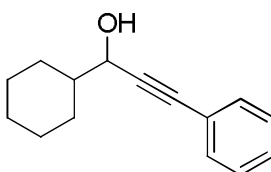
128.4, 123.0, 88.9, 86.1, 61.1, 20.8 ppm; HRMS  $m/z$  Calcd. for  $C_{17}H_{16}O$ : 236.12011. Found: 236.12053.

**3-Phenyl-1-(2-thienyl)prop-2-yn-1-ol (Table 2, entry 8)<sup>2</sup>:**



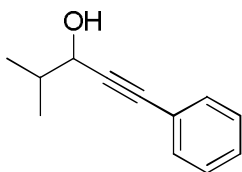
The general procedure was followed for the synthesis and purification; product was afforded as a yellow oil in 91% isolated yield.

**1-Cyclohexyl-3-phenylprop-2-yn-1-ol (Table 3, entry 1)<sup>2</sup>:**



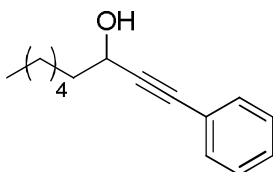
The general procedure was followed for the synthesis and purification; product was afforded as a colorless oil in 96% isolated yield.

**4-Methyl-1-phenylpent-1-yn-3-ol (Table 3, entry 2)<sup>2</sup>:**

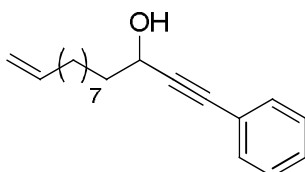


The general procedure was followed for the synthesis and purification; product was afforded as a colorless oil in 94% isolated yield.



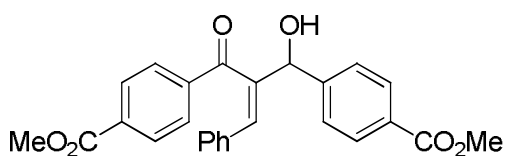
**1-Phenylnon-1-yn-3-ol (Table 3, entry 3)<sup>4</sup>:**

The general procedure was followed for the synthesis and purification; product was afforded as a colorless oil in 84% isolated yield.

**1-Phenyltridec-12-en-1-yn-3-ol (Table 3, entry 4):**

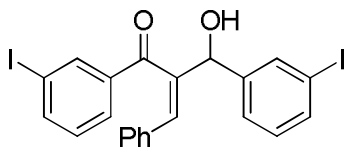
The general reaction procedure was followed for the synthesis and purification; product was afforded as colorless oil in 79% isolated yield. <sup>1</sup>H NMR (CDCl<sub>3</sub>, 400 MHz): δ 7.44–7.42 (m, 2H), 7.31–7.30 (m, 3H), 5.86–5.76 (m, 1H), 5.01–4.91 (m, 2H), 4.59 (q, 1H, *J* = 4.0 Hz), 2.03 (q, 2H, *J* = 8.0 Hz), 1.85 (d, 1H, *J* = 4.0 Hz), 1.81–1.77 (m, 2H), 1.52–1.30 (m, 12H) ppm; <sup>13</sup>C NMR (CDCl<sub>3</sub>, 100.6 MHz): δ 139.4, 131.9, 128.6, 128.5, 122.9, 114.3, 90.4, 85.1, 63.3, 38.1, 34.1, 29.7, 29.6, 29.5, 29.4, 29.2, 25.5 ppm; HRMS *m/z* Calcd. for C<sub>19</sub>H<sub>26</sub>O: 270.19835. Found: 270.19875.

**(Z)-2-(hydroxy(4-(methoxycarbonyl)phenyl)methyl)-3-phenyl-1-(4-(methoxycarbonyl)phenyl)prop-2-en-1-one (Table 4, entry 1):**



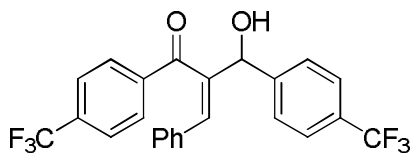
The general reaction procedure was followed for the synthesis and purification; product was afforded as yellow oil in 85% isolated yield.  $^1\text{H}$  NMR ( $\text{CDCl}_3$ , 400 MHz):  $\delta$  7.96 (d, 2H,  $J = 8.0$  Hz), 7.76 (d, 2H,  $J = 8.0$  Hz), 7.61 (d, 2H,  $J = 8.0$  Hz), 7.50 (d, 2H,  $J = 8.0$  Hz), 7.07 (s, 1H), 7.03 (s, 4H), 5.81 (s, 1H), 3.94 (s, 1H), 3.86 (s, 3H), 3.83 (s, 3H) ppm;  $^{13}\text{C}$  NMR ( $\text{CDCl}_3$ , 100.6 MHz):  $\delta$  199.8, 166.9, 166.3, 146.2, 141.1, 139.5, 134.7, 133.9, 133.9, 130.1, 129.9, 129.6, 129.3, 129.2, 128.9, 128.5, 126.6, 76.6, 52.6, 52.4 ppm; HRMS  $m/z$  Calcd. for  $\text{C}_{26}\text{H}_{22}\text{O}_2$ : 430.14164. Found: 430.14262.

**(Z)-2-(hydroxy(3-iodophenyl)methyl)-1-(3-iodophenyl)-3-phenylprop-2-en-1-one (Table 4, entry 2):**



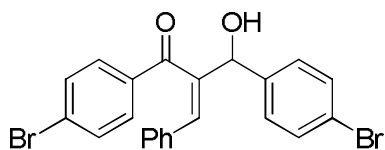
The general reaction procedure was followed for the synthesis and purification; product was afforded as colorless oil in 78% isolated yield.  $^1\text{H}$  NMR ( $\text{CDCl}_3$ , 400 MHz):  $\delta$  7.79 (s, 1H), 7.78 (s, 1H), 7.60 (d, 1H,  $J = 8.0$  Hz), 7.56–7.51 (m, 2H), 7.35 (d, 1H,  $J = 8.0$  Hz), 7.08–7.00 (m, 7H), 6.86 (t, 1H,  $J = 8.0$  Hz), 5.64 (s, 1H), 3.40 (s, 1H) ppm;  $^{13}\text{C}$  NMR ( $\text{CDCl}_3$ , 100.6 MHz):  $\delta$  198.8, 143.3, 142.1, 140.9, 138.4, 137.8, 137.3, 135.6, 134.7, 133.6, 130.5, 130.1, 129.2, 128.8, 128.8, 128.5, 126.0, 94.8, 94.2, 76.1 ppm; HRMS  $m/z$  Calcd. for  $\text{C}_{22}\text{H}_{16}\text{I}_2\text{O}_2$ : 565.92398. Found: 565.92536.

**(Z)-2-(hydroxy(4-(trifluoromethyl)phenyl)methyl)-3-phenyl-1-(4-(trifluoromethyl)phenyl)prop-2-en-1-one (Table 4, entry 3):**



The general reaction procedure was followed for the synthesis and purification; product was afforded as colorless oil in 93% isolated yield.  $^1\text{H}$  NMR ( $\text{CD}_3\text{CN}$ , 400 MHz):  $\delta$  7.83 (d, 2H,  $J = 8.0$  Hz), 7.64 (s, 4H), 7.55 (d, 3H,  $J = 8.0$  Hz), 7.18 (s, 1H), 7.13 (s, 4H), 5.79 (s, 1H), 4.26 (d, 1H, 4.0 Hz) ppm;  $^{13}\text{C}$  NMR ( $\text{CD}_3\text{CN}$ , 100.6 MHz):  $\delta$  198.4, 146.6, 142.4, 139.7, 135.2, 133.4 (q,  $J = 32.0$  Hz), 131.8, 131.7 (q,  $J = 32.0$  Hz), 129.9, 129.0, 128.5, 127.6, 125.4 (q,  $J = 4.0$  Hz), 125.3 (q,  $J = 4.0$  Hz), 124.5 (q,  $J = 273.0$  Hz), 123.9 (q,  $J = 270.0$  Hz), 75.2 ppm;  $^{19}\text{F}$  NMR ( $\text{CDCl}_3$ , 376 MHz):  $\delta$  -63.4, -64.1 ppm; HRMS  $m/z$  Calcd. for  $\text{C}_{24}\text{H}_{16}\text{F}_6\text{O}_2$ : 450.10545. Found: 450.10641.

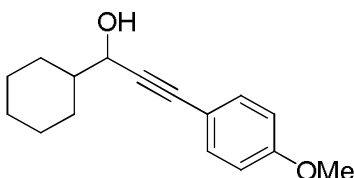
**(Z)-1-(4-bromophenyl)-2-((4-bromophenyl)(hydroxy)methyl)-3-phenylprop-2-en-1-one (Table 4, entry 4):**



The general reaction procedure was followed for the synthesis and purification; product was afforded as colorless oil in 79% isolated yield.  $^1\text{H}$  NMR ( $\text{CDCl}_3$ , 400 MHz):  $\delta$  7.48–7.42 (m, 4H), 7.31–7.26 (m, 4H), 7.08–7.06 (m, 5H), 6.97 (s, 1H), 5.67 (s, 1H), 3.28 (d, 1H,  $J = 4.0$  Hz) ppm;  $^{13}\text{C}$  NMR ( $\text{CDCl}_3$ , 100.6 MHz):  $\delta$  199.4, 141.1, 140.1, 134.9, 134.7, 133.2, 131.9,

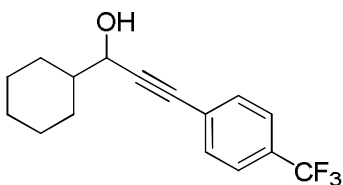
131.8, 131.0, 129.2, 128.9, 128.8, 128.5, 128.4, 122.2, 76.4 ppm; HRMS  $m/z$  Calcd. for  $C_{22}H_{16}Br_2O_2$ : 469.95170. Found: 469.95310.

**1-Cyclohexyl-3-(4-methoxyphenyl)prop-2-yn-1-ol (Table 5, entry 1):**



The general reaction procedure was followed for the synthesis and purification; product was afforded as colorless oil in 92% isolated yield.  $^1H$  NMR ( $CDCl_3$ , 400 MHz):  $\delta$  7.38 (d, 1H,  $J = 8.0$  Hz), 7.25–7.24 (m, 1H), 6.90–6.83 (m, 2H), 4.42 (d, 1H,  $J = 4.0$  Hz), 3.85 (s, 3H), 2.47 (bs, 1H), 1.94–1.66 (m, 6H), 1.24–1.17 (m, 5H) ppm;  $^{13}C$  NMR ( $CDCl_3$ , 100.6 MHz):  $\delta$  160.2, 133.8, 129.9, 120.6, 112.2, 110.8, 93.8, 82.0, 67.9, 56.0, 44.5, 28.9, 28.4, 26.7, 26.2 ppm; HRMS  $m/z$  Calcd. for  $C_{16}H_{20}O_2$ : 244.14632. Found: 244.14668.

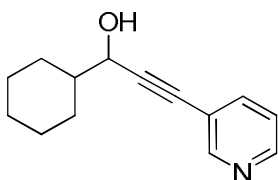
**1-Cyclohexyl-3-(4-(trifluoromethyl)phenyl)prop-2-yn-1-ol (Table 5, entry 2):**



The general reaction procedure was followed for the synthesis and purification; product was afforded as colorless oil in 84% isolated yield.  $^1H$  NMR ( $CDCl_3$ , 400 MHz):  $\delta$  7.55–7.49 (m, 4H), 4.38 (d, 1H,  $J = 4.0$  Hz), 2.37 (bs, 1H), 1.93–1.66 (m, 6H), 1.28–1.11 (m, 5H) ppm;  $^{13}C$  NMR ( $CDCl_3$ , 100.6 MHz):  $\delta$  132.1, 130.2 (q,  $J = 30.2$  Hz), 126.8, 125.4, 125.4, 125.3,

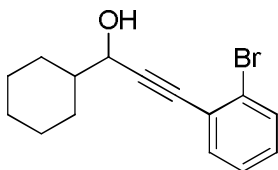
124.0 (q,  $J = 271.6$  Hz), 92.0, 84.5, 67.8, 44.4, 28.9, 28.4, 26.6, 26.1 ppm;  $^{19}\text{F}$  NMR ( $\text{CDCl}_3$ , 376 MHz):  $\delta$  -63.3 ppm; HRMS  $m/z$  Calcd. for  $\text{C}_{16}\text{H}_{17}\text{F}_3\text{O}$ : 282.12314. Found: 282.12345.

**1-Cyclohexyl-3-(pyridin-3-yl)prop-2-yn-1-ol (Table 5, entry 3):**



The general reaction procedure was followed for the synthesis and purification; product was afforded as colorless oil in 88% isolated yield.  $^1\text{H}$  NMR ( $\text{CDCl}_3$ , 400 MHz):  $\delta$  8.73 (s, 1H), 8.49 (d, 1H,  $J = 4.0$  Hz), 7.71 (d, 1H,  $J = 8.0$  Hz), 7.26–7.22 (m, 1H), 4.37 (d, 1H,  $J = 4.0$  Hz), 4.01 (bs, 1H), 1.91–1.66 (m, 6H), 1.28–1.11 (m, 5H) ppm;  $^{13}\text{C}$  NMR ( $\text{CDCl}_3$ , 100.6 MHz):  $\delta$  152.2, 148.4, 139.1, 123.3, 120.5, 115.5, 94.0, 82.0, 67.5, 44.5, 28.9, 28.6, 26.6, 26.2, 26.1 ppm; HRMS  $m/z$  Calcd. for  $\text{C}_{14}\text{H}_{17}\text{NO}$ : 215.13101. Found: 215.13147.

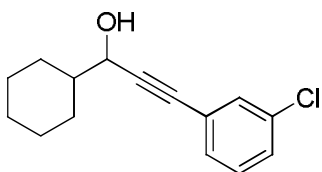
**3-(2-Bromophenyl)-1-cyclohexylprop-2-yn-1-ol (Table 5, entry 4):**



The general reaction procedure was followed for the synthesis and purification; product was afforded as yellow oil in 86% isolated yield.  $^1\text{H}$  NMR ( $\text{CDCl}_3$ , 400 MHz):  $\delta$  7.56 (d, 1H,  $J = 8.0$  Hz), 7.45 (d, 1H,  $J = 4.0$  Hz), 7.23 (t, 1H,  $J = 8.0$  Hz), 7.16 (t, 1H,  $J = 8.0$  Hz), 4.44 (s, 1H), 2.30 (d, 1H,  $J = 4.0$  Hz), 1.94–1.69 (m, 6H), 1.27–1.18 (m, 5H) ppm;  $^{13}\text{C}$  NMR ( $\text{CDCl}_3$ ,

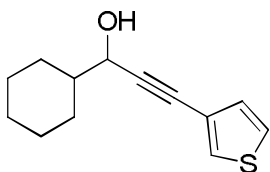
100.6 MHz):  $\delta$  133.7, 132.6, 129.7, 127.2, 125.8, 125.1, 94.3, 84.3, 67.9, 44.5, 28.9, 28.3, 26.7, 26.2, 26.1 ppm; HRMS  $m/z$  Calcd. for  $C_{15}H_{17}BrO$ : 292.04627. Found: 292.04691.

**3-(3-Chlorophenyl)-1-cyclohexylprop-2-yn-1-ol (Table 5, entry 5):**

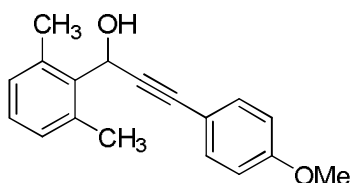


The general reaction procedure was followed for the synthesis and purification; product was afforded as yellow oil in 84% isolated yield.  $^1H$  NMR ( $CDCl_3$ , 400 MHz):  $\delta$  7.41 (s, 1H), 7.29–7.20 (m, 3H), 4.37 (s, 1H), 2.10 (s, 1H), 1.92–1.68 (m, 6H), 1.29–1.10 (m, 5H) ppm;  $^{13}C$  NMR ( $CDCl_3$ , 100.6 MHz):  $\delta$  134.3, 131.7, 130.0, 129.7, 128.8, 124.7, 90.8, 84.5, 67.8, 44.5, 28.9, 28.5, 26.6, 26.1, 26.1 ppm; HRMS  $m/z$  Calcd. for  $C_{15}H_{17}ClO$ : 248.09679. Found: 248.09739.

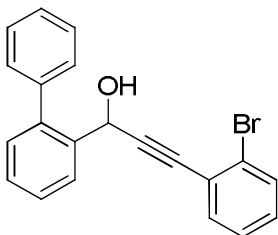
**1-Cyclohexyl-3-(thiophen-3-yl)prop-2-yn-1-ol (Table 5, entry 6):**



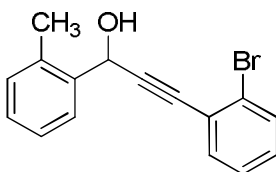
The general reaction procedure was followed for the synthesis and purification; product was afforded as yellow oil in 91% isolated yield.  $^1H$  NMR ( $CDCl_3$ , 400 MHz):  $\delta$  7.24–7.19 (m, 2H), 6.97–6.94 (m, 1H), 4.38 (d, 1H,  $J = 8.0$  Hz), 2.31 (s, 1H), 1.92–1.63 (m, 6H), 1.30–1.08 (m, 5H) ppm;  $^{13}C$  NMR ( $CDCl_3$ , 100.6 MHz):  $\delta$  132.3, 127.1, 122.9, 93.5, 79.1, 68.0, 44.4, 28.9, 28.5, 26.6, 26.1 ppm; HRMS  $m/z$  Calcd. for  $C_{13}H_{16}OS$ : 220.09218. Found: 220.09246.

**1-(2,6-Dimethylphenyl)-3-(4-methoxyphenyl)prop-2-yn-1-ol (Table 6, entry 1):**

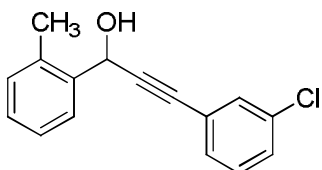
The general reaction procedure was followed for the synthesis and purification; product was afforded as yellow oil in 92% isolated yield.  $^1\text{H}$  NMR ( $\text{CDCl}_3$ , 400 MHz):  $\delta$  7.39 (d, 1H,  $J = 8.0$  Hz), 7.28 (t, 1H,  $J = 8.0$  Hz), 7.12–7.04 (m, 3H), 6.91–6.39 (m, 2H), 6.19 (s, 1H), 3.83 (s, 3H), 2.69 (s, 1H), 2.62 (s, 6H) ppm;  $^{13}\text{C}$  NMR ( $\text{CDCl}_3$ , 100.6 MHz):  $\delta$  160.4, 137.1, 136.7, 133.8, 130.2, 129.4, 128.3, 120.6, 112.2, 110.9, 93.1, 82.4, 61.2, 55.9, 20.7 ppm; HRMS  $m/z$  Calcd. for  $\text{C}_{18}\text{H}_{18}\text{O}_2$ : 266.13067. Found: 266.13699.

**1-(Biphenyl-2-yl)-3-(2-bromophenyl)prop-2-yn-1-ol (Table 6, entry 2):**

The general reaction procedure was followed for the synthesis and purification; product was afforded as colorless oil in 81% isolated yield.  $^1\text{H}$  NMR ( $\text{CDCl}_3$ , 400 MHz):  $\delta$  8.05 (d, 1H,  $J = 8.0$  Hz), 7.59 (d, 1H,  $J = 8.0$  Hz), 7.51–7.40 (m, 8H), 7.34–7.17 (m, 3H), 5.74 (s, 1H), 2.47 (s, 1H) ppm;  $^{13}\text{C}$  NMR ( $\text{CDCl}_3$ , 100.6 MHz):  $\delta$  141.2, 140.4, 138.2, 133.8, 132.6, 130.4, 129.9, 129.8, 128.5, 128.1, 127.7, 127.2, 125.9, 124.9, 94.5, 85.3, 62.5 ppm; HRMS  $m/z$  Calcd. for  $\text{C}_{21}\text{H}_{15}\text{BrO}$ : 362.03062. Found: 362.03139.

**3-(2-Bromophenyl)-1-*o*-tolylprop-2-yn-1-ol (Table 6, entry 3):**

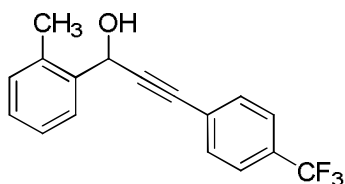
The general reaction procedure was followed for the synthesis and purification; product was afforded as yellow solid in 78% isolated yield.  $^1\text{H}$  NMR ( $\text{CDCl}_3$ , 400 MHz):  $\delta$  7.84–7.81 (m, 1H), 7.59–7.48 (m, 2H), 7.28–7.16 (m, 5H), 5.88 (d, 1H,  $J = 4.0$  Hz), 2.53 (s, 3H), 2.46 (d, 1H,  $J = 4.0$  Hz) ppm;  $^{13}\text{C}$  NMR ( $\text{CDCl}_3$ , 100.6 MHz):  $\delta$  138.3, 136.3, 133.8, 132.6, 131.0, 129.9, 128.8, 127.2, 127.0, 126.5, 125.9, 124.9, 93.4, 85.3, 63.3, 19.3 ppm; HRMS  $m/z$  Calcd. for  $\text{C}_{16}\text{H}_{13}\text{BrO}$ : 300.01497. Found: 300.01572.

**3-(3-Chlorophenyl)-1-*o*-tolylprop-2-yn-1-ol (Table 6, entry 4):**

The general reaction procedure was followed for the synthesis and purification; product was afforded as colorless oil in 72% isolated yield.  $^1\text{H}$  NMR ( $\text{CDCl}_3$ , 400 MHz):  $\delta$  7.70 (t, 1H,  $J = 4.0$  Hz), 7.45 (s, 1H), 7.34–7.20 (m, 6H), 5.82 (s, 1H), 2.49 (s, 4H) ppm;  $^{13}\text{C}$  NMR ( $\text{CDCl}_3$ , 100.6 MHz):  $\delta$  138.3, 136.2, 134.4, 131.8, 131.1, 130.1, 129.8, 129.1, 128.8, 126.8, 126.5, 124.4, 90.1, 85.3, 63.1, 19.3 ppm; HRMS  $m/z$  Calcd. for  $\text{C}_{16}\text{H}_{13}\text{ClO}$ : 256.06549. Found: 256.06600.

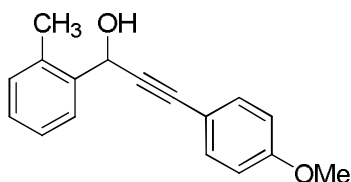
**1-*o*-Tolyl-3-(4-(trifluoromethyl)phenyl)prop-2-yn-1-ol (Table 6, entry 5):**





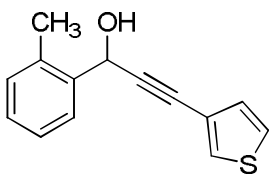
The general reaction procedure was followed for the synthesis and purification; product was afforded as colorless oil in 83% isolated yield.  $^1\text{H}$  NMR ( $\text{CDCl}_3$ , 400 MHz):  $\delta$  7.71 (t, 1H,  $J = 4.0$  Hz), 7.59–7.54 (m, 4H), 7.29–7.21 (m, 3H), 5.84 (d, 1H,  $J = 4.0$  Hz), 2.52 (d, 1H,  $J = 8.0$  Hz), 2.50 (s, 3H) ppm;  $^{13}\text{C}$  NMR ( $\text{CDCl}_3$ , 100.6 MHz):  $\delta$  138.2, 136.2, 132.4, 131.6, 130.5 (q,  $J = 33$  Hz), 128.9, 126.8, 126.6, 125.5, 125.4, 121.3 (q,  $J = 270$  Hz), 91.3, 85.3, 63.1, 19.2 ppm;  $^{19}\text{F}$  NMR ( $\text{CDCl}_3$ , 376 MHz):  $\delta$  -63.26 ppm; HRMS  $m/z$  Calcd. for  $\text{C}_{17}\text{H}_{13}\text{F}_3\text{O}$ : 290.0906. Found: 290.0918.

### 3-(4-Methoxyphenyl)-1-*o*-tolylprop-2-yn-1-ol (Table 6, entry 6):



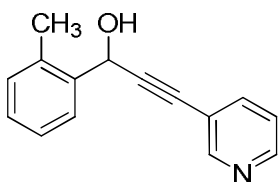
The general reaction procedure was followed for the synthesis and purification; product was afforded as yellow oil in 86% isolated yield.  $^1\text{H}$  NMR ( $\text{CDCl}_3$ , 400 MHz):  $\delta$  7.82–7.80 (m, 1H), 7.43 (d, 1H,  $J = 8.0$  Hz), 7.32–7.21 (m, 4H), 6.92–6.85 (m, 2H), 5.87 (d, 1H,  $J = 4.0$  Hz), 3.85 (s, 3H), 3.70 (d, 1H,  $J = 4.0$  Hz), 2.51 (s, 3H) ppm;  $^{13}\text{C}$  NMR ( $\text{CDCl}_3$ , 100.6 MHz):  $\delta$  160.4, 138.7, 136.4, 133.8, 130.9, 130.2, 128.5, 127.1, 126.4, 120.6, 110.9, 93.0, 83.1, 63.3, 56.0, 19.2 ppm; HRMS  $m/z$  Calcd. for  $\text{C}_{17}\text{H}_{16}\text{O}_2$ : 252.1148. Found: 252.1150.

### 3-(Thiophen-3-yl)-1-*o*-tolylprop-2-yn-1-ol (Table 6, entry 7):



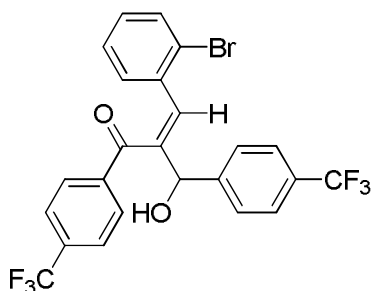
The general reaction procedure was followed for the synthesis and purification; product was afforded as yellow oil in 67% isolated yield.  $^1\text{H}$  NMR ( $\text{CDCl}_3$ , 400 MHz):  $\delta$  7.70 (t, 1H,  $J = 4.0$  Hz), 7.28–7.20 (m, 5H), 7.98 (t, 1H,  $J = 4.0$  Hz), 5.85 (d, 1H,  $J = 8.0$  Hz), 2.49 (s, 3H), 2.22 (d, 1H,  $J = 8.0$  Hz) ppm;  $^{13}\text{C}$  NMR ( $\text{CDCl}_3$ , 100.6 MHz):  $\delta$  138.3, 136.2, 132.6, 131.1, 128.8, 127.6, 127.2, 126.8, 126.5, 122.6, 92.5, 80.1, 63.4, 19.3 ppm; HRMS  $m/z$  Calcd. for  $\text{C}_{14}\text{H}_{12}\text{OS}$ : 228.0605. Found: 228.0609.

**3-(Pyridin-3-yl)-1-*o*-tolylprop-2-yn-1-ol (Table 6, entry 8):**



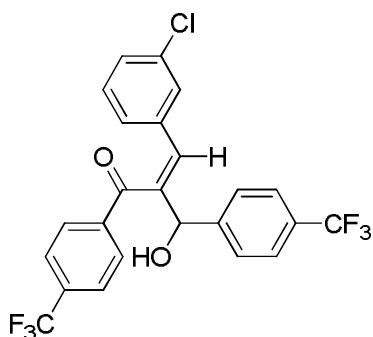
The general reaction procedure was followed for the synthesis and purification; product was afforded as yellow solid in 88% isolated yield.  $^1\text{H}$  NMR ( $\text{CDCl}_3$ , 400 MHz):  $\delta$  8.73 (s, 1H), 8.42 (d, 1H,  $J = 8.0$  Hz), 7.71–7.69 (m, 2H), 7.26–7.20 (m, 4H), 5.84 (s, 1H), 5.35 (bs, 1H), 2.48 (s, 3H) ppm;  $^{13}\text{C}$  NMR ( $\text{CDCl}_3$ , 100.6 MHz):  $\delta$  152.1, 148.4, 139.2, 138.7, 136.0, 130.9, 128.5, 126.7, 126.4, 123.4, 120.4, 93.7, 82.4, 62.5, 19.3 ppm; HRMS  $m/z$  Calcd. for  $\text{C}_{15}\text{H}_{13}\text{NO}$ : 223.0992. Found: 223.0997.

**(Z)-3-(2-Bromophenyl)-2-(hydroxy(4-(trifluoromethyl)phenyl)methyl)-1-(4-(trifluoromethyl)phenyl)prop-2-en-1-one (Table 7, entry 1):**



The general reaction procedure was followed for the synthesis and purification; product was afforded as colorless oil in 68% isolated yield.  $^1\text{H}$  NMR ( $\text{CDCl}_3$ , 400 MHz):  $\delta$  7.63–7.59 (m, 6H), 7.38–7.25 (m, 4H), 6.91 (bs, 3H), 5.89 (s, 1H), 3.33 (s, 1H) ppm;  $^{13}\text{C}$  NMR ( $\text{CDCl}_3$ , 100.6 MHz):  $\delta$  198.3, 144.9, 142.3, 139.4, 135.5, 134.6, 134.2, 131.2, 130.6 (q,  $J = 32.0$  Hz), 130.3, 129.3, 127.4, 127.0, 126.8 (q,  $J = 270.0$  Hz), 126.2 (q,  $J = 272.0$  Hz), 125.9, 124.8, 123.5, 76.5 ppm;  $^{19}\text{F}$  NMR ( $\text{CDCl}_3$ , 376 MHz):  $\delta$  -63.0, -63.8 ppm; HRMS  $m/z$  Calcd. for  $\text{C}_{24}\text{H}_{15}\text{BrF}_6\text{O}_2$ : 528.01595. Found: 528.01759.

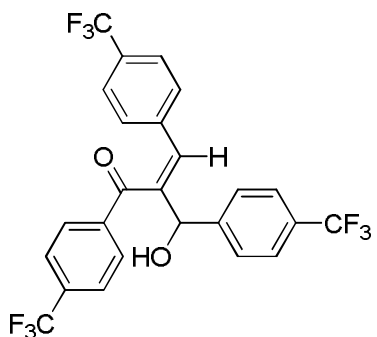
**(Z)-3-(3-Chlorophenyl)-2-(hydroxy(4-(trifluoromethyl)phenyl)methyl)-1-(4-(trifluoromethyl)phenyl)prop-2-en-1-one (Table 7, entry 2):**



The general reaction procedure was followed for the synthesis and purification; product was afforded as white solid in 74% isolated yield.  $^1\text{H}$  NMR ( $\text{CDCl}_3$ , 400 MHz):  $\delta$  7.66–7.40 (m, 8H), 7.01–6.89 (m, 5H), 5.80 (s, 1H), 3.22 (s, 1H) ppm;  $^{13}\text{C}$  NMR ( $\text{CDCl}_3$ , 100.6 MHz):  $\delta$

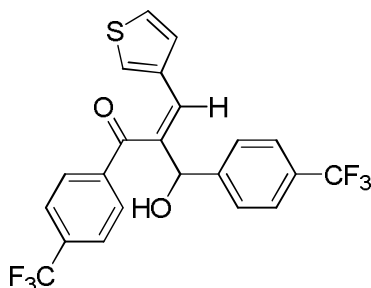
198.7, 144.5, 142.4, 138.7, 136.1, 134.8 (q,  $J = 25.0$  Hz), 134.4, 132.0, 130.7 (q,  $J = 32.0$  Hz), 129.7, 129.4, 129.0, 128.8, 126.9, 126.8 (q,  $J = 290$  Hz), 126.6 (q,  $J = 320$  Hz), 125.7, 125.4, 75.8 ppm;  $^{19}\text{F}$  NMR ( $\text{CDCl}_3$ , 376 MHz):  $\delta$  -63.1, -63.8 ppm; HRMS  $m/z$  Calcd. for  $\text{C}_{24}\text{H}_{15}\text{ClF}_6\text{O}_2$ : 484.0644. Found: 484.0665.

**(Z)-2-(hydroxy(4-(trifluoromethyl)phenyl)methyl)-1,3-bis(4-(trifluoromethyl)phenyl)prop-2-en-1-one (Table 7, entry 3):**



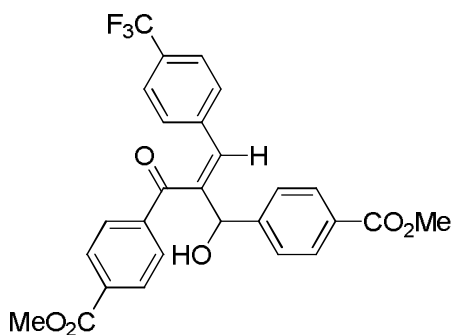
The general reaction procedure was followed for the synthesis and purification; product was afforded as yellow oil in 72% isolated yield.  $^1\text{H}$  NMR ( $\text{CDCl}_3$ , 400 MHz):  $\delta$  7.68 (d, 2H,  $J = 8.0$  Hz), 7.60–7.53 (m, 4H), 7.41 (d, 2H,  $J = 8.0$  Hz), 7.33 (d, 2H,  $J = 8.0$  Hz), 7.16 (d, 2H,  $J = 8.0$  Hz), 7.04 (s, 1H), 5.84 (d, 1H,  $J = 4.0$  Hz), 3.18 (d, 1H,  $J = 4.0$  Hz) ppm;  $^{13}\text{C}$  NMR ( $\text{CDCl}_3$ , 100.6 MHz):  $\delta$  198.5, 144.5, 143.6, 138.9, 138.1, 134.9 (q,  $J = 32.0$  Hz), 131.7, 130.7 (q,  $J = 32.0$  Hz), 130.7 (q,  $J = 32.0$  Hz), 129.6, 129.3, 127.1, 125.8, 125.4, 125.3, 124.1 (q,  $J = 271.0$  Hz), 123.8 (q,  $J = 271.0$  Hz), 123.4 (q,  $J = 271.0$  Hz), 75.9 ppm;  $^{19}\text{F}$  NMR ( $\text{CDCl}_3$ , 376 MHz):  $\delta$  -63.1, -63.5, -63.9 ppm; HRMS  $m/z$  Calcd. for  $\text{C}_{25}\text{H}_{15}\text{F}_9\text{O}_2$ : 518.09283. Found: 518.09409.

**(Z)-2-(hydroxy(4-(trifluoromethyl)phenyl)methyl)-3-(thiophen-3-yl)-1-(4-(trifluoromethyl)phenyl)prop-2-en-1-one (Table 7, entry 4):**



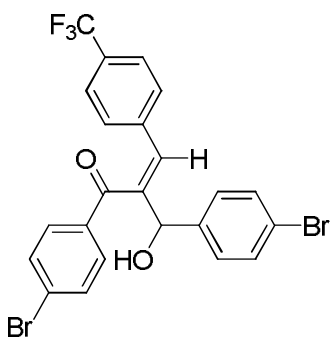
The general reaction procedure was followed for the synthesis and purification; product was afforded as green oil in 69% isolated yield.  $^1\text{H}$  NMR ( $\text{CDCl}_3$ , 400 MHz):  $\delta$  7.85 (d, 2H,  $J = 8.0$  Hz), 7.58–7.53 (m, 6H), 7.15 (d, 1H,  $J = 8.0$  Hz), 7.00 (s, 1H), 6.84–6.79 (m, 2H), 5.75 (d, 1H,  $J = 4.0$  Hz), 3.06 (d, 1H,  $J = 4.0$  Hz) ppm;  $^{13}\text{C}$  NMR ( $\text{CDCl}_3$ , 100.6 MHz):  $\delta$  198.5, 144.7, 139.3, 138.9, 137.1, 134.9 (q,  $J = 33.0$  Hz), 130.8 (q,  $J = 33.0$  Hz), 130.4, 129.8, 128.6, 128.1, 127.0, 125.7, 125.3, 124.1 (q,  $J = 270.0$  Hz), 123.61 (q,  $J = 271.0$  Hz), 76.2 ppm;  $^{19}\text{F}$  NMR ( $\text{CDCl}_3$ , 376 MHz):  $\delta$  -64.7, -65.4 ppm; HRMS  $m/z$  Calcd. for  $\text{C}_{22}\text{H}_{14}\text{F}_6\text{O}_2\text{S}$ : 456.06186. Found: 456.06315.

**(Z)-1-(4-(methoxycarbonyl)phenyl)-2-((4-(methoxycarbonyl)phenyl)(hydroxy)methyl)-3-(4-(trifluoromethyl)phenyl)prop-2-en-1-one (Table 7, entry 5):**



The general reaction procedure was followed for the synthesis and purification; product was afforded as yellow oil in 73% isolated yield.  $^1\text{H}$  NMR ( $\text{CDCl}_3$ , 400 MHz):  $\delta$  7.97 (d, 2H,  $J = 8.0$  Hz), 7.80 (d, 2H,  $J = 8.0$  Hz), 7.63 (d, 2H,  $J = 8.0$  Hz), 7.50 (d, 2H,  $J = 8.0$  Hz), 7.30 (d, 2H,  $J = 8.0$  Hz), 7.15 (d, 2H,  $J = 8.0$  Hz), 7.03 (s, 1H), 5.84 (s, 1H), 3.87 (s, 3H), 3.85 (s, 3H), 3.35 (d, 1H,  $J = 4.0$  Hz) ppm;  $^{13}\text{C}$  NMR ( $\text{CDCl}_3$ , 100.6 MHz):  $\delta$  198.9, 166.8, 166.1, 145.6, 143.8, 139.1, 134.4, 130.9, 130.3, 130.1 (q,  $J = 33.0$  Hz), 129.8, 129.2, 126.7, 125.5, 124.4, 123.8 (q,  $J = 263.0$  Hz), 76.2, 55.6, 52.4 ppm;  $^{19}\text{F}$  NMR ( $\text{CDCl}_3$ , 376 MHz):  $\delta$  -63.3 ppm; HRMS  $m/z$  Calcd. for  $\text{C}_{27}\text{H}_{21}\text{F}_3\text{O}_6$ : 498.12902. Found: 498.13023.

**(Z)-1-(4-Bromophenyl)-2-((4-bromophenyl)(hydroxy)methyl)-3-(4-(trifluoromethyl)phenyl)prop-2-en-1-one (Table 7, entry 6):**



The general reaction procedure was followed for the synthesis and purification; product was afforded as yellow oil in 65% isolated yield.  $^1\text{H}$  NMR ( $\text{CDCl}_3$ , 400 MHz):  $\delta$  7.49–7.44 (m, 4H), 7.34–7.26 (m, 6H), 7.16 (d, 2H,  $J = 8.0$  Hz), 6.94 (s, 1H), 5.69 (d, 1H,  $J = 4.0$  Hz), 3.08 (d, 1H,  $J = 4.0$  Hz) ppm;  $^{13}\text{C}$  NMR ( $\text{CDCl}_3$ , 100.6 MHz):  $\delta$  198.5, 143.8, 139.6, 138.3, 134.7, 132.2, 132.1, 132.0, 130.9, 130.4, 129.3, 128.5, 125.5, 123.9 (q,  $J = 267$  Hz), 122.5, 76.0 ppm;  $^{19}\text{F}$  NMR ( $\text{CDCl}_3$ , 376 MHz):  $\delta$  -63.2 ppm; HRMS  $m/z$  Calcd. for  $\text{C}_{23}\text{H}_{15}\text{Br}_2\text{F}_3\text{O}_2$ : 537.9358. Found: 537.9391.

### References

1. W. Su, S. Urgeonkar, P. A. McLaughlin, J. G. Verkade, *J. Am. Chem. Soc.* **2004**, *126*, 16433–16439.
2. C. W. Downey, B. D. Mahoney, V. R. Lipari, *J. Org. Chem.* **2009**, *74*, 2904–2906.
3. X. Yao, C.-J. Li, *Org. Lett.* **2005**, *7*, 4395–4398
4. H. Koyuncu, O. Dogan, *Org. Lett.* **2007**, *9*, 3477–3479.
5. G. Gao, R.-G. Xie, L. Pu, *Proc. Nat. Acad. Sci. U.S.A.* **2004**, *101*, 5417–5420.
6. Y. Asano, K. Hara, H. Ito, M. Sawamura, *Org. Lett.* **2007**, *9*, 3901–3904.

KW656, CDCL3  
400MHz  
COLORLESS OIL  
20 JUNE 2008

7.652  
7.636  
7.501  
7.427  
7.410  
7.389  
7.348

5.706

2.714

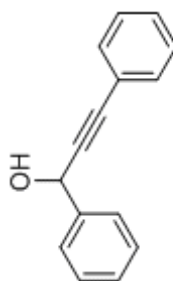
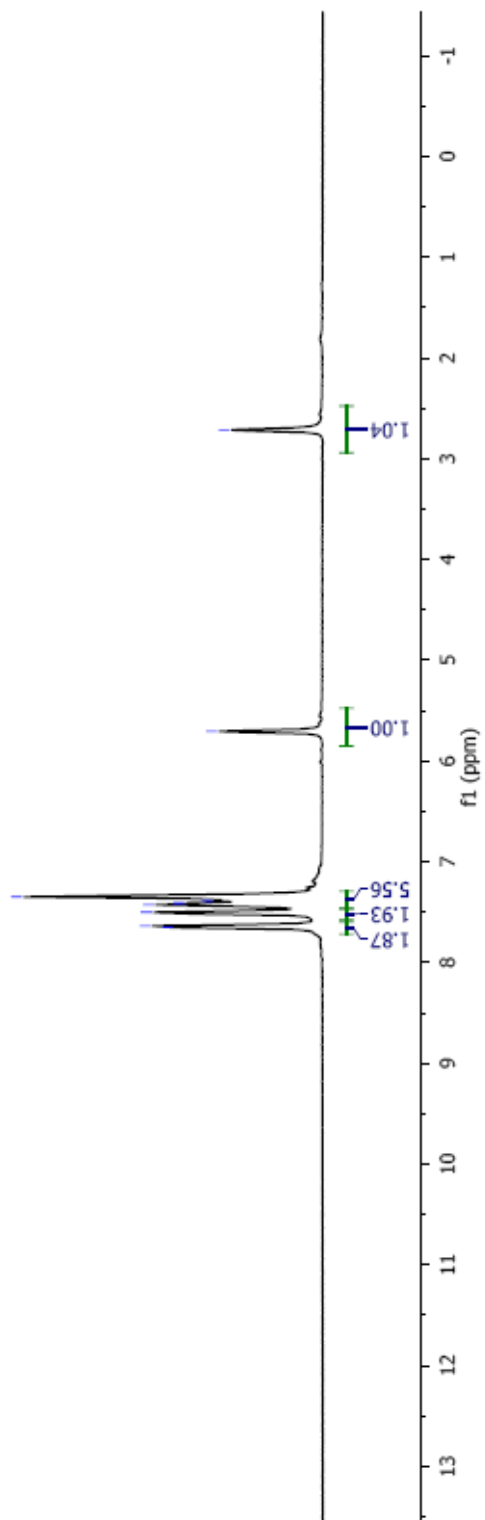


Table 1, entry 3





KW656, CDCL3  
100MHz  
COLORLESS OIL  
20 JUNE 2008

89.051  
86.912  
77.688  
77.370  
77.052  
65.329

140.883  
128.933  
128.691  
127.034  
122.674

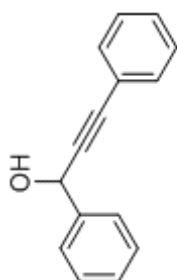
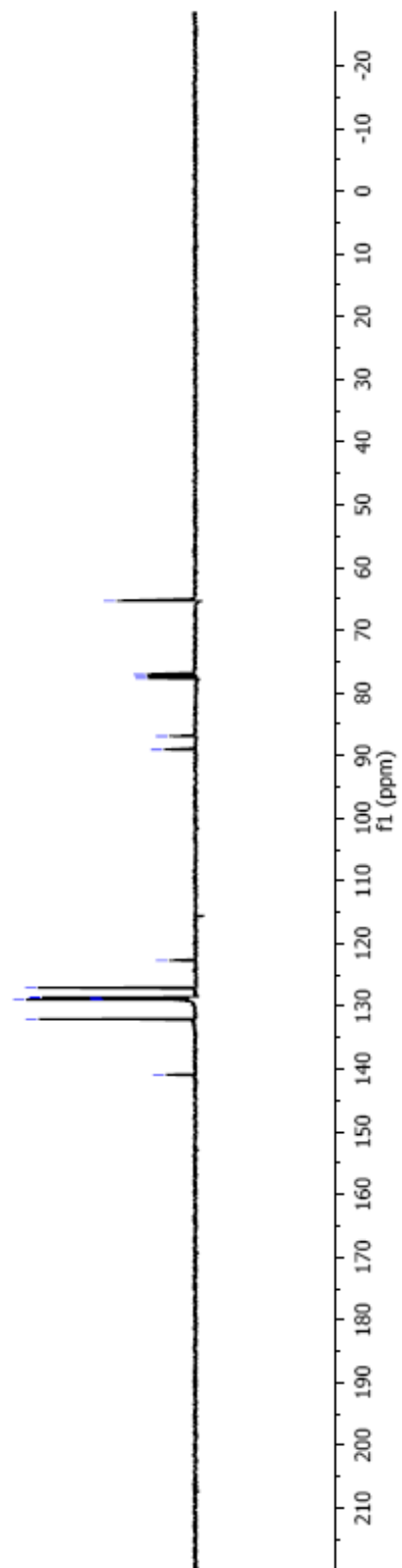
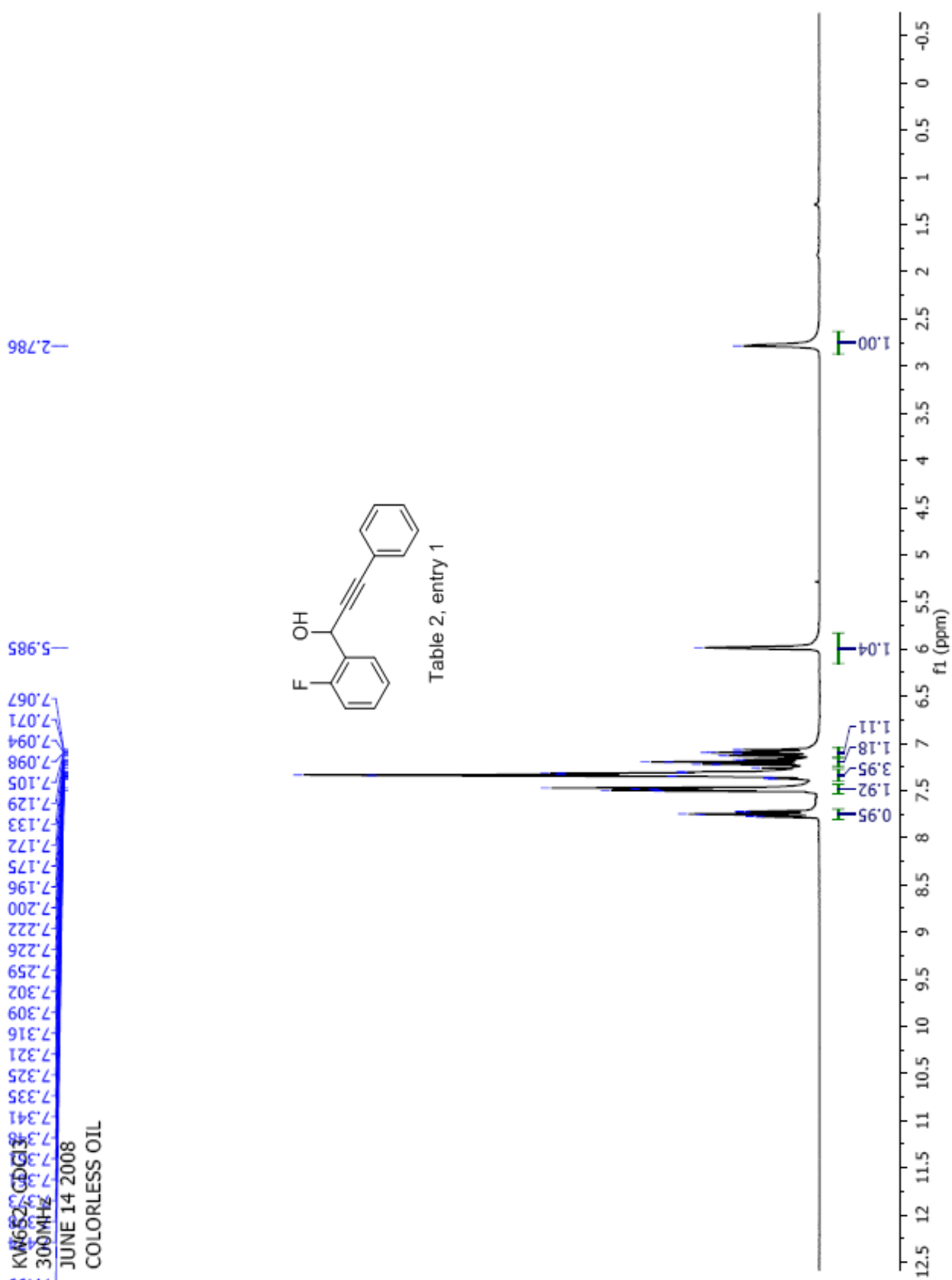


Table 1, entry 3





KW652, CDCl<sub>3</sub>  
 100MHz  
 JUNE 16 2008  
 COLORLESS OIL

161.674  
 159.207  
 132.035  
 128.695  
 128.558  
 124.672  
 124.638  
 122.488  
 116.006  
 115.797  
 87.871  
 86.810  
 77.669  
 77.351  
 77.036  
 59.768  
 59.718

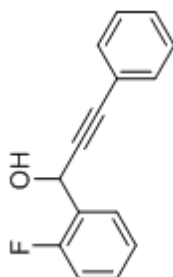
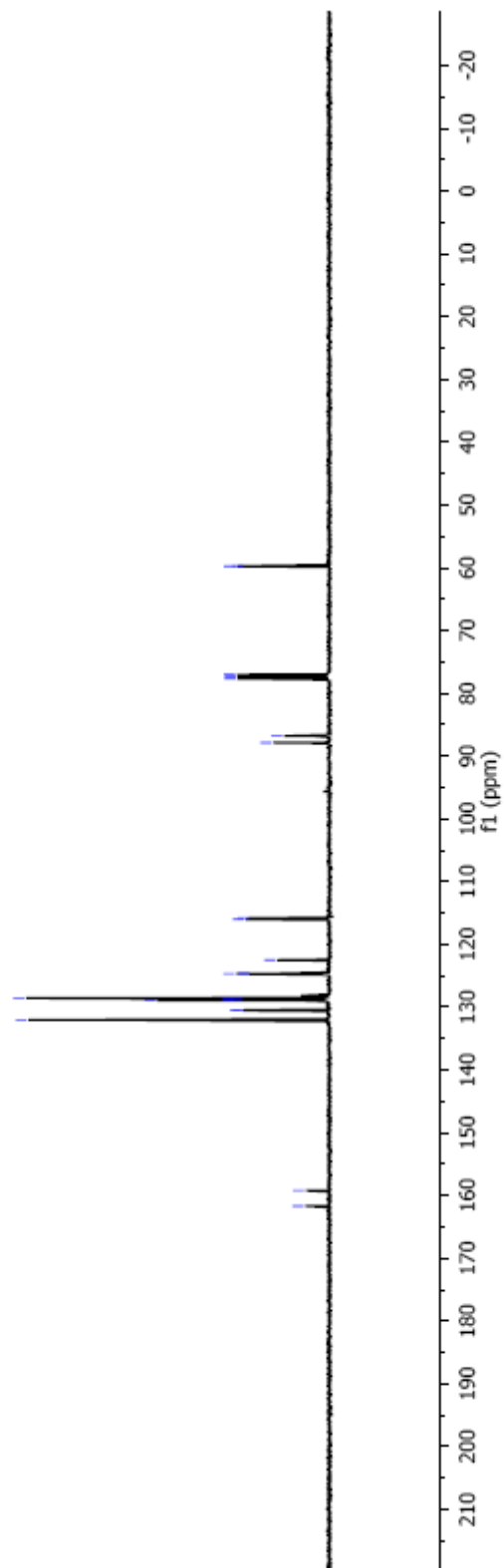


Table 2, entry 1



KW654, CDCL3  
400MHz  
YELLOW OIL  
JUNE 18 2008

2.383  
2.232

5.667

7.216  
7.235  
7.260  
7.325  
7.334  
7.338  
7.475  
7.484  
7.492  
7.497  
7.508  
7.528

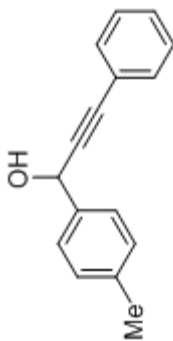
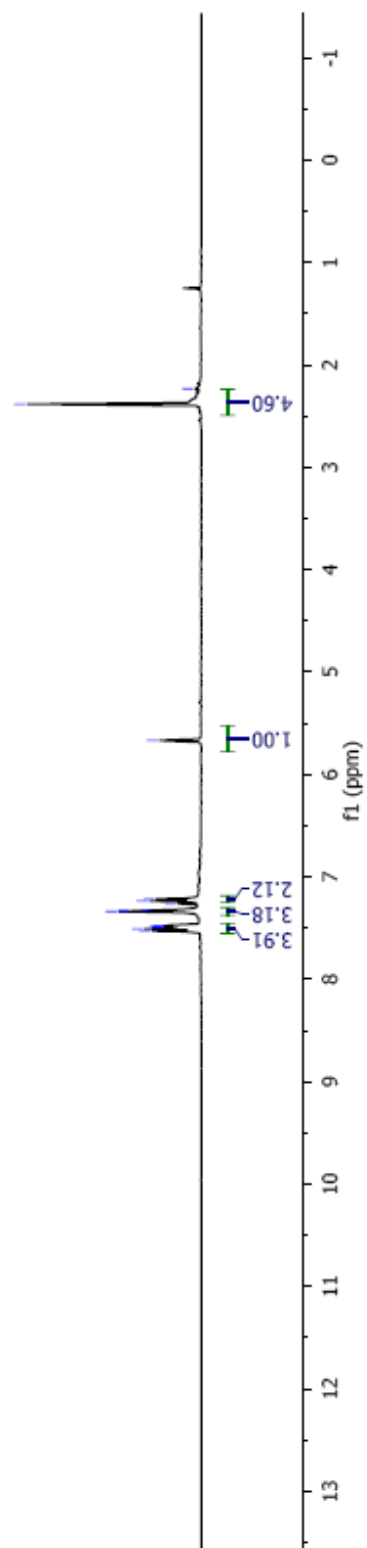


Table 2, entry 2



-21.477

-65.227

-76.976

-77.290

-77.609

-86.715

-89.107

-122.708

-126.958

-131.978

-138.009

-138.536

KW654, CDCL3  
 100MHz  
 YELLOW OIL  
 JUNE 18 2008

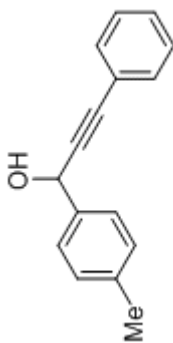
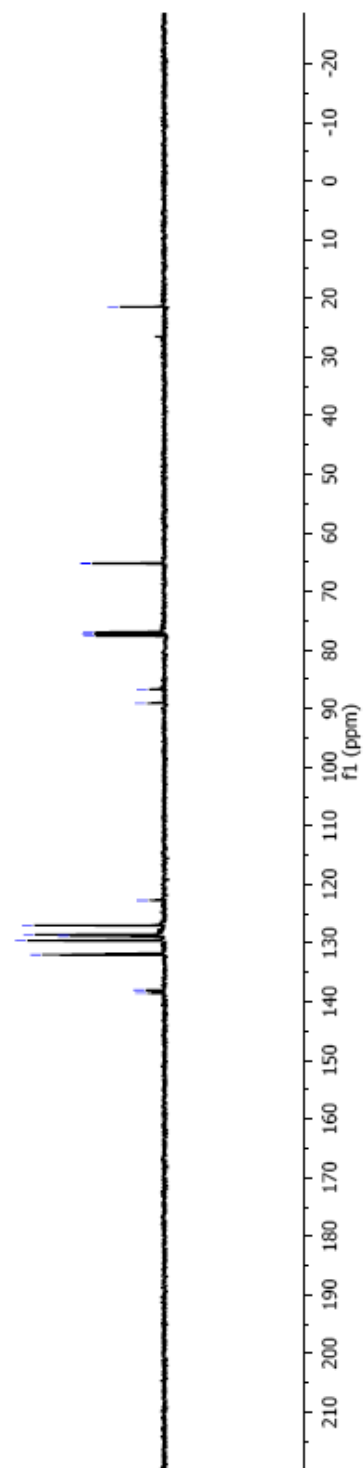


Table 2, entry 2



KW657, CDCl<sub>3</sub>  
400MHz  
COLORLESS OIL  
JUNE 20 2008

7.49  
7.48  
7.47  
7.34  
7.33  
7.33  
7.32  
7.30  
7.26  
7.22  
7.20  
6.91  
6.89  
5.68  
5.66  
3.83  
2.62

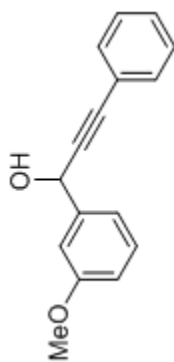
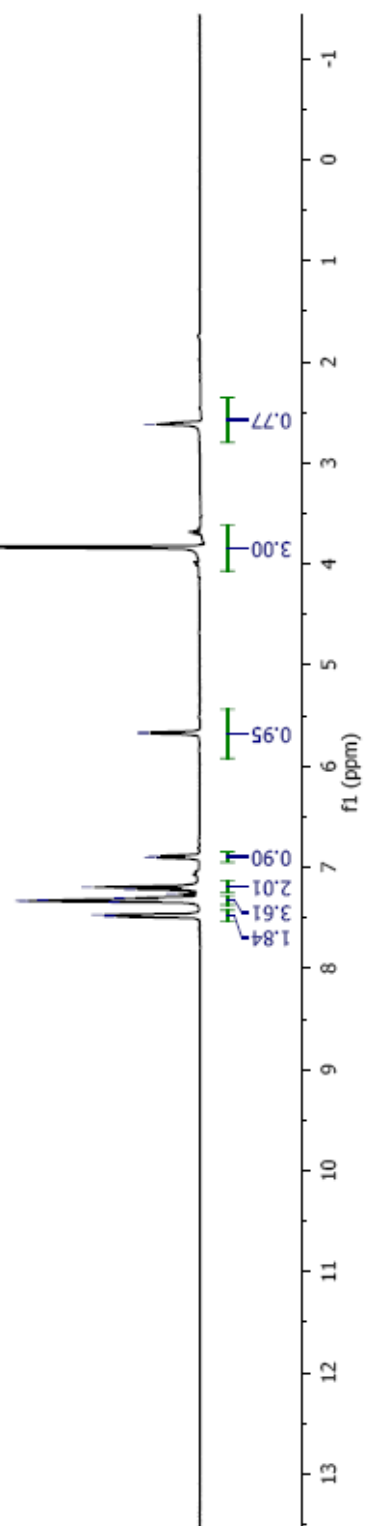
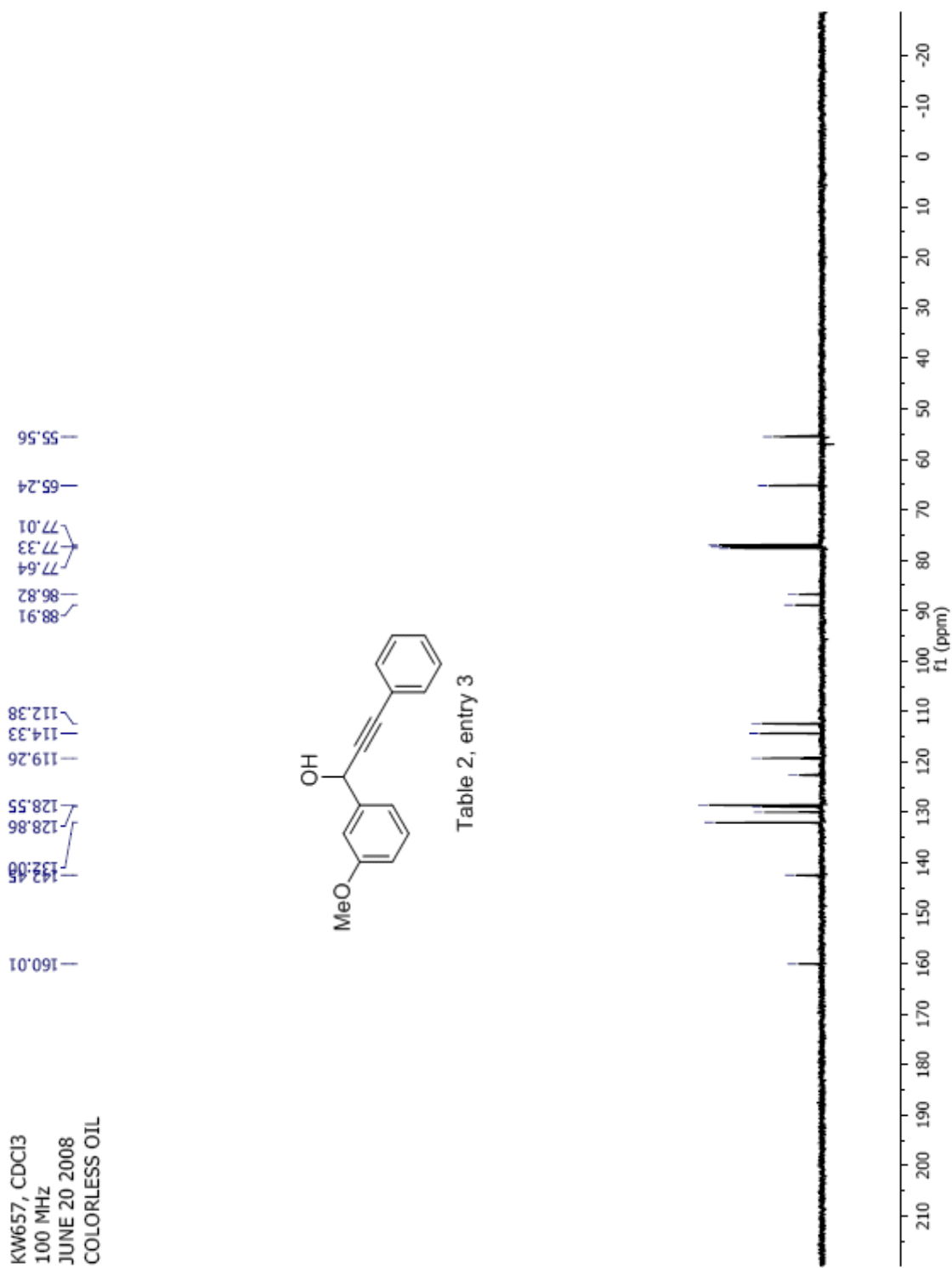


Table 2, entry 3





KW664, CDCI3  
400MHz  
COLORLESS OIL  
JUNE 27 2008

7.537  
7.518  
7.468  
7.361  
7.334  
7.314  
7.212  
7.193

2.936  
2.424

5.688

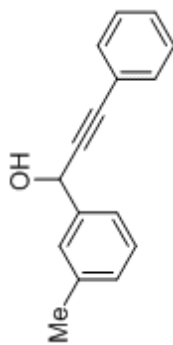
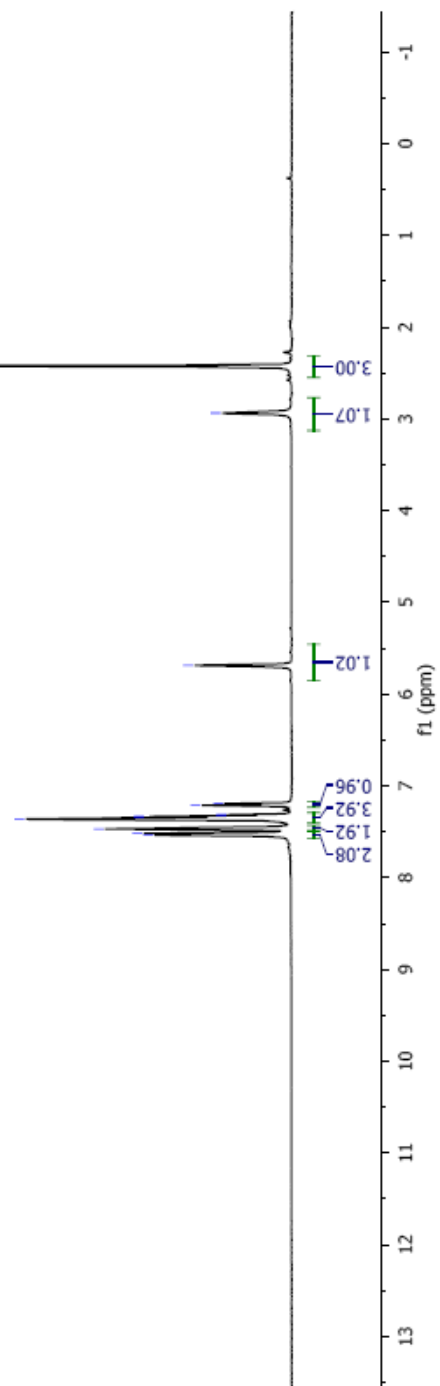


Table 2, entry 4





89.301  
86.774  
77.774  
77.455  
77.137  
65.329  
21.799

140.895  
138.649  
132.065  
128.868  
128.840  
128.596  
127.748  
124.127  
122.803

KW664, CDCI3  
100 MHz  
COLORLESS OIL  
JUNE 27 2008

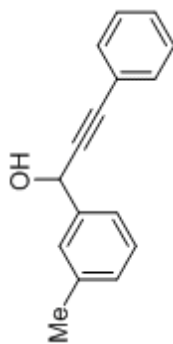
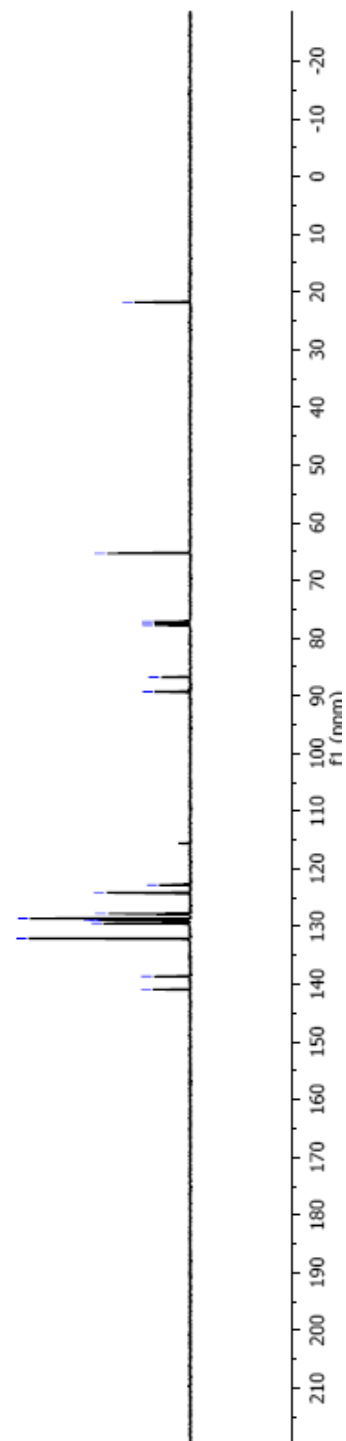


Table 2, entry 4



KW670, CDCI3  
400 MHz  
YELLOW OIL  
JULY 08 2008

8.05  
8.03  
7.50  
7.46  
7.44  
7.36  
7.26  
-5.77  
-2.71

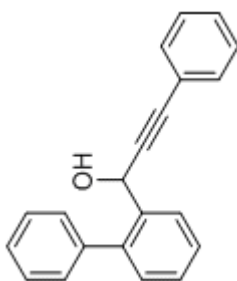
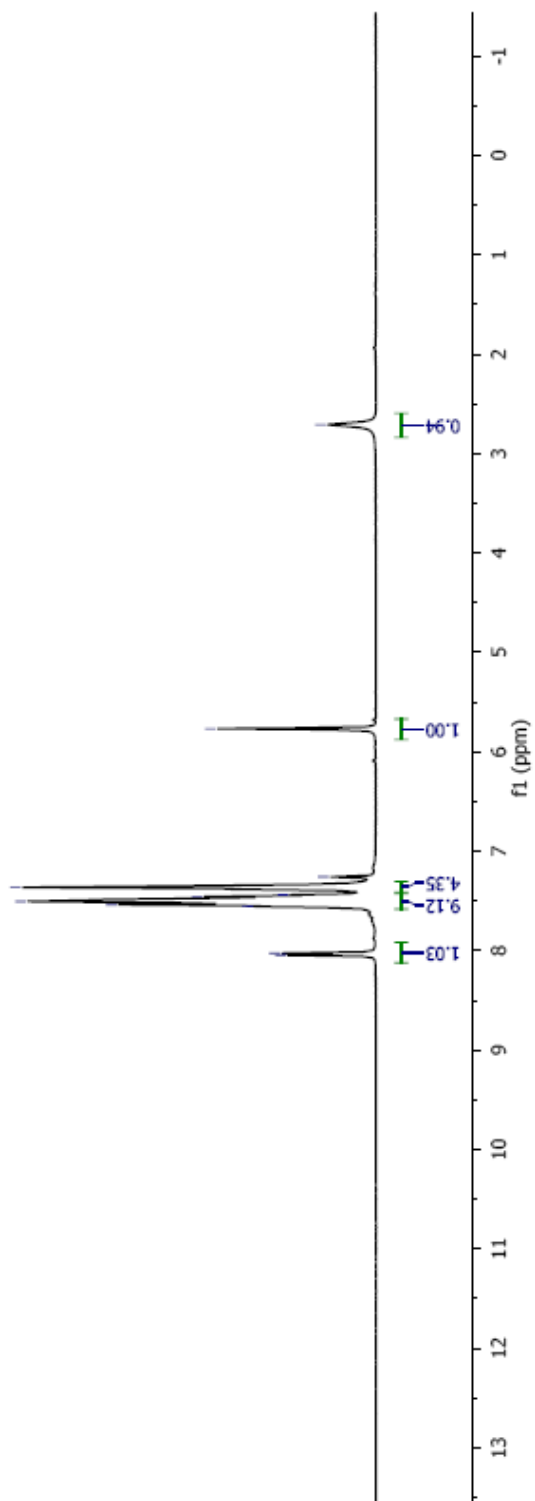


Table 2, entry 5



KW670, CDC13  
100 MHz  
YELLOW OIL  
JULY 08 2008

141.24  
140.54  
138.68  
132.02  
127.76  
122.88  
90.09  
86.69  
77.80  
77.49  
77.17  
62.47

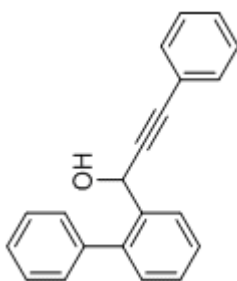
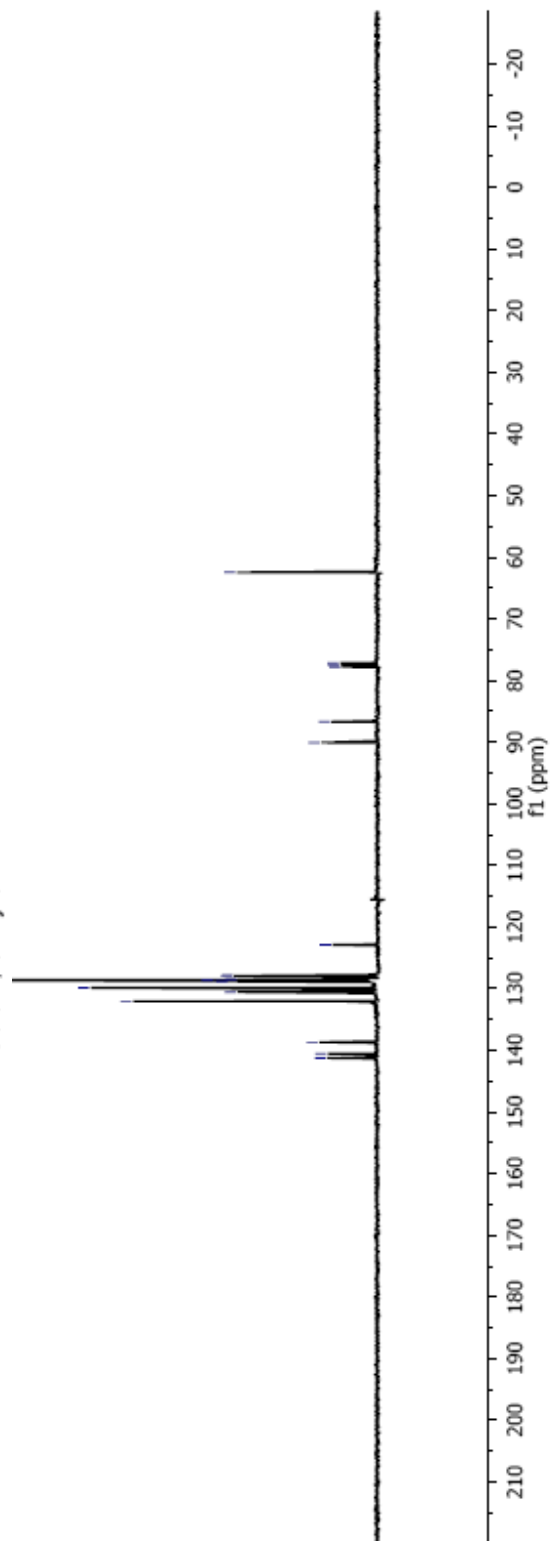


Table 2, entry 5



KW736, CDCl<sub>3</sub>  
300 MHz  
COLORLESS OIL  
NOV 21 2008

7.77  
7.75  
7.74  
7.49  
7.34  
7.30  
7.27  
7.23  
5.86  
5.84  
2.52  
2.38  
2.36

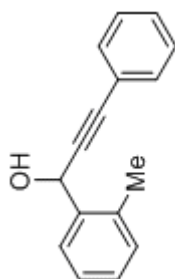
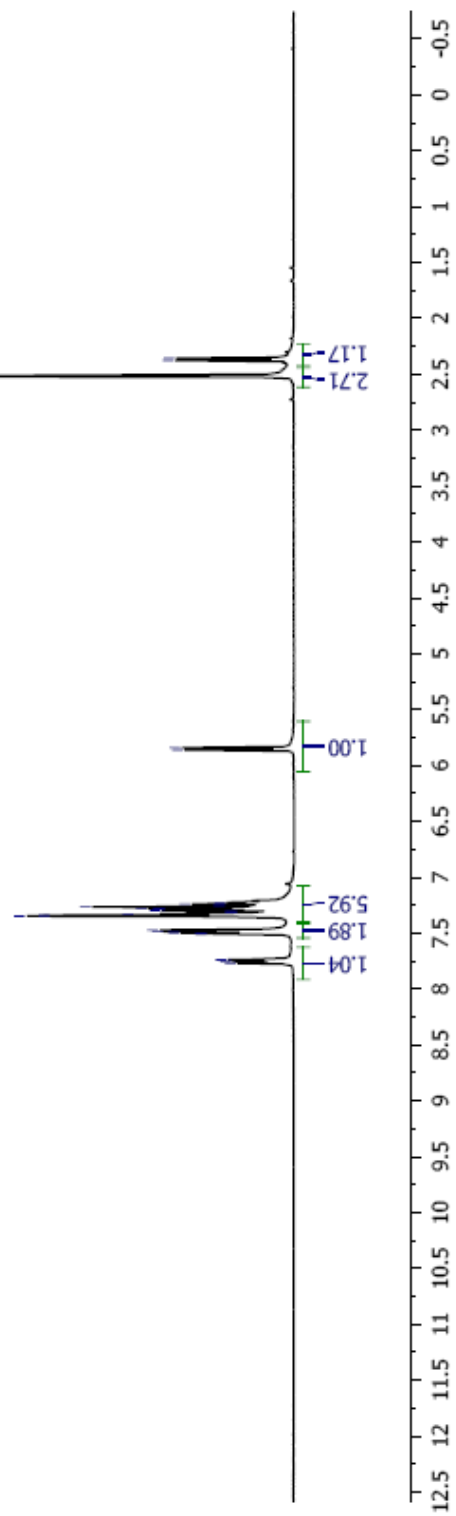


Table 2, entry 6



KW736, CDCl<sub>3</sub>  
 100 MHz  
 COLORLESS OIL  
 NOV 21 2008

138.60  
 136.27  
 131.96  
 128.71  
 128.54  
 126.83  
 126.49  
 122.75  
 88.79  
 86.75  
 77.63  
 77.31  
 76.99  
 63.19  
 19.30

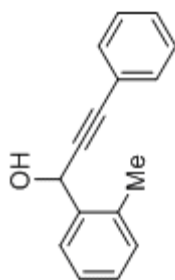
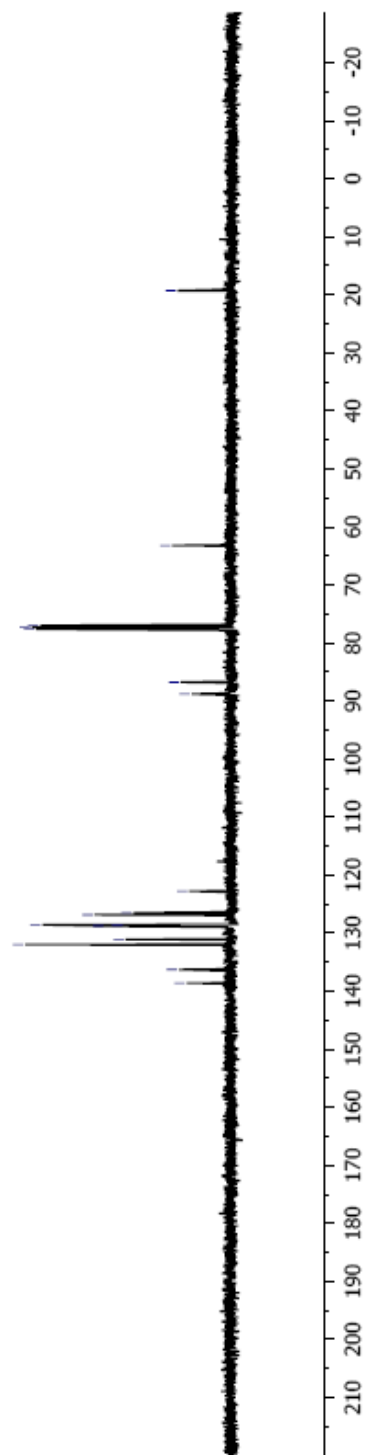


Table 2, entry 6



KW707, CDCl<sub>3</sub>  
400 MHz  
COLORLESS OIL  
SEP 25 2008

2.627  
2.522

6.165

7.486  
7.481  
7.471  
7.462  
7.341  
7.337  
7.328  
7.257  
7.164  
7.147  
7.095  
7.076

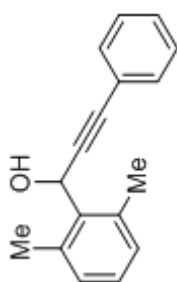
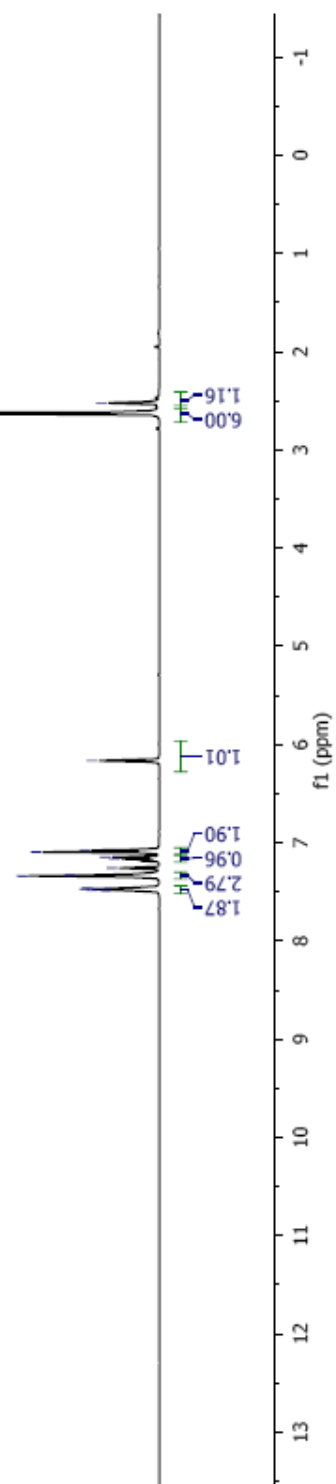


Table 2, entry 7



KW707, CDCl<sub>3</sub>  
 100 MHz  
 COLORLESS OIL  
 SEP 25 2008

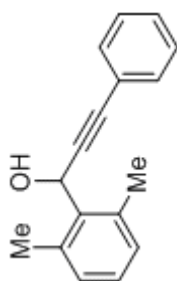
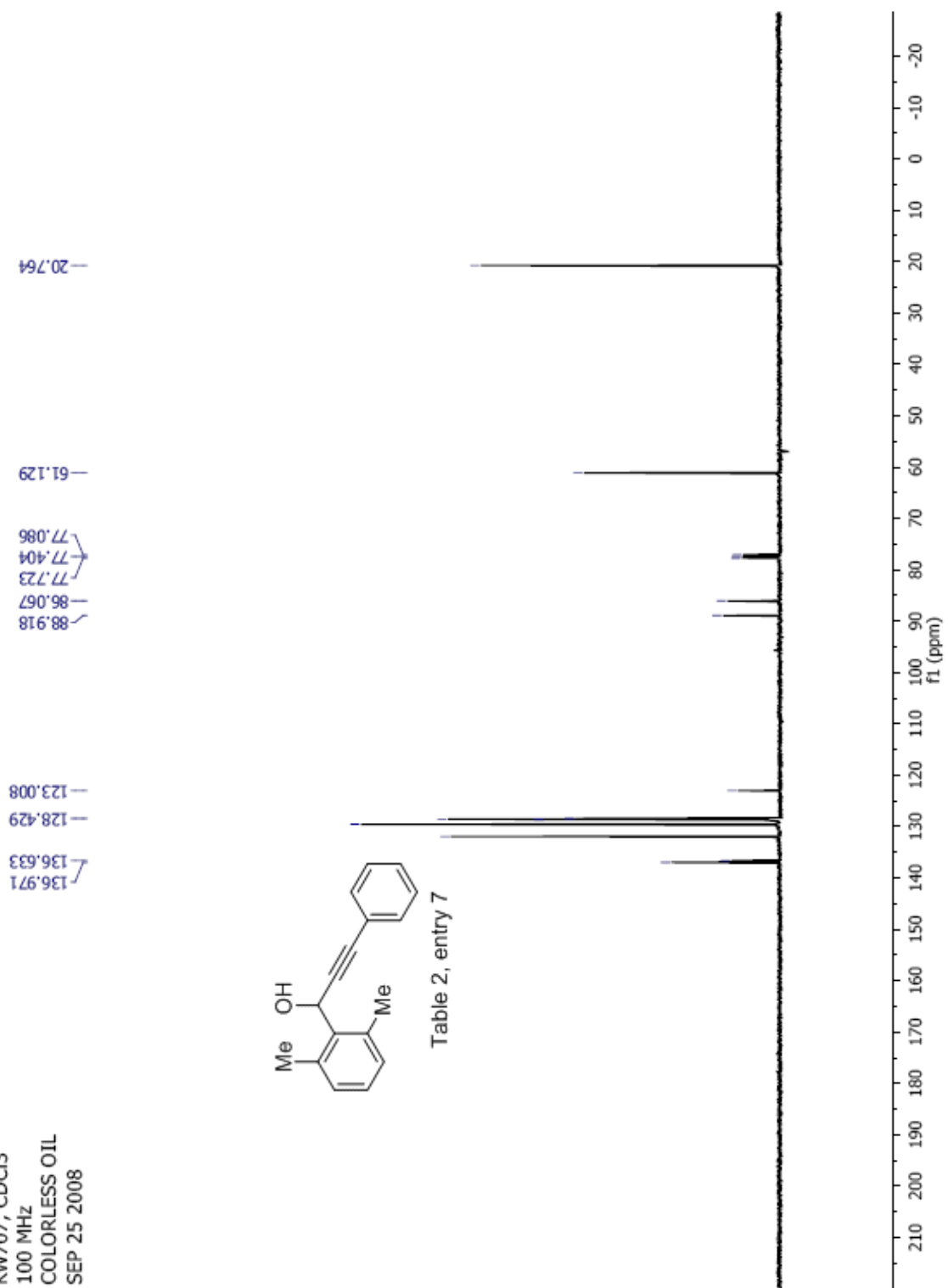


Table 2, entry 7



## Manual Peak Matching Report For Accurate Mass Determination

Theoretical mass	Experimental mass	PFK matching mass	Deviation*
236.12011	236.12053	230.98562	1.8 ppm

\* The deviation is obtained from the following equation:

$$\text{deviation} = \frac{\text{experimental mass} - \text{theoretical mass}}{\text{nominal mass}}$$

Where nominal mass takes in account only  $^{12}\text{C}$ ,  $^1\text{H}$ ,  $^{16}\text{O}$ ,  $^{14}\text{N}$  etc...

Theoretical mass correspond to the mass of the most abundant isotope peak

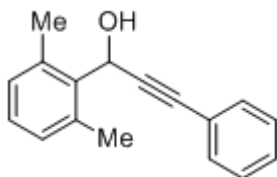


Table 2, entry 7

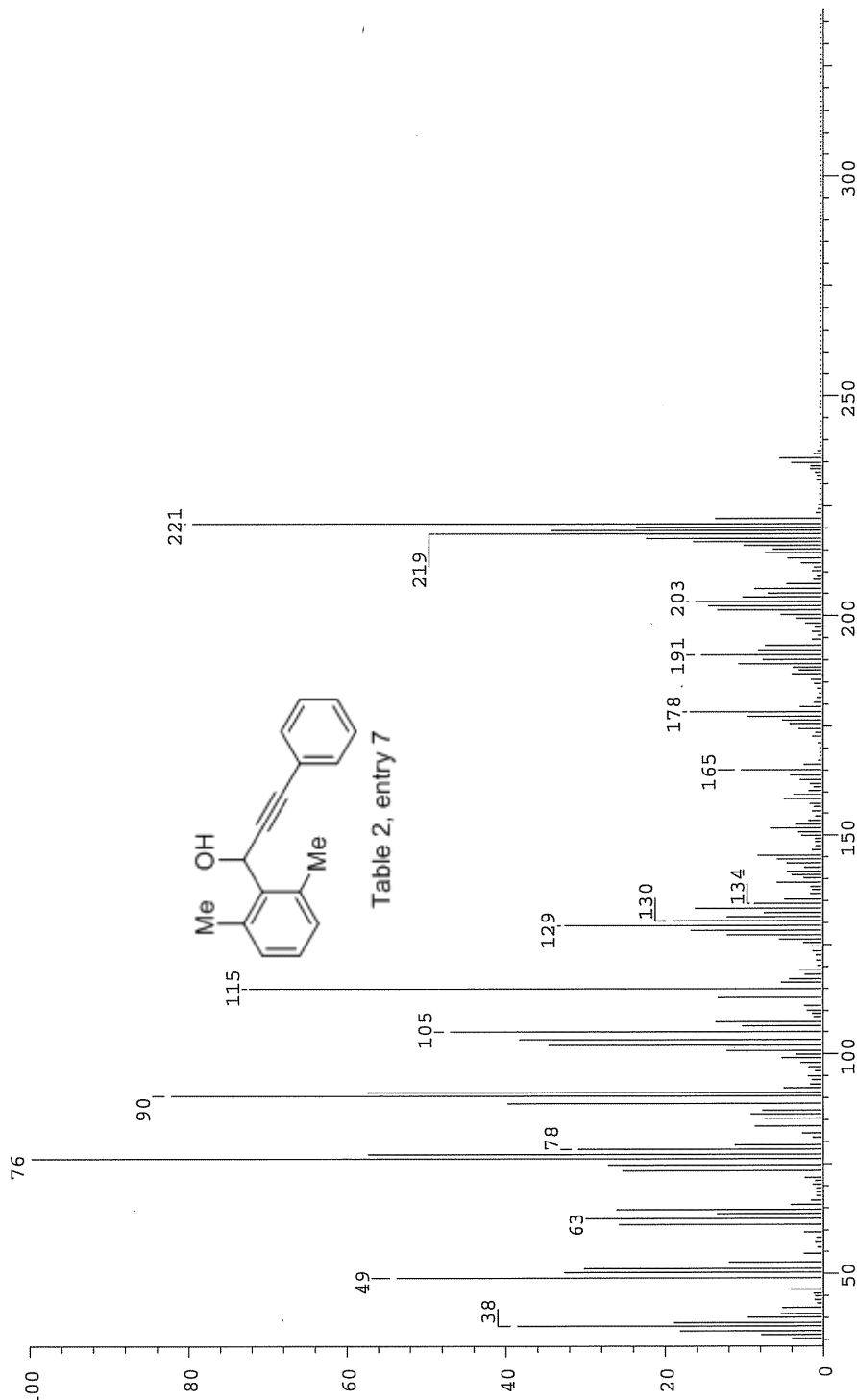
*Handwritten signature*



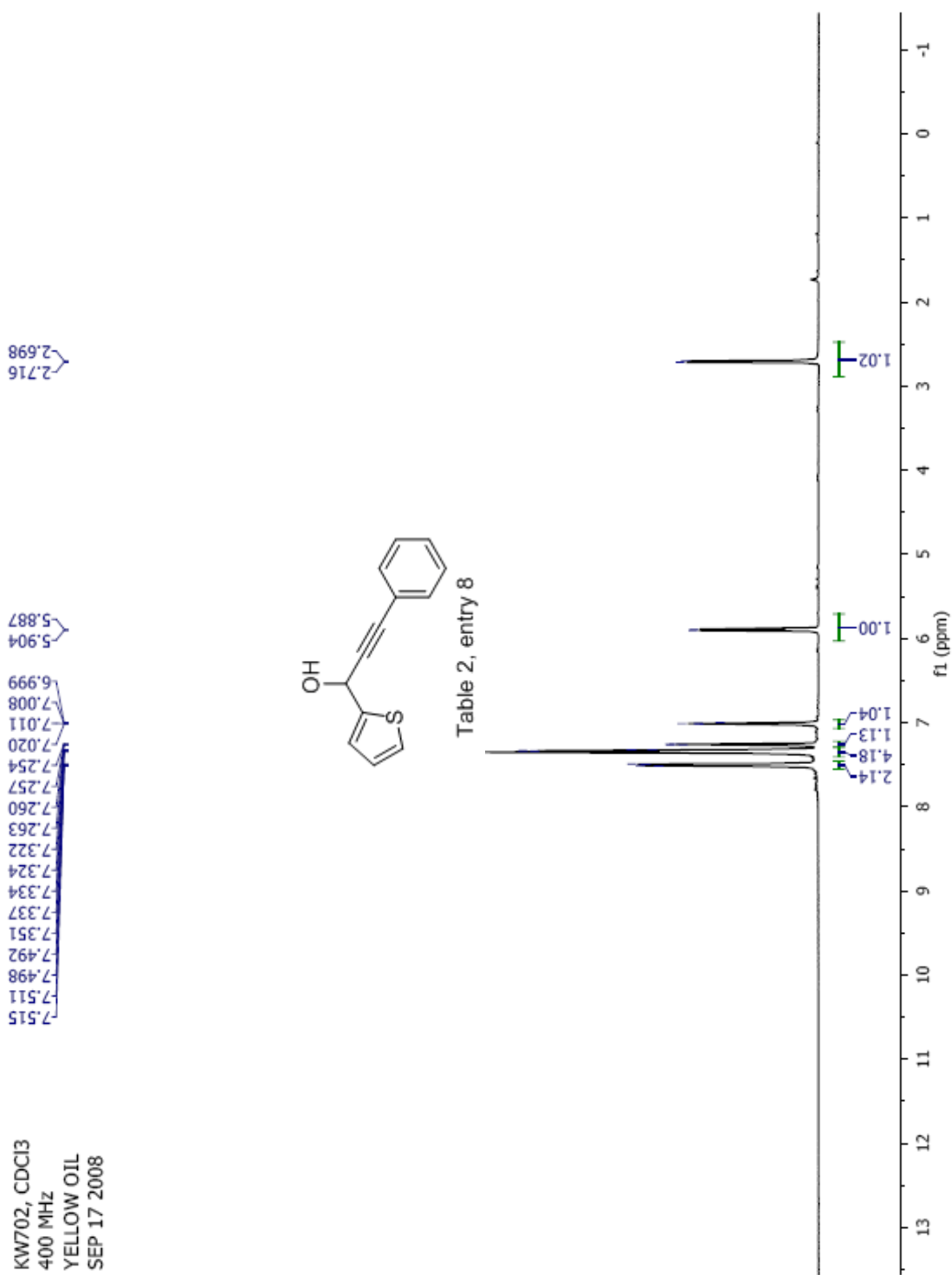
SPEC: fin083946.dat (24-OCT-08 11:08:21)  
 Samp: KW707  
 Comm: 70 eV EI  
 Oper: kh  
 Base: 76.22  
 Peak: 1000.0 mmu  
 Scan 39 @ 0.94 min (EI +QIMS LMR UP LR)

Study: ms services  
 Masses: 35.01 > 650.00  
 Intensity: 421512

Scans: 1 > 39  
 Client: Kuldup  
 #Peaks: 588  
 RIC: 7698543  
 4.2E+05



Date: Fri Oct 24 11:09:47 2008 ICIS: 8.3.0 SP2 for OSF1 (V4.0) build 98-238 from 26-Aug-98





KW702, CDCl<sub>3</sub>  
 100 MHz  
 YELLOW OIL  
 SEP 17 2008

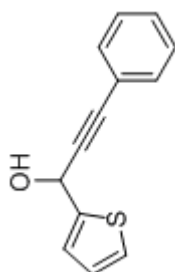
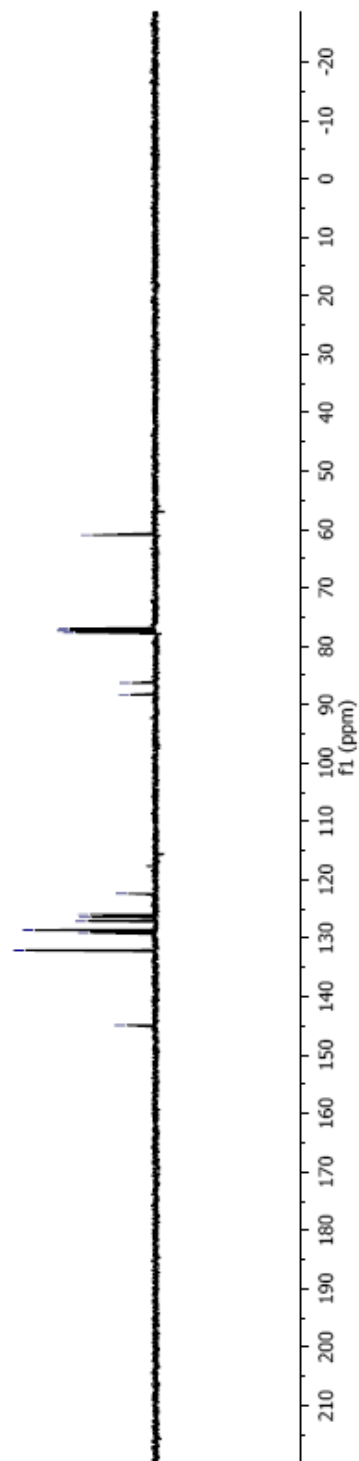


Table 2, entry 8



KW666, CDCl<sub>3</sub>  
400 MHz  
COLORLESS OIL  
JUNE 30 2008

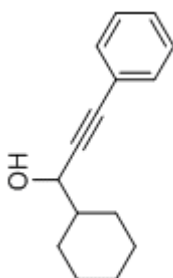
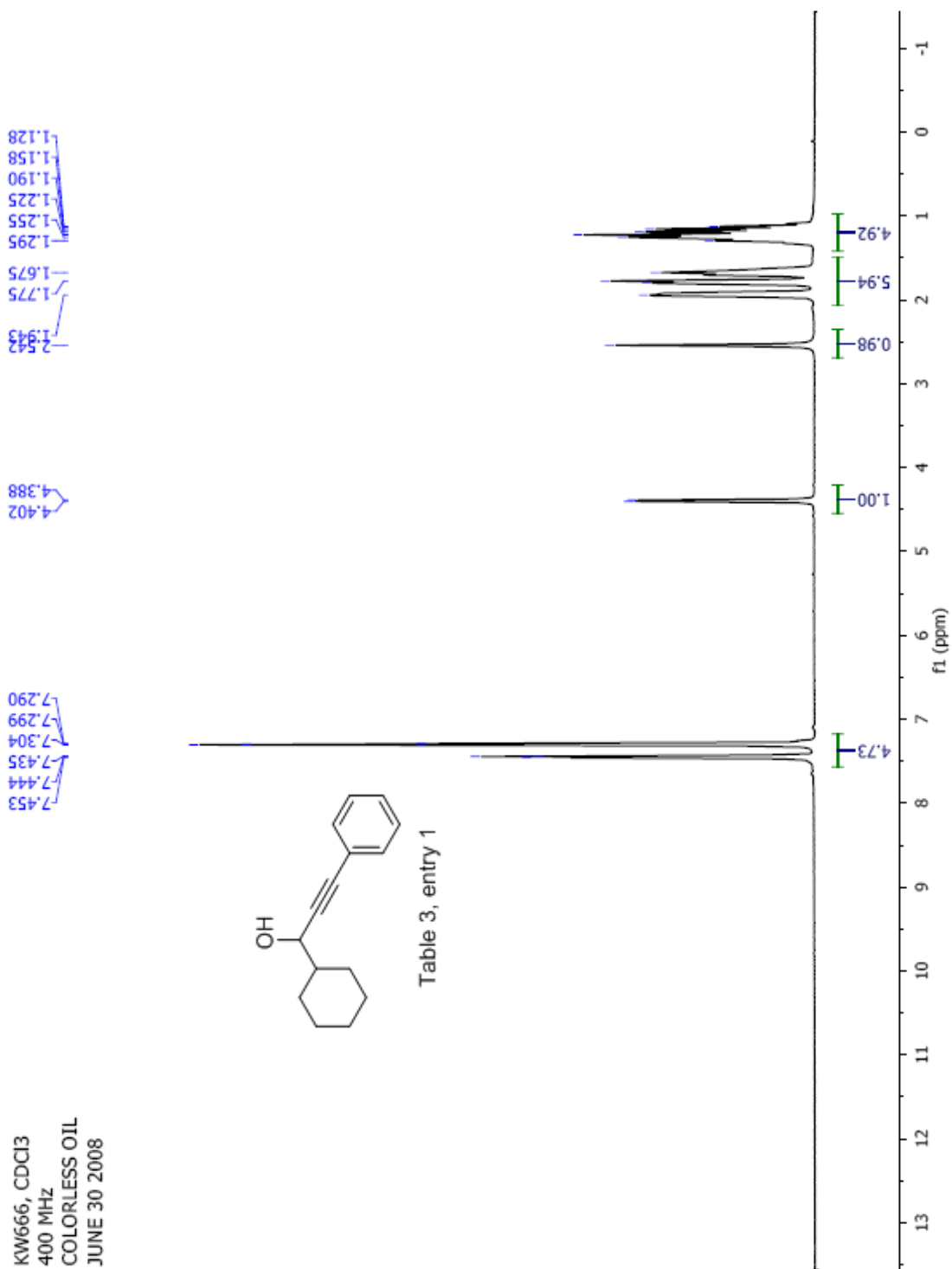


Table 3, entry 1



KW666, CDCI3  
100 MHz  
COLORLESS OIL  
JUNE 30 2008

131.935  
128.488  
123.042  
89.631  
85.839  
77.394  
77.076  
67.852  
44.542  
28.985  
28.469  
26.683  
26.210  
26.188

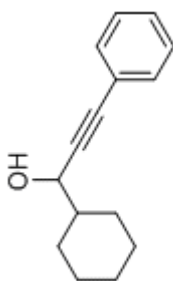
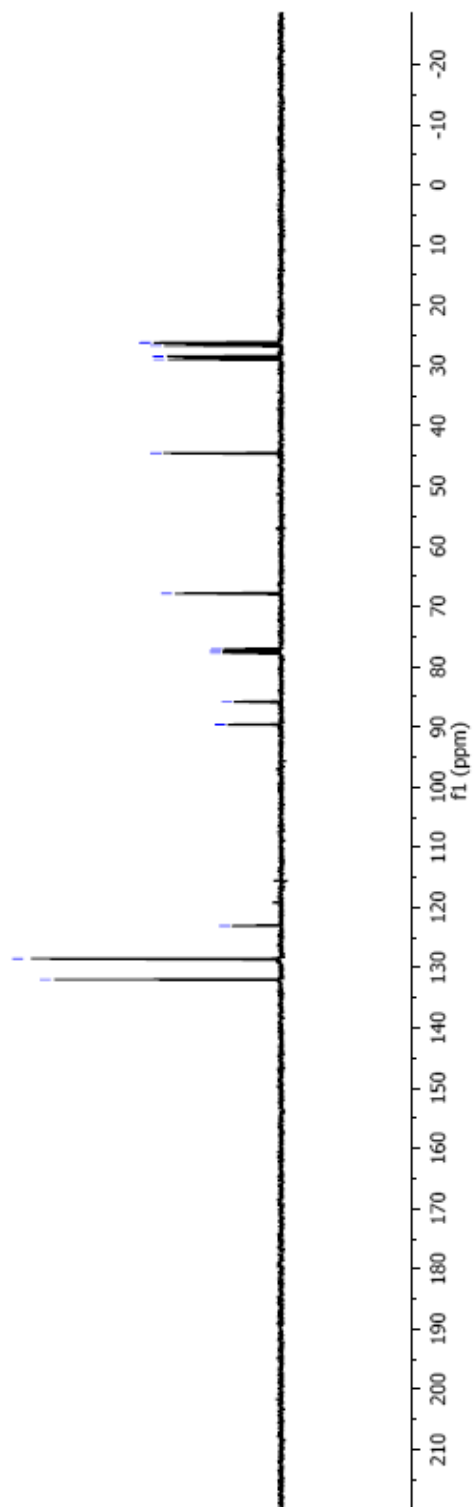


Table 3, entry 1



KW697, CDCl<sub>3</sub>  
400 MHz  
COLORLESS OIL  
SEP 12 2008

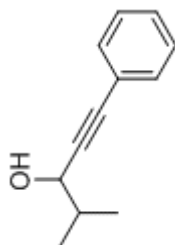
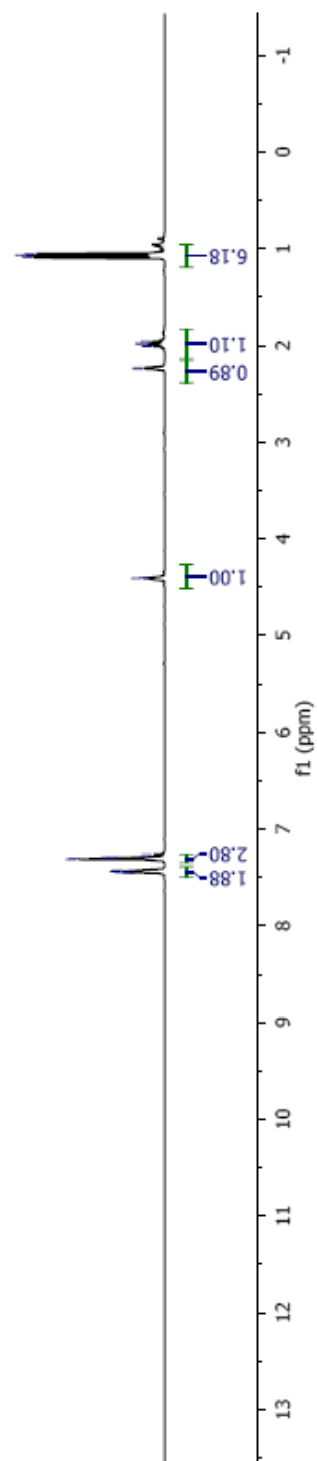


Table 3, entry 2



KW697, CDCl<sub>3</sub>  
 100 MHz  
 COLORLESS OIL  
 SEP 12 2008

131.925  
 128.554  
 128.501  
 122.951  
 89.160  
 85.798  
 77.313  
 76.995  
 68.601  
 34.939  
 18.490  
 17.819

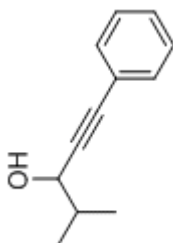
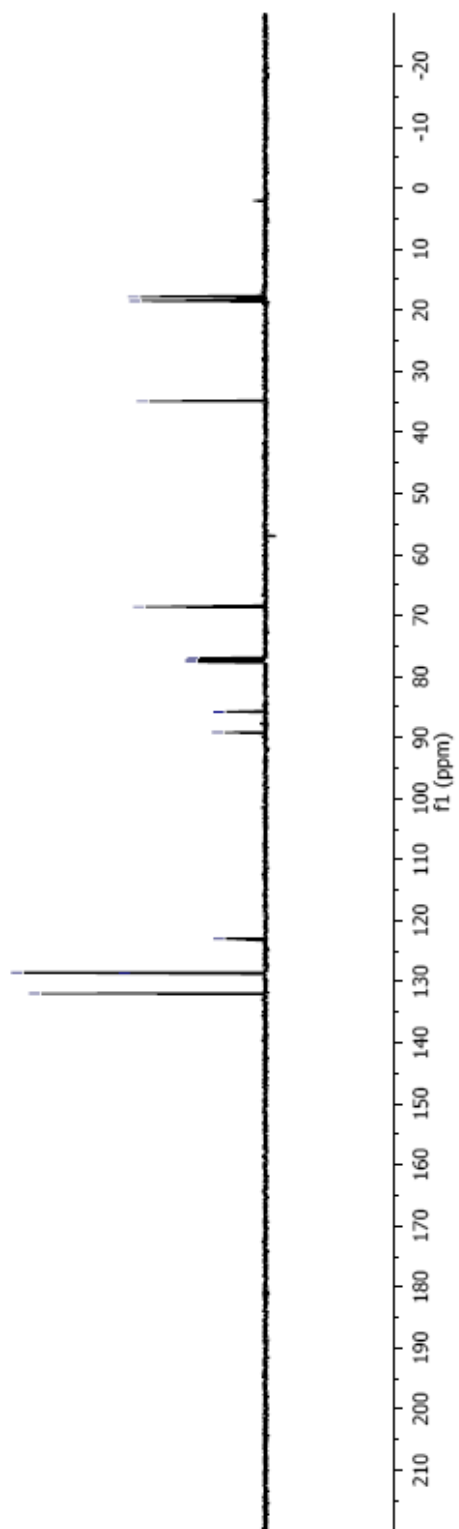


Table 3, entry 2



KW701, CDCl3  
400 MHz  
COLORLESS OIL  
SEP 22 2008

1.992  
1.816  
1.803  
1.794  
1.781  
1.763  
1.759  
1.354  
1.305  
0.913  
0.891  
0.868

4.603  
4.586  
4.565

7.445  
7.437  
7.424  
7.420  
7.412  
7.314  
7.306  
7.299  
7.292  
7.285  
7.281  
7.257

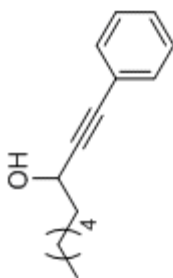
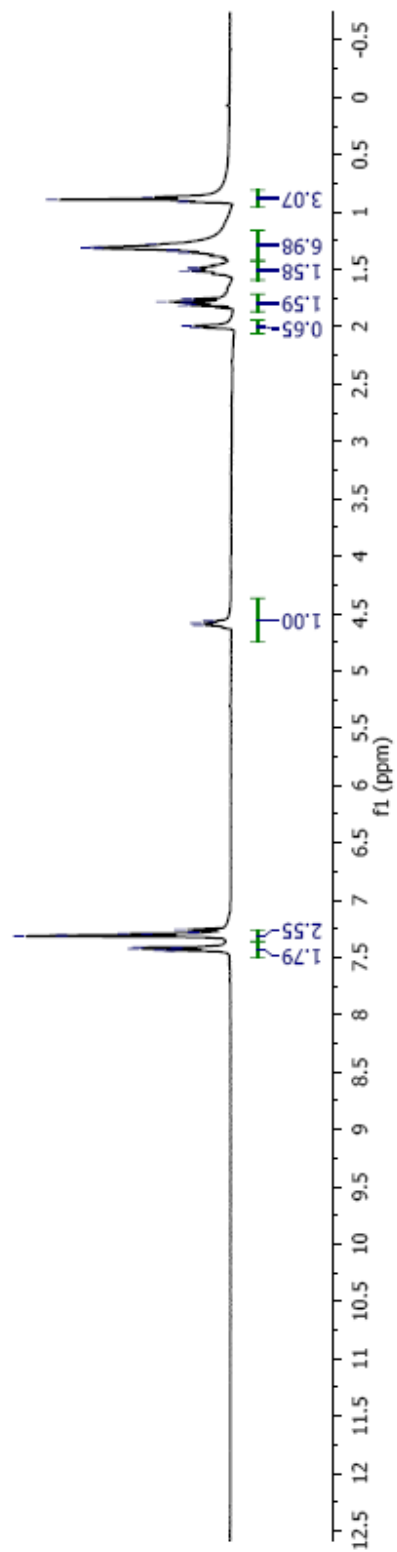


Table 3, entry 3





KW701, CDCI3  
100 MHz  
COLORLESS OIL  
SEP 22 2008

131.898  
128.564  
128.496  
122.901  
90.462  
85.023  
77.259  
76.835  
63.241  
38.135  
31.984  
29.202  
25.416  
22.823  
14.315

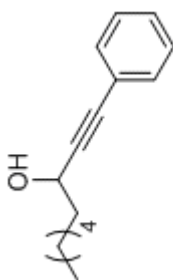
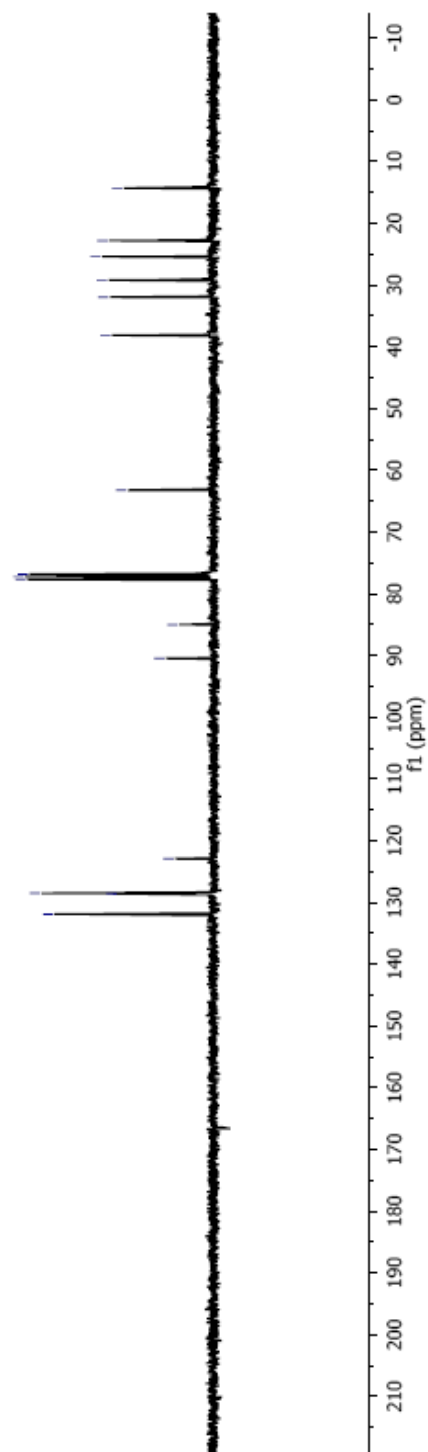


Table 3, entry 3



KW711, CDCl<sub>3</sub>  
400 MHz  
COLORLESS OIL  
OCT 02 2008

7.442  
7.436  
7.427  
7.418  
7.318  
7.312  
7.304  
7.302  
5.868  
5.829  
5.803  
5.786  
4.972  
4.916  
4.603  
4.588  
4.572  
2.064  
2.047  
2.029  
2.011  
1.867  
1.853  
1.811  
1.799  
1.782  
1.772  
1.573  
1.518  
1.501  
1.375  
1.357  
1.328  
1.306

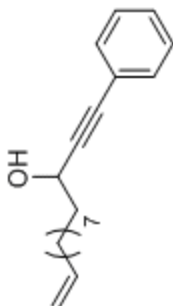
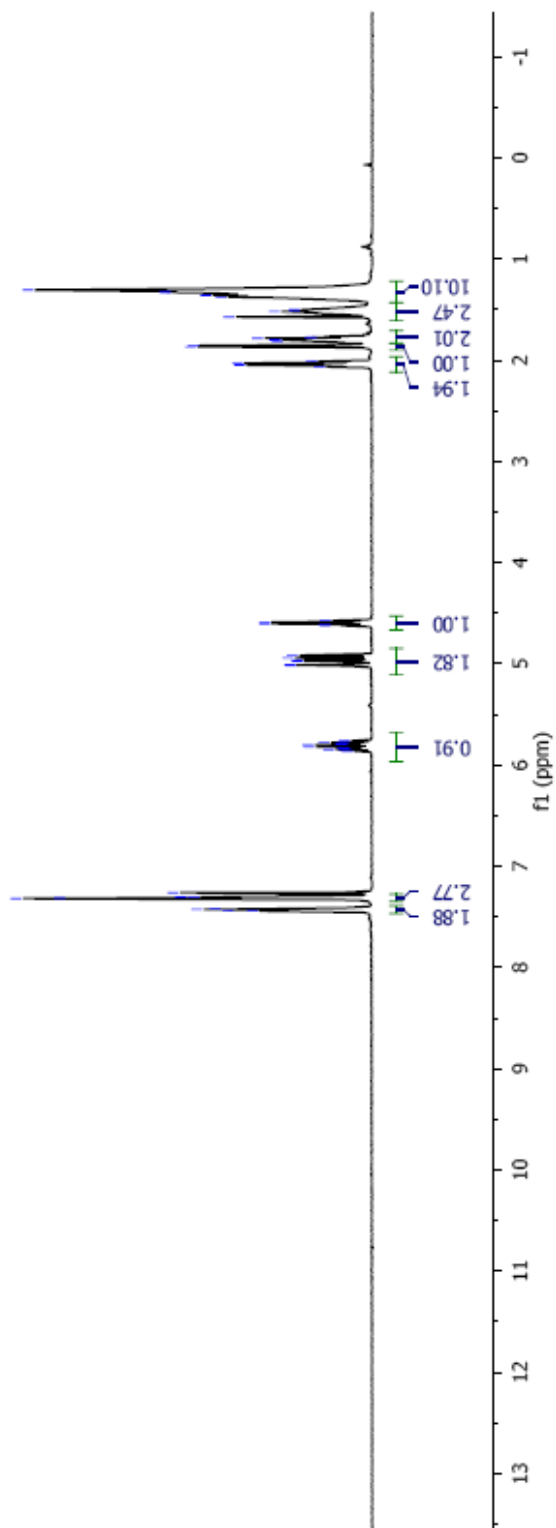


Table 3, entry 4



KW711, CDC13  
100 MHz  
COLORLESS OIL  
OCT 02 2008

139.446  
128.494  
122.864  
114.349  
90.412  
85.055  
77.252  
76.934  
63.267  
38.139  
34.060  
29.734  
29.647  
29.522  
29.363  
29.169  
25.450

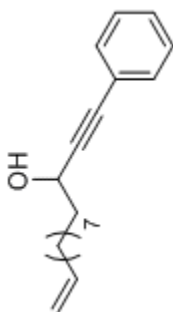
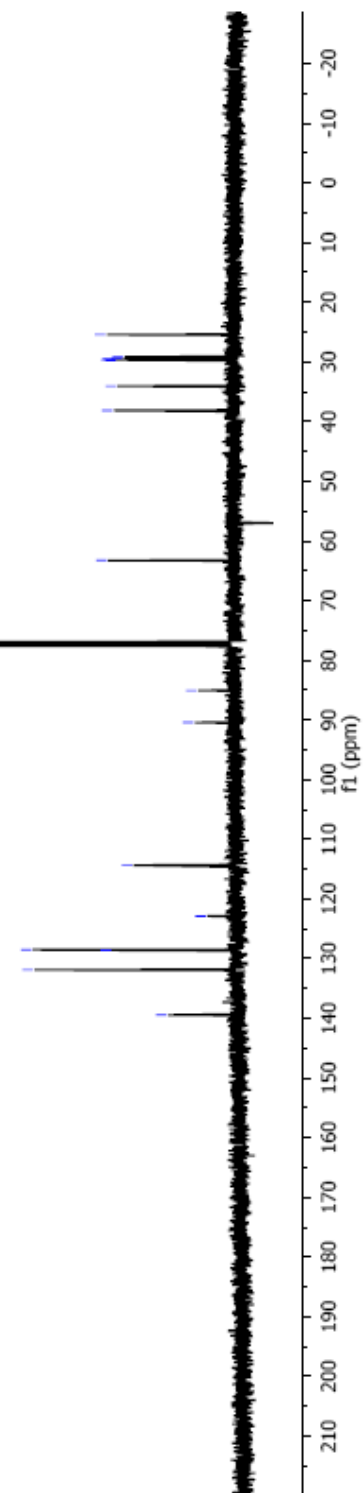


Table 3, entry 4



## Manual Peak Matching Report For Accurate Mass Determination

Theoretical mass	Experimental mass	PFK matching mass	Deviation*
270.19835	270.19875	230.98562	1.5 ppm

\* The deviation is obtained from the following equation:

$$\text{deviation} = \frac{\text{experimental mass} - \text{theoretical mass}}{\text{nominal mass}}$$

Where nominal mass takes in account only  $^{12}\text{C}$ ,  $^1\text{H}$ ,  $^{16}\text{O}$ ,  $^{14}\text{N}$  etc...

Theoretical mass correspond to the mass of the most abundant isotope peak

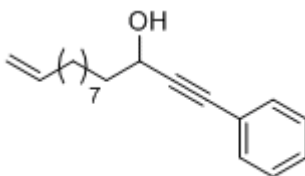
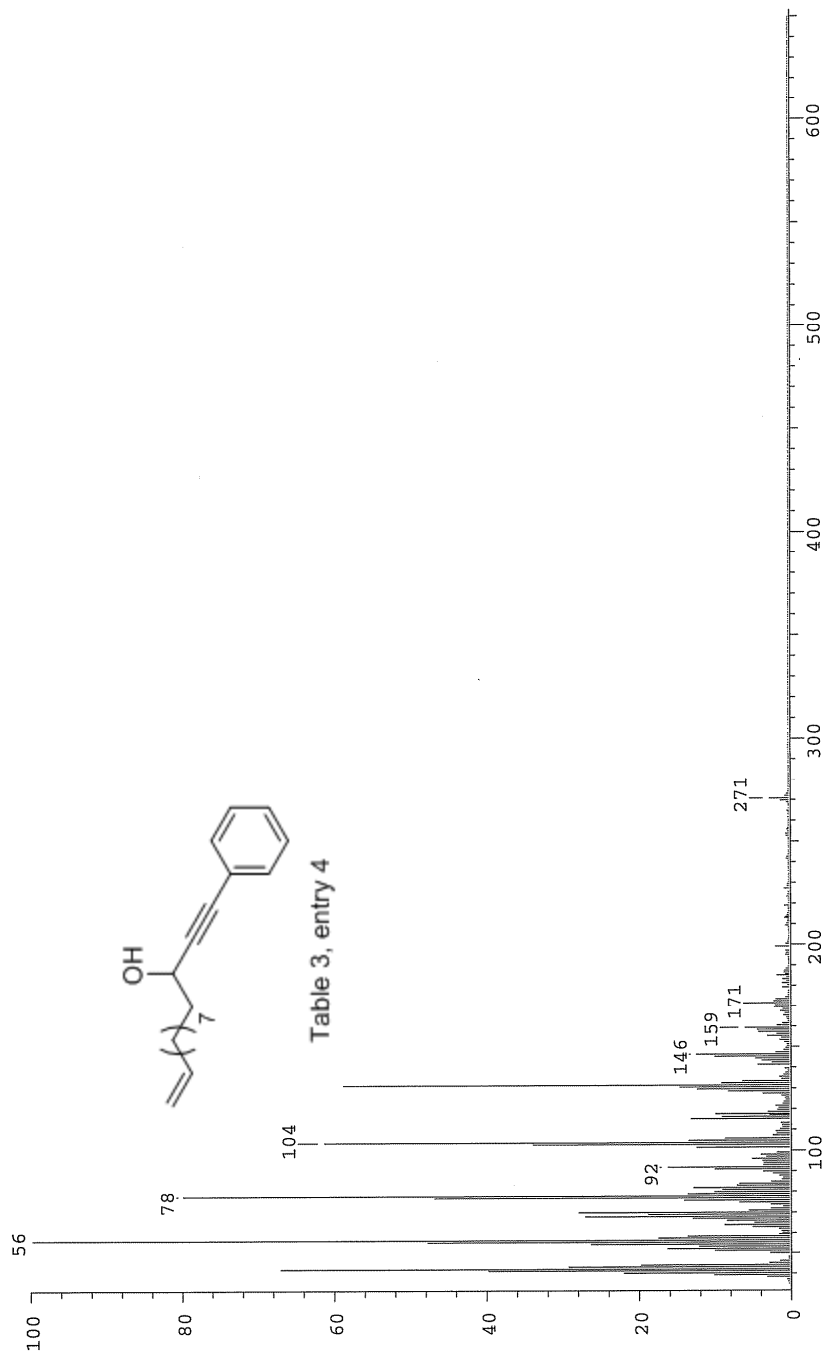


Table 3, entry 4

*Handwritten signature*

Scans: 1 > 53  
 Client: Kuldup  
 #Peaks: 612  
 RIC: 43325160  
 3.5E+06

SPFC: fin083989.dat (12-NOV-08 15:01:53)  
 Samp: KW711  
 Comm: 70 eV EI  
 Oper: KH  
 Study: MS Services  
 Masses: 35.01 > 650.00  
 Peak: 1000.0 mmu  
 Intensity: 3456369  
 Scan 28 @ 0.71 min (EI +QIMS LMR UP LR)



Date: Wed Nov 12 15:03:42 2008 ICIS: 8.3.0 SP2 for OSF1 (V4.0) build 98-238 from 26-Aug-98

KW675, CDCl<sub>3</sub>  
400 MHz  
JULY 14 2008  
YELLOW OIL

7.972  
7.952  
7.772  
7.752  
7.629  
7.609  
7.519  
7.499  
7.259  
7.072  
7.030  
5.811  
3.942  
3.869  
3.831

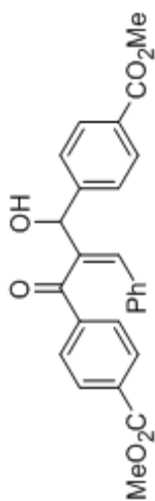
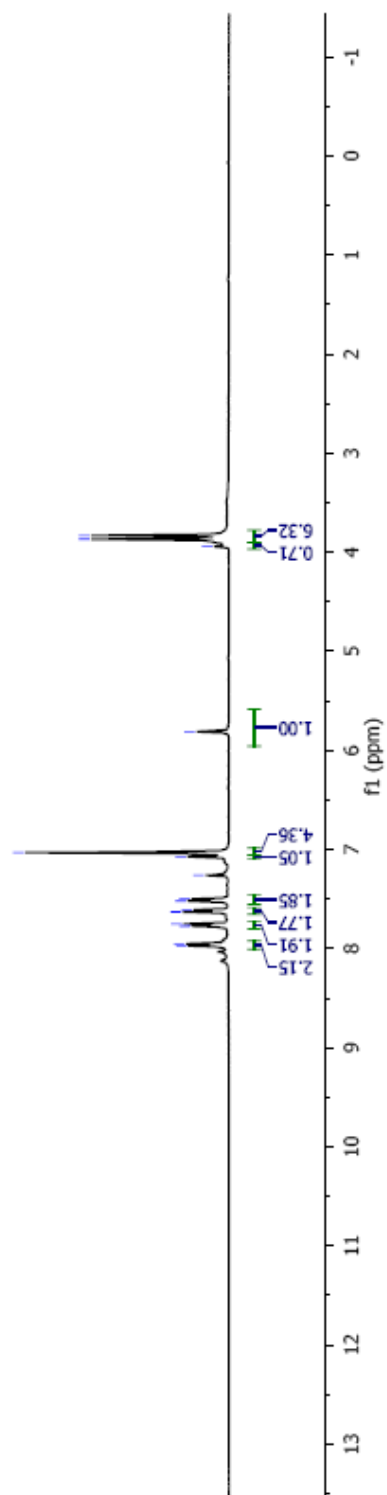
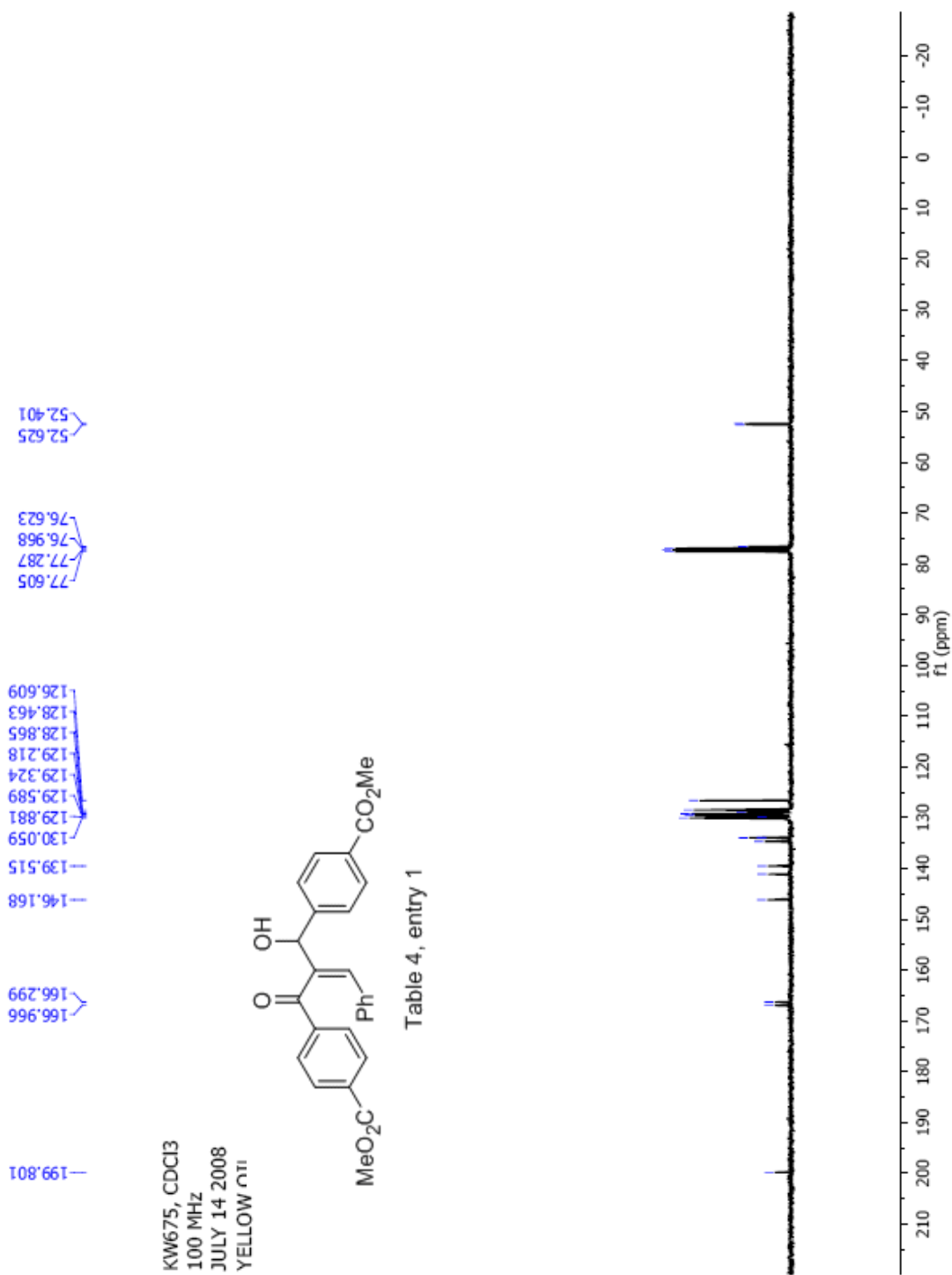


Table 4, entry 1





## Manual Peak Matching Report For Accurate Mass Determination

Theoretical mass	Experimental mass	PFK matching mass	Deviation*
430.14164	430.14262	380.97603	2.3 ppm

\* The deviation is obtained from the following equation:

$$\text{deviation} = \frac{\text{experimental mass} - \text{theoretical mass}}{\text{nominal mass}}$$

Where nominal mass takes in account only  $^{12}\text{C}$ ,  $^1\text{H}$ ,  $^{16}\text{O}$ ,  $^{14}\text{N}$  etc...

Theoretical mass correspond to the mass of the most abundant isotope peak

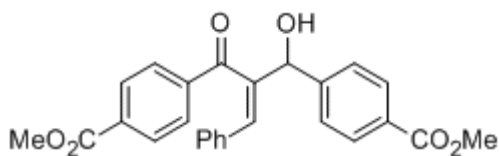


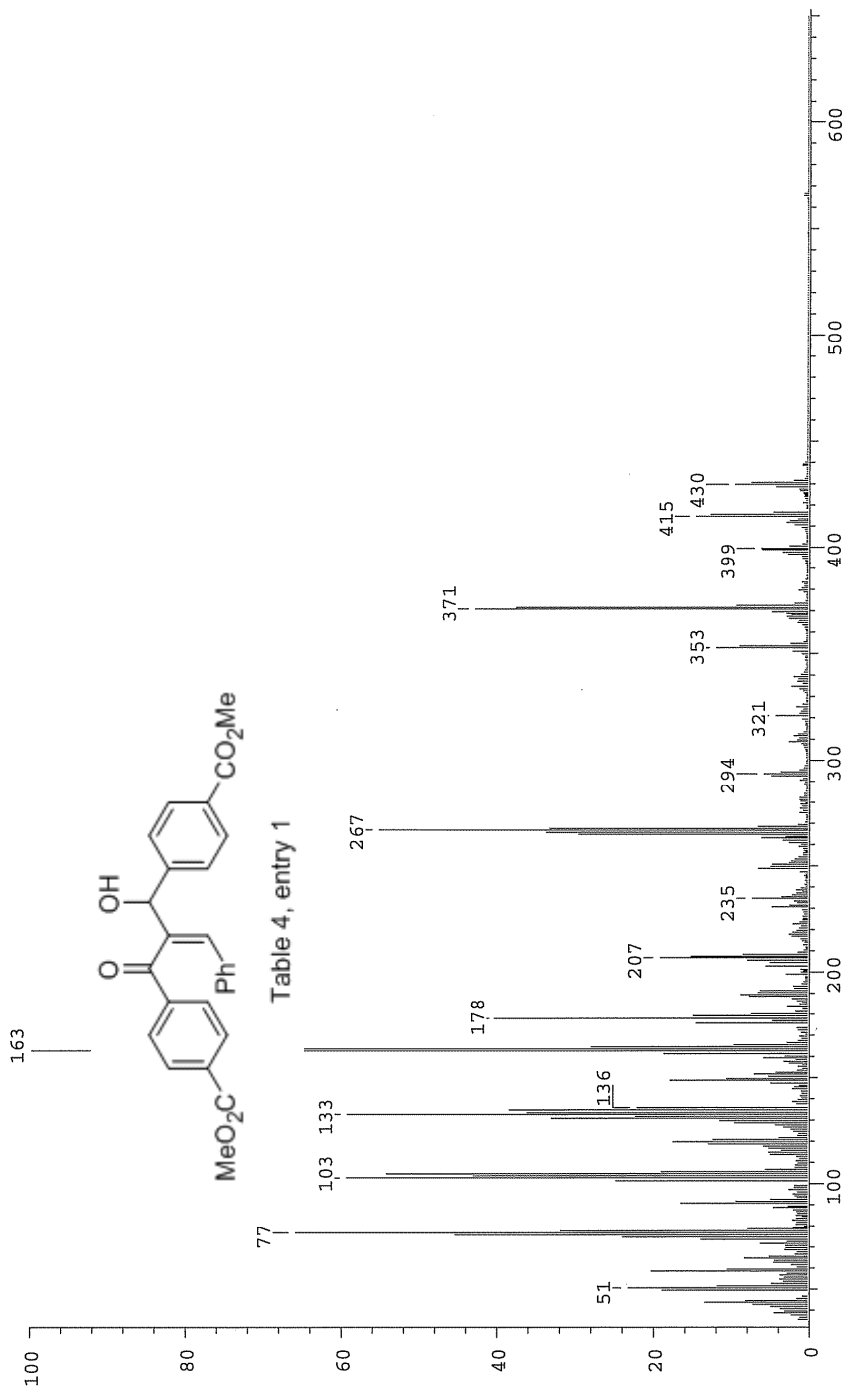
Table 4, entry 1

*Handwritten signature*



Scans: 1 > 59  
 Client: Kuldup  
 #Peaks: 650  
 RIC: 61943558  
 3.0E+06

SPEC: fin083790.dat (22-JUL-08 11:02:35)  
 Samp: KW675  
 Comm: SP 70 eV EI  
 Oper: kh  
 Study: MS services  
 Base: 162.69  
 Masses: 35.01 > 650.00  
 Peak: 1000.0 mmu  
 Intensity: 3001490  
 Scan 56 @ 1.30 min (EI +Q1MS LMR UP LR)



Date: Tue Jul 22 11:04:27 2008 ICIS: 8.3.0 SP2 for OSF1 (V4.0) build 98-238 from 26-Aug-98

7.937  
7.787  
7.617  
7.597  
7.564  
7.543  
7.532  
7.512  
7.367  
7.348  
7.258  
7.084  
7.073  
7.043  
7.035  
7.023  
7.004  
6.888  
6.868  
6.849  
5.645  
3.403

KW673, CDCl<sub>3</sub>  
400 MHz  
JULY 07 2008  
COLORLESS OIL

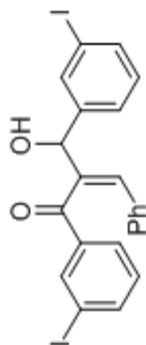
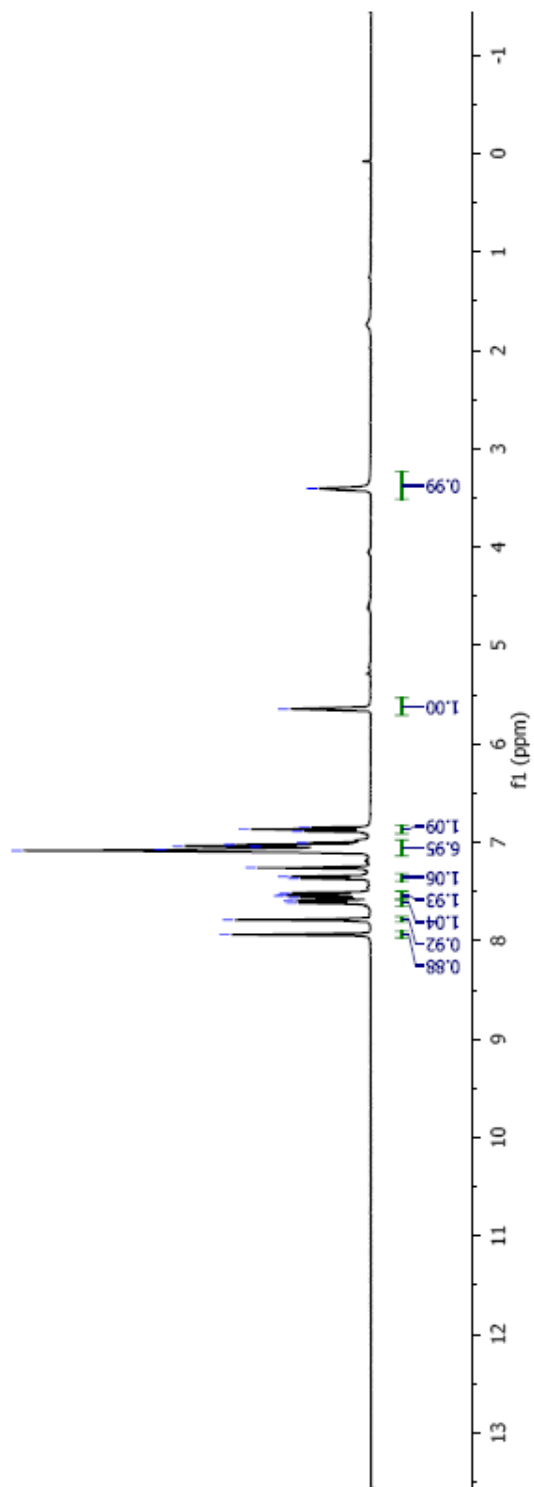


Table 4, entry 2





KW673, CDCl<sub>3</sub>  
100 MHz  
JULY 07 2008  
COLORLESS OIL

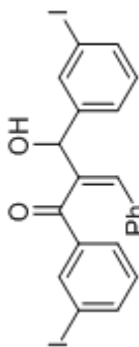
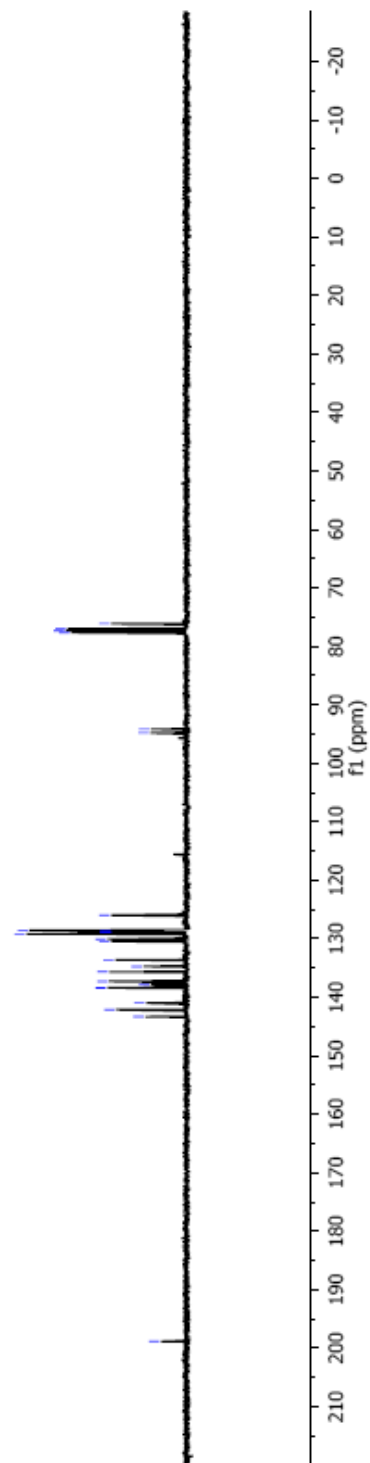
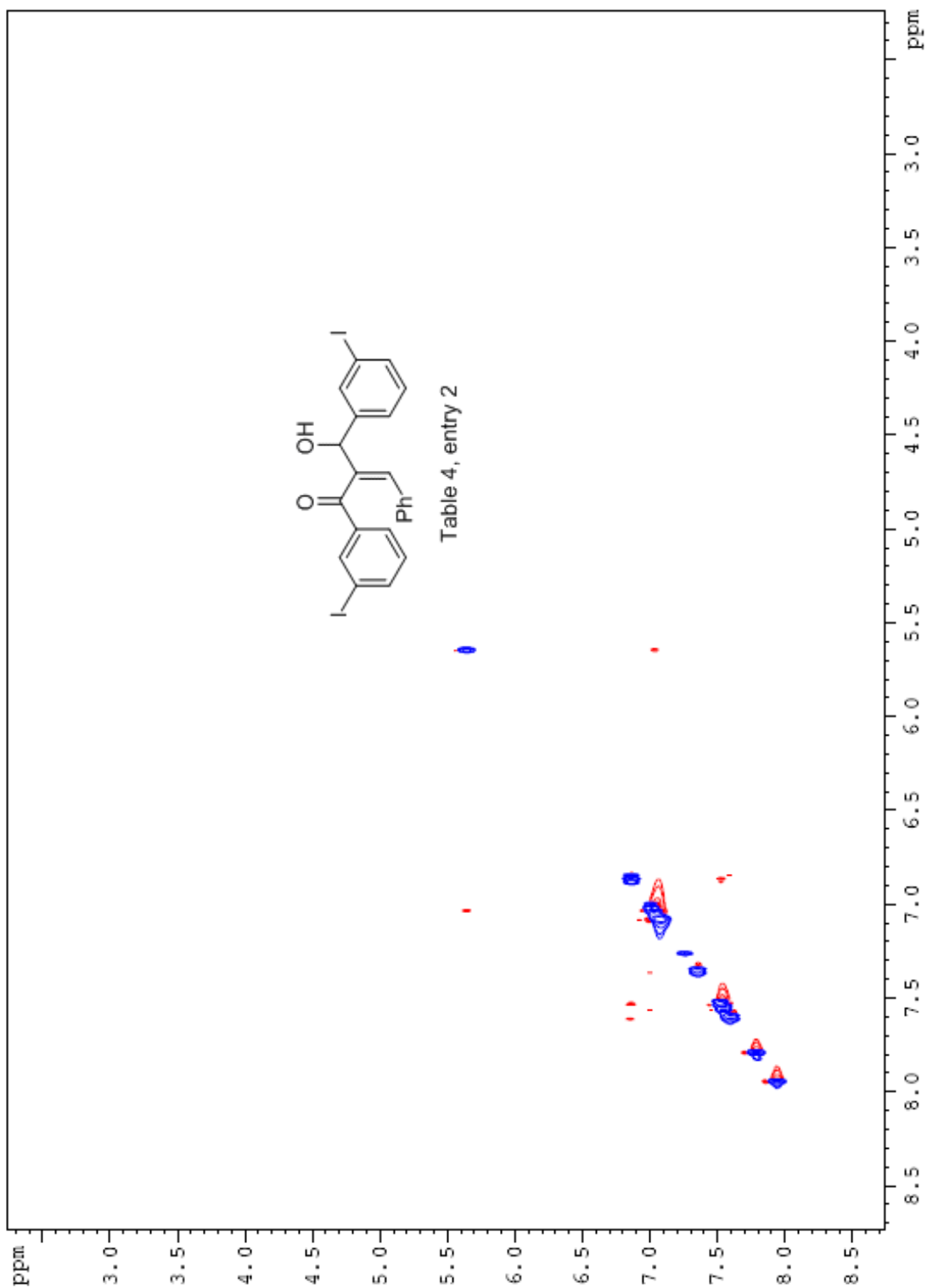


Table 4, entry 2





## Manual Peak Matching Report For Accurate Mass Determination

Theoretical mass	Experimental mass	PFK matching mass	Deviation*
565.92398	565.92536	530.96645	2.4 ppm

\* The deviation is obtained from the following equation:

$$\text{deviation} = \frac{\text{experimental mass} - \text{theoretical mass}}{\text{nominal mass}}$$

Where nominal mass takes in account only  $^{12}\text{C}$ ,  $^1\text{H}$ ,  $^{16}\text{O}$ ,  $^{14}\text{N}$  etc...

Theoretical mass correspond to the mass of the most abundant isotope peak

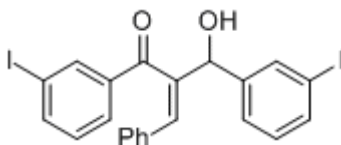
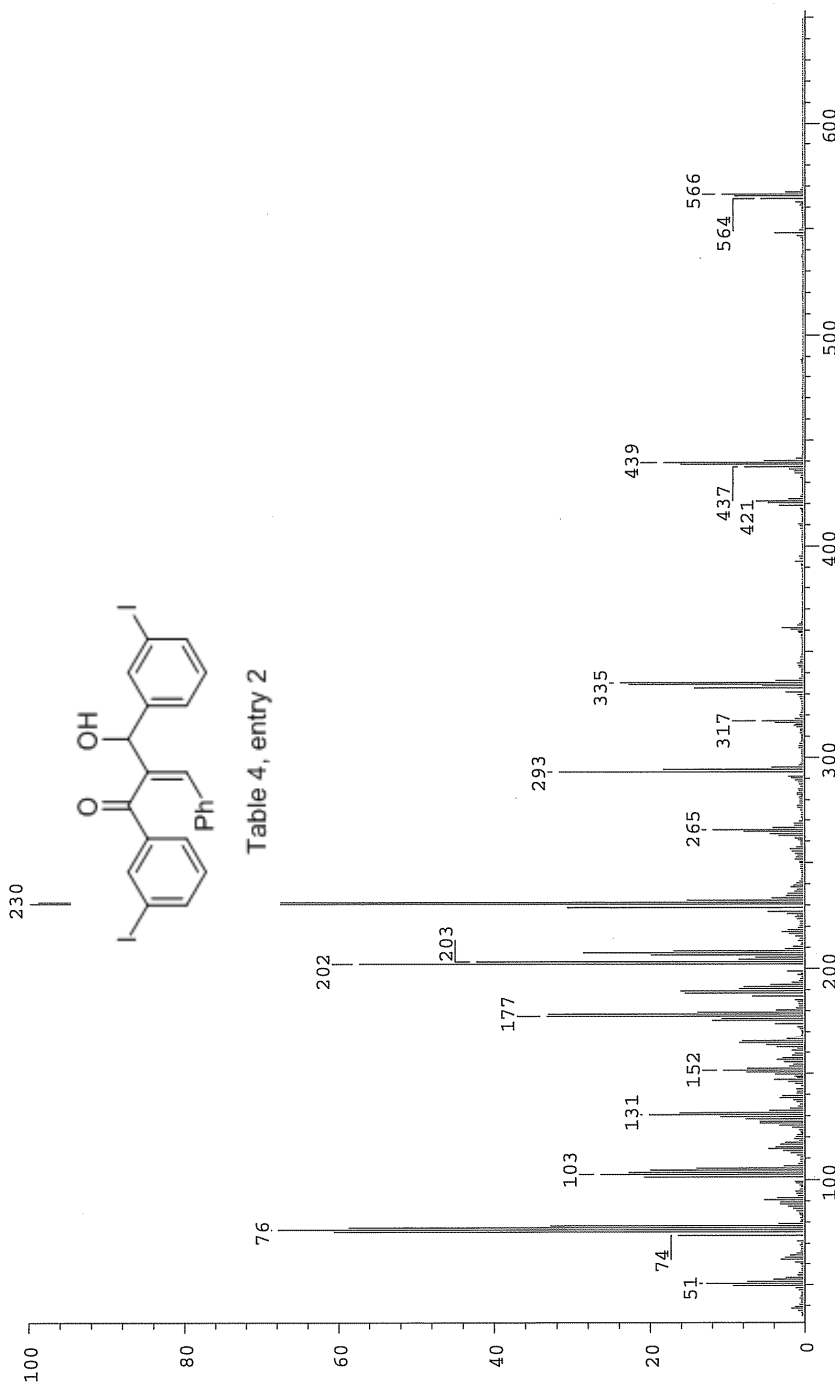


Table 4, entry 2

SPEC: fin083789.dat (22-JUL-08 10:52:27)  
 Samp: KW673  
 Comm: SP 70 eV EI  
 Oper: kh  
 Base: 230.47  
 Peak: 1000.0 mmu  
 Scan 277 @ 5.85 min (EI +Q1MS LMR UP LR)

Study: MS services  
 Masses: 35.01 > 650.00  
 Intensity: 2209958

Scans: 1 > 278  
 Client: Kuldap  
 #Peaks: 643  
 RIC: 35209654  
 2.2E+06



KW665H1, CD3CN  
 WHITE SOLID  
 JUNE 26 2008  
 400 MHz

7.8486  
 7.8284  
 7.6420  
 7.5609  
 7.5405  
 7.1852  
 7.1356  
 5.7964  
 4.2754  
 4.2642  
 2.2251

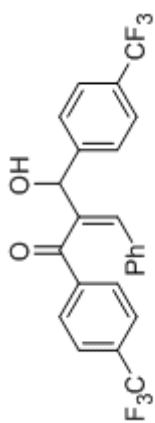
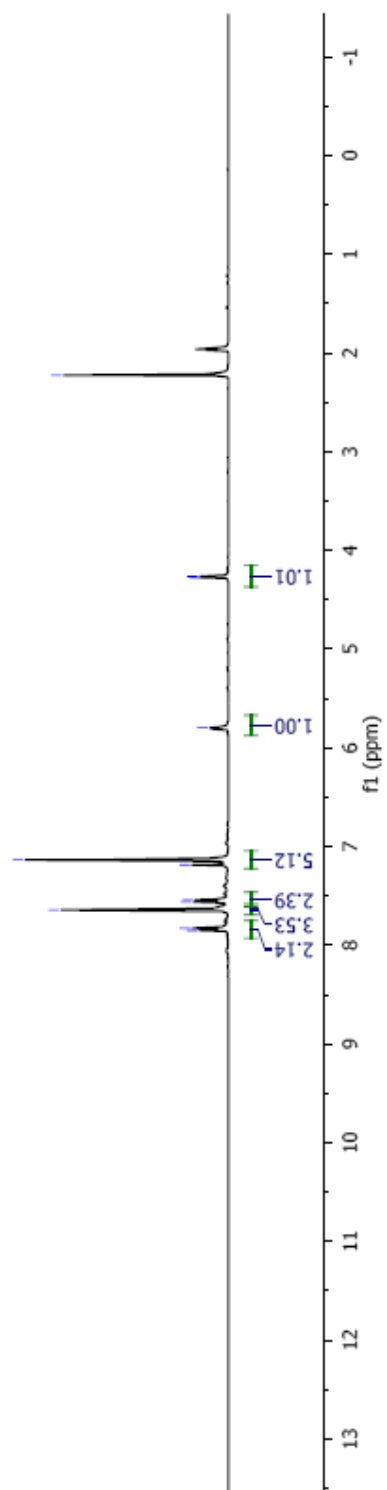
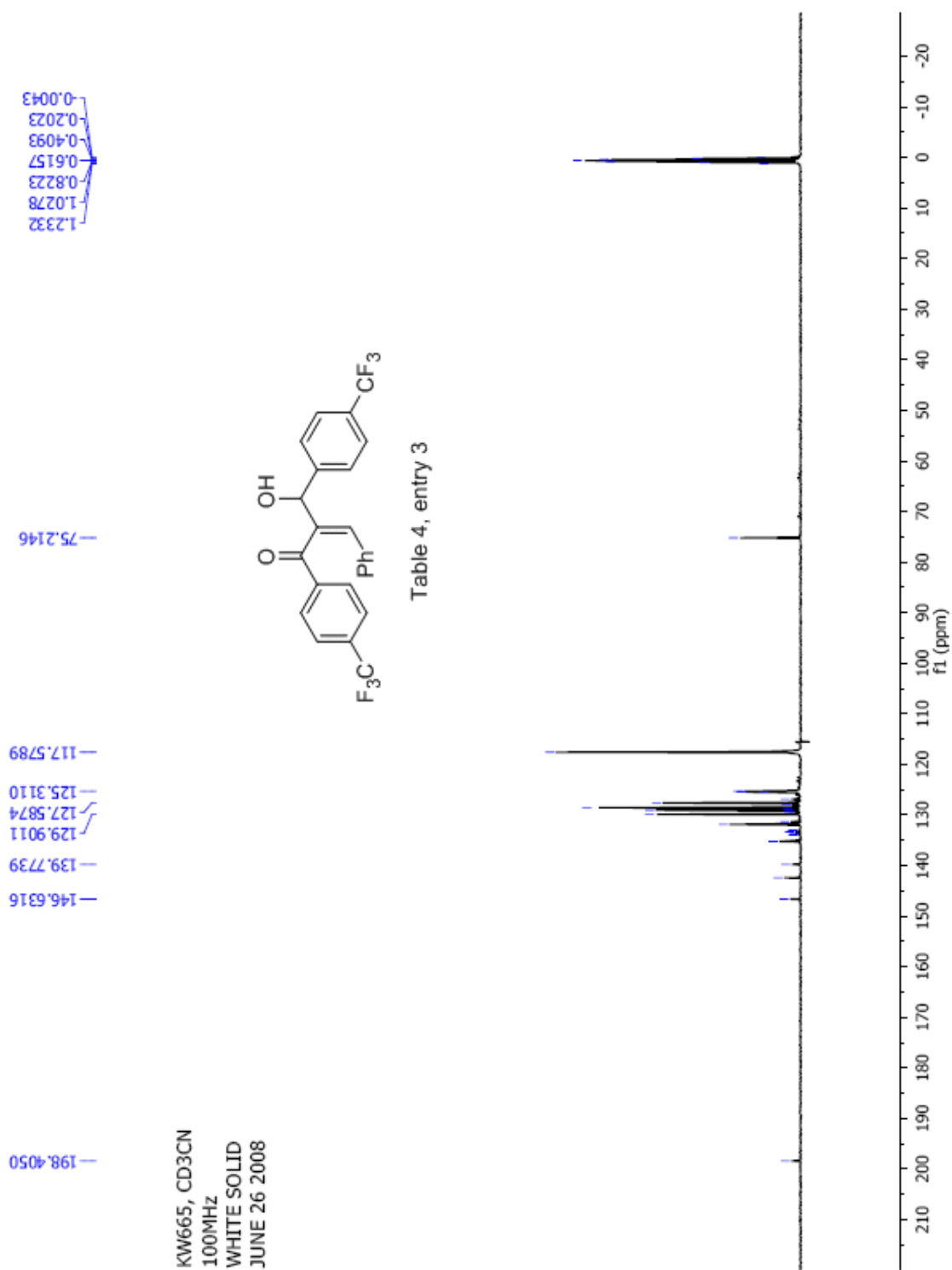


Table 4, entry 3







KW665, CD3CN  
 WHITE SOLID  
 376MHZ  
 JUNE 26 2008

63.377  
 64.154

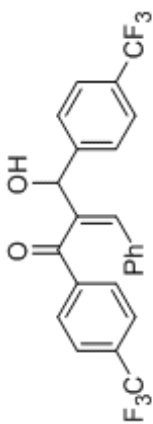
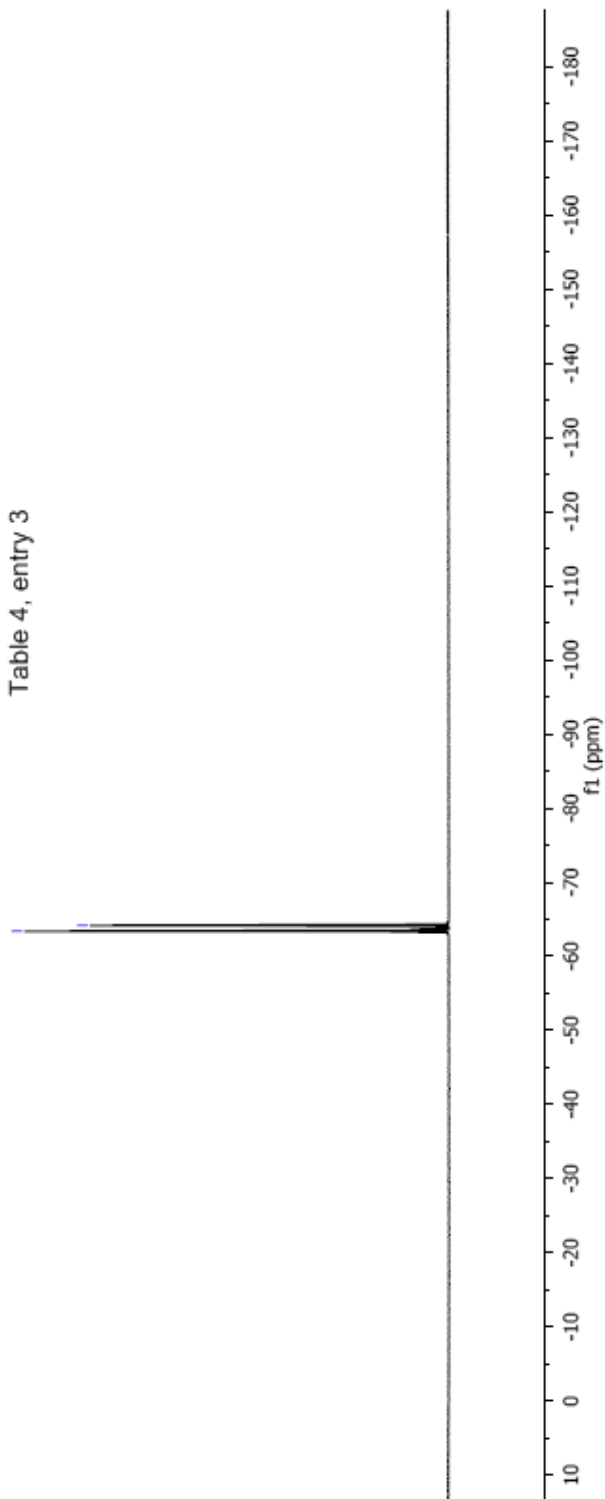


Table 4, entry 3



## Manual Peak Matching Report For Accurate Mass Determination

Theoretical mass	Experimental mass	PFK matching mass	Deviation*
450.10545	450.10641	430.97284	2.1 ppm

\* The deviation is obtained from the following equation:

$$\text{deviation} = \frac{\text{experimental mass} - \text{theoretical mass}}{\text{nominal mass}}$$

Where nominal mass takes in account only  $^{12}\text{C}$ ,  $^1\text{H}$ ,  $^{16}\text{O}$ ,  $^{14}\text{N}$  etc...

Theoretical mass correspond to the mass of the most abundant isotope peak

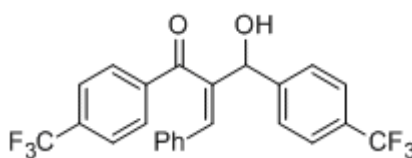
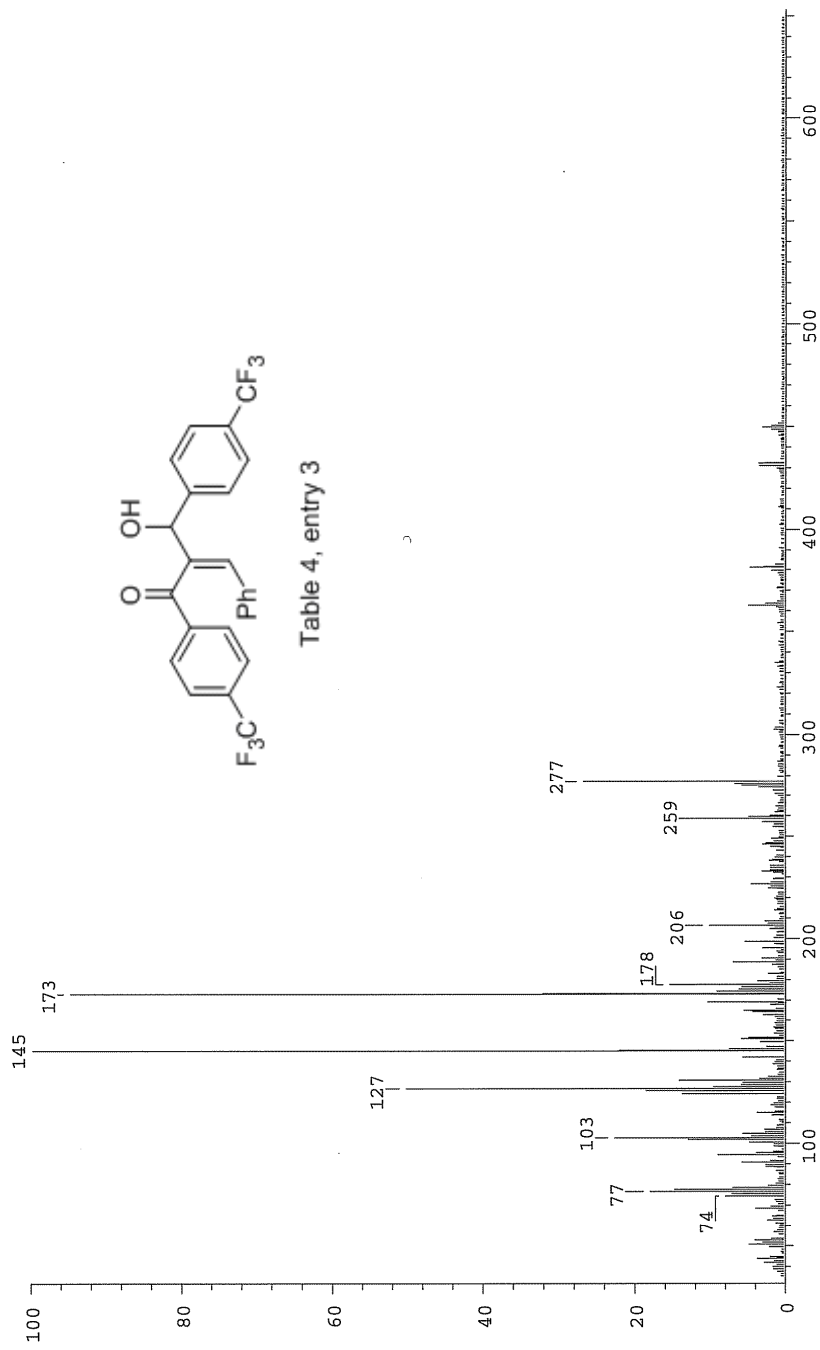


Table 4, entry 3

*HP*

SPEC: fin083770 (15-JUL-08 11:16:25)  
 Samp: 665  
 Comm: Sp 70 eV EI  
 Oper: kh  
 Base: 144.92  
 Peak: 1000.0 mmu  
 REG #9 @ 1.48 min (EI +QIMS LMR UP LR) (+64>80)  
 Study: MS services  
 Masses: 35.01 > 650.00  
 Intensity: 7773364  
 Scans: 1 > 86  
 Client: Kuldup  
 #Peaks: 627  
 RIC: 80910660  
 7.8E+06



KW708, CDCl<sub>3</sub>  
300 MHz  
SEP 24 2008  
WHITE SOLID

7.489  
7.461  
7.448  
7.421  
7.307  
7.282  
7.257  
7.086  
7.072  
7.058  
6.979  
5.671  
3.297  
3.282

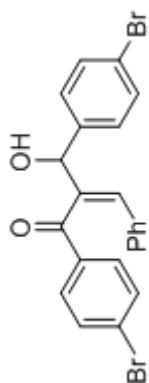
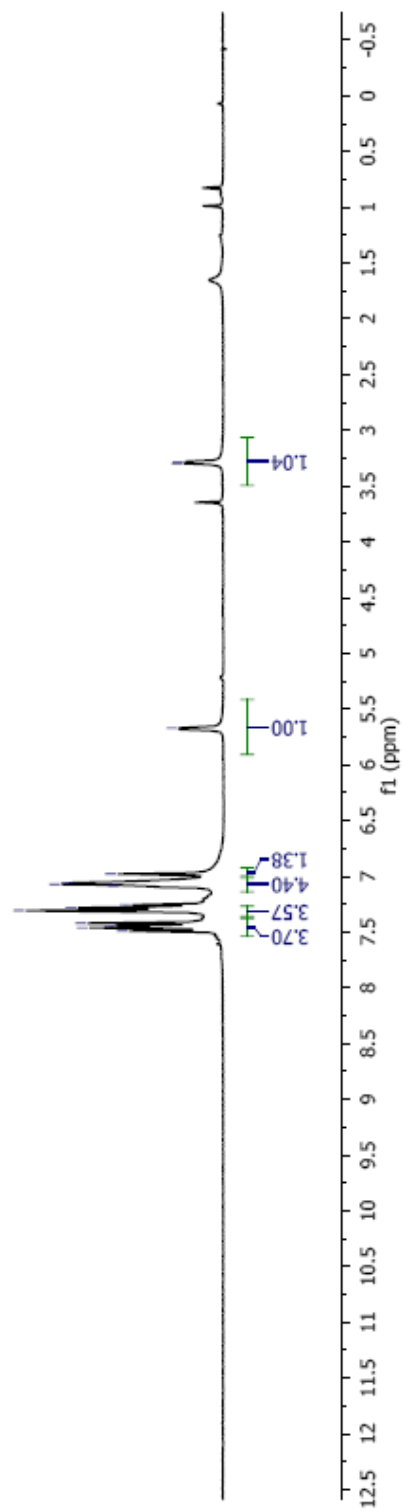
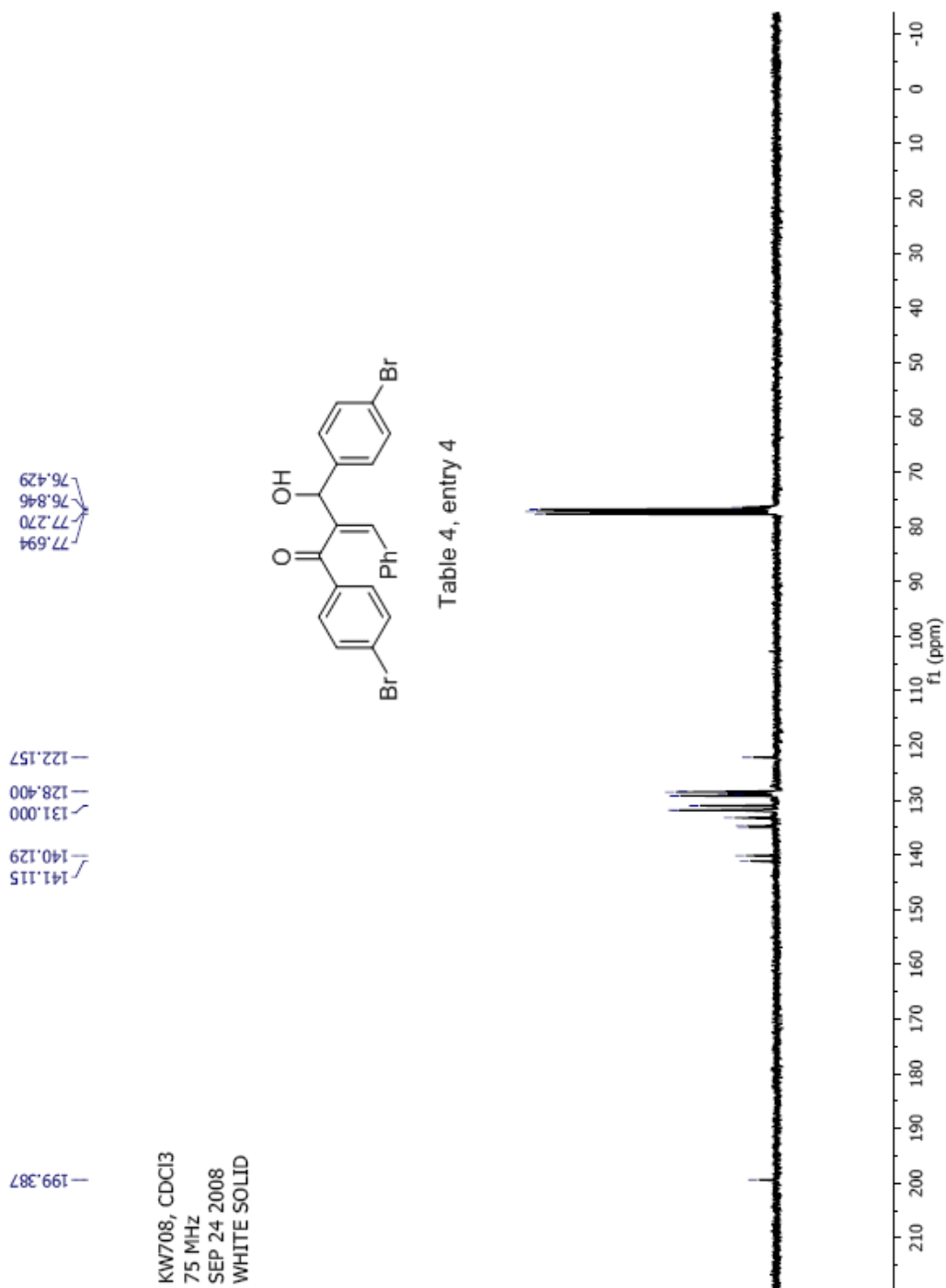


Table 4, entry 4





## Manual Peak Matching Report For Accurate Mass Determination

Theoretical mass	Experimental mass	PFK matching mass	Deviation*
469.95170	469.95310	430.97284	3 ppm

\* The deviation is obtained from the following equation:

$$\text{deviation} = \frac{\text{experimental mass} - \text{theoretical mass}}{\text{nominal mass}}$$

Where nominal mass takes in account only  $^{12}\text{C}$ ,  $^1\text{H}$ ,  $^{16}\text{O}$ ,  $^{14}\text{N}$  etc...

Theoretical mass correspond to the mass of the most abundant isotope peak

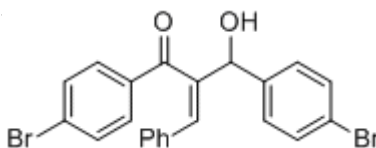


Table 4, entry 4

*MA*

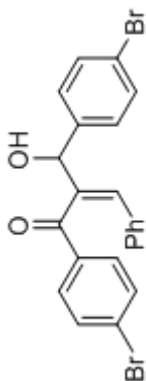
Scans: 1 > 139  
 Client: Kuldup  
 #Peaks: 547  
 RIC: 1393449  
 8.8E+04

SPEC: fir083947.dat (24-OCT-08 11:11:06)  
 Samp: KW708  
 Comm: 70 eV EI  
 Oper: kh  
 Base: 75.76  
 Peak: 1000.0 mmu  
 Scan 132 @ 2.86 min (EI +Q1MS LMR UP LR)

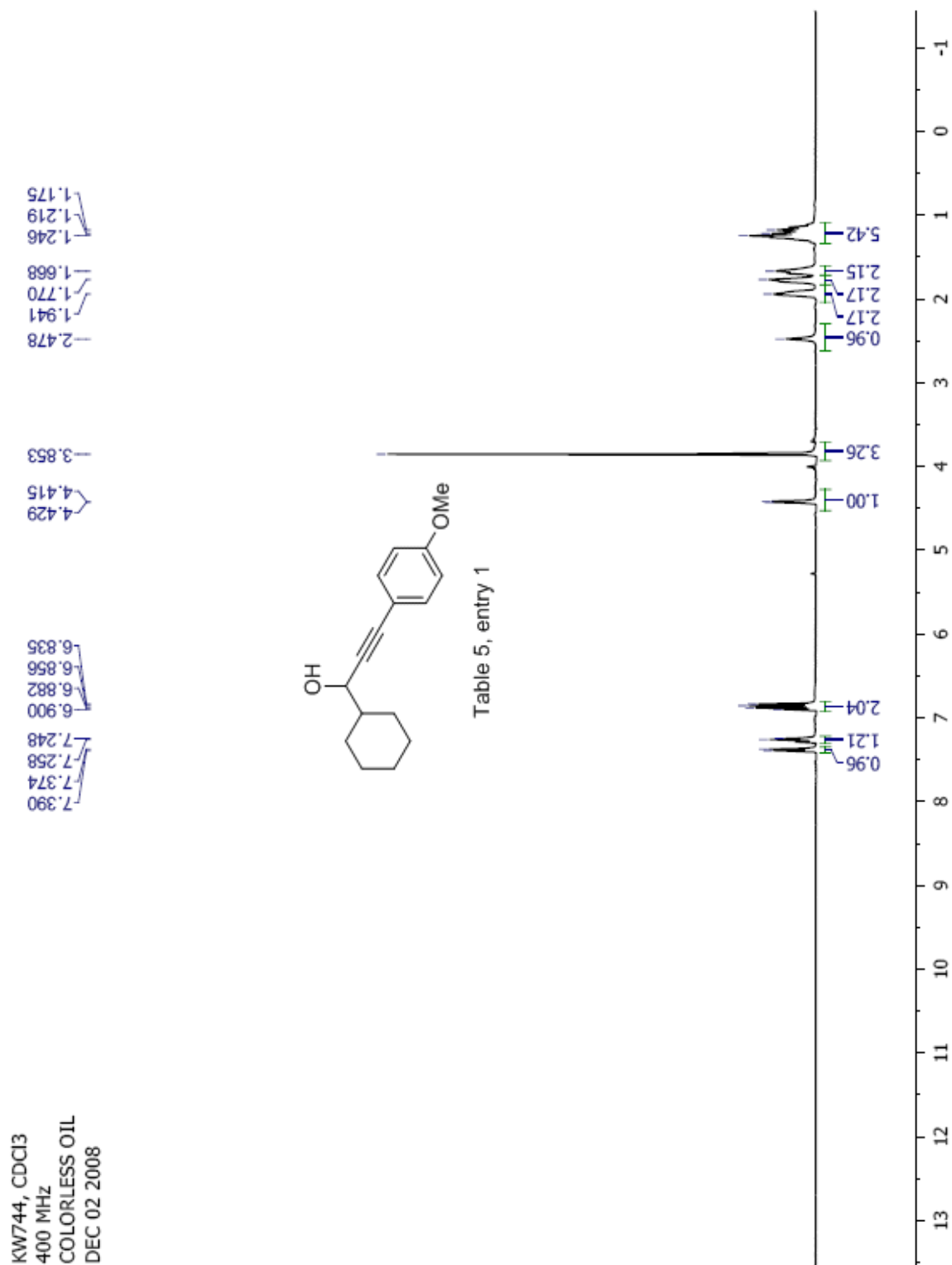
Study: ms services  
 Masses: 35.01 > 650.00  
 Intensity: 88352



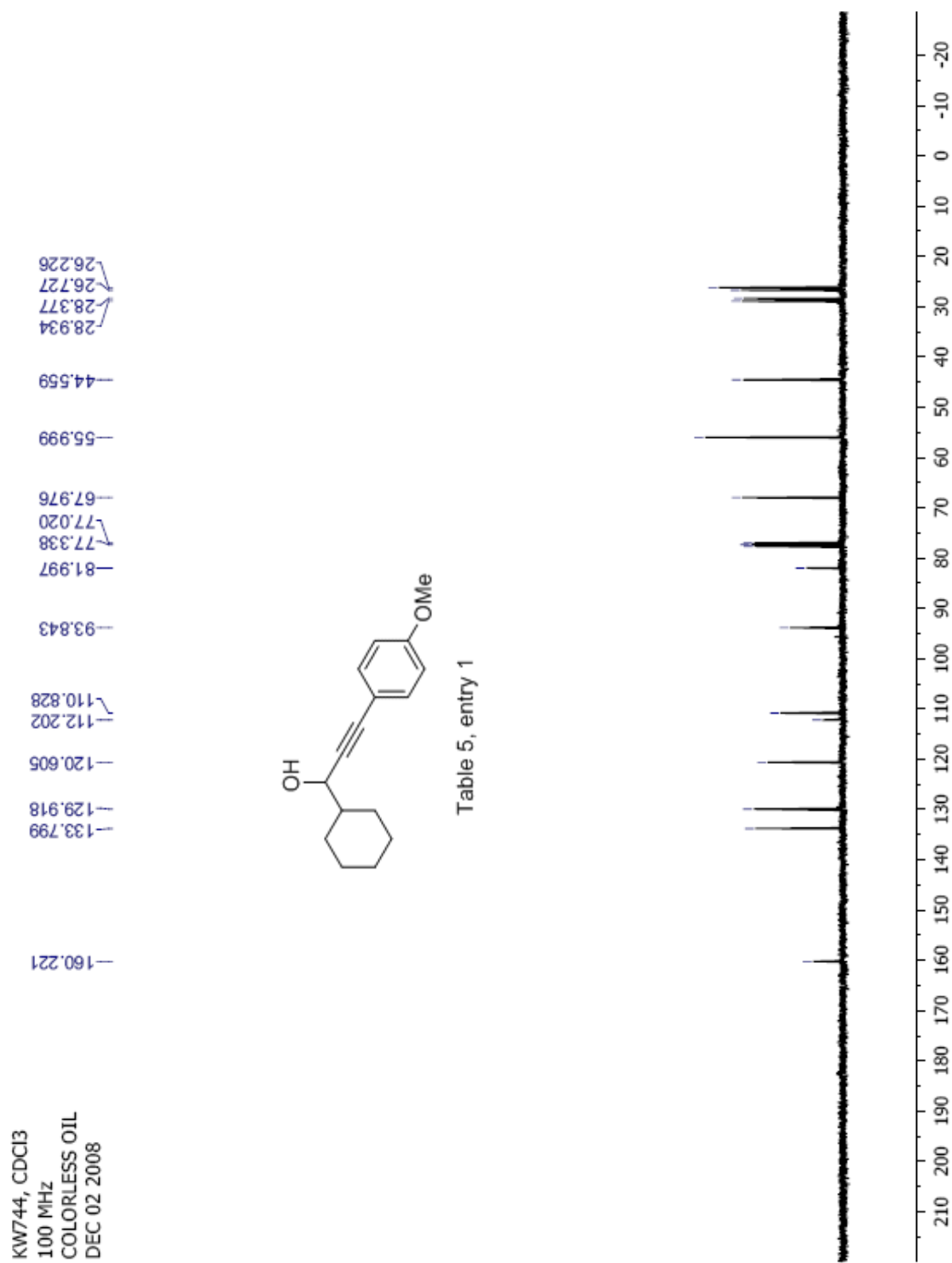
Table 4, entry 4



Date: Fri Oct 24 11:14:50 2008 ICIS: 8.3.0 SP2 for OSF1 (V4.0) build 98-238 from 26-Aug-98







## Manual Peak Matching Report For Accurate Mass Determination

Theoretical mass	Experimental mass	PFK matching mass	Deviation*
244.14632	244.14668	230.98562	2.1 ppm

\* The deviation is obtained from the following equation:

$$\text{deviation} = \frac{\text{experimental mass} - \text{theoretical mass}}{\text{nominal mass}}$$

Where nominal mass takes in account only  $^{12}\text{C}$ ,  $^1\text{H}$ ,  $^{16}\text{O}$ ,  $^{14}\text{N}$  etc...

Theoretical mass correspond to the mass of the most abundant isotope peak

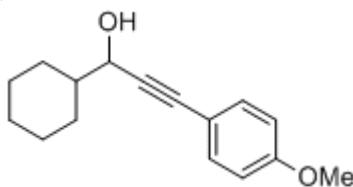


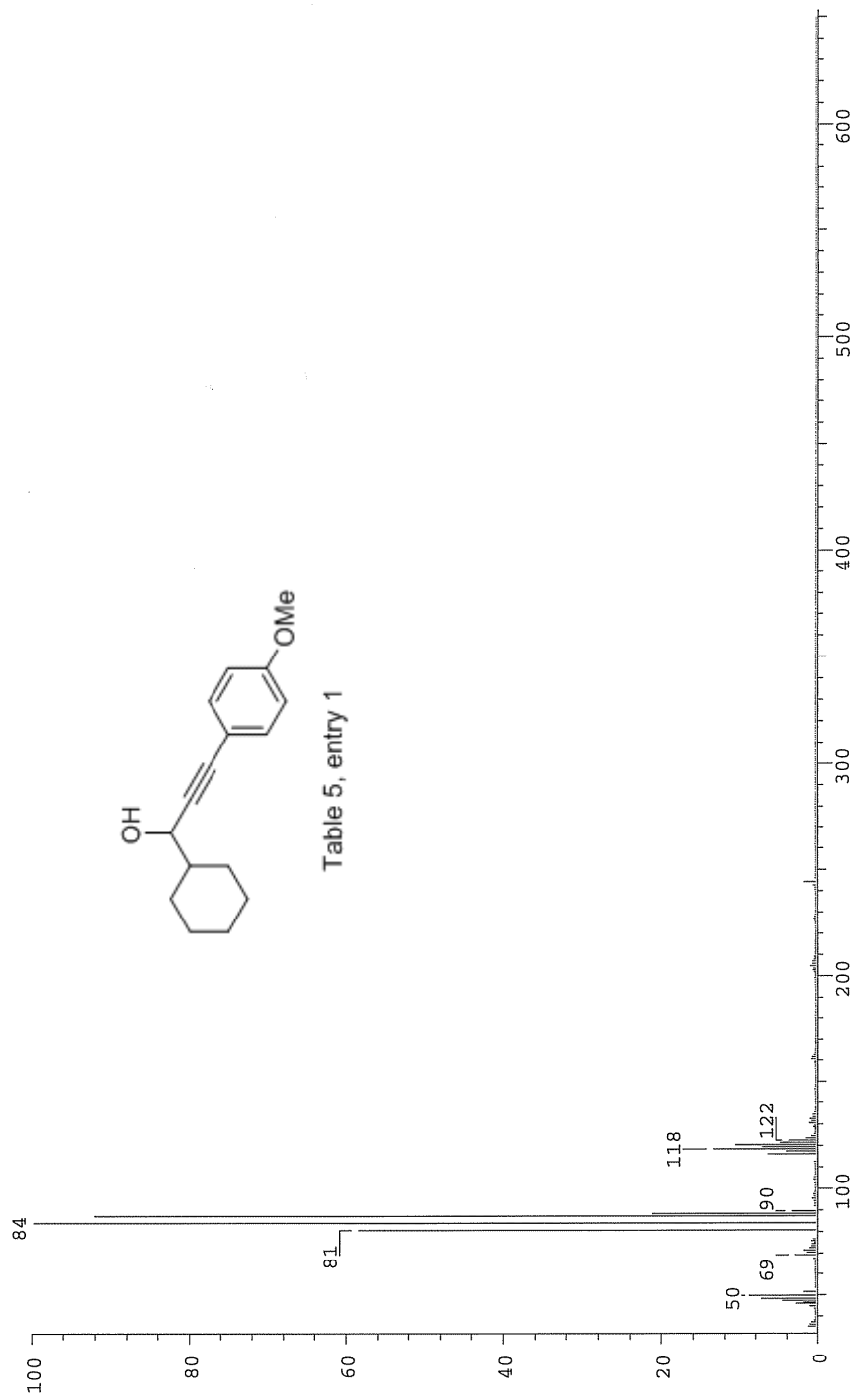
Table 5, entry 1

*h.v.*

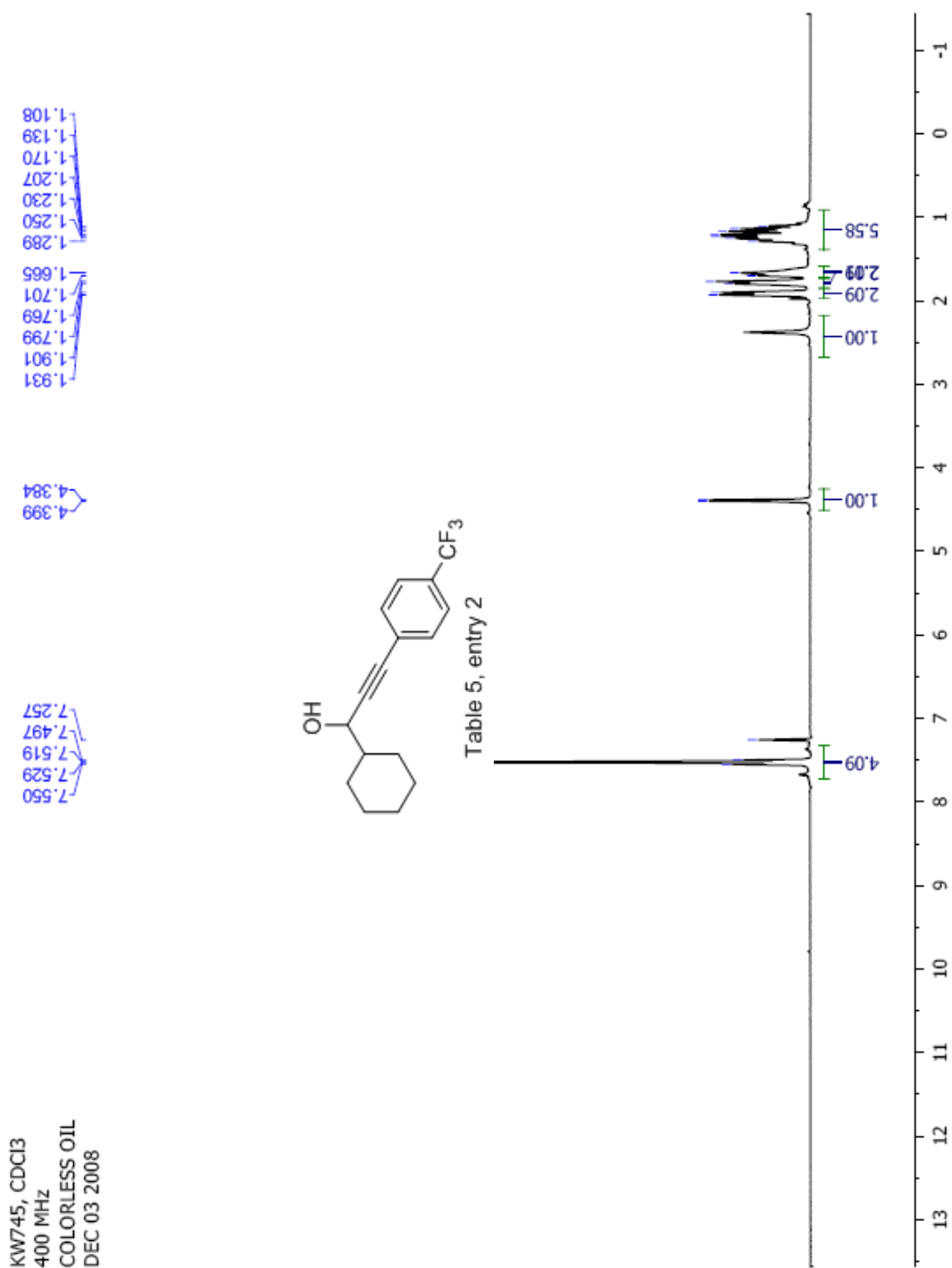
SPEC: fin084086.dat (16-DEC-08 10:29:26)  
 Samp: kw744  
 Comm: 70 eV EI  
 Oper: kh  
 Base: 84.15  
 Peak: 1000.0 mmu  
 Scan 25 @ 0.67 min (EI +QIMS LMR UP LR)

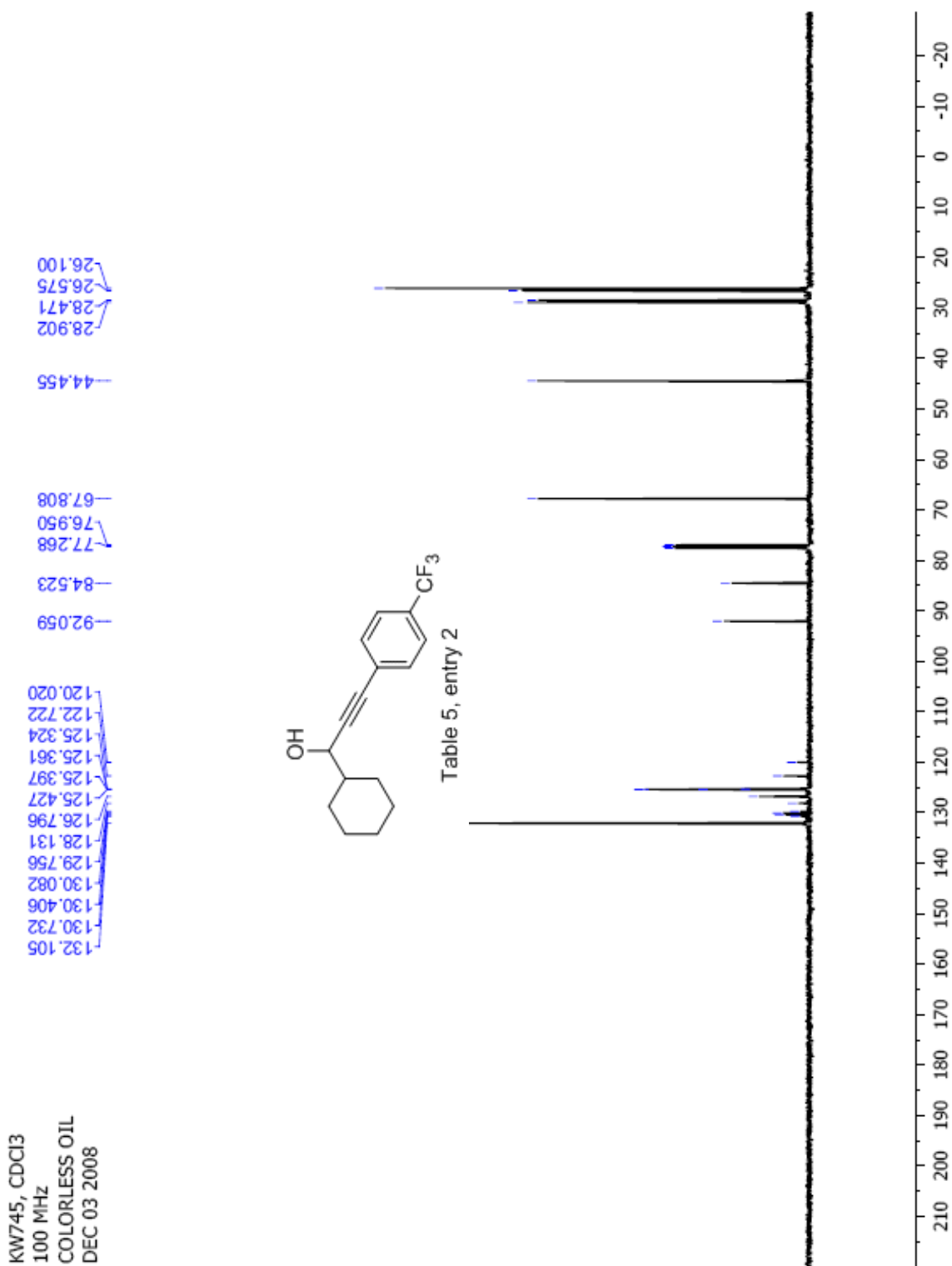
Study: ms services  
 Masses: 35.01 > 650.00  
 Intensity: 16777215

Scans: 1 > 27  
 Client: Kuldeep  
 #Peaks: 628  
 RIC: 64534449  
 1.7E+07



Date: Tue Dec 16 10:30:40 2008 ICIS: 8.3.0 SP2 for OSF1 (V4.0) build 98-238 from 26-Aug-98





KW745, CDCI3  
376 MHz  
COLORLESS OIL  
DEC 03 2008

63.315

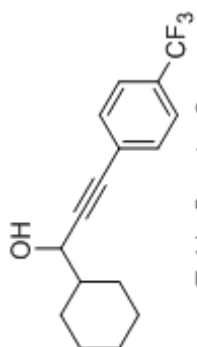
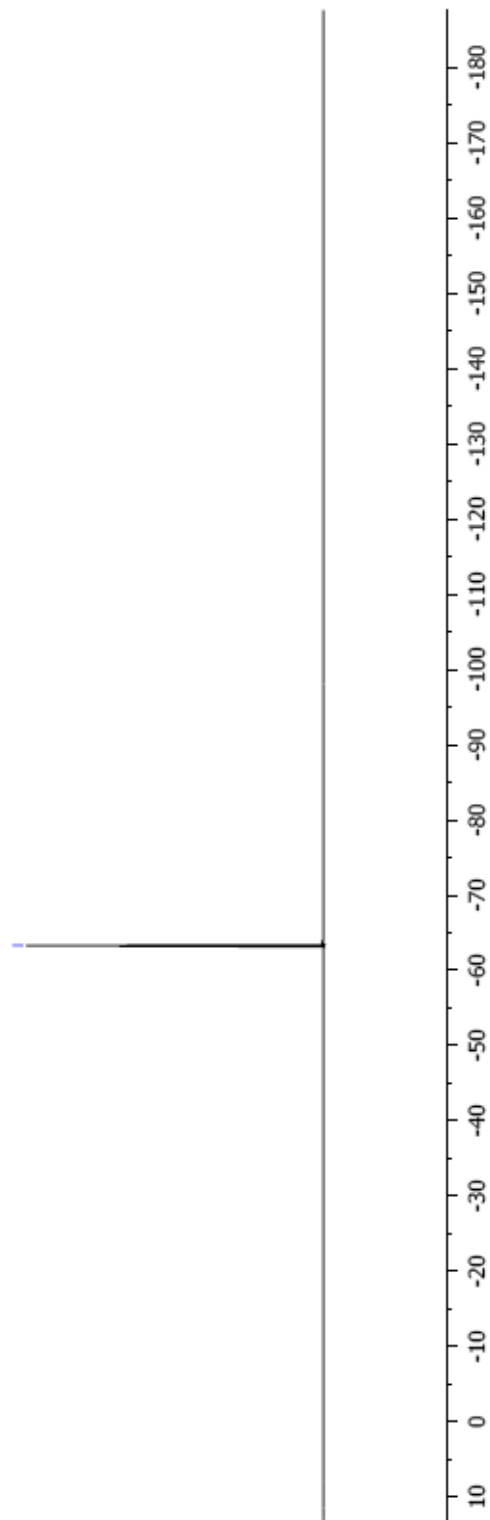


Table 5, entry 2



## Manual Peak Matching Report For Accurate Mass Determination

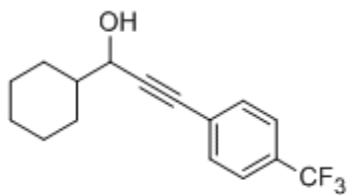
Theoretical mass	Experimental mass	PFK matching mass	Deviation*
282.12314	282.12345	268.98242	1.1 ppm

\* The deviation is obtained from the following equation:

$$\text{deviation} = \frac{\text{experimental mass} - \text{theoretical mass}}{\text{nominal mass}}$$

Where nominal mass takes in account only  $^{12}\text{C}$ ,  $^1\text{H}$ ,  $^{16}\text{O}$ ,  $^{14}\text{N}$  etc...

Theoretical mass correspond to the mass of the most abundant isotope peak



*mp*

SPEC: fin084085.dat (16-DEC-08 10:26:45)  
 Samp: kw745  
 Comm: 70 eV EI  
 Oper: kh  
 Base: 84.42  
 Peak: 1000.0 mmu  
 Scan 24 @ 0.65 min (EI +Q1MS LMR UP LR)

Study: ms services  
 Masses: 35.01 > 650.00  
 Intensity: 1.6777215

Scans: 1 > 29  
 Client: Kuldeep  
 #Peaks: 610  
 RIC: 87478930  
 1.7E+07

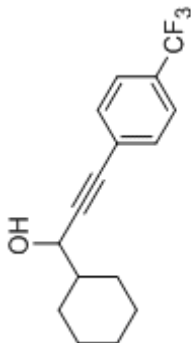
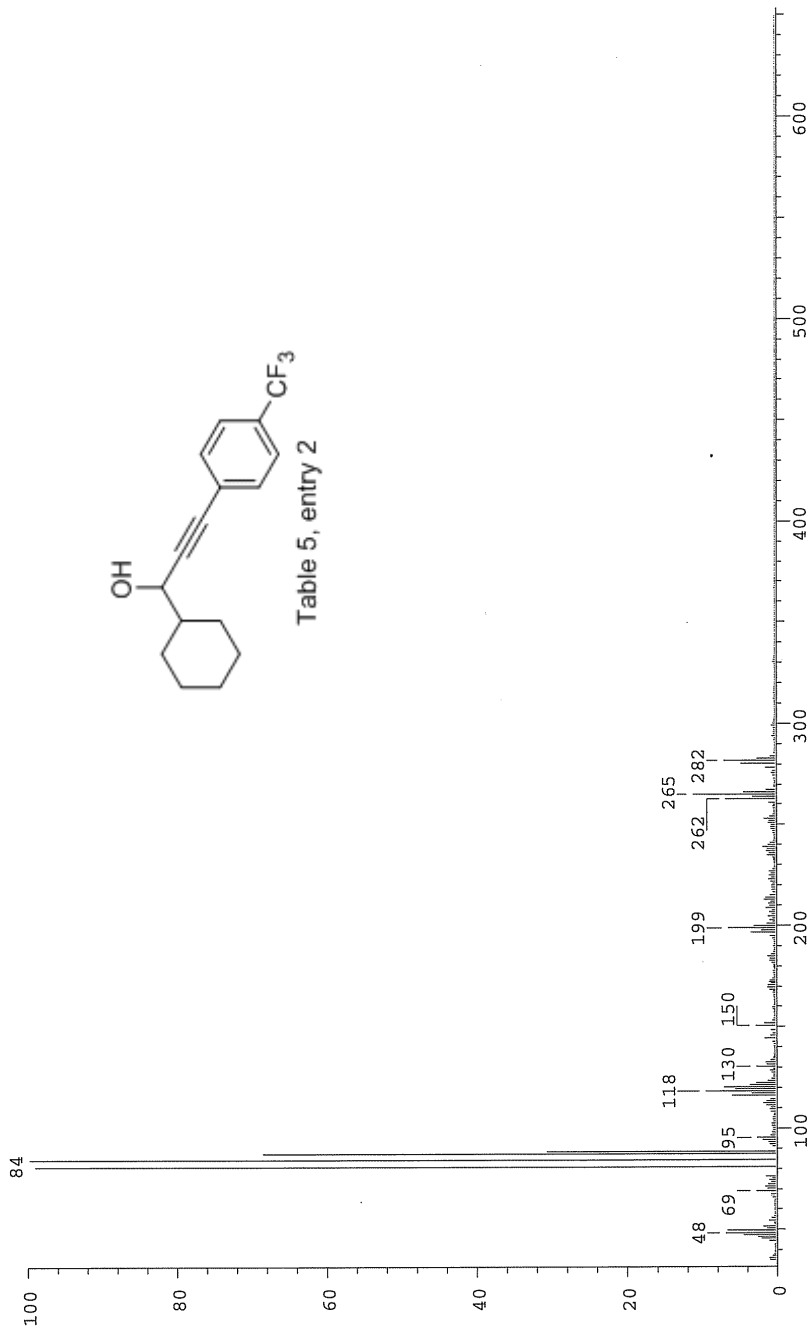
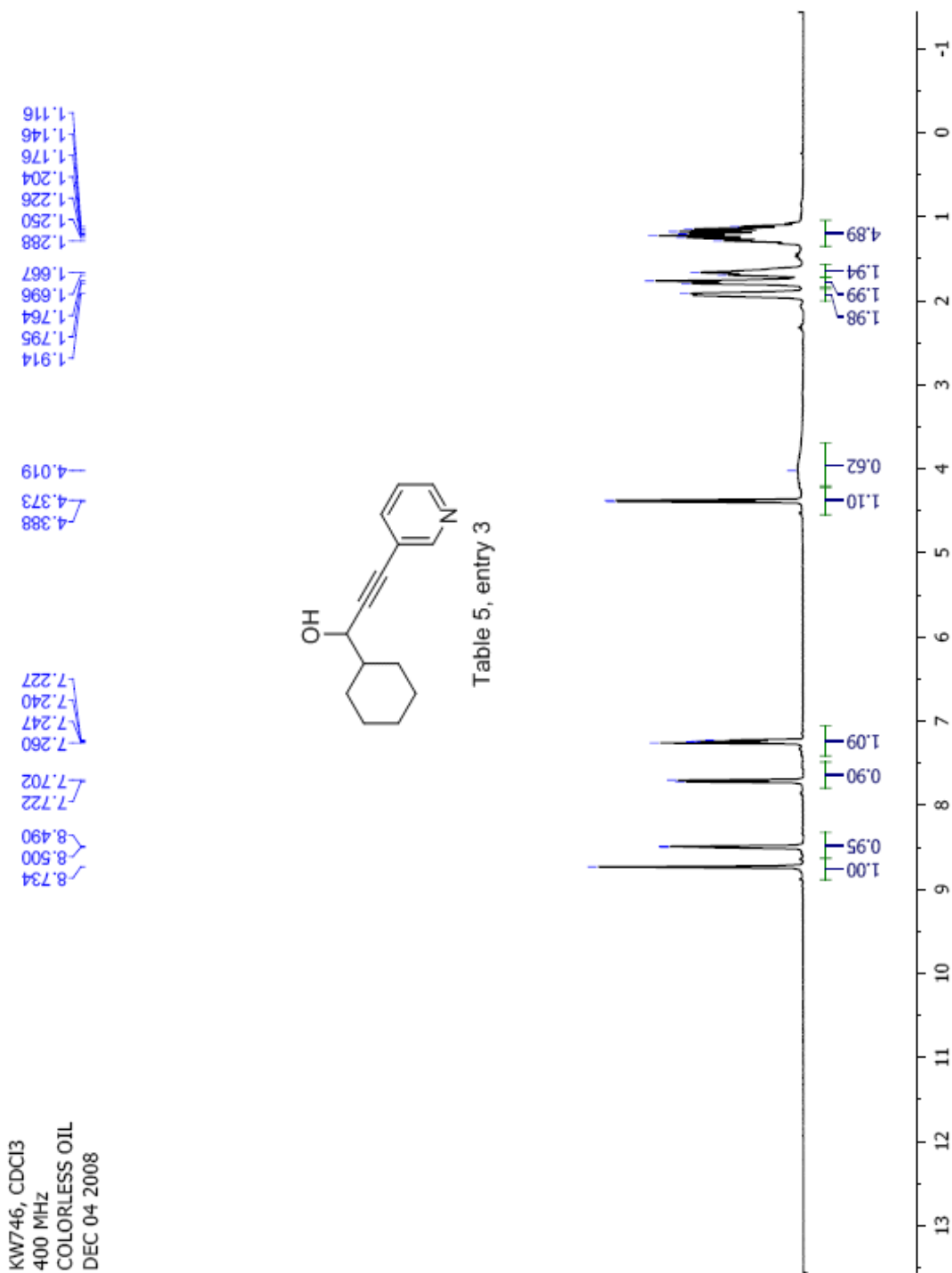


Table 5, entry 2



Date: Tue Dec 16 10:28:11 2008 ICIS: 8.3.0 SP2 for OSF1 (V4.0) build 98-238 from 26-Aug-98





KW746, CDCl<sub>3</sub>  
 100 MHz  
 COLORLESS OIL  
 DEC 04 2008

152.237  
 148.375  
 139.113  
 123.350  
 120.508  
 115.552  
 93.999  
 82.040  
 77.269  
 76.952  
 67.493  
 44.462  
 28.978  
 28.577  
 26.624  
 26.162  
 26.143

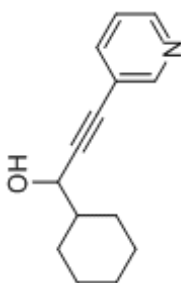
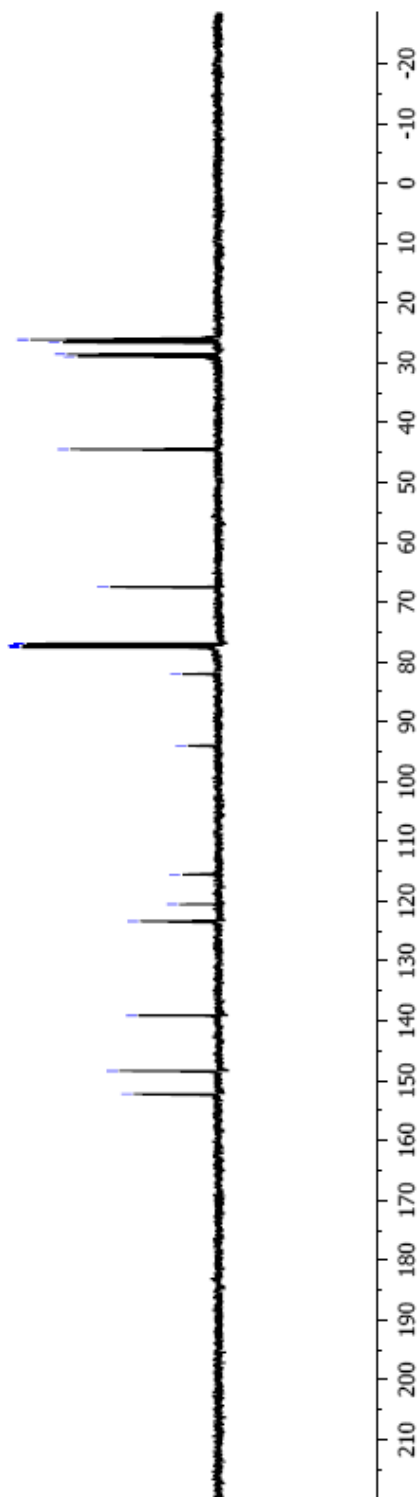


Table 5, entry 3



## Manual Peak Matching Report For Accurate Mass Determination

Theoretical mass	Experimental mass	PFK matching mass	Deviation*
215.13101	215.13147	180.98882	2.1 ppm

\* The deviation is obtained from the following equation:

$$\text{deviation} = \frac{\text{experimental mass} - \text{theoretical mass}}{\text{nominal mass}}$$

Where nominal mass takes in account only  $^{12}\text{C}$ ,  $^1\text{H}$ ,  $^{16}\text{O}$ ,  $^{14}\text{N}$  etc...

Theoretical mass correspond to the mass of the most abundant isotope peak

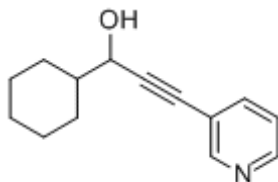


Table 5, entry 3

h 70

Scans: 1 > 107  
 Client: Kuldeep  
 #Peaks: 619  
 RIC: 19689105  
 3.0E+06

SPEC: fin084084.dat (16-DEC-08 10:22:29)  
 Samp: kw746  
 Comm: 70 eV EI  
 Oper: kh  
 Base: 83.58  
 Peak: 1000.0 mmu  
 Scan 70 @ 1.58 min (EI +QIMS LMR UP LR)

Study: ms services  
 Masses: 35.01 > 650.00  
 Intensity: 2969605

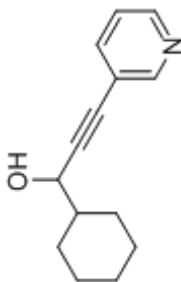
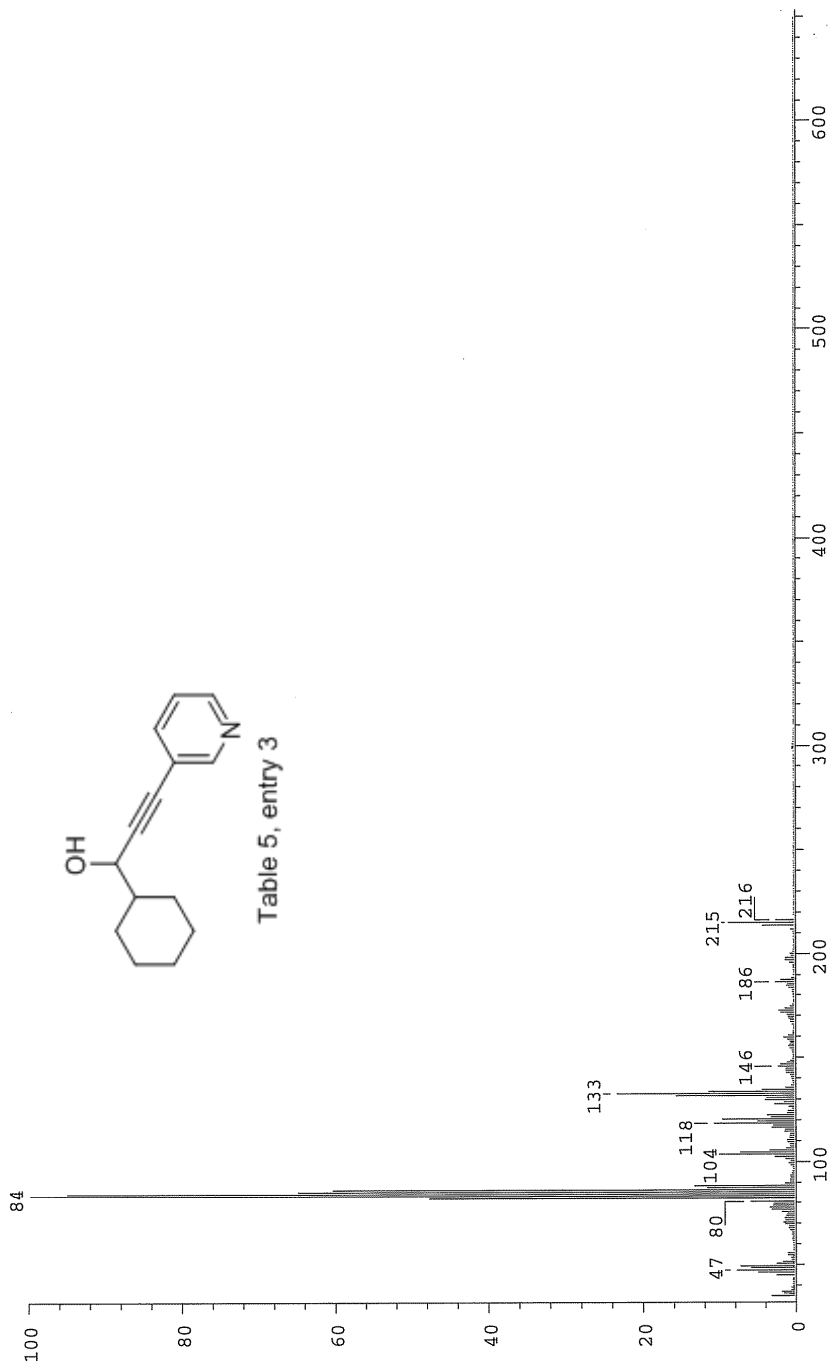


Table 5, entry 3



Date: Tue Dec 16 10:25:31 2008 ICIS: 8.3.0 SP2 for OSF1 (V4.0) build 98-238 from 26-Aug-98

KW753, CDCI3  
400 MHz  
YELLOW OIL  
DEC 15 2008

7.57  
7.56  
7.46  
7.45  
7.25  
7.23  
7.21  
7.16  
7.14  
4.44  
2.31  
2.30  
1.69  
1.27  
1.25  
1.21  
1.18

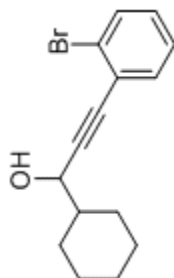
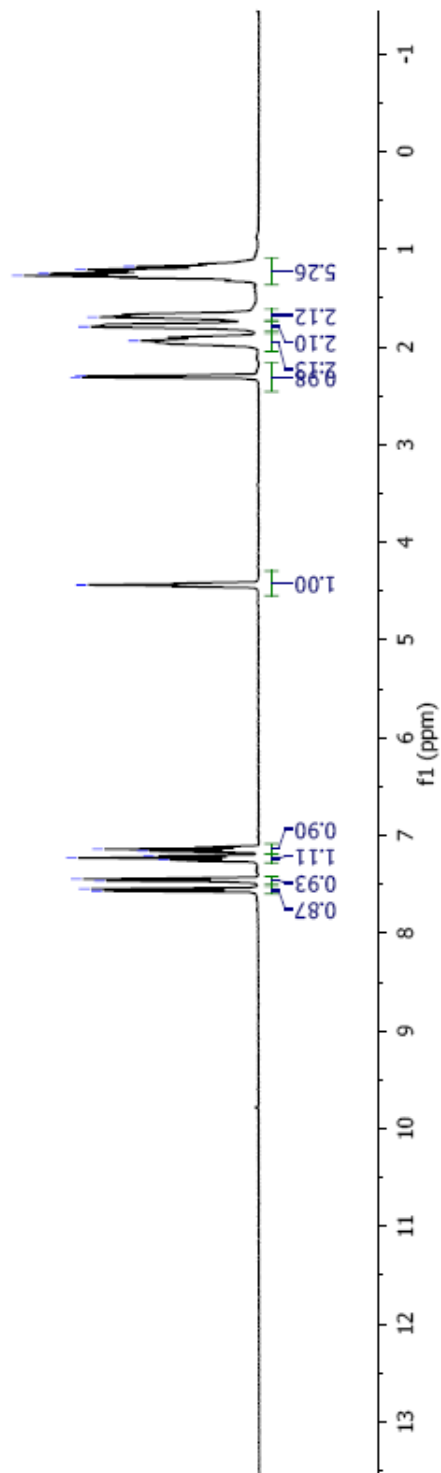


Table 5, entry 4



KW753, CDCl3  
100 MHz  
YELLOW OIL  
DEC 15 2008

133.73  
132.57  
129.67  
127.19  
125.76  
125.12  
94.28  
84.35  
77.32  
77.00  
67.96  
44.48  
28.90  
28.27  
26.68  
26.21  
26.16

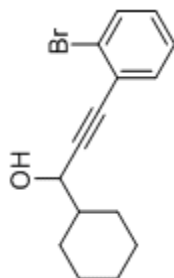
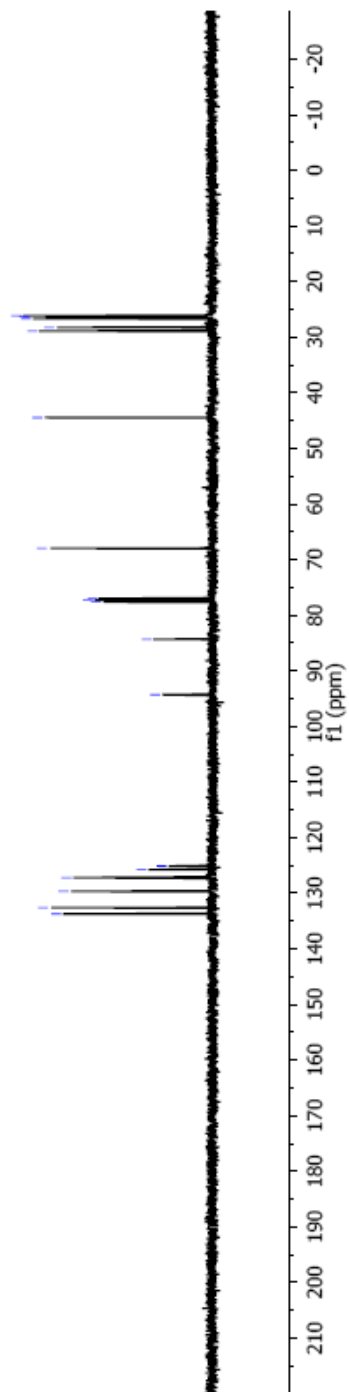


Table 5, entry 4



## Manual Peak Matching Report For Accurate Mass Determination

Theoretical mass	Experimental mass	PFK matching mass	Deviation*
292.04627	292.04691	280.98242	2.2 ppm

\* The deviation is obtained from the following equation:

$$\text{deviation} = \frac{\text{experimental mass} - \text{theoretical mass}}{\text{nominal mass}}$$

Where nominal mass takes in account only  $^{12}\text{C}$ ,  $^1\text{H}$ ,  $^{16}\text{O}$ ,  $^{14}\text{N}$  etc...

Theoretical mass correspond to the mass of the most abundant isotope peak

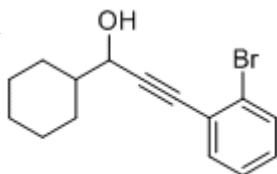


Table 5, entry 4

*MS*

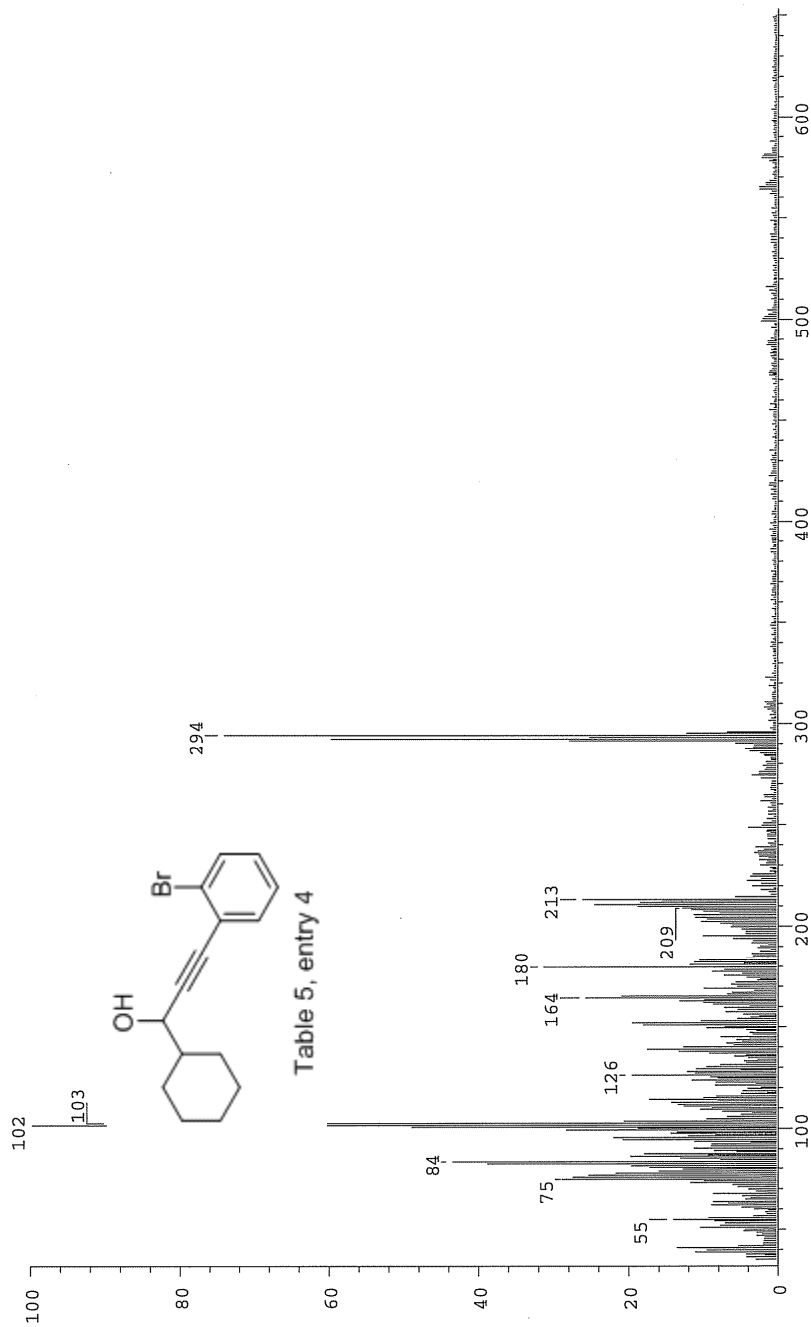
SPEC: fin084173.dat (22-JAN-09 11:08:50)  
 Stamp: kw753  
 Comm: 70 eV EI  
 Oper: kh  
 Base: 101.53  
 Peak: 1000.0 mmu  
 Scan 23 @ 0.62 min (EI +Q1MS LMR UP LR)

Study: ms services  
 Masses: 35.01 > 650.00  
 Intensity: 31091

Scans: 1 > 63

Client: Kuldup  
 #Peaks: 648  
 RIC: 773275

3.1E+04



Date: Thu Jan 22 11:11:01 2009 ICIS: 8.3.0 SP2 for OSFI (V4.0) build 98-238 from 26-Aug-98



KW755, CDCl3  
400 MHz  
YELLOW OIL  
JAN 12 2008

2.10  
1.92  
1.89  
1.80  
1.77  
1.71  
1.68  
1.29  
1.26  
1.23  
1.20  
1.17  
1.13  
1.10

4.37

7.41  
7.31  
7.29  
7.27  
7.26  
7.24  
7.22  
7.20

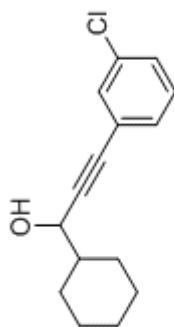
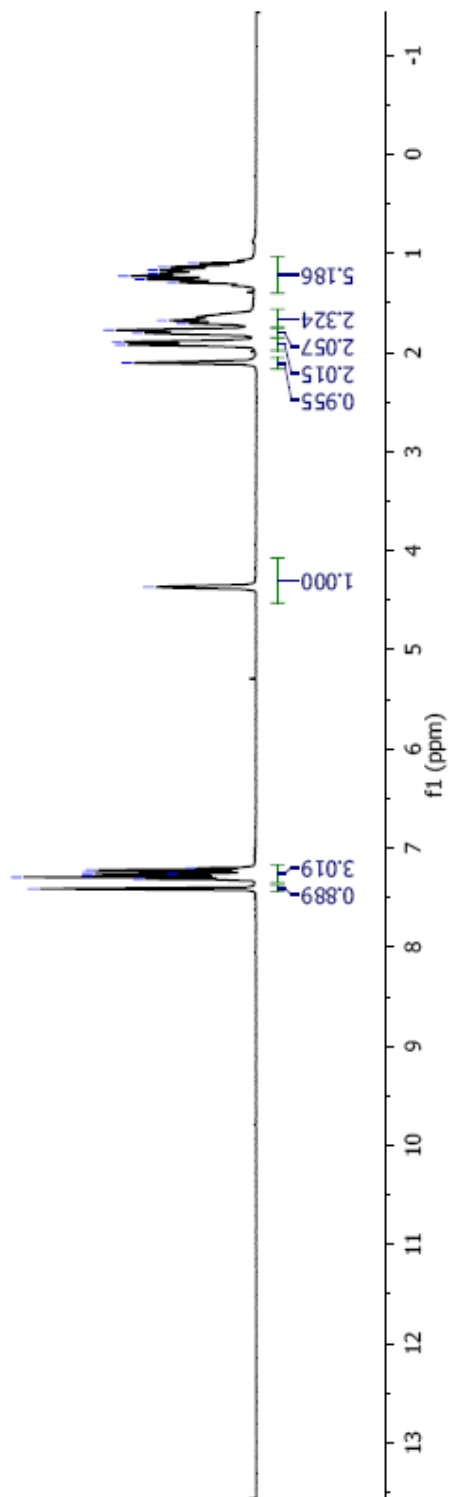


Table 5, entry 5



KW755, CDCl<sub>3</sub>  
 100 MHz  
 YELLOW OIL  
 JAN 12 2008

134.30  
 131.77  
 130.02  
 129.71  
 128.80  
 124.68  
 90.77  
 84.50  
 77.28  
 76.96  
 67.83  
 44.48  
 28.90  
 28.46  
 26.61  
 26.14  
 26.12

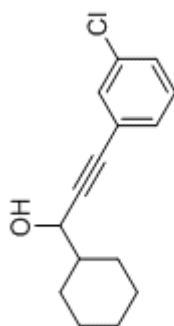
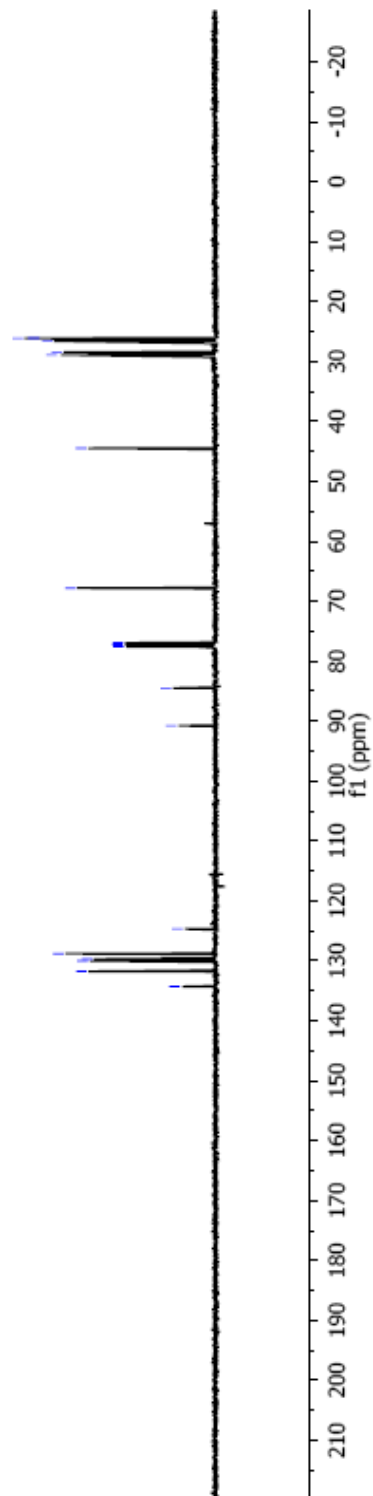


Table 5, entry 5



## Manual Peak Matching Report For Accurate Mass Determination

Theoretical mass	Experimental mass	PFK matching mass	Deviation*
248.09679	248.09739	230.98562	2.4 ppm

\* The deviation is obtained from the following equation:

$$\text{deviation} = \frac{\text{experimental mass} - \text{theoretical mass}}{\text{nominal mass}}$$

Where nominal mass takes in account only  $^{12}\text{C}$ ,  $^1\text{H}$ ,  $^{16}\text{O}$ ,  $^{14}\text{N}$  etc...

Theoretical mass correspond to the mass of the most abundant isotope peak

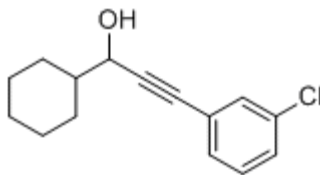


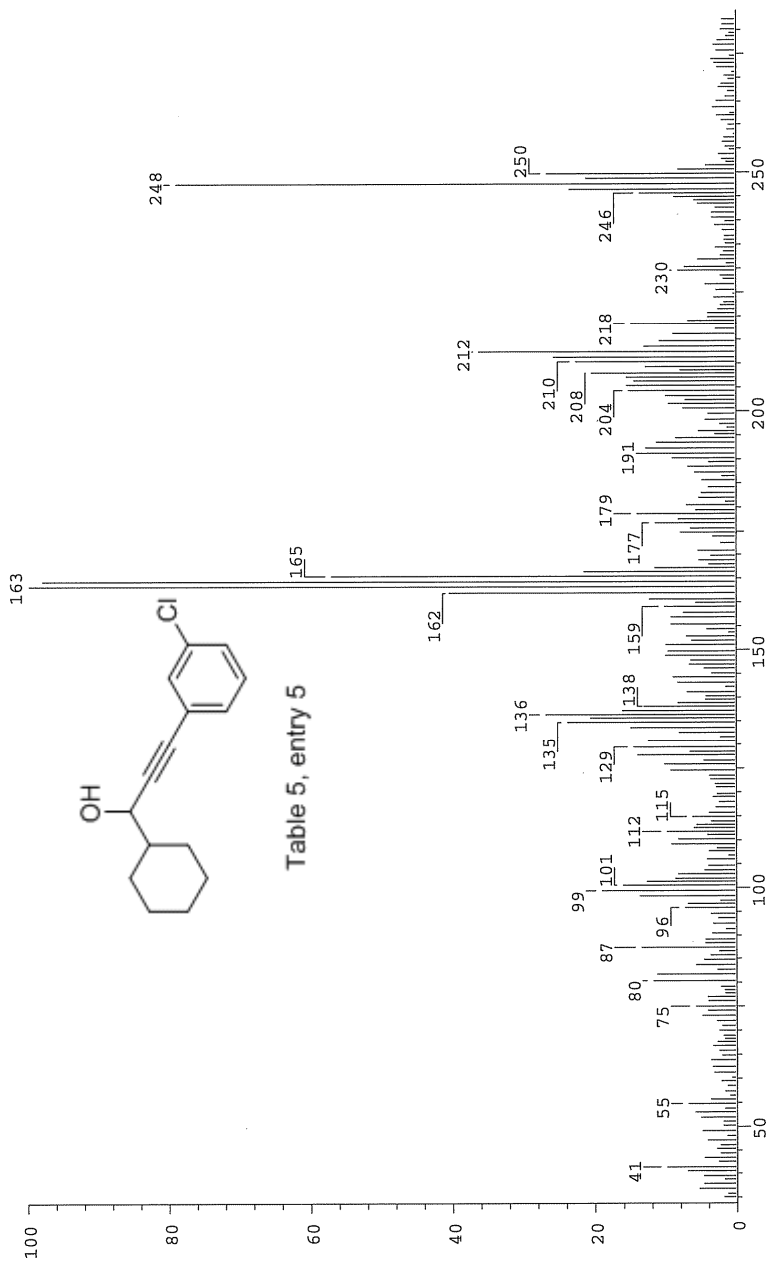
Table 5, entry 5

*Handwritten signature*

SPEC: fin084174.dat (22-JAN-09 11:12:25)  
 Samp: kw735  
 Comm: 70 eV EI  
 Oper: kh  
 Study: ms services  
 Base: 163.24  
 Masses: 35.01 > 650.00  
 Peak: 1000.0 mmu  
 Intensity: 6343  
 Scan 18 @ 0.52 min (EI +QIMS LMR UP LR)

Scans: 1 > 51

Client: Kuldup  
 #Peaks: 657  
 RIC: 152696  
 6.3E+03



Date: Thu Jan 22 11:16:20 2009 ICIS: 8.3.0 SP2 for OSF1 (V4.0) build 98-238 from 26-Aug-98

KW754, CDCl<sub>3</sub>  
400 MHz  
YELLOW OIL  
DEC 17 2008

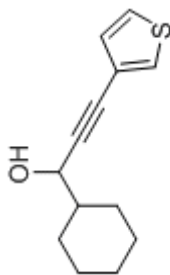
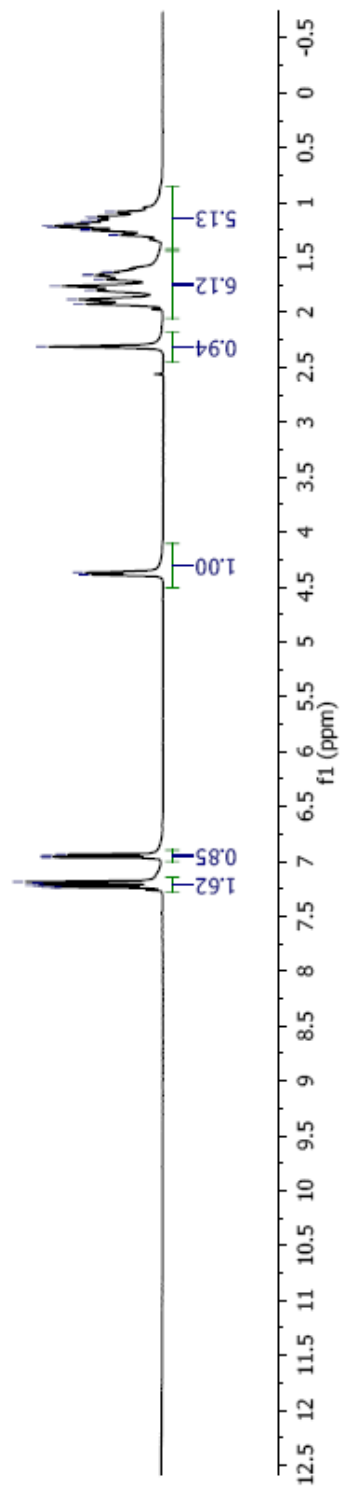


Table 5, entry 6



KW754, CDCl<sub>3</sub>  
 100 MHz  
 YELLOW OIL  
 DEC 17 2008

132.32  
 127.15  
 122.94  
 93.47  
 79.11  
 77.76  
 77.34  
 76.92  
 68.00  
 44.42  
 28.89  
 28.48  
 26.61  
 26.13

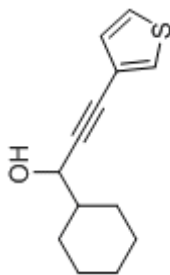
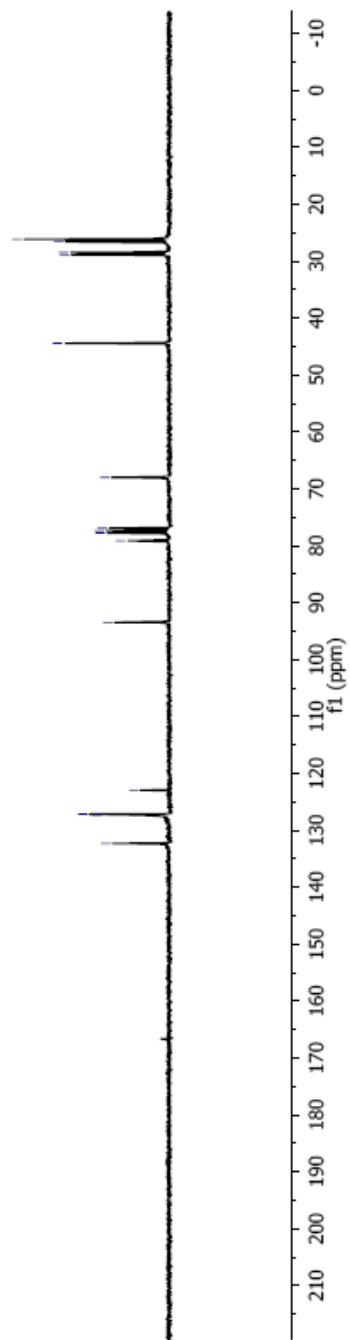


Table 5, entry 6



## Manual Peak Matching Report For Accurate Mass Determination

Theoretical mass	Experimental mass	PFK matching mass	Deviation*
220.09218	220.09246	218.98562	1.3 ppm

\* The deviation is obtained from the following equation:

$$\text{deviation} = \frac{\text{experimental mass} - \text{theoretical mass}}{\text{nominal mass}}$$

Where nominal mass takes in account only  $^{12}\text{C}$ ,  $^1\text{H}$ ,  $^{16}\text{O}$ ,  $^{14}\text{N}$  etc...

Theoretical mass correspond to the mass of the most abundant isotope peak

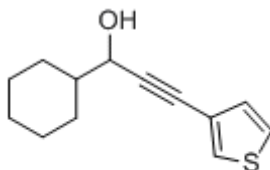
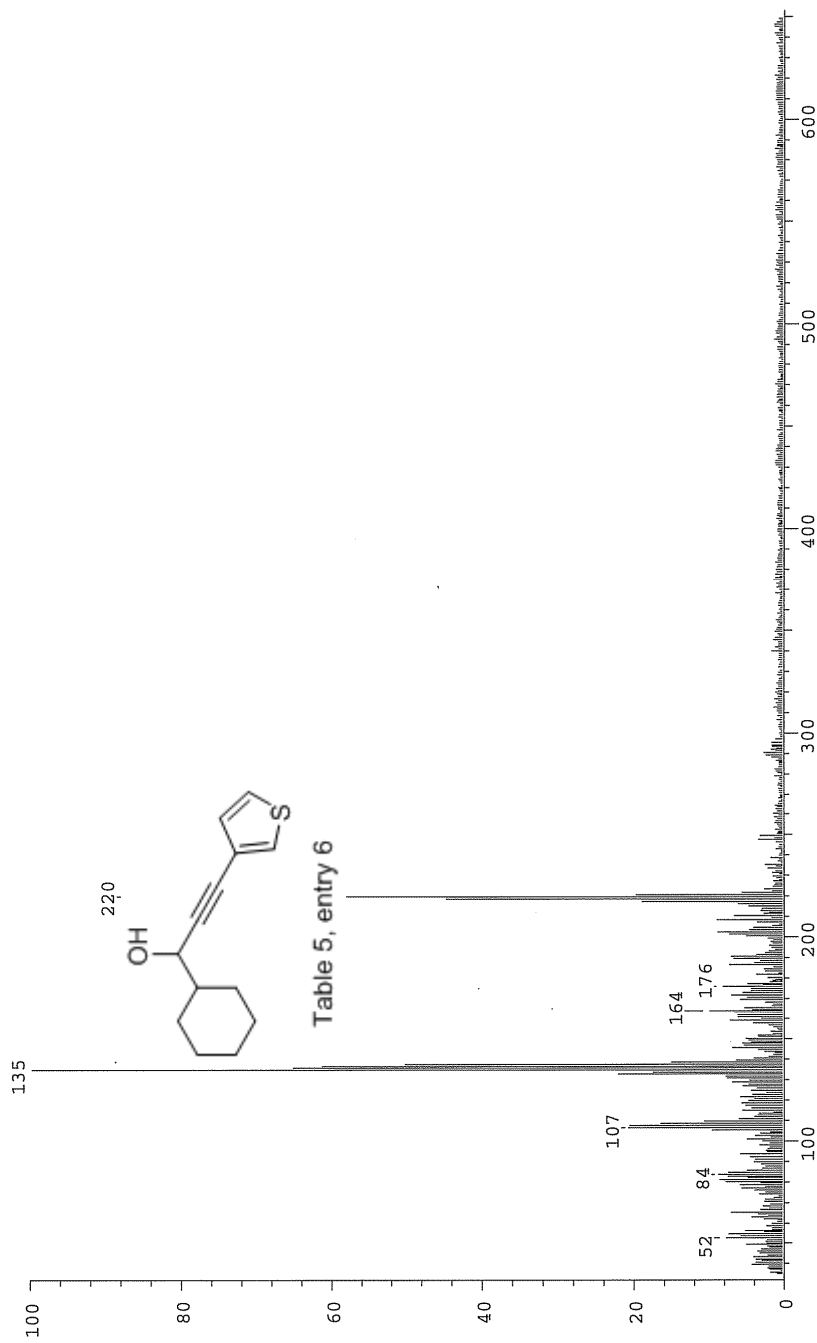


Table 5, entry 6

Scans: 1 > 44  
 Client: Kuldup  
 #Peaks: 650  
 RIC: 209195  
 1.4E+04

SPEC: fin084175.dat (22-JAN-09 11:18:09)  
 Samp: kw754  
 Comm: 70 eV EI  
 Oper: kh  
 Base: 134.82  
 Peak: 1000.0 mmu  
 Scan 12 @ 0.40 min (EI +QIMS LMR UP LR)

Study: ms services  
 Masses: 35.01 > 650.00  
 Intensity: 13965



Date: Thu Jan 22 11:19:50 2009 ICIS: 8.3.0 SP2 for OSF1 (V4.0) build 98-238 from 26-Aug-98



KW781, CDCI3  
400 MHz  
YELLOW OIL  
FEB 04 2009

7.401  
7.382  
7.285  
7.265  
7.121  
7.105  
7.059  
7.040  
6.913  
6.895  
6.876  
6.860  
6.839  
6.190  
3.837  
2.693  
2.623

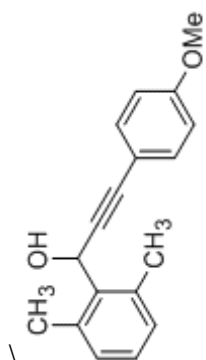
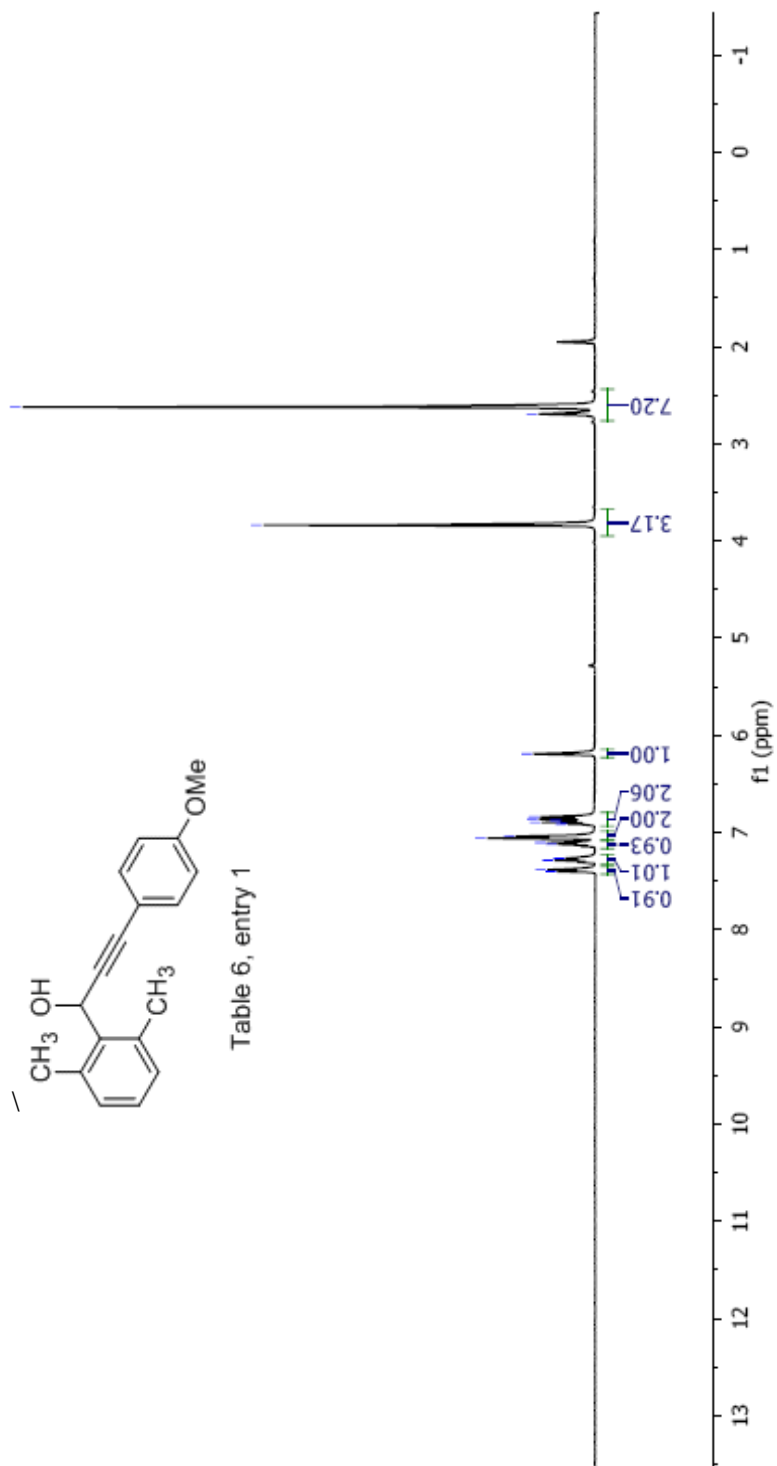


Table 6, entry 1



KW781, CDCl<sub>3</sub>  
 100 MHz  
 YELLOW OIL  
 FEB 04 2009

160.399  
 137.050  
 133.830  
 130.118  
 129.425  
 128.257  
 120.617  
 112.213  
 110.854  
 93.148  
 82.390  
 77.675  
 77.039  
 61.189  
 61.152  
 55.888  
 20.668

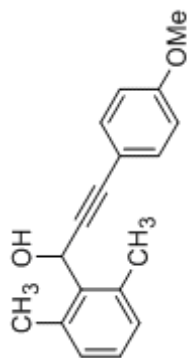
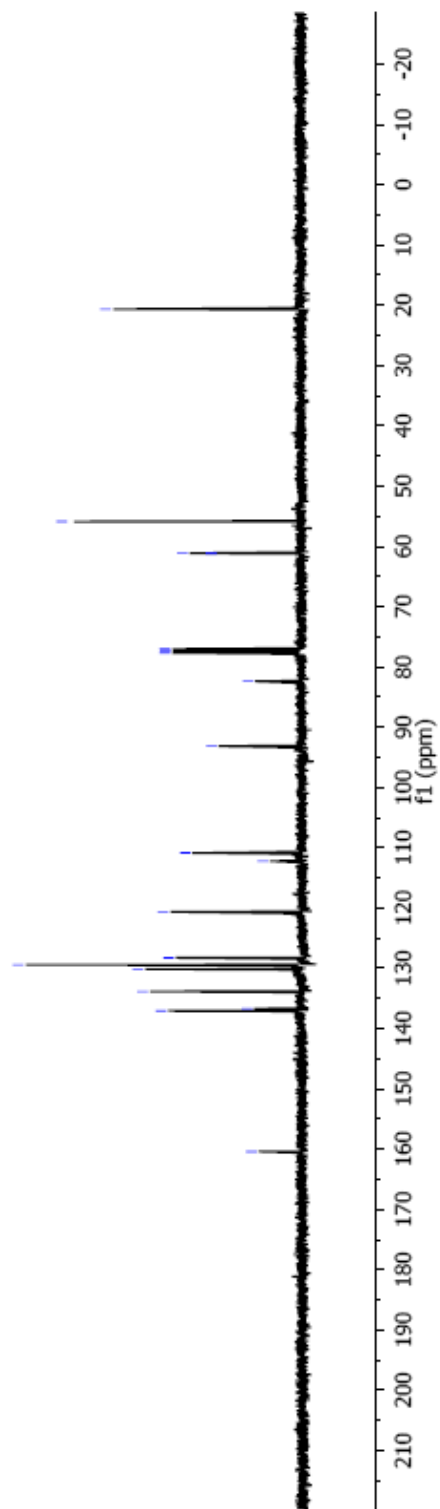


Table 6, entry 1



### Manual Peak Matching Report For Accurate Mass Determination

Theoretical mass	Experimental mass	PFK matching mass	Deviation*
266.13067	266.13179	280.98562	2.4 ppm

\* The deviation is obtained from the following equation:

$$\text{deviation} = \frac{\text{experimental mass} - \text{theoretical mass}}{\text{nominal mass}}$$

Where nominal mass takes in account only  $^{12}\text{C}$ ,  $^1\text{H}$ ,  $^{16}\text{O}$ ,  $^{14}\text{N}$  etc...

Theoretical mass correspond to the mass of the most abundant isotope peak

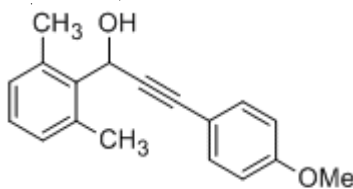
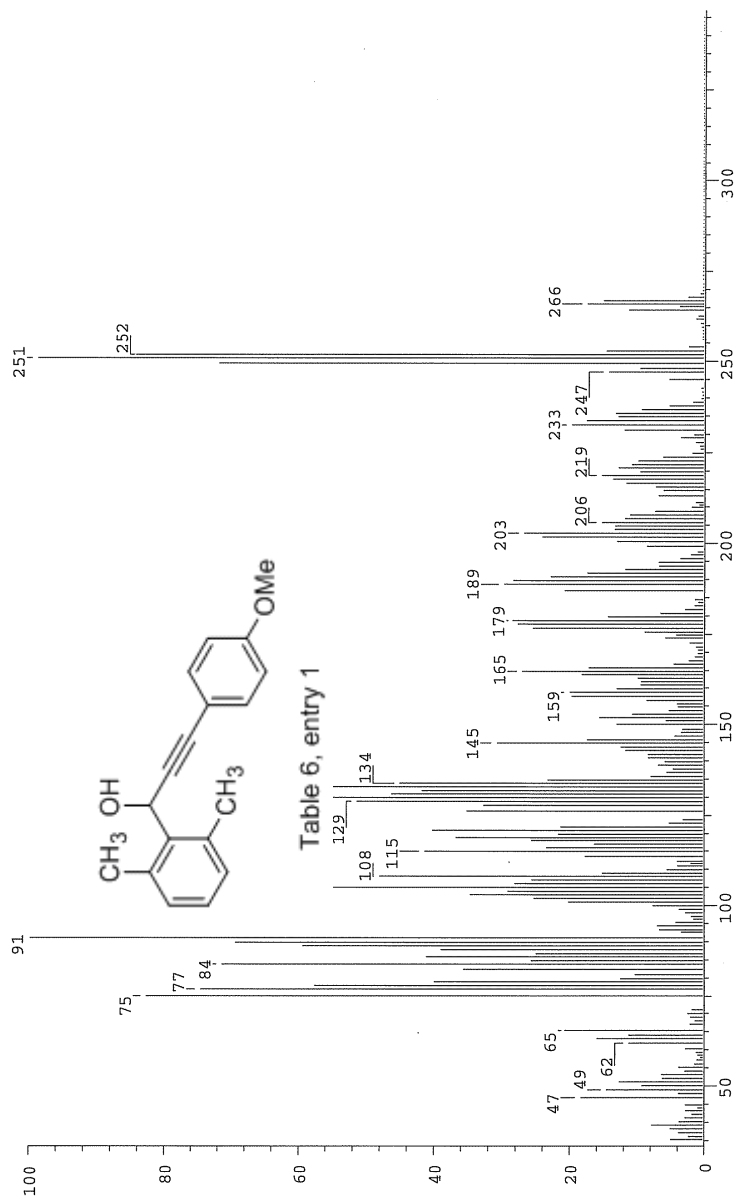


Table 6, entry 1

SPC: fin084277.dat (02-MAR-09 11:12:36)  
 Samp: kw781  
 Comm: Dp/EI  
 Oper: kh  
 Base: 91.04  
 Peak: 1000.0 mmu  
 Scan 49 @ 1.14 min (EI +QIMS LMR UP LR)

Study: ms services  
 Masses: 35.01 > 650.00  
 Intensity: 8844822

Scans: 1 > 56  
 Client: Kuldeep  
 #Peaks: 616  
 RIC: 287336684  
 8.8E+06



Date: Mon Mar 2 11:14:47 2009 ICIS: 8.3.0 SP2 for OSF1 (V4.0) build 98-238 from 26-Aug-98

KW779, CDCl<sub>3</sub>  
 400 MHz  
 COLORLESS OIL  
 FEB 02 2009

8.06  
 8.04  
 7.51  
 7.42  
 7.32  
 7.25  
 7.17  
 -5.74  
 -2.47

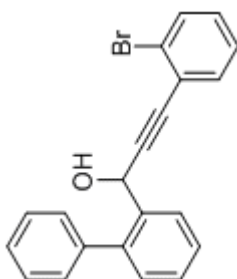
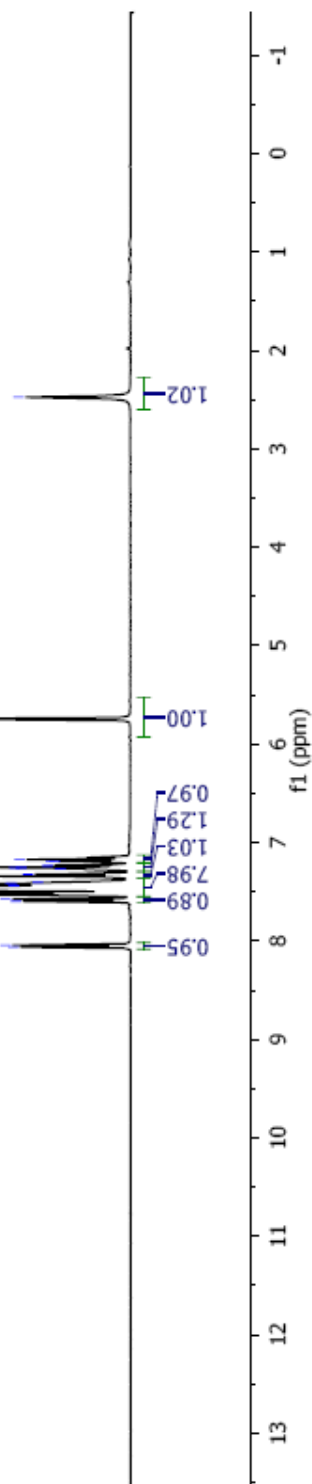


Table 6, entry 2



KW779, CDC13  
100 MHz  
COLORLESS OIL  
FEB 02 2009

141.25  
140.40  
138.25  
130.45  
129.81  
128.52  
128.07  
127.22  
124.94  
94.46  
85.27  
77.65  
77.01  
62.55  
62.51

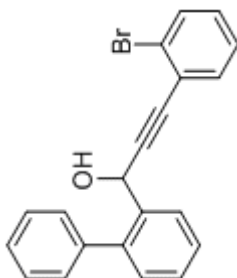
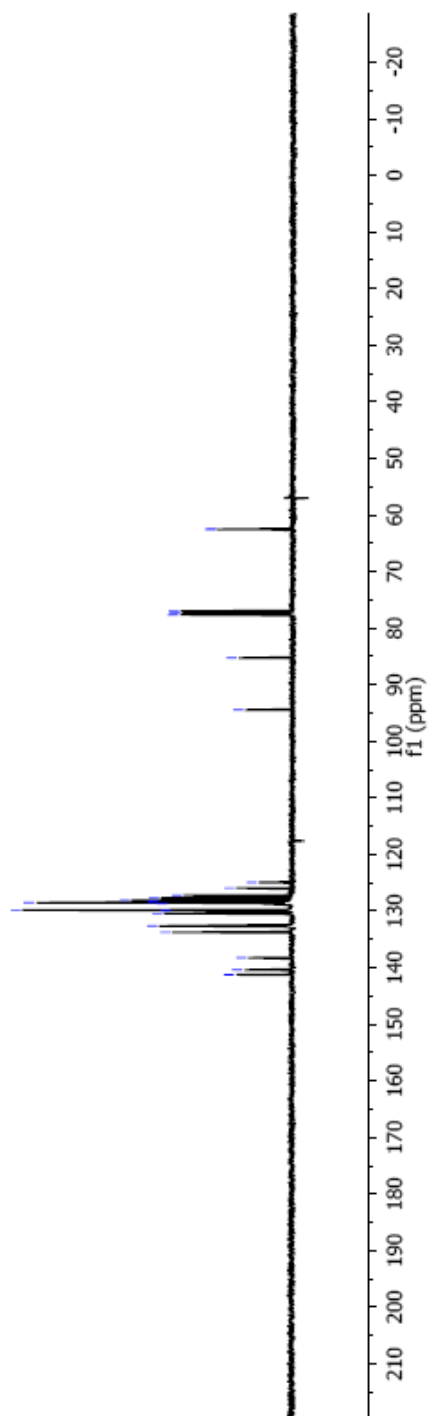


Table 6, entry 2



### Manual Peak Matching Report For Accurate Mass Determination

Theoretical mass	Experimental mass	PFK matching mass	Deviation*
362.03062	362.03139	330.97923	2.1 ppm

\* The deviation is obtained from the following equation:

$$\text{deviation} = \frac{\text{experimental mass} - \text{theoretical mass}}{\text{nominal mass}}$$

Where nominal mass takes in account only  $^{12}\text{C}$ ,  $^1\text{H}$ ,  $^{16}\text{O}$ ,  $^{14}\text{N}$  etc...

Theoretical mass correspond to the mass of the most abundant isotope peak

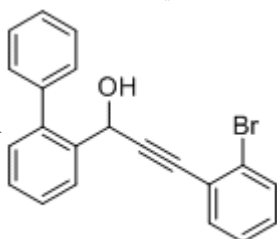


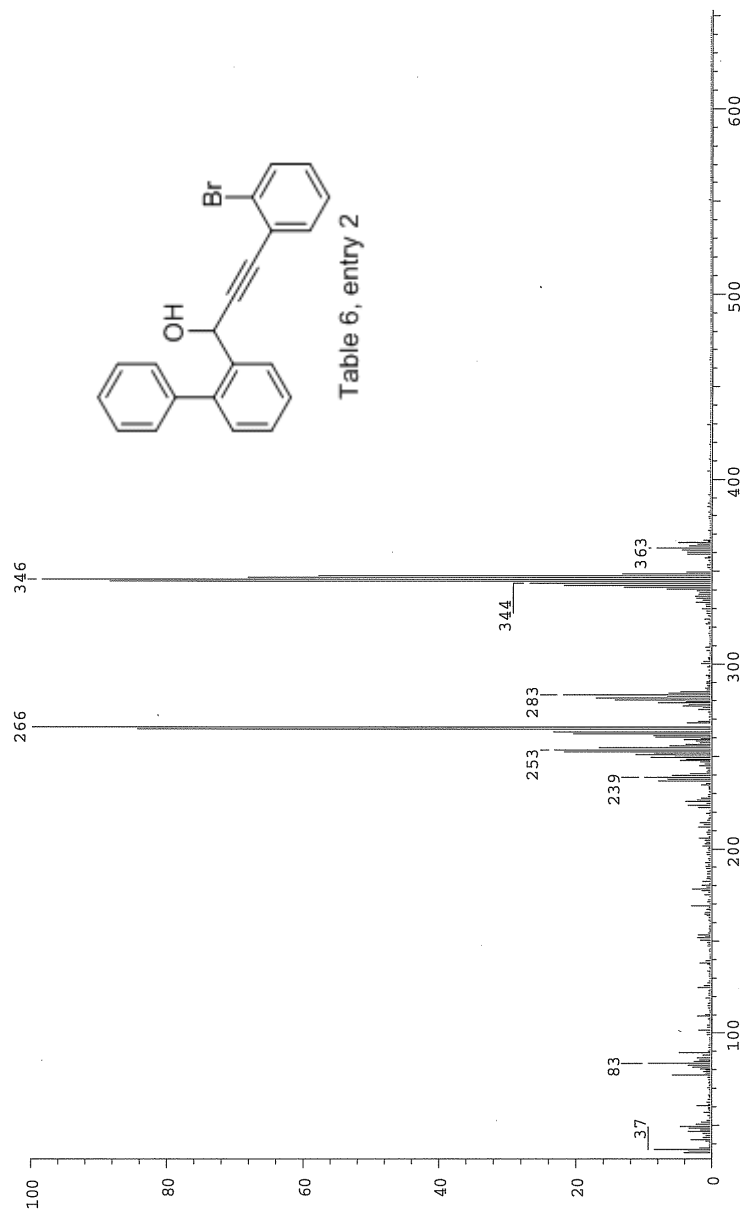
Table 6, entry 2

*JP*

SPEC: fin084266.dat (25-FEB-09 10:45:56)  
 Samp: kw779  
 Comm: DP/EI  
 Oper: Kh  
 Base: 265.70  
 Peak: 1000.0 mmu  
 Scan 30 @ 0.77 min (EI +QIMS LMR UP LR)

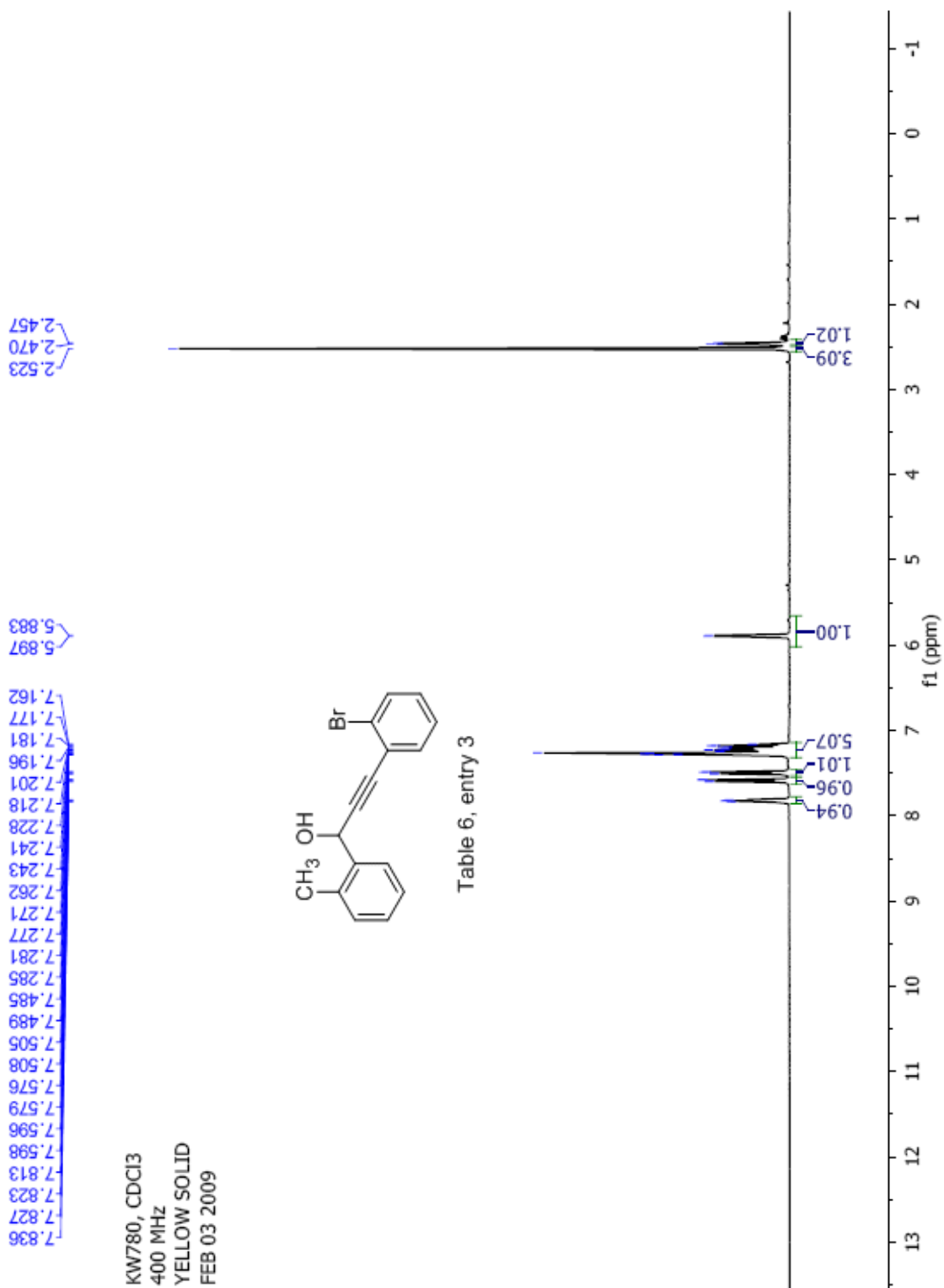
Study: ms services  
 Masses: 35.01 > 650.00  
 Intensity: 670773

Scans: 1 > 53  
 Client: Kuidup  
 #Peaks: 628  
 RIC: 7516885  
 6.7E+05



Date: Wed Feb 25 10:48:43 2009 ICIS: 8.3.0 SP2 for OSF1 (V4.0) build 98-238 from 26-Aug-98





KW780, CDCI3  
100 MHz  
YELLOW SOLID  
FEB 03 2009

138.254  
136.349  
133.812  
132.647  
131.037  
129.950  
128.792  
127.240  
127.044  
126.485  
126.858  
124.914  
93.371  
85.324  
77.314  
76.997  
63.289  
63.252  
19.323

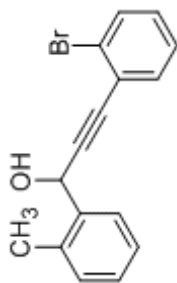
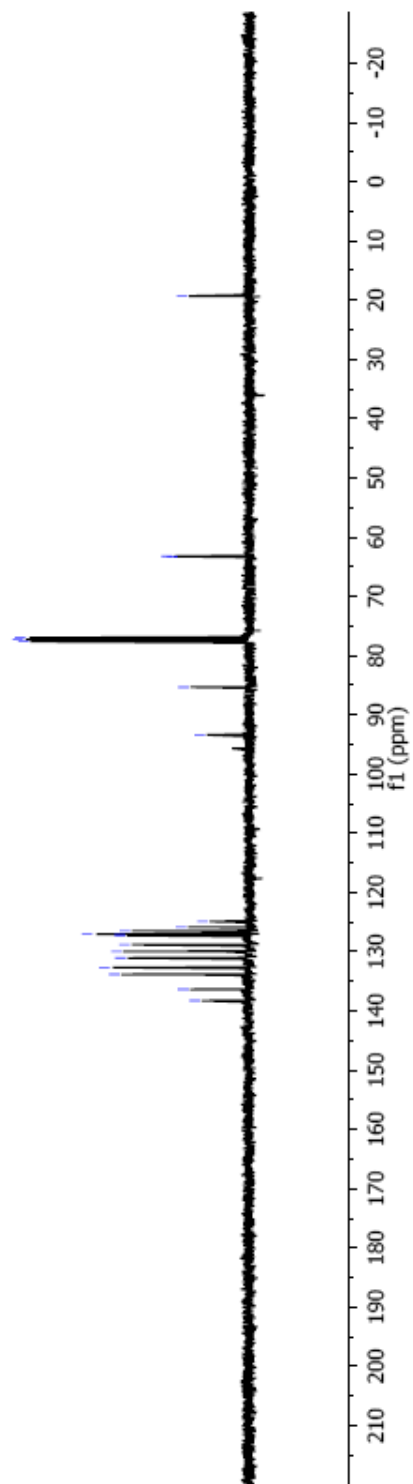


Table 6, entry 3



## Manual Peak Matching Report For Accurate Mass Determination

Theoretical mass	Experimental mass	PFK matching mass	Deviation*
300.01497	300.01572	280.98262	2.5 ppm

\* The deviation is obtained from the following equation:

$$\text{deviation} = \frac{\text{experimental mass} - \text{theoretical mass}}{\text{nominal mass}}$$

Where nominal mass takes in account only  $^{12}\text{C}$ ,  $^1\text{H}$ ,  $^{16}\text{O}$ ,  $^{14}\text{N}$  etc...

Theoretical mass correspond to the mass of the most abundant isotope peak

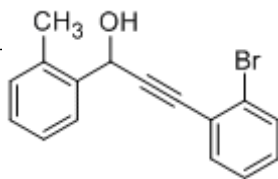


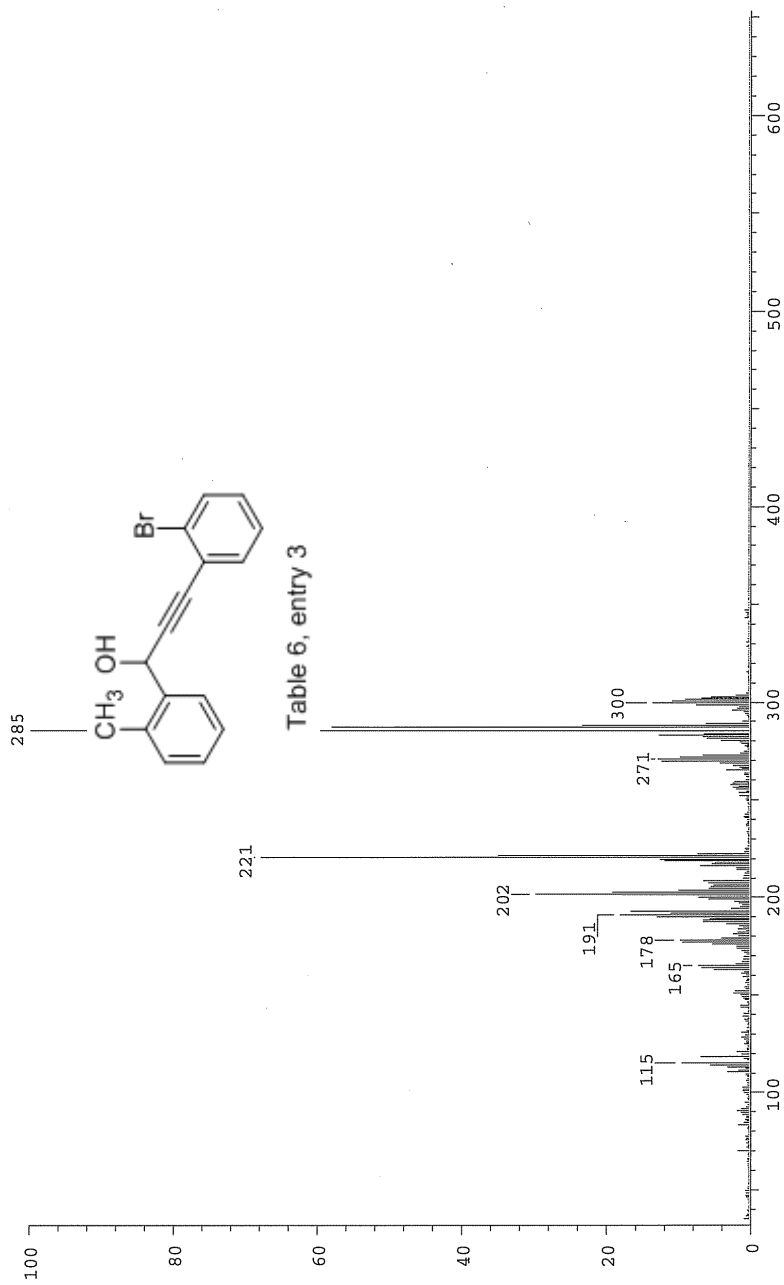
Table 6, entry 3

*Handwritten signature*

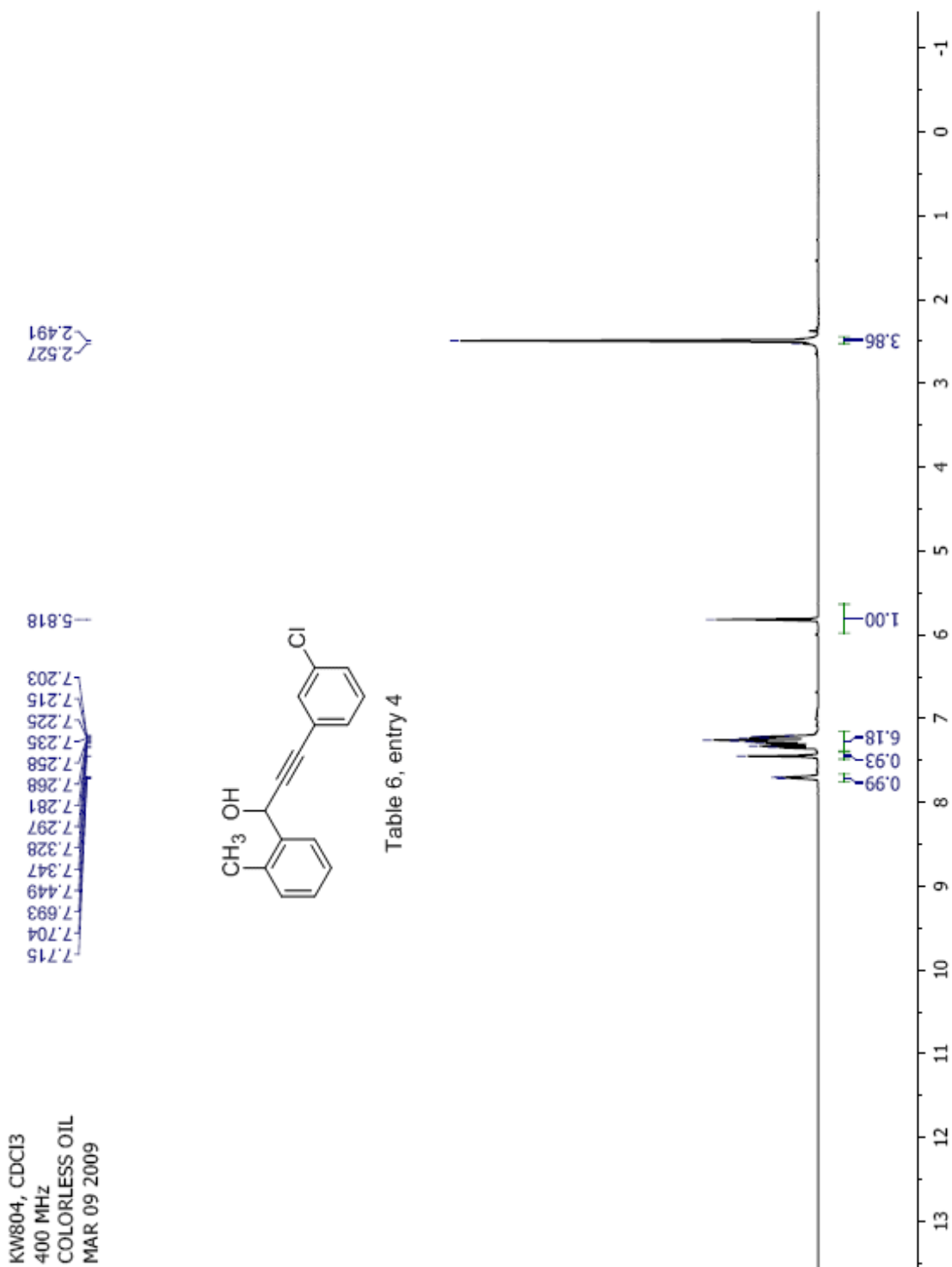
SPEC: fin084267.dat (25-FEB-09 10:50:17)  
Samp: kw780  
Comm: DP/EI  
Oper: kh  
Base: 285.11  
Peak: 1000.0 mmu  
Scan 39 @ 0.96 min (EI +Q1MS LMR UP LR)

Study: ms services  
Masses: 35.01 > 650.00  
Intensity: 1367799

Scans: 1 > 48  
Client: Kuldup  
#Peaks: 641  
RIC: 12024928  
1.4E+06



Date: Wed Feb 25 10:52:08 2009 ICIS: 8.3.0 SP2 for OSF1 (V4.0) build 98-238 from 26-Aug-98



KW804, CDCl<sub>3</sub>  
 100 MHz  
 COLORLESS OIL  
 MAR 09 2009

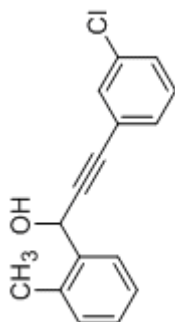
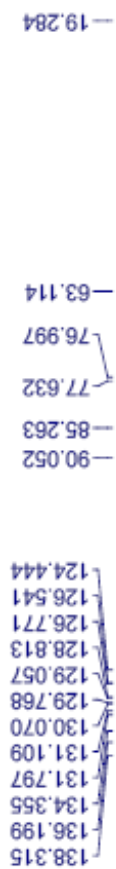
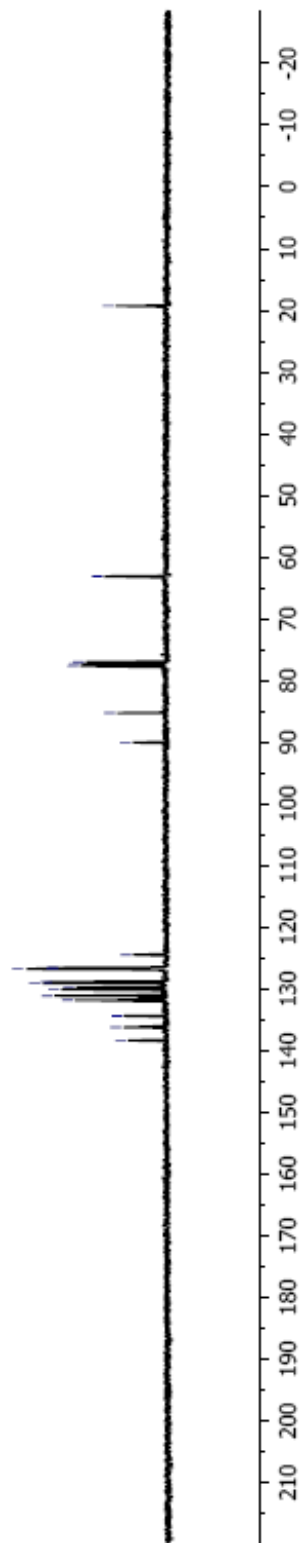


Table 6, entry 4



## Manual Peak Matching Report For Accurate Mass Determination

Theoretical mass	Experimental mass	PFK matching mass	Deviation*
256.06549	256.06600	230.98512	2 ppm

\* The deviation is obtained from the following equation:

$$\text{deviation} = \frac{\text{experimental mass} - \text{theoretical mass}}{\text{nominal mass}}$$

Where nominal mass takes in account only  $^{12}\text{C}$ ,  $^1\text{H}$ ,  $^{16}\text{O}$ ,  $^{14}\text{N}$  etc...

Theoretical mass correspond to the mass of the most abundant isotope peak

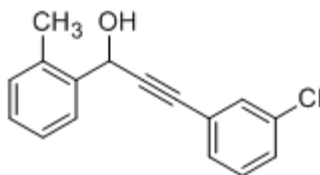


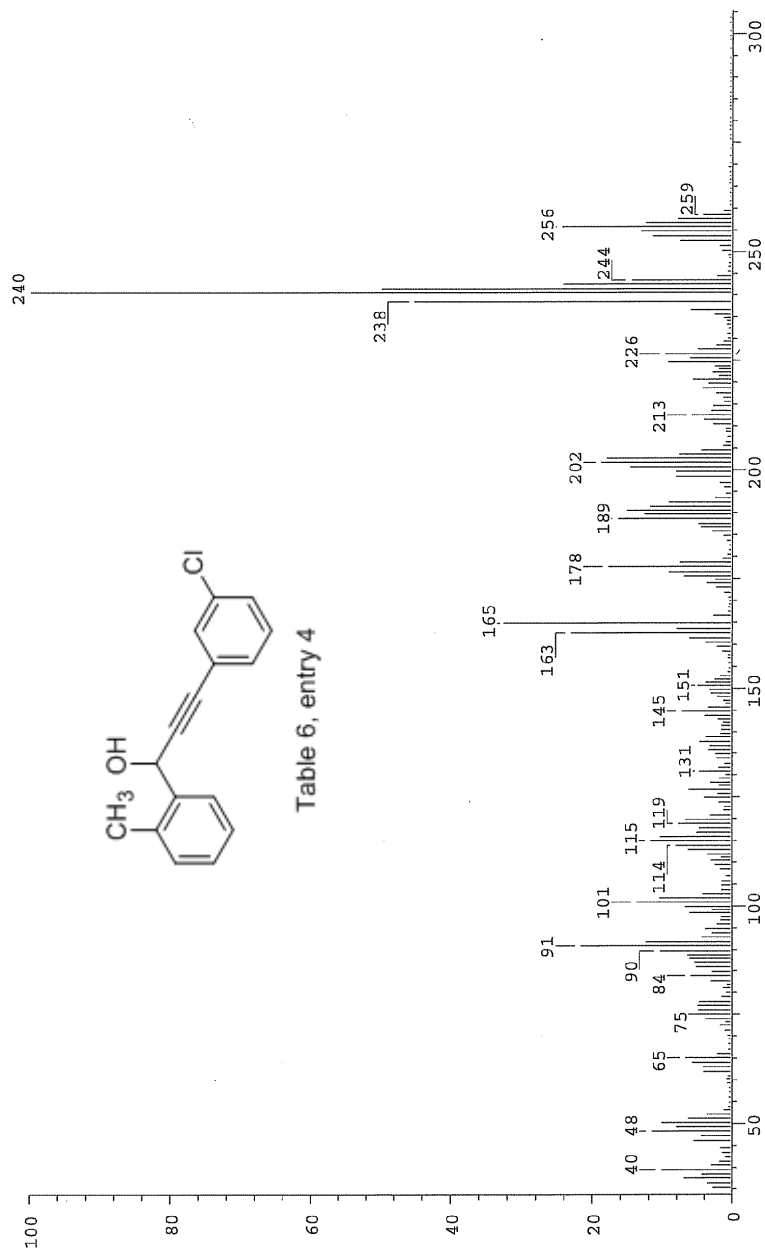
Table 6, entry 4

*J.B.*

SPC: fin084460.dat (06-MAY-09 12:38:22)  
 Samp: KW804  
 Comm: 70 eV EI  
 Oper: kh  
 Base: 240.46  
 Peak: 1000.0 mmu  
 Scan 40 @ 0.97 min (EI +QIMS LMR UP LR)

Study: ms services  
 Masses: 35.01 > 650.00  
 Intensity: 3867904

Scans: 1 > 80  
 Client: Kuldeep  
 #Peaks: 405  
 RIC: 45113379  
 3.9E+06



Date: Wed May 6 12:42:21 2009 ICIS: 8.3.0 SP2 for OSF1 (V4.0) build 98-238 from 26-Aug-98



KW802, CDCl<sub>3</sub>  
400 MHz  
COLORLESS OIL  
MAR 04 2009

2.53  
2.51  
2.50

5.85  
5.84

7.21  
7.23  
7.24  
7.26  
7.27  
7.28  
7.29  
7.54  
7.57  
7.59  
7.70  
7.71  
7.73

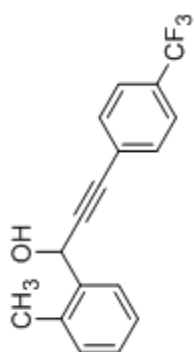
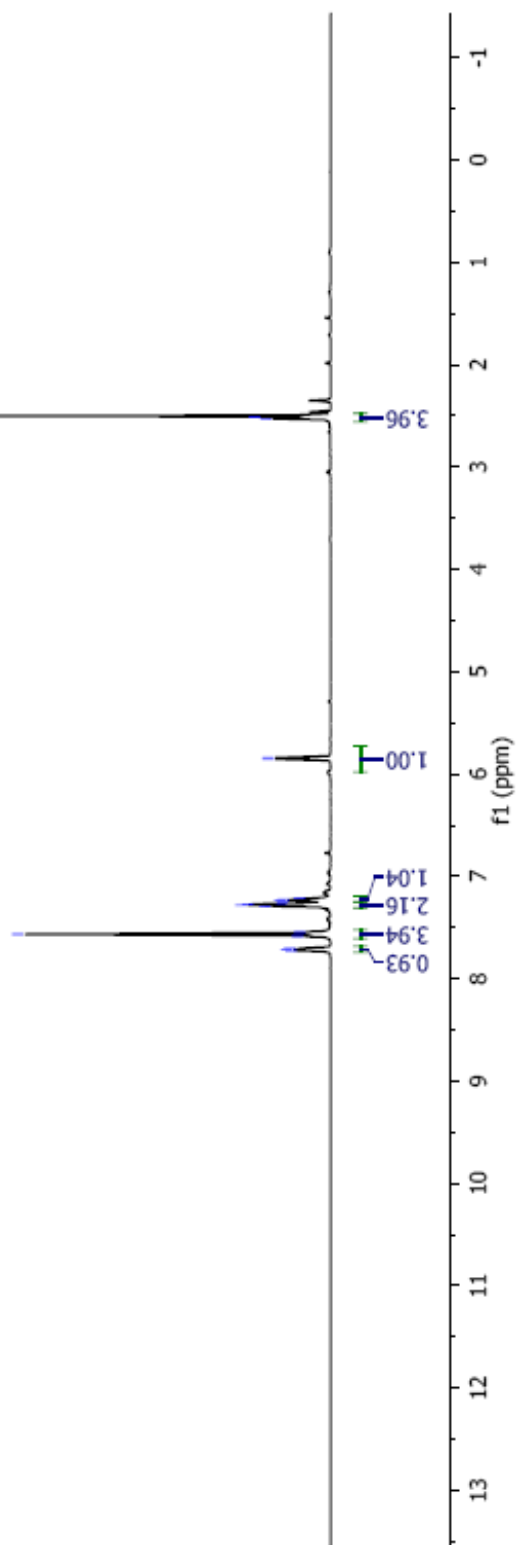
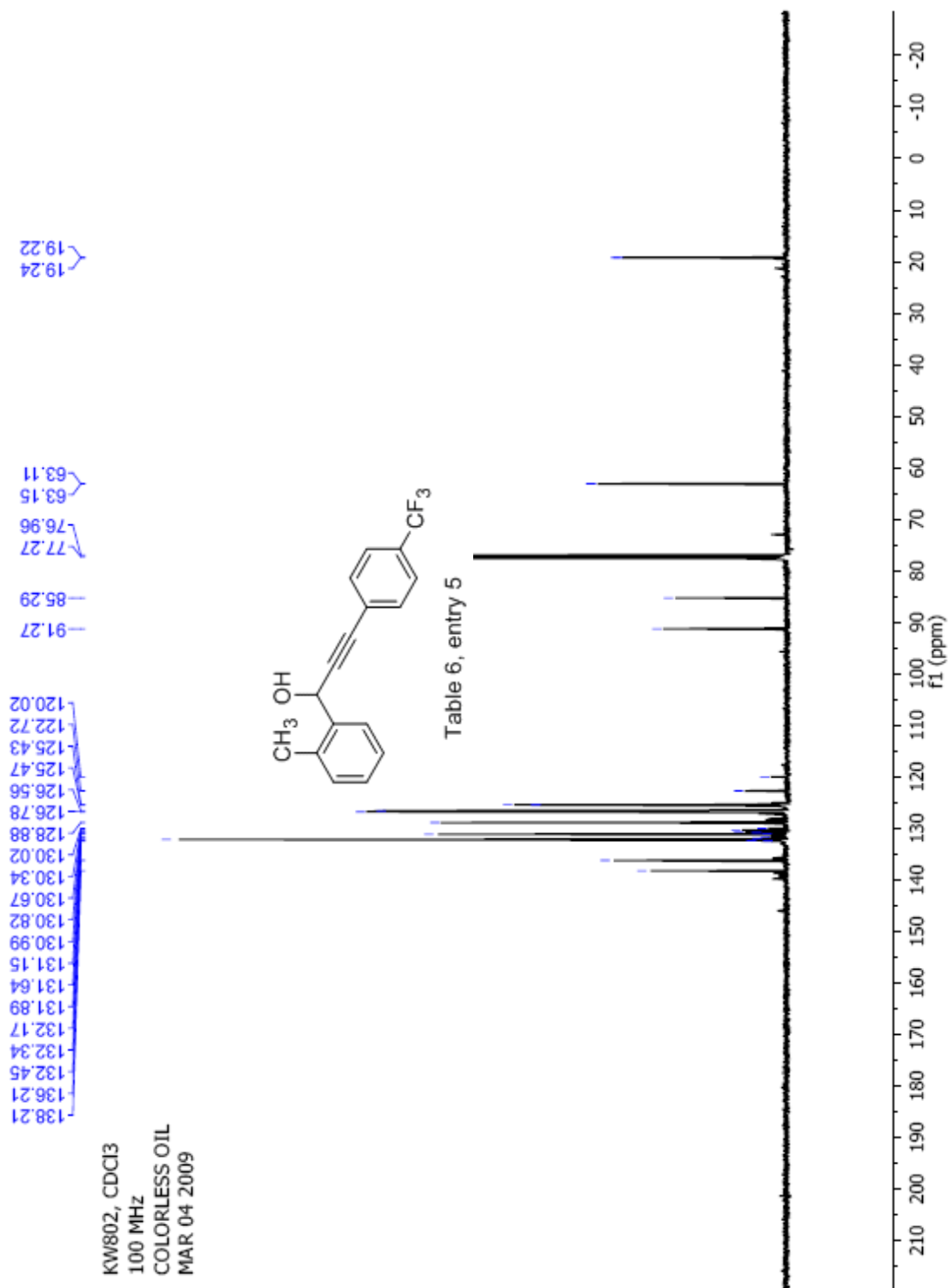


Table 6, entry 5





KW802, CDCI3  
376 MHz  
COLORLESS OIL  
MAR 04 2009

-63.26

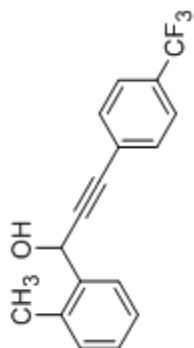
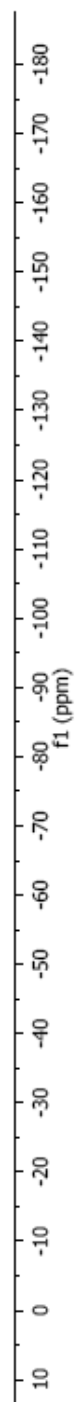


Table 6, entry 5



## Elemental Composition Report

Page 1

## Single Mass Analysis

Tolerance = 10.0 PPM / DBE: min = -1.5, max = 50.0

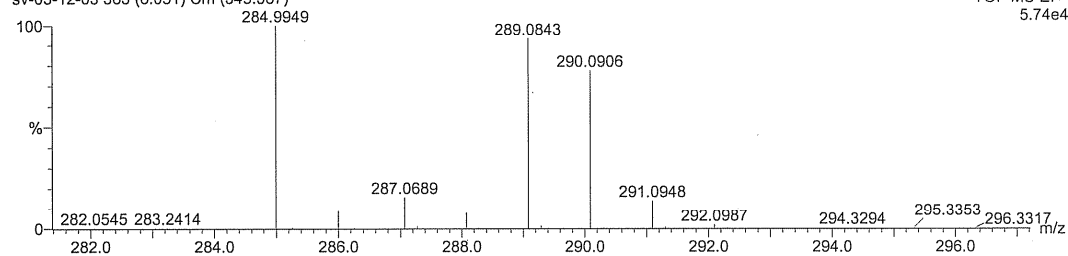
Isotope cluster parameters: Separation = 1.0 Abundance = 1.0%

Monoisotopic Mass, Odd and Even Electron Ions

74 formula(e) evaluated with 2 results within limits (up to 50 closest results for each mass)

Kuldeep KW802

sv-03-12-03 363 (6.051) Cm (349:367)

TOF MS EI+  
5.74e4

Minimum: -1.5  
Maximum: 200.0 10.0 50.0

Mass	Calc. Mass	mDa	PPM	DBE	Score	Formula
290.0906	290.0907	-0.1	-0.4	14.0	1	C20 H12 F2
	290.0918	-1.2	-4.3	10.0	2	C17 H13 O F3

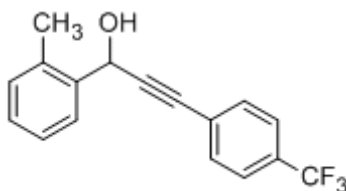
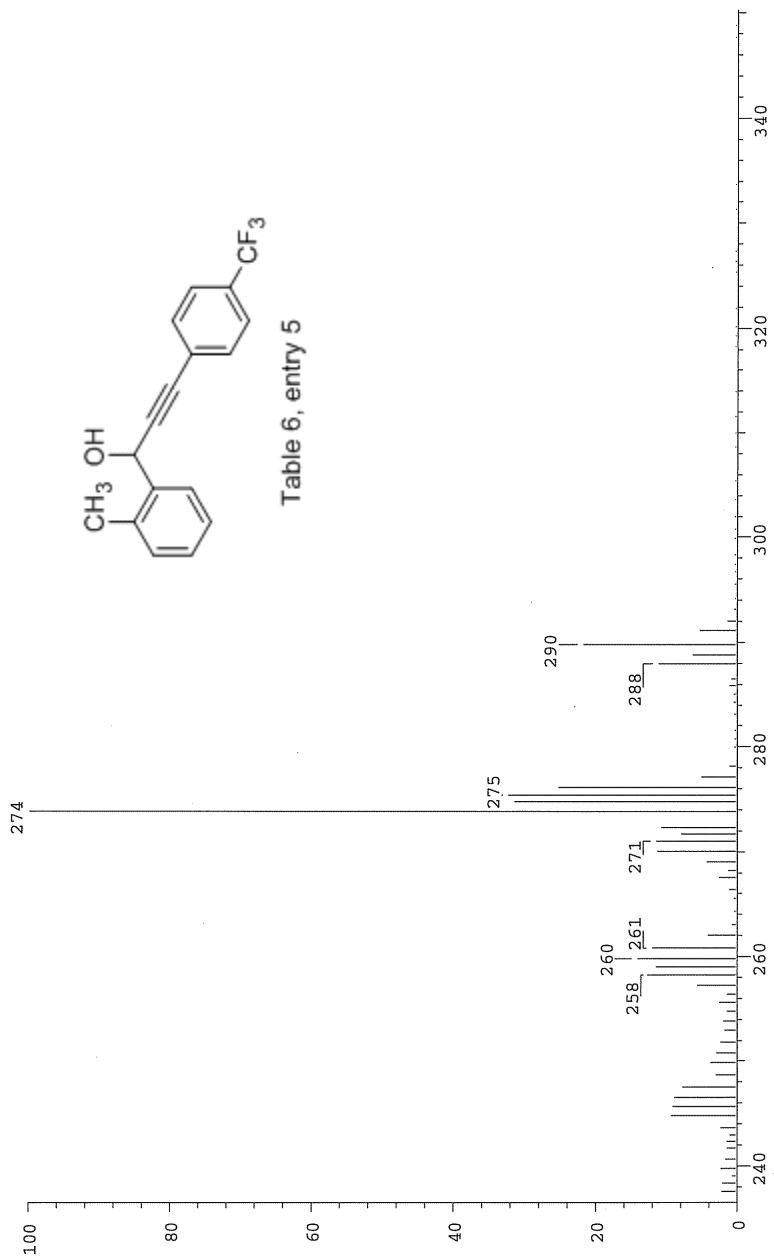


Table 6, entry 5

SPEC: fin084326.dat (12-MAR-09 11:26:59)  
 Samp: KW802  
 Comm: DP/EI  
 Oper: kh  
 Base: 90.94  
 Peak: 1000.0 mmu  
 Scan 56 @ 1.31 min (EI +QIMS LMR UP LR)

Study: ms services  
 Masses: 35.01 > 650.00  
 Intensity: 514455

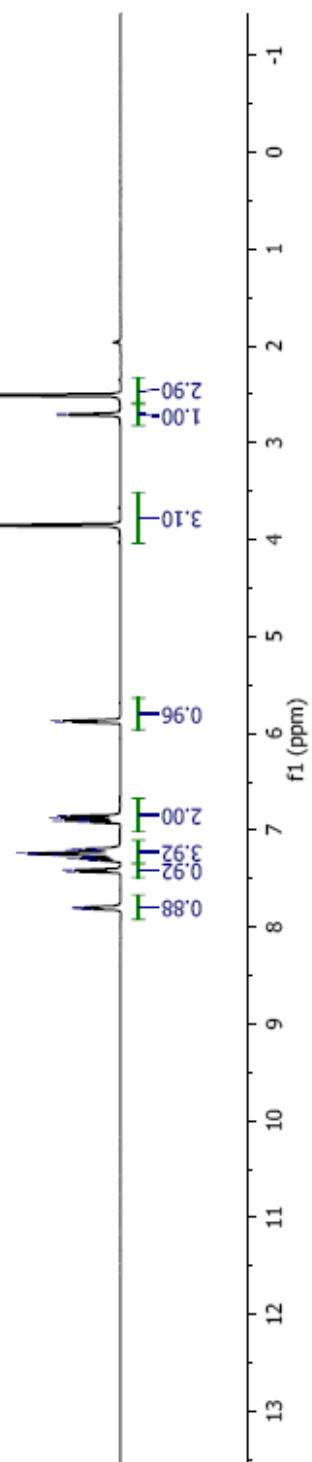
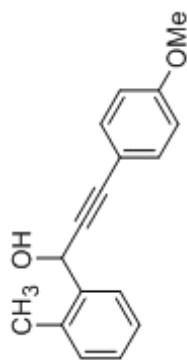
Scans: 1 > 60  
 Client: Kuldeep  
 #Peaks: 352  
 RIC: 14272035  
 3.0E+05



Date: Thu Mar 12 11:29:04 2009 ICIS: 8.3.0 SP2 for OSF1 (V4.0) build 98-238 from 26-Aug-98

KW803, CDCl<sub>3</sub>  
400 MHz  
YELLOW OIL  
MAR 06 2009

7.816  
7.807  
7.803  
7.794  
7.208  
6.920  
6.852  
5.883  
5.869  
3.854  
2.716  
2.702  
2.510



KW803, CDCI3  
 100 MHz  
 YELLOW OIL  
 MAR 06 2009

160.4  
 133.8  
 130.9  
 130.2  
 128.5  
 127.1  
 126.4  
 120.6  
 112.0  
 110.9  
 93.0  
 83.1  
 77.3  
 77.0  
 63.3  
 56.0  
 -19.2

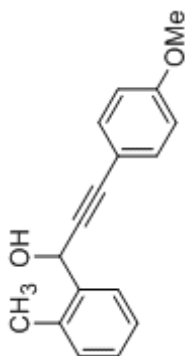
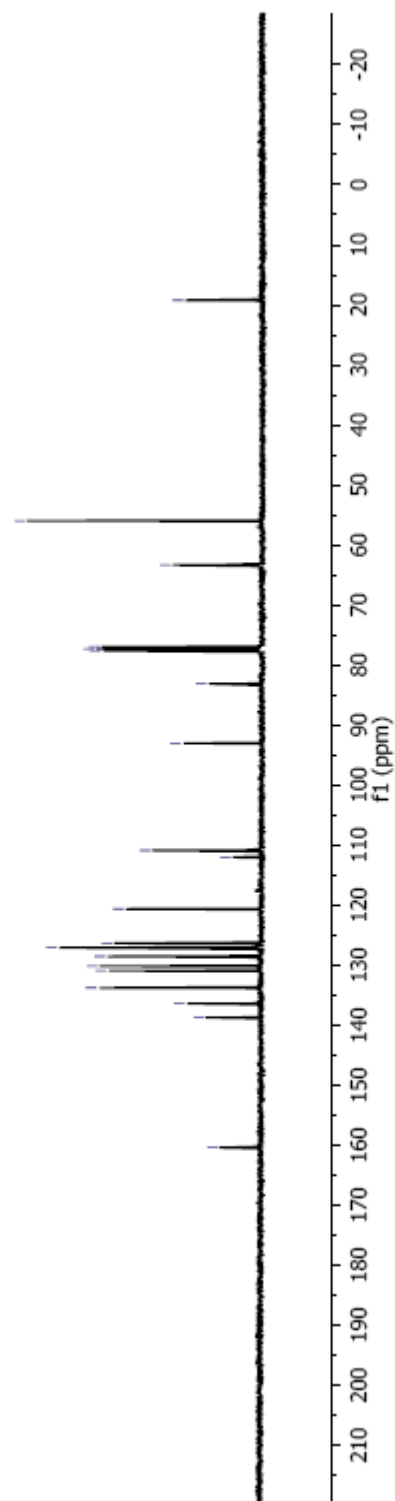


Table 6, entry 6



## Elemental Composition Report

Page 1

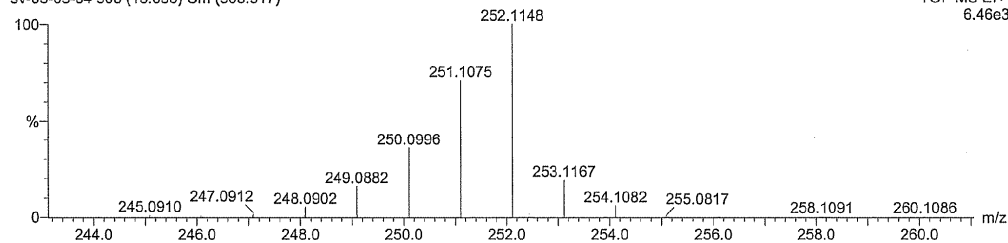
## Multiple Mass Analysis: 3 mass(es) processed

Tolerance = 10.0 PPM / DBE: min = -1.5, max = 50.0

Isotope cluster parameters: Separation = 1.0 Abundance = 1.0%

Monoisotopic Mass, Odd and Even Electron Ions

351 formula(e) evaluated with 7 results within limits (up to 50 closest results for each mass)

KW803  
sv-05-05-04 903 (15.036) Cm (903:917)TOF MS EI+  
6.46e3Minimum: 20.00  
Maximum: 100.00-1.5  
50.0

Mass	RA	Calc. Mass	mDa	PPM	DBE	Score	Formula
250.0996	35.84	250.0994	0.2	0.9	11.0	1	C17 H14 O2
		250.0980	1.6	6.2	11.5	2	C15 H12 N3 O
251.1075	71.05	251.1072	0.3	1.2	10.5	1	C17 H15 O2
		251.1059	1.6	6.5	11.0	2	C15 H13 N3 O
252.1148	100.00	252.1150	-0.2	-0.9	10.0	1	C17 H16 O2
		252.1137	1.1	4.4	10.5	2	C15 H14 N3 O
		252.1123	2.5	9.7	11.0	3	C13 H12 N6

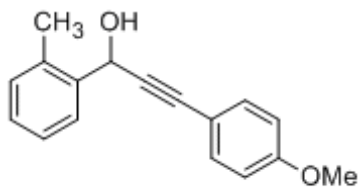
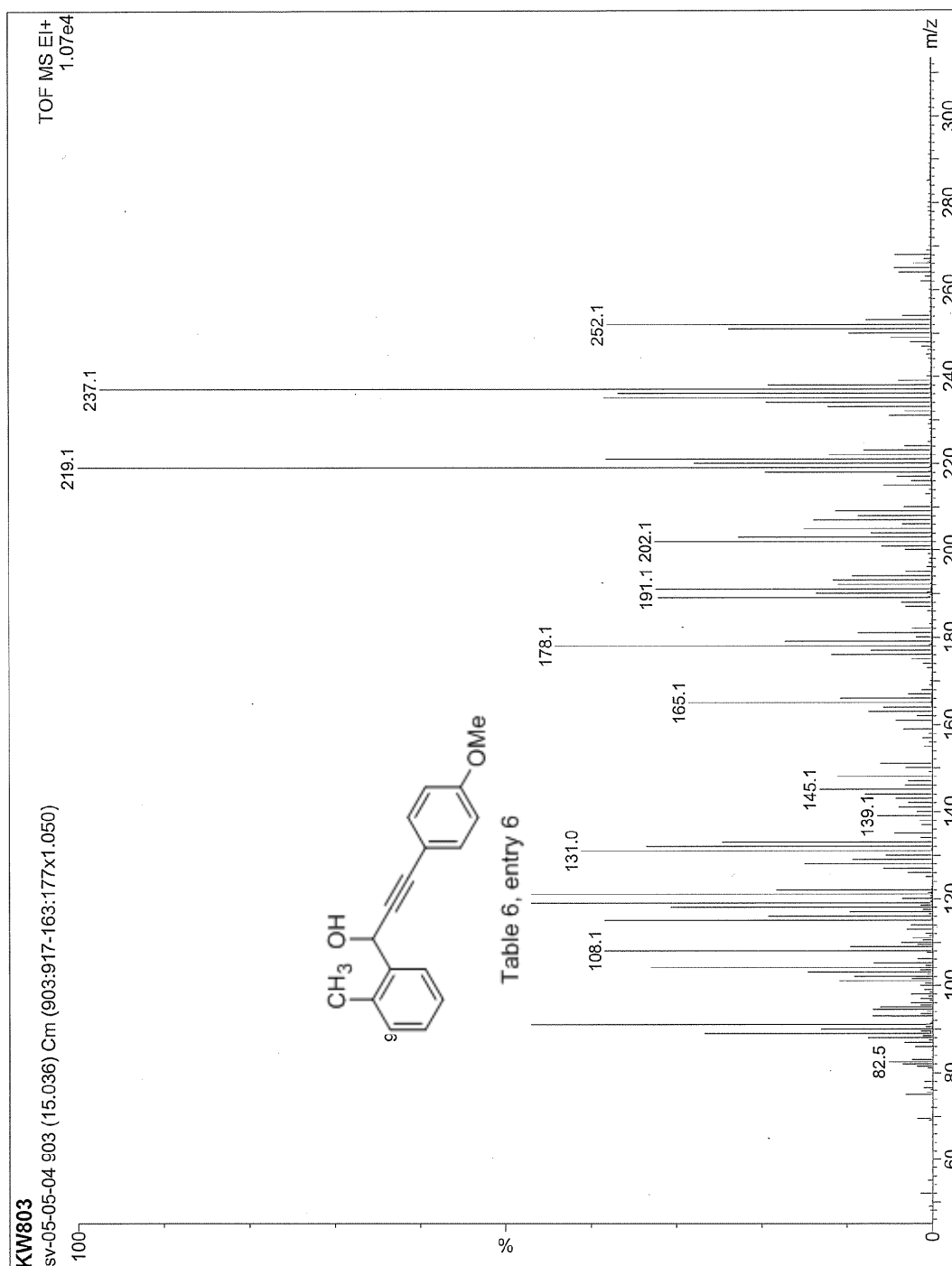


Table 6, entry 6





KW795, CDCl<sub>3</sub>  
400 MHz  
YELLOW OIL  
FEB 21 2009

7.71  
7.70  
7.69  
7.26  
7.21  
6.99  
6.97  
5.86  
5.84  
2.49  
2.23  
2.21

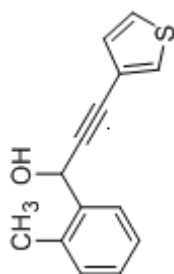
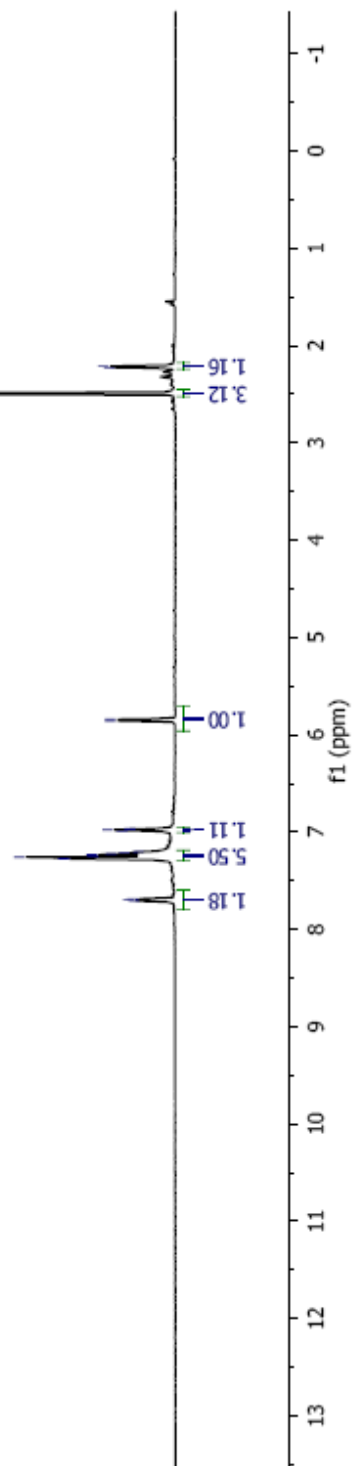


Table 6, entry 7



KW795, CDC13  
 100 MHz  
 YELLOW OIL  
 FEB 21 2009

138.29  
 136.21  
 132.62  
 131.07  
 128.76  
 127.64  
 127.17  
 126.82  
 126.51  
 122.62  
 92.53  
 80.08  
 77.56  
 77.25  
 76.93  
 63.37  
 19.27

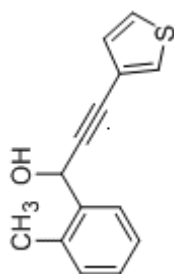
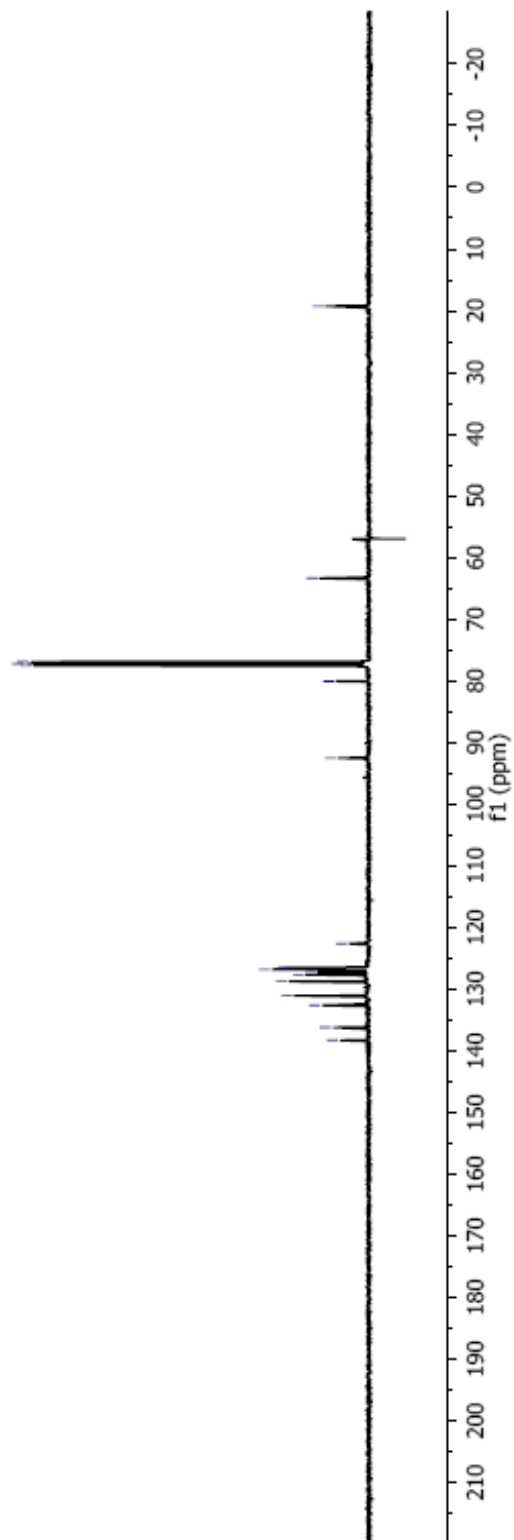


Table 6, entry 7



## Elemental Composition Report

Page 1

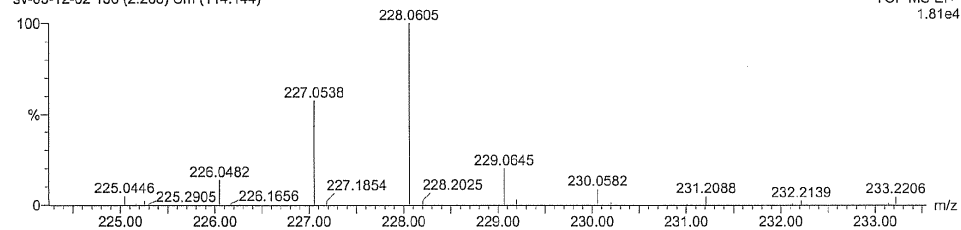
## Single Mass Analysis

Tolerance = 10.0 PPM / DBE: min = -1.5, max = 50.0

Isotope cluster parameters: Separation = 1.0 Abundance = 1.0%

## Monoisotopic Mass, Odd and Even Electron Ions

46 formula(e) evaluated with 1 results within limits (up to 50 closest results for each mass)

Kuldeep KW795  
sv-03-12-02 136 (2.266) Cm (114:144)TOF MS EI+  
1.81e4

Minimum: -1.5  
Maximum: 50.0

Mass	Calc. Mass	mDa	PPM	DBE	Score	Formula
228.0605	228.0609	-0.4	-1.7	9.0	1	C14 H12 O S

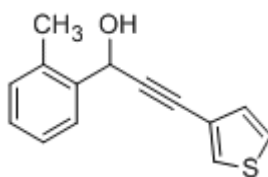
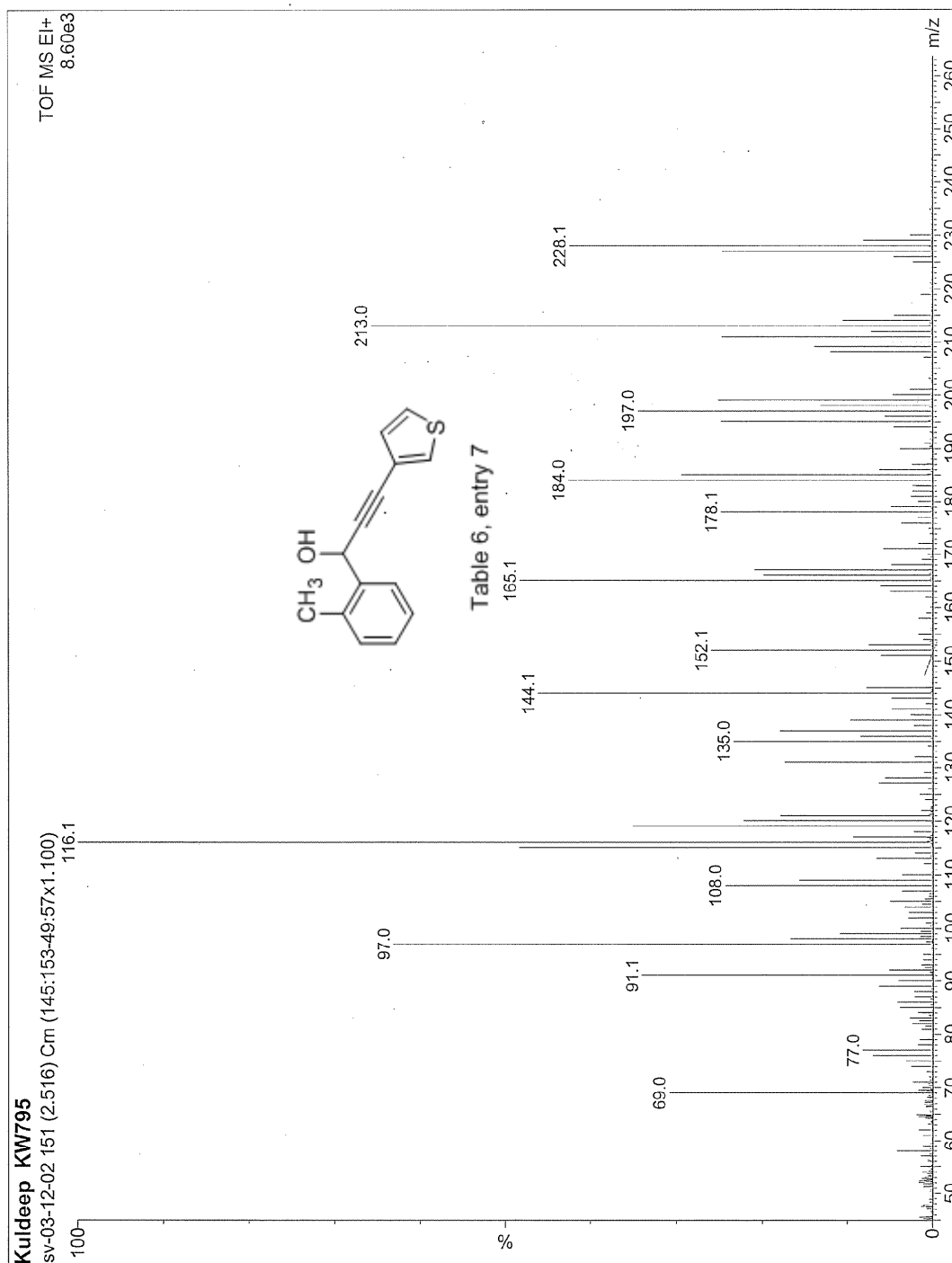


Table 6, entry 7



KW808, CDCl<sub>3</sub>  
400 MHz  
YELLOW SOLID  
MAR 13 2009

8.73  
8.41  
7.71  
7.69  
7.26  
7.23  
7.20  
5.84  
5.35  
2.48

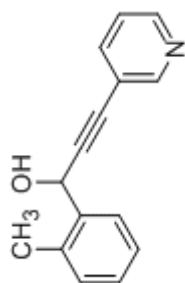
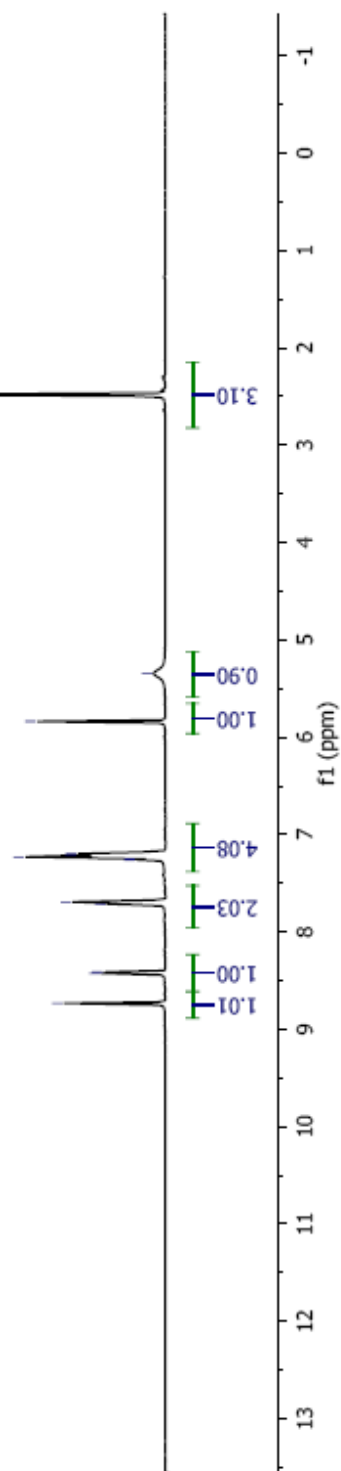


Table 6, entry 8



KW808, CDCI3  
100 MHz  
YELLOW SOLID  
MAR 13 2009

152.11  
148.40  
139.23  
136.03  
130.98  
128.52  
126.68  
126.44  
123.45  
120.42  
93.68  
82.39  
77.34  
77.02  
62.46  
19.31

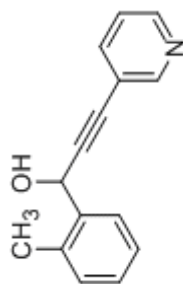
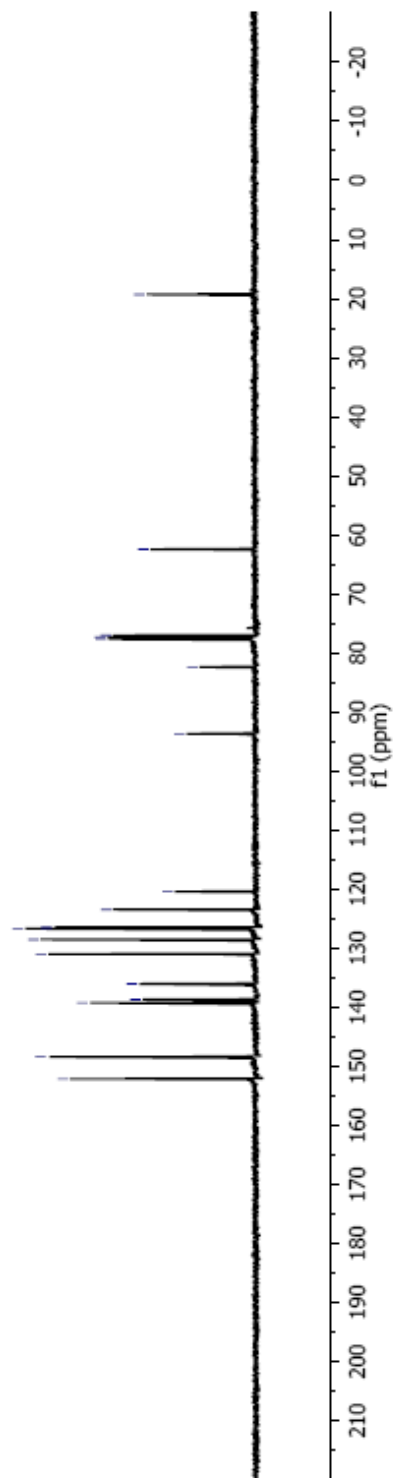


Table 6, entry 8



## Elemental Composition Report

Page 1

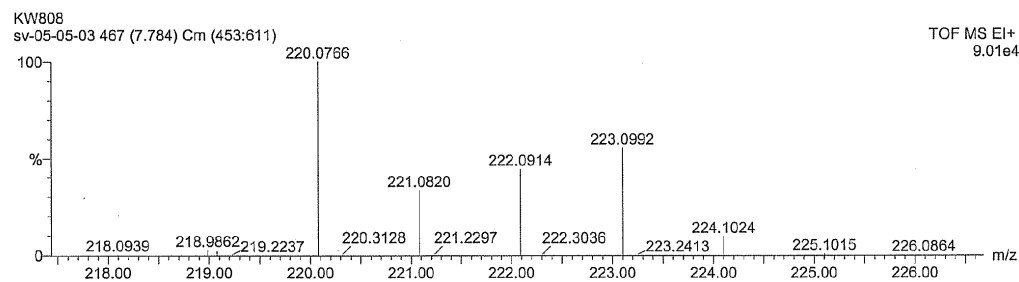
## Multiple Mass Analysis: 4 mass(es) processed

Tolerance = 7.0 PPM / DBE: min = -1.5, max = 50.0

Isotope cluster parameters: Separation = 1.0 Abundance = 1.0%

Monoisotopic Mass, Odd and Even Electron Ions

415 formula(e) evaluated with 7 results within limits (up to 50 closest results for each mass)



Minimum: 20.00  
Maximum: 100.00

Mass	RA	Calc. Mass	mDa	PPM	DBE	Score	Formula
220.0766	100.00	220.0762	0.4	1.6	11.5	1	C15 H10 N O
221.0820	33.33	221.0814	0.6	2.8	6.5	2	C12 H13 O4
		221.0827	-0.7	-3.3	11.5	1	C13 H9 N4
222.0914	44.76	222.0919	-0.5	-2.2	10.5	1	C15 H12 N O
		222.0905	0.9	3.8	11.0	2	C13 H10 N4
223.0992	55.49	223.0997	-0.5	-2.3	10.0	2	C15 H13 N O
		223.0984	0.8	3.7	10.5	1	C13 H11 N4

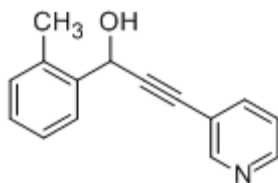
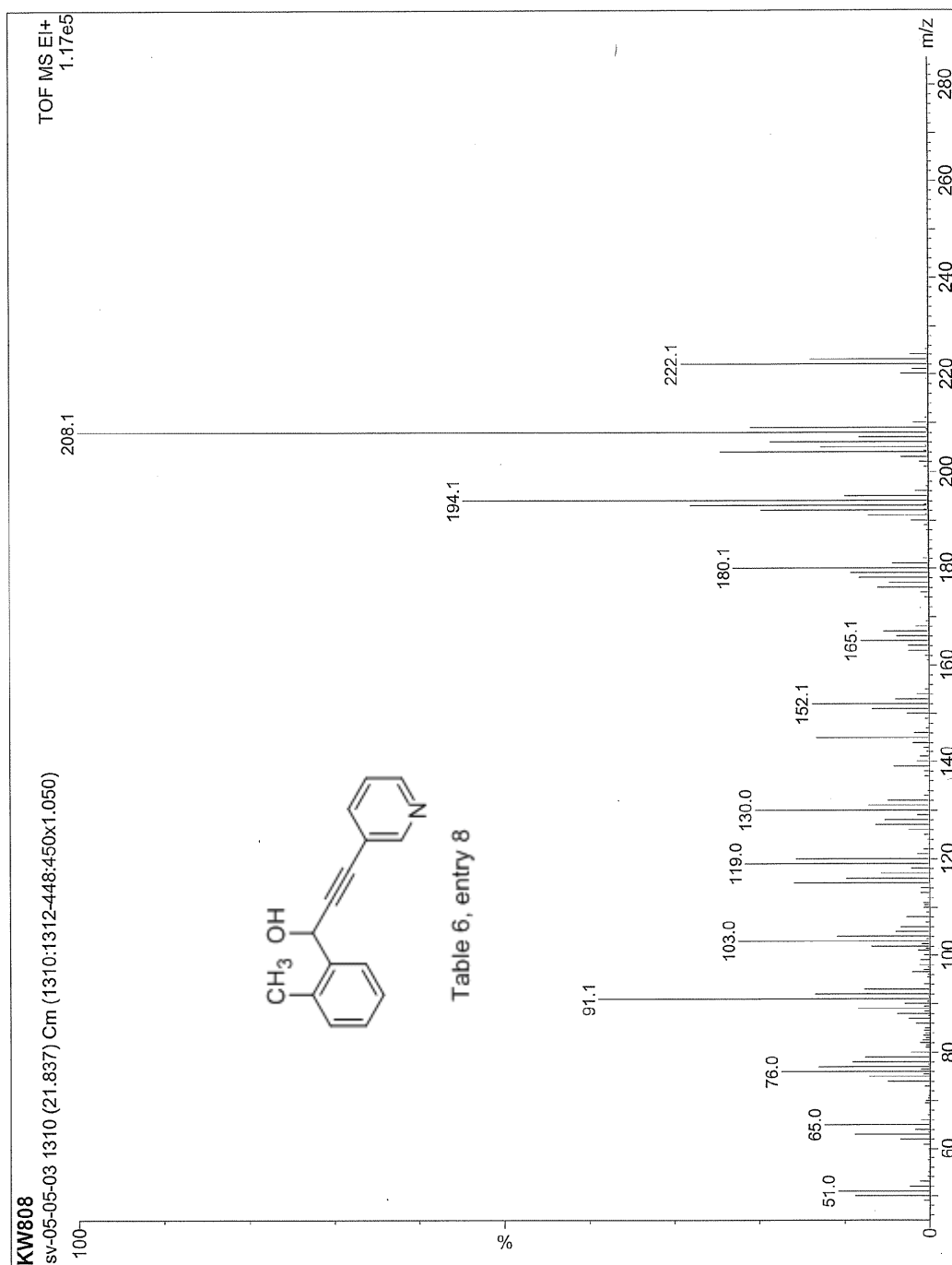


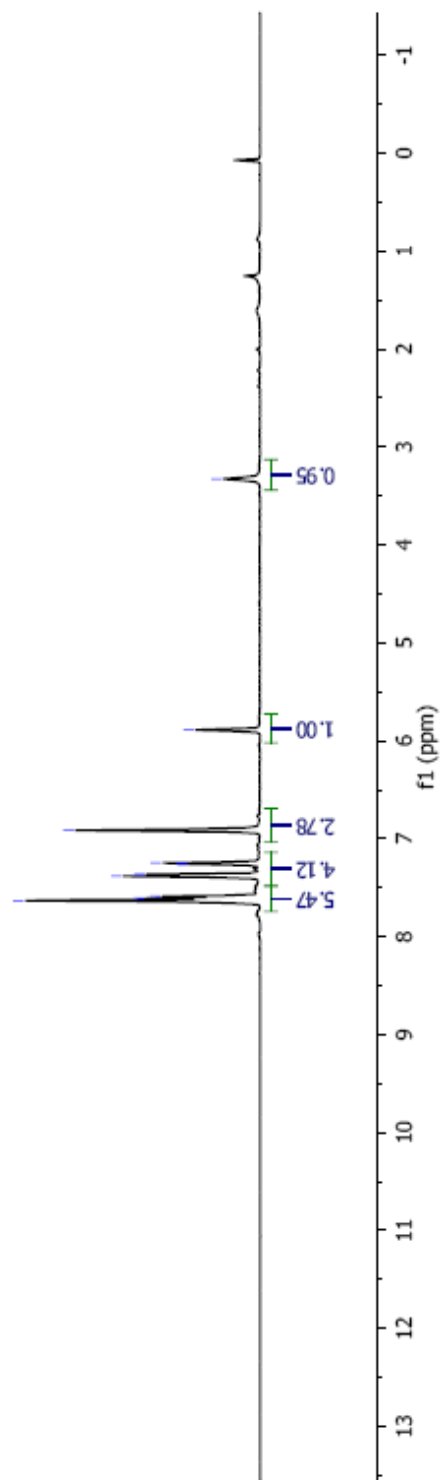
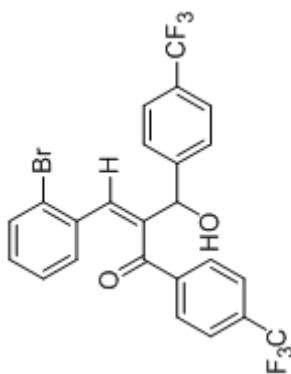
Table 6, entry 8

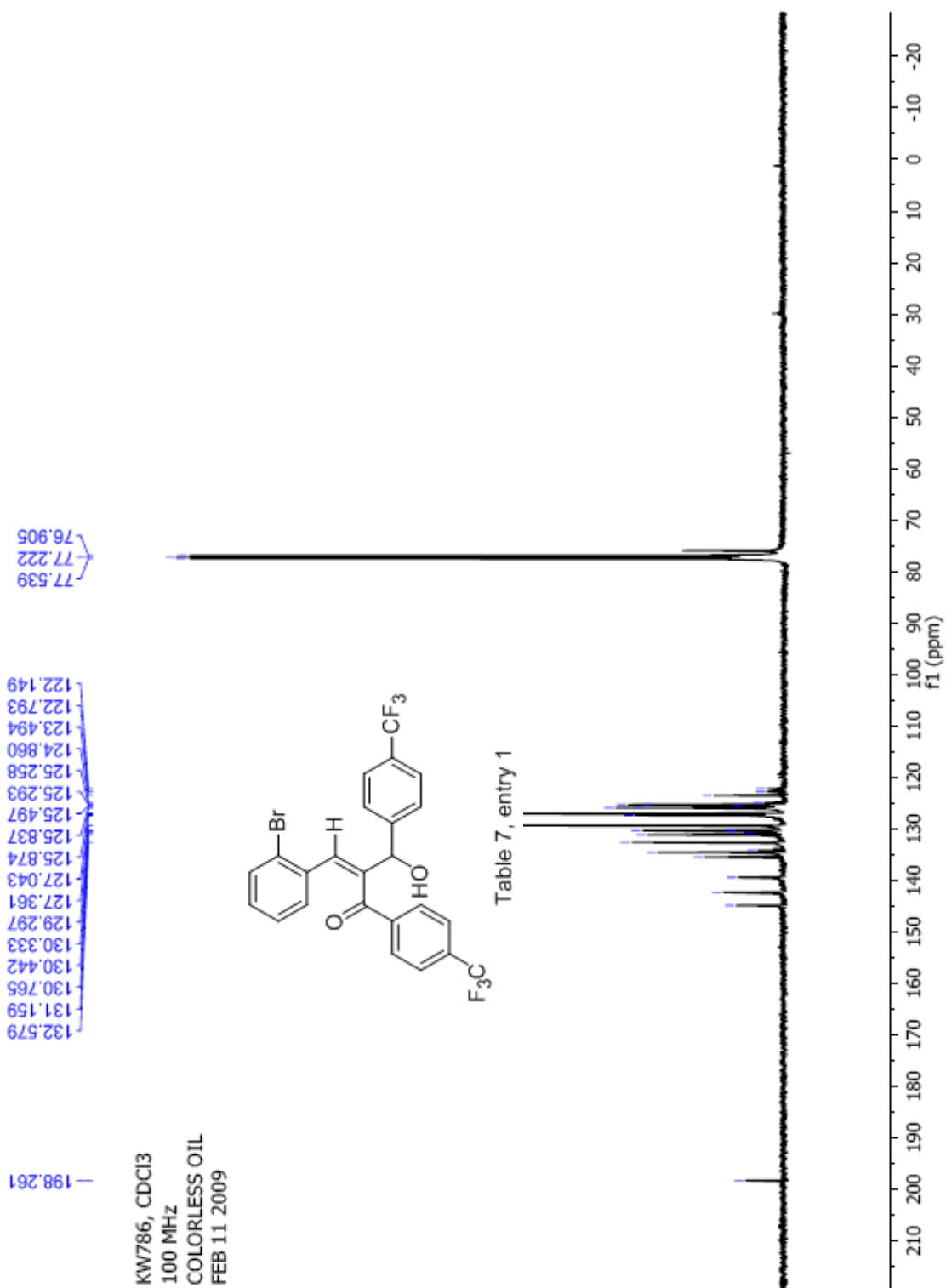




KW786, CDCl<sub>3</sub>  
400 MHz  
COLORLESS OIL  
FEB 11 2009

7.63  
7.61  
7.59  
7.38  
7.36  
7.26  
7.25  
-6.91  
-5.89  
-3.33





KW786, CDCl<sub>3</sub>  
376 MHz  
COLORLESS OIL  
FEB 11 2009

928.89  
920.99

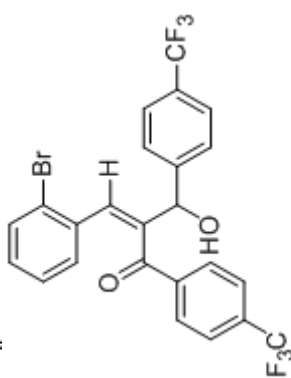
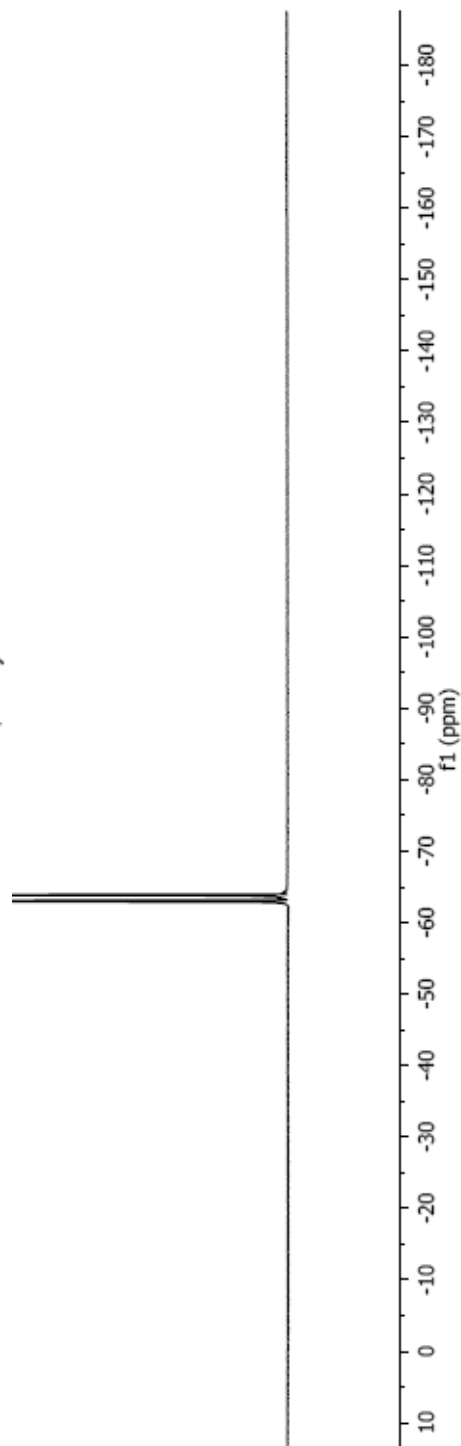


Table 7, entry 1



## Manual Peak Matching Report For Accurate Mass Determination

Theoretical mass	Experimental mass	PFK matching mass	Deviation*
528.01595	528.01759	480.96964	3 ppm

\* The deviation is obtained from the following equation:

$$\text{deviation} = \frac{\text{experimental mass} - \text{theoretical mass}}{\text{nominal mass}}$$

Where nominal mass takes in account only  $^{12}\text{C}$ ,  $^1\text{H}$ ,  $^{16}\text{O}$ ,  $^{14}\text{N}$  etc...

Theoretical mass correspond to the mass of the most abundant isotope peak

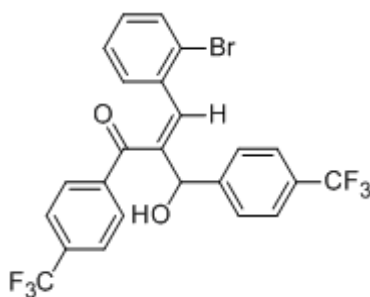


Table 7, entry 1

*MP*

Scans: 1 > 170  
 Client: Kuldip  
 #Peaks: 595  
 RIC: 846550677  
 3.1E+04

SPEC: fin084261.dat (23-FEB-09 11:34:58)

Sampl: kw786

Comm: DP/EI

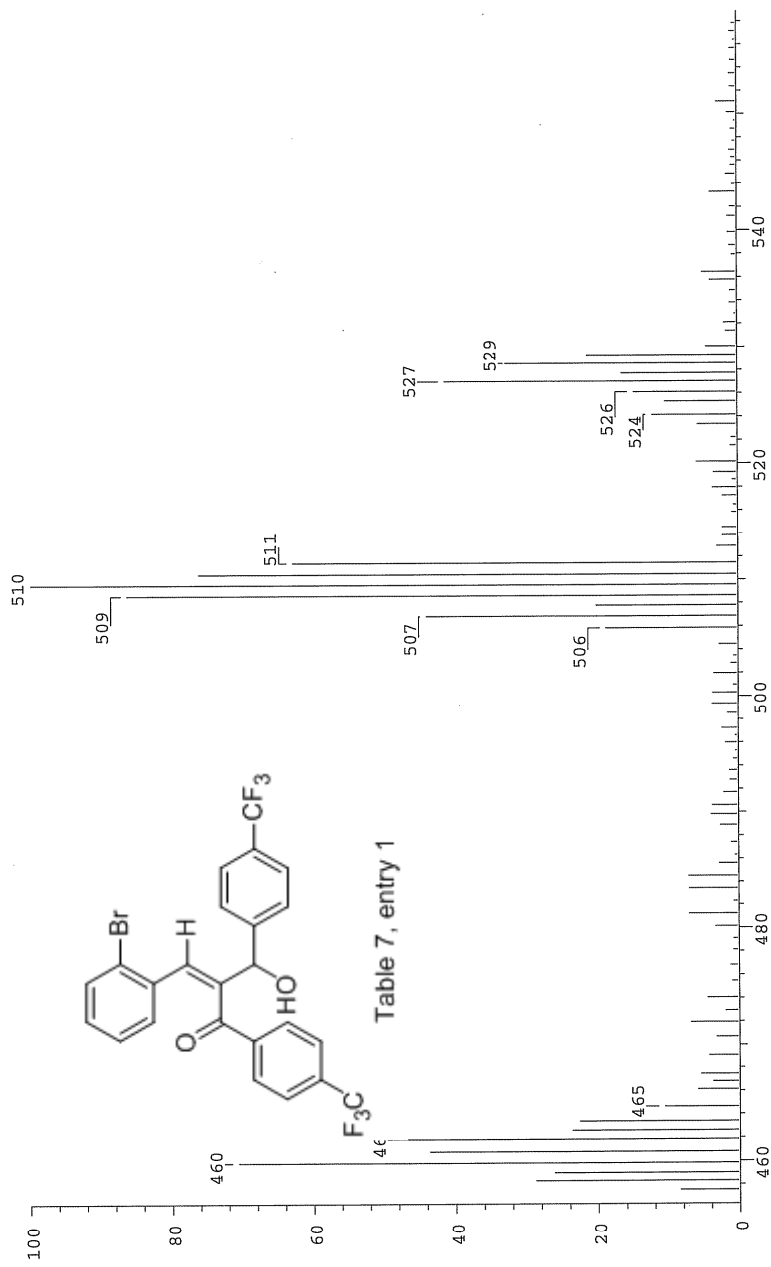
Oper: kh

Base: 173.34

Peak: 1000.0 mmu

Scan 29 @ 0.74 min (EI +Q1MS LMR UP LR)

Study: ms services  
 Masses: 35.01 > 650.00  
 Intensity: 16777215



Date: Mon Feb 23 11:39:39 2009 ICIS: 8.3.0 SP2 for OSF1 (V4.0) build 98-238 from 26-Aug-98

KW-792  
 CDCL<sub>3</sub>, 400MHZ  
 White solid  
 23 FEB 2009

3.222

5.807

6.894

6.946

7.015

7.234

7.402

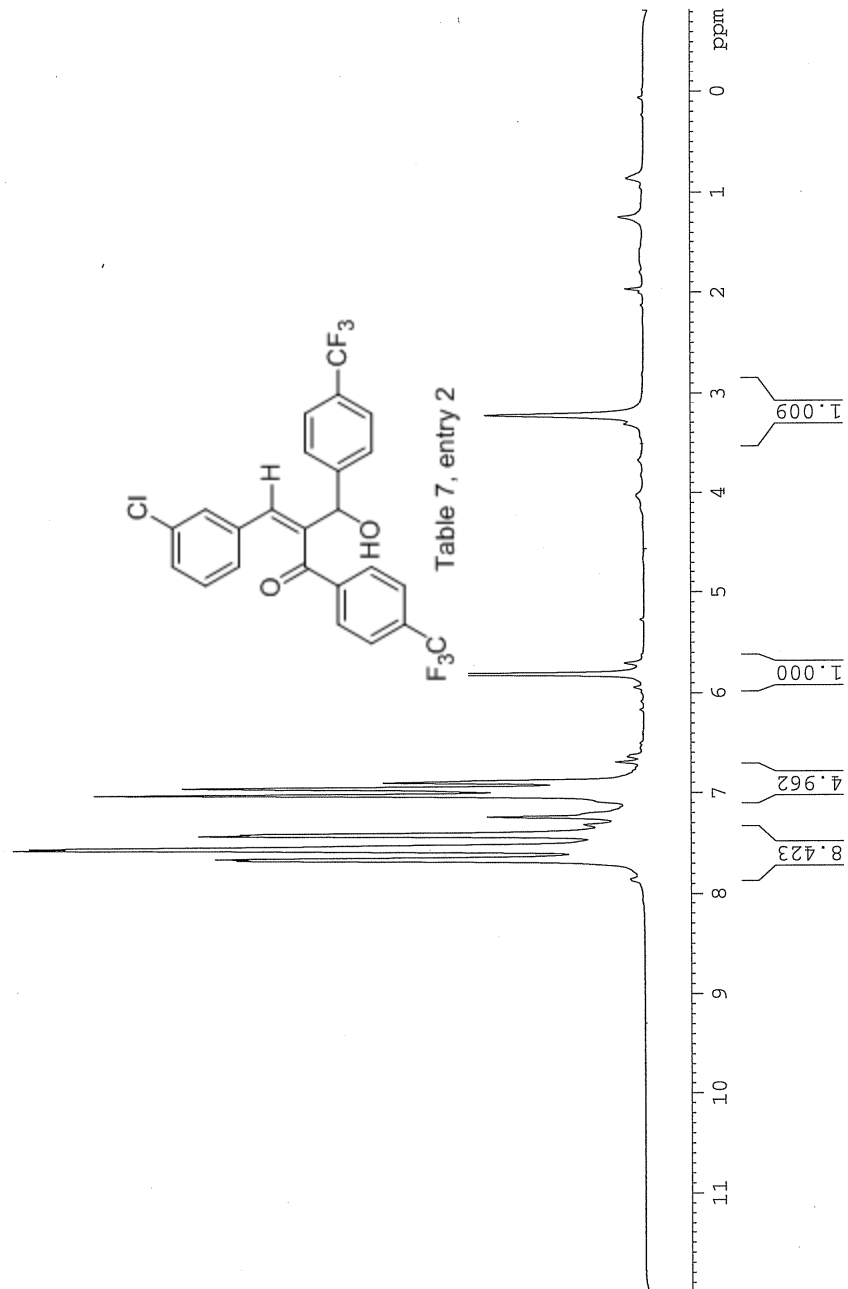
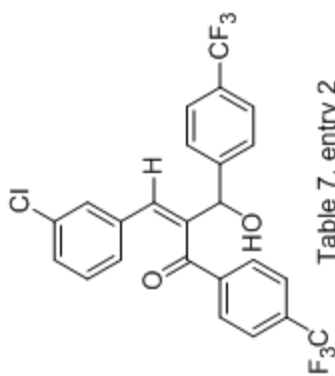
7.419

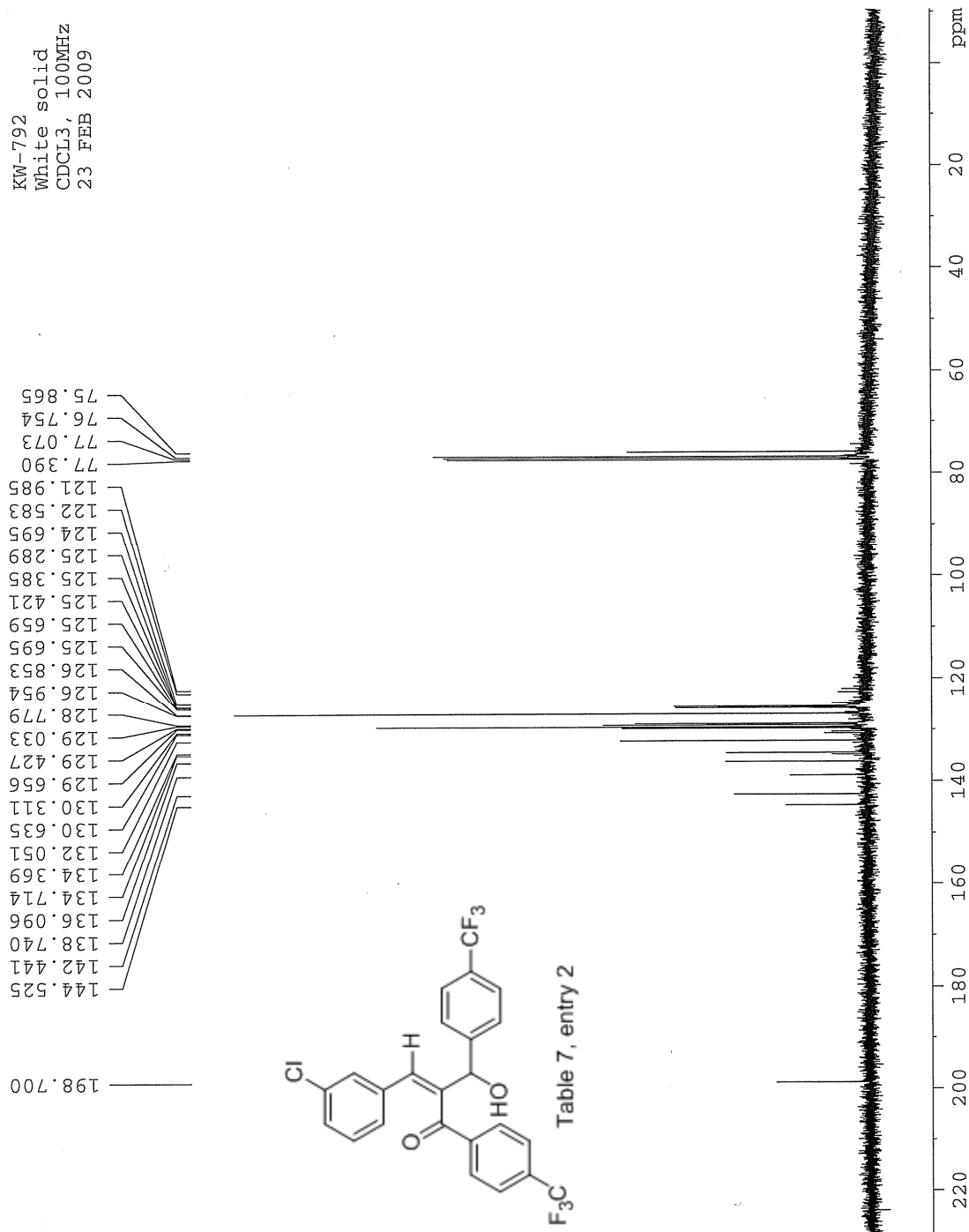
7.538

7.554

7.646

7.662







KW792, CDCl<sub>3</sub>  
376 MHz  
WHITE SOLID

63.063  
63.780

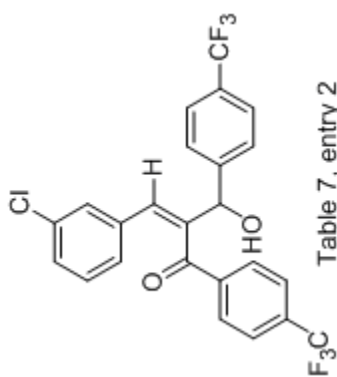
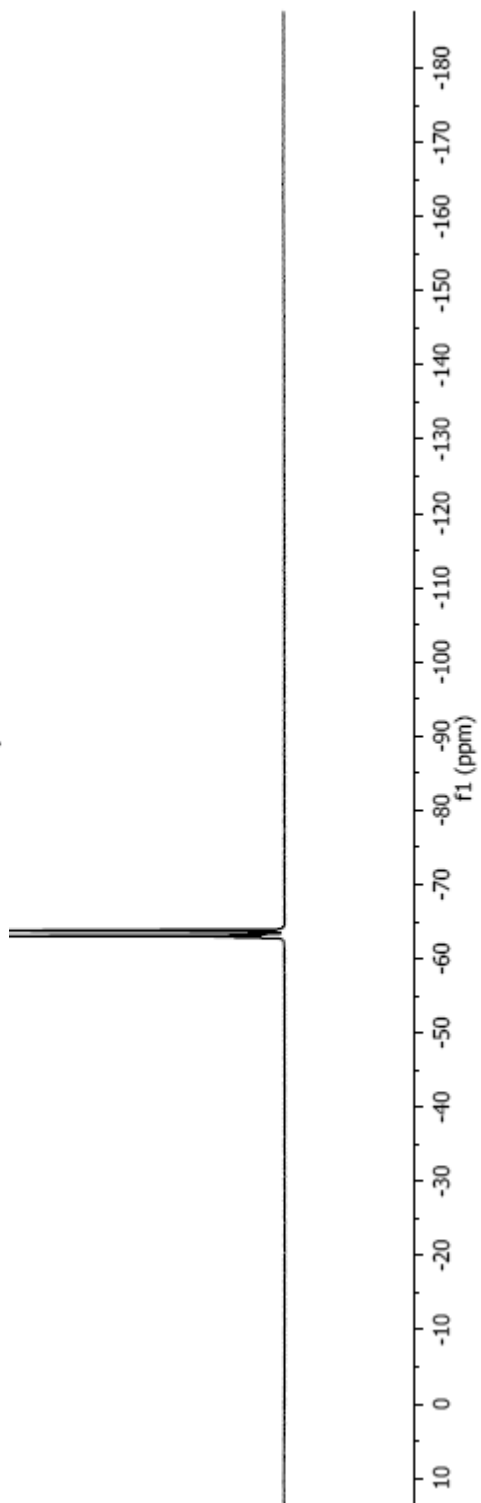


Table 7, entry 2



## Elemental Composition Report

Page 1

## Multiple Mass Analysis: 2 mass(es) processed

Tolerance = 5.0 PPM / DBE: min = -1.5, max = 50.0

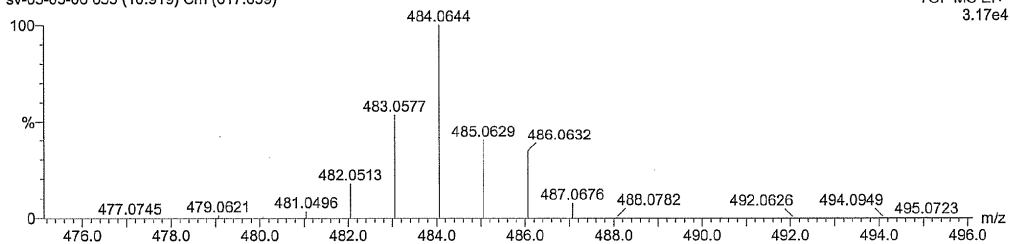
Isotope cluster parameters: Separation = 1.0 Abundance = 1.0%

Monoisotopic Mass, Odd and Even Electron Ions

737 formula(e) evaluated with 11 results within limits (up to 50 closest results for each mass)

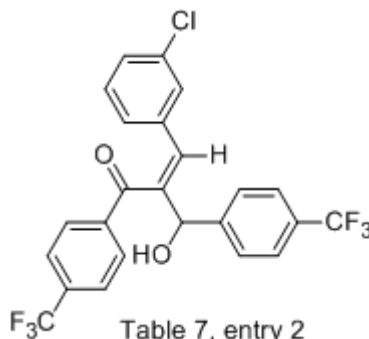
KW792

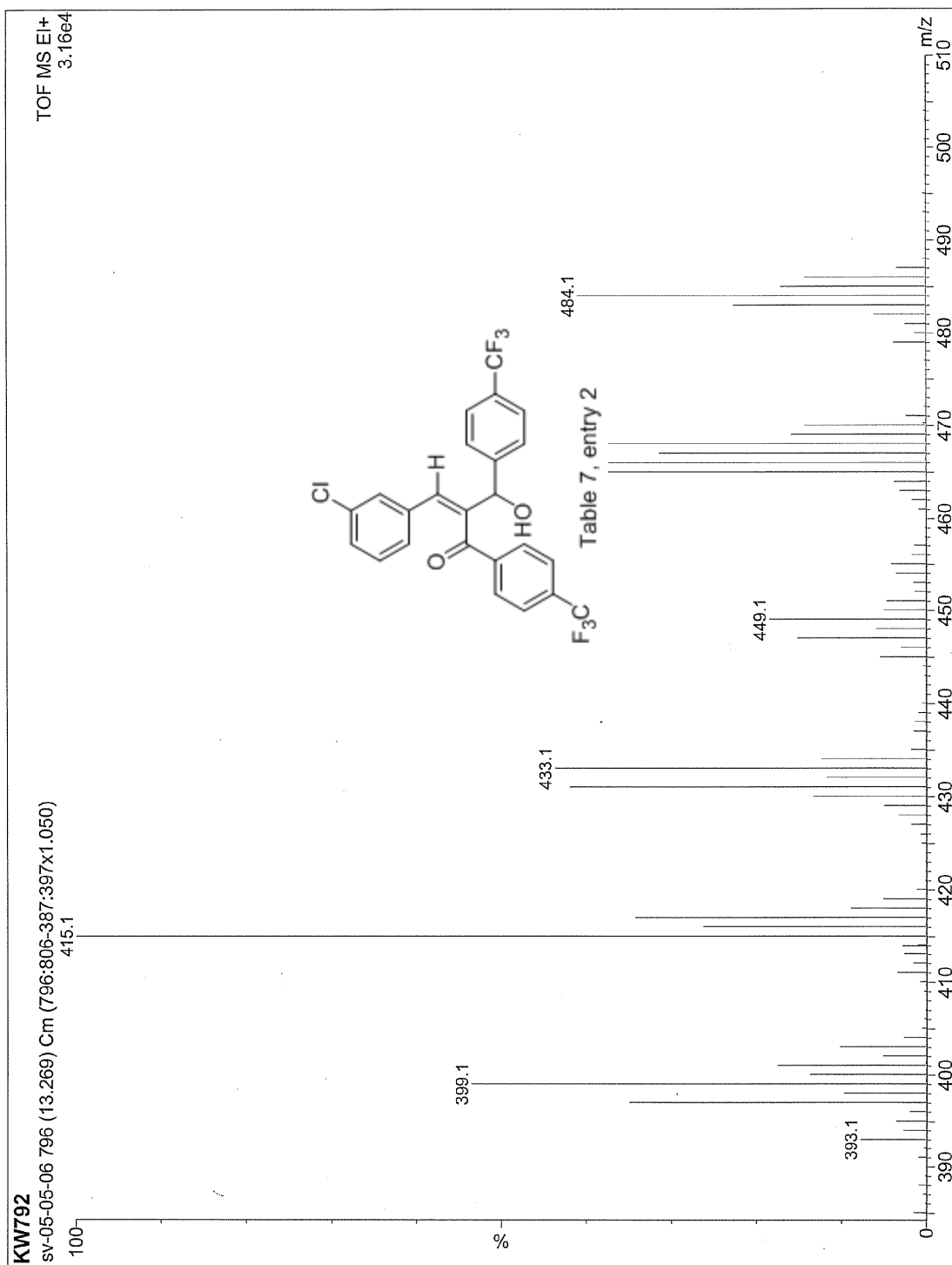
sv-05-05-06 655 (10.919) Cm (617:659)

TOF MS EI+  
3.17e4

Minimum: 50.00  
Maximum: 100.00

Mass	RA	Calc. Mass	mDa	PPM	DBE	Score	Formula
483.0577	53.70	483.0577	0.0	0.1	29.5	1	C35 H12 O Cl
		483.0575	0.2	0.4	18.5	5	C27 H13 O F5 Cl
		483.0587	-1.0	-2.0	14.5	6	C24 H14 O2 F6 Cl
		483.0588	-1.1	-2.3	25.5	2	C32 H13 O2 F Cl
		483.0564	1.3	2.8	22.5	3	C30 H12 F4 Cl
		483.0600	-2.3	-4.7	21.5	4	C29 H14 O3 F2 Cl
484.0644	100.00	484.0642	0.2	0.4	22.0	3	C30 H13 F4 Cl
		484.0653	-0.9	-1.9	18.0	4	C27 H14 O F5 Cl
		484.0655	-1.1	-2.3	29.0	1	C35 H13 O Cl
		484.0665	-2.1	-4.3	14.0	5	C24 H15 O2 F6 Cl
		484.0666	-2.2	-4.6	25.0	2	C32 H14 O2 F Cl





KW787, CDCl<sub>3</sub>  
400 MHz  
YELLOW OIL  
FEB 12 2009

7.69  
7.67  
7.60  
7.58  
7.56  
7.54  
7.44  
7.42  
7.34  
7.32  
7.17  
7.15  
7.04  
5.85  
5.84  
3.19  
3.18

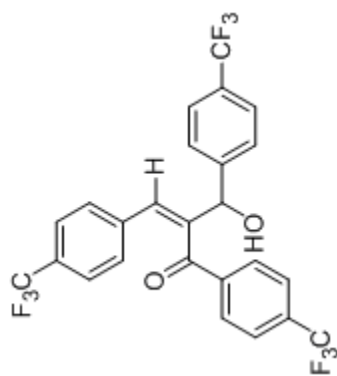
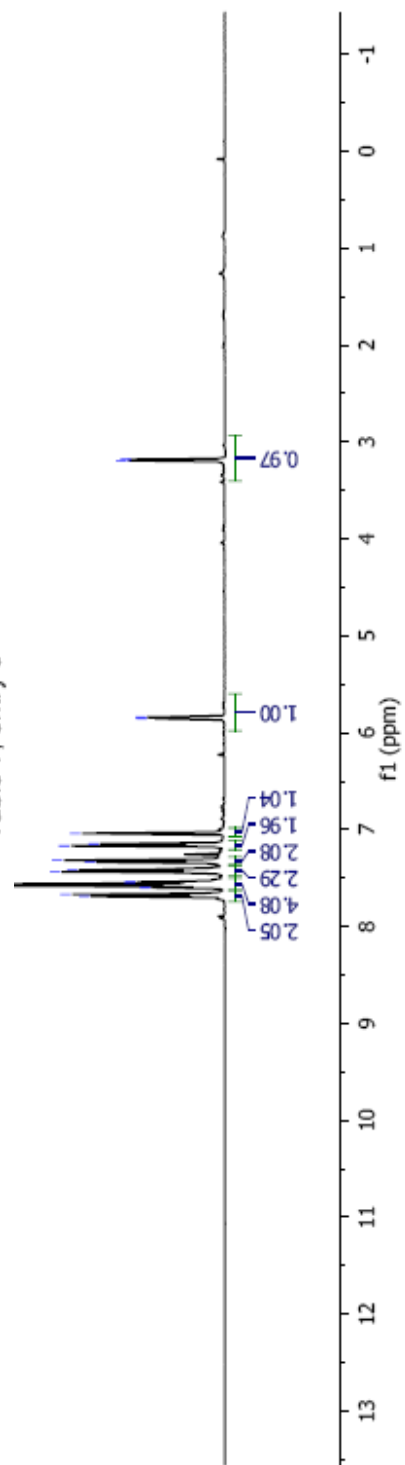
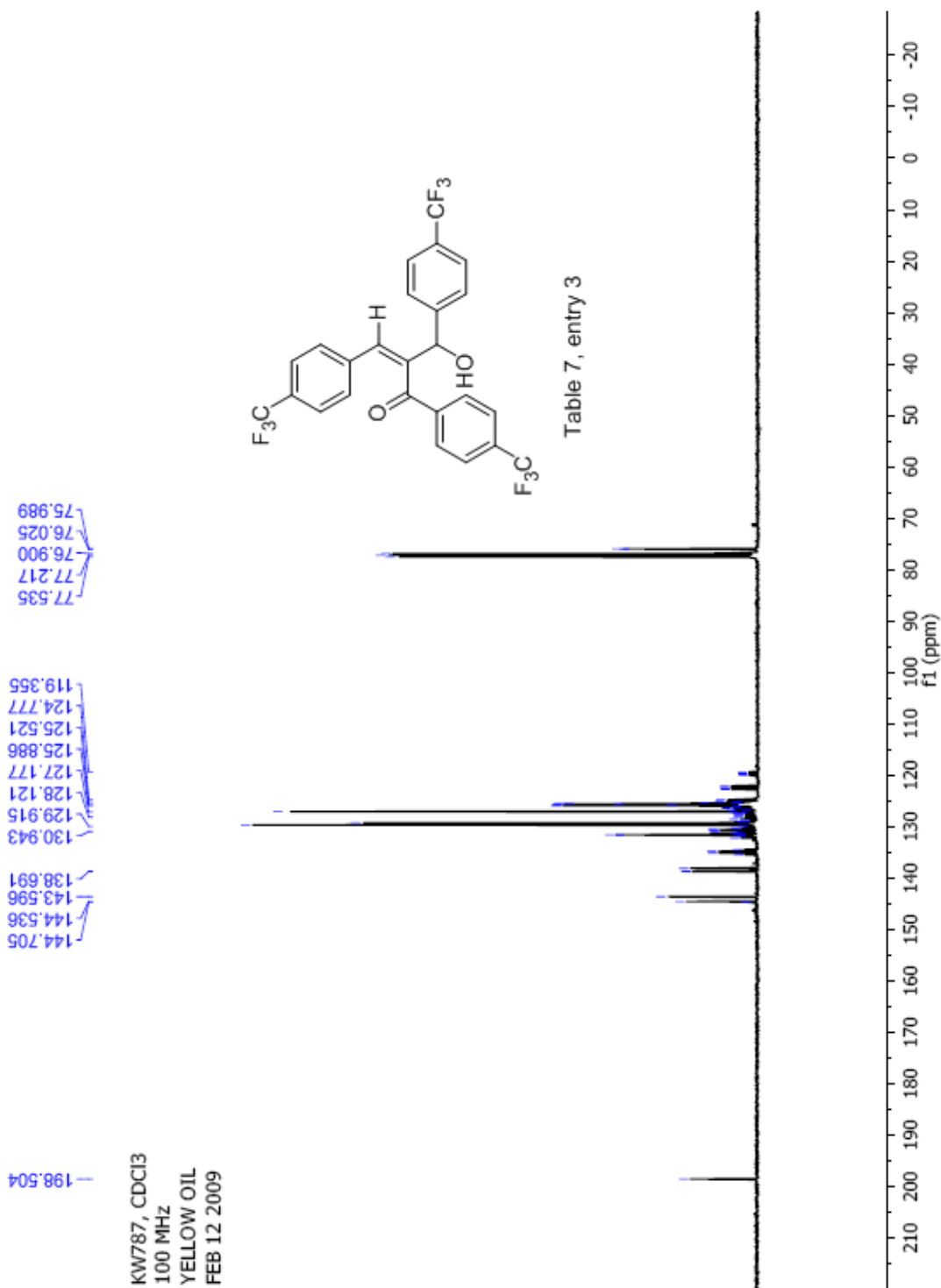


Table 7, entry 3





KW787, CDCI3  
376 MHz  
YELLOW OIL  
FEB 12 2009

63.12  
63.50  
63.94

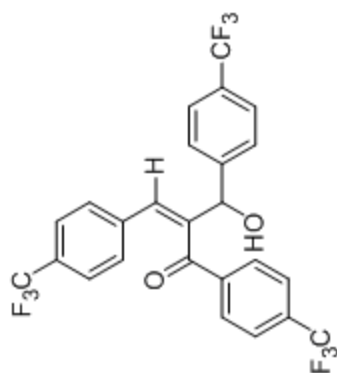
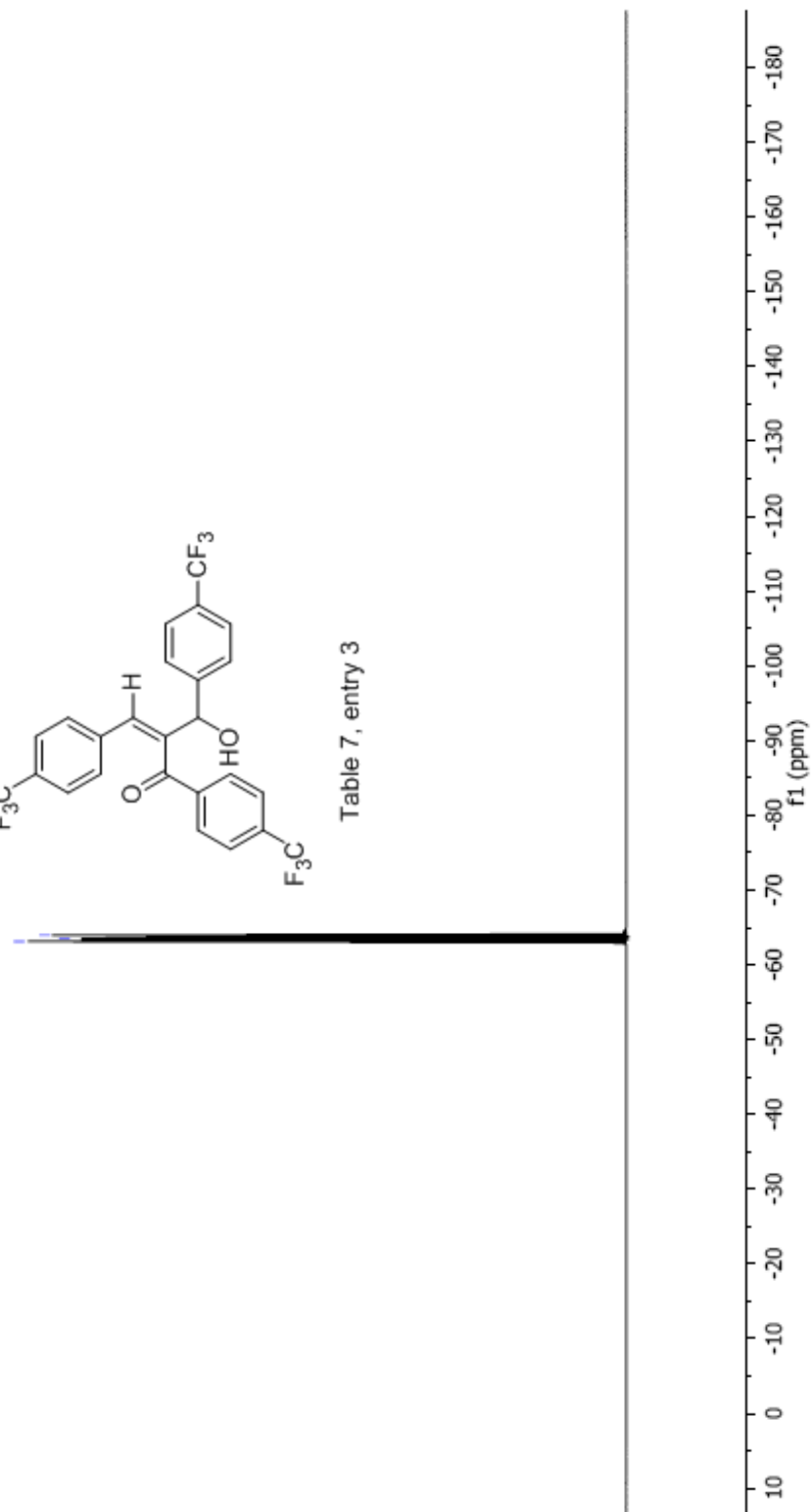


Table 7, entry 3



## Manual Peak Matching Report For Accurate Mass Determination

Theoretical mass	Experimental mass	PFK matching mass	Deviation*
518.09283	518.09409	492.96864	2.4 ppm

\* The deviation is obtained from the following equation:

$$\text{deviation} = \frac{\text{experimental mass} - \text{theoretical mass}}{\text{nominal mass}}$$

Where nominal mass takes in account only  $^{12}\text{C}$ ,  $^1\text{H}$ ,  $^{16}\text{O}$ ,  $^{14}\text{N}$  etc...

Theoretical mass correspond to the mass of the most abundant isotope peak

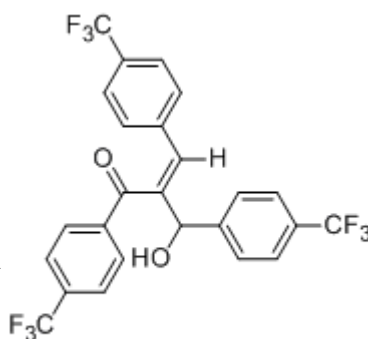


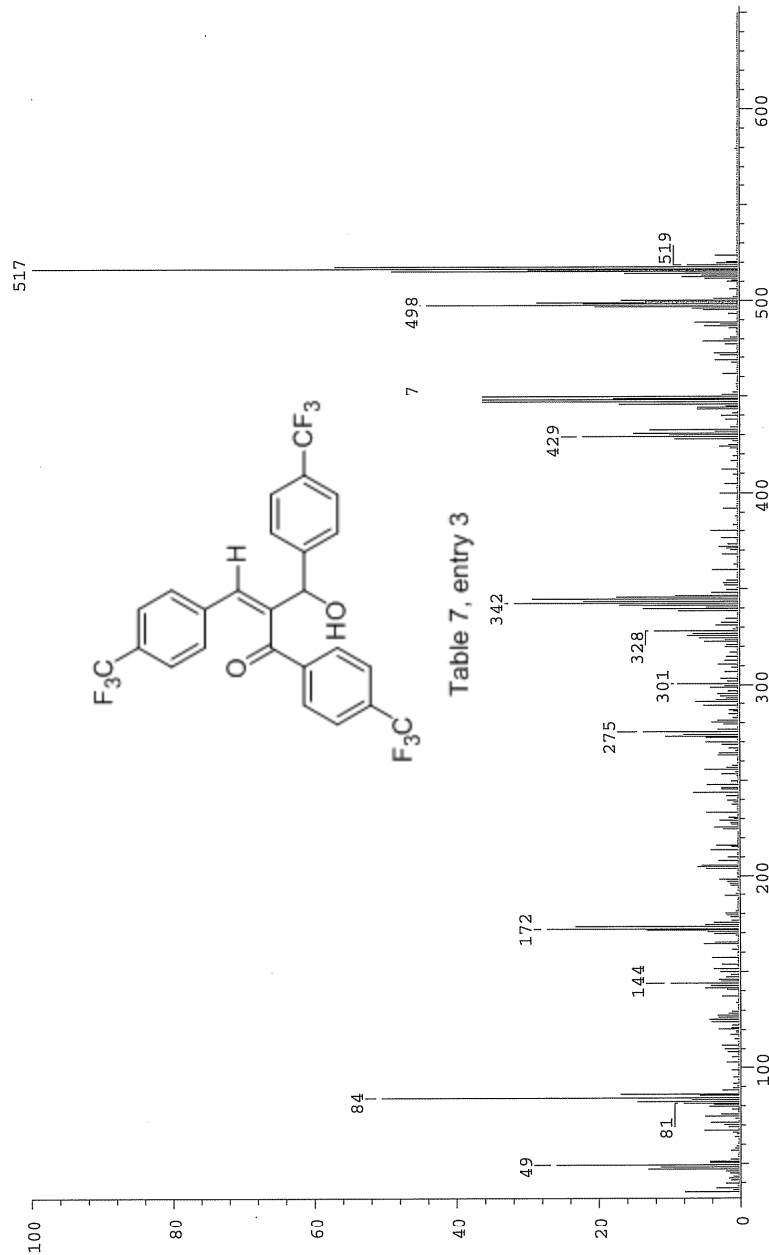
Table 7, entry 3

*bm*

SPEC: fin084254.dat (18-FEB-09 10:34:53)  
Samp: kw787  
Comm: DP 70 eV EI  
Oper: kh  
Base: 516.57  
Peak: 1000.0 mmu  
Scan 29 @ 0.74 min (EI +Q1MS LMR UP LR)

Study: ms services  
Masses: 35.01 > 650.00  
Intensity: 121516

Scans: 1 > 37  
Client: Kuldup  
#Peaks: 623  
RIC: 1940624  
1.2E+05



Date: Wed Feb 18 10:36:22 2009 ICIS: 8.3.0 SP2 for OSF1 (V4.0) build 98-238 from 26-Aug-98



KW794, CDCl<sub>3</sub>  
 400 MHz  
 GREEN OIL  
 FEB 26 2009

3.07  
 3.06

5.76  
 5.75

6.79  
 6.80  
 6.84

7.00  
 7.53

7.84  
 7.86

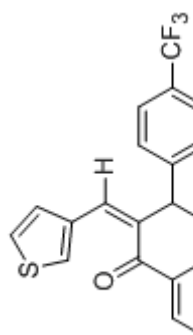
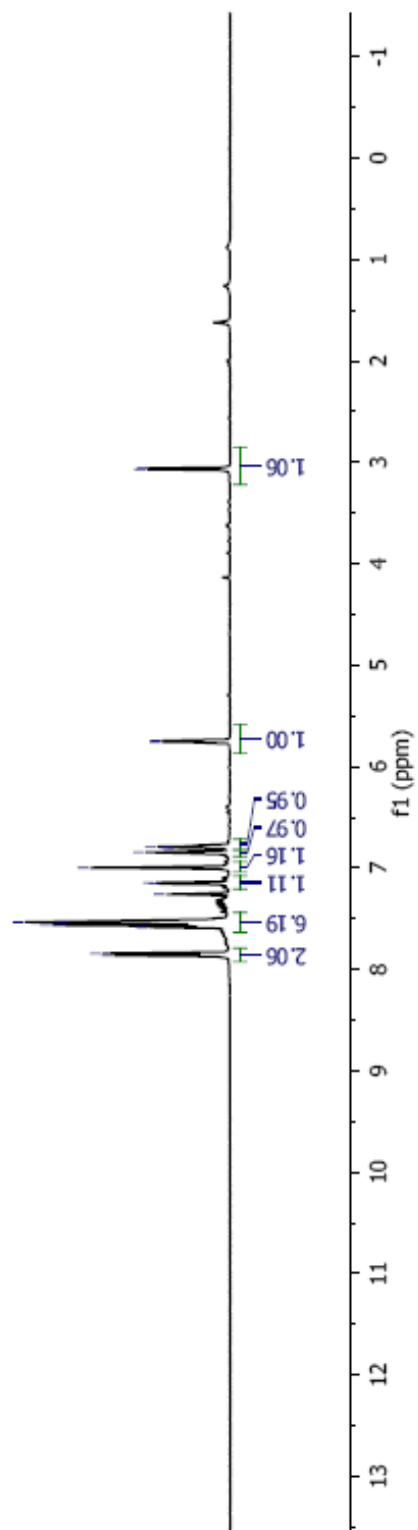
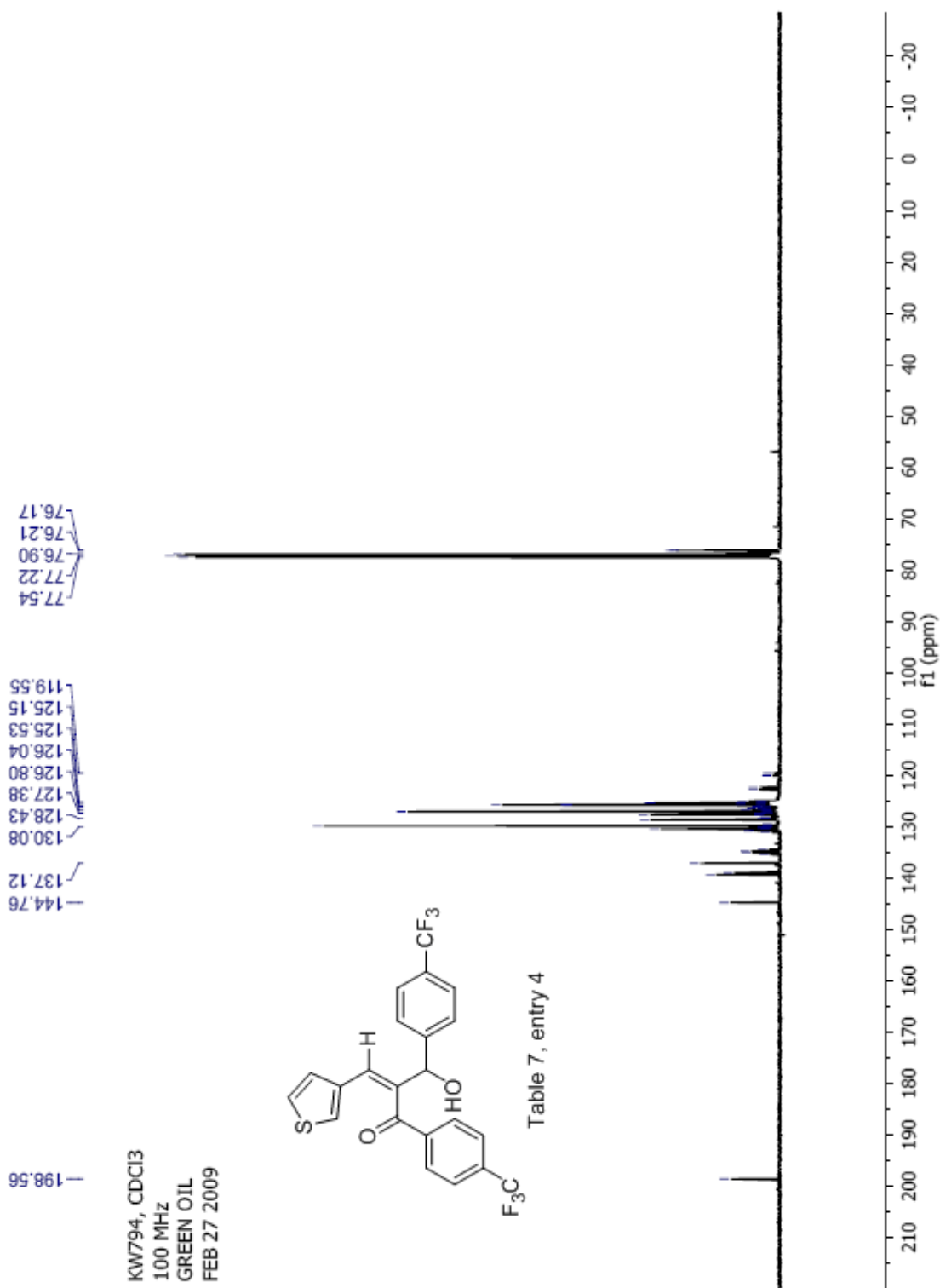


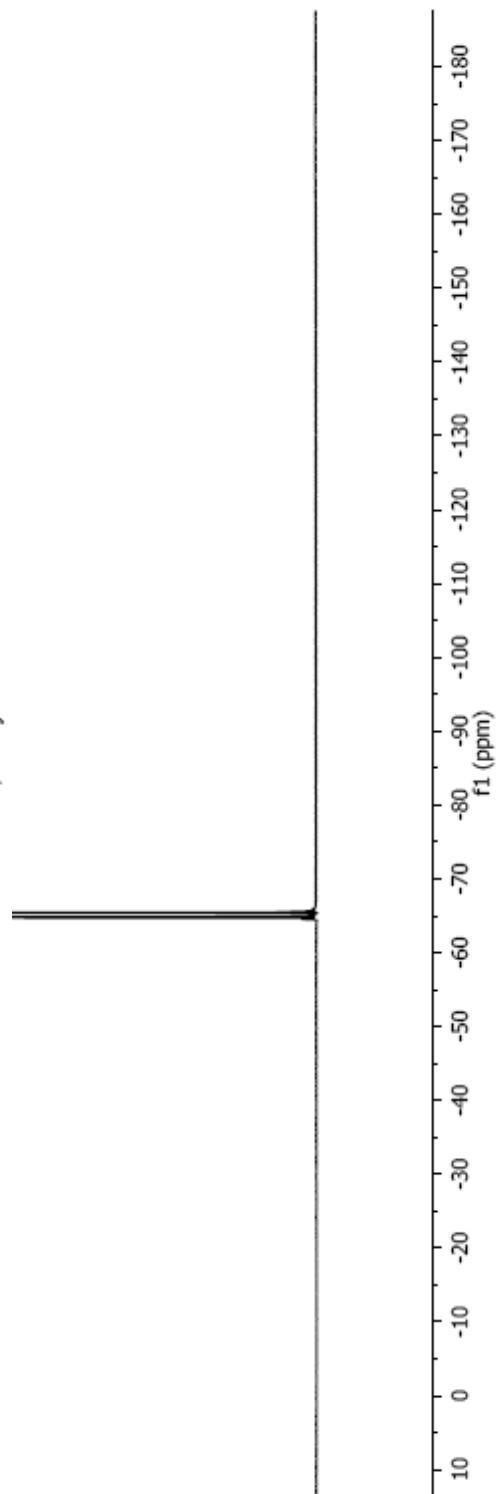
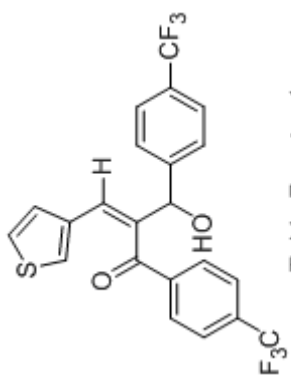
Table 7, entry 4





KW794, CDCl<sub>3</sub>  
 376 MHz  
 GREEN OIL  
 FEB 27 2009

64.78  
 65.41



## Manual Peak Matching Report For Accurate Mass Determination

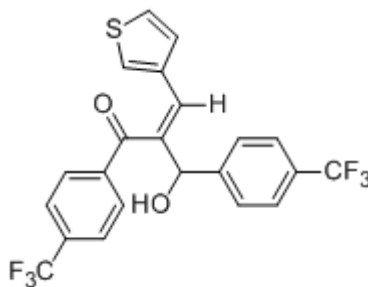
Theoretical mass	Experimental mass	PFK matching mass	Deviation*
456.06186	456.06315	430.97284	2.8 ppm

\* The deviation is obtained from the following equation:

$$\text{deviation} = \frac{\text{experimental mass} - \text{theoretical mass}}{\text{nominal mass}}$$

Where nominal mass takes in account only  $^{12}\text{C}$ ,  $^1\text{H}$ ,  $^{16}\text{O}$ ,  $^{14}\text{N}$  etc...

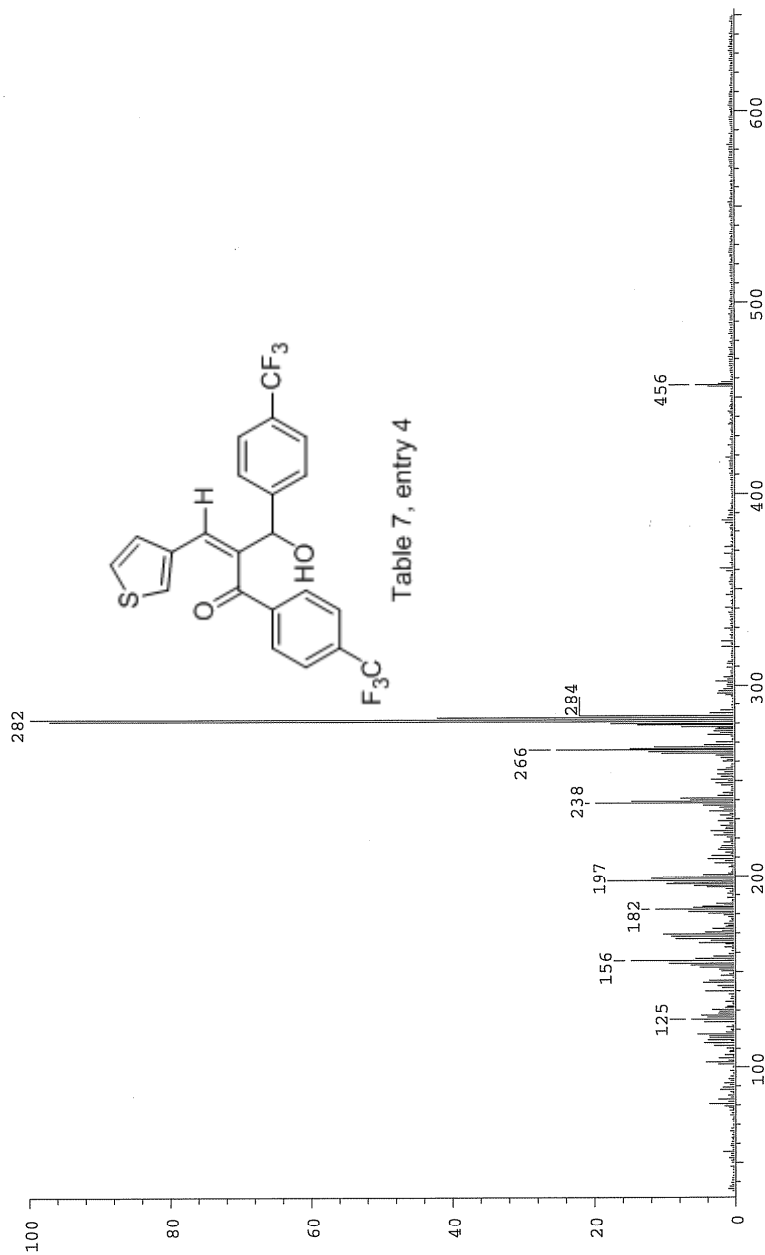
Theoretical mass correspond to the mass of the most abundant isotope peak



*ms*

Scans: 1 > 65  
 Client: Kuldeep  
 #Peaks: 622  
 RIC: 198770  
 2.0E+04

SPEC: fin084293.dat (06-MAR-09 10:55:20)  
 Samp: KW794  
 Comm: DP/EI  
 Oper: kh  
 Study: ms services  
 Masses: 35.01 > 650.00  
 Base: 281.83  
 Intensity: 19944  
 Peak: 1000.0 mmu  
 Scan 39 @ 0.96 min (EI +Q1MS LMR UP LR)



Date: Fri Mar 6 10:57:42 2009 ICIS: 8.3.0 SP2 for OSFI (V4.0) build 98-238 from 26-Aug-98

KW789, CDC13  
400 MHz  
YELLOW OIL  
FEB 17 2009

7.98  
7.96  
7.81  
7.79  
7.64  
7.62  
7.51  
7.49  
7.31  
7.29  
7.26  
7.16  
7.14  
7.03  
5.84  
5.83  
3.87  
3.85  
3.36  
3.35

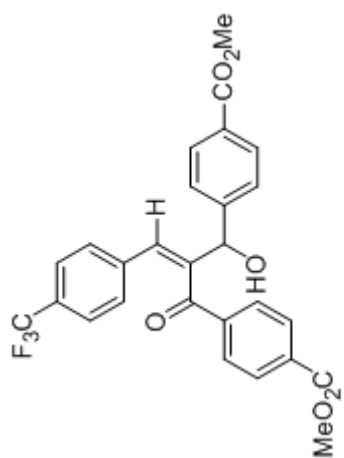
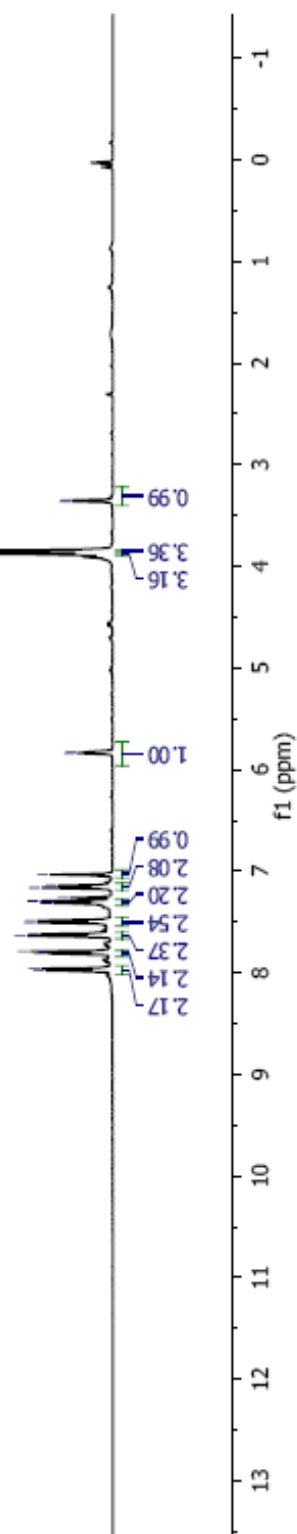


Table 7, entry 5



198.96  
166.83  
166.07  
145.64  
143.82  
139.11  
130.15  
129.25  
128.52  
126.70  
126.19  
125.45  
125.19  
119.85  
77.55  
77.24  
76.92  
76.25  
76.21  
52.62  
52.37

KW789, CDCl<sub>3</sub>  
100 MHz  
YELLOW OIL  
FEB 17 2009

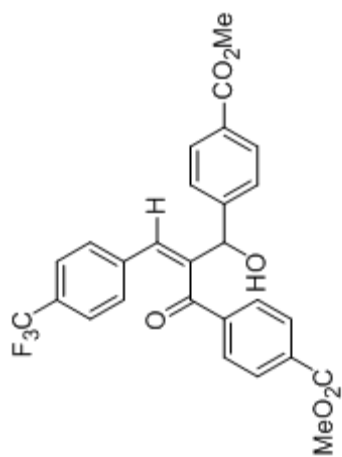
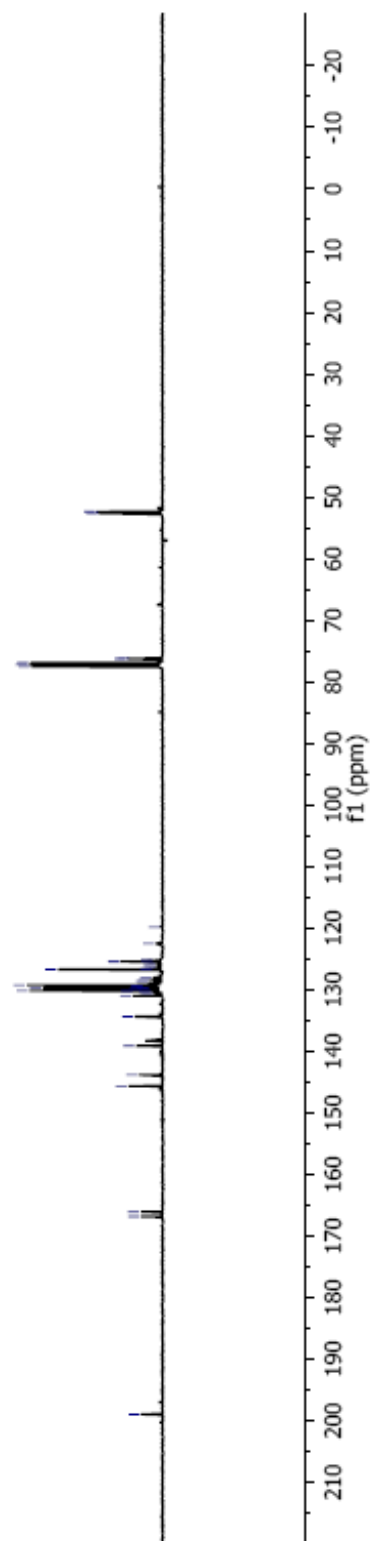
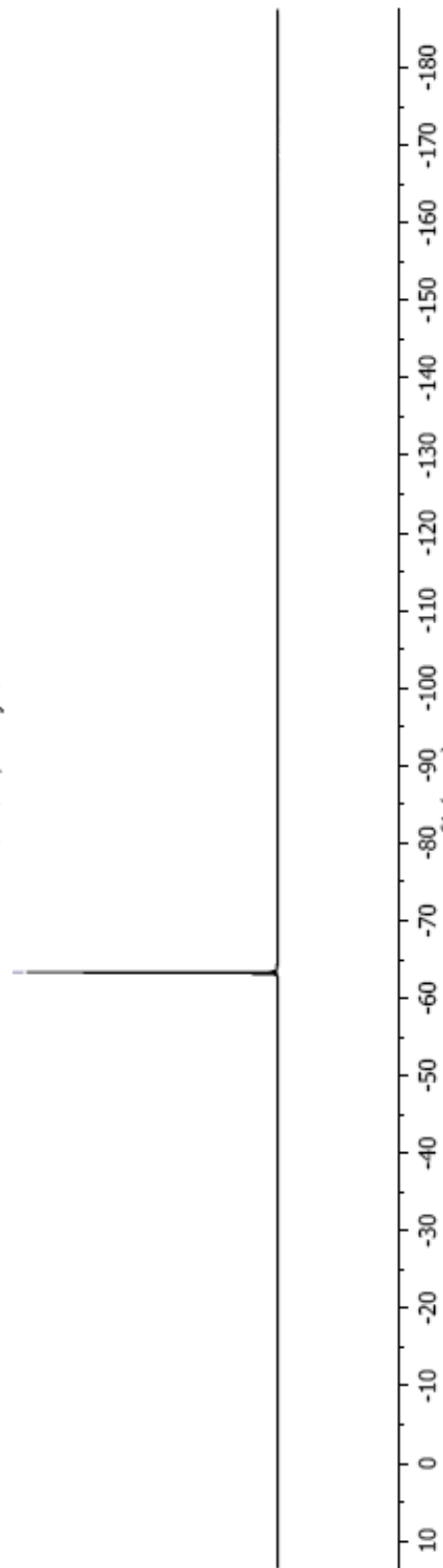
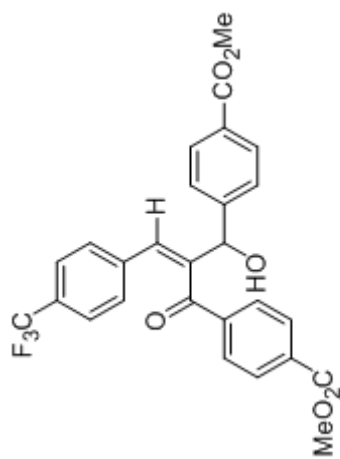


Table 7, entry 5



KW789, CDCl<sub>3</sub>  
376 MHz  
YELLOW OIL  
FEB 17 2009

63.33





## Manual Peak Matching Report For Accurate Mass Determination

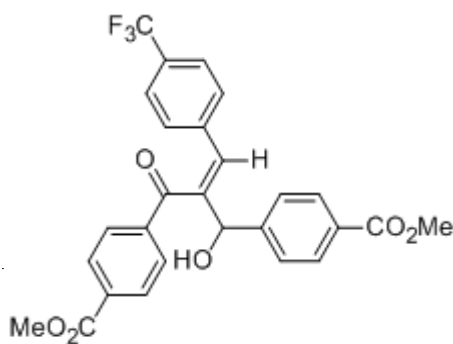
Theoretical mass	Experimental mass	PFK matching mass	Deviation*
498.12902	498.13023	498.98964	2.4 ppm

\* The deviation is obtained from the following equation:

$$\text{deviation} = \frac{\text{experimental mass} - \text{theoretical mass}}{\text{nominal mass}}$$

Where nominal mass takes in account only  $^{12}\text{C}$ ,  $^1\text{H}$ ,  $^{16}\text{O}$ ,  $^{14}\text{N}$  etc...

Theoretical mass correspond to the mass of the most abundant isotope peak

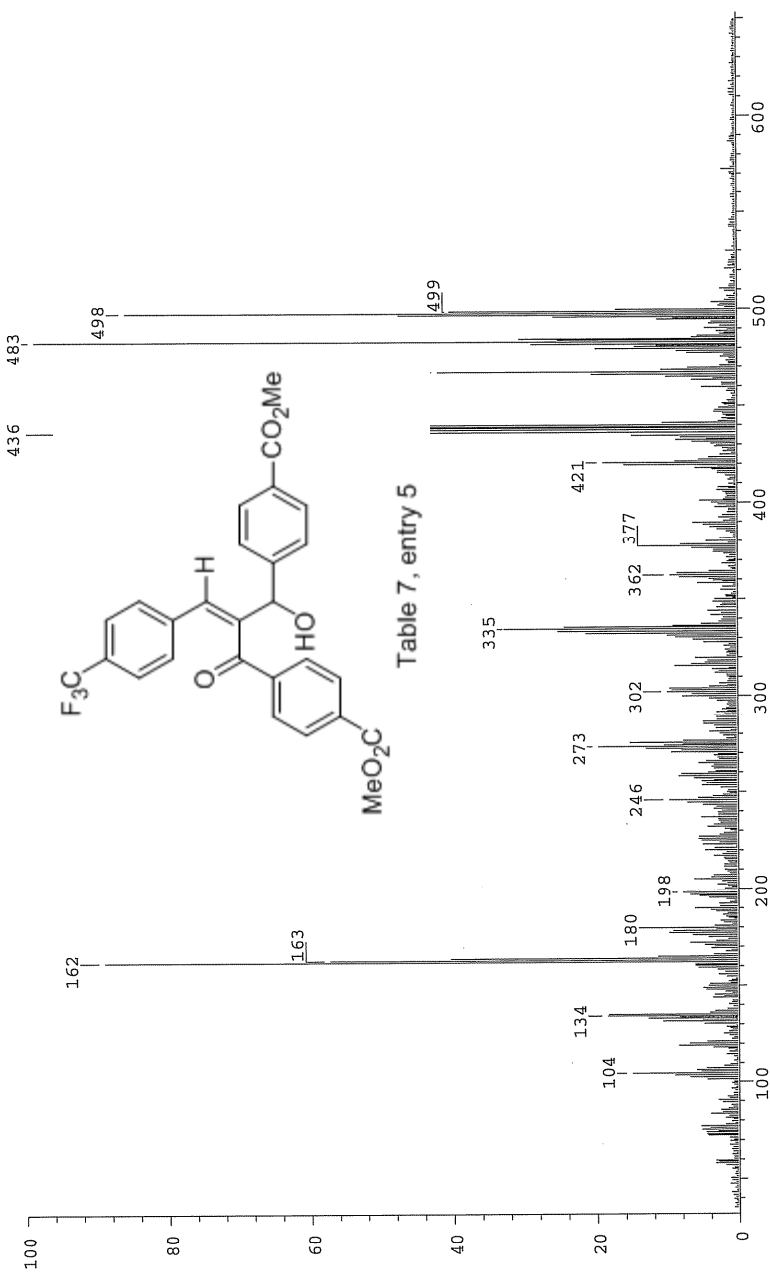


*OP*

Scans: 1 > 70  
 Client: Kuldeep  
 #Peaks: 651  
 RIC: 1781336  
 6.4E+04

SPEC: fin084276.dat (02-MAR-09 11:08:01)  
 Samp: kw789  
 Conn: DF/EI  
 Oper: kh  
 Base: 436.31  
 Peak: 1000.0 mmu  
 Scan 64 @ 1.47 min (EI +Q1MS LMR UP LR)

Study: ms services  
 Masses: 35.01 > 650.00  
 Intensity: 64483



Date: Mon Mar 2 11:10:08 2009 ICIS: 8.3.0 SP2 for OSFI (V4.0) build 98-238 from 26-Aug-98

KW809, CDCl<sub>3</sub>  
400 MHz  
YELLOW OIL  
MAR 12 2009

7.487  
7.466  
7.459  
7.438  
7.347  
7.333  
7.296  
7.275  
7.258  
7.175  
7.155  
6.944  
5.702  
3.095  
3.084

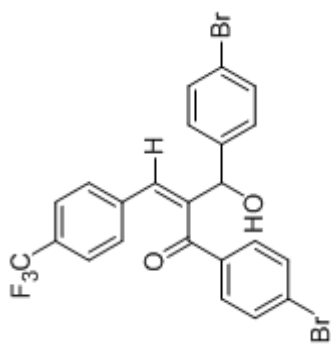
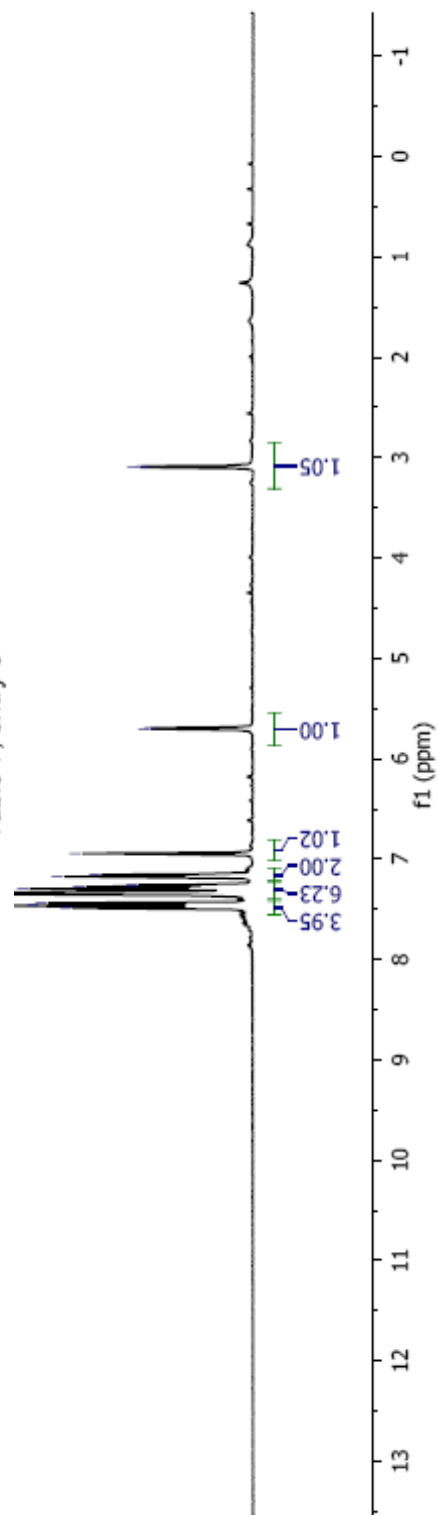


Table 7, entry 6





KW809, CDCl<sub>3</sub>  
100 MHz  
YELLOW OIL  
MAR 12 2009

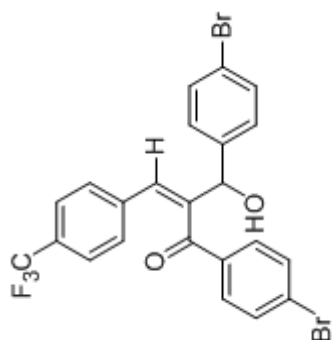
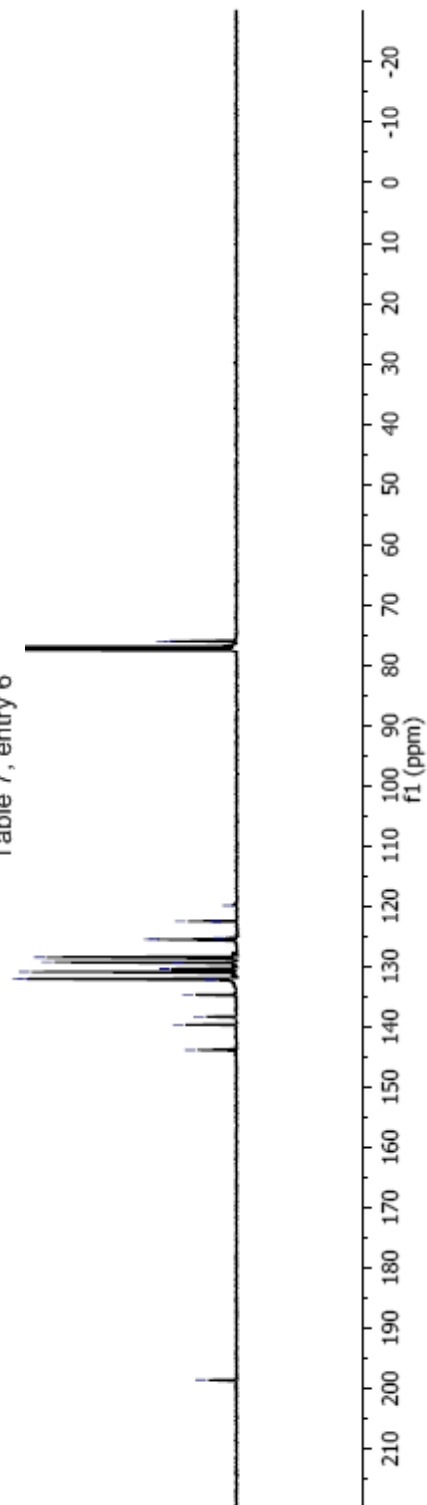


Table 7, entry 6



KW809, CDCI3  
376 MHz  
YELLOW OIL  
MAR 12 2009

63.236

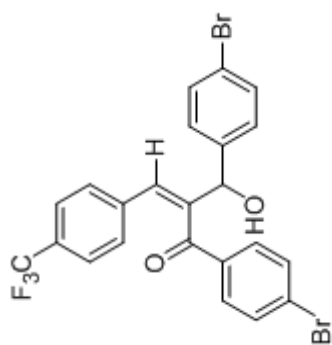
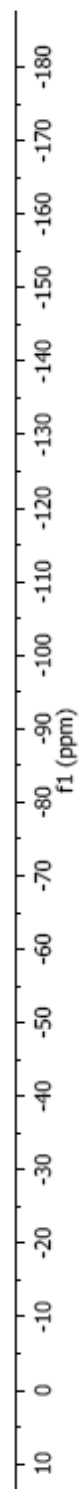


Table 7, entry 6



## Elemental Composition Report

Page 1

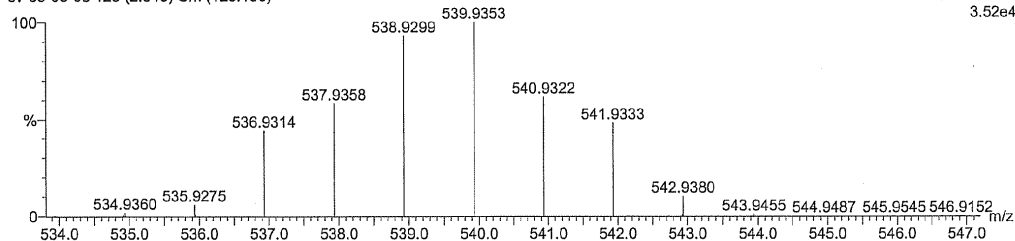
## Multiple Mass Analysis: 6 mass(es) processed

Tolerance = 20.0 PPM / DBE: min = -1.5, max = 50.0

Isotope cluster parameters: Separation = 1.0 Abundance = 1.0%

Monoisotopic Mass, Odd and Even Electron Ions

42 formula(e) evaluated with 6 results within limits (up to 50 closest results for each mass)

KW809 continued  
sv-05-05-08 123 (2,049) Cm (120:156)TOF MS EI+  
3.52e4

Mass	RA	Calc. Mass	mDa	PPM	DBE	Score	Formula
536.9314	44.31	536.9313	0.1	0.3	14.5	1	C23 H14 O2 F3 79Br2
537.9358	58.19	537.9391	-3.3	-6.1	14.0	1	C23 H15 O2 F3 79Br2
538.9299	92.95	538.9292	0.7	1.3	14.5	1	C23 H14 O2 F3 79Br
539.9353	100.00	539.9370	-1.7	-3.2	14.0	1	81Br C23 H15 O2 F3 79Br
540.9322	61.48	540.9272	5.0	9.3	14.5	1	81Br C23 H14 O2 F3 81Br2
541.9333	48.27	541.9350	-1.7	-3.1	14.0	1	C23 H15 O2 F3 81Br2

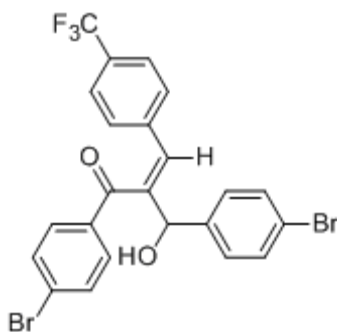
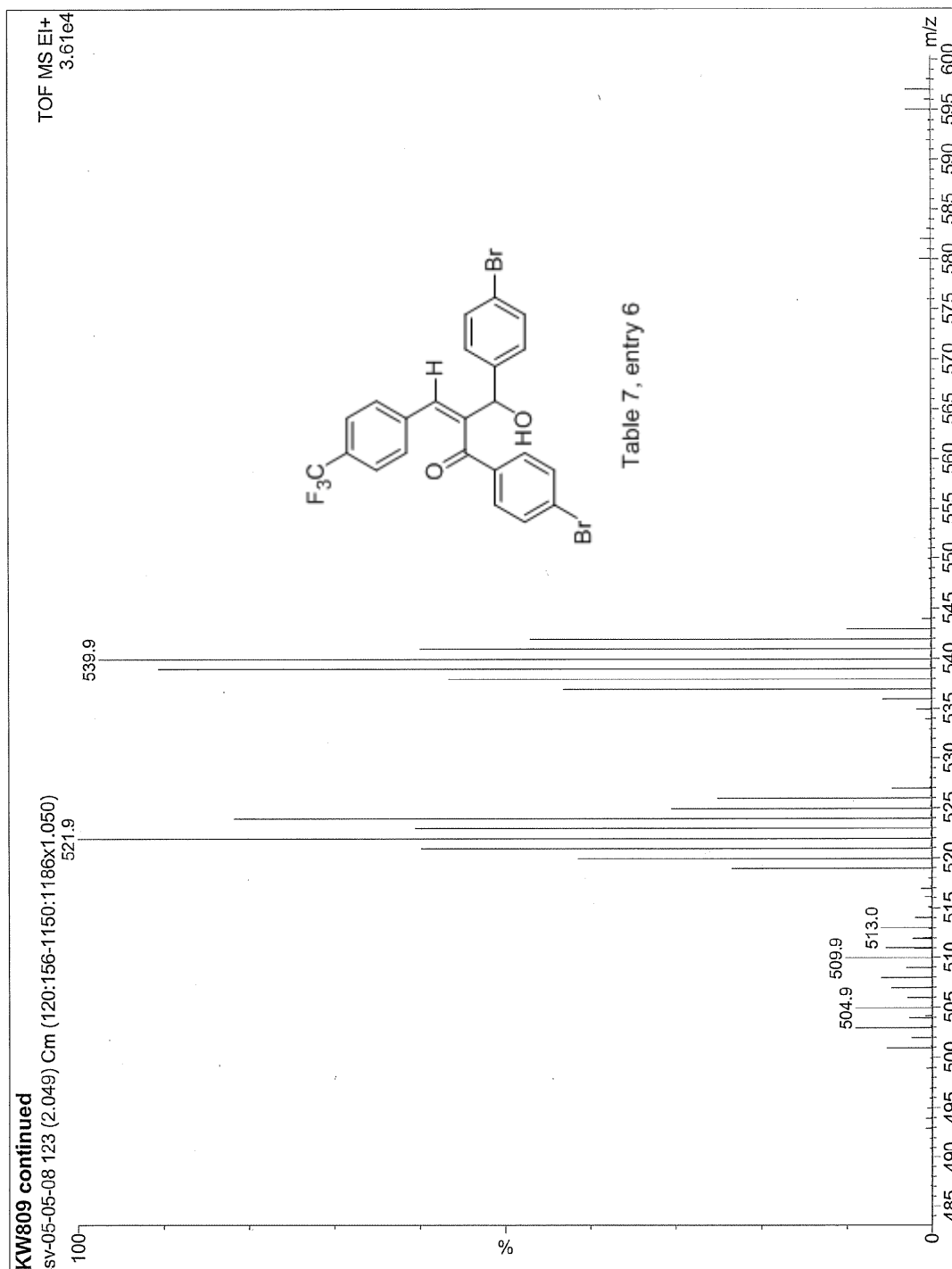
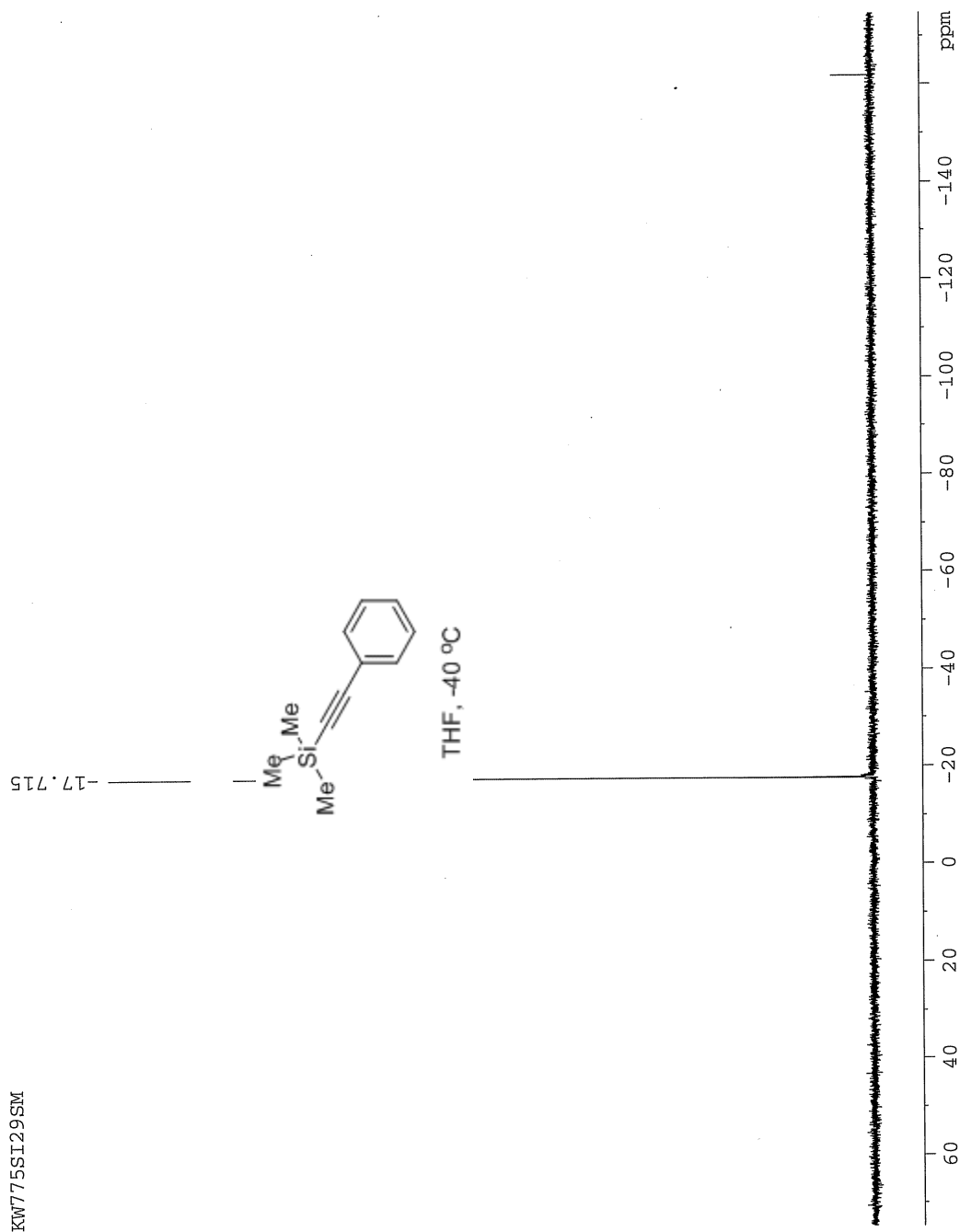


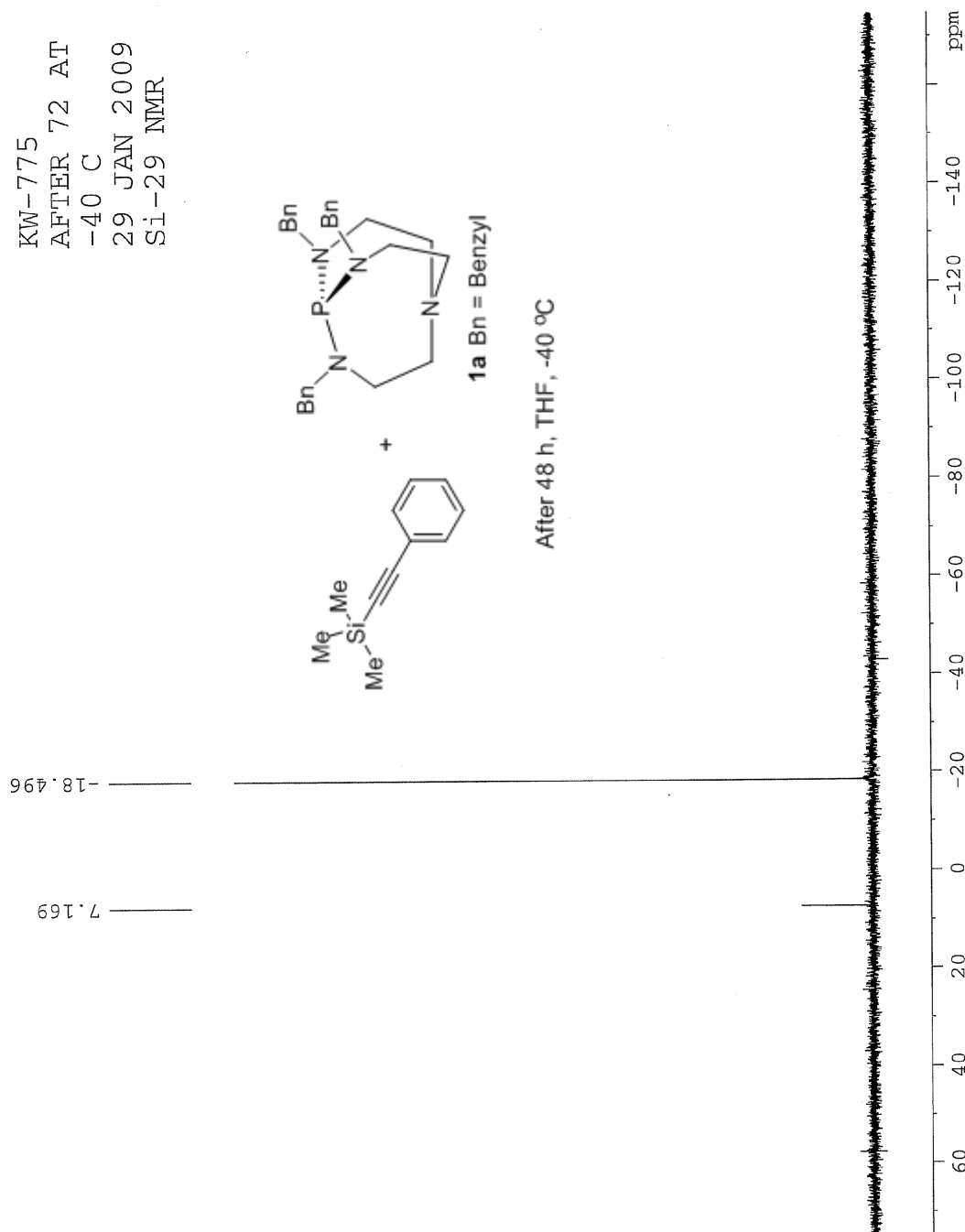
Table 7, entry 6







KW-775  
 AFTER 72 AT  
 -40 C  
 29 JAN 2009  
 Si-29 NMR



**APPENDIX E**

**CHAPTER 6**

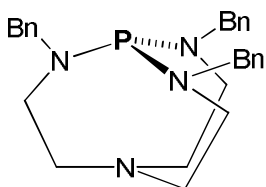
**General Information**

**References for known compounds and characterization data for the new compounds**

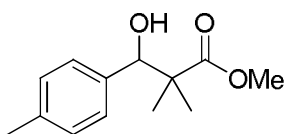
**$^1\text{H}$ ,  $^{13}\text{C}$  NMR and HRMS for all compounds**

### General Information

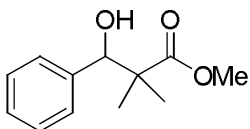
All reactions were carried out under inert atmosphere using oven dried glassware and a magnetic stirrer. THF was freshly distilled and dried over sodium/benzophenone. Trimethylsilylenolates, proazaphosphatrane **1b** and all aldehydes were purchased from commercial sources and were used without further purification. Proazaphosphatrane **1a**, **1c**, **1d** were synthesized according to our previous protocols.<sup>1</sup> An optimized procedure was reported for proazaphosphatrane **1c** in the manuscript. <sup>1</sup>H (300 or 400 Hz) and <sup>13</sup>C (100.6 MHz) NMR spectra were recorded in CDCl<sub>3</sub>; the chemical shifts are referenced to the residual peaks of CHCl<sub>3</sub> in CDCl<sub>3</sub>. <sup>31</sup>P NMR spectra were recorded at ambient temperature on a 400 MHz spectrometer using 85% H<sub>3</sub>PO<sub>4</sub> as the external standard. Thin layer chromatography (TLC) was performed using commercially prepared 60 mesh silica gel plates visualized with short-wavelength UV light (254 nm). The column chromatography was performed using (40-140 mesh) silica gel for the purification of Mukaiyama products. Electron impact ionization experiments were performed on a triple quadrupole mass spectrometer fitted with a EI/CI ion source. Accurate mass measurements were performed using a double focusing MS-50 mass spectrometer. The reported yields are isolated yields after column chromatography unless otherwise stated. All commercially available reagents were used as received.

**2,8,9-Tribenzyl-2,5,8,9-tetraaza-1-phospha-bicyclo[3.3.3]undecane (1c)<sup>1a</sup>:**

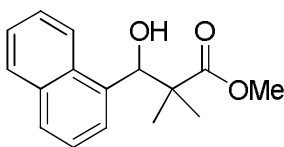
A three step optimized procedure is reported in the manuscript.

**Methyl 3-hydroxy-2,2-dimethyl-3-(4-methylphenyl)propionate (Table 1, entry 1)<sup>2</sup>:**

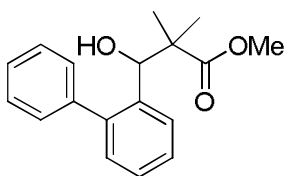
The general procedure was followed for the synthesis and purification; product was afforded as a white solid in 92% isolated yield.

**Methyl 3-hydroxy-2,2-dimethyl-3-phenylpropionate (Table 2, entry 1)<sup>2</sup>:**

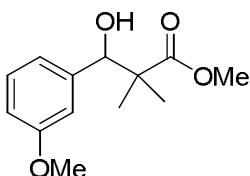
The general procedure was followed for the synthesis and purification; product was afforded as a white solid in 93% isolated yield.

**Methyl 3-hydroxy-2,2-dimethyl-3-(naphthalen-1yl)propionate (Table 2, entry 2)<sup>2</sup>:**

The general procedure was followed for the synthesis and purification; product was afforded as a yellow oil in 81% isolated yield.

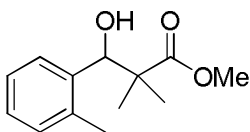
**Methyl 3-hydroxy-3-(2-biphenyl)-2,2-dimethylpropionate (Table 2, entry 3):**

The general procedure was followed for the synthesis and purification; product was afforded as a white solid in 92% isolated yield.  $^1\text{H}$  NMR ( $\text{CDCl}_3$ , 400 MHz):  $\delta$  7.58 (d, 1H,  $J = 8.0$  Hz), 7.42–7.30 (m, 7H), 7.20 (d, 1H,  $J = 7.6$  Hz), 5.27 (s, 1H), 3.75 (bs, 1H), 3.64 (s, 3H), 1.02 (s, 3H), 0.83 (s, 3H) ppm;  $^{13}\text{C}$  NMR ( $\text{CDCl}_3$ , 100 MHz):  $\delta$  178.8, 142.5, 141.9, 137.7, 130.5, 129.9, 128.5, 127.7, 127.7, 127.4, 127.1, 74.1, 52.4, 48.4, 24.2, 19.5 ppm; HRMS  $m/z$  Calcd for  $\text{C}_{18}\text{H}_{20}\text{O}_3$ : 284.14124. Found: 284.14179.

**Methyl 3-hydroxy-3-(3-methoxyphenyl)-2,2-dimethylpropionate (Table 2, entry 4):**

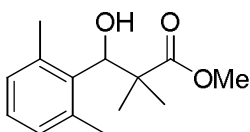
The general procedure was followed for the synthesis and purification; product was afforded as a colorless oil in 95% isolated yield.  $^1\text{H}$  NMR ( $\text{CDCl}_3$ , 400 MHz):  $\delta$  7.26–7.21 (m, 1H), 6.88–6.82 (m, 3H), 4.86 (d, 1H,  $J = 4.4$  Hz), 3.79 (s, 3H), 3.72 (s, 3H), 3.05 (d, 1H,  $J = 4.0$  Hz), 1.15 (s, 3H), 1.12 (s, 3H) ppm;  $^{13}\text{C}$  NMR ( $\text{CDCl}_3$ , 100 MHz):  $\delta$  178.3, 159.3, 141.9, 128.9, 120.3, 113.6, 113.3, 78.8, 55.4, 52.3, 47.9, 23.2, 19.4 ppm; HRMS  $m/z$  Calcd for  $\text{C}_{13}\text{H}_{18}\text{O}_4$ : 238.12050. Found: 238.12115.

**Methyl 3-hydroxy-3-(2-methylphenyl)-2,2-dimethylpropionate (Table 2, entry 5)<sup>3</sup>:**



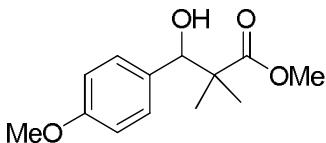
The general procedure was followed for the synthesis and purification; product was afforded as a colorless oil in 92% isolated yield.

**Methyl 3-hydroxy-3-(2,6-dimethylphenyl)-2,2-dimethylpropionate (Table 2, entry 6):**



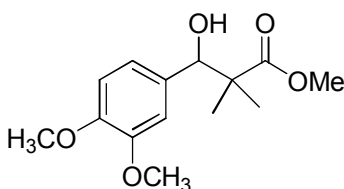
The general procedure was followed for the synthesis and purification; product was afforded as a white solid in 86% isolated yield.  $^1\text{H}$  NMR ( $\text{CDCl}_3$ , 400 MHz):  $\delta$  7.06–6.99 (m, 3H), 5.59 (s, 1H), 3.73 (s, 3H), 2.95 (s, 1H), 2.56 (s, 3H), 2.38 (s, 3H), 1.26 (s, 3H), 1.13 (s, 3H) ppm;  $^{13}\text{C}$  NMR ( $\text{CDCl}_3$ , 100 MHz):  $\delta$  178.8, 138.6, 137.5, 135.5, 131.3, 128.6, 127.4, 76.1, 52.5, 50.3, 24.2, 22.6, 20.9 ppm; HRMS  $m/z$  Calcd for  $\text{C}_{14}\text{H}_{20}\text{O}_3$ : 236.14124. Found: 236.14177.

**Methyl 3-hydroxy-3-(4-methoxyphenyl)-2,2-dimethylpropionate (Table 2, entry 7)<sup>2</sup>:**



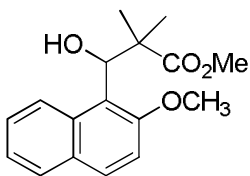
The general procedure was followed for the synthesis and purification; product was afforded as a white solid in 90% isolated yield.

**Methyl 3-hydroxy-3-(3,4-dimethoxyphenyl)-2,2-dimethylpropionate (Table 2, entry 8):**



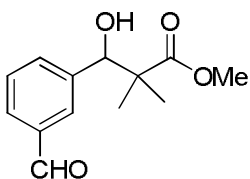
The general procedure was followed for the synthesis and purification; product was afforded as colorless oil in 91% isolated yield.  $^1\text{H}$  NMR ( $\text{CDCl}_3$ , 400 MHz):  $\delta$  6.86–6.83 (m, 2H), 6.75 (s, 1H), 5.25 (s, 1H), 3.83 (s, 3H), 3.82 (s, 3H), 3.66 (s, 3H), 1.29 (s, 3H), 1.07 (s, 3H) ppm;  $^{13}\text{C}$  NMR ( $\text{CDCl}_3$ , 100 MHz):  $\delta$  175.8, 149.2, 148.4, 129.9, 121.6, 112.2, 110.3, 68.8, 56.1, 56.1, 52.4, 49.9, 23.3, 20.3 ppm; HRMS  $m/z$  Calcd for  $\text{C}_{14}\text{H}_{20}\text{O}_5$ : 268.13107. Found: 268.13179.

**Methyl 3-hydroxy-3-(2-methoxynaphthalen-1-yl)-2,2-dimethylpropanoate (Table 2, entry 9):**



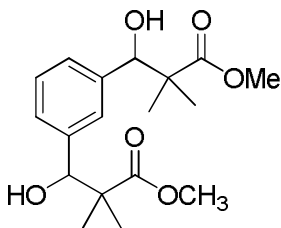
The general procedure was followed for the synthesis and purification; product was afforded as a colorless oil in 69% isolated yield.  $^1\text{H}$  NMR ( $\text{CDCl}_3$ , 400 MHz):  $\delta$  8.10 (bs, 1H), 7.81–7.74 (m, 2H), 7.46 (t, 1H,  $J = 8.0$  Hz), 7.32 (t, 1H,  $J = 8.0$  Hz), 7.27–7.23 (m, 1H), 5.90 (d, 1H,  $J = 8.0$  Hz), 4.90 (bs, 1H), 3.94 (s, 3H), 3.67 (s, 3H), 1.20 (s, 3H), 1.15 (s, 3H) ppm;  $^{13}\text{C}$  NMR ( $\text{CDCl}_3$ , 100 MHz):  $\delta$  177.5, 155.5, 133.1, 130.2, 129.3, 128.6, 126.6, 123.6, 119.9, 112.8, 75.2, 55.9, 52.0, 50.3, 24.1, 20.7 ppm; HRMS  $m/z$  Calcd for  $\text{C}_{17}\text{H}_{20}\text{O}_4$ : 288.13615. Found: 299.13656.

**Methyl 3-(3-formylphenyl)-3-hydroxy-2,2-dimethylpropanoate (Table 2, entry 10, 6a).**



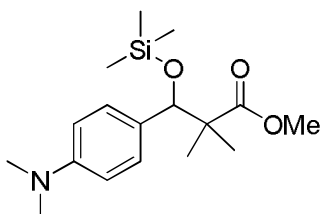
The general procedure was followed for the synthesis and purification; product was afforded as colorless oil in 49% isolated yield.  $^1\text{H}$  NMR ( $\text{CDCl}_3$ , 400 MHz):  $\delta$  9.95 (s, 1H), 7.76–7.73 (m, 2H), 7.54–7.52 (m, 1H), 7.44 (t, 1H,  $J = 8.0$  Hz), 4.93 (s, 1H), 3.67 (s, 3H), 3.48 (bs, 1H), 1.01 (s, 3H), 1.06 (s, 3H) ppm;  $^{13}\text{C}$  NMR ( $\text{CDCl}_3$ , 100 MHz):  $\delta$  192.4, 177.9, 141.2, 135.9, 133.8, 129.2, 128.9, 128.5, 76.8, 52.3, 47.7, 22.7, 19.1 ppm; HRMS  $m/z$  Calcd for  $\text{C}_{13}\text{H}_{16}\text{O}_4$ : 236.10485. Found: 236.10533.

**Dimethyl 3,3'-(1,3-phenylene)bis(3-hydroxy-2,2-dimethylpropanoate)** (Table 2, entry 10, 6b):



The general procedure was followed for the synthesis and purification; product was afforded as a colorless oil in 44% isolated yield.  $^1\text{H}$  NMR ( $\text{CDCl}_3$ , 400 MHz):  $\delta$  7.15–7.14 (m, 4H), 4.79 (d, 1H,  $J = 4.4$  Hz), 3.64 (s, 6H), 3.48 (bs, 1H), 1.05 (s, 3H), 1.04 (s, 3H), 1.02 (s, 3H), 1.01 (s, 3H) ppm;  $^{13}\text{C}$  NMR ( $\text{CDCl}_3$ , 100 MHz):  $\delta$  178.2, 139.7, 139.6, 127.2, 127.2, 127.1, 126.9, 78.5, 78.4, 52.2, 47.8, 47.8, 23.1, 22.8, 19.2, 19.1 ppm; HRMS  $m/z$  Calcd for  $\text{C}_{18}\text{H}_{26}\text{O}_6$ : 338.17293. Found: 338.17906.

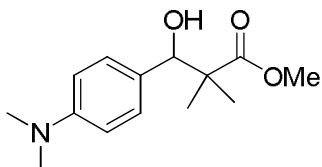
**Methyl 3-(4-(dimethylamino)phenyl)-2,2-dimethyl-3-(trimethylsilyloxy)propanoate** (Table 2, entry 11)<sup>4</sup>:





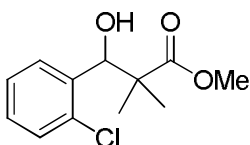
The general procedure was followed for the synthesis and purification; product was afforded as a white solid in 96% isolated yield.

**Methyl 3-hydroxy-3-(4-N,N-dimethylphenyl)-2,2-dimethylpropionate (Table 2, entry 11)<sup>5</sup>:**



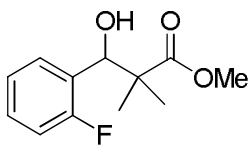
The general procedure was followed for the synthesis and purification; product was afforded as a colorless oil in 90% isolated yield.

**Methyl 3-hydroxy-3-(2-chlorophenyl)-2,2-dimethylpropionate (Table 3, entry 1):**



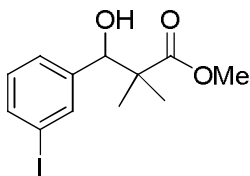
The general procedure was followed for the synthesis and purification; product was afforded as a colorless oil in 91% isolated yield. <sup>1</sup>H NMR (CDCl<sub>3</sub>, 400 MHz): δ 7.46–7.44 (m, 1H), 7.27–7.14 (m, 3H), 5.45 (s, 1H), 3.66 (s, 3H), 3.54 (bs, 1H), 1.12 (s, 3H), 1.10 (s, 3H) ppm; <sup>13</sup>C NMR (CDCl<sub>3</sub>, 100 MHz): δ 178.3, 137.9, 133.5, 129.6, 129.3, 128.8, 126.5, 73.4, 52.3, 48.6, 23.1, 18.7 ppm; HRMS *m/z* Calcd for C<sub>12</sub>H<sub>15</sub>ClO<sub>3</sub>: 242.07097. Found: 242.07153.

**Methyl 3-hydroxy-3-(2-fluorophenyl)-2,2-dimethylpropionate (Table 3, entry 2):**



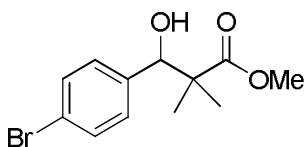
The general procedure was followed for the synthesis and purification; product was afforded as a colorless oil in 77% isolated yield.  $^1\text{H}$  NMR ( $\text{CDCl}_3$ , 400 MHz):  $\delta$  7.47–7.43 (m, 1H), 7.27–7.23 (m, 1H), 7.16–7.12 (m, 1H), 7.03–6.98 (m, 1H), 5.28 (d, 1H,  $J = 4.4$  Hz), 3.73 (s, 3H), 3.37 (d, 1H,  $J = 5.7$ Hz), 1.15 (s, 3H), 1.14 (s, 3H) ppm;  $^{13}\text{C}$  NMR ( $\text{CDCl}_3$ , 100 MHz):  $\delta$  178.4, 160.1 (d,  $J = 260$  Hz), 129.4, 129.3 (d,  $J = 4.2$  Hz), 127.4 (d,  $J = 12.9$  Hz), 124.0 (d,  $J = 3.3$  Hz), 115.2 (d,  $J = 22.8$  Hz), 71.7, 52.4, 48.2, 23.1, 18.8 ppm; HRMS  $m/z$  Calcd. for  $\text{C}_{12}\text{H}_{15}\text{FO}_3$ : 226.10052. Found: 226.10078.

**Methyl 3-hydroxy-3-(3-iodophenyl)-2,2-dimethylpropionate (Table 3, entry 3):**



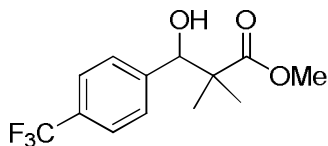
The general procedure was followed for the synthesis and purification; product was afforded as a colorless oil in 95% isolated yield.  $^1\text{H}$  NMR ( $\text{CDCl}_3$ , 400 MHz):  $\delta$  7.63–7.58 (m, 2H), 7.23 (d, 1H,  $J = 8.0$  Hz), 7.02 (t, 1H,  $J = 8.0$  Hz), 4.79 (d, 1H), 3.70 (s, 3H), 3.13(bs, 1H), 1.10 (s, 3H), 1.08 (s, 3H) ppm;  $^{13}\text{C}$  NMR ( $\text{CDCl}_3$ , 100 MHz):  $\delta$  178.1, 142.4, 136.8, 136.6, 129.5, 127.0, 93.9, 76.8, 52.3, 47.7, 22.9, 19.2 ppm; HRMS  $m/z$  Calcd. for  $\text{C}_{12}\text{H}_{15}\text{IO}_3$ : 334.00659. Found: 334.00734.

**Methyl 3-hydroxy-3-(4-bromophenyl)-2,2-dimethylpropionate (Table 3, entry 4)<sup>4</sup>:**



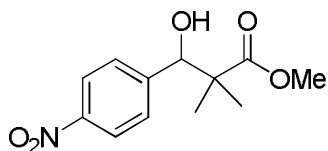
The general procedure was followed for the synthesis and purification; product was afforded as a white solid in 72% isolated yield.

**Methyl 3-hydroxy-2,2-dimethyl-3-(4-(trifluoromethyl)phenyl)propanoate (Table 3, entry 5):**



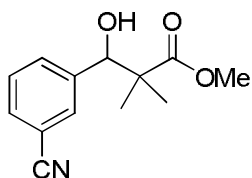
The general procedure was followed for the synthesis and purification; product was afforded as a white solid in 84% isolated yield.  $^1\text{H}$  NMR ( $\text{CDCl}_3$ , 400 MHz):  $\delta$  7.52 (d, 2H,  $J = 8.0$  Hz), 7.36(d, 2H,  $J = 8.0$  Hz), 4.87 (d, 2H,  $J = 2.8$  Hz), 3.66 (s, 3H), 3.50 (d, 2H,  $J = 4.0$  Hz), 1.08 (s, 3H), 1.04 (s, 3H) ppm;  $^{13}\text{C}$  NMR ( $\text{CDCl}_3$ , 100 MHz):  $\delta$  177.9, 144.1, 129.9 (q,  $J = 32.2$  Hz), 128.0, 124.2 (q,  $J = 270.4$  Hz), 124.6 (q,  $J = 3.7$  Hz), 77.9, 52.2, 47.6, 22.7, 19.0 ppm; HRMS  $m/z$  Calcd for  $\text{C}_{13}\text{H}_{15}\text{F}_3\text{O}_3$ : 276.09732. Found: 276.09812.

**Methyl 3-hydroxy-3-(4-nitrophenyl)-2,2-dimethylpropionate (Table 3, entry 6)<sup>2</sup>:**



The general procedure was followed for the synthesis and purification; product was afforded as a yellow oil in 62% isolated yield.

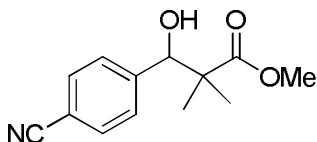
**Methyl 3-hydroxy-3-(3-cyanophenyl)-2,2-dimethylpropionate (Table 3, entry 7):**



The general procedure was followed for the synthesis and purification; product was afforded as a colorless oil in 58% isolated yield.  $^1\text{H}$  NMR ( $\text{CDCl}_3$ , 400 MHz):  $\delta$  7.58 (s, 1H), 7.55–7.50 (m, 2H), 7.40 (t, 1H,  $J = 7.6$  Hz), 4.89 (d, 1H,  $J = 3.6$  Hz), 3.69 (s, 3H), 3.53 (d,

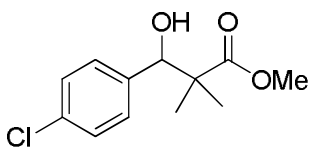
1H,  $J = 3.6$  Hz), 1.09 (s, 3H), 1.06 (s, 3H) ppm;  $^{13}\text{C}$  NMR ( $\text{CDCl}_3$ , 100 MHz):  $\delta$  177.9, 141.8, 132.4, 131.6, 131.5, 128.8, 119.0, 112.1, 77.7, 52.6, 47.9, 22.8, 19.3 ppm; HRMS  $m/z$  Calcd. for  $\text{C}_{13}\text{H}_{15}\text{NO}_3$ : 233.10519. Found: 233.10548.

**Methyl 3-hydroxy-3-(4-cyanophenyl)-2,2-dimethylpropionate (Table 3, entry 8)<sup>2</sup>:**



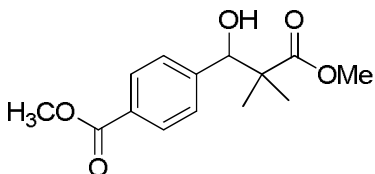
The general procedure was followed for the synthesis and purification; product was afforded as a colorless oil in 74% isolated yield.

**Methyl 3-hydroxy-3-(4-chlorophenyl)-2,2-dimethylpropionate (Table 3, entry 9)<sup>2</sup>:**

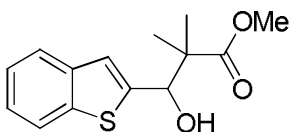


The general procedure was followed for the synthesis and purification; product was afforded as a colorless oil in 91% isolated yield.

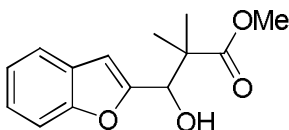
**Methyl 3-hydroxy-3-(4-methoxycarbonylphenyl)-2,2-dimethylpropionate (Table 3, entry 10)<sup>6</sup>:**



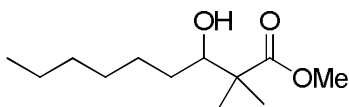
The general procedure was followed for the synthesis and purification; product was afforded as a white solid in 82% isolated yield.

**Methyl 3-(benzo[*b*]thiophen-2-yl)-3-hydroxy-2,2-dimethylpropanoate (Table 4, entry 1):**

The general procedure was followed for the synthesis and purification; product was afforded as a yellow solid in 92% isolated yield.  $^1\text{H}$  NMR ( $\text{CDCl}_3$ , 400 MHz):  $\delta$  7.79 (d, 1H,  $J = 7.6$  Hz), 7.72 (d, 1H,  $J = 8.0$  Hz), 7.36–7.29 (m, 2H), 7.18 (s, 1H), 5.15 (d, 1H,  $J = 4.0$  Hz), 3.76 (s, 3H), 3.51 (d, 1H,  $J = 4.8$  Hz), 1.28 (s, 6H) ppm;  $^{13}\text{C}$  NMR ( $\text{CDCl}_3$ , 100 MHz):  $\delta$  178.1, 145.1, 139.7, 139.4, 124.5, 124.4, 123.7, 122.5, 122.4, 76.1, 52.6, 48.1, 23.0, 20.5 ppm; HRMS  $m/z$  Calcd. for  $\text{C}_{14}\text{H}_{16}\text{O}_3\text{S}$ : 264.08202. Found: 264.08256.

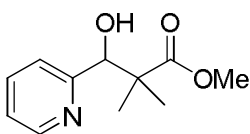
**Methyl 3-(benzofuran-2-yl)-3-hydroxy-2,2-dimethylpropanoate (Table 4, entry 2):**

The general procedure was followed for the synthesis and purification; product was afforded as a colorless oil in 89% isolated yield.  $^1\text{H}$  NMR ( $\text{CDCl}_3$ , 400 MHz):  $\delta$  7.53 (d, 1H,  $J = 7.6$  Hz), 7.44 (d, 1H,  $J = 8.4$  Hz), 7.28–7.20 (m, 2H), 6.64 (s, 1H), 4.94 (s, 1H), 3.75 (s, 3H), 3.71 (bs, 1H), 1.28 (s, 3H), 1.27 (s, 3H) ppm;  $^{13}\text{C}$  NMR ( $\text{CDCl}_3$ , 100 MHz):  $\delta$  177.8, 156.9, 154.8, 128.1, 124.4, 123.1, 121.2, 111.5, 105.0, 74.0, 52.5, 47.4, 23.1, 20.5 ppm; HRMS  $m/z$  Calcd. for  $\text{C}_{14}\text{H}_{16}\text{O}_4$ : 248.10486. Found: 248.10539.

**Methyl 3-hydroxynonanoate (Table 4, entry 3):**

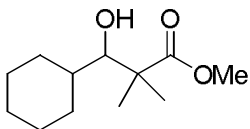
The general procedure was followed for the synthesis and purification; product was afforded as a colorless oil in 80% isolated yield.  $^1\text{H}$  NMR ( $\text{CDCl}_3$ , 400 MHz):  $\delta$  3.67 (s, 3H), 3.57 (d, 1H,  $J = 4.0$  Hz), 1.26–1.14 (m, 16H), 0.87–0.84 (m, 4H) ppm;  $^{13}\text{C}$  NMR ( $\text{CDCl}_3$ , 100 MHz):  $\delta$  178.3, 76.7, 51.9, 47.2, 31.8, 31.7, 29.3, 26.7, 22.7, 22.3, 20.4, 14.1 ppm; HRMS  $m/z$  Calcd. for  $\text{C}_{12}\text{H}_{24}\text{O}_3$ : 216.17254. Found: 216.17291.

**Methyl 3-hydroxy-2,2-dimethyl-3-(2-pyridyl)propanoate (Table 4, entry 4)<sup>6</sup>:**



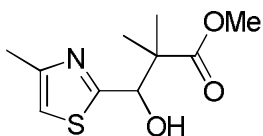
The general procedure was followed for the synthesis and purification; product was afforded as a colorless oil in 67% isolated yield.

**Methyl 3-cyclohexyl-3-hydroxypropanoate (Table 4, entry 5)<sup>7</sup>:**



The general procedure was followed for the synthesis and purification; product was afforded as a colorless oil in 67% isolated yield.

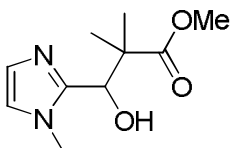
**Methyl 3-hydroxy-2,2-dimethyl-3-(4-methylthiazol-2-yl)propanoate (Table 4, entry 6):**



The general procedure was followed for the synthesis and purification; product was afforded as a yellow solid in 36% isolated yield.  $^1\text{H}$  NMR ( $\text{CDCl}_3$ , 400 MHz):  $\delta$  6.81 (s, 1H), 5.08 (d, 1H,  $J = 4.0$  Hz), 4.22 (d, 1H,  $J = 8.0$  Hz), 3.71 (s, 3H), 2.38 (s, 3H), 1.21 (s, 3H), 1.21 (s, 3H)

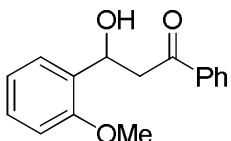
ppm;  $^{13}\text{C}$  NMR ( $\text{CDCl}_3$ , 100 MHz):  $\delta$  177.5, 170.3, 152.1, 114.0, 76.4, 52.4, 48.1, 21.6, 20.9, 17.2 ppm; HRMS  $m/z$  Calcd. for  $\text{C}_{10}\text{H}_{15}\text{NO}_3\text{S}$ : 229.07726. Found: 229.07763.

**Methyl 3-hydroxy-2,2-dimethyl-3-(1-methyl-1*H*-imidazol-2-yl)propanoate (Table 4, entry 7):**



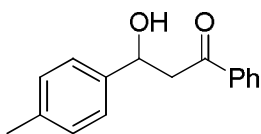
The general procedure was followed for the synthesis and purification; product was afforded as a colorless solid in 77% isolated yield.  $^1\text{H}$  NMR ( $\text{CDCl}_3$ , 400 MHz):  $\delta$  6.82 (d, 1H,  $J = 1.2$  Hz), 6.72 (d, 1H,  $J = 0.8$  Hz), 4.73 (s, 1H), 4.50 (bs, 1H), 3.66 (s, 3H), 3.65 (s, 3H), 1.23 (s, 3H), 1.22 (s, 3H) ppm;  $^{13}\text{C}$  NMR ( $\text{CDCl}_3$ , 100 MHz):  $\delta$  177.9, 147.0, 127.2, 121.5, 71.7, 52.3, 47.5, 33.5, 23.1, 21.3 ppm; HRMS  $m/z$  Calcd. for  $\text{C}_{10}\text{H}_{16}\text{N}_2\text{O}_3$ : 212.11609. Found: 212.11649.

**3-Hydroxy-3-(2-methoxy-phenyl)-1-phenyl-propan-1-one (Table 5, entry 1)<sup>8</sup>:**



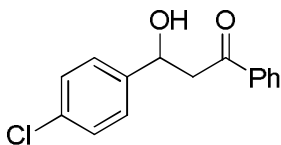
The general procedure was followed for the synthesis and purification; product was afforded as a white solid in 82% isolated yield.

**3-Hydroxy-1-phenyl-3-*p*-tolyl-propan-1-one (Table 5, entry 2)<sup>8</sup>:**



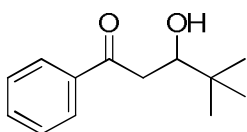
The general procedure was followed for the synthesis and purification; product was afforded as a colorless oil in 77% isolated yield.

**3-(*p*-Chlorophenyl)-3-hydroxy-1-phenylpropan-1-one (Table 5, entry 3)<sup>8</sup>:**



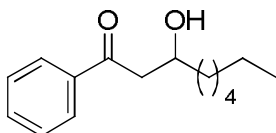
The general procedure was followed for the synthesis and purification; product was afforded as a colorless solid in 69% isolated yield.

**3-Hydroxy-4,4-dimethyl-1-phenyl-1-pentanone (Table 5, entry 4)<sup>9</sup>:**



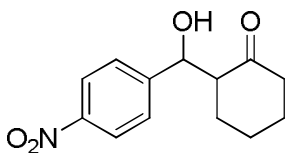
The general procedure was followed for the synthesis and purification; product was afforded as a colorless oil in 74% isolated yield.

**3-Hydroxy-1-phenyl-1-nonanone (Table 5, entry 5):**

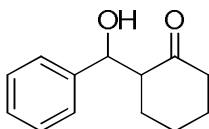


The general procedure was followed for the synthesis and purification; product was afforded as a colorless oil in 80% isolated yield. <sup>1</sup>H NMR (CDCl<sub>3</sub>, 300 MHz): δ 7.97–7.94 (m, 2H), 7.60–7.44 (m, 3H), 4.21 (bs, 1H), 3.26–2.98 (m, 3H), 1.63–1.29 (m, 10H), 0.89–0.86 (m, 3H) ppm; <sup>13</sup>C NMR (CDCl<sub>3</sub>, 75 MHz): δ 201.3, 131.9, 133.8, 128.9, 128.3, 68.0, 45.2, 36.7, 32.0, 29.5, 25.7, 22.8, 14.3 ppm; HRMS *m/z* Calcd. for C<sub>15</sub>H<sub>22</sub>O<sub>2</sub>: 234.16197. Found: 234.16226.

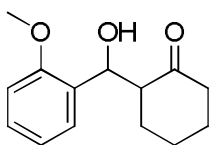


**2-[Hydroxy(4-nitrophenyl)methyl]-cyclohexanone (Table 5, entry 6)<sup>10</sup>:**

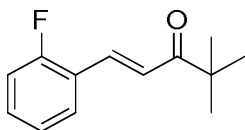
The general procedure was followed for the synthesis and purification; product was afforded as a yellow solid in 91% isolated yield.

**2-(Hydroxyphenylmethyl)-cyclohexanone (Table 5, entry 7)<sup>11</sup>:**

The general procedure was followed for the synthesis and purification; product was afforded as a white solid in 76% isolated yield.

**2-[Hydroxy(2-methoxyphenyl)methyl]-cyclohexanone (Table 5, entry 8)<sup>12</sup>:**

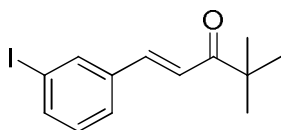
The general procedure was followed for the synthesis and purification; product was afforded as a yellow oil in 91% isolated yield.

**(E)-1-(2-Fluorophenyl)-4,4-dimethylpent-1-en-3-one (Table 6, entry 1):**

The general procedure was followed for the synthesis and purification; product was afforded as a colorless oil in 92% isolated yield. <sup>1</sup>H NMR (CDCl<sub>3</sub>, 400 MHz): δ 7.75 (d, 1H, *J* = 16 Hz), 7.54 (t, 1H, *J* = 8 Hz), 7.34–7.29 (m, 1H), 7.22 (d, 1H, *J* = 16.0 Hz), 7.13 (t, 1H, 8.0

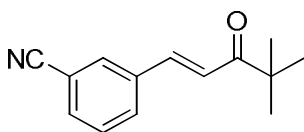
Hz), 7.07 (t, 1H,  $J = 8.0$  Hz), 1.21 (s, 9H) ppm;  $^{13}\text{C}$  NMR ( $\text{CDCl}_3$ , 100 MHz):  $\delta$  204.3, 161.8 (d,  $J = 250$  Hz), 135.8 (d,  $J = 2.0$  Hz), 131.6 (d,  $J = 9$  Hz), 129.9 (d,  $J = 3.0$  Hz), 124.6 (d,  $J = 3.0$  Hz), 123.5 (d,  $J = 7$  Hz), 123.2 (d,  $J = 12.0$  Hz), 116.4 (d, 22.0 Hz), 43.4, 26.4 ppm; HRMS  $m/z$  Calcd for  $\text{C}_{13}\text{H}_{15}\text{FO}$ : 206.11069. Found: 206.11108.

**(E)-1-(3-Iodophenyl)-4,4-dimethylpent-1-en-3-one (Table 7, entry 1):**

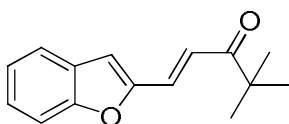


The general procedure was followed for the synthesis and purification; product was afforded as a yellow oil in 95% isolated yield.  $^1\text{H}$  NMR ( $\text{CDCl}_3$ , 400 MHz):  $\delta$  7.88 (s, 1H), 7.65 (d, 1H,  $J = 8.0$  Hz), 7.51 (d, 1H,  $J = 16.0$  Hz), 7.47 (d, 1H,  $J = 8.0$  Hz), 7.10–7.05 (m, 2H), 1.20 (s, 9H) ppm;  $^{13}\text{C}$  NMR ( $\text{CDCl}_3$ , 100 MHz):  $\delta$  204.0, 141.3, 139.0, 137.3, 136.8, 130.7, 128.0, 122.0, 95.0, 43.5, 26.5 ppm; HRMS  $m/z$  Calcd for  $\text{C}_{13}\text{H}_{15}\text{OI}$ : 314.0176. Found: 314.0168.

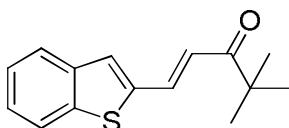
**(E)-3-(4,4-Dimethyl-3-oxopent-1-enyl)benzonitrile (Table 7, entry 2):**



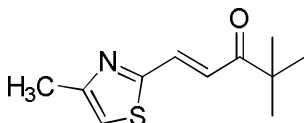
The general procedure was followed for the synthesis and purification; product was afforded as a colorless oil in 94% isolated yield.  $^1\text{H}$  NMR ( $\text{CDCl}_3$ , 400 MHz):  $\delta$  7.82 (s, 1H), 7.74 (d, 1H,  $J = 8.0$  Hz), 7.62–7.60 (m, 1H), 7.58 (d, 1H,  $J = 16.0$  Hz), 7.48 (t, 1H,  $J = 8.0$  Hz), 7.15 (d, 1H,  $J = 16.0$  Hz), 1.21 (s, 9H) ppm;  $^{13}\text{C}$  NMR ( $\text{CDCl}_3$ , 100 MHz):  $\delta$  203.8, 140.2, 136.3, 133.2, 132.6, 131.4, 129.9, 123.2, 118.4, 113.4, 43.6, 26.3 ppm; HRMS  $m/z$  Calcd for  $\text{C}_{14}\text{H}_{15}\text{NO}$ : 213.11536. Found: 213.11582.

**(E)-1-(Benzofuran-2-yl)-4,4-dimethylpent-1-en-3-one (Table 7, entry 3):**

The general procedure was followed for the synthesis and purification; product was afforded as a colorless oil in 77% isolated yield.  $^1\text{H}$  NMR ( $\text{CDCl}_3$ , 400 MHz):  $\delta$  7.53 (d, 1H,  $J = 16.0$  Hz), 7.53 (bs, 1H), 7.47 (d, 1H,  $J = 8.0$  Hz), 7.31 (dt, 1H,  $J = 8.0$  Hz,  $J = 1.2$  Hz), 7.24 (d, 1H,  $J = 16.0$  Hz), 7.20 (d, 1H,  $J = 8.0$  Hz), 6.90 (s, 1H), 1.24 (s, 9H) ppm;  $^{13}\text{C}$  NMR ( $\text{CDCl}_3$ , 100 MHz):  $\delta$  204.0, 155.6, 153.2, 129.5, 128.7, 126.6, 123.5, 121.9, 121.3, 112.0, 111.5, 43.5, 26.5 ppm; HRMS  $m/z$  Calcd for  $\text{C}_{15}\text{H}_{16}\text{O}_2$ : 228.11503. Found: 228.11549.

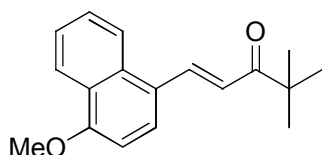
**(E)-1-(Benzo[*b*]thiophen-2-yl)-4,4-dimethylpent-1-en-3-one (Table 7, entry 4):**

The general procedure was followed for the synthesis and purification; product was afforded as a yellow oil in 83% isolated yield.  $^1\text{H}$  NMR ( $\text{CDCl}_3$ , 400 MHz):  $\delta$  7.87 (d, 1H,  $J = 16.0$  Hz), 7.79–7.74 (m, 2H), 7.49 (s, 1H), 7.39–7.33 (m, 2H), 6.95 (d, 1H,  $J = 16.0$  Hz), 1.24 (s, 9H) ppm;  $^{13}\text{C}$  NMR ( $\text{CDCl}_3$ , 100 MHz):  $\delta$  203.9, 140.4, 140.1, 139.8, 136.1, 129.5, 126.4, 125.0, 124.6, 122.6, 122.2, 43.4, 26.5 ppm; HRMS  $m/z$  Calcd for  $\text{C}_{15}\text{H}_{16}\text{OS}$ : 244.09219. Found: 244.09266.

**(E)-4,4-Dimethyl-1-(4-methylthiazol-2-yl)pent-1-en-3-one (Table 7, entry 5):**

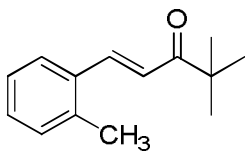
The general procedure was followed for the synthesis and purification; product was afforded as a yellow oil in 94% isolated yield.  $^1\text{H}$  NMR ( $\text{CDCl}_3$ , 400 MHz):  $\delta$  7.60 (d, 1H,  $J = 16.0$  Hz), 7.35 (d, 1H,  $J = 16.0$  Hz), 6.96 (s, 1H), 2.45 (s, 3H), 1.18 (s, 9H) ppm;  $^{13}\text{C}$  NMR ( $\text{CDCl}_3$ , 100 MHz):  $\delta$  203.8, 163.2, 155.3, 133.8, 124.2, 116.7, 43.6, 26.3, 17.4 ppm; HRMS  $m/z$  Calcd for  $\text{C}_{11}\text{H}_{15}\text{NO}$ : 209.08743. Found: 209.08770.

**(E)-1-(4-Methoxynaphthalen-1-yl)-4,4-dimethylpent-1-en-3-one (Table 7, entry 6):**



The general procedure was followed for the synthesis and purification; product was afforded as a white solid in 78% isolated yield.  $^1\text{H}$  NMR ( $\text{CDCl}_3$ , 400 MHz):  $\delta$  8.49 (d, 1H,  $J = 15.6$  Hz), 8.31 (d, 1H,  $J = 8.0$  Hz), 8.20 (d, 1H,  $J = 8.0$  Hz), 7.79 (d, 1H,  $J = 8.0$  Hz), 7.61–7.50 (m, 2H), 7.14 (d, 1H,  $J = 16.0$  Hz), 6.83 (d, 1H,  $J = 8.0$  Hz), 4.04 (s, 3H), 1.27 (s, 9H) ppm;  $^{13}\text{C}$  NMR ( $\text{CDCl}_3$ , 100 MHz):  $\delta$  204.4, 157.6, 140.0, 133.0, 125.8, 124.9, 123.5, 122.8, 121.3, 103.8, 55.9, 43.4, 26.7 ppm; HRMS  $m/z$  Calcd for  $\text{C}_{18}\text{H}_{20}\text{O}_2$ : 268.14632. Found: 268.14673.

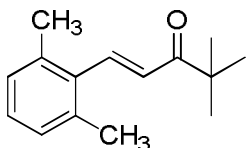
**(E)-4,4-Dimethyl-1-o-tolylpent-1-en-3-one (Table 7, entry 7):**



The general procedure was followed for the synthesis and purification; product was afforded as a white solid in 90% isolated yield.  $^1\text{H}$  NMR ( $\text{CDCl}_3$ , 400 MHz):  $\delta$  7.99 (d, 1H,  $J = 16.0$  Hz), 7.60 (d, 1H,  $J = 8.0$  Hz), 7.27–7.19 (m, 3H), 7.05 (d, 1H,  $J = 16.0$  Hz), 2.44 (s, 3H),

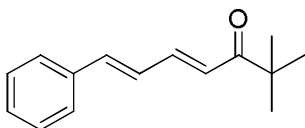
1.24 (s, 9H) ppm;  $^{13}\text{C}$  NMR ( $\text{CDCl}_3$ , 100 MHz):  $\delta$  204.5, 140.7, 138.4, 134.2, 131.1, 130.1, 126.5, 126.4, 122.1, 43.5, 26.6, 20.1 ppm; HRMS  $m/z$  Calcd for  $\text{C}_{14}\text{H}_{18}\text{O}$ : 202.13576. Found: 202.13610.

**(E)-1-(2,6-Dimethylphenyl)-4,4-dimethylpent-1-en-3-one (Table 7, entry 8):**



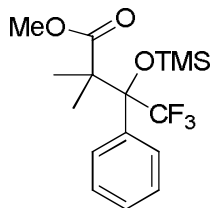
The general procedure was followed for the synthesis and purification; product was afforded as a white solid in 72% isolated yield.  $^1\text{H}$  NMR ( $\text{CDCl}_3$ , 400 MHz):  $\delta$  7.80 (d, 1H,  $J = 16.0$  Hz), 7.12–7.06 (m, 3H), 6.74 (dd, 1H,  $J = 16.0$  Hz,  $J = 1.2$  Hz), 2.34 (s, 6H), 1.21 (s, 9H) ppm;  $^{13}\text{C}$  NMR ( $\text{CDCl}_3$ , 100 MHz):  $\delta$  204.4, 141.4, 136.9, 135.1, 128.4, 128.3, 127.1, 43.4, 26.3, 21.3 ppm; HRMS  $m/z$  Calcd for  $\text{C}_{15}\text{H}_{20}\text{O}$ : 216.15141. Found: 216.15173.

**(4E,6E)-2,2-Dimethyl-7-phenylhepta-4,6-dien-3-one (Table 7, entry 9):**



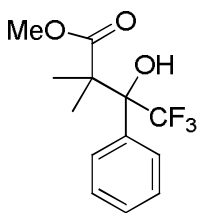
The general procedure was followed for the synthesis and purification; product was afforded as a yellow oil in 95% isolated yield.  $^1\text{H}$  NMR ( $\text{CDCl}_3$ , 400 MHz):  $\delta$  7.50–7.46 (m, 3H), 7.37–7.30 (m, 3H), 6.94–6.92 (m, 2H), 6.69 (d, 1H,  $J = 12.0$  Hz), 1.20 (s, 9H) ppm;  $^{13}\text{C}$  NMR ( $\text{CDCl}_3$ , 100 MHz):  $\delta$  204.6, 143.1, 141.3, 136.4, 129.2, 129.0, 127.3, 127.1, 124.5, 43.3, 26.6 ppm; HRMS  $m/z$  Calcd for  $\text{C}_{15}\text{H}_{18}\text{O}$ : 214.13576. Found: 214.13625.

**Methyl 4,4,4-trifluoro-2,2-dimethyl-3-phenyl-3-(trimethylsilyloxy)butanoate (Scheme 3, product 8):**



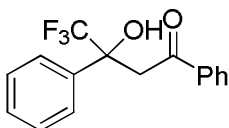
The general procedure was followed for the synthesis and purification; product was afforded as a yellow oil in 91% isolated yield.  $^1\text{H}$  NMR ( $\text{CDCl}_3$ , 400 MHz):  $\delta$  7.48–7.45 (m, 2H), 7.35–7.33 (m, 3H), 3.60 (s, 3H), 1.22 (s, 3H), 1.19 (s, 3H), 0.14 (s, 9H) ppm;  $^{13}\text{C}$  NMR ( $\text{CDCl}_3$ , 100 MHz):  $\delta$  174.8, 136.5, 128.5, 127.8, 127.3, 126.1 (q,  $J = 288$  Hz) 84.6 (q,  $J = 26.9$  Hz), 51.9, 50.9, 26.8, 22.7, 1.8 ppm; HRMS  $m/z$  Calcd for  $\text{C}_{16}\text{H}_{17}\text{F}_3\text{O}$ : 348.13686. Found: 348.13754.

**Methyl 4,4,4-trifluoro-3-hydroxy-2,2-dimethyl-3-phenylbutanoate (Scheme 3, product 9)<sup>2</sup>:**



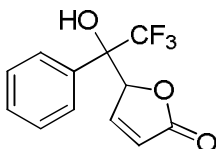
The general procedure was followed for the synthesis and purification; product was afforded as a colorless oil in 78% isolated yield.

**4,4,4-Trifluoro-3-hydroxy-1,3-diphenyl-1-butanone (Scheme 3, product 10)<sup>2</sup>:**



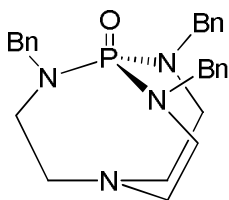
The general procedure was followed for the synthesis and purification; product was afforded as a colorless oil in 93% isolated yield.

**5-(2,2,2-Trifluoro-1-hydroxy-1-phenylethyl)furan-2(5H)-one (Scheme 3, product 11):**



The general procedure was followed for the synthesis and purification; product was afforded as a white solid in 83% isolated yield. *Syn* isomer (white solid)  $^1\text{H}$  NMR ( $\text{CDCl}_3$ , 400 MHz):  $\delta$  7.61–7.60 (m, 2H), 7.49–7.45 (m, 3H), 6.84–6.82 (m, 1H), 6.18–6.16 (m, 1H), 5.71 (t, 1H,  $J = 4.0$  Hz), 4.1 (s, 1H) ppm;  $^{13}\text{C}$  NMR ( $\text{CDCl}_3$ , 100 MHz):  $\delta$  173.0, 152.5, 133.4, 129.8, 129.2, 125.6, 124.5 (q,  $J = 280$  Hz), 124.0, 83.6, 76.6 (q,  $J = 29$  Hz) ppm; HRMS  $m/z$  Calcd for  $\text{C}_{12}\text{H}_9\text{F}_3\text{O}_3$ : 258.05038. Found: 258.05075. *Anti* isomer (yellow oil)  $^1\text{H}$  NMR ( $\text{CDCl}_3$ , 400 MHz):  $\delta$  7.56–7.54 (m, 3H), 7.42–7.39 (m, 3H), 6.04–6.02 (m, 1H), 5.58 (s, 1H), 3.66 (s, 1H) ppm;  $^{13}\text{C}$  NMR ( $\text{CDCl}_3$ , 100 MHz):  $\delta$  172.2, 152.5, 133.3, 129.8, 128.9, 126.4, 124.5 (q,  $J = 280$  Hz), 124.0, 83.2, 77.9 (q,  $J = 20$  Hz) ppm; HRMS  $m/z$  Calcd for  $\text{C}_{12}\text{H}_9\text{F}_3\text{O}_3$ : 258.05038. Found: 258.05076.

**2,8,9-Tribenzyl-2,5,8,9-tetraaza-1-phosphabicyclo[3.3.3]undecane 1-oxide (12):**



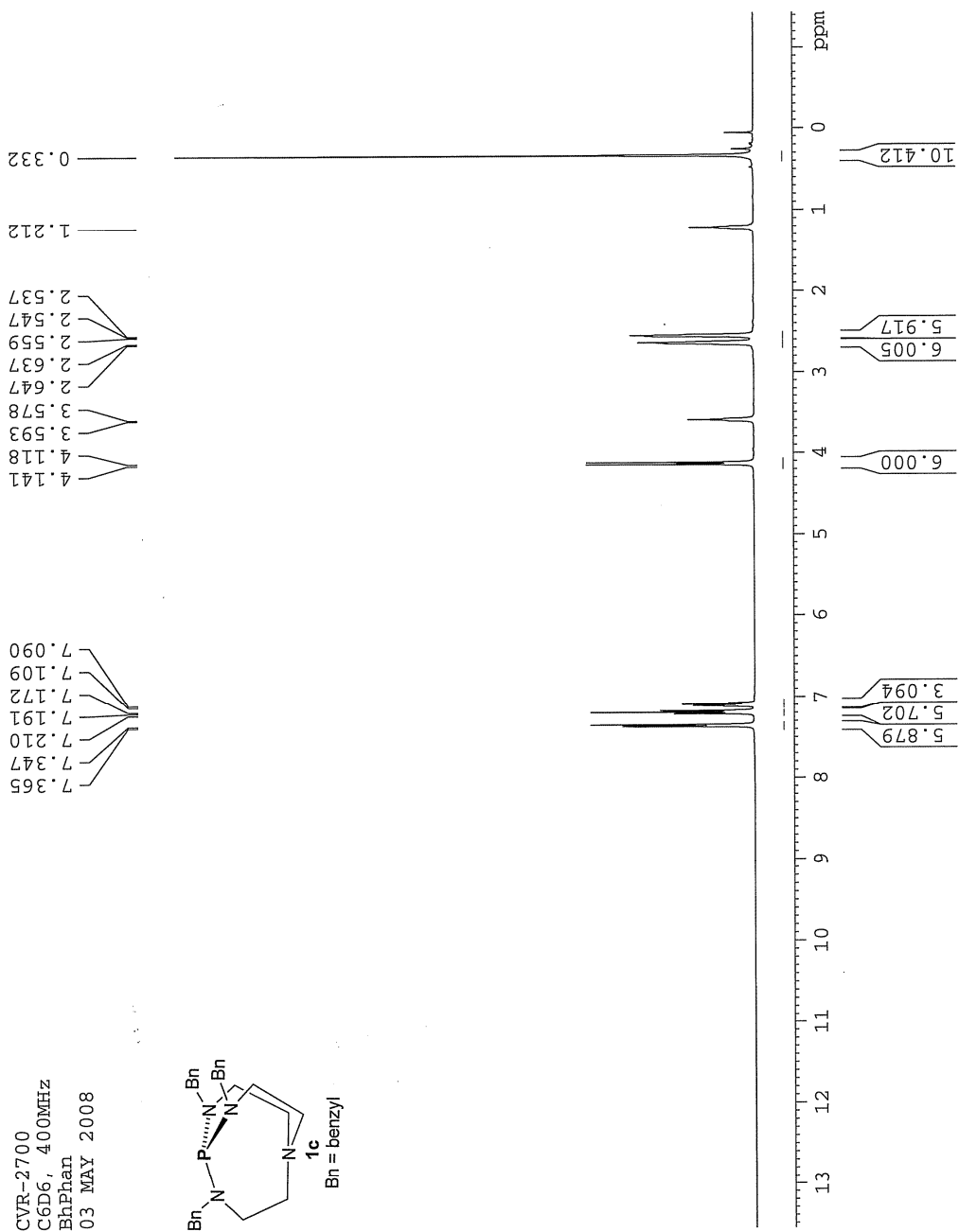
$^{31}\text{P}$  NMR ( $\text{CDCl}_3$ , 162 MHz): 24.24.  $^1\text{H}$  NMR ( $\text{CDCl}_3$ ): 7.61–7.59 (m, 6H), 7.37–7.26 (m, 9H), 4.25 (d, 6H,  $J = 8.0$  Hz), 2.88–2.79 (m, 12H) ppm.  $^{13}\text{C}$  NMR ( $\text{CDCl}_3$ ): 139.9 (d,  $J = 2.3$

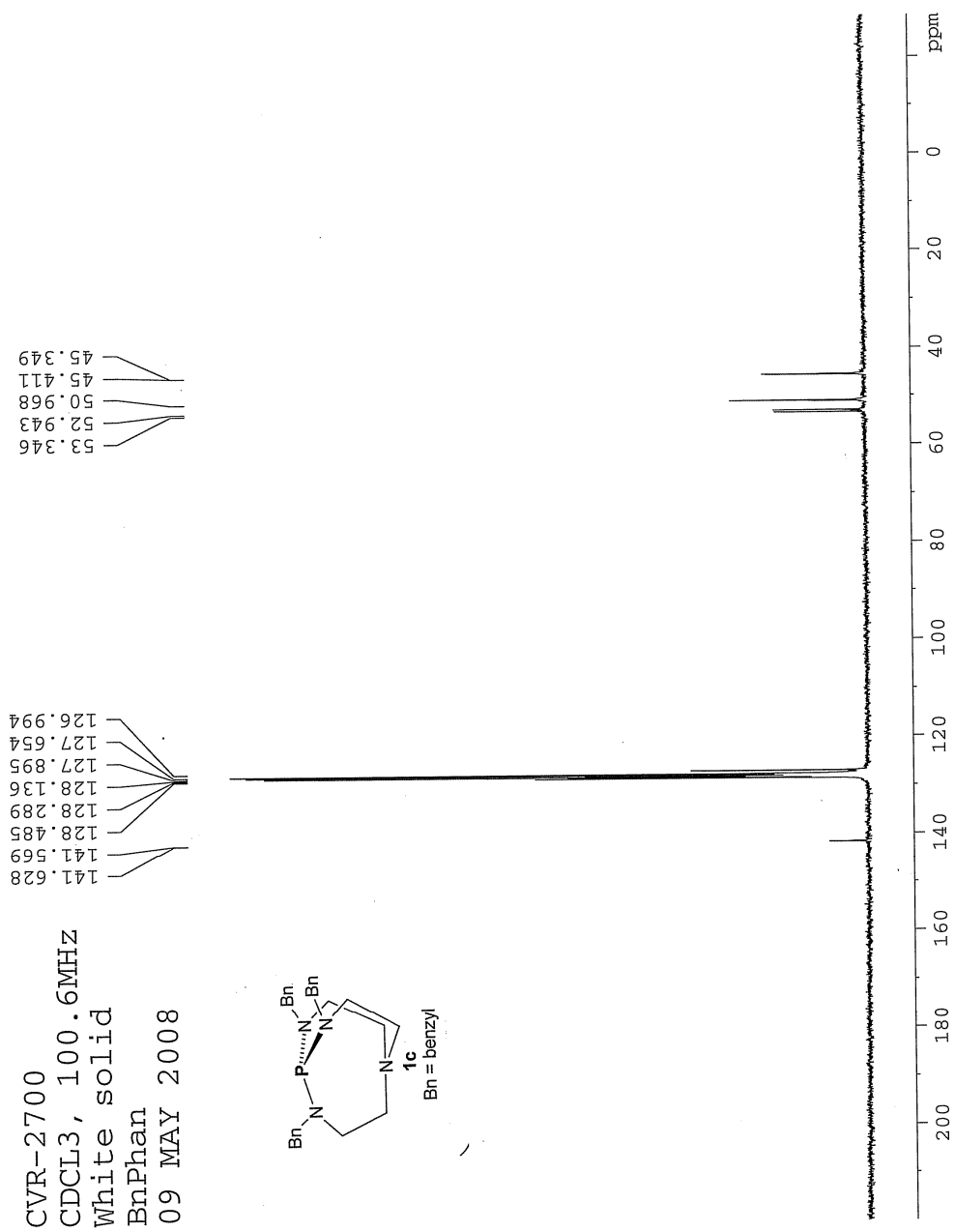
Hz), 128.9, 128.5, 127.4, 50.9 (d,  $J = 5.0$  Hz), 50.0, 47.4 (d,  $J = 3.3$  Hz) ppm. HRMS  $m/z$  calcd for  $C_{27}H_{33}N_4OP$ : 460.23919. Found: 460.24045.

## References

1. (a) Su, W.; Uргаonkar, S.; McLaughlin, P. A.; Verkade, J. G. *J. Am. Chem. Soc.* **2004**, *126*, 16433–16439. (b) Venkat Reddy, Ch.; Verkade, J. G. *J. Org. Chem.* **2007**, *72*, 3093–3096. (c) Kisanga, P. B.; Verkade, J. G. *Tetrahedron* **2001**, *57*, 467–475.
2. Song, J. J.; Tan, Z.; Reeves, J. T.; Yee, N. K.; Senanayake, C. H. *Org. Lett.* **2007**, *9*, 1013–1016.
3. Takeuchi, M.; Akiyama, R.; Kobayashi, S. *J. Am. Chem. Soc.* **2005**, *127*, 13096–13097.
4. Fujisawa, H.; Nakagawa, T.; Mukaiyama, T. *Adv. Synth. Catal.* **2004**, *346*, 1241–1246.
5. Nakagawa, T.; Fujisawa, H.; Nagata, Y.; Mukaiyama, T. *Bull. Chem. Soc. Jap.* **2004**, *77*, 1555–1567.
6. Liu, S.-Y.; Hills, I. D.; Fu, G. C. *J. Am. Chem. Soc.* **2005**, *127*, 15352–15353.
7. Heydari, A.; Khaksar, S.; Sheykhani, M.; Tajbakhsh, M. *J. Mol. Catal. A: Chemical* **2008**, *287*, 5–8.
8. Xu, H.-J.; Liu, Y.-C.; Fu, Y.; Wu, Y.-D. *Org. Lett.* **2006**, *8*, 3449–3451.
9. Mukai, C.; Hashizume, S.; Nagami, K.; Hanaoka, M. *Chem. Pharm. Bull.* **1990**, *38*, 1509–1512.
10. Fernandez-Lopez, R.; Kofoed, J.; Machuqueiro, M.; Darbre, T. *Eur. J. Org. Chem.* **2005**, *24*, 5268–5276.
11. Rohr, K.; Herre, R.; Mahrwald, R. *Org. Lett.* **2005**, *7*, 4499–4501.
12. Rodriguez, B.; Rantanen, T.; Bolm, C. *Angew. Chem, Int. Ed.* **2006**, *45*, 6924–6926.

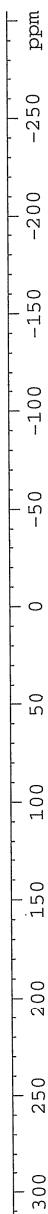
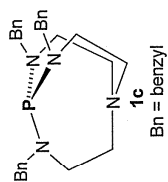


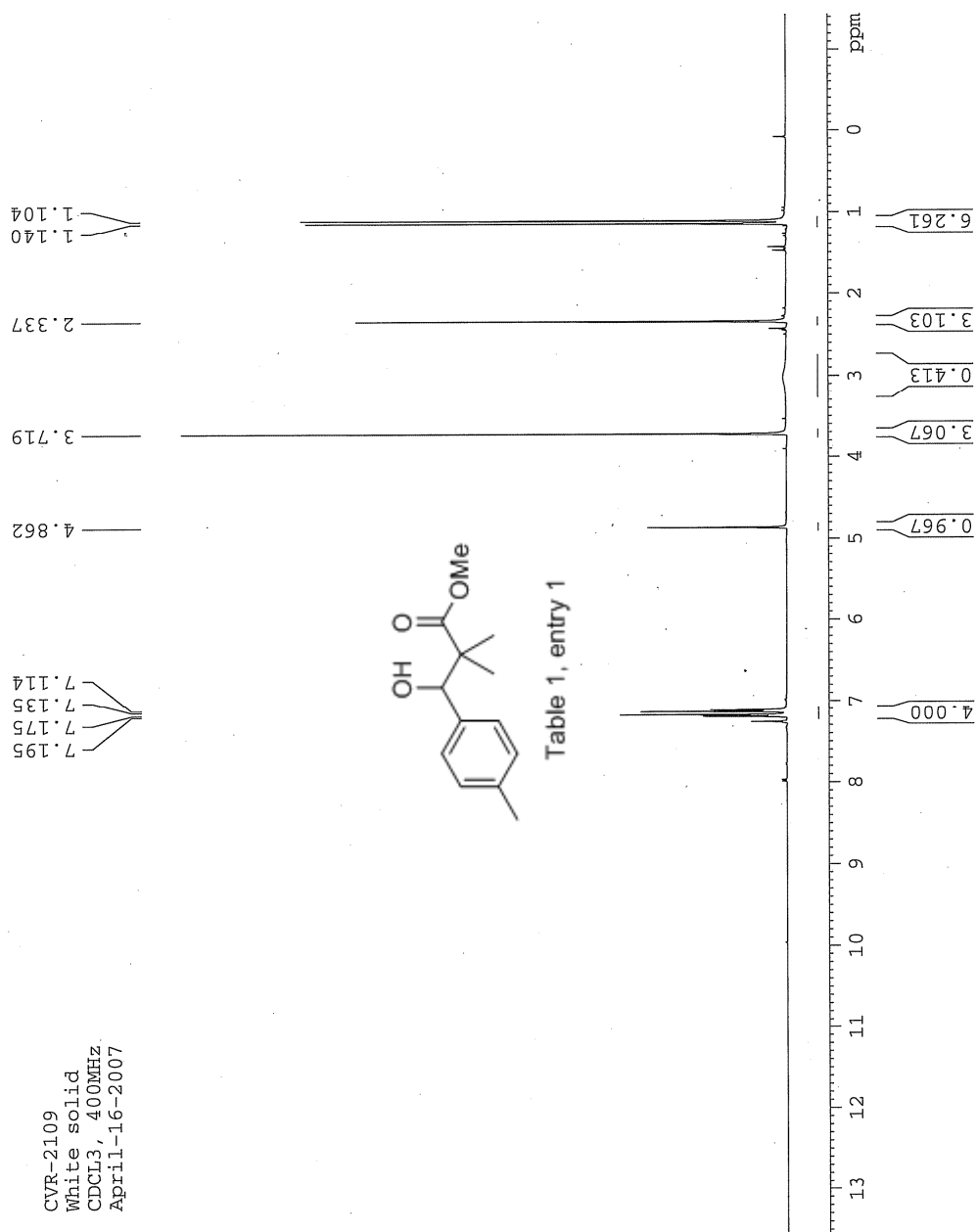


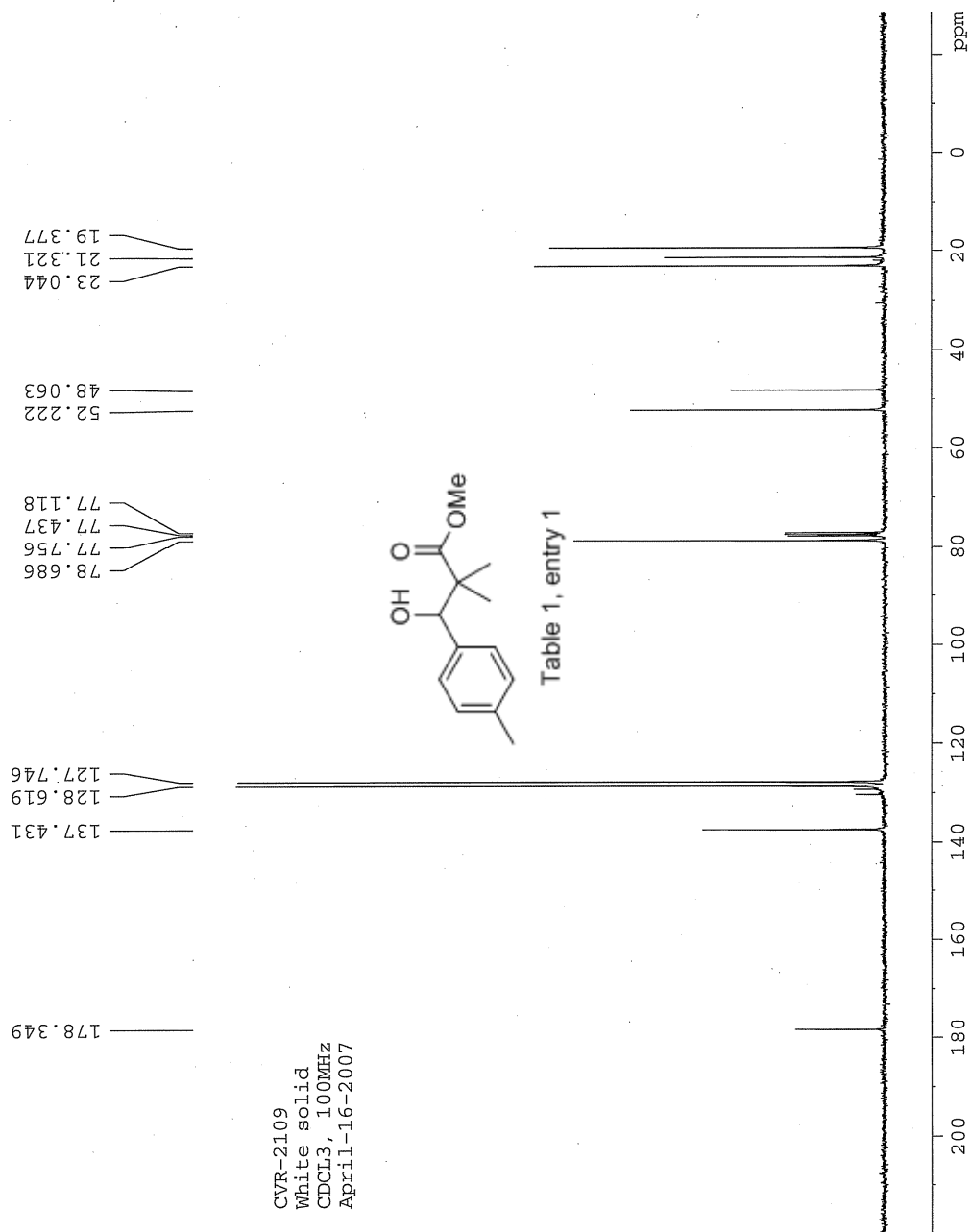


CVR-2713  
White Solid  
C6D6, 162.9MHz  
13P NMR  
9 SEP 2008

127.971







CVR-2122  
 WHITE SOLID  
 CDCl<sub>3</sub>, 300MHz  
 May-14-2007

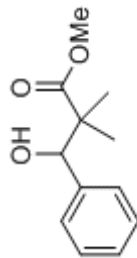
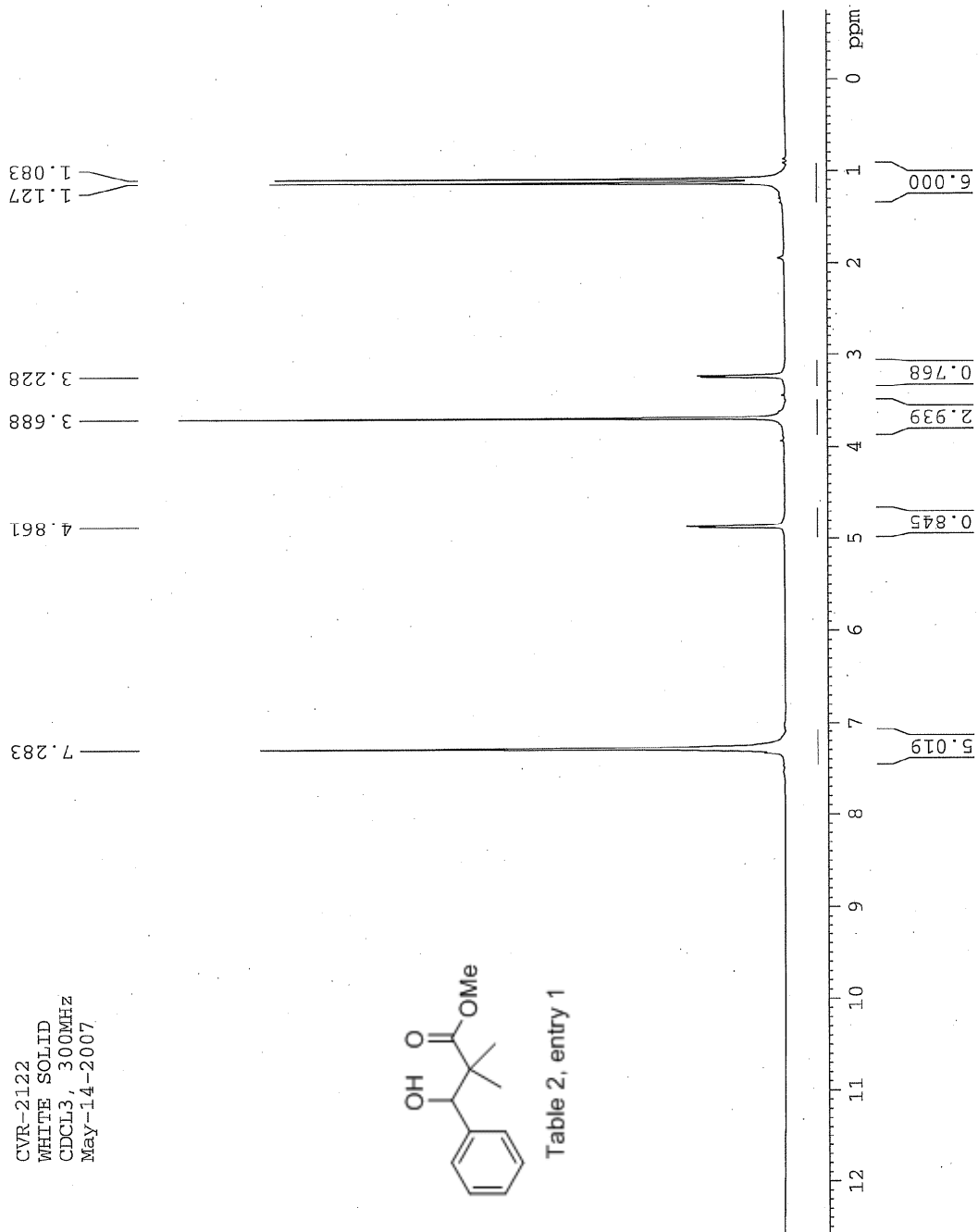
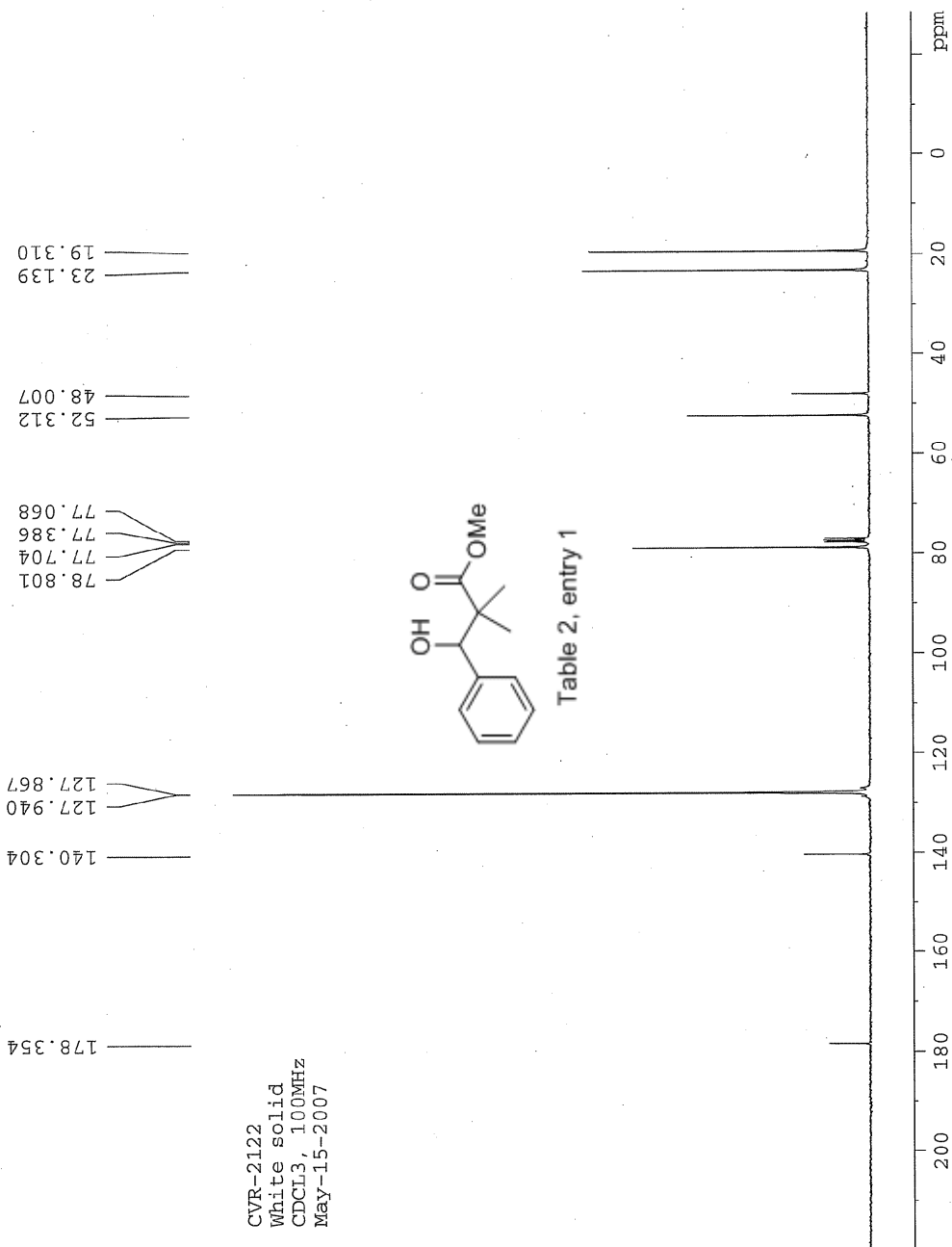
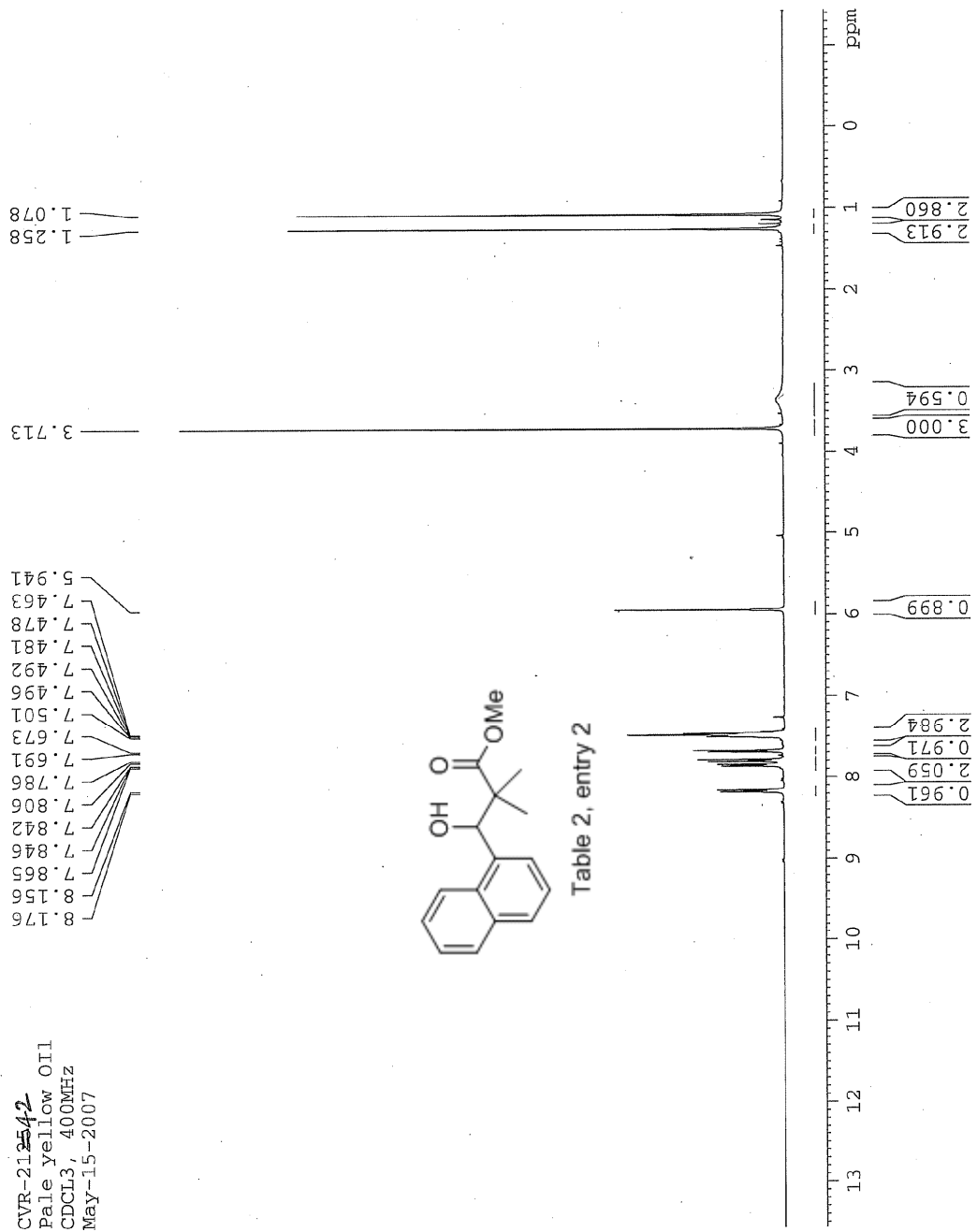


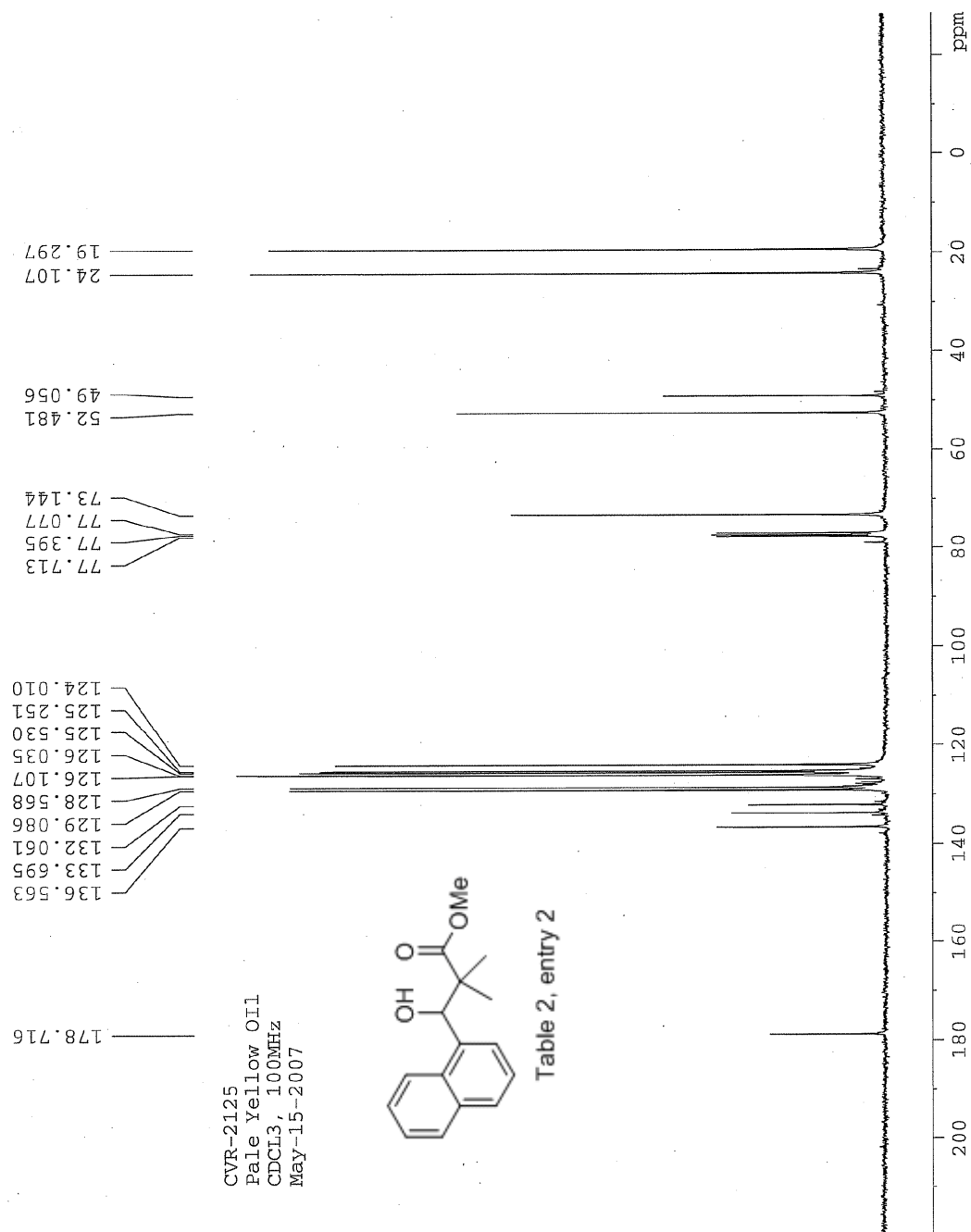
Table 2, entry 1

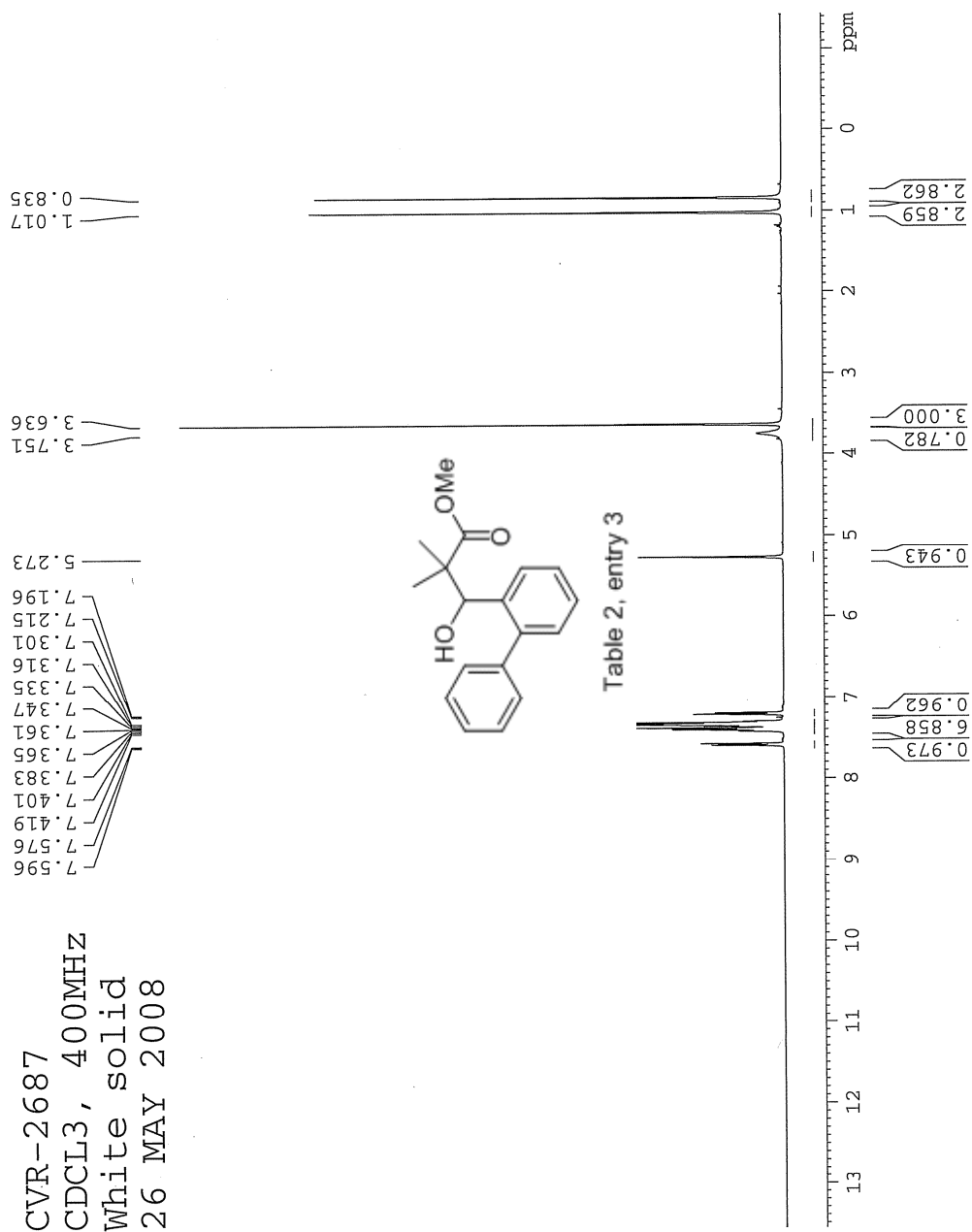


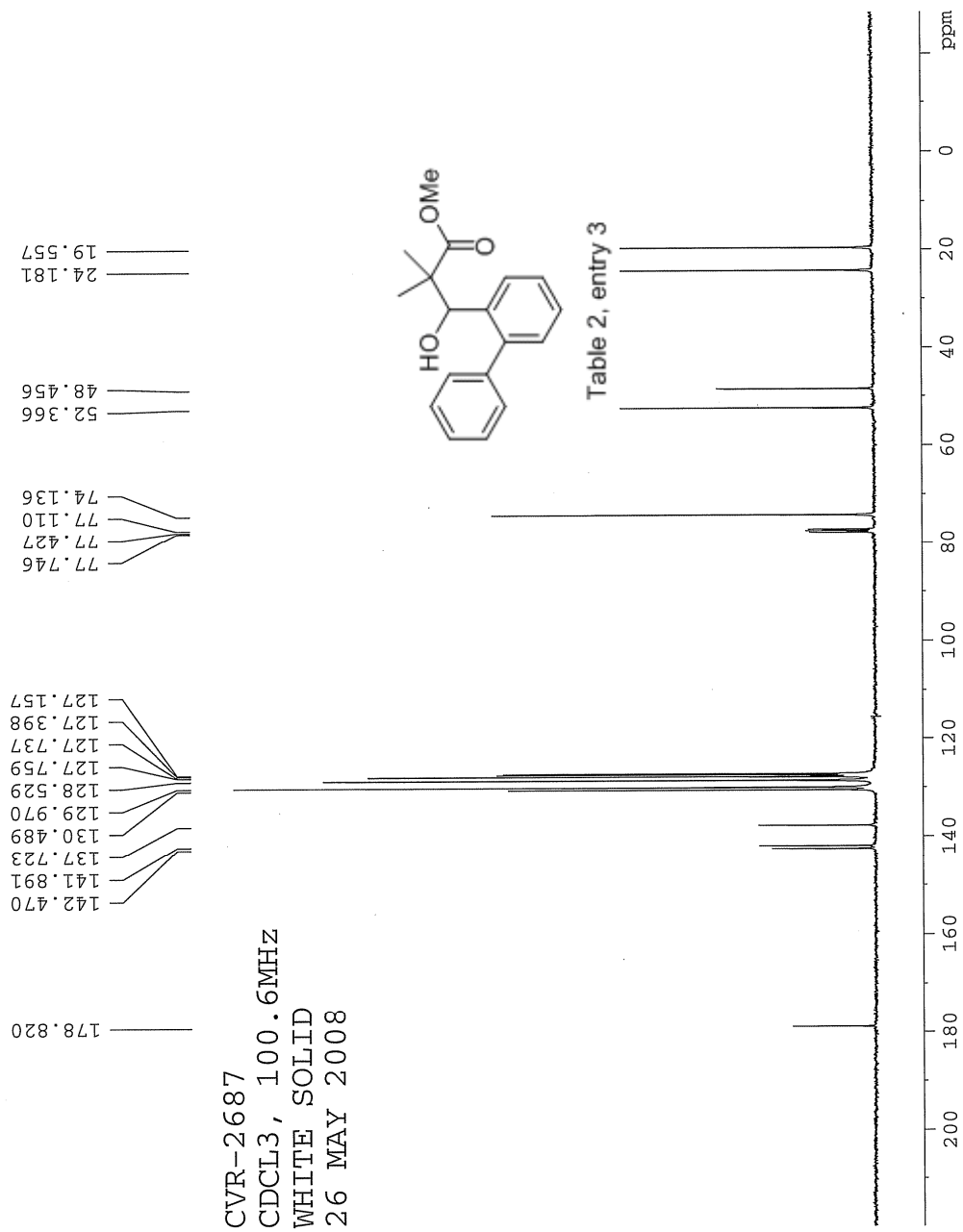












### Manual Peak Matching Report For Accurate Mass Determination

Theoretical mass	Experimental mass	PFK matching mass	Deviation*
284.14124	284.14179	280.98242	1.9 ppm

\* The deviation is obtained from the following equation:

$$\text{deviation} = \frac{\text{experimental mass} - \text{theoretical mass}}{\text{nominal mass}}$$

Where nominal mass takes in account only  $^{12}\text{C}$ ,  $^1\text{H}$ ,  $^{16}\text{O}$ ,  $^{14}\text{N}$  etc...

Theoretical mass correspond to the mass of the most abundant isotope peak

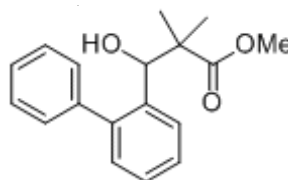
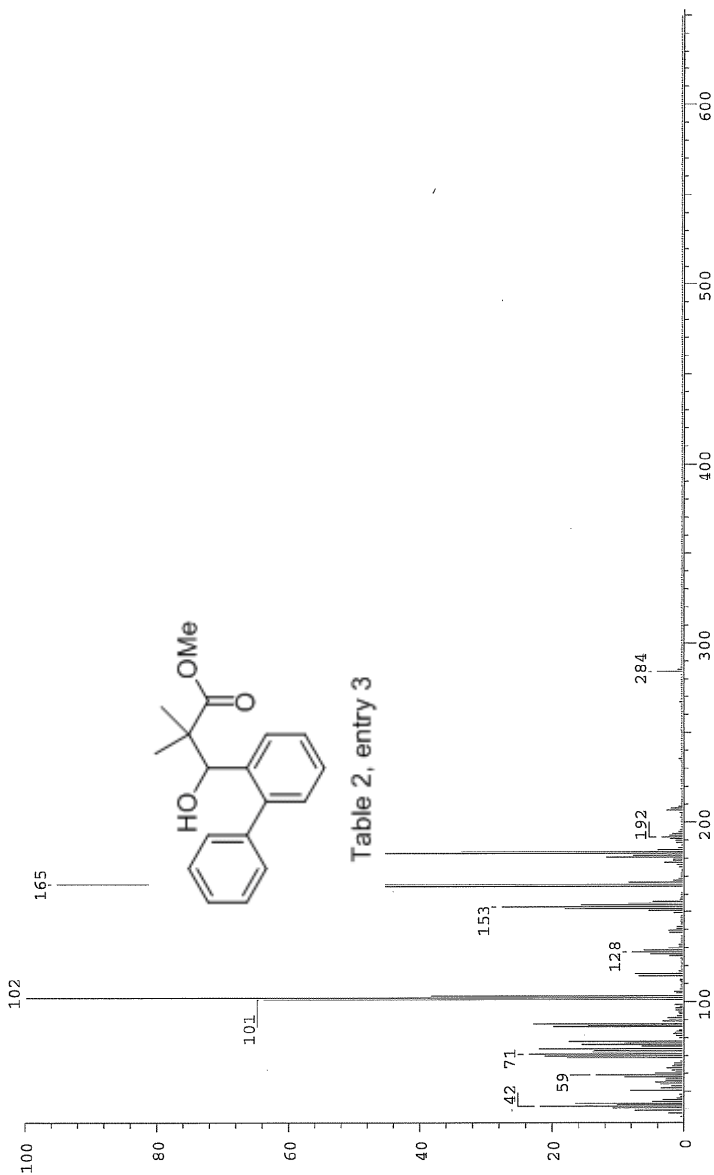


Table 2, entry 3

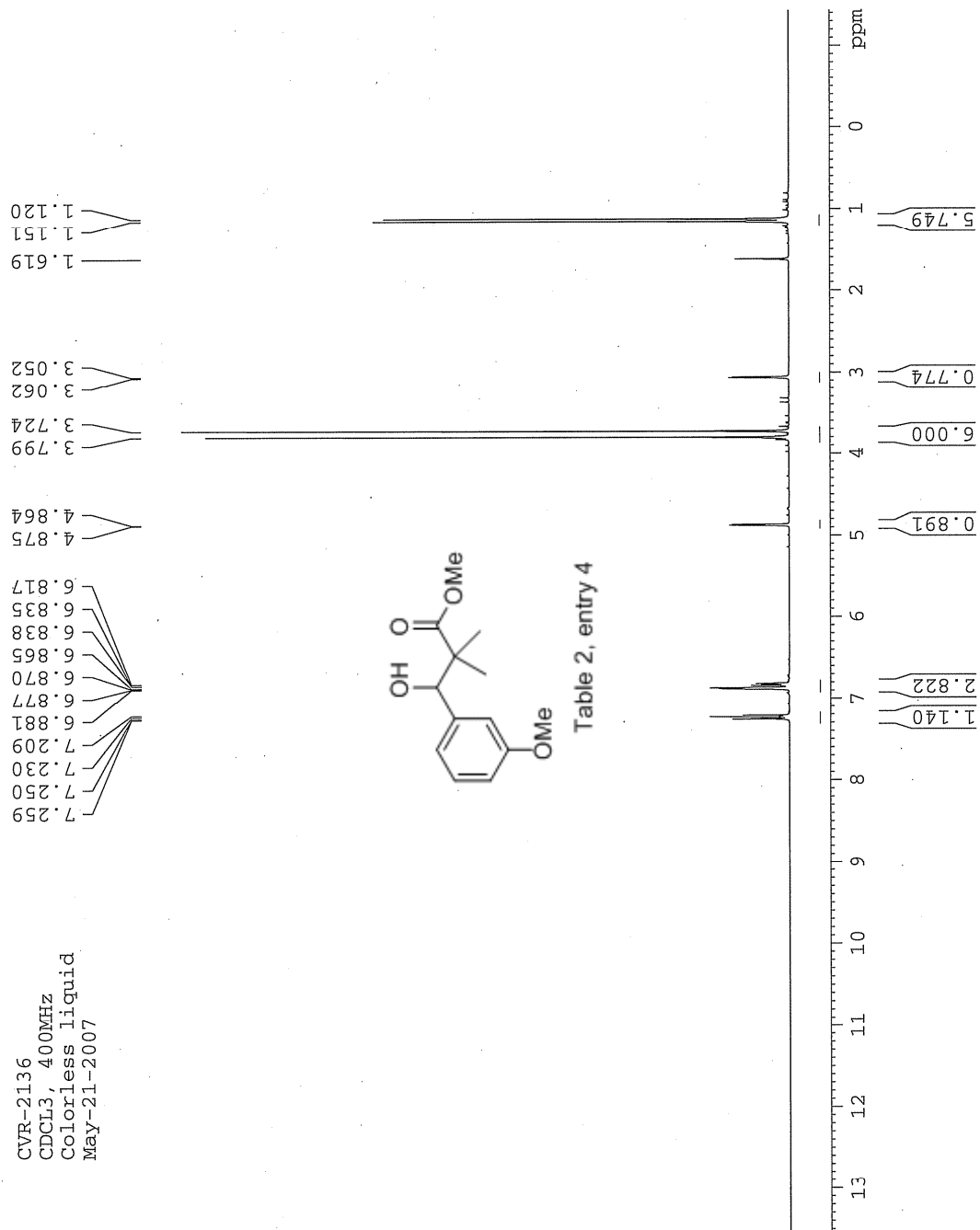
*MO*

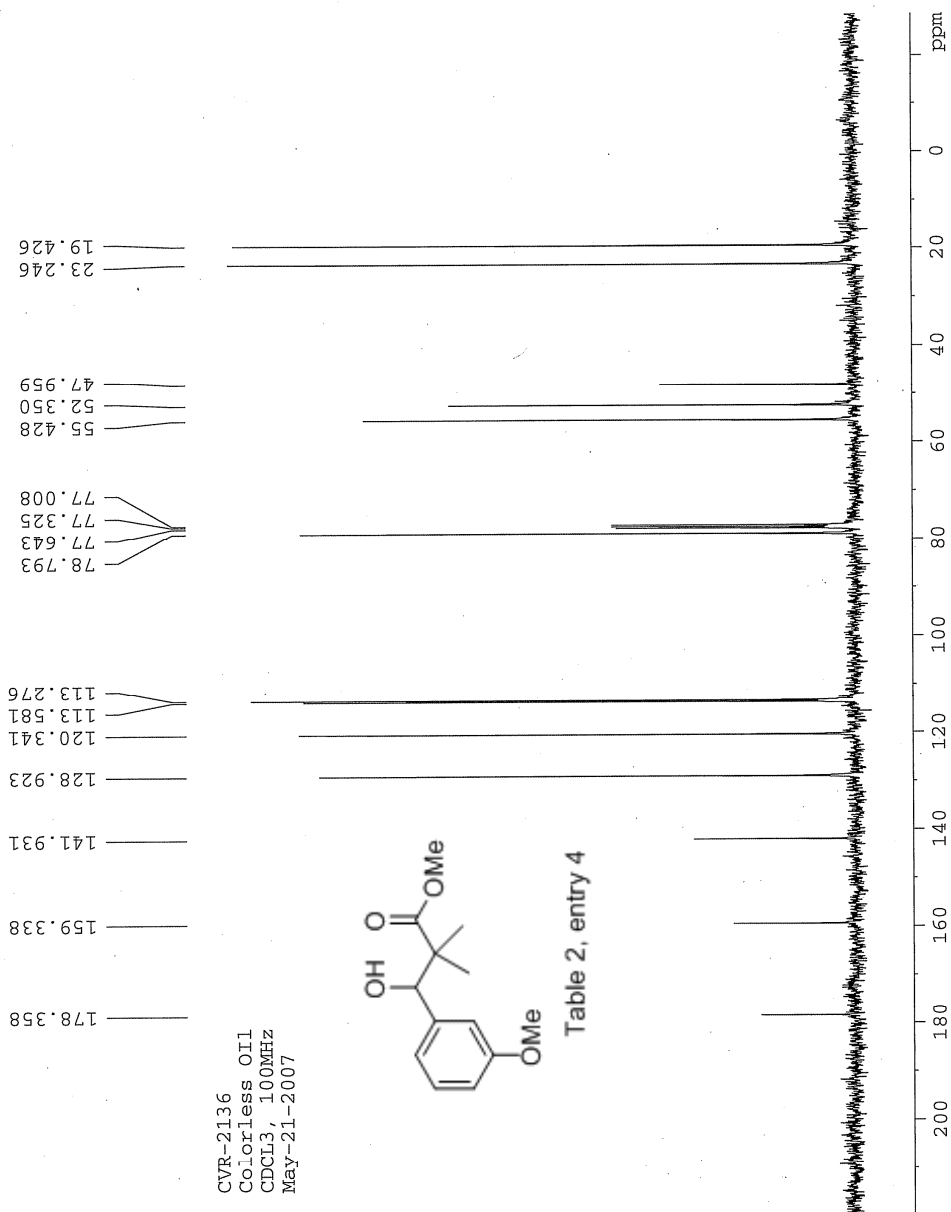
Scans: 1 > 17  
 Client: Venkat  
 #Peaks: 630  
 RIC: 10385100  
 9.6E+05

SPRC: jin063667.dat (30-MAY-08 11:09:41)  
 Samp: CVR-2687  
 Comm: 70 eV EI  
 Oper: kh  
 Study: Service  
 Masses: 35.01 > 650.00  
 Base: 102.18  
 Intensity: 956446  
 Peak: 1000.0 nmu  
 Scan 16 @ 0.48 min (EI +QIMS LMR UP LR)



Date: Fri May 30 11:11:19 2008 ICIS: 8.3.0 SP2 for OSF1 (V4.0) build 98-238 from 26-Aug-98





### Manual Peak Matching Report For Accurate Mass Determination

Theoretical mass	Experimental mass	PFK matching mass	Deviation*
238.12050	238.12115	230.98562	2.8 ppm

\* The deviation is obtained from the following equation:

$$\text{deviation} = \frac{\text{experimental mass} - \text{theoretical mass}}{\text{nominal mass}}$$

Where nominal mass takes in account only  $^{12}\text{C}$ ,  $^1\text{H}$ ,  $^{16}\text{O}$ ,  $^{14}\text{N}$  etc...

Theoretical mass correspond to the mass of the most abundant isotope peak

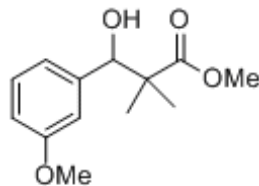


Table 2, entry 4

*Handwritten signature*



Scans: 1 > 22  
 Client: Venkat  
 #Peaks: 622  
 RIC: 2708886  
 1.8E+05

SPEC: fin084487.dat (26-MAY-09 11:39:51)  
 Samp: CVP-2136  
 Oper:  
 Base: 49.11  
 Peak: 1000.0 mmu  
 Scan 14 @ 0.44 min (EI +Q1MS LMR UP LR)

Study:  
 Masses: 35.01 > 650.00  
 Intensity: 176307

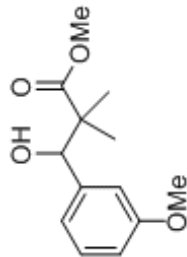
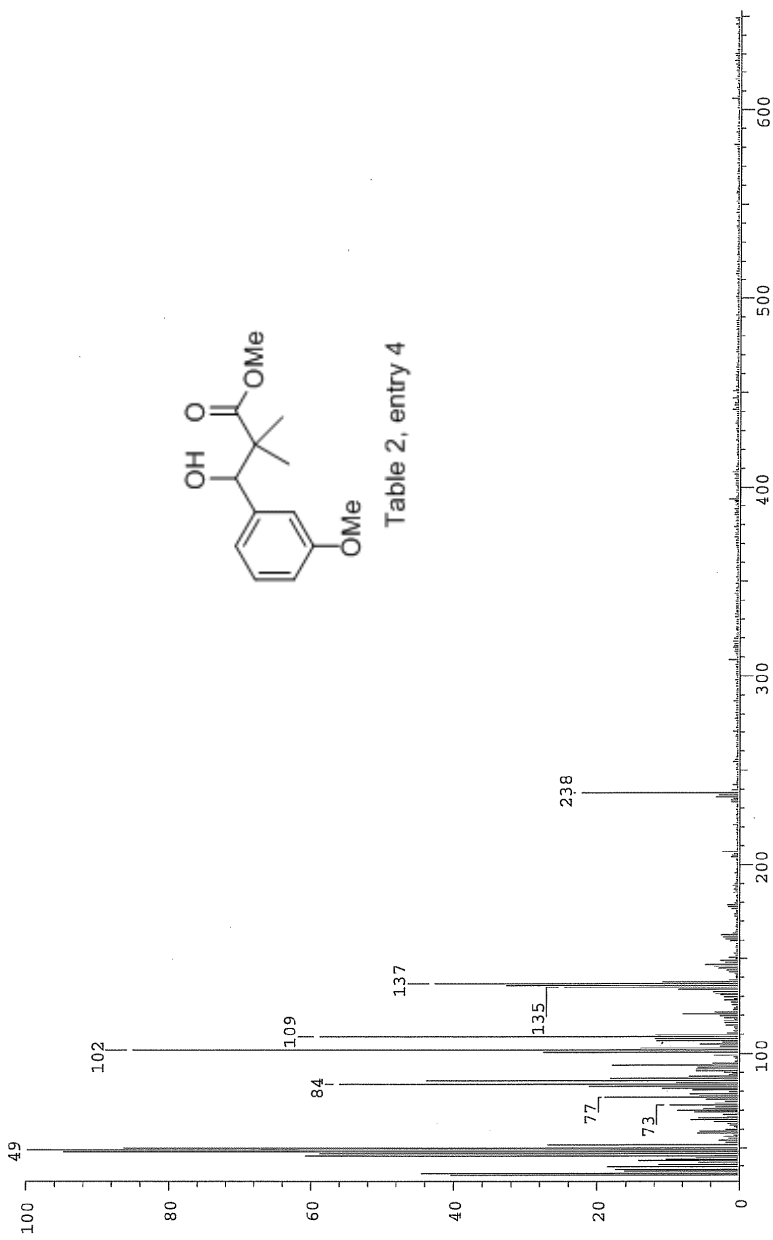
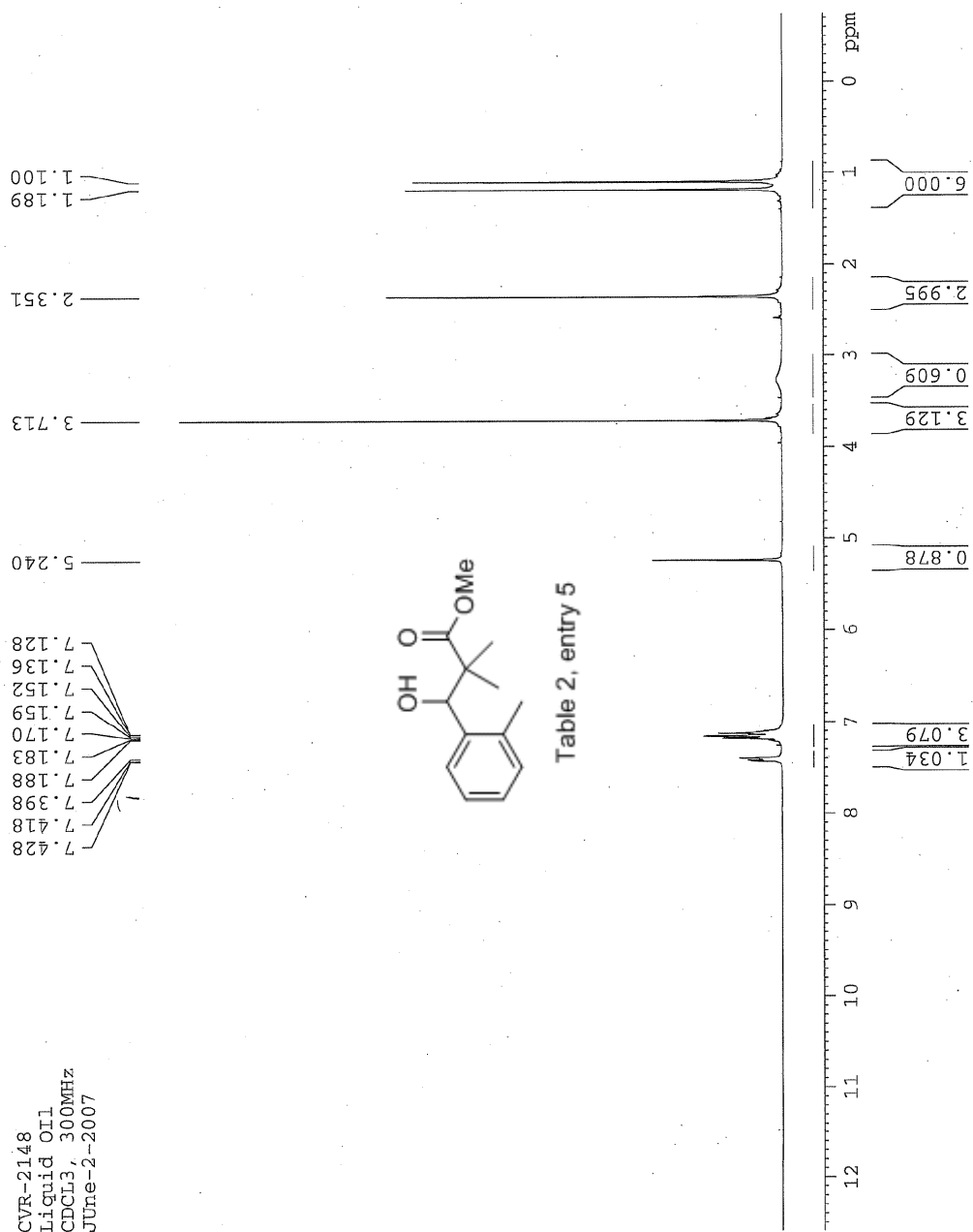
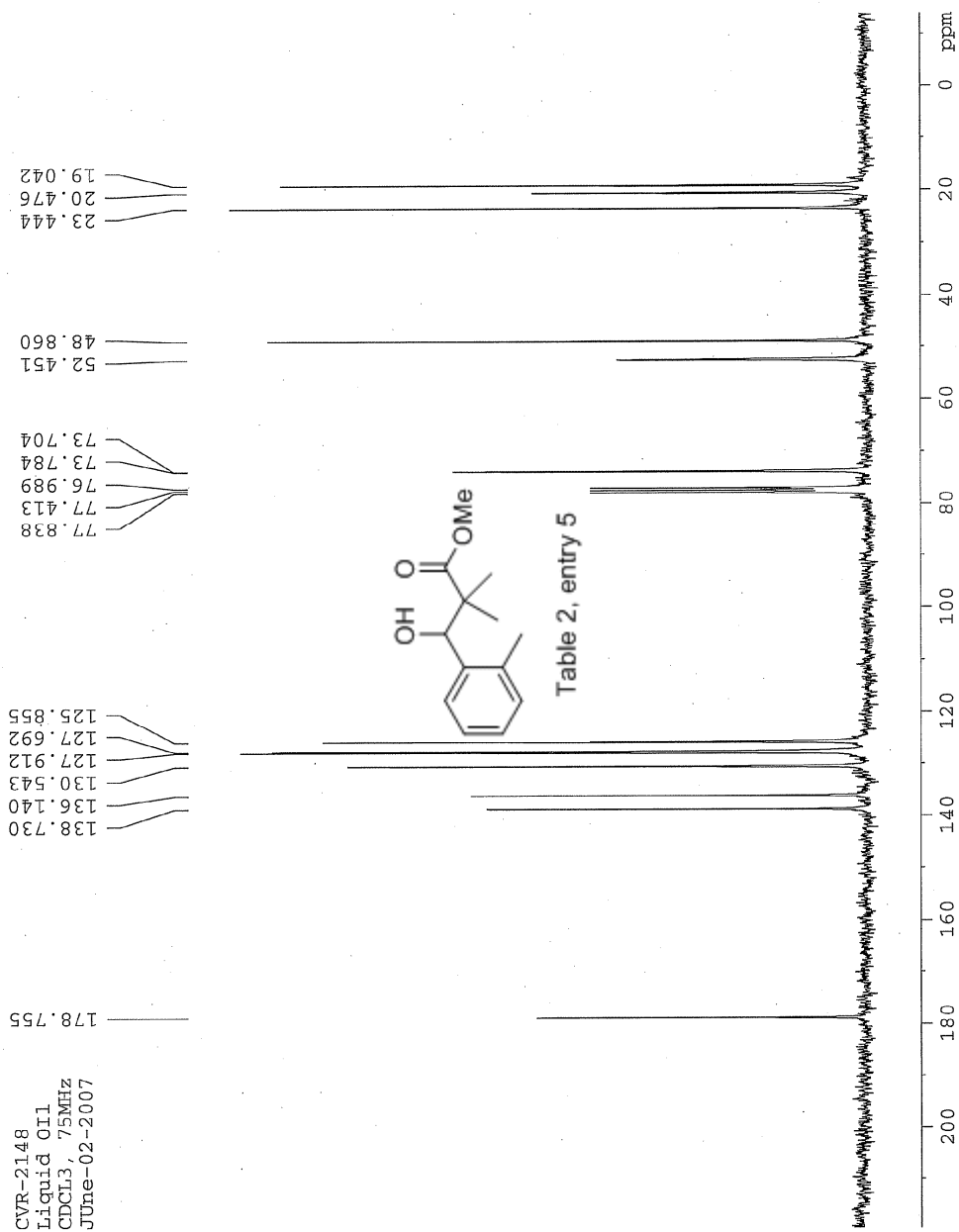
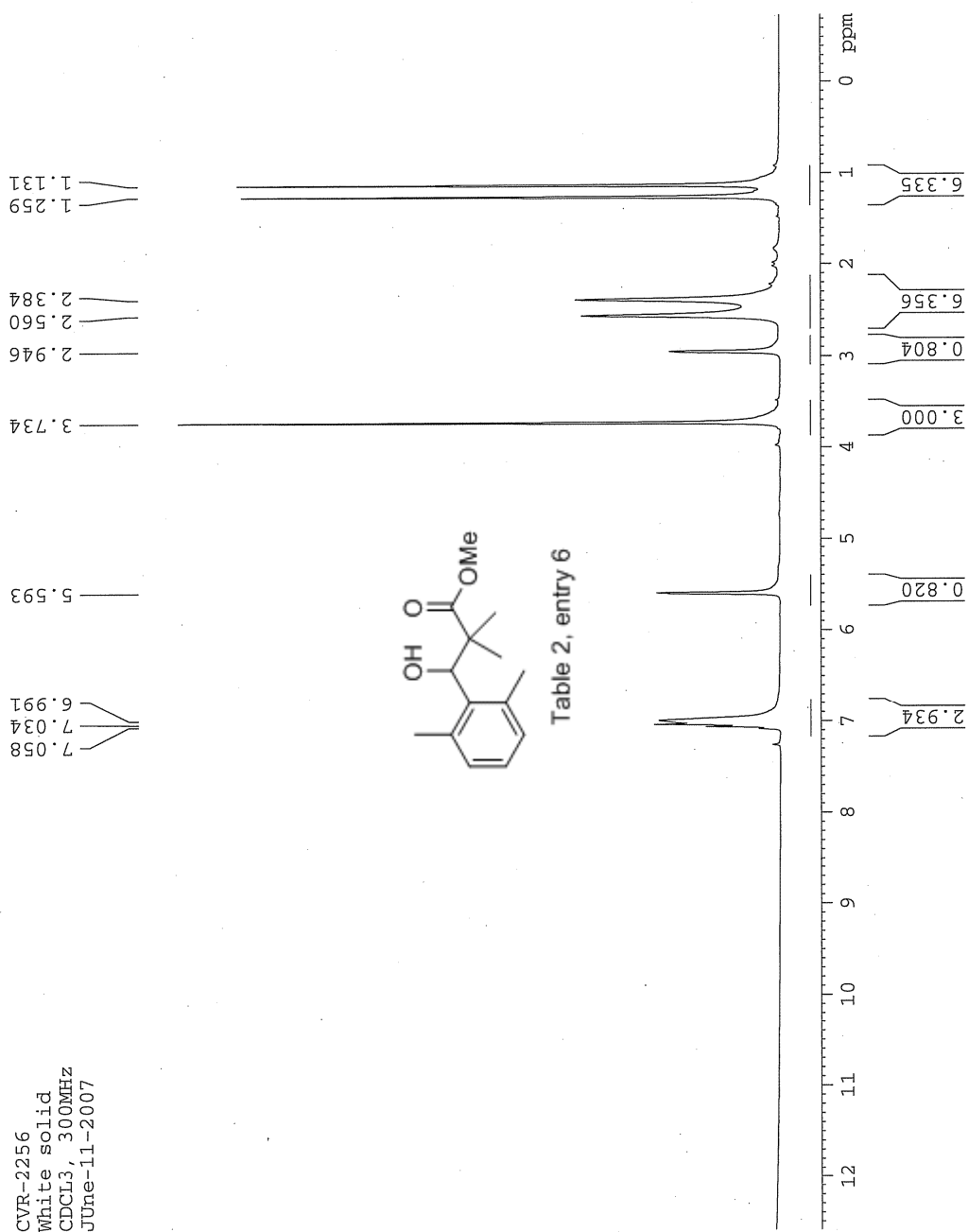


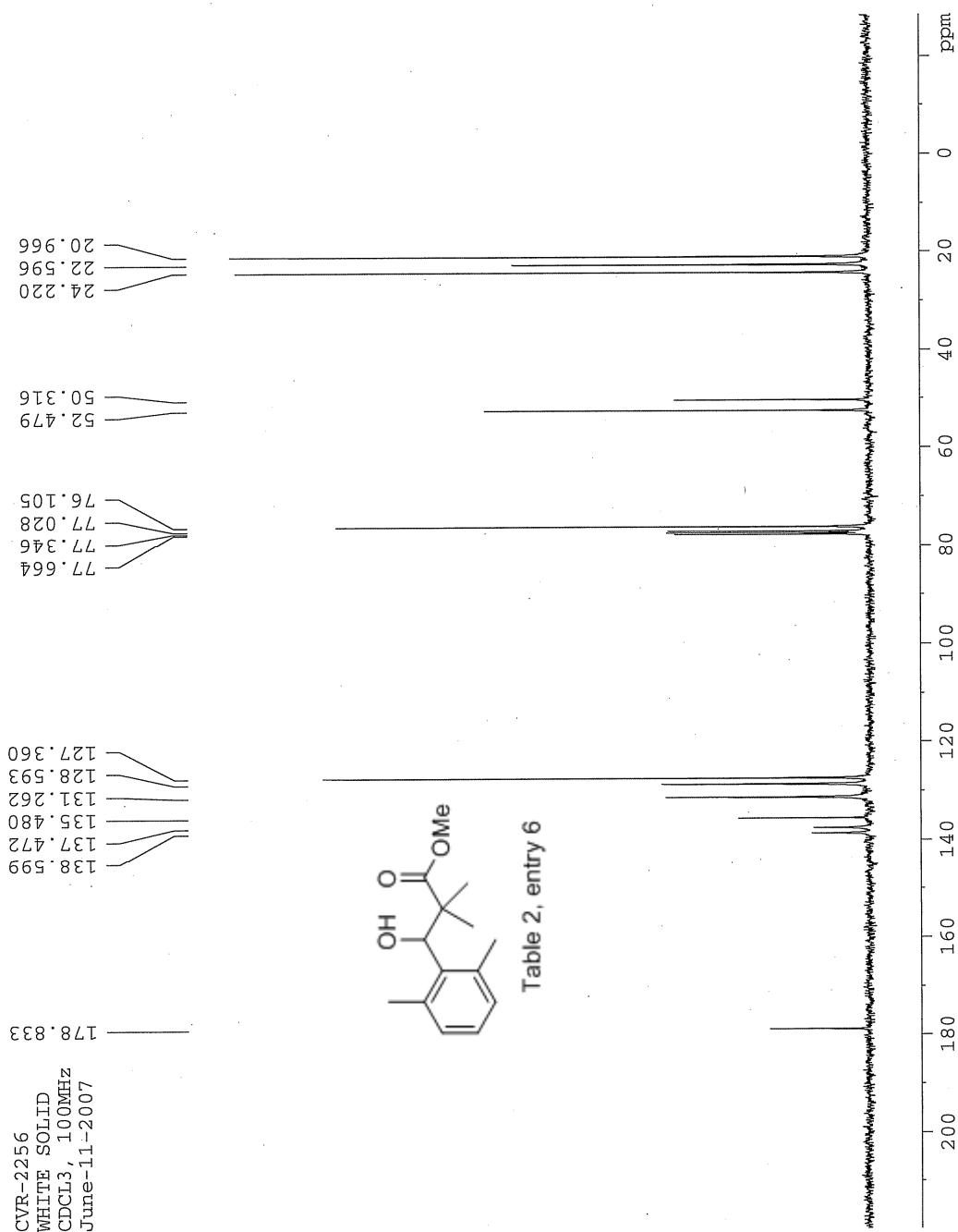
Table 2, entry 4

Date: Tue May 26 11:40:49 2009 ICIS: 8.3.0 SP2 for OSFI (V4.0) build 98-238 from 26-Aug-98









### Manual Peak Matching Report For Accurate Mass Determination

Theoretical mass	Experimental mass	PFK matching mass	Deviation*
236.14124	236.14177	230.98562	2.3 ppm

\* The deviation is obtained from the following equation:

$$\text{deviation} = \frac{\text{experimental mass} - \text{theoretical mass}}{\text{nominal mass}}$$

Where nominal mass takes in account only  $^{12}\text{C}$ ,  $^1\text{H}$ ,  $^{16}\text{O}$ ,  $^{14}\text{N}$  etc...

Theoretical mass correspond to the mass of the most abundant isotope peak

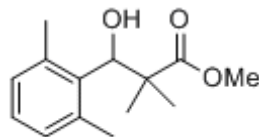
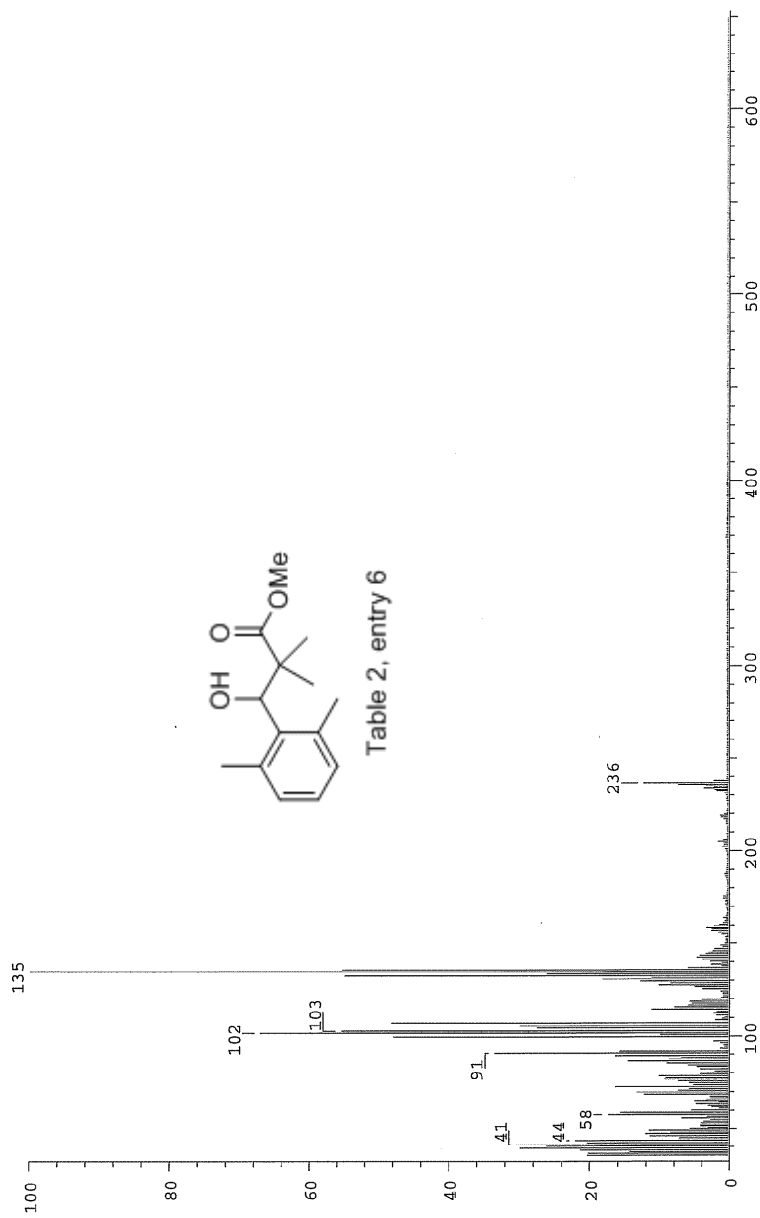


Table 2, entry 6

12/10

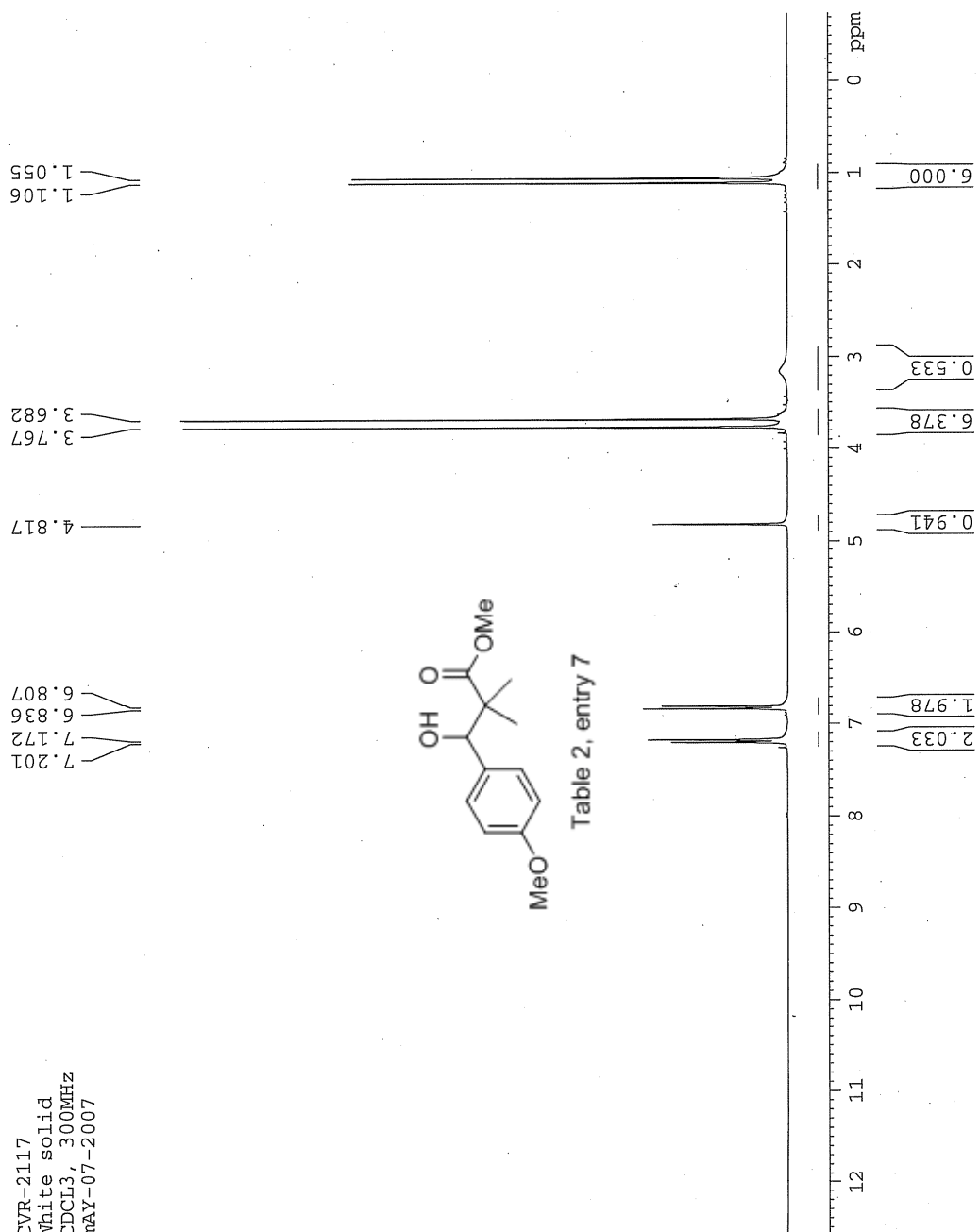
SPEC: fin084488.dat (26-MAY-09 11:44:41)  
 Samp: CVR-2256  
 Oper: 134.64  
 Base: 1000.0 mmu  
 Scan 42 @ 1.02 min (EI +Q1MS LMR UP LR)

Study: Masses: 35.01 > 650.00  
 Intensity: 433108  
 Scans: 1 > 52  
 Client: Venkat  
 #Peaks: 628  
 RIC: 5869376  
 4.3E+05

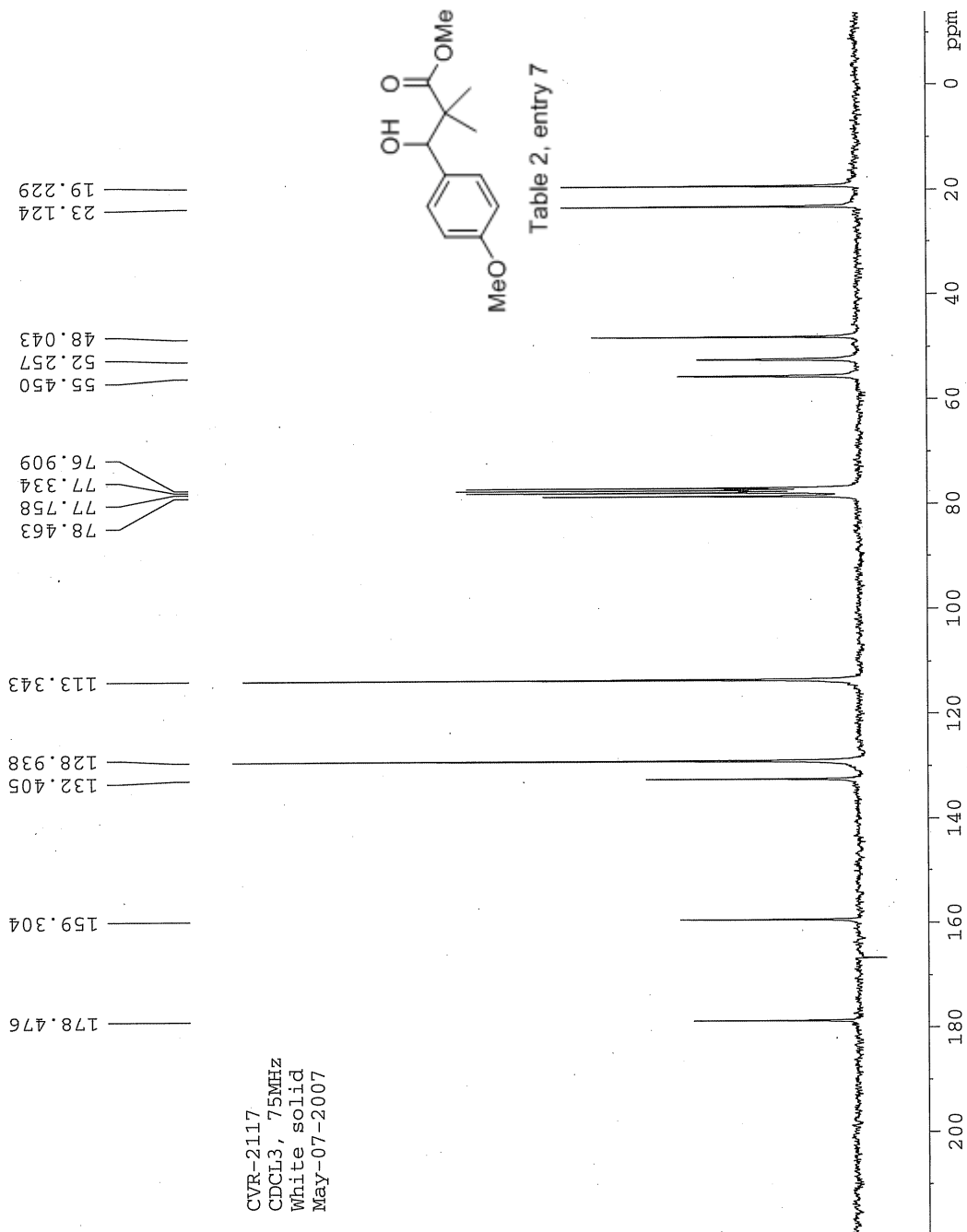


Date: Tue May 26 11:46:19 2009 ICIS: 8.3.0 SP2 for OSF1 (V4.0) build 98-238 from 26-Aug-98

CVR-2117  
 White solid  
 CDCl<sub>3</sub>, 300MHz  
 MAY-07-2007







CVR-2769  
 Oily liquid  
 CDCl<sub>3</sub>, 400MHz  
 20 AUG 2008

6.867  
6.862  
6.857  
6.852  
6.836  
6.831  
6.758  
6.737  
5.249  
3.832  
3.819  
3.660  
1.287  
1.073

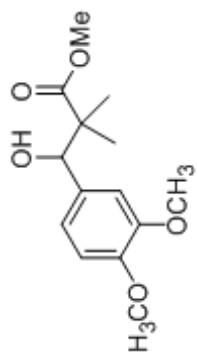
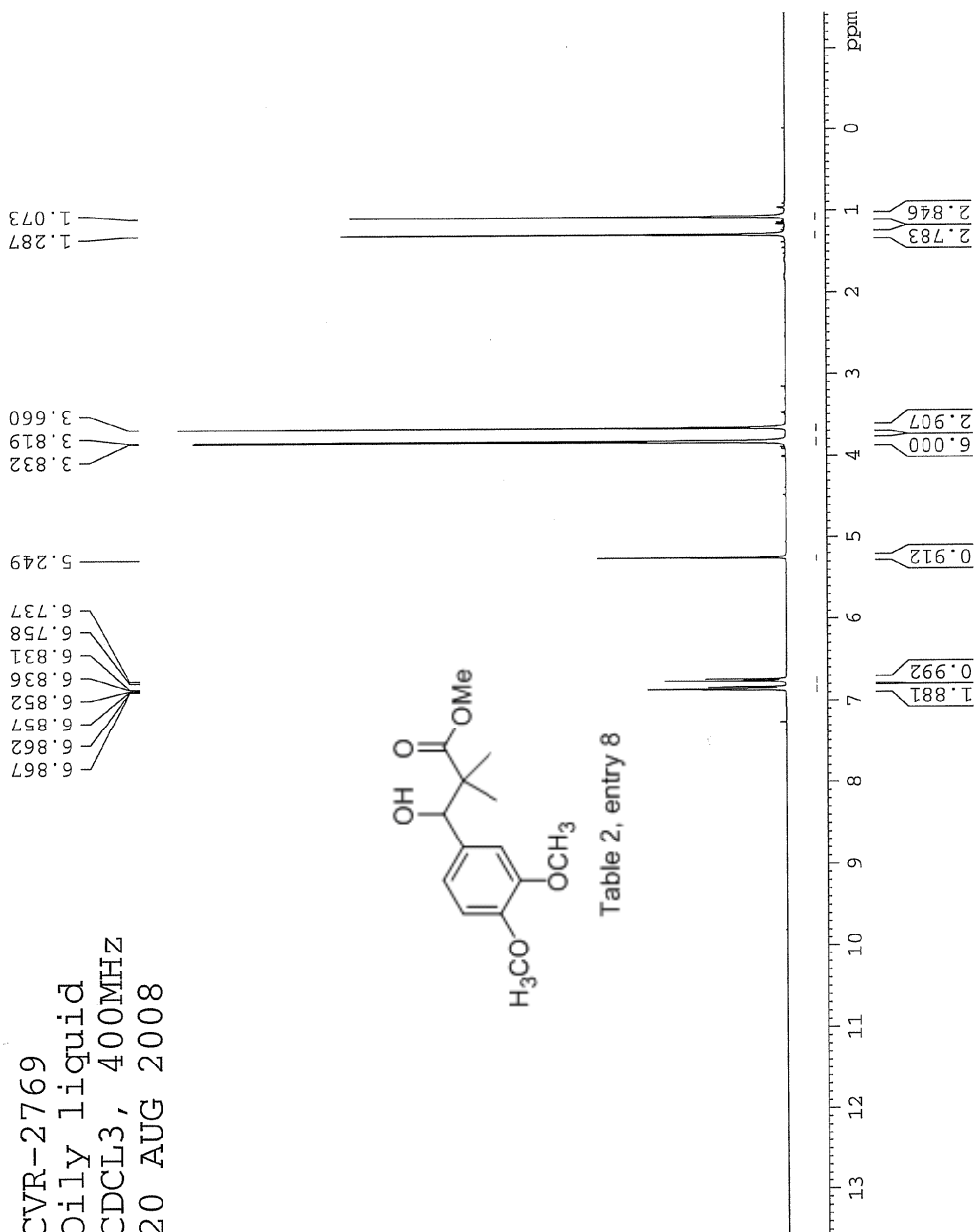
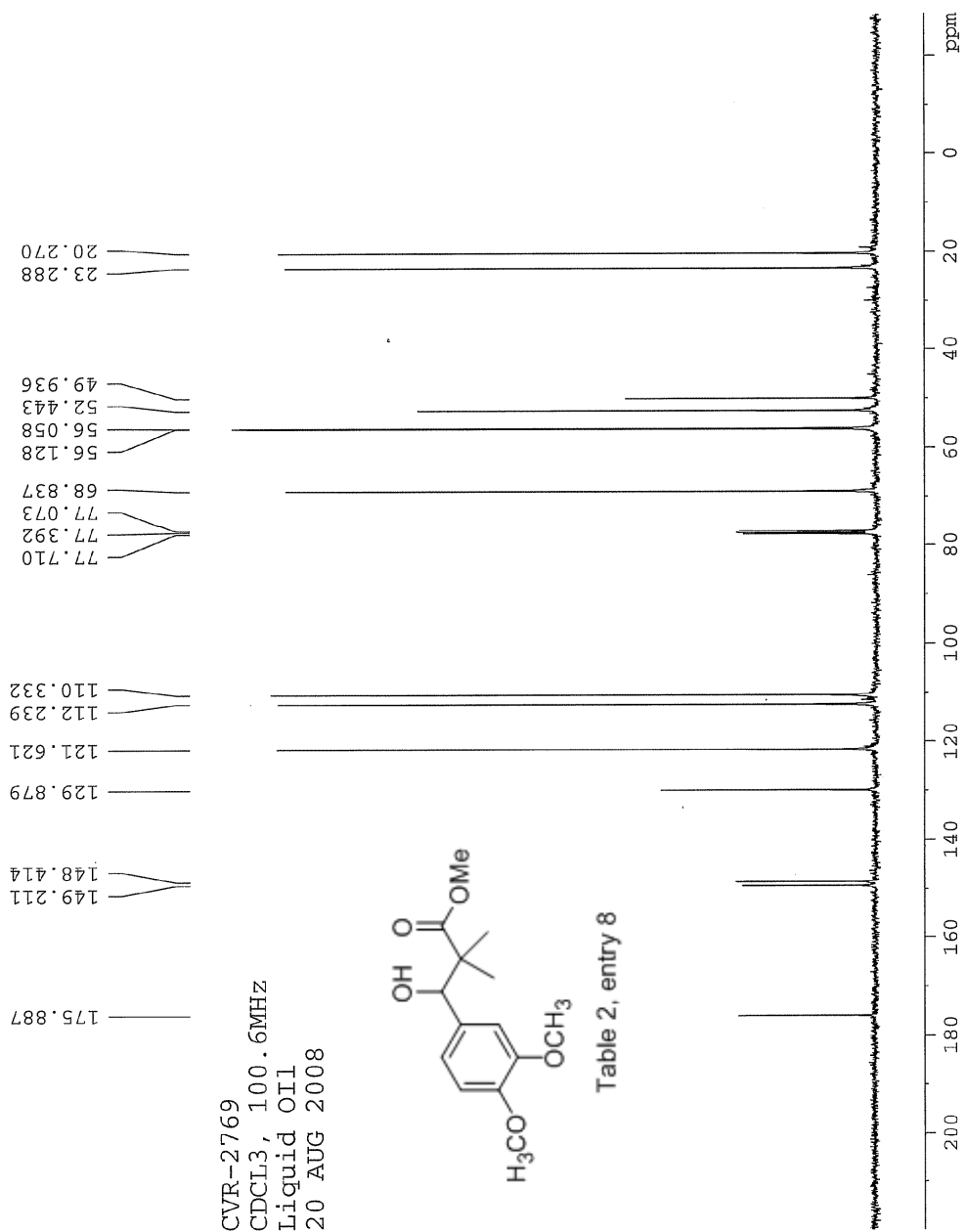


Table 2, entry 8





### Manual Peak Matching Report For Accurate Mass Determination

Theoretical mass	Experimental mass	PFK matching mass	Deviation*
268.13107	268.13179	230.98562	2.7 ppm

\* The deviation is obtained from the following equation:

$$\text{deviation} = \frac{\text{experimental mass} - \text{theoretical mass}}{\text{nominal mass}}$$

Where nominal mass takes in account only  $^{12}\text{C}$ ,  $^1\text{H}$ ,  $^{16}\text{O}$ ,  $^{14}\text{N}$  etc...

Theoretical mass correspond to the mass of the most abundant isotope peak

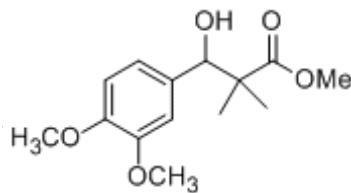


Table 2, entry 8

bo

Scans: 1 > 90  
 Client: Venkat  
 #Peaks: 623  
 RIC: 7101690  
 5.5E+05

SPEC: fin084489.dat (26-MAY-09 11:47:58)  
 Samp: CVR-2769  
 Oper: Study:  
 Base: 184.59 Masses: 35.01 > 650.00  
 Peak: 1000.0 mmu Intensity: 547788  
 Scan 65 @ 1.50 min (EI +QIMS LMR UP LR)

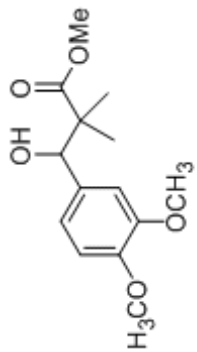
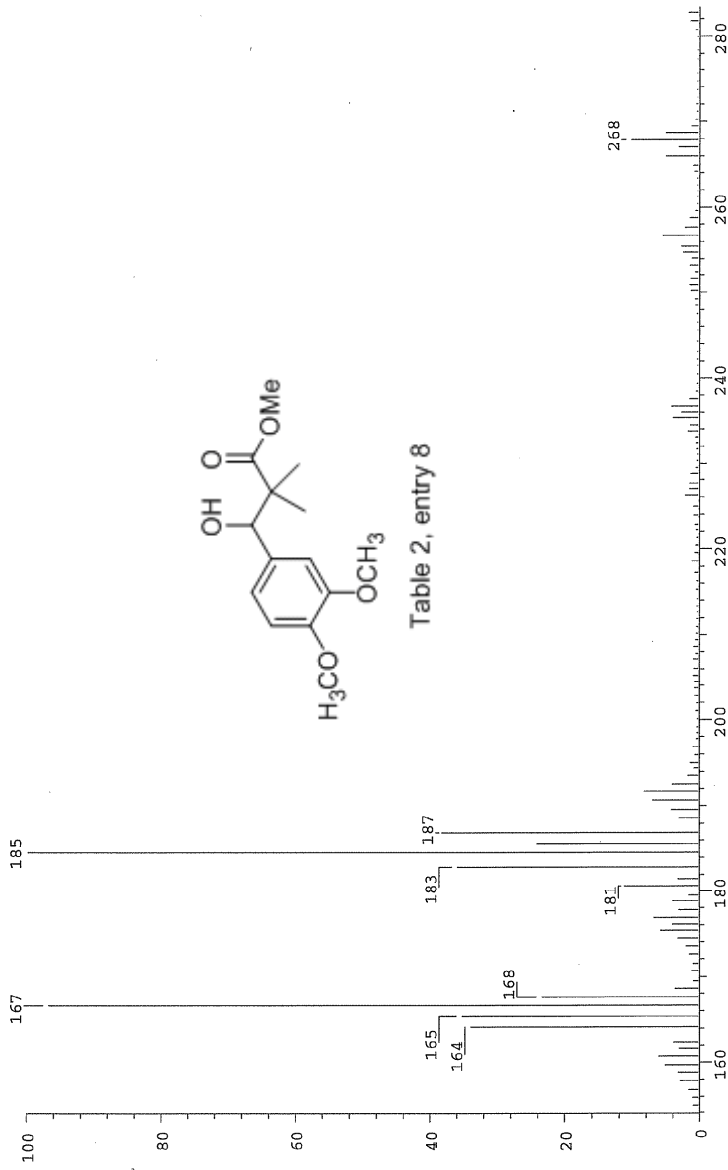
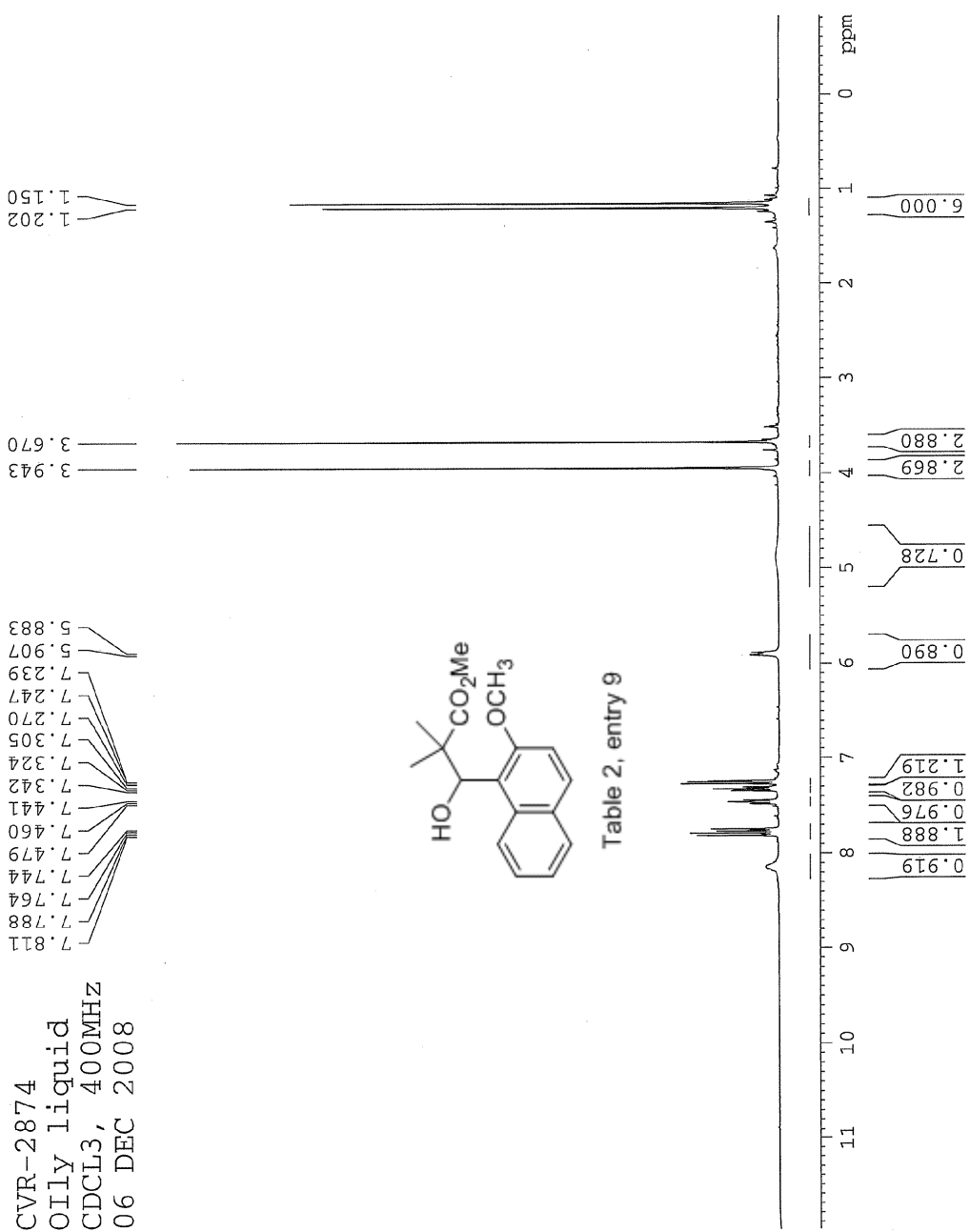
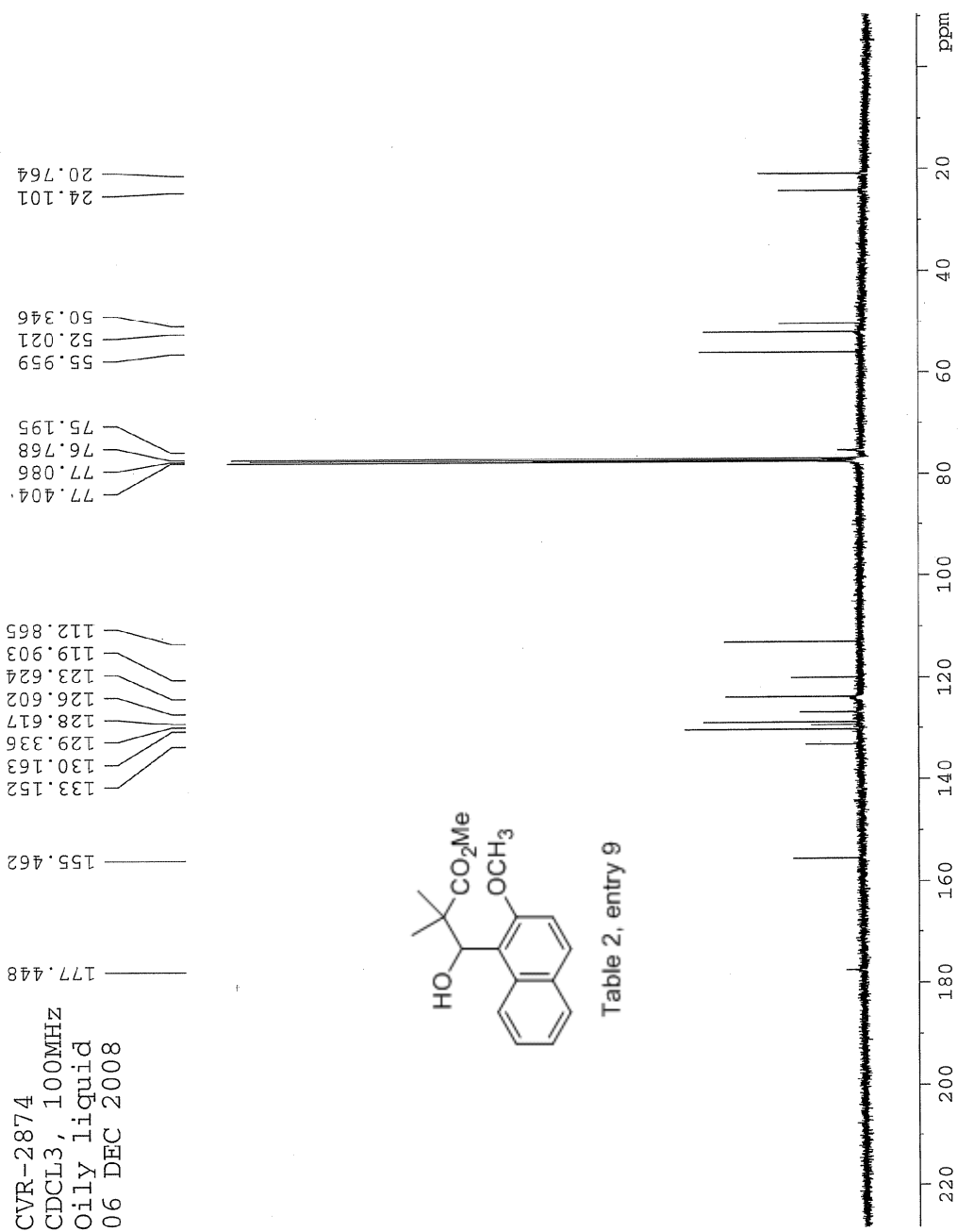


Table 2, entry 8

Date: Tue May 26 11:50:48 2009 ICIS: 8.3.0 SP2 for OSF1 (V4.0) build 98-238 from 26-Aug-98





### Manual Peak Matching Report For Accurate Mass Determination

Theoretical mass	Experimental mass	PFK matching mass	Deviation*
288.13615	288.13656	280.98242	1.4 ppm

\* The deviation is obtained from the following equation:

$$\text{deviation} = \frac{\text{experimental mass} - \text{theoretical mass}}{\text{nominal mass}}$$

Where nominal mass takes in account only  $^{12}\text{C}$ ,  $^1\text{H}$ ,  $^{16}\text{O}$ ,  $^{14}\text{N}$  etc...

Theoretical mass correspond to the mass of the most abundant isotope peak

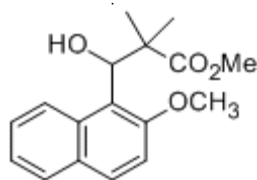


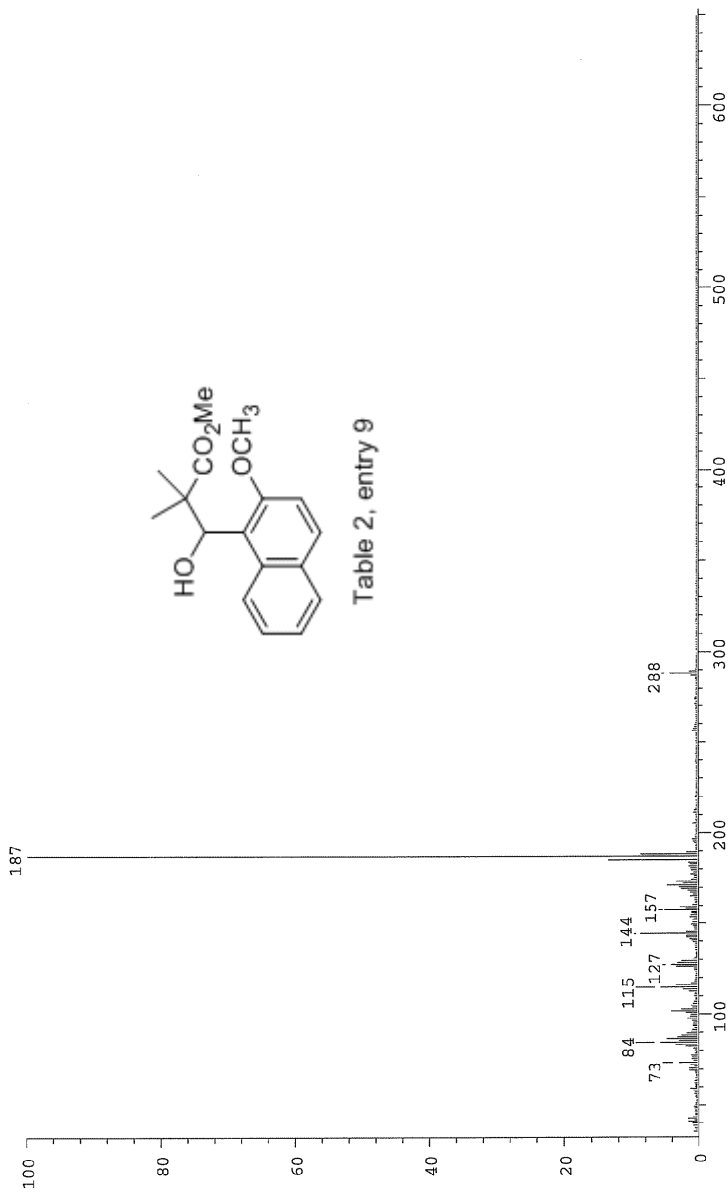
Table 2, entry 9

*Handwritten signature*

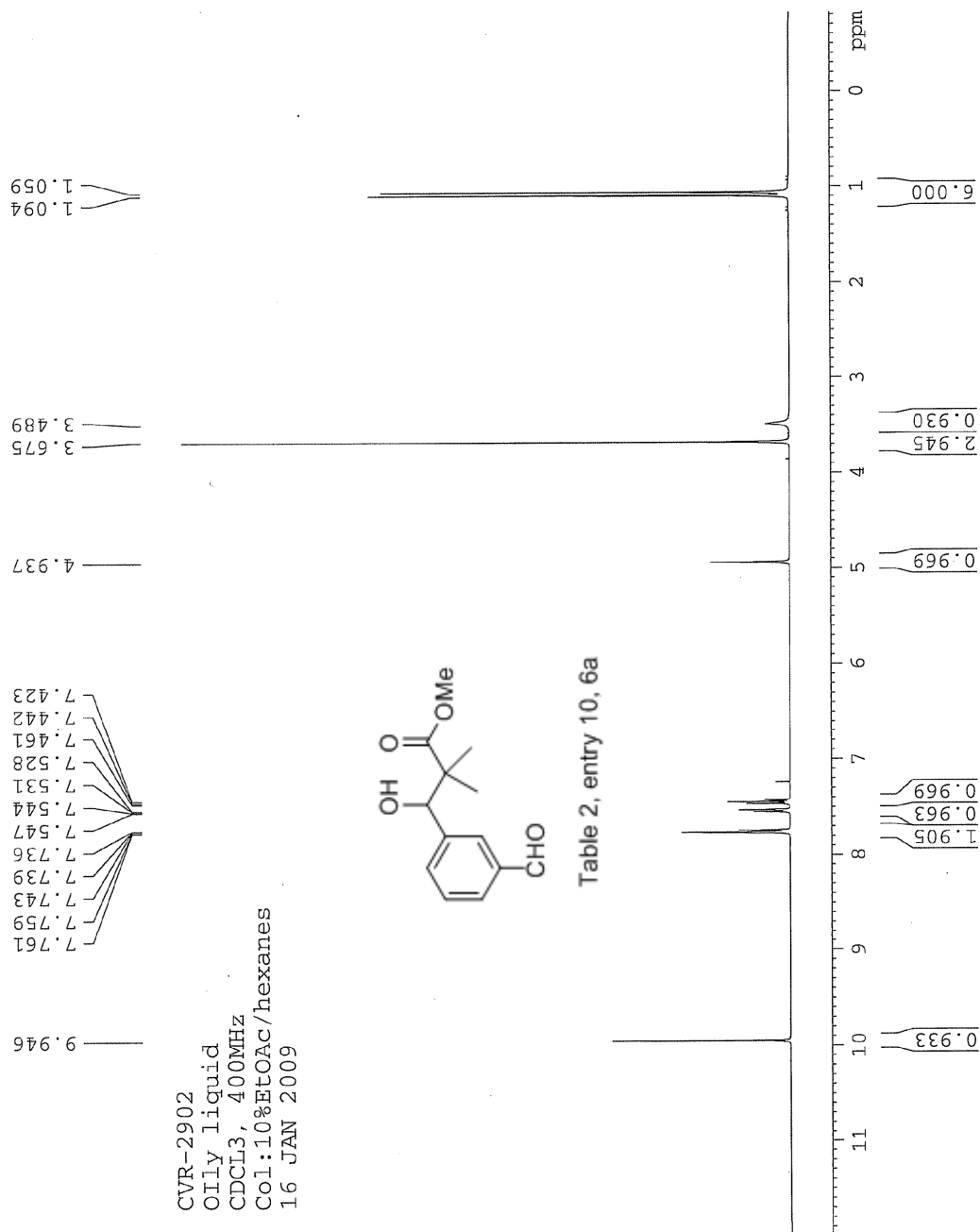


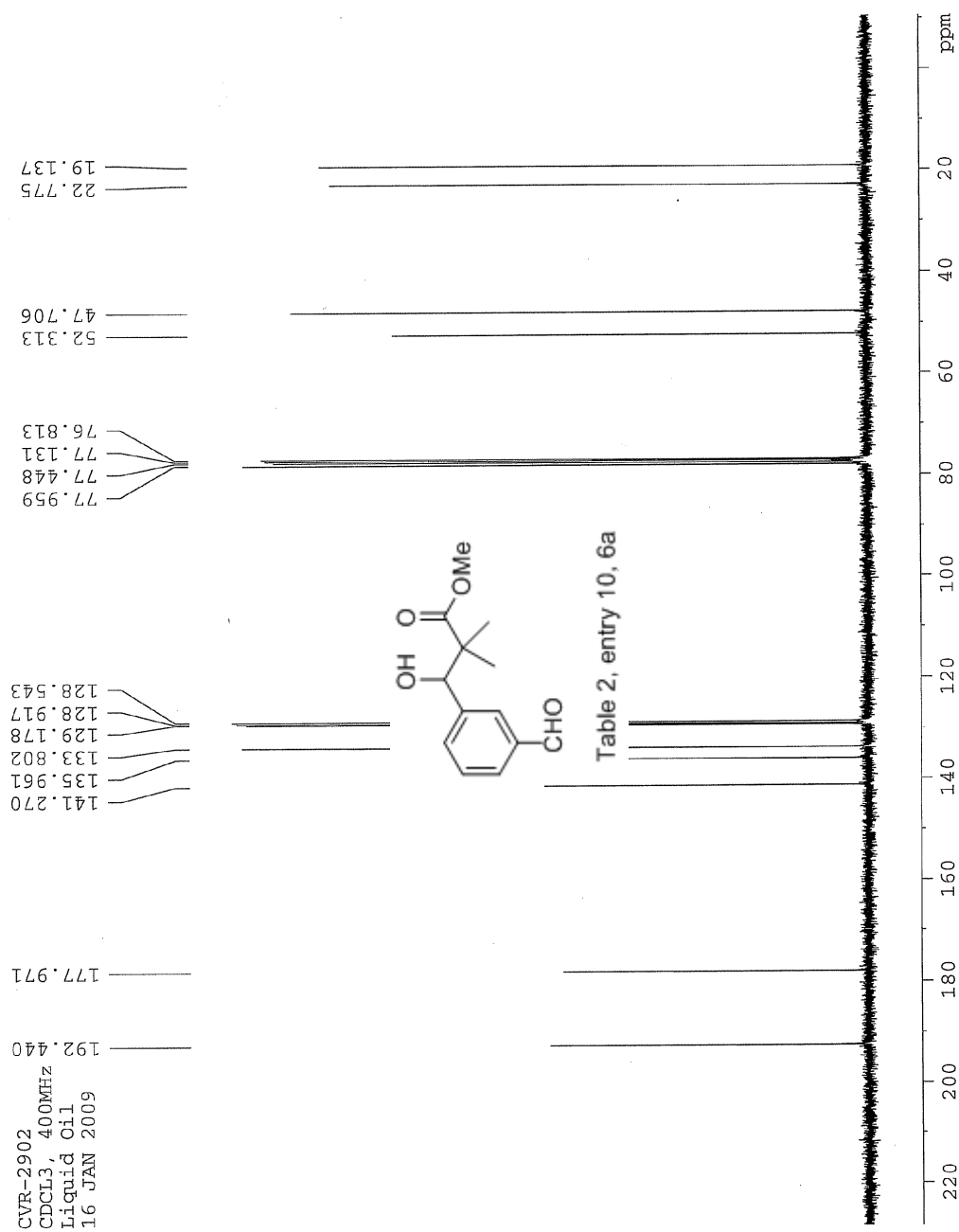
Scans: 1 > 53  
 Client: Venkat  
 #peaks: 627  
 RIC: 15007390  
 5.0E+06

SPEC: fin084061.dat (10-DEC-08 15:36:50)  
 Samp: CVR-2874  
 Comm: 70 eV EI  
 Oper: kh  
 Study: ms services  
 Masses: 35.01 > 650.00  
 Intensity: 4990774  
 Peak: 1000.0 mmu  
 Scan 51 @ 0.80 min (EI +QIMS LMR UP LR)



Date: Wed Dec 10 15:38:07 2008 ICIS: 8.3.0 SP2 for OSF1 (V4.0) build: 98-238 from 26-Aug-98





### Manual Peak Matching Report For Accurate Mass Determination

Theoretical mass	Experimental mass	PFK matching mass	Deviation*
236.10485	236.10533	230.98562	2 ppm

\* The deviation is obtained from the following equation:

$$\text{deviation} = \frac{\text{experimental mass} - \text{theoretical mass}}{\text{nominal mass}}$$

Where nominal mass takes in account only  $^{12}\text{C}$ ,  $^1\text{H}$ ,  $^{16}\text{O}$ ,  $^{14}\text{N}$  etc...

Theoretical mass correspond to the mass of the most abundant isotope peak

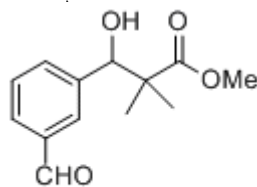


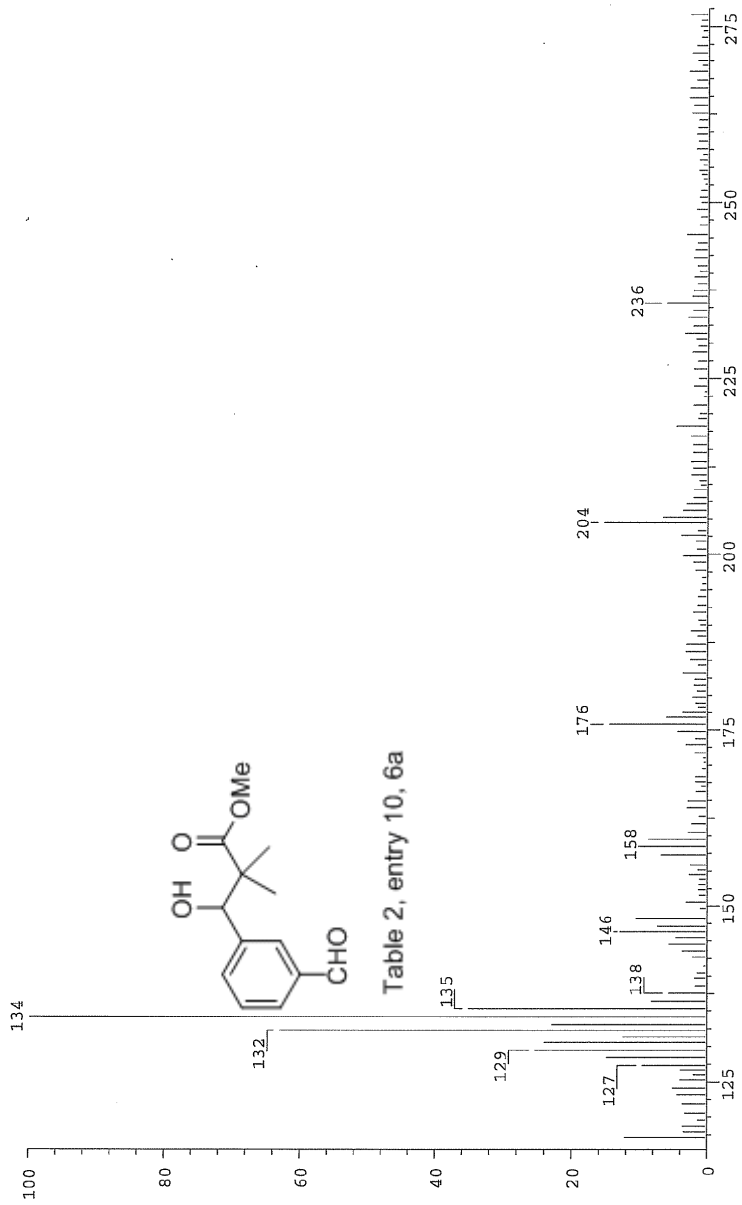
Table 2, entry 10, 6a

*hrr*

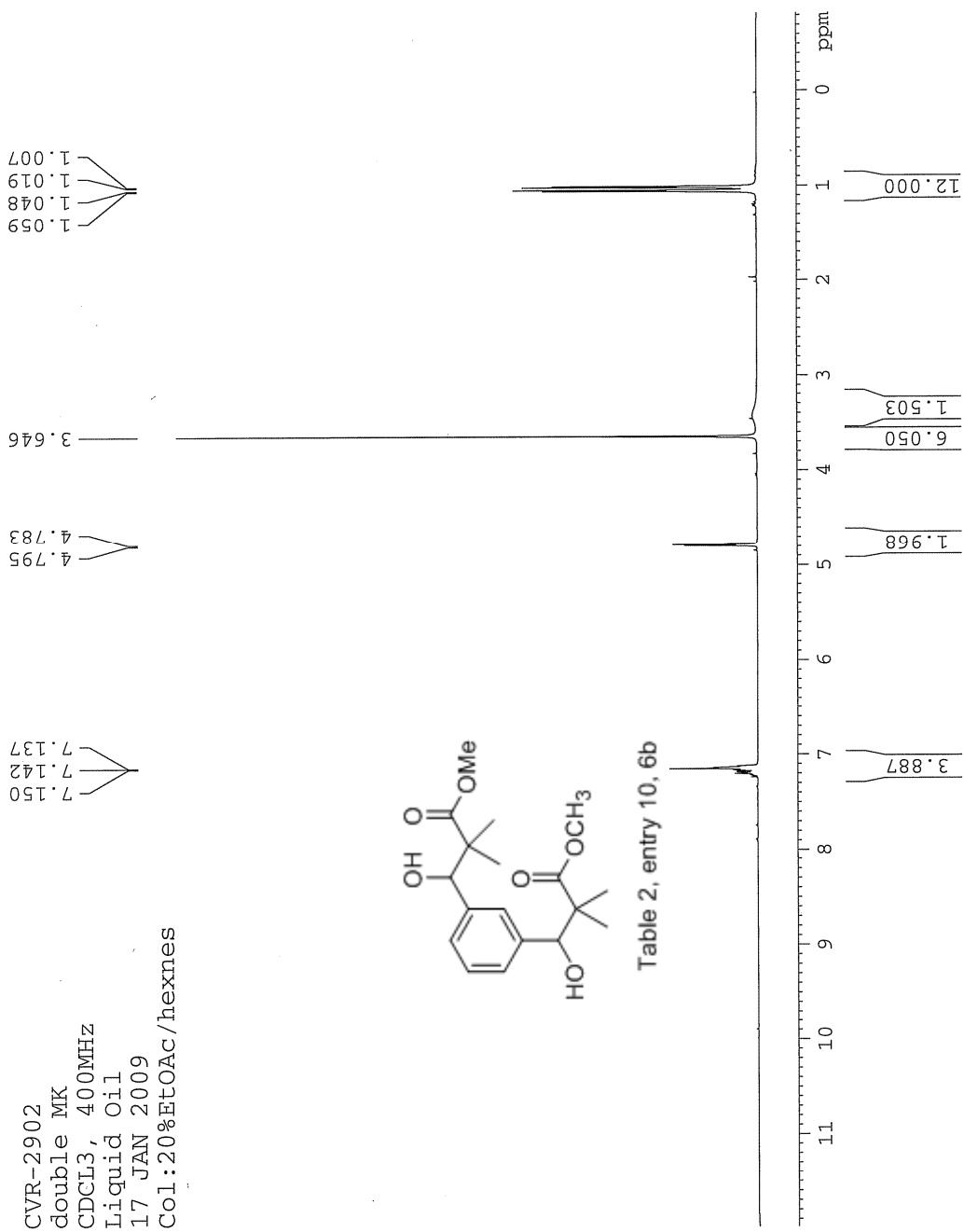
Scans: 1 > 81  
 Client: Venkat  
 #Peaks: 647  
 RIC: 203833  
 7.JE+03

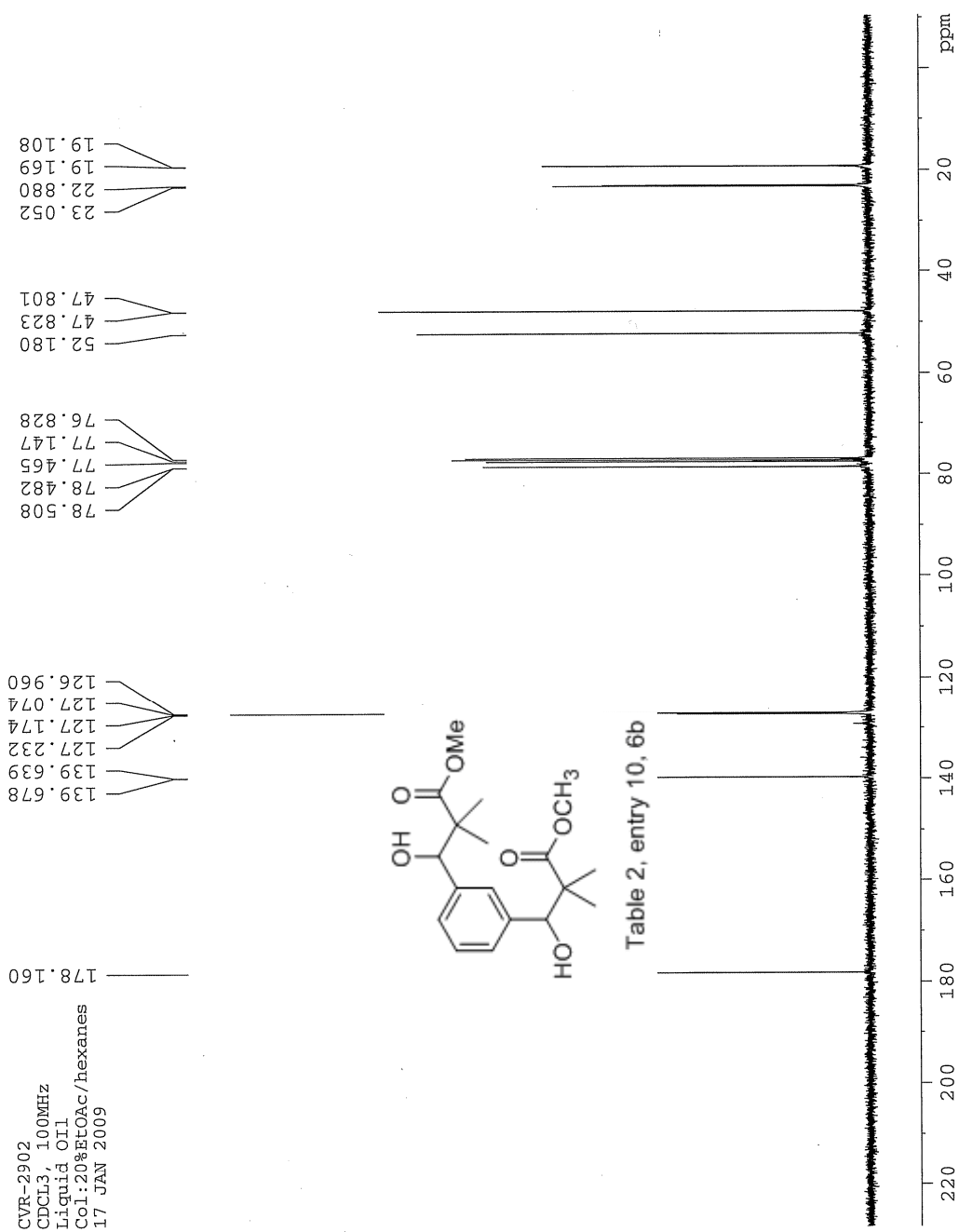
SPEC: fin084168.dat (22-JAN-09 10:16:26)  
 Samp: CVR-2902A  
 Comm: SP 70 ev EI  
 Oper: kh  
 Base: 101.28  
 Peak: 1000.0 mmu  
 Scan 69 @ 1.56 min (EI +Q1MS LMR UP LR)

Study: MS services  
 Masses: 35.01 > 650.00  
 Intensity: 24076



Date: Thu Jan 22 10:19:34 2009 ICIS: 8.3.0 SP2 for OSF1 (V4.0) build 98-238 from 26-Aug-98





## Manual Peak Matching Report For Accurate Mass Determination

Theoretical mass	Experimental mass	PFK matching mass	Deviation*
338.17293	338.17906	330.97923	1.8 ppm

\* The deviation is obtained from the following equation:

$$\text{deviation} = \frac{\text{experimental mass} - \text{theoretical mass}}{\text{nominal mass}}$$

Where nominal mass takes in account only  $^{12}\text{C}$ ,  $^1\text{H}$ ,  $^{16}\text{O}$ ,  $^{14}\text{N}$  etc...

Theoretical mass correspond to the mass of the most abundant isotope peak

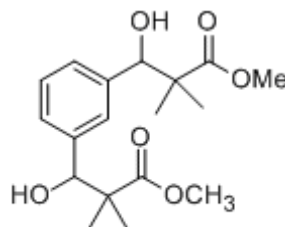


Table 2, entry 10, 6b

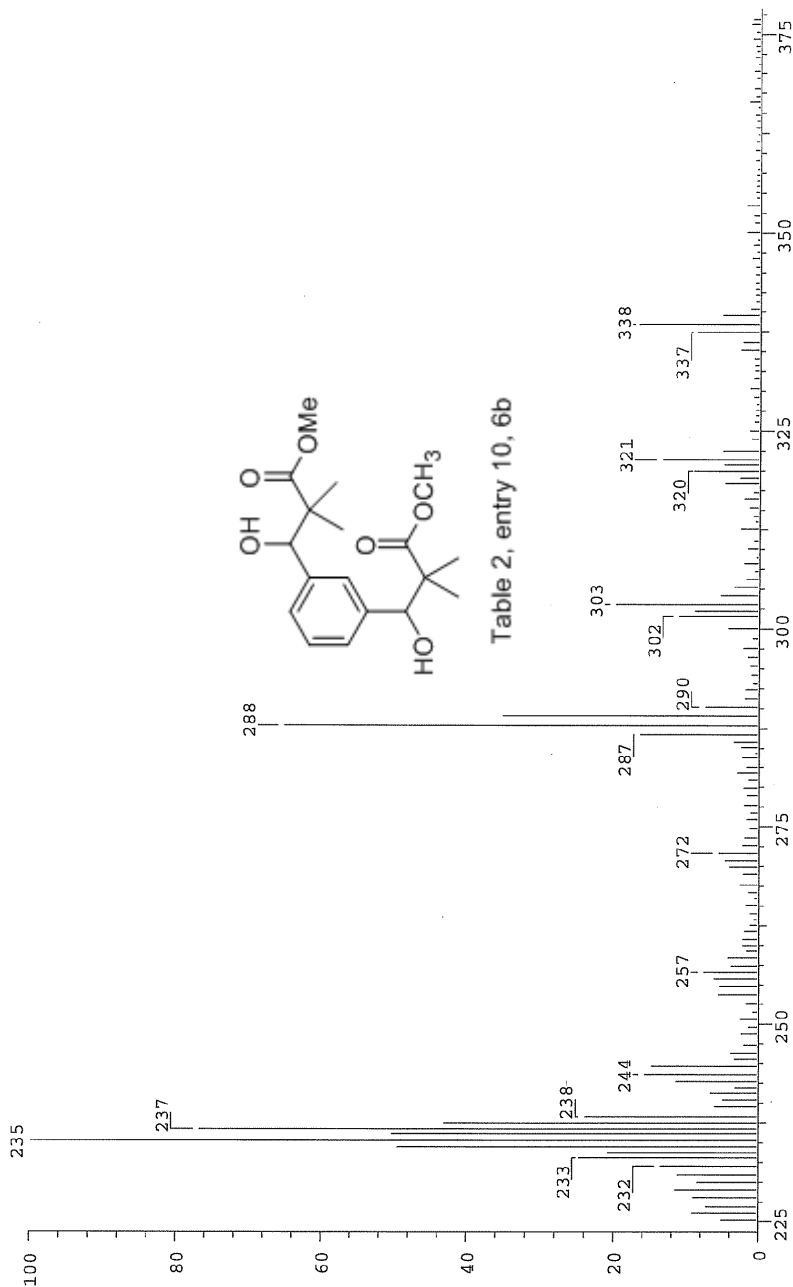
*ms*



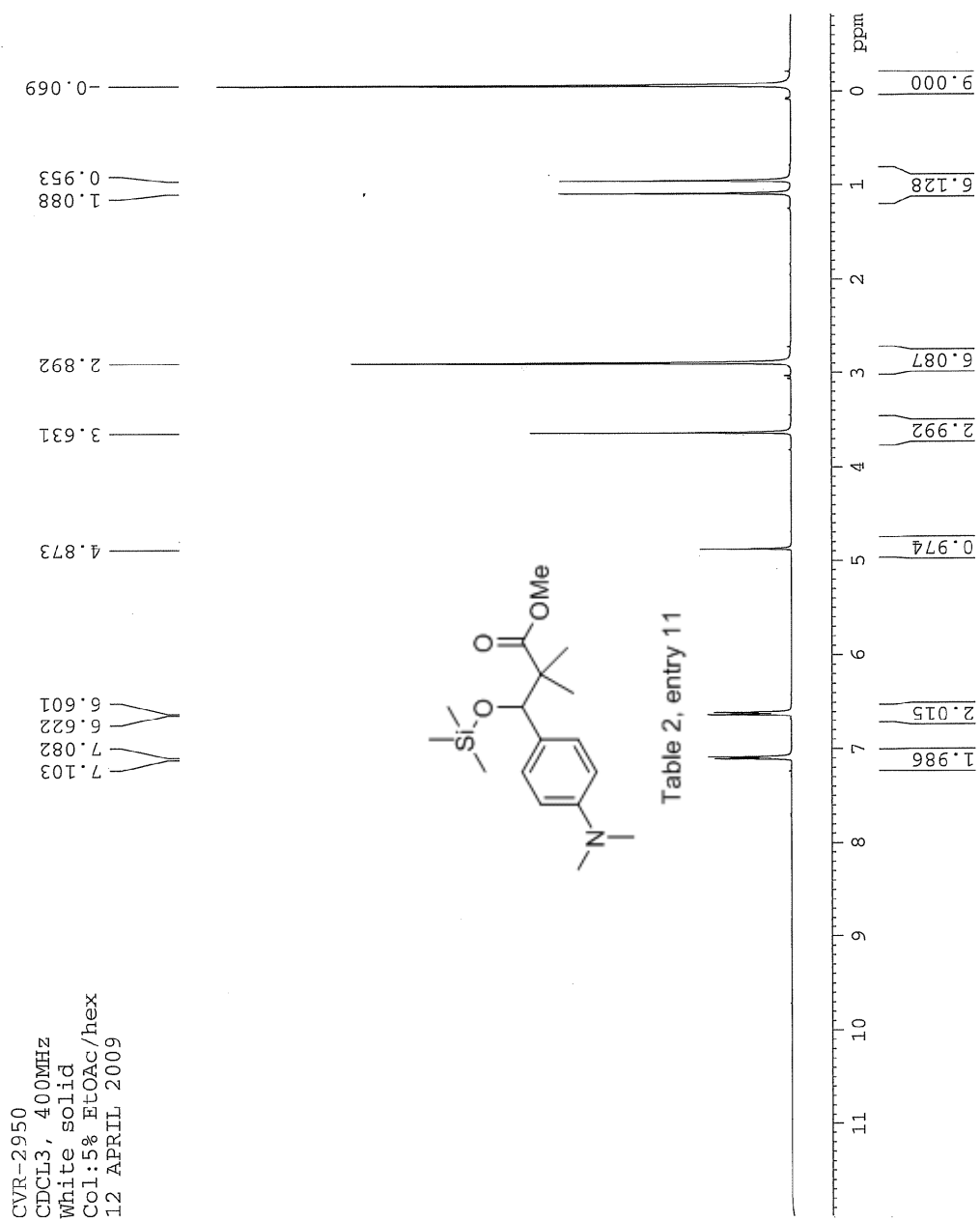
Scans: 1 > 70  
 Client: Venkat  
 #Peaks: 647  
 RIC: 3353815  
 2.3E+04

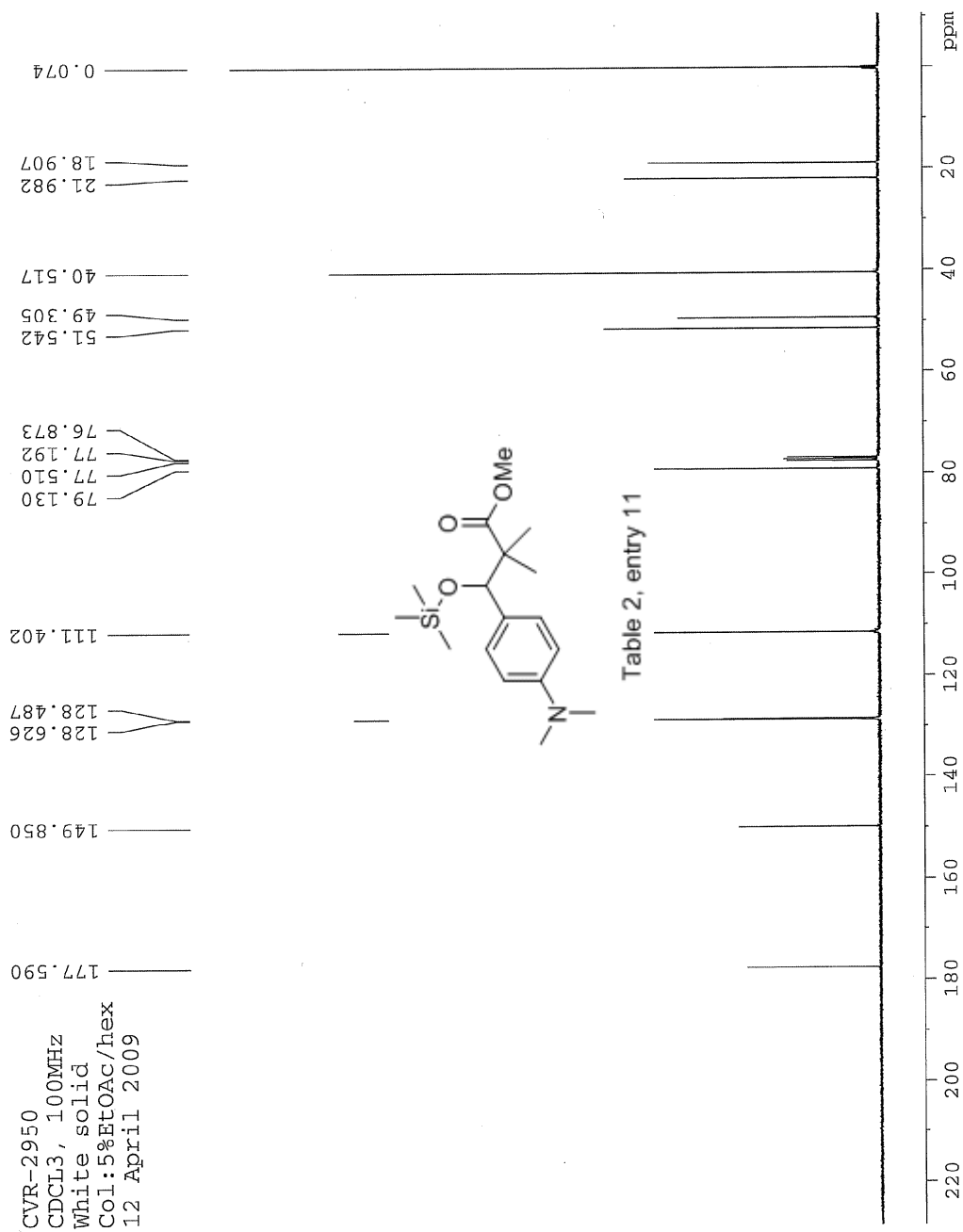
SPEC: fin084170.dat (22-JAN-09 10:48:54)  
 Samp: CVR-2902B  
 Comm: SP 70 eV EI  
 Oper: kh  
 Base: 73.43  
 Peak: 1000.0 mmu  
 Scan 31 @ 0.78 min (EI +QIMS LMR UP LR)

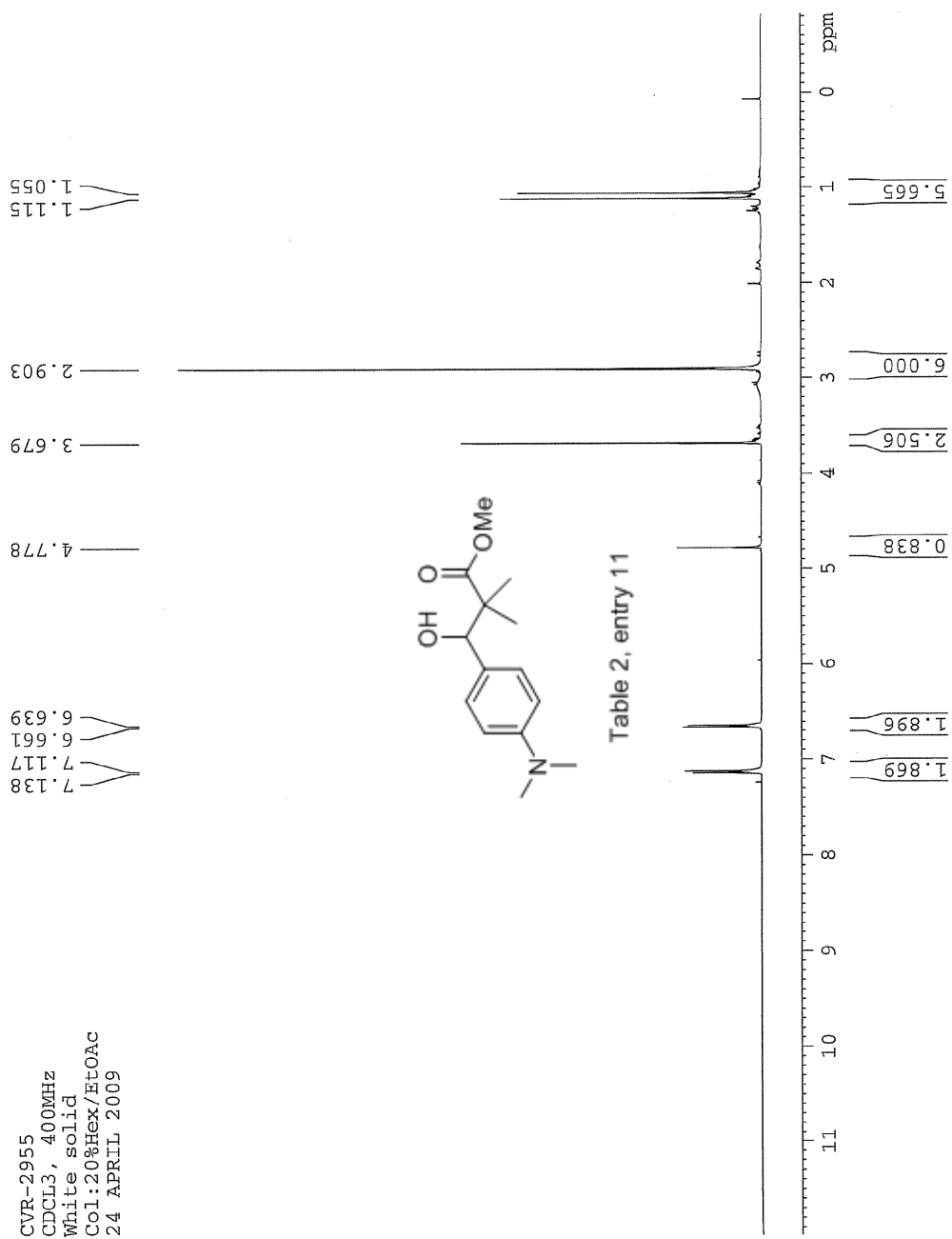
Study: MS services  
 Masses: 35.01 > 650.00  
 Intensity: 364037

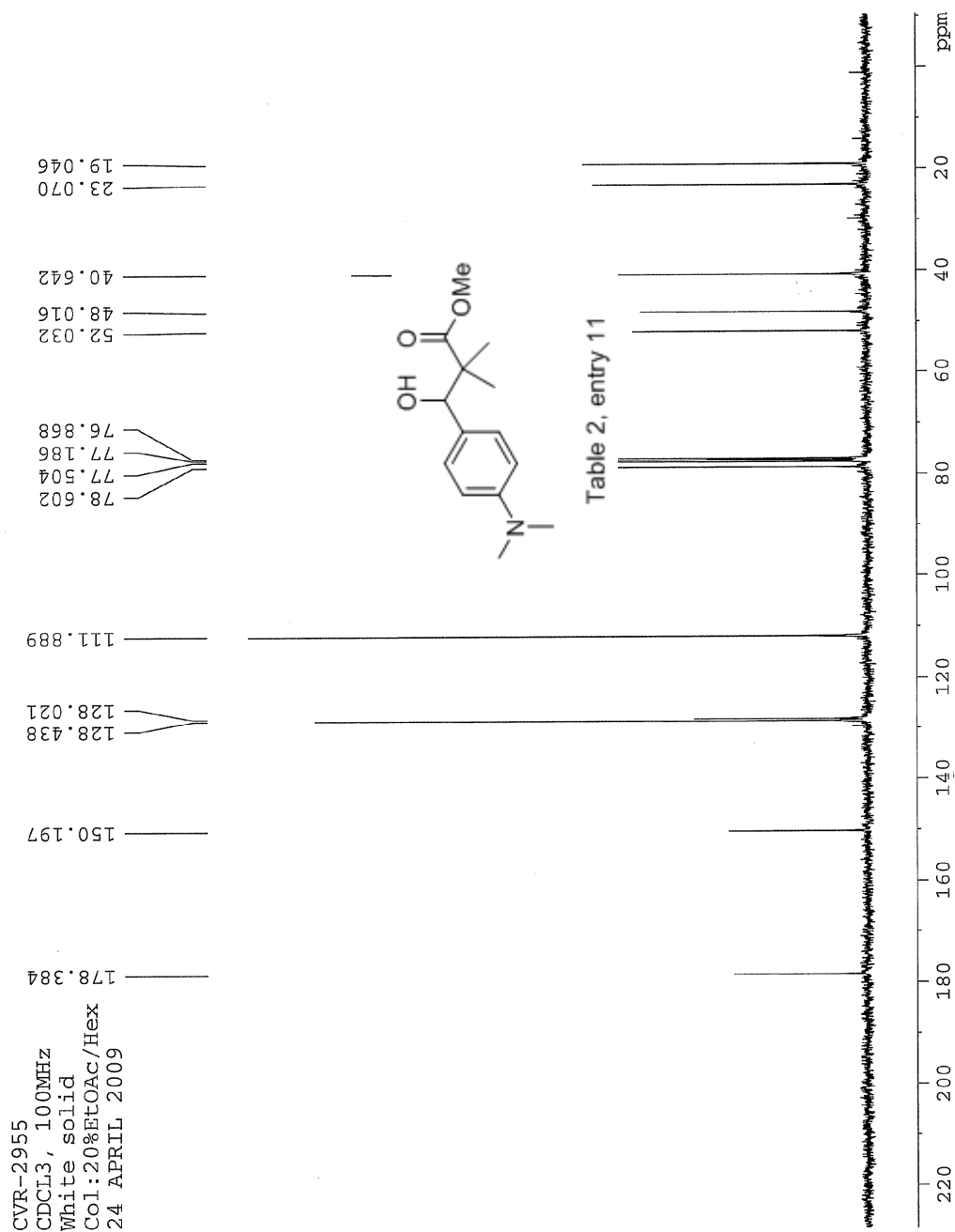


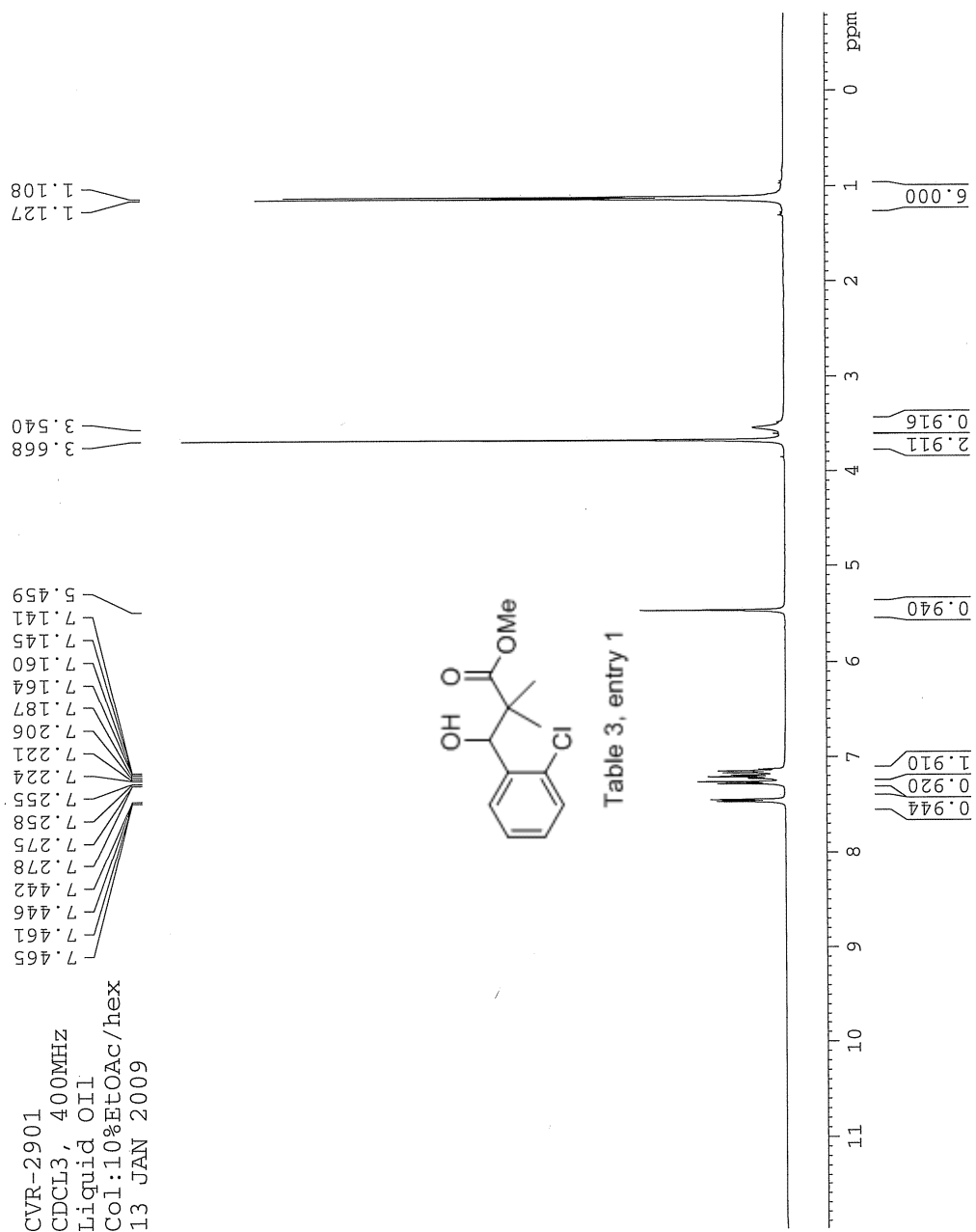
Date: Thu Jan 22 10:51:33 2009 ICIS: 8.3.0 SP2 for OSF1 (V4.0) build 98-238 from 26-Aug-98

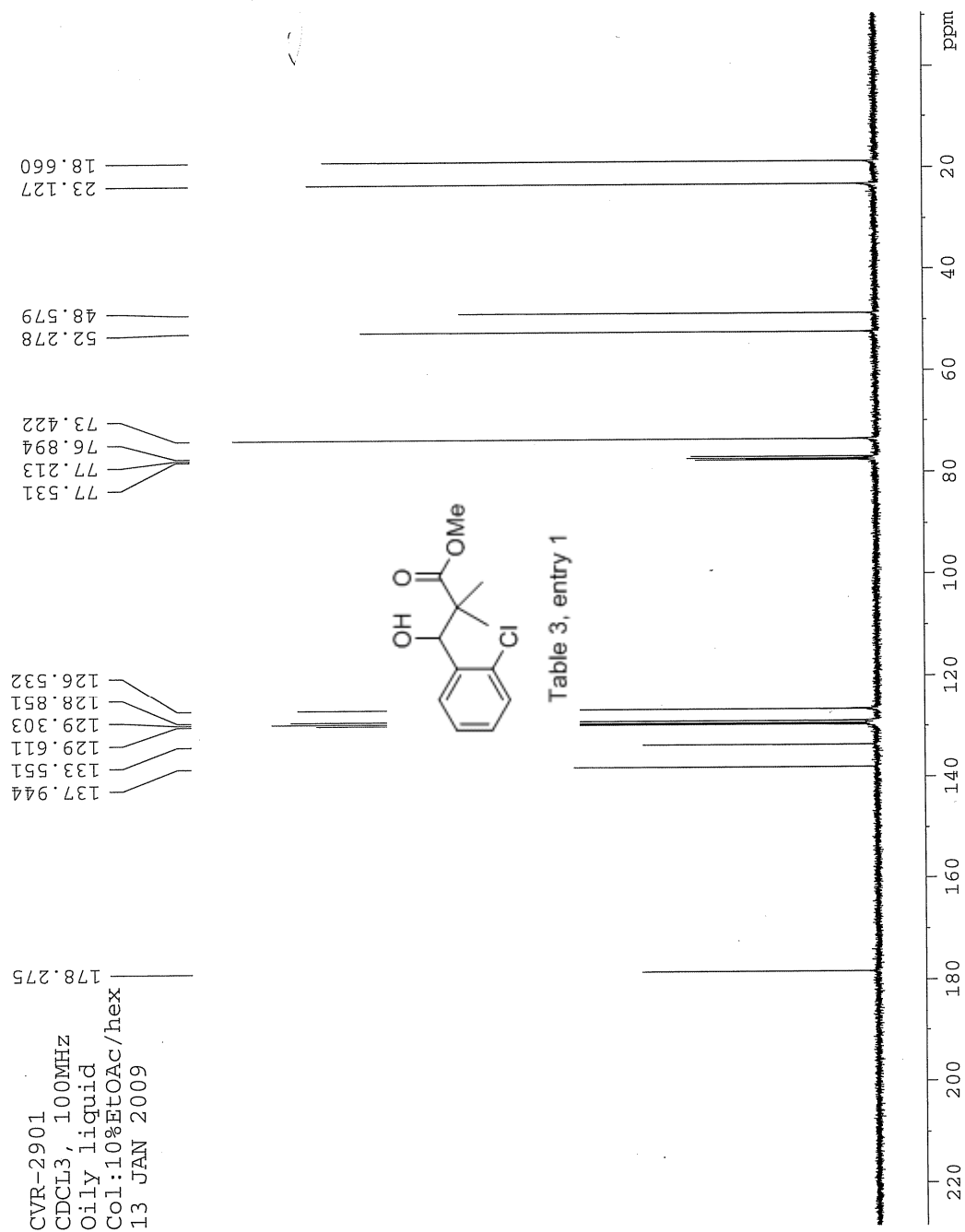












## Manual Peak Matching Report For Accurate Mass Determination

Theoretical mass	Experimental mass	PFK matching mass	Deviation*
242.07097	242.07153	230.98562	2.3 ppm

\* The deviation is obtained from the following equation:

$$\text{deviation} = \frac{\text{experimental mass} - \text{theoretical mass}}{\text{nominal mass}}$$

Where nominal mass takes in account only  $^{12}\text{C}$ ,  $^1\text{H}$ ,  $^{16}\text{O}$ ,  $^{14}\text{N}$  etc...

Theoretical mass correspond to the mass of the most abundant isotope peak

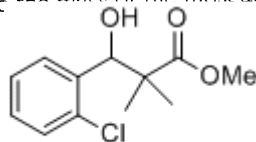


Table 3, entry 1

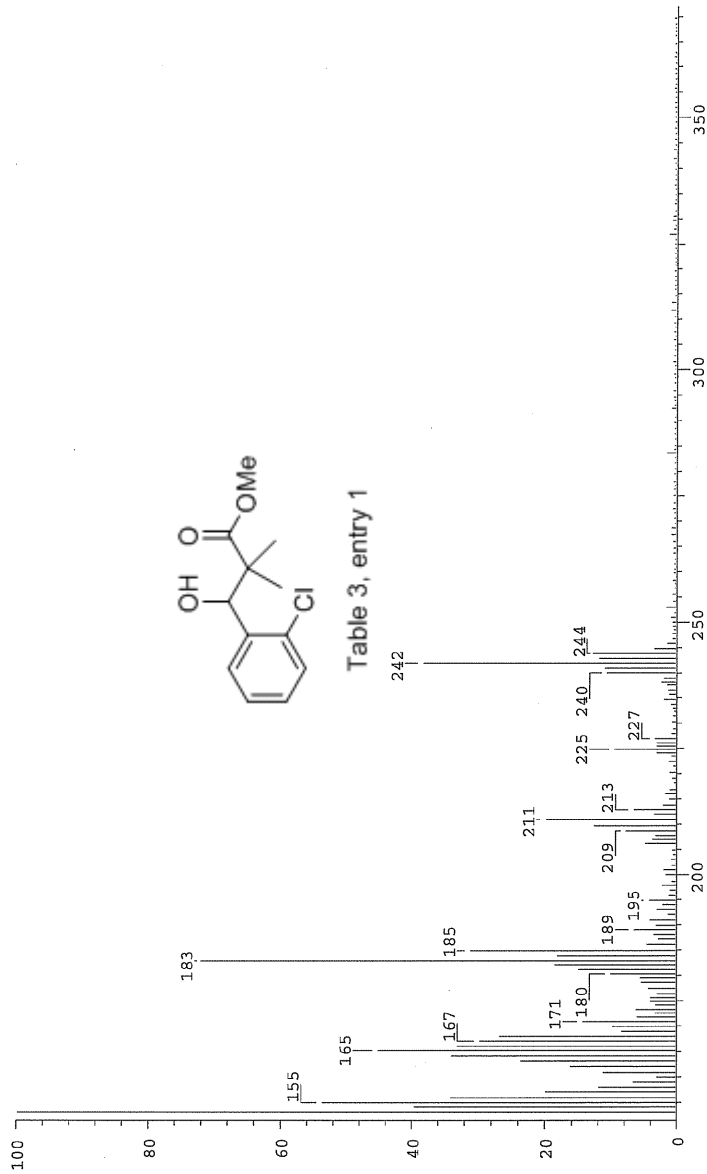
*M*



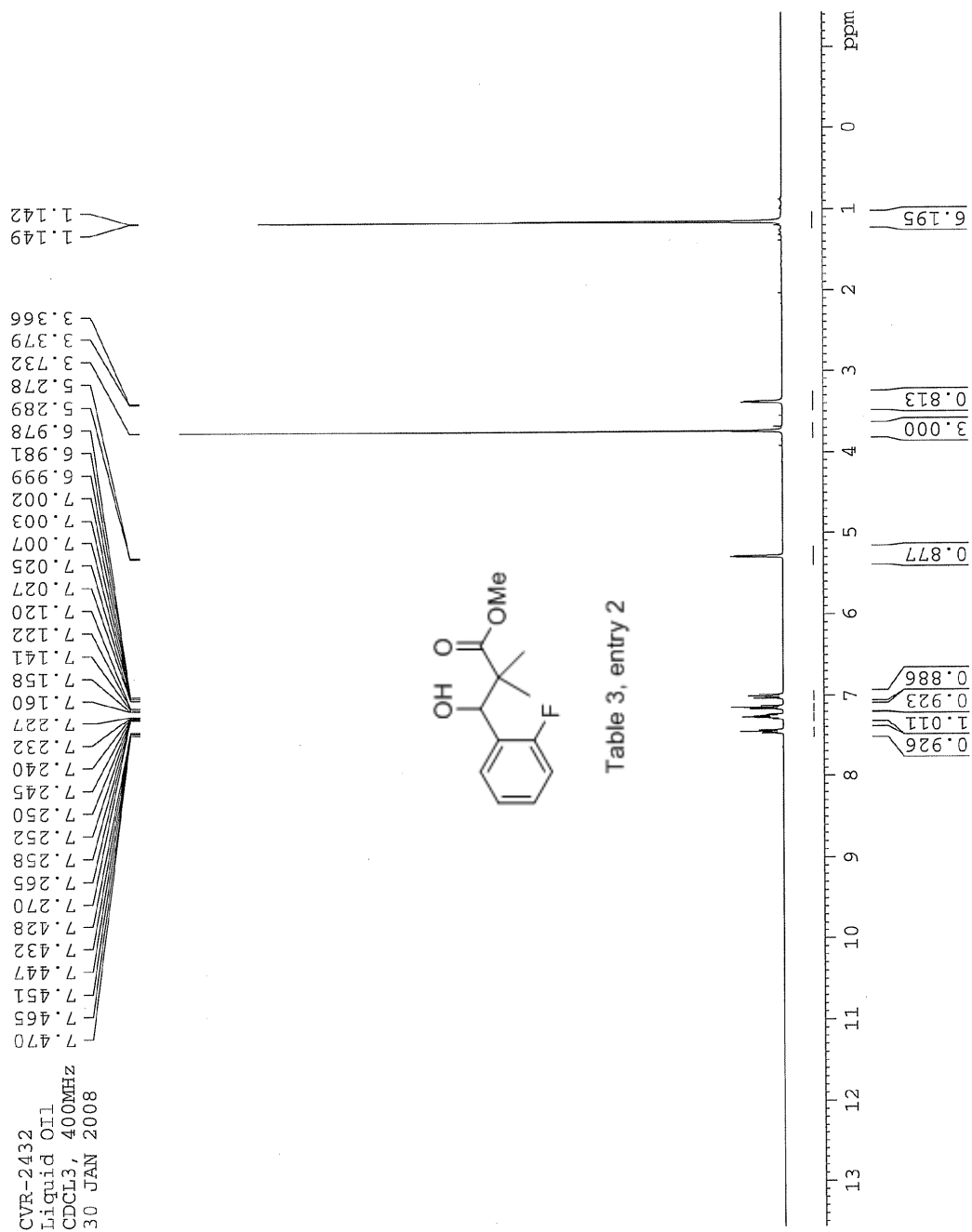
Scans: 1 > 64  
 Client: Venkat  
 #Peaks: 604  
 RIC: 20169451  
 8.7E+04

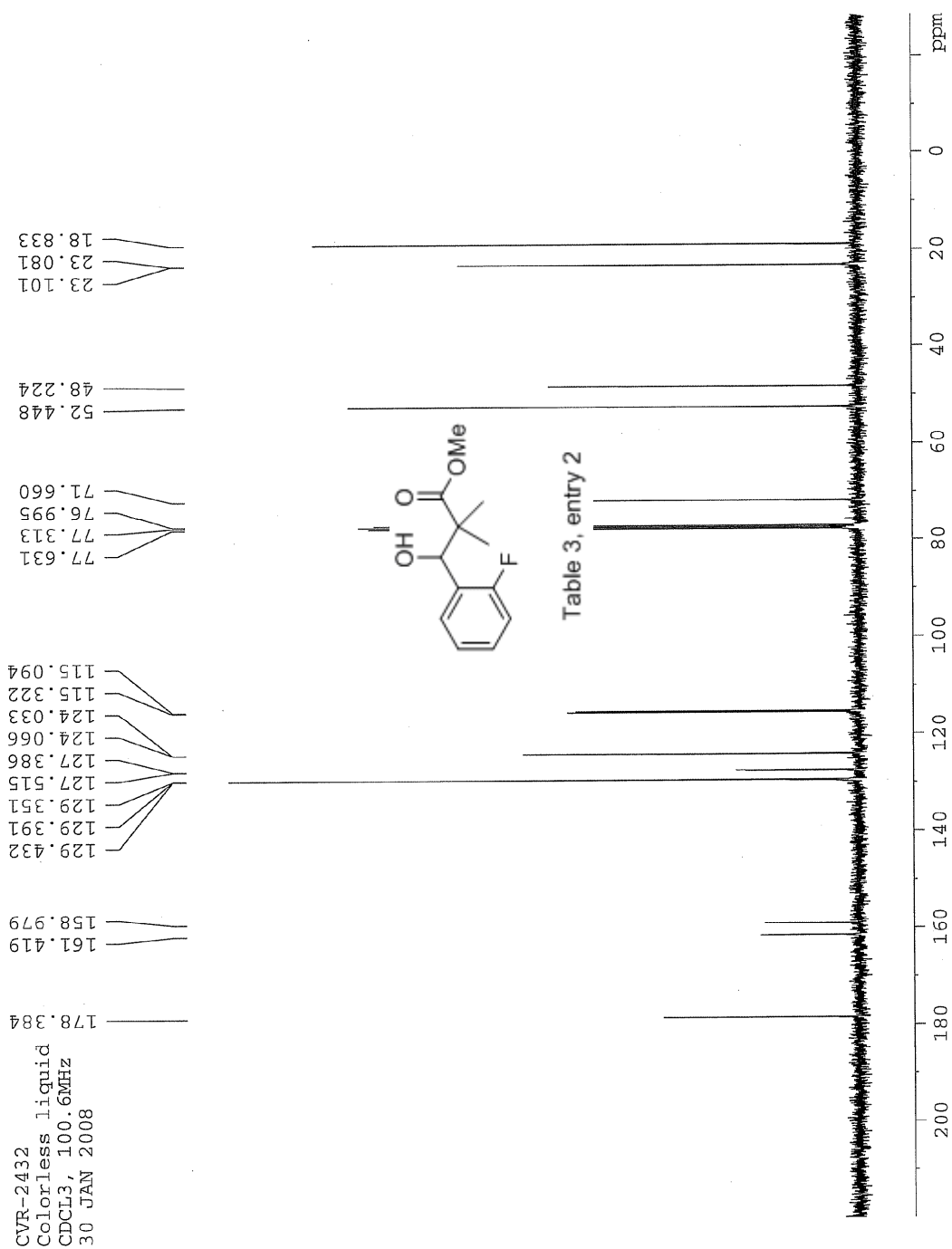
SPEC: fir084532.dat (16-JUN-09 11:00:11)  
 Samp: CVR-2901  
 Comm: DP/EI  
 Oper:  
 Base: 101.78  
 Peak: 1000.0 mmu  
 Scan 1 @ 0.18 min (EI +Q1MS LMR UP LR)

Study:  
 Masses: 35.01 > 650.00  
 Intensity: 2400208



Date: Tue Jun 16 11:02:19 2009 ICIS: 8.3.0 SP2 for OSF1 (V4.0) build 98-238 from 26-Aug-98





## Manual Peak Matching Report For Accurate Mass Determination

Theoretical mass	Experimental mass	PFK matching mass	Deviation*
226.10052	226.10078	218.98562	1.2 ppm

\* The deviation is obtained from the following equation:

$$\text{deviation} = \frac{\text{experimental mass} - \text{theoretical mass}}{\text{nominal mass}}$$

Where nominal mass takes in account only  $^{12}\text{C}$ ,  $^1\text{H}$ ,  $^{16}\text{O}$ ,  $^{14}\text{N}$  etc...

Theoretical mass correspond to the mass of the most abundant isotope peak

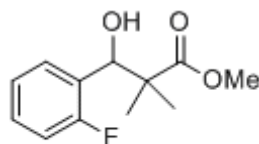


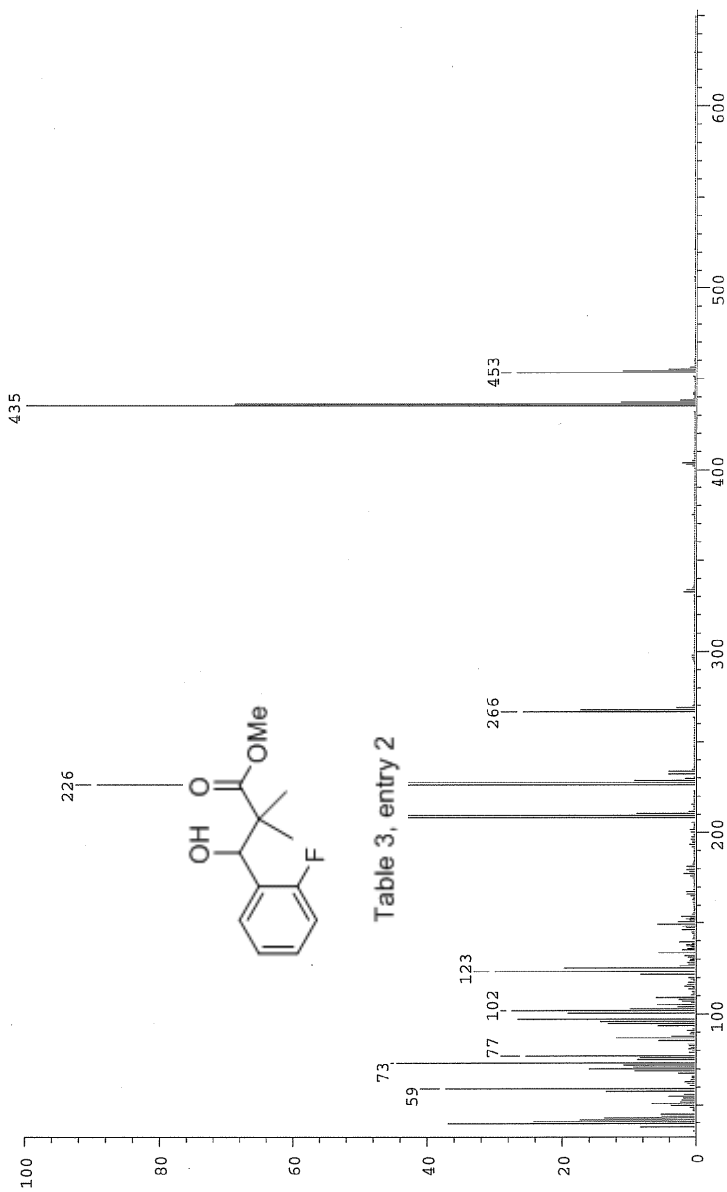
Table 3, entry 2

*BR*

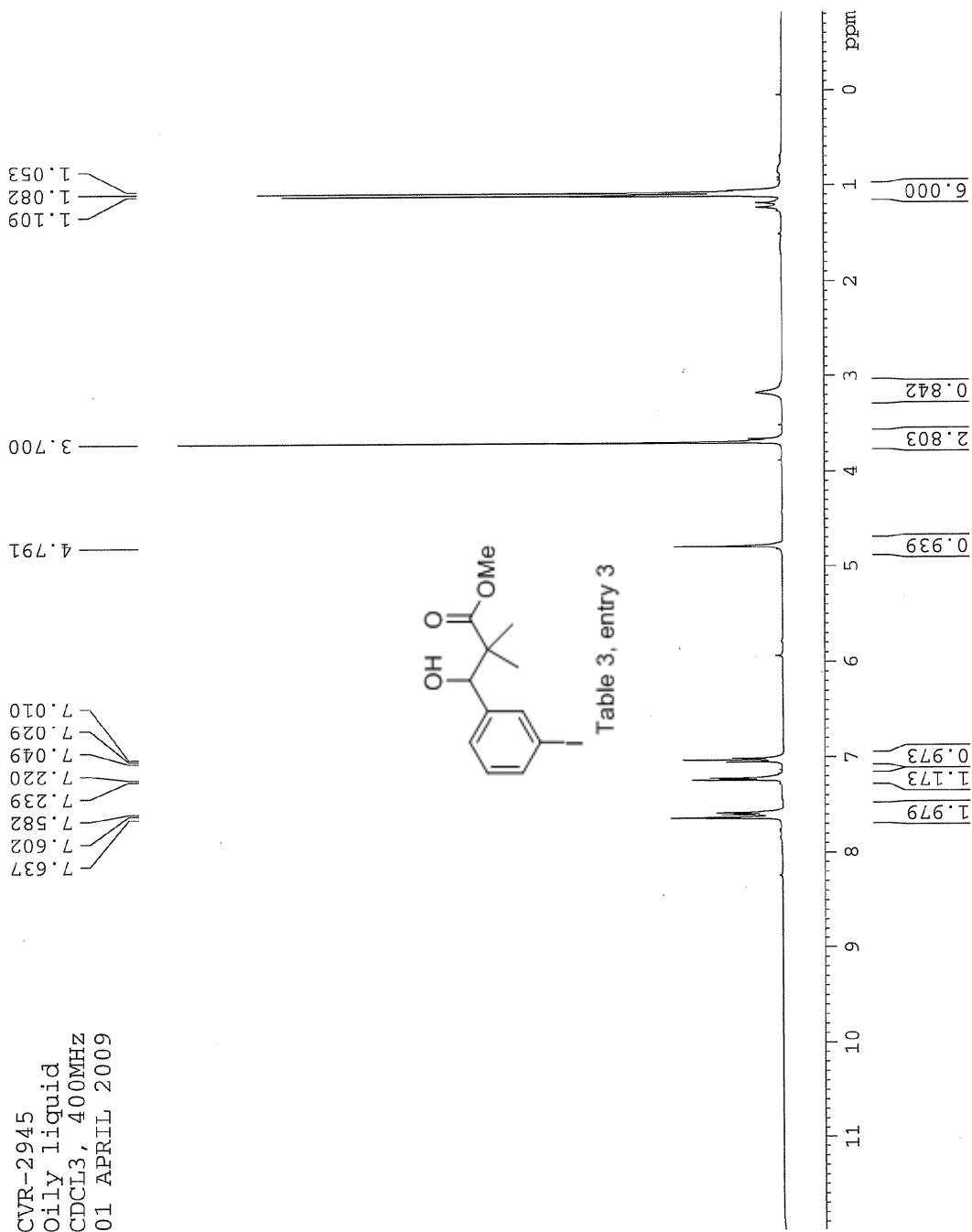
SPEC: fin063463.dat (14-FEB-08 11:25:10)  
 Samp: CVR-2432  
 Comm: 70 eV EI  
 Oper: Rh  
 Base: 435.06  
 Peak: 1000.0 mmu  
 Scan 12 @ 0.41 min (EI +QIMS LMR UP LR)

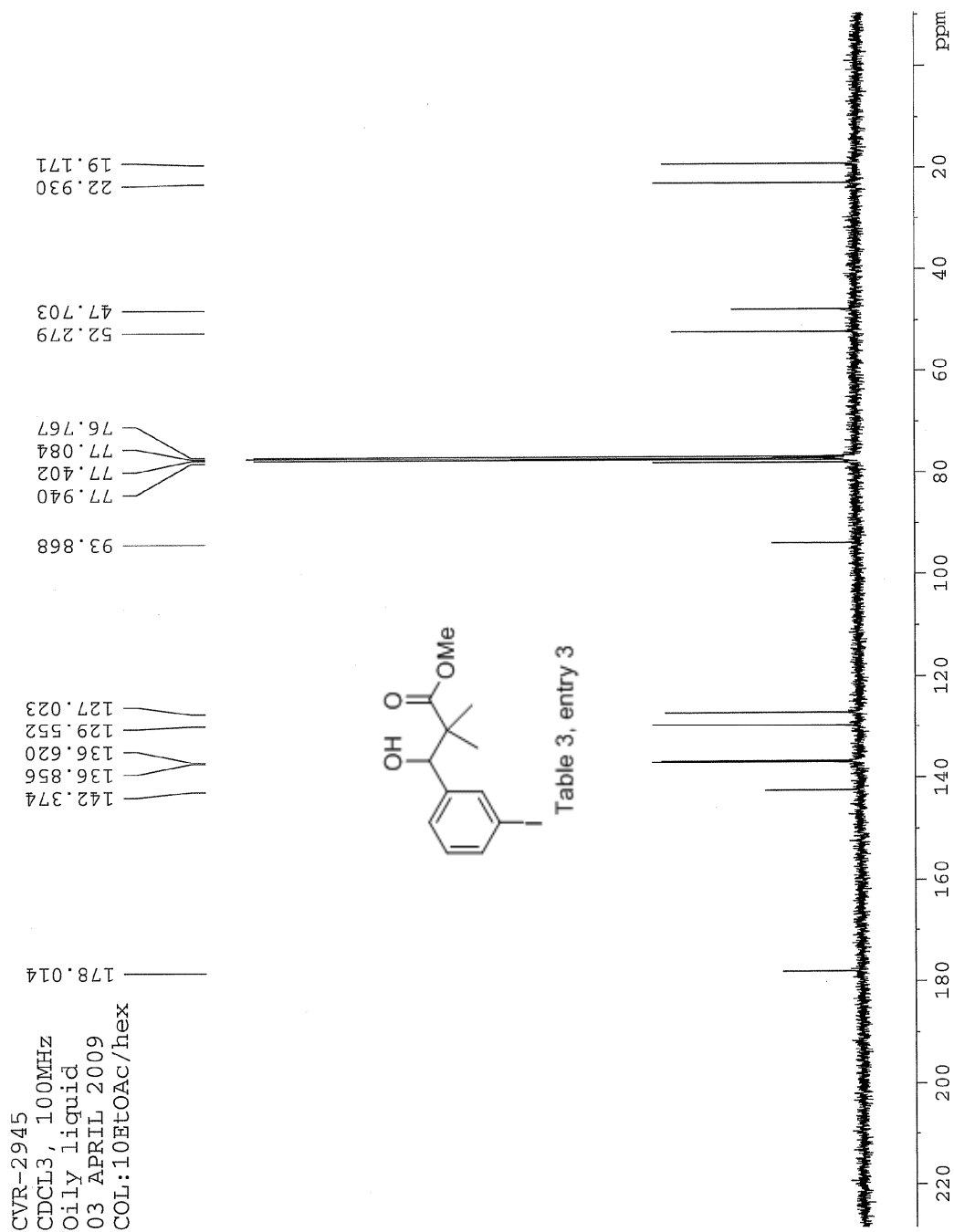
Study: MS Services  
 Masses: 35.01 > 650.00  
 Intensity: 1783560

Scans: 1 > 90  
 Client: Venkat  
 #Peaks: 619  
 RIC: 21946529  
 1.8E+06



Date: Thu Feb 14 11:27:36 2008 ICIS: 8.3.0 SP2 for OSF1 (V4.0) build 98-238 from 26-Aug-98





### Manual Peak Matching Report For Accurate Mass Determination

Theoretical mass	Experimental mass	PFK matching mass	Deviation*
334.00659	334.00734	330.97923	2.2 ppm

\* The deviation is obtained from the following equation:

$$\text{deviation} = \frac{\text{experimental mass} - \text{theoretical mass}}{\text{nominal mass}}$$

Where nominal mass takes in account only  $^{12}\text{C}$ ,  $^1\text{H}$ ,  $^{16}\text{O}$ ,  $^{14}\text{N}$  etc...

Theoretical mass correspond to the mass of the most abundant isotope peak

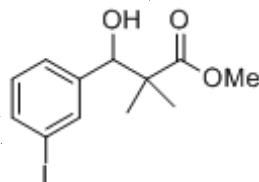
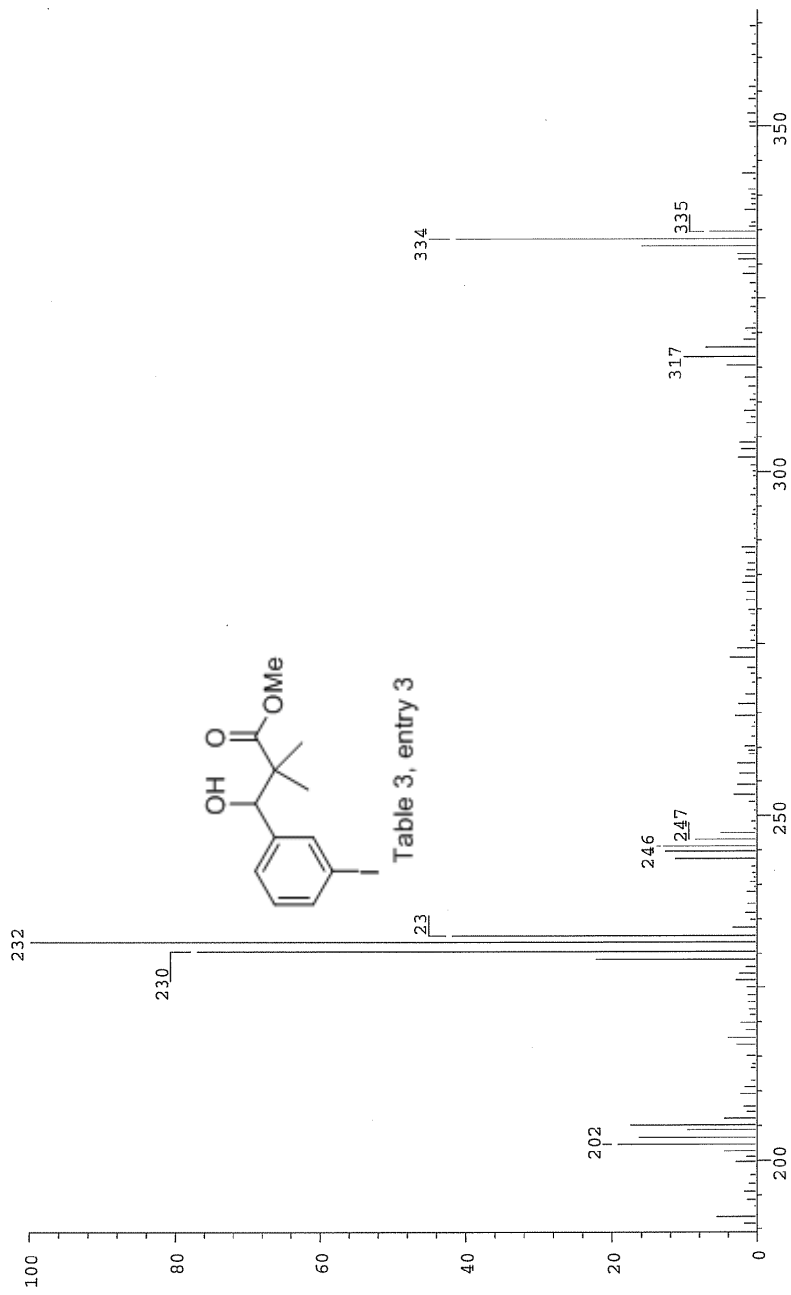


Table 3, entry 3

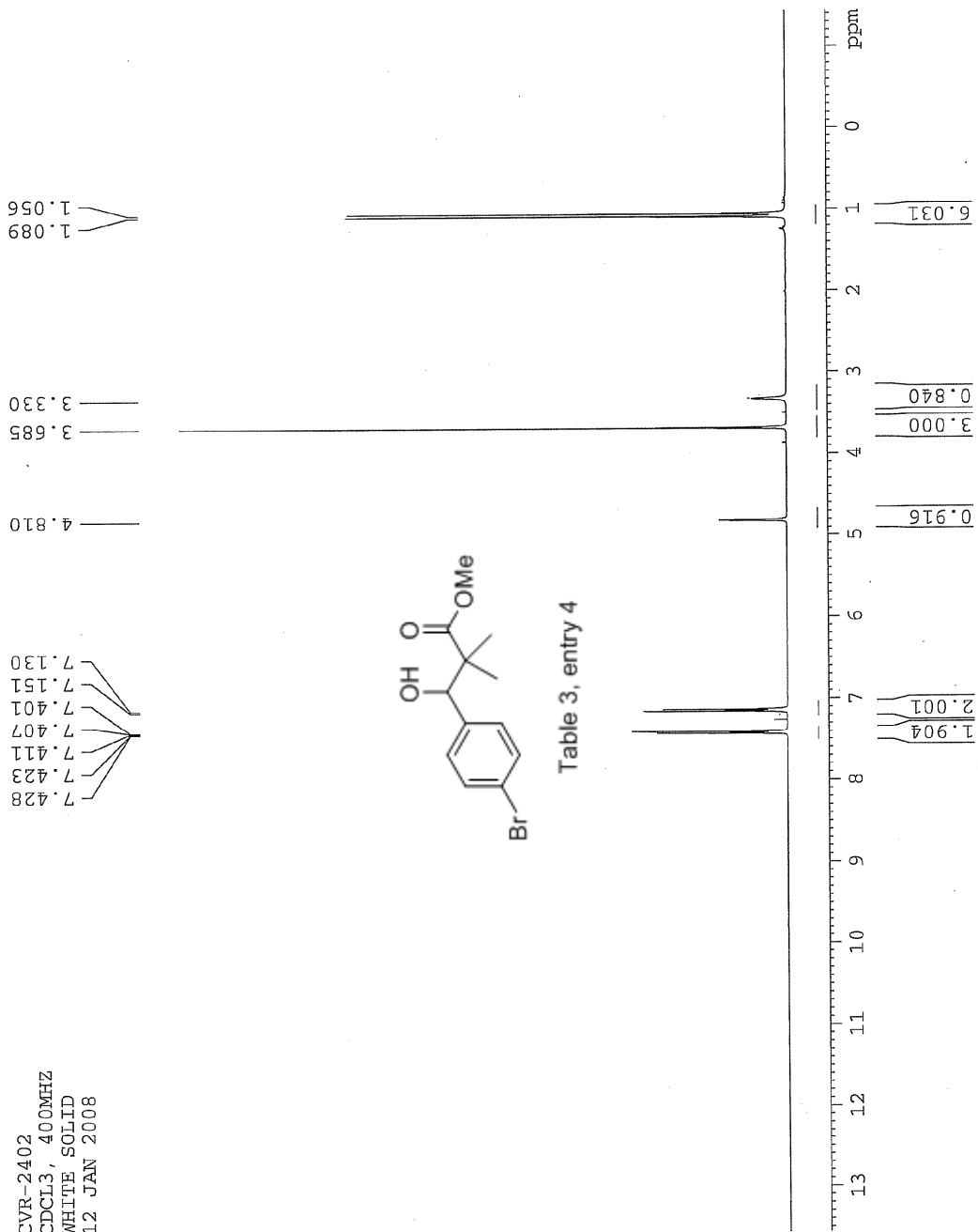


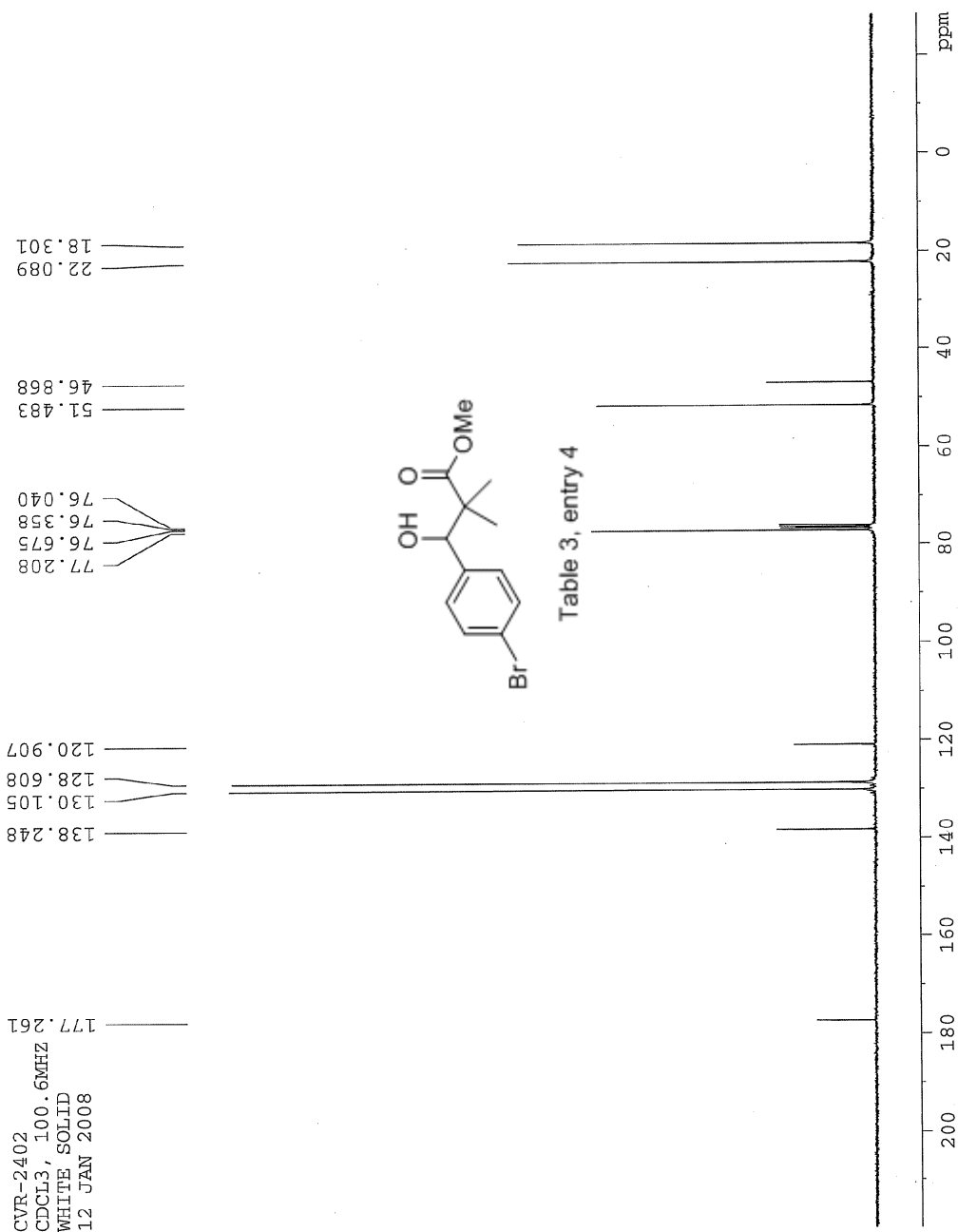
SPC: fin084373.dat (10-APR-09 10:23:57)  
 Samp: CVR-2945  
 Comm: DP/EI  
 Oper: kh  
 Base: 100.89  
 Peak: 1000.0 mmu  
 Scan 68 @ 1.54 min (EI +QIMS LMR UP LR)

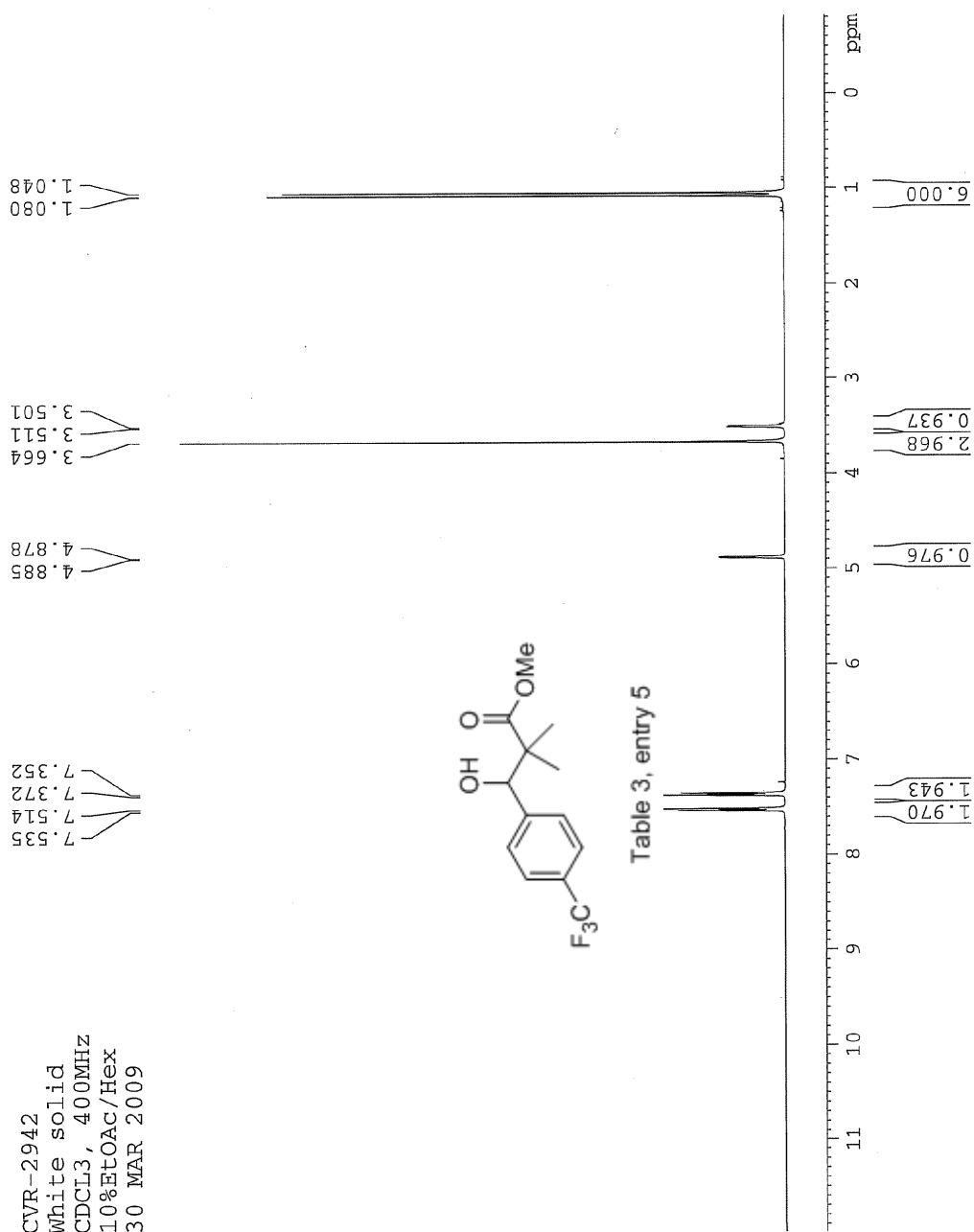
Study: ms services  
 Masses: 35.01 > 650.00  
 Intensity: 42958  
 Client: Venkat  
 #Peaks: 558  
 RIC: 292648  
 4.6E+03

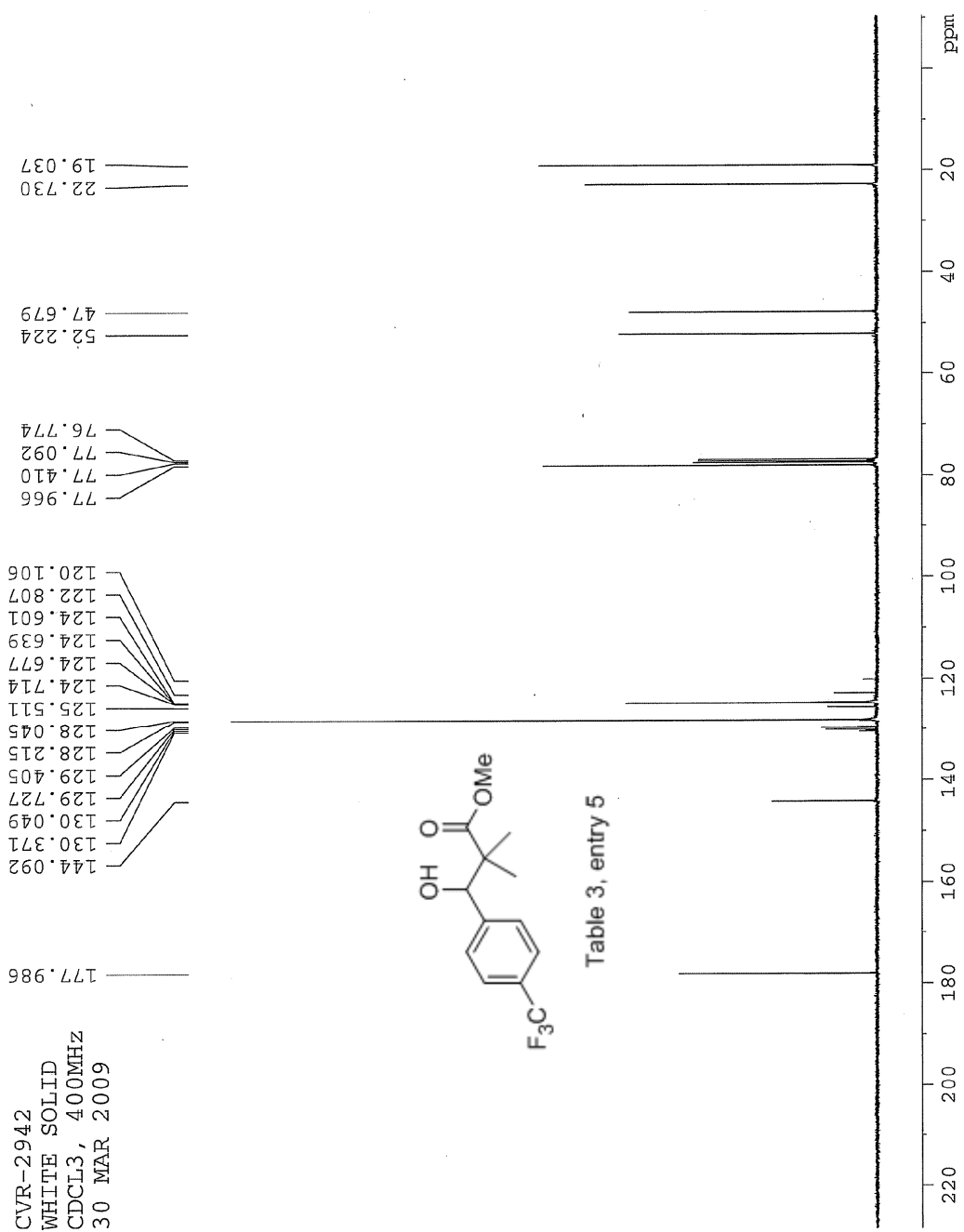


Date: Fri Apr 10 10:27:11 2009 ICIS: 8.3.0 SP2 for OSF1 (V4.0) build 98-238 from 26-Aug-98









### Manual Peak Matching Report For Accurate Mass Determination

Theoretical mass	Experimental mass	PFK matching mass	Deviation*
276.09732	276.09812	230.98562	2.9 ppm

\* The deviation is obtained from the following equation:

$$\text{deviation} = \frac{\text{experimental mass} - \text{theoretical mass}}{\text{nominal mass}}$$

Where nominal mass takes in account only  $^{12}\text{C}$ ,  $^1\text{H}$ ,  $^{16}\text{O}$ ,  $^{14}\text{N}$  etc...

Theoretical mass correspond to the mass of the most abundant isotope peak

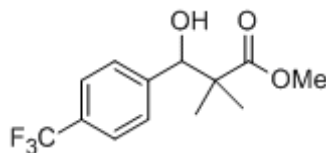


Table 3, entry 5

*Handwritten signature*

SPEC: Fin084534.dat (16-JUN-09 11:11:21)  
 Smp: CVR-2942  
 Com: DF/EI  
 Oper:  
 Base: 37.77  
 Peak: 1000.0 mmu  
 Scan 35 @ 0.86 min (EI +QIMS LMR UP LR)  
 Study:  
 Masses: 35.01 > 650.00  
 Intensity: 3571491  
 Scans: 1 > 43  
 Client: Venkat  
 #Peaks: 619  
 RIC: 24975269  
 5.5E+04

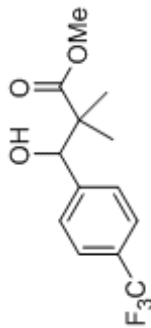
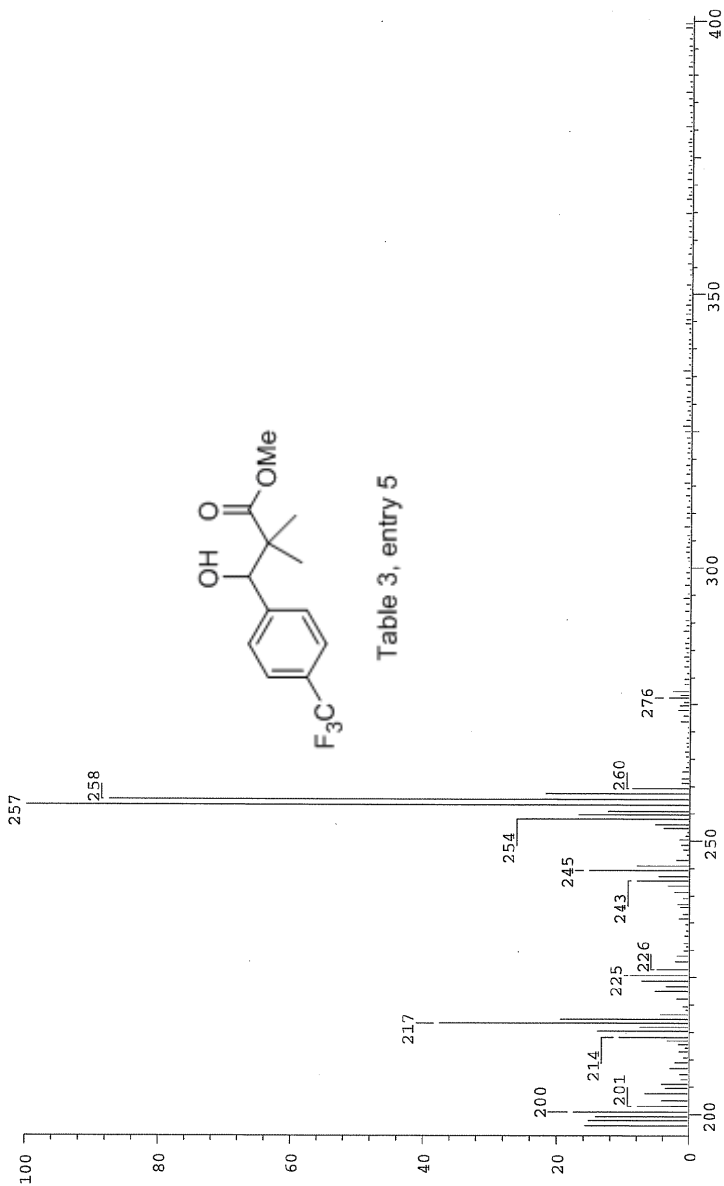
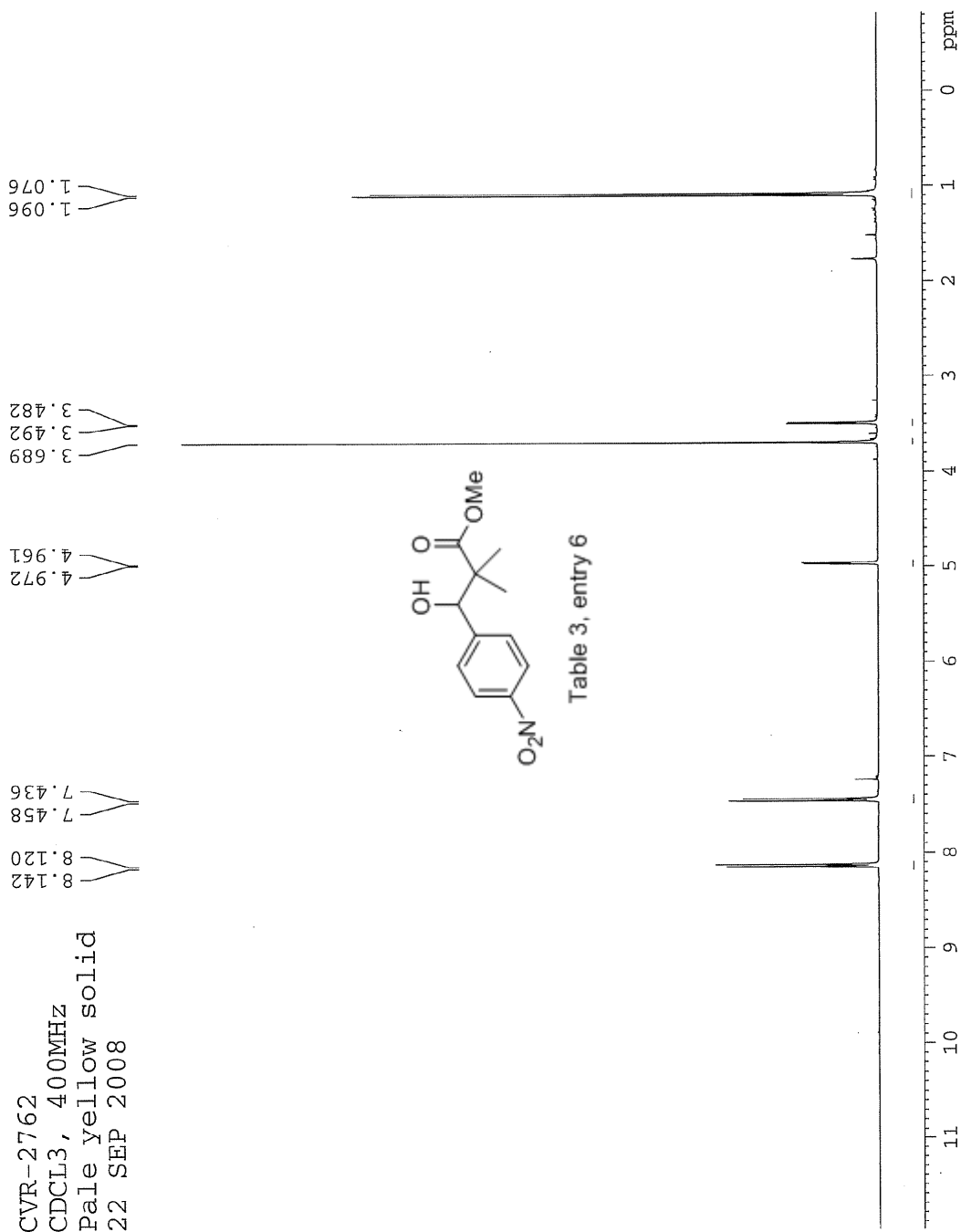
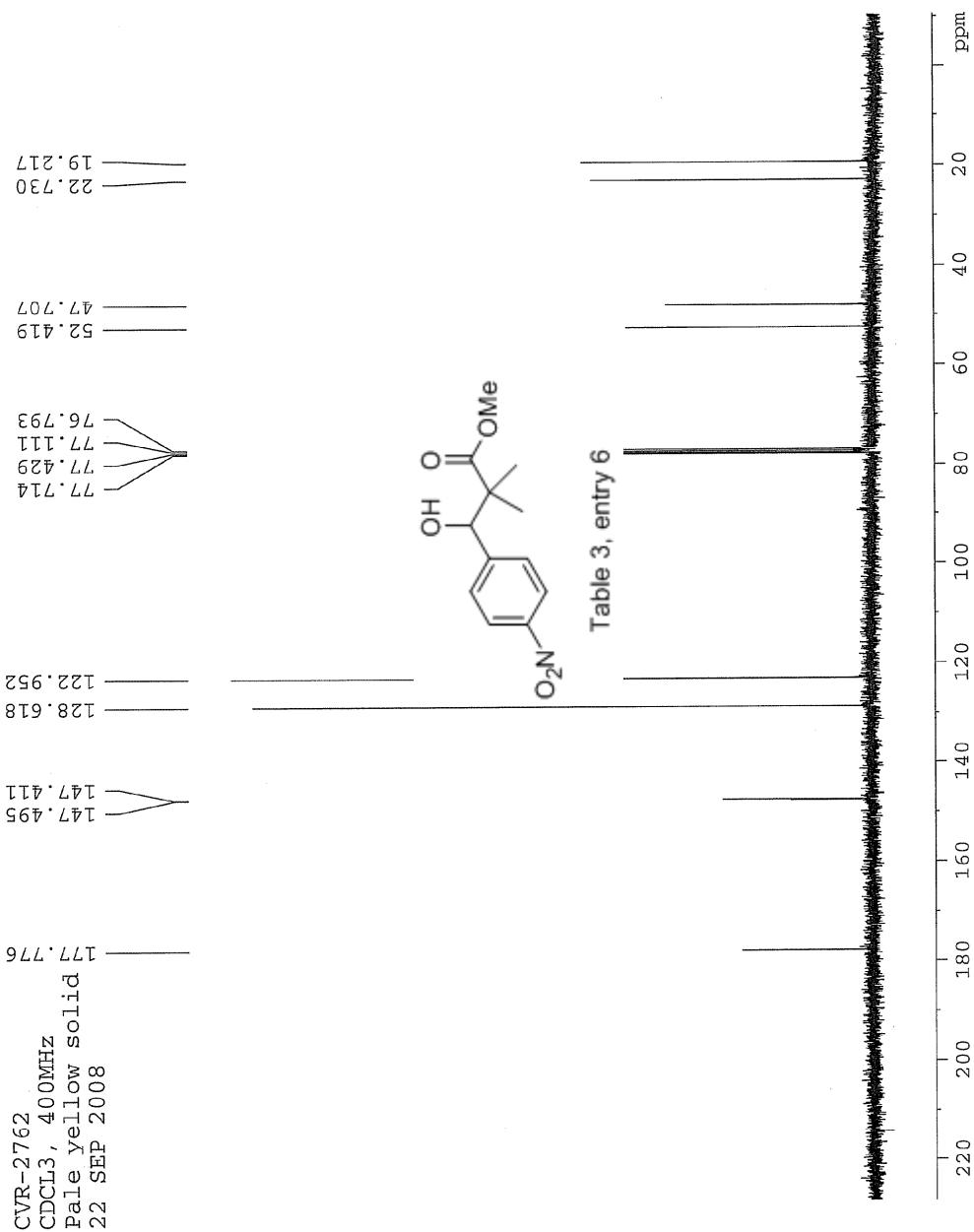


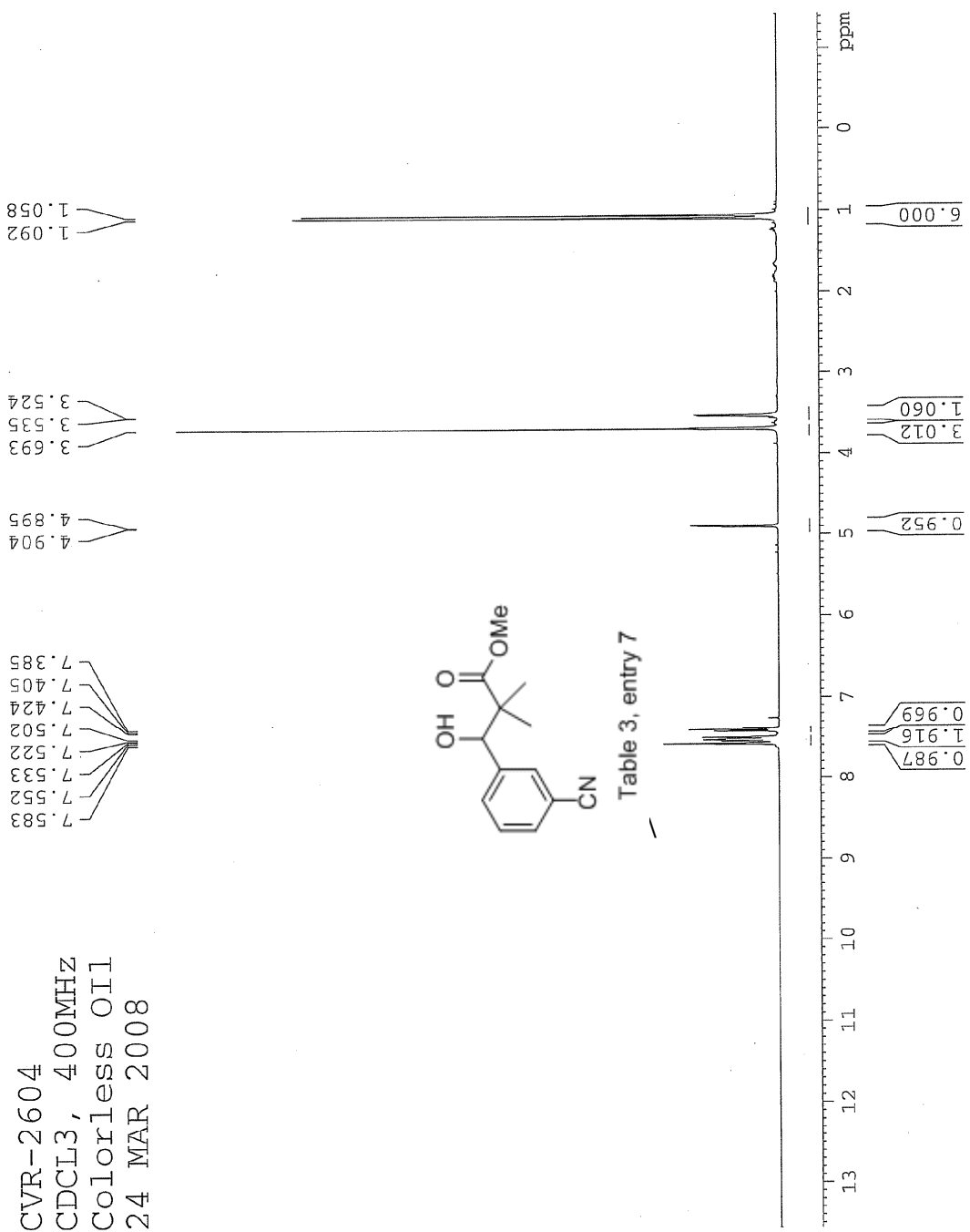
Table 3, entry 5

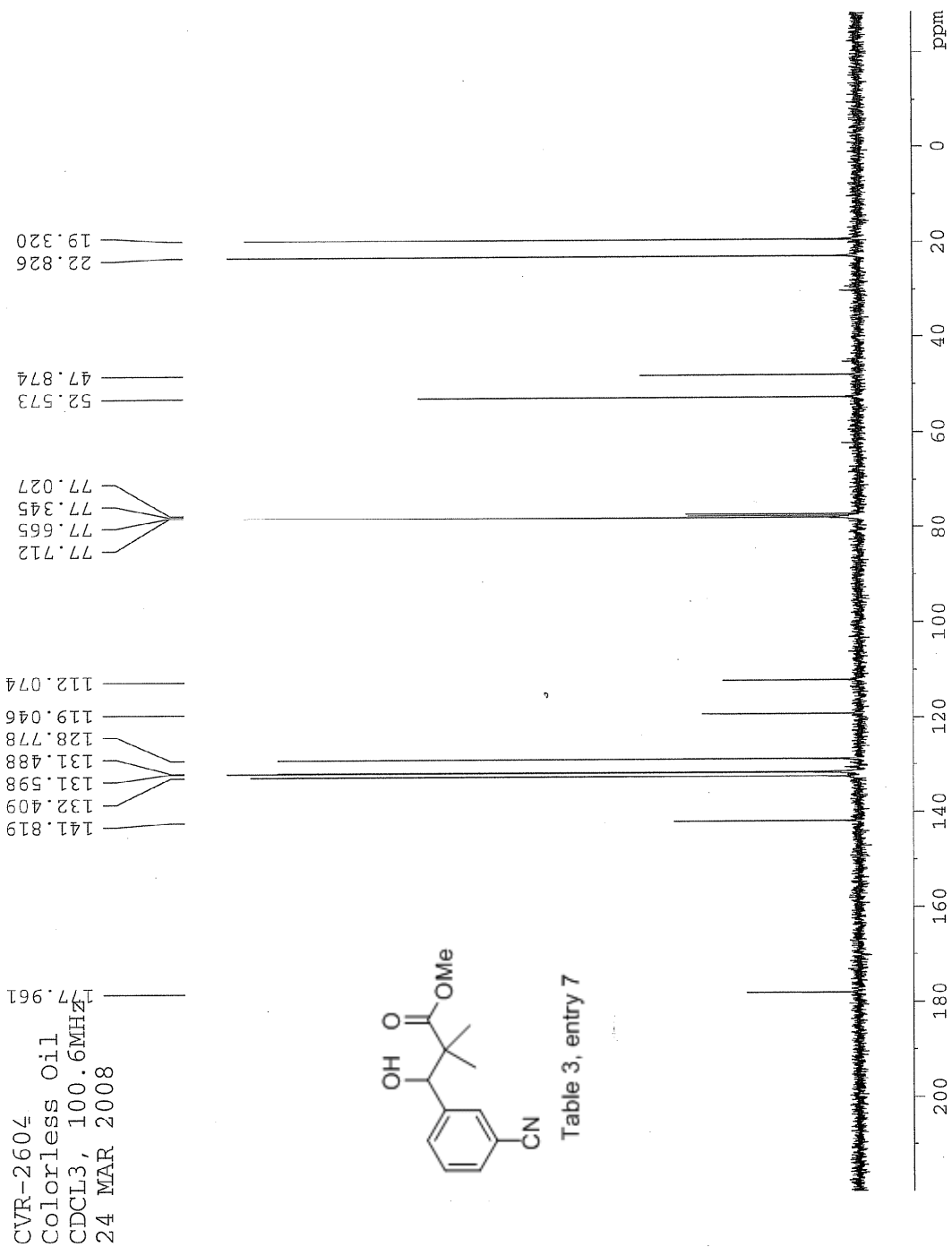
Date: Tue Jun 16 11:13:01 2009 ICIS: 8.3.0 SP2 for OSF1 (V4.0) build 98-238 from 26-Aug-98











### Manual Peak Matching Report For Accurate Mass Determination

Theoretical mass	Experimental mass	PFK matching mass	Deviation*
233.10519	233.10548	230.98562	1.3 ppm

\* The deviation is obtained from the following equation:

$$\text{deviation} = \frac{\text{experimental mass} - \text{theoretical mass}}{\text{nominal mass}}$$

Where nominal mass takes in account only  $^{12}\text{C}$ ,  $^1\text{H}$ ,  $^{16}\text{O}$ ,  $^{14}\text{N}$  etc...

Theoretical mass correspond to the mass of the most abundant isotope peak

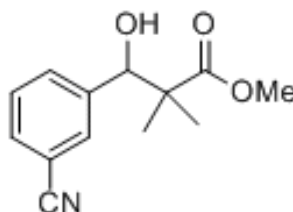


Table 3, entry 7

*MO*

SPEC: fin063552 (15-APR-08 10:57:32) Scans: 1 > 87  
 Samp: CVR-2604  
 Comm: 70 eV EI  
 Oper: kh  
 Study: MS Services  
 Base: 101.84 Masses: 35.01 > 650.00  
 Peak: 1000.0 mmu Intensity: 1966778  
 REG #9 @ 0.93 min (EI +QIMS IMR UP LR) (+38>51)

Client: Venkat

#Peaks: 635

RIC: 7285776

1.2E+05

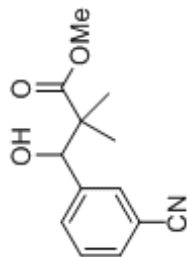
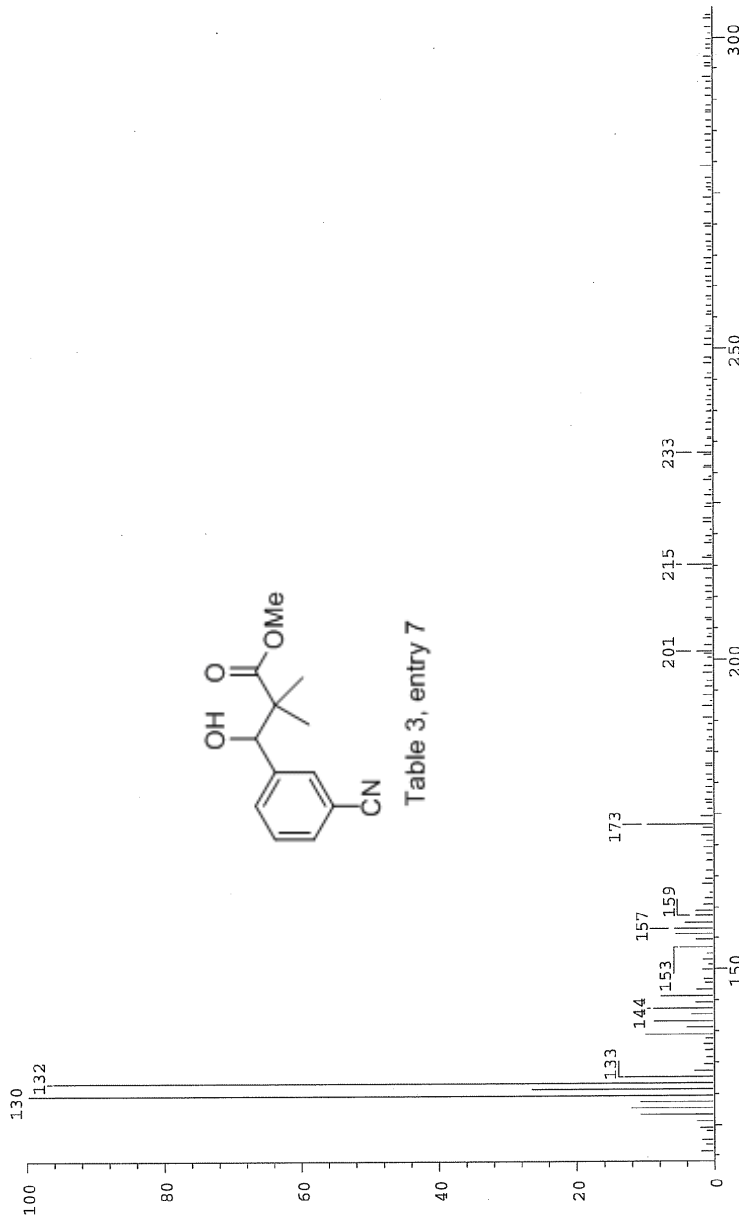
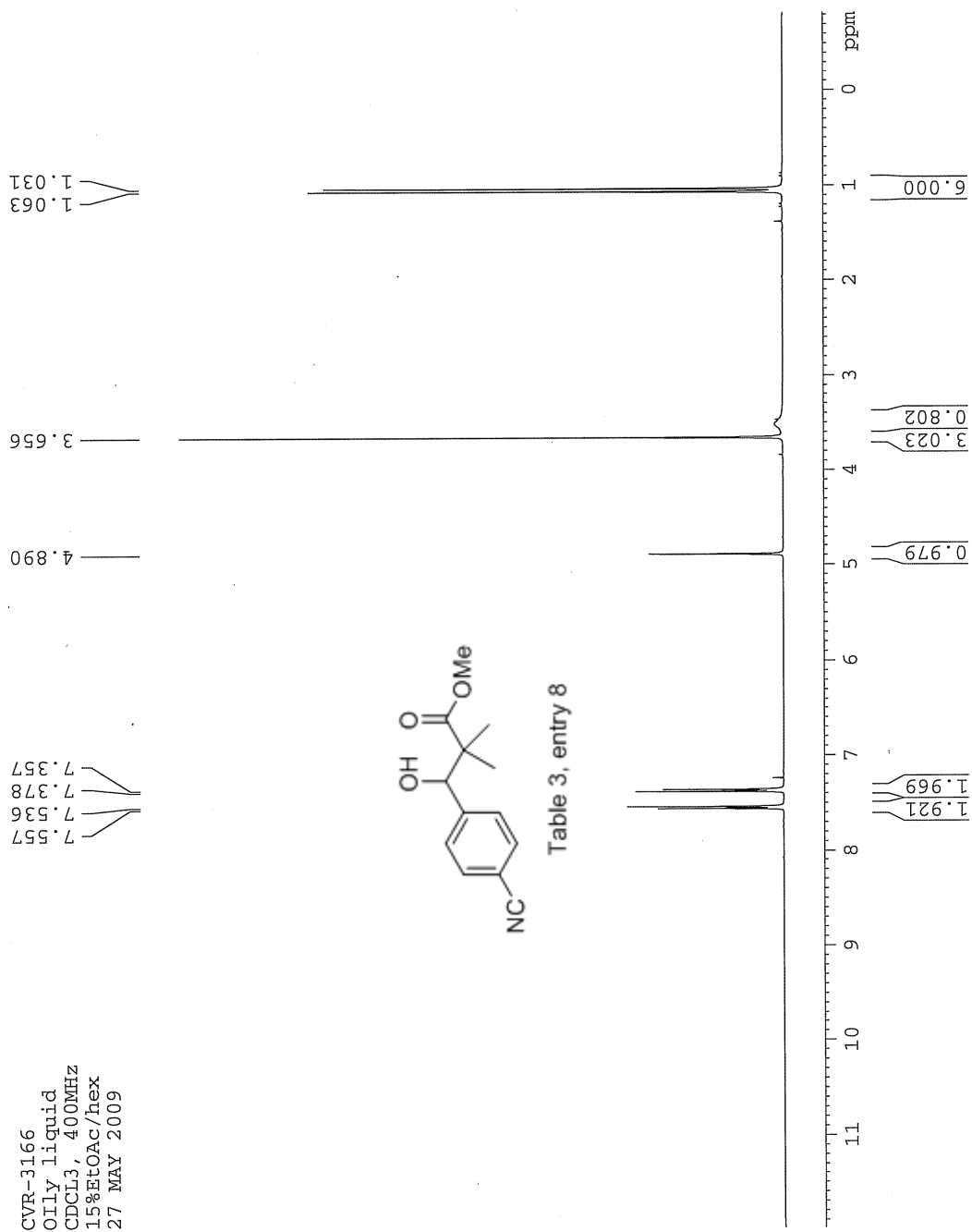
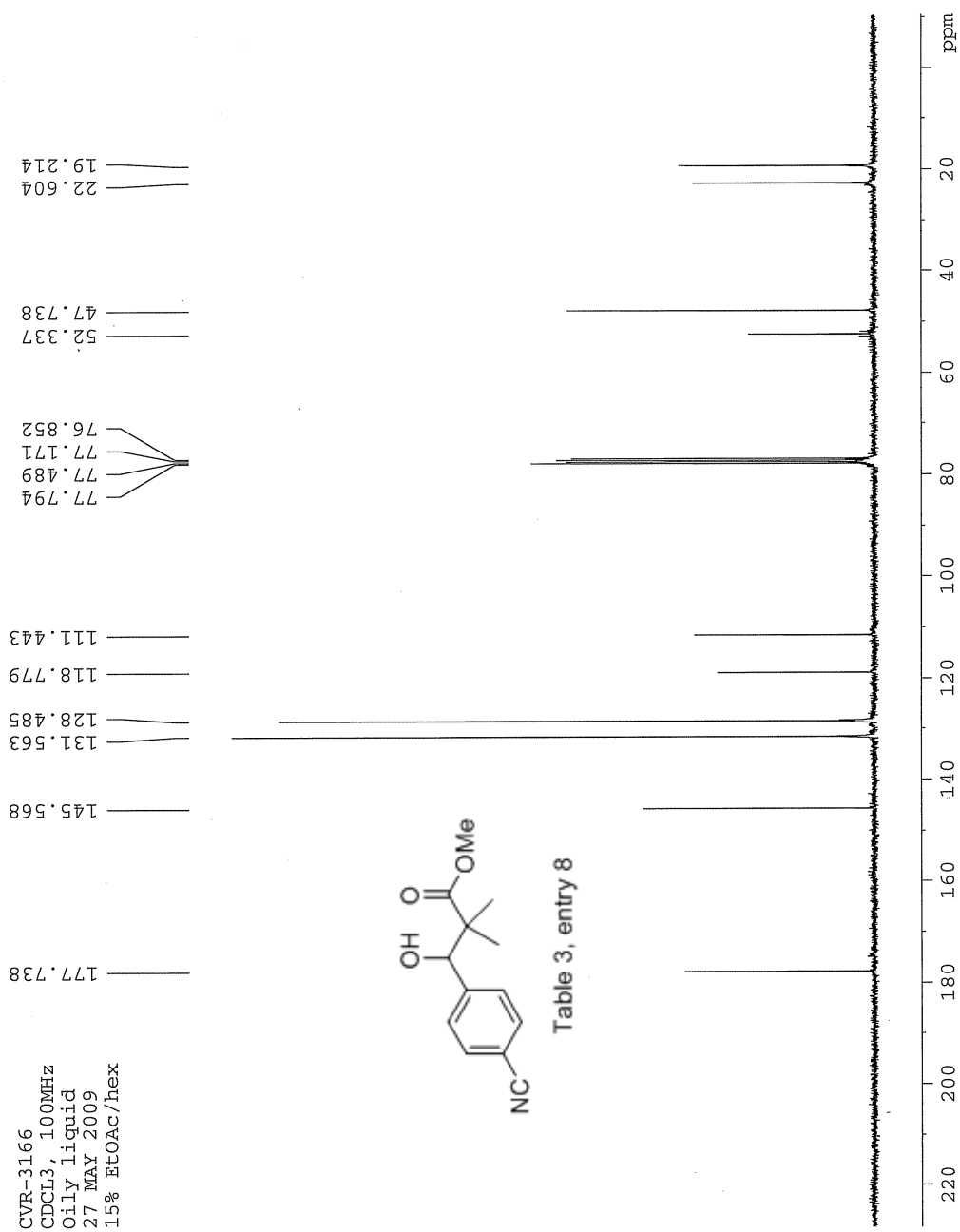
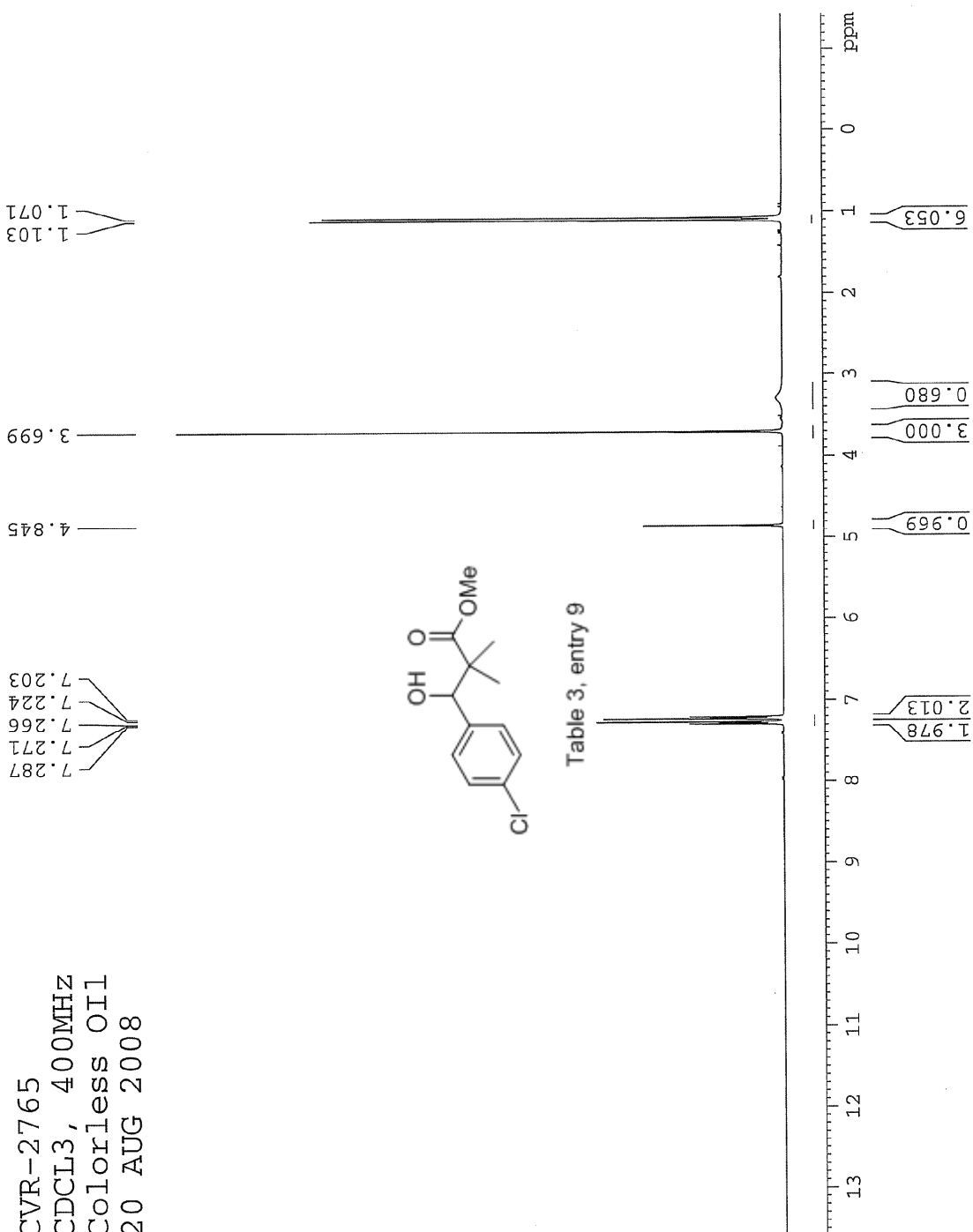


Table 3, entry 7

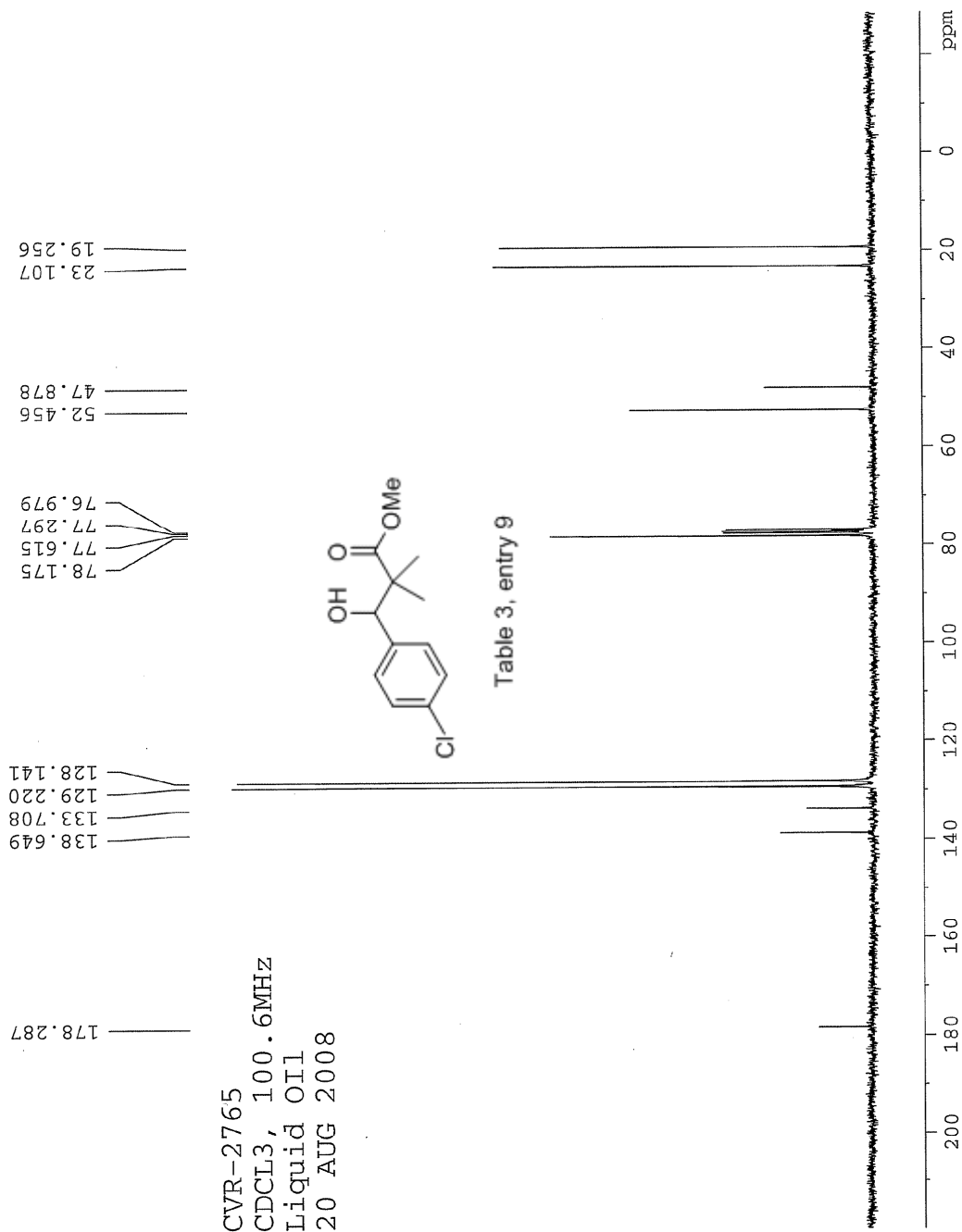
Date: Tue Apr 15 11:05:23 2008 ICIS: 8.3.0 SP2 for OSF1 (V4.0) build 98-238 from 26-Aug-98

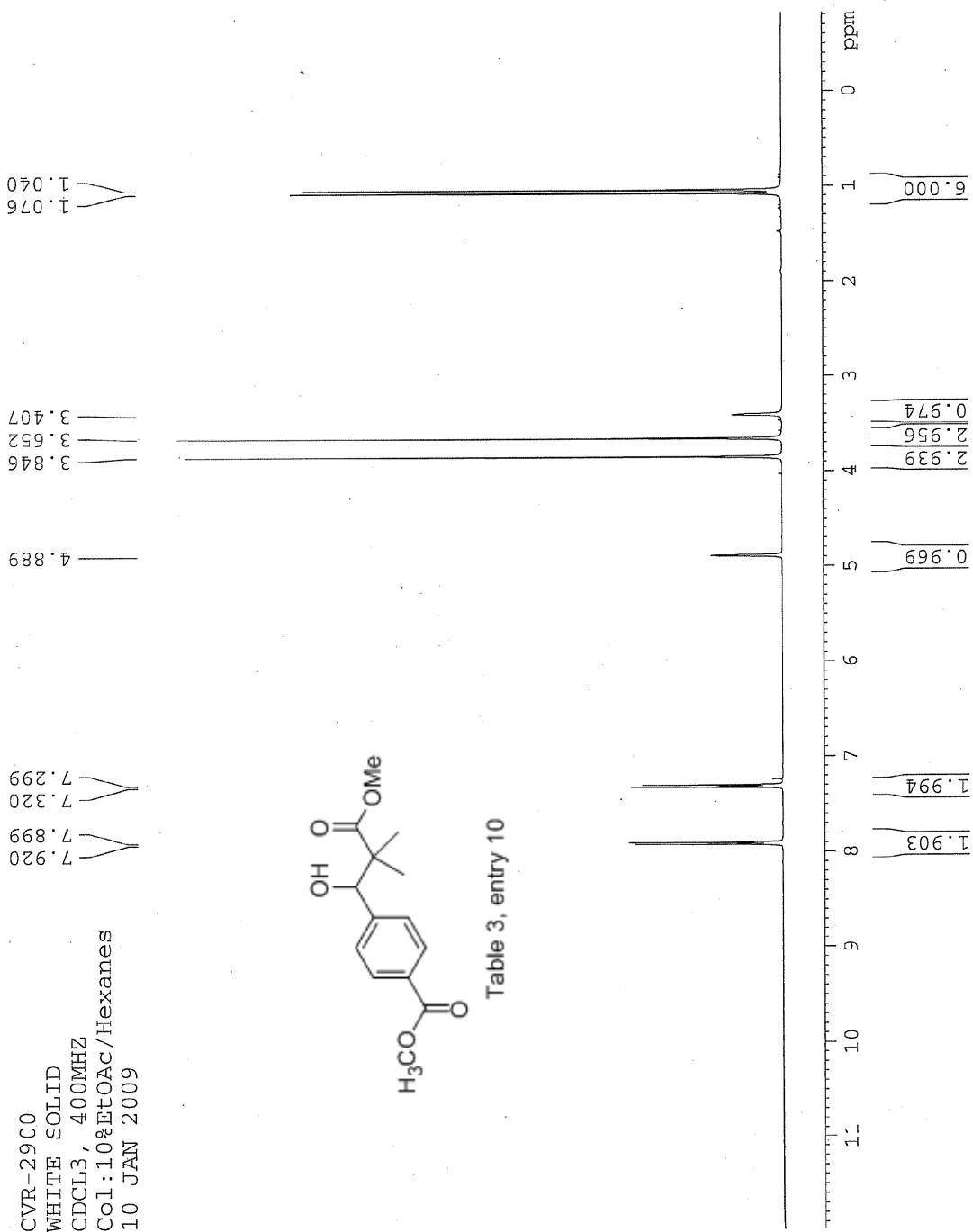


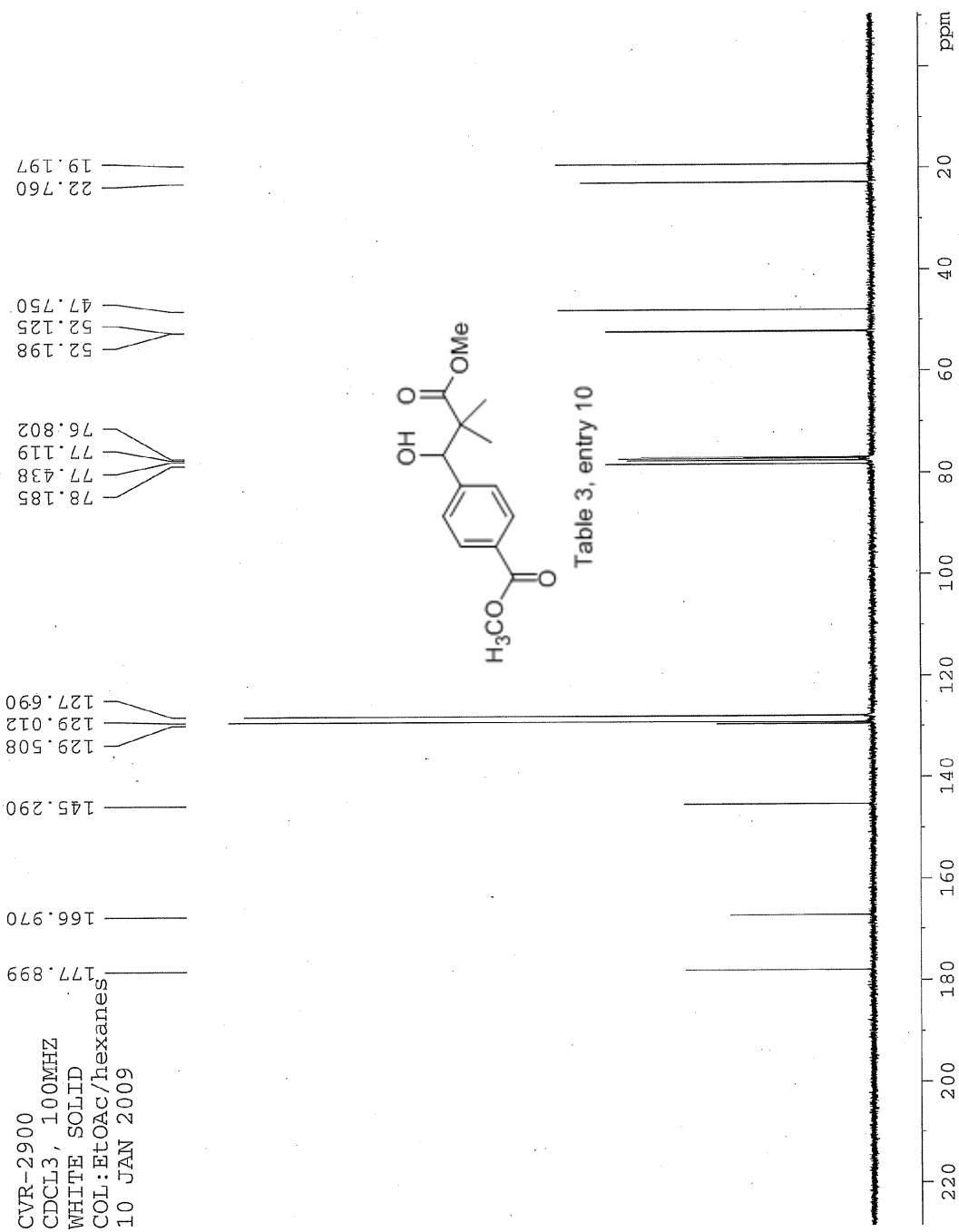


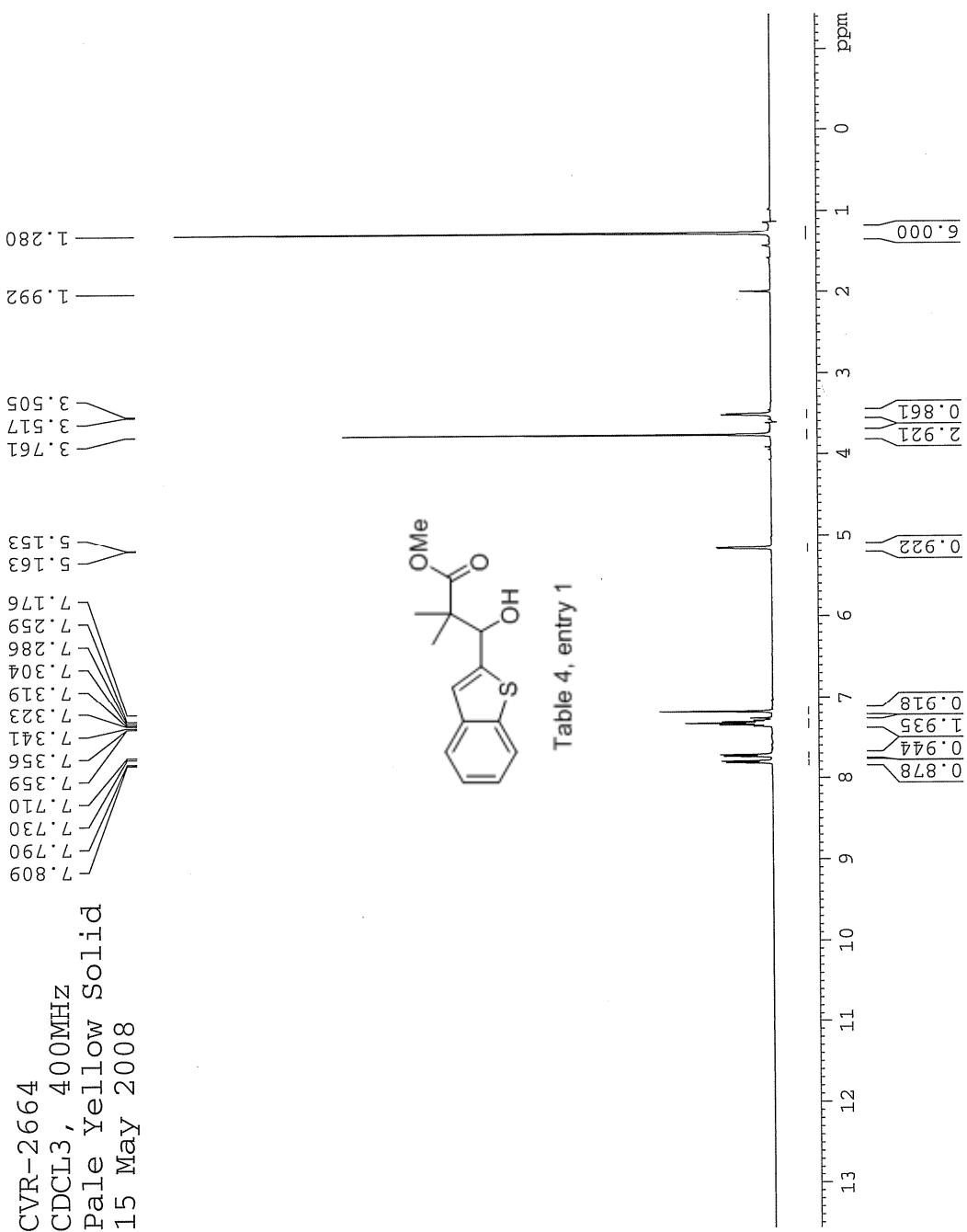


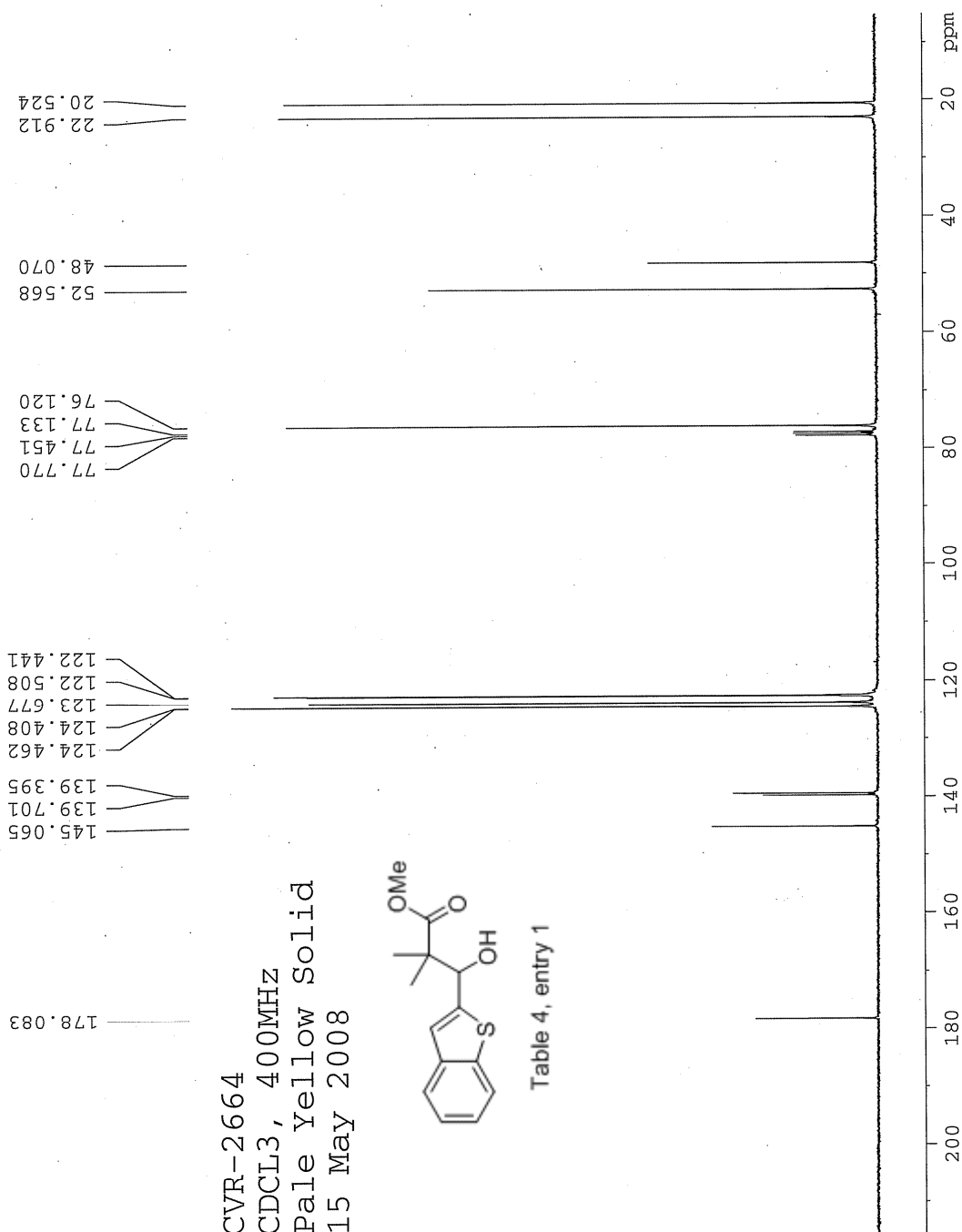












## Manual Peak Matching Report For Accurate Mass Determination

Theoretical mass	Experimental mass	PFK matching mass	Deviation*
264.08202	264.08256	230.98562	2 ppm

\* The deviation is obtained from the following equation:

$$\text{deviation} = \frac{\text{experimental mass} - \text{theoretical mass}}{\text{nominal mass}}$$

Where nominal mass takes in account only  $^{12}\text{C}$ ,  $^1\text{H}$ ,  $^{16}\text{O}$ ,  $^{14}\text{N}$  etc...

Theoretical mass correspond to the mass of the most abundant isotope peak

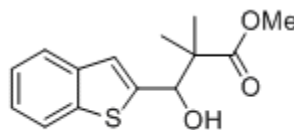


Table 4, entry 1

*Handwritten signature*

SPEC: fin063613.dat (08-MAY-08 14:51:32)  
 Samp: CVR-2660  
 Comm: 70 eV EI  
 Oper: Kh  
 Base: 162.69  
 Peak: 1000.0 mmu  
 Scan 36 @ 0.90 min (EI +QIMS LMR UP LR)

Study: Service  
 Masses: 35.01 > 650.00  
 Intensity: 901034

Scans: 1 > 41  
 Client: Venkat  
 #Peaks: 629  
 RIC: 5282802  
 9.0E+05

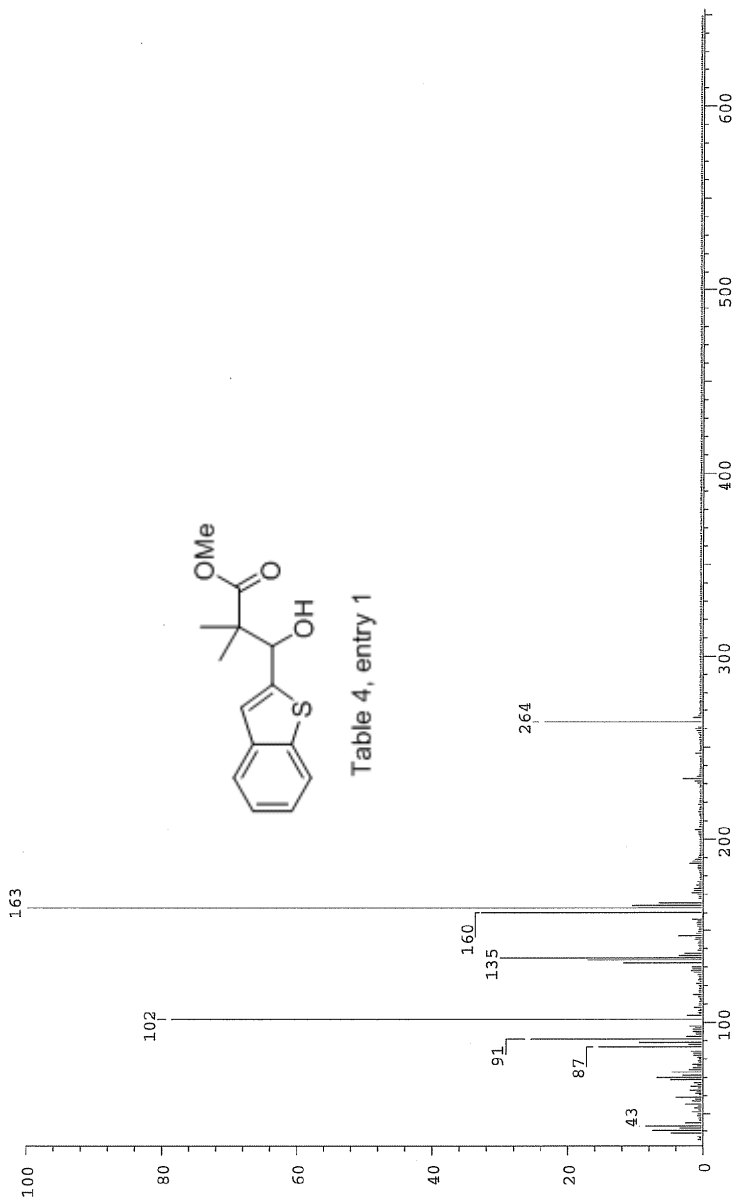


Table 4, entry 1

Date: Thu May 8 14:53:06 2008 ICIS: 8.3.0 SP2 for OSF1 (V4.0) build 98-238 from 26-Aug-98

CVR-2661  
 Liquid Oil  
 CDCL3, 400MHZ  
 05 May 2008

7.545  
7.526  
7.451  
7.430  
7.282  
7.264  
7.244  
7.234  
7.215  
7.197  
6.643  
4.942  
3.750  
3.713  
1.283  
1.274

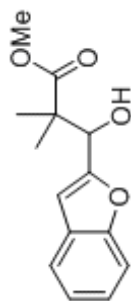
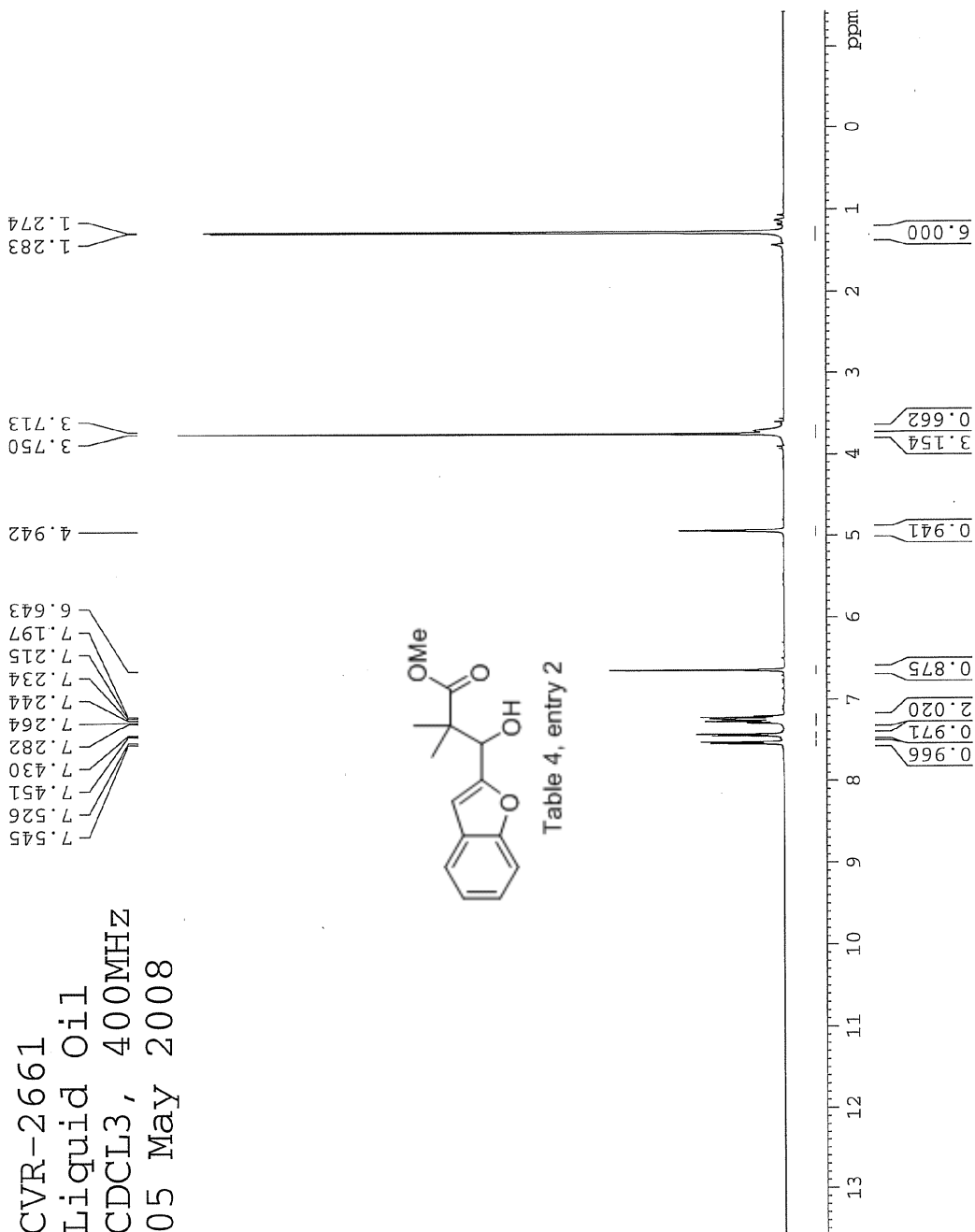
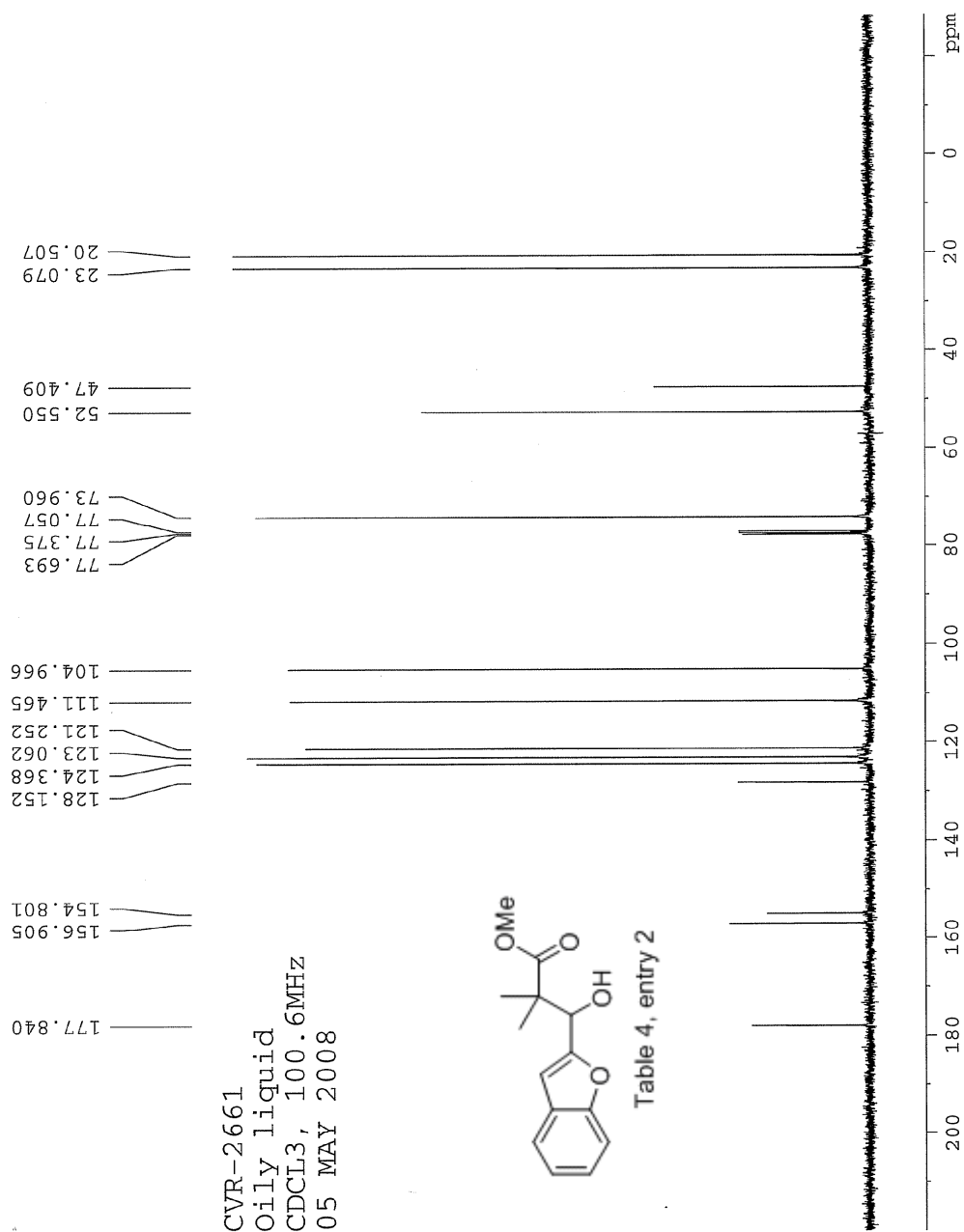


Table 4, entry 2







### Manual Peak Matching Report For Accurate Mass Determination

Theoretical mass	Experimental mass	PFK matching mass	Deviation*
248.10486	248.10539	230.98562	2.1 ppm

\* The deviation is obtained from the following equation:

$$\text{deviation} = \frac{\text{experimental mass} - \text{theoretical mass}}{\text{nominal mass}}$$

Where nominal mass takes in account only  $^{12}\text{C}$ ,  $^1\text{H}$ ,  $^{16}\text{O}$ ,  $^{14}\text{N}$  etc...

Theoretical mass correspond to the mass of the most abundant isotope peak

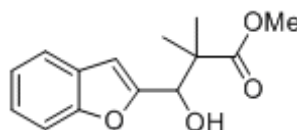


Table 4, entry 2

*Handwritten signature*

SPC: fin063614.dat (08-MAY-08 14:54:38)  
 Samp: CVR-2661  
 Comm: 70 eV EI  
 Oper: kh  
 Base: 146.89  
 Peak: 1000.0 mmu  
 Scan 37 @ 0.92 min (EI +QIMS LMR UP LR)  
 Study: Service  
 Masses: 35.01 > 650.00  
 Intensity: 2551115  
 Scans: 1 > 41  
 Client: Venkat  
 #Peaks: 612  
 RIC: 14331415 2.6E+06

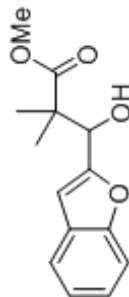
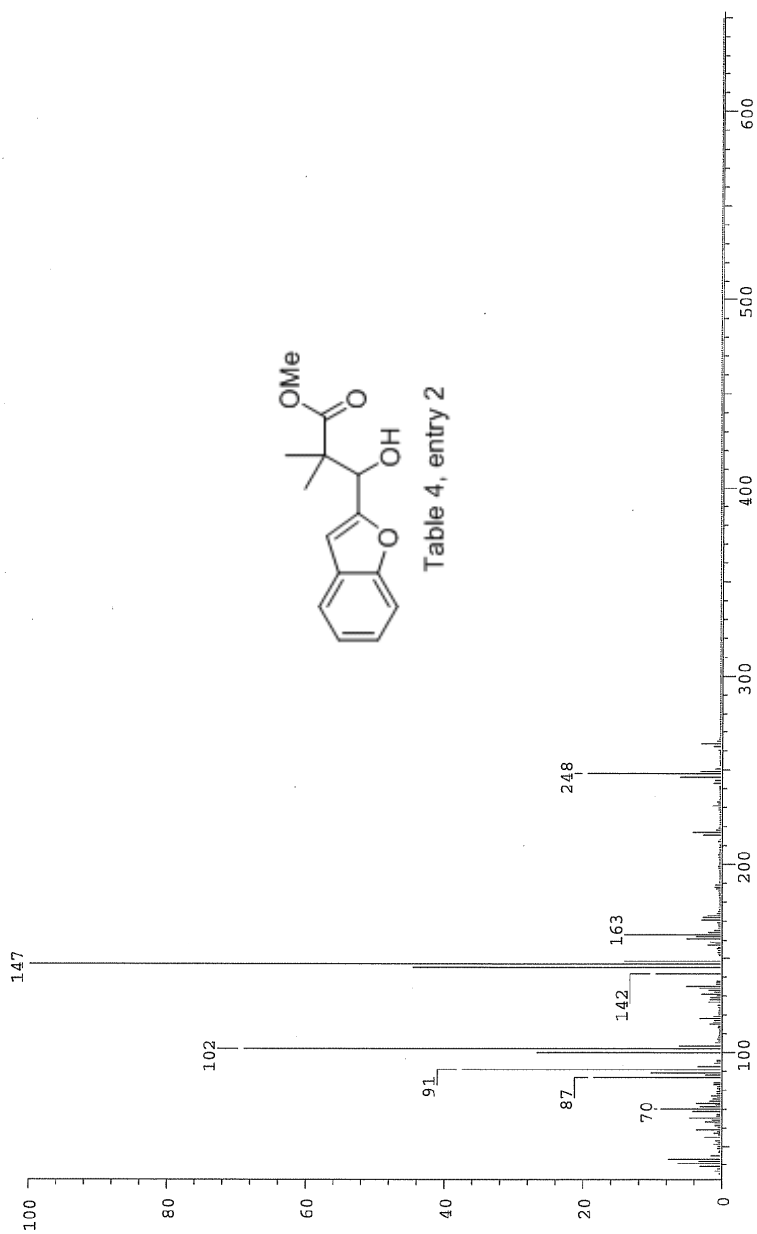
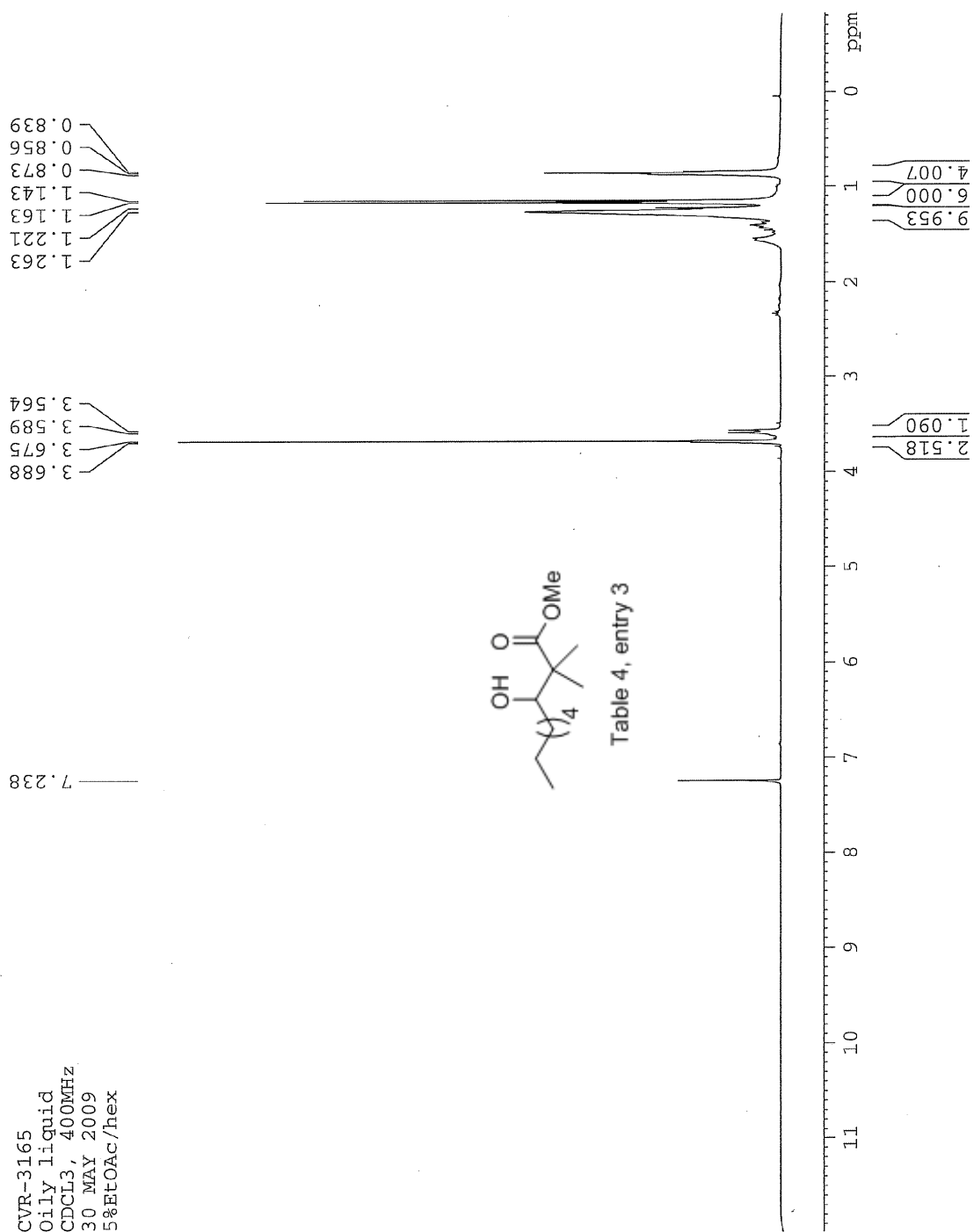
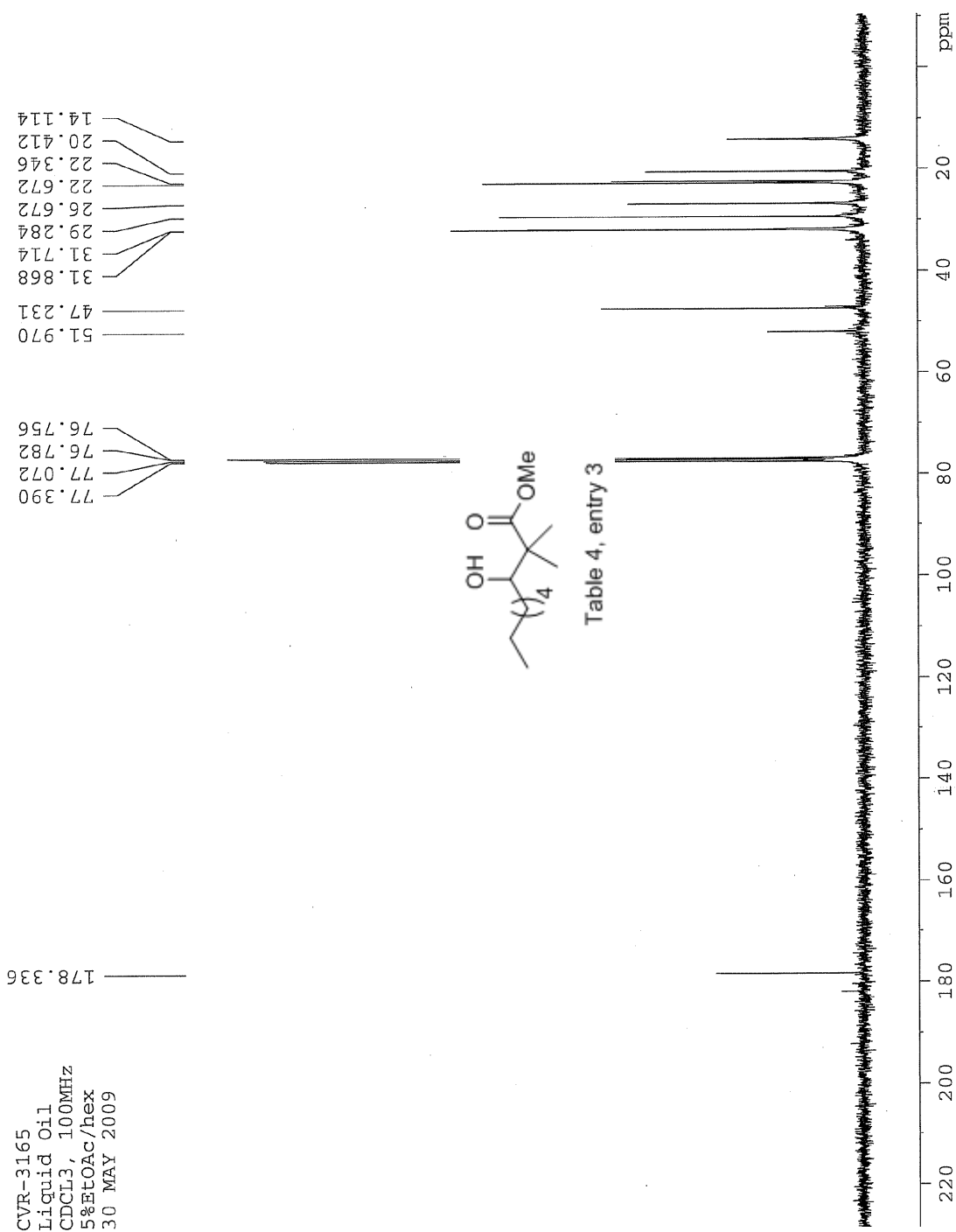


Table 4, entry 2

Date: Thu May 8 14:56:00 2008 ICIS: 8.3.0 SP2 for OSF1 (V4.0) build 98-238 from 26-Aug-98





### Manual Peak Matching Report For Accurate Mass Determination

Theoretical mass	Experimental mass	PFK matching mass	Deviation*
216.17254	216.17291	<del>216.17254</del> 180.98882	1.7 ppm

\* The deviation is obtained from the following equation:

$$\text{deviation} = \frac{\text{experimental mass} - \text{theoretical mass}}{\text{nominal mass}}$$

Where nominal mass takes in account only  $^{12}\text{C}$ ,  $^1\text{H}$ ,  $^{16}\text{O}$ ,  $^{14}\text{N}$  etc...

Theoretical mass correspond to the mass of the most abundant isotope peak

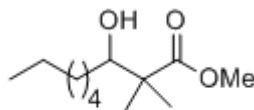


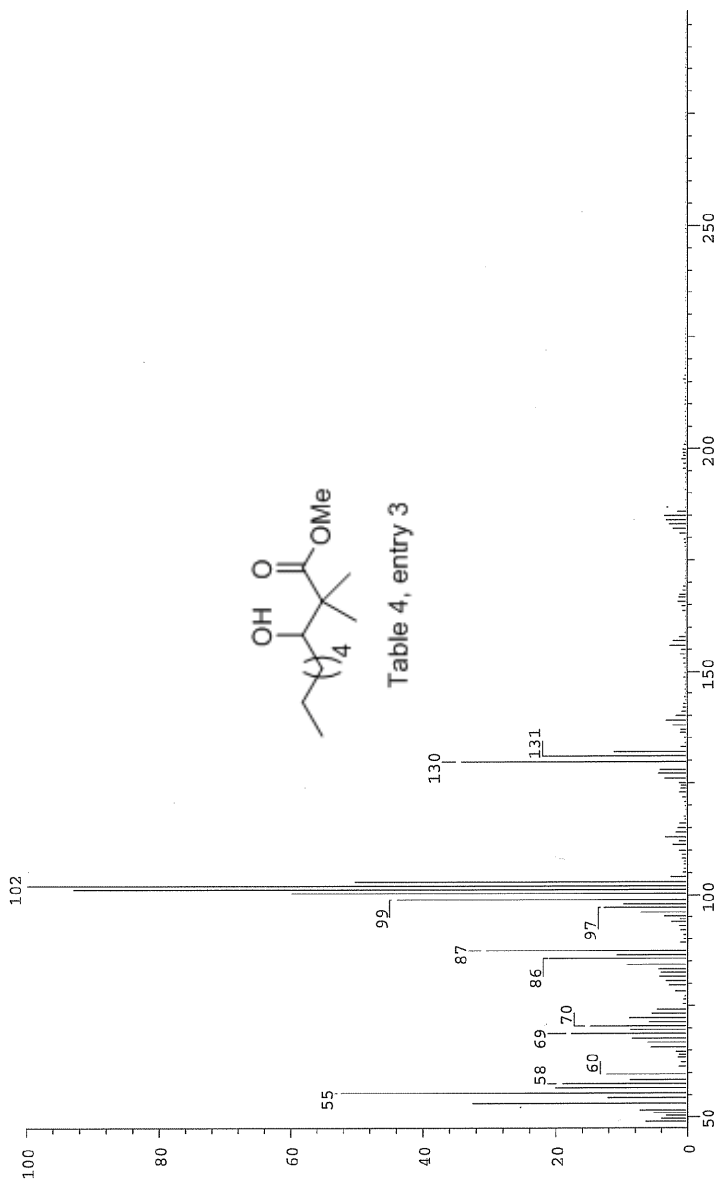
Table 4, entry 3

MO

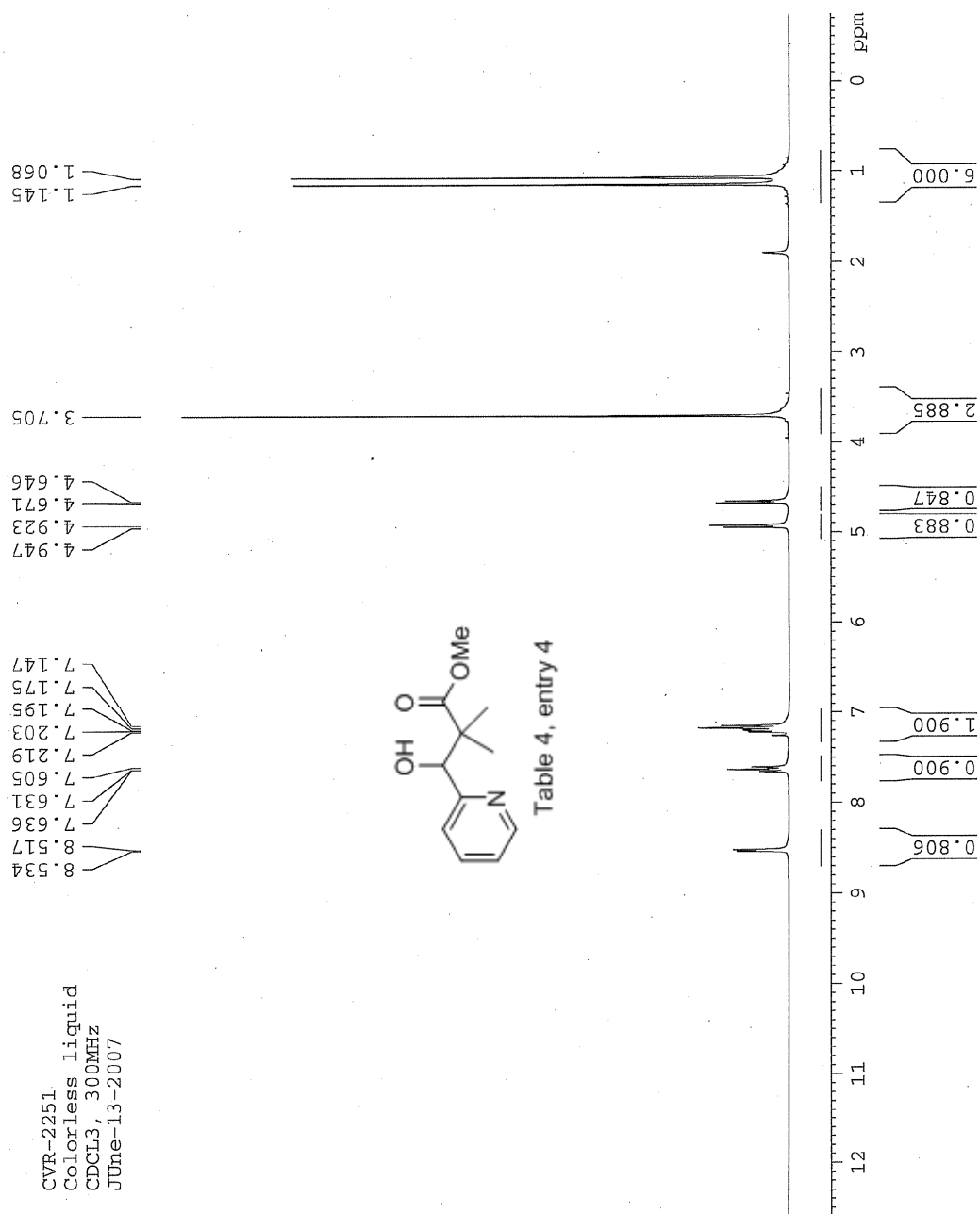
Scans: 1 > 137  
 Client: Venkat  
 #Peaks: 335  
 RIC: 49612388  
 6.0E+05

SPEC: fin084574.dat (24-JUN-09 11:04:31)  
 Samp: CVR-3165  
 Comm: DP/EI  
 Oper:  
 Base: 28.80  
 Peak: 1000.0 mmu  
 Scan 12 @ 0.28 min (EI +Q1MS LMR UP LR)

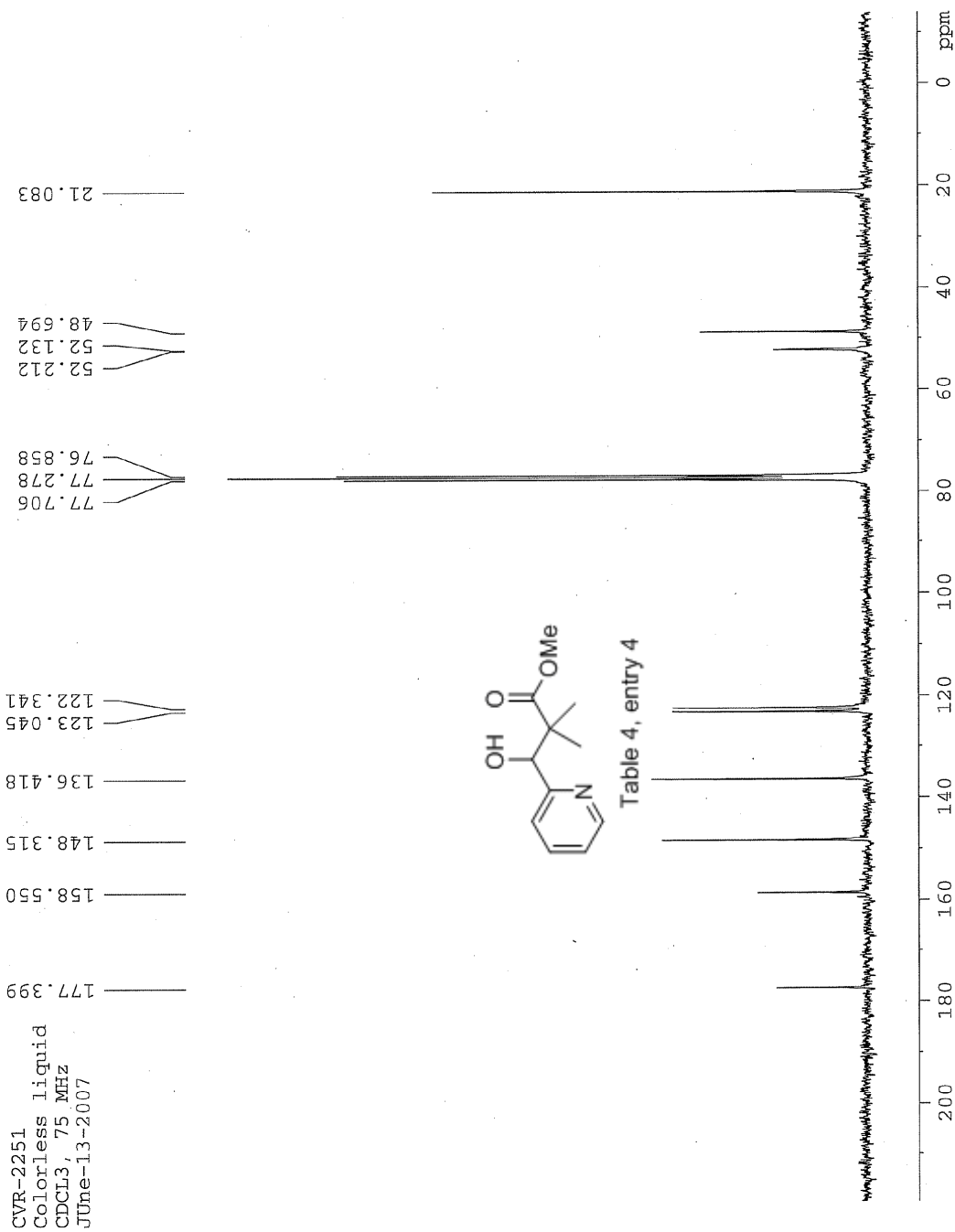
Study:  
 Masses: 23.75 > 550.02  
 Intensity: 7495031

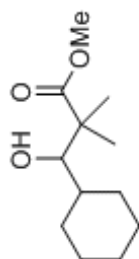
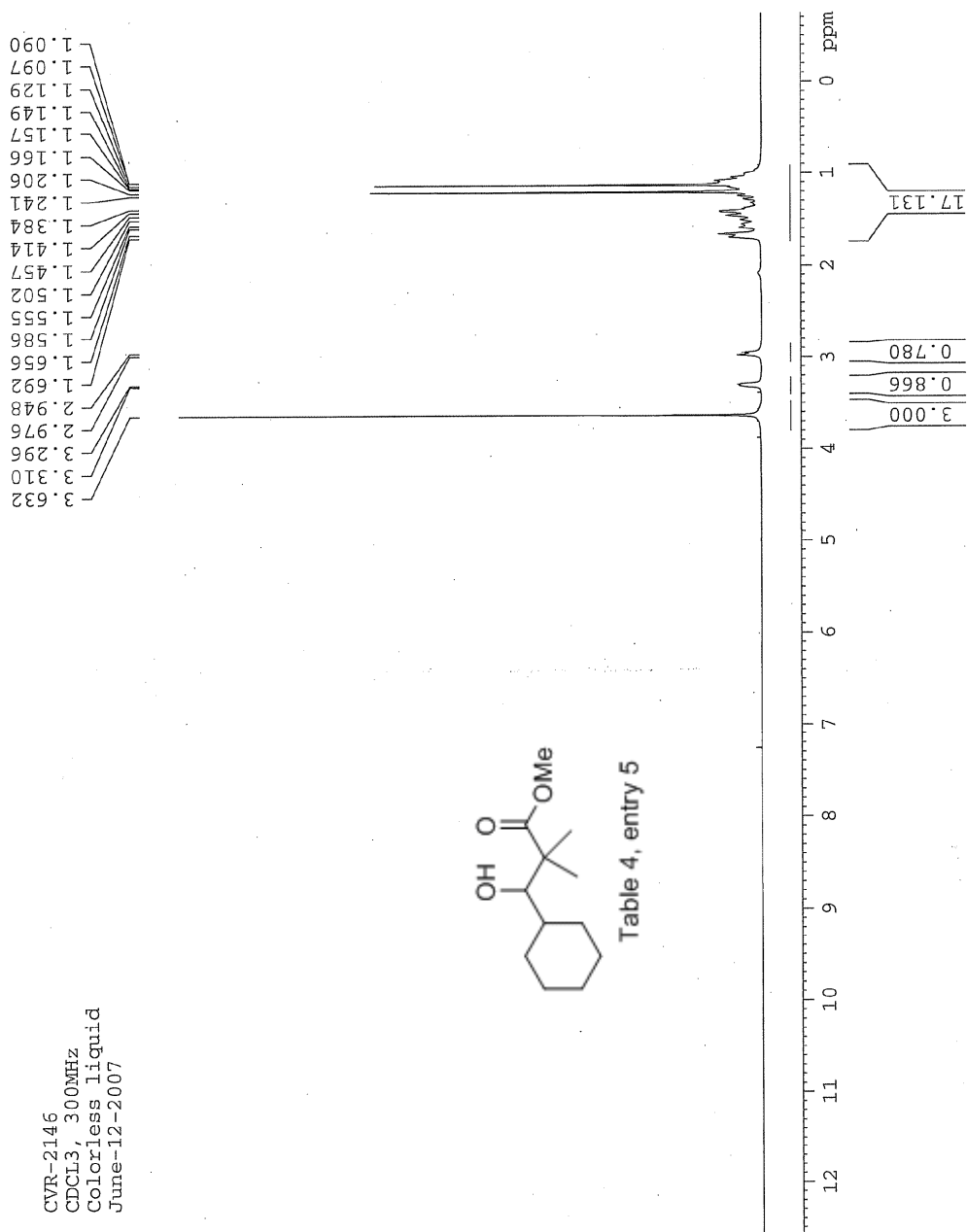


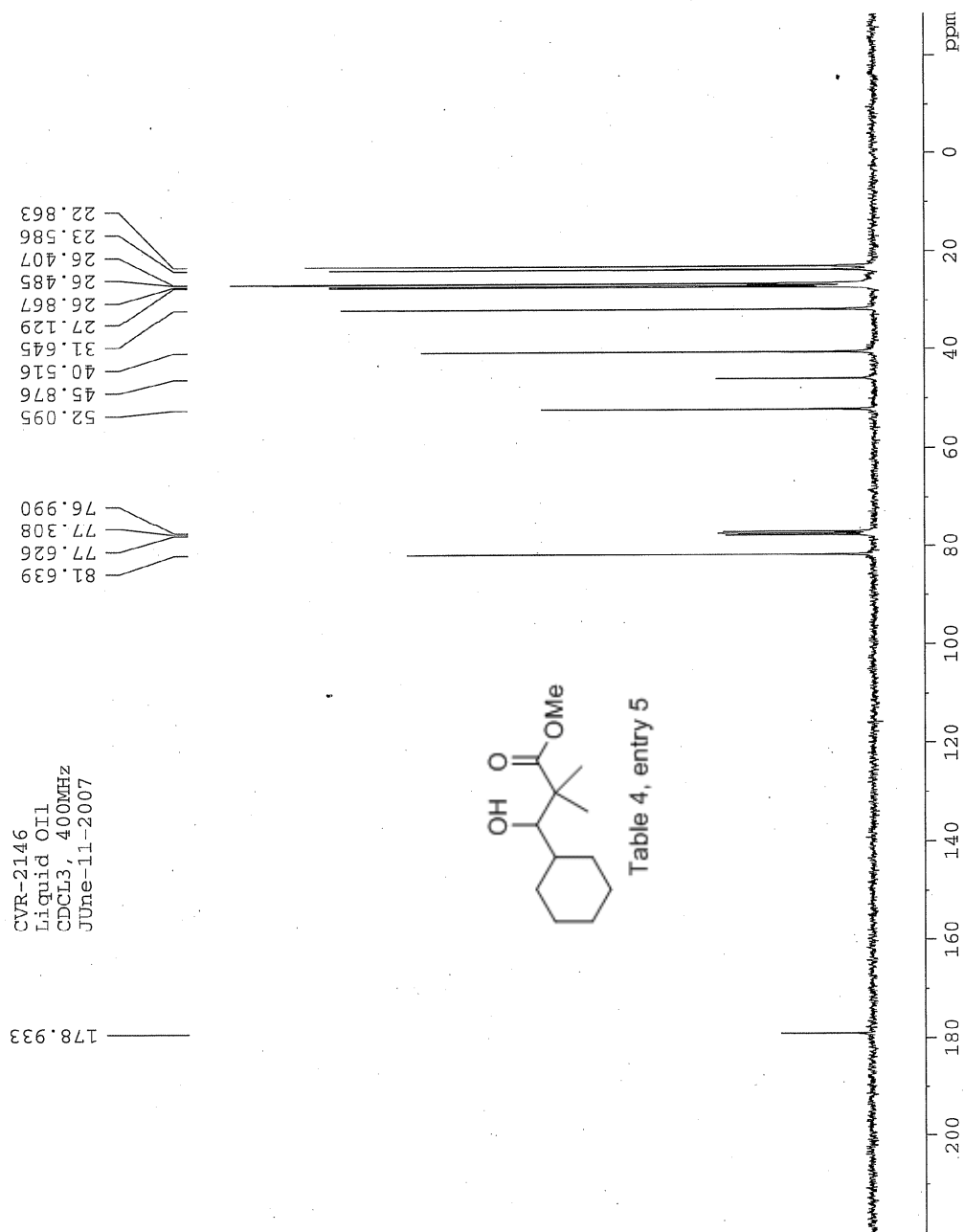
Date: Wed Jun 24 11:07:10 2009 ICIS: 8.3.0 SP2 for OSF1 (V4.0) build 98-238 from 26-Aug-98



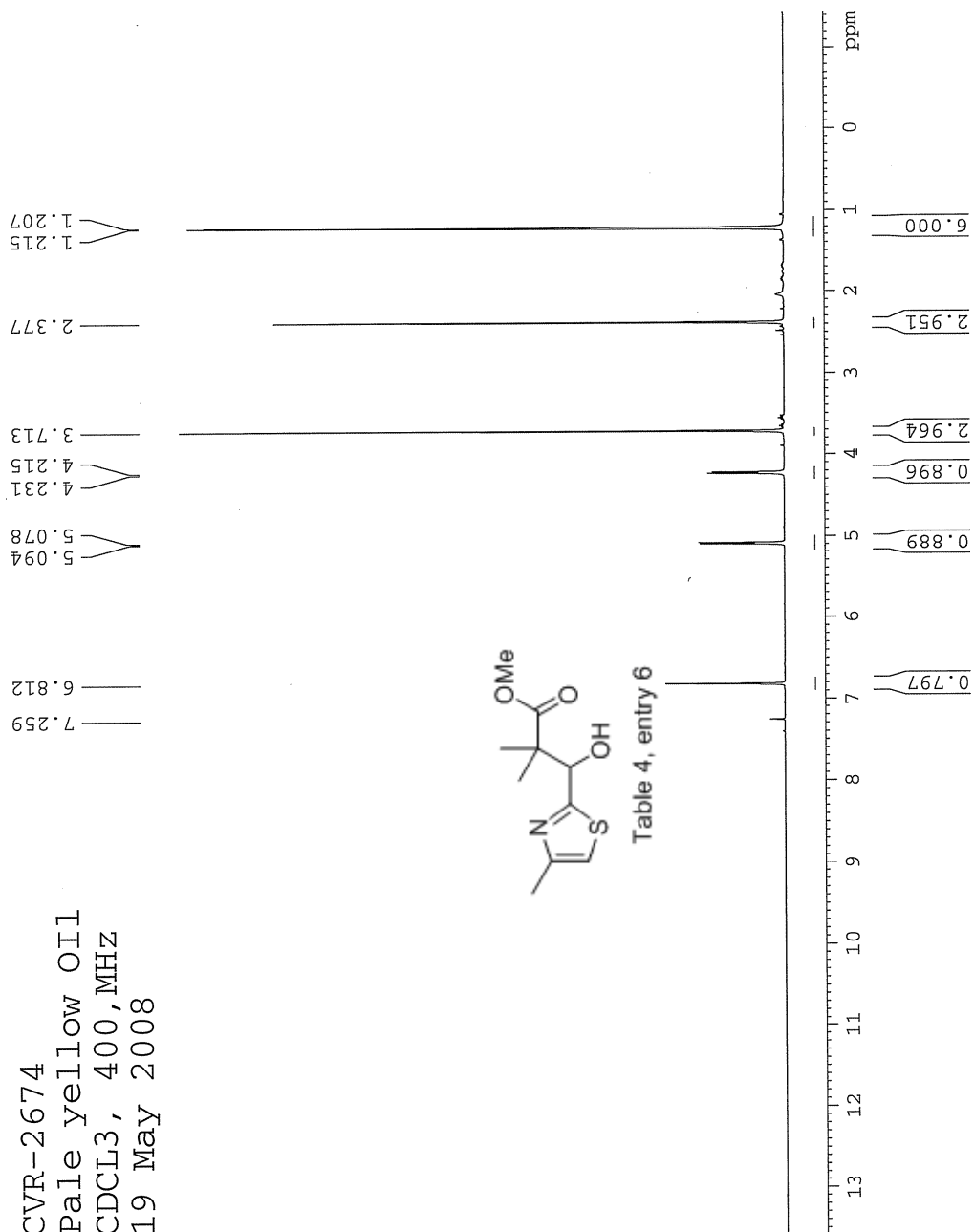


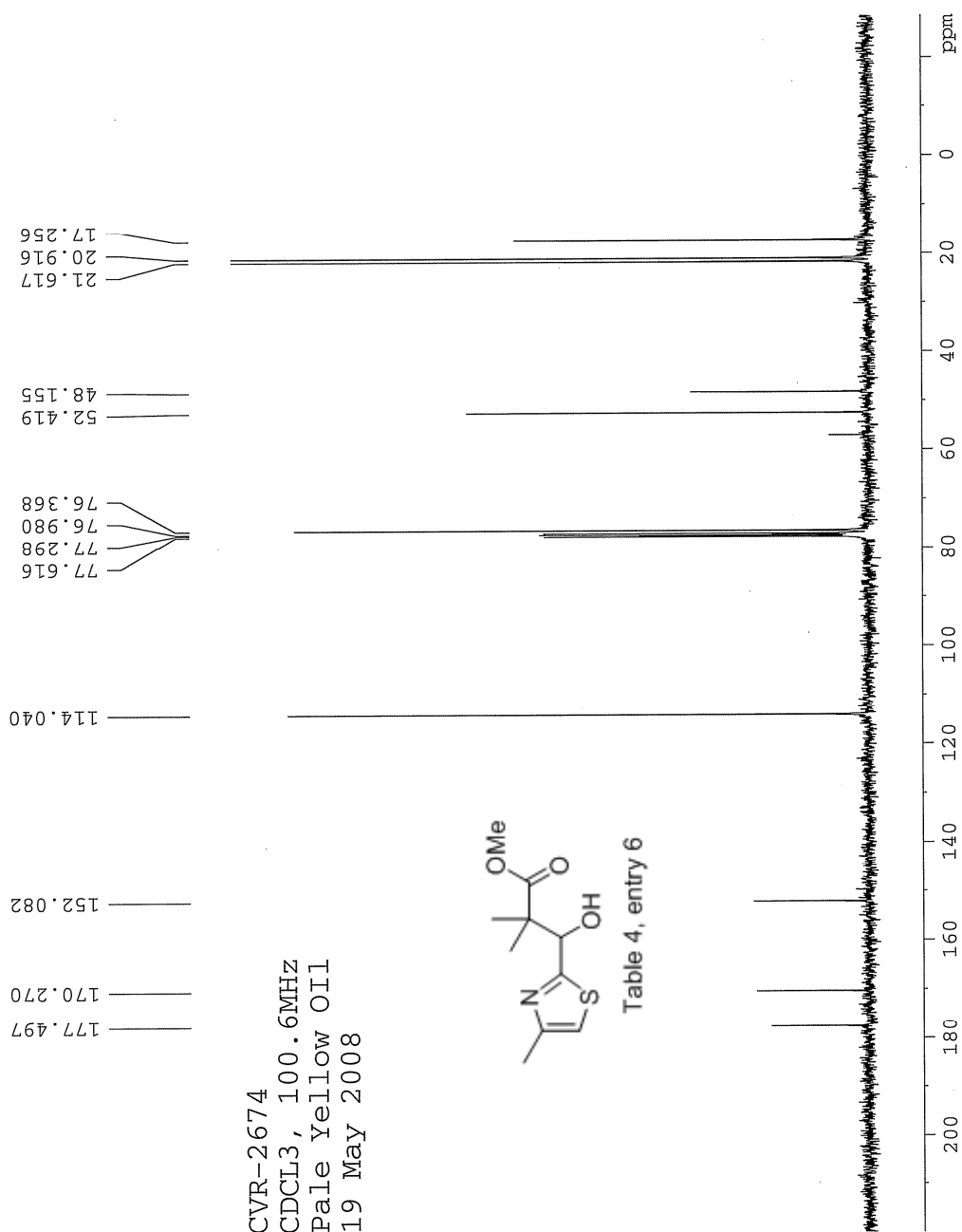






CVR-2674  
 Pale yellow Oil  
 CDCl<sub>3</sub>, 400, MHz  
 19 May 2008





## Manual Peak Matching Report For Accurate Mass Determination

Theoretical mass	Experimental mass	PFK matching mass	Deviation*
229.07726	229.07763	218.98562	1.6 ppm

\* The deviation is obtained from the following equation:

$$\text{deviation} = \frac{\text{experimental mass} - \text{theoretical mass}}{\text{nominal mass}}$$

Where nominal mass takes in account only  $^{12}\text{C}$ ,  $^1\text{H}$ ,  $^{16}\text{O}$ ,  $^{14}\text{N}$  etc...

Theoretical mass correspond to the mass of the most abundant isotope peak

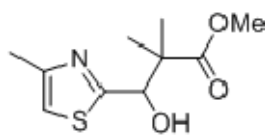


Table 4, entry 6

*M*

Scans: 1 > 22  
 Client: Rogness  
 #Peaks: 394  
 RIC: 33497681  
 6.7E+05

SPEC: fm084591.dat (26-JUN-09 16:08:41)  
 Samp: CVR-2674  
 Oper: 127.07  
 Base: 1000.0 mmu  
 Scan 16 @ 0.48 min (EI +QIMS LMR UP LR)

Study: 35.01 > 650.00  
 Masses: 6730531  
 Intensity: 6730531

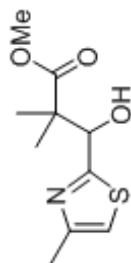
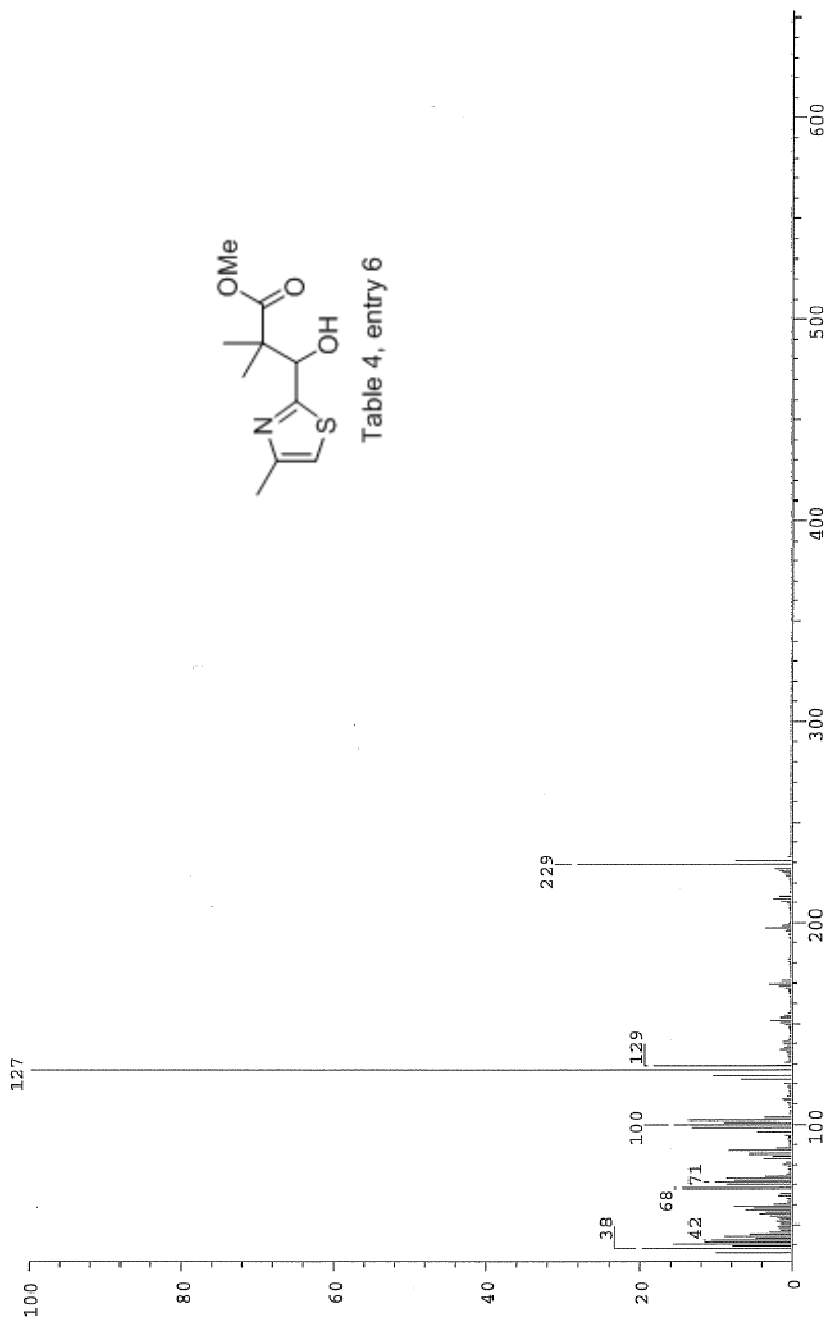
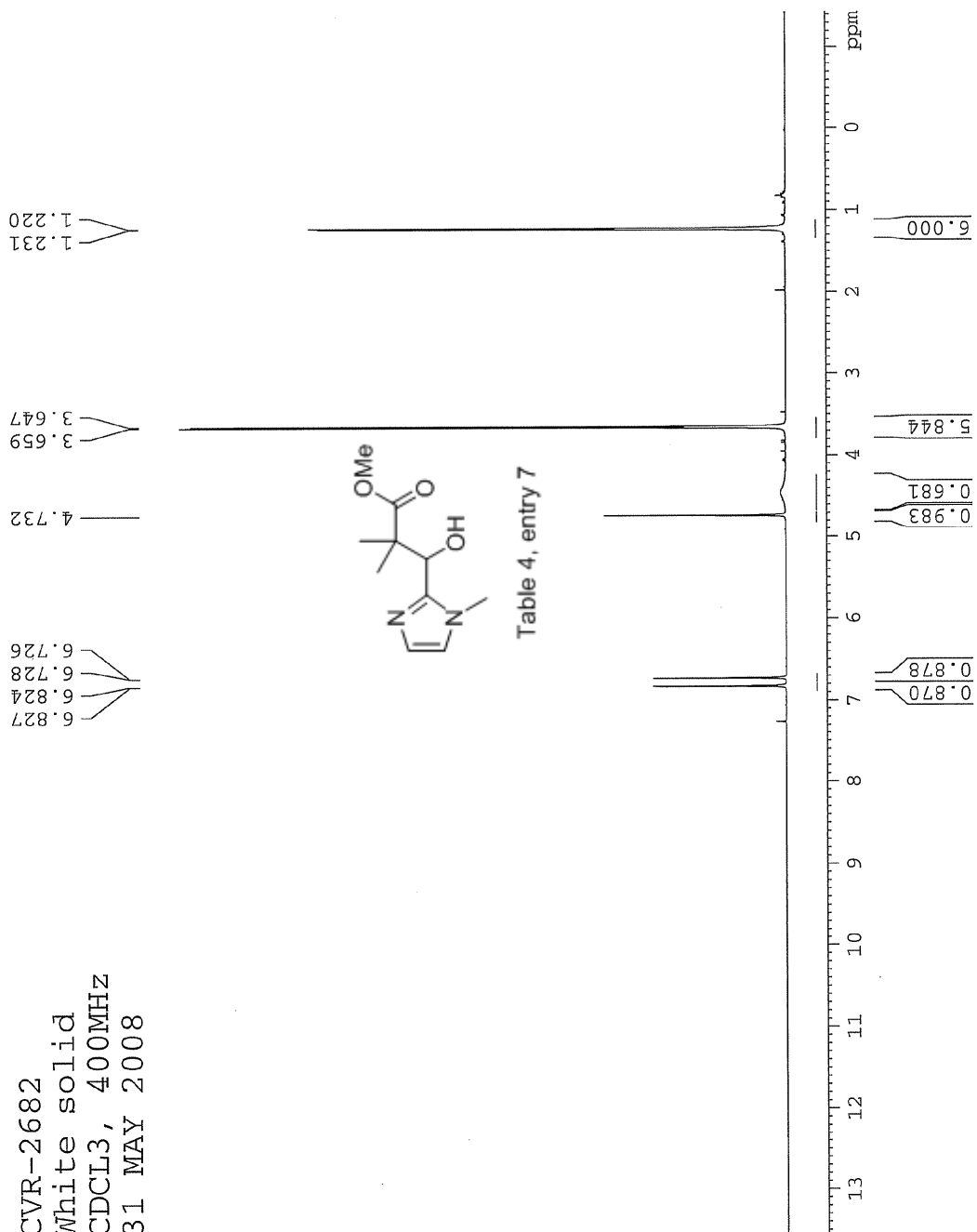


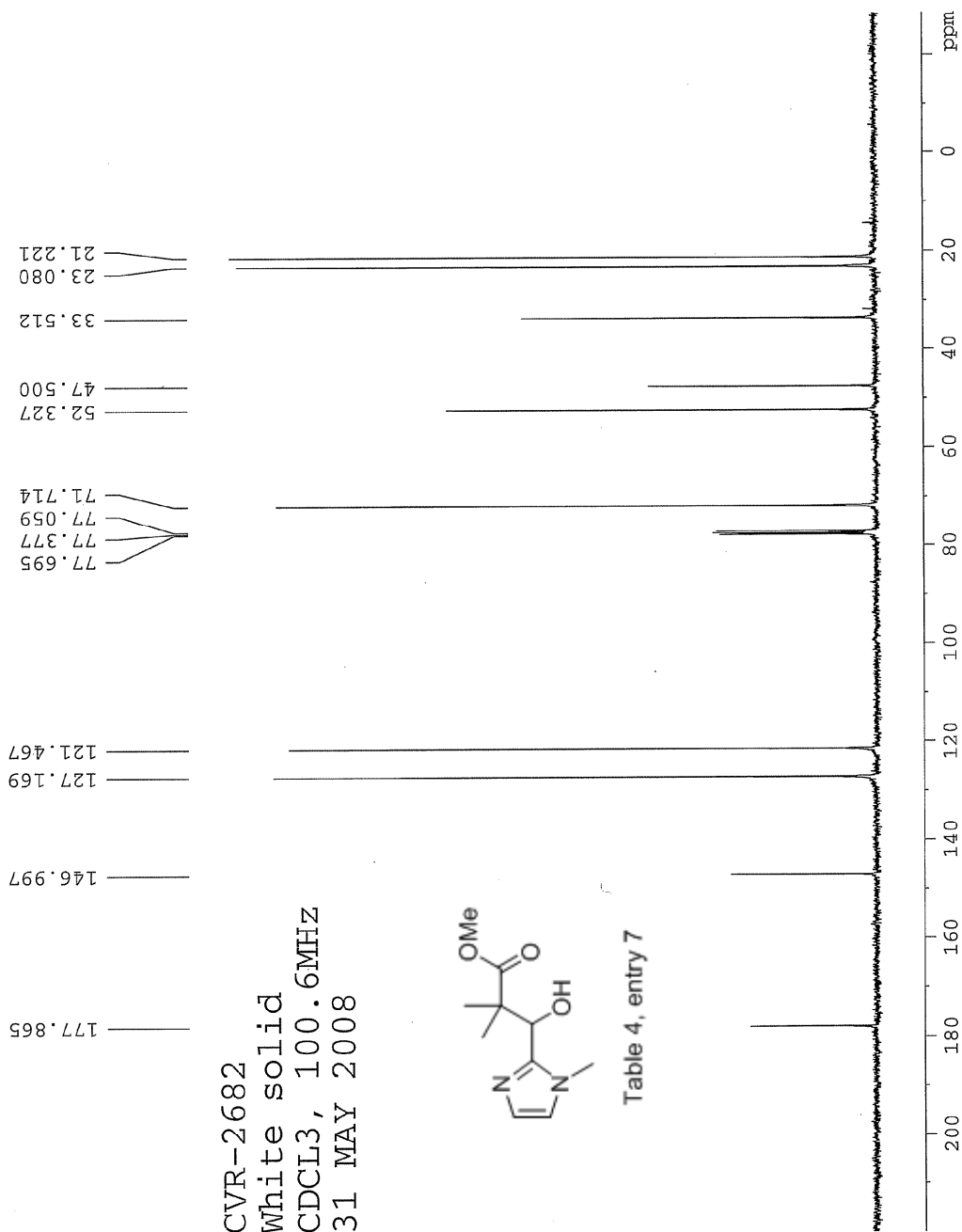
Table 4, entry 6

Date: Fri Jun 26 16:09:44 2009 ICIS: 8.3.0 SP2 for OSF1 (V4.0) build 98-238 from 26-Aug-98

CVR-2682  
 White solid  
 CDCl<sub>3</sub>, 400MHz  
 31 MAY 2008







### Manual Peak Matching Report For Accurate Mass Determination

Theoretical mass	Experimental mass	PFK matching mass	Deviation*
212.11609	212.11649	180.98882	1.9 ppm

\* The deviation is obtained from the following equation:

$$\text{deviation} = \frac{\text{experimental mass} - \text{theoretical mass}}{\text{nominal mass}}$$

Where nominal mass takes in account only  $^{12}\text{C}$ ,  $^1\text{H}$ ,  $^{16}\text{O}$ ,  $^{14}\text{N}$  etc...

Theoretical mass correspond to the mass of the most abundant isotope peak

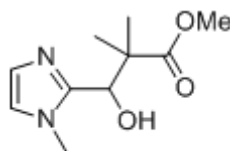


Table 4, entry 7

Scans: 1 > 38  
 Client: Venkat  
 #peaks: 622  
 RIC: 554514 2.7E+05

SPEC: fin083696.dat (10-JUN-08 11:20:17)  
 Samp: CVR-2682  
 Comm: 70 eV EI  
 Oper: kh  
 Study: MS services  
 Base: 110.80  
 Masses: 35.01 > 650.00  
 Peak: 1000.0 mmu  
 Intensity: 265718  
 Scan 35 @ 0.87 min (EI +QIMS LMR UP LR)

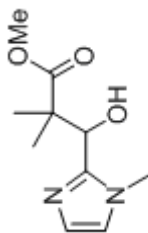
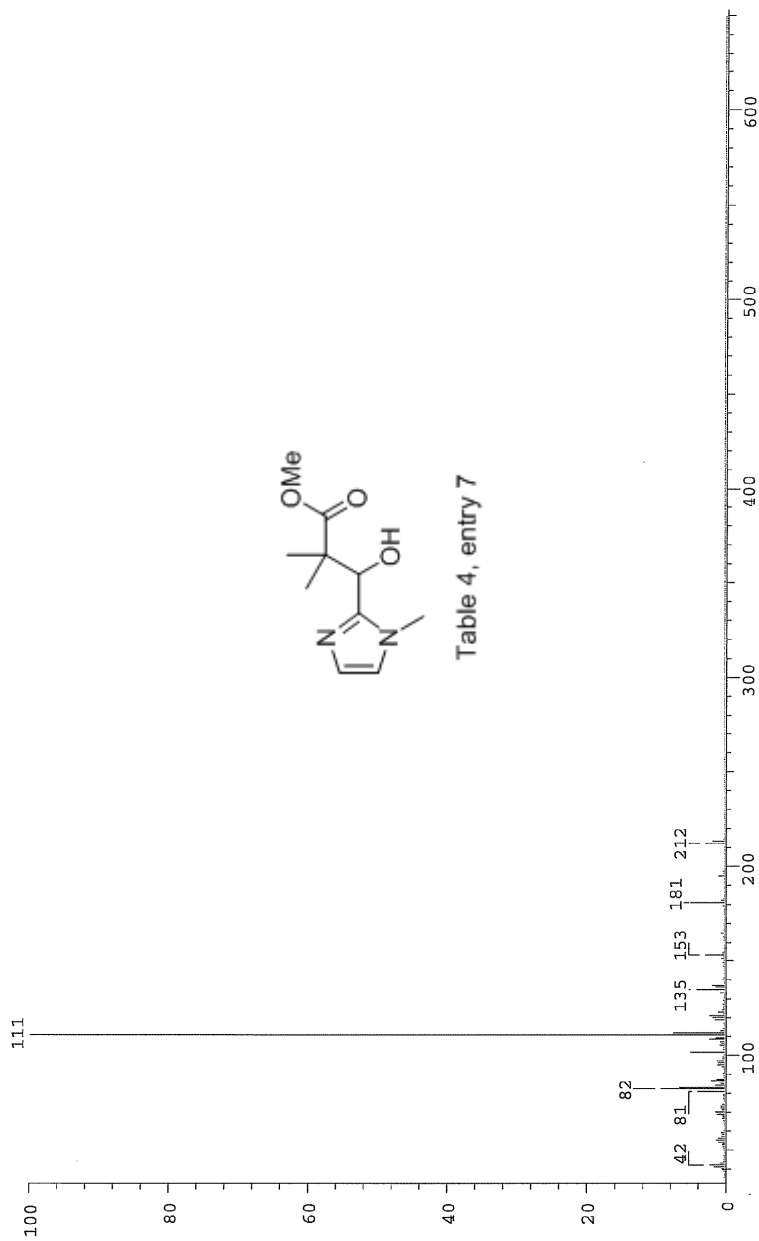
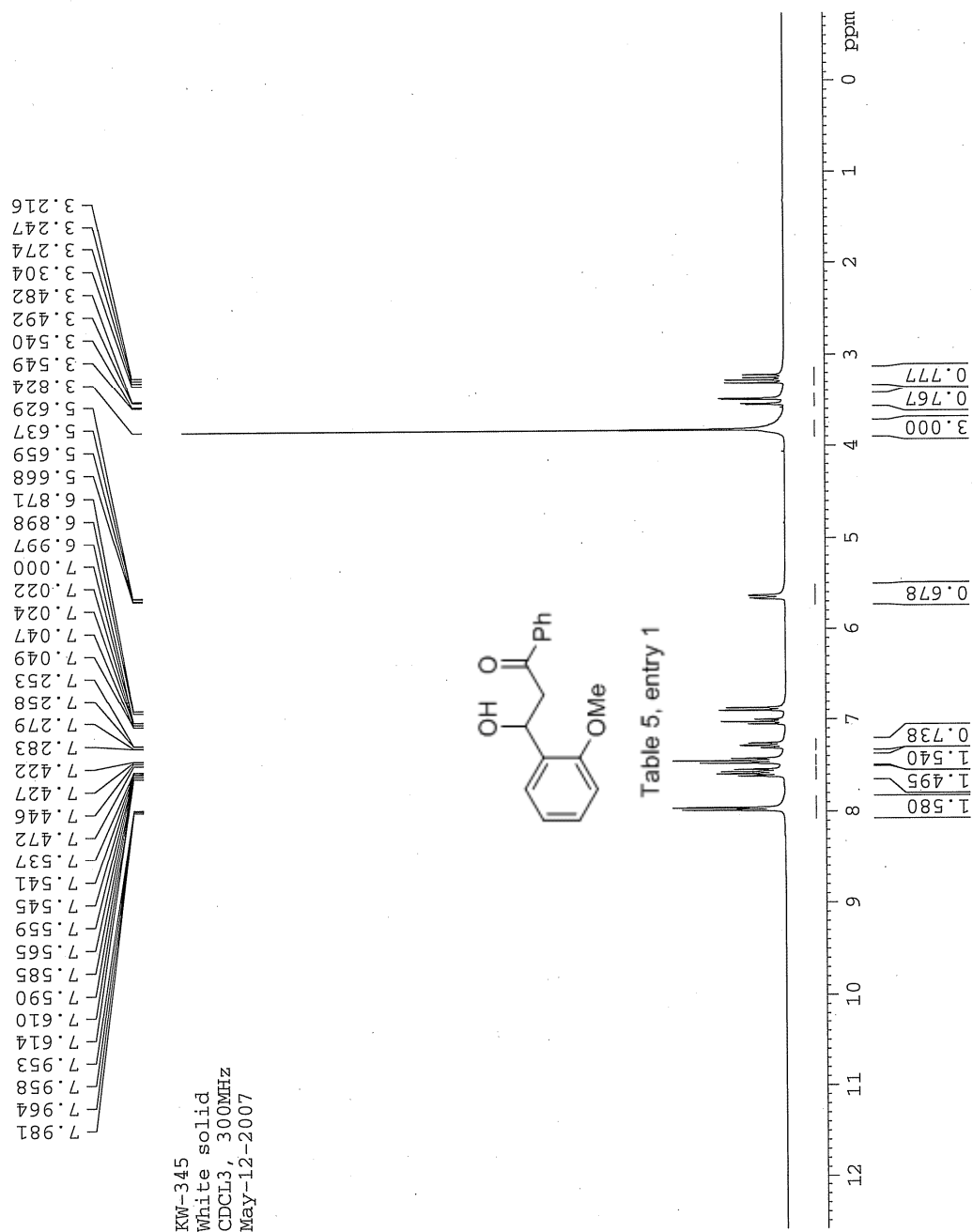
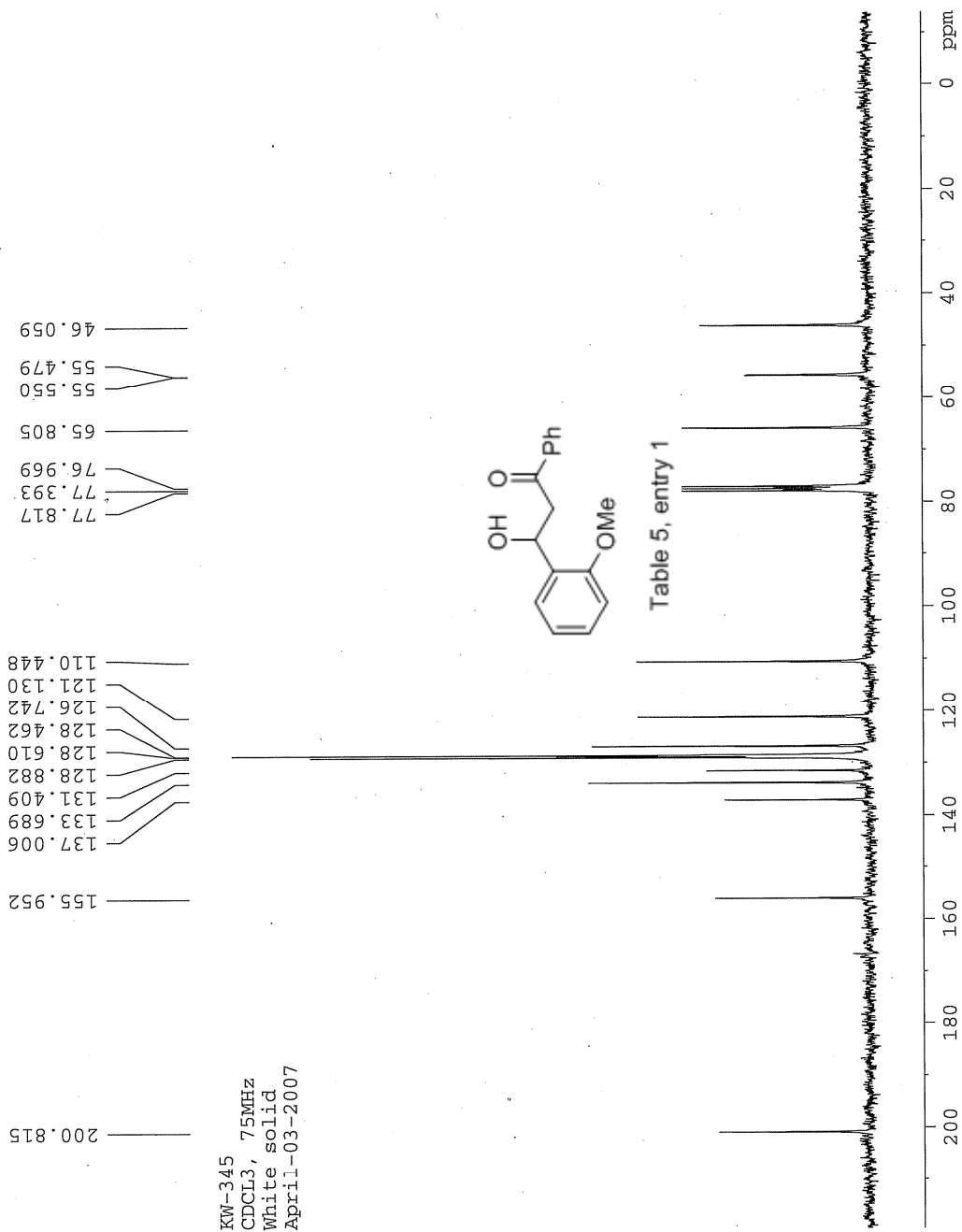
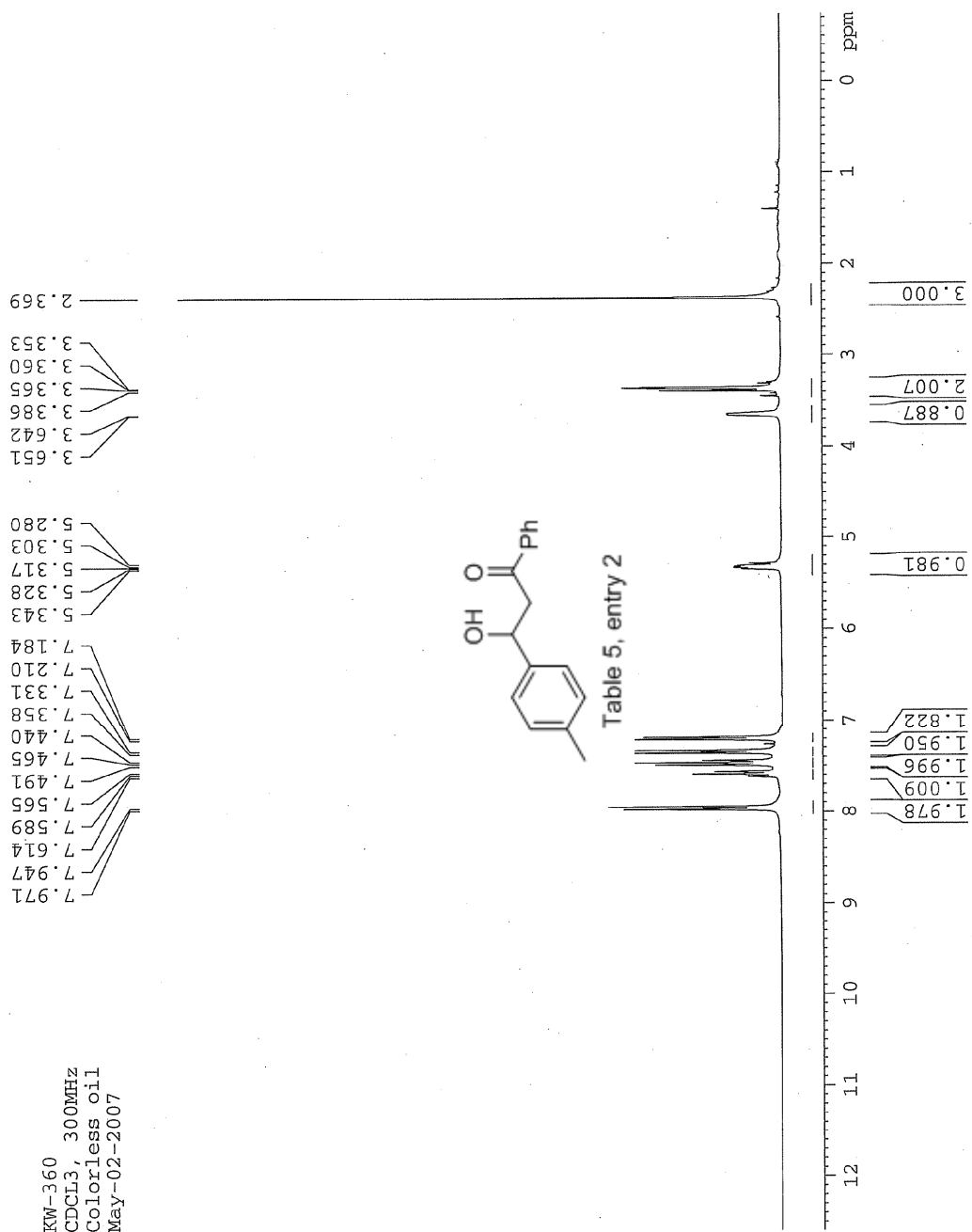


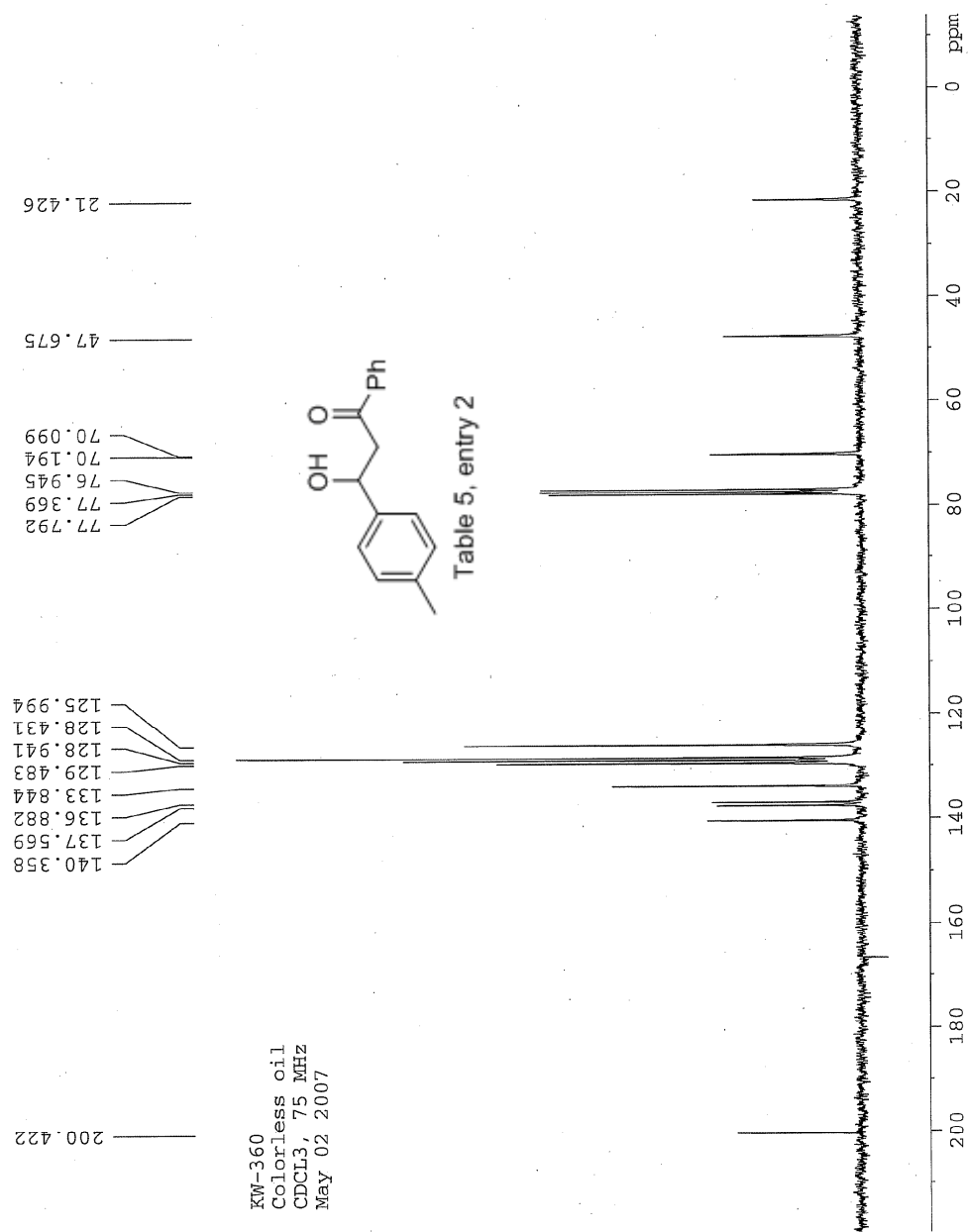
Table 4, entry 7

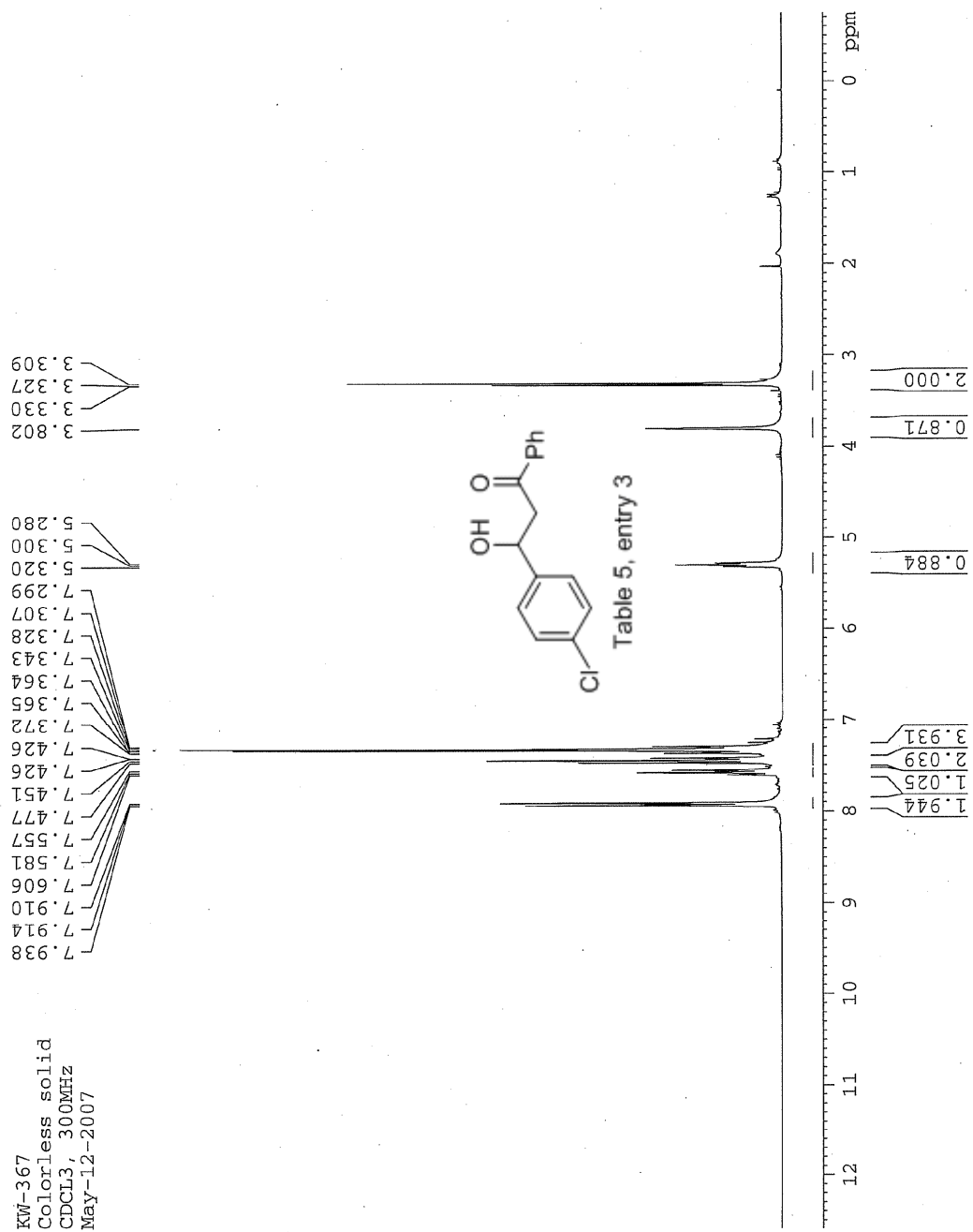
Date: Tue Jun 10 11:21:59 2008 ICIS: 8.3.0 SP2 for OSF1 (V4.0) build 98-238 from 26-Aug-98



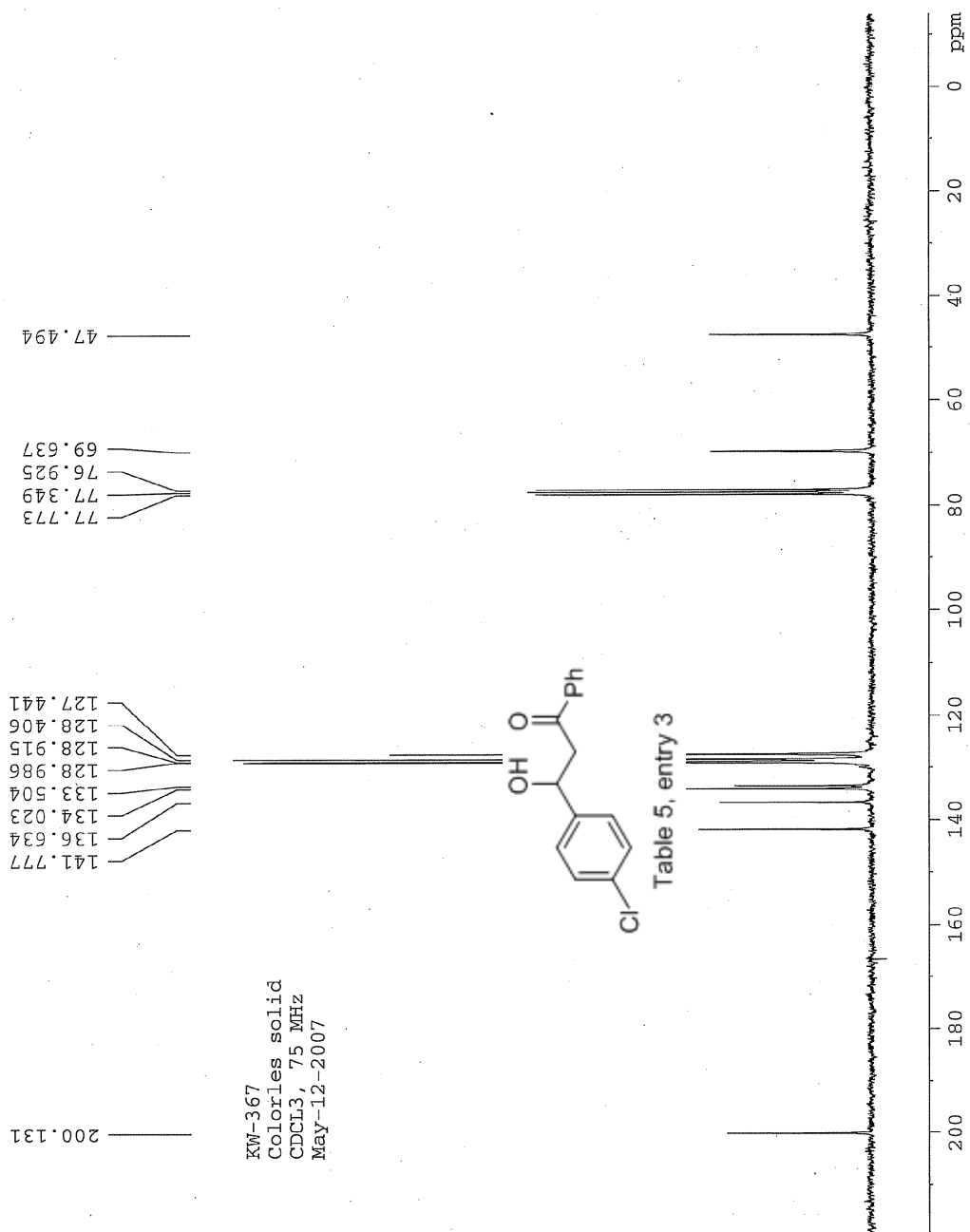


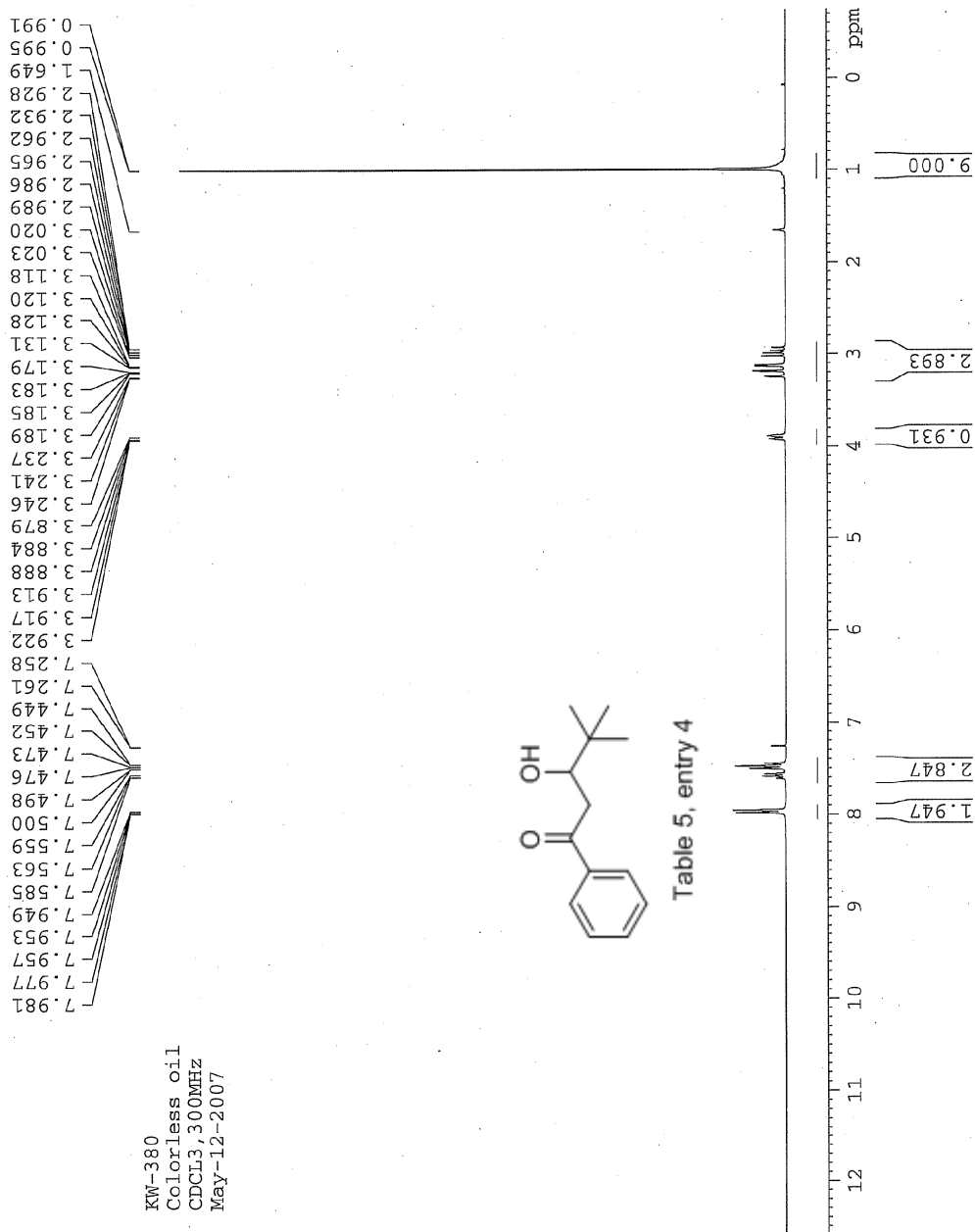


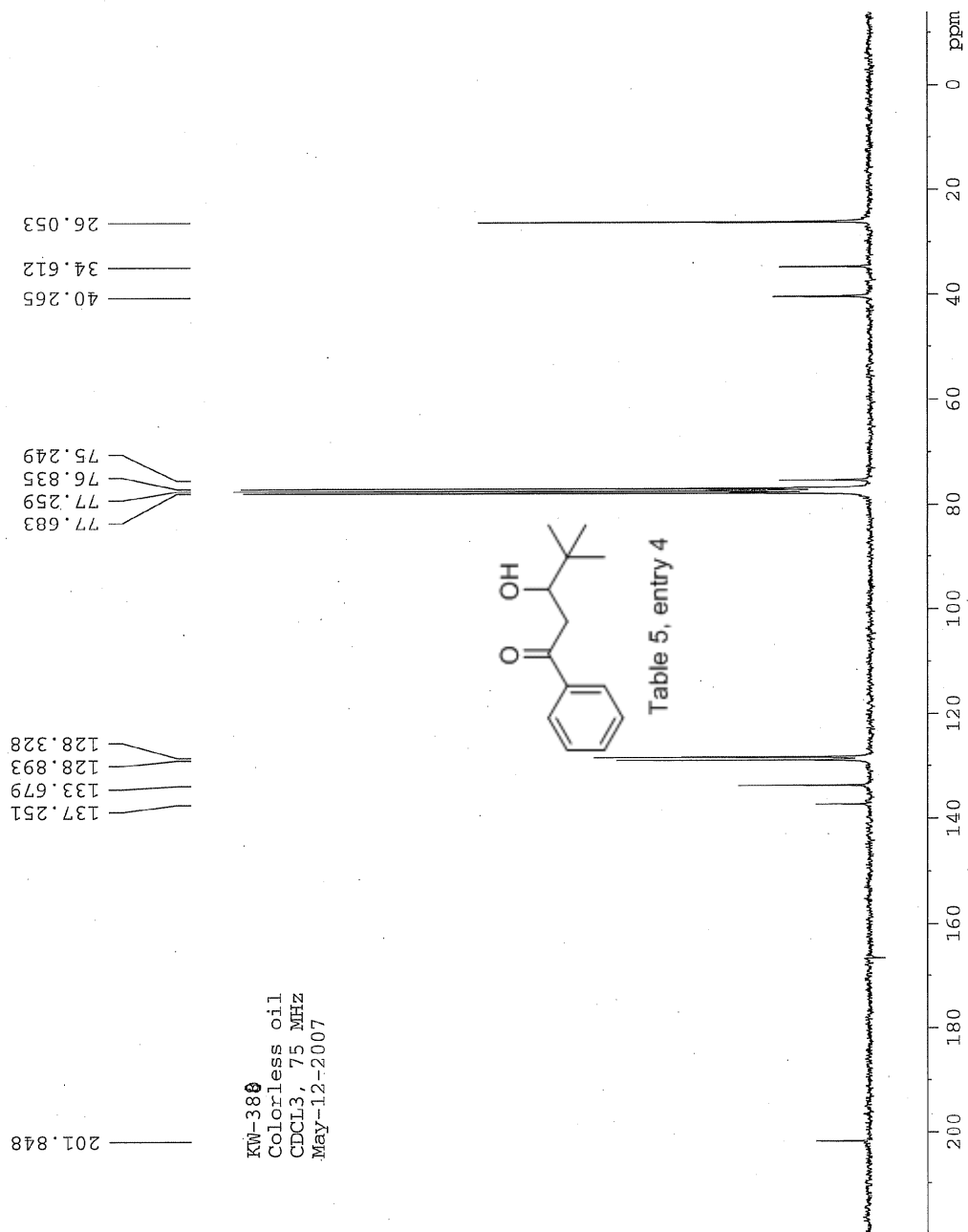


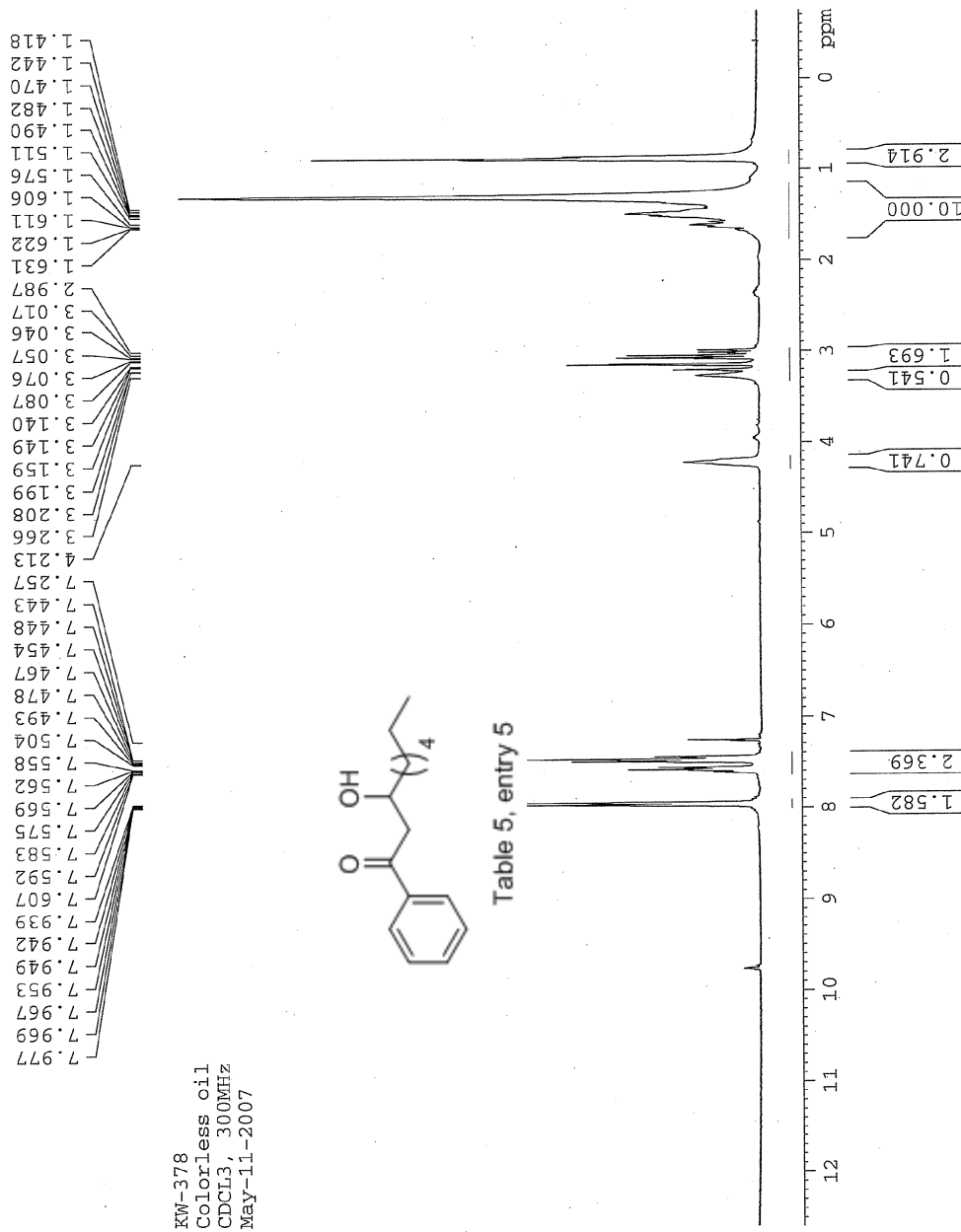


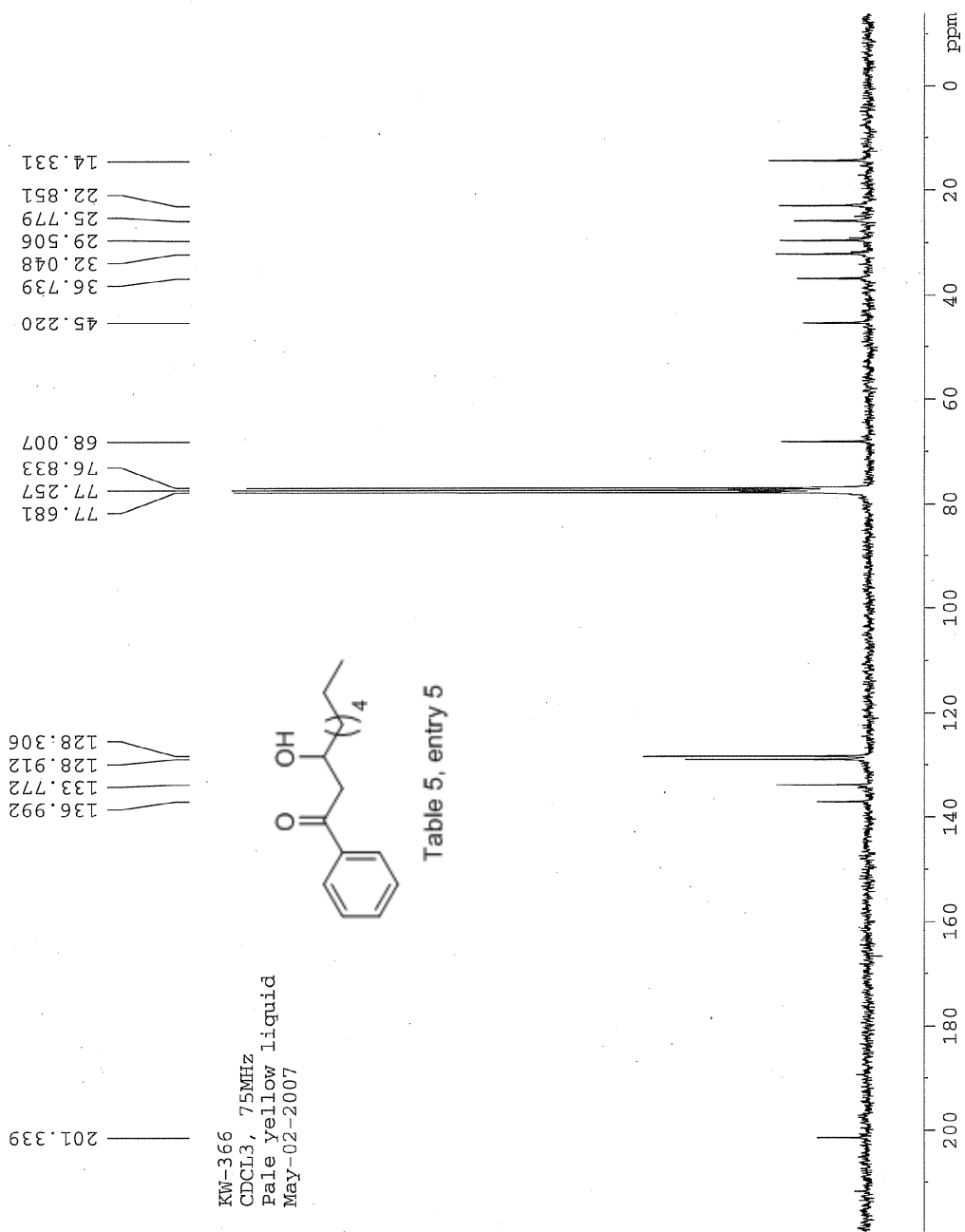












### Manual Peak Matching Report For Accurate Mass Determination

Theoretical mass	Experimental mass	PFK matching mass	Deviation*
234.16197	234.16226	230.98562	1.3 ppm

\* The deviation is obtained from the following equation:

$$\text{deviation} = \frac{\text{experimental mass} - \text{theoretical mass}}{\text{nominal mass}}$$

Where nominal mass takes in account only  $^{12}\text{C}$ ,  $^1\text{H}$ ,  $^{16}\text{O}$ ,  $^{14}\text{N}$  etc...

Theoretical mass correspond to the mass of the most abundant isotope peak

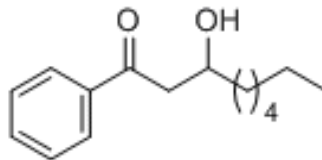


Table 5, entry 5

*Handwritten signature*

SPEC: fin084531.dat (16-JUN-09 10:55:37)  
 Samp: 378  
 Comm: DP/EI  
 Oper: Study:  
 Base: 104.87 Masses: 35.01 > 650.00  
 Peak: 1000.0 mmu Intensity: 1136950  
 Scan 28 @ 0.74 min (EI +Q1MS LMR UP LR) 1.1E+06  
 Scans: 1 > 48  
 Client: Kuldeep  
 #Peaks: 607  
 RIC: 9573930

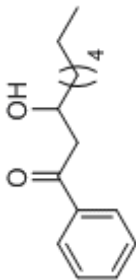
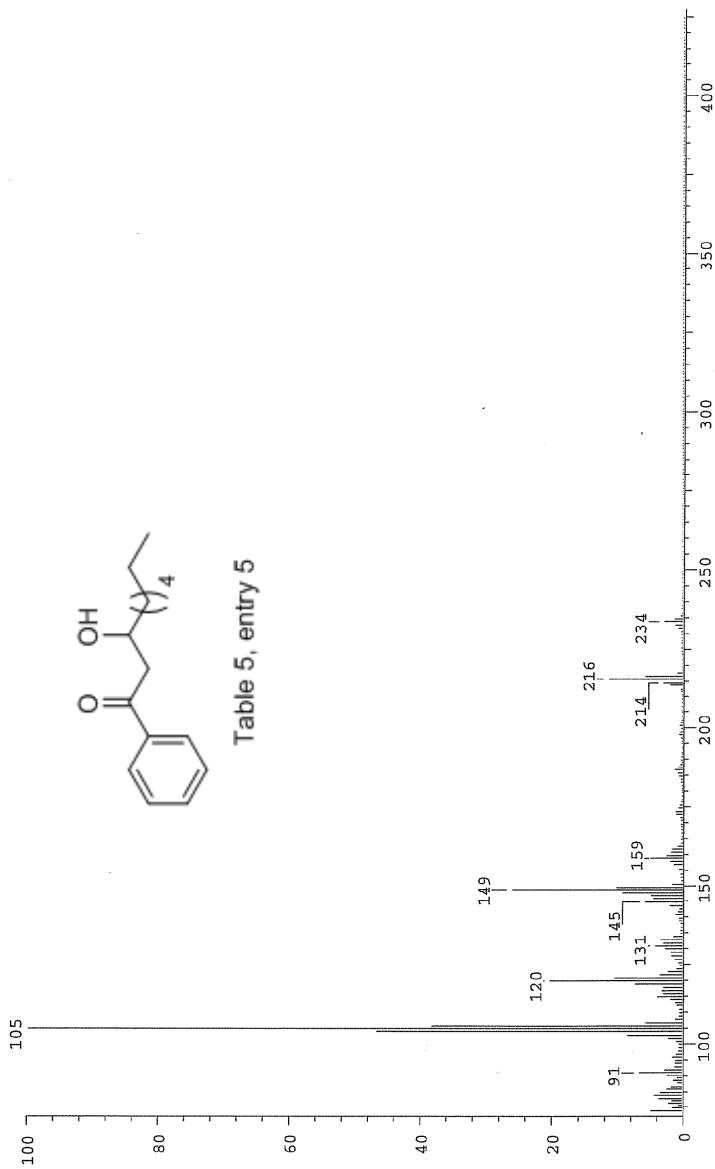
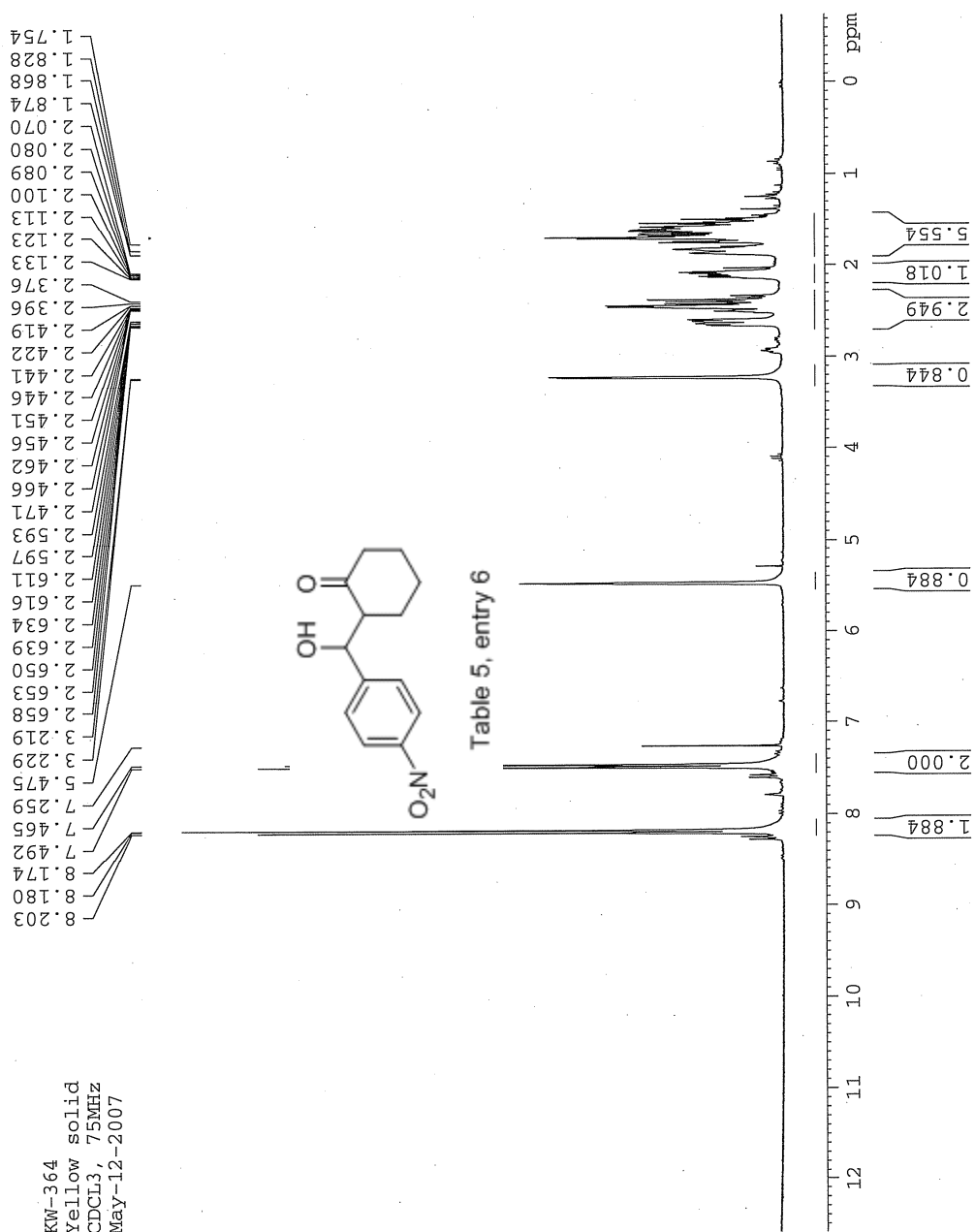
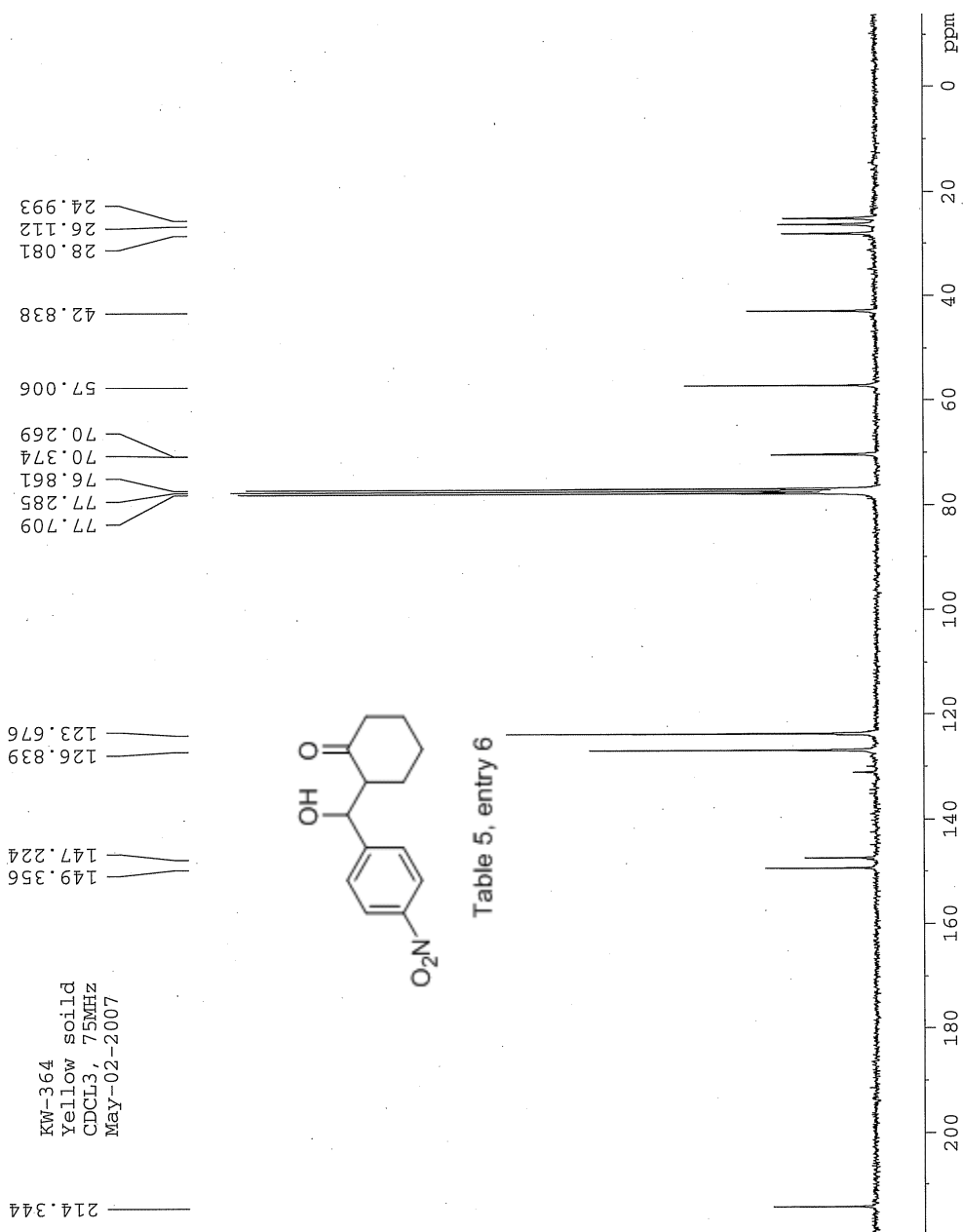


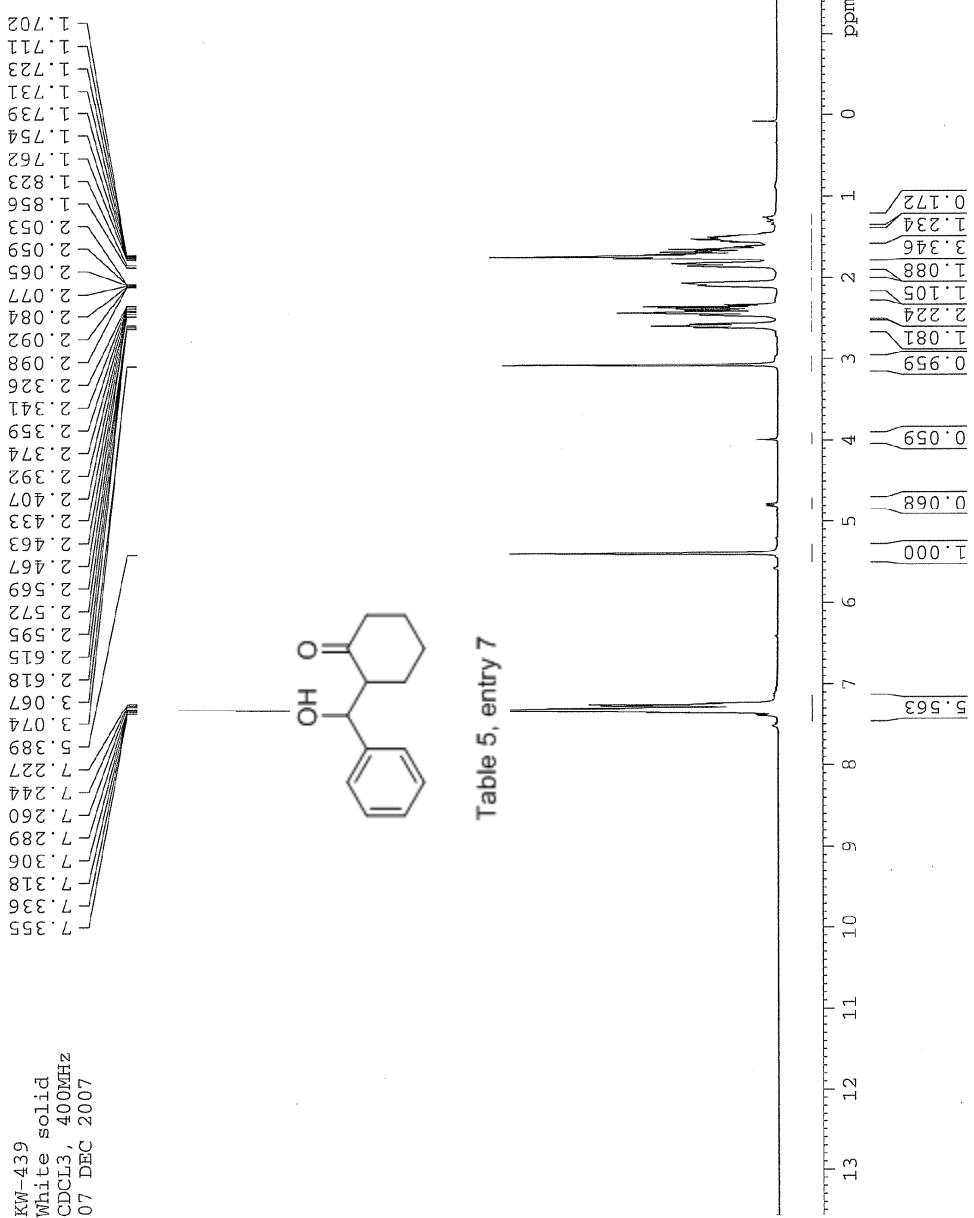
Table 5, entry 5

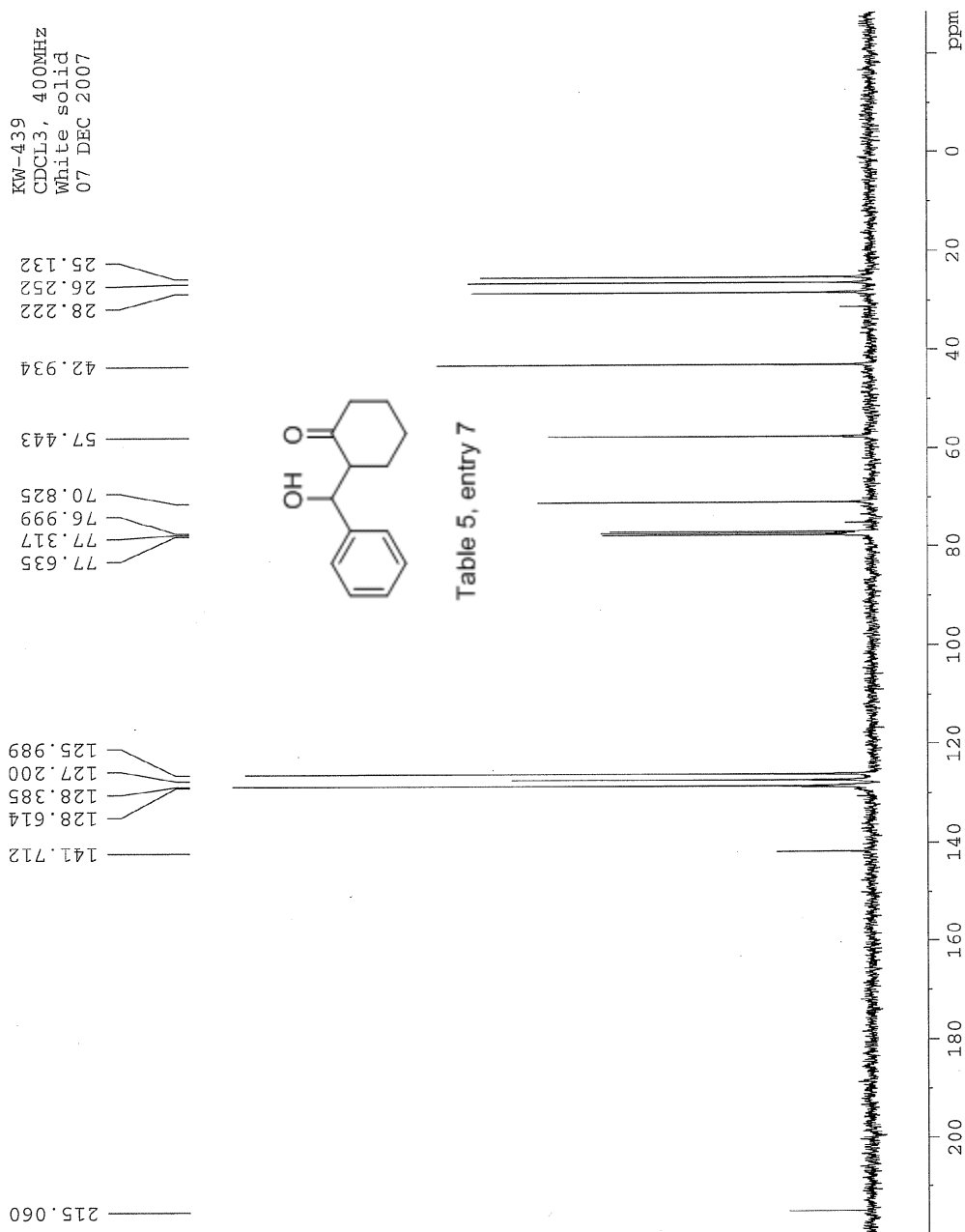
Date: Tue Jun 16 10:57:51 2009 ICIS: 8.3.0 SP2 for OSF1 (V4.0) build 98-238 from 26-Aug-98

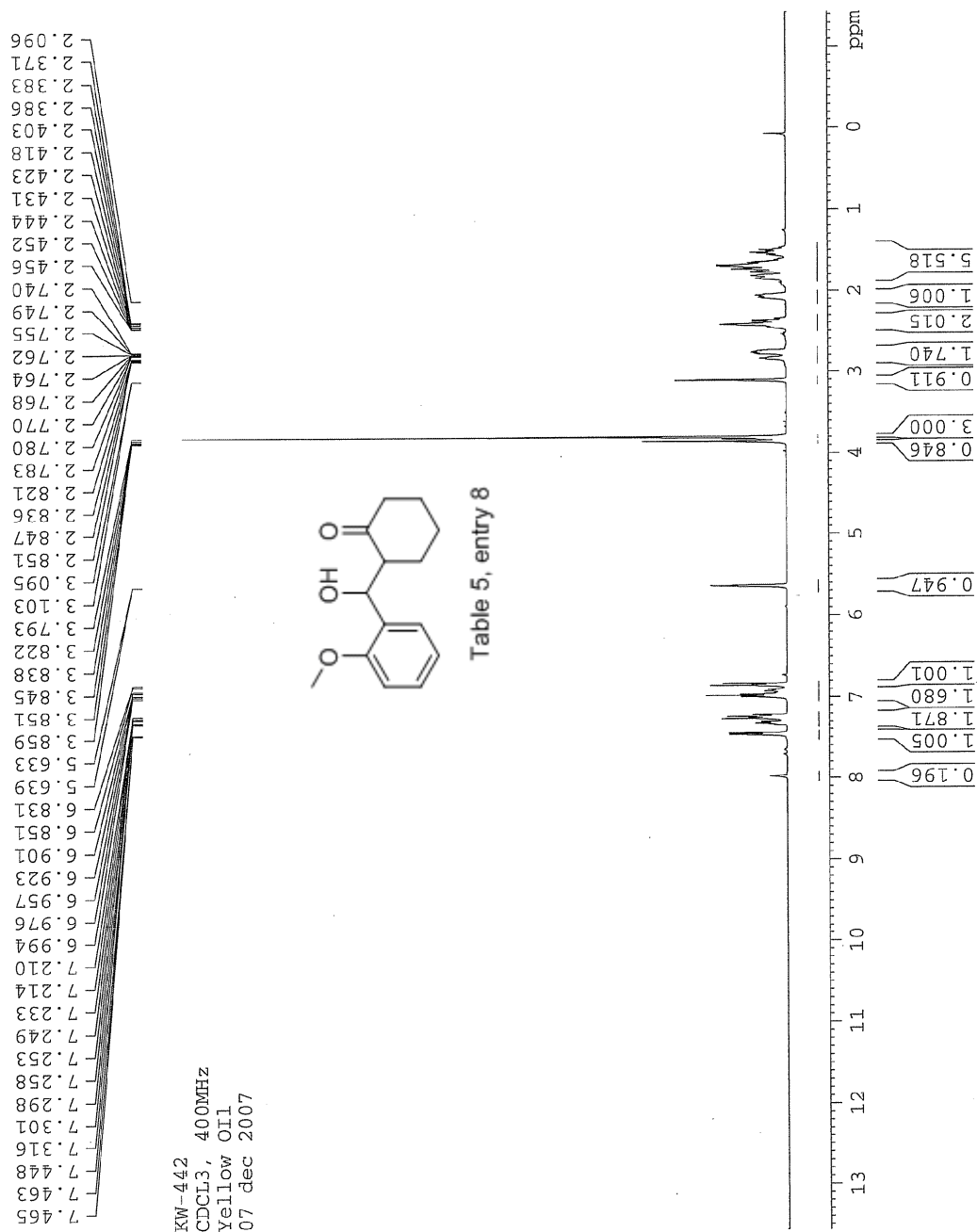


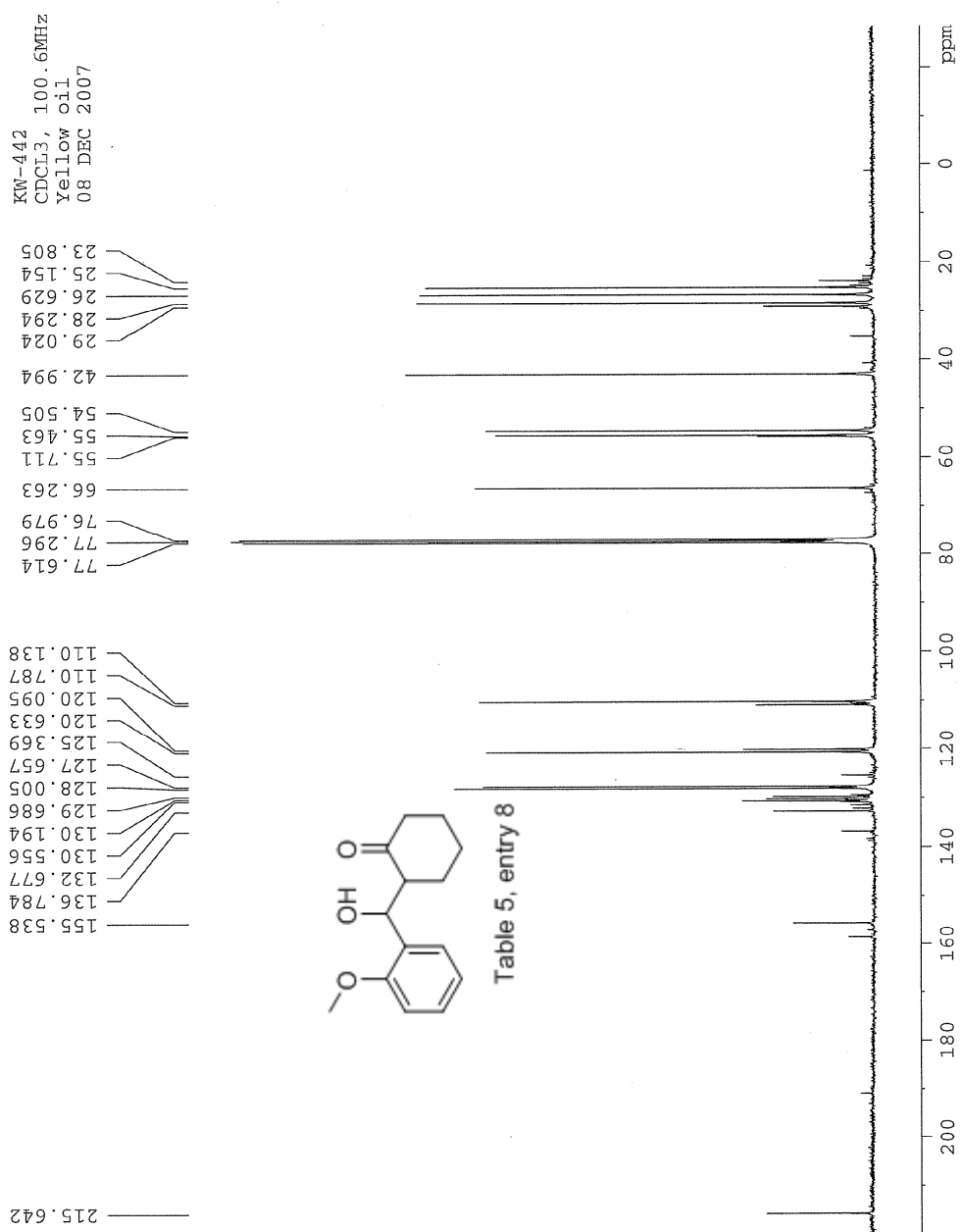


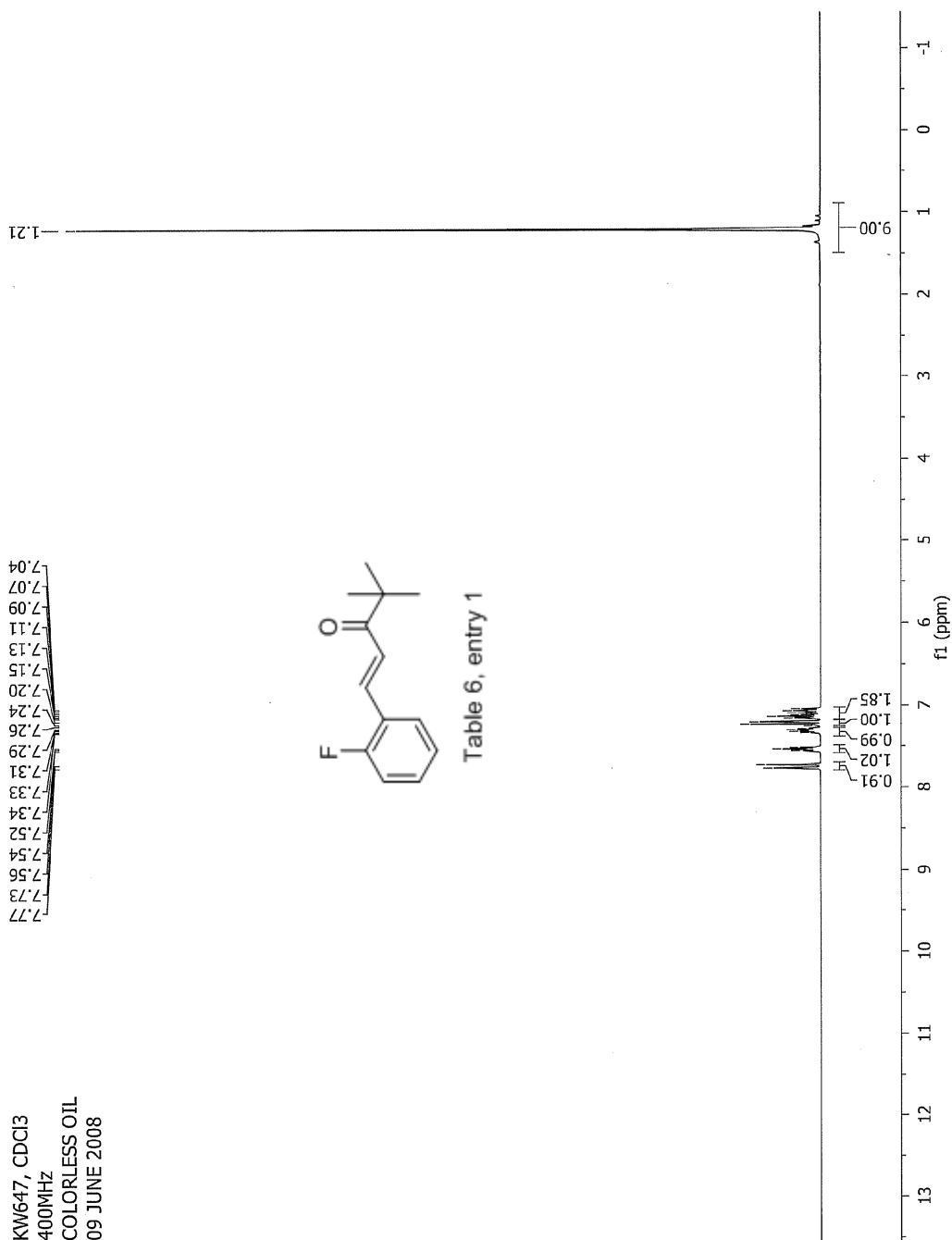


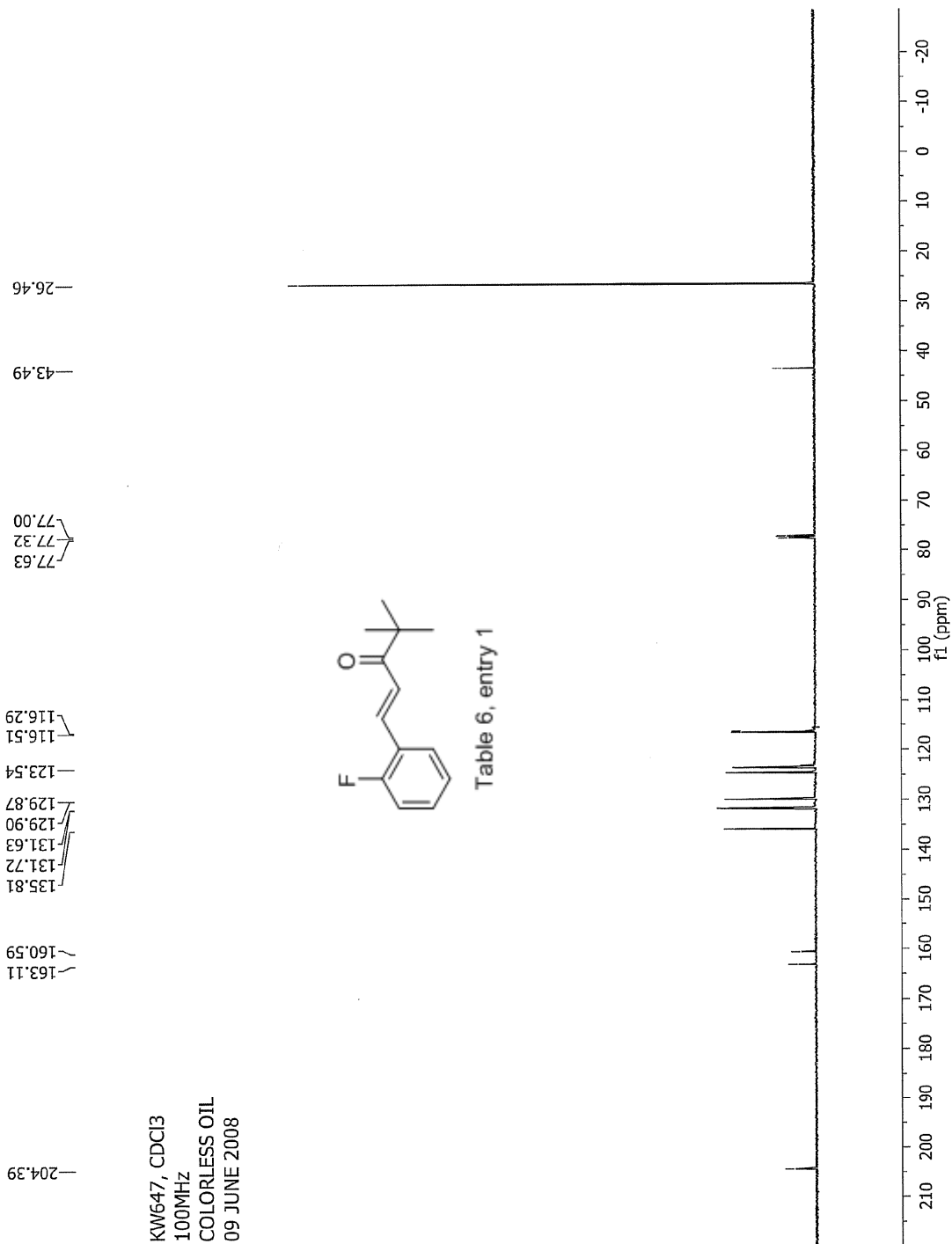












### Manual Peak Matching Report For Accurate Mass Determination

Theoretical mass	Experimental mass	PFK matching mass	Deviation*
206.11069	206.11108	180.98882	1.9 ppm

\* The deviation is obtained from the following equation:

$$\text{deviation} = \frac{\text{experimental mass} - \text{theoretical mass}}{\text{nominal mass}}$$

Where nominal mass takes in account only  $^{12}\text{C}$ ,  $^1\text{H}$ ,  $^{16}\text{O}$ ,  $^{14}\text{N}$  etc...

Theoretical mass correspond to the mass of the most abundant isotope peak

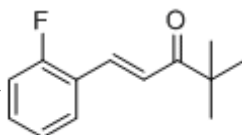
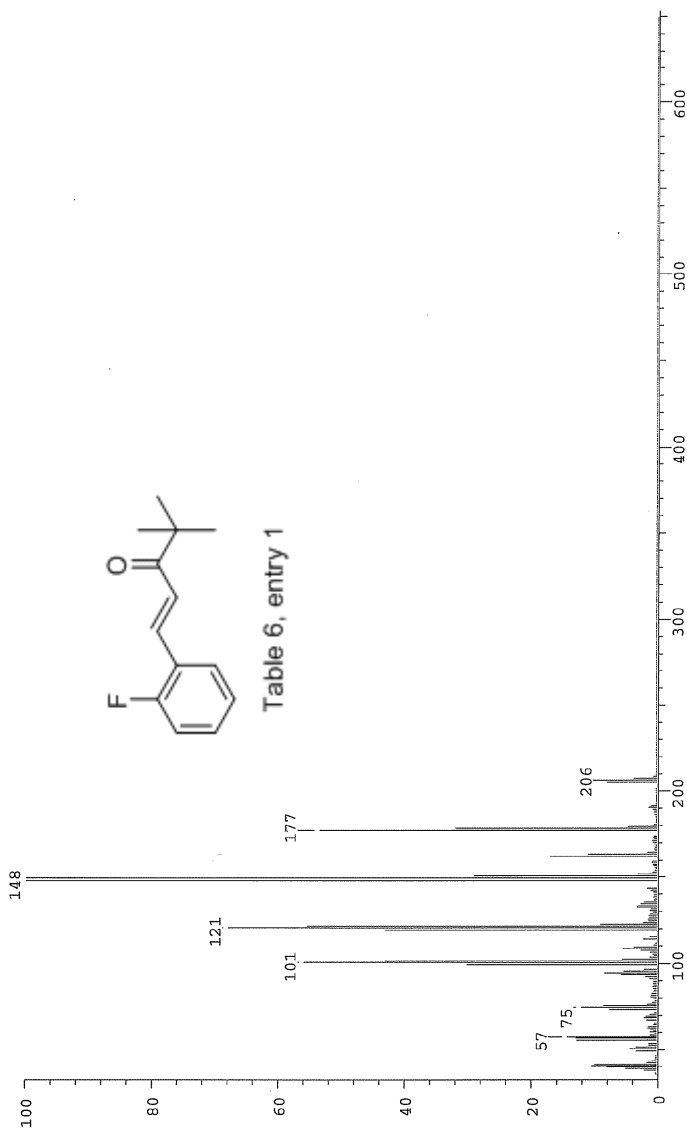


Table 6, entry 1

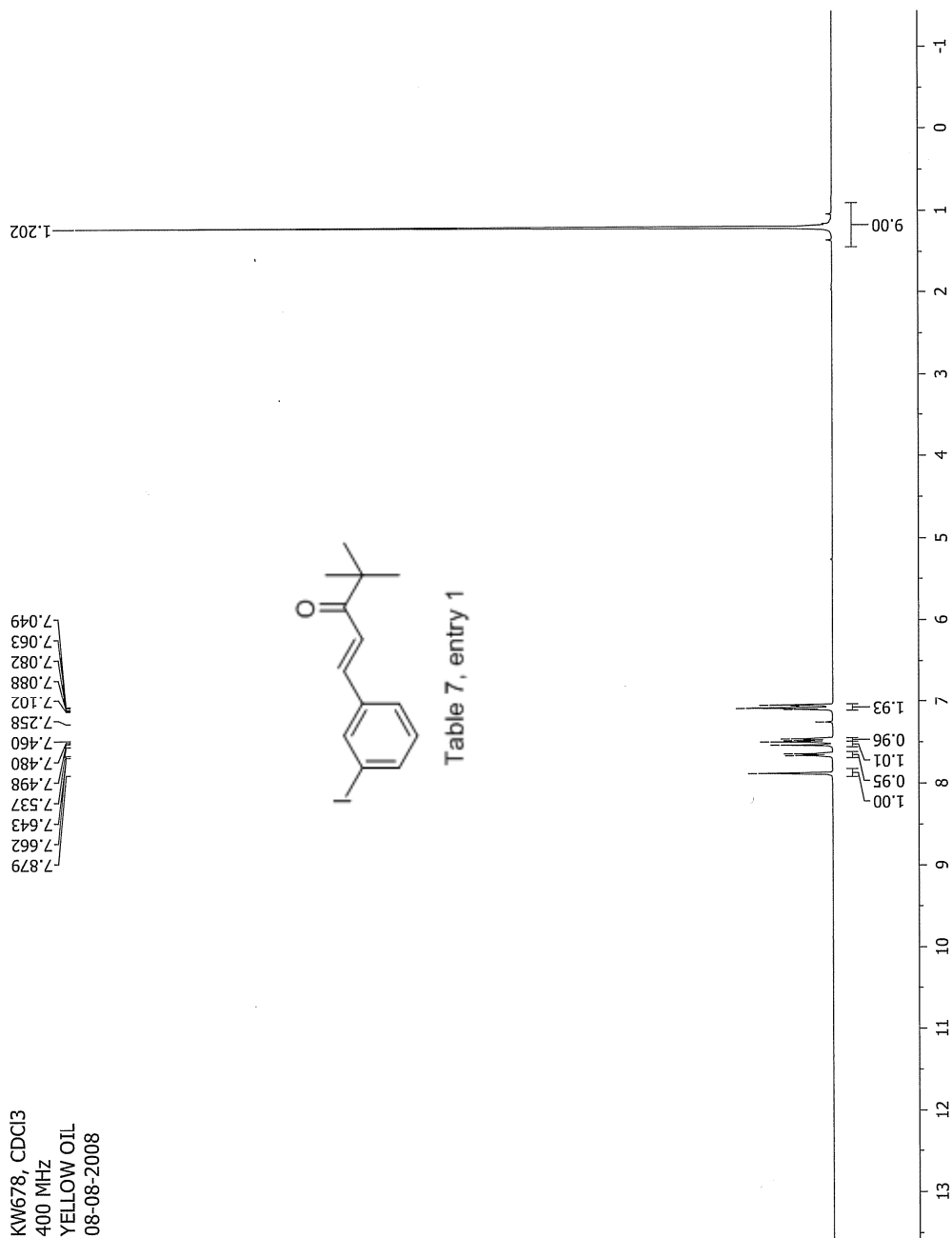
*Handwritten signature*

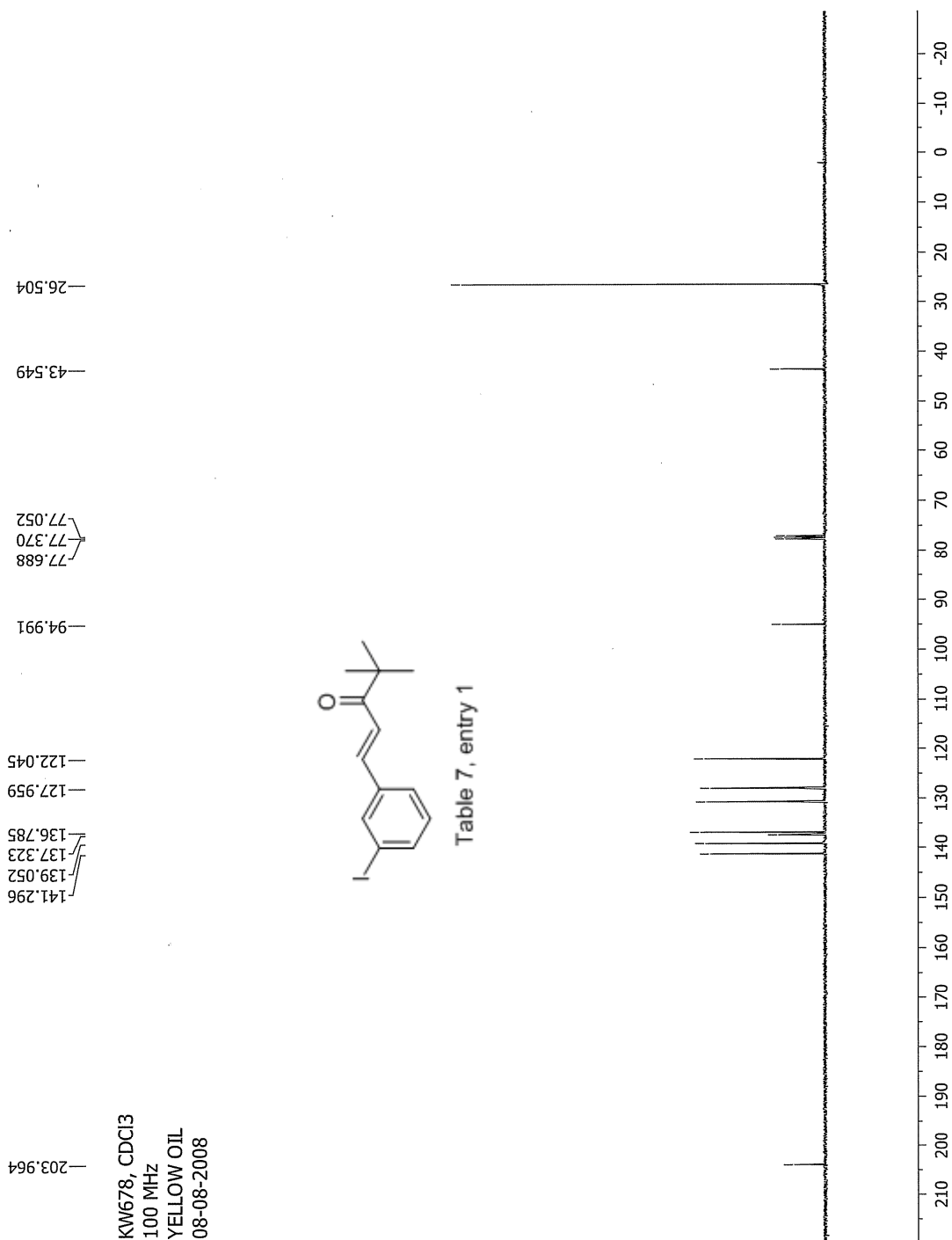


SPEC: E:\083763.dat (02-JUL-08 13:10:56)  
 Samp: KW647  
 Comm: 70 eV EI  
 Oper: kh  
 Study: MS services  
 Base: 149.32  
 Masses: 35.01 > 650.00  
 Peak: 1000.0 mmu  
 Intensity: 16777215  
 Scan 6 @ 0.29 min (EI +QIMS LMR UP LR)  
 Scans: 1 > 11  
 Client: Kuldup  
 #Peaks: 630  
 RIC: 152167114  
 1.7E+07



Date: Wed Jul 2 13:13:59 2008 ICIS: 8.3.0 SP2 for OSF1 (V4.0) build 98-238 from 26-Aug-98





## Elemental Composition Report

Page 1

## Single Mass Analysis

Tolerance = 10.0 PPM / DBE: min = -1.5, max = 50.0

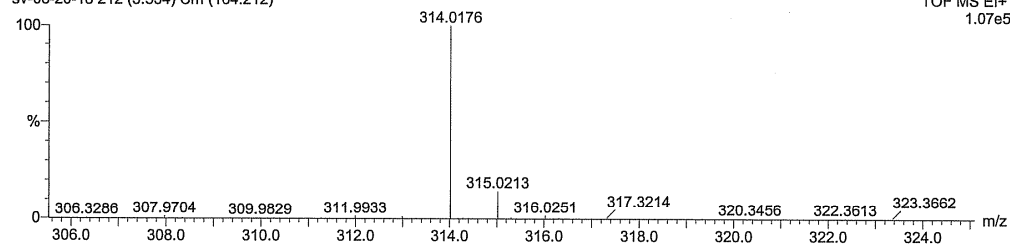
Isotope cluster parameters: Separation = 1.0 Abundance = 1.0%

Monoisotopic Mass, Odd and Even Electron Ions

39 formula(e) evaluated with 1 results within limits (up to 50 closest results for each mass)

KW 678

sv-08-20-18 212 (3.534) Cm (164:212)

TOF MS EI+  
1.07e5

Mass	Calc. Mass	mDa	PPM	DBE	Score	Formula
314.0176	314.0168	0.8	2.7	6.0	1	C13 H15 O I

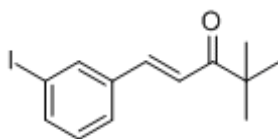
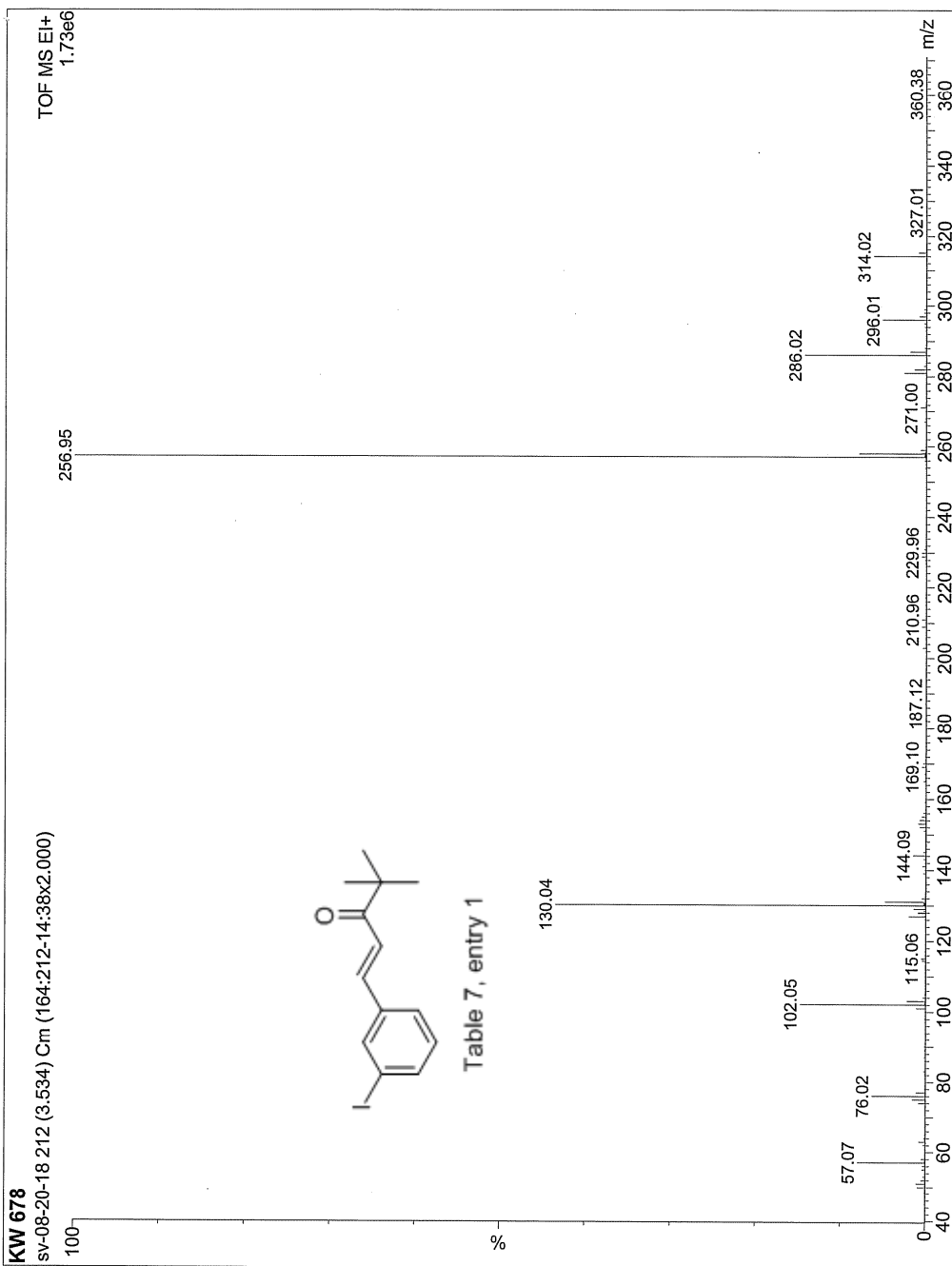
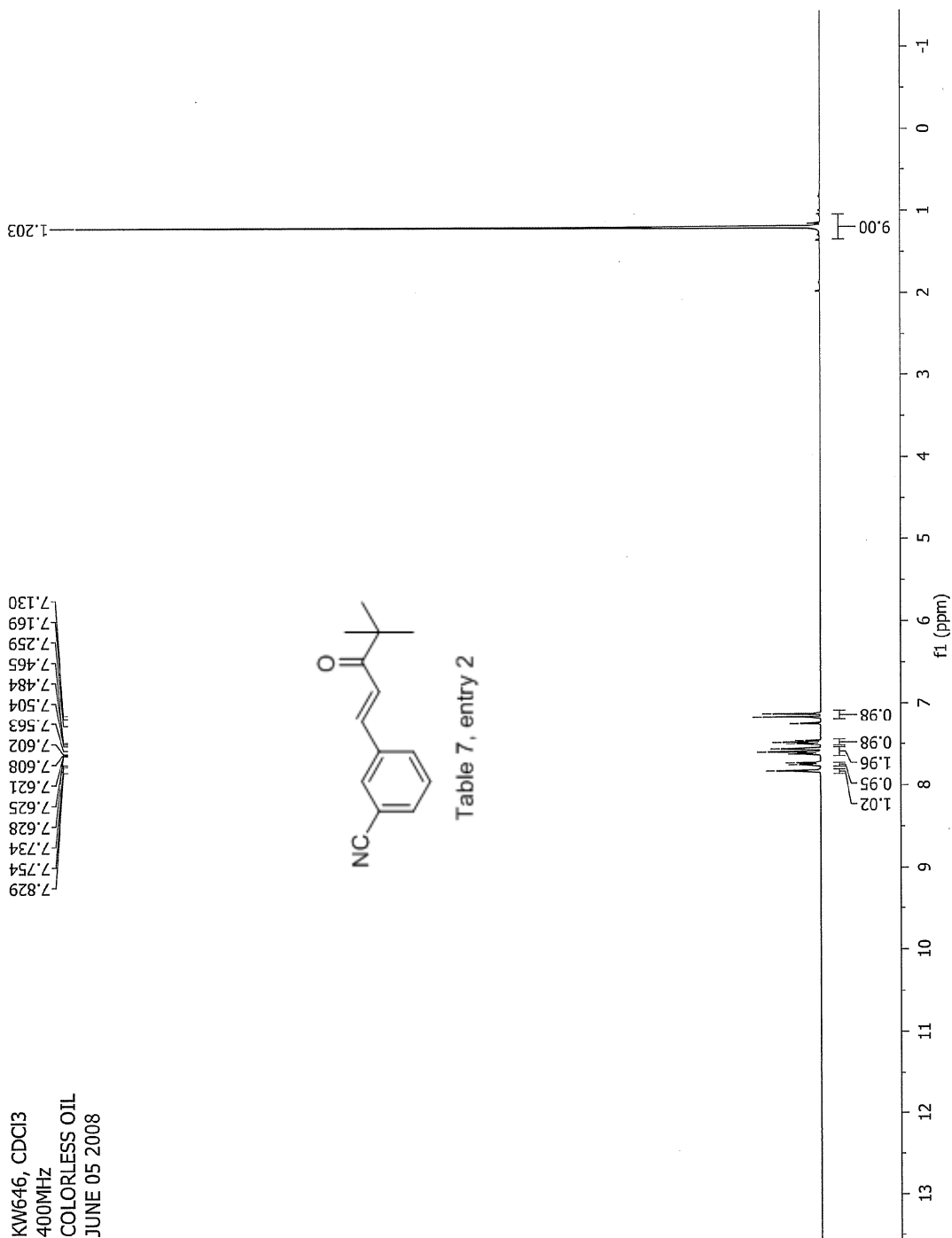
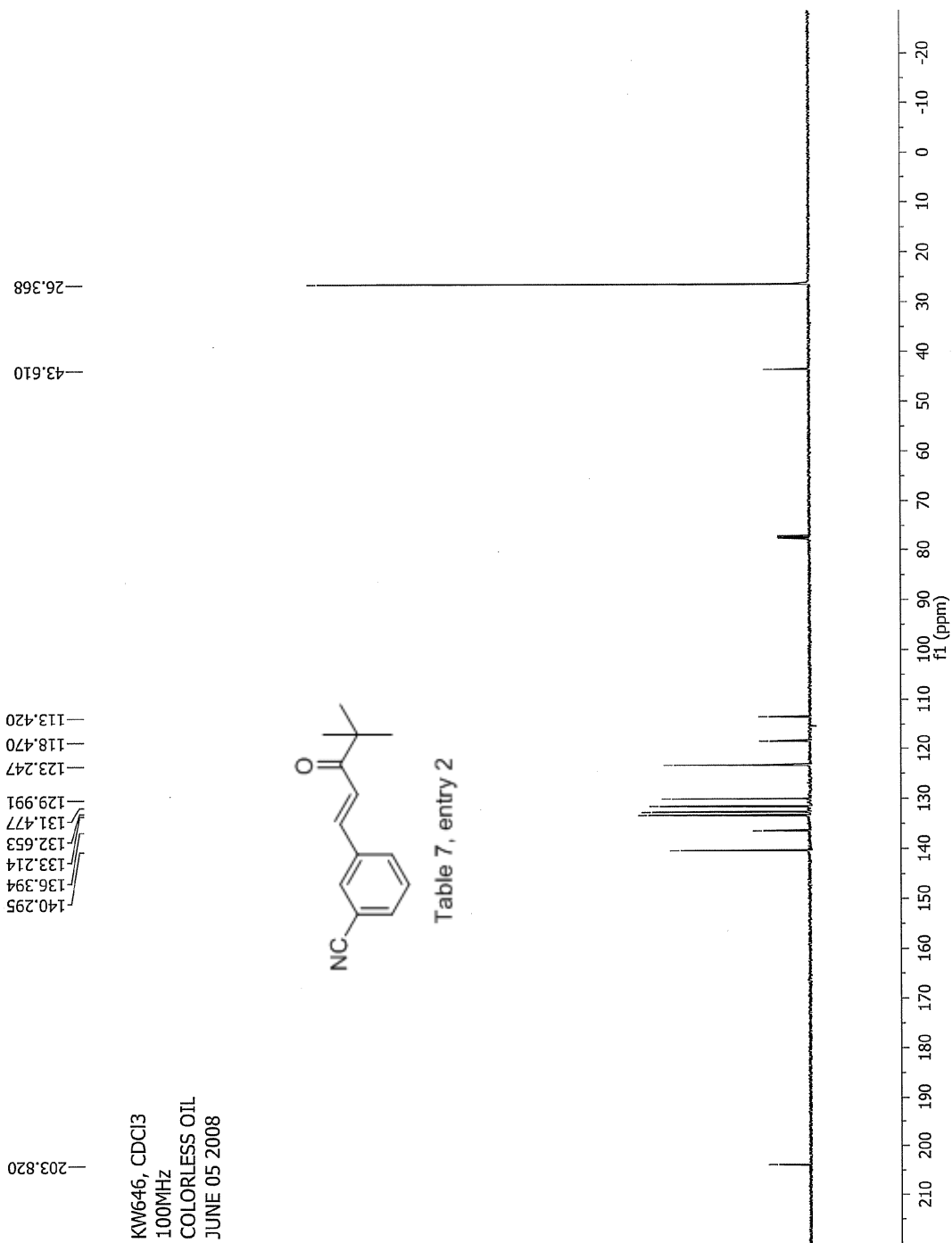


Table 7, entry 1







### Manual Peak Matching Report For Accurate Mass Determination

Theoretical mass	Experimental mass	PFK matching mass	Deviation*
213.11536	213.11582	180.98882	2.1 ppm

\* The deviation is obtained from the following equation:

$$\text{deviation} = \frac{\text{experimental mass} - \text{theoretical mass}}{\text{nominal mass}}$$

Where nominal mass takes in account only  $^{12}\text{C}$ ,  $^1\text{H}$ ,  $^{16}\text{O}$ ,  $^{14}\text{N}$  etc...

Theoretical mass correspond to the mass of the most abundant isotope peak

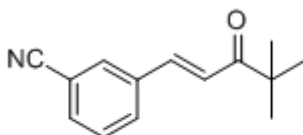


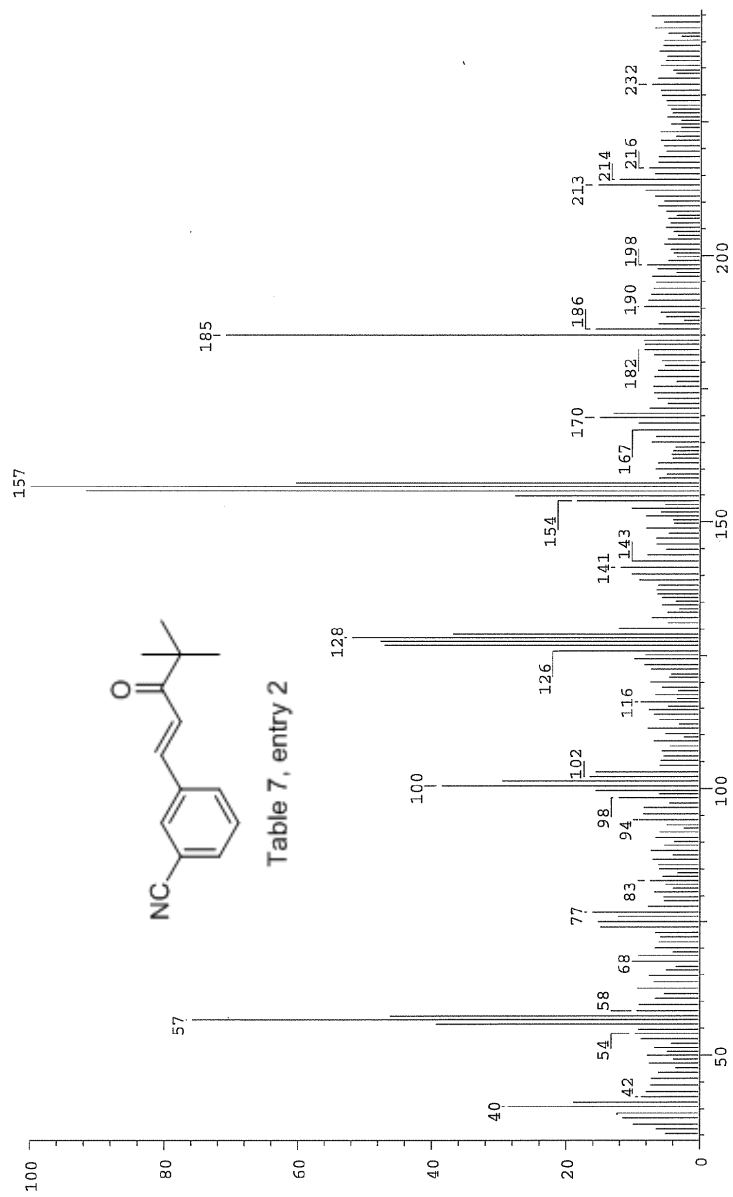
Table 7, entry 2

*W*

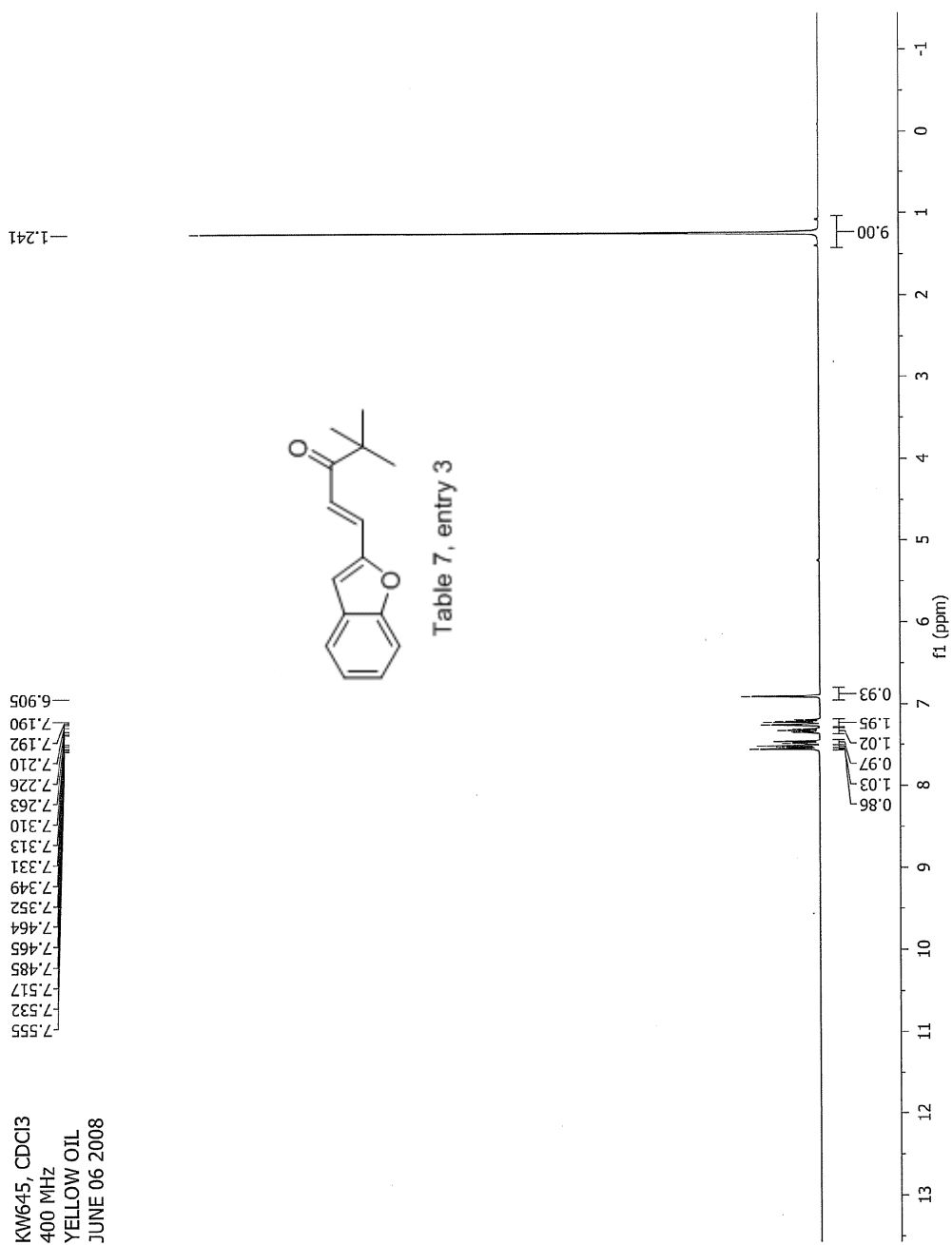


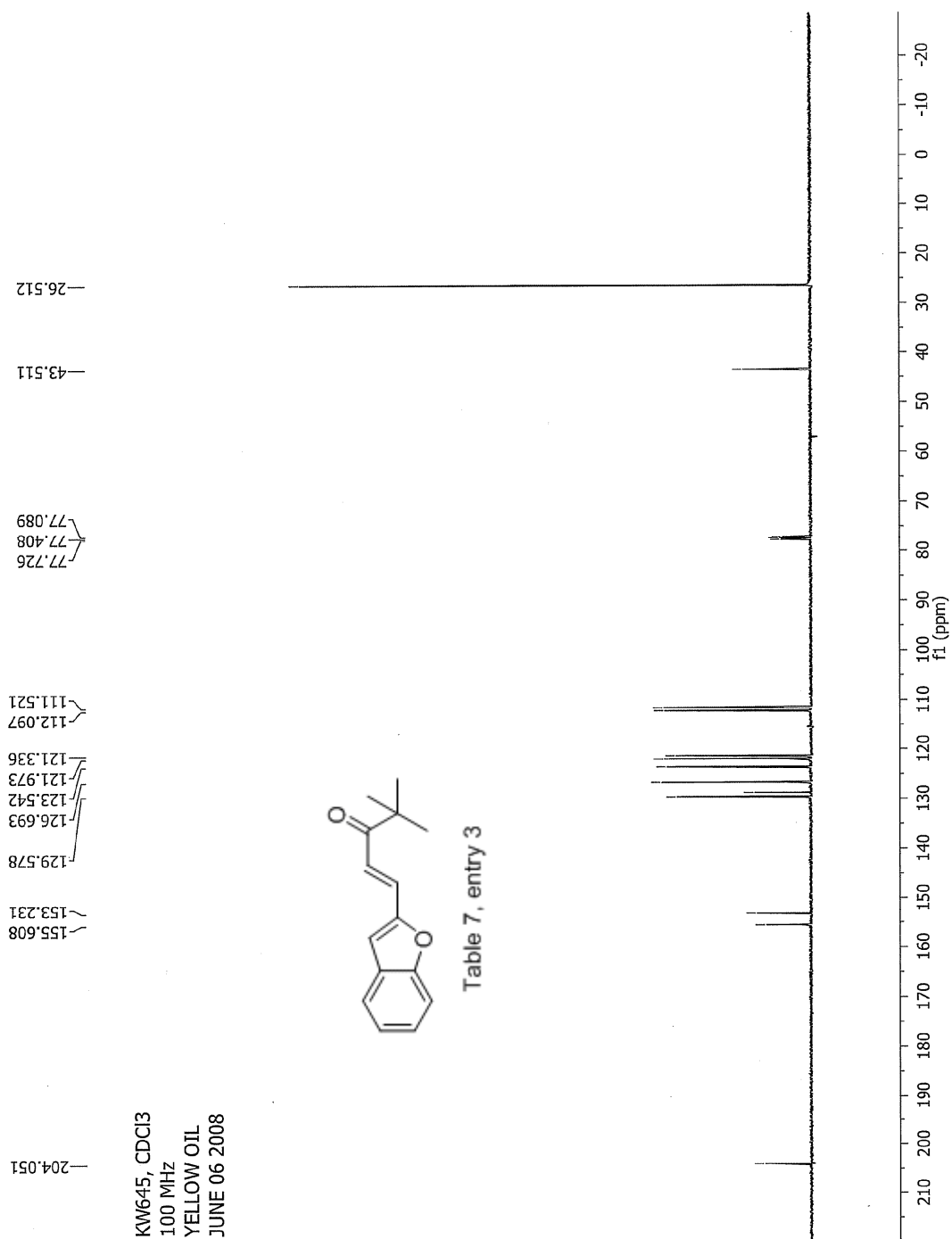
Scans: 1 > 78  
 Client: Kuldup  
 #peaks: 670  
 RIC: 876519  
 1.9E+04

SPRC: Fin083829.dat (11-AUG-08 10:48:52)  
 Samp: KW6466  
 Comm: 70 eV EI  
 Oper: kh  
 Study: ms services  
 Masses: 35.01 > 650.00  
 Base: 156.57  
 Intensity: 19368  
 Peak: 1000.0 mmu  
 Scan 33 @ 0.84 min (EI +QIMS LMR UP LR)



Date: Mon Aug 11 10:51:45 2008 ICIS: 8.3.0 SP2 for OSFI (V4.0) build 98-238 from 26-Aug-98





### Manual Peak Matching Report For Accurate Mass Determination

Theoretical mass	Experimental mass	PFK matching mass	Deviation*
228.11503	228.11549	218.98562	2 ppm

\* The deviation is obtained from the following equation:

$$\text{deviation} = \frac{\text{experimental mass} - \text{theoretical mass}}{\text{nominal mass}}$$

Where nominal mass takes in account only  $^{12}\text{C}$ ,  $^1\text{H}$ ,  $^{16}\text{O}$ ,  $^{14}\text{N}$  etc...

Theoretical mass correspond to the mass of the most abundant isotope peak

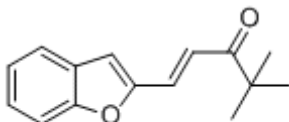


Table 7, entry 3

*Handwritten signature*

SPEC: fir083762.dat (02-JUL-08 13:07:39)  
 Samp: KW645  
 Comm: 70 eV EI  
 Oper: kh  
 Base: 171.20  
 Peak: 1000.0 mmu  
 Scan 63 @ 1.45 min (EI +QIMS LMR UP LR)  
 Study: MS services  
 Masses: 35.01 > 650.00  
 Intensity: 15459899  
 Scans: 1 > 65  
 Client: Kuldup  
 #Peaks: 657  
 RIC: 74620157  
 1.5E+07

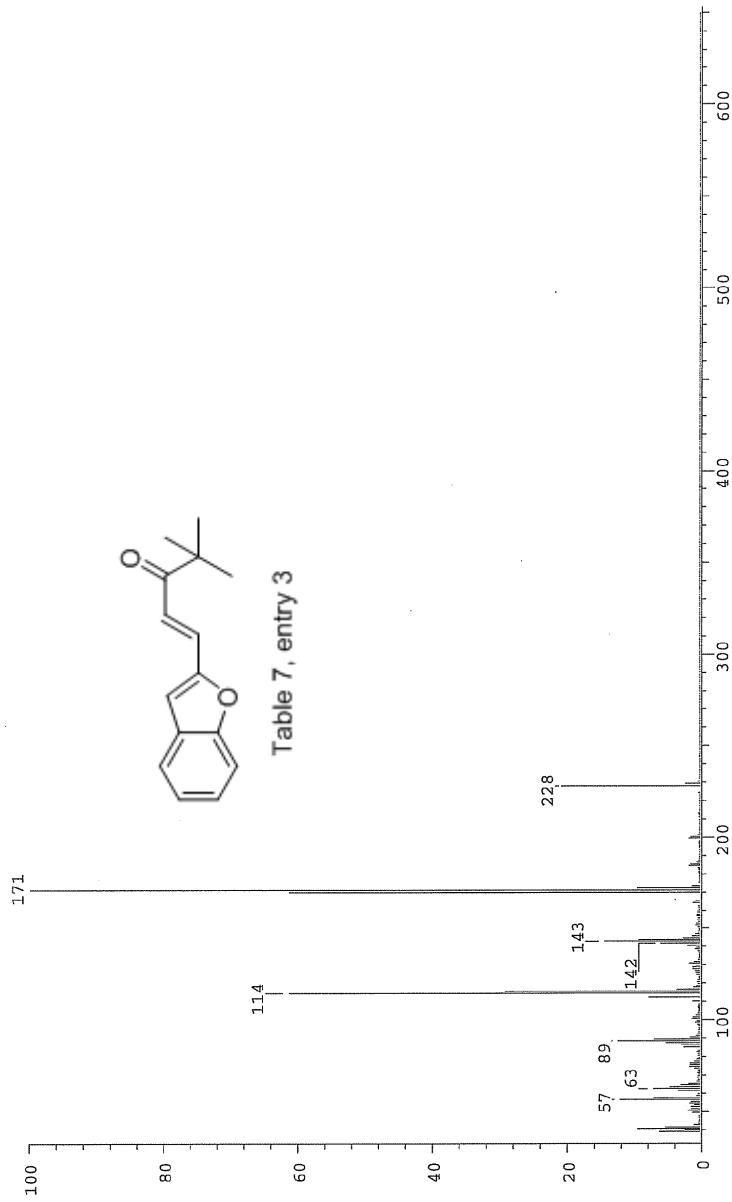
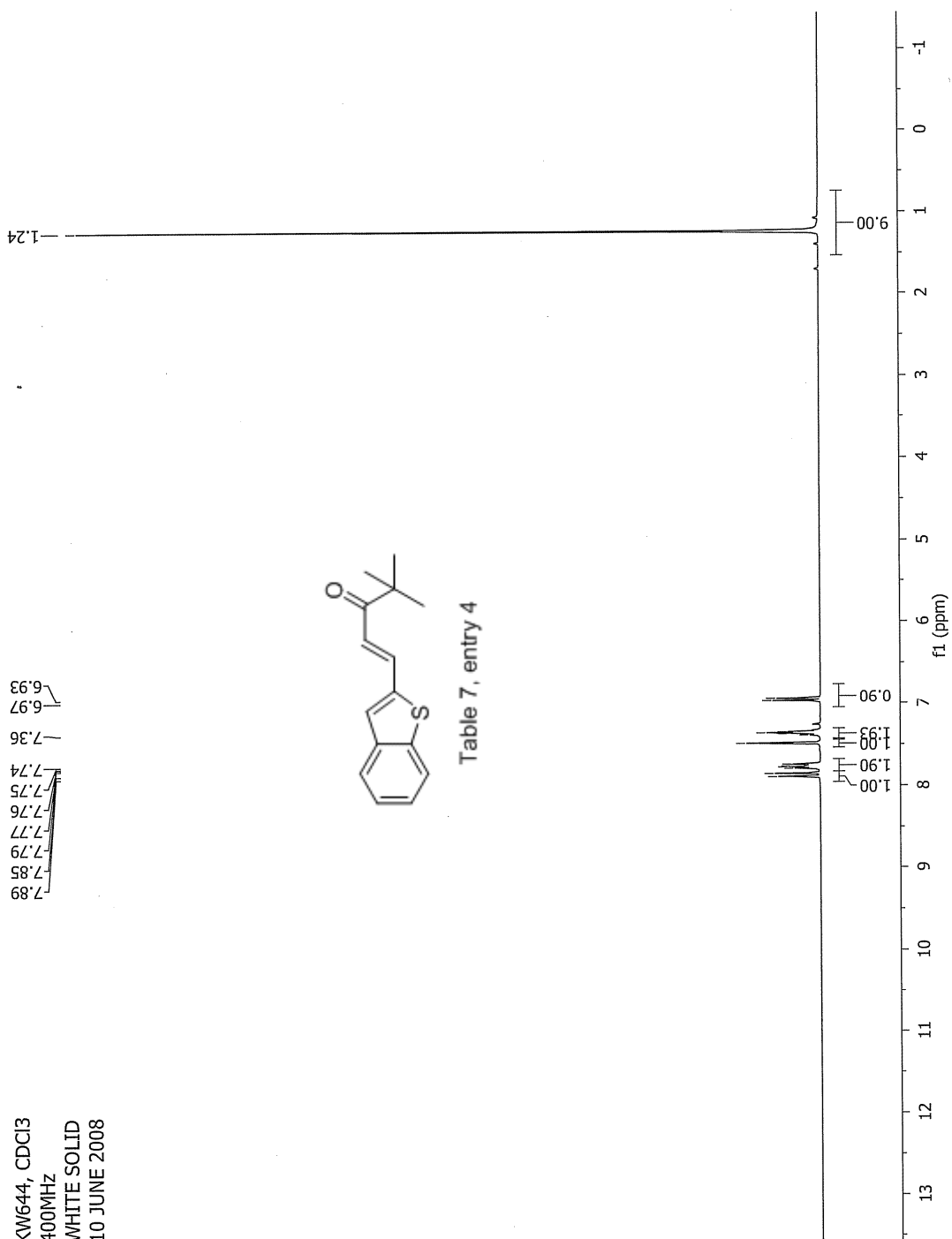
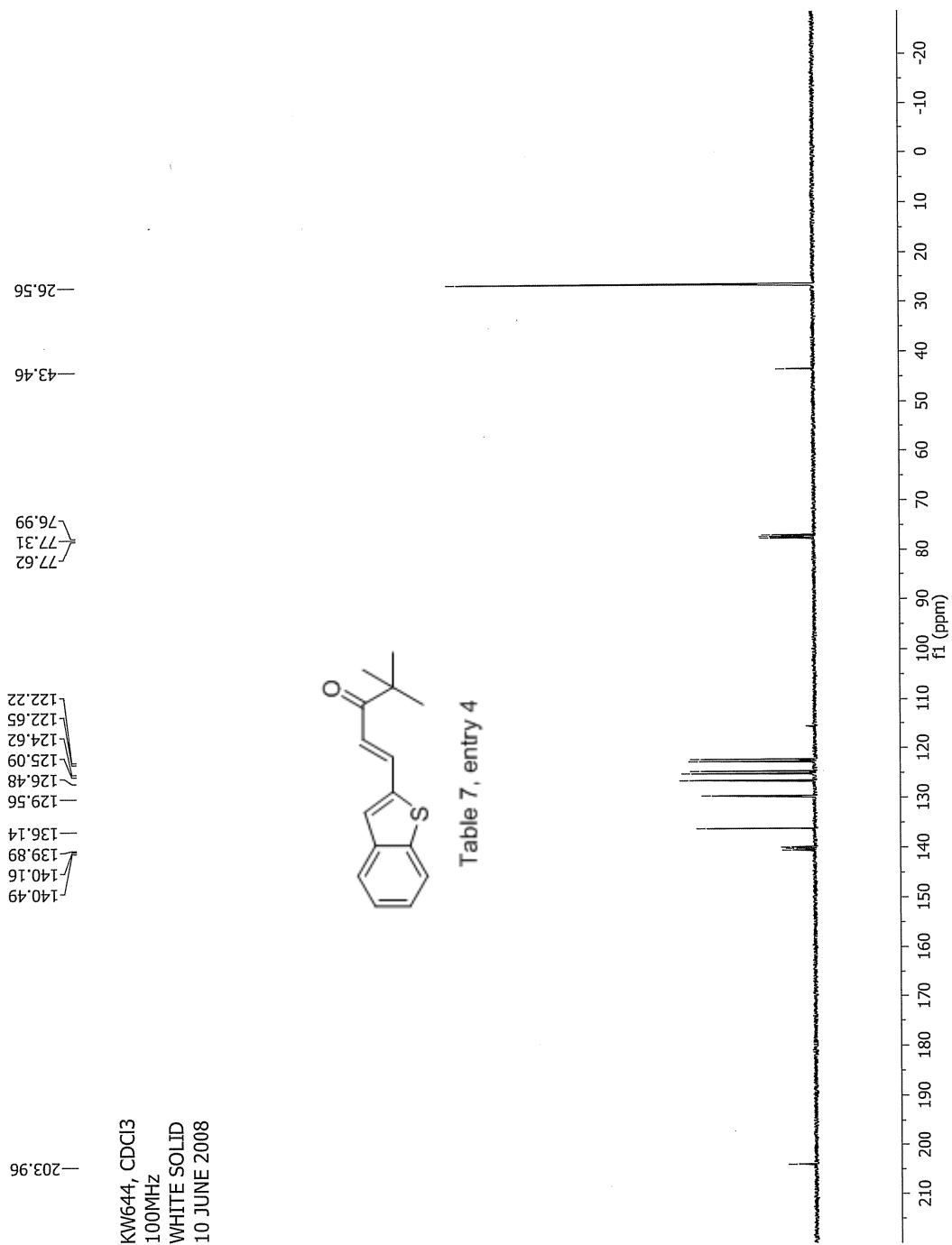


Table 7, entry 3

Date: Wed Jul 2 13:09:35 2008 ICIS: 8.3.0 SP2 for OSF1 (V4.0) build 98-238 from 26-Aug-98





### Manual Peak Matching Report For Accurate Mass Determination

Theoretical mass	Experimental mass	PFK matching mass	Deviation*
244.09219	244.09266	230.98562	1.9 ppm

\* The deviation is obtained from the following equation:

$$\text{deviation} = \frac{\text{experimental mass} - \text{theoretical mass}}{\text{nominal mass}}$$

Where nominal mass takes in account only  $^{12}\text{C}$ ,  $^1\text{H}$ ,  $^{16}\text{O}$ ,  $^{14}\text{N}$  etc...

Theoretical mass correspond to the mass of the most abundant isotope peak

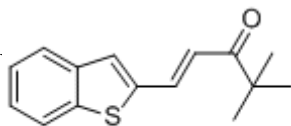
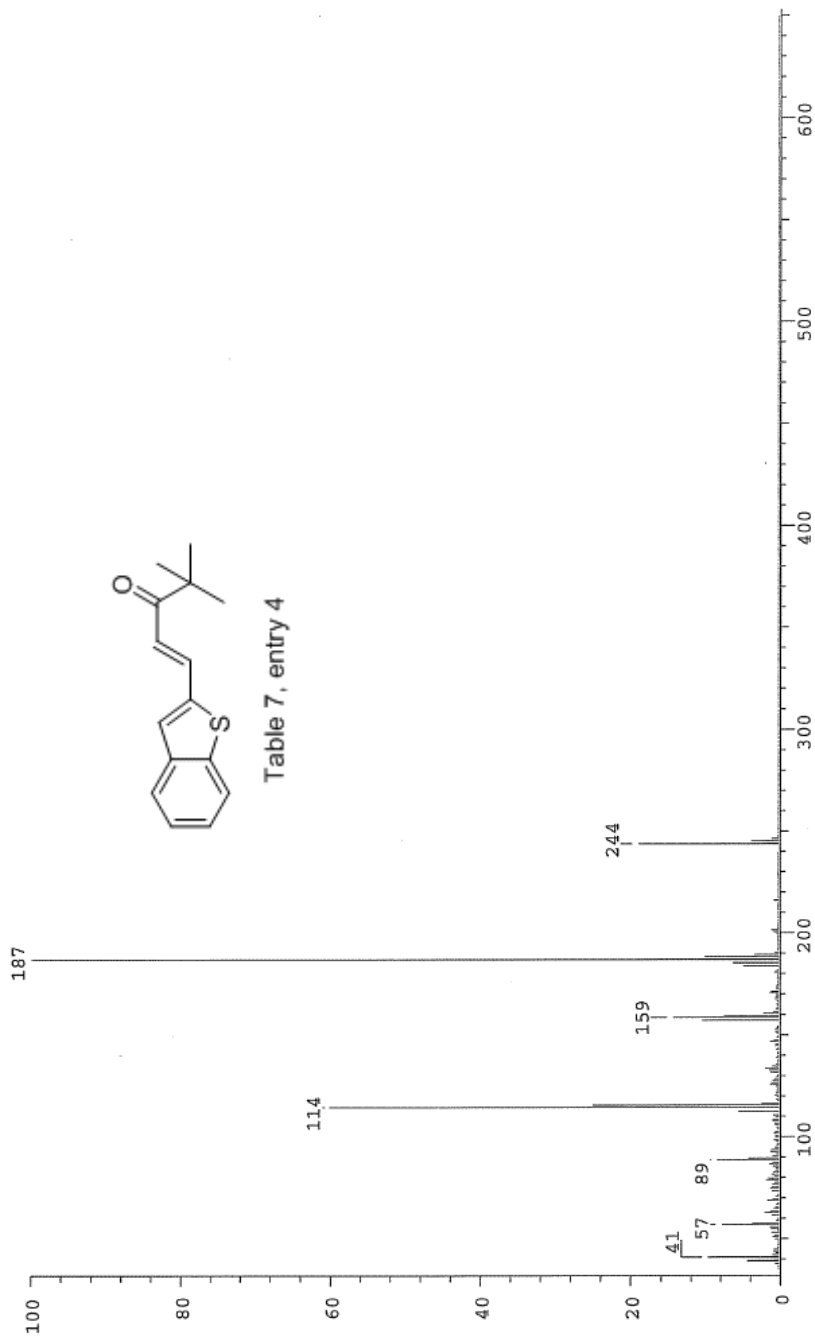


Table 7, entry 4

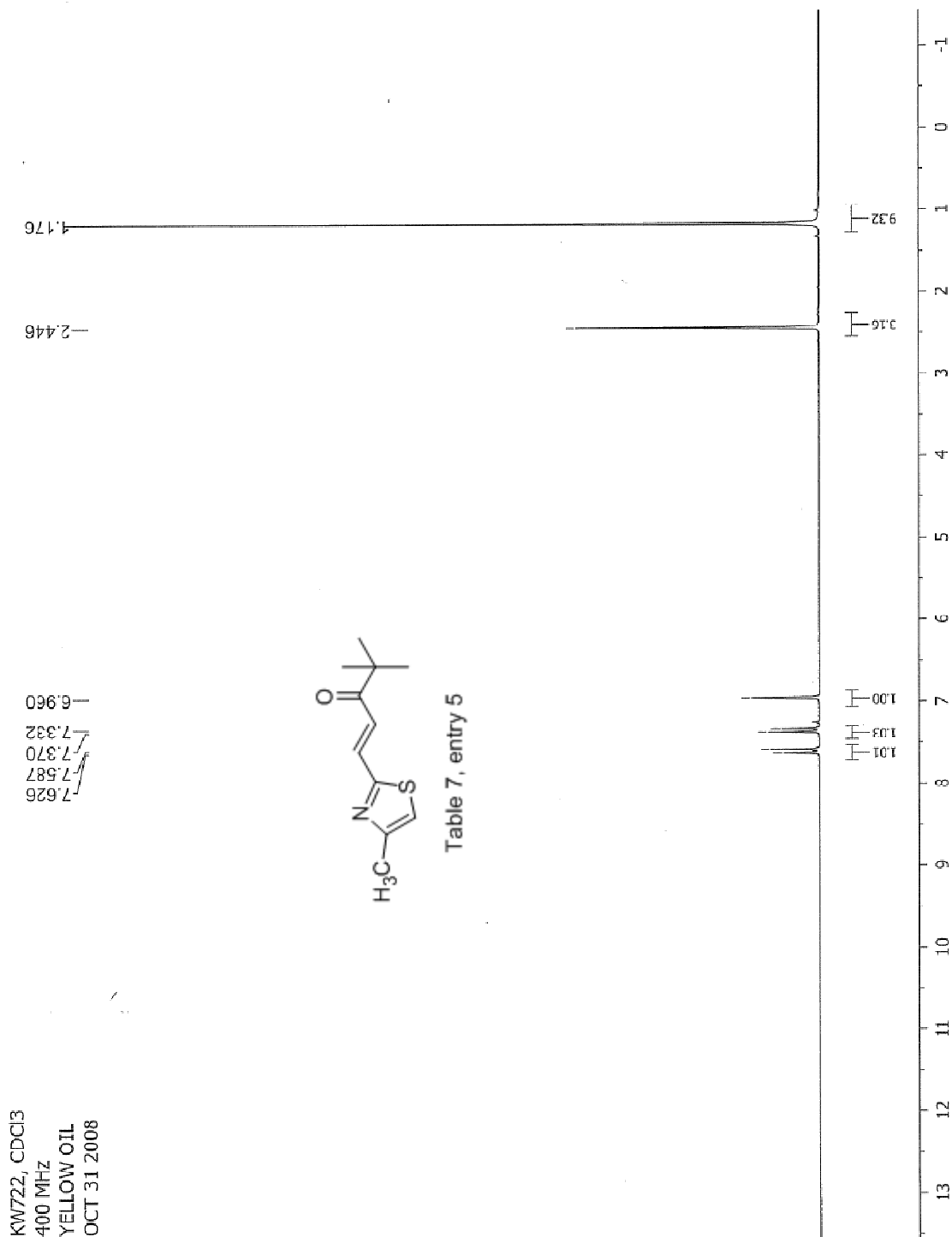
*MP*

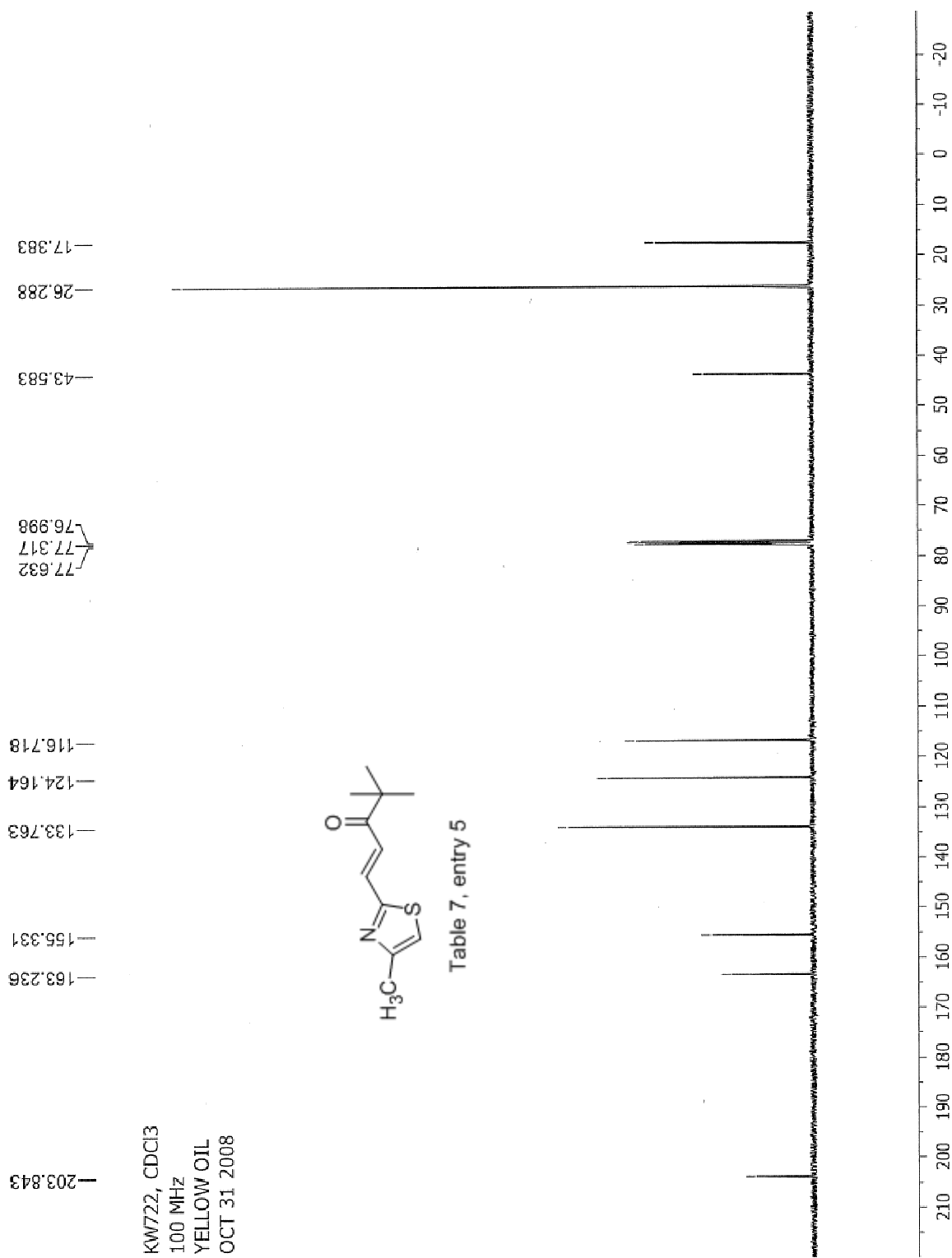


SPEC: fin083761.dat (02-JUL-08 13:03:19)  
 Samp: KW644  
 Comm: 70 eV EI  
 Oper: Kh  
 Base: 186.96  
 Peak: 1000.0 mmu  
 Scan 88 @ 2.16 min (EI +QIMS LMR UP LR)  
 Study: MS services  
 Masses: 35.01 > 650.00  
 Intensity: 15341367  
 Scans: 1 > 94  
 Client: Kuldup  
 #Peaks: 635  
 RIC: 59185932  
 1.5E+07



Date: Wed Jul 2 13:06:03 2008 ICIS: 8.3.0 SP2 for OSF1 (V4.0) build 98-238 from 26-Aug-98





### Manual Peak Matching Report For Accurate Mass Determination

Theoretical mass	Experimental mass	PFK matching mass	Deviation*
209.08743	209.08770	180.98882	1.3 ppm

\* The deviation is obtained from the following equation:

$$\text{deviation} = \frac{\text{experimental mass} - \text{theoretical mass}}{\text{nominal mass}}$$

Where nominal mass takes in account only  $^{12}\text{C}$ ,  $^1\text{H}$ ,  $^{16}\text{O}$ ,  $^{14}\text{N}$  etc...

Theoretical mass correspond to the mass of the most abundant isotope peak

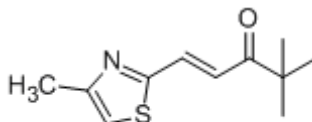


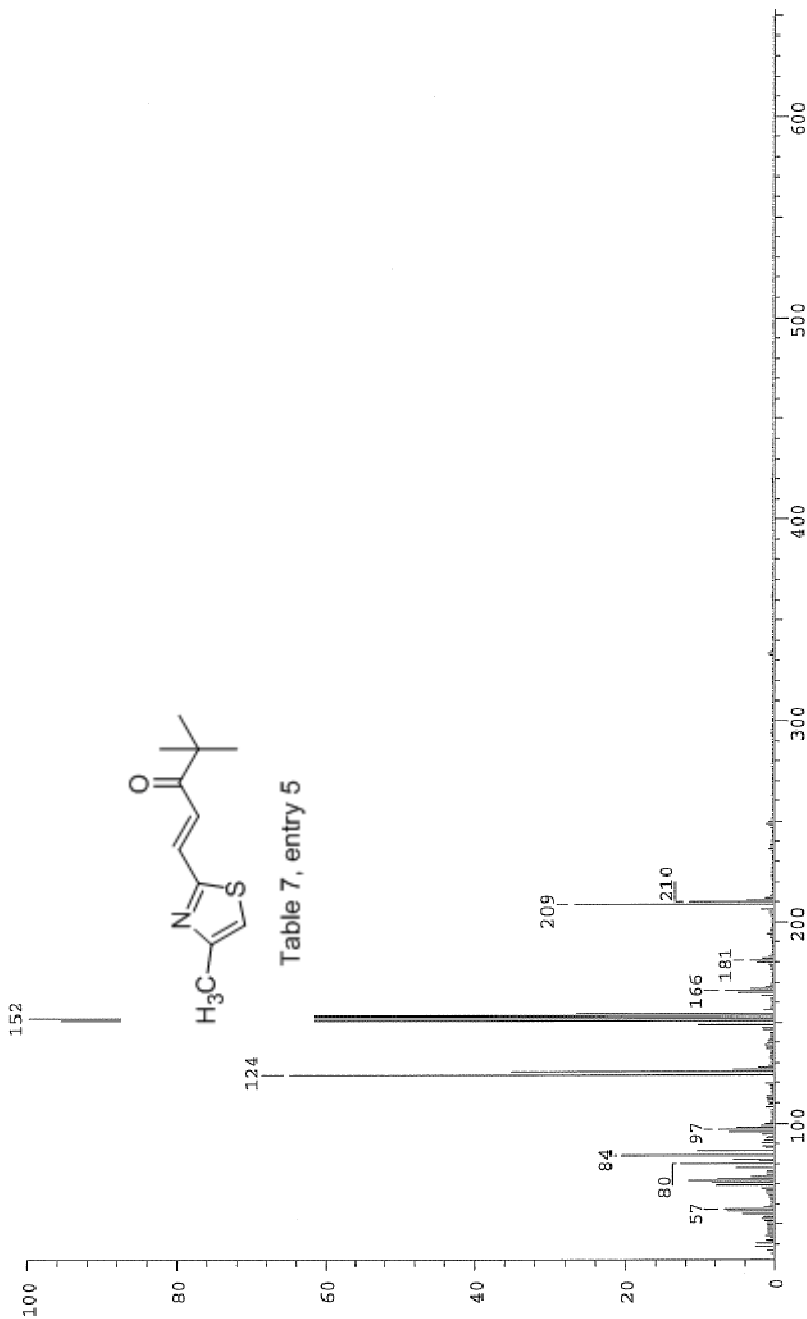
Table 7, entry 5

ba

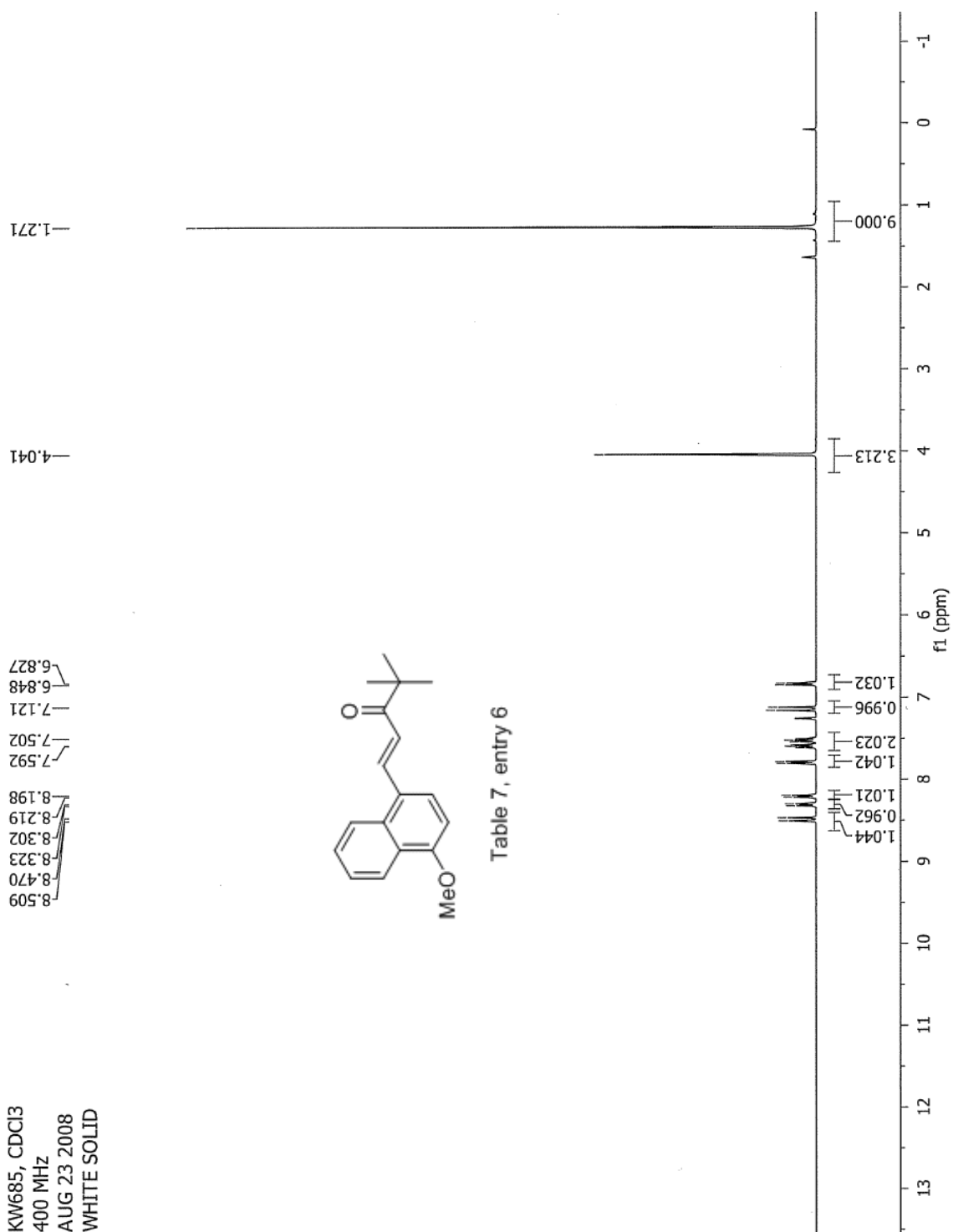
Scans: 1 > 79  
 Client: Kuiddeep  
 #Peaks: 611  
 RIC: 96034918  
 1.4E+07

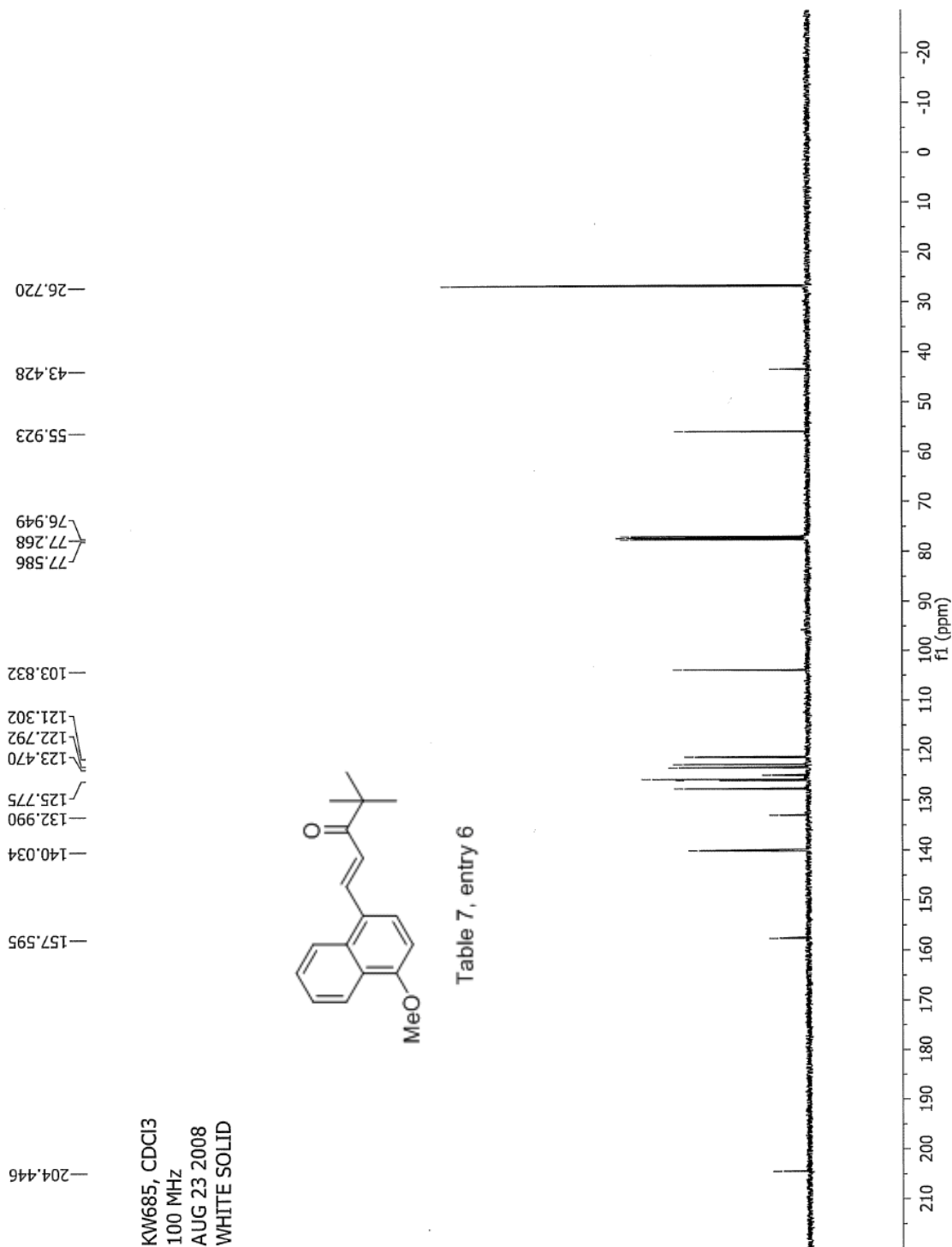
SPEC: fin084087.dat  
 Samp: kw722  
 Comm: 70 eV EI  
 Oper: Kh  
 Base: 152.11  
 Peak: 1000.0 mmu  
 Scan 65 @ 1.49 min (EI +Q1MS LMR UP LR)

Study: ms services  
 Masses: 35.01 > 650.00  
 Intensity: 14495213



Date: Tue Dec 16 10:33:42 2008 ICIS: 8.3.0 SP2 for OSFI (V4.0) build 98-238 from 26-Aug-98





Theoretical mass	Experimental mass	PFK matching mass	Deviation*
268.14632	268.14673	230.98562	1.5 ppm

\* The deviation is obtained from the following equation:

$$\text{deviation} = \frac{\text{experimental mass} - \text{theoretical mass}}{\text{nominal mass}}$$

Where nominal mass takes in account only  $^{12}\text{C}$ ,  $^1\text{H}$ ,  $^{16}\text{O}$ ,  $^{14}\text{N}$  etc...

Theoretical mass correspond to the mass of the most abundant isotope peak

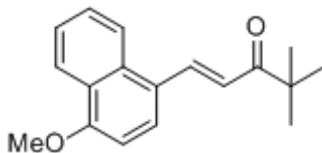
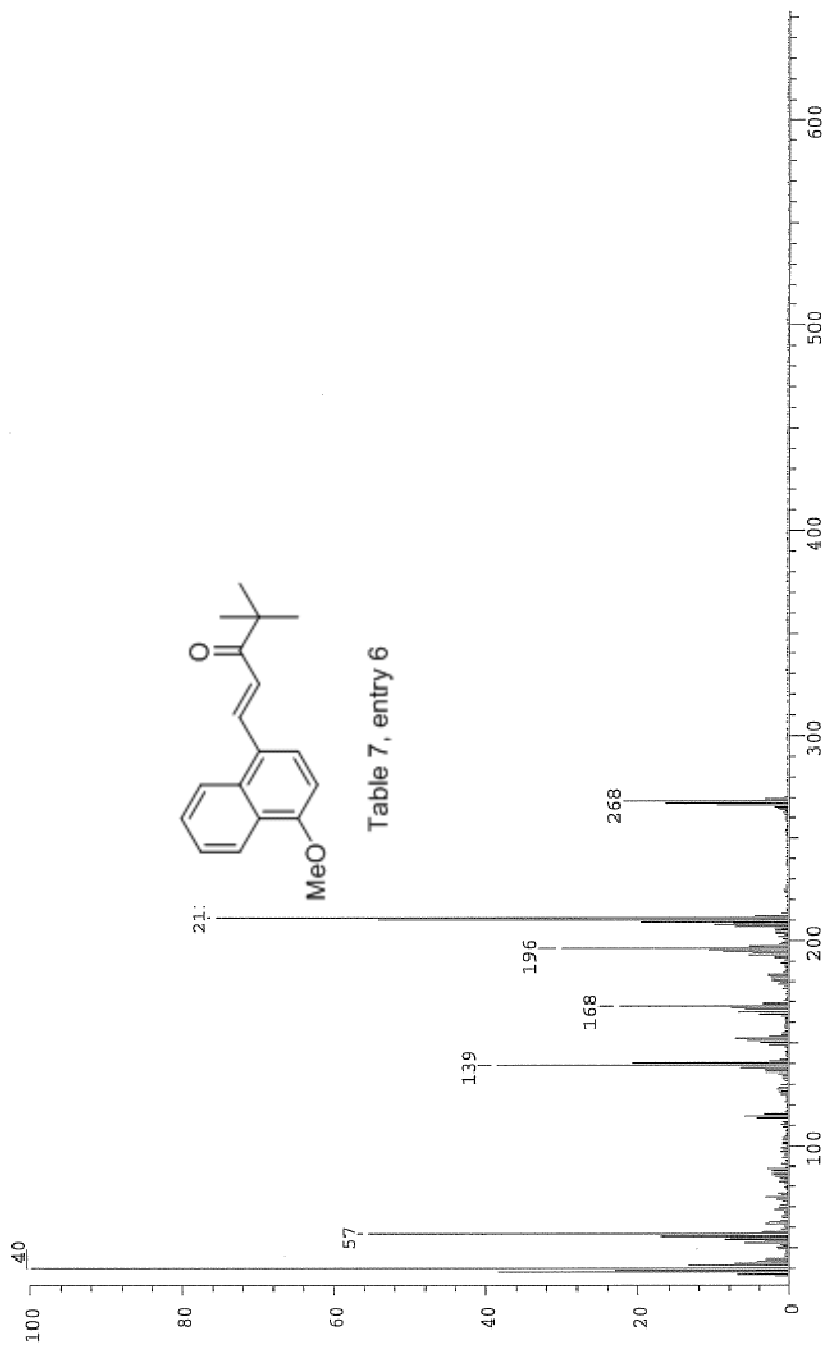


Table 7, entry 6

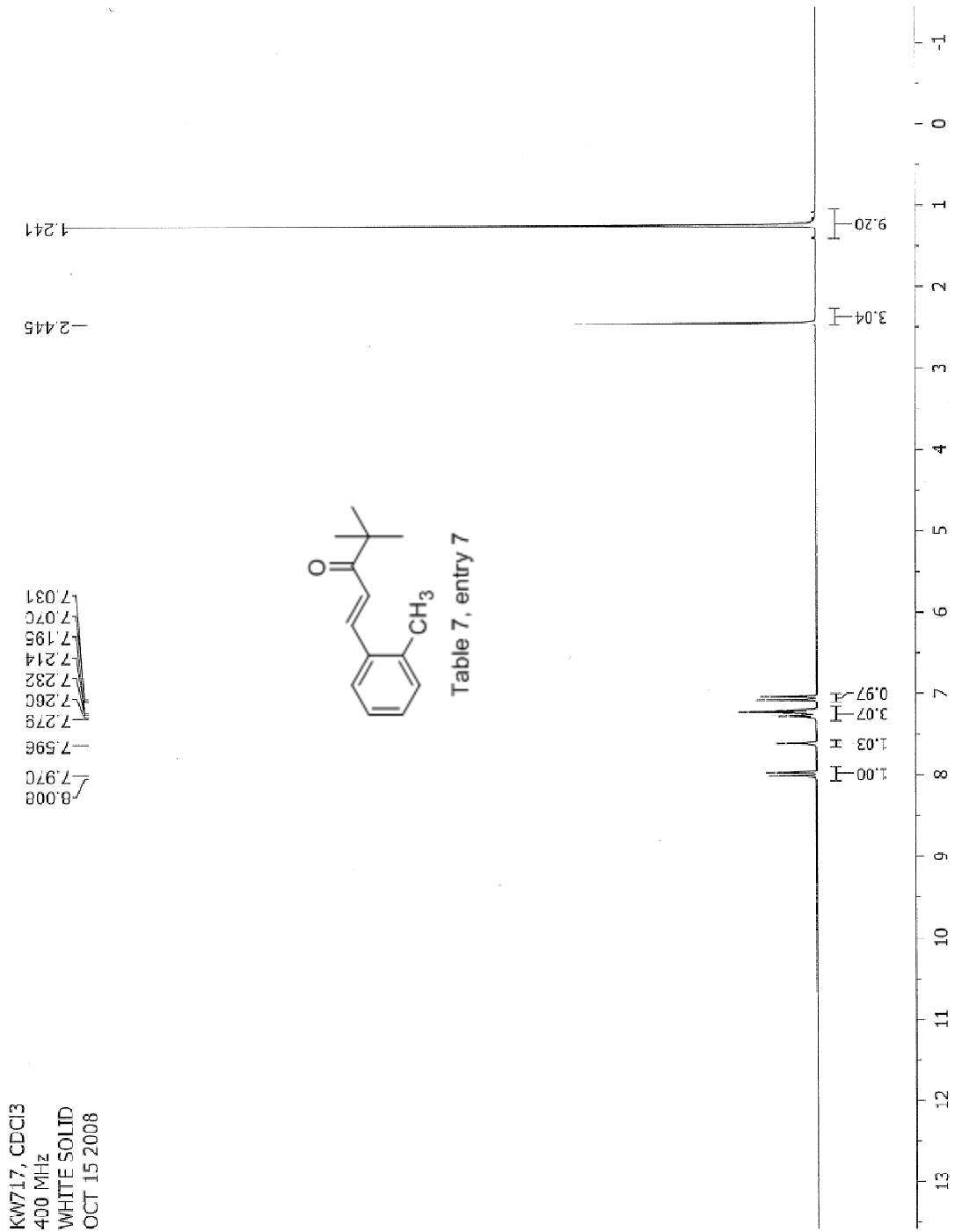
*Handwritten signature*

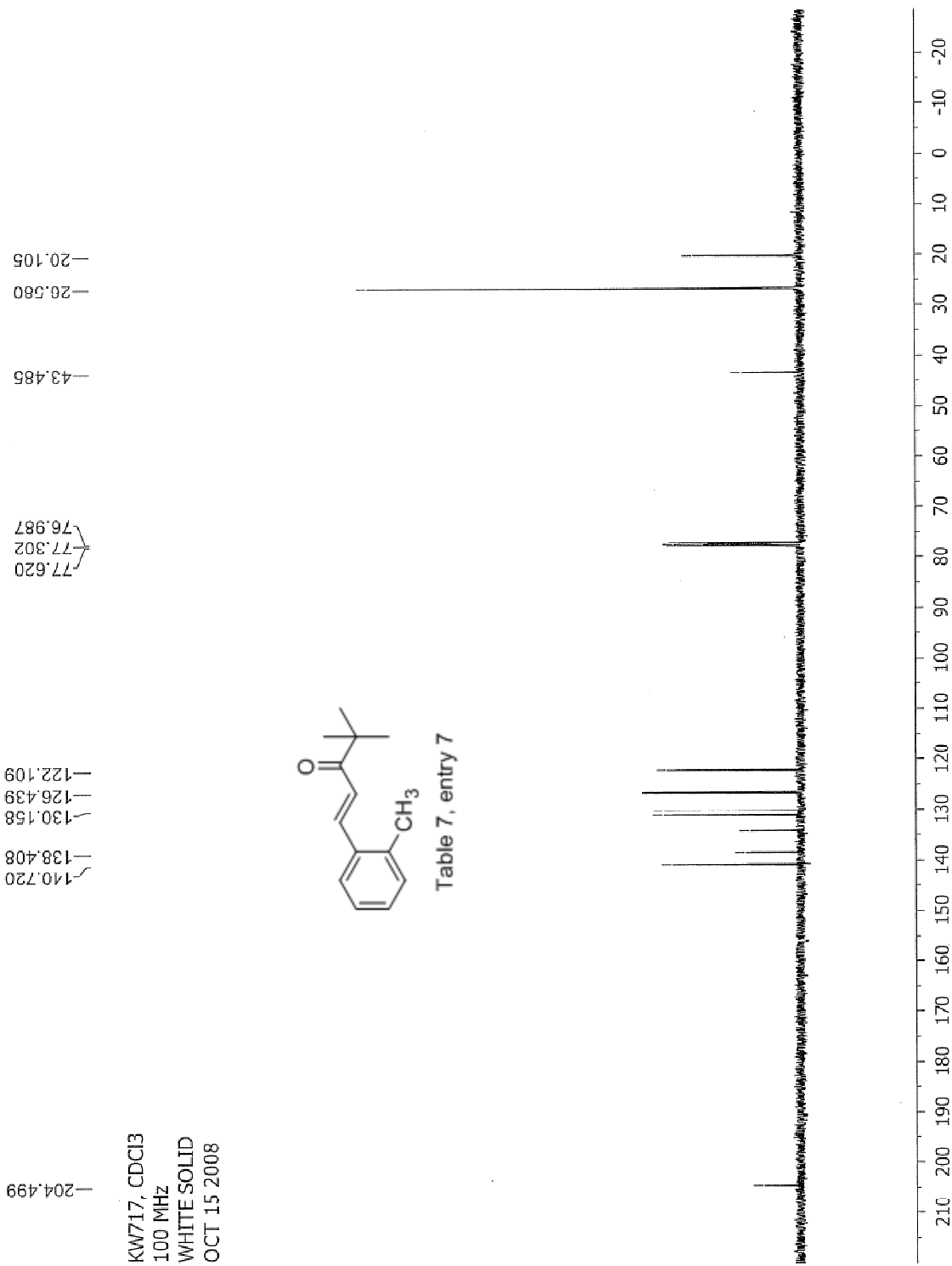


SPC: fin083944.dat (24-OCT-08 11:01:50) Scans: 1 > 14  
 Samp: KW684  
 Comm: 70 eV EI  
 Oper: kh  
 Study: MS services  
 Base: 40.19 Masses: 35.01 > 650.00  
 Peak: 1000.0 mmu Intensity: 108456  
 Scan 12 @ 0.40 min (EI +QMS EMR UP IR) 1.1E+05



Date: Fri Oct 24 11:02:43 2008 ICIS: 8.3.0 SP2 for OSFI (V4.0) build 98-238 from 26-Aug-98





## Manual Peak Matching Report For Accurate Mass Determination

Theoretical mass	Experimental mass	PFK matching mass	Deviation*
202.13576	202.13610	180.98882	1.7 ppm

\* The deviation is obtained from the following equation:

$$\text{deviation} = \frac{\text{experimental mass} - \text{theoretical mass}}{\text{nominal mass}}$$

Where nominal mass takes in account only  $^{12}\text{C}$ ,  $^1\text{H}$ ,  $^{16}\text{O}$ ,  $^{14}\text{N}$  etc...

Theoretical mass correspond to the mass of the most abundant isotope peak

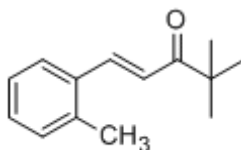


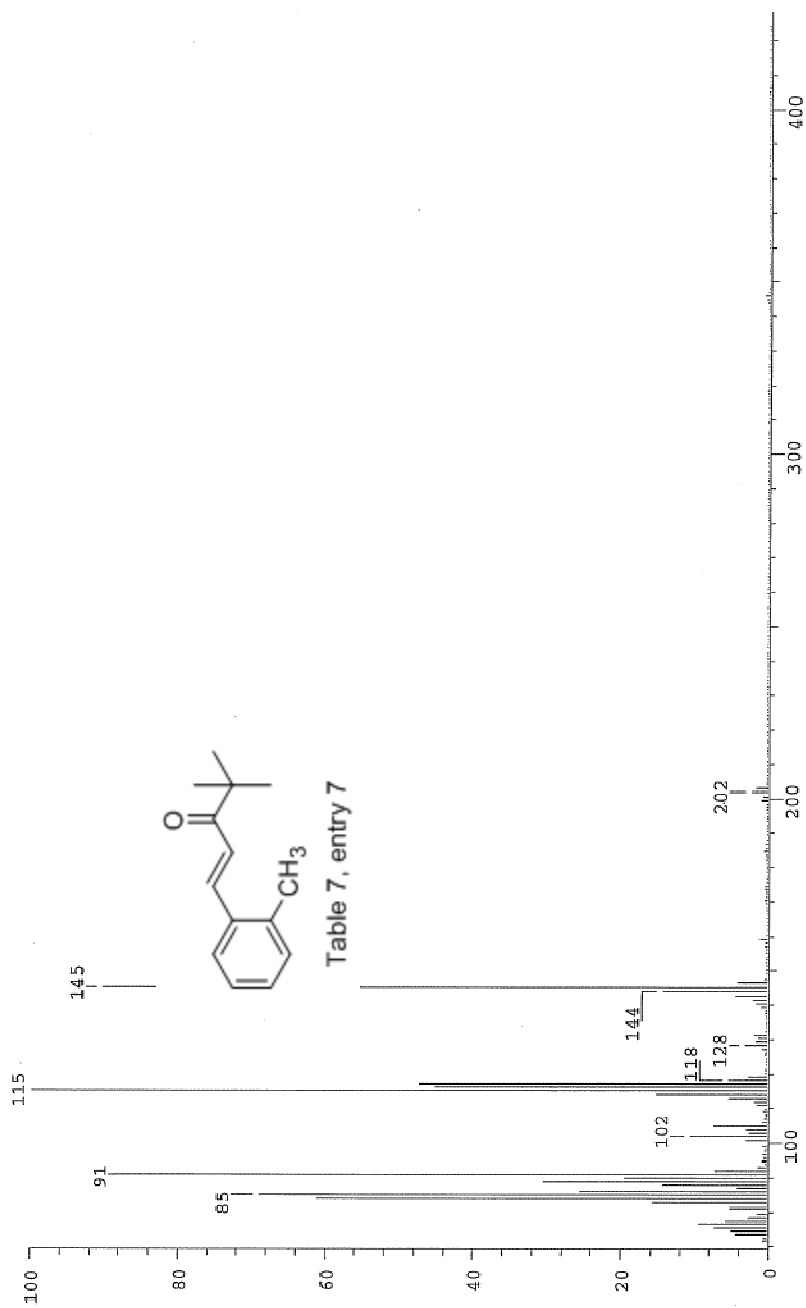
Table 7, entry 7

*Handwritten signature*

SPPC: fin083949.dat (24-OCT-08 11:20:43)  
 Samp: KW717  
 Comm: 70 eV EI  
 Oper: kh  
 Base: 39.53  
 Peak: 1000.0 mmu  
 Scan 2 @ 0.19 min (EI +QIMS LMR UP IR)

Study: ms services  
 Masses: 35.01 > 650.00  
 Intensity: 4534520

Scans: 1 > 7  
 Client: Kuldap  
 #Peaks: 537  
 RIC: 51137035  
 2.3E+06



Date: Fri Oct 24 11:21:29 2008 ICIS: 8.3.0 SP2 for OSF1 (V4.0) build 98-238 from 26-Aug-98

KW721, CDCl<sub>3</sub>  
 300 MHz  
 WHITE SOLID  
 OCT 29 2008

7.837  
 7.783  
 7.257  
 7.110  
 7.081  
 6.771  
 6.768  
 6.717  
 6.715

2.345

1.218

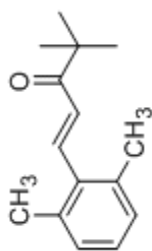
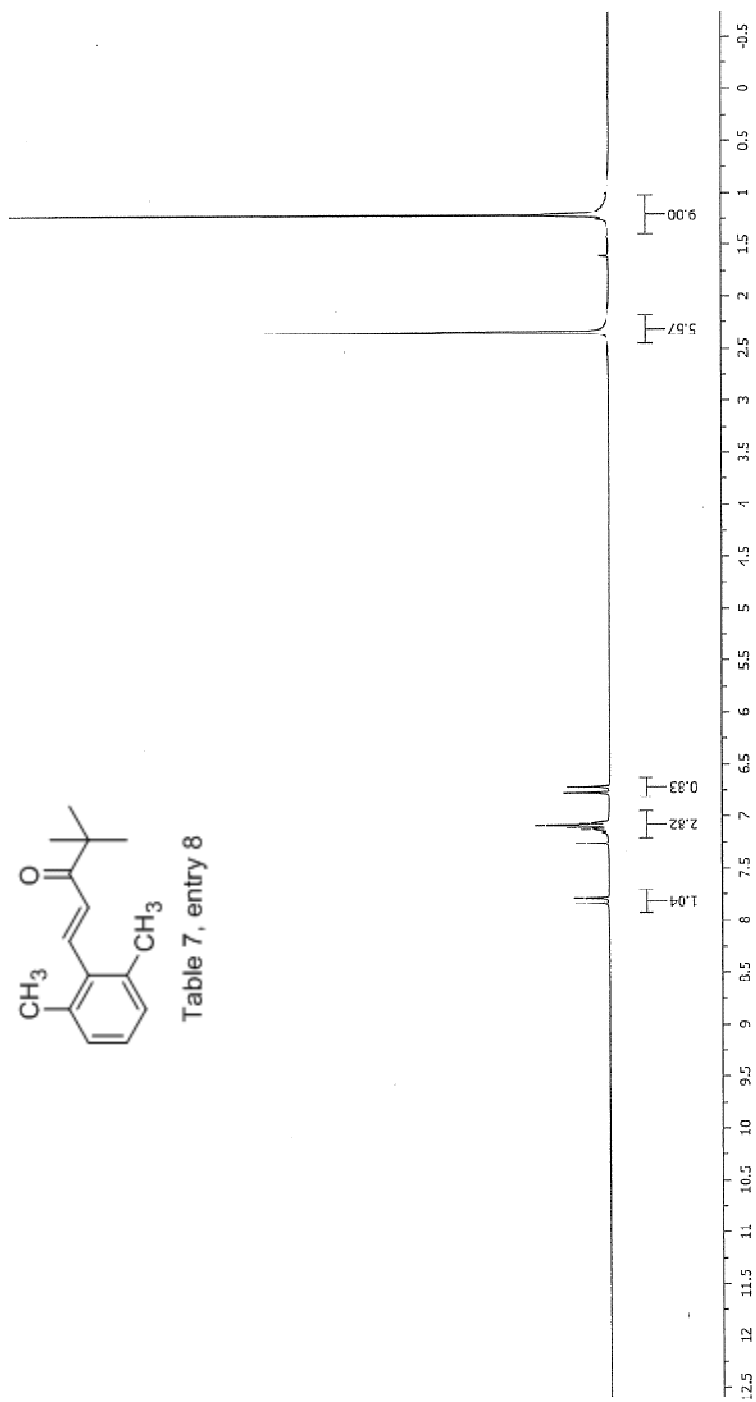
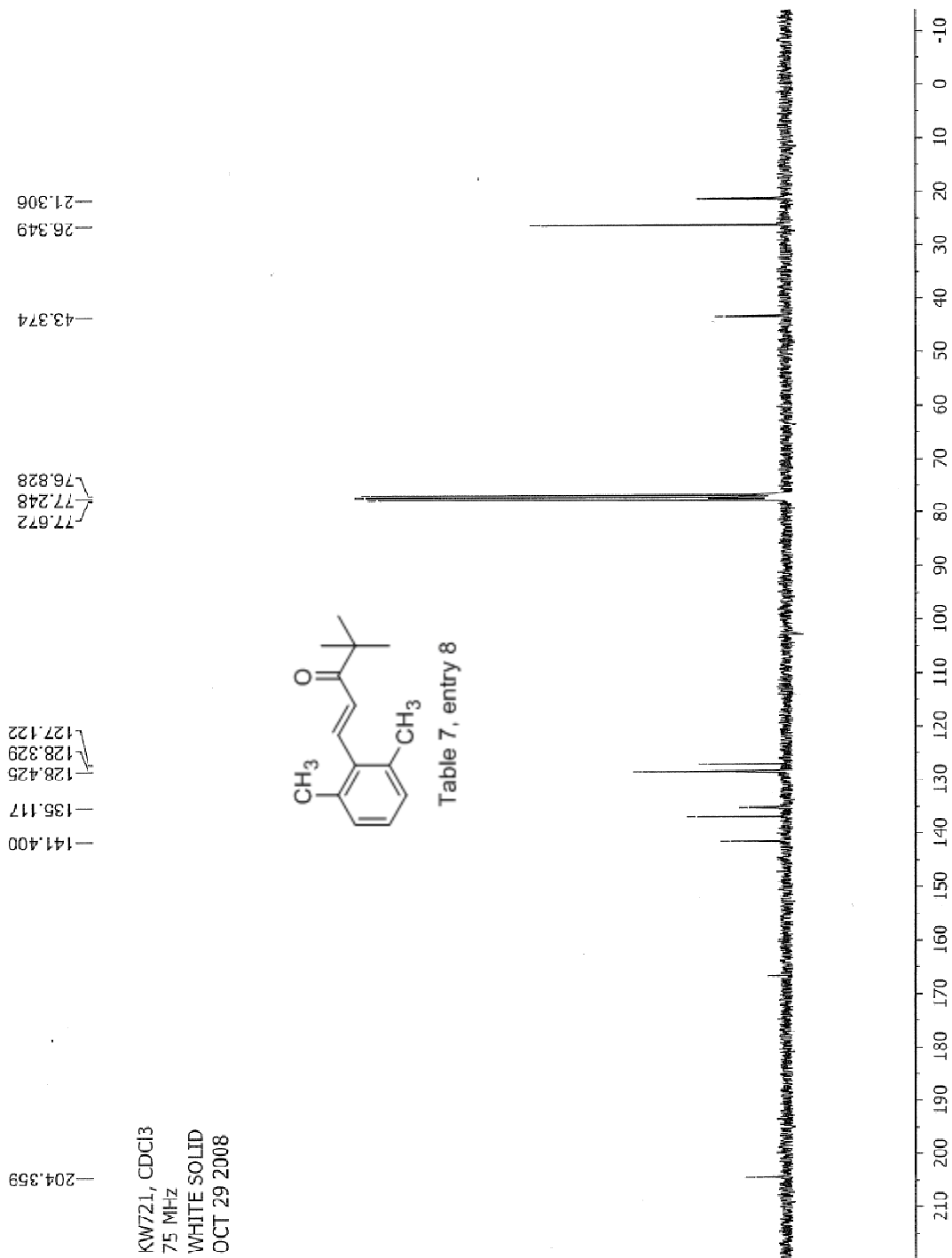


Table 7, entry 8





### Manual Peak Matching Report For Accurate Mass Determination

Theoretical mass	Experimental mass	PFK matching mass	Deviation*
216.15141	216.15173	180.98882	1.5 ppm

\* The deviation is obtained from the following equation:

$$\text{deviation} = \frac{\text{experimental mass} - \text{theoretical mass}}{\text{nominal mass}}$$

Where nominal mass takes in account only  $^{12}\text{C}$ ,  $^1\text{H}$ ,  $^{16}\text{O}$ ,  $^{14}\text{N}$  etc...

Theoretical mass correspond to the mass of the most abundant isotope peak

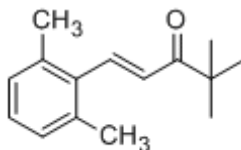


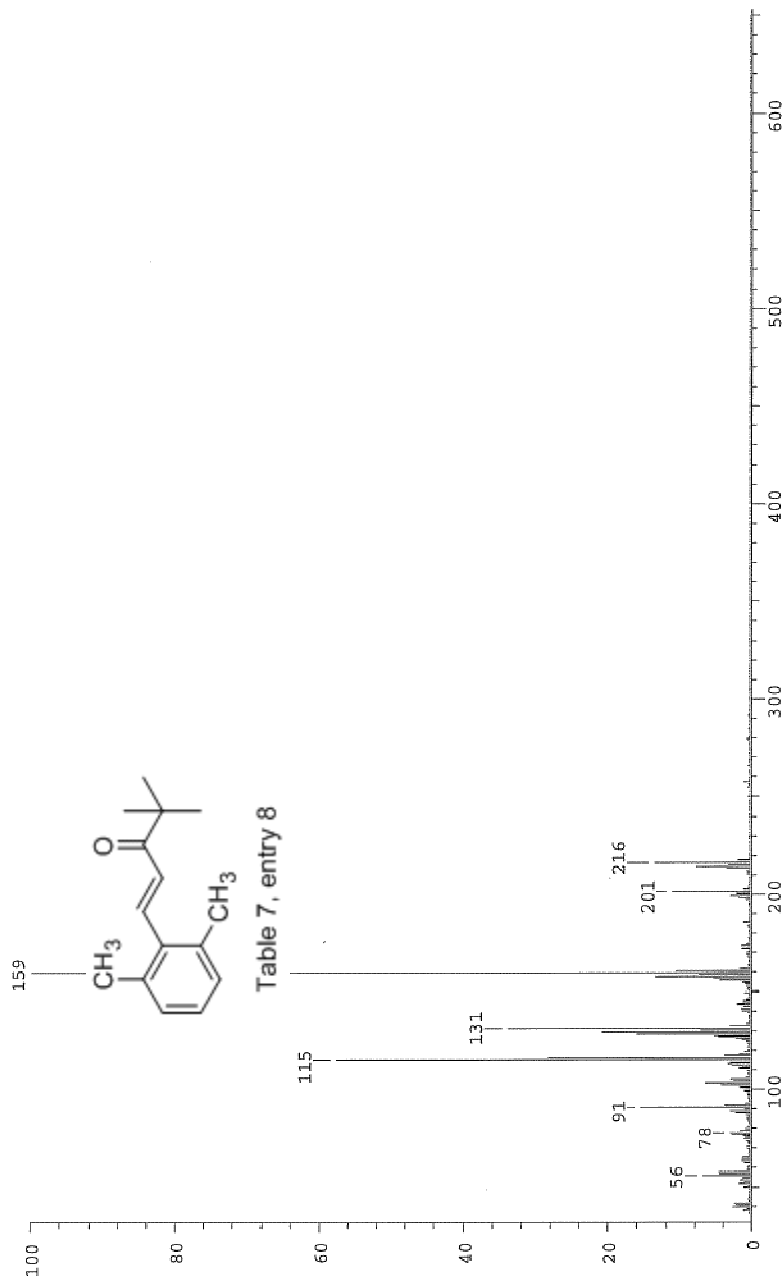
Table 7, entry 8

*Handwritten signature*

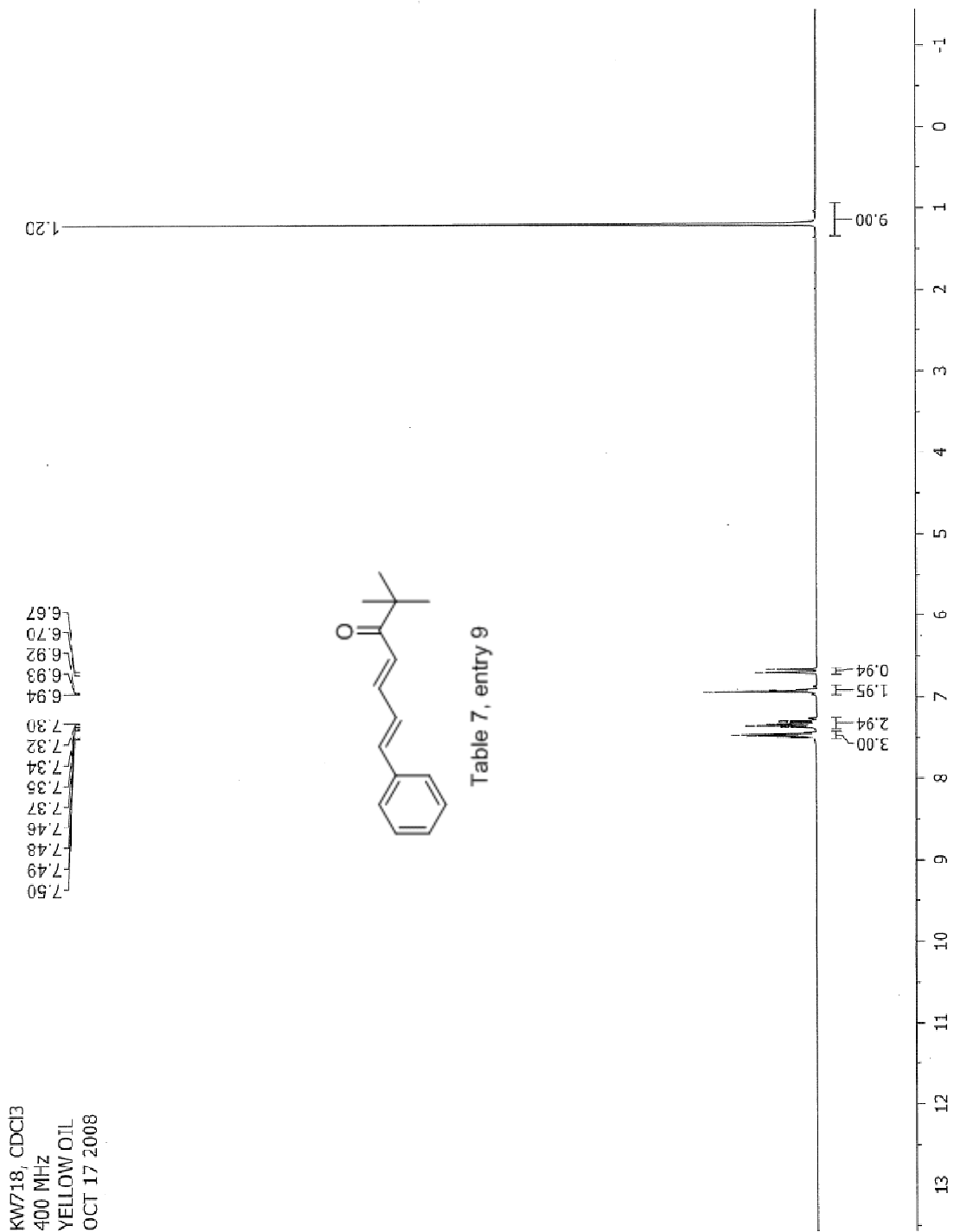


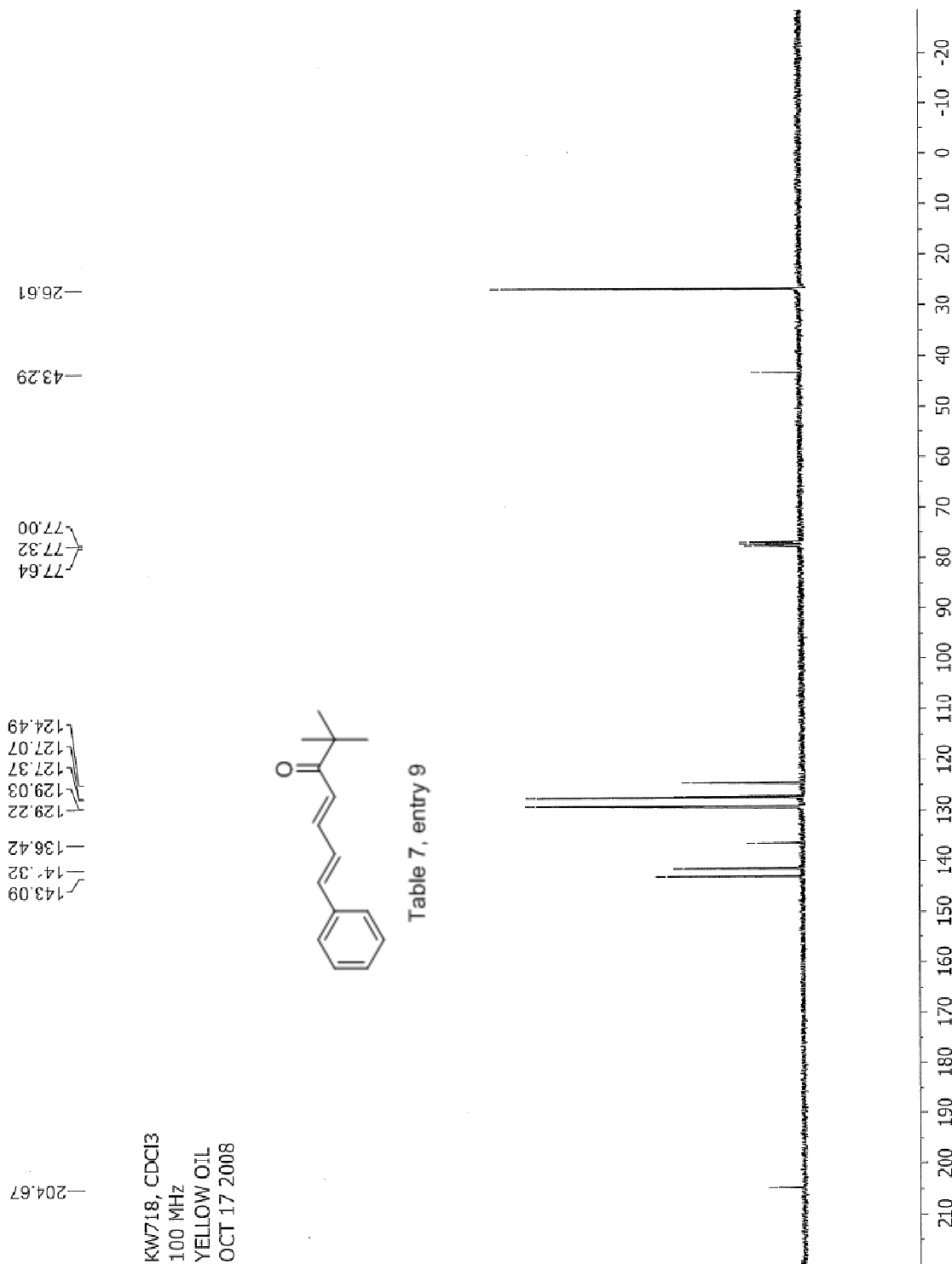
Scans: 1 > 29  
 Client: Kuldeep  
 #Peaks: 619  
 RIC: 2538287  
 4.9E+05

SPEC: fin084089.dat (16-DEC-08 10:38:07)  
 Samp: kw721  
 Comm: 70 eV EI  
 Oper: kh  
 Study: ms services  
 Base: 159.45  
 Masses: 35.01 > 650.00  
 Peak: 1000.0 mmu  
 Intensity: 491388  
 Scan 21 @ 0.58 min (EI +Q1MS LMR UP LR)



Date: Tue Dec 16 10:39:41 2008 ICIS: 8.3.0 SP2 for OSF1 (V4.0) build 98-238 from 26-Aug-98





### Manual Peak Matching Report For Accurate Mass Determination

Theoretical mass	Experimental mass	PFK matching mass	Deviation*
214.13576	214.13625	180.98882	2.3 ppm

\* The deviation is obtained from the following equation:

$$\text{deviation} = \frac{\text{experimental mass} - \text{theoretical mass}}{\text{nominal mass}}$$

Where nominal mass takes in account only  $^{12}\text{C}$ ,  $^1\text{H}$ ,  $^{16}\text{O}$ ,  $^{14}\text{N}$  etc...

Theoretical mass correspond to the mass of the most abundant isotope peak

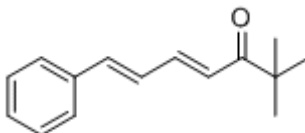
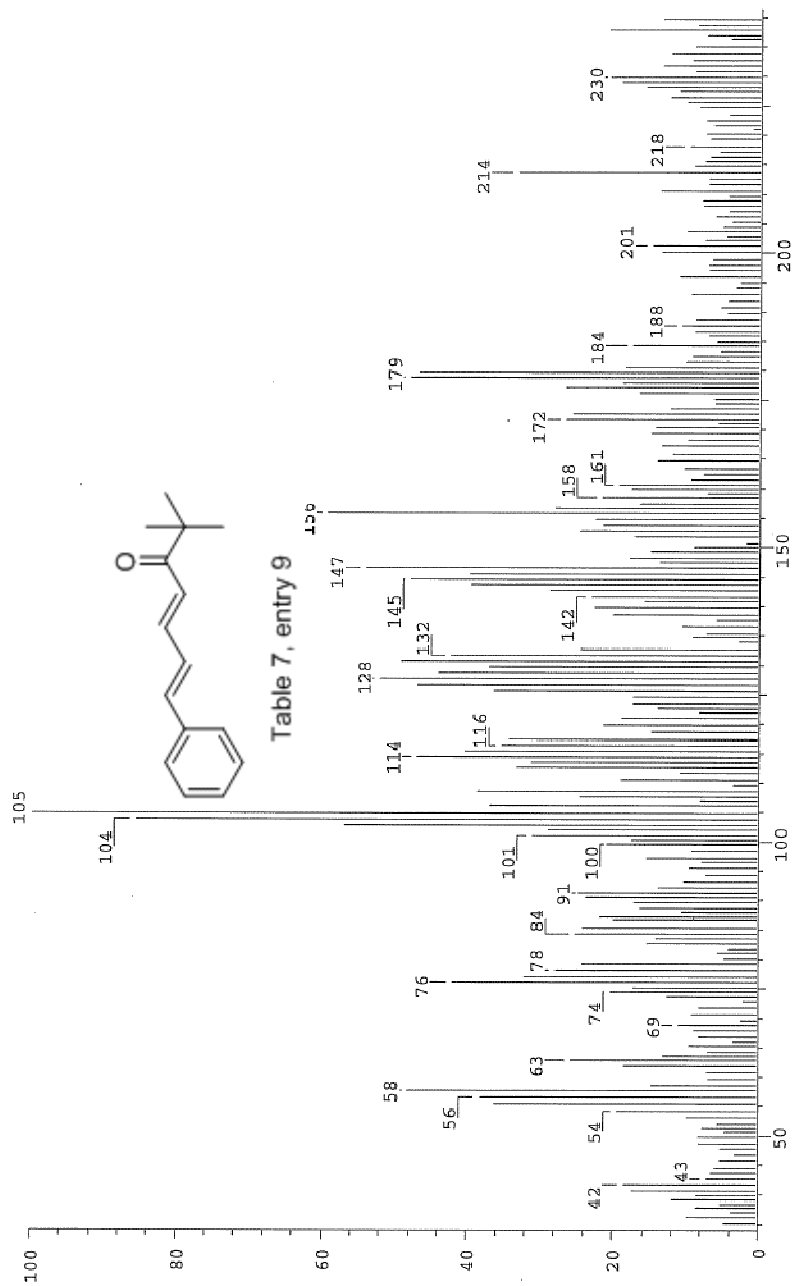


Table 7, entry 9

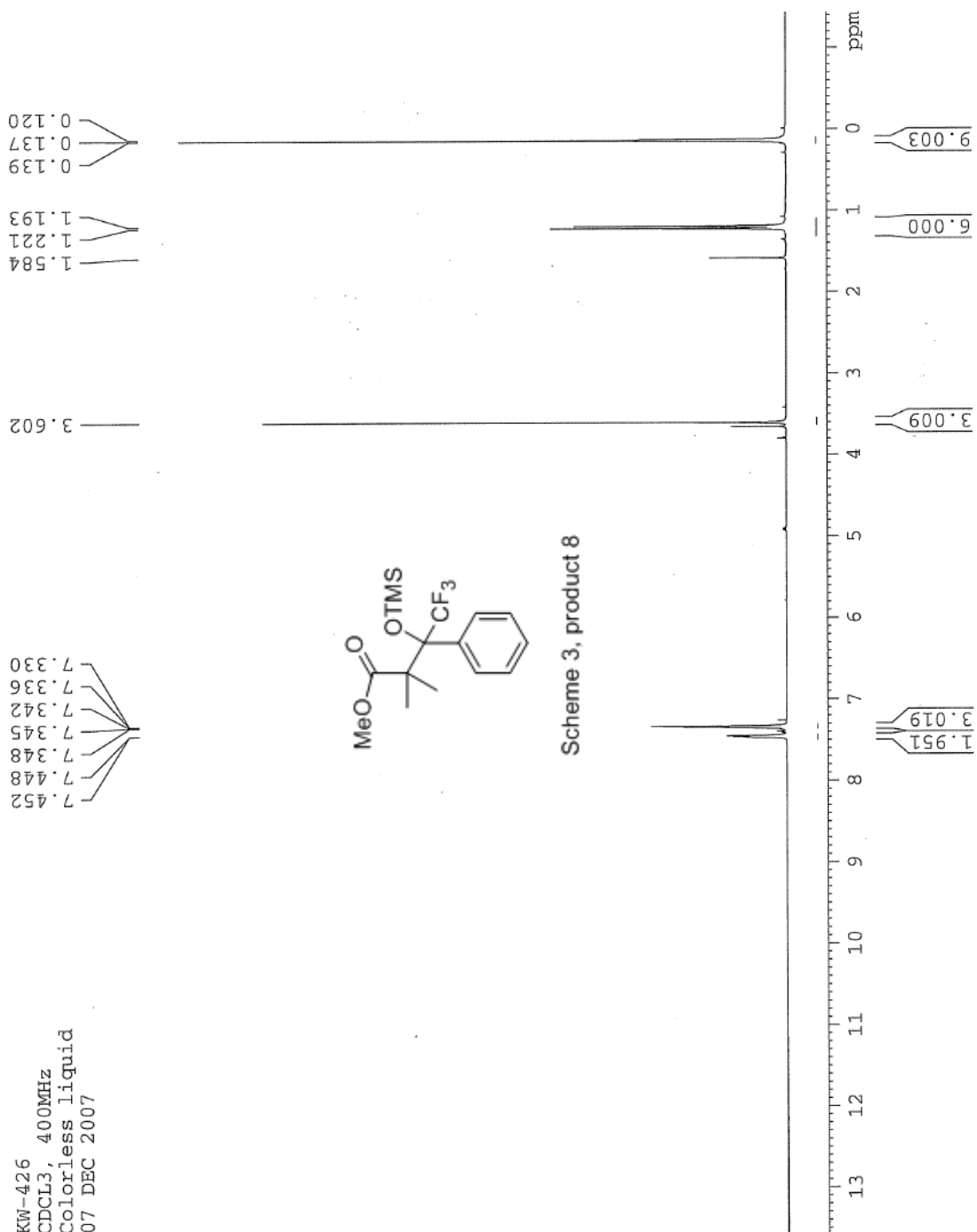
bn

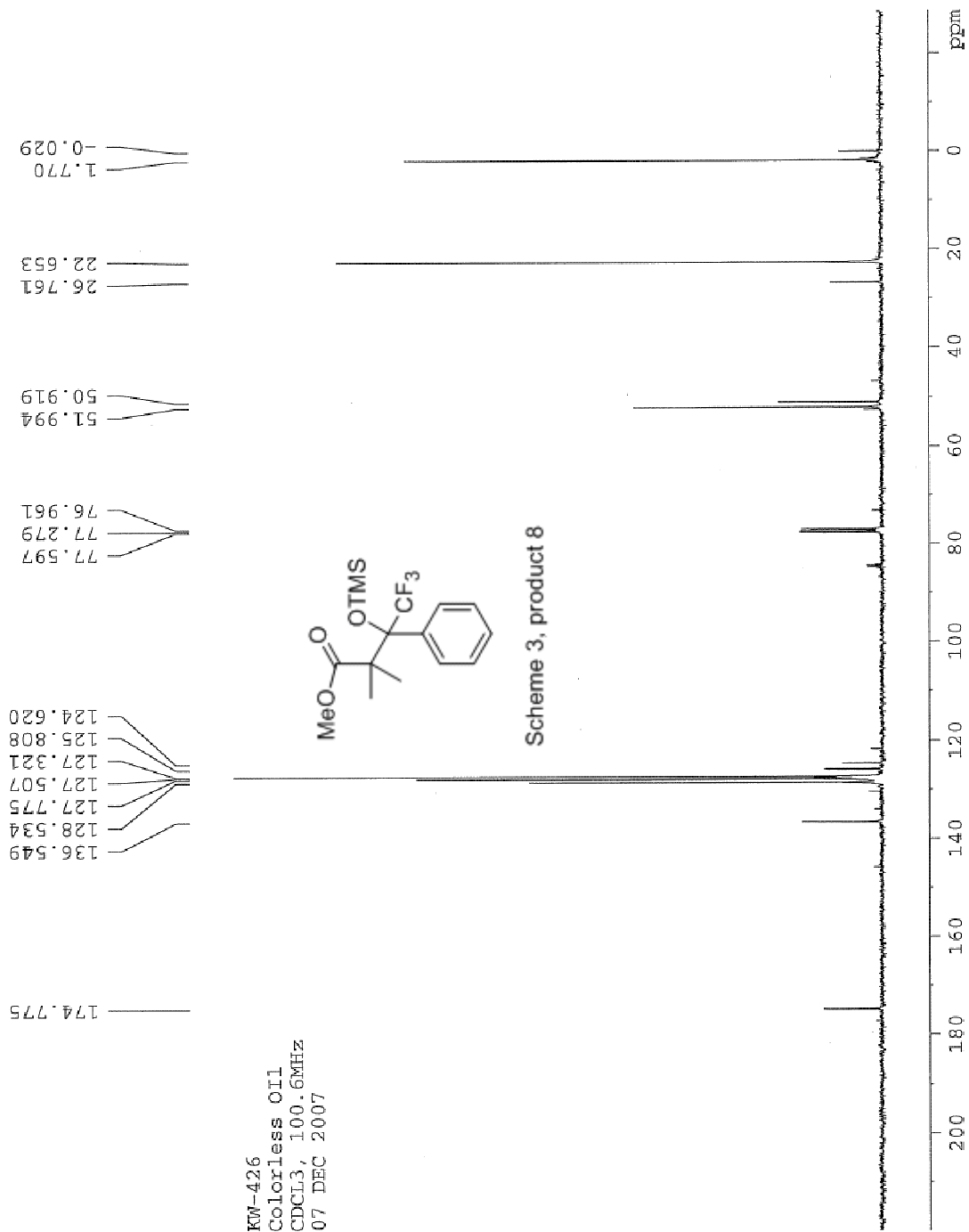
SPC: fin084172.dat (22-JAN-09 11:01:41)  
 Samp: kv718  
 Comm: 70 eV EI  
 Study: ms services  
 Oper: kh  
 Base: 104.76  
 Peak: 1000.0 mmu  
 Intensity: 3313  
 Scan: 31 @ 0.80 min (EI +QIMS LMR UP LR)  
 Scans: 1 > 157  
 Client: Kuldup  
 #Peaks: 651  
 RIC: 179934  
 3.3E+03



Date: Thu Jan 22 11:06:11 2009 ICIS: 8.3.0 SP2 for OSF1 (V4.0) build 98-238 from 26-Aug-98

KW-426  
 CDCl<sub>3</sub>, 400MHz  
 Colorless liquid  
 07 DEC 2007





### Manual Peak Matching Report For Accurate Mass Determination

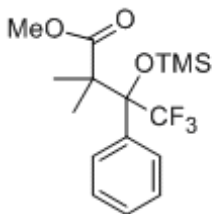
Theoretical mass	Experimental mass	PFK matching mass	Deviation*
348.13686	348.13754	330.97923	1.9 $\mu\text{m}$

\* The deviation is obtained from the following equation:

$$\text{deviation} = \frac{\text{experimental mass} - \text{theoretical mass}}{\text{nominal mass}}$$

Where nominal mass takes in account only  $^{12}\text{C}$ ,  $^1\text{H}$ ,  $^{16}\text{O}$ ,  $^{14}\text{N}$  etc...

Theoretical mass correspond to the mass of the most abundant isotope peak



Scheme 3, product 8

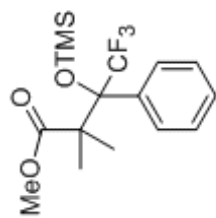
10



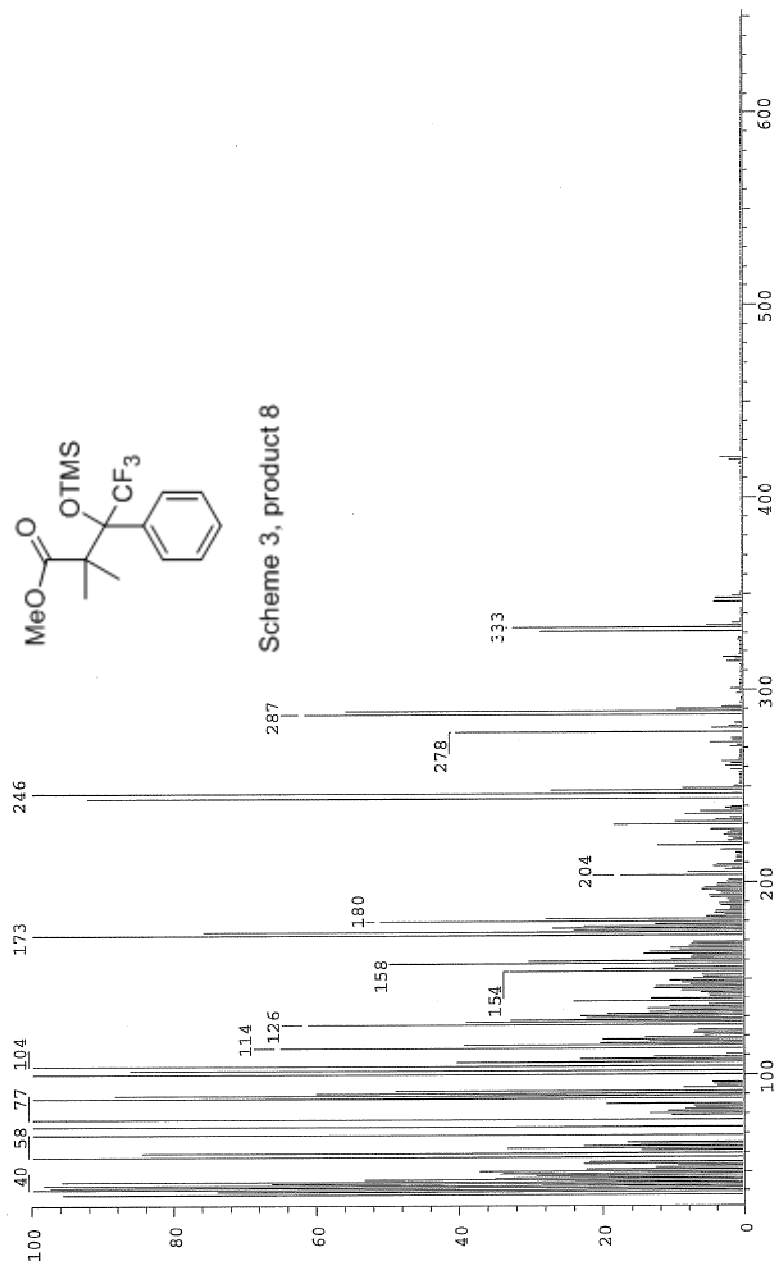
Scans: 1 > 59  
 Client: KW  
 #Peaks: 575  
 RIC: 704821906  
 1.7E+07

SPEC: fir063392.dat (12-DEC-07 11:19:03)  
 Samp: KW426  
 Comm: 70 ev EI  
 Oper: kh  
 Base: 246.31  
 Peak: 1000.0 mmu  
 Scan 15 @ 0.47 min (EI +Q)MS LMR UP LR)

Study: MS Services  
 Masses: 35.01 > 650.00  
 Intensity: 16777215

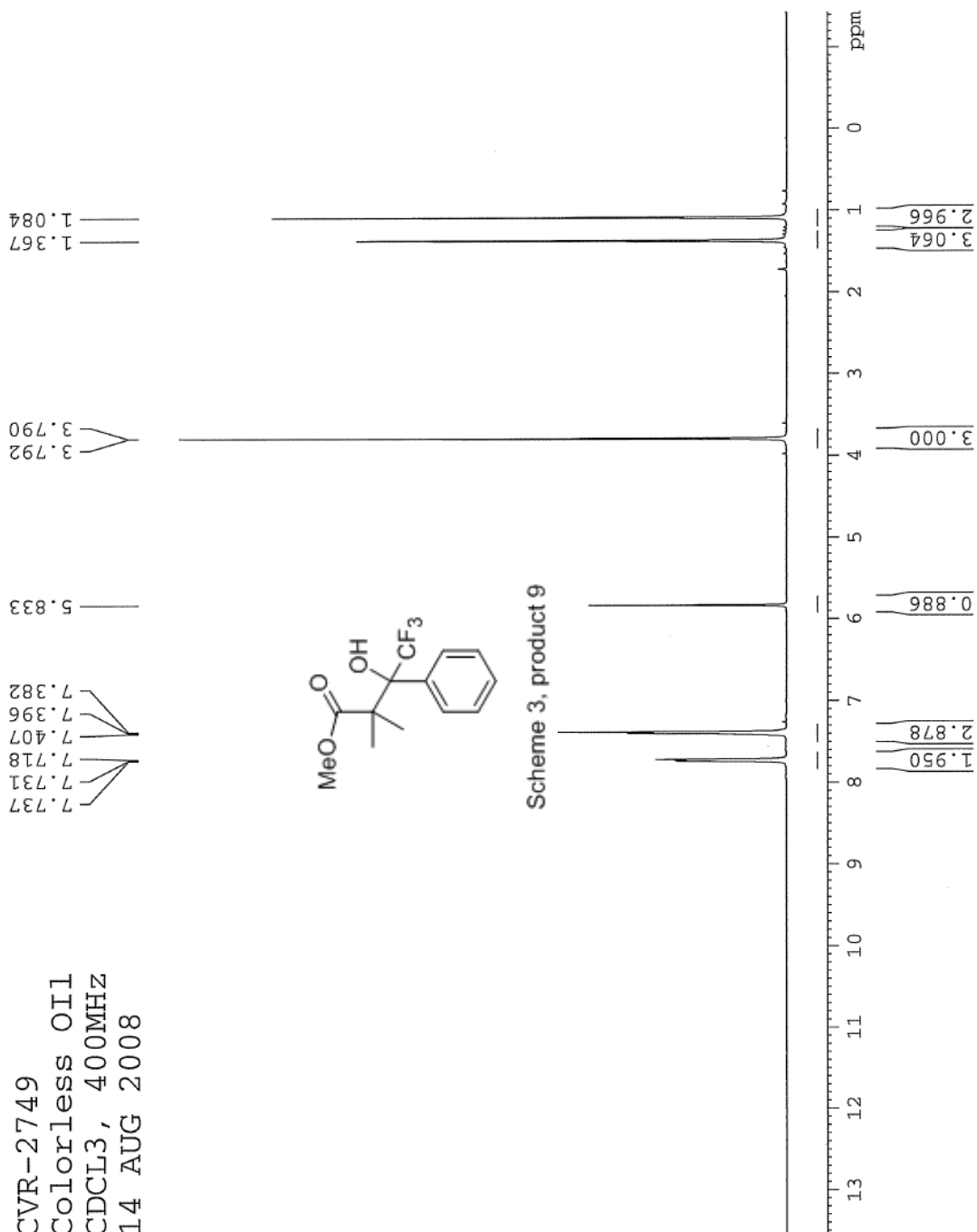


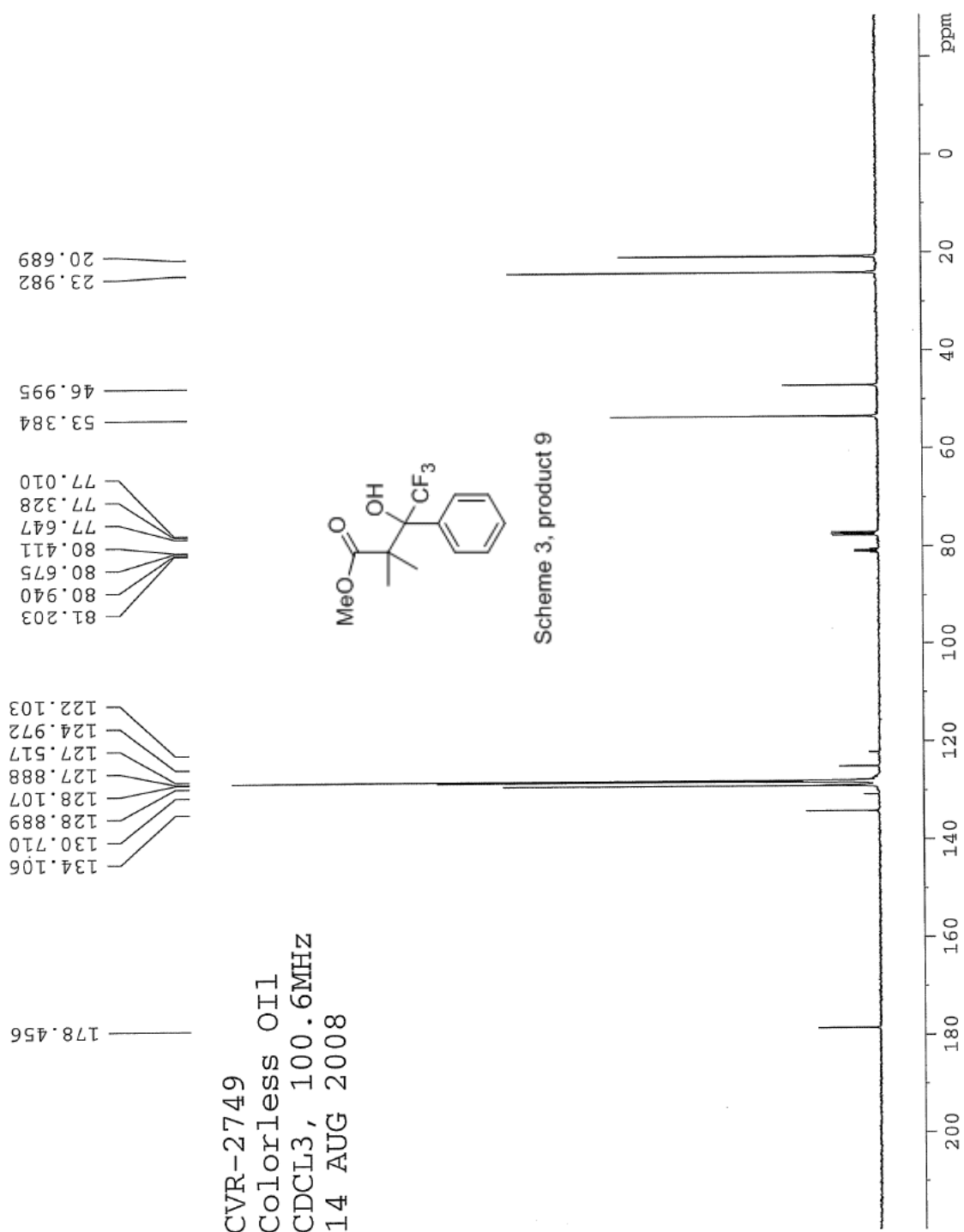
Scheme 3, product 8

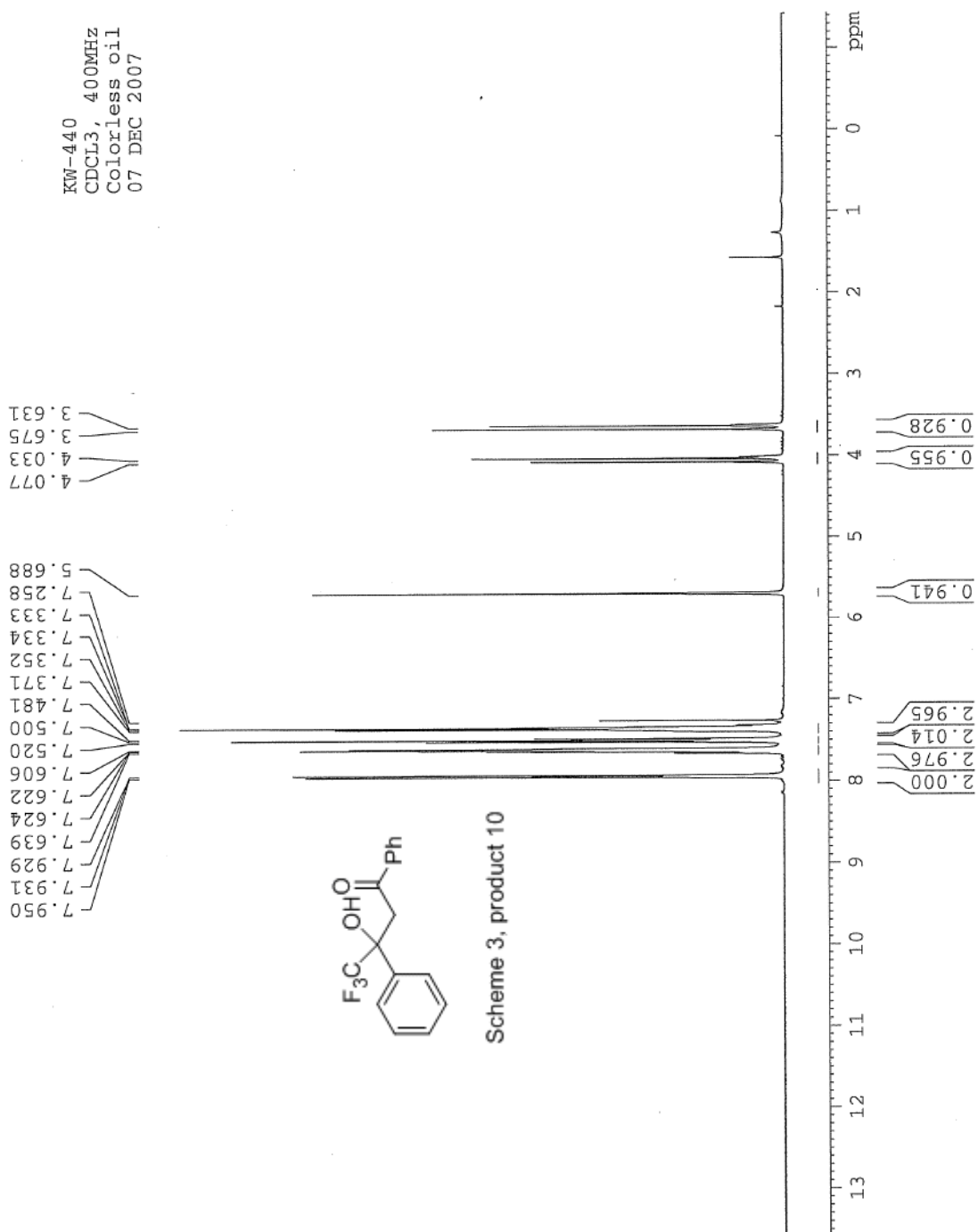


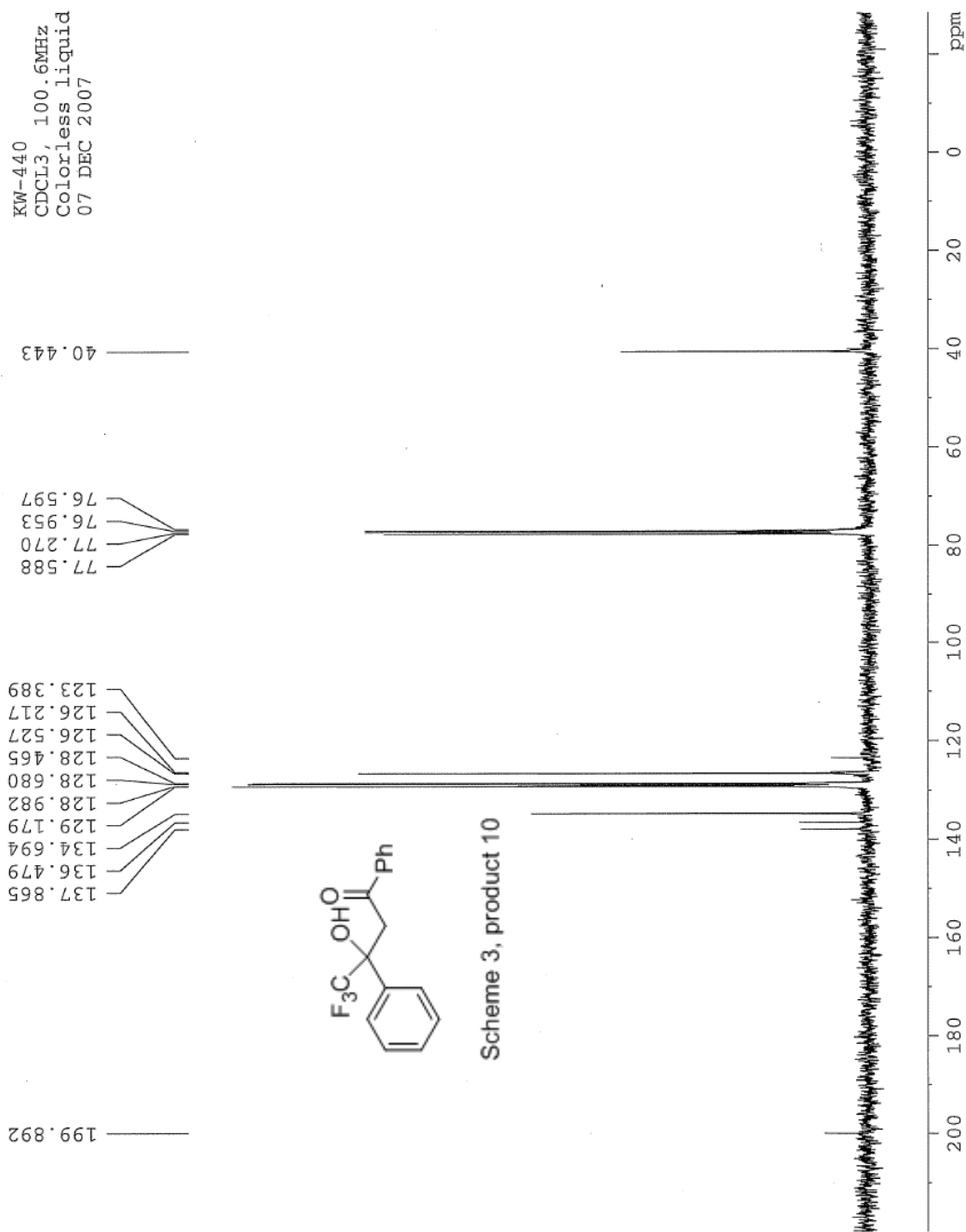
Date: Wed Dec 12 11:38:01 2007 ICIS: 8.3.0 SP2 for OSF1 (V4.0) build 98-238 from 26-Aug-98

CVR-2749  
 Colorless Oil  
 CDCl<sub>3</sub>, 400MHz  
 14 AUG 2008



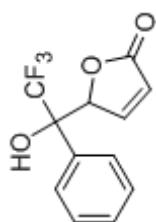




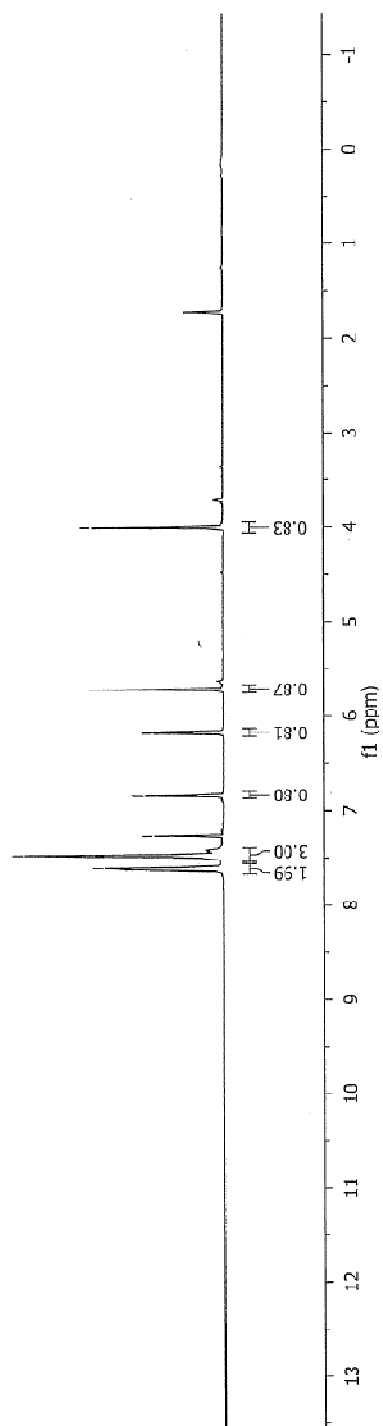


KW473-A, CDCl<sub>3</sub>  
400MHz  
WHITE SOLID

7.620  
7.614  
7.601  
7.479  
7.472  
7.465  
7.460  
7.258  
6.841  
6.838  
6.178  
6.161  
5.718  
5.714  
4.002

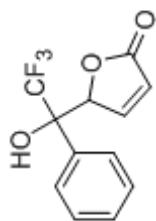


Scheme 3, product 11, syn isomer

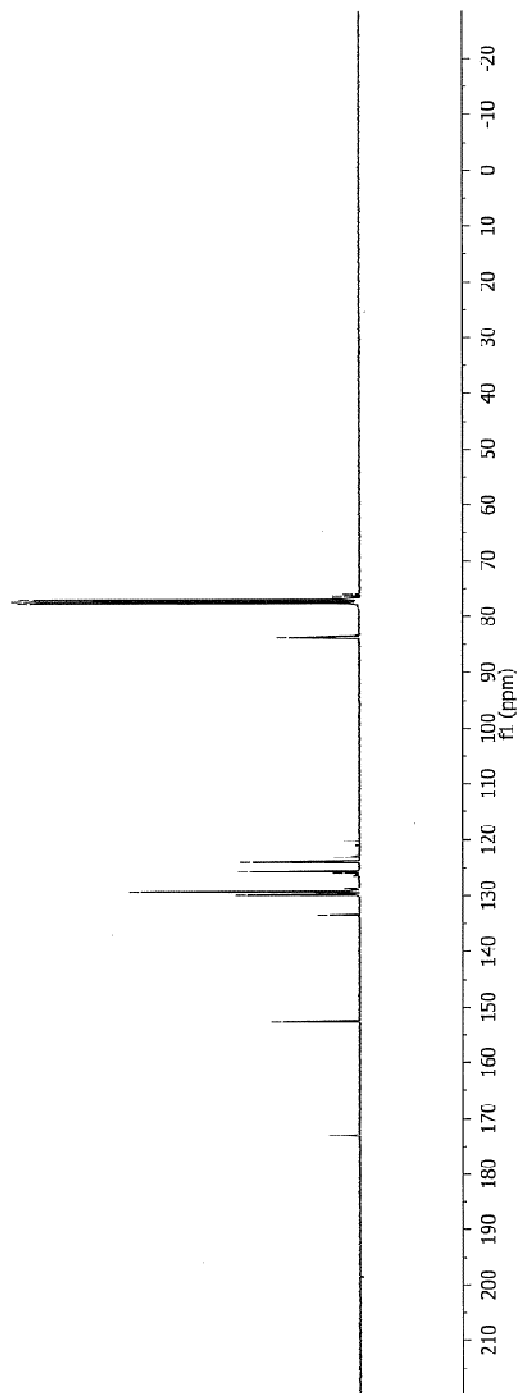


KW473A, CDCl<sub>3</sub>  
100 MHz  
AUG 16 2008

173.006  
152.548  
133.398  
129.836  
129.252  
125.994  
125.592  
123.983  
123.139  
120.284  
83.631  
77.574  
77.257  
76.939  
76.720  
76.433  
76.146



Scheme 3, product 11, syn isomer



### Manual Peak Matching Report For Accurate Mass Determination

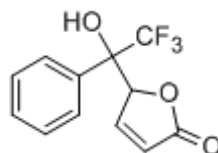
Theoretical mass	Experimental mass	PFK matching mass	Deviation*
258.05038	258.05075	242.98562	1.5 ppm

\* The deviation is obtained from the following equation:

$$\text{deviation} = \frac{\text{experimental mass} - \text{theoretical mass}}{\text{nominal mass}}$$

Where nominal mass takes in account only  $^{12}\text{C}$ ,  $^1\text{H}$ ,  $^{16}\text{O}$ ,  $^{14}\text{N}$  etc...

Theoretical mass correspond to the mass of the most abundant isotope peak

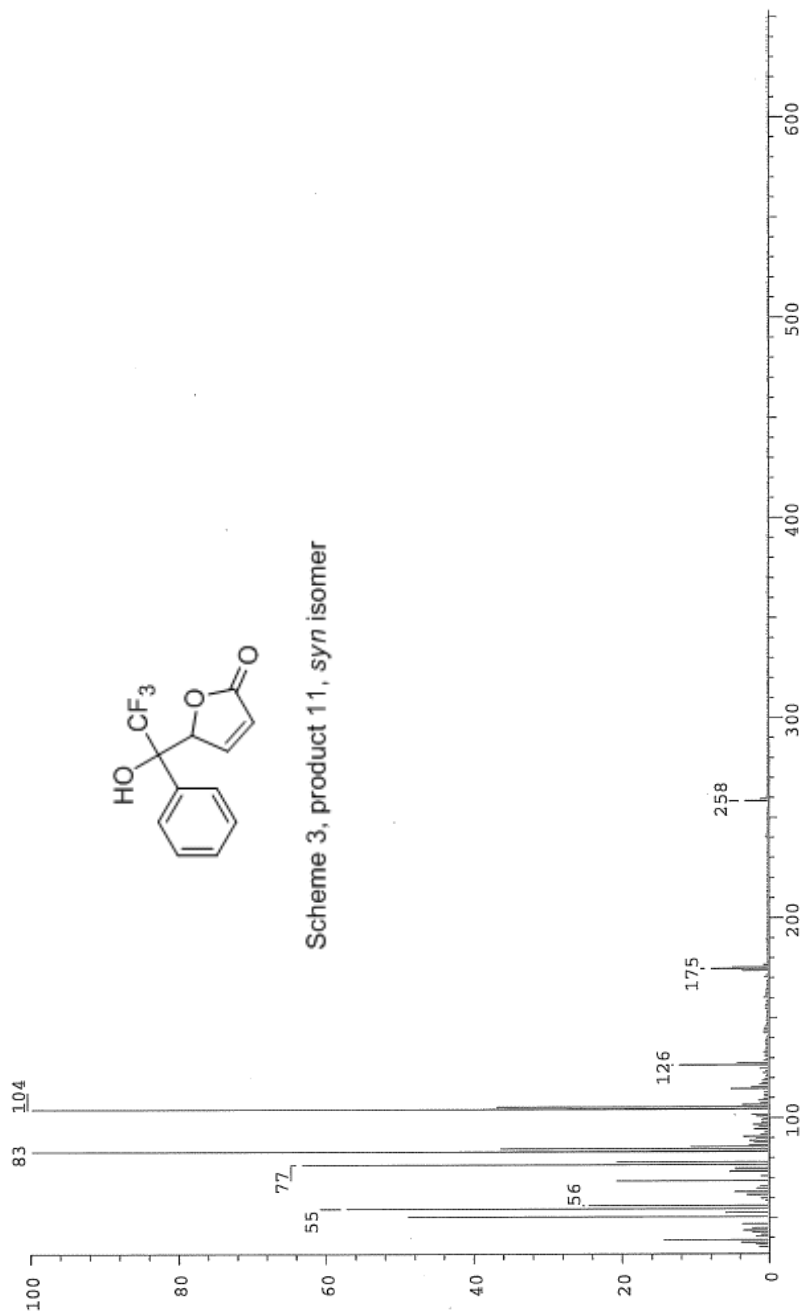


Scheme 3, product 11, syn isomer

*Handwritten signature*



SPEC: fin063540.dat (18-MAR-08 14:04:43)  
 Samp: KW-473A  
 Comm: 70 eV EI  
 Oper: kh  
 Base: 104.45  
 Peak: 1000.0 mmu  
 Scan 29 @ 0.75 min (EI +QIMS LMR UP LR)  
 Study: MS Services  
 Masses: 35.01 > 650.00  
 Intensity: 16777215  
 Scans: 1 > 35  
 Client: Kuldup  
 #Peaks: 471  
 RIC: 112602599  
 1.7E+07

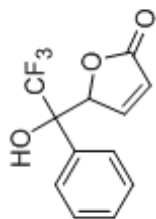


Scheme 3, product 11, syn isomer

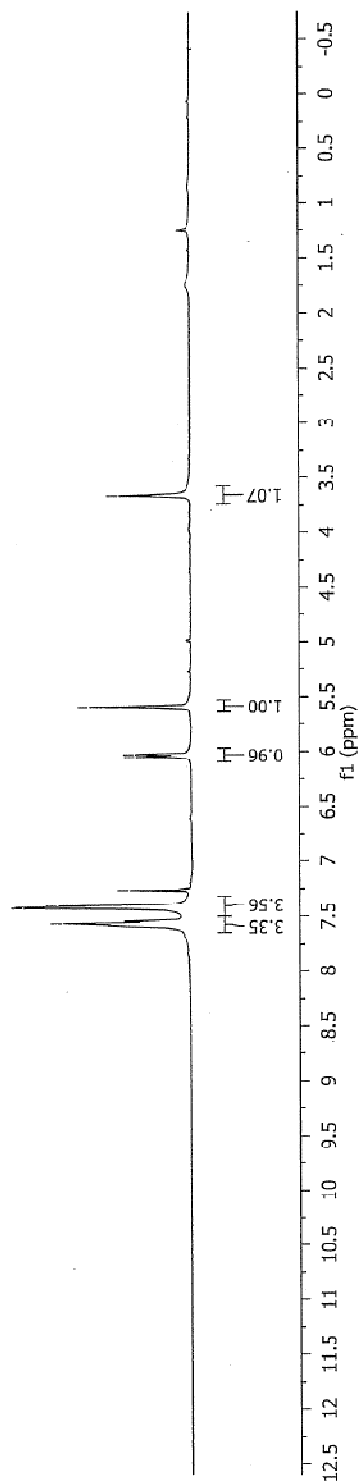
Date: Tue Mar 18 14:06:18 2008 ICIS: 8.3.0 SP2 for OSF1 (V4.0) build 98-238 from 26-Aug-98

KW473H1-B, CDCl<sub>3</sub>  
300MHz  
YELLOW SOLID

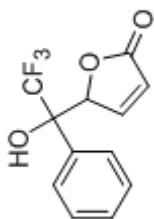
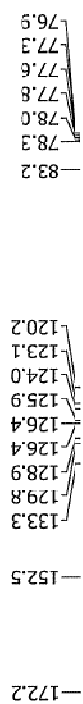
7.560  
7.420  
7.409  
7.398  
7.257  
6.046  
6.026  
5.587  
3.663



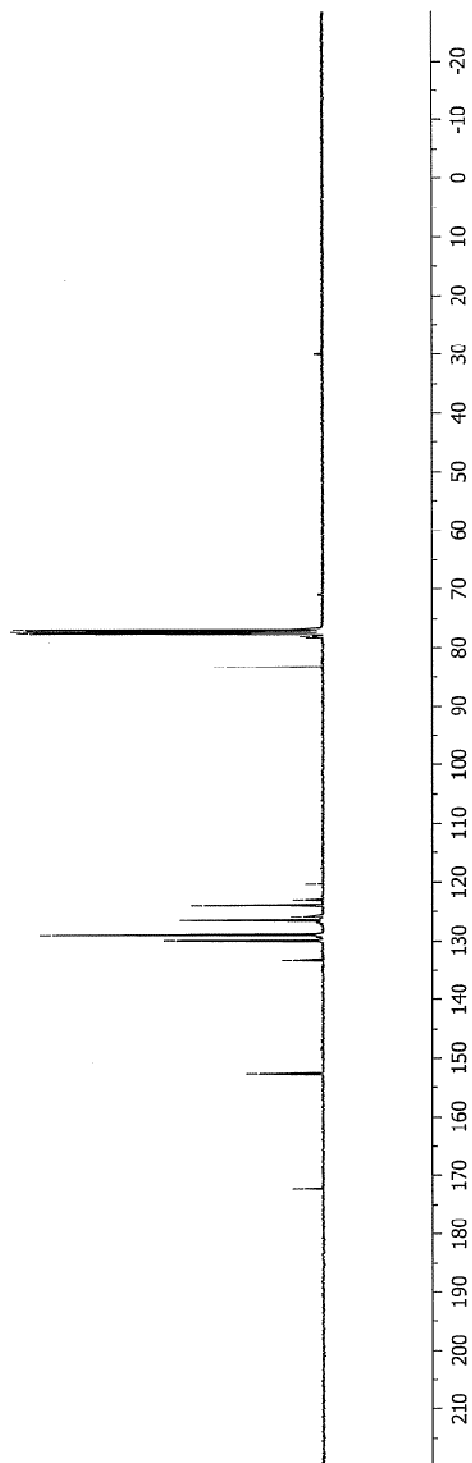
Scheme 3, product 11, *anti* isomer



KW473B, CDCl<sub>3</sub>  
100 MHz  
AUG 12 2008



Scheme 3, product 11, *anti* isomer



### Manual Peak Matching Report For Accurate Mass Determination

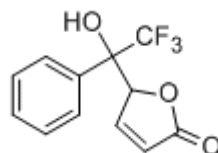
Theoretical mass	Experimental mass	PFK matching mass	Deviation*
258.05038	258.05076	230.98562	1.5 ppm

\* The deviation is obtained from the following equation:

$$\text{deviation} = \frac{\text{experimental mass} - \text{theoretical mass}}{\text{nominal mass}}$$

Where nominal mass takes in account only  $^{12}\text{C}$ ,  $^1\text{H}$ ,  $^{16}\text{O}$ ,  $^{14}\text{N}$  etc...

Theoretical mass correspond to the mass of the most abundant isotope peak



Scheme 3, product 11, *anti* isomer

W

Scans: 1 > 67  
 Client: Kuldub  
 #Peaks: 258  
 RIC: 34372  
 4.2R+03

SPRC: fin063541.dat (18-MAR-08 14:08:09)

Samp: KM-473B

Comm: 70 eV EI

Oper: kh

Base: 104.74

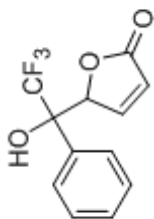
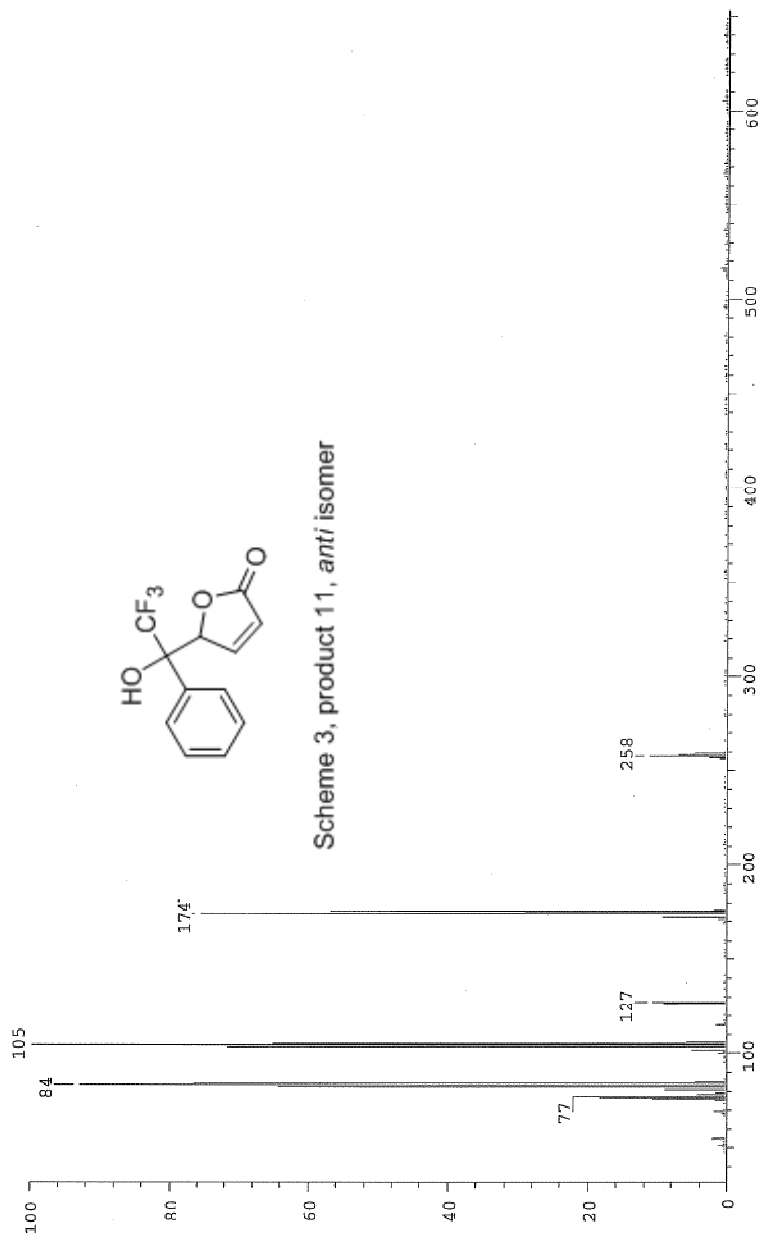
Peak: 1000.0 mmu

Scan 63 @ 1.44 min (EI +OLMS INR UP LR)

Study: MS Services

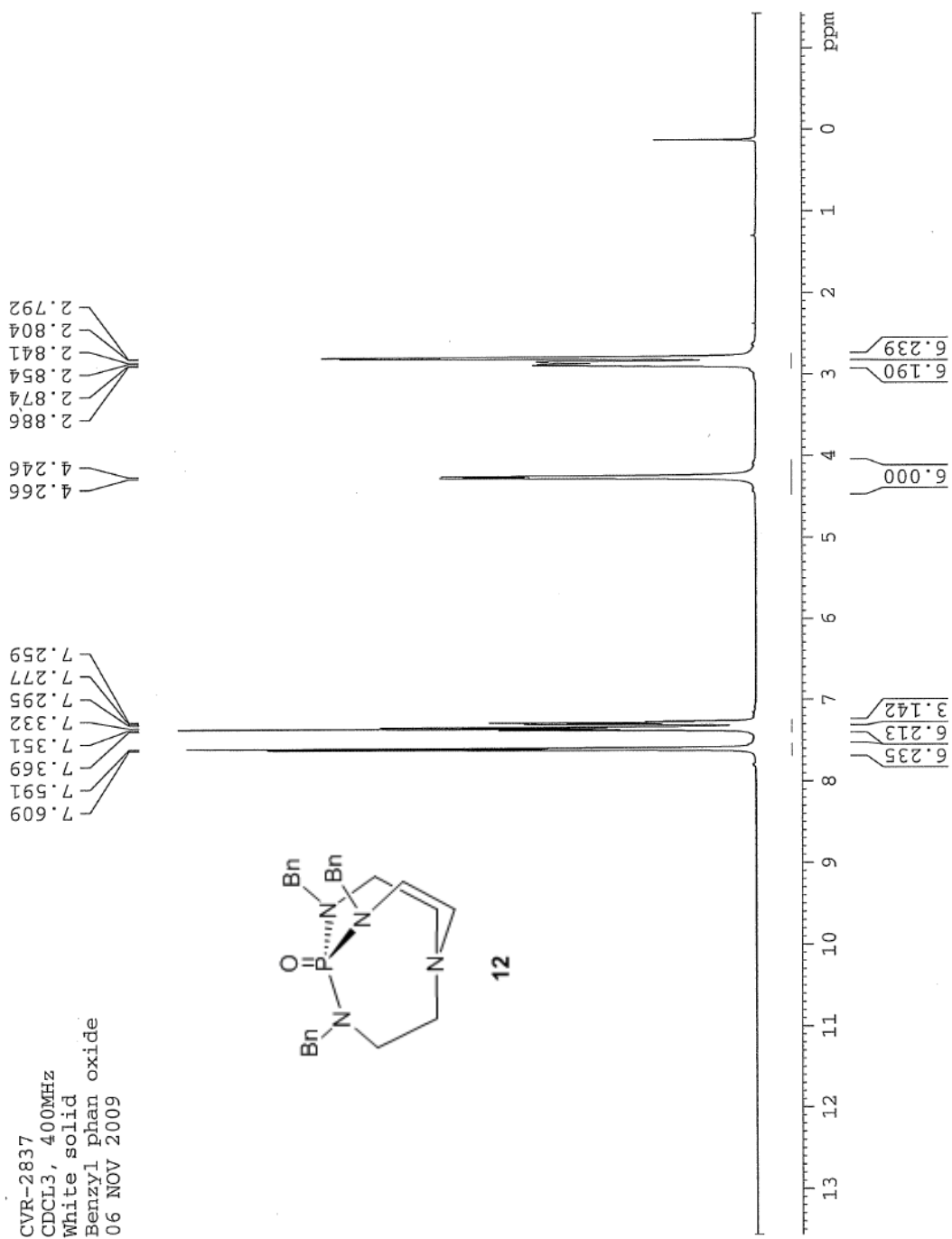
Masses: 35.01 > 650.00

Intensity: 4196

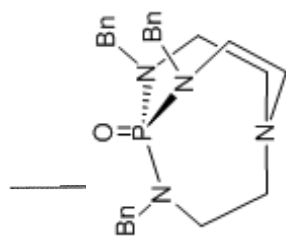
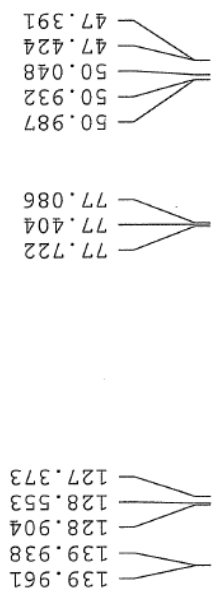


Scheme 3, product 11, *anti* isomer

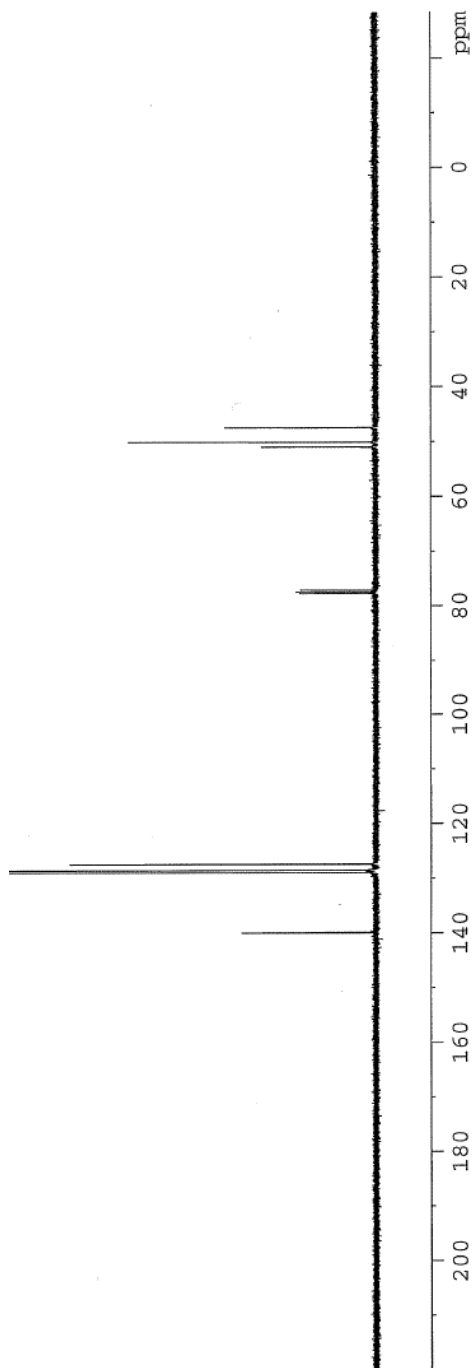
Date: Tue Mar 18 14:10:45 2008 TQMS: 3.3.0 SP2 for OSF1 (V4.0) build 98-238 from 26-Aug-98



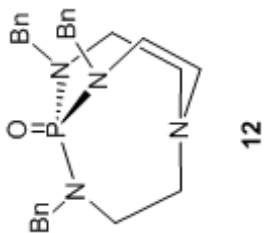
CVR-2837  
 CDCL<sub>3</sub>, 100MHz  
 Benzylphosphan Oxide  
 06 NOV 2009



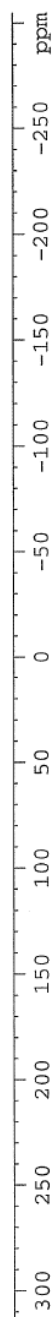
12



CVR-2837  
CDCl<sub>3</sub>, 162 MHz  
White solid  
Benzylphosphane oxide  
06 NOV 2009



24.247





## Manual Peak Matching Report For Accurate Mass Determination

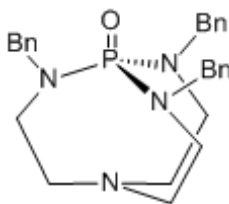
Theoretical mass	Experimental mass	PFK matching mass	Deviation*
460.23919	460.24046	430.97284	2.7 ppm

\* The deviation is obtained from the following equation:

$$\text{deviation} = \frac{\text{experimental mass} - \text{theoretical mass}}{\text{nominal mass}}$$

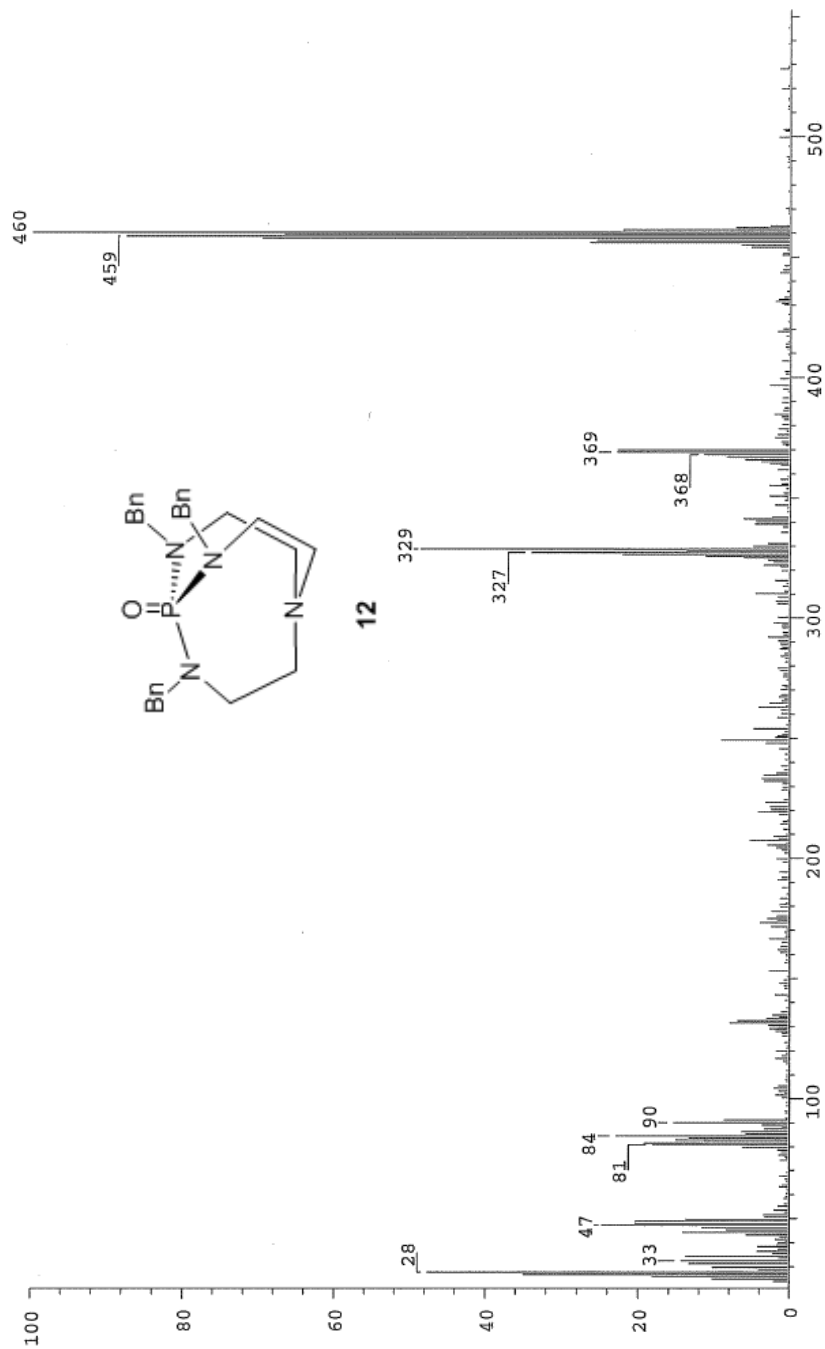
Where nominal mass takes in account only  $^{12}\text{C}$ ,  $^1\text{H}$ ,  $^{16}\text{O}$ ,  $^{14}\text{N}$  etc...

Theoretical mass correspond to the mass of the most abundant isotope peak



12

SPEC: fin084572.dat (23-JUN-09 12:06:09)  
 Samp: BFO  
 Comm: DP/EI  
 Oper: Study:  
 Base: 460.29 Masses: 23.75 > 550.02  
 Peak: 1000.0 mmu Intensity: 24175  
 Scan 80 @ 1.00 min (EI +QIMS LMR UP LR) 2.4E+04



Date: Tue Jun 23 12:07:50 2009 ICIS: 8.3.0 SP2 for OSF1 (V4.0) build 98-238 from 26-Aug-98